frontiers | Research Topics

The interaction between food ingredients and gut microbiome on health and disease

Edited by
Guiguo Zhang, Mohammad Altamimi, Yunkyoung Lee and Junling Shi

Published in
Frontiers in Microbiology
Frontiers in Microbiomes

FRONTIERS EBOOK COPYRIGHT STATEMENT

The copyright in the text of individual articles in this ebook is the property of their respective authors or their respective institutions or funders. The copyright in graphics and images within each article may be subject to copyright of other parties. In both cases this is subject to a license granted to Frontiers.

The compilation of articles constituting this ebook is the property of Frontiers.

Each article within this ebook, and the ebook itself, are published under the most recent version of the Creative Commons CC-BY licence. The version current at the date of publication of this ebook is CC-BY 4.0. If the CC-BY licence is updated, the licence granted by Frontiers is automatically updated to the new version.

When exercising any right under the CC-BY licence, Frontiers must be attributed as the original publisher of the article or ebook, as applicable.

Authors have the responsibility of ensuring that any graphics or other materials which are the property of others may be included in the CC-BY licence, but this should be checked before relying on the CC-BY licence to reproduce those materials. Any copyright notices relating to those materials must be complied with.

Copyright and source acknowledgement notices may not be removed and must be displayed in any copy, derivative work or partial copy which includes the elements in question.

All copyright, and all rights therein, are protected by national and international copyright laws. The above represents a summary only. For further information please read Frontiers' Conditions for Website Use and Copyright Statement, and the applicable CC-BY licence.

ISSN 1664-8714
ISBN 978-2-8325-7799-8
DOI 10.3389/978-2-8325-7799-8

Generative AI statement
Any alternative text (Alt text) provided alongside figures in the articles in this ebook has been generated by Frontiers with the support of artificial intelligence and reasonable efforts have been made to ensure accuracy, including review by the authors wherever possible. If you identify any issues, please contact us.

About Frontiers

Frontiers is more than just an open access publisher of scholarly articles: it is a pioneering approach to the world of academia, radically improving the way scholarly research is managed. The grand vision of Frontiers is a world where all people have an equal opportunity to seek, share and generate knowledge. Frontiers provides immediate and permanent online open access to all its publications, but this alone is not enough to realize our grand goals.

Frontiers journal series

The Frontiers journal series is a multi-tier and interdisciplinary set of open-access, online journals, promising a paradigm shift from the current review, selection and dissemination processes in academic publishing. All Frontiers journals are driven by researchers for researchers; therefore, they constitute a service to the scholarly community. At the same time, the *Frontiers journal series* operates on a revolutionary invention, the tiered publishing system, initially addressing specific communities of scholars, and gradually climbing up to broader public understanding, thus serving the interests of the lay society, too.

Dedication to quality

Each Frontiers article is a landmark of the highest quality, thanks to genuinely collaborative interactions between authors and review editors, who include some of the world's best academicians. Research must be certified by peers before entering a stream of knowledge that may eventually reach the public - and shape society; therefore, Frontiers only applies the most rigorous and unbiased reviews. Frontiers revolutionizes research publishing by freely delivering the most outstanding research, evaluated with no bias from both the academic and social point of view. By applying the most advanced information technologies, Frontiers is catapulting scholarly publishing into a new generation.

What are Frontiers Research Topics?

Frontiers Research Topics are very popular trademarks of the *Frontiers journals series*: they are collections of at least ten articles, all centered on a particular subject. With their unique mix of varied contributions from Original Research to Review Articles, Frontiers Research Topics unify the most influential researchers, the latest key findings and historical advances in a hot research area.

Find out more on how to host your own Frontiers Research Topic or contribute to one as an author by contacting the Frontiers editorial office: frontiersin.org/about/contact

The interaction between food ingredients and gut microbiome on health and disease

Topic editors

Guiguo Zhang — Shandong Agricultural University, China
Mohammad Altamimi — An-Najah National University, Palestine
Yunkyoung Lee — Jeju National University, Republic of Korea
Junling Shi — Northwestern Polytechnical University, China

Citation

Zhang, G., Altamimi, M., Lee, Y., Shi, J., eds. (2026). *The interaction between food ingredients and gut microbiome on health and disease*. Lausanne: Frontiers Media SA. doi: 10.3389/978-2-8325-7799-8

Table of contents

07 Editorial: The interaction between food ingredients and gut microbiome on health and disease
Guiguo Zhang, Mohammad Altamimi, Junling Shi and Yunkyoung Lee

12 Dietary supplementation with proanthocyanidins and rutin alleviates the symptoms of type 2 diabetes mice and regulates gut microbiota
Yue Gao, Binbin Huang, Yunyi Qin, Bing Qiao, Mengfei Ren, Liqing Cao, Yan Zhang and Maozhen Han

28 Metagenomic analysis of goat feces from Ogliastra (Sardinia, Italy)
Monica Rosaria Molotzu, Piera Angela Cabras, Lisa Di Marcantonio, Rossano Atzeni, Nicolò Pietro Paolo Macciotta and Antonella Canu

43 Macronutrient balance determines the human gut microbiome eubiosis: insights from *in vitro* gastrointestinal digestion and fermentation of eight pulse species
Da Bin Lee and In Seon Hwang

58 Cecum microbiota composition, fermentation characteristics, and immunometabolic biomarkers of Yunshang black goat fed varying dietary energy and protein levels
Binlong Fu, Xiaoqi Zhao, Muhammad Khan, Yanting Jiang, Weijuan Li, Maida Mushtaq, Baiji Danzeng, Xiaojun Ni, Zobia Azeem, Qingyong Shao, Bai Xue and Yina Ouyang

70 *Dachaihu* decoction ameliorates abnormal behavior by regulating gut microbiota in rats with propionic acid-induced autism
Yangyang Zhang, Hang Li, Bolin Li, Yizhuang Li, Xuejun Chai, Sheng Li, Xia Xue, Honglei Li, Yonghong Zhao, Youcai Tang, Baoqi Yin, Pengju Zhao, Enyao Li and Pengya Feng

88 Unveiling roles of beneficial gut bacteria and optimal diets for health
Suresh Kumar, Riya Mukherjee, Pratibha Gaur, Élcio Leal, Xiaoming Lyu, Saheem Ahmad, Paridhi Puri, Chung-Ming Chang, V. Samuel Raj and Ramendra Pati Pandey

102 Pasteurized *Akkermansia muciniphila* Timepie001 ameliorates DSS-induced ulcerative colitis in mice by alleviating intestinal injury and modulating gut microbiota
Huan Han, Hui Xiong, Zengli Liu, Xunzhi Liu, Hailin Wang, Jiaxiang Kou, Dewei Yi, Ying Shi, Hao Wu and Jianjun Qiao

115 *Amomum tsaoko* flavonoids attenuate ulcerative colitis by inhibiting TLR4/NF-κB/NLRP3 signaling pathway and modulating gut microbiota in mice
Zelin Huang, Yan Zhao, Weixing Yang, Chunfen Duan, Jun Sheng, Yang Tian, Lei Peng and Xiaoyu Gao

130 Galacto-oligosaccharides alleviate experimental lactose intolerance associated with gut microbiota in mice
Qianxi Li, Xinlei Wang, Siyu Guo, Tongtong Wang, Heng Cao, Yunhe Cao and Bing Dong

143 Dietary fatty acids promote gut health in weaned piglets by regulating gut microbiota and immune function
Zongze Fan, Lei Lei, Xingyue Wu, Ronghui Xing, Pengfei Du, Ziyang Wang, Huijuan Zhao, Yanqun Huang, Wen Chen and Xuemeng Si

157 Influence of gut microbiota and immune markers in different stages of colorectal adenomas
Xianmei Wang, Hang Chen, Meng Yang, Minshan Huang, Dan Zhang, Mingke Li, Hui Wang, Qingqing Zhou, Lihong Lu, Yu Li, Jiangkun Yu and Lanqing Ma

170 *Paederia scandens* extract alleviates obesity via modulating the gut microbiota and serum metabolome disorder
Yuanyuan Yang, Jinglei Si, Jiayuan Mo, Jin Li, Bin Pan, Yi Pan, Lihe Jiang, Decai Wang and Xueping Feng

183 Impact of bacteroides uniformis on fatty liver hemorrhagic syndrome in dawu golden phoenix laying hens: modulation of gut microbiota and arachidonic acid metabolism
Yu Zhang, Rongfei Ma, Xicui Du, Xin He, Yan Zhang, Ning Ma, Hailong Liu and Xinghua Zhao

195 Associations between gut microbiota and diet composition of three arid-adapted rodent species from the Inner Mongolia grassland
Muha Cha, Yunga Wu, Duhu Man and Xianfeng Yi

208 *Clostridium Butyricum 337279* shapes the gut microbiota to attenuate metabolic disorder in diet-induced obese mice
Xuejiao Zhang, Zhiyu Li, Junjun Cao, Haipeng Sun and Wenyan Niu

223 Synthetic vs. non-synthetic sweeteners: their differential effects on gut microbiome diversity and function
Alex Kidangathazhe, Theresah Amponsah, Abhijit Maji, Seidu Adams, Maria Chettoor, Xiuqing Wang and Joy Scaria

232 Relationship between high-fat diet, gut microbiota, and precocious puberty: mechanisms and implications
Nan Wu, Ke Ning, Yanan Liu, Qinghua Wang, Ning Li and Lei Zhang

246 Dietary *Codonopsis pilosula* polysaccharides promote gut health and enhance immunity in Hu sheep
Qing Zhao, Wanning Li, Zilong Liu, Qiao Li and Youji Ma

258 Metagenomic insights into the effects of Chive seed flavonoid on intestinal fermentation, morphology, and microbiota composition in sheep
Xujie Li, Dengpan Li, Chunhui Wang, Qiao Li, Yajing Nie, Liming Zhang, Jin Xu and Youji Ma

276 The human gut microbiota is associated with host lifestyle: a comprehensive narrative review
Qin Zeng, Xianqiong Feng, Yanling Hu and Shaoyu Su

287 Effect of supplementation with *L*-Citrulline on rumen microbiota structure, plasma metabolites, reproductive hormones, and antioxidant capacity of Hu ewes
Renping Liu, Peiyao Li, Chen Fan, Shanshan Wang, Zhiqiang Liu, Guodong Zhao and Kailun Yang

308 Exploring the influence of gut microbiota metabolites on vitiligo through the gut-skin axis
Chuanjian Yuan, Lyuye Liu, Duorong Zeng, Jinxiang Yuan, Liyuan Guo and Junling Zhang

322 Dissecting the molecular interactions between botanical extracts and the human gut microbiota
Leonardo Mancabelli, Chiara Tarracchini, Giulia Longhi, Giulia Alessandri, Marco Ventura and Francesca Turroni

336 Ferulic acid and N-Feruloylserotonin ameliorate LPS-induced intestinal inflammation via modulation of gut microbiota, metabolome, and transcriptome
Xiangdong Hu, Xuebing Han, Gang Liu, Guiping Guan and Chenmei Xia

352 Exploring the fate of *Listeria monocytogenes* in an *in vitro* digestion and fecal fermentation model: insights into survival during digestion and interaction with gut microbiota
Dong Woo Kim, Saloni Singh, Ui In Kim, So Hyeon An, Hyeon Ji Je, Dong Young Lee, Eun Ju Yun and Ok Kyung Koo

363 Effectiveness of personalized granola tailored to the gut microbiota for improving gut environment and mood states
Hiroyuki Sasaki, Hirofumi Masutomi, Yohsuke Yamauchi, Katsuyuki Ishihara and Shinji Fukuda

383 Bisphenol F exposure induced vascular toxicity through intestinal microbiota imbalance
Jianlong Yan, Yanbin Pan, Huadong Liu, Jie Yuan, Jie Chen, Yannan Gao, Chaolan Lin, Feng Lin, Rongning Wang, Yaqiong He, Caiping Wang, Cong Xu, Tangzhiming Li, Peng Zhang, Yu Lan, Wenming Shao, Xinli Pang, Da Yin, Xin Sun and Weixiang Luo

396 Effect of dietary zinc supplementation on the gastrointestinal microbiome and host gene expression in the *Shank3B*$^{-/-}$ mouse model of autism spectrum disorder
Giselle C. Wong, Yewon Jung, Kevin Lee, Chantelle Fourie, Kim M. Handley, Johanna M. Montgomery and Michael W. Taylor

413 *Lactiplantibacillus plantarum* ZP-6 mitigates polystyrene nanoplastics-induced liver damage in colitis mice via the gut-liver axis
Lili Zhao, Zihan Wei, Yibin Wang, Wanrong Chen, Wenjing Zhang, Mengfei Xie, Hong Chen, Yiping Zhang, Haiyan Gao and Xiaobing Jiang

430 Gut microbiome regulation in equine animals: current understanding and future perspectives
Fenglin Li, Xiangyu Kong, Muhammad Zahoor Khan, Lin Wei, Jinjin Wei, Mingxia Zhu, Guiqin Liu, Bingjian Huang, Changfa Wang and Zhenwei Zhang

448 Guiren Runchang granules alleviate slow transit constipation in mice by modulating gut microbiota and short-chain fatty acids
Xinfeng Bai, Yachao Wang, Kai Wang, Weihua Chu and Tianyu Bai

461 Unraveling the mysteries of the gut-kidney axis: the protective role of traditional Chinese medicine in chronic kidney disease
Jiahui Li, Lijia Diao, Menglin Li, Fugang Huang and Ke Sun

488 The role of gut microbiota in diarrhea and its alleviation through microbiota-targeted interventions
Rui Tian, Chu-Jun Chong, Ya-Ya Bai, Ni Chen, Rui-Rui Qiao, Kan Wang, Yu-Wei Wang, Peng Zhao, Chong-Bo Zhao, Yu-Ping Tang, Li Zhang and Qiao Zhang

513 *Amomum tsao-ko Crevost et Lemarie* extract targets the gut-liver axis to combat atherosclerosis in ApoE$^{-/-}$ mice
Qianqian Wang, Yuanyuan Niu, Jiawei Huang, Junhong Huang, Jiamin Zhang, Boyi Zhang, Zixuan Guo and Shuying Feng

527 Chewable tablets containing rape bee pollen and maca attenuate testosterone propionate–induced benign prostatic hyperplasia in Sprague–Dawley rats by regulating the gut microbiota and modulating the IL-6/JAK2/STAT3 signaling pathway
Xiaoqiang Huang, Guohua Ru, Hengyun Tian, Pengbo Zhang, Hongchang Zhao, Shouren Zhang, Sijie Wang, An Jia and Wanli Zhao

frontiers in Microbiology

TYPE Editorial
PUBLISHED 27 March 2026
DOI 10.3389/fmicb.2026.1809622

Check for updates

OPEN ACCESS

EDITED AND REVIEWED BY
M. Pilar Francino,
Fundación para el Fomento de la Investigación Sanitaria y Biomédica de la Comunitat Valenciana (FISABIO), Spain

*CORRESPONDENCE
Guiguo Zhang
✉ zhanggg@sdau.edu.cn
Yunkyoung Lee
✉ lyk1230@jejunu.ac.kr

RECEIVED 12 February 2026
ACCEPTED 27 February 2026
PUBLISHED 27 March 2026

CITATION
Zhang G, Altamimi M, Shi J and Lee Y (2026) Editorial: The interaction between food ingredients and gut microbiome on health and disease.
Front. Microbiol. 17:1809622.
doi: 10.3389/fmicb.2026.1809622

COPYRIGHT
© 2026 Zhang, Altamimi, Shi and Lee. This is an open-access article distributed under the terms of the Creative Commons Attribution License (CC BY). The use, distribution or reproduction in other forums is permitted, provided the original author(s) and the copyright owner(s) are credited and that the original publication in this journal is cited, in accordance with accepted academic practice. No use, distribution or reproduction is permitted which does not comply with these terms.

Editorial: The interaction between food ingredients and gut microbiome on health and disease

Guiguo Zhang[1,2]*, Mohammad Altamimi[3], Junling Shi[4] and Yunkyoung Lee[2,5]*

[1]Department of Animal Nutrition, Shandong Agricultural University, Taian, China, [2]China-South Korea International Joint Laboratory of Functional Polysaccharides in Shandong Province, Taian, China, [3]Department of Nutrition and Food Technology, Faculty of Agriculture Engineering and Veterinary Medicine, An-Najah National University, Nablus, Palestine, [4]School of Life Sciences, Northwestern Polytechnical University, Xi'an, China, [5]Department of Food Science and Nutrition, Jeju National University, Jeju, Republic of Korea

KEYWORDS
disease, food ingredients, gut microbiome, interaction, metabolites

Editorial on the Research Topic
The interaction between food ingredients and gut microbiome on health and disease

Introduction

The intricate and dynamic ecosystem of microorganisms residing in the human gastrointestinal tract, collectively known as the gut microbiome, has emerged as a central player in human health and disease (Ley et al., 2006). This complex community, comprising trillions of bacteria, archaea, viruses, and fungi, does not merely exist in a passive commensal relationship with the host (Guo et al., 2025). Instead, it engages in a continuous, bidirectional crosstalk, profoundly influencing host physiology, metabolism, and immunity (Li et al., 2021; Liu et al., 2023). Among the myriad factors shaping the composition and function of the gut microbiome, diet stands out as one of the most potent and modifiable (Koh et al., 2016; Sonnenburg and Bäckhed, 2016).

The specific food ingredients consumed by host act as both substrates and signals for the gut microbiota, thereby modulating the production of a vast array of microbial metabolites (Zmora et al., 2019). These metabolites, including short-chain fatty acids (SCFAs), bile acids, vitamins, and neurotransmitters, serve as key messengers in the gut-host axis, impacting systems far beyond the intestines, from hepatic function to cerebral health (Koh et al., 2016; Li et al., 2021). The Research Topic "*The Interaction Between Food Ingredients and Gut Microbiome on Health and Disease*" brings together a compelling Research Topic of original research and reviews that delve deep into this critical interaction, exploring how diverse dietary components, from traditional herbs and prebiotics to food contaminants, can be leveraged to promote health or, conversely, contribute to pathophysiology.

The growing body of evidence reveals that dietary interventions targeting the gut microbiome hold immense promise for preventing and treating a spectrum of conditions, including metabolic disorders, inflammatory diseases, and even neurological conditions (Zhang et al., 2025; Zhao et al., 2020). This paradigm shift toward microbiome-targeted therapeutics is fueled by the understanding that dietary precision, moving beyond one-size-fits-all recommendations, could be the future of nutritional science (Levé et al., 2025; Zeevi et al., 2015). However, unraveling the precise mechanisms underlying the diet-microbiome-host interaction is a formidable challenge, necessitating a multidisciplinary approach that integrates microbiology, metabolomics, immunology, and bioinformatics (Choi et al., 2021; Wali et al., 2023).

This Research Topic serves as a testament to these efforts, presenting cutting-edge research that moves from correlation to causation, employing sophisticated models to dissect the molecular pathways involved. The findings highlighted in this issue not only reinforce the established roles of dietary fibers and fermented foods but also shed light on the potential of underutilized botanical extracts and the risks posed by modern environmental pollutants, thereby painting a more comprehensive picture of our dietary landscape's impact on gut ecological stability. Furthermore, the concept of personalized nutrition, driven by an individual's unique microbial blueprint, is gaining traction, suggesting that the efficacy of a food ingredient is inherently tied to the pre-existing gut microbial community structure. This editorial introduces and contextualizes the 36 articles (8 reviews and 28 original research articles) that form the cornerstone of this topical Research Topic, each contributing a vital piece to the complex puzzle of how what we eat dictates who we are, through the lens of our gut microbes.

Our synthesis of the published contributions reveals clear research trends while also underscoring persistent gaps in the field. The dominant themes spans dietary fibers/polysaccharides, polyphenols and botanicals, probiotics and postbiotics, broader dietary patterns, and macronutrients, environmental, or foodborne exposures, alongside several integrative reviews. Across these studies, commonly reported readouts of microbiome modulation include SCFAs, inflammatory markers, gut barrier integrity, immune, and neurological endpoints, and metabolic indicators.

Despite this progress, important gaps remain, most notably in methodological standardization and transparent reporting. Moreover, relatively few studies establish causal, mechanistic links between specific dietary components, microbiome remodeling, and downstream host physiology (Martens et al., 2011; Zhao et al., 2018). Although multi-omics designs are increasingly used, proposed connections among microbial shifts, metabolite changes, and clinical or metabolic improvements often remain inferential (Li et al., 2026; Wang et al., 2024). Strengthening causal inference will require functional validation (e.g., fecal microbiota transplantation (FMT), germ-free/gnotobiotic models, and targeted intervention experiments), so that frequently invoked frameworks such as the gut-liver axis move from plausible models to demonstrated mechanisms.

Summary of articles published in the Research Topic

This Research Topic brings together 36 contributions examining the dynamic interplay among dietary factors, gut microbial communities, and host health. The Research Topic spans animal experiments, human clinical work, and comprehensive reviews, highlighting the gut microbiome as a central mediator in metabolic, neurological, inflammatory, and systemic conditions. Below, we briefly outline each of the 36 papers, noting the focal ingredient or intervention, the main outcomes, and the broader relevance of findings.

Animal experiments collectively underscore the therapeutic promise of diverse ingredients and strategies. Work on plant polyphenols reported that both proanthocyanidins and rutin improved type 2 diabetes in mice, with proanthocyanidins showing greater efficacy, accompanied by distinct gut microbiota shifts (Gao et al.). Likewise, flavonoids from *Amomum tsaoko* (ATF) mitigated ulcerative colitis by suppressing inflammatory signaling and enriching beneficial taxa such as *Akkermansia, Bifidobacterium and* unclassified_f_*Atopobiaceae*, via the gut microbiota-LPS/TLR4/NF-κB/NLRP3 axis (Huang et al.). In a related botanical study, an extract from *Amomum tsao-ko Crevost et Lemarie* attenuated atherosclerosis by influencing the gut-liver axis, lowering serum cholesterol, reshaping the gut microbial composition, and reducing systemic inflammation and oxidative stress (Wang Q. et al.). Additional plant-derived interventions were also effective: *Paederia scandens* extract countered obesity-associated dysbiosis by restoring microbial diversity and shifting serum metabolites linked to amino acid and energy metabolism (Yang Y. et al.). In livestock, *Codonopsis pilosula* polysaccharides supported intestinal health and immunity in Hu sheep, enhancing microbial diversity and upregulating gut barrier proteins (Zhao Q. et al.). Furthermore, ferulic acid and its derivative N-feruloylserotonin reduced intestinal inflammation through a multi-omics mechanism involving microbiota remodeling, enrichment of beneficial metabolites (e.g., 1-naphthalenesulfonic acid), and regulation of NF-κB and MAPK signaling (Hu et al.). Traditional formulas further broadened the mechanistic landscape. *Dachaihu* decoction improved autism spectrum disorder-related outcomes in rats and in a human trial, consistent with gut-brain axis modulation, including enrichment of beneficial taxa (e.g., *Adlercreutzia*), reduced inflammation and oxidative stress, and improved barrier integrity (Zhang, Li et al.). Separately, Guiren Runchang Granules (GRG) improved slow transit constipation by rebalancing gut microbial ecology, increasing SCFA production, and normalizing motility-related hormones (e.g., serotonin and motilin) (Bai et al.).

Probiotic, postbiotic, and prebiotic approaches featured prominently across multiple disease settings. Notably, pasteurized *Akkermansia muciniphila* (a postbiotic) outperformed the live strain in murine colitis model, strengthening barrier function and dampening inflammation (Han et al.). For metabolic outcomes, *Clostridium butyricum* improved obesity and glucose intolerance by restoring barrier integrity, reducing systemic inflammation, and lowering microbially derived branched-chain amino acids (Zhang X. et al.). In poultry, *Bacteroides uniformis* counteracted

diet-induced fatty liver disease in laying hens by reconfiguring the gut microbiome and correcting arachidonic acid metabolism, thereby reducing hepatic lipid deposition (Zhang, Ma et al.). A separate study addressed environmental toxicants, showing that *Lactiplantibacillus plantarum* ZP-6 lessened nanoplastic-induced liver and colon damage by promoting fecal excretion (via adsorption) and reinforcing the intestinal barrier through the gut-liver axis (Zhao L. et al.). Dietary substrates were likewise informative. Galacto-oligosaccharides (GOS) improved lactose intolerance in mice in a microbiota-dependent manner, enriching lactose-metabolizing bacteria (notably *Lactobacillus* and *Bifidobacterium*), enhancing barrier function, and reducing inflammation (Li Q. et al.). In contrast, an evaluation of sweeteners found that synthetic compounds (sucralose and saccharin) substantially reduced microbial diversity and enriched potential pathogens (e.g., *Enterobacteriaceae*), whereas non-synthetic alternatives (Rebaudioside A and xylitol) were less disruptive and in some cases strengthened beneficial microbial networks (Kidangathazhe et al.).

Micronutrients and supplements were also explored. In a neurodevelopmental framework, dietary zinc improved autism-like behaviors in Shank3B-/- mice by reshaping bacterial and fungal communities and affecting host genes involved in metabolism and microbe-host interactions (Wong et al.). In ruminant nutrition, L-citrulline enhanced reproductive performance (estrus rate) in Hu ewes through rumen microbiota shifts, improved antioxidant capacity, and stimulation of reproductive hormone secretion (Liu et al.). A blend of medium- and short-chain fatty acids (MCFA/SCFA) promoted gut health in weaned piglets as a zinc oxide alternative by reducing diarrhea, improving antioxidant status, and enriching beneficial taxa such as *Lactobacillus* and *Roseburia* (Fan et al.). Another phytochemical intervention, chive seed flavonoid improved intestinal morphology, increased volatile fatty acid production, and expanded microbial diversity in sheep, consistent with enhanced gut development and function (Li X. et al.). Extending beyond intestinal outcomes, a chewable tablet containing rapeseed bee pollen and maca alleviated benign prostatic hyperplasia in rats by restoring microbiota balance and inhibiting IL-6/JAK2/STAT3 signaling, demonstrating a gut-organ axis mechanism (Huang et al.).

Work on ecological and pathological interactions clarified how diet, management, and infection shape gut communities in animal systems. An intervention of arid-adapted rodents indicated that host phylogeny and dietary composition were key drivers of gut community structure, with plant-based foods enhancing microbial diversity and animal-based consumption reducing it (Cha et al.). In goats, husbandry-related drivers were also evident. One report showed how high dietary energy and protein shifted cecal fermentation, increased microbial diversity, and altered host gene expression linked to nutrient absorption and intestinal immunity (Fu et al.). Another study associated Caprine Arthritis Encephalitis virus infection with distinct fecal microbiome signatures and identified intensive farming (relative to pasture-based systems) as an additional factor influencing microbial composition (Molotzu et al.).

In vitro platforms provided higher-resolution views of microbiome dynamics. One study delineated how *Aloe vera* and dandelion extracts exert prebiotic effects, such as enriching *Akkermansia muciniphila* and *Bifidobacterium*, in a taxon-dependent manner shaped by cross-feeding networks involving key members such as *Bacteroides* spp. (Mancabelli et al.). Another *in vitro* model tracked the fate of the foodborne pathogen *Listeria monocytogenes*, showing that clinical isolates were more resistant to simulated digestion than food-borne strains and that infection reconstructed the microbiota, increasing ethanol-producing groups (Kim et al.). Bridging models systems and environmental health, a translational analysis proposed a gut-vascular axis for bisphenol F (BPF), demonstrating in patients and rats that BPF exposure promotes vascular calcification via dysbiosis and downstream inflammatory responses (Yan et al.).

Human clinical studies added findings with direct translational relevance. In colorectal adenoma (CRA) progression, stage-specific microbial patterns were observed, including depletion of protective, SCFA-producing genera (e.g., *Anaerostipes* and *Blautia*) in advanced lesions, alongside a progressive rise in PD-L1 pointing to candidate microbiome-based biomarkers for earlier detection (Wang X. et al.). Complementing this, an *in vitro* nutritional experiment suggested that microbial responses to foods are shaped less by single nutrients than macronutrient balance; pulses such as red and mung beans (with more favorable ratio) most strongly supported eubiosis and reduced pathobionts such as *Escherichia-Shigella* (Lee and Hwang). Consistent with individualized responsiveness, a personalized nutrition trial reported that microbiota-tailored granola increased beneficial taxa (including *Bifidobacterium*), enhanced SCFA production, and was associated with measurable improvements in mood among participants (Sasaki et al.).

In addition to the original articles, eight reviews synthesized broader evidence across diverse contexts, each examining how diet-microbiome interactions intersect with specific disease pathways. One narrative review consolidated evidence on lifestyle factors, diet, sleep, and exercise, showing that high-fiber diets and regular physical activity support beneficial SCFA-producing communities, whereas circadian disruption favors pro-inflammatory shifts and reduced microbial diversity (Zeng et al.). Another review assessed mechanistic links between high-fat diets, microbiota disruption, and precocious puberty, highlighting potential roles for microbial metabolites in endocrine signaling (Wu et al.). A further synthesis discussed the gut-brain axis in Alzheimer's disease, positioning diet as a modifiable determinant in pathogenesis (Siripaopradit et al., 2024). Beyond neurological outcomes, one review described how microbiota-derived metabolites (including SCFAs and bile acids) may contribute to vitiligo through gut-skin axis signaling and immune modulation (Yuan et al.). Shifting to animal health, another review examined the equine gut microbiome, detailing how diet and management practices influence its composition and function (Li F. et al.). From a clinical perspective, one article summarized microbiota-directed strategies, probiotics, FMT, and bacteriophage therapy, for alleviating diarrhea by re-establishing microbial balance (Tian et al.). Finally, a review highlighted beneficial taxa and dietary patterns that promote health, including recent advances in personalized nutrition and AI-enabled approaches for microbiome modulation (Kumar et al.). Collectively, these reviews offer a multi-faceted perspective on how dietary factors engage the gut

microbiome to influence health and disease across species and life stages.

Critical appraisal and future directions

The collective works presented in this Research Topic represent a significant leap forward in our mechanistic understanding of the diet-gut microbiome axis. The research moves beyond simple correlations, employing germ-free models, gnotobiotic animals, sophisticated *in-vitro* fermentation systems, and multi-omics integration to establish causality and elucidate pathways. The consistent theme across numerous studies is the potent efficacy of plant-derived compounds (polyphenols, flavonoids, and polysaccharides from herbs like Amomum tsao-ko, Codonopsis pilosula, and Paederia scandens) in ameliorating conditions from metabolic syndrome to neuroinflammation, primarily through microbial modulation. This reinforces the immense value of exploring traditional pharmacopeias for novel microbiome-targeting therapies. Furthermore, the studies on personalized nutrition and the strain-specific effects of botanical extracts powerfully underscore a critical paradigm: the host's baseline microbiota is a key determinant of nutritional response, pushing the field toward personalized approaches.

Despite these advances, several challenges and opportunities for future research remain. First, while animal models are indispensable, there is a pressing need for more long-term, well-controlled human intervention studies to validate these findings and determine effective doses for human application. Second, the sheer complexity of the interactions, where a single dietary component can simultaneously alter dozens of microbial taxa and host pathways, calls for more sophisticated computational and systems biology approaches to move from descriptive lists to predictive models of host-microbiome dynamics. A notable gap in the current Research Topic, and the field at large, is the limited exploration of non-bacterial members of the microbiome, such as fungi (the mycobiome), viruses (the virome), and archaea. Their roles in mediating the effects of diet are likely substantial but remain underexplored.

Future research should also focus on the temporal dynamics of microbial responses to dietary interventions. Understanding the resilience of the microbiome and the sustainability of dietary-induced changes is crucial for developing long-term strategies (Ko et al., 2025; Lin et al., 2025). Finally, translating this knowledge into public health and clinical practice requires the development of robust biomarkers of microbiome health and the integration of microbiome data into dietary guidelines- a formidable but essential task for the future of precision nutrition (Mann et al., 2024; Rondinella et al., 2026).

In conclusion, this Research Topic successfully captures the vibrancy and depth of contemporary research on the interaction between food ingredients and the gut microbiome. The collected articles provide compelling evidence that dietary manipulation of the gut microbiota is a powerful and viable strategy for promoting health and combating disease. From elucidating the mechanisms of ancient herbs to highlighting the risks of modern pollutants and pioneering personalized nutrition, the work presented here charts a course for future discovery. The key takeaway is that the future of nutritional science lies in embracing complexity-acknowledging the individuality of our microbial partners, the multi-kingdom nature of the gut ecosystem, and the dynamic interplay between diet, microbes, and host physiology. The insights garnered from this Research Topic firmly establish the gut microbiome not as a passive passenger, but as a central mediator of dietary health effects, opening exciting new avenues for therapeutic innovation.

Author contributions

GZ: Writing – original draft, Writing – review & editing, Conceptualization, Funding acquisition, Methodology, Visualization. MA: Formal analysis, Methodology, Resources, Writing – review & editing. JS: Investigation, Methodology, Resources, Writing – review & editing. YL: Conceptualization, Formal analysis, Funding acquisition, Writing – review & editing, Writing – original draft, Supervision.

Funding

The author(s) declared that financial support was received for this work and/or its publication. This study was supported by the National Key R&D Program of China-Korea cooperative project, the key project for foreign experts of Shandong Province (WRS2023075), the National Research Foundation Grant of Korea (2020R1A2C2004144 and RS-2024-00334577), the Forage Industrial Innovation Team Project (SDAIT-23-05), and the Key R&D Program of Shandong Province (2022TZXD0018 and YDZX2023077).

Acknowledgments

We thank the authors for submitting their work to this Research Topic and the reviewers who provided valuable comments to the individual contributions.

Conflict of interest

The author(s) declared that this work was conducted in the absence of any commercial or financial relationships that could be construed as a potential conflict of interest.

Generative AI statement

The author(s) declared that generative AI was not used in the creation of this manuscript.

Any alternative text (alt text) provided alongside figures in this article has been generated by Frontiers with the support of artificial intelligence and reasonable efforts have been made to ensure accuracy, including review by the authors wherever possible. If you identify any issues, please contact us.

Publisher's note

All claims expressed in this article are solely those of the authors and do not necessarily represent those of their affiliated organizations, or those of the publisher, the editors and the reviewers. Any product that may be evaluated in this article, or claim that may be made by its manufacturer, is not guaranteed or endorsed by the publisher.

References

Choi, B. S. Y., Daniel, N., Houde, V. P., Ouellette, A., Marcotte, B., Varin, T. V., et al. (2021). Feeding diversified protein sources exacerbates hepatic insulin resistance via increased gut microbial branched-chain fatty acids and mTORC1 signaling in obese mice. *Nat. Commun.* 12:3377. doi: 10.1038/s41467-021-23782-w

Guo, C., Ma, D., Zhang, C., Wang, Y., Ullah, F., Wang, X., et al. (2025). Dietary Jerusalem artichoke polysaccharide supplementation alters the growth performance, ruminal microbes and metabolites, muscle fatty acid and amino acid profiles in fattening lambs. *Anim. Nutr.* 22, 139–153. doi: 10.1016/j.aninu.2025.02.007

Ko, K., Guo, C., Kim, E., Zhang, G., and Lee, Y. (2025). Structural features of galacturonic acid-rich polysaccharides from Ziziphus jujuba and their protective effects against insulin resistance and muscle atrophy. *Int. J. Biol. Macromol.* 322:146287. doi: 10.1016/j.ijbiomac.2025.146287

Koh, A., De Vadder, F., Kovatcheva-Datchary, P., and Bäckhed, F. (2016). From dietary fiber to host physiology: short-chain fatty acids as key bacterial metabolites. *Cell* 165, 1332–1345. doi: 10.1016/j.cell.2016.05.041

Levé, M., Manghi, P., Bredon, M., Lefevre, A., Manara, S., Armanini, F., et al. (2025). Metabolomics and metagenomics in mice reveal the role of the gut microbiota in tryptophan metabolism. *iScience* 28:113751. doi: 10.1016/j.isci.2025.113751

Ley, R. E., Turnbaugh, P. J., Klein, S., and Gordon, J. I. (2006). Microbial ecology: human gut microbes associated with obesity. *Nature* 444, 1022–1023. doi: 10.1038/4441022a

Li, D., Feng, Y., Tian, M., Ji, J., Hu, X., and Chen, F. (2021). Gut microbiota-derived inosine from dietary barley leaf supplementation attenuates colitis through PPARγ signaling activation. *Microbiome* 9:83. doi: 10.1186/s40168-021-01028-7

Li, Z., Kang, M., Ko, K., Song, Y., Lee, Y., and Zhang, G. (2026). Dietary inulin improves growth performance and systemic health of fattening goats by modulating rumen microbiome and metabolome. *Anim. Feed Sci. Technol.* 334:116641. doi: 10.1016/j.anifeedsci.2026.116641

Lin, Y., Wu, J., Huang, H., Zeng, Z., Zhang, W., Wang, L., et al. (2025). Mechanisms of Laminaria japonica polysaccharide digestion and absorption: structure, in vivo fluorescence imaging, and gut microbiota. *J. Agric. Food Chem.* 73, 21148–21161. doi: 10.1021/acs.jafc.5c03896

Liu, A., Kim, E., Cui, J., Li, J., Lee, Y., and Zhang, G. (2023). Laminaria japonica polysaccharide improved the productivities and systemic health of ducks by mediating the gut microbiota and metabolome. *J. Agric. Food Chem.* 71, 7382–7395. doi: 10.1021/acs.jafc.2c08731

Mann, E. R., Lam, Y. K., and Uhlig, H. H. (2024). Short-chain fatty acids: linking diet, the microbiome and immunity. *Nature Rev. Immunol.* 24, 577–595. doi: 10.1038/s41577-024-01014-8

Martens, E. C., Lowe, E. C., Chiang, H., Pudlo, N. A., Wu, M., McNulty, N. P., et al. (2011). Recognition and degradation of plant cell wall polysaccharides by two human gut symbionts. *PLoS Biol.* 9:e1001221. doi: 10.1371/journal.pbio.1001221

Rondinella, D., Margarita, E., Raoul, P. C., Galli, F. S., Severino, A., Porcari, S., et al. (2026). The impact of diet on gut microbiome composition: implications for immune-mediated diseases. *Clin. Immunol. Commun.* 9, 1–11. doi: 10.1016/j.clicom.2025.12.001

Siripaopradit, Y., Chatsirisakul, O., Ariyapaisalkul, T., and Sereemaspun, A.(2024). Exploring the gut-brain axis in AlzheimerŠs disease treatment via probiotics: evidence from animal studies-a systematic review and meta-analysis. *BMC Neurol.* 24:481. doi: 10.1186/s12883-024-03978-5

Sonnenburg, J. L., and Bäckhed, F. (2016). Diet–microbiota interactions as moderators of human metabolism. *Nature* 535, 56–64. doi: 10.1038/nature18846

Wali, J. A., Ni, D., Facey, H. J. W., Dodgson, T., Pulpitel, T. J., Senior, A. M., et al. (2023). Determining the metabolic effects of dietary fat, sugars and fat-sugar interaction using nutritional geometry in a dietary challenge study with male mice. *Nat. Commun.* 14:4409. doi: 10.1038/s41467-023-40039-w

Wang, K., Zhou, Y., Li, M., Chen, Z., Wu, Z., Ji, W., et al. (2024). Structural elucidation and immunomodulatory activities in vitro of type I and II arabinogalactans from different origins of Astragalus membranaceus. *Carbohydr. Polym.* 333:121974. doi: 10.1016/j.carbpol.2024.121974

Zeevi, D., Korem, T., Zmora, N., Israeli, D., Rothschild, D., Weinberger, A., et al. (2015). Personalized nutrition by prediction of glycemic responses. *Cell* 163, 1079–1094. doi: 10.1016/j.cell.2015.11.001

Zhang, L., Marfil-Sánchez, A., Kuo, T.-H., Seelbinder, B., van Dam, L., Depetris-Chauvin, A., et al. (2025). Gut microbiome-mediated transformation of dietary phytonutrients is associated with health outcomes. *Nat. Microbiol.* 11, 94–110. doi: 10.1038/s41564-025-02197-z

Zhao, F., Liu, Q., Cao, J., Xu, Y., Pei, Z., Fan, H., et al. (2020). A sea cucumber (*Holothuria leucospilota*) polysaccharide improves the gut microbiome to alleviate the symptoms of type 2 diabetes mellitus in Goto-Kakizaki rats. *Food Chem. Toxicol.* 135:110886. doi: 10.1016/j.fct.2019.110886

Zhao, L., Zhang, F., Ding, X., Wu, G., Lam, Y. Y., Wang, X., et al. (2018). Gut bacteria selectively promoted by dietary fibers alleviate type 2 diabetes. *Science* 359, 1151–1156. doi: 10.1126/science.aao5774

Zmora, N., Suez, J., and Elinav, E. (2019). You are what you eat: diet, health and the gut microbiota. *Nat. Rev. Gastro Hepat.* 16, 35–56. doi: 10.1038/s41575-018-0061-2

frontiers | Frontiers in Microbiology

TYPE Original Research
PUBLISHED 06 January 2025
DOI 10.3389/fmicb.2024.1513935

Check for updates

OPEN ACCESS

EDITED BY
Mohammad Altamimi,
An-Najah National University, Palestine

REVIEWED BY
Ruchika Rajput,
Oak Ridge National Laboratory (DOE), United States
Dan Cheng,
Guangdong Longsee Medical, China

*CORRESPONDENCE
Maozhen Han
✉ hanmz@ahmu.edu.cn
Yan Zhang
✉ zhangyanwind@163.com

†These authors have contributed equally to this work

RECEIVED 19 October 2024
ACCEPTED 10 December 2024
PUBLISHED 06 January 2025

CITATION
Gao Y, Huang B, Qin Y, Qiao B, Ren M, Cao L, Zhang Y and Han M (2025) Dietary supplementation with proanthocyanidins and rutin alleviates the symptoms of type 2 diabetes mice and regulates gut microbiota. *Front. Microbiol.* 15:1513935. doi: 10.3389/fmicb.2024.1513935

COPYRIGHT
© 2025 Gao, Huang, Qin, Qiao, Ren, Cao, Zhang and Han. This is an open-access article distributed under the terms of the Creative Commons Attribution License (CC BY). The use, distribution or reproduction in other forums is permitted, provided the original author(s) and the copyright owner(s) are credited and that the original publication in this journal is cited, in accordance with accepted academic practice. No use, distribution or reproduction is permitted which does not comply with these terms.

Dietary supplementation with proanthocyanidins and rutin alleviates the symptoms of type 2 diabetes mice and regulates gut microbiota

Yue Gao[1,2,3†], Binbin Huang[4†], Yunyi Qin[1], Bing Qiao[1], Mengfei Ren[1], Liqing Cao[1], Yan Zhang[2*] and Maozhen Han[1,3*]

[1]School of Life Sciences, Anhui Medical University, Hefei, Anhui, China, [2]School of Life Sciences, Hefei Normal University, Hefei, Anhui, China, [3]Microbial Medicinal Resources Development Research Team, Anhui Provincial Institute of Translational Medicine, Hefei, Anhui, China, [4]School of Public Health, Anhui Medical University, Hefei, Anhui, China

Background: Obesity and high fasting blood glucose (FBG) resulting from high-fat diets (HFDs) have emerged as significant public health concerns, garnering increasing attention. Recently, gut microbiota has been linked with metabolic diseases such as type 2 diabetes (T2DM), and its mediating role in dietary supplements has been confirmed. Seeking various dietary supplements to lose body weight (BW) and decrease FBG and explaining the underlying mechanism have become the research hotspots in T2DM studies.

Methods: In this study, rutin and proanthocyanidins (PA) were selected as dietary supplements (200 mg/kg × day, oral gavage, 6 weeks) in T2DM mice induced with HFD to assess their efficacy in weight loss, FBG reduction, gut microbiota alterations, and the associated underlying mechanisms.

Results: Our findings indicate that rutin was more effective than PA in relieving inflammation and fat hypertrophy, although both significantly reduced BW and FBG within 2 weeks after the intervention. Analysis of 16S rRNA amplicons revealed substantial alterations in the gut microbial community composition of mice administered with PA and rutin compared to HFD-fed mice. Importantly, several core microbes, particularly a series of probiotics, such as *Akkermansia*, *Lactococcus*, *Odoribacter*, *Faecalibaculum*, and *Roseburia* were identified, which were significantly correlated with the changes in BW and FBG.

Conclusion: Overall, our study highlights that rutin and PA can reduce BW, FBG, and inflammation by modulating the gut microbiota composition, providing novel perspectives for managing and treating weight and FBG concerns in obesity and T2DM patients through dietary supplements in clinical treatment.

KEYWORDS

type 2 diabetes, gut microbiota, rutin, proanthocyanidins, body weight, fasting blood glucose

Introduction

Obesity is a chronic metabolic disorder, which significantly elevates the susceptibility to various diseases, including type 2 diabetes (T2DM) (Fryk et al., 2021), fatty liver (Eslam et al., 2020), hypertension (DeMarco et al., 2014; Eslam et al., 2020), myocardial infarction (Yusuf et al., 2005), and cancer (Hopkins et al., 2016). According to the World Health Organization, more than 1 billion people worldwide suffer from obesity and its derived metabolic syndromes including T2DM (World Health Organization., 2021). Consideration of T2DM is a global epidemic characterized by metabolic disorders and harboring many complications caused by genetic background and environmental factors, such as overnutrition (Donath and Shoelson, 2011), and the number of cases could exceed 642 million by 2040 without intervention (Ogurtsova et al., 2017). Hence, our present study focuses on T2DM as a disease model to explore the treatment strategy from the perspectives of microbiome approach and dietary supplementation.

In past decades, previous studies have confirmed that gut microbiota and its metabolites play an important role in the metabolism of the body and are closely associated with metabolic diseases (Fan and Pedersen, 2021). In particular, scientists have proven that the dysbiosis of gut microbiota is an important contributor to the prevalence and development of metabolic diseases such as obesity and T2DM (de Vos et al., 2022; Han et al., 2022; Ley et al., 2006) and proposed several new strategies from the perspectives of dietary, probiotics, and prebiotics for the treatment of metabolic diseases, including T2DM (Asemi et al., 2016; Delzenne et al., 2015; Kim et al., 2018; Yang et al., 2021; Yoo and Kim, 2016). It is noteworthy that various studies have highlighted the influence of diet as a pivotal factor in shaping the taxonomical and functional compositions of gut microbial communities (Sonnenburg and Bäckhed, 2016). Recent findings have underscored the anti-diabetic properties of dietary natural products, which harbor the ability to support the maintenance of gut microbial balance (de Vos et al., 2022). Several dietary natural products, such as 6-shogaol (Jiao et al., 2023), tea polyphenol (Wen et al., 2023), resveratrol (Jeyaraman et al., 2020), and myricetin (Zhao et al., 2022), have demonstrated the ability to modulate gut microbiota, enhance gut integrity, regulate host metabolism, and alleviate obesity and T2DM (Chen et al., 2019; Delzenne et al., 2011). Nowadays, although dietary natural products are promising nutritional interventions with minimal side effects in treating T2DM, exploring more dietary supplements with functional properties and benchmarking the effects of different dietary supplements are urgently needed, and the underlying mechanism should be investigated.

Polyphenols, including tea polyphenols, grape seed proanthocyanidins, and resveratrol, are famous natural dietary compounds that are enriched in plant and human foods. For example, the largest dietary sources of proanthocyanidins (PA) are pulses, grains, nuts, cocoa, tea, wine, and fruits, such as blueberries [(179.8 ± 50.8 ~331.9 ± 14.0) mg/100 g fresh weight], plums (215.9 ± 50.7 mg/100 g fresh weight), grapes (81.5 ± 15.0 mg/100 g fresh weight), and apples [(47.2 ± 0.6 ~ 141.0 ± 26.1) mg/100 g fresh weight] (Gu et al., 2004; Salvadó et al., 2015). The function of polyphenols in alleviating the metabolic syndrome associated with obesity has been confirmed (Tomás-Barberán et al., 2016). PA has been suggested to account for a significant portion of polyphenols consumed in the Western diet because of its ubiquity (Prior and Gu, 2005). Moreover, research studies have revealed that approximately 11% of PA can be identified in the feces after consuming PA daily for 10 days. This finding suggests the gastrointestinal health benefits of the stable presence of ingested PA in the gut (Choy et al., 2013). Several studies have demonstrated the function of PA supplementation and explored the mechanism relying on gut microbiota in-depth (Redondo-Castillejo et al., 2023), providing potential for the prevention and treatment of gut microbiota disorders (Campos et al., 2021; Gonzalez-Abuin et al., 2015; Hameed et al., 2020; Liu W. et al., 2017). More importantly, current toxicological studies showed that PA have no observable toxicity to humans when used appropriately (Zeng et al., 2020). In contrast, rutin is famous as one of the natural polyphenol flavonoids that can be obtained from diverse plants, such as buckwheat (up to 396 mg/100 g), amaranth leaves [up to 24.5 g/kg (dry weight)], elderflower tea (around 10.9 g/kg of dry flowers' weight), unfermented rooibos tea (about 1.69 mg/g), and acacias (Gullón et al., 2017). It has been reported to have a wide range of biological activities and pharmacological effects, including reducing fasting blood glucose (FBG) and body weight (BW), anti-inflammatory and antioxidant properties, and neuroprotection (Ghorbani, 2017; Kamalakkannan and Prince, 2006; Ola et al., 2015; Tung et al., 2021; Yeh et al., 2014; Yuan et al., 2017). Increasing evidence confirms that rutin is a type of naturally occurring flavonoid, which is widely found in vegetables and fruits; it has beneficial effects on diabetes as a dietary supplement to improve glycemic control, lipid profile, and antioxidant status with no apparent toxicity and poor bioavailability in rodents (Bazyar et al., 2023; Ghorbani, 2017; Liu Q. et al., 2017; Valentová et al., 2014), suggesting that rutin is a potential substrate or dietary supplement in clinical trial. Notably, the pharmacological properties of rutin are gradually explored, such as substantial anti-inflammatory and antioxidant effects. However, no evidence could confirm that rutin can modulate the gut microbiota in high-fat diet (HFD)-induced T2DM mice. Besides, few studies focused on the comparison of the effects of PA and rutin (both plant polyphenols and available dietary supplements) on weight loss and reduction in FBG levels and their comparative abilities to repair the gut microbiota.

Therefore, to decipher and compare the possible mechanisms by which dietary supplementation with PA or rutin reduces BW and FBG levels in HFD-induced T2DM mice by modulating the gut microbiota, we established a T2DM mouse model derived from obesity induced by HFD and subsequent oral administration of PA or rutin (both 200 mg/kg × day), comparing them with normal and positive control groups. During the intervention process, the BW and FBG levels of mice were measured with a high-frequency strategy to directly revel the effects of rutin and PA. Whereas the feces of mice were collected at two time points, namely, the time of successful modeling and 6 weeks after the intervention (week 10). The V3-V4 region of the 16S rRNA was sequenced to investigate the alterations of gut microbiota. Besides, the oral glucose tolerance tests (OGTT) and intraperitoneal glucose tolerance tests (IPITT) were conducted at the end of the intervention and the pancreatic (PAN), liver, and adipose tissues of mice were collected for weighing and hematoxylin and eosin (H&E) staining to compare the effects of rutin and PA. Our results showed that rutin and PA harbor the ability to significantly lose BW and decrease FBG

levels in T2DM mice. The results of 16S rRNA amplicon analysis revealed that the gut microbiota underwent dynamic changes in the groups administered orally with PA and rutin. Particularly, our results identified several probiotics, such as *Akkermansia*, *Lactococcus*, *Odoribacter*, *Faecalibaculum*, and *Roseburia*, which were significantly associated with the changes in BW and FBG. Moreover, the results of H&E staining suggested that rutin is more effective than PA in relieving inflammation and fat hypertrophy.

In conclusion, our study demonstrated that the function and mechanism of rutin and PA in anti-inflammatory, BW loss, and FBG level decrease rely on the modulation of the gut microbiota. Furthermore, the therapeutic effects of rutin are better than those of PA. Finally, the application scenarios in which they maximize their function may differ. Overall, our results provide new insights from the perspectives of the gut microbiome and dietary supplements into the clinical management and treatment of BW and FBG in patients with obesity and T2DM.

Materials and methods

Experimental animals and treatments

A total of 20 4-week-old male specific-pathogen-free (SPF) C57BL/6 mice were purchased from the Experimental Animal Center of Anhui Medical University (Hefei, China). Five mice were housed per cage with free access to food and sterile drinking water in a temperature-controlled room (21°C ± 2°C) under a 12-h light-dark cycle. Initially, the mice were acclimated to the new environment by being fed a standard chow diet (CD) for 1 week (defined as week 0). Following the adaptation period, the mice were randomly divided into two groups based on CD (13.5% of energy from fat; LabDiet 5001; LabDiet, USA) and HFD (45% of energy from fat; D12451; Research DIETS, USA): CD (N = 5) and HFD (N = 15) groups. Subsequently, by feeding the mice HFD for 4 weeks and measuring FBG after giving the mice overnight fasting for 12 h, with FBG > 9.5 mmol/L, the T2DM mouse model was successfully constructed (Cheng et al., 2019; Pang et al., 2016; Yu et al., 2019), the HFD group was further subdivided into three groups and there was no significant difference in BW and FBG among these three groups ($p > 0.05$, t-test). Prior research investigating the efficacy of PA in treating obesity involved a 7-week administration of a 300 mg/kg dosage (Liu W. et al., 2017). In contrast, other studies employed varying dosages (75, 150, and 300 mg/kg) over a 4-week period (Liu et al., 2022) and intervened with rutin (200 mg/kg) in HFD-fed mice for 4 weeks was found to be effective in combating obesity and improving lipid metabolism (Liu Q. et al., 2017). Considering these variables, we administered a daily oral dose of 200 mg/kg/day of PA (>95% purity; Aladdin; HFD+PA group), another received 200 mg/kg/day of rutin (>95% purity; Aladdin; HFD+Rutin group), while the third group was given stroke-physiological saline solution (SPSS) as the negative control (HFD+SPSS group). Meanwhile, the CD mice were given an equal volume of SPSS as the normal control (CD+SPSS group). At week 10, the mice were euthanized through cervical dislocation under isoflurane inhalation anesthesia. The PAN, liver tissue, and adipose tissue were collected and soaked in 4% paraformaldehyde. Fecal samples were collected at the time of successful construction of the T2DM mouse model at week 4 of the experiment and at the time of successful treatment at week 10 of the experiment, and the fecal samples were stored at −80°C (Figure 1). Ethical approval for the animal experiments was obtained from the Experimental Animal Ethics Committee of Anhui Medical University (approval no: LLSC20210503).

Measurement of BW, FBG, OGTT, and IPITT

The BW and FBG levels of each mouse were measured weekly in accordance with the description of Hosomi et al. (2022) to estimate the therapeutic effects of PA and rutin in reducing BW and decreasing FBG levels. The FBG level was measured by sampling blood from the tail tip with a Roche Accu-Chek Performa (Roche Diagnostics, Mannheim, Germany) (Dhatt et al., 2011). Furthermore, the changes in BW and FBG during the intervention process were calculated using the following formulas:

$$\Delta BW = \overline{BW}_{10w} - \overline{BW}_{4w} \quad (1)$$

$$\Delta FBG = \overline{FBG}_{10w} - \overline{FBG}_{4w} \quad (2)$$

where $\overline{BW}_{10w}$ and $\overline{BW}_{4w}$ represent the average BW of five mice at weeks 10 and 4, respectively; $\overline{FBG}_{10w}$ and $\overline{FBG}_{4w}$ represent the average FBG of five mice at weeks 10 and 4, respectively; and ΔBW and ΔFBG represent the value of weight loss and blood glucose decrease between weeks 10 and 4, respectively.

Additionally, to evaluate the metabolic status of mice and determine the therapeutic effects of rutin and PA, OGTT and IPITT experiments were performed at weeks 8 and 9, respectively. For the OGTT at week 8, mice underwent a 16-h overnight fast, while for the IPITT at week 9, a 6-h fast was employed. The end time of the measurement of FBG for each mouse was defined as its start time (0 min). Then, the FBG levels in the OGTT and IPITT experiments were measured at 15, 30, 60, and 120 min after oral administration of D-(+)-glucose (1.5 g/kg-BW) and intraperitoneal injection of insulin (0.5 U/kg-BW), respectively. The results of OGTT and IPITT were presented by the area under the curve (AUC) (Yao et al., 2021).

Weighing and H&E staining of tissues

At the end of the intervention experiment, PAN, liver, and adipose tissues including inguinal adipose tissue (IAT) and gonadal adipose tissue (GAT), of mice were collected and kept for weighing and H&E staining. These tissues were first washed with phosphate-buffered saline (PBS), and then their weight was measured and recorded. Next, H&E staining was conducted by the procedure of Zhang et al. (2020). Eventually, the cell nucleus of these tissues was stained with hematoxylin, and the cytoplasm was stained with eosin. The results of H&E staining were observed and visualized with a microscope (Leica DM2500).

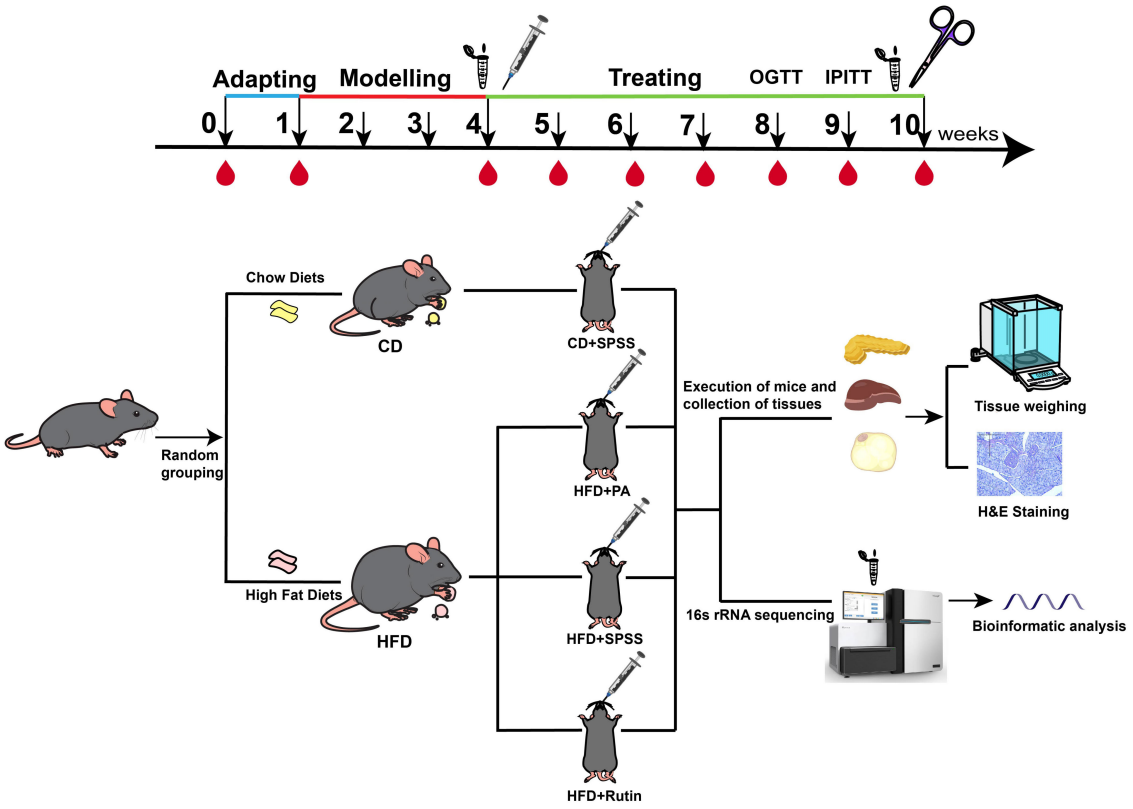

FIGURE 1
Experimental design and procedure for comparing the effects and underlying mechanisms of PA and rutin in reducing BW and decreasing FBG levels. C57BL/6 mice were acclimated for 1 week, designated as week 0. The T2DM model was induced by continuous HFD feeding over 4 weeks. Subsequently, the T2DM mice were divided into three groups: HFD+SPSS, HFD+PA, and HFD+Rutin groups. The intervention experiment lasted 6 weeks. BW and FBG were measured weekly across the entire period of the experiment. During the period of the model construction model and intervention experiment, fecal samples were collected from each mouse at the time of successful model construction (week 4) and the end of intervention (week 10) and stored at −80°C. The PAN, liver, and adipose tissues were collected and soaked in 4% paraformaldehyde for downstream analysis, including H&E staining and weighing. In addition, OGTT was performed at week 8 and IPITT at week 9.

Collection of fecal samples and 16S rRNA amplicon sequencing

During the entire experiment, the fecal samples were collected at two time points: the time of successful model construction (week 4) and the end of intervention (week 10). Thus, a total of 30 fecal samples were collected. The total DNA was extracted according to the instruction of the PowerSoil DNA Isolation Kit (MoBio, USA) and then all extracted DNA was dissolved in TE buffer and stored at −20°C. Next, the eligible DNA of samples was used as a PCR template for obtaining the V3-V4 hypervariable region of the 16S rRNA gene of microbes. Specifically, 5–50 ng DNA was used as a template for amplifying the V3-V4 amplicon by using the forward (5′-CCTACGGRRBGCASCAGKVRVGAAT-3′) and reverse primers (5′-GGACTACNVGGGTWTCTAATCC-3′). Indexed adapters were added to the ends of 16S rDNA amplicons via limited cycle PCR and the sequencing library was constructed using the MetaVxTM Library Preparation kit. DNA libraries were verified and quantified by an Agilent 2100 Bioanalyzer (Agilent Technologies, Palo Alto, CA, USA) and Qubit® 2.0 (Applied Biosystems, Carlsbad, CA, USA). All sequencing reactions were performed on the Illumina MiSeq platform with a paired-end sequencing strategy by GENEWIZ (Inc., South Plainfield, and NJ, USA).

Bioinformatic analysis

In this study, 16S rRNA amplicon analysis was conducted in QIIME2 (version: 2021.11) platform (Bokulich et al., 2018; Hall and Beiko, 2018). First, quality control, denoise, chimera removal, and splicing of raw paired-end sequencing reads were performed with the DADA2 module of QIIME2. Second, the representative sequences of microbe features were selected against the trained classifier silva-138-99-nb-classifier.qza by using the command 'rep-seqs.qza', and then the taxonomical annotations of these representative sequences were annotated with the command 'taxonomy. qza'. The relative abundance of each taxa was calculated and summarized in a table and then the taxonomical compositions of the gut microbiota at phylum, class, order, family, genus, and species levels were summarized on R (Prevel et al., 2022).

Furthermore, based on the high quality of 16S rRNA genes and their abundances, PICRUSt2 (version: 2.5.0) was applied to investigate the dynamic changes of functional composition of gut microbial communities during the intervention

experiment (Douglas et al., 2020). Two output documents, namely KO_predicted.tsv and pathway_predicted.tsv, were used to explore the alterations of functional traits of gut microbial communities. Besides, to obtain an in-depth understanding of the alterations of gut microbiota, Linear discriminate analysis effect size (LEfSe) (Segata et al., 2011) was applied to identify biomarkers among the CD+SPSS, HFD+SPSS, HFD+PA, and HFD+Rutin groups based on the composition of gut microbiota at week 10. The threshold for the logarithmic LDA score for discriminative features was set to 3.

Additionally, the genera with significant differences ($p < 0.05$, t-test) were identified based on the taxonomical compositions of gut microbial communities at weeks 4 (mPA) and 10 (cPA) with the treatment of PA, and those between weeks 4 (mRutin) and 10 (cRutin) with the treatment of rutin. The genera with significant differences presented in the intervention process of PA and rutin were defined as key microbes. Based on the compositions of gut microbial communities of CD+SPSS, HFD+SPSS, HFD+PA, and HFD+Rutin groups, the correlations among genera were calculated using the "corr.test" function of the "psych" package of R, and the corresponding co-occurrence network was visualized in Cytoscape (version: 3.6.1).

In particular, by the calculation formula of Euclidean distance between two points, a novel strategy was proposed to quantitatively illustrate the shift of the gut microbiota between two different groups in this study. Specifically, based on the composition of gut microbiota, principal coordinate analysis (PCoA) was first conducted with the "dudi.pca" function of the "vegan" package, and the values of PCo1 and PCo2 of each sample were obtained. Next, the average values of PCo1 and PCo2 in each group were calculated and defined as the coordinates of the center point of each group. Afterward, the distance of two center points was calculated as described using Formula 3, and it represents the offset of the gut microbial communities between two groups (GM_{offset}).

$$GM_{offset(g1-g2)} = \sqrt{\left(\overline{PCo1_{g1}} - \overline{PCo1_{g2}}\right)^2 + \left(\overline{PCo2_{g1}} - \overline{PCo2_{g2}}\right)^2} \quad (3)$$

where $\overline{PCo1}_{gn}$ and $\overline{PCo2}_{gn}$ represent the average values of PCo1 and PCo2 in the gut microbiota of group n, respectively, and $GM_{offset(g1-g2)}$ represents the offset of gut microbial communities between group 1 and group 2.

Statistical analysis

Statistical analysis was performed mainly on the R platform (version: 4.2.2) and GraphPad Prism software (version: 8.0.2, USA). Shannon and Simpson indices were calculated using the "estimate_richness" function of "phyloseq" package and selected to estimate the changes of α-diversity of gut microbial communities with the Kruskal-Wallis test. Based on the taxonomical composition of microbial communities at the genus level, the Bray–Curtis dissimilarities were calculated and compared with the "anosim" function of the "vegan" package. PCoA was performed and visualized with the "dudi.pca" function of "ade4" and "ggplot2" packages, respectively. The heatmaps presented in this study were visualized with the "pheatmap" package.

Results

Verified function of PA and rutin in reducing BW and decreasing FBG in T2DM mice

Several previous studies have demonstrated that PA has the potential to lose BW and decrease FBG (Bertoia et al., 2016), possibly through modulating gut microbiota. However, the function and underlying mechanism of rutin, a plant polyphenol, in obesity and T2DM remains elusive and needs further verification. Hence, a T2DM model of C57BL/6 mice with HFD for 4 weeks was constructed, and the intervention experiment was performed for 6 weeks to clarify whether rutin can alter BW and FBG in patients with obesity and T2DM. As shown in Figure 2A, the BW of the HFD group was significantly higher than that of the CD group at the end of the model construction (all $p < 0.01$, t-test). Subsequently, the T2DM mice were orally administrated with PA or rutin for 6 weeks, and the results showed that the BW of HFD+Rutin and HFD+PA groups underwent significant differences across the entire process (Figure 2B and Supplementary Table 1).

On the one hand, the BW of the CD+SPSS and HFD+SPSS groups at week 10 (CD+SPSS: 26.00 ± 2.92 g, HFD+SPSS: 35.20 ± 4.87 g) were significantly higher than that at week 4 (CD+SPSS: 22.65 ± 0.95 g, HFD+SPSS: 29.68 ± 2.40 g, all $p < 0.05$, t-test, Figure 2B). However, the BW of HFD+PA and HFD+Rutin groups at week 10 (HFD+PA: 23.00 ± 2.45 g, HFD+Rutin: 24.80 ± 1.30 g) were not significantly higher than that at week 4 (HFD+PA: 26.12 ± 2.26 g, HFD+Rutin: 25.39 ± 1.98 g, all $p > 0.05$, t-test, Figure 2B). On the other hand, the BW of the mice fed with HFD was significantly higher than that of the mice fed with CD during the intervention process, particularly at week 10 ($p < 0.01$, ordinary one-way ANOVA, Figure 2C). The BW of the HFD+PA (23.00 ± 2.45 g) and HFD+Rutin groups (24.80 ± 1.30 g) was significantly lower than that of the HFD+SPSS (35.20 ± 4.87 g) group (all $p < 0.001$, ordinary one-way ANOVA, Figure 2C). On the contrary, no significant differences were found among the CD+SPSS (26.00 ± 2.92 g), HFD+PA, and HFD+Rutin groups at week 10 (all $p > 0.05$, ordinary one-way ANOVA, Figure 2C).

Besides, we calculated ΔBW and ΔFBG values to estimate the dynamic changes in BW and FBG for CD+SPSS, HFD+SPSS, HFD+PA, and HFD+Rutin groups and highlight the effects of rutin and PA. The results showed that the BW of the HFD+SPSS group ($\Delta BW_{(HFD+SPSS)}$ = 5.52 g) increased by 2.17 g (39.3%) compared with that of the CD+SPSS group ($\Delta BW_{(CD+SPSS)}$ = 3.35 g). Importantly, we observed that the BW of HFD+PA and HFD+Rutin groups both decreased ($\Delta BW_{(HFD+Rutin)}$ = −0.594 g and $\Delta BW_{(HFD+PA)}$ = −3.116 g) at the end of the intervention experiment. These results suggested that PA and rutin can effectively decrease the BW of T2DM mice, and PA's effect on reducing weight is better than that of rutin.

Similarly, the FBG levels of the CD+SPSS, HFD+SPSS, HFD+PA, and HFD+Rutin groups were monitored during the entire experiment, and the results showed that the FBG levels of HFD+PA and HFD+Rutin groups significant differed (Supplementary Table 2). Specifically, the FBG levels of the HFD group were significantly higher than that of the CD group at the pre-intervention stage (week 4, $p < 0.001$, t-test, Figure 2D). After

10.3389/fmicb.2024.1513935

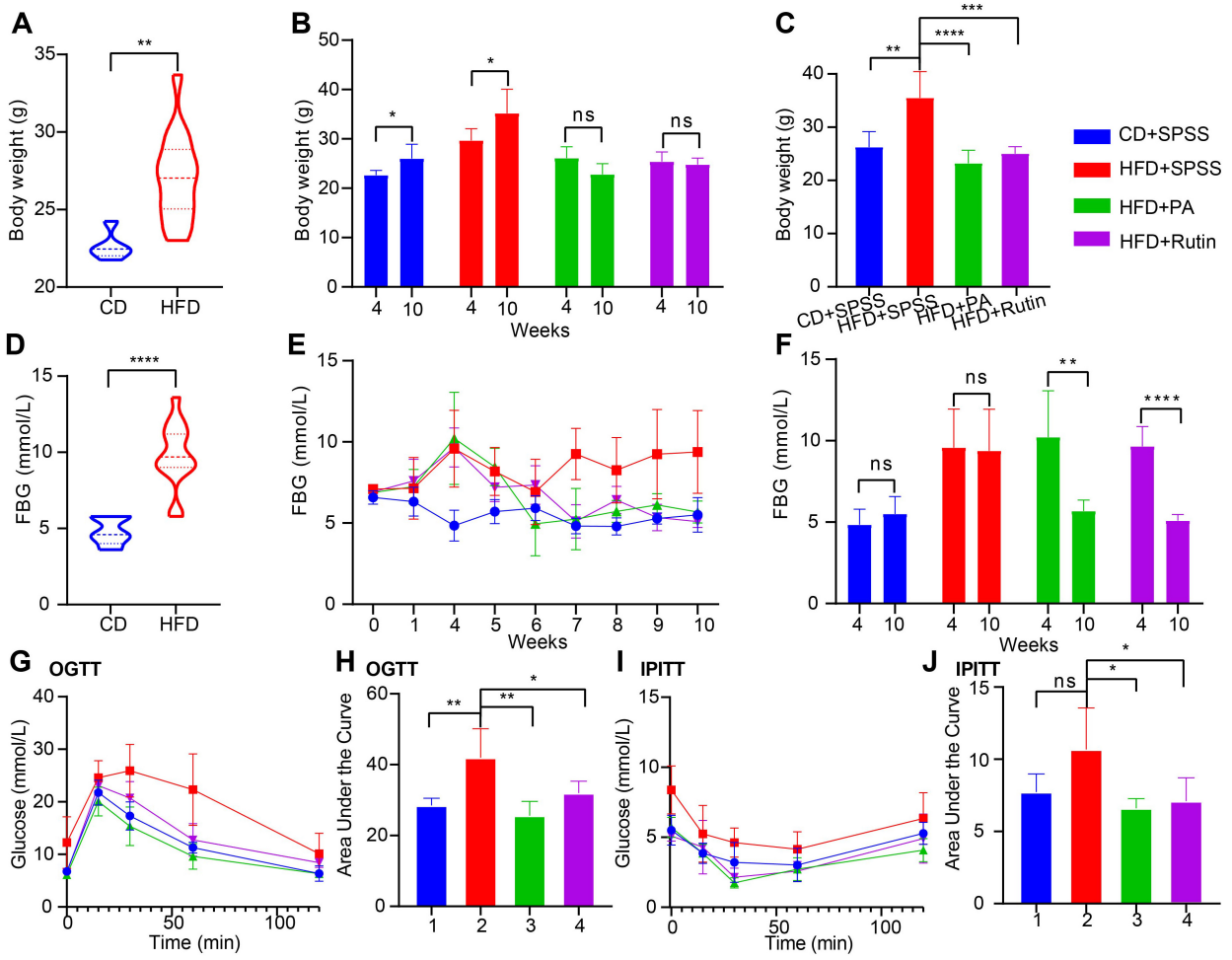

FIGURE 2
Prompt weight loss and decrease blood glucose in T2DM mice by oral gavage of PA or rutin. **(A)** The BW of CD and HFD groups has a significant difference before the oral administration of PA and rutin (week 4). **(B)** The intervention experiment with oral gavage of PA or rutin to T2DM mice showed that the BW of HFD+PA and HFD+Rutin groups had no significant differences between weeks 10 and 4, respectively, whereas that of CD+SPSS and HFD+SPSS groups significantly increased. **(C)** After oral administration of PA or rutin, the BW of HFD+PA and HFD+Rutin groups were both significantly lower than that of CD+SPSS and HFD+SPSS groups at week 10. **(D)** The FBG levels of CD and HFD groups had a significant difference at week 4. **(E)** Dynamic changes in the FBG of CD+SPSS, HFD+SPSS, HFD+PA, and HFD+Rutin groups across the entire experiment were shown. **(F)** After oral administration of PA or rutin, the FBG levels of HFD+PA and HFD+Rutin groups were significantly lower than those of CD+SPSS and HFD+SPSS groups at week 10. **(G)** OGTT showed the dynamic changes in FBG of CD+SPSS, HFD+SPSS, HFD+PA, and HFD+Rutin groups. **(H)** The AUC values of CD+SPSS and HFD+SPSS groups were significantly higher than those of HFD+PA and HFD+Rutin groups according to OGTT. **(I)** IPITT showed the dynamic changes in the FBG of CD+SPSS, HFD+SPSS, HFD+PA, and HFD+Rutin groups. **(J)** The AUC values of CD+SPSS and HFD+SPSS groups were significantly higher than those of HFD+PA and HFD+Rutin groups according to IPITT.

oral gavage of PA and rutin was administered, the FBG levels of the HFD+PA and HFD+Rutin groups both subsequently decreased, and they can return to a similar level as those in the CD+SPSS group, compared with those in the HFD+SPSS group (Figure 2E). Furthermore, the statistical results of FBG levels among these four groups between weeks 4 and 10 proved that PA and rutin can decrease the FBG levels of T2DM mice (Figure 2F). To estimate the effects of PA and rutin in decreasing FBG levels, we quantified the changes in FBG levels between weeks 10 and 4 for these four groups ($\Delta FBG_{(HFD+SPSS)} = -0.2$, $\Delta FBG_{(CD+SPSS)} = 0.66$, $\Delta FBG_{(HFD+Rutin)} = -4.56$, $\Delta FBG_{(HFD+PA)} = -4.54$), respectively. The results suggested that the ability of PA and rutin to decrease FBG levels did not show significant differences.

Additionally, to explore the effects of PA and rutin on glucose metabolism, OGTT, and IPITT were conducted at weeks 8 and 9, respectively. The OGTT results revealed that the FBG levels of the HFD+SPSS group at 0, 15, 30, 60, and 120 min were significantly higher than those of the HFD+PA, HFD+Rutin, and CD+SPSS groups (all $p < 0.05$, t-test, Figure 2G) at the same time points during the test process. Meanwhile, the AUC of the HFD+SPSS group was significantly higher than that of the HFD+PA, HFD+Rutin, and CD+SPSS groups (all $p < 0.05$, t-test, Figure 2H). Besides, we found that the AUC of the HFD+Rutin group was higher than that of the HFD+PA group (Figure 2H). The results of IPITT showed a similar pattern and trend to those of OGTT (Figures 2I, J). Overall, these results demonstrated that administering oral gavage of dietary supplements, namely, PA and rutin, to T2DM mice can restore the ability to modulate blood glucose levels and thereby lose BW and decrease FBG levels.

10.3389/fmicb.2024.1513935

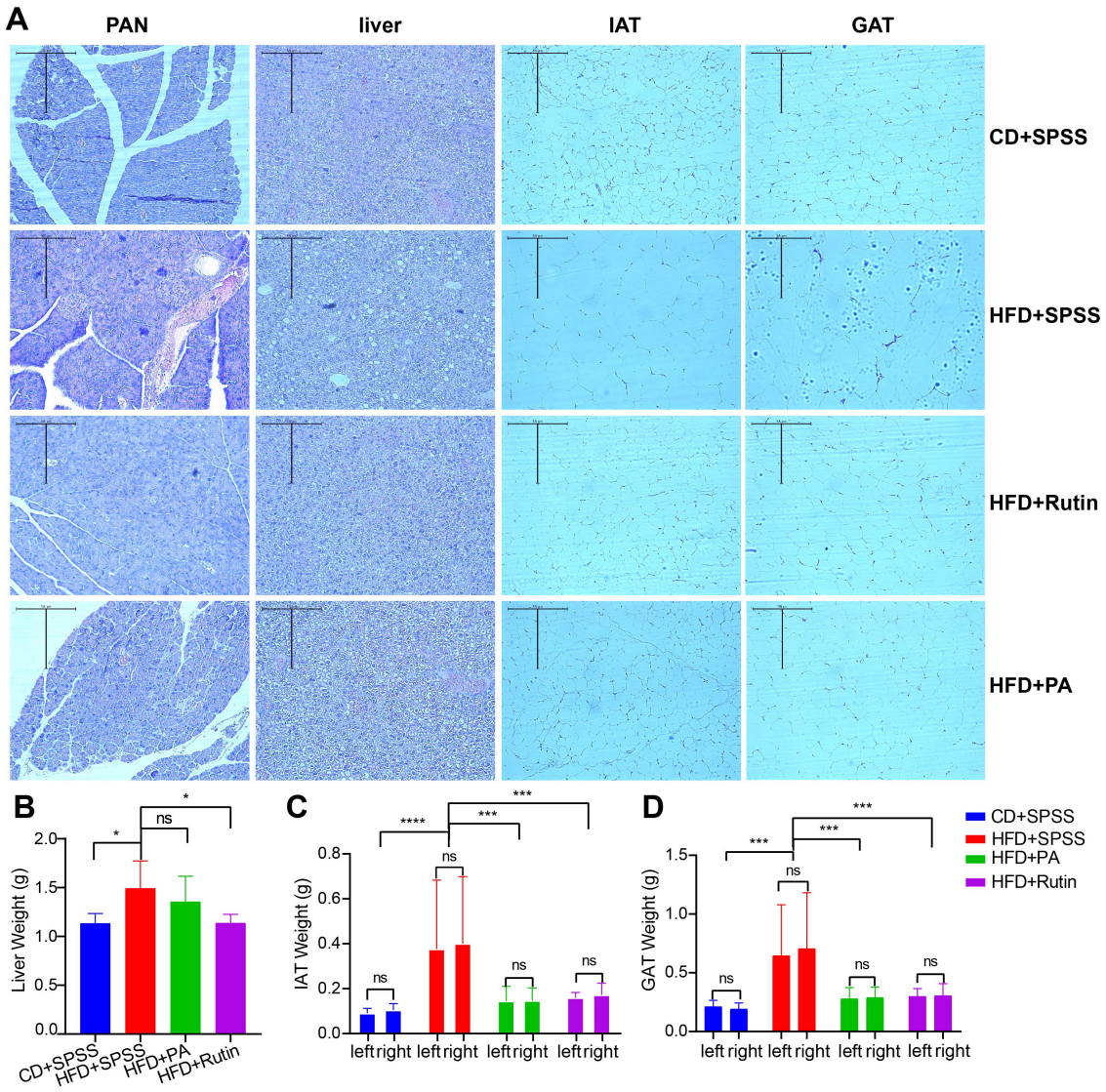

FIGURE 3
Estimation of histopathological effects of PA and rutin in reducing weight and decreasing blood glucose levels. **(A)** Four kinds of tissues, namely, PAN, liver tissue, IAT, and GAT, were collected and used for H&E staining (10 × 10) for CD+SPSS, HFD+SPSS, HFD+PA, and HFD+Rutin groups. The weight of panel **(B)** liver tissue, **(C)** IAT, and **(D)** GAT among CD+SPSS, HFD+SPSS, HFD+PA, and HFD+Rutin groups were measured and compared to explore the effects of PA and rutin on T2DM mice.

Recovery of T2DM mice tissues after oral administration of PA or rutin from a histopathological perspective

To explore the effects and underlying mechanisms of PA and rutin in reducing BW and decreasing FBG, four kinds of tissues were collected, including PAN, liver tissue, IAT, and GAT. Histopathological examination using H&E staining was conducted, and the weight of these tissues was measured for the CD+SPSS, HFD+SPSS, HFD+PA, and HFD+Rutin (Figure 3). The results showed that the tissue histopathology of different groups changed dramatically, revealing the recovery of function in the tissues after the treatment of PA and rutin. The H&E staining results showed that the cell nuclei deviated, more islet cells degenerated, the arrangement of islet cells was disordered, and intracytoplasmic vesicular structures increased in the physiological tissues of the HFD+SPSS group in comparison with that of the CD+SPSS group (Figure 3A). The liver tissues of the HFD+SPSS group showed obvious fat infiltration and contained many fat vacuoles in the visual field. In particular, fatty degeneration was found in the hepatocytes. By contrast, the hepatocytes of the CD+SPSS group were neatly arranged and structurally intact with clear cell borders and the cell nuclei were in the center of the cells (Figure 3A). The tissue histopathological changes revealed the damage to the physiological function of T2DM mice.

After oral gavage of PA and rutin was administered to T2DM mice for 6 weeks, we were surprised to find that histopathology transformation occurred in the HFD+PA and HFD+Rutin groups. For example, the number of focal vacuolar lesions of islet cells and degenerated islet cells in the HFD+PA group decreased

in comparison with that in the HFD+SPSS group (Figure 3A). Furthermore, the islet cells in the HFD+Rutin group showed a neat arrangement, abundant and uniform cell cytoplasm, the disappearance of vacuolar degeneration in the islet cells, and significant improvement in the degree of lesions (Figure 3A). Besides, although the hepatocytes were more structurally intact, the degree of fatty degeneration greatly reduced, and the number of fat vacuoles in the liver of the HFD+PA and HFD+Rutin groups significantly decreased compared with that in the HFD+SPSS group. Fat vacuoles were still present in the liver of these two groups and the proportions in the HFD+PA group were higher than in the HFD+Rutin group. Moreover, the tissue histopathological structures of the HFD+Rutin group were more similar to those of the CD+SPSS group (Figure 3A). These results showed that the oral gavage of PA and rutin in T2DM mice can recover the function of tissues. However, the recovery effectiveness of PA and rutin differ.

Additionally, the results of weight measurement of the liver tissue, IAT, and GAT among the CD+SPSS, HFD+SPSS, HFD+PA, and HFD+Rutin groups showed that the effects on the weight loss of tissues with the treatment of PA and rutin remarkably differed (Supplementary Table 3). Although the liver weight of the HFD+PA (1.36 ± 0.26 g) and HFD+Rutin (1.14 ± 0.09 g) groups decreased compared with that of the HFD+SPSS group (1.49 ± 0.28 g), a significant difference was observed between these two groups ($p < 0.05$, t-test), compared with the HFD+PA and HFD+SPSS groups (Figure 3B). In terms of IAT and GAT, the weight of their left and right parts was measured and compared among CD+SPSS, HFD+SPSS, HFD+PA, and HFD+Rutin groups. The results showed that the IAT and GAT weight of the HFD+PA (IAT: 0.146 ± 0.057 g; GAT: 0.284 ± 0.088 g) and HFD+Rutin (IAT: 0.166 ± 0.039 g; GAT: 0.302 ± 0.081 g) groups significantly decreased (IAT: 0.389 ± 0.285 g; GAT: 0.676 ± 0.431 g, all $p < 0.0001$, ordinary one-way ANOVA) in comparison with that of the HFD+SPSS group; no remarkable differences were found in these two groups and with the CD+SPSS group (Figures 3C, D). These results suggested that PA and rutin can decrease the weight of the liver tissue, IAT, and GAT, and the effects of rutin are better than those of PA.

Together, the comparison of histopathological changes and tissue measurements showed that PA and rutin by oral gavage in T2DM mice significantly altered the conformation of the tissue structure and transitioned it from a pathological to a normal state. Moreover, the effects of rutin on fatty metabolism and the weight and morphological structures of the liver were more remarkable than those of PA. Hence, the therapeutic effects of rutin were speculated to be better than those of PA from the perspective of histopathology.

The significant shift in taxonomical structure of gut microbial communities of T2DM mice after oral gavage of PA and rutin

To investigate the alterations of gut microbiota of T2DM mice caused by PA and rutin and explore the in-depth mechanism, the fecal samples of T2DM mice were collected, the meta-DNA of these samples was extracted, and the V3-V4 region of 16S rRNA was sequenced. Thus, a total of 1,658,576 high-quality sequences were obtained from 30 samples, and the 16S rRNA amplicon dataset was analyzed with the DADA2 tool within QIIME2. The result of the sparsity curve analysis suggested that the sequencing depth was sufficient, and most microbes in each sample were captured (Supplementary Figure 1). Next, the results of α diversity analysis showed that the Shannon and Simpson indices in the gut microbiota of the HFD+Rutin group significantly increased in comparison with those of the HFD+SPSS group ($p < 0.05$, t-test, Figures 4A, B). Meanwhile, the Shannon and Simpson indices in the gut microbiota of the HFD+PA group did not significantly differ from that of the HFD+SPSS group ($p > 0.05$, t-test, Figures 4A, B). To further illustrate the dynamic changes of α diversities, the α diversities of gut microbial communities between the pre-intervention (mRutin, week 4) and post-intervention (cRutin, week 10) were compared. Similarly, the α diversities in the gut microbial communities of T2DM mice significantly increased with the oral gavage of rutin within 6 weeks ($p < 0.05$, t-test, Figures 4C, D), whereas no significant difference was found after the oral administration of PA (mPA and cPA groups, Figures 4E, F). These results suggested that the oral gavage of rutin (200 mg/kg × day) to T2DM mice can significantly alter the α diversity of gut microbial communities, but not PA.

Subsequently, the differences in gut microbial communities among the CD+SPSS, HFD+SPSS, HFD+PA, and HFD+Rutin groups were verified. The results showed that the taxonomical compositions of gut microbial communities at the genus level in the HFD+PA and HFD+Rutin groups significantly differed in comparison with those in the HFD+SPSS group (ANOVA, $p < 0.05$, Figure 4G) at the end of the intervention. Importantly, significant differences were presented in the gut microbial communities of T2DM mice during the process of intervention with PA or rutin (ANOVA, all $p < 0.05$, Figures 4H, I). Moreover, PCoA showed obvious separations in the gut microbial communities of the CD+SPSS, HFD+SPSS, HFD+PA, and HFD+Rutin groups (Figure 4J) and pre-intervention and post-intervention of PA (Figure 4K) and rutin (Figure 4L). These results suggested that oral gavage of rutin (200 mg/kg × day) and PA (200 mg/kg × day) to T2DM mice can significantly change the taxonomical compositions of gut microbial communities in T2DM mice.

Particularly, to further estimate the abilities of PA and rutin to modulate the taxonomical composition of gut microbial communities, the offset value between the two groups was calculated using Formula 3. The results demonstrated that the offset of gut microbial communities between the CD+SPSS and HFD+SPSS groups was 6.68 [$GM_{offset(CD-HFD)} = 6.68$], which suggested that the taxonomical compositions of gut microbial communities of the HFD+SPSS group were changed compared to those of the CD+SPSS group. Similarly, the offset values of gut microbial communities among different groups were calculated, and the following values were obtained: $GM_{offset(HFD+PA-HFD+SPSS)} = 1.79$, $GM_{offset(HFD+Rutin-HFD+SPSS)} = 7.39$, $GM_{offset(cPA-mPA)} = 6.20$, and $GM_{offset(cRutin-mRutin)} = 6.54$. Furthermore, ΔFBG exhibited a significant positive correlation with the changes in the gut microbiota of the HFD+Rutin group ($R = 0.92$, $p < 0.05$, Supplementary Figure 2), suggesting that the decrease in FBG levels was significantly correlated with the dynamic changes in gut microbial communities during the treatment of rutin. Since

10.3389/fmicb.2024.1513935

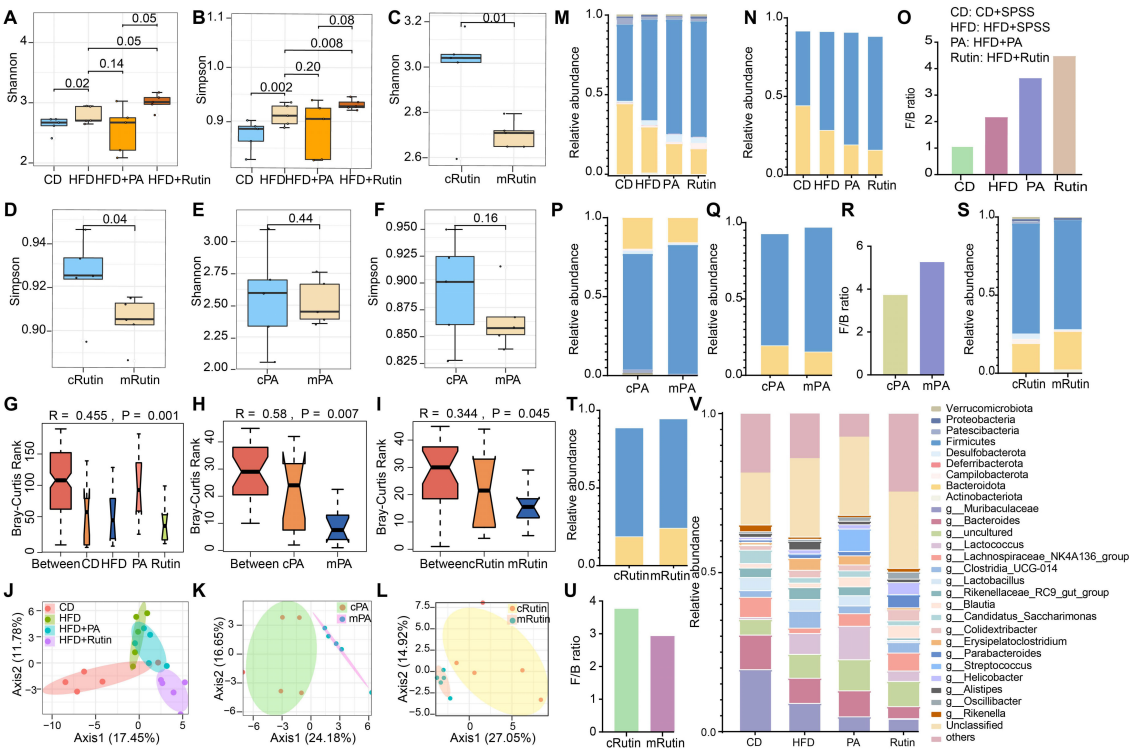

FIGURE 4

Significant alteration in the taxonomical compositions of gut microbial communities of T2DM mice after oral gavage of PA and rutin. The α diversities, including **(A)** Shannon and **(B)** Simpson indices, of gut microbial communities between the CD+SPSS, HFD+SPSS, HFD+PA, and HFD+Rutin groups were compared. The α diversities, including **(C)** Shannon and **(D)** Simpson indices, of gut microbial communities between mRutin and cRutin groups were compared. The α diversities, including **(E)** Shannon and **(F)** Simpson indices, of gut microbial communities between mPA and cPA groups were compared. The significant differences in the composition of gut microbial communities **(G)** between CD+SPSS, HFD+SPSS, HFD+PA, and HFD+Rutin groups at week 10; **(H)** between pre-intervention (mPA, week 4) and post-intervention (cPA, week 10) groups intervened with PA; and **(I)** between pre-intervention (mRutin, week 4) and post-intervention (cRutin, week 10) groups intervened with rutin were compared by their Bray–Curtis dissimilarity. Principal coordinate analyses **(J)** among CD+SPSS, HFD+SPSS, HFD+PA, and HFD+Rutin groups; **(K)** between cPA and mPA groups; and **(L)** between cRutin and mRutin groups were conducted. **(M)** The taxonomical structure of gut microbial communities for CD+SPSS, HFD+SPSS, HFD+PA, and HFD+Rutin groups was profiled at the phylum level. **(N)** The relative abundances of *Firmicutes* and *Bacteroidota* in CD+SPSS, HFD+SPSS, HFD+PA, and HFD+Rutin groups were visualized. **(O)** The ratios of *Firmicutes* and *Bacteroidota* of CD+SPSS, HFD+SPSS, HFD+PA, and HFD+Rutin groups were calculated and visualized. **(P)** The taxonomical structure of gut microbial communities for cPA and mPA groups was profiled at the phylum level. **(Q)** The relative abundances of *Firmicutes* and *Bacteroidota* in cPA and mPA groups were visualized. **(R)** The ratios of *Firmicutes* and *Bacteroidota* in cPA and mPA groups were visualized. **(S)** The taxonomical compositions of gut microbial communities in cRutin and mRutin groups were profiled at the phylum level. The relative abundances of *Firmicutes* and *Bacteroidota* in panel **(T)** cRutin and mRutin groups were visualized. **(U)** The ratios of *Firmicutes* and *Bacteroidota* in cRutin and mRutin groups were calculated and displayed. **(V)** The top 20 genera were selected and visualized to display the alterations in the taxonomical compositions of gut microbial communities at the genus level.

$GM_{offset(HFD+PA-HFD+SPSS)} < GM_{offset(HFD+Rutin-HFD+SPSS)}$, and $GM_{offset(cPA-mPA)} < GM_{offset(cRutin-mRutin)}$, the results of these offset values and linear fit analyses suggest that rutin may be superior to PA in its ability to modulate the composition of the gut microbial communities (Figures 4J–L).

Moreover, to investigate the dynamic changes in gut microbial communities, the taxonomical compositions of gut microbial communities were profiled at the phylum and genus levels. First, nine phyla, namely *Actinobacteriota*, *Bacteroidota*, *Campilobacterota*, *Deferribacterota*, *Desulfobacterota*, *Firmicutes*, *Patescibacteria*, *Proteobacteria*, and *Verrucomicrobiota*, were found to be the dominant taxa in gut microbial communities. The relative abundances of *Firmicutes* and *Bacteroidota* in T2DM mice significantly increased and decreased, respectively, during the entire process in comparison with those in normal mice in the CD+SPSS group (Figures 4M, N), consistent with the changes in these two phyla in the gut microbial communities of HFD-induced obese mice (Daniel et al., 2014). The *Firmicutes*/*Bacteroidota* (F/B) ratio in the HFD+SPSS group increased in comparison with that in the CD+SPSS group (Figure 4O). After the oral gavage of PA and rutin was administered, the relative abundances of *Firmicutes* and *Bacteroidota* continually increased and decreased (Figures 4M, N), respectively, and the *F/B* ratio in the HFD+PA and HFD+Rutin groups increased (Figure 4O). In particular, the *F/B* ratio in the HFD+Rutin group was higher than that in the HFD+PA (Figure 4O). Subsequently, the dynamic changes in the taxonomical compositions of gut microbial communities between pre-intervention and post-intervention samples for PA and rutin were compared at the phylum level. As for the T2DM mice administered with PA, the relative abundances of *Firmicutes* and *Bacteroidota* decreased and increased (Figures 4P, Q), respectively, and the F/B ratio decreased (Figure 4R). Interestingly, the dynamic patterns of the relative abundances of *Firmicutes* and *Bacteroidota* and the F/B ratio were inverse

in the gut microbial communities of mice intervened with rutin (Figures 4S–U). Furthermore, a total of 66 genera were identified, and seven taxa, including *Muribaculaceae*, *Bacteroides*, *Lactococcus*, *Lachnospiraceae_NK4A136_group*, *Clostridia_UCG-014*, *Lactobacillus*, and *Rikenellaceae_RC9_gut_group*, dominated in the gut microbial communities (Figure 4V). These results revealed that the taxonomical structures of gut microbial communities were significantly altered, coupled with the loss of BW and the decrease in FBG, with the intervention of PA and rutin.

Identification of key gut microbiota, co-occurrence network analysis, and their interactions with BW and FBG during the intervention process of rutin and PA

In the previous section of our results, we primarily focused on the dynamic changes of taxa at the phylum and genus levels and ignored the roles of microbes with significantly altered gut microbial communities of T2DM mice during the intervention process of PA and rutin. Hence, we further identified the key microbiota, explored the interactions and associations among these microbes, and linked them with the changes of BW and FBG to elucidate the potential mechanisms of PA and rutin in reducing BW and decreasing FBG.

First, the distribution of core and specific genera of gut microbial communities were visualized and 23 core genera were identified during the intervention of PA and rutin (Figure 5A). Then, the significantly differed taxon at the genus level was identified among different groups with LEfSe. The results showed that *Roseburia* and *Odoribacter* harbored powerful discrimination for the HFD group, whereas *Eubacterium_siraeum_group*, *Prevotellaceae_ucg-001*, *Anaeroplasma*, *Monoglobus*, and *Ruminococcus* were suitable to the CD+SPSS group (Figure 5B). Moreover, a series of gut probiotics and short-chain-fatty-acid-producing bacteria, such as *Lactococcus*, *Streptococcus*, *Lachnospiraceae_UCG-006*, and *Anaerotruncus* were determined to be powerful discrimination taxa in the HFD+PA and HFD+Rutin groups compared with the HFD+SPSS group after the oral gavage of PA and rutin (Figure 5B and Supplementary Figure 3). Several significantly different taxa, including *Roseburia* and *Parabacteroides*, were identified in T2DM mice with the intervention of PA and rutin (Figure 5B).

Second, co-occurrence networks between the taxonomic composition of gut microbiota at the genus level and body characteristics (including BW and FBG) and the weights of three tissues were constructed at week 10 (Supplementary Figure 4). The ratio of the abundance of the same taxon and the ratio of body features between cPA and mPA groups and between cRutin and mRutin groups were calculated and visualized (Figures 5C, D), respectively. The results showed that the relative abundances of *Colidextribacter*, *Faecalibaculum*, *A2*, *Anaerotruncus*, *Tuzzerella*, *Rikenella*, *Bilophila*, *Alistipes*, *Lachnospiraceae_NK4A136_group*, and *Roseburia* in the gut microbiota communities of T2DM mice increased, and then after the oral gavage of PA, their abundances significantly decreased (all $p < 0.05$, Kruskal–Wallis test, Figure 5C). Similarly, the relative abundances of *Roseburia*, *Lactococcus*, *Bifidobacterium*, *Romboutsia*, *Tuzzerella*, *Rikenella*, *Alistipes*, *Bacteroides*, *Lactobacillus*, *Lachnospiraceae_NK4A136_group*, *Rikenellaceae_RC9_gut_group*, *A2*, and *Anaerotruncus* in the gut microbiota communities of T2DM mice increased, and then after the oral gavage of rutin, their abundances significantly decreased (all $p < 0.05$, Kruskal–Wallis test, Figure 5D). The results suggested that the relative abundances of *Roseburia*, *Tuzzerella*, *Lachnospiraceae_NK4A136_group*, *Rikenella*, *Alistipes*, *A2*, and *Anaerotruncus*, decreased after the intervention of PA and rutin. Inversely, the dynamic change patterns of *Helicobacter*, *Erysipelatoclostridium*, *Clostridia_vadinBB60_group*, *Blautia*, *Odoribacter*, *Candidatus_Saccharimonas*, *Lactococcus*, *Parabacteroides*, and *Muribaculaceae* in T2DM mice with the oral gavage of PA and those of *Parabacteroides*, *Akkermansia*, *Bilophila*, *Helicobacter*, *Clostridia_vadinBB60_group*, *Blautia*, *Muribaculaceae*, *Candidatus_Saccharimonas*, and *Oscillibacter* with the oral gavage of rutin significantly increased (all $p < 0.05$, Kruskal–Wallis test, Figures 5C, D). The abundance of *Helicobacter*, *Muribaculaceae*, *Parabacteroides*, *Clostridia_vadinBB60_group*, *Blautia*, *Candidatus_Saccharimonas,* and *Odoribacter* increased after the intervention of PA and rutin.

Third, the linkage between the alterations in mice's body features and gut microbiota was investigated. The Pearson correlations among the gut microbiota and BW, FBG, IAT, GAT, and liver tissue were determined, and the interaction network was conducted. The results showed that *Faecalibaculum*, *Christensenellaceae_R-7_group*, *Clostridium_sensu_stricto_1*, *Coriobacteriaceae_UCG-002*, *Mucispirillum*, and *Roseburia* were significantly positively correlated with BW, whereas *NK4A214_group* was significantly negatively correlated (all $p < 0.05$, Supplementary Figure 5). Additionally, *Christensenellaceae_R-7_group*, *Clostridium_sensu_stricto_1*, *Coriobacteriaceae_UCG-002*, *Faecalibaculum*, *Mucispirillum*, and *Roseburia* were significantly positively correlated with FBG ($p < 0.05$, Supplementary Figure 5), and the relative abundance of *Roseburia* was significantly positively correlated the changes in the weight of liver tissue ($R = 0.484$, $p < 0.05$, Supplementary Figure 6). Besides, *Faecalibaculum*, *Christensenellaceae_R-7_group*, *Mucispirillum*, *Clostridium_sensu_stricto_1*, *Clostridia_vadinBB60_group*, *Coriobacteriaceae_UCG-002*, and *Roseburia*, were significantly positively correlated with the changes in IAT and GAT. In particular, *Roseburia* was strongly positively correlated with the dynamic changes in body features, including BW, FBG, IAT, GAT, and liver tissue. Our findings suggest that weight loss and FBG reduction in T2DM mice under sustained intervention with PA and rutin are strongly associated with changes in the gut microbiota.

Identification of potential functional traits of gut microbial communities that contribute to the role of rutin and PA

To obtain an in-depth understanding of the potential mechanism of PA and rutin, the functional compositions of gut microbial communities were profiled and the linkages between the

10.3389/fmicb.2024.1513935

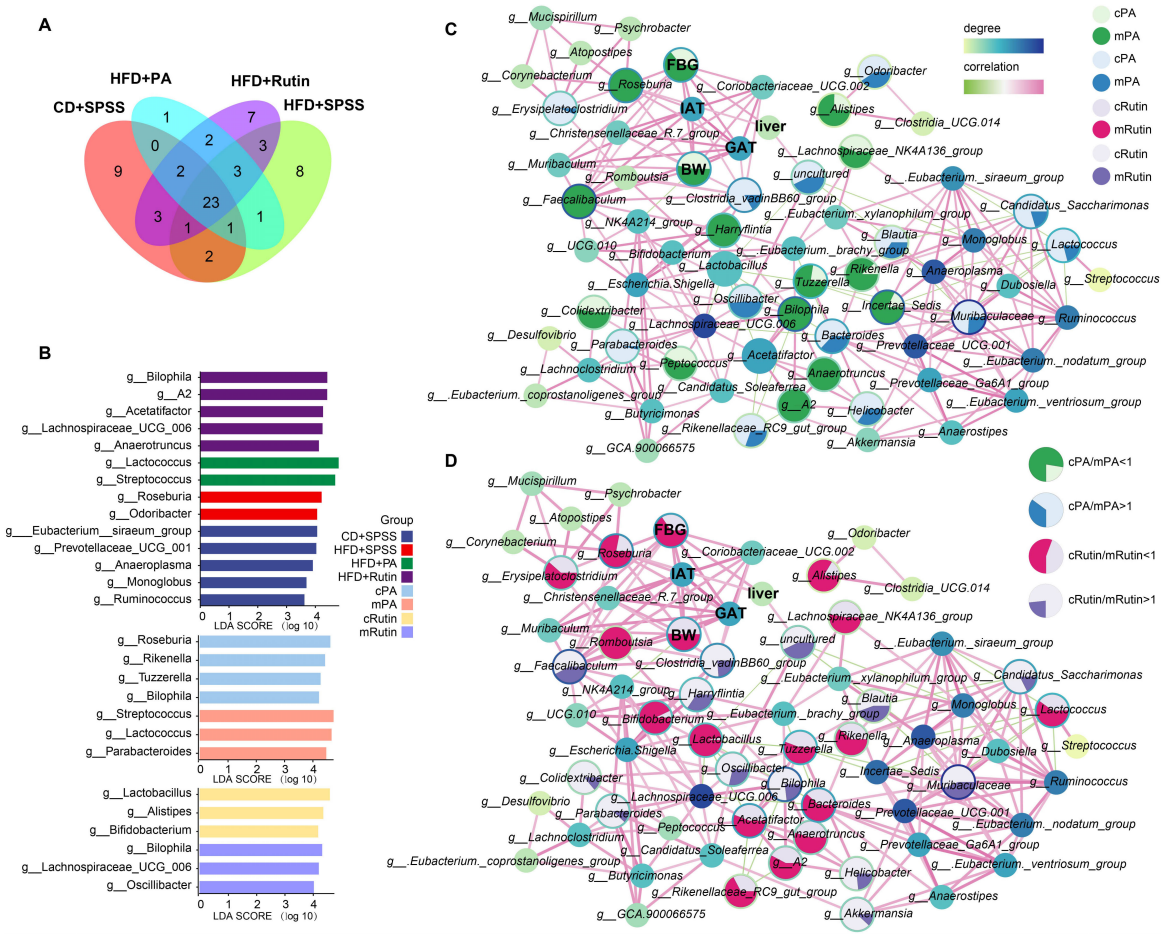

FIGURE 5
Identification of key microbes and biomarkers and construction of interaction network to reveal the potential mechanisms of PA and rutin in reducing BW and FBG. **(A)** Veen plot showed the distribution of gut microbes among groups at the genus level. **(B)** Taxonomic biomarkers for CD+SPSS, HFD+SPSS, HFD+PA, and HFD+Rutin groups and pre-intervention and post-intervention of PA and rutin were identified. Network analysis showed the interactions between gut microbes and mouse body features and the alterations of gut microbiota for the intervention with panel **(C)** PA and **(D)** rutin. The area of each circle is divided into two parts dark green and dark blue (enriched in the mPA group), and light green and light blue (enriched in the cPA group). The area of each circle is divided into two parts labeled with dark pink, dark purple (enriched in the mRutin group), and light pink and light purple (enriched in the cRutin group).

dominant functional traits and key gut microbes were constructed with multiple comparisons based on Spearman's rank correlations (Figure 6). The results showed that the associations between the discriminated taxa (biomarkers) of each group and the dominant KOs (Figure 6A) were different. Such as *Lactococcus* and *Streptococcus*, which are two biomarkers for the HFD+PA group, were significantly associated with K07024, K00059, K02030, K02004, K02003, K02529, K01992, and K06180, which are mainly involved in starch and sucrose metabolism, fatty acid metabolism, amino acid transport system, ABC transport system, *Lac*I family transcription regulatory factors, and ribosome biosynthesis (Figure 6A). Meanwhile, the biomarkers for the HFD+Rutin group, such as *Acetatifactor* and *Bilophila*, were significantly associated with abundant KOs, including K03205, K03091, K04759, K03497, K03496, K00615, K03657, K01448, K03169, K03655, K03088, and K01915, which mainly participate in the function of the secretory system, iron transport, protein signaling, *Par*B family transcription processes, chromosome segmentation proteins, pentose phosphate pathways, nucleotide excision repair, DNA replication, and amino acid metabolism (Figure 6A). Subsequently, the correlations among the top 30 KOs were calculated and visualized (Figure 6B). Then, the enrichment of KOs in the intervention of PA and rutin was compared and the functional traits of gut microbial communities were found to be mainly involved in glucose metabolism, fatty acid metabolism, amino acid metabolism, and protein transport system after PA and rutin treatment (Figures 6C, D). Overall, the results suggested that the alterations in gut microbes of the microbial communities of T2DM mice after the intervention with PA and rutin led to the enrichment of functional traits, such as the metabolism of glucose, fatty acid, and amino acids, which contributed to the role of PA and rutin in reducing BW and decreasing FBG.

Discussion

In our present study, we verified the function of rutin in reducing weight and decreasing blood glucose levels, compared

10.3389/fmicb.2024.1513935

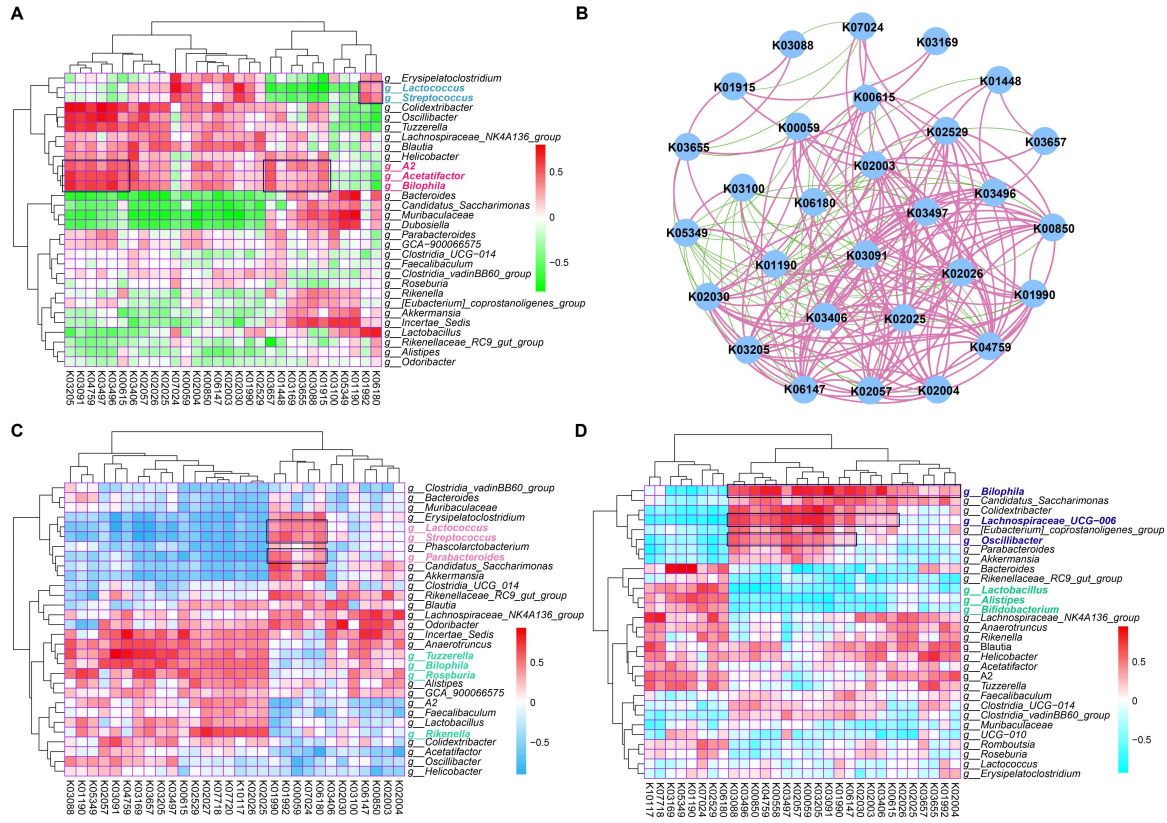

FIGURE 6

Identification of potential functional traits of gut microbial communities that contribute to the role of PA and rutin. **(A)** The heatmap showed the Spearman correlations between dominant KOs and the genus taxa based on the genus composition of gut microbial communities in CD+SPSS, HFD+SPSS, HFD+PA, and HFD+Rutin groups (week 10). **(B)** The Spearman correlations among the top 30 KOs were visualized based on the functional composition of gut microbial communities in CD+SPSS, HFD+SPSS, HFD+PA, and HFD+Rutin groups (week 10). **(C)** The Spearman correlations between dominant KOs and the genus taxa of cPA and mPA groups were determined. **(D)** The Spearman correlations between dominated KOs and the genus taxa of cRutin and mRutin groups were determined.

the effects between the oral gavage of PA and rutin in animal experiments, and investigated the potential mechanisms from the perspective of gut microbiota. Our results demonstrated that PA and rutin harbor the ability to lose BW and decrease FBG levels in T2DM mice, and enhance glucose tolerance and insulin sensitivity. In particular, the weight loss effect of PA was superior to that of rutin $\{\Delta BW_{(HFD+Rutin)} = -0.59,\ \Delta BW_{(HFD+PA)} = -3.116,$ and $abs[\Delta BW_{(HFD+PA)}] > abs[\Delta BW_{(HFD+Rutin)}]\}$, whereas the FBG decrease effect of rutin was superior to that of PA $\{\Delta FBG_{(HFD+Rutin)} = -4.56,\ \Delta FBG_{(HFD+PA)} = -4.54,$ and $abs[\Delta FBG_{(HFD+Rutin)}] > abs[\Delta FBG_{(HFD+PA)}]\}$. These results suggested that although PA and rutin harbor the ability to lose BW and decrease FBG levels, the application scenarios in which they maximize their function may differ. That is to say, the advantages of PA are rapidly reducing BW and decreasing FBG levels, and quickly controlling BW and FBG is suitable, benefiting obese populations with T2DM. Meanwhile, the advantages of rutin are slowly reducing BW and rapidly decreasing the FBG levels, benefiting patients with T2DM but without obesity. Additionally, the results of OGTT and IPITT showed that PA and rutin can enhance glucose tolerance and insulin resistance in T2DM mice, and the effects of PA are better than those of rutin.

Moreover, the histopathological results showed that the tissues of T2DM mice recovered after the oral gavage of PA and rutin, indicating the transformation of these tissues from a pathological state to a normal state. The H&E staining results of the four kinds of tissues, including PAN, liver tissue, IAT, and GAT, revealed the alterations in cells and proved that PA and rutin can improve chronic inflammation. Besides, the H&E staining results of adipose tissue sections and the measurement of liver weight indicated that PA and rutin can significantly reduce adipocyte hypertrophy. A combination of the results of PAN and liver tissue sections and the comparison results of the weight of tissues indicated that rutin is more effective in alleviating pancreatic histopathology and improving the cytopathy of liver tissue than PA.

Furthermore, previous studies have proven that the mechanism of PA in reducing BW and decreasing FBG is achieved through modulating the gut microbiota (Ferreira et al., 2023). Hence, in the present study, to elucidate the mechanism of rutin and investigate the effect variations between PA and rutin in gut microbiota remodeling, we conducted the 16S rRNA amplicon sequencing, profiled the taxonomical and functional compositions, and linked the alterations of gut microbiota with the changes of body features. Our results showed that the composition of gut microbial communities changed significantly after the oral gavage of PA or

rutin. However, according to the formula offset between the two groups, we calculated the offsets of gut microbial communities for different comparative strategies and found that the changes in gut microbial communities caused by rutin were more intense than those caused by PA. Interestingly, we found the alterations in FBG were significantly positively correlated with the dynamic changes in the gut microbiota of the HFD+Rutin group ($p < 0.05$). Besides, the dynamic changes of gut microbes were explored at the phylum and genus levels. The results demonstrated that the relative abundances of *Firmicutes* and *Bacteroides* underwent significant alteration. The Firmicutes/Bacteroidetes (F/B) ratio is widely accepted to have an important influence in maintaining normal gut homeostasis (Stojanov et al., 2020). The *F/B* ratio, which is a classical index (Pammi et al., 2017), was assessed, and we found that the *F/B* ratio in the HFD+SPSS group increased compared with that in the CD+SPSS group, whereas the *F/B* ratios in the HFD+PA and HFD+Rutin groups did not decrease. Remarkably, the *F/B* ratio decreased after the oral gavage of PA and increased after the oral gavage of rutin. These results suggested that although the potential mechanisms of PA and rutin are associated with the reconstruction of gut microbiota, the affected gut microbes differ.

Besides, based on the taxonomical composition of gut microbial communities and the data of body features during the oral gavage of PA and rutin, a series of key microbes significantly linked with body features were identified, such as *Roseburia*, *Lactococcus*, *Streptococcus*, *Lachnospiraceae_UCG-006*, *Anaerotruncus*, *Bifidobacterium*, *Akkermansia*, *Bilophila*, *Faecalibaculum*, *Parabacteroides*, and *Oscillibacter*. Additionally, these key microbes were strongly correlated with several metabolic pathways, including starch and sucrose metabolism, fatty acid metabolism, amino acid transport system, and amino acid metabolism. Previous studies have reported the linkage of these taxa to T2DM and the potential mechanism was also discussed. For example, the relative abundance of *Lactococcus* in the gut microbial community was increased and negatively associated with obesity after the administration of probiotics (Kong et al., 2019). This phenomenon was observed in the HFD+PA group. Additionally, the famous gut microbiota and the next generation probiotics, *Akkermansia muciniphila*, also undergo a significant increase in the gut microbial communities after the intervention with PA in our present study, which consistent with the result in human cohort of obesity and T2DM (Zhang et al., 2021). Previous studies have shown that the relative abundance of the gut probiotics *Akkermansia* and *Lactococcus* increased, their derived metabolites, such as short-chain fatty acids (SCFAs), also significantly increased(Cai et al., 2023; Kim et al., 2023). And the function of SCFAs in the regulation of the metabolic syndrome and the maintenance of energy homeostasis and host insulin sensitivity has been confirmed (Fu et al., 2019; Liu et al., 2019). Moreover, the abundances of a series of other SCFAs-producing gut microbes, such as *Odoribacter*, *Lactococcus*, *Streptococcus*, *Lachnospiraceae*, and *Anaerotruncus* (Dai et al., 2019; Lin et al., 2020; Wang et al., 2024), were also increased. Besides, the relative abundance of *Faecalibaculum* increased significantly after the intervention of rutin, and it was strongly correlated with BW. In a previous study, the growth of *Faecalibaculum* was notably found to alleviate obesity-induced metabolic disorders by reducing the number of pro-inflammatory Thl7 cells (Kawano et al., 2022). In addition, it has been demonstrated in previous studies that PA can be catabolized and metabolized when interacting with gut microbes to produce metabolites that enhance bioactivity and bioavailability, and that these metabolites may have a positive effect on ameliorating the metabolic syndrome (Gui et al., 2023; Redondo-Castillejo et al., 2023). Rutin has also been demonstrated to alleviate colonic lesions and modulate gut microbiota in diabetic mice (Cai et al., 2023). Therefore, we speculated that PA and rutin can positively affect metabolic health in patients with T2DM and obesity by regulating the gut microbiota, affecting related metabolic pathways and metabolites, and alleviating inflammatory response. Subsequent animal experiments and human clinical trial studies still need to be conducted to explore the potential of PA and rutin in alleviating inflammation and T2DM through the modulation of gut microbiota (Mathrani et al., 2023).

Conclusion

Our results showed that PA and rutin harbor the ability to significantly lose BW and decrease FBG levels in T2DM mice. The treatment of PA and rutin on T2DM can assist with the transformation of tissues and cells, resulting in the relief of inflammation and fat hypertrophy, and the therapeutic effects of rutin are more effective than those of PA. The results of the gut microbial community suggested that the taxonomical and functional compositions of T2DM mice administered with PA and rutin underwent significant change, and FBG exhibited a significant correlation with the offset values of gut microbial communities in rutin treatment. In addition, our findings suggest that the mechanisms of PA and rutin in reducing weight and decreasing FBG depend on the dynamic changes in several key microbes, such as *Akkermansia*, *Lactococcus*, *Odoribacter*, *Faecalibaculum*, and *Roseburia*; these microbes were significantly associated with the changes in BW and FBG, and the changes in functional traits, such as sucrose metabolism, fatty acid metabolism, amino acid transport system, and amino acid metabolism. Although PA and rutin could lower BW and reduce FBG, the application scenarios in which they maximize their function may differ, and the underlying mechanisms involve the regulation of the gut microbiota in T2DM mice. Our results provide new insights into the clinical management and treatment of BW and FBG in patients with obesity and T2DM from the perspective of gut microbiota and dietary supplements.

Data availability statement

Sequencing datasets for 30 fecal samples in our study have been deposited into NCBI's Sequence Read Archive (SRA) database with the BioProject number: PRJNA961702.

Ethics statement

The present study was approved by the Experimental Animal Ethics Committee of Anhui Medical University (approval no.

LLSC20210503). The study was conducted in accordance with the local legislation and institutional requirements.

Author contributions

YG: Methodology, Software, Validation, Visualization, Writing – original draft, Writing – review and editing. BH: Methodology, Supervision, Visualization, Writing – original draft. YQ: Methodology, Visualization, Writing – original draft. BQ: Methodology, Software, Visualization, Writing – original draft. MR: Methodology, Visualization, Writing – original draft. LC: Data curation, Resources, Supervision, Writing – original draft. YZ: Project administration, Software, Supervision, Writing – review and editing. MH: Methodology, Project administration, Supervision, Visualization, Writing – original draft, Writing – review and editing.

Funding

The author(s) declare financial support was received for the research, authorship, and/or publication of this article. This work was partially supported by the National Natural Science Foundation of China (82300645 and 82103857), Outstanding Youth Program of Anhui Provincial Natural Science Foundation (2408085Y039), Key Project for cultivating outstanding young teachers of Higher Education in Anhui Province (YQZD202406), Research Fund of Anhui Institute of Translational Medicine (2022zhyx-B15), Grants for Scientific Research of BSKY (XJ201916) from Anhui Medical University, and Research Fund of Anhui Engineering Laboratory for Medicinal, Natural Science Foundation of Higher Education in Anhui Province (KJ2021ZD0113), and Food Homologous Natural Resources Exploration (YSTY2022007).

Conflict of interest

The authors declare that the research was conducted in the absence of any commercial or financial relationships that could be construed as a potential conflict of interest.

Generative AI statement

The authors declare that no Generative AI was used in the creation of this manuscript.

Publisher's note

All claims expressed in this article are solely those of the authors and do not necessarily represent those of their affiliated organizations, or those of the publisher, the editors and the reviewers. Any product that may be evaluated in this article, or claim that may be made by its manufacturer, is not guaranteed or endorsed by the publisher.

Supplementary material

The Supplementary Material for this article can be found online at: https://www.frontiersin.org/articles/10.3389/fmicb.2024.1513935/full#supplementary-material

References

Asemi, Z., Alizadeh, S. A., Ahmad, K., Goli, M., and Esmaillzadeh, A. (2016). Effects of beta-carotene fortified synbiotic food on metabolic control of patients with type 2 diabetes mellitus: a double-blind randomized cross-over controlled clinical trial. *Clin. Nutr.* 35, 819–825. doi: 10.1016/j.clnu.2015.07.009

Bazyar, H., Moradi, L., Zaman, F., and Zare Javid, A. (2023). The effects of rutin flavonoid supplement on glycemic status, lipid profile, atherogenic index of plasma, brain-derived neurotrophic factor (BDNF), some serum inflammatory, and oxidative stress factors in patients with type 2 diabetes mellitus: a double-blind, placebo-controlled trial. *Phytother. Res.* 37, 271–284. doi: 10.1002/ptr.7611

Bertoia, M. L., Rimm, E. B., Mukamal, K. J., Hu, F. B., Willett, W. C., Cassidy, A., et al. (2016). Dietary flavonoid intake and weight maintenance: three prospective cohorts of 124,086 US men and women followed for up to 24 years. *BMJ* 352:i17. doi: 10.1136/bmj.i17

Bokulich, N. A., Kaehler, B. D., Rideout, J. R., Dillon, M., Bolyen, E., Knight, R., et al. (2018). Optimizing taxonomic classification of marker-gene amplicon sequences with QIIME 2's q2-feature-classifier plugin. *Microbiome* 6:90. doi: 10.1186/s40168-018-0470-z

Cai, C., Cheng, W., Shi, T., Liao, Y., Zhou, M., Liao, Z., et al. (2023). Rutin alleviates colon lesions and regulates gut microbiota in diabetic mice. *Sci. Rep.* 13:4897. doi: 10.1038/s41598-023-31647-z

Campos, F., Peixoto, A. F., Fernandes, P. A. R., Coimbra, M. A., Mateus, N., de Freitas, V., et al. (2021). The antidiabetic effect of grape pomace polysaccharide-polyphenol complexes. *Nutrients* 13:4495. doi: 10.3390/nu13124495

Chen, L., Gnanaraj, C., Arulselvan, P., El-Seedi, H., and Teng, H. (2019). A review on advanced microencapsulation technology to enhance bioavailability of phenolic compounds: based on its activity in the treatment of Type 2 Diabetes. *Trends Food Sci. Tech.* 85, 149–162. doi: 10.1016/j.tifs.2018.11.026

Cheng, Y., Yu, X., Zhang, J., Chang, Y., Xue, M., Li, X., et al. (2019). Pancreatic kallikrein protects against diabetic retinopathy in KK Cg-A(y)/J and high-fat diet/streptozotocin-induced mouse models of type 2 diabetes. *Diabetologia* 62, 1074–1086. doi: 10.1007/s00125-019-4838-9

Choy, Y. Y., Jaggers, G. K., Oteiza, P. I., and Waterhouse, A. L. (2013). Bioavailability of intact proanthocyanidins in the rat colon after ingestion of grape seed extract. *J. Agric. Food Chem.* 61, 121–127. doi: 10.1021/jf301939e

Dai, S., Pan, M., El-Nezami, H. S., Wan, J. M. F., Wang, M. F., Habimana, O., et al. (2019). Effects of lactic acid bacteria-fermented soymilk on isoflavone metabolites and short-chain fatty acids excretion and their modulating effects on gut microbiota. *J. Food Sci.* 84, 1854–1863. doi: 10.1111/1750-3841.14661

Daniel, H., Gholami, A. M., Berry, D., Desmarchelier, C., Hahne, H., Loh, G., et al. (2014). High-fat diet alters gut microbiota physiology in mice. *ISME J.* 8, 295–308. doi: 10.1038/ismej.2013.155

de Vos, W. M., Tilg, H., Van Hul, M., and Cani, P. D. (2022). Gut microbiome and health: mechanistic insights. *Gut* 71, 1020–1032. doi: 10.1136/gutjnl-2021-326789

Delzenne, N. M., Cani, P. D., Everard, A., Neyrinck, A. M., and Bindels, L. B. (2015). Gut microorganisms as promising targets for the management of type 2 diabetes. *Diabetologia* 58, 2206–2217. doi: 10.1007/s00125-015-3712-7

Delzenne, N. M., Neyrinck, A. M., Bäckhed, F., and Cani, P. D. (2011). Targeting gut microbiota in obesity: effects of prebiotics and probiotics. *Nat. Rev. Endocrinol.* 7, 639–646. doi: 10.1038/nrendo.2011.126

DeMarco, V. G., Aroor, A. R., and Sowers, J. R. (2014). The pathophysiology of hypertension in patients with obesity. *Nat. Rev. Endocrinol.* 10, 364–376. doi: 10.1038/nrendo.2014.44

Dhatt, G. S., Agarwal, M. M., Othman, Y., and Nair, S. C. (2011). Performance of the Roche Accu-Chek active glucose meter to screen for gestational diabetes mellitus using fasting capillary blood. *Diabetes Technol. Ther.* 13, 1229–1233. doi: 10.1089/dia.2011.0097

Donath, M. Y., and Shoelson, S. E. (2011). Type 2 diabetes as an inflammatory disease. *Nat. Rev. Immunol.* 11, 98–107. doi: 10.1038/nri2925

Douglas, G. M., Maffei, V. J., Zaneveld, J. R., Yurgel, S. N., Brown, J. R., Taylor, C. M., et al. (2020). PICRUSt2 for prediction of metagenome functions. *Nat. biotechnol.* 38, 685–688. doi: 10.1038/s41587-020-0548-6

Eslam, M., Newsome, P. N., Sarin, S. K., Anstee, Q. M., Targher, G., Romero-Gomez, M., et al. (2020). A new definition for metabolic dysfunction-associated fatty liver disease: an international expert consensus statement. *J. Hepatol.* 73, 202–209. doi: 10.1016/j.jhep.2020.03.039

Fan, Y., and Pedersen, O. (2021). Gut microbiota in human metabolic health and disease. *Nat. Rev. Microbiol.* 19, 55–71. doi: 10.1038/s41579-020-0433-9

Ferreira, Y. A. M., Jamar, G., Estadella, D., and Pisani, L. P. (2023). Proanthocyanidins in grape seeds and their role in gut microbiota-white adipose tissue axis. *Food Chem.* 404:134405. doi: 10.1016/j.foodchem.2022.134405

Fryk, E., Olausson, J., Mossberg, K., Strindberg, L., Schmelz, M., Brogren, H., et al. (2021). Hyperinsulinemia and insulin resistance in the obese may develop as part of a homeostatic response to elevated free fatty acids: a mechanistic case-control and a population-based cohort study. *Ebiomedicine* 65:103264. doi: 10.1016/j.ebiom.2021.103264

Fu, X., Liu, Z., Zhu, C., Mou, H., and Kong, Q. (2019). Nondigestible carbohydrates, butyrate, and butyrate-producing bacteria. *Crit. Rev. Food Sci. Nutr.* 59, S130–S152. doi: 10.1080/10408398.2018.1542587

Ghorbani, A. (2017). Mechanisms of antidiabetic effects of flavonoid rutin. *Biomed. Pharmacother.* 96, 305–312. doi: 10.1016/j.biopha.2017.10.001

Gonzalez-Abuin, N., Pinent, M., Casanova-Marti, A., Arola, L., Blay, M., Ardevol, A., et al. (2015). Procyanidins and their healthy protective effects against type 2 diabetes. *Curr. Med. Chem.* 22, 39–50. doi: 10.2174/0929867321666140916115519

Gu, L., Kelm, M. A., Hammerstone, J. F., Beecher, G., Holden, J., Haytowitz, D., et al. (2004). Concentrations of proanthocyanidins in common foods and estimations of normal consumption. *J. Nutr.* 134, 613–617. doi: 10.1093/jn/134.3.613

Gui, H., Sun, L., Liu, R., Si, X., Li, D., Wang, Y., et al. (2023). Current knowledge of anthocyanin metabolism in the digestive tract: absorption, distribution, degradation, and interconversion. *Crit. Rev. Food Sci. Nutr.* 63, 5953–5966. doi: 10.1080/10408398.2022.2026291

Gullón, B., Lú-Chau, T. A., Moreira, M. T., Lema, J. M., and Eibes, G. (2017). Rutin: a review on extraction, identification and purification methods, biological activities and approaches to enhance its bioavailability. *Trends Food Sci. Tech* 67, 220–235. doi: 10.1016/j.tifs.2017.07.008

Hall, M., and Beiko, R. G. (2018). 16S rRNA gene analysis with QIIME2. *Methods Mol. Biol. (Clifton, N.J.)* 1849, 113–129. doi: 10.1007/978-1-4939-8728-3_8

Hameed, A., Galli, M., Adamska-Patruno, E., Krętowski, A., and Ciborowski, M. (2020). Select polyphenol-rich berry consumption to defer or deter diabetes and diabetes-related complications. *Nutrients* 12:2538. doi: 10.3390/nu12092538

Han, M., Huang, Y., Gui, H., Xiao, Y., He, M., Liu, J., et al. (2022). Dynamic changes in host immune system and gut microbiota are associated with the production of SARS-CoV-2 antibodies. *Gut* 72, 1996–1999. doi: 10.1136/gutjnl-2022-327561

Hopkins, B. D., Goncalves, M. D., and Cantley, L. C. (2016). Obesity and cancer mechanisms: cancer metabolism. *J. Clin. Oncol.* 34, 4277–4283. doi: 10.1200/jco.2016.67.9712

Hosomi, K., Saito, M., Park, J., Murakami, H., Shibata, N., Ando, M., et al. (2022). Oral administration of Blautia wexlerae ameliorates obesity and type 2 diabetes via metabolic remodeling of the gut microbiota. *Nat. Commun.* 13:4477. doi: 10.1038/s41467-022-32015-7

Jeyaraman, M. M., Al-Yousif, N. S. H., Singh Mann, A., Dolinsky, V. W., Rabbani, R., Zarychanski, R., et al. (2020). Resveratrol for adults with type 2 diabetes mellitus. *Cochr. Datab. Syst. Rev.* 1:Cd011919. doi: 10.1002/14651858.CD011919.pub2

Jiao, W., Sang, Y., Wang, X., and Wang, S. (2023). Metabonomics and the gut microbiome analysis of the effect of 6-shogaol on improving obesity. *Food Chem.* 404:134734. doi: 10.1016/j.foodchem.2022.134734

Kamalakkannan, N., and Prince, P. S. (2006). Antihyperglycaemic and antioxidant effect of rutin, a polyphenolic flavonoid, in streptozotocin-induced diabetic wistar rats. *Basic Clin. Pharmacol. Toxicol.* 98, 97–103. doi: 10.1111/j.1742-7843.2006.pto_241.x

Kawano, Y., Edwards, M., Huang, Y., Bilate, A. M., Araujo, L. P., Tanoue, T., et al. (2022). Microbiota imbalance induced by dietary sugar disrupts immune-mediated protection from metabolic syndrome. *Cell* 185, 3501.e–3519.e. doi: 10.1016/j.cell.2022.08.005

Kim, W. K., Min, S. G., Kwon, H., Park, S., Jo, M. J., Ko, G., et al. (2023). Lactobacillus rhamnosus KBL2290 ameliorates gut inflammation in a mouse model of dextran sulfate sodium-induced colitis. *J. Microbiol. (Seoul, Korea)* 61, 673–682. doi: 10.1007/s12275-023-00061-5

Kim, Y. A., Keogh, J. B., and Clifton, P. M. (2018). Probiotics, prebiotics, synbiotics and insulin sensitivity. *Nutr. Res. Rev.* 31, 35–51. doi: 10.1017/s095442241700018x

Kong, C., Gao, R., Yan, X., Huang, L., and Qin, H. (2019). Probiotics improve gut microbiota dysbiosis in obese mice fed a high-fat or high-sucrose diet. *Nutrition* 60, 175–184. doi: 10.1016/j.nut.2018.10.002

Ley, R. E., Turnbaugh, P. J., Klein, S., and Gordon, J. I. (2006). Microbial ecology: human gut microbes associated with obesity. *Nature* 444, 1022–1023. doi: 10.1038/4441022a

Lin, R., Sun, Y., Mu, P., Zheng, T., Mu, H., Deng, F., et al. (2020). Lactobacillus rhamnosus GG supplementation modulates the gut microbiota to promote butyrate production, protecting against deoxynivalenol exposure in nude mice. *Biochem. Pharmacol.* 175:113868. doi: 10.1016/j.bcp.2020.113868

Liu, C. S., Liang, X., Wei, X. H., Jin, Z., Chen, F. L., Tang, Q. F., et al. (2019). Gegen Qinlian decoction treats diarrhea in piglets by modulating gut microbiota and short-chain fatty acids. *Front. Microbiol.* 10:825. doi: 10.3389/fmicb.2019.00825

Liu, M., Huang, B., Wang, L., Lu, Q., and Liu, R. (2022). Peanut skin procyanidins ameliorate insulin resistance via modulation of gut microbiota and gut barrier in type 2 diabetic mice. *J.Sci. Food Agric.* 102, 5935–5947. doi: 10.1002/jsfa.11945

Liu, Q., Pan, R., Ding, L., Zhang, F., Hu, L., Ding, B., et al. (2017). Rutin exhibits hepatoprotective effects in a mouse model of non-alcoholic fatty liver disease by reducing hepatic lipid levels and mitigating lipid-induced oxidative injuries. *Int. Immunopharmacol.* 49, 132–141. doi: 10.1016/j.intimp.2017.05.026

Liu, W., Zhao, S., Wang, J., Shi, J., Sun, Y., Wang, W., et al. (2017). Grape seed proanthocyanidin extract ameliorates inflammation and adiposity by modulating gut microbiota in high-fat diet mice. *Mol. Nutr. Food Res.* 61, doi: 10.1002/mnfr.201601082

Mathrani, A., Yip, W., Sequeira-Bisson, I. R., Barnett, D., Stevenson, O., Taylor, M. W., et al. (2023). Effect of a 12-week polyphenol rutin intervention on markers of pancreatic β-cell function and gut microbiota in adults with overweight without diabetes. *Nutrients* 15:3360. doi: 10.3390/nu15153360

Ogurtsova, K., da Rocha Fernandes, J. D., Huang, Y., Linnenkamp, U., Guariguata, L., Cho, N. H., et al. (2017). IDF diabetes atlas: global estimates for the prevalence of diabetes for 2015 and 2040. *Diabetes Res. Clin. Pract.* 128, 40–50. doi: 10.1016/j.diabres.2017.03.024

Ola, M. S., Ahmed, M. M., Ahmad, R., Abuohashish, H. M., Al-Rejaie, S. S., Alhomida, A. S., et al. (2015). Neuroprotective effects of rutin in streptozotocin-induced diabetic rat retina. *J. Mol. Neurosci.* 56, 440–448. doi: 10.1007/s12031-015-0561-2

Pammi, M., Cope, J., Tarr, P. I., Warner, B. B., Morrow, A. L., Mai, V., et al. (2017). Intestinal dysbiosis in preterm infants preceding necrotizing enterocolitis: a systematic review and meta-analysis. *Microbiome* 5:31. doi: 10.1186/s40168-017-0248-8

Pang, X. X., Bai, Q., Wu, F., Chen, G. J., Zhang, A. H., Tang, C. S., et al. (2016). Urotensin II induces ER stress and EMT and increase extracellular matrix production in renal tubular epithelial cell in early diabetic mice. *Kidney Blood Pressure Res.* 41, 434–449. doi: 10.1159/000443445

Prevel, R., Enaud, R., Orieux, A., Camino, A., Berger, P., Boyer, A., et al. (2022). Gut bacteriobiota and mycobiota are both associated with Day-28 mortality among critically ill patients. *Crit. Care* 26:105. doi: 10.1186/s13054-022-03980-8

Prior, R. L., and Gu, L. (2005). Occurrence and biological significance of proanthocyanidins in the American diet. *Phytochemistry* 66, 2264–2280. doi: 10.1016/j.phytochem.2005.03.025

Redondo-Castillejo, R., Garcimartín, A., Hernández-Martín, M., López-Oliva, M. E., Bocanegra, A., Macho-González, A., et al. (2023). Proanthocyanidins: impact on gut microbiota and intestinal action mechanisms in the prevention and treatment of metabolic syndrome. *Int. J. Mol. Sci.* 24:5369. doi: 10.3390/ijms24065369

Salvadó, M. J., Casanova, E., Fernández-Iglesias, A., Arola, L., and Bladé, C. (2015). Roles of proanthocyanidin rich extracts in obesity. *Food Funct.* 6, 1053–1071. doi: 10.1039/c4fo01035c

Segata, N., Izard, J., Waldron, L., Gevers, D., Miropolsky, L., Garrett, W. S., et al. (2011). Metagenomic biomarker discovery and explanation. *Genome Biol.* 12:R60. doi: 10.1186/gb-2011-12-6-r60

Sonnenburg, J. L., and Bäckhed, F. (2016). Diet-microbiota interactions as moderators of human metabolism. *Nature* 535, 56–64. doi: 10.1038/nature18846

Stojanov, S., Berlec, A., and Štrukelj, B. (2020). The influence of probiotics on the firmicutes/bacteroidetes ratio in the treatment of obesity and inflammatory bowel disease. *Microorganisms* 8:1715. doi: 10.3390/microorganisms8111715

Tomás-Barberán, F. A., Selma, M. V., and Espín, J. C. (2016). Interactions of gut microbiota with dietary polyphenols and consequences to human health. *Curr. Opin. Clin. Nutr. Metab. Care* 19, 471–476. doi: 10.1097/mco.0000000000000314

Tung, Y. T., Zeng, J. L., Ho, S. T., Xu, J. W., Li, S., Wu, J. H., et al. (2021). Anti-NAFLD effect of Djulis hull and its major compound, rutin, in mice with High-Fat Diet (HFD)-induced obesity. *Antioxidants (Basel)* 10:1694. doi: 10.3390/antiox10111694

Valentová, K., Vrba, J., Bancířová, M., Ulrichová, J., and Křen, V. (2014). Isoquercitrin: pharmacology, toxicology, and metabolism. *Food Chem. Toxicol.* 68, 267–282. doi: 10.1016/j.fct.2014.03.018

Wang, Q., Zhang, Y., Lu, R., Zhao, Q., and Gao, Y. (2024). The multiple mechanisms and therapeutic significance of rutin in metabolic dysfunction-associated

fatty liver disease (MAFLD). *Fitoterapia* 178:106178. doi: 10.1016/j.fitote.2024.106178

Wen, J. J., Li, M. Z., Chen, C. H., Hong, T., Yang, J. R., Huang, X. J., et al. (2023). Tea polyphenol and epigallocatechin gallate ameliorate hyperlipidemia via regulating liver metabolism and remodeling gut microbiota. *Food Chem.* 404:134591. doi: 10.1016/j.foodchem.2022.134591

World Health Organization. (2021). *Obesity and Overweight*. Geneva: World Health Organization.

Yang, G., Wei, J., Liu, P., Zhang, Q., Tian, Y., Hou, G., et al. (2021). Role of the gut microbiota in type 2 diabetes and related diseases. *Metabolism* 117:154712. doi: 10.1016/j.metabol.2021.154712

Yao, M. J., Teng, H., Lv, Q., Gao, H., Guo, T., Lin, Y., et al. (2021). Anti-hyperglycemic effects of dihydromyricetin in streptozotocin-induced diabetic rats. *Food Sci. Hum. Well* 10, 155–162. doi: 10.1016/j.fshw.2021.02.004

Yeh, C. H., Yang, J. J., Yang, M. L., Li, Y. C., and Kuan, Y. H. (2014). Rutin decreases lipopolysaccharide-induced acute lung injury via inhibition of oxidative stress and the MAPK-NF-κB pathway. *Free Radic. Biol. Med.* 69, 249–257. doi: 10.1016/j.freeradbiomed.2014.01.028

Yoo, J. Y., and Kim, S. S. (2016). Probiotics and prebiotics: present status and future perspectives on metabolic disorders. *Nutrients* 8:173. doi: 10.3390/nu8030173

Yu, J., Dong, R., Da, J., Li, J., Yu, F., Zha, Y., et al. (2019). High-mobility group nucleosome-binding protein 1 mediates renal fibrosis correlating with macrophages accumulation and epithelial-to-mesenchymal transition in diabetic nephropathy mice model. *Kidney Blood Pressure Res.* 44, 331–343. doi: 10.1159/000499877

Yuan, X., Wei, G., You, Y., Huang, Y., Lee, H. J., Dong, M., et al. (2017). Rutin ameliorates obesity through brown fat activation. *FASEB J.* 31, 333–345. doi: 10.1096/fj.201600459RR

Yusuf, S., Hawken, S., Ounpuu, S., Bautista, L., Franzosi, M. G., Commerford, P., et al. (2005). Obesity and the risk of myocardial infarction in 27,000 participants from 52 countries: a case-control study. *Lancet* 366, 1640–1649. doi: 10.1016/s0140-6736(05)67663-5

Zeng, Y. X., Wang, S., Wei, L., Cui, Y. Y., and Chen, Y. H. (2020). Proanthocyanidins: components, pharmacokinetics and biomedical properties. *Am. J. Chin. Med.* 48, 813–869. doi: 10.1142/s0192415x2050041x

Zhang, C., Ma, S., Wu, J., Luo, L., Qiao, S., Li, R., et al. (2020). A specific gut microbiota and metabolomic profiles shifts related to antidiabetic action: the similar and complementary antidiabetic properties of type 3 resistant starch from Canna edulis and metformin. *Pharmacol. Res.* 159:104985. doi: 10.1016/j.phrs.2020.104985

Zhang, J., Ni, Y., Qian, L., Fang, Q., Zheng, T., Zhang, M., et al. (2021). Decreased abundance of akkermansia muciniphila leads to the impairment of insulin secretion and glucose homeostasis in lean type 2 diabetes. *Adv. Sci.* 8:e2100536. doi: 10.1002/advs.202100536

Zhao, Z., Chen, Y., Li, X., Zhu, L., Wang, X., Li, L., et al. (2022). Myricetin relieves the symptoms of type 2 diabetes mice and regulates intestinal microflora. *Biomed. Pharmacother.* 153:113530. doi: 10.1016/j.biopha.2022.113530

frontiers | Frontiers in Microbiomes

TYPE Original Research
PUBLISHED 21 January 2025
DOI 10.3389/frmbi.2024.1474497

Check for updates

OPEN ACCESS

EDITED BY
Junling Shi,
Northwestern Polytechnical University, China

REVIEWED BY
Smith Etareri Evivie,
University of Benin, Nigeria
Fariborz Soheili,
University of Ottawa Heart Institute, Canada

*CORRESPONDENCE
Monica Rosaria Molotzu
monica.molotzu@izs-sardegna.it
Antonella Canu
antonella.canu@izs-sardegna.it

†These authors have contributed equally to this work

RECEIVED 01 August 2024
ACCEPTED 09 December 2024
PUBLISHED 21 January 2025

CITATION
Molotzu MR, Cabras PA, Di Marcantonio L, Atzeni R, Macciotta NPP and Canu A (2025) Metagenomic analysis of goat feces from Ogliastra (Sardinia, Italy).
Front. Microbiomes 3:1474497.
doi: 10.3389/frmbi.2024.1474497

COPYRIGHT
© 2025 Molotzu, Cabras, Di Marcantonio, Atzeni, Macciotta and Canu. This is an open-access article distributed under the terms of the Creative Commons Attribution License (CC BY). The use, distribution or reproduction in other forums is permitted, provided the original author(s) and the copyright owner(s) are credited and that the original publication in this journal is cited, in accordance with accepted academic practice. No use, distribution or reproduction is permitted which does not comply with these terms.

Metagenomic analysis of goat feces from Ogliastra (Sardinia, Italy)

Monica Rosaria Molotzu [1*†], Piera Angela Cabras [2], Lisa Di Marcantonio [3], Rossano Atzeni [4], Nicolò Pietro Paolo Macciotta [5] and Antonella Canu [1*†]

[1]Struttura Complessa Controllo Microbiologico e Ispezione Alimenti, Istituto Zooprofilattico Sperimentale della Sardegna "G. Pegreffi", Sassari, Italy, [2]Nuoro Complex Structure-Tortolì Territorial Center, Istituto Zooprofilattico Sperimentale della Sardegna "G. Pegreffi", Tortolì, Italy, [3]Struttura Complessa Batteriologia e Sviluppo Antigeni Batterici, Istituto Zooprofilattico Sperimentale dell'Abruzzo e del Molise "G. Caporale", Teramo, Italy, [4]Dipartimento Quantum e Calcolo ad Alte Prestazioni, Bioscienze e Studi Superiori, Centro di Ricerca CRS4 Sardegna, Pula, Cagliari, Italy, [5]Dipartimento di Agraria, Università degli Studi di Sassari, Sassari, Italy

With its constitutive and functional characteristics, the intestinal microbiota plays a crucial role in the health condition of the animals. Variations in the composition and gene expression of the intestinal microbiota are associated with the risk of the onset of various pathologies of the gastrointestinal tract and chronic inflammatory intestinal diseases. The objectives of this study were to evaluate the variability in the composition of the intestinal microbiota of goats of different breeds (Sarda, Maltese, and Alpine) farmed in different flocks of the region of Ogliastra (Sardegna, Italy) and to assess whether the type of feeding (natural pasture grazing-based versus intensive) could affect the intestinal bacterial composition. We also evaluated possible differences in the composition of the intestinal microbiota between healthy and Caprine arthritis encephalitis (CAE)-affected goats. The economic damage caused by this pathology is due to the reduction in milk production, with infected animals having greater susceptibility to contract diseases. The results of our study highlighted a statistically significant difference (P = 0.001–0.005) in the intestinal bacterial composition between the intensively managed flock and the other natural pasture-based flock.g In particular, a significantly greater abundance of *Acidoaminococcaceae* in the intensive flock was obgserved. Furthermore, a significantly greater abundance of *Prevotellaceae* was found in two localities in which, out of a total of 29 animals, only four tested negative for CAE. From these data, we deduced that the presence of *Prevotellaceae* can be an indication of the disease. This difference could be attributed to the farming system, the Cardedu farm being the only intensive one, and to the geographical distance of this location from the other sampling sites. Therefore, the results of the present study suggest that extensive or intensive farm management may affect the intestinal microbiota of goats.

KEYWORDS

goats, CAE, metagenomic, galaxy, Ogliastra

1 Introduction

The microbiome describes a dynamic community of microorganisms that colonize organisms from birth onward. The microbiome can vary according to different factors such as host species, age, diet, health, reproductive status, and the external environment. Moreover, it is directly linked to the host's health status, including metabolism, immunity, and development (Feng et al., 2018). The fecal microbiome is modified in response to transient changes in the host, but the abundance of some major groups of microorganisms is relatively stable throughout the life of the host. Thus, relative proportions of these groups may act as a signature of health and wellbeing, which is known as the host environment (Muegge et al., 2012). In particular, the relative ratio between the two dominant phyla in mammalian fecal microbiomes, *Firmicutes* and *Bacteroidetes*, can be used to distinguish between carnivorous and herbivorous mammals, as each group is responsible for different metabolic demands (Kreisinger et al., 2018).

Monitoring the composition of the fecal microbiome throughout the life of animals can help assess their health status (Bahrndorff et al., 2016). For example, many domestic mammal species suffer from poor health, at least partially related to dysbiosis of the fecal microbiome and to a reduced microbial diversity (McKenzie et al., 2017).

Research on this topic has evolved rapidly thanks to new technologies using next-generation sequencing platforms, which have allowed the study of communities of microorganisms (metagenomics) (Satam et al., 2023). The gastrointestinal tract is a complex system that includes a fecal content characterized by more than 10^{12} bacteria per gram of feces, which is named the "microbiota" (Randeni et al., 2024). The genome of the intestinal microbiota is at least 100 times greater than that of the entire individual, and it is defined as the "microbiome." The term metagenomics refers to the application of modern gene sequencing techniques to the study of microbial communities directly in their natural environment, thus bypassing the need to isolate and cultivate them in the laboratory (Chaudhari et al., 2023; Nam et al., 2023). These techniques have allowed the reconstruction of a large number of metagenome-associated genomes (MAGs) in different animal organisms, including goats, cattle, pigs, sheep, rodents, and poultry, and the detection of associations with host health and some illnesses (Consiglio Superiore di Sanità – Sezione III, 2018).

The 16S ribosomal RNA is a sequence that is shared universally by all prokaryotes, and it has extremely conserved regions interspersed with highly variable regions V1–V9 characterized by variable length and degree of diversity (Bertolo et al., 2024; Hrovat et al., 2024). These can be amplified and sequenced thanks to the use of degenerate primers designed on their flanking regions. The sequencing of hypervariable regions of bacterial 16S rRNA allows for the so-called metataxonomy or *phylotyping* of the microbial community itself, with the identification and assignment of the relative distributions of the so-called "taxonomic operational units" (OTUs) at different phylogenetic levels and the estimation of their relative abundances (Willis et al., 2019).

Ruminants are herbivorous hoofed mammals with specialized anatomical and physiological adaptations that make them able to perform cellulolytic fermentation of plant materials with a high content of fiber fractions. The study of the fecal microbiome of ruminant species could provide useful tools for developing strategies aimed at improving the animal health status, enhancing the ability to adapt to environmental changes, and preventing disease and parasite epidemics (McKenzie et al., 2017). Caprine arthritis encephalitis (CAE) is an infectious disease first reported in 1974 caused by a virus from the retrovirus family (Crawford et al., 1980; Narayan et al., 1980). The economic consequences of CAE are manifold. Apart from the reduction of milk production, infected animals are more susceptible to several diseases. Such a higher vulnerability not only enhances the risk of secondary infections but also increases the need for veterinary interventions, leading to an increase in operational costs for farmers. Moreover, this affliction contributes to the reduction of the longevity of infected animals, diminishing their overall productive life and, therefore, further enhancing the negative economic impact. Addressing the multifaceted challenges posed by CAE-related viral encephalitis arthritis requires a comprehensive approach that considers both the immediate losses in milk production and the long-term consequences for the health and productivity of livestock (Peterhans et al., 2004; Le Jan et al., 2005).

The study focused on the metagenomic analysis of goat feces, mainly of the Sarda breed, from six locations considered representative of the Ogliastra region, an area of Sardinia where the breeding of the Sarda goat is widespread: Baunei, Cardedu, Perdasdefogu, Talana, Urzulei, and Villagrande.

The study was carried out in the municipalities of Ogliastra (central-eastern Sardinia), included in a blue zone (demographic and/or geographical areas of the world, identified by the scholar Prof. Gianni Pes in which a higher concentration of centenarians is recorded) (Pes and Pouland, 2014). Currently, purebred Sardinian goats are farmed mostly in marginal areas, and crossbreeding with selected breeds (e.g., Murciano-Granadina and Alpine) is a common practice for improving milk yield and slaughter weight of kids. This breed, present on the island since the Neolithic, is characterized by a relevant genetic heterogeneity due to selection performed by shepherds and crosses with other breeds. In particular, three subpopulations differing in size (large, medium, and small), somatic features, and production levels can be distinguished (Macciotta et al., 2002). The Sarda breed goat is well adapted to the harsh environment of some areas of Sardinia where, despite the very difficult farming conditions (Usai et al., 2004), it produces milk and meat of excellent quality.

The aim of the study was to evaluate the differences between the microbial communities present and how the intestinal bacterial composition could be differentiated according to geographical location, type of feeding management (pasture-based or intensive), and CAE status (positive or negative).

10.3389/frmbi.2024.1474497

2 Materials and methods

2.1 Sampling

The study area was the Ogliastra, in central-eastern Sardinia (Italy), with an extension of 1,855 km^2 and a population of approximately 58,000 inhabitants, distributed in 23 localities of particular naturalistic interest.

Sampling was carried out between 07 August 2019 and 24 June 2021 on 19 goat flocks distributed in six different localities, representative of the goat farming system of the considered area. (Details on the animals analyzed for each farm and the sampling areas are described in Table 1 and Figure 1).

In most of the farms, the animals were fed natural pastures, with concentrate supplementation during the manual milking or when animals were kept in the barn. An exception was the farm located in Cardedu, characterized by intensive management, with mechanical milking and the use of antibiotics and pesticides. Natural pastures were characterized by a high presence of Mediterranean scrub. Most represented plant species were *Erica*, *Arbutus unedo*, *Pistacia lentiscus*, *Myrtus communis*, *Allium subhirsutum*, *Ferula communis*, *Phillies angustifolia*, *Genista Corsica*, *Calycotome villosa*, *Olea europea*, *Pyrus amygdaliformis*, *Quercus ilex*, *Quercus suber*, *Rosmarinus officinalis*, and *Thymus capitatus*. *Cistus* species are chemically characterized by a high content of cellulose and xylan (Duarte et al., 2013).

TABLE 1 Sampling data.

Sampling data						
Sample	Sampling date	Locality	Sex	Age	Kind	CAE
1	29/03/2021	Baunei	Female	6	Sardinian	Negative
2	29/03/2021	Baunei	Female	3	Sardinian	Negative
3	29/03/2021	Baunei	Female	7	Sardinian	Negative
4	29/03/2021	Baunei	Female	3	Sardinian	Negative
6	29/03/2021	Baunei	Female	7	Sardinian	Positive
7	29/03/2021	Baunei	Male	3	Sardinian	Positive
8	18/03/2021	Baunei	Female	6	Sardinian	Negative
9	18/03/2021	Baunei	Female	5	Sardinian	Negative
10	18/03/2021	Baunei	Female	2	Sardinian	Positive
11	18/03/2021	Baunei	Female	4	Sardinian	Negative
12	18/03/2021	Baunei	Female	5	Sardinian	Positive
13	05/03/2021	Baunei	Female	5	Sardinian	Negative
14	05/03/2021	Baunei	Female	3	Sardinian	Negative
15	05/03/2021	Baunei	Female	6	Sardinian	Negative
16	05/03/2021	Baunei	Female	4	Sardinian	Negative
17	05/03/2021	Baunei	Female	3	Sardinian	Negative
19	05/03/2021	Baunei	Female	13	Sardinian	Positive
20	05/03/2021	Baunei	Female	12	Sardinian	Positive
21	05/03/2021	Baunei	Female	8	Sardinian	Positive
22	05/03/2021	Baunei	Female	3	Sardinian	Positive
24	16/03/2021	Talana	Female	3	Sardinian	Positive
25	16/03/2021	Talana	Female	4	Sardinian	Positive
26	16/03/2021	Talana	Female	3	Sardinian	Positive
27	16/03/2021	Talana	Female	6	Sardinian	Positive
28	16/03/2021	Talana	Female	5	Sardinian	Positive
29	16/03/2021	Talana	Female	6	Sardinian	Positive
30	16/03/2021	Talana	Female	6	Sardinian	Positive

(Continued)

10.3389/frmbi.2024.1474497

TABLE 1 Continued

Sampling data						
Sample	Sampling date	Locality	Sex	Age	Kind	CAE
31	16/03/2021	Talana	Female	5	Sardinian	Positive
32	16/03/2021	Talana	Female	6	Sardinian	Positive
33	16/03/2021	Talana	Female	5	Sardinian	Negative
34	25/03/2021	Urzulei	Female	6	Sardinian	Positive
35	25/03/2021	Urzulei	Female	3	Sardinian	Positive
36	25/03/2021	Urzulei	Female	3	Sardinian	Positive
37	25/03/2021	Urzulei	Female	4	Sardinian	Positive
38	25/03/2021	Urzulei	Female	3	Sardinian	Positive
39	25/03/2021	Urzulei	Female	1	Sardinian	Positive
40	25/03/2021	Urzulei	Female	5	Sardinian	Positive
41	25/03/2021	Urzulei	Female	3	Sardinian	Positive
42	25/03/2021	Urzulei	Female	6	Sardinian	Positive
43	31/03/2021	Urzulei	Female	2	Sardinian	Positive
44	31/03/2021	Urzulei	Female	8	Sardinian	Positive
45	31/03/2021	Urzulei	Female	4	Sardinian	Positive
46	31/03/2021	Urzulei	Female	2	Sardinian	Positive
47	31/03/2021	Urzulei	Female	5	Sardinian	Negative
48	07/04/2021	Urzulei	Female	3	Sardinian	Positive
49	07/04/2021	Urzulei	Female	5	Sardinian	Positive
50	07/04/2021	Urzulei	Female	7	Sardinian	Positive
51	07/04/2021	Urzulei	Female	3	Sardinian	Positive
52	07/04/2021	Urzulei	Female	3	Sardinian	Negative
53	07/04/2021	Urzulei	Female	5	Sardinian-Samen	Positive
54	01/03/2021	Villagrande	Female	7	Sardinian	Positive
55	01/03/2021	Villagrande	Female	6	Sardinian	Negative
56	01/03/2021	Villagrande	Female	4	Sardinian	Positive
57	01/03/2021	Villagrande	Female	6	Sardinian	Positive
58	01/03/2021	Villagrande	Female	3	Sardinian	Negative
59	01/03/2021	Villagrande	Female	16	Sardinian	Positive
60	12/03/2021	Villagrande	Female	4	Sardinian	Negative
61	12/03/2021	Villagrande	Female	5	Sardinian	Positive
62	12/03/2021	Villagrande	Female	7	Sardinian	Positive
63	12/03/2021	Villagrande	Female	3	Sardinian	Positive
3	12/03/2021	Villagrande	Female	5	Sardinian	Positive
66	12/03/2021	Villagrande	Female	N.D	Sardinian	Positive
67	12/03/2021	Villagrande	Female	N.D	Sardinian	Positive
68	12/03/2021	Villagrande	Female	N.D	Sardinian	Positive
69	12/03/2021	Villagrande	Female	2	Sardinian	Positive

(Continued)

TABLE 1 Continued

Sampling data						
Sample	Sampling date	Locality	Sex	Age	Kind	CAE
70	12/03/2021	Villagrande	Female	4	Sardinian	Positive
71	24/03/2021	Cardedu	Female	4	Alpine	Positive
72	24/03/2021	Cardedu	Female	5	Maltese-Suede	Positive
73	24/03/2021	Cardedu	Female	6	Maltese	Positive
74	24/03/2021	Cardedu	Female	2	Saanen-Suede	Positive
75	24/03/2021	Cardedu	Female	3	Maltese-Saanen	Positive
76	09/04/2021	Talana	Female	5	Sardinian	Positive
77	09/04/2021	Talana	Female	1	Sardinian	Negative
78	09/04/2021	Talana	Female	2	Sardinian	Positive
79	09/04/2021	Talana	Female	7	Sardinian	Positive
80	09/04/2021	Talana	Female	2	Sardinian	Negative
81	14/04/2021	Perdasdefogu	Female	4	Sardinian	Positive
82	14/04/2021	Perdasdefogu	Female	5	Sardinian	Positive
83	14/04/2021	Perdasdefogu	Female	3	Sardinian	Positive
84	14/04/2021	Perdasdefogu	Female	5	Sardinian	Positive
85	14/04/2021	Perdasdefogu	Female	4	Sardinian	Negative
86	14/04/2021	Perdasdefogu	Female	5	Sardinian	Positive
98	05/11/2019	Arzana	Female	3	Sardinian	Positive
99	24/06/2021	Baunei	Female	8	Sardinian cross	Negative
100	24/06/2021	Baunei	Female	3	Sardinian	Negative
101	24/06/2021	Baunei	Female	4	Sardinian	Negative
102	24/06/2021	Baunei	Female	8	Sardinian	Negative
103	24/06/2021	Baunei	Female	5	Sardinian	Negative

Individual blood samples were collected using two vacutainer tubes. Stool samples were taken from the rectal ampoule of each animal. The samples were transported to the lab at a controlled temperature of 4°C.

2.2 CAE detection

The detection of the CAE virus was performed in serum samples using indirect ELISA with specific anti-small ruminant lentivirus (SRLV) antibodies. SRLVs are a group of genetically and antigenically heterogeneous RNA viruses belonging to the *Retroviridae* family and the *Lentivirus* genus. The viruses responsible for ovine Maedi-visna (MVV) and CAE, respectively, are grouped under the denomination of SRLVs (WOAH, 2021).

2.3 Processing, extraction, and library preparation for metagenomics

Metagenomic analysis was performed on the feces of 87 dairy goats (Supplementary Material 1) frozen at −80°C after collection. After thawing, 300 mg of feces was weighed, and 800 µL of NucliSENS Lysis Buffer from bioMérieux (Florence, Italy) (Bartels et al., 2003; Loens et al., 2003; Van Deursen et al., 2003) was added. The tubes were incubated at 90°C for 10 min with shaking at 1,400 rpm. Samples were centrifuged at 12,000 rpm for 4 min, and 500 µL of supernatant was then taken and subjected to nucleic acid extraction following the instructions provided by the manufacturing company bioMerièux. The DNA concentration of the samples was measured by a "Qubit® 3.0 Fluorometer" using the "High sensitivity assay kit Qubit® dsDNA" kit (Invitrogen, Carlsbad, CA, USA) (Qubit™ 4 Fluorometer Catalog Number Q33226 Publication Number MAN0017209 Revision D.0,

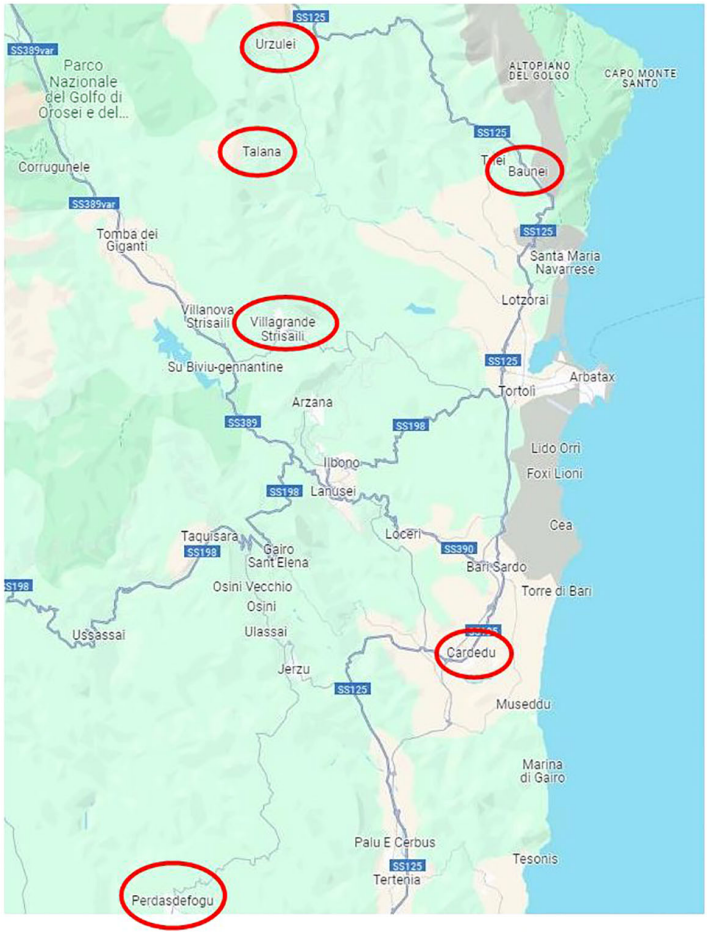

FIGURE 1
Sampling map.

Invitrogen). We performed several experiments starting from 100 mg of feces and 500 µL of lysis buffer up to 300 mg of feces, 800 µL of lysis buffer, and 100 µL of silica. This preparation allowed us to reach 3 ng/µL, necessary for metagenomic sequencing as required by the library preparation manual.

A concentration of 3 ng/µL genomic DNA (gDNA) was used for the amplification of the specific DNA region of the extracted samples, using the ranges V 2-4-8 and V 3-6-7 as primer sets –9 of the hypervariable region of the ribosomal 16S. The preparation of the libraries was carried out using the instructions of the manufacturer Thermo Fisher Scientific (Waltham, Massachusetts, USA) and the following kits: Ion 16S Metagenomics Kit, Ion Plus Fragment Library Kit, Agencourt™ AMPure, 70% ethanol, and a high-sensitivity assay kit (Qubit® dsDNA) (Ion 16S™ Metagenomics Kit Catalog Number A26216 Publication Number MAN0010799 Revision C.0, Thermofisher).

2.4 Metagenomic sequencing

Six chips of Ion Chip 318 v2 prepared with the Ion Chef™ Instrument were used. Sequencing was performed with the Ion Personal Genome Machine (PGM) (Ion Chef™ Instrument user guide Maintenance, calibration, and troubleshooting Catalog Number 4484177 Publication number MAN0018668 Revision A.0, Thermofisher; Ion Personal Genome Machine™ (PGM™) System reference guide Catalog Number 4462921, Publication number MAN0009783 Revision A.0, Thermofisher).

2.5 Bioinformatic and statistical analysis

The data analysis was performed using different platforms as described below.

Ion Reporter v. 5.20.2.0 was used in the data analysis. The QIIME2 software suite v2021.4.0 was used to analyze the amplicon data of the 16S rRNA gene. A "manifest file" was created using the "Fastq manifest" command to import the raw FASTQ data. The DADA2 pipeline was used to denoise the sequences and remove chimeric sequences. The Silva database (arb-silva.de) was used to BLAST search the obtained sequences and determine the phylogeny of the OTUs. The naive Bayes classifier trained on the SILVA 99% consensus taxonomy was employed to assign taxonomy into OTUs, which can be accessed at https://data.qiime2.org/2021.4/common/silva-138-99-nb-classifier.qza. To evaluate the completeness of the microbial communities, we conducted a rarefaction analysis using

10.3389/frmbi.2024.1474497

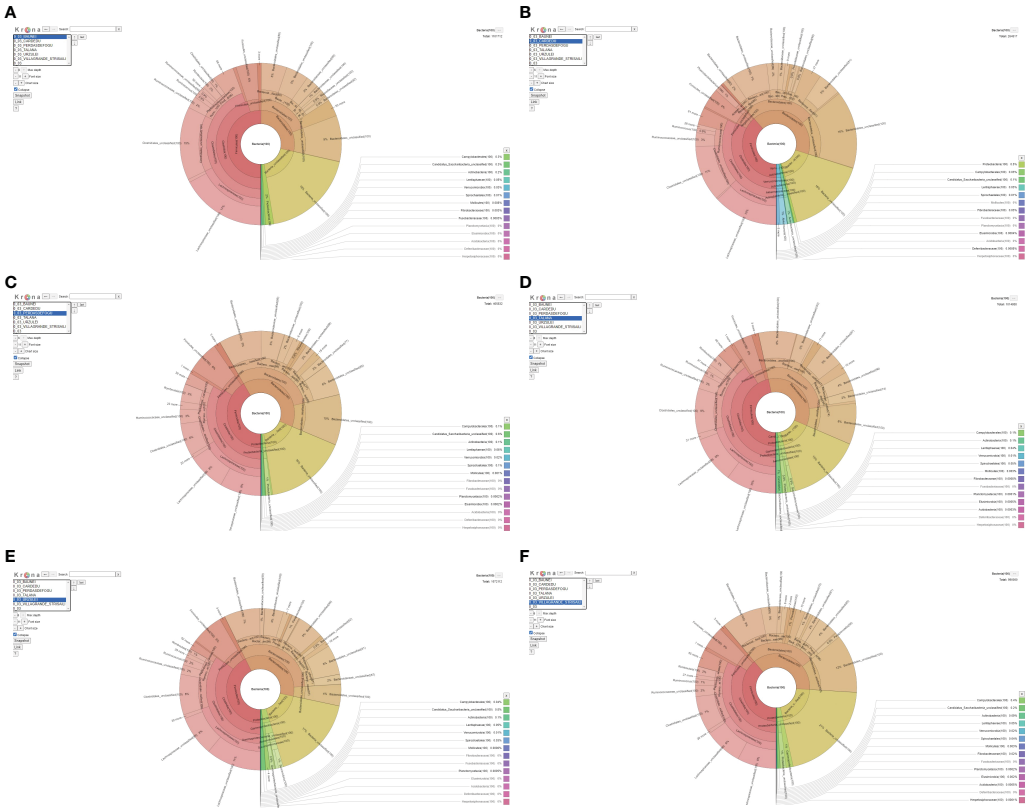

FIGURE 2
(A–F) Krona.

Faith's PD, Shannon, and observed OTU indices. The alpha diversity indices (observed OTU and Chao1) were computed, and the beta diversity metrics with unweighted UniFrac distances were calculated (Pielou, 1966).

We utilized the Emperor tool to generate Emperor plots for unweighted UniFrac distance and explored the principal coordinate (PCoA) plots in the context of the sample metadata (Vázquez-Baeza et al., 2013).

To calculate the group significance between the alpha and beta diversity indices, we used the Kruskal–Wallis (pairwise) test for the beta-group significance command. Furthermore, the beta-group significance command in the diversity plugin was utilized to test the distances between samples within a group. Finally, the statistical analysis was conducted using PERMANOVA with 999 permutations (Anderson, 2001).

In our study, we employed Mothur version 1.39.5, which was integrated into the Galaxy version 22.05 platform (Schloss et al., 2009; Schloss, 2020; The Galaxy Community, 2022). Following Mothur's recommended guidelines, we adopted the "Chappid" pipeline (Chappidi et al., 2019) to structure our metagenomic analysis with established best practices.

First, we organized FASTQ files by geographic origin in a Galaxy workspace. Quality control involved FastQC (version 0.11.9) (https://www.bioinformatics.babraham.ac.uk/projects/fastqc/), followed by

TABLE 2 Phylum percentages obtained from the Krona graph.

Phylum percentages obtained from the Krona graph						
	Baunei	Cardedu	Perdasdefogu	Talana	Urzulei	Villagrande Strisaili
Firmicutes	50	36	42	47	43	39
Bacteroidetes	28	41	40	35	36	37
Proteobacteria	2	0.50	1	3	4	3
Actinobacteria	0.20	1	0.1	0.1	0.1	0.09
Verrucomicrobia	0.03	2	0.02	0.1	0.01	0.02

10.3389/frmbi.2024.1474497

TABLE 3 Percentage of bacterial families divided by locality.

	Percentage of bacterial families divided by locality														
	Gracilibacteraceae	*Erysipelotrichaceae*	*Clostridiales Family XI. Incertae Sedis*	*Christensenellaceae*	*Acidaminococcaceae*	*Peptostreptococcaceae*	*Clostridiaceae*	*Porphyromonadaceae*	*Prevotellaceae*	*Flavobacteriaceae*	*Eubacteriaceae*	*Ruminococcaceae*	*Lachnospiraceae*	*Rikenellaceae*	*Synergistaceae*	*Bacteroidaceae*
Baunei	41.05	27.47	30.70	42.26	31.31	33.13	33.95	27.98	27.39	23.84	27.57	32.78	31.92	29.87	39.26	29.28
Cardedu	31.19	25.27	19.01	19.31	112.07	5.44	25.63	60.69	32.78	60.00	33.14	23.28	20.04	23.83	22.86	35.26
Perdasdefogu	18.38	78.18	27.12	8.64	28.99	80.00	27.04	28.27	49.92	51.30	43.91	31.44	37.51	53.00	12.16	65.90
Talana	23.63	61.65	34.06	15.69	39.28	70.66	37.43	14.62	24.99	39.21	48.41	36.27	42.37	21.65	18.11	60.60
Urzulei	12.47	78.44	23.28	8.55	38.37	22.00	24.22	21.19	29.01	27.92	30.42	27.99	33.22	19.88	12.00	57.50
Villagrande	17.90	45.06	38.60	15.47	37.38	33.74	32.11	44.03	45.22	52.31	44.86	34.43	36.15	40.26	21.48	41.45
Total	426993.17	912717.22	193546.29	65498?.33	188681.25	345908.74	313187?.20	396834.62	1243367.90	838260.23	1770284.92	2622805.10	1959362.02	436662.14	94912.87	401861?.04

TrimGalore (version 0.6.7) (https://github.com/FelixKrueger/TrimGalore.com/fenderglass/Flye) for removing low-quality reads and adapters (using default parameters with a quality threshold of 20; QPhred).

For multisample analysis, we created a group file in FASTA format using Mothur's Make.group. Removal of duplicate sequences was done with Mothur's unique.seqs. Abundance tables for taxonomic classification and OTUs were generated using count.seqs (Schloss, 2013).

The data quality was assessed using summary.seqs, revealing sequences predominantly within the 125 to 290 base range. Subsequent data cleaning steps included screen.seqs for the systematic removal of low-quality reads and sequences.

After aligning with the Silva database (Quast et al., 2012), we observed most sequences between positions 6,212 and 13,871. To ensure complete overlap, we employed screen.seqs, filter.seqs, unique.seqs, and pre.cluster.

Chimera identification was performed with chimera.vsearch, and removal utilized remove.seqs. Taxonomic assignments via classify.seqs utilized the RDP reference taxonomy (Cole et al., 2013). Lineages were removed using remove.lineage for specific groups.

Cluster.split at the order level, Make.shared, and classify.otu provided OTU information (Wooley et al., 2010).

Krona was visualized by converting the Mothur taxonomy to Krona format and using the Krona pie charts and plots per sample (Ondov et al., 2011).

Normalization involved counting sequences per sample and subsampling using subsamples. Alpha diversity estimation was performed using rarefaction curves generated by Rarefaction.single and visualized with Galaxy's plotting tool. A comprehensive summary report was produced by Summary.single, including metrics such as observed richness, coverage, the inverse Simpson index, and the total number of sequences.

For beta diversity, the thetaYC and Jaccard indices were calculated using Dist.shared, with visualization through Heatmap.sim. Venn diagrams and dendrograms were generated using the Venn and Tree.shared tools (Cuccuru et al., 2014) (Supplementary Material 1).

3 Results

Six runs were carried out with Ion PGM, which generated 20,590,826 reads with an average of 225,670 reads per sample.

We used the V2-4-8 and V3-6-7 regions because they were included in the sequencing kit. Initially, we analyzed the V4 region alone, which is widely used in the literature, but found the data to be less informative compared to the combined analysis of all regions. The quality of the sequences, assessed using the summary.seqs command, confirmed that most reads fell within the range of 125–290 bases. This multiregion approach enhanced taxonomic resolution and community representativeness, justifying its use despite being less conventional.

The microbiota of goat feces was mainly composed of the phyla *Firmicutes* and *Bacteroidetes*. In all the farms, except the one in

10.3389/frmbi.2024.1474497

TABLE 4 Percentage of bacterial genus divided by locality.

Percentage of bacterial genus divided by locality				
	Ruminococcus	*Eubacterium*	*Roseburia*	*Clostridium*
Baunei	20.82	14.14	15.95	13.61
Cardedu	18.61	11.13	9.38	9.97
Perdasdefogu	31.55	16.07	10.80	12.97
Talana	43.55	13.95	21.95	20.58
Urzulei	28.83	11.12	12.80	11.71
Villagrande	35.82	19.45	13.17	17.56

TABLE 5 Percentage of bacterial species divided by locality.

Percentage of bacterial species divided by locality						
	Ruminococcus_sp.	*Ruminococcus_gauvreauii*	*Roseburia_faecis*	*Eubacterium_hallii*	*Clostridium_lavalense*	*Ruminococcus_faecis*
Baunei	9.65	13.94	18.64	18.01	13.74	15.65
Cardedu	9.37	7.08	14.59	19.02	3.26	8.69
Perdasdefogu	36.93	17.83	13.75	20.61	26.63	11.03
Talana	23.15	29.57	26.07	14.55	25.59	20.74
Urzulei	9.58	13.06	15.45	13.02	16.57	26.92
Villagrande	11.33	18.51	11.50	14.80	14.22	16.96

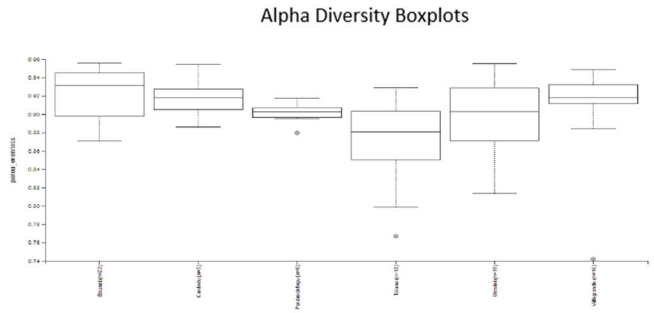

Kruskal-Wallis (all groups)

	Hsmlt
H	17.12493591715861
p-value	0.004268847193454476

Kruskal-Wallis (pairwise)

Group 1	Group 2	H	p-value	q-value
Baunei (n=23)	Cardedu (n=5)	0.108846	0.741462	0.855533
	Perdasdefogu (n=6)	2.968116	0.084921	0.195561
	Talana (n=15)	11.897659	0.000562	0.008431
	Urzulei (n=19)	4.668352	0.030723	0.121966
	Villagrande (n=16)	0.235598	0.627404	0.784255
Cardedu (n=5)	Perdasdefogu (n=6)	2.133333	0.144127	0.240212
	Talana (n=15)	3.857143	0.049535	0.148604
	Urzulei (n=19)	1.062316	0.302688	0.412756
	Villagrande (n=16)	0.000000	1.000000	1.000000
Perdasdefogu (n=6)	Talana (n=15)	1.751515	0.185686	0.278530
	Urzulei (n=19)	0.004049	0.949266	1.000000
	Villagrande (n=16)	4.570652	0.032524	0.121966
Talana (n=15)	Urzulei (n=19)	2.601203	0.106783	0.200217
	Villagrande (n=16)	7.656250	0.005658	0.042432
Urzulei (n=19)	Villagrande (n=16)	2.851974	0.091262	0.195561

FIGURE 3
Alpha diversity boxplots.

10.3389/frmbi.2024.1474497

Group significance plots

	PERMANOVA results
method name	PERMANOVA
test statistic name	pseudo-F
sample size	84
number of groups	6
test statistic	2.651964
p-value	0.001
number of permutations	999

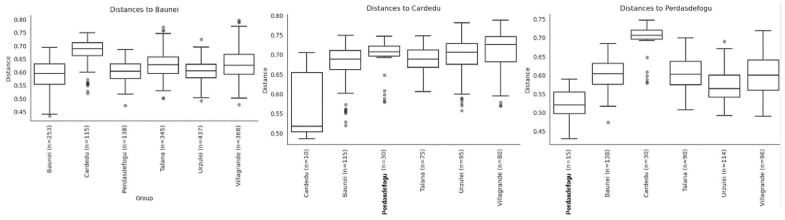

Pairwise permanova results

		Sample size	Permutations	pseudo-F	p-value	q-value
Group 1	Group 2					
Baunei	Cardedu	28	999	3.786526	0.001	0.002143
	Perdasdefogu	29	999	2.333034	0.003	0.004091
	Talana	38	999	3.216136	0.001	0.002143
	Urzulei	42	999	2.653694	0.001	0.002143
	Villagrande	39	999	1.997065	0.004	0.005000
Cardedu	Perdasdefogu	11	999	4.225272	0.005	0.005357
	Talana	20	999	3.686101	0.001	0.002143
	Urzulei	24	999	4.793803	0.001	0.002143
	Villagrande	21	999	3.267418	0.001	0.002143
Perdasdefogu	Talana	21	999	2.189486	0.003	0.004091
	Urzulei	25	999	1.671493	0.002	0.003750
	Villagrande	22	999	1.309700	0.120	0.120000
Talana	Urzulei	34	999	2.611004	0.001	0.002143
	Villagrande	31	999	2.155257	0.003	0.004091
Urzulei	Villagrande	35	999	1.766145	0.005	0.005357

FIGURE 4
Group significance plots.

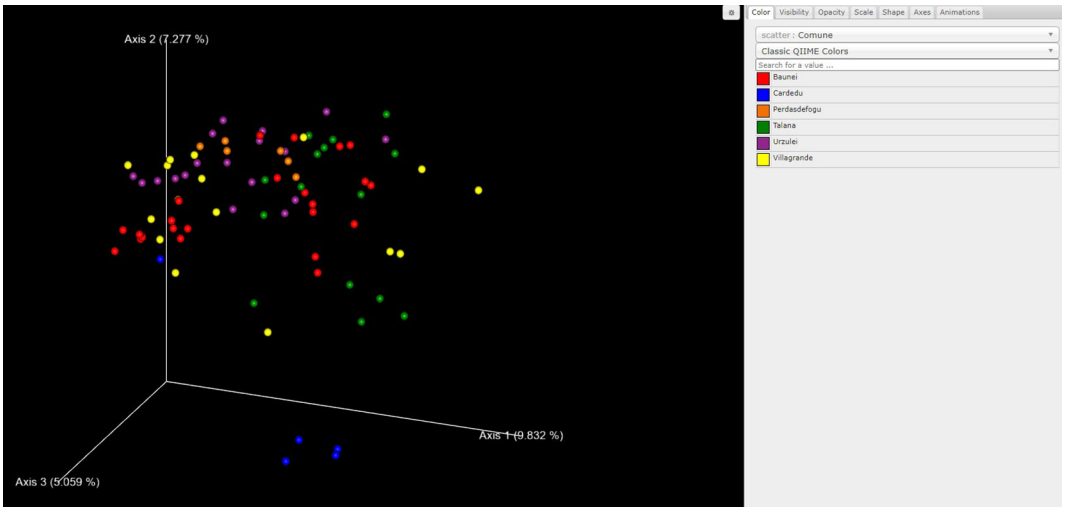

FIGURE 5
Beta diversity calculated with the weighted UniFrac metric to determine the distance between samples and PCoA to visualize the data.

Cardedu, an abundance of *Firmicutes* was noted compared to *Bacteroidetes*; in the farm in Baunei, the ratio was strongly unbalanced in favor of *Firmicutes*. In all the farms, there was a lower abundance of *Proteobacteria*, *Actinobacteria*, and *Verrucomicrobia*, except the farm in Cardedu, which has a slightly higher percentage than the others (Figure 2; Table 2).

The most represented families were as follows: *Gracilibacteraceae*, *Erysipelotrichaceae*, *Clostridiales Family XI. Incertae Sedis*, *Christensenellaceae*, *Acidaminococcaceae*, *Peptostreptococcaceae*, *Clostridiaceae*, *Porphyromonadaceae*, *Prevotellaceae*, *Flavobacteriaceae*, *Eubacteriaceae*, *Ruminococcaceae*, *Lachnospiraceae*, *Rikenellaceae*, *Synergistaceae*, and *Bacteroidaceae*. The *Erysipelotrichaceae* family has a higher abundance in the Talana, Urzulei, and Perdasdefogu farms. The *Acidaminococcaceae* and *Porphyromonadaceae* families were very abundant in the Cardedu farm. The *Peptostreptococcaceae* family had a higher abundance in the Talana and Perdasdefogu farms, while *Peptostreptococcaceae* were present in very low percentages in the Cardedu farm. The *Prevotellaceae* family had a higher abundance in the Perdasdefogu and Villagrande farms (Table 3).

The most represented genera were *Ruminococcus*, *Eubacterium*, *Roseburia*, and *Clostridium*. For the genera *Ruminococcus*, *Roseburia*, and *Clostridium*, a greater abundance was noted in the Talana farm and a lower abundance in the Cardedu farm. For the genus *Eubacterium*, no significant difference was noted in the various farms (Table 4).

The most represented species were *Ruminococcus faecis*, *Ruminococcus gauvreauii*, *Eubacterium hallii*, *Roseburia faecis*, and *Clostridium lavalense*. For the species *R. faecis*, *R. gauvreauii*, and *C. lavalense*, there were a greater abundance in the Talana and Perdasdefogu farms and a lower abundance in the Cardedu farm. For the species *R. faecis*, there was a greater abundance in the Talana farm (Table 5).

Significant differences in the relative abundance of taxa were detected between the samples from Baunei and Talana ($P = 0.0005$) and Cardedu and Talana ($P = 0.04$) farms (Figure 3).

As far as beta diversity is concerned, the Cardedu farm was significantly different from the other sites, with *P*-values ranging from 0.001 to 0.005; similar results were obtained for the Baunei farm (Figure 4). A multidimensional sorting graph (Figure 5), where each sample is a point and the distance between the points represents the similarity, highlighted a cluster made up of the Cardedu locality. Beta diversity was significantly different between the CAE-positive and CAE-negative samples ($P = 0.017$) (Figure 6). On the farms in the localities of Perdasdefogu and Villagrande, *Prevotellaceae* were abundant; *Peptostreptococcaceae* and *Erysipelotrichaceae* were abundant in the localities of Perdasdefogu, Talana, Urzulei, and Villagrande. A significant abundance of *Acidaminococcaceae* on the Cardedu farm compared to that of the other families, a high abundance of *Porphyromonadaceae* and *Flavobacteriaceae*, and a decreased presence of *Peptostreptococcaceae* were detected (Table 3).

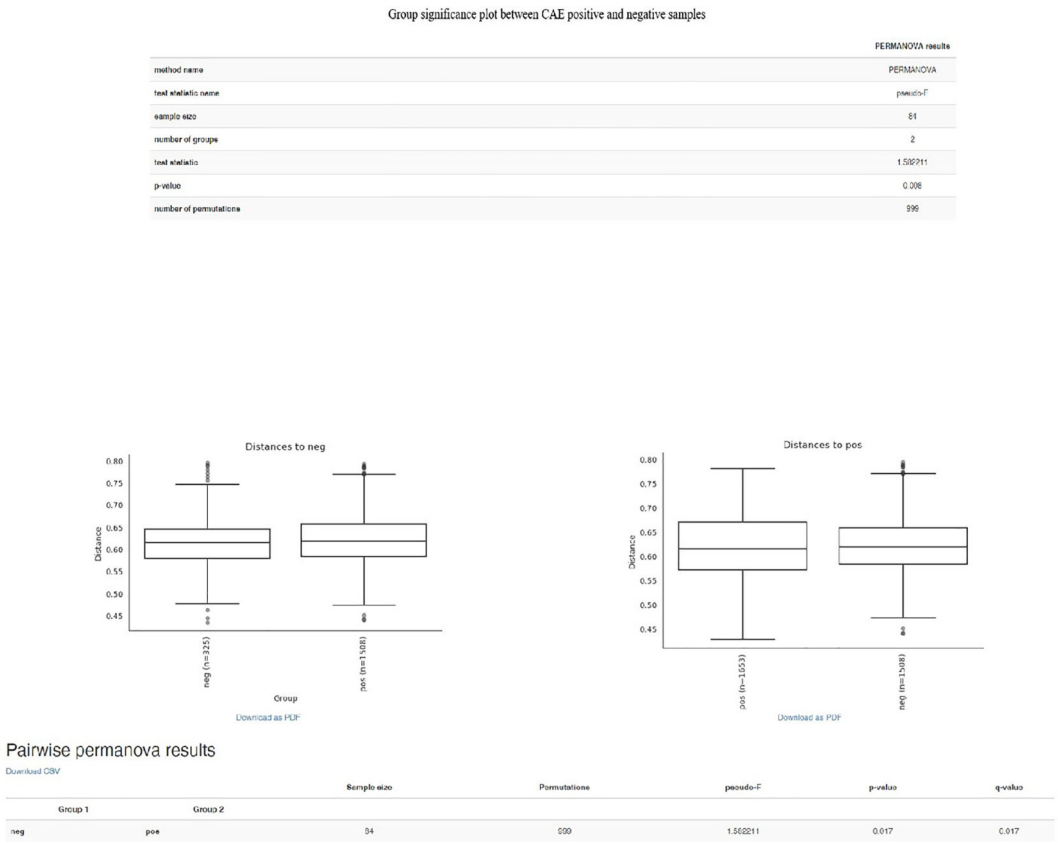

FIGURE 6
Group significance plot between CAE-positive and CAE-negative samples.

10.3389/frmbi.2024.1474497

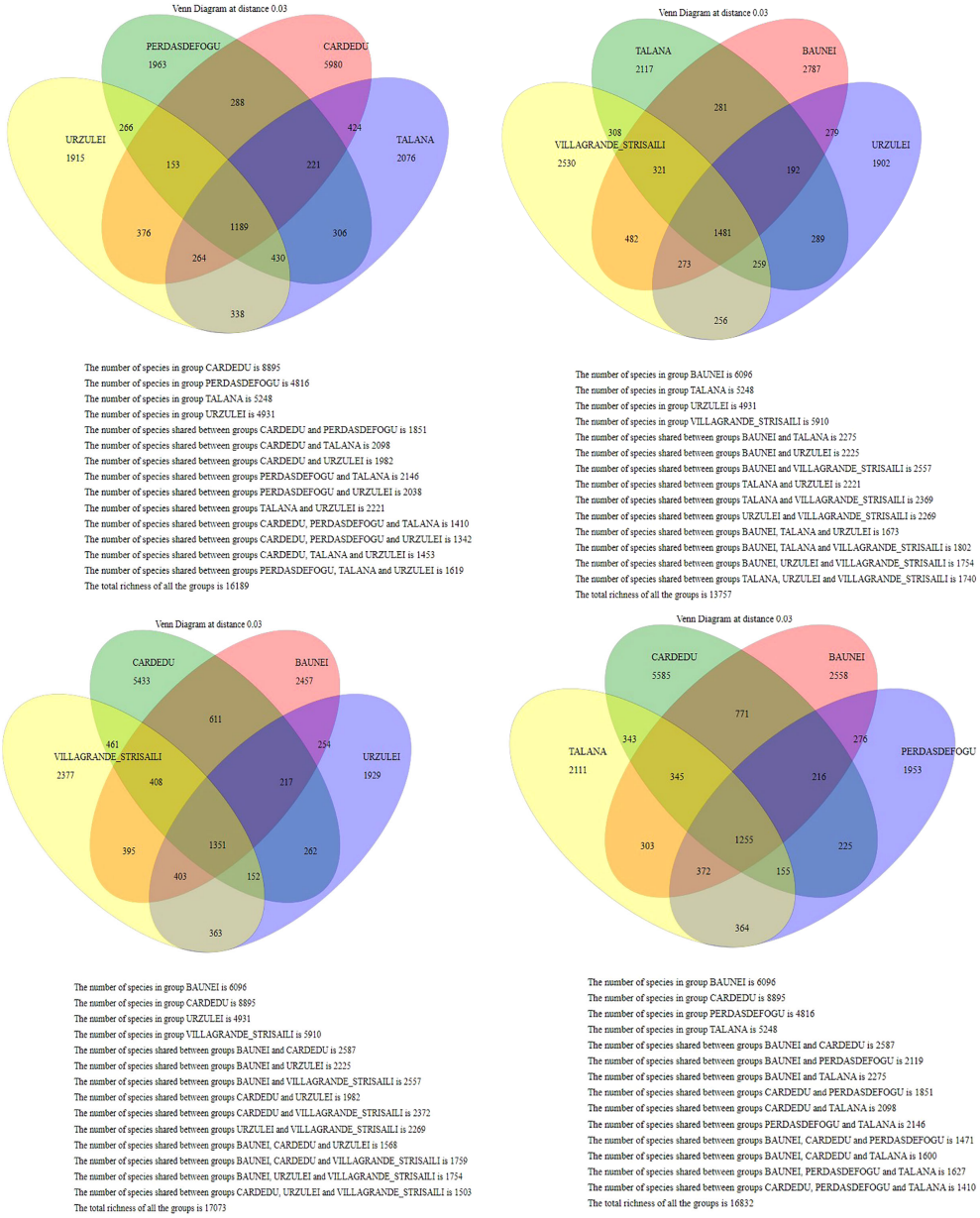

FIGURE 7
Venn diagram at a distance of 0.03; the Cardedu samples show a statistically significant difference compared to the other localities.

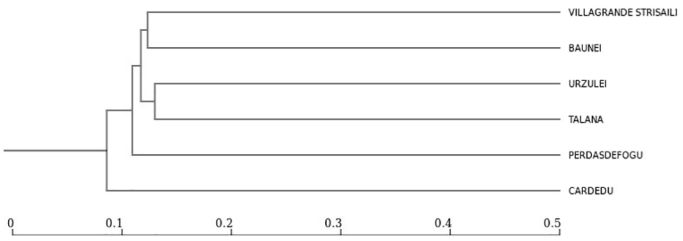

FIGURE 8
Dendrogram showing 4 clusters with greater distances between Cardedu and the other locality.

In the samples from the locality of Talana, there was a prevalence of the *Roseburia* genus and *R. faecis* (Tables 4, 5).

4 Discussion

Prevotellaceae was found in the localities of Perdasdefogu and Villagrande (Kim et al., 2014), where 4 out of 29 goats tested positive for CAE. From these data, we deduced that the presence of *Prevotellaceae* can be an indication of the disease, as highlighted by human clinical literature. The intestinal microbiome can exhibit bacterial hyperproliferation in rheumatoid arthritis (RA), which can be related to the onset or course of the disease. In particular, individuals affected by RA showed a high prevalence of *Prevotella* and *Prevotella* spp. The presence of these specific bacteria suggests a potential association between the intestinal microbiota and the development or exacerbation of this disease. Understanding the complex pattern of the relationship between the microbiome and RA could provide useful knowledge for the development of new therapeutic strategies targeting the intestinal flora, thus offering new perspectives for the management and treatment of this disease (Horta-Baas et al., 2017; Attur et al., 2022). Compared to FDR controls [first-degree relatives of RA patients (RA-FDR) have a higher risk of developing RA than the general population], individuals at risk of RA with systemic autoimmunity and/or RA-associated symptoms have an enrichment of *Prevotella* spp. The findings support the hypothesis of a mucosal origin in the development of RA. Intestinal dysbiosis could act as an early environmental modulator and may be a target of future preventive interventions (Alpizar-Rodriguez et al., 2019). These data may be related to the findings of studies on human individuals at risk of rheumatoid arthritis with systemic autoimmunity and/or symptoms associated with rheumatoid arthritis in which an increase in *Prevotella* spp. was found (Alpizar-Rodriguez et al., 2019). It could be hypothesized that the same scenario also occurs in goats affected by arthritic diseases, such as those analyzed.

Of interest is also the abundance of the genus *Roseburia* observed in the samples collected in the locality of Talana, higher than in other localities (Supplementary Material 6). Species belonging to the *Roseburia* genus are important inhabitants of the intestinal microbiome, and they are capable of fermenting complex polysaccharides into butyrate, a short-chain fatty acid that regulates the transepithelial transport of fluids, improves the oxidative and inflammatory state of the mucosa, influences human physiology, and serves as an energy source for colonocytes (Hillman et al., 2020).

The only intensive farm located in Cardedu was statistically different from the other locations. In fact, out of a total of 8,895 identified species, only 3,310 were shared with other locations (Figures 7, 8). In particular, the presence of *Acidoaminococcaceae* was significant (Table 3). This difference could be attributed to the farming system, the Cardedu farm being the only intensive one, and to the geographical distance of this location from the other sampling sites (Figure 1).

5 Conclusions

There are few studies in the literature regarding the fecal microbiome of goats and no studies with the same environmental and experimental conditions.

Therefore, the results of the present study suggest that extensive or intensive management of the farm can influence the intestinal microbiota of goats. The diversity of the farm of Talana could be attributed to the peculiarities of the rough and stony territory with many mines rich in copper, carbonate, and some veins of silver pyrite.

In the future, it would be interesting to compare the results obtained in the present work with those of other areas of Sardinia. To deepen the comparison between wild and intensive farming systems, further sampling would be necessary considering that in the present work, it was possible to analyze a limited number of samples for intensive farming.

It would also be desirable to monitor the goats from birth until a possible positivity for CAE to investigate the changes in the composition of the intestinal microbiome and the increase of *Prevotellaceae* to have new perspectives in the management of the disease.

Data availability statement

The original contributions presented in the study are publicly available. This data can be found here: Galaxy Server instance https://izs3.crs4.it/. To access the datasets, enter Email Address "guest@izs3.crs4.it" and Password "gU3st1ZS3CR$4". Once logged in, click "Shared Data". This will open a dropdown menu allowing access to Data Libraries and Histories.

Ethics statement

Ethical approval was not required for the studies involving animals in accordance with the local legislation and institutional requirements because the study was performed on the feces and blood of the animals. The animals were not subjected to any invasive treatment. Written informed consent was obtained from the owners for the participation of their animals in this study.

Author contributions

MM: Conceptualization, Data curation, Formal analysis, Investigation, Methodology, Supervision, Visualization, Writing – original draft, Writing – review & editing. PC: Investigation, Writing – original draft, Funding acquisition, Project administration. LD: Writing – original draft, Formal analysis, Methodology. RA: Formal analysis, Methodology, Writing – original draft. NM: Funding acquisition, Project administration, Writing – review & editing. AC: Writing – review & editing,

Conceptualization, Data curation, Formal analysis, Investigation, Methodology, Supervision, Visualization, Writing – original draft.

Funding

The author(s) declare financial support was received for the research, authorship, and/or publication of this article. This research was supported by funds from the Istituto Zooprofilattico Sperimentale della Sardegna and funded by the Ministry of Labour, Health and Social Policies.

Conflict of interest

The authors declare that the research was conducted in the absence of any commercial or financial relationships that could be construed as a potential conflict of interest.

Publisher's note

All claims expressed in this article are solely those of the authors and do not necessarily represent those of their affiliated organizations, or those of the publisher, the editors and the reviewers. Any product that may be evaluated in this article, or claim that may be made by its manufacturer, is not guaranteed or endorsed by the publisher.

Supplementary material

The Supplementary Material for this article can be found online at: https://www.frontiersin.org/articles/10.3389/frmbi.2024.1474497/full#supplementary-material

SUPPLEMENTARY MATERIAL 1
Pipeline GALAXY.

References

Alpizar-Rodriguez, D., Lesker, T. R., Gronow, A., Gilbert, Benoît, Raemy, E., Lamacchia, C., et al. (2019). Prevotella covers in individuals at risk for rheumatoid arthritis. *Rheumatoid Arthritis* 78, 590–593. doi: 10.1136/annrheumdis-2018-214514

Anderson, M. J. (2001). A new method for nonparametric multivariate analysis of variance. *Austral Ecol.* doi: 10.1111/j.1442-9993.2001.01070.pp.x

Attur, M., Scher, J. U., Abramson, S. B., and Attur, M. (2022). Role of intestinal dysbiosis and nutrition in rheumatoid arthritis. *Cells* 11, 2436. doi: 10.3390/cells11152436

Bahrndorff, S., Alemu, T., Alemneh, T., and Lund Nielsen, J. (2016). The microbiome of animals: implications for conservation biology. *Int. J. Genomics*. doi: 10.1155/2016/5304028

Bartels, L., Onland, G., Boel che,, and van den Brule, A. J. C. (2003). Isolation of Enterovirus RNA from clinical samples using magnetic silica particles. *J. Microbiol. Methods* 55, 535. 14.

Bertolo, A., Valido, E., and Stoyanov, J. (2024). Optimized bacterial community characterization through full-length 16S rRNA gene sequencing utilizing MinION nanopore technology. *BMC Microbiol.* 24, 58. doi: 10.1186/s12866-024-03208-5

Chappidi, S., Villa, C. E., and Cantarel, B. L. (2019). Using Mothur to determine bacterial community composition and structure in 16S ribosomal RNA datasets. *Curr. Bioinform. Protocol.* 67, 83. doi: 10.1002/cpbi.83

Chaudhari, H. G., Prajapati, S., Wardah, Z. H., Raol, G., Prajapati, V., Patel, R., et al. (2023). Decoding the microbial universe with metagenomics: a brief insight. *Front. Genet.* 14. doi: 10.3389/fgene.2023.1119740

Cole, J. R., Wang, Q., Fish, J. A., Chai, B., McGarrell, D. M., et al. (2013). Ribosome database project: data and tools for high-throughput rRNA analysis. *Nucleic Acid Res.* 42, D633–D642. doi: 10.1093/nar/gkt1244

Consiglio Superiore di Sanità – Sezione III (2018). *Il Microbiota umano: dalla ricerca alle applicazioni cliniche. Raccomandazioni e Linee di indirizzo*.

Crawford, T. B., Adams, D. S., Cheevers, W. P., and Cork, L. C. (1980). Chronic arthritis in goats caused by a retrovirus. *Science* 207, 997–999. doi: 10.1126/science.6153243

Cuccuru, G., Orsini, M., Pinna, A., Sbardellati, A., Soranzo, N., Travaglione, A., et al. (2014). Orion, a web-based framework for NGS analysis in microbiology. *Bioinformatics* 30, 1928–1929. doi: 10.1093/bioinformatics/btu135

Duarte, G. V., Moura, A. I., Moreira, R., Nunes, J., Figueiredo, M. M., and Carvalho, M. G. (2013). Evaluation of several forest residues as potential raw material for bioethanol production in Portugal. *J. Bioprocess Eng. Biorefinery* 2, 73–78. doi: 10.1166/jbeb.2013.1035

Feng, Q., Chen, W.-D., and Wang, Y.-D. (2018). Gut microbiota: an integral moderator in health and disease. *Front. Microbiol.* 9. doi: 10.3389/fmicb.2018.00151

Hillman, E. T., Kozik, A. J., Hooker, C. A., Burnett, J. L., Heo, Y., Kiesel, V. A., et al. (2020). Comparative genomics of the genus Roseburia reveals divergent biosynthetic pathways that may influence colonic competition among species. *Microb. Genom.* 6, mgan000399. doi: 10.1099/mgen.0.000399

Horta-Baas, G., Romero-Figueroa, M. D. S., Montiel-Jarquín, A. J., Pizano-Zárate, M. L., García-Mena, J., and Ramírez-Durán, N. (2017). Intestinal dysbiosis and rheumatoid arthritis: A link between gut microbiota and the pathogenesis of rheumatoid arthritis. *J. Immunol. Res.* 2017, 4835189. doi: 10.1155/2017/4835189

Hrovat, K., Dutilh, B. E., Medema, M. H., and Melkonian, C. (2024). Taxonomic resolution of different 16S rRNA variable regions varies strongly across plant-associated bacteria. *ISME Commun.* 4, ycae034. doi: 10.1093/ismeco/ycae034

Kim, M., Kim, J., Kuehn, L. A., Bono, J. L., Berry, E. D., Kalchayanand, N., et al. (2014). Investigation of bacterial diversity in the feces of cattle fed different diets. *J. Anim. Sci.* 92, 683–694. doi: 10.2527/jas.2013-6841

Kreisinger, J., Schmiedová, L., Petrželková, A., Tomášek, O., Adámková, M., Michálková, R., et al. (2018). Fecal microbiota associated with phytohaemagglutinin-induced immune response in nestlings of a passerine bird. *Ecol. Evol.* 8, 9793-9802. doi: 10.1002/ece3.4454

Le Jan, C., Bellaton, C., Greenland, T., and Mornex, J. F. (2005). Mammary transmission of caprine arthritis encephalitis virus: a 3D model for *in vitro* study. *Reprod. Nutr. Dev.* 45, 513–523. doi: 10.1051/rnd:2005035

Loens, K., Beck, T., van Deursen, P., et al. (2003). Comparison of magnetic and conventional Boom RNA extraction using respiratory samples. *J. Microbiol. Methods* 55, 509.

Macciotta, N. P. P., et al. (2002). Somatic variability of Sardinian goat breed analysed by multivariate methods. *Livestock Product. Sci.* 75, 51–58. doi: 10.1016/S0301-6226(01)00309-8

McKenzie, V. J., Song, S. J., Delsuc, F., Perst, T. L., Oliverio, A. M., Korpita, T. M., et al. (2017). The effects of captivity on the mammalian gut microbiome. *Integr. Comp. Biol.* 57. doi: 10.1093/icb/icx090

Muegge, B. D., Kuczynski, J., Knights, D., Clemente, J. C., González, A., Fontana, L., et al. (2012). Diet drives convergence in gut microbiome functions across mammalian phylogeny and within humans. *Science* 332, 970-974. doi: 10.1126/science.119871

Nam, N. N., Do, H. D. K., Loan Trinh, K. T., and Lee, N. Y. (2023). Metagenomics: an effective approach for exploring microbial diversity and functions. *Foods* 12, 2140. doi: 10.3390/foods12112140

Narayan, O., Clements, J. E., Strandberg, J. D., Cork, L. C., and Griffin, D. E. (1980). Biological characterization of the virus causing leukoencephalitis and arthritis in goats. *J. Gen. Virol.* 50, 69–79. doi: 10.1099/0022-1317-50-1-69

Ondov, B. D., Bergman, N. H., and Phillippy, A. M. (2011). Interactive metagenomics visualization in a web browser. *BMC Bioinf.* 12, (1). doi: 10.1186/1471-2105-12-385

Pes, G., and Pouland, M. (2014). *Longevità e identità in Sardegna. L'identificazione della "Zona Blu" dei centenari in Ogliastra*. Ed. F. Angeli

Peterhans, E., Greenland, T., Badiola, J., Harkiss, G., Bertoni, G., Amorena, B., et al. (2004). Routes of transmission and consequences of small ruminant lentiviruses (SRLVs) infection and eradication schemes. *Vet. Res.* 35, 257–274. doi: 10.1051/vetres:2004014

Pielou, E. C. (1966). The measurement of diversity in different types of biological collections. *J. Theor. Biol.* 13, 131–144. doi: 10.1016/0022-5193(66)90013-0

Quast, C., Pruesse, E., Yilmaz, P., Gerken, J., Schweer, T., et al. (2012). The SILVA ribosomal RNA gene database project: improved data processing and web-based tools. *Nucleic Acid Res.* 41, D590–D596. doi: 10.1093/nar/gks1219

Randeni, N., Bordiga, M., and Xu, B. (2024). A comprehensive review of the triangular relationship among diet-gut microbiota-inflammation. *Int. J. Mol. Sci.* 25, 9366. doi: 10.3390/ijms25179366

Satam, H., Joshi, K., Mangrolia, U., Waghoo, S., Zaidi, G., Rawool, S., et al. (2023). Next-generation sequencing technology: current trends and advancements. *Biology* 12, 997. doi: 10.3390/biology12070997

Schloss, P. D. (2013). Secondary structure improves OTU assignments of 16S rRNA gene sequences. *ISME J.* 7, 457–460. doi: 10.1038/ismej.2012.102

Schloss, P. D. (2020). Reintroduction month: 10 years later. *Appl. Environ. Microbiol.* 86, e02343–e02319. doi: 10.1128/AEM.02343-19

Schloss, P. D., Westcott, S. L., Ryabin, T., Hall, J. R., Hartmann, M., Hollister, E. B., et al. (2009). Introducing mothur: open-source, platform-independent, community-supported software for describing and comparing microbial communities. *Appl. Environ. Microbiol.* 75, 7537–7541. doi: 10.1128/AEM.01541-09

The Galaxy Community (2022). The galaxy platform for accessible, reproducible, and collaborative biomedical analysis: 2022 update. *Nucleic Acids Res.* 50, W345–W351. doi: 10.1093/nar/gkac247

Usai, M. G., et al. (2004). "Survey on the goat farming system in Sardinia," in *Procedure XVI SIPAOC Siena National Congress*.

Van Deursen, P., de Bie, P., Verhoeven, A., et al. (2003). *Nucleic acid isolation using magnetic silica particles. Poster 71c at the European Meeting of Molecular Diagnostics* (Scheveningen, The Netherlands).

Vázquez-Baeza, Y., Pirrung, M., Gonzalez, A., and Knight, R. (2013). EMPeror: A tool for visualizing high-throughput microbial community data. *GigaScience* 2, art. no. 16. doi: 10.1186/2047-217X-2-16

Willis, C., Desai, D., and LaRoche, J. (2019). Influence of 16S rRNA variable region on perceived diversity of marine microbial communities of the Northern North Atlantic. *FEMS Microbiol. Lett.* 366, fnz152. doi: 10.1093/femsle/fnz152

WOAH. (2021). Caprine arthritis/encephalitis and Maedi-visna. In *Manual of diagnostic test and vaccines for terrestrial animals*. (World Organisation for Animal Health, Paris).

Wooley, J. C., Godzik, A., and Friedberg, I. (2010). A primer on metagenomics (P.E. Bourne, ed.). *Comput. Biol. PloS* 6, e1000667. doi: 10.1371/journal.pcbi.1000667

frontiers | Frontiers in Microbiology

TYPE Original Research
PUBLISHED 30 January 2025
DOI 10.3389/fmicb.2024.1512217

Check for updates

OPEN ACCESS

EDITED BY
Mohammad Altamimi,
An-Najah National University, Palestine

REVIEWED BY
Francisco Jose Roig,
Universidad San Jorge, Spain
Rui Li,
Chinese Academy of Sciences (CAS), China

*CORRESPONDENCE
In Seon Hwang
✉ suni0845@gmail.com

RECEIVED 22 October 2024
ACCEPTED 26 December 2024
PUBLISHED 30 January 2025

CITATION
Lee DB and Hwang IS (2025) Macronutrient balance determines the human gut microbiome eubiosis: insights from *in vitro* gastrointestinal digestion and fermentation of eight pulse species.
Front. Microbiol. 15:1512217.
doi: 10.3389/fmicb.2024.1512217

COPYRIGHT
© 2025 Lee and Hwang. This is an open-access article distributed under the terms of the Creative Commons Attribution License (CC BY). The use, distribution or reproduction in other forums is permitted, provided the original author(s) and the copyright owner(s) are credited and that the original publication in this journal is cited, in accordance with accepted academic practice. No use, distribution or reproduction is permitted which does not comply with these terms.

Macronutrient balance determines the human gut microbiome eubiosis: insights from *in vitro* gastrointestinal digestion and fermentation of eight pulse species

Da Bin Lee and In Seon Hwang*

Food and Nutrition Division, Department of Agri-food Resources, National Institute of Agricultural Sciences, Wanju, Republic of Korea

The interactions between macronutrients, the human gut microbiome, and their metabolites (short-chain fatty acids) were comprehensively investigated via an *in vitro* digestion and fermentation model subjected to eight pulse species. 16S rRNA sequencing and taxonomic analysis of pulse digesta fermented for up to 24 h revealed an increase in the relative abundance of gut health-detrimental genera represented by *Escherichia-Shigella* in kidney bean, soybean, cowpea, chickpea, and black bean samples. In contrast, the relative abundance of health-positive genera, including *Bacteroides*, *Eubacterium*, and *Akkermansia*, was elevated in red bean, mung bean, and Heunguseul. At the same time, the proportion of the pathogenic *Escherichia-Shigella* decreased. Concurrently, these three species exhibited an increase in microbial diversity as evidenced by the calculation of α-diversity (Shannon index) and β-diversity (Bray-Curtis distance). Despite the lower nutrient contents in the three pulses, represented by carbohydrates, amino acids, and fatty acids, network analysis revealed that the nutrient contents in the pulse digesta possess complex positive or negative correlations with a variety of bacteria, as well as their metabolites. These correlations were more pronounced in red bean, mung bean, and Heunguseul than in the other pulses. It was postulated that the overall potential to nourish gut environments in these species was due to the balance of their nutritional components. The linear regression analysis demonstrated that there was a negative association between carbohydrate and amino acid contents and the increase in Shannon indices. Furthermore, the ratio of carbohydrates to fatty acids and amino acids to fatty acids displayed negative correlations with the diversity increase. The ratio of carbohydrates to amino acids showed a weak positive correlation. It is noteworthy that a diet comprising foods with a balanced nutritional profile supports the growth of beneficial gut microbes, thereby promoting microbial eubiosis. Consistent work on different ingredients is essential for precise insight into the interplay between food and the human microbiome in complex dietary patterns.

KEYWORDS

gut fermentation, *in vitro* digestion, human microbiome, pulse, diversity

1 Introduction

In response to the growing efforts of various industries to achieve carbon neutrality amidst climate change, the food industry has witnessed a notable surge in demand for plant-based diets as alternatives to conventional animal-derived foods (Sandua, 2024). In comparison to animal-based foods, those derived from plants are rich in phytochemicals, micronutrients, and dietary fibers. Additionally, they contain minimal amounts of saturated fats and trans fats, which have been linked to adverse effects on cardiovascular health (Gong et al., 2020). However, plant-based foods have certain limitations. For instance, they often have restricted amount of micronutrients that are predominantly found in meat or seafood, as well as a lower quantity and quality of protein (Tso and Forde, 2021).

To address these shortcomings, pulses have been employed extensively as a pivotal ingredient in plant-based diets. In addition to their high protein and dietary fiber content, pulses contain beneficial unsaturated fatty acids, such as omega-3, which qualifies them as a nutritionally valuable food source (Karolkowski et al., 2021; Didinger and Thompson, 2022). Globally, pulse products are widely consumed, with notable examples including tofu, natto, tempeh, and soy sauce. Given the recent interest in the gut microbiome as a key factor for maintaining human health, there is a growing recognition of the potential of fermented foods made from pulses to nurture the growth of beneficial bacteria, including *Streptococcus* sp. and *Faecalibacterium* sp. (Valentino et al., 2024). This is attributed to the presence of prebiotic components, such as polysaccharides, and probiotic species that are abundant in these foods.

To elucidate the precise relationship between food and the microbiome, it is essential to identify the impacts of each ingredient, before the combinations of foods, on the growth or reduction of gut bacteria. One of the limiting factors of exploiting microbiome-informed precision nutrition strategies is the difficulty of identifying the effect of a single food in our complex dietary intake (Valles-Colomer et al., 2023). As complex individual diets in clinical studies hinder the comprehension of the effects of specific dietary components on the gut microbiota, dietary metadata is needed for the advancement of microbiome-targeted therapies (Ross et al., 2024). However, there is a paucity of knowledge regarding how food ingredients, in addition to a single nutrient or dietary pattern, influence the gut microbiota. A number of recent studies have consistently reported that the intake of dietary fibers and polysaccharides from food consumption (Deehan et al., 2020; Coker et al., 2021) or certain diet types, such as the Mediterranean diet (Meslier et al., 2020; Rinott et al., 2022), can improve the diversity of the human microbiome and support the proliferation of beneficial bacteria, thereby exerting positive health effects.

This approach presents a challenge in current practices due to the inherent limitations of the self-reporting dietary assessment technique, which is dependent on an individual's memory (Johnson et al., 2020). To overcome these challenges and assess the specific impact of individual ingredients on the human microbiome, an *in vitro* digestion and colonic fermentation method was developed by multiple researchers (Xavier and Mariutti, 2021). This system simulates the digestive process of food through the human mouth, upper gastrointestinal tract, and colonic fermentation process under controlled conditions, thereby providing standardized results in a time- and cost-effective manner compared to human trials. Consequently, the system allows for the rapid and accurate evaluation of the effects of a variety of daily consumed ingredients on the gut microbiota. As the INFOGEST protocol has been validated for *in vitro* digestion studies of foods, it has been utilized in current studies examining a range of food items, such as leafy vegetables and pulses (Lee et al., 2019; Kim et al., 2021; Bae et al., 2021). Meanwhile, the final destination of consumed food, gut fermentation, has not been sufficiently investigated in the majority of research, which has been limited to the simulation of the digestion process and the measurement of the bioaccessibility of food ingredients. The combined model of *in vitro* digestion and gut fermentation system allows for the prediction of the ultimate health effects of food consumption.

This study aimed to investigate the impact of commonly consumed pulses in Korea on the human gut microbiota and metabolite profiles. Pulses constitute a principal component of the Korean diet, with a diverse range of pulses being consumed in Korea. In this study, the following pulses were selected as analytic samples: soybean, kidney bean, cowpea, black bean, red bean, mung bean, Heunguseul, and chickpea. The last one is a non-domestic species whose consumption has recently increased, though it is not cultivated in Korea. The digested products of pulses prepared using an *in vitro* digestion model were cultured in an *in vitro* gut fermentation model simulating the human colon environment to observe the effects on gut microbiota. Modifications were made to the INFOGEST protocol in order to accurately simulate the digestion of nutrients. These included the addition of the BBMV (brush border membrane vesicles) enzyme, which was extracted from the porcine small intestine and subjected in the final stage of digestion. Furthermore, given that pulses are a food source that typically contains macronutrients (carbohydrates, proteins, and fats), the study also analyzed the interrelationships between these components in pulses and changes in the gut microbiota, as well as their metabolites. This was done to ascertain the nutritional factors that contribute to the prebiotic effects of pulse samples.

2 Materials and methods

2.1 Preparing pulses in edible form

Eight types of pulses commonly consumed in Korea were selected for analysis as follows: soybeans (*Glycine max*, SB), kidney beans (*Phaseolus vulgarius*, KB), cowpeas (*Vigna unguiculata*, CB), chickpeas (*Cicer arietinum*, CP), black beans (*Rhynchosia nulubilis*, BB), mung beans (*Vigna radiate*, MB), Heunguseul (*Vigna anaularis L. Heunguseul*, HS), and red beans (*Vigna anaularis L.*, RB). The samples were prepared in a consumable form by applying the most common cooking methods suggested by the National Standard Food Composition Table (provided by the Rural Development Administration, 10th version). Consequently, each sample was subjected to either boiling or stir-frying, with the specific methods outlined as follows: The SBs (Sangju, Gyeongsangbuk-do, Korea) were boiled for 40 min in water at three times their weight after a 4-hour soaking. CBs (Gurye, Jeollanam-do, Korea) were boiled for 50 min in water at 10 times their weight after soaking for 8 h. The KBs (Geochang, Gyeongsangnam-do, Korea), HSs (Wanju, Jeollabuk-do,

Korea), MBs (Muan, Jeollanam-do, Korea), and RBs (Muan, Jeollanam-do, Korea) were boiled for 1 h in water at 10 times of their weight without prior soaking. The CP samples (USA) were boiled for 15 min in water at 10 times their weight, following a 6-hour soaking. The roasted BBs (Sangju, Gyeongsangbuk-do, Korea) were obtained from a commercial market.

2.2 Simulated digestion using *in vitro* gastrointestinal model

A gastrointestinal model was constructed and simulated to examine the alteration of nutrient contents throughout the digestive process, which encompasses the oral, gastric, intestinal, and BBMV phases (Minekus et al., 2014). In the oral phase, cooked pulses were mixed with a 1:1 solution of simulated salivary fluid (KCl (Potassium chloride P9333, Sigma Aldrich Co, Seoul, Korea) 15.1 mmol/L, KH_2PO_4 (Potassium phosphate monobasic P0662, Sigma Aldrich Co.) 3.7 mmol/L, $NaHCO_3$ (Sodium bicarbonate S5761, Sigma Aldrich Co.) 13.6 mmol/L, $MgCl_2(H_2O)_6$ (Magnesium chloride hexahydrate 63,068, Sigma Aldrich Co.) 0.15 mmol/L, $(NH_4)_2CO_3$ (Ammonium carbonate 207,861, Sigma Aldrich Co.) 0.06 mmol/L, pH 7.0) and enzyme (75 U/mL salivary α-amylase solution (α-Amylase from human saliva A0521, Sigma Aldrich Co.), 0.3 M $CaCl_2$ (Calcium chloride C1016, Sigma Aldrich Co.), water). The solution was digested at 37°C for 2 min. The gastric phase entailed the mixture of the oral digested samples and a 1:1 solution of simulated gastric fluid (KCl 6.9 mmol/L, KH_2PO_4 0.9 mmol/L, $NaHCO_3$ 25 mmol/L, NaCl (Sodium chloride S9888, Sigma Aldrich Co.) 47.2 mmol/L, $MgCl_2(H_2O)_6$ 0.1 mmol/L, $(NH_4)_2CO_3$ 0.5 mmol/L, pH 3.0) and enzyme (2000 U/mL porcine pepsin stock solution (Pepsin from porcine gastric mucosa P7000, Sigma Aldrich Co.), 0.3 M $CaCl_2$, 1 M HCl (Hydrochloric acid 4095–3705, Daejung, Seoul, Korea), water). The solution was incubated at 37°C for 120 min. Similarly, the intestinal phase was conducted through the mixing of gastric digested samples with a 1:1 solution of simulated intestinal fluid (KCl 6.8 mmol/L, KH_2PO_4 0.8 mmol/L, $NaHCO_3$ 85 mmol/L, NaCl 38.4 mmol/L, $MgCl_2(H_2O)_6$ 0.33 mmol/L, $(NH_4)_2CO_3$ 0.6 mmol/L, pH 7.0) and enzyme (200 U/mL pancreatin from porcine pancreas [Pancreatin from porcine pancreas P7545, Sigma Aldrich Co.]), 160 mM bile salts (Bile extract porcine B8631, Sigma Aldrich Co.), 0.3 M $CaCl_2$, water and reacting at 37°C for 120 min. As the final digestive phase, 77.3 U/mL of BBMV was added for the digesta to react at 37°C for 180 min (Oku et al., 2011). Subsequently, the mixture was heated at 100°C for 10 min to inhibit further digestion.

2.3 Dialysis process

The samples that underwent *in vitro* digestion were collected and placed in a 1 kDa molecular weight cut-off cellulose membrane (Spectra/Por® 6 Standard RC Pre-Wetted Dialysis Tubing). They were then soaked in 10 mM NaCl at 37°C for 24 h to remove low-molecular-weight components (Shiowatana et al., 2006; Bouayed et al., 2011; Hettiarachchi et al., 2021). Once the dialysis process was complete, the digested material was transferred to the *in vitro* gut fermentation model.

2.4 Determination of the nutrient content in digested pulses

The cooked pulses were subjected to oral, gastric, small intestinal digestion, and dialysis phases, and the major nutrient contents of each fully digested pulse sample were analyzed. A total of six types of saccharides, including oligosaccharides, disaccharides, and monosaccharides, were determined. In addition, 22 essential and non-essential amino acids and 6 fatty acids were quantified. These nutrients serve as energy sources for the gut microbiota in the simulated human gut, and the analysis data were used to examine the correlation between nutrient content and microbial growth.

2.4.1 Analysis of free saccharides in digested samples

The levels of six free saccharides were determined for the pulse samples treated by the digestion and dialysis process. All samples were filtered (0.45 μm) and were analyzed using a Dionex Ultimate 3,000 (Thermo Dionex, Germany) and Sugar-pak (Waters, 300 mm × 6.5 mm) column. Standards for glucose (Junsei chem, 98%), galactose (Sigma, 99%), arabinose (Aldrich, 99%), xylose (Aldrich, 99%), fructose (Sigma, 99%), mannose (Sigma, 99%), sucrose (Sigma, 99.5%), maltose monohydrate (Junsei chem, 99%), lactose monohydrate (Junsei chem, 99%), raffinose (Sigma, 99%), and stachyose (Sigma, 99%) were used.

2.4.2 Analysis of free amino acids in digested samples

Twenty-two amino acids were quantified for the digested samples. They were diluted with a buffer (0.1 M perchloric acid, 0.1% meth-phosphoric acid) for ultrasonic extraction for 1 h and were homogenized for 1 h at room temperature. Samples were filtered (0.2 μm) and were analyzed on a Dionex Ultimate 3,000 (Thermo Dionex, Germany) and Inno C18 column (Younjin biochrom, 4.6 mm × 150 mm, 5 μm). Standards for aspartic acid (Asp, Agilent 5061-3330), glutamic acid (Glu, Agilent 5061-3330), serine (Ser, Agilent 5061-3330), histidine (His, Agilent 5061-3330), glycine (Gly, Agilent 5061-3330), threonine (Thr, Agilent 5061-3330), alanine (Ala, Agilent 5061-3330), arginine (Arg, Agilent 5061-3330), GABA (Sigma), taurine (Tau, Sigma), tyrosine (Tyr, Agilent 5061-3330), valine (Val, Agilent 5061-3330), methionine (Met, Agilent 5061-3330), phenylalanine (Phe, Agilent 5061-3330), isoleucine (Ile, Agilent 5061-3330), leucine (Leu, Agilent 5061-3330), lysine (Lys, Agilent 5061-3330), proline (Pro, Agilent 5061-3330), cysteine (Cys, Agilent 5061-3330), glutamine (Gln, Agilent 5062-2478), asparagine (Asn, Agilent 5062-2478), and tryptophan (Trp, Agilent 5062-2478) were used.

2.4.3 Analysis of free fatty acids in digested samples

The amounts of six fatty acids (palmitic acid, stearic acid, arachidic acid, oleic acid, linoleic acid, α-linolenic acid [Supelco 37 Component FAME Mix, Supelco, United States)] were determined. Freeze-dried samples were mixed with 340 μL of methylation mixture (MeOH: benzen: DMP: H_2SO_4 = 39:20:5:2) and 200 μL of heptane for extraction at 80°C for 2 h. The supernatants were analyzed at room temperature using an Agilent 7890A GC–MS (Agilent, USA) and a DB-23 column (Agilent, 60 mm × 0.25 mm × 0.25 mm). FID (280°C, H2 35, Air 350, He 35 mL/min) was used as the detector.

2.5 Quantification of human microbiome abundance and metabolite contents

2.5.1 *In vitro* human gut fermentation

The *in vitro* batch fermentation process was performed according to the method established by Mandalari et al. (2008). The fecal slurry used to simulate the human intestinal environment was the mixture of fresh feces from 10 healthy adults who had not consumed prebiotics or probiotics for 6 months prior to sample collection (approved by the Institutional Review Board of the National Institute of Agricultural Sciences, BR-202307-01). The fecal slurry diluted with 0.1 M PBS at pH 7.0 was left in an anaerobic condition for a period of time, after which the supernatant was injected into the culture medium. The fermentation medium was prepared with peptone water (2 g/L), yeast extract (1 g/L), NaCl (0.1 g/L), K_2HPO_4 (0.04 g/L), KH_2PO_4 (0.04 g/L), $MgSO_4{\cdot}7H_2O$ (0.01 g/L), $CaCl_2{\cdot}2H_2O$ (0.01 g/L), $NaHCO_3$ (2 g/L), bile salts (0.5 g/L), L-cysteine hydrochloride (0.5 g/L), hemin (50 mg/L), vitamin K_1(10 μL/L), and Tween 80 (2 mL/L). After 15 mL of the fecal slurry was injected into 135 mL of the medium, pulse digesta was added to make 1% (w/v) of the total mixture, which was fermented under anaerobic conditions maintained by the oxygen-free nitrogen gas (15 mL/min). The fermentation was maintained at pH 6.7 at 37°C, and samples were retrieved every 0, 12, and 24 h. Non-substrate samples were produced as controls in which the pulse digesta was replaced with the distilled water. Additionally, fecal samples collected without the pretreatment process were analyzed for their microbiome abundance to verify that the *in vitro* model functioned appropriately and reflected the characteristics of the original fecal microbiota.

2.5.2 16S amplicon and shotgun metagenome sequencing for taxonomy analysis

Microbial sequencing and taxonomy profiling were performed by Macrogen, Inc. (Seoul, Korea) and Life Mining Lab., GIST (Gwangju, Korea). DNA was extracted using a DNeasyPowerSoil Kit (Qiagen, Germany) according to the manufacturer's instructions. The extracted DNA was quantified using Quant-IT PicoGreen (Invitrogen).

For 16S analysis, the sequencing libraries were prepared according to the Illumina 16S Metagenomic Sequencing Library protocols to amplify the V3 and V4 regions. The input gDNA 2 ng was PCR amplified with 5× reaction buffer, 1 mM of dNTP mix, 500 nM each of the universal F/R PCR primer, and Herculase II fusion DNA polymerase (Agilent Technologies, United States). The cycle condition for the first PCR was 3 min at 95°C for heat activation, and 25 cycles of 30 s at 95°C, 30 s at 55°C and 30 s at 72°C, followed by a 5-min final extension at 72°C. The universal primer pair with Illumina adapter overhang sequences used for the first amplifications were as follows: V3-F: 5′-TCGTCGGCAGCGTCAGATGTGTATAAGAGACAGCCTACGGGNGGCWGCAG-3′, V4-R: 5′-GTCTCGTGGGCTCGGAGATGTGTATAAGAGACAGGACTACHVGGGTATCTAATCC-3′. The first PCR product was purified with AMPure beads (Agencourt Bioscience, USA). Following purification, the 2 μL of the first PCR product was PCR amplified for final library construction containing the index using NexteraXT Indexed Primer. The cycle condition for the second PCR was the same as the first except for 10 cycles. The PCR product was purified with AMPure beads. The final purified product was then quantified using qPCR according to the quantification protocol guide (KAPA Library Quantification kits for IlluminaSequencing platforms) and qualified using the TapeStation D1000 ScreenTape (Agilent Technologies, Germany). The paired-end (2 × 300 bp) sequencing was performed by the Macrogen using the MiSeq™ platform (Illumina, USA). After sequencing, Cutadapt (v3.2) was utilized to remove adapter and primer sequences from the raw data, with forward and reverse reads trimmed to 250 bp and 200 bp. To generate Amplicon Sequence Variants (ASV) sequences, the reads were performed error-correction, merging, and denoising processes with DADA2 (v1.18.0). Sequences with expected errors of two or more were excluded. Erroneous reads were denoised based on an established error model. Following error correction, paired-end reads were merged by overlapping. Chimeric sequences were eliminated using the consensus method with the removeBimeraDenovo function in DADA2. ASVs with lengths shorter than 350 bp were filtered out using R (v4.0.3). The resulting ASVs were utilized for downstream analysis using QIIME (v1.9.0). Each ASV was aligned to the organism with the highest similarity in the corresponding Reference Database (NCBI_16S), using algorithms such as Bayesian classifier (DADA2_v1.18.0, confidence value: 50). Alpha and beta diversity metrices were calculated to elucidate the complexity and compositional changes of microbial genus both within and between individual samples. Alpha diversity was employed to quantify the richness and evenness of microbial communities within each sample, while beta diversity was utilized to assess the differences in microbial composition across samples.

For three pulse samples that exhibited a significant increase in genus-level diversity, additional species-level analysis was conducted using Shotgun method. The sequencing libraries were prepared according to the manufacturer's instructions of TruSeq Nano DNA High Throughput Library Prep Kit (Illumina). Briefly, 100 ng of genomic DNA was sheared using adaptive focused acoustic technology (Covaris) and the fragmented DNA is end-repaired to create 5′-phosphorylated, blunt-ended dsDNA molecules. Following end-repair, DNA was size selected with bead-based method. These DNA fragments go through the addition of a single 'A' base, and ligation of the TruSeq DNA UD Indexing adapters. The products are then purified and enriched with PCR to create the final DNA library. The libraries were quantified using qPCR according to the qPCR Quantification Protocol Guide (KAPA Library Quantification kits for Illumina Sequencing platforms) and qualified using the Agilent Technologies 4200 TapeStation D1000 screentape (Agilent technologies). Then we sequenced using the NovaSeq (Illumina). DNA Illumina HiSeq/NovaSeq raw data was demultiplexed by index sequences, and paired-end FASTQ files were generated for each sample after sequencing. Adapter sequences and data with an average phred quality score less than 20 were removed using Trimmomatic (v0.39) of the Kneaddata (v0.10.0) pipeline (option: SLIDINGWINDOW:4:20). Then, bowtie2 (v2.4.5) was used to remove the human genome sequences using the hg37dec_v0.1 reference (*Homo sapiens* reference genome). The pre-processed data were analyzed using MetaPhlAn4 (v4.0.0) for ~1 million microorganisms composed of NCBI reference genomes and species-level genome bins (SGBs). The reads were mapped to the specific marker genes of the microbial species, and the species abundance was calculated based on the average number of reads mapped to the marker genes. At this time, marker genes that mapped to less than 33% were removed as the species were considered absent. The taxonomic composition derived from the species abundance was presented by Krona (Ondov et al., 2011), a tool for calculating the relative proportions (%) of species

within each microbial genus. This analysis served as a reference for the subsequent discussions regarding the potential health implications associated with specific microbial genera.

2.5.3 Analysis of short-chain fatty acids (SCFAs) as microbial metabolites

Acetic acid, butyric acid, and propionic acid in the pulse digesta after intestinal fermentation were determined using HPLC Ultimate3000 (Thermo Dionex, United States) and RI detector (ERC, RefractoMAX520, Japan) at UV 210 nm. 10 μL aliquots of 0, 12, and 24 h fermentation samples were injected onto an ICSep Coregel 87H3 column (7.8 mm × 300 mm, concise separations, United States). The mobile phase was 0.01 N H_2SO_4 at a flow rate of 0.5 mL/min and an oven temperature of 40°C. Volatile organic acid mixture (AccuStandard FAMQ-004, 10 mM) containing formic, acetic, propionic, isobutyric, butyric, isovaleric, valeric, isocaproic, caproic, and heptanoic acid was the standard material for the analysis.

2.6 Statistical approach

All experiments were conducted in triplicate, and data entry, descriptive statistics, and the construction of bar graphs of the relative abundance of genera for each sample were performed using Microsoft Excel 2016 (Microsoft Corporation, Redmond, Washington, United States). All statistical tests, analyses, and visualizations, except those practiced by Excel were performed using RStudio (2023.12.1. +402 for Windows). To analyze differences in relative microbial abundances during colonic fermentation of digested pulse, a Wilcoxon rank-sum test (at the 95% confidence level) was used. For comparisons of α-diversity and β-diversity, the Shannon index (SI) was calculated for 0, 12, and 24 h fermentation samples of each pulse sample, and Bray-Curtis distances were used for multidimensional scaling (MDS) visualization. Significant differences in the nutrient contents and the SIs between samples were tested by ANOVA and Tukey's method ($p < 0.05$) and presented in a box plot. Principal component analysis (PCA) was performed to identify the distribution of nutrient content—carbohydrates, amino acids, and fatty acids—within the digested pulse samples, selecting principal components with an accumulated variance greater than 80% and generating a biplot expressing loadings and scores. Primary variables for the network analysis were chosen from the factor analysis conducted on the carbohydrates, amino acid, and fatty acid content, as well as on the difference in absolute microbial abundance between 0 h and 12 h samples. Variables with a loading of ≥0.5 were selected, and only edges with a correlation >0.5 were included in the positive correlation network, while edges with a correlation < −0.5 were included in the negative correlation network. The centrality of each variable in the network analysis was calculated and represented by the size of the nodes. Communities within the network were identified using the Infomap method and displayed in different colors.

3 Results

3.1 Free carbohydrate, amino acid, and fatty acid contents in digested pulses

The degraded forms of carbohydrates in the pulses subjected to digestion were quantified, followed by the oral, gastric, small intestinal phases, and dialysis phases (Supplementary Table S1). During the digestive process, carbohydrates with high molecular weight were broken down into monosaccharides, and most of the low molecular weight compounds were eliminated by dialysis. However, some undigested oligosaccharides, such as stachyose, remained in the samples. The stachyose content in the digested samples of CB, CP, and BB was 63.84 ± 1.80 μg, 58.56 ± 0.99 μg, and 42.17 ± 0.45 μg, respectively, while 9.14 ± 0.57 μg of raffinose remained only in the digested BB. The monosaccharide glucose was detected in the digested samples of KB, CP, and CB at concentrations of 246.77 ± 1.93 μg, 228.95 ± 1.24 μg, and 206.96 ± 0.77 μg, respectively. Based on the PCA biplot (Figure 1A), samples other than KB, CP, CB, and BB contained relatively lower amounts of free saccharides.

Free amino acid content was also examined after proteins were degraded during the digestion process and subsequently filtered through dialysis phases. The consistent directionality of the loading vectors on the PCA biplot (Figure 1B) corresponding to each amino acid suggests a positive correlation in amino acid content across the samples. Notably, the loading vectors for glutamine, ornithine, and citrulline deviated slightly from the direction observed for other

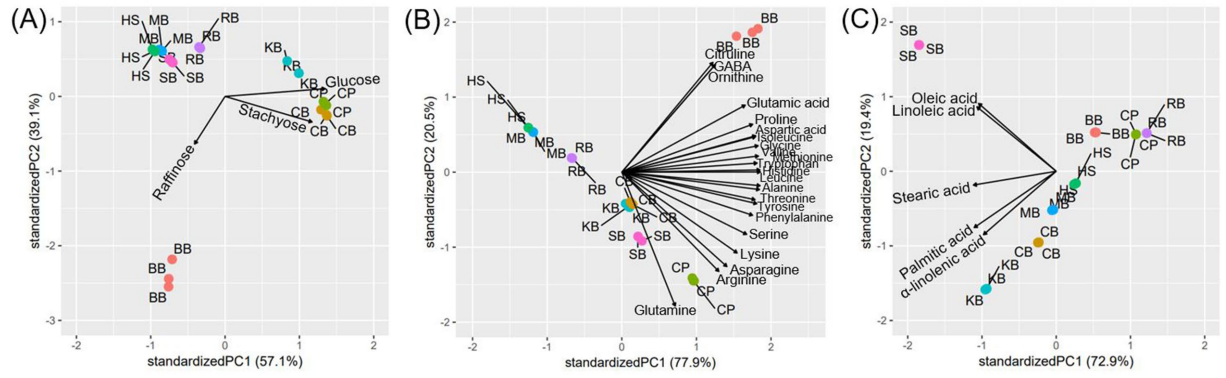

FIGURE 1
PCA biplot of the content of free saccharides **(A)**, amino acids **(B)**, and fatty acids **(C)** contents in the digested samples of eight pulses.

amino acids, indicating the possibility of differential levels of these amino acids in some pulses. Overall amino acid levels in eight pulses were high at glutamine, arginine, phenylalanine, and leucine (Supplementary Table S2). Specifically, glutamine showed particularly high levels, with contents of 92.05 ± 3.93 μg, 30.76 ± 0.13 μg, 23.80 ± 0.26 μg, 23.53 ± 0.36 μg, 20.54 ± 0.19 μg in the digested samples of BB, CP, CB, SB, and KB. Arginine also showed high concentrations of 27.60 ± 0.18 μg and 19.99 ± 0.23 μg in the digested CP and SB samples, while phenylalanine was present at levels of 21.76 ± 0.19 and 17.57 ± 0.73 in the CP and BB samples. Similarly, leucine was found in high concentrations of 27.62 ± 1.19 μg, and 23.39 ± 0.09 μg in BB and CP digesta, indicating that CP and BB digesta contained the highest overall levels of amino acids. As confirmed by the PCA plot (Figure 1B), relatively lower levels of amino acids were observed in samples from RB, KB, MB, and HS. Ornithine and citrulline were exclusively detected in the digested BB sample.

For free fatty acids, they were largely eliminated after dialysis, with only trace amounts remaining in the samples. According to the PCA plot (Figure 1C), the digested samples of BB, RB, and CP had the lowest fatty acid contents. In contrast, the digested SB sample contained the highest levels of oleic acid (10.02 ± 0.01 μg) and linoleic acid (25.27 ± 0.01 μg) (Supplementary Table S3). The digested KB sample also had a relatively high level of free fatty acids, with palmitic acid (3.67 ± 0.00 μg) and α-linolenic acid (5.51 ± 0.01 μg) present at higher levels compared to the other pulses.

3.2 Microbial taxonomic analysis of *in vitro* fermentation samples

The eight different digested pulses were cultured using an *in vitro* gut fermentation model, and products were collected at 0, 12, and 24 h in each pulse digesta. After collection, the genus-level 16S (V3-V4) rRNA sequencing and taxonomic profiling were performed, and the relative abundance of microbes was visualized in a bar plot chart (Figure 2). In the initial (0 h) colonic fermentation of the BB digesta, *Enterobacter* represented approximately 40% of the total gut microbiota, while the *Prevotella 9* lineage accounted for around 15%. However, as the fermentation progressed, both *Enterobacter* and *Prevotella 9* decreased in their portion, while *Escherichia-Shigella*, *Fusobacterium*, and *Bacteroides* increased, resulting in a simplified microbial community.

Besides, in the CB digesta, the initial microbial composition displayed a distribution of the diverse genus, including *Prevotella 9*, *Faecalibacterium*, *Blautia*, and *Bacteroides*, each representing about 15% of the community. But, over fermentation time, *Escherichia-Shigella*, *Bifidobacterium*, and *Bacteroides* dominated the community. This trend of simplification of the microbial composition was particularly pronounced in the CP digesta, with a remarkable increase in *Escherichia-Shigella* and *Bacteroides*, which came to account for a large portion of the microbial community. Similar patterns were observed during the fermentation of the KB digesta, where the relative abundance of *Bifidobacterium* increased.

Although the SB digesta initially contained a diverse community, with *Alistipes*, *Akkermansia*, *Bacteroides*, *Aquamonas*, and various *Eubacterium* groups comprising a substantial proportion, the *Eubacterium* groups increasingly constituted the community as fermentation progressed. In particular, *Akkermansia* gradually decreased during fermentation. Overall, a common trend was observed in the fermentation of BB, CB, CP, and KB digesta, characterized by an increase in the relative abundance of *Escherichia-Shigella*, *Bacteroides*, and *Clostridium sensu stricto 1*, along with a decrease in *Blautia*.

In the fermentation of HS digesta, a marked decrease in the relative abundance of *Escherichia-Shigella*, which comprised about

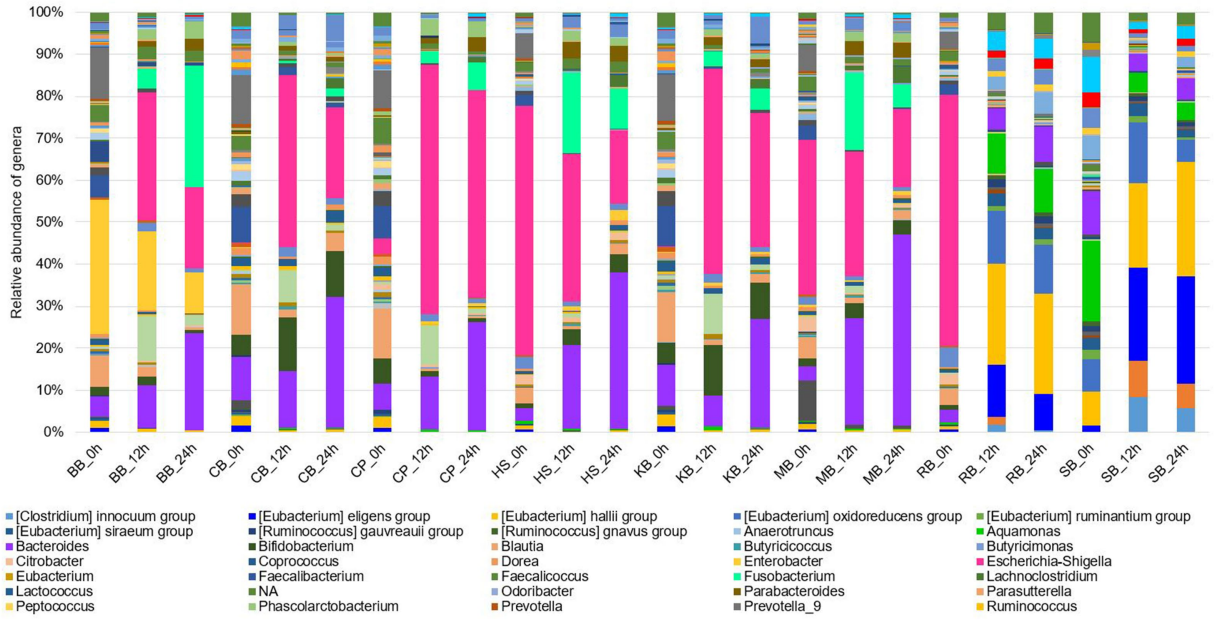

FIGURE 2
Composition of the gut microbiota of *in vitro* fermentation samples (0 h, 12 h, 24 h) of eight pulses at the genus level.

60% of the primary microbial community, was observed over time. Concurrently, the proportions of *Bacteroides*, *Fusobacterium*, and *Bifidobacterium* increased. A similar pattern was found in the fermentation of MB digesta, with a decline in the relative abundance of *Bacillus* and an increase in *Bifidobacterium*. An inverse relationship between the relative abundances of *Escherichia-Shigella* and *Bacteroides* was identified in most pulse digesta.

During the fermentation of RB digesta, the relative abundance of *Escherichia-Shigella* decreased significantly, while the portions of *Bacteroides* and the *Eubacterium* groups increased. This trend was consistent with the results seen in the SB digesta where *Eubacterium oxidoreducens*, *Eubacterium hallii*, and *Eubacterium eligens* groups collectively accounted for approximately 45% of the microbial community at the 12 h and 24 h time points. Furthermore, unlike the other pulses, RB digesta showed an increase in the relative abundance of *Aquamonas*, *Alistipes*, and *Akkermansia*. While *Aquamonas* is prevalent in environmental materials such as water and has not been studied in the context of human health or food samples, the positive health effects of *Alistipes* and *Akkermansia* are described in the discussions of Table 1.

Furthermore, diversity analyses were conducted to provide a quantitative framework the patterns of microbial variability among the samples that were illustrated in the aforementioned bar plot. The α-diversity (SI) of the pulse samples at each *in vitro* fermentation time was calculated to assess the genus complexity of the fecal microbiota within each pulse (Figure 3). In most samples, there was a decrease in

TABLE 1 The relative abundance of genera which exhibited a significant increase at 12 or 24 h of fermentation compared to the initial time point (0 h) for three pulse samples.

Genus[a]	RB %	HS %	MB %
Bacteroides	6.94 ± 1.62	28.57 ± 8.51	35.44 ± 10.02
Bifidobacterium	0.04 ± 0.01	4.07 ± 0.42	3.42 ± 0.05
Fusobacterium	0.06 ± 0.01	14.43 ± 4.76	11.84 ± 6.72
Parabacteroides	ND[b]	3.83 ± 0.26	3.63 ± 0.02
Parasutterella	ND[b]	0.10 ± 0.00	0.08 ± 0.02
Phascolarctobacterium	ND[b]	2.21 ± 0.29	2.04 ± 0.06
Sutterella	ND[b]	2.80 ± 0.18	2.57 ± 0.26
Alistipes	4.54 ± 0.30	0.60 ± 0.34[c]	0.66 ± 0.15
Butyricimonas	0.09 ± 0.00[c]	0.10 ± 0.02	0.08 ± 0.00[c]
Enterobacter	0.11 ± 0.01	1.74 ± 0.69	0.35 ± 0.29[c]
Coprococcus	–	0.77 ± 0.45[c]	0.76 ± 0.19[c]
Odoribacter	ND[b]	0.08 ± 0.02[c]	0.27 ± 0.11
Akkermansia	2.11 ± 0.30[c]	0.09 ± 0.01	0.30 ± 0.01
Lachnoclostridium	ND[b]	1.59 ± 1.30[c]	2.48 ± 1.32

[a]Listed all genus taxa in RB or HS or MB that had a significant increase in relative abundance after 12 or 24 h of fermentation compared to 0 h (Wilcoxon's rank-sum test, $p < 0.05$).
[b]ND, Not Detected.
[c]There was no significant increase in the relative abundance at 12 or 24 h in comparison to 0 h.

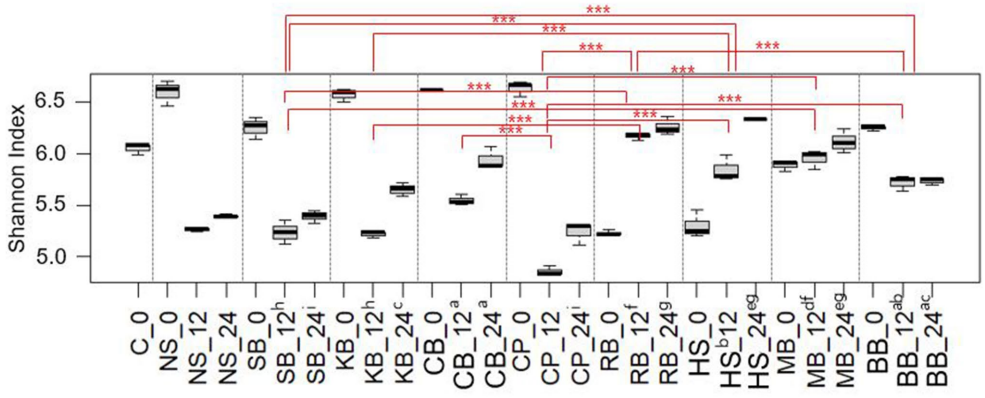

FIGURE 3
The change in Shannon indices of each pulse sample over fermentation hour (0 h, 12 h, 24 h). Samples with significant differences in Shannon indices at both 12 h and 24 h fermentation were connected by red lines and are indicated with their significance levels (***$p < 0.001$). Samples without significant differences were designated with the same alphabet. The C (control) and NS (non-substrate) samples were excluded from the significance test.

diversity at 12 h of colonic fermentation compared to 0 h, with a slight increase observed at 24 h. However, in RB, HS, and MB, diversity consistently increased over time. The mean SIs at 0 h and 12 h for each sample were as follows: SB 6.25 and 5.24, KB 6.57 and 5.22, CB 6.60 and 5.54, CP 6.63 and 4.86, and BB 6.24 and 5.72, with a similar range of decrease. In contrast, the diversity increased from 5.23 to 6.17 in RB, from 5.30 to 5.84 in HS, and from 5.89 to 5.95 in MB, indicating an upward trend in these three pulses.

The β-diversity of the microbial communities was analyzed using Bray-Curtis distances between samples (Figure 4). Based on the calculated distances, a general distribution was observed by the MDS method, which exerted significant shifts in the composition of the gut microbiota at either 12 or 24 h of fermentation compared to 0 h in all pulse samples. Since KB, CB, CP, BB, and SB showed a decrease also in α-diversity as fermentation progressed, it was suggested that the digestive residues of these samples reduced the richness of the microbial distribution in the colon, simultaneously altering the composition of the microbiota. However, RB, HS, and MB digesta positively influenced the distribution of a variety of microorganisms during colonic digestion.

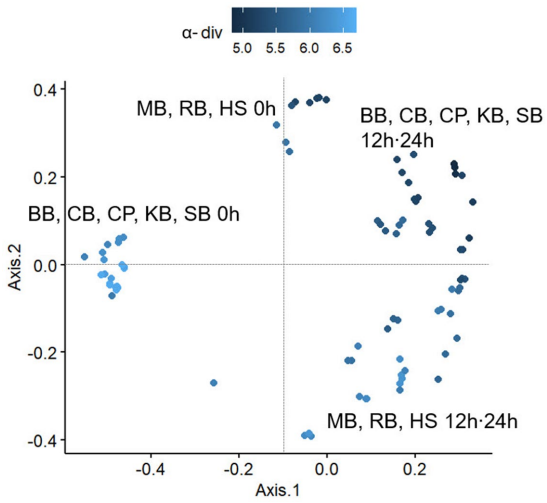

FIGURE 4
The plot based on a multidimensional scaling (MDS) analysis of the Bray-Curtis distances between pulse samples taken at each fermentation hour (0 h, 12 h, 24 h). BB, black bean; CB, cowpea; CP, chickpea; HS, Heunguseul; KB, kidney bean; MB, mung bean; RB, red bean; SB, soybean.

Changes in gut microbiome genera were observed in three pulses where health-positive bacteria increased during colonic digestion (Table 1). As the relative abundances of *Bacteroides*, *Bifidobacterium*, and *Fusobacterium* were found to be increased by colonic fermentation in all three samples, the relative growth of *Coprococcus* and *Lachnoclostridium* was uniquely depicted in RB, while *Odoribacter* and *Akkermansia* were specifically increased in MB. The species-level analysis performed by Shotgun whole genome sequencing for these genera (Figure 5) showed that these genera contained only *O. splanchnicus* and *A. muciniphila*, respectively. Meanwhile, the proportions of *Alistipes* and *Lachnoclostridium* increased in both RB and MB. *Alistipes* belongs to a relatively recently discovered sub-branch genus within the phylum Bacteroidetes. The Shotgun sequencing identified the following four species for *Alistipes*: *A. onderdonkii* (69%), *A. shahii* (19%), *A. senegalensis* (5%), and *A. finegoldii* (4%).

The relative abundances of *Sutterella* and *Akkermansia* also increased in MB and HS, while the relative growth of *Enterobacter* was promoted in RB and HS. In the case of *Enterobacter*, only *E. hormaechei* constituted a minute fraction, comprising 0.003% of the entire Enterobacteriaceae family.

3.3 Comprehensive correlations between nutrients, microbiome growth, and metabolite production

3.3.1 Positive correlation networks

A network analysis was conducted to explore positive interrelationships between nutrient content of eight digested pulses, microbiome changes, and metabolite production in the pulses after 12-h colonic fermentation (Figure 6A). The analysis revealed

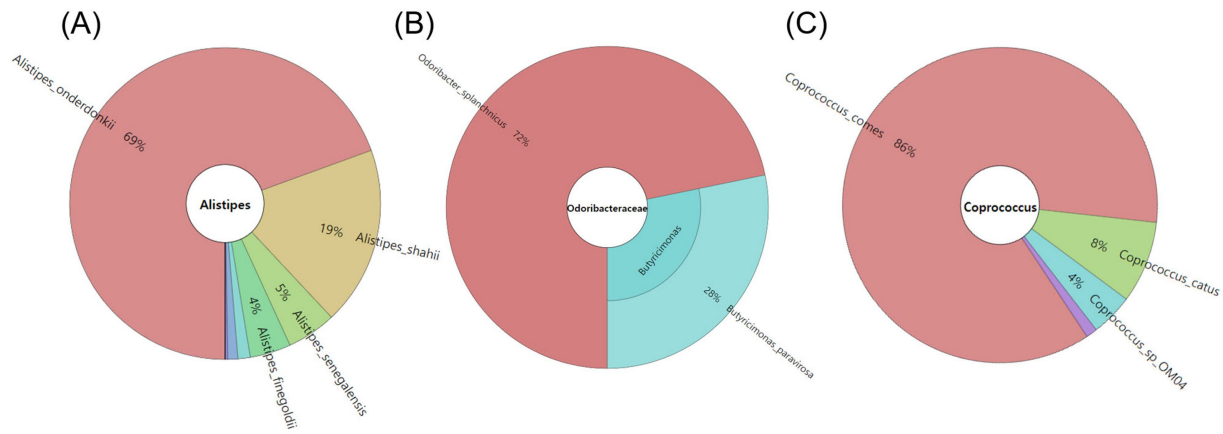

FIGURE 5
The taxonomic classification of species within the genus demonstrated a significant increase in relative abundance during the fermentation of HS **(A)**, MB **(B)**, and RB **(C)** digesta.

significant interconnectivity among nutrients, particularly amino acids and sugars, which exhibited high centrality and strong positive correlations.

In terms of changes in the microbiome, two major communities were identified. The first community, comprising *Faecalibacterium*, *Bifidobacterium*, *Agathobacter*, *Fusicatenibacter*, *Butyricoccus*, *Desulfovibrio*, *Catenibacterium*, *Coprococcus*, and *Prevotella 9*, demonstrated complex positive correlations both within the group and with nutrient components. Notably, *Fusicatenibacter*, *CAG-56*, and *Bifidobacterium* showed positive correlations with α-linolenic acid (ALA), while *Anaerostipes* was influenced by amino acids, subsequently affecting the growth of *Blautia*, *Monoglobus*, and *Fusicatenibacter*. The second community, centered around *Pseudocitrobacter*, including *Lactococcus*, *Prevotella*, *Phascolarctobacterium*, *Escherichia-Shigella*, and *Citrobacter*, no strong correlations with the nutrients were observed. Among the metabolites, acetic acid exhibited strong positive correlations with amino acids and *Enterococcus*, while butyric acid was more strongly associated with microbial changes than nutrient components.

Further analysis of RB, MB, and HS samples, which showed markedly increased microbial diversity, revealed distinct patterns (Figure 6C). In comparison to the complete network, the *Pseudocitrobacter*-centered and fatty acid-based communities merged in these samples, displaying strong direct correlations between fatty

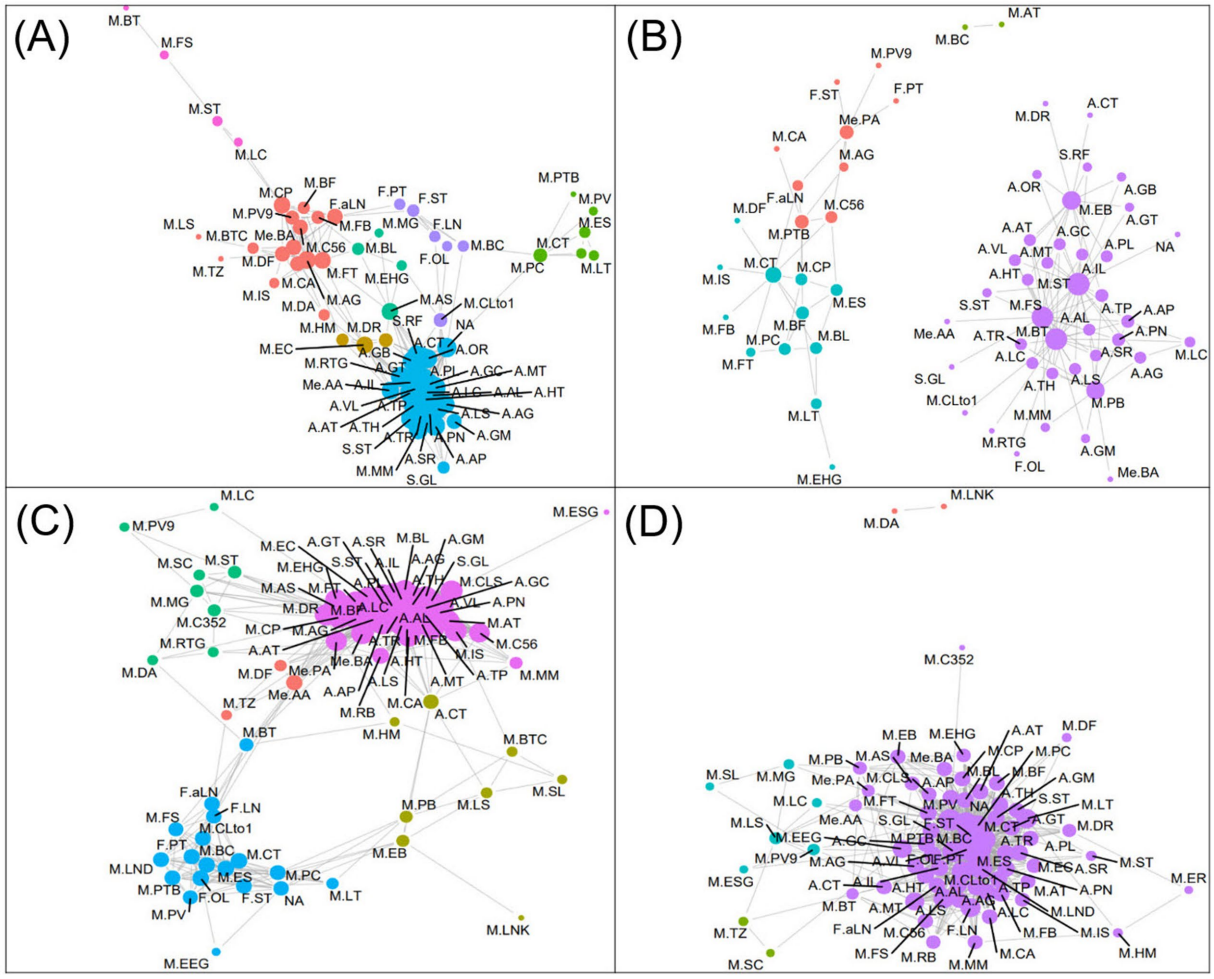

FIGURE 6
Positive **(A,C)** and negative **(B,D)** network analysis between the nutrient contents, microbial abundance changes (0 h–12 h), and metabolite contents produced by microbiota. The size of the nodes is indicative of the centrality of each variable, while the edges represent the correlation linkage. S.GL, glucose; S.ST, stachyose; S.RF, raffinose; A.GM, glutamine; A.LS, lysine; A.SR, serine; A.PN, phenylalanine; A.AP, asparagine; A.AG, arginine; A.TR, tyrosine; A.MT, methionine; A.AL, alanine; A.LC, leucine; A.TH, threonine; A.HT, histidine; A.TP, tryptophane; A.IL, isoleucine; A.AT, aspartate; A.OR, ornithine; A.CT, citrulline; A.GT, glutamate; A.GB, GABA; A.PL, proline; A.VL, valine; F.OL, oleic acid; F.LN, linoleic acid; F.ST, stearic acid; F.PT, palmitic acid; F.aLN, α-linolenic acid; M.AG, agathobacter; M.AT, alistipes; M.AS, anaerostipes; M.BC, bacillus; M.BT, bacteroides; M.BF, bifidobacterium; M.BL, blautia; M.BTC, butyricoccus; M.C352, CAG-352; M.C56, CAG-56; M.CA, catenibacterium; M.CT, citrobacter; M.CLto1, clostridium sensu stricto1; M.CLS, collinsella; M.CP, coprococcus; M.DF, desulfovibrio; M.DA, dialister; M.DR, dorea; M.EB, enterobacter; M.EC, enterococcus; M.ER, erysipelotrichaceae UCG-003; M.ES, escherichia-shigella; M.FB, faecalibacterium; M.FT, fusicatenibacter; M.FS, fusobacterium; M.HM, holdemanella; M.IS, incertae sedis; M.LC, lachnoclostridium; M.LS, lachnospira; M.LND, lachnospiraceae ND3007 group; M.LNK, lachnospiraceae NK4A136 group; M.LT, lactococcus; M.MM, megamonas; M.MG, monoglobus; NA, not identified; M.PB, parabacteroides; M.PTB, phascolarctobacterium; M.PV, prevotella; M.PV9, prevotella_9; M.PC, pseudocitrobacter; M.RB, romboutsia; M.SC, streptococcus; M.SL, subdoligranulum; M.ST, sutterella; M.TZ, tyzzerella; M.EEG, *eubacterium eligens* group; M.EHG, *eubacterium hallii* group; M.ESG, *eubacterium siraeum* group; M.RTG, ruminococcus torque group; Me.AA, acetic acid; Me.PA, propionic acid; Me.BA, butyric acid.

acids and microorganisms. Nutrient-microbe interactions were more frequent, indicating dense positive effects of nutrients on multiple microorganisms. Additionally, three metabolites had strong positive relations with amino acids and were particularly influenced by fatty acids such as α-linolenic acid.

In conclusion, the network analysis for RB, MB, and HS illustrated higher connectivity between communities and more extensive microbe-nutrient interactions compared to the complete network. This increase connectivity and interaction may explain the elevated microbial diversity observed in these three pulses, highlighting the complex interplay between nutrient composition and microbial ecology in pulse digestion and fermentation processes.

3.3.2 Negative correlation networks

The negative network revealed two distinct communities, with the most significant centrality observed in a community dominated by *Bacteroides*, *Fusobacterium*, *Sutterella*, and *Enterobacter*. These four bacteria were commonly associated with eight amino acids: aspartate, glycine, histidine, isoleucine, methionine, proline, tryptophan, and valine. *Sutterella* and *Enterobacter* also exhibited negative correlations with glutamate, GABA, and ornithine. It is noteworthy that despite the known ability of these microorganisms to metabolize amino acids as a primary energy source, they demonstrated strong negative correlations with these nutrients.

On the other hand, fewer microorganisms showed negative correlations with fatty acids. Notable examples included *Citrobacter* and *Phascolarctobacterium*, which negatively correlated with *α*-linolenic acid, and *Bacteroides*, which showed a negative association with oleic acid. Among metabolites, propionic acid had negative correlations with *Agathobacter*, *CAG-56*, and *Prevotella_9*, as well as with fatty acids such as α-linolenic acid, palmitic acid, and stearic acid. Additionally, acetic acid and butyric acid had direct negative correlations with *Fusobacterium* and *Parabacteroides*.

The negative correlation network analysis for RB, MB, and HS samples (Figure 6D) revealed a different pattern compared to the overall network. In these samples, there was no clear community separation, and the centrality of fatty acids was the most prominent. Unlike the general network (Figure 6B), strong negative correlations were observed between fatty acids and amino acids in RB, MB, and HS. This analysis also supported the findings from the positive network, indicating that the nutrient composition of RB, MB, and HS digesta played a significant role in negatively influencing the growth of several microorganisms. These results emphasize the complex and counterintuitive relationships between nutrients and microbial communities in pulse digestion and fermentation processes.

3.3.3 The linear relationship between nutrient composition and microbial diversity

In fact, nutrient analysis of the digesta from RB, MB, and HS demonstrated relatively small differences in fatty acid and amino acid content compared to the other pulses. For example, the average range of fatty acid content in the digesta of RB, MB, and HS was 0.04–0.16, 0.64–5.07, 0.22–1.70 μg, respectively, while KB, CB, and BB showed similar fatty acid content (0.82–5.51, 0.55–4.22, 0.41–3.10 μg) (Supplementary Table S3). However, the average amino acid content of KB, CB, and BB was significantly higher (1.85–20.54, 1.65–14.99, 0.10–92.05 μg) than that of RB, MB, and HS (0.24–10.38, 0.16–4.30, 0.14–2.78 μg) (Supplementary Table S2). Thus, it is suspected that a balanced nutrient profile, rather than one dominated by a single nutrient, may promote diverse and active microbial interactions.

To further investigate the quantitative relationship between nutrient balance and microbial diversity implied by the network analysis, linear regression analyses were performed (Figure 7). The coefficient of determination between changes in the SI from 0 h to 12 h and the principle component score (PC1) of each nutrient group (sugars, S_PC; amino acids, A_PC; fatty acids, F_PC) was examined. Results showed a strong inverse correlation between SI changes and

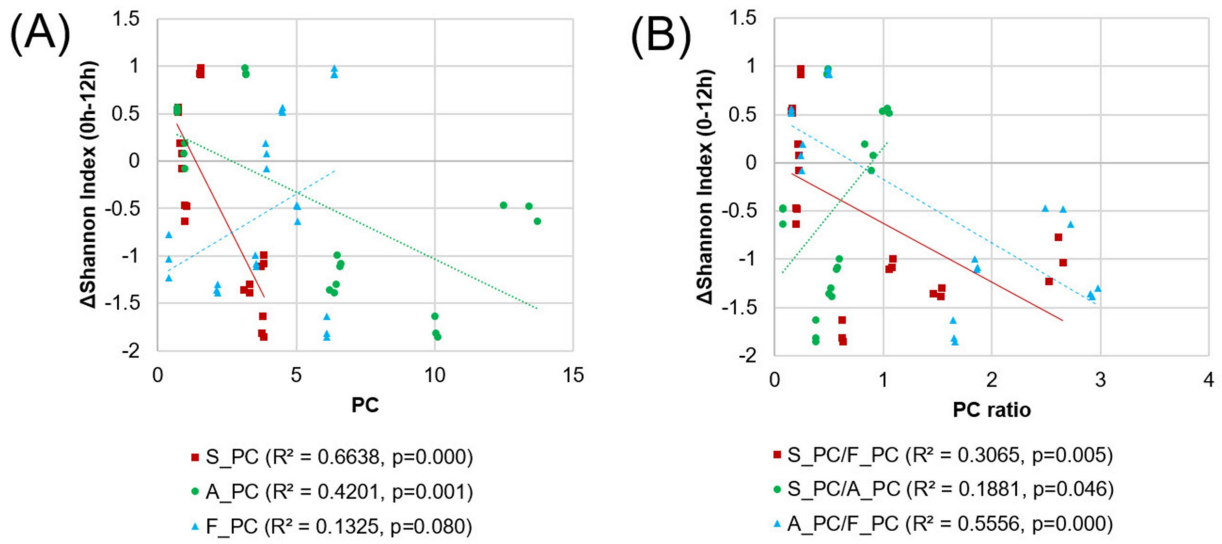

FIGURE 7
The linear regression analysis between the changes in the Shannon index for each pulse sample and the principal components of each nutrient **(A)** or their ratios **(B)**. The amino acid content data for SBs were identified as outliers and were subsequently excluded from the analysis.

sugars ($R^2 = 0.6638$, $p = 0.000$) and a moderate correlation with amino acids ($R^2 = 0.4201$, $p = 0.001$).

While the fatty acid content itself has a limited correlation with diversity ($R^2 = 0.1325$, $p = 0.080$), its ratio with other nutrients significantly influenced the gut environment (Figure 7B). The ratio of S_PC to F_PC had a moderate negative correlation with the SI change ($R^2 = 0.3065$, $p = 0.005$), while the A_PC to F_PC ratio was inversely related to SI change ($R^2 = 0.5556$, $p = 0.000$). The S_PC to A_PC ratio had a weak positive correlation ($R^2 = 0.1881$, $p = 0.046$). These results from quantitative analyses reinforce the findings from network analysis, implying the importance of nutrient balance in shaping microbial diversity.

4 Discussions

4.1 Health-affecting bacterial growth of *in vitro* gut fermentation samples

16S (V3-V4) rRNA sequencing and taxonomic profiling unveiled an enriched microbial community in RB, MB, and HS samples along with the fermentation time. Furthermore, there was a decrease in the relative abundance of health-negative genera such as *Escherichia-Shigella*, with an increase in beneficial bacteria including *Bacteroides* and *Eubacterium* groups. The term *Escherichia-Shigella* refers to both *Escherichia coli* and *Shigella*, which are genetically similar and difficult to be distinguished by 16S rRNA analysis. While most strains of *E. coli* are nonpathogenic and symbiotic in the human gut, *Shigella* is known to cause dysentery through intestinal infection (Wright et al., 2015; Xu et al., 2022). On the other hand, *Bacteroides*, although functionally diverse at the species level, plays a critical role in degrading complex carbohydrates in the gut, which supports intestinal immune function and homeostasis. Research has demonstrated that individuals with inflammatory bowel diseases (IBD), such as Crohn's disease and ulcerative colitis, tend to have higher *Escherichia-Shigella* and lower *Bacteroides* levels (Wright et al., 2015).

Eubacterium oxidoreducens is known to participate in the oxidation–reduction reactions of various organic compounds in the gut and has been studied for its health-promoting role in cancer research, including esophageal (Li et al., 2024) and small cell lung cancer (Yang et al., 2024). *Eubacterium hallii* is an important gut bacterium that produces short-chain fatty acids (SCFAs), such as butyrate and propionate, which serve as an energy source for intestinal cells (Engels et al., 2016) and have been reported to contribute to anti-inflammatory effects and improved insulin sensitivity (Mukherjee et al., 2020; Seegers et al., 2021). *Eubacterium eligens*, known for its anti-inflammatory properties, regulates intestinal immune responses in the gut and may have protective effects against inflammatory bowel disease (IBD) (Chung et al., 2017; Olendzki et al., 2022). All of these species are known to metabolize complex carbohydrates and dietary fiber as energy sources, suggesting that measuring the dietary fiber and oligosaccharide content of RB may help identify the specific factors influencing the growth of these microorganisms.

While RB, HS, and MB positively influenced the distribution of a variety of microorganisms during colonic digestion, diversity analyses revealed that both α- and β-diversity varied among the initial fermentation samples (0 h). It has been previously reported that environments with high microbial diversity are known to be resilient to microbial perturbations, and ecological theory posits that environments with low microbial diversity are inherently less receptive to the colonization of new microbial species, as reduced diversity limits the availability of ecological niches and competitive opportunities (Lozupone et al., 2012; Bourdeau-Julien et al., 2023). Nevertheless, the present results, where samples with initially high diversity experienced a decrease while those with low diversity saw an increase, illustrated that RB, MB, and HS may have significant factors that promote a favorable gut environment compared to the others.

Not only was diversity enhanced in the three pulses, but there was also a recognized growth of multiple health-promoting microbiota including *Bacteroides, Bifidobacterium*, and *Coprococcus*. *Bacteroides* spp. protect the gut microbiome from pathogens and provide an energy source (Zafar and Saier, 2021). Approximately 50% of the carbohydrate in pulses is starch, which is converted to resistant starch (RS) during heat treatment. The metabolic capabilities of the gut microbiota vary depending on structural differences in RS, with RS4 consumption specifically known to increase the abundance of *Bacteroides* and *Bifidobacterium* (Kadyan et al., 2022).

Meanwhile, SCFA-producing *Coprococcus* (Nogal et al., 2021) has been found to grow with high quality diets. Since SCFAs are produced by the metabolism of anti-inflammatory bacteria that participate in energy synthesis in the human body, increasing the abundance of *Coprococcus* may help the growth of beneficial gut microbiomes (Laitinen and Mokkala, 2019). *Coprococcus* and *Lachnoclostridium*, along with *Lachnospira*, belong to the family *Lachnospiraceae*, which, according to NCBI, consists of 58 genera and several unclassified strains (Vacca et al., 2020). *C. comes*, consisting of 86% of *Coprococcus* genera, is a beneficial butyrate-producing bacterium found in the human gut. Butyrate, one of its major metabolic byproducts, plays a pivotal role in maintaining the intestinal barrier, reducing inflammation, and facilitating gut health. Studies have linked *C. comes* to positive outcomes in mental health, particularly in reducing symptoms of depression, due to its involvement in the gut-brain axis (Notting et al., 2023). Moreover, butyrate production by *C. comes* has been associated with anticancer properties, particularly in protecting against colorectal cancer by supporting the gut epithelium and regulating inflammatory processes (Liu et al., 2024). *Clostridium symbiosum*, the only species detected in the genus *Lachnoclostridium*, contributes to the fermentation of dietary fiber and aids in the production of SCFAs such as butyrate, which supports gut barrier function and reduces inflammation. By producing SCFAs, it can regulate metabolism and immune responses, playing a protective role in metabolic conditions like type 2 diabetes and colorectal cancer (Wang et al., 2012; Ren et al., 2024). However, overgrowth of *C. symbiosum* has been observed in conditions of gut dysbiosis, which may be associated with diseases such as obesity and inflammatory bowel disease (IBD) (Rodríguez et al., 2020).

The fermentation of MB digesta led to an enhanced relative abundance of *Odoribacter*, while HS digesta promoted the proliferation of *Butrycimonas*. Previous studies have indicated that *Odoribacter*, *Butyricimonas*, and *Bacteroides* are positively related with human cognitive function and contribute to the anti-inflammatory pathway and the modulation of the immune system (Zeng et al., 2021). The beneficial gut bacterium *O. splanchnicus* is known to utilize dietary fiber and resistant starch as its primary energy source, producing short-chain fatty acids (SCFAs)

(Hiippala et al., 2020; Ren et al., 2024). During the fermentation of RB and MB, *Alistipes* showed a significant increase, with *Alistipes onderdonkii* emerging as the predominant species within this genus, and is recognized as a characteristic member of the gut microbiome with anti-inflammatory properties and involvement in the inhibition of tumor necrosis factor (TNF). It has been reported to play a beneficial role in cancer immunotherapy by modulating the tumor microenvironment (Parker et al., 2020; Li et al., 2023).

The genera *Sutterella* and *Enterobacter*, which showed increased abundance in HS and MB, and HS and RB respectively, are gut microbes with similar potential impacts on human health. *Sutterella* has been associated with inflammatory conditions such as irritable bowel syndrome (IBS) and autism spectrum disorders, suggesting that it may play a role in gut inflammation and immune modulation (Hiippala et al., 2016). On the other hand, *Enterobacter* species are opportunistic pathogens causing infection and dysbiosis, especially in immunocompromised individuals (Moreira de Gouveia et al., 2024). Both genera can affect gut homeostasis and contribute to disease states.

Besides, the relative abundance of *Akkermansia* significantly increased in HS and MB. *Akkermansia muciniphila* is one of the most abundant single species in the human gut microbiota, comprising 0.5–5% of the total bacteria. It degrades the mucin layer of the intestinal mucosa and produces beneficial metabolites such as acetate and propionate. Through this mechanism, *A. muciniphila* has been shown to reduce body fat mass and adipose tissue inflammation while improving insulin sensitivity, thereby enhancing gut barrier function (Cani and de Vos, 2017).

4.2 Nutrient-microbiome-metabolite network claims importance of nutrient balance for gut health

Protein degradation during pulse digestion led to a consistent increase in amino acid levels. The high interconnectivity between amino acids and sugars observed in the network analysis suggested that the pulses used in the experiment had proportional amounts of protein and carbohydrates. Fatty acids did not have direct positive networks with amino acids or sugars, indicating that the fat content of the pulses does not necessarily align with protein or carbohydrate level and may vary among the pulses.

In the positive correlation network of the eight pulses, few links were observed between microbes and nutrients. *Fusicatenibacter*, *CAG-56*, and *Bifidobacterium* were positively correlated with the fatty acid α-linolenic acid (ALA), while *Anaerostipes* was influenced by amino acids and associated with the growth of *Blautia*, *Monoglobus*, and *Fusicatenibacter*. Coakley et al. (2009) reported the ability of *Bifidobacterium* strains to convert linoleic acid to c9, t11-conjugated linoleic acid (CLA) and grow in the presence of anti-inflammatory ALA. Since the anti-inflammatory properties may create a favorable gut environment that is likely to foster the proliferation of SCFA-producing bacteria (Yang et al., 2023), the growth of SCFA-producing *Fusicatenibacter* (Pihelgas et al., 2024) might have been affected by ALA. *Anaerostipes*, a butyrate-producing genus, interacts with amino acids such as glutamate and lysine, which serve as substrates for SCFA production, especially butyrate, known for its anti-inflammatory effects (Singh et al., 2023) which can in turn promote the growth of *Fusicatenibacter*.

Cross-feeding interactions explain the correlations within this bacterial community, where one microbe's byproducts support the growth of others. These interactions, several bacteria degrade dietary components into intermediate metabolites such as acetate or lactate, which are then sequentially used as nutrient substrates by butyrate-producing bacteria. Rivière et al. (2016) reported relationships between acetate- or lactate-producing *Bifidobacterium* and butyrate-producing colonic bacteria, such as *Faecalibacterium prausnitzii* (clostridial cluster IV) and *Anaerostipes*. Accordingly, positive associations of the SCFA metabolite content with microbial alteration were more frequent than those with nutrient content. This may stress that the composition and activity of the gut microbiota are of paramount importance in determining the production of key metabolites.

Therefore, optimizing microbial conditions may yield greater advantages to gut health than focusing solely on individual nutrient contents. Recent studies have highlighted the potential of dietary interventions in modulating the gut microbiome by enhancing beneficial microbial populations or increasing the production of SCFA. For instance, Purdel et al. (2023) reported that fasting and/or time-restricted regimens can achieve gut health. Time-restricted fasting, intermittent fasting, and Ramadan fasting protocols were shown to increase *Akkermansia muciniphila* and *Bacteroidetes*, associated with improved metabolic health and reduced gut inflammation. Caloric restriction and alternate day fasting resulted in increased microbial diversity and promoted *Bacteroides* and SCFA production. In addition, water-only fasting and fasting-mimicking diets led to a high abundance of beneficial microbes like *Lactobacillus* and *Bifidobacterium*, improving immune function and gut health.

The synergistic role of prebiotics—indigestible dietary fibers that provide food for beneficial bacteria—with probiotics in promoting a diverse and stable gut microbiome has also been emphasized (Shang et al., 2024). Combining probiotic-rich meals with prebiotic fibers enhances intestinal permeability defenses through SCFA production, maintaining stability in gut flora despite dietary or environmental changes. A previous study by Starke et al. (2023) reported that amino acid-cross-feeding bacteria contribute to the compositional stability of the gut microbiome, with no evidence that dietary amino acid intake affects the frequency of auxotrophy, suggesting that simple manipulation of nutrient content may not be sufficient to regulate microbial-nutrient metabolic pathways.

In the negative network analysis of the eight pulses, a community centered around *Bacteroides*, *Fusobacterium*, *Sutterella*, and *Enterobacter* exhibited the greatest centrality and had strong correlations with amino acids. These findings were on the opposite side with previous studies that have identified various taxa involved in amino acid metabolism, including nitrogen metabolism and the tricarboxylic acid (TCA) cycle (Kanehisa et al., 2023), implying the positive relationships between those microbes and amino acids. For example, some *Enterobacter* and *Sutterella* species are engaged in the glutamate metabolism of the TCA cycle, producing glutamine as a byproduct. The pathway also includes the conversion of glutamate to GABA, suggesting that a decrease in glutamate might lead to a reduced GABA level (Kanehisa et al., 2023). Given

that no relationships were recognized for these bacteria with amino acids even in the positive network of present study, it was discerned that an imbalance in the overall nutritional state provoked by amino acids may have created an unfavorable gut environment for bacterial growth. Despite their reliance on amino acids for energy, their metabolism can produce toxic byproducts such as ammonia and hydrogen sulfide. These substances can disrupt gut homeostasis, contribute to dysbiosis, and negatively affect the balance of microbial populations (Lin et al., 2017).

4.3 Quantitative relationships among carbohydrates, amino acids, and fatty acids modulating the gut environment depend on context-rule

The positive and negative networks for RB, MB, and HS had higher connectivity between communities, with a broader range of microbes interacting directly or indirectly with fatty acids and amino acids compared to the complete network. This could interpret the improved microbial diversity observed in these three pulses. Since the three pulses comprising the subset network were not identified for their nutrient abundance, it was proposed that the overall nutritional status in RB, MB, and HS influenced the nutrient-microbe interactions.

Evidence from this study insists that facilitating a gut environment driven by the comprehensive nutrient balance, rather than individual nutrients, promotes eubiosis, thereby enhancing microbial diversity and stimulating the growth of beneficial microorganisms. In fact, the linear regression demonstrated the quantitative relationship between nutrient content and microbial diversity. Excess sugars and amino acids were found to negatively affect the gut environment, with a weak correlation between fatty acids and the SI. However, fatty acid content as a ratio to sugars or amino acids significantly influenced gut microbial diversity. Consequently, the nutritional context-dependence for maintaining gut health was highlighted by elucidating the importance of avoiding overconsumption of sugars and amino acids while maintaining a balance with fatty acids. In the human colon, an overload of certain nutrients can promote the overgrowth of specific microorganisms, which can disrupt the environment for others and reduce overall microbial diversity. Amino acids, in particular, can facilitate the growth of pathogenic amino-acid-degrading bacteria, such as *Clostridium*, and produce metabolites such as ammonia, phenols, and amines that can alter gut pH.

A previous opinion by Rios-Covian et al. (2017) suggested the metabolic remodeling of the host and *Bacteroides* in response to dietary organic nitrogen/carbohydrate combinations. In addition, a study in mice by Holmes et al. (2017) described that the pattern of protein and carbohydrate intake drives diet-microbiome interactions. The interdependence of sugars and amino acids in the digested pulses used in this study obscured the association of the ratio of carbohydrates to amino acids with microbiota, which also emphasized the relevance of the context of the food matrices in determining microbiome metabolism. Although this study concluded that balancing fatty acids with sugars or amino acids is relevant to a healthy microbiome, the context-based effect may not be distinguished when examining food groups in which carbohydrates are predominant, such as fruits and vegetables. Therefore, elucidating the multidirectional connections between nutrients and microbes using a variety of food ingredients might notify the way to combine foods that complement each ingredient's nutritional benefits for gut microbiota health.

Several limitations need to be discussed in further studies. Although the primary energy source of microorganisms – saccharides, amino acids, and fatty acids—was quantified in this study, the content of complex carbohydrates such as dietary fiber, resistant starch, or a variety of oligosaccharides also needs to be analyzed. Functional food components including isoflavones could also be the other candidates, as their effects on human microbiome changes were reported (Aboushanab et al., 2022; Narduzzi et al., 2022). Furthermore, since a single food group, pulses, was studied in the present research, other food groups with diverse matrices containing various proportions of macronutrients should be examined to demonstrate the multifaceted interactions between nutrient components and microbial diversity.

5 Conclusion

This study elucidated the effects of nutrient intake from pulse consumption on the human microbiome and metabolite changes. Following the application of *in vitro* digestion and fermentation to pulses, 16S rRNA analysis revealed a reduction in harmful pathogenic microorganisms and a specific increase in beneficial bacteria in the RB, HS, and MB samples. In addition, SI and Bray-Curtis distance calculations indicated that these pulses enhanced gut microbial diversity that differed from the others. Network analysis and linear regressions examining the interaction between changes in microbial communities and the nutrient content of each sample suggested that this effect was due to the balanced nutrient profiles of the three pulses. However, this should not be interpreted to mean that other pulses are detrimental to gut health. As the present study was primarily limited to pulse digesta, this can be overcome in real-life dietary contexts by consuming a variety of food groups beyond pulses. Nevertheless, our research demonstrated that maintaining a diet rich in nutrient-balanced foods, including RB, HS, and MB, supports gut microbial diversity and an environment conducive to the growth of health-positive bacteria, such as *Alistipes*, *Akkermansia*, *Coprococcus*, and *Eubacterium* groups.

This pioneering study quantitatively investigated the extensive interdependence between key nutrients and gut microbiota dynamics. By applying food ingredients in their consumed forms to the replicated model of human digestion and gut microbiota, their contribution to microbial shifts and metabolite production could be explored, reflecting real-world conditions. There is a need to further examine the effects of commonly consumed individual ingredients in everyday meals—such as meat, fish, dairy products, fruits, and vegetables—on the gut microbiota. As more data accumulate, it may be possible to identify optimal food combinations for improving gut health. Additionally, *in vitro* fermentation model that simulates gastrointestinal conditions in patients with gut disorders could potentially provide tailored dietary recommendations for therapeutic purposes.

Data availability statement

The original contributions presented in the study are publicly available. This data can be found here: https://www.ncbi.nlm.nih.gov/, PRJNA1212984.

Ethics statement

The studies involving humans were approved by National Institute of Agricultural Sciences, Republic of Korea. The studies were conducted in accordance with the local legislation and institutional requirements. The participants provided their written informed consent to participate in this study.

Author contributions

DL: Data curation, Investigation, Methodology, Validation, Writing – original draft, Writing – review & editing. IH: Conceptualization, Data curation, Formal analysis, Project administration, Supervision, Visualization, Writing – original draft, Writing – review & editing.

Funding

The author(s) declare that financial support was received for the research, authorship, and/or publication of this article. This study was carried out with the support of the "Research Program for Agricultural Science & Technology Development (PJ016762)" by the National Institute of Agricultural Sciences. Rural Development Administration, Republic of Korea.

Conflict of interest

The authors declare that the research was conducted in the absence of any commercial or financial relationships that could be construed as a potential conflict of interest.

Generative AI statement

The authors declare that no Gen AI was used in the creation of this manuscript.

Publisher's note

All claims expressed in this article are solely those of the authors and do not necessarily represent those of their affiliated organizations, or those of the publisher, the editors and the reviewers. Any product that may be evaluated in this article, or claim that may be made by its manufacturer, is not guaranteed or endorsed by the publisher.

Supplementary material

The Supplementary material for this article can be found online at: https://www.frontiersin.org/articles/10.3389/fmicb.2024.1512217/full#supplementary-material

References

Aboushanab, S. A., Khedr, S. M., Gette, I. F., Danilova, I. G., Kolberg, N. A., Ravishankar, G. A., et al. (2022). Isoflavones derived from plant raw materials: bioavailability, anti-cancer, anti-aging potentials, and microbiome modulation. *Crit. Rev. Food Sci. Nutr.* 63, 261–287. doi: 10.1080/10408398.2021.1946006

Bae, H. G., Kim, S., Lee, J. C., and Kim, M. J. (2021). Evaluation of antioxidant activity and lipid oxidative stability of roasted buckwheat according to in vitro digestive system. *Korean Journal of Food Preservation.* 28, 612–620. doi: 10.11002/kjfp.2021.28.5.612

Bouayed, J., Hoffmann, L., and Bohn, T. (2011). Total phenolics, flavonoids, anthocyanins and antioxidant activity following simulated gastro-intestinal digestion and dialysis of apple varieties: bioaccessibility and potential uptake. *Food Chem.* 128, 14–21. doi: 10.1016/j.foodchem.2011.02.052

Bourdeau-Julien, I., Castonguay-Paradis, S., Rochefort, G., Perron, J., Lamarche, B., Flamand, N., et al. (2023). The diet rapidly and differentially affects the gut microbiota and host lipid mediators in a healthy population. *Microbiome.* 11:26. doi: 10.1186/s40168-023-01469-2

Cani, P. D., and de Vos, W. M. (2017). Next-generation beneficial microbes: the case of *Akkermansia muciniphila*. *Front. Microbiol.* 8:1765. doi: 10.3389/fmicb.2017.01765

Chung, W. S. F., Meijerink, M., Zeuner, B., Holck, J., Louis, P., Meyer, A. S., et al. (2017). Prebiotic potential of pectin and pectic oligosaccharides to promote anti-inflammatory commensal bacteria in the human colon. *FEMS Microbiol. Ecol.* 93:fix127. doi: 10.1093/femsec/fix127

Coakley, M., Banni, S., Johnson, M. C., Mills, S., Devery, R., Fitzgerald, G., et al. (2009). Inhibitory effect of conjugated α-linolenic acid from bifidobacteria of intestinal origin on SW480 cancer cells. *Lipids* 44, 249–256. doi: 10.1007/s11745-008-3269-z

Coker, J. K., Moyne, O., Rodionov, D. A., and Zengler, K. (2021). Carbohydrates great and small, from dietary fiber to sialic acids: how glycans influence the gut microbiome and affect human health. *Gut Microbes* 13, 1–18. doi: 10.1080/19490976.2020.1869502

Deehan, E. C., Yang, C., Perez-Muñoz, M. E., Nguyen, N. K., Cheng, C. C., Triador, L., et al. (2020). Precision microbiome modulation with discrete dietary fiber structures directs short-chain fatty acid production. *Cell Host Microbe* 27, 389–404.e6. doi: 10.1016/j.chom.2020.01.006

Didinger, C., and Thompson, H. J. (2022). The role of pulses in improving human health: a review. *Legume Sci.* 4:e147. doi: 10.1002/leg3.147

Engels, C., Ruscheweyh, H. J., Beerenwinkel, N., Lacroix, C., and Schwab, C. (2016). The common gut microbe *Eubacterium hallii* also contributes to intestinal propionate formation. *Front. Microbiol.* 7:713. doi: 10.3389/fmicb.2016.00713

Gong, X., Li, X., Xia, Y., Xu, J., Li, Q., Zhang, C., et al. (2020). Effects of phytochemicals from plant-based functional foods on hyperlipidemia and their underpinning mechanisms. *Trends Food Sci. Technol.* 103, 304–320. doi: 10.1016/j.tifs.2020.07.026

Han, X., Tian, H., Yang, L., and Ji, Y. (2024). Bidirectional Mendelian randomization to explore the causal relationships between the gut microbiota and male reproductive diseases. *Sci. Rep.* 14:18306. doi: 10.1038/s41598-024-69179-9

Hettiarachchi, H. A. C. O., Gunathilake, K. D. P. P., and Jayatilake, S. (2021). Effect of in-vitro gastrointestinal digestion and dialysis process on phenolic compounds and antioxidant capacity of selected underutilized fruits in Sri Lanka. *Trop. Agric. Res.* 32, 212–218. doi: 10.4038/tar.v32i2.8468

Hiippala, K., Barreto, G., Burrello, C., Diaz-Basabe, A., Suutarinen, M., Kainulainen, V., et al. (2020). Novel Odoribacter splanchnicus strain and its outer membrane vesicles exert immunoregulatory effects in vitro. *Frontiers in microbiology.* 11:575455. doi: 10.3389/fmicb.2020.575455

Hiippala, K., Kainulainen, V., Kalliomäki, M., Arkkila, P., and Satokari, R. (2016). Mucosal prevalence and interactions with the epithelium indicate commensalism of *Sutterella spp*. *Front. Microbiol.* 7:1706. doi: 10.3389/fmicb.2016.01706

Holmes, A. J., Chew, Y. V., Colakoglu, F., Cliff, J. B., Klaassens, E., Read, M. N., et al. (2017). Diet-microbiome interactions in health are controlled by intestinal nitrogen source constraints. *Cell Metab.* 25, 140–151. doi: 10.1016/j.cmet.2016.10.021

Jaagura, M., Viiard, E., Karu-Lavits, K., and Adamberg, K. (2021). Low-carbohydrate high-fat weight reduction diet induces changes in human gut microbiota. *Microbiologyopen.* 10:e1194. doi: 10.1002/mbo3.1194

Johnson, A. J., Zheng, J. J., Kang, J. W., Saboe, A., Knights, D., and Zivkovic, A. M. (2020). A guide to diet-microbiome study design. *Front. Nutr.* 7:79. doi: 10.3389/fnut.2020.00079

Kadyan, S., Sharma, A., Arjmandi, B. H., Singh, P., and Nagpal, R. (2022). Prebiotic potential of dietary beans and pulses and their resistant starch for aging-associated gut and metabolic health. *Nutrients* 14:1726. doi: 10.3390/nu14091726

Kanehisa, M., Furumichi, M., Sato, Y., Kawashima, M., and Ishiguro-Watanabe, M. (2023). KEGG for taxonomy-based analysis of pathways and genomes. *Nucleic Acids Res.* 51, D587–D592. doi: 10.1093/nar/gkac963

Karolkowski, A., Guichard, E., Briand, L., and Salles, C. (2021). Volatile compounds in pulses: a review. *Food Secur.* 10:3140. doi: 10.3390/foods10123140

Kim, H. S., Oh, K. Y., Lee, S. M., Kim, J. Y., Lee, S. H., Jang, J. S., et al. (2021). Effect of extraction methods on the quality of pomegranate juice and physiological activity. *Journal of Korean Society of Food Science and Nutrition.* 50, 136–148. doi: 10.3746/jkfn.2021.50.2.136

Laitinen, K., and Mokkala, K. (2019). Overall dietary quality relates to gut microbiota diversity and abundance. *Int. J. Mol. Sci.* 20. doi: 10.3390/ijms20081835

Lee, S. M., Park, H. J., Kim, H. S., Kim, J. Y., Lee, S. H., Jang, J. S., et al. (2019). Quality characterization by various juice extraction method and changes in physiological activities by in vitro digestion of Angelica keiskei, Brassica oleracea, and Oenanthe javanica vegetable juices. *Journal of Korean Society of Food Science and Nutrition.* 48, 718–727. doi: 10.3746/jkfn.2019.48.7.718

Li, Z., Rasic, M., Kwan, M., Sepulveda, M., McIntosh, C., Shastry, V., et al. (2023). Oral administration of the commensal Alistipes onderdonkii prolongs allograft survival. *American Journal of Transplantation.* 23, 272–277. doi: 10.1016/j.ajt.2022.11.011

Li, J., Gao, X., Sun, X., Li, H., Wei, J., Lv, L., et al. (2024). Investigating the causal role of the gut microbiota in esophageal cancer and its subtypes: a two-sample Mendelian randomization study. *BMC Cancer* 24:416. doi: 10.1186/s12885-024-12205-w

Lin, R., Liu, W., and Piao, M. (2017). A review of the relationship between the gut microbiota and amino acid metabolism. *Amino Acids* 49, 2083–2090. doi: 10.1007/s00726-017-2493-3

Liu, G., Tang, J., Zhou, J., and Dong, M. (2024). Short-chain fatty acids play a positive role in colorectal cancer. *Discov. Oncol.* 15:425. doi: 10.1007/s12672-024-01313-5

Lozupone, C. A., Stombaugh, J. I., Gordon, J. I., Jansson, J. K., and Knight, R. (2012). Diversity, stability, and resilience of the human gut microbiota. *Nature* 489, 220–230. doi: 10.1038/nature11550

Mandalari, G., Faulks, R. M., Rich, G. T., Lo Turco, V., Picout, D. R., Lo Curto, R. B., et al. (2008). Release of protein, lipid, and vitamin E from almond seeds during digestion. *J. Agric. Food Chem.* 56, 3409–3416. doi: 10.1021/jf073393v

Meslier, V., Laiola, M., De Filippis, F., Roume, H., Quinquis, B., Giacco, R., et al. (2020). Mediterranean diet intervention in overweight and obese subjects lowers plasma cholesterol and causes changes in the gut microbiome and metabolome independently of energy intake. *Gut* 69, 1258–1268. doi: 10.1136/gutjnl-2019-320438

Minekus, M., Alminger, M., Alvito, P., Ballance, S., Bohn, T. O. R. S. T. E. N., Bourlieu, C., et al. (2014). A standardised static in vitro digestion method suitable for food–an international consensus. *Food Funct.* 5, 1113–1124. doi: 10.1039/C3FO60702J

Moreira de Gouveia, M. I., Bernalier-Donadille, A., and Jubelin, G. (2024). Enterobacteriaceae in the human gut: dynamics and ecological roles in health and disease. *Biology* 13:142. doi: 10.3390/biology13030142

Mukherjee, A., Lordan, C., Ross, R. P., and Cotter, P. D. (2020). Gut microbes from the phylogenetically diverse genus *Eubacterium* and their various contributions to gut health. *Gut Microbes* 12:1802866. doi: 10.1080/19490976.2020.1802866

Narduzzi, L., Agulló, V., Favari, C., Tosi, N., Mignogna, C., Crozier, A., et al. (2022). (Poly) phenolic compounds and gut microbiome: new opportunities for personalized nutrition. *Microbiome Res. Rep.* 1:16. doi: 10.20517/mrr.2022.06

Nogal, A., Louca, P., Zhang, X., Wells, P. M., Steves, C. J., Spector, T. D., et al. (2021). Circulating levels of the short-chain fatty acid acetate mediate the effect of the gut microbiome on visceral fat. *Front. Microbiol.* 12:711359. doi: 10.3389/fmicb.2021.711359

Notting, F., Pirovano, W., Sybesma, W., and Kort, R. (2023). The butyrate-producing and spore-forming bacterial genus *Coprococcus* as a potential biomarker for neurological disorders. *Gut Microbiome* 4:e16. doi: 10.1017/gmb.2023.14

Oku, T., Tanabe, K., Ogawa, S., Sadamori, N., and Nakamura, S. (2011). Similarity of hydrolyzing activity of human and rat small intestinal disaccharidases. *Clin. Exp. Gastroenterol.* 4, 155–161. doi: 10.2147/CEG.S19961

Olendzki, B., Bucci, V., Cawley, C., Maserati, R., McManus, M., Olednzki, E., et al. (2022). Dietary manipulation of the gut microbiome in inflammatory bowel disease patients: pilot study. *Gut Microbes* 14:2046244. doi: 10.1080/19490976.2022.2046244

Ondov, B. D., Bergman, N. H., and Phillippy, A. M. (2011). Interactive metagenomic visualization in a web browser. *BMC Bioinformatics* 12:385. doi: 10.1186/1471-2105-12-385

Parker, B. J., Wearsch, P. A., Veloo, A. C. M., and Rodriguez-Palacios, A. (2020). The genus *Alistipes*: gut bacteria with emerging implications to inflammation, cancer, and mental health. *Front. Immunol.* 11:906. doi: 10.3389/fimmu.2020.00906

Pihelgas, S., Ehala-Aleksejev, K., Adamberg, S., Kazantseva, J., and Adamberg, K. (2024). The gut microbiota of healthy individuals remains resilient in response to the consumption of various dietary fibers. *Sci. Rep.* 14:22208. doi: 10.1038/s41598-024-72673-9

Purdel, C., Margină, D., Adam-Dima, I., and Ungurianu, A. (2023). The beneficial effects of dietary interventions on gut microbiota—an up-to-date critical review and future perspectives. *Nutrients* 15:5005. doi: 10.3390/nu15235005

Ren, Y. M., Zhuang, Z. Y., Xie, Y. H., Yang, P. J., Xia, T. X., Xie, Y. L., et al. (2024). BCAA-producing *Clostridium symbiosum* promotes colorectal tumorigenesis through the modulation of host cholesterol metabolism. *Cell Host Microbe* 32, 1519–1535.e7. doi: 10.1016/j.chom.2024.07.012

Rinott, E., Meir, A. Y., Tsaban, G., Zelicha, H., Kaplan, A., Knights, D., et al. (2022). The effects of the green-Mediterranean diet on cardiometabolic health are linked to gut microbiome modifications: a randomized controlled trial. *Genome Med.* 14:29. doi: 10.1186/s13073-022-01015-z

Rios-Covian, D., Salazar, N., Gueimonde, M., and de los Reyes-Gavilan, C. G. (2017). Shaping the metabolism of intestinal bacteroides population through diet to improve human health. *Front. Microbiol.* 8:376. doi: 10.3389/fmicb.2017.00376

Rivière, A., Selak, M., Lantin, D., Leroy, F., and de Vuyst, L. (2016). Bifidobacteria and butyrate-producing colon bacteria: importance and strategies for their stimulation in the human gut. *Front. Microbiol.* 7:979. doi: 10.3389/fmicb.2016.00979

Rodríguez, C., Romero, E., Garrido-Sanchez, L., Alcaín-Martínez, G., Andrade, R. J., Taminiau, B., et al. (2020). Microbiota insights in *Clostridium difficile* infection and inflammatory bowel disease. *Gut Microbes* 12:1725220. doi: 10.1080/19490976.2020.1725220

Ross, F. C., Patangia, D., Grimaud, G., Lavelle, A., Dempsey, E. M., Ross, R. P., et al. (2024). The interplay between diet and the gut microbiome: implications for health and disease. *Nat. Rev. Microbiol.* 22, 671–686. doi: 10.1038/s41579-024-01068-4

Sandua, D. (2024). The plant-based revolution. Independently published.

Seegers, J. F., Bui, T. P. N., and de Vos, W. M. (2021). Remarkable metabolic versatility of the commensal bacteria Eubacterium hallii and Intestinimonas butyriciproducens: Potential next-generation therapeutic microbes. *Probiotic Bacteria and Postbiotic Metabolites: Role in Animal and Human Health.*, 139–151. doi: 10.1007/978-981-16-0223-8_5

Shang, Z., Pai, L., and Patil, S. (2024). Unveiling the dynamics of gut microbial interactions: a review of dietary impact and precision nutrition in gastrointestinal health. *Front. Nutr.* 11:1395664. doi: 10.3389/fnut.2024.1395664

Shiowatana, J., Kitthikhun, W., Sottimai, U., Promchan, J., and Kunajiraporn, K. (2006). Dynamic continuous-flow dialysis method to simulate intestinal digestion for in vitro estimation of mineral bioavailability of food. *Talanta* 68, 549–557. doi: 10.1016/j.talanta.2005.04.068

Singh, V., Lee, G. D., Son, H. W., Koh, H., Kim, E. S., Unno, T., et al. (2023). Butyrate producers, "the sentinel of gut": their intestinal significance with and beyond butyrate, and prospective use as microbial therapeutics. *Front. Microbiol.* 13:1103836. doi: 10.3389/fmicb.2022.1103836

Starke, S., Harris, D. M., Zimmermann, J., Schuchardt, S., Oumari, M., Frank, D., et al. (2023). Amino acid auxotrophies in human gut bacteria are linked to higher microbiome diversity and long-term stability. *ISME J.* 17, 2370–2380. doi: 10.1038/s41396-023-01537-3

Sugihara, K., and Kamada, N. (2024). Metabolic network of the gut microbiota in inflammatory bowel disease. *Inflamm. Regen.* 44:11. doi: 10.1186/s41232-024-00321-w

Tso, R., and Forde, C. G. (2021). Unintended consequences: nutritional impact and potential pitfalls of switching from animal-to plant-based foods. *Nutrients* 13:2527. doi: 10.3390/nu13082527

Vacca, M., Celano, G., Calabrese, F. M., Portincasa, P., Gobbetti, M., and de Angelis, M. (2020). The controversial role of human gut lachnospiraceae. *Microorganisms.* 8:573. doi: 10.3390/microorganisms8040573

Valentino, V., Magliulo, R., Farsi, D., Cotter, P. D., O'Sullivan, O., Ercolini, D., et al. (2024). Fermented foods, their microbiome and its potential in boosting human health. *Microbial biotechnology.* 17:e14428. doi: 10.1111/1751-7915.14428

Valles-Colomer, M., Menni, C., Berry, S. E., Valdes, A. M., Spector, T. D., and Segata, N. (2023). Cardiometabolic health, diet, and the gut microbiome: a meta-omics perspective. *Nat. Med.* 29, 551–561. doi: 10.1038/s41591-023-02260-4

Wang, J., Qin, J., Li, Y., Cai, Z., Li, S., Zhu, J., et al. (2012). A metagenome-wide association study of gut microbiota in type 2 diabetes. *Nature* 490, 55–60. doi: 10.1038/nature11450

Wright, E. K., Kamm, M. A., Teo, S. M., Inouye, M., Wagner, J., and Kirkwood, C. D. (2015). Recent advances in characterizing the gastrointestinal microbiome in Crohn's disease: a systematic review. *Inflammatory bowel diseases.* 21, 1219–1228. doi: 10.1097/mib.0000000000000382

Xavier, A. A., and Mariutti, L. R. (2021). Static and semi-dynamic in vitro digestion methods: state of the art and recent achievements towards standardization. *Curr. Opin. Food Sci.* 41, 260–273. doi: 10.1016/j.cofs.2021.08.002

Xu, X., Ocansey, D. K. W., Hang, S., Wang, B., Amoah, S., Yi, C., et al. (2022). The gut metagenomics and metabolomics signature in patients with inflammatory bowel disease. *Gut Pathogens.* 14:26. doi: 10.1186/s13099-022-00499-9

Yang, J., Liu, S., Zhao, Q., Li, X., and Jiang, K. (2023). Gut microbiota-related metabolite alpha-linolenic acid mitigates intestinal inflammation induced by oral infection with *toxoplasma gondii*. *Microbiome.* 11:273. doi: 10.1186/s40168-023-01681-0

Yang, W., Fan, X., Li, W., and Chen, Y. (2024). Causal influence of gut microbiota on small cell lung cancer: a Mendelian randomization study. *The Clinical Respiratory Journal.* 18:e13764. doi: 10.1111/crj.13764

Zafar, H., and Saier, M. H. (2021). Gut bacteroides species in health and disease. *Gut Microbes* 13, 1–20. doi: 10.1080/19490976.2020.1848158

Zeng, Q., Yang, Z., Wang, F., Li, D., Liu, Y., Wang, D., et al. (2021). Association between metabolic status and gut microbiome in obese populations. *Microb. Genom.* 7:000639. doi: 10.1099/mgen.0.000639

frontiers | Frontiers in Microbiology

TYPE Original Research
PUBLISHED 04 February 2025
DOI 10.3389/fmicb.2025.1523586

Check for updates

OPEN ACCESS

EDITED BY
Mohammad Altamimi,
An-Najah National University, Palestine

REVIEWED BY
Hao Lizhuang,
Qinghai University, China
Irfan Ahmed,
Islamia University of Bahawalpur, Pakistan

*CORRESPONDENCE
Qingyong Shao
✉ shaoqingyong@163.com
Bai Xue
✉ xuebai68@163.com
Yina Ouyang
✉ yinaouyang@126.com

†These authors have contributed equally to this work

RECEIVED 06 November 2024
ACCEPTED 13 January 2025
PUBLISHED 04 February 2025

CITATION
Fu B, Zhao X, Khan M, Jiang Y, Li W, Mushtaq M, Danzeng B, Ni X, Azeem Z, Shao Q, Xue B and Ouyang Y (2025) Cecum microbiota composition, fermentation characteristics, and immunometabolic biomarkers of Yunshang black goat fed varying dietary energy and protein levels. *Front. Microbiol.* 16:1523586. doi: 10.3389/fmicb.2025.1523586

COPYRIGHT
© 2025 Fu, Zhao, Khan, Jiang, Li, Mushtaq, Danzeng, Ni, Azeem, Shao, Xue and Ouyang. This is an open-access article distributed under the terms of the Creative Commons Attribution License (CC BY). The use, distribution or reproduction in other forums is permitted, provided the original author(s) and the copyright owner(s) are credited and that the original publication in this journal is cited, in accordance with accepted academic practice. No use, distribution or reproduction is permitted which does not comply with these terms.

Cecum microbiota composition, fermentation characteristics, and immunometabolic biomarkers of Yunshang black goat fed varying dietary energy and protein levels

Binlong Fu[1†], Xiaoqi Zhao[1†], Muhammad Khan[1†], Yanting Jiang[1], Weijuan Li[1], Maida Mushtaq[1], Baiji Danzeng[1], Xiaojun Ni[1], Zobia Azeem[2], Qingyong Shao[1*], Bai Xue[3*] and Yina Ouyang[1*]

[1]Yunnan Animal Sciences and Veterinary Institute, Kunming, China, [2]Department of Zoology, University of Veterinary and Animal Sciences, Lahore, Pakistan, [3]Animal Nutrition Institute, Sichuan Agricultural University, Chengdu, China

Introduction: Ruminants including goats have diverse microcosms of microbiota involved in diet digestion, absorption, and assimilation. Moreover, it is well known that changes in dietary regimens including nutrient levels result in varied gut microbiota composition, and ultimately, the performance and health of these animals.

Methods: The current study examined the effects of varying dietary energy and protein levels on the cecal fermentation, immune biomarkers, and microbiota characteristics of 80 male Yunshan Black Goats (6 months, ~35.82 $\pm$ 2.79 kg), divided into four diets: 1) High Energy-High Protein (HEHP), 2) High Energy-Low Protein (HELP), 3) Low Energy-High Protein (LEHP), and 4) Low Energy-Low Protein (LELP). Twenty goats (five from each treatment group) were randomly slaughtered after a 50-day feeding trial, and cecal digesta and tissue were sampled for microbial analysis.

Results: The cecal content revealed that the high-energy groups (HEHP, HELP) had lower pH levels than the LEHP group ($p < 0.05$) and significantly higher valeric and isovaleric acid concentrations in HEHP. Although species richness (Chao1 index) remained consistent, the HEHP group showed higher diversity (Shannon and Simpson indices) than LEHP ($p < 0.05$). Dominant phyla included *Bacteroidetes* and *Firmicutes*; LEHP and LELP had significantly higher *Bacteroidetes* abundance than HELP, while HELP had higher *Firmicutes* abundance than LEHP ($p < 0.05$). *Verrucomicrobia* abundance was lower in LEHP than in HELP and LELP ($p < 0.05$). At the genus level, 311 genera were identified, with *Clostridium*, *Prevotella*, *unidentified_BS11*, and others showing significant variation. The HELP group had lower *unidentified_BS11* than LEHP and LELP, and higher *unidentified_Ruminococcaceae*, *Clostridium*, and *Lachnospiraceae* than LEHP ($p < 0.05$). VFA metabolism, absorption, cytokine expression, and tight junction protein mRNA in cecal tissue were also analyzed. Genes like MCT-1 and SLC16A4, linked to VFA absorption, positively correlated with *Paludibacter*, which was associated with immune markers (TLR-3, TLR-4, IFN-γ) and Occludin expression. In contrast, VFA-related genes and tight junction proteins negatively correlated with *unidentified Fibrobacterales*, suggesting a microbial role in adaptive immunity.

Conclusion: This study demonstrated that dietary energy and protein levels significantly influenced cecal fermentation, immune biomarkers, and microbiota composition in Yunshan Black Goats.

KEYWORDS

Yunshang black goat, dietary energy and protein, cecal microbiota composition, fermentation characteristics, immunometabolic biomarkers

1 Introduction

Ruminants including goats have multi-comparted stomach, which host a diverse and ecologically complex microbiome that is crucial to their digestive efficiency, health, and performance. In the rumen, this microbiome ferments a variety of carbohydrates sugars, starch, cellulose, hemicellulose, and pectin yielding carbon dioxide, methane, hydrogen, and volatile fatty acids (VFAs) (Salgado-Flores et al., 2016). However, accumulating evidence highlights the significant role of the hindgut and its microbial residents in maintaining ruminant health and productive efficiency (Gressley et al., 2011). Understanding the interactions between host and microbiome in the hindgut, particularly in the cecum, is critical as these relationships impact nutrient utilization, animal health, and reproductive performance (Gressley et al., 2011).

The cecum, a major fermentation site within the ruminant hindgut, is vital for nutrients digestion and intestinal health. Upon entry into the hindgut, undigested fiber components, such as cellulose and hemicellulose, undergo secondary fermentation by the cecal microbiome, producing VFAs that supply additional energy to the host and enhance feed utilization efficiency (Gressley et al., 2011). Additionally, the cecum contributes significantly to overall animal health, productivity, and welfare (Salgado-Flores et al., 2016). Unlike the rumen, the cecum lacks natural buffering mechanisms like protozoa and saliva, possesses a distinct epithelial structure, and has a limited capacity to neutralize low pH (Gressley et al., 2011).

The metagenomic studies have revealed that high-grain diets alter the composition and metabolism of the cecal microbiome and can induce mucosal damage (Slyter, 1976). The effects of nutritional imbalances on the cecal microbiome, epithelial metabolism, and immune responses in pregnant sheep are well established (Xie et al., 2021). However, the interactions between the cecal microbiome and fatty acid production, and the microbiome's response to dietary changes in protein and energy levels, remain poorly understood (Wu et al., 2023). Dietary protein levels that exceed the small intestine's absorptive capacity may increase bacterial protein fermentation in the hindgut, producing inflammatory metabolites linked to hindgut acidosis (Liu et al., 2014). Therefore, the current study hypothesized to investigate how changes in dietary energy and protein affect the composition and function of the cecal microbiome and their implications for gene expression in cecal epithelial tissues. Through quantitative PCR, we measure the expression of genes involved in VFA absorption and metabolism, cytokine production, and tight junction proteins. The current study aimed to deepen understanding of host-microbiome interactions in response to dietary shifts and offer valuable insights for optimizing the nutritional management of Yunshang black goats.

2 Materials and methods

2.1 Experimental site, animals, and study design

The current experiment was conducted at the Yunnan Academy of Animal Husbandry and Veterinary Sciences research facility, after approval from the ethical committee of the Yunnan Academy of Animal Husbandry and Veterinary Sciences (201911004). In this study, 80 male Yunshang Black Goats (approx. 6 months old, 35.82 ± 2.79 kg) were assigned to four diets in a completely randomized 2 × 2 factorial design: (1) high energy-high protein (HEHP), (2) high energy-low protein (HELP), (3) low energy-high protein (LEHP), and (4) low energy-low protein (LELP). The high-energy diets provided 9.74–9.76 MJ/kg, and high-protein diets contained 12.99–13.04% protein, while low-energy diets provided 8.14–8.18 MJ/kg, and low-protein diets contained 10.01–10.05% protein. After a 14-day adaptation, a 50-day feeding trial was conducted. Goats, housed individually in 1.5 × 2.0 m pens, had *ad libitum* feed and water access, with feed offered twice daily at 08:00 and 17:00, adjusting by 5% daily to ensure sufficient intake.

2.2 Slaughtering and sample collection

After the feeding trial, twenty goats (five from each treatment group) were randomly chosen, and were transported to the slaughtering facility early in the morning after a 24 h feed and water withdrawal. The goats were then electrically stunned and slaughtered following animal welfare guidelines. The digestive tract was dissected, and the cecum was isolated immediately. Cecal digesta samples were collected, with pH measured on-site using a pH meter (Testo-205, Germany). Samples were diluted with distilled water, centrifuged at 2000 g for 10 min, and the supernatant mixed with 25% (wt/vol) metaphosphoric acid (5 mL supernatant and 1 mL acid) before storage at -20°C for VFAs analysis via gas chromatography (GC-14B; Shimadzu, Japan). Cecal epithelium samples were washed with ice-cold phosphate-buffered saline and divided. One portion, cut into 0.4 × 0.4 cm sections, was stored at -80°C for RNA extraction, while the other was fixed in 4% paraformaldehyde for histomorphometric microscopy. Briefly, about 7 cm of cecum, was washed the chime on each tissue block with normal saline, and then fixed in 4% formaldehyde solution. The cecal sections were made by paraffin and hematoxylin–eosin (HE) staining, and the morphology of the cecal epithelium was observed by panoramic section scanner (3DHISTECH, PANNORAMIC, Hungary).

2.3 Cecal fermentation analysis

Cecal digesta VFAs were analyzed by gas chromatography (GC-14B; Shimadzu, Japan). Briefly, samples were diluted 1:5 with distilled water, centrifuged at 2000 g for 10 min, and the supernatant was mixed with 25% (w/v) metaphosphoric acid to assess VFA concentrations. The gas chromatograph, fitted with a 30 m × 0.32 mm × 0.25 μm capillary column, operated at a column temperature of 130°C, vaporization temperature of 180°C, and a flame ionization detector at 180°C. VFA molar proportions were calculated by dividing individual VFA concentrations by the total VFA concentration.

2.4 16S rRNA gene sequencing analysis of cecal digesta

Microbial RNA from cecal digesta was extracted using the cetyltrimethylammonium bromide (CTAB) method. The V3–V4 region of the 16S rRNA gene was amplified with universal primers 341F and 806R. Amplicons were purified with the AxyPrep DNA Gel Extraction Kit (Axygen Biosciences, United States), and sequencing libraries were prepared using the Illumina TruSeq DNA Sample Preparation Kit. Cluster generation, template hybridization, and amplification were performed with the TruSeq PE Cluster Kit and TruSeq SBS Kit, and sequencing was conducted on an Illumina MiSeq platform. Raw data were processed in QIIME (v1.9.0), with operational taxonomic units (OTUs) clustered at 97% similarity using UPARSE (v7.1) and chimeras removed via UCHIME. Taxonomic analysis of OTUs representatives was completed using the RDP Classifier (v2.2) with reference to the SILVA database (v132).

2.5 RNA extraction, reverse transcription, and qPCR analysis

All digesta and mucosa samples were thawed at 4°C. Approximately 200 mg of each sample was placed into 2 mL centrifuge tubes containing 0.2 g of bead powder. By the provided instructions, total RNA was extracted by employing the RNAiso Plus Total RNA Extraction Kit (TaKaRa, Dalian, China), and its integrity was examined via 1.5% agarose gel electrophoresis (Biowest Agarose, Spain). The concentration and OD value were determined using the NanoDrop 2000 UV–Visible Spectrophotometer (Thermo Fisher Scientific, Waltham, MA, United States). Eventually, cDNA was synthesized with the utilization of Oligo $(dT)_{18}$ primer (50 pmol/μL) and M-MLV reverse transcriptase (TaKaRa, Dalian, China) following the instructions (Table 1). The three internal reference genes, namely ACTB (entry number: NM_001290932), GAPDH (entry number: XM_006065800), and RPS23 (entry number: XM_006059350), were employed as controls in this study. Each PCR Strip & Caps tube was supplemented with 10 μL of dib® SYBR qPCR SuperMix Plus (Data Invention Biotech, ABC Biochemistry, China). Additionally, 0.8 μL of upstream and downstream primers (1 μM), 2 μL of template cDNA (100 ng/μL), and 6.4 μL of ddH_2O were prepared using the iQ^5 Real-Time PCR system (Bio-Rad Laboratories, United States) for RT-qPCR analysis with three replicates for all data. The experimental procedure involved predenaturation at 95°C for 30 s, denaturation at 95°C for 5 s, annealing at 60°C for 30 s, and extension at 72°C for 30 s over a total of 40 cycles. Finally, the calculation method of $2^{-\triangle\triangle Ct}$ was used for relative quantitative analysis. Relative quantitative analysis was conducted using the ΔΔCt method, where $\Delta Ct = Ct_{(target\ gene)} - Ct_{(geometric\ mean\ of\ internal\ reference\ gene)}$ and $\Delta\Delta Ct = \Delta Ct - \Delta Ct_{(median)}$.

2.6 Bioinformatics and statistical analysis

The Shapiro–Wilk and Bartlett tests were performed using R software version 3.5.1 (R Core Team, Vienna, Austria) to evaluate the normality and homogeneity of variance across all data distributions. Initial data processing was conducted in Excel 2016, followed by analysis using SPSS v24 statistical software. For the α diversity index, Student's *t*-test was applied. Additionally, a one-way analysis of variance (ANOVA) was conducted, with the least significant difference (LSD) test employed for multiple comparisons. Spearman's correlation coefficient was calculated to assess correlations between microbial species and intestinal metabolites. Data of qPCR were analyzed using GraphPad Prism (Version 9.0.0, San Diego, California, United States) for visualization purposes, and an independent sample T-test was utilized to determine statistical significance ($p < 0.05$).

3 Results

3.1 Cecal fermentation characteristic

The dietary protein and energy levels have influenced ($p < 0.05$) the cecal fermentation of the goats (Figure 1). The pH levels in the HEHP and HELP groups were notably lower compared to the LEHP group ($p < 0.05$), while no significant differences were observed between the LELP group and the others ($p > 0.05$) (Figure 1A). The propionate concentration in the LEHP group was significantly lower than in the LELP group ($p < 0.05$). Additionally, the HEHP group exhibited significantly higher concentrations of butyric, isobutyric, valeric, and isovaleric acids compared to the LEHP group ($p < 0.05$) (Figure 1B). Acetate was the predominant VFA across all groups, comprising approximately 70.0% of the total VFAs, followed by propionate at about 18.0% (Figure 1D). Notably, the proportion of acetate in the HELP group was significantly lower than in the other three groups, while the LELP group showed a significantly higher proportion of propionate compared to the others ($p < 0.05$) (Figure 1D). The HELP group also had significantly higher proportions of butyric acid compared to the low-energy groups (LEHP and LELP), with the HEHP group also exhibiting significantly higher proportions of butyric acid than the LELP group ($p < 0.05$) (Figure 1D). However, the total VFAs, acetate, and caproate concentrations were similar ($p > 0.05$) across the groups (Figure 1C).

3.2 Cecal microbial profiling and differential analysis

Venn diagram identified the OTUs across four test groups (HEHP, HELP, LEHP, LELP), with counts of 7,818, 8,858, 9,818, and 9,483 OTUs, respectively, totaling 1,124 unique OTUs (Figure 2A). Alpha diversity analysis showed no significant difference in the Chao1 index (species richness) across groups ($p > 0.05$), though Shannon and Simpson indices (diversity) were higher in HEHP than LEHP ($p < 0.05$), indicating increased microbiota diversity in HELP diets. Principal Coordinate Analysis (PCoA) revealed no significant differences in β diversity among diets ($p > 0.05$), showing stable community structure (Figures 2B,C). At the phylum level, *Bacteroidetes* and *Firmicutes* were predominant, with LEHP and LELP showing higher *Bacteroidetes* than HELP ($p < 0.05$), and HELP showing higher *Firmicutes* than LEHP ($p < 0.05$) (Figures 2D,E). *Verrucomicrobia* abundance was lower in LEHP compared to HELP and LELP ($p < 0.05$). At the genus level, 311 genera were identified, with key differences in *Clostridium, Prevotella, unidentified_BS11, unidentified_Lachnospiraceae, unidentified_Ruminococcaceae*, and *unidentified_S24-7*. Specifically, *unidentified_BS11* was lower in HELP than low-energy groups, while *unidentified_Ruminococcaceae*, *Clostridium*, and

10.3389/fmicb.2025.1523586

TABLE 1 Primer sequence used for qPCR analysis.

Genes	Primer (5′ → 3′)	Source	Size (bp)	Temperature (°C)
Claudin-1F	TGCCCCAGTGGAAGGTTTAC	XM_005675123.3	266	60
Claudin-1R	CTTCTGTGCCTCGTCGTCTT			
Claudin-4 F	CGTGCTATTGTCGGTGGTGG	XM_005697785.2	300	60
Claudin-4 R	GAGTAGGGCTTGTTGTTTCGTG			
Occludin F	GCGGTAACTTGGAGACGCTTTC	XM_018065677.1	107	60
Occludin R	GCCTCCCGTCGTGTAGTCTGTT			
ZO-1 F	TTGAACGCAAGTTTGAAAGTCCT	XM_018066118.1	121	60
ZO-1 R	TGTGCAGACTTCAGGAGGGTTT			
BDH-1 F	CCAGGACTACGGCAGGAAGTA	XM_018046459.1	143	60
BDH-1 R	GGTGGTAGCGAGTGTAGGGAGT			
BDH-2 F	AAGGCGTTGTGAACAGGTGC	XM_005681356.3	182	60
BDH-2 R	CAGTGCCTCTTCAGGATTTGGT			
HMGCL F	CTAAAGTCGCTGAGGTCTCCAAG	XM_005676858.2	225	60
HMGCL R	AGTCCACGACACTCACTCCCAT			
HMGCS1 F	CGATGGTGTAGACGCTGGAAAG	XM_005694739.3	150	60
HMGCS1 R	CGCCCAATGCAGTCATAAGAAA			
DRA F	AATTGTGGGCTATTAAAGAGGACC	NM_001314188.1	230	60
DRA R	CATGATGTCCAGGTTGGCTTTC			
NHE1F	CTGGACATTTGTTATCAGCACCCT	XM_018056627.1	177	60
NHE1R	AGGAGGTAGCCCAGGGAGAA			
SLC9A2 F	TTCGGGAGAACCAACCCAAG	XM_018054964.1	224	60
SLC9A2 R	CAAGGTTCGCTGACGGATCT			
SLC9A3 F	CCCGGCAGGAGTACAAACAT	XM_018065648.1	125	60
SLC9A3 R	CTTGGCCGACTTGAAGGACT			
MCT1F	CCCTCAACCAGGCTTTCTTTAT	XM_013962525.2	116	60
MCT1R	CTTTGGCCCTATTGGTCTCATC			
SLC16A4 F	GGAGCTATCACATTGCATCTGGTT	XM_013962551.2	115	60
SLC16A4 R	CTGGACCACTTGGAGACAAACTACT			
TLR3 F	ATCTGTCCCTGAGCAGCAACC	XM_018041934.1	131	60
TLR3 R	GGCAAAGGAGTCATTACCCATC			
TLR4 F	CTTCCCAACCTGGAGCACTT	NM_001285574.1	128	60
TLR4 R	TCTAAAGGGTTCAGGGACAAATCTA			
IFN-γF	TGGAAAGAGGAGAGTGACAAAAAG	NM_001285682.1	101	60
IFN-γR	CTCCTTTGAATGACCTGGTTATCT			
IL-6 F	TGAAGGAAAAGATCGCAGGTCTAA	NM_001285640.1	100	60
IL-6 R	ACCTTTGCGTTCTTTACCCACT			

unidentified_Lachnospiraceae were higher in HELP compared to LEHP ($p < 0.05$), and *Prevotella* was higher in LELP compared to HEHP ($p < 0.05$) (Figures 3A,B).

3.3 Correlation analysis between cecal microbiota and acids

Among the 331 identified bacterial genera, the top 20 with significant differences between groups were selected, and the correlation between cecal fermentation parameters and cecal microbiota was analyzed using Spearman's correlation coefficient (Figure 4). The results showed that butyric acid, valeric acid, isovaleric acid, caproic acid, and pH had significant or extremely significant correlations with cecal microorganisms ($p < 0.05$). In contrast, acetic acid, propionic acid, isobutyric acid, and total VFA did not show significant correlations with cecal microorganisms. The relative abundances of *unidentified_Ruminococcaceae* and *unidentified_Lachnospiraceae* were significantly or extremely significantly positively correlated with valeric acid and isovaleric acid ($p < 0.05$). The relative abundance of *Shuttleworthia* was significantly or extremely significantly

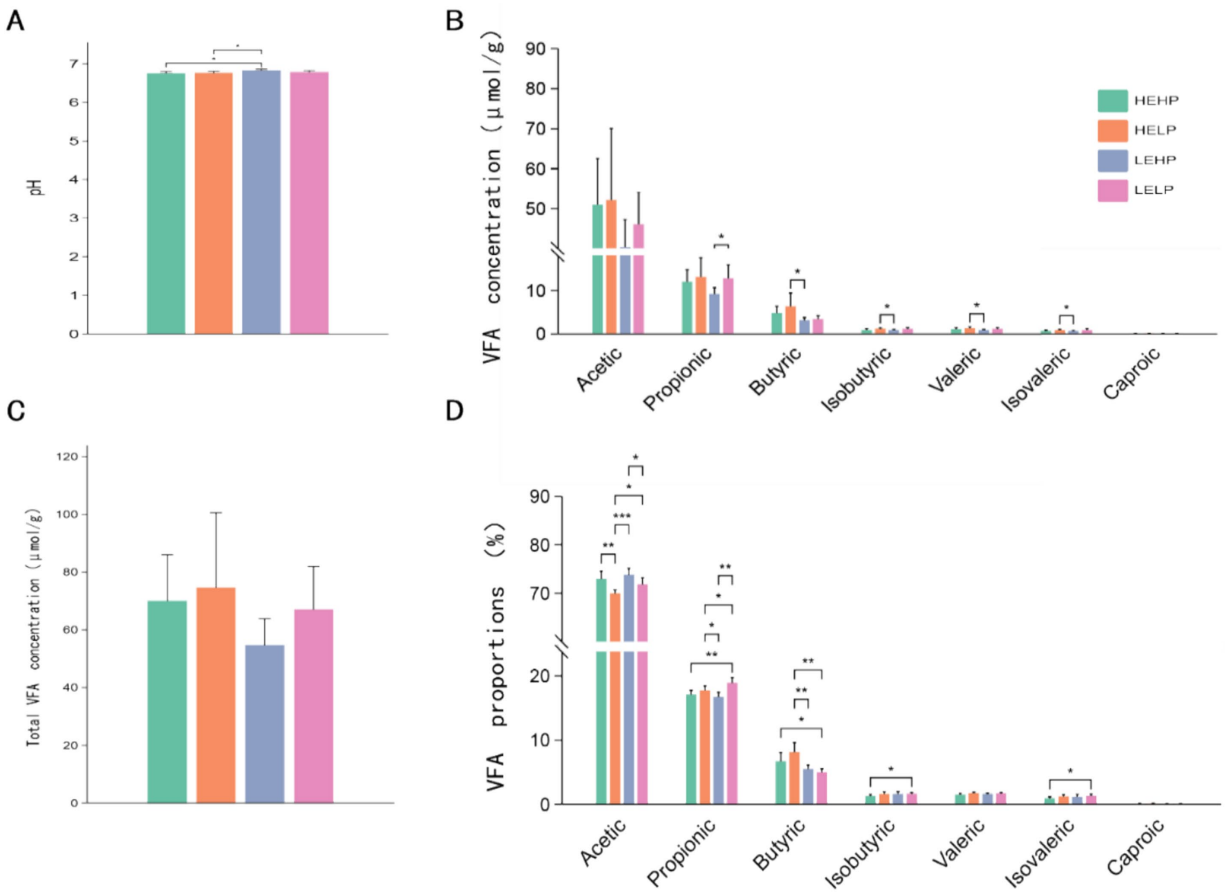

FIGURE 1
The effect of dietary protein and energy levels on pH **(A)**, relative concentration **(B)**, total VFA content **(C)**, and proportions of acetic acid, propionic acid, butyric acid, isobutyric acid, valeric acid, and caproic acid **(D)** in goat cecal digesta. Significant differences between treatments were determined using the Kruskal-Wallis test. *, **, and ***represent $p < 0.05$, $p < 0.01$, and $p < 0.001$, respectively.

positively correlated with butyric acid and valeric acid ($p < 0.05$). Conversely, the relative abundance of TG5 was significantly or extremely significantly negatively correlated with butyric acid, valeric acid, and caproic acid ($p < 0.05$). The relative abundance of *Clostridium* was significantly positively correlated with isovaleric acid ($p < 0.05$), while the relative abundance of *Blautia* was significantly negatively correlated with pH ($p < 0.05$).

3.4 VFA absorption, VFA metabolism, relative expression of cytokines, and tight junction protein mRNA in cecum

Due to the unique physiological structure of the cecum, excessive VFA can induce cecal inflammation. To further investigate this, we collected cecal epithelial tissues to analyze VFA absorption, VFA metabolism, and the relative mRNA expression levels of cytokines and tight junction proteins (Figure 5A). We did not observe significant differences in the mRNA abundances of genes related to VFA absorption or intracellular pH regulation ($p > 0.05$), such as DRA, NHE1, SLC9A2, MCT1, and SLC16A4. Similarly, VFA metabolism in the epithelium showed that genes associated with ketogenesis, such as BDH1, BDH2, and HMGCS1, were not affected by the dietary treatments. However, the mRNA abundance of HMGCL was lower in LELP-fed animals compared to LEHP. Interleukin-6 (IL-6), a pro-inflammatory cytokine, was significantly upregulated in HEHP-fed and HELP-fed animals compared to the LELP after 50 days of feeding ($p < 0.05$). Additionally, we detected the tight junction proteins Claudin-1, Claudin-4, Occludin, and ZO-1, but no significant differences were observed among the four groups ($p > 0.05$). These results suggest that a high-energy (HEHP and HELP) diet may affect the function of the cecal epithelium and induce an inflammatory response. This is supported by light microscopy cross-sections showing sloughing of the cecal epithelial surface in animals fed the high-grain (HG) diet (Figure 5B).

3.5 Correlation analysis

The results showed that VFA absorption-related genes, such as MCT-1 and SLC16A4, were positively correlated with the relative abundance of *Paludibacter* (Figure 5C). Additionally, the relative abundance of *Paludibacter* was also positively correlated with cytokines (such as TLR-3, TLR-4, and IFN-γ) and the tight junction protein Occludin. Furthermore, our study found that VFA absorption-related genes (such as SLC9A2, MCT-1, and

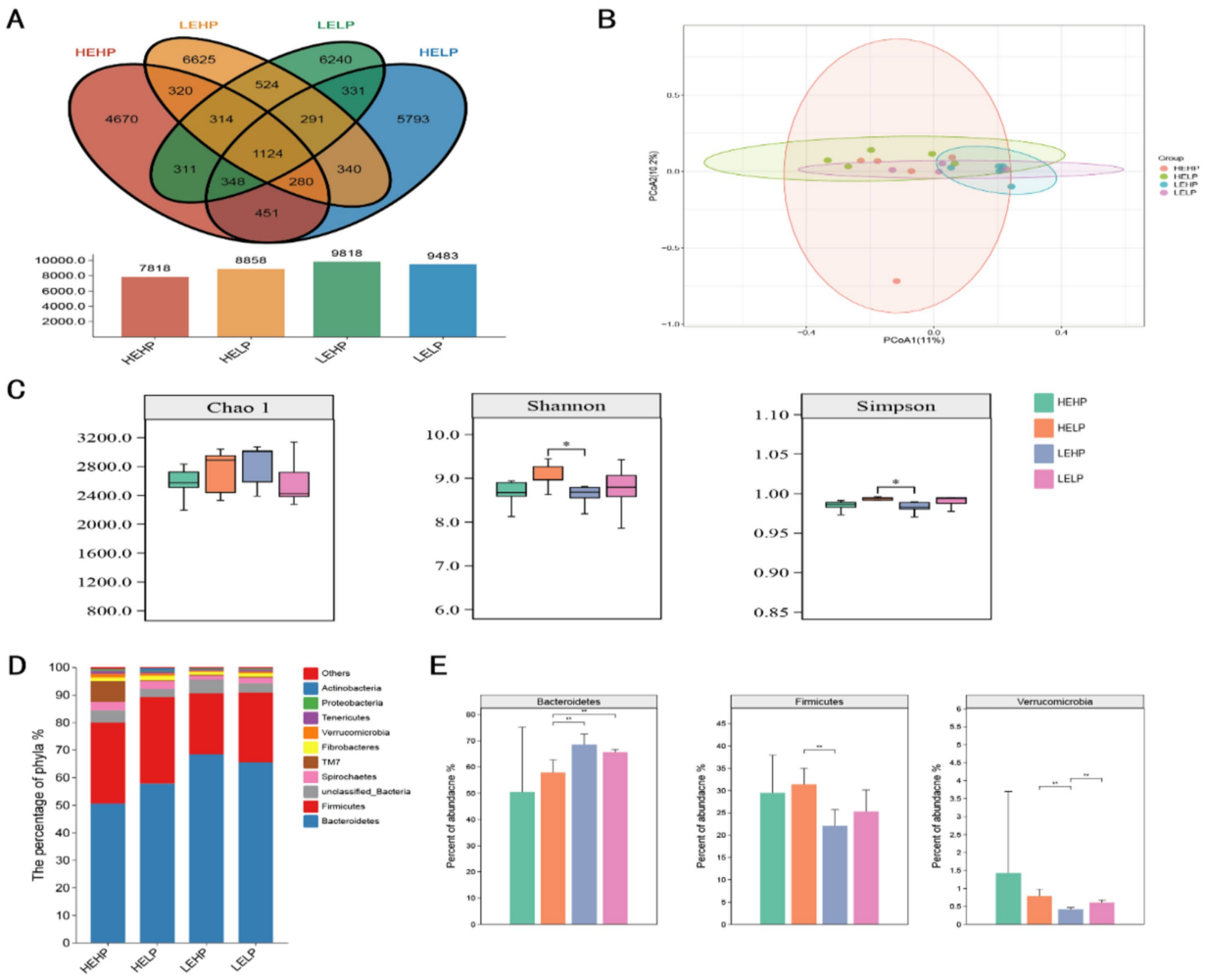

FIGURE 2
The cecal microbial profile (Venn plot **A**; principal coordinate analysis **B**) and differential analysis (alpha and beta diversities **C**; relative abundance of top 10 phyla **D**,**E**) of goats fed various energy and protein levels.

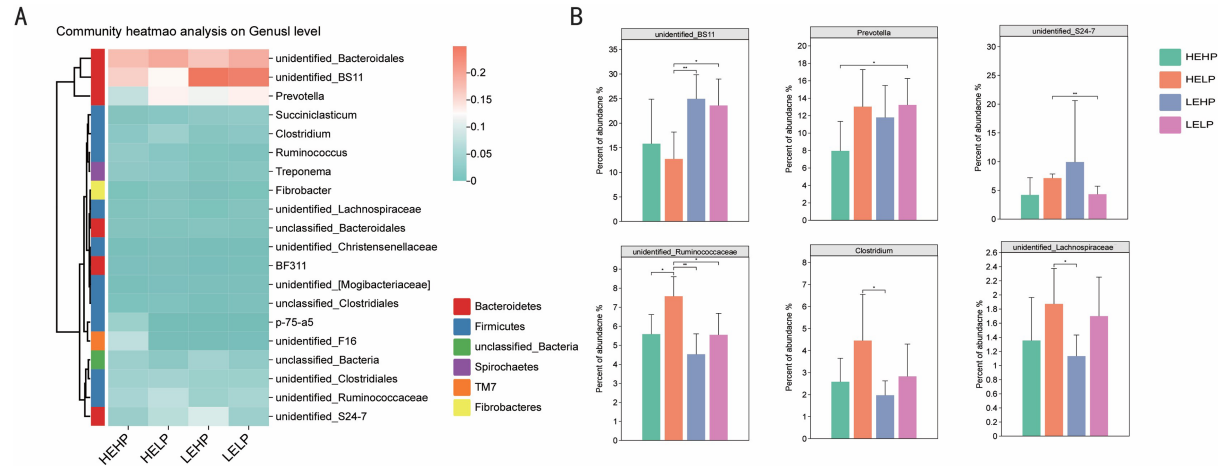

FIGURE 3
Cecal microbiota composition analysis (heatmap **A**; and relative abundance of top 20 genera **B**) of goats fed different energy and protein levels.

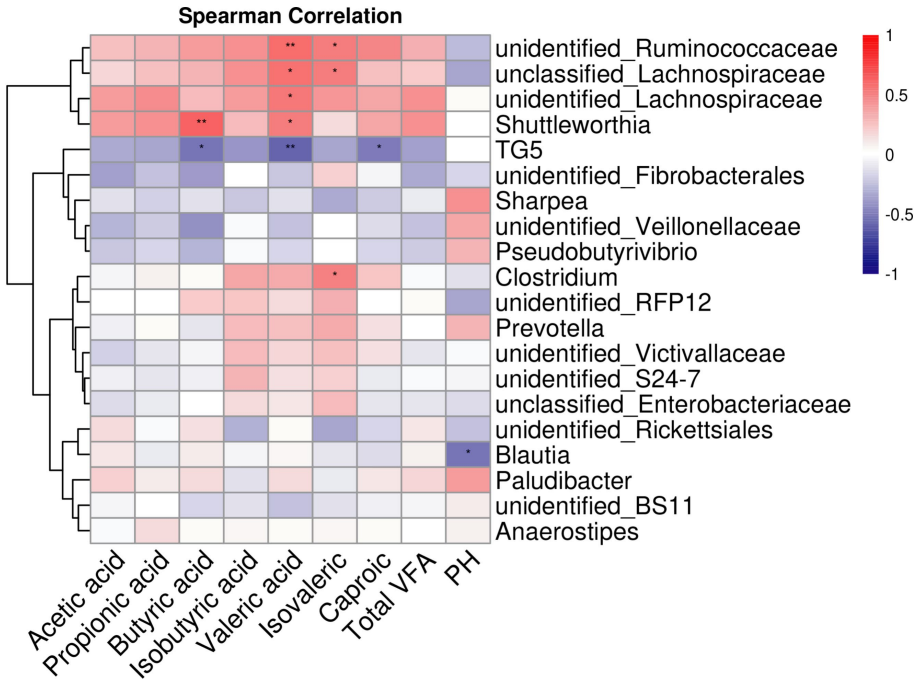

FIGURE 4
Heat map analysis of cecum fermentation parameters and top-20 microorganisms of genus level of goats fed different dietary energy and protein levels.

SLC16A4), VFA metabolism-related genes (such as BDH-1, HMGCL, and HMGCS1), cytokines, and tight junction proteins (Occludin and ZO-1) were negatively correlated with the relative abundance of unidentified *Fibrobacterales*. This suggests that the microbial community plays a critical role in host adaptive immunity. These findings indicate that perturbations in the hindgut microbiota can alter the host's immune system, thereby regulating inflammation.

4 Discussion

In this study, changes in the cecal fermentation of goats fed different dietary energy and protein levels were investigated in detail. The pH values in the HEHP and HELP groups were lower than in the LEHP group. Additionally, butyric acid and isobutyric acid concentrations were affected by varying dietary energy and protein levels, with the HELP group showing higher levels compared to the LEHP group. It is well known that feeding increasing levels of dietary energy such as higher inclusion of grain in diets results in the concentrations of total VFA, acetic acid, propionic acid, butyric acid, and lactic acid in the gut of the animals (Zoetendal et al., 1998; Siciliano-Jones and Murphy, 1989) and thus this increasing VFA production poses a greater challenge to maintaining the balance of the gastrointestinal ecosystem (Mertens, 1997). Moreover, a higher accumulation of these organic acids can lead to a decrease in rumen pH and drastic changes in the rumen microbiota, potentially resulting in subacute rumen acidosis (Kleen et al., 2003). A study by DeGregorio et al. (1982) reported that feeding 80% corn grains on a dry basis resulted in cecum engorgement with total VFA contents, along with significantly reduced butyric acid ratios, lactic acid concentrations, acetic acid to propionic acid ratios, and pH. Similarly, another study found increased total VFAs in the cecum when rabbits were transitioned from a low-protein to a high-protein diet (Trocino et al., 2013). In the current study, dietary energy and protein levels did not affect the total VFA content in the cecum of the goats. This may be because the effect of energy levels on the cecum in this study was less pronounced and species differences. Goats have well-developed rumen (primary site of fermentation) and dietary energy substances, such as starch, are primarily fermented into VFAs in the rumen, and any unfermented starch enters the small intestine, where it can be digested and absorbed as glucose, reducing the need for liver gluconeogenesis. Approximately 30% of glucose metabolic requirements can be absorbed from the gut, which helps to increase energy reserves. Our study also revealed that at the same energy level, the proportion of acetic acid increased with the rise in crude protein levels. Our results are consistent with previous research (Manzanilla et al., 2009), which reported that feeding high protein levels increased the cecum acetate of the piglet. Overall, the fermentation parameters of the four groups differed, likely due to variations in the composition of the cecal microbiota suggesting that dietary energy and protein levels influenced the cecum fermentation.

The large and complex microbial ecosystem plays a crucial role in the degradation of feed and the production of end products such as VFAs, microbial proteins, and B vitamins. A study by Zhang et al. (2017) found that a high-grain diet significantly reduced the number of OTUs. The results also indicated that the number of OTUs of rumen epithelial-associated bacteria showed a quadratic significant change over the feeding period with the HG diet. Our findings suggest that feeding the HEHP diet reduced the number of OTUs, whereas

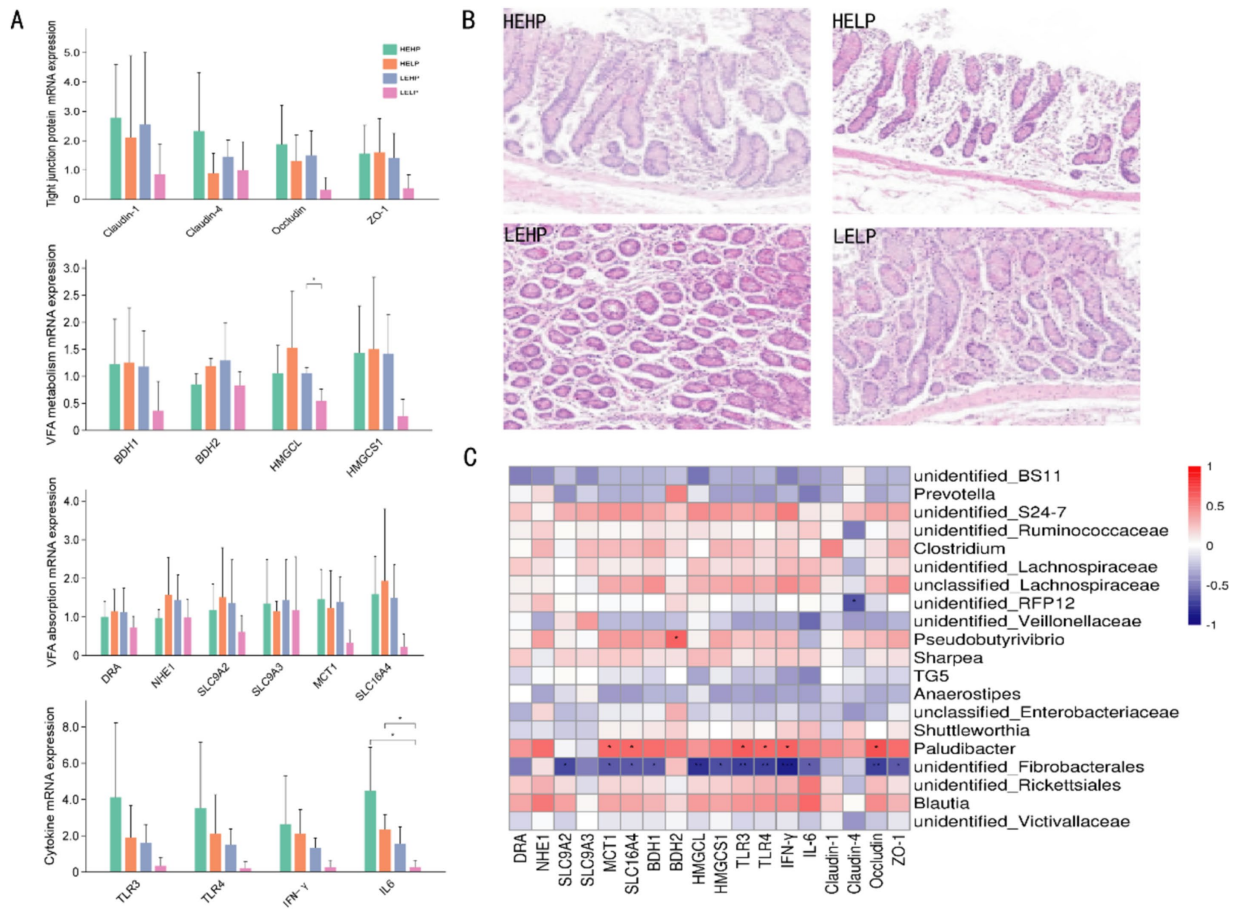

FIGURE 5
Morphology and related mRNA expression of cecal epithelium. **(A)** mRNA abundances of genes, cytokines, and tight junction proteins associated with VFA uptake and metabolism among the four groups. **(B)** Optical transactions of cecal epithelial tissue of goats fed diets with different energy and protein levels. **(C)** Heat map analysis of mRNA expression of cecal microbiota and associated genes with differences between groups.

giving the LEHP diet increased them. Similarly, at the same protein level, increased energy decreased the number of OTUs. One possible explanation for these changes in the composition of the gastrointestinal bacterial community could be the increase in rapidly fermentable carbohydrates, which can cause a sharp decrease in pH and dynamic changes in the concentrations of butyrate, lactate, and total short-chain fatty acids, as discussed above. The development and nutrient metabolism of the hindgut are closely related to the structure and quantity of the intestinal flora. It has been concluded that feeding patterns, the ratio of dietary concentrate, and the level of dietary nutrients can affect the bacterial diversity and the composition of dominant bacteria in the rumen (Zhang et al., 2020; Liu et al., 2019; Bi et al., 2018). In our study, we performed PCoA analysis on the OTUs and found that the four groups were not highly differentiated. There was no significant difference in the Chao 1 index, but both the Shannon and Simpson indices were significantly higher in the HELP group compared to the LEHP group. This difference in microbial population structure may be due to the increased amount of fermentable substrates in the diet, which are conducive to microbial growth. Additionally, proteins and carbohydrates that are not fully utilized by the small intestine will enter the large intestine and be further fermented and reused by microorganisms. This process results in the production of short-chain fatty acids, which have important physiological functions such as regulating the intestinal flora, enhancing intestinal function, and supplying energy to the host, particularly the intestinal epithelia. In the gastrointestinal tract, it is clear that dietary components play a key role in shaping the prevalence of bacterial phyla and specific intestinal compartments. Dietary factors are indeed key determinants affecting the relative abundance of microorganisms (Petri et al., 2013). The microbial differences between different parts of the gastrointestinal tract may be because when microorganisms flow into the intestine with chyme, the acidic environment can dissolve microbial cells, leading to the degradation or even death of some bacteria. Consequently, the number of rumen microorganisms reaching the hindgut decreases, resulting in changes in the composition of the gastrointestinal microbiota. The cecum is relatively rich in microbial species, with *Firmicutes* and *Bacteroidetes* as the core phyla, accounting for more than 90% of the total intestinal bacteria (O'Hara et al., 2020). *Firmicutes* primarily degrade fibrous substances, while *Bacteroidetes* mainly degrade non-fibrous carbohydrates. The results of this study showed that *Firmicutes* and *Bacteroidetes* were the dominant phyla in the cecum, consistent with other studies using 16S rDNA sequencing (Hook et al., 2011). In this study, the cecal pH of animals in the high-energy diet group was lower, and previous studies have shown that a low-pH gastrointestinal environment is conducive to the growth of *Firmicutes* (Hook et al.,

2011), which was also verified in our experiment. Additionally, we found differences in *Verrucomicrobia* at the phylum level. Studies (Sun et al., 2024) have shown that these bacteria may participate in lipid metabolism and are associated with triglycerides and total cholesterol. These results suggest that cecal microbiota are adapting to diets with different energy and protein levels, or they need to become more adaptive over time to changes in the cecal environment caused by feeding with different nutrient levels. Other factors like animal species, physiological stage, and environment may also influence the cecal microflora structure. Moreover, the current study showed that among the top 20 most abundant bacteria, the different genera included *unidentified_BS11*, *Prevotella*, *unidentified_S24-7*, *unidentified_Ruminococcaceae*, *Clostridium*, and *unidentified_Lachnospiraceae* were abundant at the genus level. All these different bacterial genera belong to *Firmicutes* and *Bacteroidetes*. Notably, although the highest relative abundance in the goat cecum was in *Ruminococcus* and *BS_11* (which were not classified), the relative abundance of *Prevotella* was higher in all samples. In healthy animals, *Prevotella* is a dominant microbe in the gastrointestinal tract (Dias et al., 2024), which is consistent with the findings in this study. *Prevotella* can almost complete the degradation of proteins, carbohydrates, and other nutrients by itself, and its distribution in different parts of the gastrointestinal tract is related to its high genetic variation (Stevenson and Weimer, 2007; Mullins et al., 2013). Some bacteria in the family *Ruminococcus* can produce cellulase, amylase, and other carbohydrate-degrading enzymes. *Ruminococcus* helps in the intestinal degradation of cellulose and hemicellulose, producing short-chain fatty acids such as butyric acid and acetic acid, which promote lipid metabolism, produce short-chain fatty acids and lipid products, and facilitate body fat deposition (Niu et al., 2015). Additionally, *Ruminococcus albus* and *Ruminococcus flavefaciens*, both belonging to the *Ruminococcaceae* family, can secrete large amounts of cellulase and hemicellulase, indicating that *Ruminococcaceae* microorganisms have a wide range of carbohydrate degradation activities. In this experiment, the highest relative abundance of microorganisms in the goat cecum was *f_Ruminococcaceae*, which was not classified, and the relative abundance of *g_Ruminococcus* was also high in all samples. Gu et al. (2013) found that *Ruminococcaceae* is the dominant bacterial group in the large intestine and feces of mice, and the results of this experiment are similar to those findings. Our results suggest that there may be active carbohydrate fermentation in the hindgut of goats. Additionally, *Trichomillaceae* were the most abundant phylum in fecal samples of the current study. This phylum can degrade fiber and protein and is associated with improved feed efficiency (Lopes et al., 2019).

Intestinal microbiota can enhance the host's nutrient absorption and thus promote overall health. In this experiment, the *Ruminococcaceae* family had the highest abundance, and the *Ruminococcus* genus was particularly abundant in cecal contents. *Trichospirillaceae* can digest fibrous substances in the gut to form VFAs, which can reduce gut pH and inhibit harmful microorganisms, thereby maintaining a relatively stable microbial community (Greer et al., 2013). In this study, *unclassified f_Bacteroidaceae, unclassified f_Lachnospiraceae,* and *g_Clostridium* were the dominant bacterial groups in the cecum. Studies have shown that *Bacteroides fragilis*, a member of the Bacteroides genus, can promote the development of the intestinal immune system (Rhee et al., 2004).

It has also been found that *Trichospiraceae* has anti-enteritis properties (Surana and Kasper, 2017). Additionally, several genera within *Lachnospiraceae* are butyricogenic bacteria, capable of producing butyric acid through the fermentation of fiber. Butyric acid can promote the expression of cecal defensin genes, effectively inhibiting the invasion of pathogenic microorganisms (Pryde et al., 2002; Sunkara et al., 2011). *Clostridium* includes *Clostridium butyricum*, a probiotic commonly found in the mammalian intestinal tract. *C. butyricum* can stimulate mucosal immune responses by fermenting fiber and metabolizing butyric acid, thereby inhibiting the growth of harmful intestinal bacteria (Mo et al., 2015). These results suggest that cecal microbes play a crucial role in maintaining gut health. Furthermore, all three of these microorganisms secrete cellulase, which aids the host in digesting cellulose (Bian et al., 2013; Zeng et al., 2015; Daly et al., 2012; Zhu et al., 2011). Additionally, our study found that the TG5 genus, belonging to *Dethiosulfovibrionaceae*, was negatively correlated with VFA content. Previous studies have indicated that an increased abundance of *Dethiosulfovibrionaceae* can serve as a potential biomarker for myocardial fibrosis (Marcinkiewicz et al., 2017). Moreover, the growth of *Desulfovibrio* is inhibited in low-pH environments (Huang et al., 2019). The results of this study once again suggest that there may be active carbohydrate fermentation in the cecum of goats. Previous research has shown that the hindgut of ruminants can compensate for the fibrous material not fully digested in the rumen (Wang et al., 2017; Jiao et al., 2014). This suggests that cecal microorganisms may regulate intestinal immune function primarily by affecting digestive metabolites.

The gastrointestinal tract of ruminants hosts a rich variety of microbial flora, with different regions emphasizing distinct microbial functions. For example, rumen microorganisms primarily focus on digesting and degrading nutrients, especially fibrous materials, while intestinal microorganisms play a crucial role in maintaining the host's intestinal health, in addition to compensating for and digesting nutrients not fully broken down in the rumen (Dodd et al., 2017; Kadoki et al., 2017; Cervantes-Barragan et al., 2017; Koppel et al., 2017; Bauer et al., 2018). Furthermore, digestive tract microorganisms are closely linked to local and systemic immune responses, preventing the invasion of pathogenic bacteria and maintaining intestinal homeostasis (Kataoka, 2016). Previous studies have also shown that mice fed a high-protein diet can experience increased severity of inflammatory bowel disease (Ng and Ananthakrishnan, 2019), and a high-fat diet can promote neuroinflammation (Kim et al., 2019). In this study, we observed changes in VFA content and microbial composition in the cecum when feeding diets with different energy and protein levels. We found that the tight junctions between cecal epithelial tissues in the experimental group showed erosion and cell necrosis. Previous research has indicated that high levels of hindgut fermentation can lead to inflammation and laminitis, which may be induced by amines, endotoxins, or bacteria capable of penetrating the intestinal barrier (Gozho et al., 2006; Crawford et al., 2007). In this study, we did not find any significant differences in the mRNA abundance of genes related to VFA absorption among the four groups. However, HMGCL, a gene related to VFA metabolism, was down-regulated in the LELP group, which may be related to the change in cecal pH. Additionally, we measured the mRNA expression of genes related to cytokines and inflammatory factors. The mRNA expression of the cytokine IL-6 in the LELP group was significantly

down-regulated compared to the HEHP and HELP groups, suggesting that immune system activation may be involved in the adaptation of the cecal epithelium to a high-nutrient diet. IL-6 is a multifunctional, pleiotropic cytokine involved in the regulation of immune response, acute phase response, and inflammation (Chang et al., 2014). Generally, the occurrence of inflammation affects the mRNA expression of genes related to tight junction proteins, but no such phenomenon was observed in this study. We speculate that this might be due to the adaptation of microorganisms to changes in nutrient levels, with the carbon metabolism of the cecal microbiome being altered by the introduction of a high-energy, high-protein diet, and adapting over time. Previous studies have reported that ruminants can adapt to a high-grain diet, which requires at least 3 weeks of rumen microbial adaptation (Tajima et al., 2001) and rumen epithelial morphological and functional adaptation (Górka et al., 2017). A highly interdependent relationship exists between the microbes in the gut microbiota system and the host, and the diversity of gut microbes has been proposed as a new marker to assess gut health and metabolic capacity (Clarke et al., 2014). The interaction between intestinal symbionts and the immune system plays an active role in maintaining overall health by promoting the growth of immune cells, shaping immune responses, and maintaining the integrity of the intestinal barrier (Zhou et al., 2024; Rinninella et al., 2019). To investigate the correlation between gene expression and cecal microbial abundance, we conducted a heatmap analysis. The results showed that *Pseudobutyrivibrio* belongs to the *Trichospirillum* genus, which is part of the *Trichospirillaceae* family. This family is a major producer of short-chain fatty acids and is known to enhance epithelial integrity, protect the barrier, and inhibit inflammation (Sun et al., 2021; Sun et al., 2021). Additionally, our study found that *Paludibacter* was positively correlated with the expression of genes related to VFA absorption, as well as genes associated with inflammatory factors and tight junction proteins. Previous studies have shown that *Paludibacter* is significantly correlated with feed utilization efficiency (Myer et al., 2017), and can help the host capture more protein and energy materials (Huang et al., 2022; Zhang et al., 2020). Furthermore, in our study, *unidentified_Fibrobacterales* was associated with RPF12 and had an effect on the expression of VFA-related genes in the cecum and intestinal health. Specifically, *unidentified_Fibrobacterales* were correlated to varying degrees with VFA absorption and transport genes, cytokines, and tight junction proteins. This indicates a long-term interdependence and restriction relationship between the microorganisms in the cecum and the host, as well as between different microorganisms. The dynamic relationship among these microorganisms is closely related to the absorption and transport of nutrients in the body. The intestinal microbiota also provides other beneficial functions to the host, such as balancing immune function, stabilizing the intestinal environment, and improving the health level of animals (Shapira, 2016; Hasegawa and Inohara, 2014).

5 Conclusion

Based on the results, feeding different energy and protein levels altered the cecal microbiota composition. The dominant phyla were *Bacteroidetes* and *Firmicutes* across the groups. At the genus level, 311 genera were identified, with *Clostridium*, *Prevotella*, *unidentified_BS11*, and others showing significant variation. Additionally, the analysis of VFA metabolism, absorption, cytokine expression, and tight junction protein mRNA in cecal tissue revealed that MCT-1 and SLC16A4 genes are linked to VFA absorption, positively correlated with *Paludibacter*, which was associated with immune markers (TLR-3, TLR-4, IFN-γ) and Occludin expression. In contrast, VFA-related genes and tight junction proteins negatively correlated with *unidentified Fibrobacterales*, suggesting a microbial role in adaptive immunity. The results of this study provide theoretical guidance for the practical application of diets with varying energy and protein levels in fattening goats.

Data availability statement

The data presented in the study are deposited in the NCBI BioProject database with accession number PRJNA1214186. The data can be assessed by using this link: https://www.ncbi.nlm.nih.gov/bioproject/1214186.

Ethics statement

The animal studies were approved by the Yunnan Academy of Animal Husbandry and Veterinary Sciences research facility after approval from the ethical committee of Yunnan Academy of Animal Husbandry and Veterinary Sciences (201911004). The studies were conducted in accordance with the local legislation and institutional requirements. Written informed consent was obtained from the owners for the participation of their animals in this study.

Author contributions

BF: Methodology, Writing – original draft, Data curation, Investigation. XZ: Data curation, Methodology, Writing – original draft. MK: Conceptualization, Formal analysis, Methodology, Visualization, Writing – original draft, Writing – review & editing. YJ: Investigation, Methodology, Software, Writing – original draft. WL: Formal analysis, Investigation, Validation, Writing – review & editing. MM: Formal analysis, Investigation, Software, Validation, Visualization, Writing – review & editing. BD: Formal analysis, Software, Visualization, Writing – original draft. XN: Data curation, Software, Validation, Writing – original draft. ZA: Software, Validation, Writing – review & editing. QS: Conceptualization, Methodology, Project administration, Supervision, Writing – original draft, Writing – review & editing. BX: Conceptualization, Funding acquisition, Project administration, Supervision, Writing – review & editing, Methodology, Writing – original draft. YO: Conceptualization, Funding acquisition, Methodology, Project administration, Supervision, Writing – review & editing.

Funding

The author(s) declare that financial support was received for the research, authorship, and/or publication of this article. This study was

supported by the Major Science and Technology Project of Yunnan Province (20202102AE090039), the Xingdian Elite Support Plan of Yunnan Province – Industrial Innovation Talents Project (YFGRC202426), the Technology Innovation Talents Project of Yunnan Province (202405AD350042) and the Basic Research Foundation Key Project of Yunnan Province (202001AS070002).

Conflict of interest

The authors declare that the research was conducted in the absence of any commercial or financial relationships that could be construed as a potential conflict of interest.

Generative AI statement

The authors declare that no Gen AI was used in the creation of this manuscript.

Publisher's note

All claims expressed in this article are solely those of the authors and do not necessarily represent those of their affiliated organizations, or those of the publisher, the editors and the reviewers. Any product that may be evaluated in this article, or claim that may be made by its manufacturer, is not guaranteed or endorsed by the publisher.

References

Bauer, P. V., Duca, F. A., Waise, T., Rasmussen, B. A., Abraham, M. A., Dranse, H. J., et al. (2018). Metformin alters upper small intestinal microbiota that impact a glucose-SGLT1-sensing Glucoregulatory pathway. *Cell Metab.* 27, 101–117.e5. doi: 10.1016/j.cmet.2017.09.019

Bi, Y., Zeng, S., Zhang, R., Diao, Q., and Tu, Y. (2018). Effects of dietary energy levels on rumen bacterial community composition in Holstein heifers under the same forage to concentrate ratio condition. *BMC Microbiol.* 18:69. doi: 10.1186/s12866-018-1213-9

Bian, G., Ma, L., Su, Y., and Zhu, W. (2013). The microbial community in the feces of the white rhinoceros (*Ceratotherium simum*) as determined by barcoded pyrosequencing analysis. *PLoS One* 8:e70103. doi: 10.1371/journal.pone.0070103

Cervantes-Barragan, L., Chai, J. N., Tianero, M. D., di Luccia, B., Ahern, P. P., Merriman, J., et al. (2017). *Lactobacillus reuteri* induces gut intraepithelial CD4(+) CD8alphaalpha(+) T cells. *Science* 357, 806–810. doi: 10.1126/science.aah5825

Chang, P. V., Hao, L., Offermanns, S., and Medzhitov, R. (2014). The microbial metabolite butyrate regulates intestinal macrophage function via histone deacetylase inhibition. *Proc. Natl. Acad. Sci. USA* 111, 2247–2252. doi: 10.1073/pnas.1322269111

Clarke, S. F., Murphy, E. F., O'Sullivan, O., Lucey, A. J., Humphreys, M., Hogan, A., et al. (2014). Exercise and associated dietary extremes impact on gut microbial diversity. *Gut* 63, 1913–1920. doi: 10.1136/gutjnl-2013-306541

Crawford, C., Sepulveda, M. F., Elliott, J., Harris, P. A., and Bailey, S. R. (2007). Dietary fructan carbohydrate increases amine production in the equine large intestine: implications for pasture-associated laminitis. *J. Anim. Sci.* 85, 2949–2958. doi: 10.2527/jas.2006-600

Daly, K., Proudman, C. J., Duncan, S. H., Flint, H. J., Dyer, J., and Shirazi-Beechey, S. P. (2012). Alterations in microbiota and fermentation products in equine large intestine in response to dietary variation and intestinal disease. *Br. J. Nutr.* 107, 989–995. doi: 10.1017/S0007114511003825

DeGregorio, R. M., Tucker, R. E., Mitchell, G. J., and Gill, W. W. (1982). Carbohydrate fermentation in the large intestine of lambs. *J. Anim. Sci.* 54, 855–862. doi: 10.2527/jas1982.544855x

Dias, E., de Carvalho, F. E., Polizel, G., Cançado, F. A. C. Q., Furlan, É., Fernandes, A. C., et al. (2024). Fetal programming influence on microbiome diversity and ruminal and Cecal epithelium in beef cattle. *Animals (Basel)* 14:870. doi: 10.3390/ani14060870

Dodd, D., Spitzer, M. H., van, W., Merrill, B., Hryckowian, A., Higginbottom, S., et al. (2017). A gut bacterial pathway metabolizes aromatic amino acids into nine circulating metabolites. *Nature* 551, 648–652. doi: 10.1038/nature24661

Górka, P., Schurmann, B. L., Walpole, M. E., Błońska, A., Li, S., Plaizier, J. C., et al. (2017). Effect of increasing the proportion of dietary concentrate on gastrointestinal tract measurements and brush border enzyme activity in Holstein steers. *J. Dairy Sci.* 100, 4539–4551. doi: 10.3168/jds.2016-12162

Gozho, G. N., Krause, D. O., and Plaizier, J. C. (2006). Rumen lipopolysaccharide and inflammation during grain adaptation and subacute ruminal acidosis in steers. *J. Dairy Sci.* 89, 4404–4413. doi: 10.3168/jds.S0022-0302(06)72487-0

Greer, R. L., Morgun, A., and Shulzhenko, N. (2013). Bridging immunity and lipid metabolism by gut microbiota. *J. Allergy Clin. Immunol.* 132, 253–262, 263. doi: 10.1016/j.jaci.2013.06.025

Gressley, T. F., Hall, M. B., and Armentano, L. E. (2011). Ruminant nutrition symposium: productivity, digestion, and health responses to hindgut acidosis in ruminants. *J. Anim. Sci.* 89, 1120–1130. doi: 10.2527/jas.2010-3460

Gu, S., Chen, D., Zhang, J. N., Lv, X., Wang, K., Duan, L. P., et al. (2013). Bacterial community mapping of the mouse gastrointestinal tract. *PLoS One* 8:e74957. doi: 10.1371/journal.pone.0074957

Hasegawa, M., and Inohara, N. (2014). Regulation of the gut microbiota by the mucosal immune system in mice. *Int. Immunol.* 26, 481–487. doi: 10.1093/intimm/dxu049

Hook, S. E., Steele, M. A., Northwood, K. S., Dijkstra, J., France, J., Wright, A. D. G., et al. (2011). Impact of subacute ruminal acidosis (SARA) adaptation and recovery on the density and diversity of bacteria in the rumen of dairy cows. *FEMS Microbiol. Ecol.* 78, 275–284. doi: 10.1111/j.1574-6941.2011.01154.x

Huang, K., Liu, Y., Tang, H., Qiu, M., Li, C., Duan, C., et al. (2019). Glabridin prevents doxorubicin-induced cardiotoxicity through gut microbiota modulation and colonic macrophage polarization in mice. *Front. Pharmacol.* 10:107. doi: 10.3389/fphar.2019.00107

Huang, X., Mi, J., Denman, S. E., Basangwangdui, Pingcuozhandui, Zhang, Q., et al. (2022). Changes in rumen microbial community composition in yak in response to seasonal variations. *J. Appl. Microbiol.* 132, 1652–1665. doi: 10.1111/jam.15322

Jiao, J., Wang, P., He, Z., Tang, S., Zhou, C., Han, X., et al. (2014). In vitro evaluation on neutral detergent fiber and cellulose digestion by post-ruminal microorganisms in goats. *J. Sci. Food Agric.* 94, 1745–1752. doi: 10.1002/jsfa.6485

Kadoki, M., Patil, A., Thaiss, C. C., Brooks, D. J., Pandey, S., Deep, D., et al. (2017). Organism-level analysis of vaccination reveals networks of protection across tissues. *Cell* 171, 398–413.e21. doi: 10.1016/j.cell.2017.08.024

Kataoka, K. (2016). The intestinal microbiota and its role in human health and disease. *J. Med. Investig.* 63, 27–37. doi: 10.2152/jmi.63.27

Kim, J. D., Yoon, N. A., Jin, S., and Diano, S. (2019). Microglial UCP2 mediates inflammation and obesity induced by high-fat feeding. *Cell Metab.* 30, 952–962.e5. doi: 10.1016/j.cmet.2019.08.010

Kleen, J. L., Hooijer, G. A., Rehage, J., and Noordhuizen, J. P. T. M. (2003). Subacute ruminal acidosis (SARA): a review. *J. Vet. Med. A Physiol. Pathol. Clin. Med.* 50, 406–414. doi: 10.1046/j.1439-0442.2003.00569.x

Koppel, N., Maini, R. V., and Balskus, E. P. (2017). Chemical transformation of xenobiotics by the human gut microbiota. *Science* 356:eaag2770. doi: 10.1126/science.aag2770

Liu, H., Xu, T., Xu, S., Ma, L., Han, X., Wang, X., et al. (2019). Effect of dietary concentrate to forage ratio on growth performance, rumen fermentation and bacterial diversity of tibetan sheep under barn feeding on the Qinghai-tibetan plateau. *PeerJ* 7:e7462. doi: 10.7717/peerj.7462

Liu, J., Xu, T., Zhu, W., and Mao, S. (2014). High-grain feeding alters caecal bacterial microbiota composition and fermentation and results in caecal mucosal injury in goats. *Br. J. Nutr.* 112, 416–427. doi: 10.1017/S0007114514000993

Lopes, D., La Reau, A. J., Duarte, M. S., Detmann, E., Bento, C. B. P., Mercadante, M. E. Z., et al. (2019). The bacterial and fungal microbiota of Nelore steers is dynamic across the gastrointestinal tract and its fecal-associated microbiota is correlated to feed efficiency. *Front. Microbiol.* 10:1263. doi: 10.3389/fmicb.2019.01263

Manzanilla, E. G., Pérez, J., Martín, M., Blandón, J., Baucells, F., Kamel, C., et al. (2009). Dietary protein modifies effect of plant extracts in the intestinal ecosystem of the pig at weaning1. *J. Anim. Sci.* 87, 2029–2037. doi: 10.2527/jas.2008-1210

Marcinkiewicz, A. L., Peter, K., and Yi-Pin, L. (2017). There is a method to the madness: strategies to study host complement evasion by Lyme disease and relapsing fever spirochetes. *Front. Microbiol.* 8:328. doi: 10.3389/fmicb.2017.00328

Mertens, D. R. (1997). Creating a system for meeting the fiber requirements of dairy cows. *J. Dairy Sci.* 80, 1463–1481. doi: 10.3168/jds.S0022-0302(97)76075-2

Mo, S., Kim, B. S., Yun, S. J., Lee, J. J., Yoon, S. H., and Oh, C. H. (2015). Genome sequencing of *Clostridium butyricum* DKU-01, isolated from infant feces. *Gut Pathog.* 7:8. doi: 10.1186/s13099-015-0055-3

Mullins, C. R., Mamedova, L. K., Carpenter, A. J., Ying, Y., Allen, M. S., Yoon, I., et al. (2013). Analysis of rumen microbial populations in lactating dairy cattle fed diets

varying in carbohydrate profiles and *Saccharomyces cerevisiae* fermentation product. *J. Dairy Sci.* 96, 5872–5881. doi: 10.3168/jds.2013-6775

Myer, P. R., Freetly, H. C., Wells, J. E., Smith, T. P. L., and Kuehn, L. A. (2017). Analysis of the gut bacterial communities in beef cattle and their association with feed intake, growth, and efficiency. *J. Anim. Sci.* 95, 3215–3224. doi: 10.2527/jas.2016.1059

Ng, S. C., and Ananthakrishnan, A. N. (2019). New approaches along the IBD course: diet, tight control and stem cells. *Nat. Rev. Gastroenterol. Hepatol.* 16, 82–84. doi: 10.1038/s41575-018-0088-4

Niu, Q., Li, P., Hao, S., Zhang, Y., Kim, S. W., Li, H., et al. (2015). Dynamic distribution of the gut microbiota and the relationship with apparent crude fiber digestibility and growth stages in pigs. *Sci. Rep.* 5:9938. doi: 10.1038/srep09938

O'Hara, E., Neves, A., Song, Y., and Guan, L. L. (2020). The role of the gut microbiome in cattle production and health: driver or passenger? *Annu. Rev. Anim. Biosci.* 8, 199–220. doi: 10.1146/annurev-animal-021419-083952

Petri, R. M., Schwaiger, T., Penner, G. B., Beauchemin, K. A., Forster, R. J., McKinnon, J. J., et al. (2013). Characterization of the core rumen microbiome in cattle during transition from forage to concentrate as well as during and after an acidotic challenge. *PLoS One* 8:e83424. doi: 10.1371/journal.pone.0083424

Pryde, S. E., Duncan, S. H., Hold, G. L., Stewart, C. S., and Flint, H. J. (2002). The microbiology of butyrate formation in the human colon. *FEMS Microbiol. Lett.* 217, 133–139. doi: 10.1111/j.1574-6968.2002.tb11467.x

Rhee, K. J., Sethupathi, P., Driks, A., Lanning, D. K., and Knight, K. L. (2004). Role of commensal bacteria in development of gut-associated lymphoid tissues and preimmune antibody repertoire. *J. Immunol.* 172, 1118–1124. doi: 10.4049/jimmunol.172.2.1118

Rinninella, E., Raoul, P., Cintoni, M., Franceschi, F., Miggiano, G. A. D., Gasbarrini, A., et al. (2019). What is the healthy gut microbiota composition? A changing ecosystem across age, environment, diet, and diseases. *Microorganisms* 7:14. doi: 10.3390/microorganisms7010014

Salgado-Flores, A., Hagen, L. H., Ishaq, S. L., Zamanzadeh, M., Wright, A. D. G., Pope, P. B., et al. (2016). Rumen and cecum microbiomes in reindeer (*Rangifer tarandus tarandus*) are changed in response to a lichen diet and may affect enteric methane emissions. *PLoS One* 11:e155213. doi: 10.1371/journal.pone.0155213

Shapira, M. (2016). Gut microbiotas and host evolution: scaling up Symbiosis. *Trends Ecol. Evol.* 31, 539–549. doi: 10.1016/j.tree.2016.03.006

Siciliano-Jones, J., and Murphy, M. R. (1989). Production of volatile fatty acids in the rumen and cecum-colon of steers as affected by forage: concentrate and forage physical form. *J. Dairy Sci.* 72, 485–492. doi: 10.3168/jds.S0022-0302(89)79130-X

Slyter, L. L. (1976). Influence of acidosis on rumen function. *J. Anim. Sci.* 43, 910–929. doi: 10.2527/jas1976.434910x

Stevenson, D. M., and Weimer, P. J. (2007). Dominance of Prevotella and low abundance of classical ruminal bacterial species in the bovine rumen revealed by relative quantification real-time PCR. *Appl. Microbiol. Biotechnol.* 75, 165–174. doi: 10.1007/s00253-006-0802-y

Sun, D., Bai, R., Zhou, W., Yao, Z., Liu, Y., Tang, S., et al. (2021). Angiogenin maintains gut microbe homeostasis by balancing alpha-Proteobacteria and Lachnospiraceae. *Gut* 70, 666–676. doi: 10.1136/gutjnl-2019-320135

Sun, C., Xiong, X., Liu, M., Liang, Q., Zhao, Q., Wei, G., et al. (2024). *Bacteroides ovatus* alleviates high-fat and high-cholesterol-induced nonalcoholic fatty liver disease via gut-liver axis. *Biomed. Pharmacother.* 178:117156. doi: 10.1016/j.biopha.2024.117156

Sunkara, L. T., Achanta, M., Schreiber, N. B., Bommineni, Y. R., Dai, G., Jiang, W., et al. (2011). Butyrate enhances disease resistance of chickens by inducing antimicrobial host defense peptide gene expression. *PLoS One* 6:e27225. doi: 10.1371/journal.pone.0027225

Surana, N. K., and Kasper, D. L. (2017). Moving beyond microbiome-wide associations to causal microbe identification. *Nature* 552, 244–247. doi: 10.1038/nature25019

Tajima, K., Aminov, R. I., Nagamine, T., Matsui, H., Nakamura, M., and Benno, Y. (2001). Diet-dependent shifts in the bacterial population of the rumen revealed with real-time PCR. *Appl. Environ. Microbiol.* 67, 2766–2774. doi: 10.1128/AEM.67.6.2766-2774.2001

Trocino, A., Fragkiadakis, M., Majolini, D., Tazzoli, M., Radaelli, G., and Xiccato, G. (2013). Soluble fibre, starch and protein level in diets for growing rabbits: effects on digestive efficiency and productive traits. *Anim. Feed Sci. Technol.* 180, 73–82. doi: 10.1016/j.anifeedsci.2013.01.007

Wang, Y., Liu, J., Yin, Y., Zhu, W., and Mao, S. (2017). Rumen microbial and fermentation characteristics are affected differently by acarbose addition during two nutritional types of simulated severe subacute ruminal acidosis in vitro. *Anaerobe* 47, 39–46. doi: 10.1016/j.anaerobe.2017.04.003

Wu, W., Lu, H., Cheng, J., Geng, Z., Mao, S., and Xue, Y. (2023). Undernutrition disrupts Cecal microbiota and epithelium interactions, epithelial metabolism, and immune responses in a pregnant sheep model. *Microbiol. Spectr.* 11:11. doi: 10.1128/spectrum.05320-22

Xie, F., Xu, L., Wang, Y., Mao, S., Chen, L., and Dill-McFarland, K. (2021). Metagenomic sequencing reveals that high-grain feeding alters the composition and metabolism of cecal microbiota and induces cecal mucosal injury in sheep. *mSystems* 6:e91521. doi: 10.1128/msystems.00915-21

Zeng, Y., Zeng, D., Zhang, Y., Ni, X., Tang, Y., Zhu, H., et al. (2015). Characterization of the cellulolytic bacteria communities along the gastrointestinal tract of Chinese Mongolian sheep by using PCR-DGGE and real-time PCR analysis. *World J. Microbiol. Biotechnol.* 31, 1103–1113. doi: 10.1007/s11274-015-1860-z

Zhang, L., Jiang, X., Li, A., Waqas, M., Gao, X., Li, K., et al. (2020). Characterization of the microbial community structure in intestinal segments of yak (*Bos grunniens*). *Anaerobe* 61:102115. doi: 10.1016/j.anaerobe.2019.102115

Zhang, X. L., Xu, T. W., Wang, X. G., Geng, Y. Y., Liu, H. J., Hu, L. Y., et al. (2020). The effect of transitioning between feeding methods on the gut microbiota dynamics of yaks on the Qinghai-Tibet plateau. *Animals (Basel)* 10, 9:1641. doi: 10.3390/ani10091641

Zhang, R., Ye, H., Liu, J., and Mao, S. (2017). High-grain diets altered rumen fermentation and epithelial bacterial community and resulted in rumen epithelial injuries of goats. *Appl. Microbiol. Biotechnol.* 101, 6981–6992. doi: 10.1007/s00253-017-8427-x

Zhou, P., Chen, C., Patil, S., and Dong, S. (2024). Unveiling the therapeutic symphony of probiotics, prebiotics, and postbiotics in gut-immune harmony. *Front. Nutr.* 11:1355542. doi: 10.3389/fnut.2024.1355542

Zhu, L., Wu, Q., Dai, J., Zhang, S., and Wei, F. (2011). Evidence of cellulose metabolism by the giant panda gut microbiome. *Proc. Natl. Acad. Sci. USA* 108, 17714–17719. doi: 10.1073/pnas.1017956108

Zoetendal, E. G., Akkermans, A. D., and De Vos, W. M. (1998). Temperature gradient gel electrophoresis analysis of 16S rRNA from human fecal samples reveals stable and host-specific communities of active bacteria. *Appl. Environ. Microbiol.* 64, 3854–3859. doi: 10.1128/AEM.64.10.3854-3859.1998

frontiers | Frontiers in Microbiology

TYPE Original Research
PUBLISHED 13 February 2025
DOI 10.3389/fmicb.2025.1535451

Check for updates

OPEN ACCESS

EDITED BY
Junling Shi,
Northwestern Polytechnical University, China

REVIEWED BY
Gaofeng Wu,
Xi'an Jiaotong University, China
Shuai Zhao,
Henan University of Technology, China

*CORRESPONDENCE
Enyao Li
✉ Lienyao@zzu.edu.cn
Pengya Feng
✉ fengpy@zzu.edu.cn

†These authors have contributed equally to this work

RECEIVED 27 November 2024
ACCEPTED 23 January 2025
PUBLISHED 13 February 2025

CITATION
Zhang Y, Li H, Li B, Li Y, Chai X, Li S, Xue X, Li H, Zhao Y, Tang Y, Yin B, Zhao P, Li E and Feng P (2025) *Dachaihu* decoction ameliorates abnormal behavior by regulating gut microbiota in rats with propionic acid-induced autism.
Front. Microbiol. 16:1535451.
doi: 10.3389/fmicb.2025.1535451

COPYRIGHT
© 2025 Zhang, Li, Li, Li, Chai, Li, Xue, Li, Zhao, Tang, Yin, Zhao, Li and Feng. This is an open-access article distributed under the terms of the Creative Commons Attribution License (CC BY). The use, distribution or reproduction in other forums is permitted, provided the original author(s) and the copyright owner(s) are credited and that the original publication in this journal is cited, in accordance with accepted academic practice. No use, distribution or reproduction is permitted which does not comply with these terms.

Dachaihu decoction ameliorates abnormal behavior by regulating gut microbiota in rats with propionic acid-induced autism

Yangyang Zhang[1†], Hang Li[2†], Bolin Li[3], Yizhuang Li[4], Xuejun Chai[5], Sheng Li[6], Xia Xue[2], Honglei Li[1], Yonghong Zhao[1], Youcai Tang[1,7], Baoqi Yin[1], Pengju Zhao[1], Enyao Li[1]* and Pengya Feng[1,2]*

[1]Department of Children Rehabilitation, Henan Key Laboratory of Rehabilitation Medicine, The Fifth Affiliated Hospital of Zhengzhou University, Zhengzhou, China, [2]Henan Key Laboratory for Helicobacter Pylori and Digestive Tract Microecology, The Fifth Affiliated Hospital of Zhengzhou University, Zhengzhou, China, [3]College of Traditional Chinese Medicine, Fujian University of Traditional Chinese Medicine, Fuzhou, China, [4]Department of Neurology, The Fifth Affiliated Hospital of Zhengzhou University, Zhengzhou, China, [5]School of Basic Medical Science, The Shaanxi Key Laboratory of Brain Disorders, Xi'an Medical University, Xi'an, China, [6]School of Life Sciences, Westlake University, Hangzhou, China, [7]Henan Provincial Outstanding Overseas Scientists Chronic Liver Injury Workshop, Zhengzhou Key Laboratory of Metabolism-Associated Fatty Liver Disease, The Fifth Affiliated Hospital of Zhengzhou University, Zhengzhou, China

Background: Autism spectrum disorder (ASD) is an early-onset neurodevelopmental disorder, usually accompanied by gut microbiota dysregulation. Gut microbiota homeostasis is considered effective for ASD. Reportedly, *Dachaihu* decoction (DCHD) can efficiently regulate gut microbiota and inflammation. However, the mechanisms underlying the effects of DCHD in the treatment of ASD remain unclear.

Objective: This study investigated the potential effects and mechanisms of DCHD in treating ASD.

Methods: In the animal experiment, propionic acid was administered to construct an ASD rat model. The ASD rats were treated with DCHD, and the efficacy was assessed using the behavioral detections, such as open field test, elevated plus maze test, novel object recognition test. Additionally, the levels of IL-6, TNF-α, IL-10, T-SOD, MDA, GSH and CAT were determined using kits, and histological staining was used to evaluate brain morphology. Moreover, tight junction proteins (ZO-1 and occludin) expression levels were evaluated using RT-qPCR, whereas Iba1 expression level was assessed by immunofluorescence staining. The 16S rRNA sequencing and metabolomic analysis of feces revealed the potential targets of DCHD against ASD. In a small human trail, the clinical scales ADOS-2 and Autism Behavior Checklist (ABC) assessed autism severity. Gastrointestinal problems and brain function were evaluated based on food intolerance and event-related potential, respectively.

Results: DCHD significantly improved autism-like behaviors and increased antioxidant enzyme activity, decreased inflammation and enhanced the intestinal barrier by the animal experiment. Furthermore, the DCHD treatment altered the gut microbiota profile, with increased probiotics *Adlercreutzia*, *Parvibacter*, *Turicibacter*, and *Christensenellaceae*. Further, DCHD increased the beneficial metabolite indole-3-acetate and decreased the cognitive impairment-related metabolites asymmetric dimethylarginine and homogentisic acid. Meanwhile, the small clinical trial revealed that DCHD significantly alleviated the core

10.3389/fmicb.2025.1535451

symptoms of ASD, with decreased ADOS-2 and ABC scale scores. DCHD also decreased the levels of specific egg white/yolk and milk IgG antibodies and shortened the MMN and P3b latencies.

Conclusion: This study demonstrated that DCHD may alleviate ASD via inhibiting oxidative stress, reducing inflammation, and modulating the gut microbiota in rats. Combined with human trial, DCHD may be a promising drug for treating ASD. This study provides a scientific rationale for treating mental disorders related to gut microbiota dysbiosis.

KEYWORDS

autism spectrum disorder, dachaihu decoction, 16S rRNA sequencing, metabolomic analysis, gut microbiota

1 Introduction

Autism spectrum disorder (ASD) is a group of neurodevelopmental conditions commencing early in life and is characterized by impaired social communication and interactions and stereotyped, repetitive behavior. In western countries, the prevalence of ASD among children and adolescents is 2.76% (1/36) (Maenner et al., 2023). In China, ASD affects 0.7% of children, making it the most prevalent mental disorder (Jiang et al., 2024). The increasing incidence of ASD is a public health concern globally (Bougeard et al., 2024), yet there are no effective drugs to treat ASD. Risperidone and aripiprazole have been approved by the US Food and Drug Administration to treat ASD-associated symptoms in children; however, these drugs may lead to gastrointestinal disorders, irritability, excessive salivation, and other undesirable effects (Biswas et al., 2023). Behavioral psychotherapy is often used to treat ASD, but it is costly and has gradual effects (Qin et al., 2024). Thus, investigating strategies for safely and effectively treating ASD is crucial.

Reportedly, the gut microbiota is an important modulator of host physiology (Fischbach and Segre, 2016), including the endophenotypes associated with ASD (Sherwin et al., 2019), and is known to influence brain physiology and social behavior by participating in the microbiota–gut–brain axis (Sherwin et al., 2019), including immune activation, production of microbial metabolites and peptides, and production of various neurotransmitters and neuromodulators (Sherwin et al., 2019). Many strategies for treating ASD involving interventions in the gut microbiota are being identified, such as fecal microbiota transplantation (FMT), probiotics and prebiotics (Poupard et al., 2024). Human trials (Guidetti et al., 2022; Lin et al., 2024; Mazzone et al., 2024; Wan et al., 2024) have indicated that FMT and probiotics can remarkably improve gastrointestinal symptoms in children with ASD by increasing the abundance of beneficial bacteria. For example, *Limosilactobacillus reuteri* (Mazzone et al., 2024) and *Lactiplantibacillus plantarum* PS128 (Ma et al., 2024) can enhance social behavior in children with ASD, including increasing adaptive social functioning and reducing their social deficits. Reportedly, FMT can reshape the composition and structure of the gut microbiota in patients with ASD, thereby improving

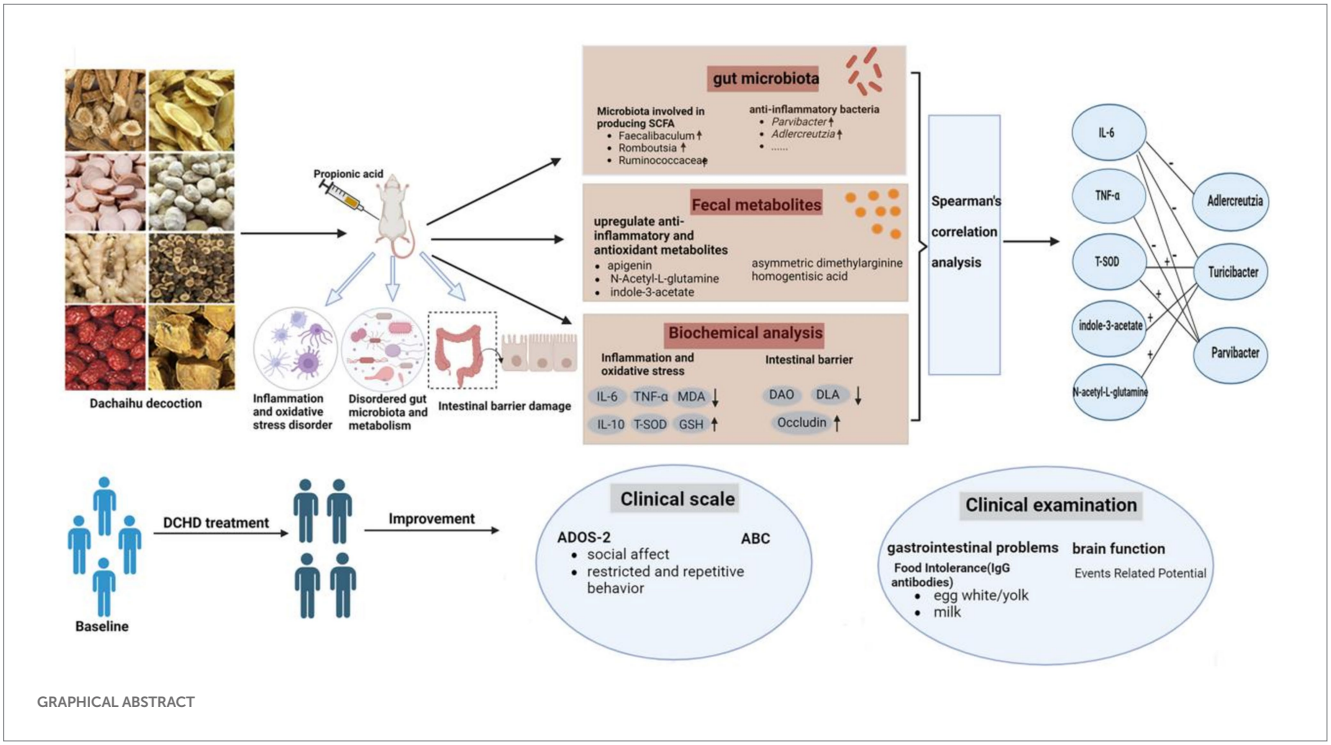

GRAPHICAL ABSTRACT

gastrointestinal symptoms and ASD-related behavioral symptoms (Kang et al., 2017; Li et al., 2021). Although these methods effectively treat ASD, they are not well promoted because of limitations such as FMT being expensive and complex to perform and probiotics showing individual variability in responses and interactions with medications (Poupard et al., 2024; Tan et al., 2021; Zhang et al., 2023). Thus, exploring novel pharmaceuticals that can preserve the equilibrium of the gut microbiota as a therapeutic approach for ASD is crucial.

Traditional Chinese medicine, recognized for its multitarget approach and low cellular toxicity, comprises numerous promising therapeutics (Wang et al., 2024). Dachaihu decoction (DCHD) comes from the Treatise on Cold Damage and Miscellaneous Diseases (*Shang Han Za Bing Lun*) by *Zhongjing Zhang*. DCHD, a classical formula in ancient China (Cui et al., 2020), effectively regulates mood disorders and depressive symptoms and is effective for exerting anti-inflammatory effects and improving the function of the gastrointestinal tract (Shi et al., 2024). Clinically, DCHD has demonstrated efficacy in treating the "shao-yang signs," which include symptoms like fever and chills, as well as "yang-ming signs," characterized by abdominal pain and fullness. In addition, DCHD is also utilized in the treatment of digestive disorders, including inflammatory bowel disease, hepatitis, and gallbladder-related conditions (Duan et al., 2024). Reportedly, DCHD can ameliorate septic gut injury, kidney injury in diabetic mice and high-fat-diet-induced nonalcoholic fatty liver disease by modulating the gut microbiota, glutathione and serum metabolism (Cui et al., 2020; Huang et al., 2023). Hence, DCHD might have great therapeutic potential for ASD by regulating the gut microbiota. However, to our knowledge, no studies have explored the biological basis of DCHD's action and potential interaction between DCHD and gut microbiota in ASD.

Herein, we investigated the protective effects of DCHD against ASD and the role of crosstalk between DCHD and gut microbiota in preventing ASD using a rat model with propionic acid (PPA)-induced autism. DCHD reversed ASD-associated gut dysbiosis by enriching probiotics and beneficial metabolites, further improving gut–brain barrier function and modulating inflammatory factors. Finally, we elucidated potential interactions between gut microbiota and DCHD metabolites that modulate the efficacy of DCHD in ASD. Altogether, DCHD potentially prevents ASD, the effects of which involve its interaction with gut microbiota.

2 Materials and methods

2.1 Participants

Children with ASD treated at the Fifth Affiliated Hospital of Zhengzhou University between August 2023 and August 2024 were included. All participants provided written informed consent before enrollment. The clinical trial was approved by the Scientific Ethics and Safety Committee of the Fifth Affiliated Hospital of Zhengzhou University (KY2023077). Patients with ASD conforming to the ASD diagnostic criteria in the Diagnostic and Statistical Manual of Mental Disorders, 5th Edition (DSM-5); whose diagnosis had been made by a senior child psychiatrist based on the patient's medical history, clinical assessment, and established diagnostic criteria; with 2–6 years of age; and whose parents/guardians had permitted their participation were included. However, those with comorbid other mental illness or cognitive impairment; Abnormal mental behavior caused by organic diseases; Patients with other undiagnosed diseases were excluded. A total of 30 young children (between 24 and 72 months) with ASD were included. The average age was 42.36 (± 14.71) months.

2.2 Clinical assessment

The characteristics and severity of the clinical symptoms in children with ASD were evaluated using Autism Diagnostic Observation Schedule (ADOS) and Autism Behavior Checklist (ABC). The ADOS scale was divided into two modules: social affect (SA) and restricted and repetitive behavior (RRB). Each module had a corresponding cutoff score.

2.3 Food intolerance

Upon enrollment of the patients, 2 mL of fasting venous blood was collected in the morning using an EDTA-K_2 anticoagulant tube and centrifuged at 3,500 rpm for a duration of 15 min. The obtained supernatant was stored in a freezer at −80°C. The concentrations of 14 food-specific IgG antibodies were determined using ELISA at the clinical laboratory of the Fifth Affiliated Hospital of Zhengzhou University. The obtained results were categorized into positive groups (+, >50 U/mL) and negative groups (−, <50 U/mL).

2.4 Event-related potential

Patients were admitted within 10 days to undergo an event-related potential test using the Nihon Kohden electromyogram and evoked potential device (MEB-2306C). The test was conducted in accordance with the 10–20 system for electrode placement, which facilitated recording of cerebral electrical activity of patients. Reference electrodes—A1 and A2—were positioned over the left and right earlobes. A ground electrode was situated at the forehead midline. The electrode–skin impedance was maintained below 5 kΩ, and the filtering was 0.5–100 Hz. To assess mismatch negativity (MMN), the latencies of the Cz and Fz waveforms were meticulously documented. The mean of these measurements was calculated, and the related potential evoked by the standard stimulus was subtracted from that evoked by the deviant stimulus. MMN was identified as the most prominent negative phase wave within 100–250 ms. Similarly, for the P300 measurement, the latencies of the Cz and Fz waveforms were recorded. P300 was confirmed as the most significant positive phase wave observed within 250–450 ms poststimulus.

2.5 *Dachaihu* decoction and ultrahigh-performance liquid chromatography–mass spectrometry analysis

DCHD were provided by Henan Zhangzhongjing Pharmacy Co., Ltd. for the animal experiment. Its components and their proportions are shown in Table 1. The eight herbs components of

TABLE 1 The information sheet of *Dachaihu* decoction.

Generic name	Botanical name	Medication batch number	Weight (g)
Chaihu	*Bupleurum chinense* DC.	211,203	15
Huangqin	*Scutellaria baicalensis* Georgi	231,001	9
Zhishi	*Citrus aurantium* L.	22,110,301	9
Shaoyao	*Paeonia lactiflora* Pall.	230,901	9
Ban Xia	*Pinellia pedatisecta* Schott	230,701	9
Dahuang	*Rheum officinale* Baill.	220,901	6
Shengjiang	*Zingiber officinale* Roscoe	/	15
Dazao	*Ziziphus jujuba* Mill	230,902–1	12

DCHD were meticulously measured and combined, subsequently, 500 mL of water was introduced to the blend. The solution was heated vigorously to reach boiling point, after which the heat was reduced to let it simmer gently for a duration of 25 min. The solution was filtered to obtain a 250 mL decoction, and decocted at low heat for 25 min to obtain a 125 mL decoction, which represented a single dose of DCHD (equivalent to 0.79 g/mL herbal materials). The decoction was concentrated at 62.5 mL to obtain two doses of DCHD (equivalent to 1.58 g/mL herbal materials). DCHD was analyzed using ACQUITY UPLC I-Class HF with ACQUITY UPLC HSS T3 (100 mm × 2.1 mm, 1.8 μm). Mobile phase A was 0.1% formic acid–water, whereas mobile phase B was acetonitrile, meticulously conducted in accordance with the predefined elution parameters. The main mass spectroscopy conditions were as follows: spray voltage 3,000 V (−) and 3,800 V (+), mass range 125–1,000 m/z, Aux. gas heater temperature 350°C; sheath gas flow rate 35 Arb; and Aux. gas flow rate 8 Arb. The PDA scanning range was 210–400 nm. The process was conducted by Lu-Ming Biotech Co., Ltd. (Shanghai, China).

2.6 Animal experiment

A total of 30 healthy male SD rats (bodyweight 150 ± 50 g) were purchased from the Experimental Animal Center of Zhengzhou University. They were housed in the animal room of the medical campus of Zhengzhou University of Chinese Medicine (temperature 20°C–22°C, humidity 50–60%), with a 12-h light/dark cycle, and all rats had unrestricted access to food and water. This experiment was approved by the Medical and Experimental Animal Ethics Committee of Academy of Medical Sciences of Zhengzhou University [ZZU-LAC20221111(04)]. The rats were randomly assigned to five groups: control, ASD model, DCHD only, DCHD at a low dose (DCH_L), and DCHD at a high dose (DHD_H) ($n = 6$ per group). All groups, except for control and DCHD-only, were subcutaneously administered with PPA (250 mg/kg/day, pH 7.4) for 5 days to induce ASD (Benitah et al., 2023). The daily doses of the DCH_L and DCH_H groups were 4 and 16 g/kg body weight, respectively (Cui et al., 2020). Meanwhile, the control and DCHD-only groups were given normal saline. After 4 weeks of the DCHD treatment, the rats underwent behavioral analysis for 4 weeks. Subsequently, the feces were collected and the rats were sacrificed.

2.7 Behavioral assessments

A researcher, blinded to the group assignments, conducted the behavioral evaluations. ASD-like behavior was scored using the Smart 3.0 tracking software (PanLab, United States). The behavioral assessments were carried out during the day between 09:00 and 18:00 h.

2.8 Open field test

For this test, the rats were placed in a 100 cm × 100 cm × 40 cm black plastic box. The box was divided into central and peripheral areas. An overhead camera system was used to record its path, and the Smart3.0 software was employed to determine the frequency of entries and the time duration within the central area. The open field test (OFT) is common assay for evaluating both anxiety-like and motor behaviors for animals (Kraeuter et al., 2019).

2.9 Three-chamber social test

The experiment was carried out in a connected transparent three-chamber chamber, a classic way of assessing social skills in rats (Buffington et al., 2016). Prior to the test, the rat is placed in the test environment for acclimatization for 2 h. For the social experiment, the left metal box was placed into the stranger rat 1, and the experimental rat was observed for 10 min. The Smart3.0 software analysis system was used to calculate the residence time of the tested rat in S1 and the empty cage (E1). In the social preference experiment, the left metal box was placed into the stranger rat 2 (S2) and the S1. The test time was 10 min, and the residence time of the tested rats on both sides was analyzed.

2.10 Elevated plus maze test

According to the experiment, each rat was positioned on the central platform (15 cm × 15 cm), facing the direction of the open arm (45 cm × 15 cm). The activities of each rat in both the open arm and the closed arm (45 cm × 15 cm × 30 cm) were meticulously observed. Conducted in dim lighting and a quiet environment, the experiment lasted for 5 min. During this period, the movement track of each rat

in the elevated cross maze, as well as the time spent and distance traveled in the open arm, were carefully monitored. The elevated plus maze (EPM) experiment is designed to investigate the anxiety state of animals by utilizing their innate tendency to explore new environments and their conflicting behavior stemming from fear of the high, open, and suspended spaces.

2.11 Novel object recognition test

For this experiment, the rats were initially allowed to acclimate to the surroundings by being placed in the laboratory for 1 day before the test. The novel object recognition test consisted of three stages. First, two identical objects [old object (O) and familiar object (F)] were placed on opposite sides of the testing box of $60 \times 60 \times 60$ cm^3, each approximately 10 cm from the walls of box. The rats were placed the box and allow them to explore freely for a 5 min period before removing them. Following each rat was tested, clean the box with 75% ethanol to eliminate any residual odor. Twenty-four hours later, one of the familiar objects in the test box was randomly substituted with a novel object (N) of comparable size but differing in shape and color, while the positions of both objects remained unchanged. The rats were then placed back into the experimental box to explore for 5 min before being removed.

2.12 Biochemical analysis

Serum samples were collected following centrifugation at 3,500 rpm for 15 min. The GSH, T-SOD, MDA, AST, ALT, and BUN levels were measured using the corresponding biochemical kits (Nanjing Jiancheng Institute of Biotechnology, Nanjing, China). The level of IL-6, IL-10, and TNF-α also were measured by the rat ELISA kits (Fankel, Shanghai, China), per the manufacturer's instructions. Moreover, a microplate reader was used to measure absorbance (PerkinElmer, Germany).

2.13 Hematoxylin and eosin staining and immunohistochemistry

For histopathological analysis, samples from the liver, kidney, and hippocampus were routinely fixed in 4% paraformaldehyde and then embedded in paraffin wax, cut into 5-μm-thick slices, and subsequently subjected to dehydration, embedding, and sectioning. Further, the sections were observed using a Nikon imaging system (TS2). For immunohistochemistry, paraffin-embedded sections of brain tissue were heated at 60°C, dewaxed with water, subjected to antigen retrieval, and closed at room temperature. The primary anti-Iba1 (17,198, 12,000; Cell Signaling Technology) was added, followed by incubation at 4°C overnight. Subsequently, rinse them with PBS five times, allowing 5 min for each rinse. Afterwards, rabbit secondary antibody (HRP-labeled) (Servicebio, China) was added, followed by incubation in the dark for 1 h, rinsing with PBS, color development by DAB, dehydration, and sealing. The immunohistochemistry samples were photographed under an upright microscope and analyzed using ImageJ (version: 1.8.0.112).

2.14 Immunofluorescence analysis

The dewaxed coronal sections were subjected to antigen retrieval. The primary antibody rabbit antirat Iba1 (Cell Signaling Technology, 17,198), prepared at a 1:100 ratio with PBS, was added dropwise to the sections, which were then incubated at 4°C overnight. The secondary antibody anti-rabbit IgG was diluted in 4% BSA in PBS and incubated at room temperature for 1 h. The cell nucleus was stained with DAPI at room temperature for 10 min, avoiding light. Fluorescence images were obtained using a confocal laser scanning microscope (DMI8 DFC7000T; Leica Microsystems).

2.15 mRNA expression analysis by RT-qPCR

Total RNA was extracted from the colon using Trizol reagent (Thermo Fisher) and processed per the PrimeScript RT Reagent Kit (Vazamy, Nanjing, China) instructions to synthesize cDNA. qPCR was performed in an RT-qPCR instrument (MA-Smart) per the SYBR Premix Ex Taq II Reagent (Vazamy, Nanjing, China) instructions. GAPDH was used as an internal reference gene, and the $2^{-\Delta\Delta CT}$ relative quantitation method was used to analyze gene expression. The used primers were synthesized by Shanghai Shenggong Technology Co., Ltd., and Table 2 contains the primers listed for qRT-PCR analysis.

2.16 16S rRNA sequencing and bioinformatic analysis

Approximately 1.0 g of midstream fecal samples were collected from PPA-treated rats and preserved at a temperature of −80°C for subsequent analysis. DNA was extracted from these samples using the Tiangen Biochemical Technology Co., Ltd. (Beijing, China) Fecal Genome DNA Extraction Kit (DP328-02). The V3-V4 regions of the 16S rRNA gene were targeted for amplification using the primers 341F (CCTACGGGNGGCWGCAG) and 785R (GACTACHVGGGTA TCTAATCC). Following amplification, the PCR products were purified and subjected to agarose gel electrophoresis to isolate the amplicon. The target DNA fragment was then excised, purified, and prepared for sequencing. The purified DNA libraries were sequenced on the Illumina

TABLE 2 Sequences of primers used in the study.

Gene	Forward primer (5′- > 3′)	Reverse primer (5′- > 3′)
GAPDH	CCTGGAGAAACCTGCCAAG	CACAGGAGACAACCTGGTCC
Occludin	AGCGAAGAGTACATGGCTGC	TCACTTCTCCAGCAACCAGC
ZO-1	GGAGCGGGGACAAGATGAAG	GAGGATGGAGTTACCCACAGC

Novaseq 6,000 platform using a paired-end (PE250) sequencing strategy. Post-sequencing, the cutadapt software was employed to remove primer sequences from the raw reads, and vsearch was used to merge the paired-end sequences. Sequences with a similarity of 97% or greater were clustered into operational taxonomic units (OTUs). These OTUs, representing the core sequences within each cluster, were then utilized for taxonomic annotation and further classification analysis. Alpha diversity was determined using QIIME2. Beta diversity was analyzed by principal coordinate analysis (PCoA). Linear discriminant analysis (LDA) coupled with effect size (LEfSe) was applied to evaluate the taxa with differences in abundance between the groups. Bacterial groups exhibiting an LDA score of 2.00 or higher were deemed to be significantly abundant within a specific group. The 16S rRNA analysis data presented in the study are deposited in the National Center for Biotechnology Information Sequence Read Archive database, accession numbber PRJNA1131930; The metabolomic analysis data presented in the study are deposited in the MetaboLights database (accession code: MTBLS3435).

2.17 Metabolomic analysis

The 50 mg fecal sample was precisely weighed and transferred into a 2 mL centrifuge tube. To this, 600 μL of methanol containing 2-chloro-L-phenylalanine was added, and the mixture was vortexed for 30 s to ensure thorough mixing. Subsequently, 100 mg of glass beads were introduced into a tissue grinder, and the sample was ground at a frequency of 60 Hz for 90 s. Following grinding, the sample was subjected to ultrasonication at room temperature for 10 min to further aid in the extraction process. After ultrasonication, the sample was centrifuged at 12,000 rpm for 10 min at a temperature of 4°C to separate the supernatant from the solid particles. The supernatant was then passed through a 0.22 μm membrane filter to remove any remaining particulates and collect the resulting filtrate. The LC/MS system for untargeted metabolomic analysis comprised Waters Acquity I-Class PLUS ultrahigh-performance liquid tandem Waters Xevo G2-XS QT high-resolution mass spectrometer. Raw data collected using MassLynx were processed by R XCMS (v3.12.0) software. Metabolites with RSD > 30% in QC samples were filtered and used for subsequent data analysis. Subsequently, the identified compounds were used as queries for searches for classification and pathway information in HMDB (Wishart et al., 2007), MassBank (Horai et al., 2010), KEGG (Ogata et al., 1999), LipidMaps (Sud et al., 2007), mzcloud (Abdelrazig et al., 2020), and the metabolite database built by Panomix Biomedical Tech Co., Ltd. (Shuzhou, China). PCoA was used to judge the repeatability of the samples within groups. The R package ropls was used to perform OPLS-DA modeling, and 200× permutation tests were performed to confirm model reliability. The significantly enriched KEGG pathways among the differential metabolites were calculated using the hypergeometric distribution test. The 16S rRNA analysis data presented in the study are deposited in the National Center for Biotechnology Information Sequence Read Archive database, accession numbber PRJNA1131930; The metabolomic analysis data presented in the study are deposited in the MetaboLights database (accession code: MTBLS3435).

2.18 Statistical analysis

All data are presented as mean ± SD. Two groups were compared using unpaired Student's t-test or Mann–Whitney U test. Categorical variables were compared between two groups using the χ^2 or Fisher's exact test. Multiple groups were compared by Wilcoxon's test or one-way ANOVA. All statistical analyses were conducted using GraphPad Prism (version 9.5.0) or R package. Pearson's correlation analysis was used to determine the correlation between different parameters. Spearman's correlation analysis was used to explore the relationships of gut microbiota exhibiting differential expression between groups with social behaviors, serum physiological measures, and differentially expressed metabolites. All p values were two-sided, and $p < 0.05$ was regarded as indicative of statistical significance ($^*p < 0.05$, $^{**}p < 0.01$, $^{***}p < 0.001$, $^{****}p < 0.0001$, ns, not significant).

3 Results

3.1 Ultrahigh-performance liquid chromatography–mass spectrometry chromatogram analysis of multiple active ingredients in DCHD

Ultrahigh-performance liquid chromatography–mass spectrometry was employed to analyze the 11 primary active ingredients of DCHD (Cui et al., 2020). From the positive-ion mode results, 1, 2, 3, 4, 5, 6, 7, and 8 were identified as synephrine, albiflorin, paeoniflorin, naringin, neohesperidin, baicalin, saiko saponin A, and [6]-gingerol, respectively (Supplementary Figure S1B). From the negative-ion mode results, 1, 2, and 3 were identified as succinic acid, hesperidin, and emodin, respectively (Supplementary Figure S1C).

3.2 *Dachaihu* decoction improved autism-like behavior in rats with propionic acid-induced autism spectrum disorder

To explore the therapeutic effect of DCHD in ASD, several social behavior tests—open field test (OFT), elevated plus maze (EPM), novel object recognition (NOR) test, and three-chamber sociability tests(TCT)—were conducted (Figure 1A). Compared with the control, PPA-treated rats displayed impaired ASD-related behaviors, as reflected by the decreased total distance of movement (Figure 1B), fewer open-arm entries and less time spent in open arms (Figure 1C), the poor recognition of novelty (Figure 1D), and lack of preference for the stranger and novel rats in the sociability and social novelty tests (Figure 1E); this was consistent with previous results(Liu et al., 2024). However, after 4 weeks of DCH_H treatment, the total traveled distance had significantly increased ($p < 0.05$) in the OFT (Figure 1B). Meanwhile, in the EPM test, the rats treated with DCH_H exhibited more numerous entries and more time to the open arms than those the ASD group (Figure 1C), suggesting decreased anxiety. Moreover, in the NOR test (Figure 1D), rats in the DCH_H group were more inclined to explore new objects than those in the ASD group ($p < 0.05$), indicating improved learning and memory skills. In the three-chamber sociability test (Figure 1E), rats with autism treated with DCH_H possessed better socialization skills, with increased exposure to new rats

10.3389/fmicb.2025.1535451

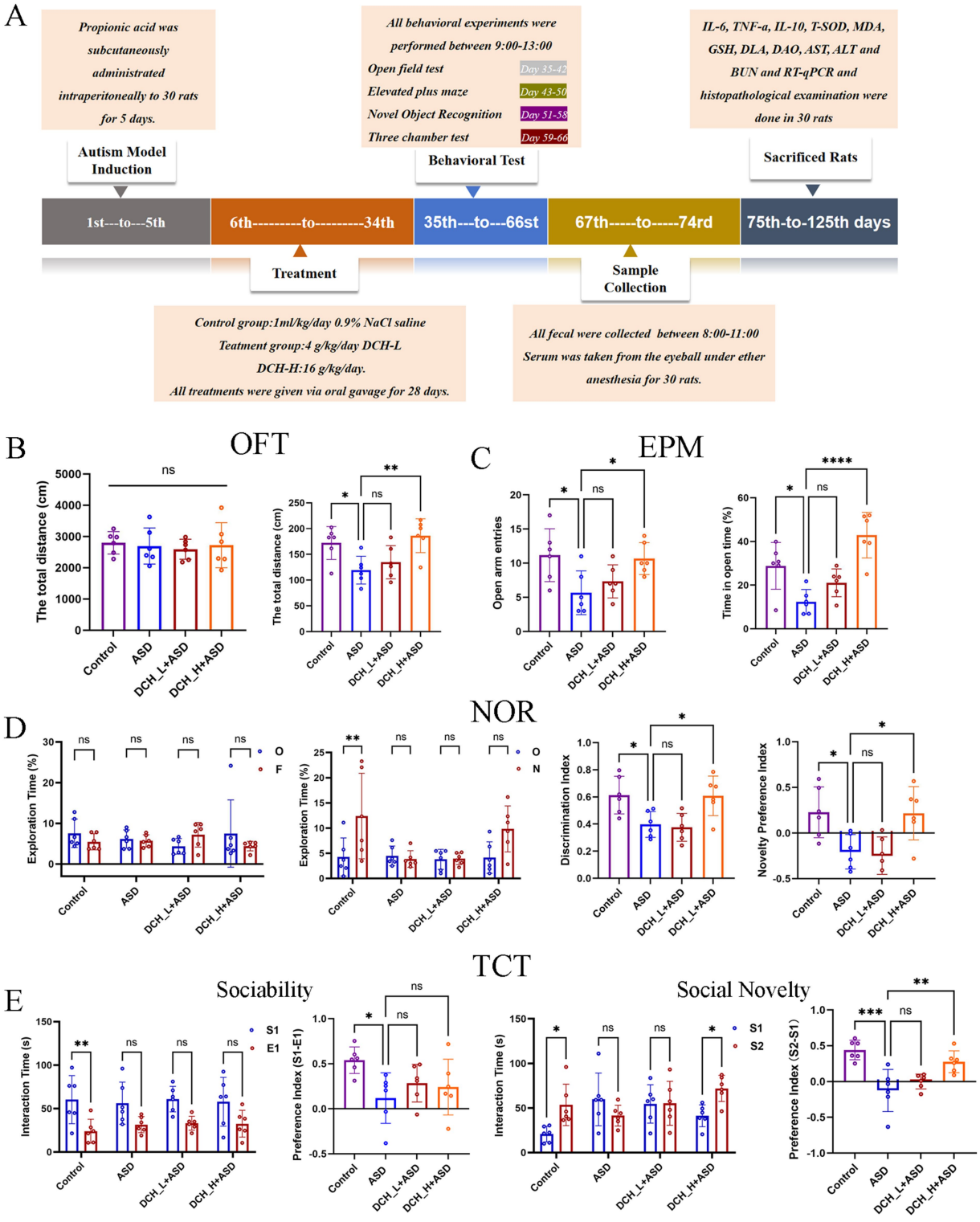

FIGURE 1
Experimental protocol and results of rat behavioral experiments. **(A)** Schematic of the animal study protocol. **(B)** Results of OFT in rats after 4 weeks of DCHD treatment. **(C)** Results of EPM test in rats after 5 weeks of DCHD treatment. **(D)** Results of NOR test in rats after 6 weeks of DCHD treatment. **(E)** Results of TCT in rats after 7 weeks of DCHD treatment.One-way ANOVA followed by Tukey's *post hoc* test was used for multiple pairwise comparison. *$p < 0.05$, **$p < 0.01$, ***$p < 0.001$, ns, not significant.

and exhibiting strong socialization abilities ($p < 0.05$), suggesting that DCH_H administration improved socialization in autistic rats. For all behavioral tests, no significant differences were found between the DCH_L treatment and ASD group. Thus, 4 weeks of treatment with DCH_H but not DCH_L reversed the social deficits in rats with PPA-induced autism.

3.3 *Dachaihu* decoction attenuated/mitigated inflammation, oxidative stress, and intestinal permeability of autistic rats

The key indicators of oxidative stress (GSH, T-SOD, and MDA) and levels of inflammatory factors (TNF-α, IL-6, and IL-10) were determined to evaluate the pharmacodynamic effect of DCHD for improving ASD. There were significantly increased in IL-6, TNF-α, and MDA levels (p = 0.0044, 0.0073, and 0.0080, respectively) in the PPA-induced ASD group (432.60 ± 11.18 pg/mL, 282.66 ± 36.96 ng/L, and 5.75 ± 0.89 nmol/mL) compared with those in the control group (415.34 ± 5.48 pg/mL, 213.20 ± 27.24 ng/L, and 3.82 ± 0.53 nmol/mL). Meanwhile, the induction of autism by PPA resulted in significantly decreased in the serum levels of IL-10 (p = 0.0031), GSH (p = 0.0322), and T-SOD activity (p = 0.0207) (21.48 ± 4.90 ng/L, 6.68 ± 2.51 μmol/L, and 72.27 ± 13.85 U/mL) compared with those in the control group (40.25 ± 7.57 ng/L, 14.45 ± 5.03 μmol/L, and 106.38 ± 22.22 U/mL) (Figures 2A–F). With the antioxidant and anti-inflammatory effects of DCHD, IL-6 and TNF-α levels were significantly decreased after 4 weeks of DCH_H treatments (p = 0.0119), compared with the findings in the ASD group. Furthermore, DCH_H treatment significantly reversed the changes in the serum levels of IL-10, MDA, and GSH (p = 0.0137, 0.0349 and 0.0295), as well as T-SOD activity (p = 0.0113), relative to those in the ASD group. Moreover, theeffects of DCHD on the liver and kidney were explored. Biomarkers (serum AST, ALT, and BUN) indicated that DCHD was not hepatotoxic or nephrotoxic to the rats (Supplementary Figures S2B–D). Furthermore, there were no obvious histopathological distinctions between the DCHD treatment and control group in liver and kidney sections (Supplementary Figure S2A).

Increased gut barrier permeability can translocate various luminal contents into the circulatory system, potentially triggering immune responses and neuroinflammation, which could in turn affect brain function and behavior(Chelakkot et al., 2018). This can also activate the microglia of the central nervous system and release proinflammatory cytokines(Alexandrov et al., 2020; Kelly et al., 2015). To evaluate whether DCHD can impact gut barrier function, we tested serum DAO and DLA, biomarkers of gut barrier integrity, that significantly increased upon the induction of autism by administering PPA (DAO, 214.60 ± 32.71 pg/mL, p = 0.0283; DLA, 54.69 ± 6.88 μmol/L, p = 0.0110) compared with the control group (DAO, 142.47 ± 16.78 pg/mL; DLA, 43.13 ± 6.41 μmol/L). However, DCH_H treatment markedly decreased the DAO and DLA levels (DAO, p = 0.0118; DLA, p = 0.0405; Figure 3A). Accordingly, the expression of ZO-1 and occludin, declined in the autistic rats, but was elevated in the DCH_H-treated rats, as determined by RT-qPCR (Figure 3B). These findings indicated that DCHD might contribute to restoring the function of the gut barrier.

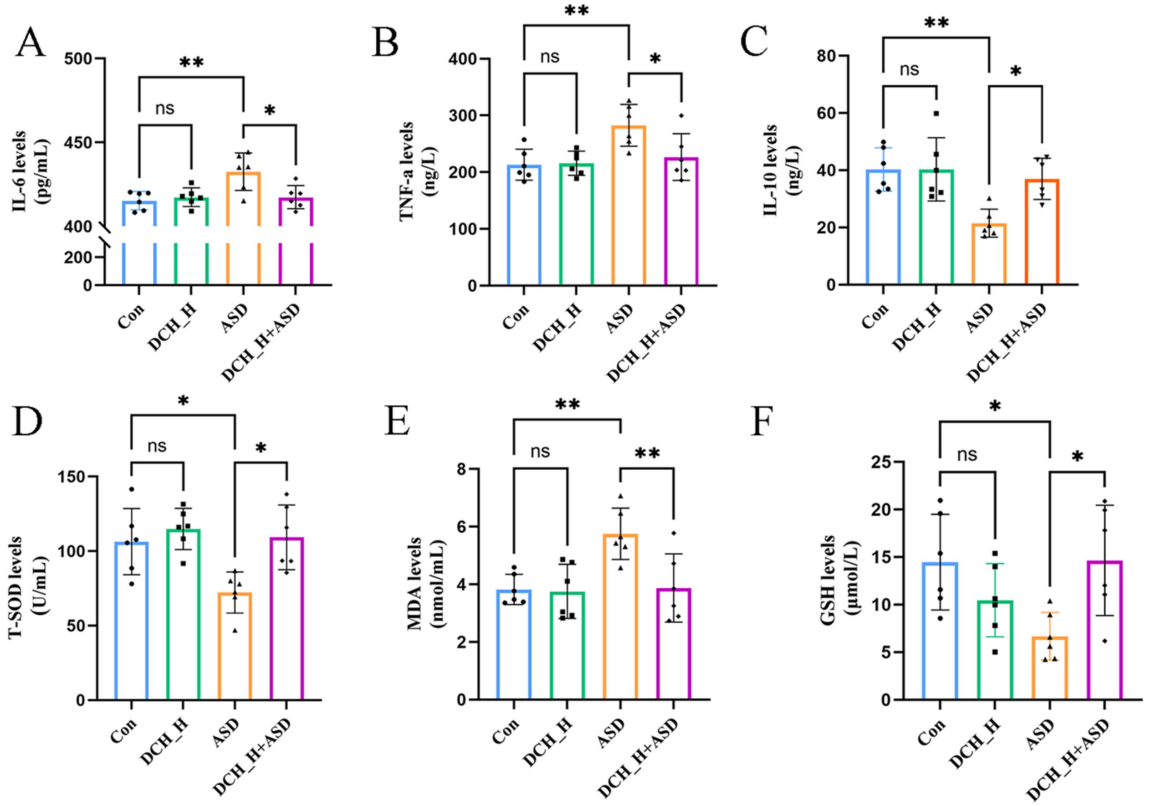

FIGURE 2
Dachaihu decoction effectively relieved inflammation, oxidative stress, and intestinal permeability in rats with PPA-induced autism. **(A–F)** Serum levels of IL-6, TNF-α, IL-10, T-SOD, MDA, and GSH.One-way ANOVA followed by Tukey's post hoc test was used for multiple pairwise comparison. *p < 0.05, **p < 0.01, ***p < 0.001, ns, not significant.

10.3389/fmicb.2025.1535451

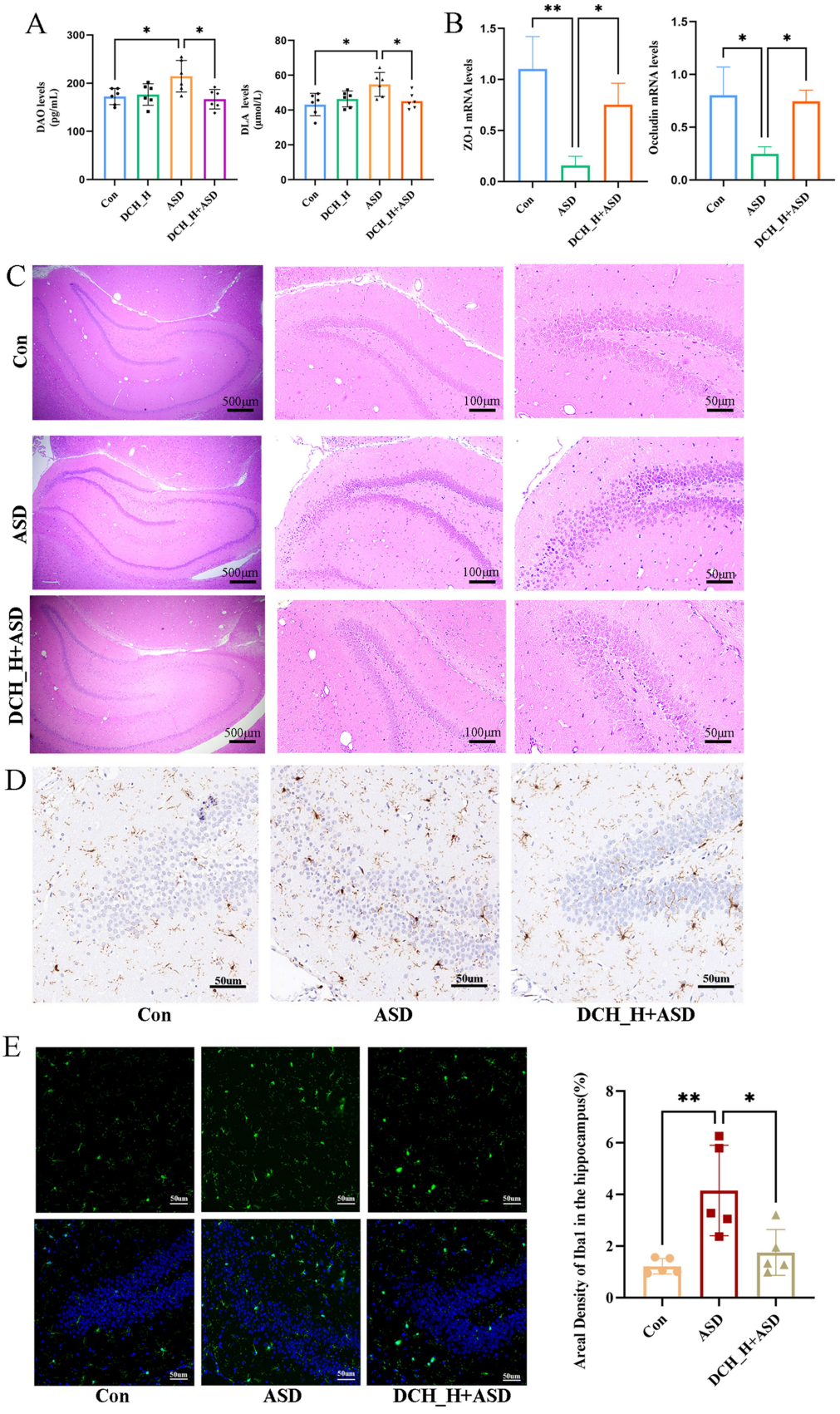

FIGURE 3
Dachaihu decoction effectively relieved intestinal permeability in rats with PPA-induced autism. **(A)** DAO and DLA levels. **(B)** ZO-1 and occludin mRNA expression in colon (n = 3, each group) assessed by RT-qPCR. **(C-E)** Brain tissue sections underwent hematoxylin and eEosin (H&E) staining, and immunohistochemical and immunofluorescence studies for histopathological analysis (n = 5, each group). One-way ANOVA followed by Tukey's post hoc test was used for multiple pairwise comparison.*p < 0.05, **p < 0.01, ***p < 0.001, ns, not significant.

Hippocampal lesions are reportedly associated with the social memory deficits in ASD (Banker et al., 2021). Herein, hematoxylin and eosin staining showed that the ASD group exhibited a loose arrangement of neurons and necrotic neurons in the DG region of the hippocampus, in contrast to the control group, whereas DCH_H treatment slowed down cell atrophy, as evidenced by more tightly arranged neurons (Figure 3C). Consequently, the number of microglia in the hippocampal DG regions was significantly increased in rats with PPA-induced autism but was decreased by DCHD treatment (Figures 3D,E). Thus, the number of microglia in the hippocampus, density of Iba-1, and branches of the microglia were consistently restored by DCH_H, as revealed by immunofluorescence staining ($p < 0.05$). These results suggested that DCHD might improve hippocampal function through the gut–brain axis.

3.4 *Dachaihu* decoction modulated propionic acid-induced gut dysbiosis in autistic rats

Alterations in the gut microbiota reportedly correlates with behavioral problems in patients with autism(Chen et al., 2022). To determine if DCHD intervention changs the gut microbiota thereby involved in improved ASD-like behaviors, we profiled the gut microbiota composition of rats through 16S rRNA sequencing. A Venn diagram at the OTU level shows 2,360 common OTUs among the four groups, with each group harboring unique OTUs (Figure 4A). Results from the PCoA of β-diversity plots indicate that DCH_H, without impacting microbial α-diversity (Figure 4B), modified the structural composition of the gut microbial community (ASD vs. Control, $p = 0.018$; DCH_H vs. ASD, $p = 0.031$ by Adonis analysis; Figure 4C). At the phylum level, the *Firmicutes/Bacteroidetes* ratio was significantly higher in rats with ASD (2.8912 ± 1.6552) than in control rats (0.9075 ± 0.4564), whereas the *Firmicutes/Bacteroidetes* ratio was partially restored (1.9489 ± 1.2763) after 4 weeks of DCH_H treatment (Figure 4D). The LEfSe revealed that the ASD rats were characterized by high levels of *Pasteurellaceze*, *Pasteurellales*, and *Rodentibacter*, while DCH_H treatment was associated with high levels of *Peptostreptococcaceae*, *Romboutsia*, *Tyzzerella*, *Parvibacter*, and *Adlercreutzia* (Supplementary Figure S3). A heatmap of gut microbial genera showed that DCH_H holistically altered the PPA-induced composition of microbiota (Figure 4E). Notably, DCHD treatment reversed the decreases in the beneficial bacteria *Adlercreutzia* and *Christensenellaceae*_uncultured in the ASD group (Figure 4F). Meanwhile, the relative abundance of the beneficial bacteria *Muribaculaceae_ge* and *Odoribacter* significantly decreased in the PPA-induced rats group compared with the control group (Figure 4F). Conversely, genera such as the harmful bacteria *Erysipelatoclostridium* and *Clostridiales*_unclassified increased in the ASD group (Figure 4F). Furthermore, the levels of the probiotics *Faecalibaculum*, *Dubosiella, Parvibacter*, *Romboutsia*, *Turicibacter*, and *Ruminococcaceae*_UCG-007 were significantly increased in the ASD rats after DCHD treatment (Figure 4F). Considerably, DCHD treatment affected the gut microbiota profile and optimized the bacterial composition in ASD rats.

3.5 *Dachaihu* decoction corrects gut microbiota metabolite imbalances/ modulates gut metabolites in autistic rats

Gut microbiota can regulate the development and function of the host nervous system through its metabolites (Xiao et al., 2022; Zheng et al., 2021). Thus, we performed metabolomic analysis of the gut microbiota. The fecal samples from distinct groups were largely separated by partial least-squares discriminant analysis (PLS-DA) and Orthogonal Partial Least Squares Discriminant Analysis (OPLS-DA) (Figure 5A), suggesting distinct metabolic modes. KEGG enrichment analysis of differential metabolites between the Con and ASD groups and between the DCH_H and ASD groups (Figures 5B,C). Subsequent bioinformatic analysis identified 20 significantly enriched KEGG pathways between the DCH_H and ASD groups (Figure 5C), among which aldosterone synthesis and secretion (ID: rno04925, $p = 0.021$), Linoleic acid metabolism (ID: rno00591, $p = 0.033$), Inflammatory mediator regulation of TRP channels (ID: rno04750, $p = 0.049$), Serotonergic synapse (ID: rno04726, $p = 0.068$), and Lysine degradation (ID: rno00310, $p = 0.092$) were notable for containing the most differentially expressed metabolites, and among which GABAergic synapse (ID: rno04727, $p = 0.088712694$) showed the highest significance. Meanwhile, 39 distinct metabolites (FC > 1, VIP > 1, and $p < 0.05$) were identified between the PPA-induced rats group and control group, which included 26 and 13 metabolites up- and down-regulated in ASD (Figure 5D). Meanwhile, 34 distinct metabolites were identified between the DCHD-treated and ASD groups (FC > 1, VIP > 1, and $p < 0.05$), 12 and 22 of which were up- and down-regulated, respectively (Figure 5D). Notably, the findings on the differential metabolites in the feces revealed that DCHD upregulated metabolites such as indole-3-acetate, apigenin, erythritol, and N-acetyl-L-glutamine, while down regulating metabolites such as asymmetric dimethylarginine, homogentisic acid, m-cresol and caprylic acid, and arachidonic acid (Figure 5E).

3.6 Correlations of the altered gut microbiota with behaviors, serum biochemical parameters, and gut metabolites in autistic rats

Gut microbiota is considered closely related to autistic behaviors (Zarimeidani et al., 2024). Herein, Spearman's correlation analysis showed that the genera *Parvibacter* and *Dubosiella* were a strong correlation to improved social behaviors, followed by *Romboutsia* and *Christensenellaceae*_uncultured. Such behaviors included the increased total distance of movement, the more open-arm entries and longer time spent in open arms, the better novelty performance, and the improved preference for the stranger rat in the sociability test and for the novel rat in the social novelty test (Figure 6A). Overall, DCHD regulation of social behaviors is linked to specific gut microbiota, suggesting that DCHD can regulate the gut microbiota of PPA-induced rats and improve social behaviors.

Herein, correlations were found between the differential gut microbiota and serum chemical parameters, including inflammatory response indices IL-6, TNF-α, and IL-10; oxidative stress indices T-SOD, GSH, and MDA; and intestinal barrier markers DAO and DLA (Figure 6A). In addition, the results showed that most DCHD-promoted beneficial bacteria, such as *Adlercreutzia*, *Faecalibaculum*,

10.3389/fmicb.2025.1535451

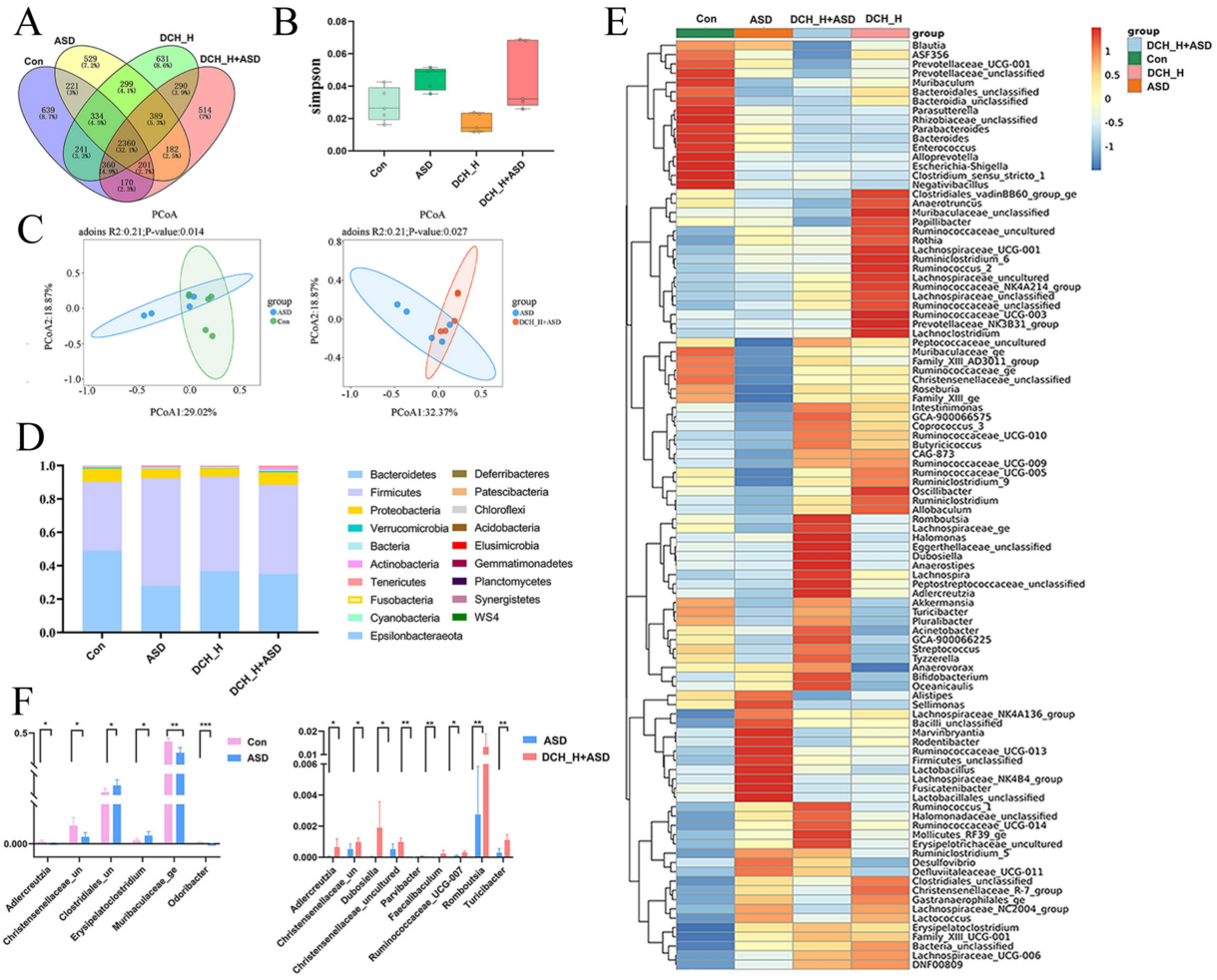

FIGURE 4
DCHD regulated gut microbiota dysbiosis in rats with PPA-induced autism after 4 weeks of treatment. **(A)** Venn diagram showing the overlap of OTUs among the four groups. **(B)** Simpson index (α-diversity) and **(C)** Principal component analysis (PCoA) (*β*-diversity) of the gut microbiota. **(D)** Histogram of relative abundance of the gut microbiota at the phylum level. **(E)** Heatmap of gut microbial genera among the four groups. **(F)** Bacteria with differential abundance between the ASD and control groups, and between the DCHD-treated and ASD groups. One-way ANOVA followed by Tukey's post hoc test was used for multiple pairwise comparison. *$p < 0.05$, **$p < 0.01$, and ***$p < 0.001$.

Dubosiella, *Romboutsia*, *Christensenellaceae*_unclassified, *Ruminococcaceae*_UCG-007, and *Parvibacter*, were negatively associated with serum IL-6 level. Meanwhile, the levels of *Christensenellaceae*_unclassified, *Dubosiella*, *Peptostreptococcaceae*_unclassified, *Romboutsia*, *Ruminococcaceae*_UCG-007, and *Parvibacter* were positively associated with IL-10, T-SOD, and GSH. Additionally, the genera *Adlercreutzia*, *Dubosiella*, and *Parvibacter* were negatively associated with either serum DAO or DLA content.

The gut microbiota significantly contributes to the regulation of metabolism. To investigate the potential links between the changes in the gut microbiota and metabolites, we used Spearman's correlation analysis to creat a correlation matrix (Figure 6B). Some bacteria are strongly correlated with many metabolites (cor > 0.5 or cor < −0.5). For example, *Adlercreutzia*, *Coriobacteriaceae*_UCG-002, *Dubosiella*, *Eggerthellaceae*_unclassified and *Faecalibaculum* were positively correlated with apigenin. Meanwhile, *Adlercreutzia, Dubosiella, Romboutsia*, *Turicibacter*, and *Christensenellaceae*_uncultured were positively correlated with erythritol. In addition, *Parvibacter* and *Christensenellaceae* were negatively correlated with asymmetric dimethylarginine. However, *Turicibacter* and *Ruminococcaceae*_UCG-007 were positively correlated with indole-3-acetate. *Parvibacter* was negatively correlated with m-cresol. Furthermore, *Adlercreutzia*, *Faecalibaculum*, and *Dubosiella* were negatively correlated with aldosterone. *Christensenellaceae, Turicibacter, Romboutsia*, and *Peptostreptococcaceae*_unclassified were positively correlated with serotonin. Finally, *Ruminococcaceae*_UCG-007 and *Turicibacter* were positively correlated with N-acetyl-L-glutamine. Therefore, DCHD may improve PPA-induced disordered social behaviors by regulating gut microbiota, potentially by influencing inflammatory response, oxidative stress, intestinal barrier function, and gut microbial metabolism.

3.7 *Dachaihu* decoction significantly improves the clinical symptoms of autism spectrum disorder

To explore the therapeutic effect of DCHD in children with ASD, we performed a small clinical study, revealing that 6 months of DCHD

10.3389/fmicb.2025.1535451

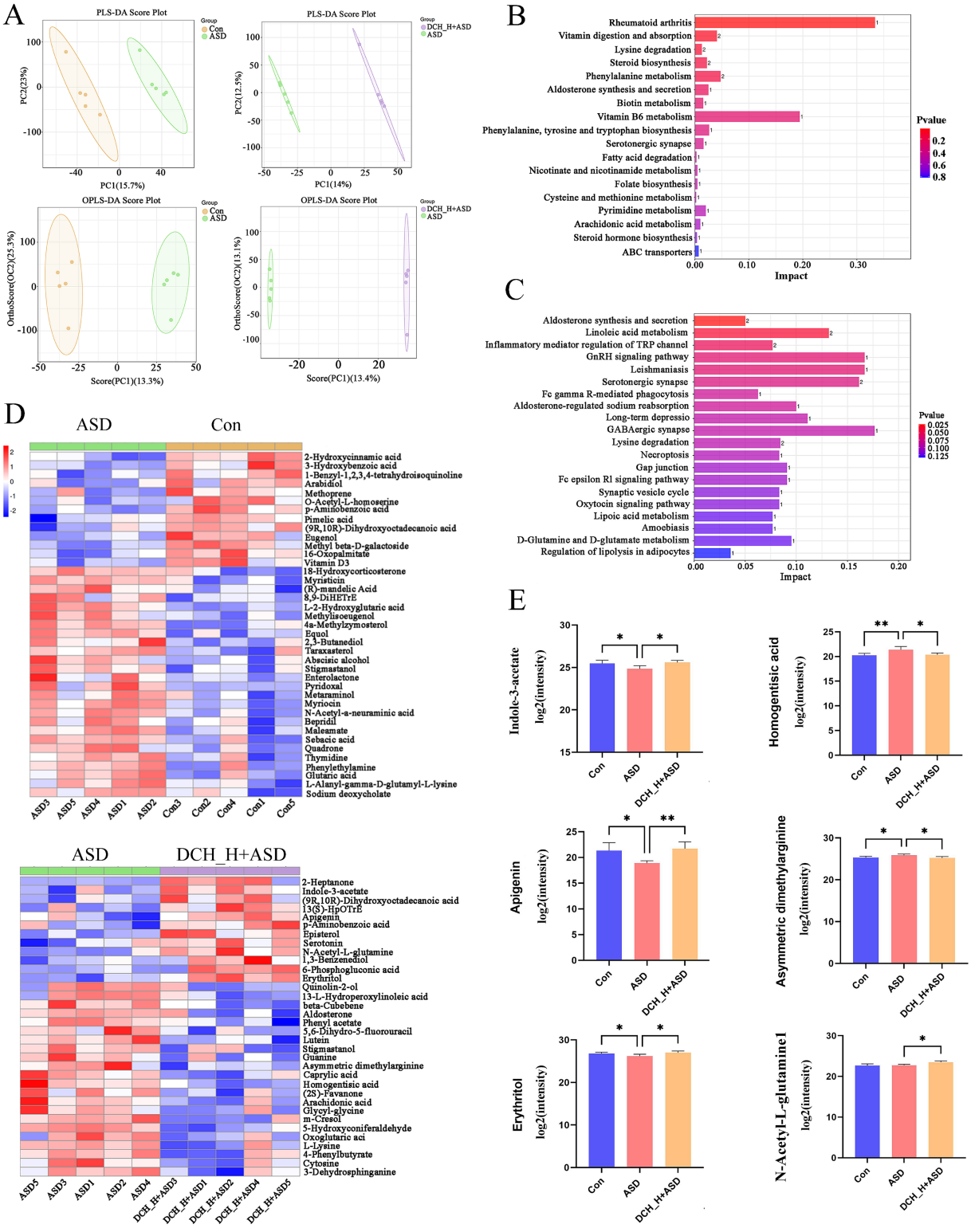

FIGURE 5
DCHD regulated metabolic processes in gut microbiota of rats with PPA-induced autism. **(A)** Clustering analyses of partial least-squares discriminant analysis (PLS-DA) and orthogonal partial least-squares discriminant analysis (OPLS-DA). **(B)** KEGG enrichment analysis of differential metabolites between the Con and ASD groups. **(C)** KEGG enrichment analysis of differential metabolites between the DCH_H and ASD groups. **(D)** Different metabolites between the ASD and control groups and different metabolites between the ASD + DCH_H and ASD groups. **(E)** Gut metabolism is regulated by DCHD, *$p < 0.05$, **$p < 0.01$. Metabolites with >1-fold change, with VIP > 1 and $p < 0.05$ (*t*- test).

10.3389/fmicb.2025.1535451

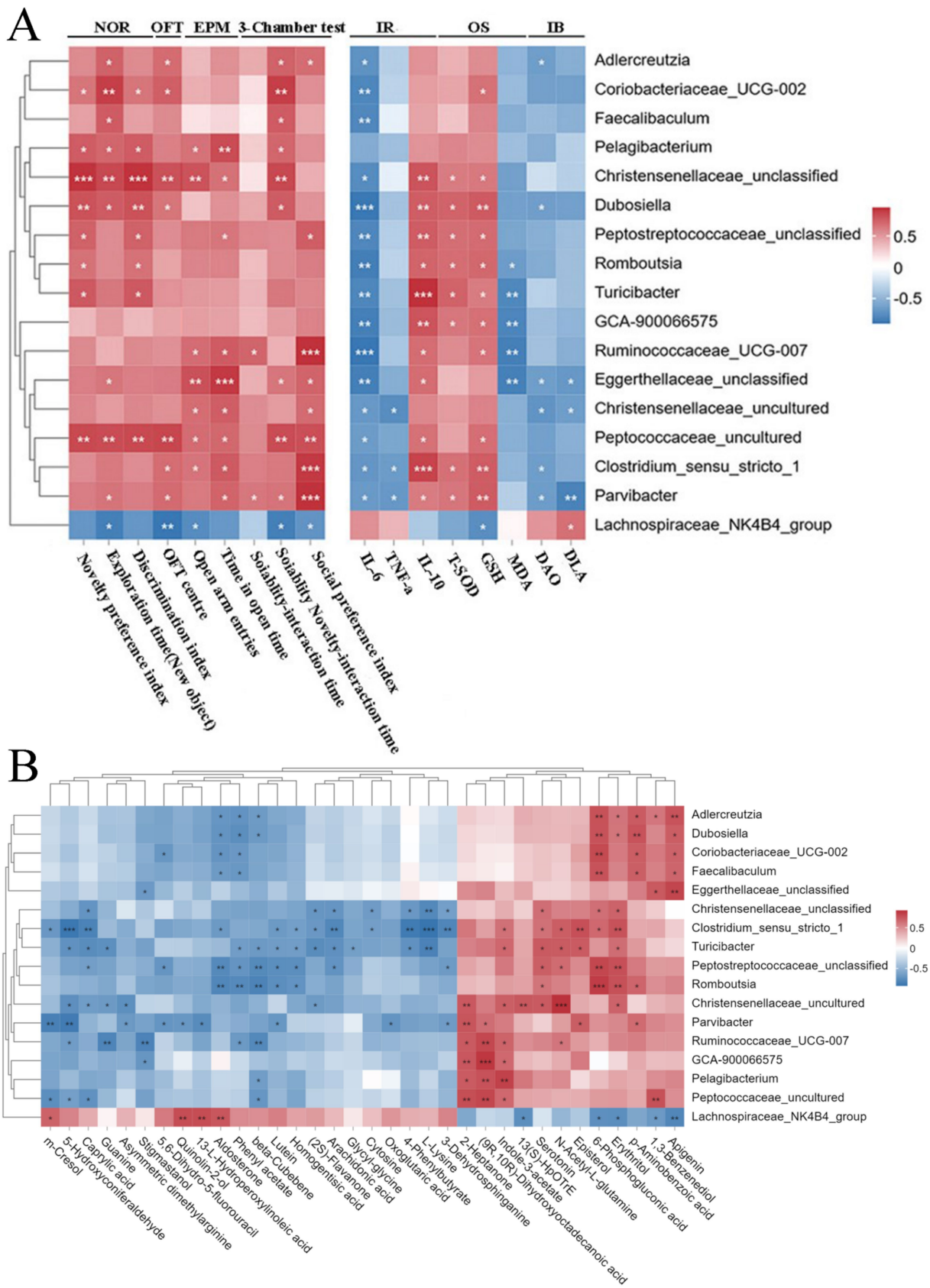

FIGURE 6
Spearman's correlation analysis. **(A)** Correlations between the differential genera and ASD-related behaviors and serum biochemical parameters of ASD rats after DCHD treatment.+ **(B)** Correlations between the differential genera and metabolites in feces of ASD rats after DCHD treatment. The different genera detected in 16S rRNA sequencing data between DCHD_H and ASD groups (Metastats analysis, $p < 0.05$). IR, inflammatory response; OS,

(Continued)

FIGURE 6 (Continued)
oxidative stress; IB, intestinal barrier. Metabolites with >1-fold change, with VIP > 1 and $p < 0.05$ (*t*- test) between DCHD_H and ASD groups. The correlation coefficient is indicated by a color gradient from blue (negative correlation) to brick-red (positive correlation). *p* values were corrected for multiple testing using the Benjamini–Hochberg false discovery rate. *$p < 0.05$, **$p < 0.01$, and ***$p < 0.001$.

application as ASD treatment achieved better results (Figure 7), primarily evidenced by improved overall symptom severity as assessed by the ABC score and ADOS-2 (Figures 7B,C). Furthermore, the latencies of MMN and P3b were significantly reduced, suggesting the enhanced capacity to process social and emotional information upon treating ASD-affected children with DCHD (Figure 7D). Meanwhile, DCHD treatment significantly decreased the food intolerance by reducing the concentrations of total IgG antibodies and specifically the IgG antibodies of egg white/yolk and milk (Figure 7E). Notably, no adverse effects were observed in ASD-affected children treated with DCHD in this trial. DCHD had no effects on serum AST, ALT and γ-GT(liver function) and BUN and CREA(kidney function) (Supplementary Figure S4), suggesting its safety.

4 Discussion

ASD is one of the most common neurodevelopmental disorders in children, with a prevalence rate of >2% in western countries (Maenner et al., 2023). The gut microbiota could be a promising therapeutic target for the interventions in ASD. The TCM formula DCHD reportedly exerts regulatory effects on the gut microbiota, which may be beneficial in ASD. However, the specific efficacy and mechanisms of DCHD in treating ASD remain unclear. Herein, DCHD significantly improved ASD-like behaviors, decreased inflammation and oxidative stress, restored gut barrier function, and modulated the gut microbiota in a PPA-induced rat model of ASD. Moreover, the DCHD dose that achieved such improvements was safe and well tolerated; this was consistent with the findings of a previous study (Cui et al., 2020), suggesting that DCHD is safe and effective for treating ASD.

The gut–brain axis is a complex bidirectional communication system between the gastrointestinal tract and the central nervous system, which has been implicated in various neurological disorders, including ASD (Morton et al., 2023). Gut barrier dysfunction, characterized by increased tight junction permeability and loss of tight junction proteins, is common in ASD (Dargenio et al., 2023). The changes in epithelial barrier function induced by DCHD were investigated here. Decreased serum levels of DAO and DLA, along with increased protein expression of the gut -barrier associated marker ZO-1 and occludin in the colon, were observed in DCHD-treated rats. Moreover, compared with ASD rats, DCHD treatment decreased the number of microglia and arranged more tightly neurons in the DG region of the hippocampus, indicating the memory and learning deficits was partially restored (Liu et al., 2023). The results suggested that DCHD might improve gut barrier and hippocampal function, alleviating ASD symptoms via the gut–brain axis.

Given that ASD is inextricably linked to alterations in the gut microbiota, the crosstalk between DCHD and the gut microbiota was analyzed here. The 16S rRNA sequencing showed that DCH_H treatment significantly attenuated gut dysbiosis in autistic rats (Figure 4). DCH_H treatment reversed the changes in *Firmicutes*/*Bacteroidetes* ratio, which was reported to increase in an ASD rat model (Jingyi et al., 2024). Moreover, the decreases in the probiotics *Adlercreutzia* and *Christensenellaceae*_unclassified induced by PPA were significantly reversed by treatment with DCH_H. Additionally, other probiotics such as *Faecalibaculum*, *Dubosiella*, *Parvibacter*, *Romboutsia*, *Turicibacter*, and *Ruminococcaceae*_UCG-007 were enriched by the DCH_H treatment. *Adlercreutzia* has reportedly played an active role in controlling inflammation and protecting the intestinal barrier (Wang et al., 2024), and to be negatively correlated with anxiety-like behavior (Xu et al., 2019). Moreover, *Faecalibaculum*, *Romboutsia*, and *Ruminococcaceae* are reportedly associated with enhanced gut motility and gut epithelial barrier by producing SCFAs (Li et al., 2021; Li et al., 2019; Li et al., 2022). Furthermore, the anti-inflammatory bacteria *Parvibacter*, *Christensenellaceae*, and *Dubosiella* are negatively correlated with IL-6 and TNF-α, and positively correlated with IL-10 (Figure 6A), which is consistent with the findings in previous reports(Chen et al., 2024; Gao et al., 2018; Wan et al., 2021). In addition, the abundance of *Turicibacter* is decreased in ASD-affected children compared with that in typically developing controls (Mehra et al., 2023). Notably, DCHD treatment significantly increased the relative abundance of *Turicibacter*, a critical component of the gut microbiota that plays a potential role in gut health (Wang et al., 2023). Considerably, DCHD treatment increased beneficial microbiota and inhibited inflammation and intestinal barrier damage, potentially contributing to improved ASD-like social behaviors.

The systematicity of metabolomics is similar to the holistic nature of TCM (Wang et al., 2024). Indeed, upon its administration, TCM can cause changes in the gut microbiota metabolome. Herein, the metabolomic analysis revealed that numerous metabolites were upregulated in DCHD-treated rats, including indole-3-acetate, apigenin, erythritol, and N-acetyl-L-glutamine. Of these, apigenin (Jayaprakash et al., 2024), N-acetyl-L-glutamine (Wu et al., 2023), and indole-3-acetate (Wei et al., 2024) are known for their anti-inflammatory, antioxidant, and gut–barrier protective effects. Specifically, apigenin and erythritol alleviate autistic-like stereotyped repetitive behaviors by mitigating oxidative stress and curbing excessive proliferation of the gut microbiota in ASD model mice (Cannon et al., 2020; Soltani et al., 2024). N-Acetyl-L-glutamine possess neuroprotective effects in various nervous system disorders, such as hemiplegia, brain trauma, and cerebral apoplexy sequelae (Ding et al., 2015; Wu et al., 2023). Meanwhile, indole-3-acetate is reduced in fecal samples from children with ASD compared with the levels in control group (Peralta-Marzal et al., 2021). In addition, the present findings revealed that DCHD downregulates asymmetric dimethylarginine and homogentisic acid. These compounds are known to elevate oxidative stress, potentially increasing ROS generation and resulting in redox imbalance, which can cause cerebral endothelial dysfunction and contribute to cognitive disorders (Braconi et al., 2010; Braconi et al., 2015; Jiang et al., 2024). Our results indicate that alterations in the gut microbiota metabolome may contribute to the increased antioxidant ability and

10.3389/fmicb.2025.1535451

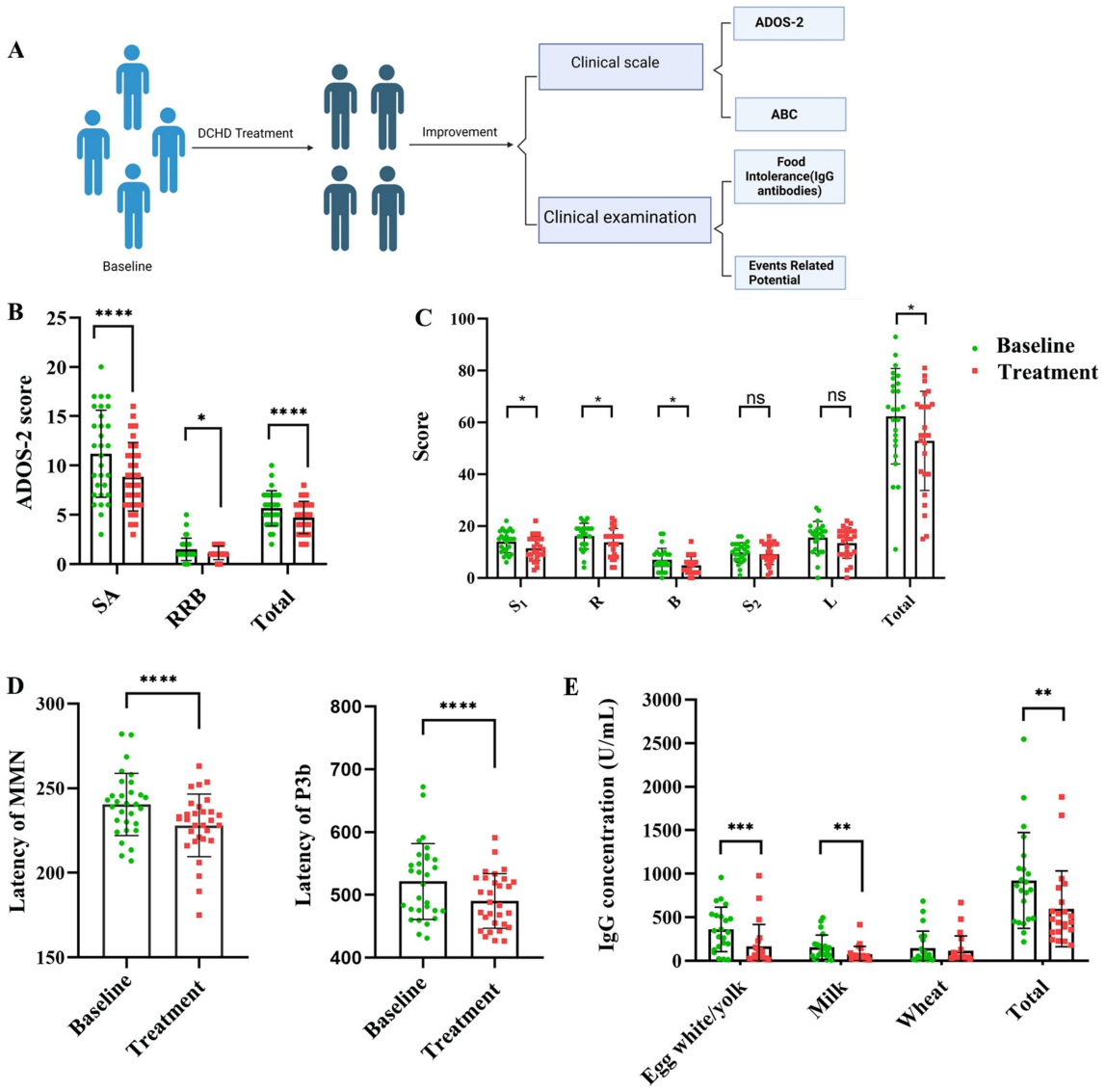

FIGURE 7
(A) Schematic of the small clinical study protocol. **(B,C)** DCHD effectively alleviates core ASD symptoms. **(D)** P3b latency and MMN latency, and **(E)** Food intolerance in children with ASD; n = 25–30, each group; social affect, SA; restricted and repetitive behavior, RRB. Two-sided Wilcoxon's matched-pairs signed-rank test was used for multiple pairwise comparison. Sensory: S_1; Relating: R; Body and object use: B; Social and selfhelp: S_2; Language: L. *$p < 0.05$, **$p < 0.01$, ***$p < 0.001$, ****$p < 0.0001$, ns, not significant.

decreased inflammatory response, thereby improving the ASD-like symptoms observed in rats with PPA-induced ASD. The altered metabolites identified in the metabolomic analysis may serve as major players in the effectiveness of DCHD treatment. Our findings suggested possible crosstalk between DCHD and the gut microbiota metabolome improves social behaviors in autistic rats.

Integrative gut microbiome and metabolome analysis revealed that the anti-inflammatory and antioxidant bacteria *Adlercreutzia* and *Faecalibaculum* were positively correlated with apigenin and erythritol in our study. Such metabolism can reduce repetitive behaviors of mice with ASD. Another anti-inflammatory bacterial taxon, the genus *Parvibacter*, was negatively correlated with asymmetric dimethylarginine, a metabolite associated with exacerbating oxidative stress. In addition, the abundances of *Parvibacter*, *Romb*outsia, and Christensenellaceae_uncultured are linked to improved social behaviors (Figure 6A). Herein, the abundances of *Adlercreutzia*, *Faecalibaculum*, *Parvibacter*, *Romboutsia*, and *Christensenellaceae*_uncultured were significantly increased by DCHD, suggesting that DCHD may improve abnormal behavior in mice with ASD by remodeling the gut microbiota and improving inflammatory responses. Thus, the protective role of DCHD in ASD involves modified gut microbiota and metabolites, highlighting the interplay between DCHD and gut microbiota in alleviating ASD symptoms. These findings may provide new insights into therapeutic interventions for ASD.

Our small clinical trial further demonstrated that DCHD significantly alleviated core symptoms of ASD, resulting in improvements in overall symptom severity, social communication, and motivation among children with ASD. DCHD also ameliorated gastrointestinal problems, as evidenced by decreased levels of FI-specific IgG antibody and total IgG antibody (Li

et al., 2020). Additionally, the MMN (Chien et al., 2024) and P3b latencies (Zhou et al., 2023) were significantly shortened by DCHD treatment, indicating improved cognitive impairment and brain responses for discriminating novelty. Given the clinical data about children with ASD, DCHD treatment may be promising for improving the main symptoms of ASD without side effects. In future studies, we plan to adopt multisource targeted metabolomics, metagenomics, and FMT to explore the association between differences in gut microbiota variations and metabolite changes in ASD patients after DCHD administration.

5 Conclusion

Combining clinical data from children with ASD and findings from interventional experiments in rats, this study confirmed the safety and efficacy of DCHD for treating ASD. The mechanism of action could be associated with reducing oxidative stress and modulating inflammatory reactions, protecting the intestinal barrier, balancing gut microbiota, and modulating gut microbial metabolism. This study provided crucial directions for the discovery and advancement of therapeutic agents for treating ASD and other psychiatric conditions at the gut microbiota and metabolic levels.

Data availability statement

The datasets presented in this study can be found in online repositories. The names of the repository/repositories and accession number(s) can be found in the article/Supplementary material.

Ethics statement

The studies involving humans were approved by the Scientific Ethics and Safety Committee of the Fifth Affiliated Hospital of Zhengzhou University. The studies were conducted in accordance with the local legislation and institutional requirements. Written informed consent for participation in this study was provided by the participants' legal guardians/next of kin. The animal studies were approved by The Scientific Ethics and Safety Committee of the Academy of Medical Sciences of Zhengzhou University. The studies were conducted in accordance with the local legislation and institutional requirements. Written informed consent was obtained from the owners for the participation of their animals in this study.

Author contributions

YZ: Data curation, Investigation, Visualization, Formal analysis, Writing – original draft. HL: Formal analysis, Data curation, Validation, Visualization, Writing – original draft. BL: Formal analysis, Data curation, Validation, Writing – original draft. YL: Investigation, Data curation, Writing – original draft. XC: Writing – review & editing. SL: Writing – review & editing. XX: Data curation, Software, Writing – review & editing. HL: Data curation, Writing – original draft. YZ: Data curation, Writing – review & editing. YT: Resources, Writing – review & editing. BY: Resources, Writing – review & editing. PZ: Resources, Writing – review & editing. EL: Supervision, Conceptualization, Funding acquisition, Project administration, Writing – review & editing. PF: Conceptualization, Methodology, Supervision, Writing – original draft, review & editing.

Funding

The author(s) declare that financial support was received for the research, authorship, and/or publication of this article. This work was funded by the fund of Henan Provincial Science and Technology Research Project (No. 232102311068, 242102311189, and 242102311176), the Henan Provincial Medical Science and Technology Research Joint Venture Project (No. SBGJ202403038) and the Key Research and Development Project of Henan Province (No. 241111210500).

Conflict of interest

The authors declare that the research was conducted in the absence of any commercial or financial relationships that could be construed as a potential conflict of interest.

Generative AI statement

The authors declare that no Gen AI was used in the creation of this manuscript.

Publisher's note

All claims expressed in this article are solely those of the authors and do not necessarily represent those of their affiliated organizations, or those of the publisher, the editors and the reviewers. Any product that may be evaluated in this article, or claim that may be made by its manufacturer, is not guaranteed or endorsed by the publisher.

Supplementary material

The Supplementary material for this article can be found online at: https://www.frontiersin.org/articles/10.3389/fmicb.2025.1535451/full#supplementary-material

References

Abdelrazig, S., Safo, L., Rance, G. A., Fay, M. W., Theodosiou, E., Topham, P. D., et al. (2020). Metabolic characterisation of *Magnetospirillum gryphiswaldense* MSR-1 using LC-MS-based metabolite profiling. *RSC Adv.* 10, 32548–32560. doi: 10.1039/D0RA05326K

Alexandrov, P. N., Hill, J. M., Zhao, Y., Bond, T., Taylor, C. M., Percy, M. E., et al. (2020). Aluminum-induced generation of lipopolysaccharide (LPS) from the human gastrointestinal (GI)-tract microbiome-resident *Bacteroides fragilis*. *J. Inorg. Biochem.* 203:110886. doi: 10.1016/j.jinorgbio.2019.110886

Banker, S. M., Gu, X., Schiller, D., and Foss-Feig, J. H. (2021). Hippocampal contributions to social and cognitive deficits in autism spectrum disorder. *Trends Neurosci.* 44, 793–807. doi: 10.1016/j.tins.2021.08.005

Benitah, K. C., Kavaliers, M., and Ossenkopp, K. P. (2023). The enteric metabolite, propionic acid, impairs social behavior and increases anxiety in a rodent ASD model: examining sex differences and the influence of the estrous cycle. *Pharmacol. Biochem. Behav.* 231:173630. doi: 10.1016/j.pbb.2023.173630

Biswas, M., Vanwong, N., and Sukasem, C. (2023). Pharmacogenomics and non-genetic factors affecting drug response in autism spectrum disorder in Thai and other populations: current evidence and future implications. *Front. Pharmacol.* 14:1285967. doi: 10.3389/fphar.2023.1285967

Bougeard, C., Picarel-Blanchot, F., Schmid, R., Campbell, R., and Buitelaar, J. (2024). Prevalence of autism Spectrum disorder and co-morbidities in children and adolescents: a systematic literature review. *Focus (Am Psychiatr Publ)* 22, 212–228. doi: 10.1176/appi.focus.24022005

Braconi, D., Laschi, M., Taylor, A. M., Bernardini, G., Spreafico, A., Tinti, L., et al. (2010). Proteomic and redox-proteomic evaluation of homogentisic acid and ascorbic acid effects on human articular chondrocytes. *J. Cell. Biochem.* 111, 922–932. doi: 10.1002/jcb.22780

Braconi, D., Millucci, L., Bernardini, G., and Santucci, A. (2015). Oxidative stress and mechanisms of ochronosis in alkaptonuria. *Free Radic. Biol. Med.* 88, 70–80. doi: 10.1016/j.freeradbiomed.2015.02.021

Buffington, S. A., Di Prisco, G. V., Auchtung, T. A., Ajami, N. J., Petrosino, J. F., and Costa-Mattioli, M. (2016). Microbial reconstitution reverses maternal diet-induced social and synaptic deficits in offspring. *Cell* 165, 1762–1775. doi: 10.1016/j.cell.2016.06.001

Cannon, M. L., Merchant, M., Kabat, W., Unruh, B., and Ramones, A. (2020). Inhibition of autism Spectrum disorder associated Bacteria and *C. difficile* by polyols. Edelweiss applied. *Sci. Technol.* 33-36, 33–36. doi: 10.33805/2576-8484.176

Chelakkot, C., Ghim, J., and Ryu, S. H. (2018). Mechanisms regulating intestinal barrier integrity and its pathological implications. *Exp. Mol. Med.* 50, 1–9. doi: 10.1038/s12276-018-0126-x

Chen, Y. C., Lin, H. Y., Chien, Y., Tung, Y. H., Ni, Y. H., and Gau, S. S. (2022). Altered gut microbiota correlates with behavioral problems but not gastrointestinal symptoms in individuals with autism. *Brain Behav. Immun.* 106, 161–178. doi: 10.1016/j.bbi.2022.08.015

Chen, D., Wang, Y., Yang, J., Ou, W., Lin, G., Zeng, Z., et al. (2024). Shenling Baizhu san ameliorates non-alcoholic fatty liver disease in mice by modulating gut microbiota and metabolites. *Front. Pharmacol.* 15:1343755. doi: 10.3389/fphar.2024.1343755

Chien, Y. L., Hsieh, M. H., and Gau, S. S. (2024). Mismatch negativity and P3a in unaffected siblings of individuals with autism Spectrum disorder and the exploration on the neurocognitive implications. *J. Autism Dev. Disord.* 2024:520. doi: 10.1007/s10803-024-06520-1

Cui, H., Li, Y., Wang, Y., Jin, L., Yang, L., Wang, L., et al. (2020). Da-chai-Hu decoction ameliorates high fat diet-induced nonalcoholic fatty liver disease through remodeling the gut microbiota and modulating the serum metabolism. *Front. Pharmacol.* 11:584090. doi: 10.3389/fphar.2020.584090

Dargenio, V. N., Dargenio, C., Castellaneta, S., De Giacomo, A., Laguardia, M., Schettini, F., et al. (2023). Intestinal barrier dysfunction and microbiota-gut-brain Axis: possible implications in the pathogenesis and treatment of autism Spectrum disorder. *Nutrients* 15:620. doi: 10.3390/nu15071620

Ding, L., Dong, G., Zhang, D., Ni, Y., and Hou, Y. (2015). The regional function of cGAS/STING signal in multiple organs: one of culprit behind systemic lupus erythematosus? *Med. Hypotheses* 85, 846–849. doi: 10.1016/j.mehy.2015.09.026

Duan, Z. W., Liu, Y., Zhang, P. P., Hu, J. Y., Mo, Z. X., Liu, W. Q., et al. (2024). Da-chai-Hu-Tang formula inhibits the progression and metastasis in HepG2 cells through modulation of the PI3K/AKT/STAT3-induced cell cycle arrest and apoptosis. *J. Ethnopharmacol.* 331:118293. doi: 10.1016/j.jep.2024.118293

Fischbach, M. A., and Segre, J. A. (2016). Signaling in host-associated microbial communities. *Cell* 164, 1288–1300. doi: 10.1016/j.cell.2016.02.037

Gao, L., Li, J., Zhou, Y., Huang, X., Qin, X., and Du, G. (2018). Effects of Baicalein on cortical Proinflammatory cytokines and the intestinal microbiome in senescence accelerated mouse prone 8. *ACS Chem. Neurosci.* 9, 1714–1724. doi: 10.1021/acschemneuro.8b00074

Guidetti, C., Salvini, E., Viri, M., Deidda, F., Amoruso, A., Visciglia, A., et al. (2022). Randomized double-blind crossover study for evaluating a probiotic mixture on gastrointestinal and behavioral symptoms of autistic children. *J. Clin. Med.* 11:263. doi: 10.3390/jcm11185263

Horai, H., Arita, M., Kanaya, S., Nihei, Y., Ikeda, T., Suwa, K., et al. (2010). MassBank: a public repository for sharing mass spectral data for life sciences. *J. Mass Spectrom.* 45, 703–714. doi: 10.1002/jms.1777

Huang, N., Wei, Y., Liu, M., Yang, Z., Yuan, K., Chen, J., et al. (2023). Dachaihu decoction ameliorates septic intestinal injury via modulating the gut microbiota and glutathione metabolism as revealed by multi-omics. *J. Ethnopharmacol.* 312:116505. doi: 10.1016/j.jep.2023.116505

Jayaprakash, P., Isaev, D., Yang, K. S., Beiram, R., Oz, M., and Sadek, B. (2024). Apigenin alleviates autistic-like stereotyped repetitive behaviors and mitigates brain oxidative stress in mice. *Pharmaceuticals (Basel)* 17:482. doi: 10.3390/ph17040482

Jiang, X., Chen, X., Su, J., and Liu, N. (2024). Prevalence of autism spectrum disorder in mainland China over the past 6 years: a systematic review and meta-analysis. *BMC Psychiatry* 24:404. doi: 10.1186/s12888-024-05729-9

Jiang, J., Miao, W., Guo, H., and Tian, W. (2024). Effects of rosuvastatin on serum asymmetric dimethylarginine levels and incidence of long-term cardiovascular events in patients with hyperlipidaemia and H-type hypertension. *Br. J. Hosp. Med. (Lond.)* 85, 1–10. doi: 10.12968/hmed.2024.0115

Jingyi, L., Lin, W., Yuan, C., Lingling, Z., Qianqian, J., Anlong, X., et al. (2024). Intravenous transplantation of bone marrow-derived mesenchymal stem cells improved behavioral deficits and altered fecal microbiota composition of BTBR mice. *Life Sci.* 336:122330. doi: 10.1016/j.lfs.2023.122330

Kang, D.-W., Adams, J. B., Gregory, A. C., Borody, T., Chittick, L., Fasano, A., et al. (2017). Microbiota transfer therapy alters gut ecosystem and improves gastrointestinal and autism symptoms: an open-label study. *Microbiome* 5:10. doi: 10.1186/s40168-016-0225-7

Kelly, J. R., Kennedy, P. J., Cryan, J. F., Dinan, T. G., Clarke, G., and Hyland, N. P. (2015). Breaking down the barriers: the gut microbiome, intestinal permeability and stress-related psychiatric disorders. *Front. Cell. Neurosci.* 9:392. doi: 10.3389/fncel.2015.00392

Kraeuter, A. K., Guest, P. C., and Sarnyai, Z. (2019). The open field test for measuring locomotor activity and anxiety-like behavior. *Methods Mol. Biol.* 1916, 99–103. doi: 10.1007/978-1-4939-8994-2_9

Li, N., Chen, H., Cheng, Y., Xu, F., Ruan, G., Ying, S., et al. (2021). Fecal microbiota transplantation relieves gastrointestinal and autism symptoms by improving the gut microbiota in an open-label study. Frontiers in cellular and infection. *Microbiology* 11:376. doi: 10.3389/fcimb.2021.801376

Li, J. W., Fang, B., Pang, G. F., Zhang, M., and Ren, F. Z. (2019). Age- and diet-specific effects of chronic exposure to chlorpyrifos on hormones, inflammation and gut microbiota in rats. *Pestic. Biochem. Physiol.* 159, 68–79. doi: 10.1016/j.pestbp.2019.05.018

Li, G., Lin, J., Zhang, C., Gao, H., Lu, H., Gao, X., et al. (2021). Microbiota metabolite butyrate constrains neutrophil functions and ameliorates mucosal inflammation in inflammatory bowel disease. *Gut Microbes* 13:1968257. doi: 10.1080/19490976.2021.1968257

Li, C., Liu, Y., Fang, H., Chen, Y., Weng, J., Zhai, M., et al. (2020). Study on aberrant eating behaviors, food intolerance, and stereotyped behaviors in autism Spectrum disorder. *Front. Psych.* 11:493695. doi: 10.3389/fpsyt.2020.493695

Li, Y., Xia, D., Chen, J., Zhang, X., Wang, H., Huang, L., et al. (2022). Dietary fibers with different viscosity regulate lipid metabolism via ampk pathway: roles of gut microbiota and short-chain fatty acid. *Poult. Sci.* 101:101742. doi: 10.1016/j.psj.2022.101742

Lin, C. H., Zeng, T., Lu, C.-W., Li, D.-Y., Liu, Y.-Y., Li, B.-M., et al. (2024). Efficacy and safety of *Bacteroides fragilis* BF839 for pediatric autism spectrum disorder: a randomized clinical trial. *Front. Nutr.* 11:59. doi: 10.3389/fnut.2024.1447059

Liu, Y., Li, H., Wang, X., Huang, J., Zhao, D., Tan, Y., et al. (2023). Anti-Alzheimers molecular mechanism of icariin: insights from gut microbiota, metabolomics, and network pharmacology. *J. Transl. Med.* 21:277. doi: 10.1186/s12967-023-04137-z

Liu, Q. Q., Mi, J., Du, Y. Y., Rong, Z., Qin, Y., Jiang, W., et al. (2024). Lotusine ameliorates propionic acid-induced autism spectrum disorder-like behavior in mice by activating D1 dopamine receptor in medial prefrontal cortex. *Phytother. Res.* 38, 1089–1103. doi: 10.1002/ptr.8098

Ma, Y. Z., Zhang, Y. S., Cao, J. X., Chen, H. C., Su, X. M., Li, B., et al. (2024). Aberration of social behavior and gut microbiota induced by cross-fostering implicating the gut-brain axis. *Brain Behav. Immun.* 120, 499–512. doi: 10.1016/j.bbi.2024.06.026

Maenner, M. J., Warren, Z., Williams, A. R., Amoakohene, E., Bakian, A. V., Bilder, D. A., et al. (2023). Prevalence and characteristics of autism Spectrum disorder among children aged 8 years - autism and developmental disabilities monitoring network, 11 sites, United States, 2020. Morbidity and mortality weekly report. *MMWR Surveill Summ* 72, 1–14. doi: 10.15585/mmwr.ss7202a1

Mazzone, L., Dooling, S. W., Volpe, E., Uljarević, M., Waters, J. L., Sabatini, A., et al. (2024). Precision microbial intervention improves social behavior but not autism severity: a pilot double-blind randomized placebo-controlled trial. *Cell Host Microbe* 32, 106–116.e6. doi: 10.1016/j.chom.2023.11.021

Mehra, A., Arora, G., Sahni, G., Kaur, M., Singh, H., Singh, B., et al. (2023). Gut microbiota and autism Spectrum disorder: from pathogenesis to potential therapeutic perspectives. *J. Tradit. Complement. Med.* 13, 135–149. doi: 10.1016/j.jtcme.2022.03.001

Morton, J. T., Jin, D. M., Mills, R. H., Shao, Y., Rahman, G., McDonald, D., et al. (2023). Multi-level analysis of the gut-brain axis shows autism spectrum disorder-associated molecular and microbial profiles. *Nat. Neurosci.* 26, 1208–1217. doi: 10.1038/s41593-023-01361-0

Ogata, H., Goto, S., Sato, K., Fujibuchi, W., Bono, H., and Kanehisa, M. (1999). KEGG: Kyoto encyclopedia of genes and genomes. *Nucleic Acids Res.* 27, 29–34. doi: 10.1093/nar/27.1.29

Peralta-Marzal, L. N., Prince, N., Bajic, D., Roussin, L., Naudon, L., Rabot, S., et al. (2021). The impact of gut microbiota-derived metabolites in autism Spectrum disorders. *Int. J. Mol. Sci.* 22:52. doi: 10.3390/ijms221810052

Poupard, L., Page, G., Thoreau, V., and Kaouah, Z. (2024). Relationships between gut microbiota and autism Spectrum disorders: development and treatment. *Clin Psychopharmacol Neurosci* 22, 554–564. doi: 10.9758/cpn.24.1179

Qin, L., Wang, H., Ning, W., Cui, M., and Wang, Q. (2024). New advances in the diagnosis and treatment of autism spectrum disorders. *Eur. J. Med. Res.* 29:322. doi: 10.1186/s40001-024-01916-2

Sherwin, E., Bordenstein, S. R., Quinn, J. L., Dinan, T. G., and Cryan, J. F. (2019). Microbiota and the social brain. *Science* 366:2016. doi: 10.1126/science.aar2016

Shi, H., Sun, M., Wang, S., He, F., Yang, R., Li, Z., et al. (2024). Jiawei Dachaihu decoction protects against mitochondrial dysfunction in atherosclerosis (AS) mice with chronic unpredictable mild stress (CUMS) via SIRT1/PGC-1alpha/TFAM/LON signaling pathway. *J. Ethnopharmacol.* 330:118150. doi: 10.1016/j.jep.2024.118150

Soltani, Z., Shariatpanahi, M., Aghsami, M., Owliaey, H., and Kheradmand, A. (2024). Investigating the effect of exposure to monosodium glutamate during pregnancy on development of autism in male rat offspring. *Food Chem. Toxicol.* 185:114464. doi: 10.1016/j.fct.2024.114464

Sud, M., Fahy, E., Cotter, D., Brown, A., Dennis, E. A., Glass, C. K., et al. (2007). LMSD: LIPID MAPS structure database. *Nucleic Acids Res.* 35, D527–D532. doi: 10.1093/nar/gkl838

Tan, Q., Orsso, C. E., Deehan, E. C., Kung, J. Y., Tun, H. M., Wine, E., et al. (2021). Probiotics, prebiotics, synbiotics, and fecal microbiota transplantation in the treatment of behavioral symptoms of autism spectrum disorder: a systematic review. *Autism Res.* 14, 1820–1836. doi: 10.1002/aur.2560

Wan, F., Han, H., Zhong, R., Wang, M., Tang, S., Zhang, S., et al. (2021). Dihydroquercetin supplement alleviates colonic inflammation potentially through improved gut microbiota community in mice. *Food Funct.* 12, 11420–11434. doi: 10.1039/D1FO01422F

Wan, L., Wang, H., Liang, Y., Zhang, X., Yao, X., Zhu, G., et al. (2024). Effect of oral faecal microbiota transplantation intervention for children with autism spectrum disorder: a randomised, double-blind, placebo-controlled trial. *Clin. Transl. Med.* 14:e70006. doi: 10.1002/ctm2.70006

Wang, J., Cao, Y., Hou, W., Bi, D., Yin, F., Gao, Y., et al. (2023). Fecal microbiota transplantation improves VPA-induced ASD mice by modulating the serotonergic and glutamatergic synapse signaling pathways. *Transl. Psychiatry* 13:17. doi: 10.1038/s41398-023-02307-7

Wang, N., Chen, S., Xie, Y., Liu, X., Xi, Z., Li, J., et al. (2024). The Sanbi decoction alleviates intervertebral disc degeneration in rats through intestinal flora and serum metabolic homeostasis modulation. *Phytomedicine* 127:155480. doi: 10.1016/j.phymed.2024.155480

Wei, W., Liu, Y., Hou, Y., Cao, S., Chen, Z., Zhang, Y., et al. (2024). Psychological stress-induced microbial metabolite indole-3-acetate disrupts intestinal cell lineage commitment. *Cell Metab.* 36, 466–483.e7. doi: 10.1016/j.cmet.2023.12.026

Wishart, D. S., Tzur, D., Knox, C., Eisner, R., Guo, A. C., Young, N., et al. (2007). HMDB: the human metabolome database. *Nucleic Acids Res.* 35, D521–D526. doi: 10.1093/nar/gkl923

Wu, L., Chen, S., He, B., Zhou, G., Xu, Y., Zhu, G., et al. (2023). Acetylglutamine facilitates motor recovery and alleviates neuropathic pain after brachial plexus root avulsion in rats. *J. Transl. Med.* 21:563. doi: 10.1186/s12967-023-04399-7

Xiao, W., Su, J., Gao, X., Yang, H., Weng, R., Ni, W., et al. (2022). The microbiota-gut-brain axis participates in chronic cerebral hypoperfusion by disrupting the metabolism of short-chain fatty acids. *Microbiome* 10:62. doi: 10.1186/s40168-022-01255-6

Xu, Z., Wang, C., Dong, X., Hu, T., Wang, L., Zhao, W., et al. (2019). Chronic alcohol exposure induced gut microbiota dysbiosis and its correlations with neuropsychic behaviors and brain BDNF/Gabra1 changes in mice. *Biofactors* 45, 187–199. doi: 10.1002/biof.1469

Zarimeidani, F., Rahmati, R., Mostafavi, M., Darvishi, M., Khodadadi, S., Mohammadi, M., et al. (2024). Gut microbiota and autism Spectrum disorder: a Neuroinflammatory mediated mechanism of pathogenesis? *Inflammation* 2024:2061. doi: 10.1007/s10753-024-02061-y

Zhang, J., Zhu, G., Wan, L., Liang, Y., Liu, X., Yan, H., et al. (2023). Effect of fecal microbiota transplantation in children with autism spectrum disorder: a systematic review. *Front. Psych.* 14:1123658. doi: 10.3389/fpsyt.2023.1123658

Zheng, H., Xu, P., Jiang, Q., Xu, Q., Zheng, Y., Yan, J., et al. (2021). Depletion of acetate-producing bacteria from the gut microbiota facilitates cognitive impairment through the gut-brain neural mechanism in diabetic mice. *Microbiome* 9:145. doi: 10.1186/s40168-021-01088-9

Zhou, X., Lin, Z., Yang, W., Xiang, M., Zhou, B., and Zou, Z. (2023). The differences of event-related potential components in patients with comorbid depression and anxiety, depression, or anxiety alone. *J. Affect. Disord.* 340, 516–522. doi: 10.1016/j.jad.2023.08.049

frontiers | Frontiers in Microbiology

TYPE Review
PUBLISHED 18 February 2025
DOI 10.3389/fmicb.2025.1527755

Check for updates

OPEN ACCESS

EDITED BY
Junling Shi,
Northwestern Polytechnical University, China

REVIEWED BY
Malgorzata Ziarno,
Warsaw University of Life Sciences, Poland
Suman Kharb,
Givaudan, Canada

*CORRESPONDENCE
Ramendra Pati Pandey
✉ ramendra.pandey@gmail.com
Suresh Kumar
✉ drsureshkumarmohil@gmail.com
V. Samuel Raj
✉ directorcd4@srmuniversity.ac.in

RECEIVED 18 November 2024
ACCEPTED 03 February 2025
PUBLISHED 18 February 2025

CITATION
Kumar S, Mukherjee R, Gaur P, Leal É, Lyu X, Ahmad S, Puri P, Chang C-M, Raj VS and Pandey RP (2025) Unveiling roles of beneficial gut bacteria and optimal diets for health.
Front. Microbiol. 16:1527755.
doi: 10.3389/fmicb.2025.1527755

COPYRIGHT
© 2025 Kumar, Mukherjee, Gaur, Leal, Lyu, Ahmad, Puri, Chang, Raj and Pandey. This is an open-access article distributed under the terms of the Creative Commons Attribution License (CC BY). The use, distribution or reproduction in other forums is permitted, provided the original author(s) and the copyright owner(s) are credited and that the original publication in this journal is cited, in accordance with accepted academic practice. No use, distribution or reproduction is permitted which does not comply with these terms.

Unveiling roles of beneficial gut bacteria and optimal diets for health

Suresh Kumar[1]*, Riya Mukherjee[2,3], Pratibha Gaur[4,5], Élcio Leal[6], Xiaoming Lyu[7], Saheem Ahmad[8], Paridhi Puri[9], Chung-Ming Chang[2,3,10], V. Samuel Raj[5,6]* and Ramendra Pati Pandey[5,6]*

[1]National Institute of Biologicals, Ministry of Health & Family Welfare, Govt. of India, Noida, India, [2]Graduate Institute of Biomedical Sciences, Chang Gung University, Taoyuan, Taiwan, [3]Department of Medical Biotechnology and Laboratory Science, Chang Gung University, Taoyuan, Taiwan, [4]Centre for Drug Design Discovery and Development (C4D), SRM University Delhi-NCR, Sonepat, India, [5]Department of Biotechnology and Microbiology, SRM University Delhi-NCR, Sonepat, India, [6]Laboratório de Diversidade Viral, Instituto de Ciências Biológicas, Universidade Federal Do Pará, Belém, Brazil, [7]Department of Laboratory Medicine, The Third Affiliated Hospital, Southern Medical University, Guangzhou, China, [8]Department of Medical Laboratory Sciences, College of Applied Medical Sciences, University of Hail, Ha'il, Saudi Arabia, [9]University Centre for Research and Development, Chandigarh University, Mohali, India, [10]Master & Ph.D Program in Biotechnology Industry, Chang Gung University, Taoyuan, Taiwan

The gut microbiome plays a pivotal role in human health, influencing digestion, immunity, and disease prevention. Beneficial gut bacteria such as *Akkermansia muciniphila*, *Adlercreutzia equolifaciens*, and *Christensenella minuta* contribute to metabolic regulation and immune support through bioactive metabolites like short-chain fatty acids (SCFAs). Dietary patterns rich in prebiotics, fermented foods, and plant-based bioactive compounds, including polyphenols and flavonoids, promote microbiome diversity and stability. However, challenges such as individual variability, bioavailability, dietary adherence, and the dynamic nature of the gut microbiota remain significant. This review synthesizes current insights into gut bacteria's role in health, emphasizing the mechanisms by which dietary interventions modulate microbiota. Additionally, it highlights advancements in microbiome-targeted therapies and the transformative potential of personalized nutrition, leveraging microbiota profiling and artificial intelligence (AI) to develop tailored dietary strategies for optimizing gut health and mitigating chronic inflammatory disorders. Addressing these challenges requires a multidisciplinary approach that integrates scientific innovation, ethical frameworks, and practical implementation strategies.

KEYWORDS

healthy gut bacteria, phytochemicals, prebiotic foods and probiotic foods, probiotics, fatty acid

1 Introduction

The human gut is a fascinating ecosystem that harbors trillions of microorganisms collectively known as gut microbiota that play a crucial role in several physiological functions through their derived metabolites such as nutrient metabolism, immune system regulation, vitamin production, mental health, and brain function that contribute to overall maintaining of health. There is a wide distribution of microbes in the gut which is essential for better health (Figure 1). Some of the key gut bacteria, including *Akkermansia muciniphila, Adlercreutzia equolifaciens, Barnesiella, Christensenella minuta, and Oxalobacter formigenes*, *Lactobacillus,*

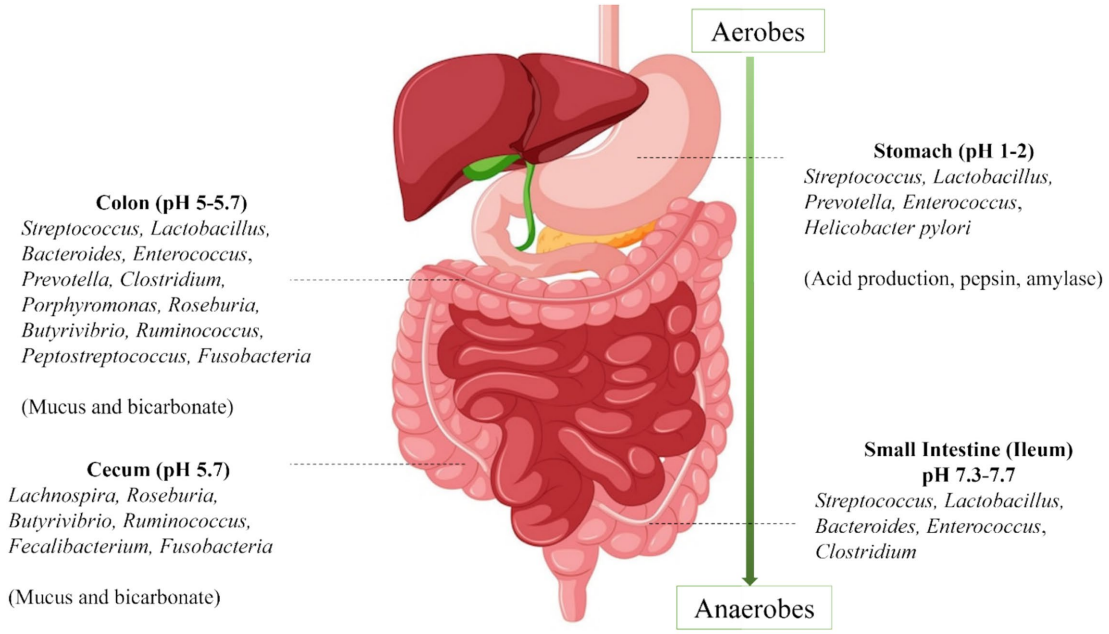

FIGURE 1
Distribution of gut microbiota.

Bifidobacterium, *Faecalibacterium prausnitzii*, *Roseburia* spp. contribute to unusual health benefits such as improved gut barrier function, better glucose metabolism, reduced inflammation, weight management, and prevention of kidney stone formation (Anhê et al., 2016; Maruo et al., 2008; Ubeda et al., 2013; Ang et al., 2023; Kaufman et al., 2008).

The dietary sources such as polyphenols, alkaloids, capsaicin, and polysaccharides are essential constituents that support the growth of these beneficial bacteria, leading to improved digestive health and overall well-being (Chenbo et al., 2022; Othman et al., 2019). The metabolites are small molecules that produced by the gut microbiota as byproducts can target directly as well as indirectly both the bacteria themselves and the host, regulating the composition and function of the gut microbiota (Liu et al., 2022; Jandhyala et al., 2015). In recent years, the significance of gut microbiota and their metabolites in influencing human health has garnered significant attention.

The role of gut microbiota in disease initiation is gaining significant attention. Dysbiosis, an imbalance in microbial composition, is strongly associated with the onset of conditions such as inflammatory bowel disease (IBD), metabolic syndrome, and neurodegenerative disorders. Altered microbial populations lead to reduced production of beneficial metabolites like SCFAs and increased levels of pro-inflammatory compounds such as lipopolysaccharides (LPS), disrupting gut barrier integrity and systemic homeostasis (Tan et al., 2014). Additionally, microbial interactions with dietary components such as fibers, polyphenols, and omega-3 fatty acids further influence health outcomes by modulating inflammation, immune signaling, and metabolic pathways (Sultan et al., 2021).

Several studies have focused on elucidating the specific functions and mechanisms of these microorganisms in relation to various diseases (Lavelle and Sokol, 2020; Parada Venegas et al., 2019; Liu et al., 2022). There is currently a lack of a comprehensive summarization regarding the most beneficial gut bacteria, their derived metabolites, and their dietary sources that contribute to maintaining overall health. In this review, we provide the potential role of microbiota in human health. We also discuss the essential gut bacteria and emphasize the derived metabolites of these gut bacteria especially the functions of regulating the local and systemic immune system, energy metabolism, and neural activity. Finally, we discuss how dietary approaches impacts the gut microbial ecology, and foods that promote healthier and more resilient intestinal gut bacteria.

2 Impact of microbiota on human health

The microbial balance in the intestine is closely related to human diseases and wellness. Extensive research has uncovered the crucial link between gut bacteria and fundamental human biological functions. Because of the varied metabolic genes encoding distinct enzymes and biochemical pathways, the microbiota plays critical roles in energy and nutrition extraction from food (Hou et al., 2022). Furthermore, the creation of bioactive compounds, including vitamins, amino acids, and lipids, is heavily reliant on gut bacteria (Roberfroid et al., 2009). The human microbiota not only protects the host from external pathogens by creating antimicrobial compounds but also plays an essential role in the development of intestinal mucosa and the immune system.

One of the key mechanisms by which the gut microbiota influences health is through the production of short-chain fatty acids (SCFAs), primarily acetate, propionate, and butyrate, which are generated via the fermentation of dietary fibers. SCFAs play a multifaceted role in maintaining gut homeostasis. Butyrate serves as the primary energy source for colonocytes, promoting tight junction integrity and reducing gut permeability, thereby reinforcing the gut barrier. Propionate and acetate, on the other hand, influence systemic

metabolism by modulating gluconeogenesis and lipid biosynthesis in the liver (Tan et al., 2014). Beyond metabolic regulation, SCFAs exert anti-inflammatory effects by interacting with G-protein-coupled receptors (GPCRs) and inhibiting histone deacetylases (HDACs), which regulate immune and inflammatory pathways (Yao et al., 2024; Liu et al., 2023).

The immune regulatory role of the microbiota is also mediated through the modulation of nuclear factor kappa B (NF-κB), a critical transcription factor that governs the expression of pro-inflammatory cytokines and antimicrobial peptides. Dysbiosis, or an imbalance in gut microbiota, can lead to overactivation of NF-κB, driving chronic inflammation and increasing susceptibility to inflammatory bowel disease and other gut-related disorders. SCFAs, particularly butyrate, have been shown to inhibit NF-κB activation by preventing the phosphorylation and degradation of inhibitor proteins (IκBs), thereby mitigating inflammatory responses and promoting gut homeostasis (Yao et al., 2024; Liu et al., 2023).

The gut microbiota demonstrates stability, resilience, and symbiotic relationships with the host in healthy environments. Its composition varies significantly across different anatomical sections of the gastrointestinal tract. For example, *Akkermansia muciniphila* resides in the mucus layer of the large intestine and is involved in maintaining intestinal integrity by stimulating mucin production and regulating gut permeability. *Adlercreutzia equolifaciens* is commonly found in the colon, where it metabolizes soy isoflavones into bioactive equol, a compound with antioxidant and estrogenic properties. *Barnesiella* has been discovered in multiple sections of the gastrointestinal tract, including the cecum, colon, and feces, where it contributes to the breakdown of complex carbohydrates and the modulation of immune responses (Afzaal et al., 2022).

Such discrepancies in microbial distribution are primarily attributable to differences in local conditions. The small intestine, for instance, has a rapid transit time and high bile content, while the colon exhibits slower flow rates, a gentler pH, and larger microbial communities dominated by anaerobic species (Afzaal et al., 2022). Aside from regional variation, gut microbiota composition also changes with age. Microbial diversity typically increases from childhood to adulthood and gradually declines after the age of 70, contributing to age-associated vulnerabilities in immune and metabolic health.

3 Optimal foods for nurturing gut bacteria

The composition and functionality of gut microbiota are profoundly influenced by specific dietary choices, with certain foods playing a pivotal role in promoting the growth of beneficial bacteria. Microbiota-accessible carbohydrates (MACs), including dietary fibers such as resistant starch, inulin, and pectin, serve as fermentable substrates for gut bacteria, particularly *Bifidobacterium* and *Faecalibacterium prausnitzii*. These fibers stimulate the production of short-chain fatty acids (SCFAs), which are essential for gut homeostasis. For example, resistant starch found in foods like legumes and whole grains has been shown to increase butyrate production, supporting colonic health and reducing gut inflammation. Similarly, inulin, a naturally occurring polysaccharide present in chicory root and Jerusalem artichoke, selectively enhances the abundance of *Bifidobacterium*, contributing to improved gut barrier function and immune modulation (Baxter et al., 2019) (Murga-Garrido et al., 2021).

Polyphenols, bioactive compounds abundant in plant-based foods such as berries, cocoa, and green tea, also play a critical role in supporting gut health. These compounds interact with gut microbiota to produce bioactive metabolites that exert anti-inflammatory and antioxidant effects. For instance, anthocyanins in blueberries have been shown to increase the abundance of *Akkermansia muciniphila*, a bacterium linked to enhanced metabolic health and reduced markers of systemic inflammation (Cano et al., 2024). However, the efficacy of these foods can be significantly influenced by processing methods. High-temperature cooking or refining can degrade fibers and polyphenols, reducing their availability to gut microbes. Minimally processed foods, such as raw fruits, vegetables, and whole grains, retain higher levels of beneficial compounds and are therefore more effective in nurturing gut bacteria (Sejbuk et al., 2024).

Prebiotics, defined as substrates selectively utilized by host microorganisms to confer health benefits, are fundamental to promoting gut health. Common prebiotics include inulin, fructooligosaccharides (FOS), galactooligosaccharides (GOS), and resistant starch, all of which foster the growth of beneficial bacterial taxa such as *Bifidobacterium* and *Faecalibacterium* (Krumbeck et al., 2018). Inulin, naturally present in foods like onions, garlic, and asparagus, is known for its ability to selectively enhance *Bifidobacterium* populations (Davani-Davari et al., 2019). Similarly, FOS, found in bananas, leeks, and artichokes, promotes microbial diversity and supports the production of SCFAs, which are crucial for maintaining gut barrier integrity and reducing inflammation. GOS, commonly derived from dairy products or synthesized for commercial use, has demonstrated particular benefits in infant gut microbiota, simulating the effects of human milk oligosaccharides (Davani-Davari et al., 2019).

Resistant starch, present in foods such as potatoes, green bananas, and legumes, has a unique role in promoting butyrate production. This SCFA is particularly beneficial for colonic health, as it serves as an energy source for colonocytes and reduces intestinal inflammation. However, the efficacy of prebiotics can be influenced by food processing. For example, cooking methods like boiling or steaming generally preserve prebiotic content, whereas high-temperature frying or prolonged storage may degrade these beneficial fibers, reducing their fermentability (Queen and Queen, 2020). To maximize the benefits of prebiotic-rich foods, dietary interventions should prioritize minimally processed options and explore novel methods for enhancing the stability of prebiotics during food preparation (Queen and Queen, 2020).

4 Role of microbiota in disease induction

The intestinal mucosal barrier, which consists of physical, chemical, microbial, and immunological components, serves as one of the body's major defensive barriers. It protects against bacterial invasion, prevents the entry of foreign antigens and toxins into the circulation, and minimizes water and nutrient loss. This barrier also regulates molecular exchange while supporting the coexistence and colonization of gut bacteria. Disruptions to the gut microbiota's

composition can have significant repercussions, influencing the development of major diseases (Figure 2).

Dysbiosis, characterized by a loss of beneficial microbes and an overgrowth of pathogenic species, plays a central role in disease induction. The intestinal mucosal barrier becomes compromised, leading to increased gut permeability and systemic inflammation. For instance, in inflammatory bowel disease (IBD), the weakened mucus layer of the digestive tract allows luminal bacteria to penetrate epithelial cells (Bull and Plummer 2015), triggering proliferative and inflammatory processes (Parekh et al., 2015). Dysbiosis also affects the production of key microbial metabolites, such as short-chain fatty acids (SCFAs). Reduced levels of butyrate, a critical SCFA, impair gut barrier integrity and exacerbate inflammation, further contributing to the pathogenesis of IBD (Chae et al., 2024).

Emerging evidence has also highlighted the gut's influence on systemic diseases such as obesity and type 2 diabetes (T2D). Obesity is associated with an increased Firmicutes to Bacteroides/Prevotella ratio, which elevates microbial genes involved in polysaccharide breakdown and raises SCFA production. This enhanced energy extraction from food contributes to weight gain. Additionally, microbial digestion of dietary choline and carnitine, common in Western diets, produces trimethylamine-N-oxide (TMAO), a compound linked to increased cardiovascular disease (CVD) risk. In T2D, dysbiosis results in a proliferation of Proteobacteria, Bacteroidetes, and Firmicutes, disrupting glucose metabolism and contributing to insulin resistance (Muscogiuri et al., 2017).

The gut microbiota's role extends beyond metabolic and inflammatory disorders to include infectious diseases such as COVID-19. Studies suggest a strong gut-lung axis, wherein the gut microbiota upregulates the synthesis of ACE2, a receptor used by the SARS-CoV-2 virus to enter cells (Wang et al., 2023). Nutraceuticals, including polyphenols and probiotics, have been proposed to support immune responses and potentially mitigate disease severity.

Neurodegenerative diseases, such as Alzheimer's and Parkinson's, have also been linked to dysbiosis. Alterations in gut microbiota composition affect the gut-brain axis through microbial metabolites like SCFAs and tryptophan derivatives, influencing neuroinflammation and neurotransmitter synthesis (Junyi et al., 2024). For example, elevated levels of lipopolysaccharides (LPS) in dysbiotic states can disrupt the blood–brain barrier and activate microglia, exacerbating neurodegeneration.

5 Gut-brain axis in neurodegenerative diseases

The gut-brain axis represents a dynamic bidirectional communication network linking the gut microbiota and the central nervous system (CNS). This intricate system operates through multiple mechanisms, including microbial metabolites such as short-chain fatty acids (SCFAs), immune signaling, the vagus nerve, and neuroendocrine pathways via the hypothalamic–pituitary–adrenal (HPA) axis. Recent studies underscore the significant role of this axis in influencing brain function, mood regulation, and the pathophysiology of neurodegenerative diseases (Schneider et al., 2024).

Neurodegenerative diseases such as Alzheimer's disease (AD) and Parkinson's disease (PD) have been closely linked to gut dysbiosis, a condition characterized by imbalances in microbial composition (Schneider et al., 2024; Kulkarni et al., 2024; Caradonna et al., 2024).

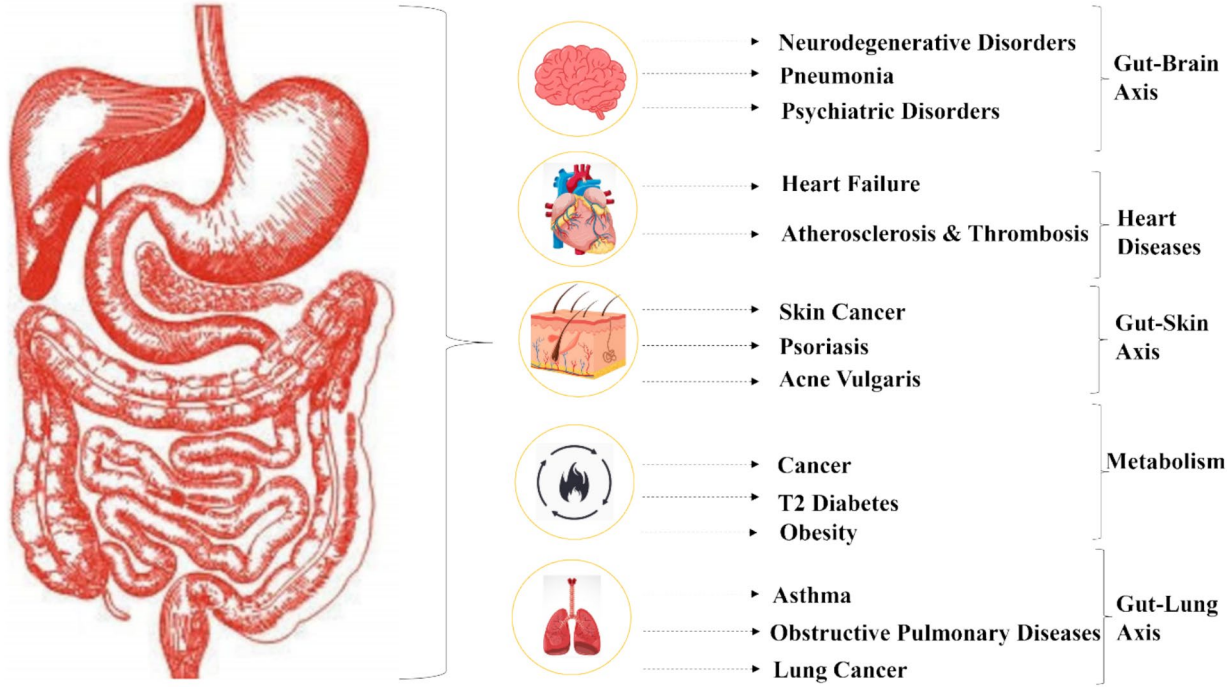

FIGURE 2
Dysbiosis of the human microbiota.

In Alzheimer's disease, gut dysbiosis contributes to increased systemic inflammation through the release of microbial metabolites like lipopolysaccharides (LPS), which compromise the blood–brain barrier integrity. This allows amyloid-beta peptides to accumulate, exacerbating neuroinflammation and neuronal damage (Kulkarni et al., 2024; Caradonna et al., 2024). Similarly, Parkinson's disease is associated with alterations in gut microbiota composition, particularly a reduction in anti-inflammatory taxa such as *Akkermansia muciniphila*. These changes are thought to facilitate the misfolding and aggregation of α-synuclein, a hallmark of PD pathology, and promote its transmission from the enteric nervous system to the CNS via the vagus nerve (Kulkarni et al., 2024; Caradonna et al., 2024).

Microbial metabolites play a pivotal role in modulating neuroinflammatory pathways. SCFAs, including butyrate and propionate, have been shown to regulate microglial activation, which is critical for maintaining CNS homeostasis. A reduction in SCFA levels, often observed in dysbiotic states, is correlated with increased neuroinflammation and cognitive decline (Fodor et al., 2023). Moreover, tryptophan metabolites derived from gut bacteria influence serotonin and kynurenine pathways, both of which are integral to mood regulation and cognitive processes. For instance, studies have highlighted the role of *Bacteroides* species in promoting the synthesis of indole derivatives, which have neuroprotective effects (Fodor et al., 2023).

6 Essential gut-friendly bacteria and their byproducts

6.1 *Akkermansia muciniphila*

Akkermansia muciniphila is an anaerobic gram-negative anti-obesity bacterium that grows singly or in pairs in mucin-rich medium (Liu et al., 2022). *Akkermansia muciniphila* has garnered significant attention due to its ability to degrade mucus that considers a protective layer that lines the gut and maintains a healthy balance that serves as a barrier against harmful microorganisms as excessive mucus production can lead to a range of health issues, including inflammatory bowel disease (IBD) and obesity (Geerlings et al., 2018; Kim et al., 2021). Mucin layer is primarily made up of gelatinous mucins secreted by goblet cells and also consist of a peptide backbone modified by O-linked glycans. The presence of proline and threonine in the peptide backbone contributes to the unique properties of mucin, including its gel-like consistency and protective function (Pelaseyed et al., 2014). Further, the production of butyrate, a short-chain fatty acid by *Akkermansia muciniphila* not only provides an energy source for the cells lining the colon but also contributes to reducing inflammation and improving gut barrier function (Portincasa et al., 2022). Another metabolite produced by *Akkermansia muciniphila* is propionate, which also has anti-inflammatory effects and regulate glucose metabolism. It also stimulates the production of molecules that promote the growth of beneficial bacteria in the gut, leading to a more diverse and balanced gut microbiota (Rodrigues et al., 2022).

6.2 Adlercreutzia equolifaciens

Adlercreutzia equolifaciens is a Gram-positive bacterium that thrives in an anaerobic environment, slightly acidic pH range of 6.0 to 6.5 by using culture medium, such as Reinforced Clostridial Medium (RCM). This bacterium is of particular interest due to its ability to produce equol, a metabolite of the soy isoflavone daidzein, which is found in soy products and other legumes. Research has shown that equol has estrogenic and antioxidant properties, which may help alleviate symptoms associated with hormonal imbalances, such as menopause, hot flashes and night sweats (Mayo et al., 2019). Further equol have anti-inflammatory and anti-cancer effects. Individuals who consume a diet rich in soy products are more likely to have a higher abundance of *Adlercreutzia equolifaciens* in their gut (Tuli et al., 2022).

6.3 Barnesiella

Barnesiella is an obligate anaerobic bacterium that can be cultivated under both anaerobic and microaerophilic conditions at a temperature range of 37–42°C in nutrient-rich media, such as brain-heart infusion (BHI) or tryptic soy broth (TSB), supplemented with appropriate carbon and nitrogen sources (Ubeda et al., 2013). *Barnesiella* is a commensal bacterium that found reasonably low level in the gastrointestinal tract of humans help in the breakdown of complex carbohydrates, production of SCFAs, modulation of immune responses, facilitate the clearance of intestinal VRE colonization and prevent the spread of highly antibiotic-resistant bacteria (Tao et al., 2021; Ubeda et al., 2013; Aindelis and Chlichlia, 2020).

6.4 *Christensenella minuta*

Christensenella minuta is an obligate anaerobe that could be grow optimally under mesophilic conditions, between 30°C to 37°C by using a suitable culture medium, such as a nutrient-rich broth, to support its growth (Kropp et al., 2021; Ang et al., 2023). One of the unique metabolic features of *Christensenella minuta* is its ability to produce butyrate, a short-chain fatty acid linked with various health benefits, including anti-inflammatory and anti-cancer properties. Studies suggest that individuals with higher levels of *Christensenella minuta* may have a lower risk of type 2 diabetes, inflammatory bowel disease and obesity which sparked interest in the use in the development of probiotics and prebiotics (Mazier et al., 2021; Ang et al., 2023). In addition, this bacterium can influence the host's response to certain medications, such as antidiabetic drugs and suggested that it may contribute to inter-individual differences in drug response and could potentially be targeted for personalized medicine approaches.

6.5 *Oxalobacter formigenes*

Oxalobacter formigenes is a unique bacterium that can be grow in anaerobic environment by using Oxalate-Minimal Medium, which consists of oxalate, mineral salts, vitamins and buffer system (Duncan et al., 2002; Daniel et al., 2021). This bacterium resides in the human gastrointestinal tract known for its unique ability to break down and metabolize oxalate, a compound that can form kidney stones in some individuals. Studies have shown that individuals with a higher abundance of *Oxalobacter formigenes* in their gut have a lower risk of developing kidney stones (Chmiel et al., 2022). This bacterium

produces an enzyme called oxalyl-CoA decarboxylase, which converts oxalate into a less harmful compound called formate (Karamad et al., 2022).

7 Optimal foods for nurturing the growth of gut-friendly bacteria

Research has consistently shown that our dietary choices have a direct impact on the health and resilience of our gut microbiome (Singh et al., 2017; Su and Liu, 2021). The incorporation of prebiotic rich foods, fermented foods, and a wide variety of plants and fruits promote the thriving of these gut microbiome as detailed in Table 1 (Nambiar et al., 2023; Leeuwendaal et al., 2022). The colorful plant foods are not only visually appealing, but they also provide a wide range of health benefits for the microbiome and metabolism. One of the key benefits of colorful foods is their high content of phytochemicals bioactive compounds such as carotenoids, flavonoids, and anthocyanins that have been shown to have numerous health-promoting effects (Samtiya et al., 2021; Khoo et al., 2017).

The microbiome is a living dynamic environment where the relative abundance of species may fluctuate daily, weekly, and monthly depending on diet, medication, exercise, and a host of other environmental exposures (Monda et al., 2017; York, 2019).

7.1 Carotenoids

Gut microbiota breaks down the carotenoid's rich foods, into various beneficial gut metabolites such as apocarotenoids and SCFAs having anti-inflammatory, antioxidant, and anticancer properties that contribute to decrease the risk of the development of chronic diseases, cardiovascular diseases, type 2 diabetes, obesity, brain-related diseases and certain types of cancer (Rowles and Erdman, 2020; Rocha et al., 2023; Eroglu et al., 2023; Min et al., 2023). They also act as antioxidants, protecting the body's cells from damage caused by harmful free radicals. Their ability to protect against lipid peroxidation and damage caused by ROS makes them valuable in maintaining overall health and reducing the risk of chronic diseases (Lobo et al., 2010; Rocha et al., 2023).

Apo-carotenoids exhibit unique characteristics, including higher aqueous solubility and higher electrophilicity, which make them particularly suitable for targeting transcription factors such as NF-κB, PPARγ, and RAR/RXRs (Eroglu et al., 2023). These compounds hold potential for therapeutic applications in the fields of inflammation, metabolic disorders, and cell differentiation. Studies have found that carotenoids can directly influence the composition of the gut microbiota in a positive manner (Rocha et al., 2023). Beta-carotene such as carrots and sweet potatoes can increase the abundance of certain beneficial bacteria, such as *Bifidobacteria* and *Lactobacillus* (Rinninella et al., 2019; Zhiguo et al., 2023; Li et al., 2022a). Lycopene, found in tomatoes, has been shown to increase the levels of bacteria that produce short-chain fatty acids, which are beneficial for gut health (Eroglu et al., 2023). A. Lutein, found in leafy greens, has been associated with a more diverse gut microbiota (Dinsmoor et al., 2019).

7.2 Flavonoids

Flavonoid-rich foods including fruits like berries, citrus fruits, vegetables, dark chocolate and tea, can lead to an increase in the diversity and abundance of gut metabolites that break down the

TABLE 1 Various dietary sources that produce and nourish good gut bacteria.

S. No.	Beneficial bacteria	Substances	Sources	References
1.	*Akkermansia muciniphila*	Polyphenols	Caffeic acid, chlorogenic acid, salvianolic acid A, ferulic, Concord grape polyphenols, puerarin, resveratrol, epigallocatechin gallate, black tea, red wine, grape juice, aronia juice, *Canarium album* extract, arctic berries, flavonoids	Zhou (2017), Visioli et al. (2003), Anhê et al. (2016), Roopchand et al. (2015), Kajla et al. (2015) and Chenbo et al. (2022)
		Alkaloids	Berberine, curcumin caffeine, chlorogenic acid and betaine	
		Capsaicin	Chili peppers	
		Plant-derived carbohydrates	Nonfermentable fiber, wheat dietary fiber, konjac glucomannan, bran, fiber-rich common beans, oligofructose, Inulin-type fructan, stachyose, polysaccharides from spirulina platensis, *Lycium barbarum* polysaccharide and fucoidan	
		Others	Oily fish, walnuts bamboo shoots, rhubarb extract and flaxseed	
2.	*Adlercreutzia equolifaciens*	Isoflavone diet	Tofu, tempeh, and soy milk	Jensen et al. (2021)
3.	*Barnesiella*	Polyphenols	Cherry juices Black raspberry-rich diet *Ganoderma lucidum* mushroom	Ubeda et al. (2013), Daillère et al. (2016), Gu et al. (2019), and Miaoyu et al. (2021)
		Prebiotics		
4.	*Christensenella minuta*	Polyphenols	Red grapes, cranberries, strawberries and blueberries	Mazier et al. (2021), Ang et al. (2023) and Waters and Ley (2019)
5.	*Oxalobacter formigenes*	Prebiotic foods	Prebiotic foods like kimchi, sauerkraut, kefi, spinach, legumes, tea and celery	Kaufman et al. (2008) and Chmiel et al. (2022)

flavonoids through fermentation processes into various metabolites compounds that have anti-inflammatory and antioxidant properties and reduce the risk of metabolic disorders such as cardiovascular disease by improving the insulin sensitivity (Joaquim et al., 2023; Wang et al., 2022; Pan et al., 2023). One important group of flavonoids known as flavan-3-ols has been shown to increase the levels of short-chain fatty acids (SCFAs) such as butyrate, which provide energy for the gut epithelial cells and have anti-inflammatory effects (Fotschki et al., 2015). Another bioactive compound flavanols associated with increase the production of urolithins metabolites in the gut that have been shown to have anti-inflammatory, antioxidant, and anticancer properties (Singh et al., 2019). Further flavonoids have also been found to increase the production phenolic acids, benzoic acid derivatives, and microbial-derived compounds that can influence various physiological processes in the body (Rahman et al., 2021). Previous research reported that flavonoids have the ability to modulate the relative abundance by increasing the relative abundance *of Bifidobacterium*, *Lactobacillus*, while decreasing the relative abundance of *Lachnoclostridium* and *Bilophila*, highlights their potential as dietary supplements or functional food ingredients to promote a healthy gut microbiota (Baky et al., 2022; Pan et al., 2023).

7.3 Anthocyanins

Anthocyanins that are responsible for bright red, purple, and blue colors to fruits like blueberries, blackberries, purple cabbage and cherries have been shown to have anti-inflammatory and antioxidant effects, as well as potential anti-cancer properties (Khoo et al., 2017; Bahare et al., 2020). They may also help regulate blood sugar levels and improve insulin sensitivity (Fernandes, 2019). One metabolite that has been extensively studied in relation to Anthocyanins increase nitric oxide (NO) metabolite known as signaling molecule that helps in the regulation of blood flow, neurotransmission, and immune responses Geum et al. (2020). Increased levels of nitric oxide relax and dilate blood vessels, leading to improved blood flow and reduced risk of hypertension, heart disease and diabetes (da Silva et al., 2021; Kumar et al., 2022). Studies have consistently shown that anthocyanin leads to an increase in the presence of beneficial bacteria such as *Lactobacillus*, *Bifidobacterium*, *Blautia, Faecalibacterium*, *Prevotella*, *Akkermansia* and stimulate the production SCFAs particularly butyrate (Verediano et al., 2021; Zhong et al., 2023; Liang et al., 2023).

7.4 Polyphenols

Polyphenols are a group of compounds that are naturally found in many plant-based foods and beverage that undergo various transformations by the gut bacteria and converted into a wide range of metabolites having antioxidant and anti-inflammatory properties (Gizem et al., 2020; Bertelli et al., 2021). Studies have shown that certain polyphenols, such as those found in green tea, berries, and cocoa, can increase the production of short-chain fatty acids (SCFAs) and branched-chain amino acids (BCAAs) and could be useful in the treatment and prevention of various gastrointestinal disorders (Manach et al., 2004; Kumar Singh et al., 2019; Lippolis et al., 2023). Furthermore, polyphenols have been shown to modulate the composition of the gut microbiota, promoting the growth of beneficial bacteria like *Lactobacillus*, *Lactiplantibacillus* and *Bifidobacterium* while hindering the proliferation of pathogenic strains like *Clostridium* and *Fusobacterium* (Corrêa et al., 2019; Wang et al., 2022; Lippolis et al., 2023; Rahman et al., 2021).

7.5 Alkaloids

Alkaloids have been known to possess various biological activities and have been used in traditional medicine for centuries (Heinrich et al., 2021). Studies have shown that certain alkaloids promote the growth of beneficial bacteria that leads to an increase in the production of short-chain fatty acids, such as butyrate, which have numerous health benefits (Feng et al., 2018; Dehau et al., 2023). Furthermore, alkaloids found in coffee, such as caffeine and chlorogenic acid, have been shown to increase the production of certain bile acids in the gut (Iriondo-DeHond et al., 2020; Chen et al., 2023). Bile acids are important for the digestion and absorption of dietary fats and also have regulatory roles in lipid and glucose metabolism (González-Regueiro et al., 2017). Research has shown that berberine has antimicrobial properties, specifically targeting harmful bacteria like *Escherichia coli* (*E. coli*) and *Clostridium difficile* (*C. difficile*), while promoting the growth of beneficial bacteria like Bifidobacterium and *Lactobacillus* (Cheng et al., 2022; Zhang et al., 2021; Peng et al., 2019).

7.6 Capsaicin

Research has shown that capsaicin can stimulate the production of certain gut metabolites such as SCFAs known to have various beneficial effects, such as reducing inflammation and improving insulin sensitivity (Song et al., 2017; Kang et al., 2017). Furthermore, capsaicin has been shown to enhance the activity of certain enzymes such as enzyme lipase, which is responsible for breaking down dietary fat (Liu et al., 2021). This increased enzyme activity can lead to a more efficient digestion and utilization of nutrients, ultimately affecting the production of gut metabolites (Menden et al., 2022; Chandra et al., 2020). In addition to its direct effects on gut metabolites, capsaicin has also been found to influence the composition of the gut microbiota and increase the abundance of *Akkermansia muciniphila* (Li et al., 2022b).

8 Dietary strategies for optimizing gut microbiota

The composition and functionality of the gut microbiota are profoundly influenced by dietary choices, making nutrition a cornerstone for maintaining microbial health. Specific dietary strategies, including the incorporation of fermented foods, synbiotic combinations, and anti-inflammatory diets, have been shown to promote microbial diversity, enhance the production of beneficial metabolites like short-chain fatty acids (SCFAs), and reduce inflammation. These approaches not only support digestive health but also play a critical role in systemic immunity and metabolic regulation. By tailoring dietary interventions to the unique needs of individuals,

it is possible to foster a balanced gut microbiota that contributes to overall well-being and resilience against chronic diseases.

8.1 Prebiotic-rich foods

Prebiotics can be found in a variety of foods, including fruits, vegetables, whole grains, and legumes. Some common examples of prebiotic fibers include inulin, fructooligosaccharides (FOS), and galactooligosaccharides (GOS) (Lockyer and Stanner, 2019). The primary benefits of prebiotics are their ability to selectively stimulate the growth of beneficial bacteria, such as *Bifidobacteria, Lactobacilli* and enhance the production of beneficial metabolites like short-chain fatty acids (Markowiak and Śliżewska, 2017; Davani-Davari et al., 2019). Prebiotic rich foods such as Chicory root and Jerusalem Artichokes are excellent sources of inulin, a fiber that serves as a fuel for the beneficial gut bacteria (Carlson et al., 2018). Similarly, the content of pectin in apples and resistant starch in bananas acts as nourishment for good bacteria (Englyst and Cummings, 1986; Leonel and Alvarez-Leite, 2012).

Other prebiotic foods like oats, barley, and quinoa promote healthy gut bacteria by providing good source of prebiotic fibers (Slavin, 2013). Legumes foods, including lentils, chickpeas, and beans, are known for their high nutritional value and are an excellent source of prebiotics that promote the growth of beneficial bacteria in the gut (Kadyan et al., 2022). The content of fructooligosaccharides (FOS) in garlic and onions, and inulin and oligofructose in asparagus vegetables act as prebiotics by stimulating the growth of beneficial gut bacteria (Zhang et al., 2013; Guillamón et al., 2021).

8.2 Fermented foods

Fermented foods are a rich source of probiotics that enhance gut health by introducing beneficial bacteria and improving microbial diversity. Popular examples include yogurt, kimchi, and sauerkraut. These foods support gut integrity by increasing levels of *Lactobacillus* and *Bifidobacterium*, which produce metabolites like short-chain fatty acids (SCFAs) that reduce inflammation and strengthen the gut barrier (Dimidi et al., 2019). In addition to these widely studied examples, global fermented foods such as miso and natto from Japanese cuisine, kefir from Eastern Europe, and dosa from India provide unique probiotic strains and bioactive compounds. Miso and natto, for instance, contain *Bacillus subtilis*, which has been shown to promote immune regulation and reduce markers of systemic inflammation (Oshiro et al., 2021). Kefir is particularly rich in lactic acid bacteria and yeast, offering a broad spectrum of probiotics with antimicrobial and gut-stabilizing properties (Tingirikari et al., 2024).

Fermented foods provide a natural and delicious way to support a healthy gut microbiome. With their probiotic properties, they offer numerous benefits, including improved digestive health, enhanced immune function, increased nutrient availability, and potential mental well-being (Leeuwendaal et al., 2022). Yogurt is a widely consumed fermented dairy product that augments beneficial bacteria, such as *Lactobacillus* and *Bifidobacterium* (Lisko et al., 2017). Kimchi is mainly produced by fermented vegetables, including cabbage, radishes, and garlic that contain *Lactobacillus* bacteria, which are known to promote gut health and improve digestion (Dimidi et al., 2019).

Another fermented food known as Kombucha made from a fermented tea beverage that is rich in bioactive compounds and a variety of beneficial acetic acid bacteria and yeasts, contributing to a healthy gut microbiome (Kitwetcharoen et al., 2023). A previous study conducted on rats revealed that tempeh, a fermented soybean product, has the potential to enhance the production of immunoglobulin A (IgA) and modulate the composition of gut microbiota. In addition to the study on rats, research involving supplementation of tempeh in humans for 16 days led to a significant increase in the abundance of beneficial gut bacteria like *Akkermansia muciniphila* (Stephanie et al., 2017).

Practical dietary recommendations include incorporating a variety of fermented foods into daily meals. For example, pairing kimchi with rice or adding yogurt to smoothies can provide both flavor and health benefits. Future research should explore the synergistic interactions between probiotics in fermented foods and the resident gut microbiota to optimize therapeutic applications.

8.3 Synbiotic foods

Synbiotic foods provide a convenient and effective way to support a healthy gut microbiome (Jiang et al., 2022). By combining prebiotics and probiotics, these foods offer numerous health benefits, including improved digestion, enhanced immune function, increased nutrient absorption, and reduced inflammation (Yadav et al., 2022). Incorporating synbiotic foods into a balanced diet can be a valuable strategy for promoting overall health and well-being (Pandey et al., 2015). Synbiotic food having a combination of arabinose, lactulose and *Lactobacillus plantarum*, have gained attention for their potential to effectively regulate blood glucose, blood lipid, and body weight in patients with Type 2 Diabetes Mellitus (T2DM) (Jiang et al., 2022). Another preparation known as a banana smoothie made with kefir or yogurt is a delicious and nutritious beverage that maximizes the benefits for gut bacteria. Stir-fry made with tempeh, asparagus, garlic, and leeks prompts, you can actively healthy gut microbiome. The combination of yogurt and fruits such as blueberries creates a synbiotic effect, where the probiotics from yogurt and the prebiotics from blueberries work together to promote the growth and activity of healthy gut bacteria (Fernandez and Marette, 2017).

8.4 Anti-inflammatory foods

Anti-inflammatory foods such as fatty fish, fruits, vegetables, whole grains, and spices have long been recognized for their potential health benefits by supporting a diverse and balanced gut microbiome, reducing inflammation and promoting overall gut health (Bagheri et al., 2022). Fish like salmon, sardines, and anchovies in diet can have a positive impact on gut health. Their omega-3 fatty acids and ability to increase healthy gut bacteria make them a valuable addition to an anti-inflammatory diet (Costantini et al., 2017). Flax seeds are rich in dietary fiber, including both soluble and insoluble fiber that act as prebiotics and provide nourishment for the beneficial bacteria in the gut (Kajla et al., 2015; Mueed et al., 2022). When the gut bacteria ferment the fiber from flax seeds, they produce short-chain fatty acids (SCFAs), such as butyrate that help in maintaining a healthy gut environment (Arora et al., 2019).

9 Impact of diet on microbial ecology in the gut

Diet plays a pivotal role in shaping the composition, diversity, and metabolic activity of the gut microbiota. Long-term dietary patterns, including plant-based and high-protein diets, create distinct microbial environments that influence host health. Microbiota-accessible carbohydrates (MACs), a subset of dietary fibers, serve as the primary energy source for gut bacteria, fostering the growth of beneficial taxa and stimulating the production of short-chain fatty acids (SCFAs) (De Filippo et al., 2010). MACs are composed of complex polysaccharides, such as resistant starches, inulin, and pectin, that are indigestible by host enzymes but fermentable by gut microbes. These carbohydrates selectively enhance the abundance of health-promoting bacteria like *Bifidobacterium* and *Faecalibacterium prausnitzii*, both of which are associated with anti-inflammatory effects and improved gut barrier integrity (Hills et al., 2019). For example, resistant starch found in legumes and whole grains increases butyrate production, which supports colonic health. Similarly, inulin from chicory root and Jerusalem artichokes promotes the proliferation of *Bifidobacterium*, contributing to gut homeostasis and reduced systemic inflammation. These carbohydrates are made up of monosaccharides linked together by various forms of glycosidic connections. Any major differences in their chemical makeup, solubility, and size classify these carbohydrates into a wide range of biological niches. Dietary fibers are crucial sources of energy for the bacteria that live in the colon and cecum. In addition to reducing microbial diversity and short chain fatty acid (SCFA) production, a low intake of dietary fiber causes the gut microbial metabolism to shift toward the use of less advantageous substrates. The mucus barrier is harmed by a protracted absence of dietary fibers, which is also linked to an increase in the number of bacteria that break down mucins, like *Akkermansia muciniphila* (Makki et al., 2018).

As a result, a lack of dietary fibre and an increase in sugar and fat in human diets may lead to the extinction of particular bacterial species. These changes may lead to dysfunctions, which could exacerbate existing conditions like IBD, allergies, colorectal cancer, autoimmune illnesses, obesity, etc. A diet high in fiber helps to maintain a healthy gut microbiota that is more diverse and performs activities like producing short-chain fatty acids (SCFAs) (Figure 3). Low fiber intake, a diet high in protein and sugar, and an industrialized diet all contribute to altered gut bacterial function, including a significant decrease in their capacity to produce SCFAs, which is linked to the emergence of chronic inflammatory diseases (Makki et al., 2018).

10 Microbiome-targeted therapies

Advancements in microbiome research have led to the development of innovative therapies aimed at modulating gut microbiota to improve health outcomes, including CNS-related disorders. Microbiome-targeted therapies encompass probiotics, prebiotics, postbiotics, dietary interventions, and fecal microbiota transplantation (FMT), each offering unique mechanisms to restore microbial balance and enhance host health (Loh et al., 2024).

Probiotics, defined as live microorganisms that confer health benefits when consumed in adequate amounts, have garnered attention for their potential to influence the gut-brain axis. Specific strains, such as *Lactobacillus rhamnosus* and *Bifidobacterium longum*, have shown promise in alleviating symptoms of anxiety and depression by modulating the HPA axis and reducing systemic inflammation (Schächtle and Rosshart, 2021). Moreover, these probiotics enhance the production of neuroactive compounds like gamma-aminobutyric acid (GABA), which exerts calming effects on the CNS (Schächtle and Rosshart, 2021; Loh et al., 2024).

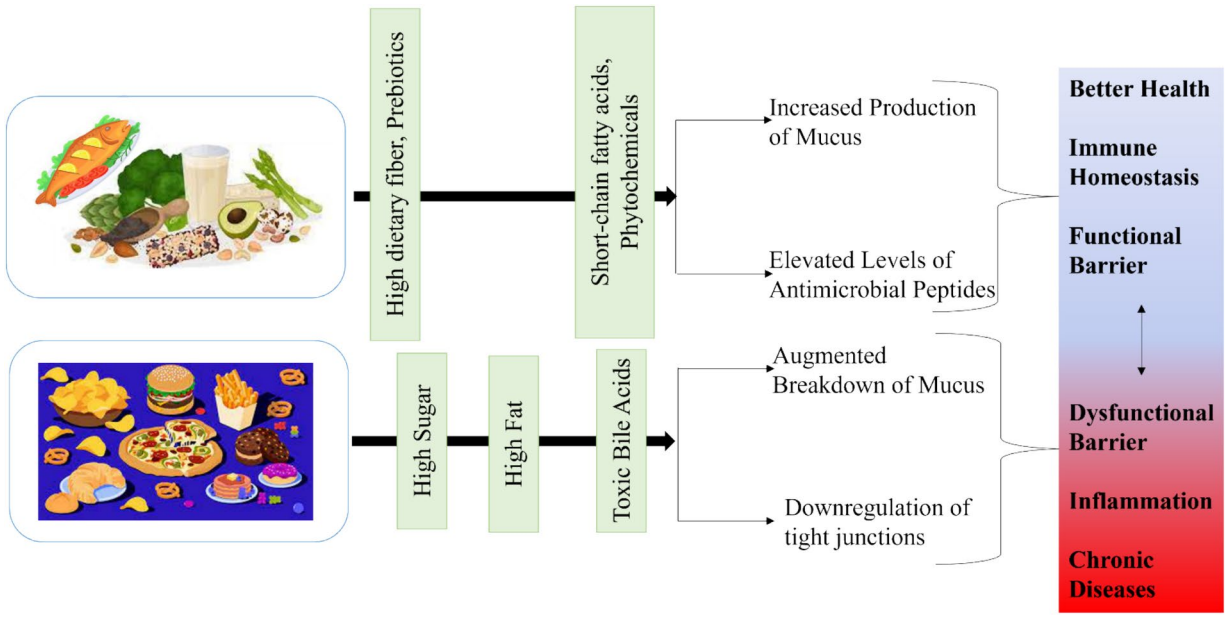

FIGURE 3
Effect of high and low fiber diet on gut microbiota.

Prebiotics, including dietary fibers and oligosaccharides, serve as substrates for beneficial gut bacteria, stimulating the production of SCFAs and other bioactive metabolites. For example, inulin and fructooligosaccharides have been shown to increase butyrate levels, which play a critical role in reducing neuroinflammation and preserving neuronal integrity (Anand et al., 2025). Prebiotic interventions also hold potential for personalized nutrition, wherein diets are tailored to enhance specific microbial taxa associated with improved CNS health.

Fecal microbiota transplantation (FMT), a procedure involving the transfer of stool from a healthy donor to a recipient, has emerged as a promising therapeutic avenue for neuropsychiatric and neurodegenerative disorders. Preliminary clinical trials suggest that FMT can restore microbial diversity and ameliorate symptoms in conditions such as autism spectrum disorder and depression (Zhang et al., 2023; Peery et al., 2024). However, the standardization of FMT protocols and the identification of specific microbial communities responsible for therapeutic effects remain critical challenges (Zhang et al., 2023).

Future research should focus on the development of "designer probiotics" tailored to target specific diseases and the integration of microbiome data with genomic and metabolomic profiles to advance precision medicine. Additionally, leveraging computational tools to model host-microbiota interactions could facilitate the identification of novel therapeutic targets, paving the way for next-generation microbiome-based treatments.

11 Conclusion

The study of the human gut microbiota has advanced significantly in recent years, revealing its profound influence on the host's metabolism, physiology, and immune system. Numerous factors, including nutrition, host genetics, age, medications, and lifestyle, shape the composition and functionality of the gut microbiota. These dynamic interactions play a pivotal role in human health, and alterations in gut microbial composition are now recognized as key contributors to the development of various diseases. A deeper understanding of the interplay between diet and microbiota holds the potential to develop tailored nutritional strategies aimed at reducing the prevalence of chronic inflammatory disorders.

Emerging evidence highlights the critical role of plant-based foods rich in phytochemicals and other specific dietary components in promoting the growth and maintenance of beneficial gut bacteria. However, challenges such as absorption, bioavailability, dietary interactions, and individual variations in metabolism can limit the efficacy of phytochemicals in fostering a healthy gut microbial community. The highly dynamic nature of gut microbiota, influenced by environmental factors, further complicates these interventions. Addressing issues such as standardization of dietary recommendations, variability in individual responses, and the long-term maintenance of dietary changes is essential for optimizing the benefits of specific foods on gut health.

In this review, we explored the intricate roles of beneficial gut bacteria and the significant impact of optimal diets on human health. Our findings underscore the transformative potential of personalized nutrition, customized to individual microbiota profiles, in revolutionizing healthcare. By leveraging the symbiotic relationship between gut bacteria and dietary patterns, targeted dietary interventions and preventive strategies can be developed to address chronic diseases. However, implementing such personalized recommendations on a large scale requires a paradigm shift in healthcare systems, moving towards individualized care. Ethical concerns, particularly related to privacy and the use of data in precision medicine, also present formidable challenges that must be carefully navigated.

Advancements in microbiome-targeted therapies, including probiotics, prebiotics, and synbiotics, along with the integration of artificial intelligence (AI), offer promising avenues for tailoring dietary interventions. AI-driven models can integrate microbiome, metabolome, and genomic data to generate precise nutritional recommendations, optimizing dietary strategies at an individual level. Future research should prioritize understanding the mechanisms underlying host-microbiota interactions, improving the bioavailability of key dietary components, and evaluating the long-term effects of dietary interventions on microbial ecology. Combining these scientific insights with robust ethical frameworks is essential to fully harness the potential of gut microbiota in promoting health and preventing disease. Through a multidisciplinary approach, we can unlock innovative solutions that bridge scientific discovery and practical implementation, advancing healthcare and improving lives.

Author contributions

SK: Conceptualization, Validation, Visualization, Writing – original draft, Writing – review & editing. RM: Validation, Visualization, Writing – original draft, Writing – review & editing. PG: Conceptualization, Validation, Writing – review & editing. ÉL: Validation, Visualization, Writing – review & editing. XL: Validation, Writing – review & editing, Investigation, Visualization. SA: Validation, Writing – review & editing. PP: Validation, Writing – review & editing, Formal analysis, Visualization. C-MC: Visualization, Writing – review & editing, Investigation, Supervision, Writing – original draft. VR: Investigation, Visualization, Writing – review & editing, Conceptualization, Validation. RP: Conceptualization, Investigation, Validation, Visualization, Writing – review & editing, Supervision, Writing – original draft.

Funding

The author(s) declare that financial support was received for the research, authorship, and/or publication of this article. This research was funded by VtR Inc-CGU (SCRPD1L0221), DOXABIO-CGU (SCRPD1K0131), and a CGU grant (UZRPD1L0011, UZRPD1M0081).

Conflict of interest

The authors declare that the research was conducted in the absence of any commercial or financial relationships that could be construed as a potential conflict of interest.

Generative AI statement

The authors declare that no Gen AI was used in the creation of this manuscript.

Publisher's note

All claims expressed in this article are solely those of the authors and do not necessarily represent those of their affiliated organizations, or those of the publisher, the editors and the reviewers. Any product that may be evaluated in this article, or claim that may be made by its manufacturer, is not guaranteed or endorsed by the publisher.

References

Afzaal, M., Saeed, F., Shah, Y. A., Hussain, M., Rabail, R., Socol, C. T., et al. (2022). Human gut microbiota in health and disease: unveiling the relationship. *Front. Microbiol.* 13:99900. doi: 10.3389/fmicb.2022.99900

Aindelis, G., and Chlichlia, K. (2020). Modulation of anti-tumour immune responses by probiotic Bacteria. *Vaccine* 8:329. doi: 10.3390/vaccines8020329

Anand, A., Manjula, S. N., Fuloria, N. K., Sharma, H., and Mruthunjaya, K. (2025). Inulin as a prebiotic and its effect on gut microbiota. *In inulin as a prebiotic and its effect on gut microbiota.* pp. 113–135. doi: 10.1007/978-981-97-9056-2_6

Ang, W. S., Law, J. W., Letchumanan, V., Hong, K. W., Wong, S. H., Ab Mutalib, N. S., et al. (2023). A keystone gut bacterium *Christensenella minuta*-a potential biotherapeutic agent for obesity and associated metabolic diseases. *Foods* 12:2485. doi: 10.3390/foods12132485

Anhê, F. F., Pilon, G., Roy, D., Desjardins, Y., Levy, E., and Marette, A. (2016). Triggering Akkermansia with dietary polyphenols: a new weapon to combat the metabolic syndrome? *Gut Microbes* 7, 146–153. doi: 10.1080/19490976.2016.1142036

Arora, T., Rudenko, O., Egerod, K. L., Husted, A. S., Kovatcheva-Datchary, P., Akrami, R., et al. (2019). Microbial fermentation of flaxseed fibers modulates the transcriptome of GPR41-expressing enteroendocrine cells and protects mice against diet-induced obesity. *Am. J. Physiol. Endocrinol. Metab.* 316, E453–E463. doi: 10.1152/ajpendo.00391.2018

Bagheri, S., Zolghadri, S., and Stanek, A. (2022). Beneficial effects of anti-inflammatory diet in modulating gut microbiota and controlling obesity. *Nutrients* 14:3985. doi: 10.3390/nu14193985

Bahare, S., Javad, S., Francesca, C., Reiner, Ž., Zorzan, D., Imran, M., et al. (2020). The therapeutic potential of Anthocyanins: current approaches based on their molecular mechanism of action. *Front. Pharmacol.* 11:1300. doi: 10.3389/fphar.2020.01300

Baky, M. H., Elshahed, M., Wessjohann, L., and Farag, M. A. (2022). Interactions between dietary flavonoids and the gut microbiome: a comprehensive review. *Br. J. Nutr.* 128, 577–591. doi: 10.1017/S0007114521003627

Baxter, N. T., Schmidt, A. W., Venkataraman, A., Kim, K. S., Waldron, C., and Schmidt, T. M. (2019). Dynamics of human gut microbiota and short-chain fatty acids in response to dietary interventions with three fermentable fibers. *mBio* 10:10.1128/mbio.02566-18. doi: 10.1128/mbio.02566-18

Bertelli, A., Biagi, M., Corsini, M., Baini, G., Cappellucci, G., and Miraldi, E. (2021). Polyphenols: from theory to practice. *Foods* 10:2595. doi: 10.3390/foods10112595

Bull, M. J., and Plummer, N. T. (2015). Part 2: Treatments for Chronic Gastrointestinal Disease and Gut Dysbiosis. *Integr. Med.* 14, 25–33.

Cano, R., Bermúdez, V., Galban, N., Garrido, B., Santeliz, R., Gotera, M. P., et al. (2024). Dietary polyphenols and gut microbiota Cross-talk: molecular and therapeutic perspectives for Cardiometabolic disease: a narrative review. *Int. J. Mol. Sci.* 25:9118. doi: 10.3390/ijms25169118

Caradonna, E., Nemni, R., Bifone, A., Gandolfo, P., Costantino, L., Giordano, L., et al. (2024). The brain–gut axis, an important player in Alzheimer and Parkinson disease: a narrative review. *J. Clin. Med.* 13:4130. doi: 10.3390/jcm13144130

Carlson, J. L., Erickson, J. M., Lloyd, B. B., and Slavin, J. L. (2018). Health effects and sources of prebiotic dietary Fiber. *Curr. Dev. Nutr.* 2:nzy005:nzy005. doi: 10.1093/cdn/nzy005

Chae, Y., Lee, Y. R., Kim, Y., and Park, H. (2024). Diet-induced gut dysbiosis and leaky gut syndrome. *J. Microbiol. Biotechnol.* 34, 747–756. doi: 10.4014/jmb.2312.12031

Chandra, P., Enespa, S. R., and Arora, P. K. (2020). Microbial lipases and their industrial applications: a comprehensive review. *Microb. Cell Fact.* 19:169. doi: 10.1186/s12934-020-01428-8

Chen, L., Wang, X. J., Chen, J. X., Yang, J. C., Lin, L., Cai, X. B., et al. (2023). Caffeine ameliorates the metabolic syndrome in diet-induced obese mice through regulating the gut microbiota and serum metabolism. *Diabetol. Metab. Syndr.* 15:37. doi: 10.1186/s13098-023-00993-3

Chenbo, Y., Chuanqi, C., Jianxin, Z., Hao, Z., Wei, C., and Qixiao, Z. (2022). Dietary strategies to promote the abundance of intestinal *Akkermansia muciniphila*, a focus on the effect of plant extracts. *J. Funct. Foods* 93:105093. doi: 10.1016/j.jff.2022.10509

Cheng, H., Liu, J., Tan, Y., Feng, W., and Peng, C. (2022). Interactions between gut microbiota and berberine, a necessary procedure to understand the mechanisms of berberine. *J. Pharm. Anal.* 12, 541–555. doi: 10.1016/j.jpha.2021.10.003

Chmiel, J. A., Carr, C., Stuivenberg, G. A., Venema, R., Chanyi, R. M., Al, K. F., et al. (2022). New perspectives on an old grouping: the genomic and phenotypic variability of *Oxalobacter formigenes* and the implications for calcium oxalate stone prevention. *Front. Microbiol.* 13:1011102. doi: 10.3389/fmicb.2022.1011102

Corrêa, T. A. F., Rogero, M. M., Hassimotto, N. M. A., and Lajolo, F. M. (2019). The two-way polyphenols-microbiota interactions and their effects on obesity and related metabolic diseases. *Front. Nutr.* 6:188. doi: 10.3389/fnut.2019.00188

Costantini, L., Molinari, R., Farinon, B., and Merendino, N. (2017). Impact of Omega-3 fatty acids on the gut microbiota. *Int. J. Mol. Sci.* 18:2645. doi: 10.3390/ijms18122645

Da Silva, G. M., da Silva, M. C., Nascimento, D. V. G., Lima Silva, E. M., Gouvêa, F. F. F., de França Lopes, L. G., et al. (2021). Nitric oxide as a central molecule in hypertension: focus on the Vasorelaxant activity of new nitric oxide donors. *Biology* 10:1041. doi: 10.3390/biology10101041

Daillère, R., Vétizou, M., Waldschmitt, N., Yamazaki, T., Isnard, C., Poirier-Colame, V., et al. (2016). Enterococcus hirae and *Barnesiella intestinihominis* facilitate cyclophosphamide-induced therapeutic immunomodulatory effects. *Immunity* 45, 931–943. doi: 10.1016/j.immuni.2016.09.009

Daniel, S. L., Moradi, L., Paiste, H., Wood, K. D., Assimos, D. G., Holmes, R. P., et al. (2021). Forty years of *Oxalobacter formigenes*, a gutsy oxalate-degrading specialist. *Appl. Environ. Microbiol.* 87:e0054421. doi: 10.1128/AEM.00544-21

Davani-Davari, D., Negahdaripour, M., Karimzadeh, I., Seifan, M., Mohkam, M., Masoumi, S., et al. (2019). Prebiotics: definition, types, sources, mechanisms, and clinical applications. *Food Secur.* 8:92. doi: 10.3390/foods8030092

De Filippo, C., Cavalieri, D., Di Paola, M., Ramazzotti, M., Poullet, J. B., Massart, S., et al. (2010). Impact of diet in shaping gut microbiota revealed by a comparative study in children from Europe and rural Africa. *Proc. Natl. Acad. Sci. USA* 107, 14691–14696. doi: 10.1073/pnas.1005963107

Dehau, T., Cherlet, M., Croubels, S., van Immerseel, F., and Goossens, E. (2023). A high dose of dietary Berberine improves Gut Wall morphology, despite an expansion of *Enterobacteriaceae* and a reduction in beneficial microbiota in broiler chickens. *mSystems* 8:e0123922. doi: 10.1128/msystems.01239-22

Dimidi, E., Cox, S., Rossi, M., and Whelan, K. (2019). Fermented foods: definitions and characteristics, impact on the gut microbiota and effects on gastrointestinal health and disease. *Nutrients* 11:1806. doi: 10.3390/nu11081806

Dinsmoor, A., Thompson, S., Edwards, C., Burd, N., Khan, N., Erdman, J., et al. (2019). Associations between serum lutein and human gut microbiota (P02-004-19). *Current developments. Nutrition* 3:nzz029. doi: 10.1093/cdn/nzz029.P02-004-19

Duncan, S. H., Richardson, A. J., Kaul, P., Holmes, R. P., Allison, M. J., and Stewart, C. S. (2002). Oxalobacter formigenes and its potential role in human health. *Appl. Environ. Microbiol.* 68, 3841–3847. doi: 10.1128/AEM.68.8.3841-3847.2002

Englyst, H. N., and Cummings, J. H. (1986). Digestion of the carbohydrates of banana (Musa paradisiaca sapientum) in the human small intestine. *Am. J. Clin. Nutr.* 44, 42–50. doi: 10.1093/ajcn/44.1.42

Eroglu, A., Al'Abri, I. S., Kopec, R. E., Crook, N., and Bohn, T. (2023). Carotenoids and their health benefits as derived via their interactions with gut microbiota. *Adv. Nutr.* 14, 238–255. doi: 10.1016/j.advnut.2022.10.007

Feng, W., Ao, H., and Peng, C. (2018). Gut microbiota, short-Chain fatty acids, and herbal medicines. *Front. Pharmacol.* 9:1354. doi: 10.3389/fphar.2018.01354

Fernandes, I. (2019). "Anthocyanins: Nutrition and health" in Bioactive Molecules in Food. Reference Series in Phytochemistry. eds. J. M. Mérillon and K. Ramawat (Cham: Springer).

Fernandez, M. A., and Marette, A. (2017). Potential health benefits of combining yogurt and fruits based on their probiotic and prebiotic properties. *Adv. Nutr.* 8, 155S–164S. doi: 10.3945/an.115.011114

Fodor, A., Cozma, A., Sitar-Taut, A., Vulturar, R., Suharoschi, R., Rusu, A., et al. (2023). The potential of epigenetic compounds in treating diabetes. Amsterdam: Elsevier.

Fotschki, B., Juśkiewicz, J., Sójka, M., Jurgoński, A., and Zduńczyk, Z. (2015). Ellagitannins and Flavan-3-ols from raspberry pomace modulate Caecal fermentation processes and plasma lipid parameters in rats. *Molecules* 20, 22848–22862. doi: 10.3390/molecules201219878

Geerlings, S. Y., Kostopoulos, I., de Vos, W. M., and Belzer, C. (2018). *Akkermansia muciniphila* in the human gastrointestinal tract: when, where, and how? *Microorganisms* 6:75. doi: 10.3390/microorganisms6030075

Geum, H. L., et al. (2020). Anthocyanins attenuate endothelial dysfunction through regulation of uncoupling of nitric oxide synthase in aged rats. *Aging Cell* 19:e13279. doi: 10.1111/acel.13279

Gizem, C., Koen, V., Luigi, L., Rocchetti, G., Delmas, D., Daglia, M., et al. (2020). Interaction of dietary polyphenols and gut microbiota: microbial metabolism of

polyphenols, influence on the gut microbiota, and implications on host health. *Food Front.* 1, 109–133. doi: 10.1002/fft2.25

González-Regueiro, J. A., Moreno-Castañeda, L., Uribe, M., and Chávez-Tapia, N. C. (2017). The role of bile acids in glucose metabolism and their relation with diabetes. *Ann. Hepatol.* 16, S21–S26. doi: 10.5604/01.3001.0010.5672

Gu, J., Thomas-Ahner, J. M., Riedl, K. M., Bailey, M. T., Vodovotz, Y., Schwartz, S. J., et al. (2019). Dietary black raspberries impact the colonic microbiome and phytochemical metabolites in mice. *Mol. Nutr. Food Res.* 63:e1800636. doi: 10.1002/mnfr.201800636

Guillamón, E., Andreo-Martínez, P., Mut-Salud, N., Fonollá, J., and Baños, A. (2021). Beneficial effects of organosulfur compounds from *Allium cepa* on gut health: a systematic review. *Foods* 10:1680. doi: 10.3390/foods10081680

Heinrich, M., Mah, J., and Amirkia, V. (2021). Alkaloids used as medicines: structural Phytochemistry meets biodiversity-an update and forward look. *Molecules* 26:1836. doi: 10.3390/molecules26071836

Hills, R. D., Pontefract, B. A., Mishcon, H. R., Black, C. A., Sutton, S. C., and Theberge, C. R. (2019). Gut microbiome: profound implications for diet and disease. *Nutrients* 11:1613. doi: 10.3390/nu11071613

Hou, K., Wu, Z., Chen, X., Wang, J., Zhang, D., and Xiao, C. (2022). Microbiota in health and diseases. *Signal Transduction and Targeted Therapy*, 7. doi: 10.1038/s41392-022-00974-4

Iriondo-DeHond, A., Uranga, J. A., Del Castillo, M. D., and Abalo, R. (2020). Effects of coffee and its components on the gastrointestinal tract and the brain-gut Axis. *Nutrients* 13:88. doi: 10.3390/nu13010088

Jandhyala, S. M., Talukdar, R., Subramanyam, C., Vuyyuru, H., Sasikala, M., and Nageshwar Reddy, D. (2015). Role of the normal gut microbiota. *World J. Gastroenterol.* 21, 8787–8803. doi: 10.3748/wjg.v21.i29.8787

Jensen, S. N., Cady, N. M., Shahi, S. K., Peterson, S. R., Gupta, A., Gibson-Corley, K. N., et al. (2021). Isoflavone diet ameliorates experimental autoimmune encephalomyelitis through modulation of gut bacteria depleted in patients with multiple sclerosis. *Sci. Adv.* 7:eabd4595. doi: 10.1126/sciadv.abd4595

Jiang, H., Cai, M., Shen, B., Wang, Q., Zhang, T., and Zhou, X. (2022). Synbiotics and gut microbiota: new perspectives in the treatment of type 2 diabetes mellitus. *Foods* 11:2438. doi: 10.3390/foods11162438

Joaquim, B., Bruno, S., Pedro, C., and Maria, H. (2023). Polyphenols in health and disease: gut microbiota, bioaccessibility, and bioavailability. *Compounds* 3, 40–72. doi: 10.3390/compounds3010005

Junyi, L., Yueyang, W., Bin, L., Xiaohong, D., Wenhui, C., Ning, Z., et al. (2024). Gut microbiota mediates Neuroinflammation in Alzheimer's disease: unraveling key factors and mechanistic insights. *Mol. Neurobiol.* 62, 3746–3763. doi: 10.1007/s12035-024-04513-w

Kadyan, S., Sharma, A., Arjmandi, B. H., Singh, P., and Nagpal, R. (2022). Prebiotic potential of dietary beans and pulses and their resistant starch for aging-associated gut and metabolic health. *Nutrients* 14:1726. doi: 10.3390/nu14091726

Kajla, P., Sharma, A., and Sood, D. R. (2015). Flaxseed-a potential functional food source. *J. Food Sci. Technol.* 52, 1857–1871. doi: 10.1007/s13197-014-1293-y

Kang, C., Wang, B., Kaliannan, K., Wang, X., Lang, H., Hui, S., et al. (2017). Gut microbiota mediates the protective effects of dietary capsaicin against chronic low-grade inflammation and associated obesity induced by high-fat diet. *MBio* 8, e00470–e00417. doi: 10.1128/mBio.00470-17

Karamad, D., Khosravi-Darani, K., Khaneghah, A. M., and Miller, A. W. (2022). Probiotic oxalate-degrading Bacteria: new insight of environmental variables and expression of the oxc and frc genes on oxalate degradation activity. *Foods* 11:2876. doi: 10.3390/foods11182876

Kaufman, D. W., Kelly, J. P., Curhan, G. C., Anderson, T. E., Dretler, S. P., Preminger, G. M., et al. (2008). *Oxalobacter formigenes* may reduce the risk of calcium oxalate kidney stones. *J. Am. Soc. Nephrol.* 19, 1197–1203. doi: 10.1681/ASN.2007101058

Khoo, H. E., Azlan, A., Tang, S. T., and Lim, S. M. (2017). Anthocyanidins and anthocyanins: colored pigments as food, pharmaceutical ingredients, and the potential health benefits. *Food Nutr. Res.* 61:1361779. doi: 10.1080/16546628.2017.1361779

Kim, S., Shin, Y. C., Kim, T. Y., Kim, Y., Lee, Y. S., Lee, S. H., et al. (2021). Mucin degrader *Akkermansia muciniphila* accelerates intestinal stem cell-mediated epithelial development. *Gut Microbes* 13, 1–20. doi: 10.1080/19490976.2021.1892441

Kitwetcharoen, H., Phung, L. T., Klanrit, P., Thanonkeo, S., Tippayawat, P., Yamada, M., et al. (2023). Kombucha healthy drink—recent advances in production chemical composition and health benefits. *Fermentation* 11:48. doi: 10.3390/fermentation9010048

Kropp, C., Le Corf, K., Relizani, K., Tambosco, K., Martinez, C., Chain, F., et al. (2021). The keystone commensal bacterium *Christensenella minuta* DSM 22607 displays anti-inflammatory properties both in vitro and in vivo. *Sci. Rep.* 11:11494. doi: 10.1038/s41598-021-90885-1

Krumbeck, J. A., Rasmussen, H. E., Hutkins, R. W., Clarke, J., Shawron, K., Keshavarzian, A., et al. (2018). Probiotic Bifidobacterium strains and galactooligosaccharides improve intestinal barrier function in obese adults but show no synergism when used together as synbiotics. *Microbiome* 6:121. doi: 10.1186/s40168-018-0494-4

Kulkarni, R., Kumari, S., Dhapola, R., Sharma, P., Singh, S. K., Medhi, B., et al. (2024). Association between the gut microbiota and Alzheimer's disease: an update on signaling pathways and translational therapeutics. *Mol. Neurobiol.* doi: 10.1007/s12035-024-04545-2

Kumar, S., Perumal, N., Yadav, P. K., Pandey, R. P., Chang, C. M., and Raj, V. S. (2022). Amoxicillin impact on pathophysiology induced by short term high salt diet in mice. *Sci. Rep.* 12:19351. doi: 10.1038/s41598-022-21270-9

Kumar Singh, A., Cabral, C., Kumar, R., Ganguly, R., Kumar Rana, H., Gupta, A., et al. (2019). Beneficial effects of dietary polyphenols on gut microbiota and strategies to improve delivery efficiency. *Nutrients* 11:2216. doi: 10.3390/nu11092216

Lavelle, A., and Sokol, H. (2020). Gut microbiota-derived metabolites as key actors in inflammatory bowel disease. *Nat. Rev. Gastroenterol. Hepatol.* 17, 223–237. doi: 10.1038/s41575-019-0258-z

Leeuwendaal, N. K., Stanton, C., O'Toole, P. W., and Beresford, T. P. (2022). Fermented foods, health and the gut microbiome. *Nutrients* 14:1527. doi: 10.3390/nu14071527

Leonel, A. J., and Alvarez-Leite, J. I. (2012). Butyrate: implications for intestinal function. *Curr. Opin. Clin. Nutr. Metab. Care* 15, 474–479. doi: 10.1097/MCO.0b013e32835665fa

Li, Z., Dai, Z., Shi, E., Wan, P., Chen, G., and Zhang, Z. (2022a). Study on the interaction between β-carotene and gut microflora using an in vitro fermentation model. *Food Science and Human Wellness*, 12, 1369–1378. doi: 10.1016/j.fshw.2022.10.030

Li, J., Liao, X., Yin, X., Deng, Z., Hu, G., Zhang, W., et al. (2022b). Gut microbiome and serum metabolome profiles of capsaicin with cognitive benefits in APP/PS1 mice. *Nutrients* 15:118. doi: 10.3390/nu15010118

Liang, A., Leonard, W., Beasley, J. T., Fang, Z., Zhang, P., and Ranadheera, C. S. (2023). Anthocyanins-gut microbiota-health axis: a review. *Critical reviews in food science and nutrition*, 1–26. *Adv. Online Pub.* 64, 7563–7588. doi: 10.1080/10408398.2023.2187212

Lippolis, T., Cofano, M., Caponio, G. R., De Nunzio, V., and Notarnicola, M. (2023). Bioaccessibility and bioavailability of diet polyphenols and their modulation of gut microbiota. *Int. J. Mol. Sci.* 24:3813. doi: 10.3390/ijms24043813

Lisko, D. J., Johnston, G. P., and Johnston, C. G. (2017). Effects of dietary yogurt on the healthy human gastrointestinal (GI) microbiome. *Microorganisms* 5:6. doi: 10.3390/microorganisms5010006

Liu, X., Shao, J., Liao, Y., Wang, L., Jia, Y., Dong, P., et al. (2023). Regulation of short-chain fatty acids in the immune system. *Front. Immunol.* 14:1186892. doi: 10.3389/fimmu.2023.1186892

Liu, S. J., Wang, J., He, T. F., Liu, H. S., and Piao, X. S. (2021). Effects of natural capsicum extract on growth performance, nutrient utilization, antioxidant status, immune function, and meat quality in broilers. *Poult. Sci.* 100:101301. doi: 10.1016/j.psj.2021.101301

Liu, M. J., Yang, J. Y., Yan, Z. H., Hu, S., Li, J. Q., Xu, Z. X., et al. (2022). Recent findings in *Akkermansia muciniphila*-regulated metabolism and its role in intestinal diseases. *Clin. Nutr.* 41, 2333–2344. doi: 10.1016/j.clnu.2022.08.029

Lobo, V., Patil, A., Phatak, A., and Chandra, N. (2010). Free radicals, antioxidants and functional foods: impact on human health. *Pharmacogn. Rev.* 4, 118–126. doi: 10.4103/0973-7847.70902

Lockyer, S., and Stanner, S. (2019). Prebiotics – an added benefit of some fibre types. *Nutr. Bull.* 44, 74–91. doi: 10.1111/nbu.12366

Loh, J. S., Mak, W. Q., Tan, L. K. S., Ng, C. X., Chan, H. H., Yeow, S. H., et al. (2024). Microbiota–gut–brain axis and its therapeutic applications in neurodegenerative diseases. *Signal transduction and targeted. Therapy* 9:743. doi: 10.1038/s41392-024-01743-1

Makki, K., Deehan, E. C., Walter, J., and Bäckhed, F. (2018). The impact of dietary fiber on gut microbiota in host health and disease. *Cell Host Microbe* 23, 705–715. doi: 10.1016/j.chom.2018.05.012

Manach, C., Scalbert, A., Morand, C., Rémésy, C., and Jiménez, L. (2004). Polyphenols: food sources and bioavailability. *Am. J. Clin. Nutr.* 79, 727–747. doi: 10.1093/ajcn/79.5.727

Markowiak, P., and Śliżewska, K. (2017). Effects of probiotics, prebiotics, and Synbiotics on human health. *Nutrients* 9:1021. doi: 10.3390/nu9091021

Maruo, T., Sakamoto, M., Ito, C., Toda, T., and Benno, Y. (2008). *Adlercreutzia equolifaciens* gen. Nov., sp. nov., an equol-producing bacterium isolated from human faeces, and emended description of the genus Eggerthella. *Int. J. Syst. Evol. Microbiol.* 58, 1221–1227. doi: 10.1099/ijs.0.65404-0

Mayo, B., Vázquez, L., and Flórez, A. B. (2019). Equol: a bacterial metabolite from the Daidzein Isoflavone and its presumed beneficial health effects. *Nutrients* 11:2231. doi: 10.3390/nu11092231

Mazier, W., Le Corf, K., Martinez, C., Tudela, H., Kissi, D., Kropp, C., et al. (2021). A new strain of *Christensenella minuta* as a potential biotherapy for obesity and associated metabolic diseases. *Cells* 10:823. doi: 10.3390/cells10040823

Menden, A., Hall, D., Hahn-Townsend, C., Broedlow, C. A., Joshi, U., Pearson, A., et al. (2022). Exogenous lipase administration alters gut microbiota composition and ameliorates Alzheimer's disease-like pathology in APP/PS1 mice. *Sci. Rep.* 12:4797. doi: 10.1038/s41598-022-08840-7

Miaoyu, L., Leilei, Y., Jianxin, Z., Hao, Z., Wei, C., Qixiao, Z., et al. (2021). Role of dietary edible mushrooms in the modulation of gut microbiota. *J. Funct. Foods* 83:104538. doi: 10.1016/j.jff.2021.104538

Min, W., Renzhe, T., Rui, Z., Yongxiang, Q., and Dongmei, D. (2023). The protective effect of serum carotenoids on cardiovascular disease: a cross-sectional study from the general US adult population. *Front. Nutr.* 10:10. doi: 10.3389/fnut.2023.1154239

Monda, V., Villano, I., Messina, A., Valenzano, A., Esposito, T., Moscatelli, F., et al. (2017). Exercise modifies the gut microbiota with positive health effects. *Oxidative Med. Cell. Longev.* 2017:972. doi: 10.1155/2017/3831972

Mueed, A., Shibli, S., Korma, S. A., Madjirebaye, P., Esatbeyoglu, T., and Deng, Z. (2022). Flaxseed bioactive compounds: chemical composition, functional properties, food applications and health benefits-related gut microbes. *Foods* 11:3307. doi: 10.3390/foods11203307

Murga-Garrido, S. M., Hong, Q., Cross, T. L., Hutchison, E. R., Han, J., Thomas, S. P., et al. (2021). Gut microbiome variation modulates the effects of dietary fiber on host metabolism. *Microbiome* 9:117. doi: 10.1186/s40168-021-01061-6

Muscogiuri, G., Balercia, G., Barrea, L., Cignarelli, A., Giorgino, F., Holst, J. J., et al. (2017). Gut: a key player in the pathogenesis of type 2 diabetes? *Crit. Rev. Food Sci. Nutr.* 58, 1294–1309. doi: 10.1080/10408398.2016.1252712

Nambiar, R. B., Perumal, A. B., Shittu, T., Sadiku, E. R., and Sellamuthu, P. S. (2023). Editorial: probiotics, prebiotics, synbiotics, postbiotics, & paraprobiotics - new perspective for functional foods and nutraceuticals. *Front. Nutr.* 10:1164676. doi: 10.3389/fnut.2023.1164676

Oshiro, N., Wong, S. K., Chan, H. T., Chan, E. W. C., and Kezuka, M. (2021). Natto and miso: an overview on their preparation, bioactive components and health-promoting effects. Food Research (Malaysia).

Othman, L., Sleiman, A., and Abdel-Massih, R. M. (2019). Antimicrobial activity of polyphenols and alkaloids in middle eastern plants. *Front. Microbiol.* 10:911. doi: 10.3389/fmicb.2019.00911

Pan, L., Ye, H., Pi, X., Liu, W., Wang, Z., Zhang, Y., et al. (2023). Effects of several flavonoids on human gut microbiota and its metabolism by *in vitro* simulated fermentation. *Front. Microbiol.* 14:1092729. doi: 10.3389/fmicb.2023.1092729

Pandey, K. R., Naik, S. R., and Vakil, B. V. (2015). Probiotics, prebiotics and synbiotics-a review. *J. Food Sci. Technol.* 52, 7577–7587. doi: 10.1007/s13197-015-1921-1

Parada Venegas, D., De la Fuente, M. K., Landskron, G., González, M. J., Quera, R., Dijkstra, G., et al. (2019). Short Chain fatty acids (SCFAs)-mediated gut epithelial and immune regulation and its relevance for inflammatory bowel diseases. *Front. Immunol.* 10:277. doi: 10.3389/fimmu.2019.00277

Parekh, P. J., Balart, L. A., and Johnson, D. A. (2015). The influence of the gut microbiome on obesity, metabolic syndrome and gastrointestinal disease. *Clin. Transl. Gastroenterol.* 6:e91. doi: 10.1038/ctg.2015.16

Peery, A. F., Kelly, C. R., Kao, D., Vaughn, B. P., Lebwohl, B., and Altayar, O. (2024). AGA Clinical Practice Guideline on Fecal Microbiota–Based Therapies for select Gastrointestinal Diseases. *Gastroenterol.* 166, 409–434. doi: 10.1053/j.gastro.2024.01.008

Pelaseyed, T., Bergström, J. H., Gustafsson, J. K., Ermund, A., Birchenough, G. M., Schütte, A., et al. (2014). The mucus and mucins of the goblet cells and enterocytes provide the first defense line of the gastrointestinal tract and interact with the immune system. *Immunol. Rev.* 260, 8–20. doi: 10.1111/imr.12182

Peng, J., Zheng, T. T., Li, X., Liang, Y., Wang, L. J., Huang, Y. C., et al. (2019). Plant-derived alkaloids: the promising disease-modifying agents for inflammatory bowel disease. *Front. Pharmacol.* 10:351. doi: 10.3389/fphar.2019.00351

Portincasa, P., Bonfrate, L., Vacca, M., De Angelis, M., Farella, I., Lanza, E., et al. (2022). Gut microbiota and short Chain fatty acids: implications in glucose homeostasis. *Int. J. Mol. Sci.* 23:1105. doi: 10.3390/ijms23031105

Queen, R., and Queen, R. (2020). Resistant starch, butyrate and gut barrier integrity resistant starch. Resistant starch research resistant starch research and benefits explained in simple terms. Available at: https://resistantstarchresearch.com/posts/resistant-starch-butyrate-and-gut-barrier-integrity/#:~:text=Resistant%20starch's%20production%20of%20butyrate,intestinal%20inflammation%20is%20also%20beneficial

Rahman, M. M., Rahaman, M. S., Islam, M. R., Rahman, F., and Mithi, F. M.,and Alqahtani, T. (2021). Role of phenolic compounds in human disease: Current knowledge and future Prospects. *Molecules*, 27:233. doi: 10.3390/molecules27010233

Rinninella, E., Cintoni, M., Raoul, P., Lopetuso, L. R., Scaldaferri, F., Pulcini, G., et al. (2019). Food components and dietary habits: keys for a healthy gut microbiota composition. *Nutrients* 11:2393. doi: 10.3390/nu11102393

Roberfroid, M., Bornet, F., Bouley, C., and Cummings, J. (2009). Colonic microflora: nutrition and Health0. Summary and conclusions of an international Life Sciences Institute (ILSI) [Europe] workshop held in Barcelona, Spain. *Nutr. Rev.* 53, 127–130. doi: 10.1111/j.1753-4887.1995.tb01535.x

Rocha, H. R., Coelho, M. C., Gomes, A. M., and Pintado, M. E. (2023). Carotenoids diet: digestion, gut microbiota modulation, and inflammatory diseases. *Nutrients* 15:2265. doi: 10.3390/nu15102265

Rodrigues, V. F., Elias-Oliveira, J., Pereira, Í. S., Pereira, J. A., Barbosa, S. C., Machado, M. S. G., et al. (2022). *Akkermansia muciniphila* and gut immune system: a good friendship that attenuates inflammatory bowel disease, obesity, and diabetes. *Front. Immunol.* 13:934695. doi: 10.3389/fimmu.2022.934695

Roopchand, D., Carmody, R. N., Kuhn, P., Moskal, K., Rojas-Silva, P., Turnbaugh, P. J., et al. (2015). Dietary polyphenols promote growth of the gut BacteriumAkkermansia muciniphilaand attenuate high-fat diet–induced metabolic syndrome. *Diabetes* 64, 2847–2858. doi: 10.2337/db14-1916

Rowles, J. L., and Erdman, J. W. (2020). Carotenoids and their role in cancer prevention. Biochimica et biophysica acta. *Mol. Cell Biol. Lipids* 1865:158613. doi: 10.1016/j.bbalip.2020.158613

Samtiya, M., Aluko, R. E., Dhewa, T., and Moreno-Rojas, J. M. (2021). Potential health benefits of plant food-derived bioactive components: an overview. *Foods* 10:839. doi: 10.3390/foods10040839

Schächtle, M. A., and Rosshart, S. P. (2021). The microbiota-gut-brain axis in health and disease and its implications for translational research. *Front. Cell. Neurosci.* 15:698172. doi: 10.3389/fncel.2021.698172

Schneider, E., O'Riordan, K. J., Clarke, G., and Cryan, J. F. (2024). Feeding gut microbes to nourish the brain: unravelling the diet–microbiota–gut–brain axis. *Nat. Metab.* 6, 1454–1478. doi: 10.1038/s42255-024-01108-6

Sejbuk, M., Mirończuk-Chodakowska, I., Karav, S., and Witkowska, A. M. (2024). Dietary polyphenols, food processing and gut microbiome: recent findings on bioavailability, bioactivity, and gut microbiome interplay. *Antioxidants* 13:1220. doi: 10.3390/antiox13101220

Singh, R., Chandrashekharappa, S., Bodduluri, S. R., Baby, B. V., Hegde, B., Kotla, N. G., et al. (2019). Enhancement of the gut barrier integrity by a microbial metabolite through the Nrf2 pathway. *Nat. Commun.* 10:89. doi: 10.1038/s41467-018-07859-7

Singh, R. K., Chang, H. W., Yan, D., Lee, K. M., Ucmak, D., Wong, K., et al. (2017). Influence of diet on the gut microbiome and implications for human health. *J. Transl. Med.* 15:73. doi: 10.1186/s12967-017-1175-y

Slavin, J. (2013). Fiber and prebiotics: mechanisms and health benefits. *Nutrients* 5, 1417–1435. doi: 10.3390/nu5041417

Song, J. X., Ren, H., Gao, Y. F., Lee, C. Y., Li, S. F., Zhang, F., et al. (2017). Dietary capsaicin improves glucose homeostasis and alters the gut microbiota in obese diabetic Ob/Ob mice. *Front. Physiol.* 8:602. doi: 10.3389/fphys.2017.00602

Stephanie, R. N. K., Soka, S., and Suwanto, A. (2017). Effect of tempeh supplementation on the profiles of human intestinal immune system and gut microbiota. *Microbiol. Indonesia* 11, 11–17. doi: 10.5454/mi.11.1.2

Su, Q., and Liu, Q. (2021). Factors affecting gut microbiome in daily diet. *Front. Nutr.* 8:644138. doi: 10.3389/fnut.2021.644138

Sultan, S., El-Mowafy, M., Elgaml, A., Ahmed, T., Hassan, H., and Mottawea, W. (2021). Metabolic influences of gut microbiota dysbiosis on inflammatory bowel disease. *Front. Physiol.* 12:715506. doi: 10.3389/fphys.2021.715506

Tan, J., McKenzie, C., Potamitis, M., Thorburn, A. N., Mackay, C. R., and Macia, L. (2014). The role of short-chain fatty acids in health and disease. *Adv. Immunol.* 121, 91–119. doi: 10.1016/B978-0-12-800100-4.00003-9

Tao, F., Xing, X., Wu, J., and Jiang, R. (2021). Enteral nutrition modulation with n-3 PUFAs directs microbiome and lipid metabolism in mice. *PLoS One* 16:e0248482. doi: 10.1371/journal.pone.0248482

Tingirikari, J. M. R., Sharma, A., and Lee, H. (2024). Kefir: a fermented plethora of symbiotic microbiome and health. *J. Ethnic Foods* 11:252. doi: 10.1186/s42779-024-00252-4

Tuli, H. S., Kumar, A., Sak, K., Aggarwal, D., Gupta, D. S., Kaur, G., et al. (2022). Gut microbiota-assisted synthesis, cellular interactions and synergistic perspectives of Equol as a potent anticancer Isoflavone. *Pharmaceuticals* 15:1418. doi: 10.3390/ph15111418

Ubeda, C., Bucci, V., Caballero, S., Djukovic, A., Toussaint, N. C., Equinda, M., et al. (2013). Intestinal microbiota containing Barnesiella species cures vancomycin-resistant *Enterococcus faecium* colonization. *Infect. Immun.* 81, 965–973. doi: 10.1128/IAI.01197-12

Verediano, T. A., Stampini Duarte Martino, H., Dias Paes, M. C., and Tako, E. (2021). Effects of anthocyanin on intestinal health: a systematic review. *Nutrients* 13:1331. doi: 10.3390/nu13041331

Visioli, F., Risé, P., Barassi, M. C., Marangoni, F., and Galli, C. (2003). Dietary intake of fish vs. formulations leads to higher plasma concentrations of n-3 fatty acids. *Lipids* 38, 415–418. doi: 10.1007/s11745-003-1077-x

Wang, X., Qi, Y., and Zheng, H. (2022). Dietary polyphenol, gut microbiota, and health benefits. *Antioxidants* 11:1212. doi: 10.3390/antiox11061212

Wang, M., Yu, F., Zhang, Y., Chang, W., and Zhou, M. (2022). The effects and mechanisms of flavonoids on Cancer prevention and therapy: focus on gut microbiota. *Int. J. Biol. Sci.* 18, 1451–1475. doi: 10.7150/ijbs.68170

Wang, M., Zhang, Y., Li, C., Chang, W., and Zhang, L. (2023). The relationship between gut microbiota and COVID-19 progression: new insights into immunopathogenesis and treatment. *Front. Immunol.* 14:1180336. doi: 10.3389/fimmu.2023.1180336

Waters, J. L., and Ley, R. E. (2019). The human gut bacteria Christensenellaceae are widespread, heritable, and associated with health. *BMC Biol.* 17:83. doi: 10.1186/s12915-019-0699-4

Yadav, M. K., Kumari, I., Singh, B., Sharma, K. K., and Tiwari, S. K. (2022). Probiotics, prebiotics and synbiotics: safe options for next-generation therapeutics. *Appl. Microbiol. Biotechnol.* 106, 505–521. doi: 10.1007/s00253-021-11646-8

Yao, Y., Liu, Y., Xu, Q., and Mao, L. (2024). Short chain fatty acids: essential weapons of traditional medicine in treating inflammatory bowel disease. *Molecules* 29:379. doi: 10.3390/molecules29020379

York, A. (2019). Your microbiome is what you eat. *Nat. Rev. Microbiol.* 17:721. doi: 10.1038/s41579-019-0287-1

Zhang, T., Gao, G., Kwok, L., and Sun, Z. (2023). Gut microbiome-targeted therapies for Alzheimer's disease. *Gut Microbes* 15:613. doi: 10.1080/19490976.2023.2271613

Zhang, N., Huang, X., Zeng, Y., Wu, X., and Peng, X. (2013). Study on prebiotic effectiveness of neutral garlic fructan in vitro. *Food Sci. Human Wellness* 2, 119–123. doi: 10.1016/j.fshw.2013.07.001

Zhang, M., Li, A., Yang, Q., Li, J., Wang, L., Liu, X., et al. (2021). Beneficial effect of alkaloids from *Sophora alopecuroides* L. on CUMS-induced depression model mice *via* modulating gut microbiota. *Front. Cell. Infect. Microbiol.* 11:665159. doi: 10.3389/fcimb.2021.665159

Zhiguo, Z., Buyu, L., Xingquan, L., Weiwei, H., Zhang, C., Guo, Y., et al. (2023). Effects of steaming on sweet potato soluble dietary Fiber: content, structure, and *Lactobacillus* proliferation in vitro. *Food Secur.* 12:1620. doi: 10.3390/foods12081620

Zhong, H., Xu, J., Yang, M., Hussain, M., Liu, X., Feng, F., et al. (2023). Protective effect of Anthocyanins against neurodegenerative diseases through the microbial-intestinal-brain axis: a critical review. *Nutrients* 15:496. doi: 10.3390/nu15030496

Zhou, K. (2017). Strategies to promote abundance of *Akkermansia muciniphila*, an emerging probiotics in the gut, evidence from dietary intervention studies. *J. Funct. Foods* 33, 194–201. doi: 10.1016/j.jff.2017.03.045

frontiers | Frontiers in Microbiology

TYPE Original Research
PUBLISHED 19 February 2025
DOI 10.3389/fmicb.2025.1542522

Check for updates

OPEN ACCESS

EDITED BY
Guiguo Zhang,
Shandong Agricultural University, China

REVIEWED BY
Hamed I. Hamouda,
Chinese Academy of Sciences (CAS), China
Lingjun Tong,
Shandong First Medical University, China

*CORRESPONDENCE
Hao Wu
✉ dream72wh@tju.edu.cn
Jianjun Qiao
✉ jianjunq@tju.edu.cn

RECEIVED 10 December 2024
ACCEPTED 03 February 2025
PUBLISHED 19 February 2025

CITATION
Han H, Xiong H, Liu Z, Liu X, Wang H, Kou J, Yi D, Shi Y, Wu H and Qiao J (2025) Pasteurized *Akkermansia muciniphila* Timepie001 ameliorates DSS-induced ulcerative colitis in mice by alleviating intestinal injury and modulating gut microbiota.
Front. Microbiol. 16:1542522.
doi: 10.3389/fmicb.2025.1542522

COPYRIGHT
© 2025 Han, Xiong, Liu, Liu, Wang, Kou, Yi, Shi, Wu and Qiao. This is an open-access article distributed under the terms of the Creative Commons Attribution License (CC BY). The use, distribution or reproduction in other forums is permitted, provided the original author(s) and the copyright owner(s) are credited and that the original publication in this journal is cited, in accordance with accepted academic practice. No use, distribution or reproduction is permitted which does not comply with these terms.

Pasteurized *Akkermansia muciniphila* Timepie001 ameliorates DSS-induced ulcerative colitis in mice by alleviating intestinal injury and modulating gut microbiota

Huan Han[1,2], Hui Xiong[2], Zengli Liu[2], Xunzhi Liu[3], Hailin Wang[4], Jiaxiang Kou[2], Dewei Yi[2], Ying Shi[3], Hao Wu[1,2]* and Jianjun Qiao[1,2]*

[1]School of Chemical Engineering and Technology, Tianjin University, Tianjin, China, [2]Zhejiang Institute of Tianjin University, Shaoxing, China, [3]Shanghai Fuyang Biotechnology Co., Ltd., Shanghai, China, [4]College of Food and Bioengineering, Fujian Polytechnic Normal University, Fuqing, China

Introduction: *Akkermansia muciniphila* (*A. muciniphila*), known as a next-generation probiotic, has been widely recognized for its beneficial effects in various metabolic diseases. While there is not much research whether live or pasteurized *A. muciniphila* has different effects on intestinal health.

Methods: In the present study, a strain of *A. muciniphila* was isolated from healthy individuals, with the live and pasteurized *A. muciniphila* named Timepie001 and Timepie001+, respectively. They were administered to dextran sulfate sodium-induced ulcerative colitis mice to investigate their influences on the host intestinal health.

Results and conclusion: The results showed that prophylactic supplementation with live and pasteurized *A. muciniphila* alleviates ulcerative colitis symptoms by retarding weight loss, preserving intestinal tissue structure, modulating inflammatory cytokines (TNF-α, IL-1β), and enhance the colonic mucosal barrier by upregulating the expression of tight junction protein Claudin-1. Interestingly, pasteurized *A. muciniphila* has a better effect compared with live *A. muciniphila*. Moreover, pasteurized *A. muciniphila* can regulates the gut microbiome to maintain intestinal homeostasis. This provides theoretical support for the widespread application of postbiotics in the food industry.

KEYWORDS

***Akkermansia muciniphila*, Timepie001, ulcerative colitis, gut microbiota, intestinal regulation**

1 Introduction

Ulcerative colitis (UC) is a chronic inflammatory bowel disease (IBD) commonly known as "green cancer." The pathogenesis of UC is complex and not fully understood, involving oxidative stress, intestinal mucosal damage, inflammation, and microbial dysregulation (Han et al., 2023; Seni et al., 2024). Lesions typically occur in the sigmoid colon and rectum but can extend to the descending colon, or even the entire colon (Li Y. et al., 2024). UC has become a global health problem seriously affecting the quality of life of patients (Zheng et al., 2023). The

etiology of UC is multifactorial, arising from the interplay of genetic predisposition, environmental factors, unhealthy dietary habits, and autoimmune responses (Ni et al., 2017). Current treatments for UC include corticosteroids, immunosuppressants, and aminosalicylates, which despite their effectiveness, often come with significant costs and adverse side effects (Wangchuk et al., 2024). Therefore, there is a pressing need to further elucidate the underlying pathogenesis of UC and to develop safe and effective therapeutic strategies.

At present, although the pathogenesis of UC is not fully understood, an increasing number of studies indicate that the disrupted intestinal environment and gut microbiota are key factors affecting the occurrence and development of UC (Guo et al., 2021; Cheng et al., 2023; Zhang et al., 2025). Probiotics can modulate the balance of the gut microbiome, influence the metabolites produced by gut microorganisms, and play a key role in human intestinal health (Wang et al., 2024; Zhang et al., 2024). Multiple studies indicate probiotics can inhibit the proliferation of pathogenic bacteria, maintain mucosal barrier function, protect the host from pathogen-induced damage, promote the development of the intestinal immune system, and participate in immune regulation through the production of beneficial metabolites (Wu et al., 2022; Dai et al., 2024). This contributes to establishing a healthy gut microenvironment that can prevent and alleviate enteritis (Shen et al., 2018). Compared to healthy individuals, Earley et al. (2019) quantitatively analyzed the amount of *A. muciniphila* in mucus brushings from the colonic mucus, and found a significant reduction in all four areas of the colon, the caecum, transverse colon, left colon and rectum in patients with UC. Vigsnaes et al. (2012) and Wang et al. (2020) confirmed that *A. muciniphila* in stool samples was significantly reduced in patients with UC. The DSS-induced acute UC model in mice is a commonly used animal model for studying UC. Similarly, numerous studies have shown that *A. muciniphila* in animals with experimental colitis is negatively correlated with disease severity (Berry et al., 2012; Dunn et al., 2016; Zhang et al., 2016). These findings suggest that *A. muciniphila* may play a role in the pathogenesis and progression of UC and could be a potential target for therapeutic strategies.

A. muciniphila is a normal human intestinal bacterium and a strictly anaerobic gram-negative bacterium, oval-shaped organism, with 0.6–1.0 mm cell size. It is an obligate anaerobic, non-spore forming, and non-motile, belonging to the Verrucomicrobia phylum, was first isolated in 2004 by Derrien et al. (2004) from the feces of a healthy individual. *A. muciniphila* colonizes the human intestinal mucosal layer, where it degrades mucin and regulates the intestinal barrier and immune response. The abundance of *A. muciniphila* in the human intestinal tract represents 1–4% of the total fecal microbiota, and changes with age, diet, body weight and immune state throughout a life-time (Sharon et al., 2018). As the next generation of probiotics, *A. muciniphila* have been reported various beneficial properties, including protective effects against metabolic and diabetes, obesity, pulmonary fibrosis, heredity and immune conditions, colitis-associated colorectal cancer (Payahoo et al., 2019; Zhao et al., 2023; Faghfuri and Gholizadeh, 2024; Yu et al., 2024). Moreover, both animal experiments and human trials have demonstrated that exogenous supplementation with *A. muciniphila* or pasteurized *A. muciniphila* is effective, safe, and tolerated (Frank et al., 2007; Zhai et al., 2019). Depommier et al. (2019) conducted a randomized, double-blind, placebo-controlled pilot study in overweight/obese insulin-resistant volunteers. After 3 months of supplementation, they found that oral administration of pasteurized *A. muciniphila* improved insulin sensitivity by 30% compared to the placebo group, reducing insulin levels and total plasma cholesterol, while live bacteria did not exhibit these effects. The previous articles mainly focused on the field of metabolic disease, with limited research on UC. It is interesting that sometimes researchers' conclusions are contradictory. Such as, Qu et al. (2021) found that *A. muciniphila* strain BAA-835 significantly ameliorated the symptoms in DSS-induced acute colitis; Bian et al. (2019) pointed that *A. muciniphila* Muc^T can protect the gut barrier function and reduce the levels of inflammatory cytokines to ameliorates dextran sulfate sodium (DSS)-induced UC in mice. However, Seregin et al. (2017) investigated fecal samples from two genetically colitis-prone mouse model, namely IL10$^{-/-}$ and Winnie$^{-/-}$ mice. Both models exhibited more abundant *A. muciniphila* than their wild-type littermates, and gavage of *A. muciniphila* to IL-10$^{-/-}$ mice aggravated their colitis. Therefore, further research is needed to investigate the effect of *A. muciniphila* on colitis.

In this study, a strain of *A. muciniphila* was first screened and identified from healthy individuals and designated as Timepie001, while its pasteurized form was named Timepie001+. The optimal effects of live and pasteurized *A. muciniphila* intervention, as well as prophylactic supplementation, on intestinal barrier function in DSS-induced acute UC mice were then investigated. Additionally, possible mechanisms were explored through changes in inflammatory factors, expression of intercellular junction proteins and the gut microbiota.

2 Materials and methods

2.1 Preparation of Timepie001

A fecal sample from a healthy adult volunteer was freshly collected in a polyethylene bag and approximately 0.2 g fecal sample was dissolved in anaerobic PBS (pH7.2) containing 0.5 g/L of cysteine-HCL. The suspension was thoroughly mixed and serially diluted in 10-fold increments. Diluted suspensions were streaked onto brain heart infusion (BHI) agar plates supplemented with 2.5 g/L mucin. The plates were incubated at 37°C under anaerobic conditions generated by a gas mixture of 182 kPa $N_2/CO_2/H_2$ (85:10:5, v/v) for 3 days. Single colonies were then selected and re-streaked onto fresh BHI plates containing 2.5 g/L mucin until pure cultures were obtained.

To determine the phylogenetic affiliation of the purified colonies, nucleotide sequence analysis of the cloned 16S rRNA gene was performed (Gómez-Gallego et al., 2016). The 16S rRNA gene sequence was compared to sequences from GenBank using the program BLASTN 2.0, available through the National Centre for Biotechnology Information (NCBI) website.[1]

A. muciniphila was incubated at 37°C for 48 h in BHI medium contained 2.5 g/L mucin. Following incubation, *A. muciniphila* and pasteurized *A. muciniphila* (70 degrees Celsius for 30 min) subsequently centrifuged at 8,000 × g for 15 min at 4°C. The cells were washed twice by PBS and centrifuged. The washed cells were resuspended in protective medium containing 7% (w/v) skim milk, 5% (w/v) trehalose and 1.5% (w/v) natrascorb as lyoprotectors. Immediately, the cells were prefrozen at −40°C for 12 h, and then frozen at −15°C, 5 Pa for 24 h using a vacuum freeze dryer (Turuvekere Sadguruprasad and Basavaraj, 2018).

1 http://www.ncbi.nlm.nih.gov/blast/

2.2 Cell culture and anti-inflammatory activity

RAW 264.7 cells were cultured in RPMI 1640 media with 10% fetal bovine serum (FBS), 1% penicillin-streptomycin (Cytiva, SH40003.01) in an environment containing 5% CO_2 at 37°C. Once cell adhesion reached 80–90%, the cells were passaged at 1:2 ratios.

For experiments, cells were seeded into a 96-well or 6-well plate until they reached an amount of 2×10^6 cells/mL. After 24 h incubation, the cells were treated by different percentages (50, 25 and 12.5%) of live *A. muciniphila*. Cell viability was assessed using the Cell Counting Kit-8 (CCK-8) (TargetMOI, C0005). The cells were then treated with 2 μg/mL lipopolysaccharides (LPS) (Solarbio, L8880) and 25% of live and pasteurized *A. muciniphila*. After an additional 24 h of incubation, the production of nitric oxide (NO), interleukin-1β (IL-1β) and interleukin-6 (IL-6) were measured using the Griess assay (Beyotime, S0021S) and ELISA kits (Excell, EM004-96/EM001-96).

2.3 Ulcerative colitis model and treatments

The animal experimental design was drafted according to the requirements of the Guide for the Care and Use of Laboratory Animals: Eighth Edition (Astronomy and Astrophysics, 1996). Healthy male age-matched C57BL/6J mice (6–8 weeks of age) were purchased from Zhejiang Academy of Medical Sciences (Hangzhou, China). DSS (mol wt, 36,000–50,000 Da, CAS No. 9011-18-1) was purchased from MP Biomedicals (Goddard, United States). All animals were housed under specific pathogen-free conditions in IVC cages with 12 h light/dark cycles, enriched water and food feeding. Following 1 week of acclimatization, the mice were randomly assigned to four groups ($n = 6$ for each group).

Negative control group (NC): received deionized water for 7 days.

DSS group (DSS): 2.5% DSS was given as the sole source of drinking fluid and administered PBS for 7 days.

Live *A. muciniphila* (Timepie001) group: 2.5% DSS was given as the sole source of drinking fluid and administered live *A. muciniphila* (1×10^9 CFU/mouse) by oral gavage for 7 days.

Pasteurized of *A. muciniphila* (Timepie001+) group: 2.5% DSS was given as the sole source of drinking fluid, and pasteurized *A. muciniphila* (same weight as live *A. muciniphila*) was administered by oral gavage for 7 days.

During the duration of the experiment, the body weight, fecal status, and degree of fecal blood were measured daily for disease activity index (DAI) assessment. At the end of the experiment, spleens were excised, rinsed with 0.9% NaCl, and weighed. Colons were collected, rinsed with ice-cold 0.9% NaCl, placed on filter paper, and their lengths were measured using a ruler. Each colon was then divided into four large sections, which were snapped frozen at −80°C. The above process was inspected and approved by the Animal Care & Welfare Committee of Zhejiang University of Technology, China (No. ZH20240531066).

2.4 Disease activity index

The disease activity index (DAI) was assessed based on body weight loss, diarrhea, and hematochezia to evaluate the severity of colitis. Body weight loss was scored as follows: 0 (≤1%), 1 (1–5%), 2 (5–10%), 3 (10–15%), and 4 (≥15%). Diarrhea and rectal bleeding were scored daily, with rectal bleeding rated as: 0 (no bleeding), 2 (slight bleeding), and 4 (extensive bleeding); diarrhea was scored as: 0 (well-formed stools), 2 (soft and pasty stools), and 4 (watery stools). The average DAI value was calculated from these scores.

2.5 Assessment of colon inflammation

Colonic tissues were fixed in 4% paraformaldehyde solution at room temperature and then embedded in paraffin. The fixed colon was cut into 5 μm sections for hematoxylin and eosin (H&E) staining. Pathological analysis of all sections was performed using light microscopy. The specific evaluation criteria are as follows: depth of inflammation and at a range from 0 to 4 as to the amount of crypt damage or regeneration. (0: intact recess without inflammation; 1: 1/3 recess damaged; 2: 2/3 recess damage and mild inflammation; 3: large recess damage, intact mucosa, and moderate inflammation; 4: mucosal epithelium loss, erosion, severe inflammation).

2.6 RNA extraction and RT-qPCR

RNA extraction from colonic tissue was modified from previously established methods (Cheng et al., 2021). Total RNA was extracted from the colon tissue samples with RNAprep Pure Tissue Kit (TIANGEN, DP431). The RNA purity was assessed with a microspectrophotometer (Mettler Toledo UV5) and 260/280 nm of all the samples were between 1.8 and 2.1. Following the kit's instructions, RNA was reverse-transcribed into cDNA using the SPARKscript II RT Plus Kit (with gDNA Eraser) (SparkJade, AG0304-B). RT-qPCR amplification was performed using 2 × SYBR Green qPCR Mix (with ROX) (SparkJade, AG0104-B). The primer sequences for GAPDH, IL-1β, tumor necrosis factor-α (TNF-α) and zonula occludens-1 (ZO-1) were detailed in Table 1, with GAPDH serving as an internal reference gene. Relative mRNA expression levels were calculated using the $2^{-\Delta\Delta CT}$ method.

TABLE 1 Primer sequence list of the tested genes.

Gene	Sense (5′–3′)	Anti-sense (5′–3′)
GAPDH	TGGCCTTCCGTGTTCCTAC	GAGTTGCTGTTGAAGTCGCA
IL-1β	TCGCAGCAGCACATCAACAAGAG	TGCTCATGTCCTCATCCTGGAAGG
TNF-α	CAGGCGGTGCCTATGTCTC	CGATCACCCCGAAGTTCAGTAG
ZO-1	GCGAACAGAAGGAGCGAGAAGAG	GCTTTGCGGGCTGACTGGAG

2.7 Western blot analysis

Western blot analysis was performed according to modified protocols from previous studies (Lee et al., 2022). Total proteins were extracted from the colonic tissue using RIPA lysis buffer (containing protease inhibitors) (Macklin, Y10001173) and sonicated at 4°C. Protein concentrations in tissue lysates were quantitated using a BCA protein assay kit (Solarbio, PC0020). After centrifuging the lysed sample, protein concentrations were adjusted, mixed with a 5× loading buffer, and heated in a metal bath for 10 min. Proteins (10 μL) were separated using 10% SDS-PAGE and transferred to polyvinylidene fluoride (PVDF) membranes (Millipore, Billerica, MA, United States). After completion, the membranes were blocked for 1 h with 5% BSA in 1% TBST and probed with specific primary antibodies [GADPH (Affinity, AF7021), Claudin-1 (Zenbio, 343202)] at 4°C overnight. The PVDF membrane was then washed five times with 1% TBST (TBS with Tween-20) and incubated with secondary antibodies (ZSGB-BIO, ZB-2301) in 5% bovine serum albumin (BSA) at room temperature for 1 h. After the PVDF membrane was washed five times, immunoblot images were captured using a fluorescence imaging system (Tanon-5200Multi), and the band expression levels were quantified using Image J. GAPDH was used as a reference gene.

2.8 Taxonomic analyses of the gut microbiota

Fresh fecal samples were collected in sterile sampling tubes, with approximately 200 mg from the distal segment taken using a sampler and placed into a tube containing nucleic acid preservative solution, then immediately stored at −80°C until DNA extraction. Genomic DNA was extracted from all fecal samples and amplified using polymerase chain reaction (PCR) with primers specific to the 16S V3–V4 region. Libraries were constructed using the Illumina Inc. library preparation kit (Model: TruSeq DNA PCR-Free Library Preparation Kit). After quantitative assessment and qualification, sequencing was performed on the NovaSeq 6000. Sequencing reads were assembled, and sequence quality was controlled and filtered. The sequences were clustered into operational taxonomic units (OTUs) with 97% similarity and annotated using the Silva 138 database. Species abundances across different categorization levels were detected together with the composition of the gut microbiota in each sample at each level of classification (phylum, class, order, family, and genus). The number of OTUs in each group was statistically analyzed to compare the changes in the richness of the mouse intestinal microbial community. Alpha diversity was assessed using the Shannon, Simpson, Chao1, and ACE index. The composition of the microbial community was illustrated in a bar chart at the genus level and differences were analyzed.

2.9 Statistics analysis

The data are presented as Mean ± SEM with at least triplicates and $n = 6$ for each group. All analyses were performed using Graphpad Prism version 5.0 (Graphpad Software, San Diego, CA, United States). One-way analysis of variance (ANOVA) was utilized to compare multiple groups. When significant differences were identified, Tukey's *post hoc* test was applied to determine specific differences between pairs of means, with appropriate adjustments for multiple testing. In all analyses, the confidence interval was set at 95%, and p-values less than 0.05 were considered statistically significant.

3 Results

3.1 Isolation and identification of *Akkermansia muciniphila*

The strain *A. muciniphila* Timepie001 was isolated from healthy human subjects and identified through 16S rDNA analysis, which revealed a 99.93% similarity with the 16S sequence of *A. muciniphila* ATCC BAA-835, confirming its classification as *A. muciniphila* (Ouwerkerk et al., 2016). To further establish the evolutionary relationship between the two strains, whole-genome sequencing of Timepie001 was conducted, followed by average nucleotide identity (ANI) analysis comparing it to *A. muciniphila* ATCC BAA-835 (Figure 1). The ANI value obtained for Timepie001 was 97.24%, meeting the ANI threshold for species classification (greater than 95%). Subsequent experiments utilized pasteurized freeze-dried powder of the strain.

3.2 Anti-inflammatory activity *in vitro*

Macrophages are important participants in the pathogenesis of UC due to their production of many pivotal cytokines. In this study, an LPS-induced RAW 264.7 cell model was established *in vitro*. Cell viability was assessed using the CCK-8 assay and ELISA was utilized to measure the protein levels of cytokines in the supernatant of different experimental groups. The survival rates of RAW264.7 cells treated with varying concentrations of Timepie001 for 24 h are shown in Figure 2. It is evident that Timepie001 at concentrations ranging from 12.5 to 25% exhibited no cytotoxicity, with high cell viability observed. For subsequent experiments, a concentration of 25% was selected for cellular treatment, corresponding to a Timepie001 concentration of 1×10^8 CFU/mL. Figure 2 displays the effects of Timepie001 and Timepie001+ on the secretion of NO, IL-6 and IL-1β from LPS-induced RAW264.7 inflammatory cells. As illustrated in Figures 2B–D, LPS (2 μg/mL) significantly increased the secretion of NO, IL-6 and IL-1β ($p < 0.01$). Following intervention with Timepie001 and Timepie001+, compared with model group, the secretion levels of these three inflammatory factors were significantly reduced by 86.66, 81.99, 24.20 and 91.80%, 81.61 and 28.40%, respectively ($p < 0.05$). These results indicate that Timepie001 and Timepie001+ markedly inhibits the inflammatory response in LPS-stimulated RAW 264.7 cells, Timepie001+ has better anti-inflammatory effects.

3.3 Body weight and DAI scores

Food and water intake generally serves as indicator of an organism's physiological status. As shown in Figures 3A,B, there was no significant difference in water and food intake among the four groups in 4 days. However, significant differences in food and water

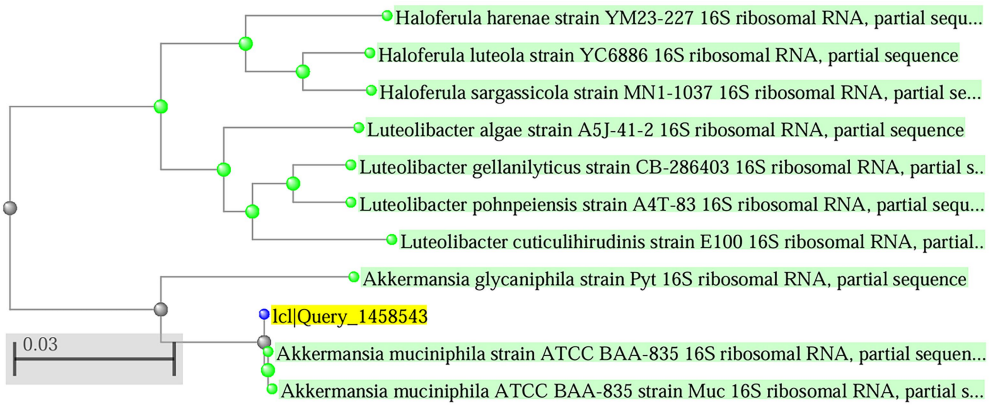

FIGURE 1
Phylogenetic tree showing the position of the determined 16S rDNA gene sequence of the strain purified among those of selected type strains. The tree was generated by the neighbor-joining method.

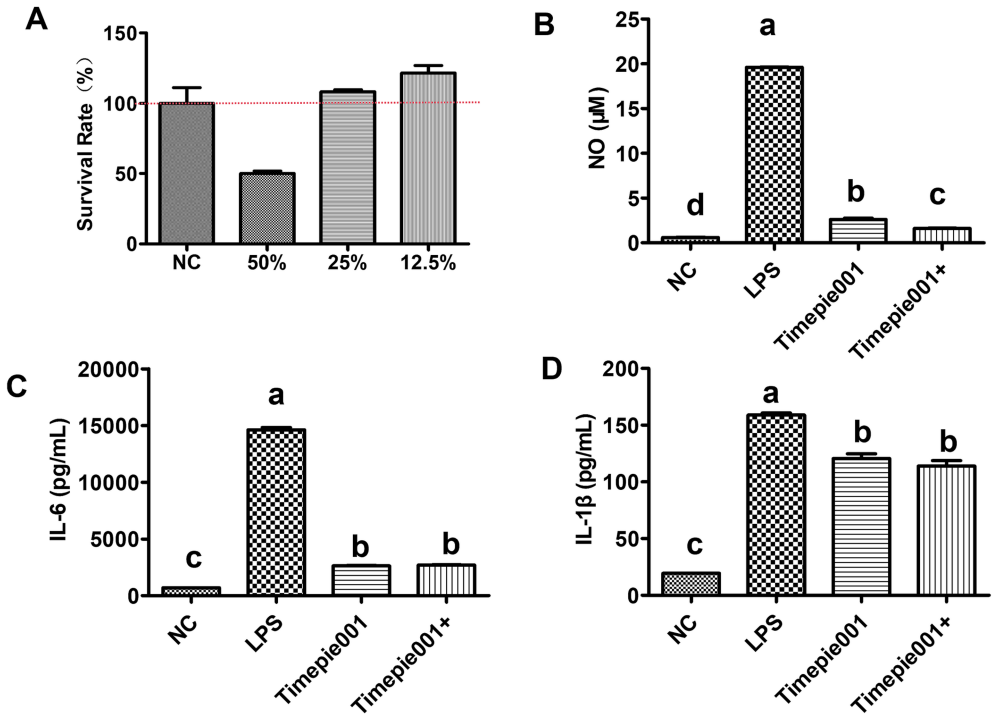

FIGURE 2
The effect of Timepie001 and Timepie001+ on the survival rate and secretion of pro-inflammatory cytokines in RAW264.7 cells. **(A)** Effects of different concentrations of Timepie001 on survival rate of RAW264.7 cells. **(B–D)** Concentrations of the NO, IL-6, and IL-1β. The results were expressed as the mean values ± SEM (n = 3). One-way ANOVA was used for statistical analysis, followed by Tukey's *post hoc* test. Different letters indicate significant differences ($p \leq 0.05$).

intake were observed among the group on the 8th day. In terms of total food intake, there was no significant difference between the Timepie001+ group and NC group ($p > 0.05$), and no significant difference between the Timepie001 group and DSS group on the 8th day. Regarding total water intake, significant differences were found between the other three groups and the NC group ($p < 0.05$), but no significant difference was ovserved among the three groups ($p > 0.05$). These results indicate that some pathological changes occurred in the three groups of mice after 5 days, the condition of mice in Timepie001+ group was slightly better than that in the Timepie001 group.

The current findings successfully established a DSS-induced mouse model of UC, characterized by typical symptoms including weight loss, diarrhea, hematochezia, and an increase in the DAI. During the experiment, the body weight of the NC group mice continued to increase over time. In contrast, both the Timepie001, Timepie001+ and DSS groups showed a significant reduction in body weight compared to the NC group mice ($p < 0.05$). By day 8, the body

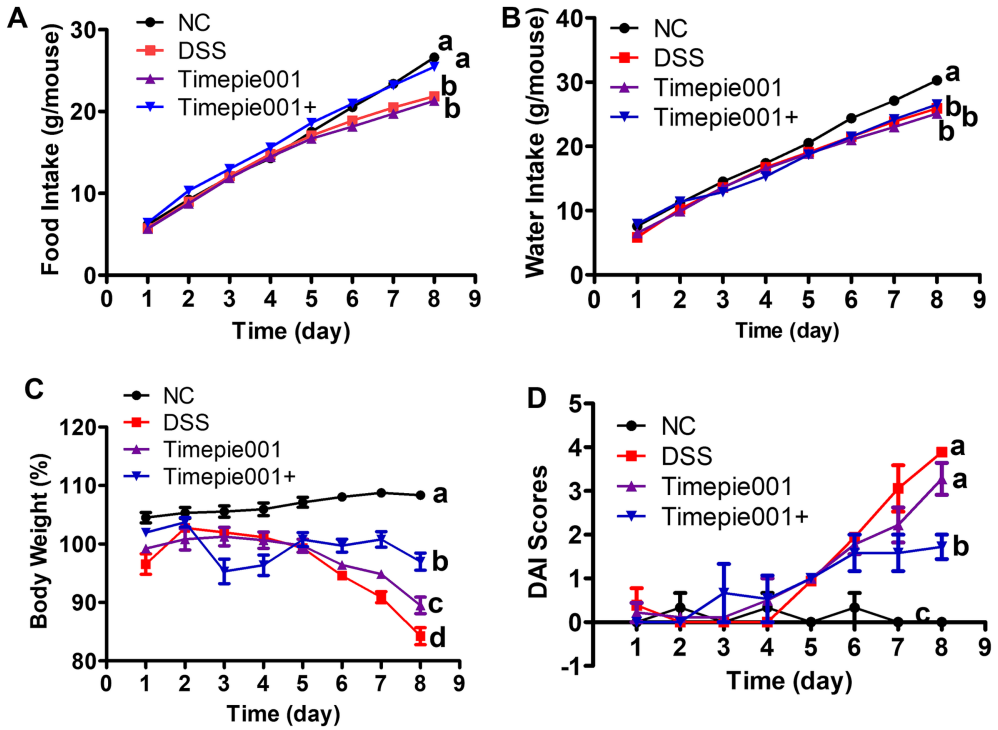

FIGURE 3
Effect of Timepie001 and Timepie001+ on the average. **(A)** Total food. **(B)** Total water intake of each mouse. **(C)** Daily body weight variation and changes in **(D)** DAI scores with DSS-induced colitis in 8 days. The mean ± SEM are shown (n = 6). [a–d]Values followed by different letters indicate significant differences ($p \leq 0.05$) between different group using one-way ANOVA followed by Tukey's test for *post hoc* analysis.

weight of DSS-induced mice had decreased by 15.77% from their initial weight. However, compared to the DSS group, the weight loss in the Timepie001 and Timepie001+ group were significantly reduced (Figure 3C), suggesting that Timepie001 and Timepie001+ effectively alleviates weight loss in DSS-induced mice. The DAI score was used to evaluate the impact of Timepie001 on colitis in mice. As illustrated in Figure 3D, the DAI index of DSS group mice increased due to DSS administration compared to the NC group, whereas the DAI index of mice receiving oral Timepie001+ was significantly reduced. The Timepie001 group did not show a similar effect.

3.4 Colon length and spleen distension size

As shown in Figure 4A, the colon tissue of the NC group exhibited normal color and thickness, with no signs of edema or congestion, and no adhesions to surrounding tissues. In contrast, mice treated with DSS displayed clear symptoms of UC, including congestion, edema, shortened colon length, as well as ulcers, localized necrosis, and melena. Notably, Timepie001+ was found to effectively alleviate colonic damage in DSS-induced colitis models. The shortening of the colon is typically associated with inflammation, and it is important to highlight that both Timepie001 and Timepie001+ significantly reduced colon shortening in colitis mice compared to the NC group, with the improvement effect of Timepie001+ being better (Figure 4B). The spleen, as the largest lymphatic organ, contains a high number of lymphocytes and macrophages involved in both humoral and cellular immune responses. Inflammatory conditions lead to splenomegaly. The normal spleen appears smooth and deep red; however, the spleens of DSS-treated mice became enlarged and darker. Following Timepie001+ treatment, the size and color of the spleens were comparable to those of the NC group (Figure 4C). The relative spleen weight of DSS-treated mice significantly increased ($p < 0.05$, as shown in Figure 4D). Timepie001 and Timepie001+ markedly countered the enlargement of the spleen, indicating its inhibitory effect on the peripheral inflammation associated with colitis. There was no significant difference in the relative weight of the spleen between Timepie001 and Timepie001+.

3.5 Histopathological alterations

The degree of colonic damage, including the status of the intestinal wall, crypt integrity, colonic tissue ulceration, and neutrophil infiltration, can be assessed using H&E staining. The effect of Timepie001 and Timepie001+ on colonic histology in colitis-affected mice is illustrated in Figure 5B. The colon mucosa of the NC mice was intact, with well-distributed glands and no ulceration or significant inflammatory cell infiltration. In the DSS group, the structure of the intestinal mucosa was disrupted, resulting in irregular shapes, sloughing, ulceration, obvious inflammatory cell infiltration and a significant increase in the histological score. After treatment with Timepie001 and Timepie001+, the colonic tissue injury of mice was significantly improved. In the Timepie001+ group, the area of mucosal ulcers in the colonic tissue was reduced, and the intestinal wall showed signs of restoration (Figure 5B). Additionally, histological examination revealed that mice in the Timepie001+ group had reduced immune cell infiltration and less disruption of the crypts,

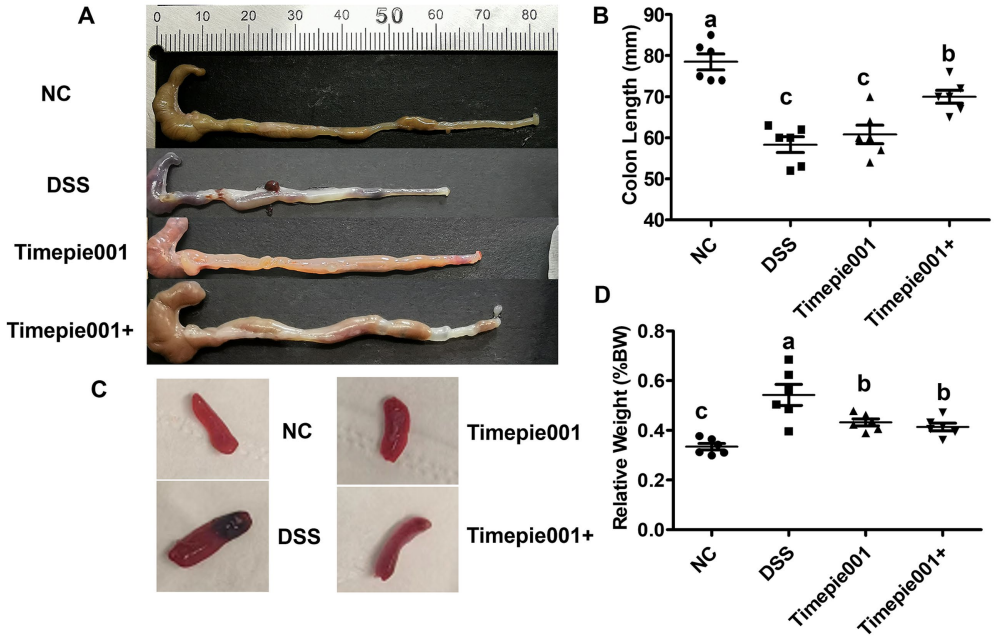

FIGURE 4
Effect of Timepie001 and Timepie001+ on the symptoms changes of colitis mice. **(A)** Macroscopic pictures of colons. **(B)** Colon length. **(C)** The morphology of the spleen. **(D)** Relative spleen weight (%BW). The values are presented as means of six mice ± SEM. $^{a-c}$Values followed by different letters indicate significant differences ($p \leq 0.05$) between different group using one-way ANOVA followed by Tukey's test for *post hoc* analysis.

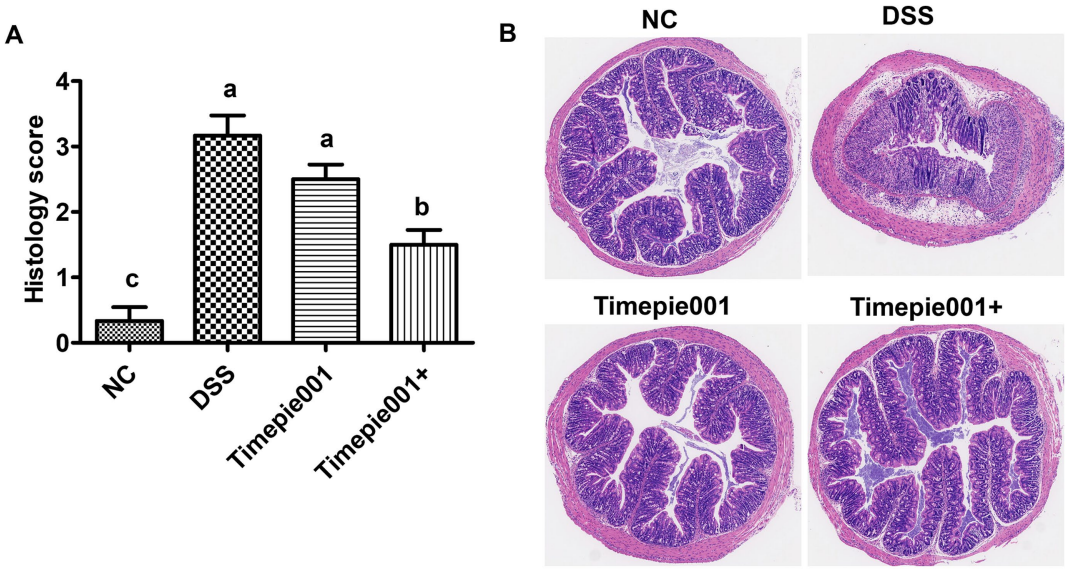

FIGURE 5
Effects of Timepie001 and Timepie001+ on histopathology changes of colon tissues in colitis mice. **(A)** The colonic histopathological score. **(B)** H&E staining (100×). The values are presented as means of 6 mice ± SEM. $^{a-c}$Values followed by different letters indicate significant differences ($p \leq 0.05$) between different group using one-way ANOVA followed by Tukey's test for *post hoc* analysis.

along with lower histological scores compared to the DSS group (Figure 5A). However, there was no significant difference in histological scores between the DSS group and the Timepie001 group ($p > 0.05$). These results indicate that treatment with Timepie001+ can ameliorate clinical symptoms, improve histological scores, and reduce inflammatory cell infiltration in a murine model of colitis.

3.6 Expression of related genes in colonic tissues

Quantitative RT-qPCR results for IL-1β, TNF-α and ZO-1 mRNA expression are presented in Figure 6. Compared to the NC group, the mRNA expression of IL-1β, TNF-α were significantly increased and

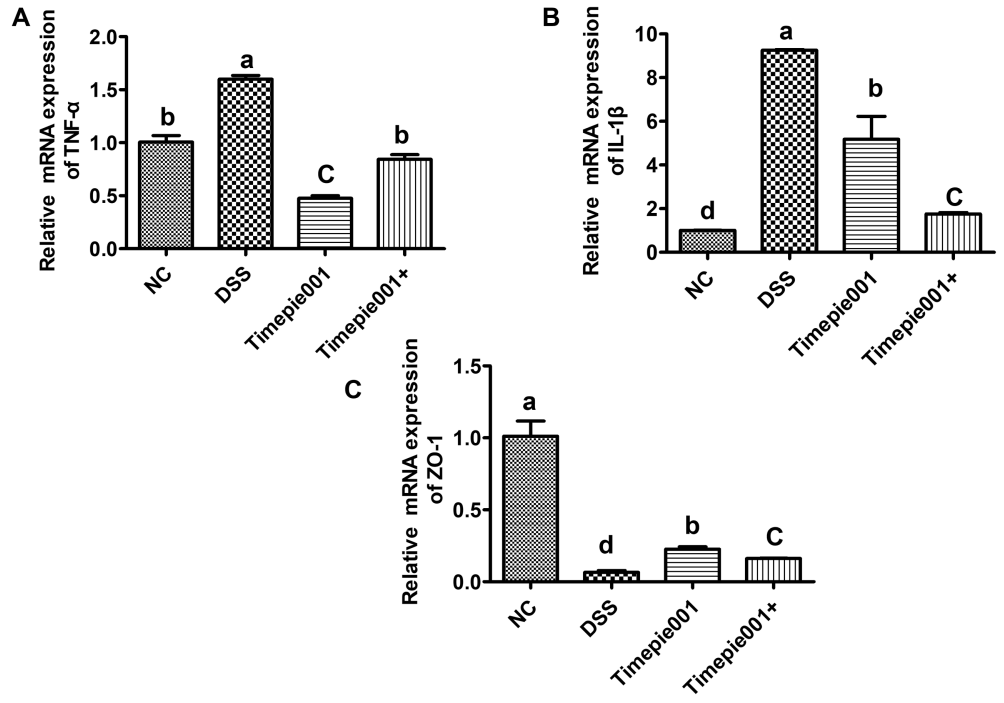

FIGURE 6
Effect of Timepie001 and Timepie001+ on expression of (TNF-α **(A)**, IL-1β **(B)**, and ZO-1 **(C)**) in colonic tissues of mice with UC induced by DSS. Dates are expressed as mean ± SEM. $^{a-d}$Values followed by different letters indicate significant differences ($p \leq 0.05$) between different group using one-way ANOVA followed by Tukey's test for *post hoc* analysis.

ZO-1 was decreased in the colon tissues of DSS-induced UC mice ($p < 0.01$). Following intervention with Timepie001 and Timepie001+, the expression of IL-1β and TNF-α was significantly reduced compared to the DSS group, with relative decreases of 44.02, 70.27 and 81.05%, 47.16%, respectively, while ZO-1 increased by 246 and 147% ($p < 0.05$). Inflammation is a major contributor to colon damage in UC. When colitis occurs, the intestinal barrier is disrupted, pathogens infiltrate the intestinal mucosa, causing a flood of pro-inflammatory cytokines to be released, which exacerbates the inflammatory response (Neurath, 2014). TNF-α and IL-1β are key pro-inflammatory cytokines that are released at elevated levels in patients with UC, intensifying the inflammatory response. These findings suggest that Timepie001+ can improve DSS-induced colitis by modulating the levels of inflammatory cytokines. Science UC is generally accompanied by an increase in intestinal permeability, and the increase in ZO-1 gene expression also indicated that Timepie001 and Timepie001+ can improve the intestinal permeability of the colon. With the improvement effect of Timepie001+ being more significant.

3.7 Expression of epithelial intercellular junction proteins

Claudin-1 protein is a crucial component of the colonic epithelial barrier. Pathogens and viruses can exploit tight junctions to infiltrate and infect cells, leading to the production of inflammatory cytokines. The disruption of the colonic epithelial barrier is a significant factor contributing to colitis. This study investigates the impact of Timepie001 and Timepie001+ on the expression of tight junction proteins in the intestines of mice with UC. As shown in Figure 7, there is a down-regulation of Claudin-1 expression in the colon of DSS-induced UC mice. However, although Timepie001 and Timepie001+ up-regulates Claudin-1 expression in UC mice ($p < 0.05$), there was no significant difference in protein expression levels between the Timepie001+ groups and the NC group. Overall, these finding suggest that Timepie001+ may mediate its protective effects against UC mice by enhancing intestinal barrier function.

From all the above results, it can be concluded that Timepie001+ group has a better improvement effect on DSS-induced UC. Therefore, in the following section on gut microbiota analysis, only the differences between the Timepie001+ group, NC group and DSS group were analyzed.

3.8 Gut microbiological analysis

The intestinal microbiota of mice with colitis often changes, and in this study, 16S rRNA gene sequencing was used to assess the composition of the intestinal microbiota. The number of OTUs in the sample detection results can reflect changes in the richness of the mouse intestinal microbial community. The NC group, DSS group and Timepie001+ group had 432, 336, and 489 OTUs, respectively (Figures 8A). The Timepie001+ group was closer to the NC group than the DSS group at the OTU level, indicating that the intestinal microbiota of the mice tended to develop at a normal level after intervention with pasteurized *A. muciniphila*, and the diversity of the intestinal microbiota of the mice was restored.

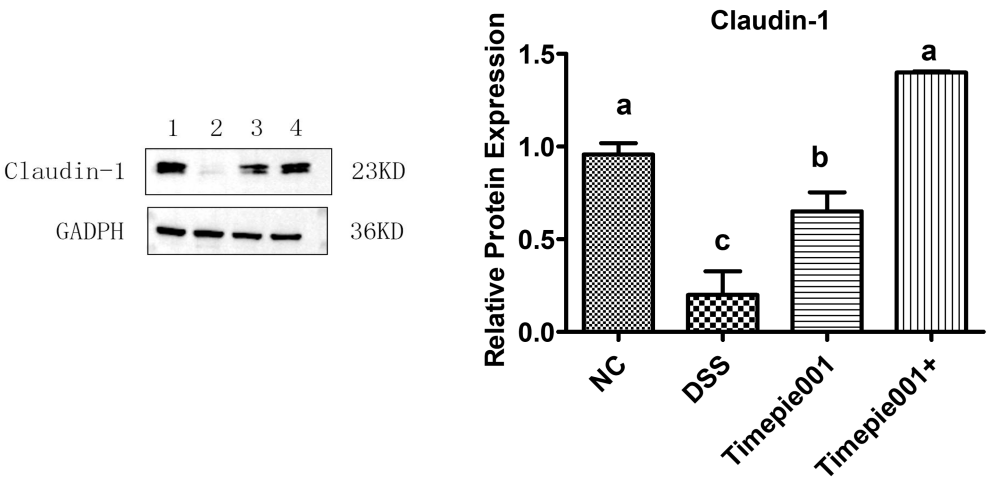

FIGURE 7
The relative protein levels of Claudin-1 in the mice colon. Dates are expressed as mean ± SEM. [a–c]Values followed by different letters indicate significant differences ($p \leq 0.05$) between different group using one-way ANOVA followed by Tukey's test for *post hoc* analysis.

Alpha diversity was compared among the three groups using ACE and Shannon index (Figures 8B,C), where the ACE index reflects species richness, and the Shannon index reflects both richness and evenness. The results indicated significant differences in alpha diversity indices among the groups, with the ACE and Shannon values in the DSS group being markedly lower than those in the NC and Timepie001+ groups. The alpha diversity indices in the Timepie001+ group were comparable to the those of NC group, with both the ACE and Shannon indices slightly exceeding those of the NC group.

Metagenomic techniques were employed to determine the composition of the gut microbiota in each group. The relative abundance of major gut microbiota in each group is represented by bar charts at the phylum and genus level (Figures 8D,E). Notable changes were observed in the composition of the gut microbiota among UC mice. At the phylum level, the abundance of Proteobacteria, Verrucomicrobiota, Desulfobacterota, Campylobacterota, and Deferribacterota increased in DSS-induced mice compared to the NC group, while Bacteroidota, Firmicutes, Patescibacteria, and Actinobacteriota decreased. The relative abundances of Bacteroidota in the NC, DSS, and Timepie001+ groups were 27.42, 7.61, and 31.29%, respectively, and for Firmicutes, they were 28.80, 10.51, and 16.28% (Figures 8D,F). Following Timepie001+ intervention, the abundance of harmful bacteria decreased while that of beneficial bacteria increased. At the genus level, DSS induction led to a decrease in the abundances of Muribaculaceae, Acinetobacer, Mammaliicoccus, Alistipes, Candidatus_Saccharimonas Enterorhabdus, Halomonas, Limosilactobacillus, Rikenella and Muribaculum, while Pseudomonas, Delftia, Akkermansia and Bacteroides increased. Timepie001+ intervention alleviated these changes (Figures 8E,F).

4 Discussion

Probiotics are active microorganisms that are beneficial to human health. They mainly exist in the human intestine and play many important roles and effects, including maintaining intestinal health, promoting digestion and absorption, enhancing immunity, improving constipation and diarrhea, and reducing cholesterol (Daglia et al., 2024; Wang D. et al., 2025; Yao et al., 2025). Postbiotics has been a rapidly growing topic in recent years (Wegh et al., 2019). Experts in the field of probiotics and prebiotics suggested a definition for the term "postbiotics" which was "preparation of inanimate microorganisms and/or their components that confers a health benefit on the host" (Eslami et al., 2024). Most previous studies have focus on the beneficial effects of probiotics and prebiotics on UC. However, postbiotics appear to be safer than probiotics. Since postbiotics consist of nonviable microbial cells, Interference inhibition by interferon, infections, or inflammatory responses known side effects of probiotics is lower with postbiotics.

A. muciniphila is known as the second-generation probiotic, It can utilizes glycoprotein mucin as its direct source of carbon and nitrogen to colonize the human intestinal mucosal layer (Zhou and Zhang, 2019), which means it has a unique survival advantage of being able to survive in nutrient deficiencies and harsh conditions (Gómez-Gallego et al., 2016). *A. muciniphila* have the characteristic of mucosal degradation and play important role in regulating the intestinal barrier and immune response, thus contributing significantly to human health and diseases. The observation of decreased levels of *A. muciniphila* in UC patients suggests that these bacterial may contribute to the pathogenesis and procession of UC, and could be potential target and promising strategy for UC therapy (Earley et al., 2019). However, its anaerobic biological characteristics limit its widespread application in dietary supplements. Research have shown that after 30 min of pasteurization at 70°C, *A. muciniphila* retains most of its beneficial effects. Pasteurized *A. muciniphila* was found to increase systemic energy expenditure and fecal energy excretion in diet-induced obese mice, as well as enhance intestinal epithelial renewal (Depommier et al., 2020). However, there are few articles on the effectiveness of using pasteurized *A. muciniphila* for UC.

DSS-induces UC symptoms characterized by weight loss, diarrhea, hematochezia, shortened colon length, colonic swelling, splenomegaly, and even death (Jang et al., 2019; Ma et al., 2020; Shi et al., 2024). Colon length, DAI scores and histological analysis showed that Timepie001+ significantly improved DSS-induced inflammatory

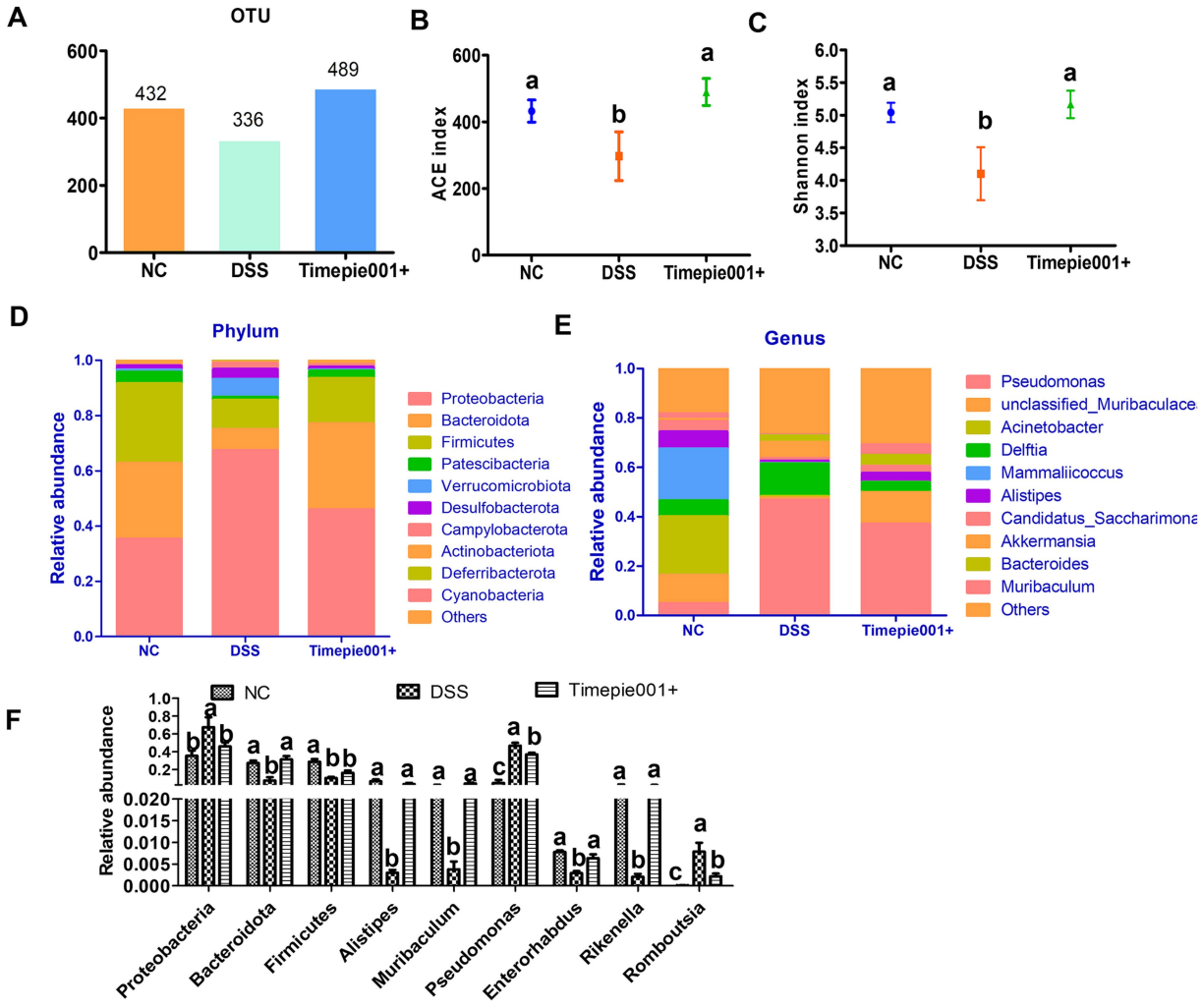

FIGURE 8
The effect of Timepie001+ on gut microbiota in colitis mice. **(A)** OTUs of gut microbiota. **(B,C)** The ACE index and Shannon index among three groups. **(D,E)** Relative abundance of taxa at the phylum, genus levels. **(F)** Relative abundance of taxa in the three groups. The values are presented as means of six mice ± SEM. $^{a-c}$Values followed by different letters indicate significant differences ($p \leq 0.05$) between different group using one-way ANOVA followed by Tukey's test for *post hoc* analysis.

infiltration, crypt damage, and mucosal injury. While Timepie001 did not show significant improvement. Based on our findings, we propose several potential mechanisms, including modulation of the inflammatory response, enhancement of the intestinal mucosal barrier, and reconfiguration of the gut microbiota.

Inflammation is a key factor in the onset of UC. The production of TNF-α and IL-1β can further amplify the inflammatory response, exacerbating UC (Hu et al., 2024; Li Y. et al., 2024). TNF-α is primarily produced by monocytes and macrophages and acts as a pro-inflammatory cytokine involved in systemic inflammation, stimulating acute inflammatory responses (El-Boghdady et al., 2023). It conveys signals to the cell nucleus via specific receptors on the cell membrane, promoting various complex biological activities such as cell proliferation, differentiation, immune regulation, and inflammation mediation. TNF-α promotes the secretion of endothelial cell adhesion factors, increases the permeability of epithelial tight junctions, and inhibits epithelial cell growth, leading to damage to the mucosa and extracellular matrix. Numerous studies have revealed the anti-inflammatory effect of *A. muciniphila* (Miao et al., 2024; Xiao et al., 2024). For instance, oral administration of *A. muciniphila* strain BAA-835 significantly ameliorated the symptoms in DSS-induced acute colitis, as evidenced by decreased body weight loss, colon length shortening, and colon histological inflammatory score. Zhai et al. (2019) studied and compared the characteristics of *A. muciniphila* ATCC BAA-835 and *A. muciniphila* strain 139, and reported interesting results. Both strains showed anti-inflammatory effects including inhibiting IL-8 production induced by TNF-α co-cultured HT-29 cells *in vitro* anti-inflammatory experiments. However, these two strains exhibited different functions in the DSS-induced UC model. Although these two strains alleviated colitis symptoms by down-regulating pro-inflammatory cytokines, only the DSS + ATCC group observed significant reductions in spleen weight and inflammation index compared to the DSS group. In our study, it can be observed that Timepie001+ can significantly reduce the production of NO, IL-1β, and IL-6 induced by LPS after interacting with macrophages RAW 264.7 cells, demonstrating good anti-inflammatory

effects. We also observed a decrease in the expression of inflammatory cytokines (TNF-α and IL-1β) in colon tissue. These results suggest that the protective effect of Timepie001+ on UC may be achieved through anti-inflammatory effects.

UC with damage to the intestinal mucosal barrier being a critical pathological mechanism (Wang J. et al., 2025; Wang Y. et al., 2025). The intestinal mucosal barrier serves as the body's first line of defense against harmful substances and pathogens, comprising chemical, biological, immune, and mechanical barriers, with the mechanical barrier playing a predominant role (Li J. et al., 2024). Previous reports indicate that the colons of UC patients or model mice are thinner compared to controls, and intestinal permeability is increased in colitis models. Madsen et al. (2010) explored the relationship between increased intestinal permeability and intestinal inflammation in IL-10 deficient mice, noting that at 2 weeks of age, these mice showed no signs of intestinal damage but exhibited increased intestinal permeability alongside elevated concentrations of TNF-α and IFN-γ. This suggests that the increase in intestinal permeability precedes the inflammatory response. Tight junction proteins are essential components of the intestinal mucosal mechanical barrier, preventing pathogenic bacterial antigens from entering the mucosal tissue and circulatory system. Key tight junction proteins include ZO-1 and Claudin-1. During the onset of UC, the expression levels of tight junction proteins decrease, leading to increased mucosal permeability and subsequent inflammatory responses and clinical symptoms. These were consistent with our results, indicating that the protective mechanism of Timepie001+ against UC operates by enhancing the functionality of the intestinal barrier.

UC is also considered a consequence of dysregulated immune responses due to an imbalance in the gut microbiota (Ni et al., 2017; Cheng et al., 2023; Hu et al., 2024). Patients with UC often exhibit a reduction in beneficial bacteria and an increase in harmful bacteria. Our findings consistently demonstrate that in the intestines of DSS-treated mice, there is a decrease in the diversity of specific bacterial taxa and changes in their relative abundances. Notably, in the group supplemented with Timepie001+, we observed a restoration of microbial α-diversity.

At the phylum level, studies have shown that the ratio of Firmicutes to Bacteroidetes should not be excessively high (Gomes et al., 2018). In our study, after intervention with Timepie001+, compared to the DSS group, there was an increase in Firmicutes and Bacteroidetes, and a decrease in Proteobacteria. The ratios for the NC, DSS, and Timepie001+ groups were 1.05, 1.38, and 0.52, respectively, indicating that the Timepie001+ group had a significantly lower ratio than the DSS group. At the genus level, Alistipes and Rikenella have been proved as the producer of short-chain fatty acids, which have a variety of physiological functions including provide energy for colon cells, maintain intestinal barrier integrity, regulate intestinal immunity etc., and play a significant role in intestinal homeostasis (Guo et al., 2021). The relative abundance of Alistipes and Rikenella in the intestines of mice with enteritis were severely insufficient compared to the healthy group. After taking Timepie001+, the abundance of Alistipes and Rikenella was restored to some extent. Muribaculum is a member of Muribaculaceae and has been proven to be the dominant microbiota in healthy mice in multiple studies (Lagkouvardos et al., 2016; Hiraishi et al., 2022), may participate in the prevention or alleviation of UC, but the specific mechanism is still unclear (Wang et al., 2022). The abundance of Enterorhabdus and Halomonas was significantly reduced in DSS group, which is consistent with previous research results (Tong et al., 2021; Wu et al., 2024). Meanwhile, we also noted the increase in the abundance of Pseudomonas, Bilophila, Erysipelatoclostridium and Romboutsia. Pseudomonas, a group of gram-negative bacteria, is recognized as an opportunistic pathogen associated with intestinal barrier dysfunction and infection. Overgrowth of Pseudomonas has been linked to intestinal inflammation and systemic inflammatory responses, and it is found in higher abundances in the intestines of UC patients, where it contributes to microbial imbalances and disease progression (Goldberg et al., 2008; Ren et al., 2021; Cao et al., 2024). The abundance of Bilophila, Erysipelatoclostridium, and Romboutsia have been reported to have a positive correlation with IBD (Tong et al., 2021; Cheng et al., 2023; Li et al., 2023), and our study has reached the same conclusion. Collectively, these results suggest that alterations in the gut microbiota may play a crucial role in the preventive effects of *A. muciniphila* against UC.

All results indicate that pasteurized *A. muciniphila* has a better effect on ameliorating UC than live *A. muciniphila*, which may be due to the following reasons: (1) specific active ingredients: such as Amuc_1100, the membrane proteins can interact with host cells or receptors, promote intestinal barrier function, regulate host immunity, and inhibit inflammation, thereby improving metabolic health; (2) colonization of live bacteria: the colonization of live *A. muciniphila* in the intestine may be inhibited by the host's gut microbiota, leading to their inability to fully exert their function. Pasteurized *A. muciniphila* do not have colonization issues and can more stably exert their beneficial components. (3) Safety and stability: pasteurized *A. muciniphila* are less likely to cause infection or adverse reactions, and have higher safety.

5 Conclusion

This study evaluated the alleviation effects of live and pasteurized *A. muciniphila* on DSS-induced colitis in mice. The results demonstrate that pasteurized *A. muciniphila* shows a more significant improvement in UC compared to live *A. muciniphila*. Due to the fact that postbiotics do not require attention to bacterial activity and is not limited by temperature, humidity, etc., their application range is more extensive. Overall, this research provides foundational insights for the development of functional foods utilizing pasteurized *A. muciniphila* in the management of UC.

Data availability statement

The original contributions presented in the study are included in the article/supplementary material, further inquiries can be directed to the corresponding authors.

Ethics statement

The animal study was approved by the Animal Care & Welfare Committee of Zhejiang University of Technology, China. The study was conducted in accordance with the local legislation and institutional requirements.

Author contributions

HH: Data curation, Formal analysis, Writing – original draft. HX: Methodology, Supervision, Writing – original draft. ZL: Data curation, Writing – original draft. XL: Conceptualization, Project administration, Writing – review & editing. HWa: Data curation, Formal analysis, Validation, Writing – review & editing. JK: Data curation, Software, Writing – review & editing. DY: Data curation, Methodology, Writing – original draft. YS: Conceptualization, Project administration, Resources, Writing – review & editing. HWu: Data curation, Resources, Writing – review & editing. JQ: Conceptualization, Funding acquisition, Methodology, Resources, Writing – review & editing.

Funding

The author(s) declare that financial support was received for the research, authorship, and/or publication of this article. This study was supported by the National Natural Science Foundation of China (Grant No. 32070073).

Conflict of interest

XL and YS were employed by Shanghai Fuyang Biotechnology Co., Ltd.

The remaining authors declare that the research was conducted in the absence of any commercial or financial relationships that could be construed as a potential conflict of interest.

Generative AI statement

The authors declare that no Gen AI was used in the creation of this manuscript.

Publisher's note

All claims expressed in this article are solely those of the authors and do not necessarily represent those of their affiliated organizations, or those of the publisher, the editors and the reviewers. Any product that may be evaluated in this article, or claim that may be made by its manufacturer, is not guaranteed or endorsed by the publisher.

References

Astronomy and Astrophysics (1996). Guide for the care and use of laboratory animals. Washington, DC: National Academies Press.

Berry, D., Schwab, C., Milinovich, G., Reichert, J., Ben Mahfoudh, K., Decker, T., et al. (2012). Phylotype-level 16S rRNA analysis reveals new bacterial indicators of health state in acute murine colitis. *ISME J.* 6, 2091–2106. doi: 10.1038/ismej.2012.39

Bian, X., Wu, W., Yang, L., Lv, L., Wang, Q., and Li, Y. (2019). Administration of Akkermansia muciniphila Ameliorates Dextran Sulfate Sodium-Induced Ulcerative Colitis in Mice. *Front Microbiol.* 10:2259. doi: 10.3389/fmicb.2019.02259

Cao, R., Fang, X., Li, Z., Li, S., Guo, Q., and Chai, Y. (2024). Effect of *Polygonatum sibiricum* saponins on gut microbiota of mice with ulcerative colitis. *Fitoterapia* 174:105855. doi: 10.1016/j.fitote.2024.105855

Cheng, R., Xu, W., Wang, J., Tang, Z., and Zhang, M. (2021). The outer membrane protein Amuc_1100 of *Akkermansia muciniphila* alleviates the depression-like behavior of depressed mice induced by chronic stress. *Biochem. Biophys. Res. Commun.* 566, 170–176. doi: 10.1016/j.bbrc.2021.06.018

Cheng, H., Zhang, D., Wu, J., Liu, J. R., Tan, Y., Feng, W., et al. (2023). *Atractylodes macrocephala* Koidz. volatile oil relieves acute ulcerative colitis via regulating gut microbiota and gut microbiota metabolism. *Front. Immunol.* 14:1127785. doi: 10.3389/fimmu.2023.1127785

Daglia, M., Drago, L., Ullah, H., Di, A., Brindisi, G., Brunese, F. P., et al. (2024). Effects of the supplementation of single and multi-strain probiotics, alone or in combination with other treatments, on asthma in children: a systematic review of the randomized, placebo-controlled clinical studies. *J. Funct. Foods* 123:106599. doi: 10.1016/j.jff.2024.106599

Dai, N., Yang, X., Pan, P., Zhang, G., Sheng, K., Wang, J., et al. (2024). *Bacillus paralicheniformis*, an acetate-producing probiotic, alleviates ulcerative colitis via protecting the intestinal barrier and regulating the NLRP3 inflammasome. *Microbiol. Res.* 287:127856. doi: 10.1016/j.micres.2024.127856

Depommier, C., Everard, A., Druart, C., Plovier, H., Van, H. M., Vieira-Silva, S., et al. (2019). Supplementation with *Akkermansia muciniphila* in overweight and obese human volunteers: a proof-of-concept exploratory study. *Nat. Med.* 25, 1096–1103. doi: 10.1038/s41591-019-0495-2

Depommier, C., Hul, M. V., Everard, A., Delzenne, N. M., Vos, W. M. D., and Cani, P. D. (2020). Pasteurized *Akkermansia muciniphila* increases whole-body energy expenditure and fecal energy excretion in diet-induced obese mice. *Gut Microbes* 11, 1231–1245. doi: 10.1080/19490976.2020.1737307

Derrien, M., Vaughan, E. E., Plugge, C. M., and de Vos, W. M. (2004). Akkermansia muciniphila gen. nov., sp. nov., a human intestinal mucin-degrading bacterium. *Int J Syst Evol Microbiol.* 54, 1469–1476. doi: 10.1099/ijs.0.02873-0

Dunn, K. A., Moore-Connors, J. M., MacIntyre, B., Stadnyk, A. W., Thomas, N. A., Noble, A. J., et al. (2016). Early changes in microbial community structure are associated with sustained remission after nutritional treatment of pediatric Crohn's disease. *Inflamm. Bowel Dis.* 22, 2853–2862. doi: 10.1097/MIB.0000000000000956

Earley, H., Lennon, G., Balfe, I., Coffey, J. C., and O'Connell, P. R. J. S. R. (2019). The abundance of *Akkermansia muciniphila* and its relationship with sulphated colonic mucins in health and ulcerative colitis. *Sci. Rep.* 9:15683. doi: 10.1038/s41598-019-51878-3

El-Boghdady, N. A., El-Hakk, S. A., and Abd-Elmawla, M. A. (2023). The lncRNAs UCA1 and CRNDE target miR-145/TLR4/NF-κB/TNF-α axis in acetic acid-induced ulcerative colitis model: the beneficial role of 3,3-diindolylmethane. *Int. Immunopharmacol.* 121:110541. doi: 10.1016/j.intimp.2023.110541

Eslami, M., Pakmehr, A., Pourghazi, F., Kami, A., Ejtahed, H.-S., Mohajeri-Tehrani, M., et al. (2024). The anti-obesity effects of postbiotics: A systematic review of pre-clinical and clinical studies. *Clin. Nutr. ESPEN* 64, 370–389. doi: 10.1016/j.clnesp.2024.10.153

Faghfuri, E., and Gholizadeh, P. (2024). The role of *Akkermansia muciniphila* in colorectal cancer: a double-edged sword of treatment or disease progression? *Biomed. Pharmacother.* 173:116416. doi: 10.1016/j.biopha.2024.116416

Frank, D., Amand, A. S. S., Feldman, R., Boedeker, E., Harpaz, N., and Pace, N. R. (2007). Molecular-phylogenetic characterization of microbial community imbalances in human inflammatory bowel diseases. *Proc. Natl. Acad. Sci. U.S.A.* 104, 13780–13785. doi: 10.1073/pnas.0706625104

Goldberg, J. B., Hancock, R. E., Parales, R. E., Loper, J., and Cornelis, P. (2008). Pseudomonas 2007. *J. Bacteriol.* 190, 2649–2662. doi: 10.1128/jb.01950-07

Gomes, A. C., Hoffmann, C., and Mota, J. F. (2018). The human gut microbiota: metabolism and perspective in obesity. *Gut Microbes* 9, 1–18. doi: 10.1080/19490976.2018.1465157

Gómez-Gallego, C., Pohl, S., Salminen, S., Vos, W. M. D., and Kneifel, W. J. B. M. (2016). *Akkermansia muciniphila*: a novel functional microbe with probiotic properties. *Benef. Microbe.* 7, 571–584. doi: 10.3920/bm2016.0009

Guo, C., Wang, Y., Zhang, S., Zhang, X., Du, Z., Li, M., et al. (2021). *Crataegus pinnatifida* polysaccharide alleviates colitis via modulation of gut microbiota and SCFAs metabolism. *Int. J. Biol. Macromol.* 181, 357–368. doi: 10.1016/j.ijbiomac.2021.03.137

Han, H., Ke, L., Xu, W., Wang, H., Zhou, J., and Rao, P. (2023). Incidental nanoparticles in black tea alleviate DSS-induced ulcerative colitis in BALB/c mice. *Food Funct.* 14, 8420–8430. doi: 10.1039/d3fo00641g

Hiraishi, K., Zhao, F., Kurahara, L. H., Li, X., Yamashita, T., Hashimoto, T., et al. (2022). Lactulose modulates the structure of gut microbiota and alleviates colitis-associated tumorigenesis. *Nutrients* 14:649. doi: 10.3390/nu14030649

Hu, Q., Xie, J., Jiang, T., Gao, P., Chen, Y., Zhang, W., et al. (2024). Paeoniflorin alleviates DSS-induced ulcerative colitis by suppressing inflammation, oxidative stress, and apoptosis via regulating serum metabolites and inhibiting CDC42/JNK signaling pathway. *Int. Immunopharmacol.* 142:113039. doi: 10.1016/j.intimp.2024.113039

Jang, Y. J., Kim, W. K., Han, D. H., Lee, K., and Ko, G. (2019). *Lactobacillus fermentum* species ameliorate dextran sulfate sodium-induced colitis by regulating the immune response and altering gut microbiota. *Gut Microbes* 10, 696–711. doi: 10.1080/19490976.2019.1589281

Lagkouvardos, I., Pukall, R., Abt, B., Foesel, B. R. U., Meier-Kolthoff, J. P., Kumar, N., et al. (2016). The mouse intestinal bacterial collection (miBC) provides host-specific insight into cultured diversity and functional potential of the gut microbiota. *Nat. Microbiol.* 1:16131. doi: 10.1038/nmicrobiol.2016.131

Lee, J., Kim, S., and Kang, C. H. (2022). Immunostimulatory activity of lactic acid bacteria cell-free supernatants through the activation of NF-κB and MAPK signaling pathways in RAW 264.7 cells. *Microorganisms* 10:2247. doi: 10.3390/microorganisms 10112247

Li, J., Wei, Y., Liu, C., Guo, X., Liu, Z., Zhang, L., et al. (2024). 2′-Fucosyllactose restores the intestinal mucosal barrier in ulcerative colitis by inhibiting STAT3 palmitoylation and phosphorylation. *Clin. Nutr.* 43, 380–394. doi: 10.1016/j.clnu. 2023.12.011

Li, K., Wu, J., Xu, S., Li, X., Zhang, Y., and Gao, X.-J. (2023). Rosmarinic acid alleviates intestinal inflammatory damage and inhibits endoplasmic reticulum stress and smooth muscle contraction abnormalities in intestinal tissues by regulating gut microbiota. *Microbiol. Spectr.* 11:e0191423. doi: 10.1128/spectrum.01914-23

Li, Y., Yue, X., Ren, X., Pang, Y., Wang, T., Huangfu, B., et al. (2024). Mare milk and fermented mare milk alleviate DSS-induced ulcerative colitis in mice by reducing inflammation and modulating intestinal flora. *J. Dairy Sci.* doi: 10.3168/jds. 2024-25181

Ma, S., Yeom, J., and Lim, Y. H. (2020). Dairy *Propionibacterium freudenreichii* ameliorates acute colitis by stimulating MUC2 expression in intestinal goblet cell in a DSS-induced colitis rat model. *Sci. Rep.* 10:5523. doi: 10.1038/s41598-020-62497-8

Madsen, K. L., Malfair, D., Gray, D., Doyle, J. S., Jewell, L. D., and Fedorak, R. N. J. I. B. D. (2010). Interleukin-10 gene-deficient mice develop a primary intestinal permeability defect in response to enteric microflora. *Inflamm. Bowel Dis.* 5, 262–270. doi: 10.1002/ibd.3780050405

Miao, Y., Wang, M., Sun, H., Zhang, Y., Zhou, W., Yang, W., et al. (2024). *Akkermansia muciniphila* ameliorates colonic injury in mice with DSS-induced acute colitis by blocking macrophage pro-inflammatory phenotype switching via the HDAC5/DAB2 axis. *Biochim. Biophys. Acta* 1871:119751. doi: 10.1016/j.bbamcr.2024.119751

Neurath, M. F. (2014). Cytokines in inflammatory bowel disease. *Nat. Rev. Immunol.* 14, 329–342. doi: 10.1038/nri3661

Ni, J., Wu, G. D., Albenberg, L., and Tomov, V. T. (2017). Gut microbiota and IBD: causation or correlation? *Nat. Rev. Gastroenterol. Hepatol.* 14, 573–584. doi: 10.1038/nrgastro.2017.88

Ouwerkerk, J. P., Aalvink, S., Belzer, C., and de Vos, W. M. (2016). *Akkermansia glycaniphila* sp. nov., an anaerobic mucin-degrading bacterium isolated from reticulated python faeces. *Int. J. Syst. Evol. Microbiol.* 66, 4614–4620. doi: 10.1099/ijsem.0.001399

Payahoo, L., Khajebishak, Y., Alivand, M. R., Soleimanzade, H., Alipour, S., Barzegari, A., et al. (2019). Investigation the effect of oleoylethanolamide supplementation on the abundance of *Akkermansia muciniphila* bacterium and the dietary intakes in people with obesity: a randomized clinical trial. *Appetite* 141:104301. doi: 10.1016/j.appet.2019.05.032

Qu, S., Fan, L., Qi, Y., Xu, C., Hu, Y., and Chen, S. (2021). Akkermansia muciniphila Alleviates Dextran Sulfate Sodium (DSS)-Induced Acute Colitis by NLRP3 Activation. *Microbiol Spectr.* 9:e0073021. doi: 10.1128/Spectrum.00730-21

Ren, Z., Pan, L. L., Huang, Y., Chen, H., Liu, Y., Liu, H., et al. (2021). Gut microbiota-CRAMP axis shapes intestinal barrier function and immune responses in dietary gluten-induced enteropathy. *EMBO Mol. Med.* 13:e14059. doi: 10.15252/emmm.202114059

Seni, K., Saini, A., Debnath, R., Singh, A., Sharma, A., Bisht, D. S., et al. (2024). Advancements in ulcerative colitis management: a critical assessment of etrasimod therapy. *Health Sci. Rev.* 12:100196. doi: 10.1016/j.hsr.2024.100196

Seregin, S. S., Golovchenko, N., Schaf, B., Chen, J., Pudlo, N. A., Mitchell, J., et al. (2017). NLRP6 protects $IL10^{-/-}$ mice from colitis by limiting colonization of *Akkermansia muciniphila*. *Cell Rep.* 19, 733–745. doi: 10.1016/j.celrep.2017.03.080

Sharon, G., Ioannis, K., Willem, D. V., and Clara, B. J. M. (2018). *Akkermansia muciniphila* in the human gastrointestinal tract: when, where, and how? *Microorganisms* 6, 75–81. doi: 10.3390/microorganisms6030075

Shen, Z. H., Zhu, C. X., Quan, Y. S., Yang, Z. Y., Wu, S., Luo, W. W., et al. (2018). Relationship between intestinal microbiota and ulcerative colitis: mechanisms and clinical application of probiotics and fecal microbiota transplantation. *Gastroenterology* 24, 5–14. doi: 10.3748/wjg.v24.i1.5

Shi, D.-C., Wang, P.-Y., Xu, L., Zhu, H., Zhang, W.-Y., Wu, Q.-Y., et al. (2024). Potential of *Dendrobium officinale* oligosaccharides to alleviate chronic colitis by modulating inflammation and gut microbiota. *Food Med. Homol.* 2024:9420077. doi: 10.26599/fmh.2025.9420077

Tong, L., Hao, H., Zhang, Z., Lv, Y., and Yi, H. J. T. (2021). Milk-derived extracellular vesicles alleviate ulcerative colitis by regulating the gut immunity and reshaping the gut microbiota. *Theranostics* 11, 8570–8586. doi: 10.7150/thno.62046

Turuvekere Sadguruprasad, L., and Basavaraj, M. (2018). Statistical modelling for optimized lyophilization of *Lactobacillus acidophilus* strains for improved viability and stability using response surface methodology. *AMB Express* 8:129. doi: 10.1186/s13568-018-0659-3

Vigsnaes, L., Brynskov, J., Steenholdt, C., Wilcks, A., and Licht, T. (2012). Gram-negative bacteria account for main differences between faecal microbiota from patients with ulcerative colitis and healthy controls. *Benefic. Microbes* 3, 287–297. doi: 10.3920/BM2012.0018

Wang, H., Cai, Y., Wu, W., Zhang, M., Dai, Y., and Wang, Q. (2024). Exploring the role of gut microbiome in autoimmune diseases: a comprehensive review. *Autoimmun. Rev.* 23:103654. doi: 10.1016/j.autrev.2024.103654

Wang, Y., Chen, Y., Zhang, H., Yu, S., Yuan, G., and Hu, H. (2025). Colon-targeted self-assembled nanoparticles loaded with berberine double salt ameliorate ulcerative colitis by improving intestinal mucosal barrier and gut microbiota. *Colloids Surf. B* 245:114353. doi: 10.1016/j.colsurfb.2024.114353

Wang, J. L., Han, X., Li, J. X., Shi, R., Liu, L. L., Wang, K., et al. (2022). Differential analysis of intestinal microbiota and metabolites in mice with dextran sulfate sodium-induced colitis. *World J. Gastroenterol.* 28, 6109–6130. doi: 10.3748/wjg.v28.i43.6109

Wang, J., Lv, X., Li, Y., Wu, H., Chen, M., Yu, H., et al. (2025). A ROS-responsive hydrogel that targets inflamed mucosa to relieve ulcerative colitis by reversing intestinal mucosal barrier loss. *J. Control. Release* 377, 606–618. doi: 10.1016/j.jconrel.2024.11.065

Wang, L., Tang, L., Feng, Y., Zhao, S., Han, M., Zhang, C., et al. (2020). A purified membrane protein from *Akkermansia muciniphila* or the pasteurised bacterium blunts colitis associated tumourigenesis by modulation of $CD8^+$ T cells in mice. *Gut* 69, 1988–1997. doi: 10.1136/gutjnl-2019-320105

Wang, D., Xu, R., Liu, S., Sun, X., Zhang, T., Shi, L., et al. (2025). Enhancing the application of probiotics in probiotic food products from the perspective of improving stress resistance by regulating cell physiological function: A review. *Food Res. Int.* 199:115369. doi: 10.1016/j.foodres.2024.115369

Wangchuk, P., Yeshi, K., and Loukas, A. (2024). Ulcerative colitis: clinical biomarkers, therapeutic targets, and emerging treatments. *Trends Pharmacol. Sci.* 45, 892–903. doi: 10.1016/j.tips.2024.08.003

Wegh, C. A. M., Geerlings, S. Y., Knol, J., Roeselers, G., and Belzer, C. (2019). Postbiotics and their potential applications in early life nutrition and beyond. *Int. J. Mol. Sci.* 20:4673. doi: 10.3390/ijms20194673

Wu, Y., Jha, R., Li, A., Liu, H., Zhang, Z., Zhang, C., et al. (2022). Probiotics (*Lactobacillus plantarum* HNU082) supplementation relieves ulcerative colitis by affecting intestinal barrier functions, immunity-related gene expression, gut microbiota, and metabolic pathways in mice. *Microbiol. Spectr.* 10:e0165122. doi: 10.1128/spectrum.01651-22

Wu, Z., Li, Y., Jiang, M., Sang, L., and Chang, B. (2024). Selenium yeast alleviates dextran sulfate sodium-induced chronic colitis in mice by reducing proinflammatory cytokines and regulating the gut microbiota and their metabolites. *J. Inflamm. Res.* 17, 2023–2037. doi: 10.2147/JIR.S449335

Xiao, X., Wu, Y., Jie, Z., Lin, L., Li, Y., Hu, W., et al. (2024). *Akkermansia Muciniphila* supplementation improves hyperlipidemia, cardiac function, and gut microbiota in high fat fed apolipoprotein E-deficient mice. *Prostaglandins Other Lipid Mediat.* 175:106906. doi: 10.1016/j.prostaglandins.2024.106906

Yao, B., Yang, Z., Zhao, X., Han, Z., Li, P., and Shang, N. (2025). Biofilm-state probiotics: advanced alternatives to traditional probiotics. *Trends Food Sci. Technol.* 156:104854. doi: 10.1016/j.tifs.2024.104854

Yu, E., Eid, J., Cheng, A., Lynch, B., and Bauter, M. (2024). Lack of genotoxicity and subchronic toxicity in safety assessment studies of *Akkermansia muciniphila* formulation. *Toxicol. Rep.* 13:101790. doi: 10.1016/j.toxrep.2024.101790

Zhai, R., Xue, X., Zhang, L., Yang, X., Zhao, L., and Zhang, C. (2019). Strain-specific anti-inflammatory properties of two *Akkermansia muciniphila* strains on chronic colitis in mice. *Front. Cell. Infect. Microbiol.* 9:239. doi: 10.3389/fcimb.2019.00239

Zhang, S.-s., Feng, D., An, J.-z., Zhao, J., Zhao, J.-y., Guo, Y., et al. (2025). Total glycosides of *Cistanche deserticola* attenuates DSS-induced inflammatory bowel disease by regulating intestinal environmental homeostasis. *Food Med. Homol.* 2:9420048. doi: 10.26599/fmh.2025.9420048

Zhang, Q., Wu, Y., Wang, J., Wu, G., Long, W., Xue, Z., et al. (2016). Accelerated dysbiosis of gut microbiota during aggravation of DSS-induced colitis by a butyrate-producing bacterium. *Sci. Rep.* 6:27572. doi: 10.1038/srep27572

Zhang, K., Zhang, Q., Qiu, H., Ma, Y., Hou, N., Zhang, J., et al. (2024). The complex link between the gut microbiome and obesity-associated metabolic disorders: mechanisms and therapeutic opportunities. *Heliyon* 10:e37609. doi: 10.1016/j.heliyon.2024.e37609

Zhao, X., Zhao, J., Li, D., Yang, H., Chen, C., Qin, M., et al. (2023). *Akkermansia muciniphila*: a potential target and pending issues for oncotherapy. *Pharmacol. Res.* 196:106916. doi: 10.1016/j.phrs.2023.106916

Zheng, M., Han, R., Yuan, Y., Xing, Y., Zhang, W., Sun, Z., et al. (2023). The role of *Akkermansia muciniphila* in inflammatory bowel disease: current knowledge and perspectives. *Front. Immunol.* 13. doi: 10.3389/fimmu.2022.1089600

Zhou, J.-C., and Zhang, X.-W. (2019). *Akkermansia muciniphila*: a promising target for the therapy of metabolic syndrome and related diseases. *Chin. J. Nat. Med.* 17, 835–841. doi: 10.1016/S1875-5364(19)30101-3

frontiers | Frontiers in Microbiology

TYPE Original Research
PUBLISHED 10 March 2025
DOI 10.3389/fmicb.2025.1557778

Check for updates

OPEN ACCESS

EDITED BY
Guiguo Zhang,
Shandong Agricultural University, China

REVIEWED BY
Muhammad Zohaib Aslam,
Tuskegee University, United States
Liming Mao,
Nantong University, China

*CORRESPONDENCE
Xiaoyu Gao
✉ 2018014@ynau.edu.cn
Lei Peng
✉ 370686911@qq.com
Yang Tian
✉ tianyang@ynau.edu.cn

†These authors have contributed equally to this work

RECEIVED 09 January 2025
ACCEPTED 25 February 2025
PUBLISHED 10 March 2025

CITATION
Huang Z, Zhao Y, Yang W, Duan C, Sheng J, Tian Y, Peng L and Gao X (2025) *Amomum tsaoko* flavonoids attenuate ulcerative colitis by inhibiting TLR4/NF-κB/NLRP3 signaling pathway and modulating gut microbiota in mice.
Front. Microbiol. 16:1557778.
doi: 10.3389/fmicb.2025.1557778

COPYRIGHT
© 2025 Huang, Zhao, Yang, Duan, Sheng, Tian, Peng and Gao. This is an open-access article distributed under the terms of the Creative Commons Attribution License (CC BY). The use, distribution or reproduction in other forums is permitted, provided the original author(s) and the copyright owner(s) are credited and that the original publication in this journal is cited, in accordance with accepted academic practice. No use, distribution or reproduction is permitted which does not comply with these terms.

Amomum tsaoko flavonoids attenuate ulcerative colitis by inhibiting TLR4/NF-κB/NLRP3 signaling pathway and modulating gut microbiota in mice

Zelin Huang[1,2,3†], Yan Zhao[4†], Weixing Yang[2], Chunfen Duan[2], Jun Sheng[3], Yang Tian[1,3*], Lei Peng[2*] and Xiaoyu Gao[1,2,3*]

[1]Yunnan Key Laboratory of Precision Nutrition and Personalized Food Manufacturing, Yunnan Agricultural University, Kunming, China, [2]College of Food Science and Technology, Yunnan Agricultural University, Kunming, China, [3]Engineering Research Center of Development and Utilization of Food and Drug Homologous Resources, Ministry of Education, Yunnan Agricultural University, Kunming, China, [4]Division of Science and Technology, Yunnan Agricultural University, Kunming, China

Ulcerative colitis (UC) is a global disease for which there is little of effective treatment options, thus creating an urgent need for the development of new drug candidates from natural and functional foods. *Amomum tsaoko* Crevost et Lemarie is a kind of medicinal and food herb that is rich in flavonoids. However, the pharmacological effects of *Amomum tsaoko* flavonoids (ATF) on UC have not yet been reported. The present study established a mouse model of UC using 3% dextran sulfate sodium (DSS), and modern molecular biology techniques such as IHC, RT-qPCR, Western blot, and 16S rRNA gene analysis were used to investigate the effect of ATF in UC mice. The results demonstrated that a high dose of ATF (100 mg/kg) led to a significant restoration of body weight, disease activity index score, and colon length, in addition to ameliorating colonic tissue damage in UC mice. ATF reduced the serum levels of lipopolysaccharides (LPS), inhibited the activation of the colonic TLR4/NF-κB/NLRP3 signaling pathway, and increased the mRNA expression of tight junction proteins such as *ZO-1*, *Occludin*, and *Claudin4*. Furthermore, ATF was found to reduce the relative abundance of the DSS-induced conditional pathogenic (*Escherichia-Shigella*, *Colidextribacter*, and *Oscillibacter*), increase the potential probiotic taxa (*Akkermansia*, *Bifidobacterium* and *unclassified_f__Atopobiaceae*). Interestingly, these genera were found to be significantly correlated with the UC core phenotypic indicators. These findings indicated that ATF may alleviate UC symptoms by modulating the gut microbiota-LPS/TLR4/NF-κB/NLRP3 axis. The present study has the potential to serve as a valuable reference point for understanding the role of natural flavonoids in the prevention of inflammatory diseases, and to expand the future applications of ATF in the fields of food and medicine.

KEYWORDS

Amomum tsaoko*, flavonoids, ulcerative colitis, *Escherichia-Shigella*, *Akkermansia*, *Bifidobacterium*, *Colidextribacter*, *Oscillibacter

1 Introduction

Ulcerative colitis (UC) is a chronic inflammatory bowel disease (IBD) that is characterized by periodic relapses, most often with recurrent abdominal pain and diarrhea, mucus-thickened blood stools, severe weight loss, and a long-term inflammatory state of the colon. These clinical manifestations increase the risk of colon cancer (Sun et al., 2021). The aetiology of UC is multifaceted and closely associated with immune dysfunction (Powell et al., 2015), impaired intestinal barrier function (Zhen and Zhang, 2019) and dysbiosis of the gut microbiota (Kim S. G. et al., 2019). At this juncture, the management of UC remains largely dependent on the utilization of pharmacological agents, predominantly anti-inflammatory drugs, immunosuppressants and biosuppression, such as sulfasalazine, azathioprine and mesalazine. However, these therapeutic modalities have been associated with an increased risk of disease exacerbation and deterioration (Klein and Eliakim et al., 2010; Pauly et al., 2017). It is therefore imperative to identify a safe and effective natural edible resource as an alternative drug for the treatment of UC.

In China, herbal medicine represents a typical and long-established intervention for the treatment of intestinal inflammation, utilizing plant-derived active ingredients. The composition of Chinese herbal medicine is complex, comprising large molecules that are primarily polysaccharides and water-soluble proteins, while small molecules may consist of flavonoids, alkaloids, amino acids, organic acids, nucleotides, and other substances. These small molecules generally exhibit fewer side effects. It has been established that the anti-UC properties of active compounds derived from herbal medicines primarily target inflammation or oxidative stress, which is associated with increased levels of anti-inflammatory cytokines (IL-4, IL-10, SOD), and decreased levels of pro-inflammatory cytokines (TNF-α, IL-1β, and IL-6 etc.) (Cao et al., 2019). These findings suggest that the study of natural drug compounds related to UC is of great value.

A substantial body of evidence from previous studies has demonstrated that flavonoids can alleviate IBD through a range of mechanisms. To illustrate, soybean isoflavones have been demonstrated to impede IκB protein phosphorylation and IKK degradation (Kim S. E. et al., 2019). Naringenin inhibits the TLR4/NF-κB pathway, inducing M2 macrophages and accelerating colonic recovery (Chaen et al., 2019). Quercetin enhances intestinal barrier function through the assembly of zonula occludens-2, occludin, and claudin-1 and the expression of claudin-4 (Suzuki and Hara, 2009). Nobiletin targets oxidative stress, NLRP3 inflammatory vesicle activation and immune responses in UC mice (Yang et al., 2024). Kaempferol alleviates colitis by restoring the gut microbiota and inhibiting the LPS-TLR4-NF-κB axis (Qu et al., 2021). The overall pharmacological mechanisms by which flavonoids alleviate UC appear to be related to the modulation of the body's immune response, inflammatory response, intestinal barrier and gut microbiota.

Amomum tsaoko Crevost et Lemarie (AT) is one of the most widely used Chinese medicinal herbs, with a multitude of applications. It is also used as a spice to remove the fishy flavor and has the effect of warming the spleen and stomach, stopping vomiting, eliminating the hostage, and expelling the cold and pain in the abdomen. Nevertheless, AT is predominantly employed as a seasoning, and its potential therapeutic benefits remain largely untapped (Hu et al., 2018). The gradual study of AT has resulted in the isolation of over 300 compounds, with flavonoids representing the primary components of AT (Yang S. et al., 2022; Cai et al., 2021). The flavonoids present in AT have been demonstrated to possess high antioxidant activity, which has been shown to significantly improve the symptoms of type II diabetic mice (Zhang et al., 2022). Moreover, these flavonoids have been demonstrated to inhibit the production of NO in LPS-stimulated RAW 264.7 murine macrophages, which have been shown to exhibit potent anti-inflammatory activity (Whan et al., 2018). The flavonoids have additionally been demonstrated to display enhanced pharmacological activity in mice with constipation (Hu et al., 2023). These previous studies implied that the flavonoids present in AT may possess ameliorative properties in the context of IBD. However, no studies have been reported on the utilization of total flavonoids in AT (ATF) in IBD. In the present study, the anti-UC properties of high-purity ATF, which had been successfully prepared in our previous work (Hu et al., 2018) were evaluated in the experimental UC mouse model induced by dextran sulfate sodium (DSS). Furthermore, the anti-UC mechanism of ATF was explored from the perspectives of inflammatory signaling pathway and intestinal microecology, with a view to providing theoretical bases for the application of ATF in functional foods or medicines.

2 Materials and methods

2.1 Preparation of ATF

The AT fruits were sourced from Gongshan County, Yunnan Province of China. The preparation of ATF was outlined in brief, with reference to the published literature of our group (Huang et al., 2025). The AT was pulverized and then extracted using a sonicator. Subsequently, a specific concentration and pH of the upper sample solution were prepared. Adsorption and desorption were conducted with HPD300 macroporous resin, and the 20 and 30% ethanol eluates were concentrated and vacuum-dried, and stored for spare parts. The ATF obtained from the preparation primarily comprised (+)-Epicatechin (30.88%), Isoquercitrin (17.33%), Astragalin (9.52%) Kaempferol-3-O-rutinoside (8.46%), Procyanidin B2 (6.82%), and other compounds.

2.2 Design of animal experiments

A total of 60 male C57/6 J mice (20–23 g) were obtained from Beijing Vital River Laboratory Animal Technology Co., Ltd. (SPF grade). The animals were housed in the Yunnan key laboratory of precision nutrition and personalized food manufacturing. All the procedures were reviewed and approved by the life science ethics committee of Yunnan agricultural university (Approval no. 202312008). The animals were maintained at a temperature of 24 ± 1°C under a 12-h light/dark cycle, on an ad libitum diet (LAD3001M, Trophic Animal Feed High-tech Co. Ltd., China.) and water, and experiments were conducted in groups after 1 week acclimatization. The average body weight of mice in each group was similar.

10.3389/fmicb.2025.1557778

Dextran sulfate sodium (DSS) is a common inducer of UC, and an acute UC model can usually be established by feeding with 3% DSS for 5–7 days. Five experimental groups were set up ad follows. (a) CON group (sterilized water, $n = 12$); (b) DSS group (3% DSS, $n = 12$); (c) DSS + LATF group (25 mg/kg·bw ATF + 3% DSS, $n = 12$); (d) DSS + MATF group (50 mg/kg·bw ATF + 3% DSS, $n = 12$); (e) DSS + HATF group (100 mg/kg·bw ATF + 3% DSS, $n = 12$). Gavage volume was set at 0.2 mL/10 g body weight. Figure 1A shows the experimental procedure. Fourteen days prior to the DSS intervention, mice were gavaged with sterilized water in the CON and DSS groups, and mice were gavaged with 25, 50, and 100 mg/kg-bw oxalic acid flavonoids in the ATF dose group, respectively. Water was freely

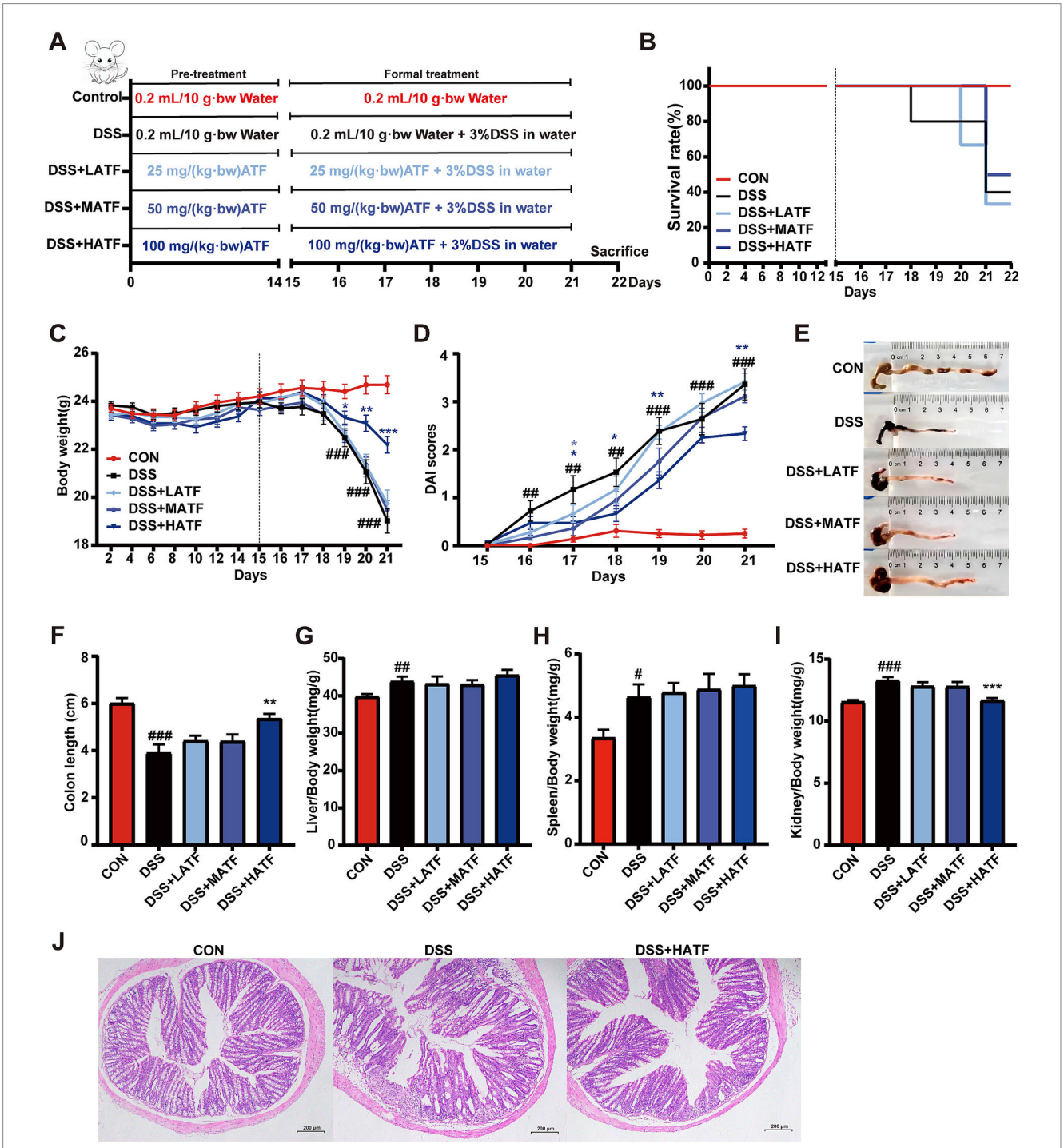

FIGURE 1
Amomum tsaoko flavonoids (ATF) is effective in alleviating symptoms of the DSS-induced colitis. **(A)** Animal experiment design; **(B)** survival curves; **(C)** mice body weights were recorded daily; **(D)** calculate the DAI score; **(E,F)** bowel images and colon length stats; **(G–I)** liver, spleen and kidney index; **(J)** images of colon sections stained with H&E. All data presented in mean ± SEMs, $n = 10–12$. # compared with the CON group; * compared with the DSS group. $^{\#}p < 0.05$, $^{\#\#}p < 0.01$, $^{\#\#\#}p < 0.001$; $^{*}p < 0.05$, $^{**}p < 0.01$, $^{***}p < 0.001$.

consumed by the mice for the rest of the time. The 3% DSS solution was provided from day 15 to 22 to all groups except the CON. On the 21st day of the experiment, it was observed that the weight loss rate of mice in the model group exceeded 20%, which was considered to be the weight loss criterion for animal ethics. The experiment was therefore terminated on the 22nd day, and the mice were euthanized. Mice were executed with CO_2 at the end day of experiment. Blood was collected and incubated to obtain serum. The livers, spleens and kidneys of the mice were weighed. The entire intestine was extracted, the mesentery and other associated tissues were excluded, and the proximal colon and cecum were harvested. The length of the colonic segments from each mouse was meticulously recorded. The colonic segments and the contents of the cecum were then collected and stored in a −80°C refrigerator for future use.

2.3 DAI score

During the course of DSS-induced UC, a daily record was kept of body weight change, fecal status and blood in stool in mice. The mean of the sum of the three scores was then used to calculate the disease activity index score (DAI). The calculation of weight loss was performed as the ratio of daily body weight change to initial body weight. The fecal status was slightly modified with reference to the Bristol stool typing method, and blood was discriminated by the instructions of the fecal occult blood kit (BC8270, Solarbio, Beijing). The detailed DAI scoring criteria are shown in Supplementary Table S1.

2.4 Serum biochemical analysis

Lipopolysaccharides, TNF-α and IL-1β in serum were detected by Mouse Lipopolysaccharides (LPS) ELISA Kit (CSB-E13066m, Cusabio, Wuhan), Mouse TNF-α ELISA Kit (E-EL-M3063, Elabscience, Wuhan) and Mouse IL-1β ELISA Kit (E-EL-M0037, Elabscience, Wuhan) were used for the assay. All the assays were performed according to the instructions of the kits.

2.5 RNA extraction, reverse transcription and real-time quantitative PCR

RNA was extracted from 10 to 20 mg of each mouse colon tissue sample using a bead-beating method and the FastPure Cell/Tissue DNA Isolation Mini Kit (RC101-01, Vazyme, Nanjing). RNA concentration and purity were determined using a spectrophotometer. Total RNA were then reverse transcribed to cDNA using HiScript III RT SuperMix for qPCR (+gDNA wiper) kit (R323-01, Vazyme, Nanjing). The obtained cDNA was stored at −30°C.

The real-time quantitative PCR reactions system was prepared according to the instructions of the ChamQ Universal SYBR qPCR Master Mix kit (Q711-02, Vazyme, Nanjing). Gene expression was determined using a LightCycler® 480 System (Roche Diagnostics, Switzerland) PCR instrument, as outlined in the Supplementary Table S2. PCR reactions were set up in duplicate. As the reference gene, RPL-19 was used to calibrate target mRNA expression. The $2^{-\Delta\Delta Ct}$ method was used to calculate the results, with primer sequences given in Supplementary Table S3.

2.6 H&E staining of colonic tissue

A 4% formaldehyde solution was used to fix the colon. After embedding, all the colons were then cut into 3 μm sections for hematoxylin and eosin (H&E) staining. Two H&E-stained sections were obtained from each mouse for analysis. H&E-stained sections were imaged using a biological microscope.

2.7 Immunohistochemistry

The 3 μm wax blocks were dewaxed in xylene and rehydrated in graded ethanol. Following quenching of endogenous peroxidase activity and blocking of non-specific binding, the sections were subjected to an overnight incubation at room temperature with F4/80, TLR4, and NLRP3 mouse monoclonal antibodies (28463-1-AP, 66350-1-Ig, and 68,102-1-Ig respectively, Proteintech, Wuhan). This was followed by an incubation for 20 min at room temperature with biotinylated secondary antibodies (Zymed Laboratories, Carlsbad, CA, United States). The slides were then incubated with reagents from the Avidin-Biotin (SP-2001, Vector Laboratories, CA, United States) and 3,3′-diaminobenzidine kits (SK-4100, Vector Laboratories, CA, United States). Images obtained using Olympus CX43 microscope and CellSens Entry. The sections were photographed top-to-bottom and left-to-right and images of undamaged tissue structure were selected for analysis. The images were digitized using Image Pro-Plus 6.0 software (Media cybernetics, United States).

2.8 16S rRNA gene sequencing

Samples of cecal content were sent to Shanghai Majorbio Bio-pharm Technology Co., Ltd. for 16S rRNA gene sequencing. The microbial DNA was extracted from the cecum contents of the mice in the CON, DSS and DSS + HATF groups using the E.Z.N.A.® Soil DNA kit (Omega Bio-tek, United States). Final DNA concentration and purity were determined using a NanoDrop 2000 UV–Vis (Thermo Scientific, United States). The DNA quality was evaluated using 1% agarose gel electrophoresis. The V3–V4 highly variable region of the bacterial 16S rRNA gene was amplified using a thermal cycling PCR system (GeneAmp 9,700, ABI, United States) and primers 338F (5′-ACTCCTACGGGGAGGCAGCAG3′) and 806R (5'- GGACTACHVG GGTWTCTAAT -3′). PCR was performed using the following procedure: denaturation at 95°C for 3 min; annealed at 95°C and 55°C for 30 s, respectively, and extended at 72°C for 45 s, 27 cycles; extended at 72°C for 10 min. PCR was conducted three times in a 20 μL mixture comprising 4 μL of 5 × FastPFU buffer, 2 μL of 2.5 mM dNTPs, 0.8 μL of each primer (5 μM), 0.4 μL of FastPFU polymerase, and 10 ng of template DNA. PCR products obtained from 2% agarose gels were purified using the Axyprep DNA Gel Extraction Kit (Axygen Biosciences, United States) and quantified using Quantifluor™-ST (Promega, United States) according to the manufacturer's protocol. The purified amplicons were pooled in equimolar amounts and subjected to paired-end sequencing (2 × 300) on the Illumina MiSeq platform (Illumina, United States). The RDP Classifier was used to classify and analyze the Silva (SSU123) 16S rRNA database. Bioinformatics analysis was conducted on Majorbio's cloud platform.

2.9 Data analysis

Data analysis were conducted using GraphPad Prism 8.0, with results expressed as the means ± standard errors of the means (SEMs). Analysis of variance was conducted using the statistical software package SPSS 26.0 (SPSS Inc., Chicago, IL, United States). Statistical analysis of the results was conducted using analysis of variance (ANOVA) with Duncan's test. Advanced Cor link was performed using the OmicStudio tools at https://www.omicstudio.cn/tool. Multivariate analyses were conducted using the Majorbio platform. Unless stated otherwise, results were statistically significant at $p < 0.05$.

3 Results

3.1 ATF relieved the DSS-induced colitis in mice

Figure 1A illustrates the flow of the animal experiment. The CON group showed no unusual symptoms during the experiment. The DSS group, the DSS + LATF group, the DSS + MATF group, and the DSS + HATF group, respectively, had mortality in 2, 2, 1, and 0 mice following DSS ingestion (Figure 1B). From day 5, DDS-treated mice lost weight ($p < 0.01$) and had diarrhea and blood in their stool. They showed a big increase in DAI score compared to the CON group ($p < 0.01$). The DSS + HATF group showed a strong effect on body weight and DAI score ($p < 0.01$, Figures 1C,D). Interestingly, low, medium, and high doses of ATF inhibited colon shortening and alleviated DSS-induced liver, spleen, and kidney swelling, with the high dose exhibiting a pronounced effect ($p < 0.01$, Figures 1E–I). Pathological sections showed severe damage to the mucosal layer of the colon in mice in the DSS group, with a marked reduction in crypt and goblet cells. The DSS + HATF group showed less inflammation than the model group, with more goblet cells and a more intact mucosal structure (Figure 1J). In sum, high doses of ATF could effectively treat UC in mice.

3.2 ATF could regulate the expression of inflammatory factors

Abnormal increases in the levels of inflammatory factors are an important feature of UC. As shown in Figure 2, serum levels TNF-α and IL-1β, plus colonic *TNF-α*, *IL-1β*, *COX-2*, and *MCP-1* mRNA levels were higher in the DSS group than CON. The ATF intervention significantly reduced the levels of these factors ($p < 0.05$, Figures 2A–F) and tended to down-regulate *IL-6*, *IFN-γ*, and *IL-18* mRNA expression, though not statistically significant ($p > 0.05$, Figures 2G–I). The findings showed that the ATF decreased the DSS-induced inflammation in UC.

Similarly, ATF intervention reversed the DSS-induced up-regulation of the mRNA expression of colonic *F4/80, CD68, CD11b, CD14,* and *Ly-6G* ($p < 0.05$), with no significant effect on *CD115* ($p > 0.05$, Figures 2J–O). Furthermore, immunohistochemistry was utilized to investigate the expression of the macrophage marker, F4/80, in mice. The analysis revealed that F4/80 expression within the colon exhibited an increase in the DSS-induced UC model, concurrent with a decrease in response to ATF treatment (Figures 2P,Q). These observations are consistent with the results obtained from RT-qPCR, suggesting that ATF exerts a regulatory effect on inflammatory responses and contributes to the preservation of colonic tissue integrity.

3.3 ATF reduced the DSS-induced endotoxaemia and damage to the intestinal barrier

The release of toxins from the body is intimately associated with disrupting the gut barrier (Di Tommaso et al., 2021). Serum LPS and TLR4 levels in the colon increased in mice in the DSS group compared to the CON group ($p < 0.01$), indicating metabolic endotoxemia. LPS and TLR4 levels were lower in the ATF group than the DSS group ($p < 0.05$). TLR4 immunohistochemistry results were similar to the ATF group and close to those of the CON group (Figures 3A–D). In parallel, the mRNA expression of *Muc2, ZO-1, Occludin* and *Claudin4* were markedly reduced in the DSS-induced colitis mice ($p < 0.05$). Despite the absence of a notable impact of ATF on *Muc2* ($p > 0.05$, Figure 3E), it was observed to stimulate the mRNA expression of *ZO-1, Occludin,* and *Claudin4* ($p < 0.05$, Figures 3F–H). In general, the ATF could modulate these genes to match control levels, reducing metabolic endotoxaemia and intestinal damage.

3.4 ATF inhibited the NF-κB/NLRP3 inflammatory pathway

Given that the DSS contributed to the increased levels of LPS and TLR4, we postulated that the NF-κB/NLRP3 pathway was activated (Liu et al., 2023). In DSS-induced colitis, the mRNA expression of *NF-κB, MyD88*, and *TRAF6* was elevated ($p < 0.05$, Figures 4A–C), while the expression of *p*-p65 was significantly up-regulated in the colons of mice in the DSS group ($p < 0.01$, Figures 4D,E). This finding suggests that the colonic NF-κB signaling pathway was activated in our UC mice. Concurrently, the mRNA expression of colonic *NLRP3, Caspase-1,* and *ASC* was elevated in the DSS group of mice compared with the CON group ($p < 0.05$, Figures 4F–H). And IHC analysis revealed that the expression level of colonic NLRP3 in mice in the DSS group was significantly higher than that in the CON group ($p < 0.01$, Figures 4I,J). Conversely, ATF was able to inhibit the expression of these genes and proteins to varying degrees, approaching the levels observed in the CON group. Overall, ATF could inhibit the activation of the NF-κB/NLRP3 signaling pathway and to reduce the expression of colonic inflammatory mediators, thereby ameliorating DSS-induced colonic inflammation.

3.5 ATF ameliorated the DSS-induced gut microbiota dysbiosis

The 16S rRNA gene was sequenced to assess the impact of ATF on the gut microbiota of the UC mice. The sparse curve of the Sobs index for each sample exhibited a tendency to flatten with an increase in the number of sequences, indicating that the sequencing depth was sufficient to reflect the diversity of the samples and that the sequencing results were credible (Figure 5A).

10.3389/fmicb.2025.1557778

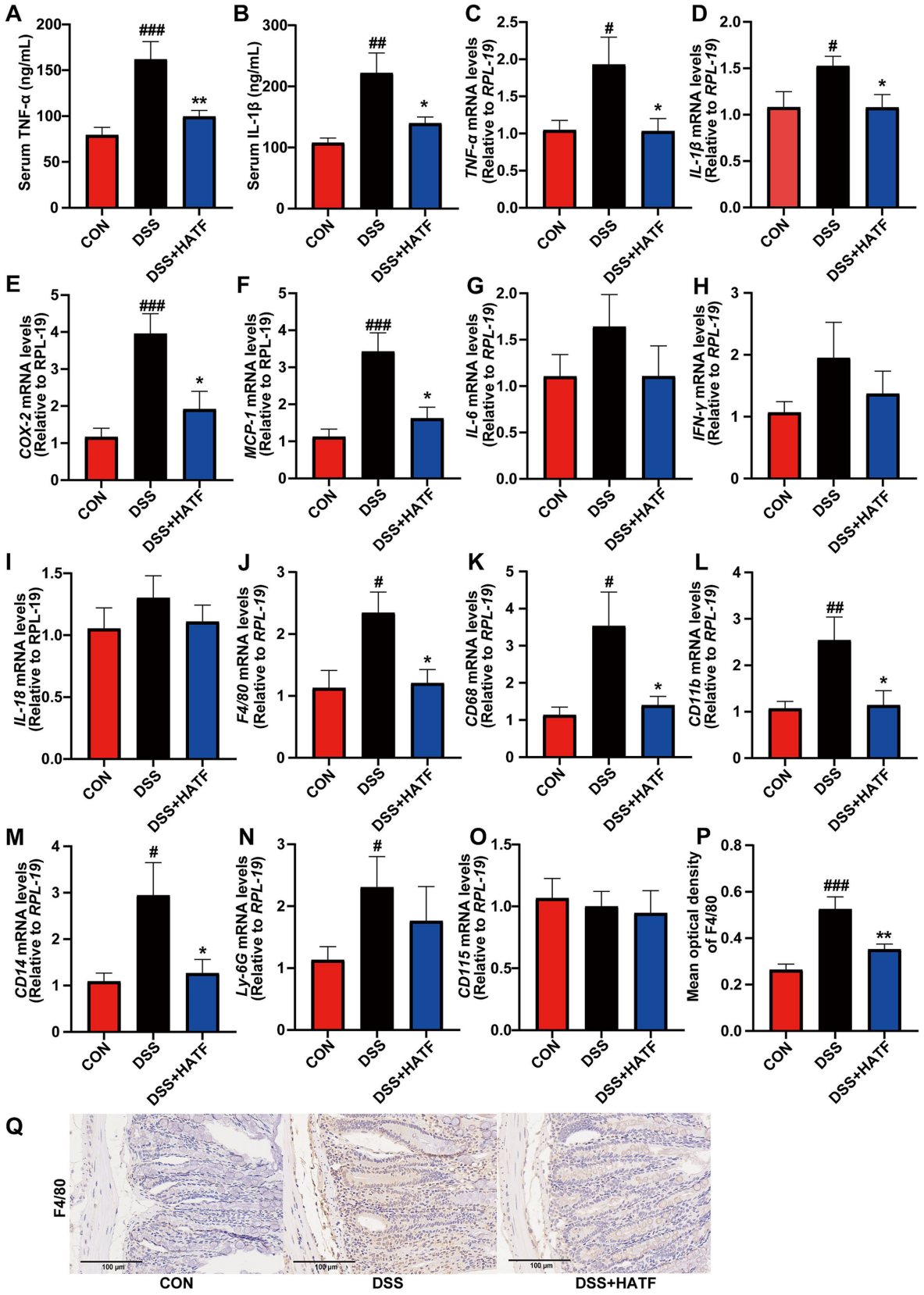

FIGURE 2
Amomum tsaoko flavonoids reversed the DSS-induced up-regulation of pro-inflammatory factors and inflammatory cell infiltration. **(A,B)** Serum levels of TNF-α and IL-1β; **(C–O)** the mRNA expression of *TNF-α*, *IL-1β*, *COX-2*, *MCP-1*, *IL-6*, *IFN-γ*, *IL-18*, *F4/80*, *CD68*, *CD11b*, *CD14*, *Ly-6G (Gr-1)*, and *CD115*. **(P,Q)** Percentage of F4/80 positive area in colonic tissue, and represented IHC images in three group. All data presented in mean ± SEMs, n = 8–10. # compared with the CON group; * compared with the DSS group. $^{\#}p < 0.05$, $^{\#\#}p < 0.01$, $^{\#\#\#}p < 0.001$; $^{*}p < 0.05$, $^{**}p < 0.01$.

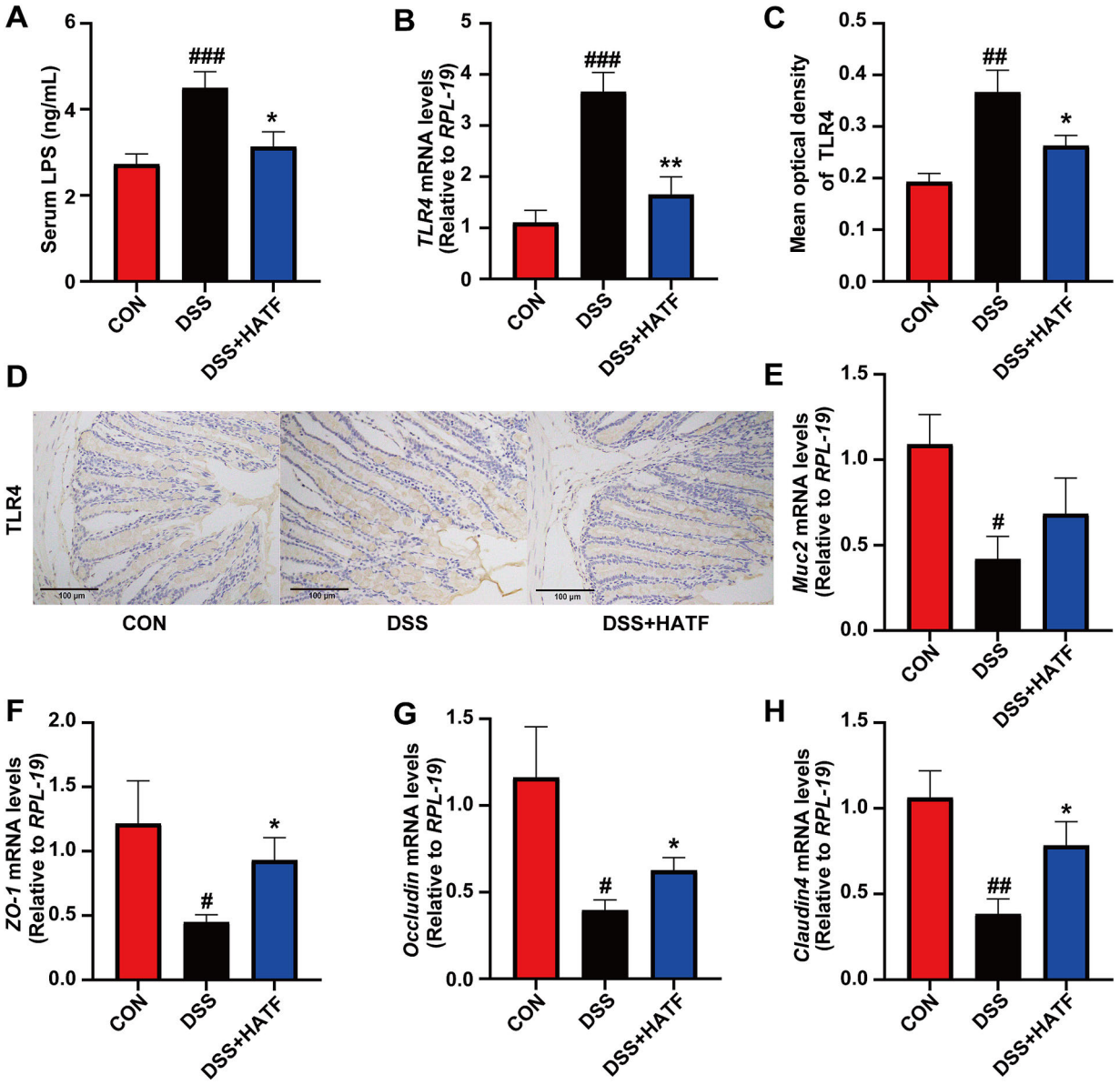

FIGURE 3
Amomum tsaoko flavonoids alleviated metabolic endotoxaemia and ameliorated intestinal barrier damage. **(A)** Serum LPS levels. **(B)** The mRNA expression of TLR4 in colon. **(C,D)** Percentage of TLR4 positive area in colon, and represented IHC images in three group. **(E–H)** The mRNA expression of Muc2, ZO-1, Occludin, and Claudin4, respectively. All data presented in mean ± SEMs, n = 8–10. # compared with the CON group; * compared with the DSS group. $^{\#}p < 0.05$, $^{\#\#}p < 0.01$, $^{\#\#\#}p < 0.001$; $^{*}p < 0.05$, $^{**}p < 0.01$.

Despite the DSS and DSS + HATF groups demonstrating no significant difference from the CON group with regard to α-diversity indices (Figure 5B), the PCoA result clearly separated the CON, DSS, and DSS + HATF group, with the DSS + HATF group demonstrating a closer proximity to the CON group (Figure 5C), suggesting that ATF altered the β-diversity of the gut microbiota in UC mice and had a restorative effect on the DSS-induced gut microbiota dysbiosis.

The LEfSe analyses similarly demonstrated the dramatic effects of loperamide and ATF on microbial taxa at different levels (Figure 5D). A total of 88 different taxa, including 4 phyla, 6 classes, 10 orders, 20 families and 48 genera, were identified in the three groups. Of these, the CON, DSS, and DSS + HATF groups had 31, 32, and 25 dominant taxa, respectively, (Figure 5D and Supplementary Figure S1). The present study focused on the taxa significantly affected by DSS and ATF, especially those significantly changed by ATF treatment.

At the phylum level, the relative abundance of *Actinobacteriota*, *Verrucomicrobiota,* and *Proteobacteria* in the cecum of mice in the DSS group was significantly different from that of the CON group ($p < 0.01$), and the ATF intervention significantly increased the relative abundance of *Actinobacteriota* and *Verrucomicrobiota* and *Bacteroidota* ($p < 0.05$), but did not restore Proteobacteria to a significant level (Figure 5E, $p > 0.05$). At the family level, DSS treatment induced a significant up-regulation of *Enterobacteriaceae* and *Anaerovoracaceae*, which was significantly reversed by ATF intervention ($p < 0.05$, Figure 5F). Furthermore, the relative

10.3389/fmicb.2025.1557778

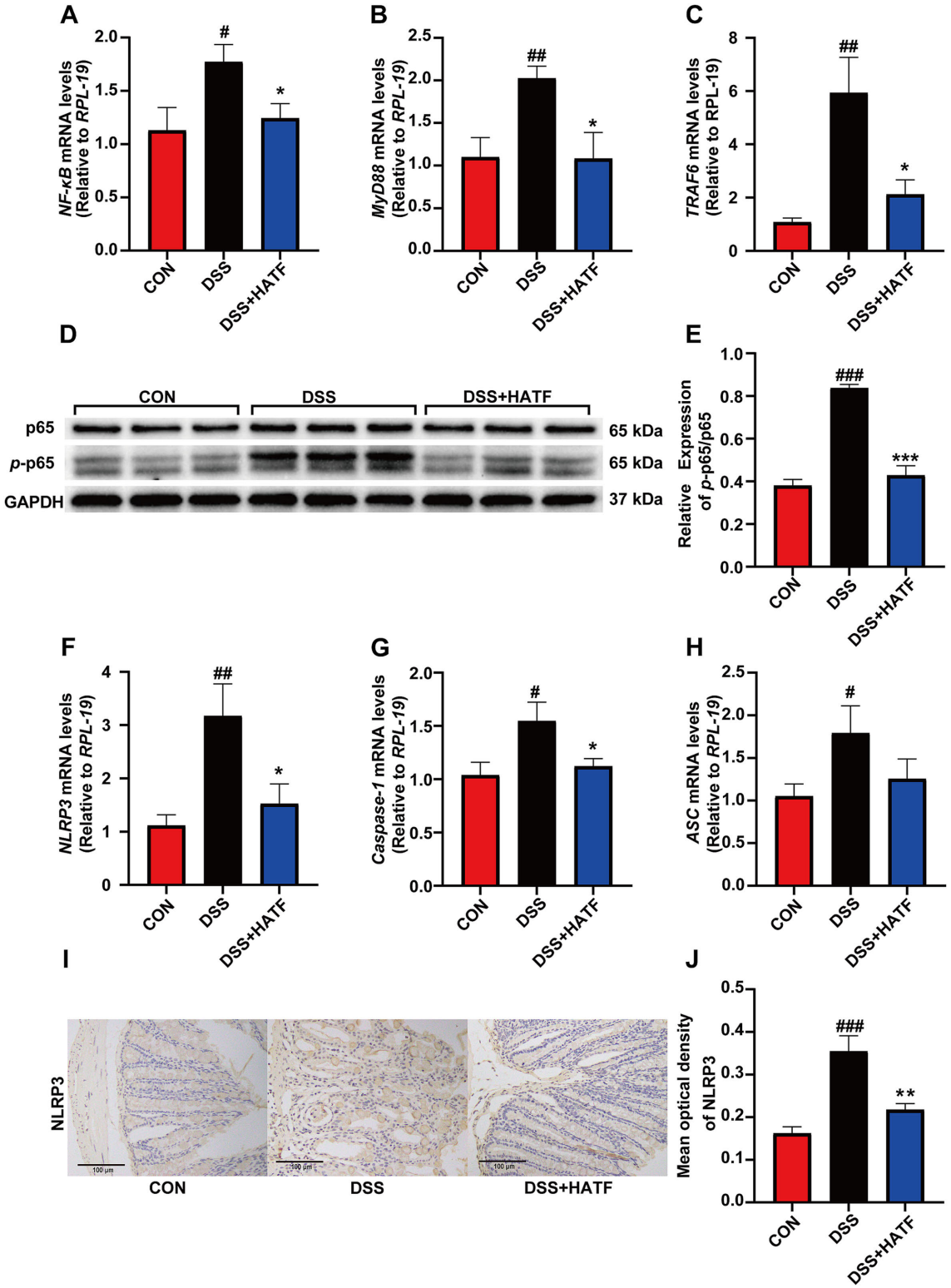

FIGURE 4
The effect of ATF on the NF-κB and NLRP3 signaling pathway. **(A–C)** The mRNA expression of *NF-κB*, *MyD88*, *TRAF6* in colon, respectively. **(D,E)** The phosphorylation of p65 was detected by Western blotting, and the relative expression of *p*-p65/p65. **(F–H)** The mRNA expression of *NLRP3*, *Caspase-1*, and *ASC* in colon, respectively. **(I,J)** Represented IHC images in three group, and percentage of NLRP3-positive area in colon. All data presented in mean ± SEMs, n = 8–10. # compared with the CON group; * compared with the DSS group. $^{\#}p < 0.05$, $^{\#\#}p < 0.01$, $^{\#\#\#}p < 0.001$; $^{*}p < 0.05$, $^{**}p < 0.01$.

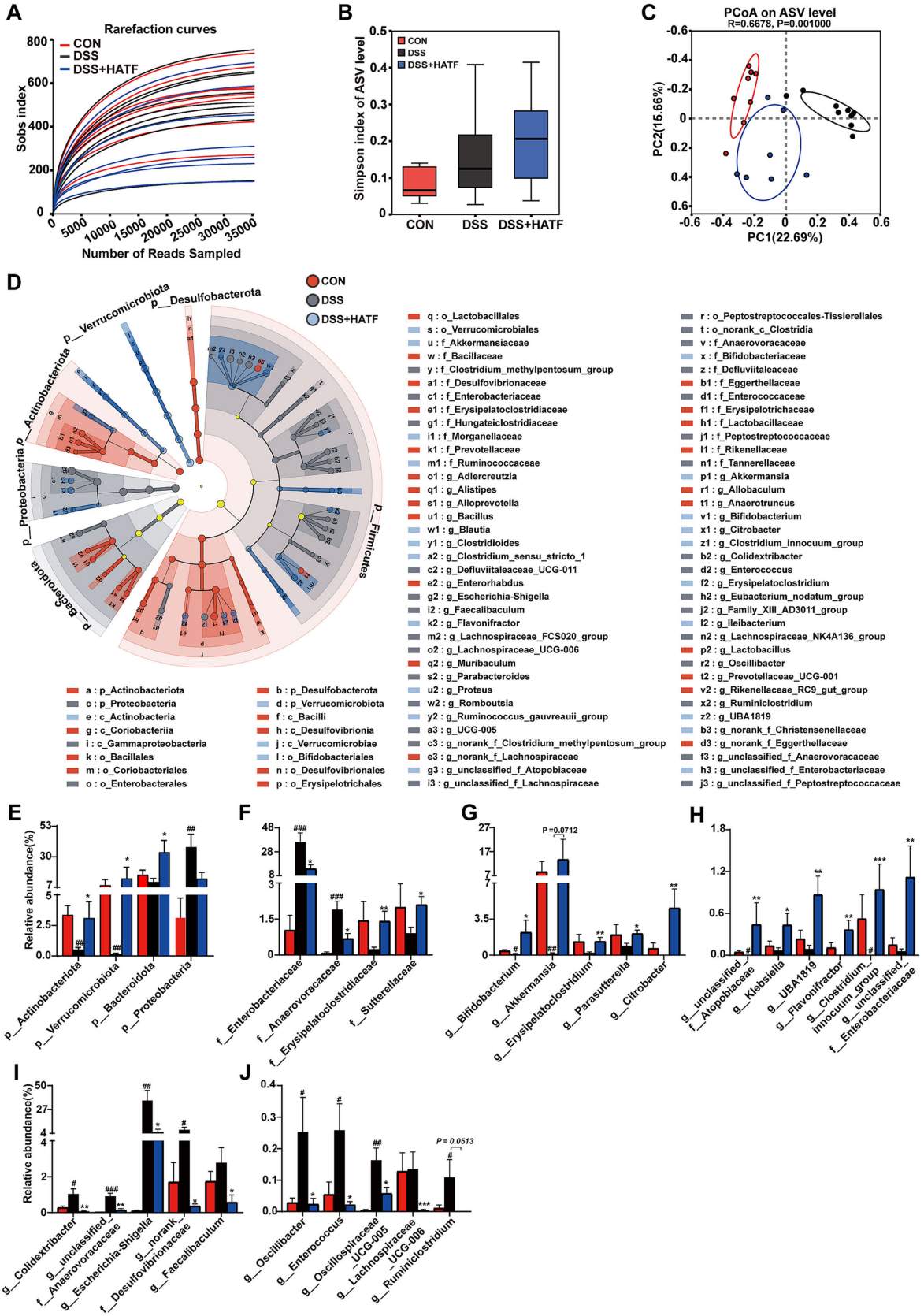

FIGURE 5
Amomum tsaoko flavonoids altered the structure and composition of the gut microbial community in UC mice. **(A)** Rank-abundance curve; **(B)** α-diversity index; **(C)** PCoA based on the Bray–Curtis distance algorithm. **(D)** Linear discriminant analysis effect size (LEfSe) analyses (LDA score > 2.0). **(E)** Relative abundance of microbes at the phylum level. **(F)** Relative abundances of microbes at the family level. **(G–J)** Relative abundances of microbes at the genus level. All data presented in mean ± SEMs, $n = 6$. # compared with the CON group; * compared with the DSS group. $^{\#}p < 0.05$, $^{\#\#}p < 0.01$, $^{\#\#\#}p < 0.001$; $^{*}p < 0.05$, $^{**}p < 0.01$, $^{***}p < 0.001$.

abundance of *Erysipelatoclostridiaceae* and *Sutterellaceae* was induced to decrease by DSS, significantly elevated by ATF intervention, and significantly suppressed the increase in relative abundance of *Anaerovoracaceae* ($p < 0.05$, Figure 5F).

At the genus level, high doses of ATF elevated the relative abundance of *Bifidobacterium*, *Akkermansia*, *Erysipelatoclostridium*, *Parasutterella,* and *Citrobacter* to a greater extent and in a statistically significant way in comparison to the DSS group, as well as significantly increasing the number of relative abundance of *unclassified_f__Atopobiaceae*, *Klebsiella*, *UBA1819*, *Flavonifractor*, *Clostridium_innocuum_group* and *unclassified__f__Enterobacteriaceae* ($p < 0.05$, Figures 5G,H). In contrast, high doses of ATF significantly suppressed the abnormal increase in the relative abundance of *Colidextribacter*, *unclassified_f__Anaerovoracaceae*, *Escherichia-Shigella*, *norank_f__Desulfovibrionaceae*, *Faecalibaculum*, *Oscillibacter*, *Enterococcus*, *Oscillospiraceae_UCG-005*, *Lachnospiraceae_UCG-006*, and *Ruminiclostridium*. It is noteworthy that in DSS-induced UC mice, the relative abundance of colonies such as *Escherichia-Shigella*, *Desulfovibrionaceae*, and *Enterococcus*, which may produce LPS, was significantly increased, whereas ATF inhibited this change ($p < 0.05$, Figures 5I,J). These findings illustrate that ATF has the capacity to reinstate the DSS-induced gut microbial dysbiosis to varying extents across multiple domains, including microbial diversity, community structure, and species composition.

3.6 Correlation analysis between specific microbiological taxa and core indicators

In order to elucidate the pivotal function of gut microbiota in the alleviation of UC by ATF, bivariate correlation analyses were employed to investigate the correlations between microbial taxa that exhibited a significant response to ATF and core indicators in UC mice.

Figure 6A shows the link between microbial taxa and pathological phenotypes in UC mice. BWCR, CL and DAI are core parameters reflecting the extent of UC disease in mice. These parameters correlated with the differential microbial taxa obtained from the screening. All three parameters demonstrated a robust correlation with *Escherichia-Shigella*, *Anaerovoracaceae* and *unclassified_f__Anaerovoracaceae* ($r \geq 0.65$ or $r \leq -0.65$, $p < 0.05$). *Oscillospiraceae_UCG-005, Proteobacteria* and *Enterobacteriaceae* were negatively correlated with BWCR ($r \leq -0.65, p < 0.05$) and positively correlated with DAI ($r \geq 0.65$, $p < 0.05$). *Colidextribacter* and CL were negatively correlated ($r = -0.6531, p < 0.05$). There is a significant positive correlation between *Actinobacterota, Verrucomicrobiota, Akkermansia, unclassified_f__Atopobiaceae, Bifidobacterium*, *Erysipelatoclostridium* and BWCR ($r < 0.65$, $p < 0.05$). A significant negative correlation was evident between these variables and DAI ($r > -0.65$, $p < 0.05$). Correlations between *Oscillibacter, Ruminiclostridium*, and *Enterococcus* and BWCR and CL were negative ($r > -0.65, p < 0.05$), while those with DAI were positive. In general, BWCR and CL showed the opposite correlation observed in DAI results, consistent with conventional pathological UC signs in mice. Notably, the microbial taxa positively correlated with BWCR and CL were up-regulated by ATF. Those negatively correlated with BWCR and CL and positively correlated with DAI were increased by DSS. ATF significantly reversed this.

The relationship between ATF and other key indicators were also investigated. Our findings revealed a significant positive correlation between *Escherichia-Shigella, Anaerovoracaceae,* and *unclassified_f__Anaerovoracaceae* and serum TNF-α, IL-1β, and colonic *CD11b* and *TLR4*. These taxa were positively correlated with colonic *TRAF6* and *NLRP3* and negatively correlated with *Occludin* and *Claudin4* (Figures 6B–D). A significant positive correlation was observed between *unclassified_f__Anaerovoracaceae* and colonic *F4/80, CD68, CD14, TNF-α, COX-2, MCP-1, MyD88,* and *Caspase-1* ($p < 0.05$). A notable inverse correlation was observed between *unclassified_f__Atopobiaceae* and serum IL-1β, colonic *TNF-α*, *CD11b, TLR4* and *TRAF6*. Conversely, *Oscillibacter, Colidextribacter and Oscillospiraceae_UCG-005* had a different correlation, with a stronger positive association. There was also a significant negative correlation with *occludin* and *claudin4* ($p < 0.05$). In addition, *Escherichia-Shigella*, *norank_f__Desulfovibrionaceae*, *Enterococcus*, *Proteobacteria*, and *Enterobacteriaceae* showed a positive correlation with LPS, while *Actinobacteriota* and *Bifidobacterium* demonstrated a negative correlation. Remarkably, only *Escherichia-Shigella* was significantly positively correlated with both LPS and TLR4 ($p < 0.05$).

In conclusion, *Escherichia-Shigella, unclassified_f__Anaerovoracaceae*, *unclassified_f__Atopobiaceae*, *Bifidobacterium, norank_f__Desulfovibrionaceae*, *Colidextribacter,* and *Oscillibacter* correlated with multiple host core indicators, suggesting that gut microbiota may play a key role in the improvement of UC by ATF.

4 Discussion

Ulcerative colitis is associated with autoimmune function abnormalities. The disease has a long-lasting impact on affected individuals, limiting their quality of life. At the present time, DSS is currently widely used in UC modeling. DSS directly stimulates intestinal cells and disrupts the intestinal barrier, causing acute enteritis, which is the same as clinical UC presentation (Gadaleta et al., 2017). In the present study, DSS caused weight loss, bloody stools and shortened colons in mice. This shows that the DSS model is effective. It has been reported that the DSS-induced UC mice frequently exhibit an imbalance in intestinal homeostasis (Pei et al., 2019; Håkansson et al., 2015). Therefore, a systematic evaluation was conducted of the effects of ATF on the DSS-induced UC mice in terms of intestinal inflammation, intestinal barrier, and gut microbiota. Our results demonstrated that ATF intervention (100 mg/kg) markedly impeded the substantial decline in body weight, the surge in DAI scores, the reduction in colon length, and the disruption of colon tissue structure in UC mice. Additionally, the expression of imbalanced inflammatory factors was diminished, the compromised intestinal barrier was replenished, the activation of the LPS/TLR4/NF-κB/NLRP3 signaling pathway was suppressed, and the disrupted gut microbiota was ameliorated. These effects collectively resulted in the effective alleviation of UC symptoms in mice.

The therapeutic efficacy of ATF in UC may be due to its active ingredients. During the pre-trial period, a plant-wide targeted metabolomics assay was conducted, which revealed that the relative abundance of flavonoids in ATF was greater than 73%. The predominant flavonoids identified were (+)-Epicatechin (30.88%), Isoquercitrin (17.33%), Astragalin (9.52%) Kaempferol-3-O-rutinoside (8.46%), Procyanidin B2 (6.82%), and others. It was found that astragalin was capable of effectively modulating the relative abundance of *Ruminococcaceae* and *Escherichia-Shigella*, while concomitantly exerting

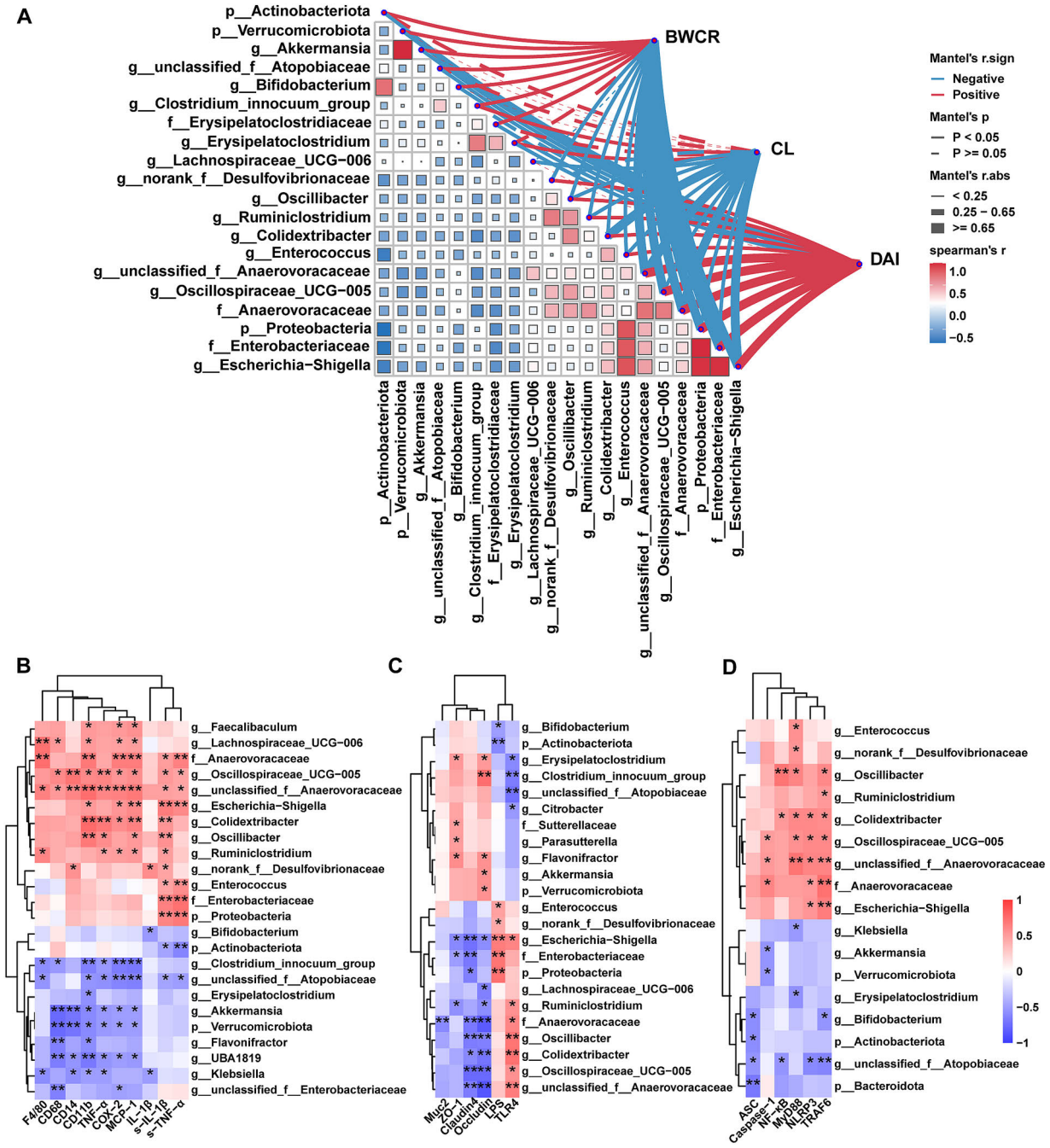

FIGURE 6
Correlations between the differential genera and core indicators of UC. **(A)** Correlations between differential genera and conventional pathological phenotypes of UC mice. **(B)** Correlations between differential genera and inflammatory factors and immune cell markers. **(C)** Correlations between differential genera and metabolic endotoxaemia and colonic barrier factors. **(D)** Correlations between differential genera and NF-κB/NLRP3 signaling pathway. BWCR, body weight change rate of mice; CL, colon length; DAI, disease activity index. S-IL-1β, IL-1β in serum; S-TNF-α, TNF-α in serum; LPS, LPS in serum; all other factors are relative expressions of mRNAs. The color at each point of intersection indicates the value of the *r* coefficient (n = 22–24). The *Benjamini–Hochberg* (BH) procedures were used to adjust p values for multiple testing. * indicates that there is a significant correlation between these two parameters ($p < 0.05$). *$p < 0.05$, **$p < 0.01$.

a capacity to inhibit NF-κB activation in mice, thereby serving to attenuate DSS-induced acute experimental colitis (Peng et al., 2020). Kaempferol administration was found to exert a protective effect on UC mice by restoring the intestinal microflora and simultaneously inhibiting the LPS-TLR4-NF-κB axis (Qu et al., 2021). Proanthocyanidin extract was found to decrease the protein levels of NF-κB and Keap-1 and increase the expression of Nrf2 and HO-1 proteins in UC mice (Wang et al., 2022). Rutin was found to prevent inflammation by inhibiting the p38/MAPKAPK2 and PI3K/Akt/GSK3β/NF-κB signaling axes in UC mice (Sharma et al., 2021). It is noteworthy that astragalin, kaempferol, proanthocyanidin, and rutin all demonstrated the capacity to impede the activation of the NF-κB-related pathway. These monomers were

identified as predominant constituents within the ATF, thereby offering substantial corroborating evidence for the findings of this study.

In the DSS-induced mouse model of colitis, it is frequently observed to occur concurrently with intestinal inflammation. Macrophage activation permits pro-inflammatory factors to assume an active role in the inflammatory process. Conversely, an excess of pro-inflammatory cytokines induces macrophage polarization, thereby intensifying the inflammatory response (Shapouri-Moghaddam et al., 2018). The present study observed that DSS stimulation increased inflammatory cell infiltration in colon of UC mice, significantly up-regulating the expression levels of inflammatory cell markers *F4/80, CD68, CD11b, CD14,* and *Ly-6G,* as well as the significant expression of the inflammatory factors *TNF-α, IL-1β, COX-2,* and *MCP-1*. This indicates that the ingestion of DSS may have triggered the secretion of pro-inflammatory factors by particular immune cells, thereby contributing to the onset of colitis. Nevertheless, flavonoids have the capacity to regulate the balance of the immune system directly. It has been demonstrated that flavonoid molecules can facilitate the conversion of macrophages from the M1 to the M2 phenotype, thereby alleviating colitis in rats (Tian et al., 2021). Moreover, these molecules have been demonstrated to inhibit the infiltration of TCD3+ cells and CD68+ macrophages in the intestinal mucosa, thereby alleviating colitis by reducing the production of pro-inflammatory cytokines TNF-α and IL6 by macrophages (Du et al., 2019). The ATF intervention was observed to significantly down-regulate the expression of macrophage markers *F4/80*, *CD68*, *CD11b,* and *CD14*, and to inhibit the expression of *TNF-α*, *IL-1β*, *COX-2*, and *MCP-1*, in a manner consistent with the findings of previous literature reports. These observations suggest that ATF may have the potential to prevent colitis by modulating immune cells and inflammatory factors (Figure 2).

A substantial body of clinical evidence indicates that the intestinal barrier plays a pivotal role in maintaining intestinal health. Macrophages within the lamina propria of the normal intestinal mucosa are devoid of CD14. In the event of LPS-induced apoptosis and necrosis of intestinal epithelial cells, a considerable number of CD14+ monocytes are recruited to the mucosal site (He et al., 2016). Concurrently, LPS is readily absorbed into the bloodstream, where it stimulates monocytes to produce substantial quantities of TNF-α and IL-1β. This, in turn, results in the onset of intestinal inflammation and disruption of the intestinal barrier (Gren and Grip, 2016). The current study demonstrated that DSS intake led to a notable elevation in serum LPS levels and a marked up-regulation in the expression of pro-inflammatory mediators, including TNF-α, IL-1β, and CD14. H&E staining results confirmed that the DSS induced the destruction of intestinal epithelial cells and a substantial infiltration of inflammatory cells. However, these effects were markedly attenuated following ATF intervention, accompanied by a notable elevation in *ZO-1*, *Occludin*, and *Claudin-4* expression (Figure 3). This finding is in accordance with the conclusions of Chen et al., who demonstrated that procyanidins can inhibit the expression of NF-κB and NLRP3 inflammatory vesicle signaling induced by LPS (Chen et al., 2018). This process serves to attenuate intestinal barrier damage in mice with colitis. Furthermore, isoquercitrin (Cibiček et al., 2016), quercetin (Wang et al., 2024), and rutin (Wu et al., 2023) have all been found to safeguard the gut barrier by suppressing the production of pro-inflammatory mediators and by enhancing the release of tight junction proteins and mucins.

TLRs/NF-κB signaling pathway represents a crucial link in the pathogenesis of IBD (Kordjazy et al., 2018). As LPS, a Gram-negative bacterial cell wall component present in the intestinal lumen, crosses the damaged intestinal barrier and enters the intestinal mucosal lamina propria, it is recognized by TLR4. Subsequent binding of LPS to TLR4 activates MyD88 and TRAF6 proteins, initiating downstream signaling and releasing NF-κB dimmers into the nucleus. This process prompts the transcription of a series of inflammation-associated genes, thereby triggering the inflammatory response. In the present study, the increase in LPS content may have contributed to the rise in the expression of its receptor TLR4, while promoting a significant rise in the expression of *NF-κB, MyD88,* and *TRAF6* in colon, implying the activation of the NF-κB signaling pathway. The activation of NF-κB has been observed to upregulate the expression of inflammatory vesicle components, including NLRP3, ASC, and the precursor of Caspase-1 (Yang Q. et al., 2022). Formononetin has been demonstrated to reduce the protein levels of the NLRP3 pathway (NLRP3, ASC, and IL-1β) in the DSS-induced acute colitis mice (Wu et al., 2018). Baicalein has been shown to attenuate TNBS-induced colitis by inhibiting the TLR4/MyD88 signaling cascade and inactivating the NLRP3 inflammasome (Luo et al., 2017). Similarly, we also found that ATF significantly inhibited the DSS-induced activation of NF-κB and NLRP3 inflammasome. From this, we speculate that ATF is able to improve UC by inhibiting the LPS/TLR4/NF-κB/NLRP3 signaling axis.

Flavonoids have been demonstrated to exert a beneficial influence on the regulation of gut microbiota (Shen et al., 2022). Our findings indicate that ATF is capable of effectively reversing the abnormalities of gut microbiota observed in UC mice (Figure 5). The specific differential taxa exhibited varying degrees of correlation with pathological phenotypic indices of UC mice, including the body weight change rate of mice (BWCR), colon length (CL), and disease activity index (DAI). It implied that these differential taxa may play a significant role in the alleviation of UC by ATF. Previous clinical data has shown that the relative abundance of *Escherichia-Shigella* in UC patients was significantly higher than that observed in normal patients (He et al., 2021). *Escherichia-Shigella* is a typical genus of Proteobacteria, and is also a major activator of the LPS/TLR4/NF-κB pathway (Tian et al., 2023). In the present study, the relative abundance of *Escherichia-Shigella* in the cecum contents of UC mice induced by DSS was found to be more than 10-fold higher than that of the control mice. ATF treatment was found to significantly reduce the relative abundance of *Escherichia-Shigella*. The relative abundance of *Escherichia-Shigella* showed a strong negative correlation with the BWCR, and the CL showed a strong negative correlation and a strong positive correlation with DAI. Notably, *Escherichia-Shigella* also exhibited a significant positive correlation with LPS, TRAF, and NLRP3, suggesting that the ameliorative effect of ATF on the DSS-induced colitis may be partly mediated by reducing the relative abundance of *Escherichia-Shigella*.

In addition to *Escherichia-Shigella, Desulfovibrio, Colidextribacter,* and *Oscillibacter* are frequently identified as pathogenic genera in UC. *Desulfovibrio* is capable of producing LPS, and studies have

demonstrated that LPS produced by *Desulfovibrio desulfuricans* enhances the transcriptional activity of the NF-κB p65 and IκBα genes in colon intestinal epithelial cells (Kapral et al., 2010). A significant increase in the relative abundance of *Colidextribacter* has been demonstrated to lead to elevated expression levels of NLRP3 inflammasome and a concomitant reduction in the expression of tight junction proteins (Gao et al., 2024). Similarly, *Oscillibacter* may contribute to severe the DSS-induced colitis (Li et al., 2018). The findings of the present study demonstrated that these genera exhibited significant correlations not only with conventional phenotypic indicators of colitis, but also with body inflammation, intestinal barrier function, and the LPS/TLR4/NF-κB/NLRP3 signaling pathway. It was speculated that these genera might also be involved in the process of amelioration of ATF in UC mice.

It has been demonstrated by preceding studies that certain flavonoid monomer components, including phloretin (Wu et al., 2019), rutin (Power et al., 2016), and proanthocyanidin (Sheng et al., 2020), have the capacity to enhance the relative abundance of beneficial bacteria, such as *Bifidobacterium, Akkermansia,* and *unclassified_f__Atopobiaceae,* within the context of the anti-colitis process. The present study found that ATF intervention was also able to significantly increase the relative abundance of these genera, which are associated with the production of short-chain fatty acids. These acids play an important role in maintaining the intestinal barrier (Zeng et al., 2017; Domingo et al., 2008). Meanwhile, *unclassified_f__Atopobiaceae*, *Bifidobacterium*, and *Akkermansia* were found to be significantly and positively correlated with BWCR in UC mice, which was contrary to the findings of DAI. Among them, *unclassified_f__Atopobiaceae* also exhibited a significant negative correlation with several inflammatory factors, including *TLR4*, *NF-κB*, and *NLRP3*. Consequently, *unclassified_f__Atopobiaceae* may be one of the key taxa for ATF in improving UC. Furthermore, in the ATF-treated group, *Akkermansia* was observed to be a highly abundant taxa, although it was not significant in comparison to the DSS group ($p = 0.0712$), *Akkermansia* demonstrated a significant negative correlation with several metrics, particularly the LPS/TLR4/NF-κB/NLRP3 inflammatory signaling pathway. This finding suggests a potential link between *Akkermansia* and ATF-treated UC. In addition to the above taxa, Anaerovoracaceae, *unclassified_f__Anaerovoracaceae*, and *Oscillospiraceae_UCG-005* also exhibited a significant correlation with the UC core indexes. Despite the fact that these taxa have been documented on rare occasions, ATF significantly reversed the aberrant changes of these taxa in UC mice.

In summary, it can be concluded that gut microbiota may play an important role in ATF alleviation of the DSS-induced UC symptoms in mice through modulation of the TLR4/NF-κB/NLRP3 inflammatory signaling pathway, and several classical conditional pathogens (*Escherichia-Shigella*, *Desulfovibrio*, *Colidextribacter* and *Oscillibacter*) and probiotic taxa (*Akkermansia*, *Bifidobacterium* and *unclassified_f__Atopobiaceae*) may be key.

5 Conclusion

In this work, high-dose of ATF (100 mg/kg·bw) has been demonstrated to significantly improve symptoms of the DSS-induced colitis. The experiments results showed that ATF may inhibit the occurrence of colitis phenomena, including weight loss, diarrhea, blood in stool, and colon shortening in UC mice by modulating the microbiota-LPS/TLR4/NF-κB/NLRP3 signaling axis. The correlation network between gut microbiota and UC core indicators provides an important basis for elucidating the important mediating role of gut microbiota in ATF alleviation of UC. Several taxa belonging to the classical conditional pathogens (*Escherichia-Shigella*, *Desulfovibrio*, *Colidextribacter* and *Oscillibacter*) and probiotic taxa (*Akkermansia*, *Bifidobacterium* and *unclassified_f__Atopobiaceae*) may be the key mediators. Despite the evidence from animal experiments demonstrating the efficacy of ATF in the treatment of UC, its application in human subjects remains to be elucidated. Furthermore, the types and levels of flavonoids obtained from ATF extracts are subject to variation, thus necessitating further research to identify the key components of ATF's anti-UC properties. Notwithstanding, this study provides novel insights into the potential of ATF to alleviate intestinal inflammation through dietary intervention, and its multi-targeted characterization of action provides a solid foundation for further research into the development of novel functional foods or plant-derived mucosal repair agents.

Data availability statement

The raw reads of the 16S rRNA gene sequence data were deposited into the NCBI Sequence Read Archive (SRA) database under BioProject accession number PRJNA1204908.

Ethics statement

All the procedures were reviewed and approved by the life science ethics committee of Yunnan agricultural university (Approval no. 202312008). The study was conducted in accordance with the local legislation and institutional requirements.

Author contributions

ZH: Data curation, Investigation, Methodology, Software, Validation, Writing – original draft. YZ: Funding acquisition, Investigation, Methodology, Software, Validation, Visualization, Writing – original draft. WY: Data curation, Software, Writing – original draft. CD: Investigation, Methodology, Writing – original draft. JS: Resources, Supervision, Writing – review & editing. YT: Funding acquisition, Supervision, Writing – review & editing. LP: Conceptualization, Resources, Software, Writing – review & editing. XG: Conceptualization, Funding acquisition, Investigation, Resources, Supervision, Writing – review & editing.

Funding

The author(s) declare that financial support was received for the research, authorship, and/or publication of this article. This research was funded by the Xingdian talent plan of Yunnan Province (Young talents project, 2022–0255), Yunnan Fundamental Research Projects (202401AT070217 and 202401AT070216), Scientific Research Fund

of Yunnan Provincial Department of Education (2024J0478), and Yunnan Province-City Integration Project (202302AN360002).

Conflict of interest

The authors declare that the research was conducted in the absence of any commercial or financial relationships that could be construed as a potential conflict of interest.

Generative AI statement

The author(s) declare that no Gen AI was used in the creation of this manuscript.

Publisher's note

All claims expressed in this article are solely those of the authors and do not necessarily represent those of their affiliated organizations, or those of the publisher, the editors and the reviewers. Any product that may be evaluated in this article, or claim that may be made by its manufacturer, is not guaranteed or endorsed by the publisher.

Supplementary material

The Supplementary material for this article can be found online at: https://www.frontiersin.org/articles/10.3389/fmicb.2025.1557778/full#supplementary-material

References

Cai, R., Yue, X., Wang, Y., Yang, Y., Sun, D., Li, H., et al. (2021). Chemistry and bioactivity of plants from the genus Amomum. *J. Ethnopharmacol.* 281:114563. doi: 10.1016/j.jep.2021.114563

Cao, S. Y., Ye, S. J., Wang, W. W., Wang, B., Zhang, T., and Pu, Y. Q. (2019). Progress in active compounds effective on ulcerative colitis from Chinese medicines. *Chin. J. Nat. Med.* 17, 81–102. doi: 10.1016/S1875-5364(19)30012-3

Chaen, Y., Yamamoto, Y., and Suzuki, T. (2019). Naringenin promotes recovery from colonic damage through suppression of epithelial tumor necrosis factor-α production and induction of M2-type macrophages in colitic mice. *Nutr. Res.* 64, 82–92. doi: 10.1016/j.nutres.2019.01.004

Chen, L., You, Q., Hu, L., Gao, J., Meng, Q., Liu, W., et al. (2018). The antioxidant procyanidin reduces reactive oxygen species signaling in macrophages and ameliorates experimental colitis in mice. *Front. Immunol.* 8:1910. doi: 10.3389/fimmu.2017.01910

Cibiček, N., Roubalová, L., Vrba, J., Zatloukalová, M., Ehrmann, J., Zapletalová, J., et al. (2016). Protective effect of isoquercitrin against acute dextran sulfate sodium-induced rat colitis depends on the severity of tissue damage. *Pharmacol. Rep.* 68, 1197–1204. doi: 10.1016/j.pharep.2016.07.007

Di Tommaso, N., Gasbarrini, A., and Ponziani, F. R. (2021). Intestinal barrier in human health and disease. *Int. J. Environ. Res. Public Health* 18:12836. doi: 10.3390/ijerph182312836

Domingo, M. C., Huletsky, A., Boissinot, M., Bernard, K. A., Picard, F. J., and Bergeron, M. G. (2008). *Ruminococcus gauvreauii* sp. nov., a glycopeptide-resistant species isolated from a human faecal specimen. *Int. J. Syst. Evol. Microbiol.* 58, 1393–1397. doi: 10.1099/ijs.0.65259-0

Du, Y., Ding, H., Vanarsa, K., Soomro, S., Baig, S., Hicks, J., et al. (2019). Low dose epigallocatechin Gallate alleviates experimental colitis by subduing inflammatory cells and cytokines, and improving intestinal permeability. *Nutrients* 11:1743. doi: 10.3390/nu11081743

Gadaleta, R. M., Garcia-Irigoyen, O., and Moschetta, A. (2017). Exploration of inflammatory bowel disease in mice: chemically induced murine models of inflammatory bowel disease (IBD). *Curr. Protoc. Mouse Biol.* 7, 13–28. doi: 10.1002/cpmo.20

Gao, Q., Tian, W., Yang, H., Hu, H., Zheng, J., Yao, X., et al. (2024). Shen-Ling-Bai-Zhu-san alleviates the imbalance of intestinal homeostasis in dextran sodium sulfate-induced colitis mice by regulating gut microbiota and inhibiting the NLRP3 inflammasome activation. *J. Ethnopharmacol.* 319:117136. doi: 10.1016/j.jep.2023.117136

Gren, S. T., and Grip, O. (2016). Role of monocytes and intestinal macrophages in Crohn's disease and ulcerative colitis. *Inflamm. Bowel Dis.* 22, 1992–1998. doi: 10.1097/MIB.0000000000000824

Håkansson, Å., Tormo-Badia, N., Baridi, A., Xu, J., Molin, G., Hagslätt, M. L., et al. (2015). Immunological alteration and changes of gut microbiota after dextran sulfate sodium (DSS) administration in mice. *Clin. Exp. Med.* 15, 107–120. doi: 10.1007/s10238-013-0270-5

He, X. X., Li, Y. H., Yan, P. G., Meng, X. C., Chen, C. Y., Li, K. M., et al. (2021). Relationship between clinical features and intestinal microbiota in Chinese patients with ulcerative colitis. *World J. Gastroenterol.* 27, 4722–4737. doi: 10.3748/wjg.v27.i28.4722

He, Y., Liu, S., Kling, D. E., Leone, S., Lawlor, N. T., Huang, Y., et al. (2016). The human milk oligosaccharide 2′-fucosyllactose modulates CD14 expression in human enterocytes, thereby attenuating LPS-induced inflammation. *Gut* 65, 33–46. doi: 10.1136/gutjnl-2014-307544

Hu, Y., Gao, X., Zhao, Y., Liu, S., Luo, K., Fu, X., et al. (2023). Flavonoids in Amomum tsaoko Crevost et Lemarie ameliorate Loperamide-induced constipation in mice by regulating gut microbiota and related metabolites. *Int. J. Mol. Sci.* 24:7191. doi: 10.3390/ijms24087191

Hu, Y. F., Zhang, X. M., Xu, S. Z., Yang, S. C., and Yang, Z. Q. (2018). Analysis of genetic diversity and genetic relationship of Amomum tsao-ko germplasm resources in Yunnan by SSR markers. *Chin. Herb Med.* 49, 5388–5395. doi: 10.7501/j.issn.0253-2670.2018.22.025

Huang, Z., Zhao, Y., Yang, W., Lang, L., Sheng, J., Tian, Y., et al. (2025). Preparation of flavonoids from *Amomum tsaoko* and evaluation of their antioxidant and α-glucosidase inhibitory activities. *Food Chem* 25:102177. doi: 10.1016/j.fochx.2025.102177

Kapral, M., Węglarz, L., Parfiniewicz, B., Lodowska, J., and Jaworska-Kik, M. (2010). Quantitative evaluation of transcriptional activation of NF-κB p65 and p50 subunits and IκBα encoding genes in colon cancer cells by *Desulfovibrio desulfuricans* endotoxin. *Folia Microbiol.* 55, 657–661. doi: 10.1007/s12223-010-0106-6

Kim, S. G., Becattini, S., Moody, T. U., Shliaha, P. V., Littmann, E. R., Seok, R., et al. (2019). Microbiota-derived lantibiotic restores resistance against vancomycin-resistant Enterococcus. *Nature* 572, 665–669. doi: 10.1038/s41586-019-1501-z

Kim, S. E., Kawaguchi, K., Hayashi, H., Furusho, K., and Maruyama, M. (2019). Remission effects of dietary soybean Isoflavones on DSS-induced murine colitis and an LPS-activated macrophage cell line. *Nutrients* 11:1746. doi: 10.3390/nu11081746

Klein, A., and Eliakim, R. (2010). Non steroidal anti-inflammatory drugs and inflammatory bowel disease. *Pharmaceuticals* 3, 1084–1092. doi: 10.3390/ph3041084

Kordjazy, N., Haj-Mirzaian, A., Haj-Mirzaian, A., Rohani, M. M., Gelfand, E. W., Rezaei, N., et al. (2018). Role of toll-like receptors in inflammatory bowel disease. *Pharmacol. Res.* 129, 204–215. doi: 10.1016/j.phrs.2017.11.017

Li, M., Wu, Y., Hu, Y., Zhao, L., and Zhang, C. (2018). Initial gut microbiota structure affects sensitivity to DSS-induced colitis in a mouse model. *Sci. China Life Sci.* 61, 762–769. doi: 10.1007/s11427-017-9097-0

Liu, H., Chen, R., Wen, S., Li, Q., Lai, X., Zhang, Z., et al. (2023). Tea (*Camellia sinensis*) ameliorates DSS-induced colitis and liver injury by inhibiting TLR4/NF-κB/NLRP3 inflammasome in mice. *Biomed. Pharmacother.* 158:114136. doi: 10.1016/j.biopha.2022.114136

Luo, X., Yu, Z., Deng, C., Zhang, J., Ren, G., Sun, A., et al. (2017). Baicalein ameliorates TNBS-induced colitis by suppressing TLR4/MyD88 signaling cascade and NLRP3 inflammasome activation in mice. *Sci. Rep.* 7:16374. doi: 10.1038/s41598-017-12562-6

Pauly, N. J., Michailidis, L., Kindred, M. G., Flomenhoft, D., Lofwall, M. R., Walsh, S. L., et al. (2017). Predictors of chronic opioid use in newly diagnosed Crohn's disease. *Inflamm. Bowel Dis.* 23, 1004–1010. doi: 10.1097/MIB.0000000000001087

Pei, L. Y., Ke, Y. S., Zhao, H. H., Wang, L., Jia, C., Liu, W. Z., et al. (2019). Role of colonic microbiota in the pathogenesis of ulcerative colitis. *BMC Gastroenterol.* 19:10. doi: 10.1186/s12876-019-0930-3

Peng, L., Gao, X., Nie, L., Xie, J., Dai, T., Shi, C., et al. (2020). Astragalin attenuates dextran sulfate sodium (DSS)-induced acute experimental colitis by alleviating gut microbiota Dysbiosis and inhibiting NF-κB activation in mice. *Front. Immunol.* 11:2058. doi: 10.3389/fimmu.2020.02058

Powell, N., Lo, J. W., Biancheri, P., Vossenkämper, A., Pantazi, E., Walker, A. W., et al. (2015). Interleukin 6 increases production of cytokines by colonic innate lymphoid cells in mice and patients with chronic intestinal inflammation. *Gastroenterology* 149, 456–67.e15. doi: 10.1053/j.gastro.2015.04.017

Power, K. A., Lu, J. T., Monk, J. M., Lepp, D., Wu, W., Zhang, C., et al. (2016). Purified rutin and rutin-rich asparagus attenuates disease severity and tissue damage following dextran sodium sulfate-induced colitis. *Mol. Nutr. Food Res.* 60, 2396–2412. doi: 10.1002/mnfr.201500890

Qu, Y., Li, X., Xu, F., Zhao, S., Wu, X., Wang, Y., et al. (2021). Kaempferol alleviates murine experimental colitis by restoring gut microbiota and inhibiting the LPS-TLR4-NF-κB Axis. *Front. Immunol.* 12:679897. doi: 10.3389/fimmu.2021.679897

Shapouri-Moghaddam, A., Mohammadian, S., Vazini, H., Taghadosi, M., Esmaeili, S. A., Mardani, F., et al. (2018). Macrophage plasticity, polarization, and function in health and disease. *J. Cell. Physiol.* 233, 6425–6440. doi: 10.1002/jcp.26429

Sharma, A., Tirpude, N. V., Kumari, M., and Padwad, Y. (2021). Rutin prevents inflammation-associated colon damage via inhibiting the p38/MAPKAPK2 and PI3K/Akt/GSK3β/NF-κB signalling axes and enhancing splenic Tregs in DSS-induced murine chronic colitis. *Food Funct.* 12, 8492–8506. doi: 10.1039/d1fo01557e

Shen, N., Wang, T., Gan, Q., Liu, S., Wang, L., and Jin, B. (2022). Plant flavonoids: classification, distribution, biosynthesis, and antioxidant activity. *Food Chem.* 383:132531. doi: 10.1016/j.foodchem.2022.132531

Sheng, K., Zhang, G., Sun, M., He, S., Kong, X., Wang, J., et al. (2020). Grape seed proanthocyanidin extract ameliorates dextran sulfate sodium-induced colitis through intestinal barrier improvement, oxidative stress reduction, and inflammatory cytokines and gut microbiota modulation. *Food Funct.* 11, 7817–7829. doi: 10.1039/d0fo01418d

Sun, Y., Zhang, Z., Zheng, C. Q., and Sang, L. X. (2021). Mucosal lesions of the upper gastrointestinal tract in patients with ulcerative colitis: a review. *World J. Gastroenterol.* 27, 2963–2978. doi: 10.3748/wjg.v27.i22.2963

Suzuki, T., and Hara, H. (2009). Quercetin enhances intestinal barrier function through the assembly of zonula [corrected] occludens-2, occludin, and claudin-1 and the expression of claudin-4 in Caco-2 cells. *J. Nutr* 139, 965–974. doi: 10.3945/jn.108.100867

Tian, G., Wang, W., Xia, E., Chen, W., and Zhang, S. (2023). Dendrobium officinale alleviates high-fat diet-induced nonalcoholic steatohepatitis by modulating gut microbiota. *Front. Cell. Infect. Microbiol.* 13:1078447. doi: 10.3389/fcimb.2023.1078447

Tian, L., Zhao, J. L., Kang, J. Q., Guo, S. B., Zhang, N., Shang, L., et al. (2021). Astragaloside IV alleviates the experimental DSS-induced colitis by remodeling macrophage polarization through STAT signaling. *Front. Immunol.* 12:740565. doi: 10.3389/fimmu.2021.740565

Wang, X., Quan, S., Li, J., Liu, Y., Sun, H., Zhang, J., et al. (2022). Protective effects of grape seed proanthocyanidin extract in preventing DSS induced ulcerative colitis based on Pharmacodynamic, pharmacokinetic and tissue distribution. *Curr. Drug Metab.* 23, 496–505. doi: 10.2174/1389200223666220609151836

Wang, X., Xie, X., Li, Y., Xie, X., Huang, S., Pan, S., et al. (2024). Quercetin ameliorates ulcerative colitis by activating aryl hydrocarbon receptor to improve intestinal barrier integrity. *Phytother. Res.* 38, 253–264. doi: 10.1002/ptr.8027

Whan, C. C., Young, S. J., Changon, S., Su, H. S., Eun-Kyung, A., Hoon, J. Y., et al. (2018). In vitro anti-inflammatory activity of the components of amomum tsao-ko in murine macrophage raw 264.7 cells. *Afr. J. Tradit. Complement. Altern. Med.* 15, 26–34. doi: 10.21010/ajtcamv15i2.4

Wu, M., Li, P., An, Y., Ren, J., Yan, D., Cui, J., et al. (2019). Phloretin ameliorates dextran sulfate sodium-induced ulcerative colitis in mice by regulating the gut microbiota. *Pharmacol. Res.* 150:104489. doi: 10.1016/j.phrs.2019.104489

Wu, W., Liu, L., Zhu, Y., Ni, J., Lu, J., Wang, X., et al. (2023). Zinc-Rutin particles ameliorate DSS-induced acute and chronic colitis via anti-inflammatory and antioxidant protection of the intestinal epithelial barrier. *J. Agric. Food Chem.* 71, 12715–12729. doi: 10.1021/acs.jafc.3c03195

Wu, D., Wu, K., Zhu, Q., Xiao, W., Shan, Q., Yan, Z., et al. (2018). Formononetin administration ameliorates dextran sulfate sodium-induced acute colitis by inhibiting NLRP3 Inflammasome signaling pathway. *Mediat. Inflamm.* 2018, 3048532–3048512. doi: 10.1155/2018/3048532

Yang, J., Xia, X., Du, M., Cheng, S., Zhu, B., and Xu, X. (2024). Highly effective Nobiletin-MPN in yeast microcapsules for targeted modulation of oxidative stress, NLRP3 Inflammasome activation, and immune responses in ulcerative colitis. *J. Agric. Food Chem.* 72, 13054–13068. doi: 10.1021/acs.jafc.3c09530

Yang, S., Xue, Y., Chen, D., and Wang, Z. (2022). Amomum tsao-ko Crevost and Lemarié: a comprehensive review on traditional uses, botany, phytochemistry, and pharmacology. *Phytochem. Rev.* 21, 1487–1521. doi: 10.1007/s11101-021-09793-x

Yang, Q., Zhang, J., Liu, F., Chen, H., Zhang, W., Yang, H., et al. (2022). *A. caviae* infection triggers IL-1β secretion through activating NLRP3 inflammasome mediated by NF-κB signaling pathway partly in a TLR2 dependent manner. *Virulence* 13, 1486–1501. doi: 10.1080/21505594.2022.2116169

Zeng, H., Huang, C., Lin, S., Zheng, M., Chen, C., Zheng, B., et al. (2017). Lotus seed resistant starch regulates gut microbiota and increases short-chain fatty acids production and mineral absorption in mice. *J. Agric. Food Chem.* 65, 9217–9225. doi: 10.1021/acs.jafc.7b02860

Zhang, X. F., Tang, Y. J., Guan, X. X., Lu, X., Li, J., Chen, X. L., et al. (2022). Flavonoid constituents of Amomum tsao-ko Crevost et Lemarie and their antioxidant and antidiabetic effects in diabetic rats – in vitro and in vivo studies. *Food Funct.* 13, 437–450. doi: 10.1039/d1fo02974f

Zhen, Y., and Zhang, H. (2019). NLRP3 Inflammasome and inflammatory bowel disease. *Front. Immunol.* 10:276. doi: 10.3389/fimmu.2019.00276

frontiers | Frontiers in Microbiology

TYPE Original Research
PUBLISHED 25 March 2025
DOI 10.3389/fmicb.2025.1530156

Check for updates

OPEN ACCESS

EDITED BY
Guiguo Zhang,
Shandong Agricultural University, China

REVIEWED BY
Jinrong Wang,
Henan University of Technology, China
Guosheng Xin,
Ningxia University, China
Dennis Savaiano,
Purdue University, United States

*CORRESPONDENCE
Bing Dong
✉ dongbing@cau.edu.cn

RECEIVED 19 November 2024
ACCEPTED 21 February 2025
PUBLISHED 25 March 2025

CITATION
Li Q, Wang X, Guo S, Wang T, Cao H, Cao Y and Dong B (2025)
Galacto-oligosaccharides alleviate experimental lactose intolerance associated with gut microbiota in mice.
Front. Microbiol. 16:1530156.
doi: 10.3389/fmicb.2025.1530156

COPYRIGHT
© 2025 Li, Wang, Guo, Wang, Cao, Cao and Dong. This is an open-access article distributed under the terms of the Creative Commons Attribution License (CC BY). The use, distribution or reproduction in other forums is permitted, provided the original author(s) and the copyright owner(s) are credited and that the original publication in this journal is cited, in accordance with accepted academic practice. No use, distribution or reproduction is permitted which does not comply with these terms.

Galacto-oligosaccharides alleviate experimental lactose intolerance associated with gut microbiota in mice

Qianxi Li, Xinlei Wang, Siyu Guo, Tongtong Wang, Heng Cao, Yunhe Cao and Bing Dong*

State Key Laboratory of Animal Nutrition and Feeding, College of Animal Science and Technology, China Agricultural University, Beijing, China

Introduction: Galacto-oligosaccharides (GOS) are beneficial for alleviating lactose intolerance (LI). GOS have the ability to modify the composition of the intestinal microbiota. The development of intestinal diseases could be influenced by the composition of the gut microbiota. Nevertheless, it remains unclear whether gut microbiota exerts an effect when GOS alleviate LI, whether alterations in composition of the intestinal microbiota influence inflammatory response and lactose digestion.

Methods: We first investigated the effects of GOS on mice with established lactose intolerance. Next, we demonstrated that prophylactic supplementation with GOS also conferred similar benefits.

Results: The results showed that GOS enhanced anti-inflammatory, antioxidant, and gut barrier function. We observed that GOS mediated a change in the gut microbiome by increasing the abundance of *Lactobacillus*. GOS pre-supplementation reduced incident LI, enhanced anti-inflammatory, antioxidant, and gut barrier function, and markedly altered the gut microbiome by significantly enriching *Bifidobacterium*. Collectively, the alleviation of LI by GOS suggests an intimate involvement of probiotics.

Discussion: This study demonstrates that GOS ameliorated LI in a gut microbiota-dependent manner. Our findings provide novel evidence that GOS substitute for lactase and serve as a potential modulator of the gut microbiota for the prevention of LI.

KEYWORDS

galacto-oligosaccharides, lactose intolerance, gut microbiota, mice, lactase

1 Introduction

Lactose intolerance (LI) is a global issue in public health management. Approximately two-thirds of the population have LI all over the world (Toca et al., 2022). The clinical manifestations of LI encompass abdominal distension, abdominal pain, nausea, increased intestinal peristalsis, and diarrhea. Accumulation of undigested lactose in the intestinal lumen leads to an elevated osmotic pressure which cause hyperosmotic diarrhea. Simultaneously, the fermentation of lactose by intestinal microbiota generates

volatile fatty acids and gases such as hydrogen, methane, and carbon dioxide (Vandenplas, 2015). Currently, the primary therapeutic strategies for LI involve restricting intake of lactose-containing dairy products (milk, soft cheese, and ice cream) or using lactase supplements concurrent with dairy consumption. Blind avoidance of dairy products results in a significant decrease in calcium intake and increased risk of chronic diseases such as low bone density, osteoporosis and their sequelae among many lactose intolerant patients (Obermayer-Pietsch et al., 2004; Ross et al., 2011). Interestingly, elevated milk intake among lactose intolerant individuals decreases risk of type 2 diabetes (Luo et al., 2024). Hence, it is of great significance to assist lactose intolerant patients in developing tolerance to lactose.

Intestinal tolerance to lactose could be established through adaptation of the intestinal microbiota (Szilagyi et al., 2010; Azcarate-Peril et al., 2021). This adaptive mechanism encompasses increasing abundance and diversity of lactose-metabolizing bacteria which induces production of β-galactosidase by microorganisms (Hertzler and Savaiano, 1996), and enhances utilization rate of hydrogen generated during fermentation (Hertzler et al., 1997). These adaptions enable rapid metabolism of lactose by the intestinal microbiota. Intestinal microbiota served as a crucial bridge between environmental factors and host health (Kamada et al., 2013). Galacto-oligosaccharides (GOS) can alter the composition of the intestinal microbiota, as a "Bifidus Factor," by increasing abundances of *Bifidobacterium* (Andersen et al., 2011). Dysbiosis of the intestinal microbiota is a characteristic of intestinal diseases. One therapeutic strategy to correct dysbiosis is to increase the proportion of beneficial bacteria in the intestinal microbiota (Zhang et al., 2020).

Researched have evaluated whether GOS alleviates clinical symptoms of LI in humans, using the hydrogen breath test (HBT) and conducting regular follow-up exams. Savaiano et al. (2013) continuously supplemented LI patients with a GOS formulation for 35 days. Subsequently, the patients reintroduced dairy products into their daily diet and underwent an additional 30-day follow-up. Chey et al. (2020) also conducted similar researches. These studies revealed patients exhibited a tendency for improvement in both lactose digestion and lactose intolerance symptoms. However, the specific mechanism remains unclear. Studies of GOS supplementation in human are useful but have significant flaws. The inconsistent diet of lactose intolerant patients, the strong subjectivity of patient reports, and the small sample size are significant limitations of human studies. Therefore, it is necessary to establish animal models to further explore the underlying mechanisms.

Lactase activity of C57BL/6 mice is extremely high before weaning, but drops sharply after weaning. Lactase activity of these mice 8 weeks postweaning is very low, and similar to that of adult humans (Detel et al., 2008). C57BL/6 mice after weaning can serve as an ideal animal model for the study of lactose intolerance.

Abbreviations: GOS, galacto-oligosaccharides; LI, lactose intolerance; BW, body weight; HBT, hydrogen breath test; SPF, specific pathogen-free; BCA, bicinchoninic acid; ELISA, enzyme-linked immunosorbent assay; ROS, reactive oxygen species; T-SOD, total superoxide dismutase; CAT, catalase; GSH-Px, glutathione peroxidase; MDA, malondialdehyde; PCoA, principal coordinate analysis.

In this study, to explore the potential alleviative effect of GOS in treatment or prevent of lactose intolerance, we investigated the effect of GOS in lactose induced LI mice and measured the indices related to intestinal inflammation, oxidative stress, and barrier dysfunction and the alteration of intestinal microbiota. The underlying mechanisms of GOS were also studied.

2 Materials and methods

2.1 Animals

Eight-week-old male mice (C57BL/6N) status (SPF Biotechnology Co., Ltd., Beijing, China), with an initial body weight of 21.56 ± 0.13 g were used in this study. Feed (AIN-93) required for the mice during the experiment was sourced from Xiaoshu Youtai Biotechnology Co., Ltd (Beijing, China). Six animals were housed in each cage and kept in the standard specific pathogen-free (SPF) facilities of China Agricultural University. The light/dark cycle in the experimental rooms was 12 h of light and 12 h of darkness daily, with a temperature of 22°C and a humidity of 50%. The experimental protocol was approved by the Animal Experiment Ethics Committee of the Experimental Animal Center of China Agricultural University, with the approval number AW91603202-1-1. The experimental process adhered to the "Authors' Guide to Consensus on Animal Ethics and Welfare" of the International Association of Veterinary Editors and local and national regulations. Mice were dosed with lactose (molecular weight 342, purity ≥ 98%, Macklin Biochemical Technology Co., Ltd, Shanghai, China). GOS (0.5 g/d, purity ≥ 98%, Macklin Biochemical Technology Co., Ltd, Shanghai, China) was administered to mice by oral gavage. The oligomers of GOS was 3 to 5. Lactase (Cangzhou SUNSON Enzyme Bioctechnology Co., Ltd, Hebei, China).

2.2 Treatments and sample collection

To ascertain the success of lactose intolerance modeling, Experiment 1 was conducted, a total of 16 mice (n = 8/group). After one-week of acclimation, mice were divided randomly into two treatment groups, with 8 mice in each group. To build the LI model, mice, fed a normal diet of AIN-93 (Supplementary Table 1), were gavaged with 200 μL saline containing lactose (50 mg/20 g BW) with the intragastric needle daily. Mice in the experimental group (lac) were gavaged orally with lactose for 7 days to build up lactose intolerance, while mice in the control group (con) were gavaged with an equal volume of saline. After 7 days, mice were sacrificed, and their histological changes, changes in concentration of blood inflammatory factors level. The intestinal tissues of the ileum and jejunum were subjected to histological examination by Hematoxylin and Eosin (H&E) staining. The diarrhea condition was measured after lactose challenging, mice were fasted for 12 h in advance, and then were allowed to access food and water. The number of defecations and the total fecal mass were recorded within 6 h after lactose administration (Li et al., 2012).

To investigate if GOS could mitigate lactose intolerance, Experiment 2 was conducted with a total of 16 mice (n = 8/group).

10.3389/fmicb.2025.1530156

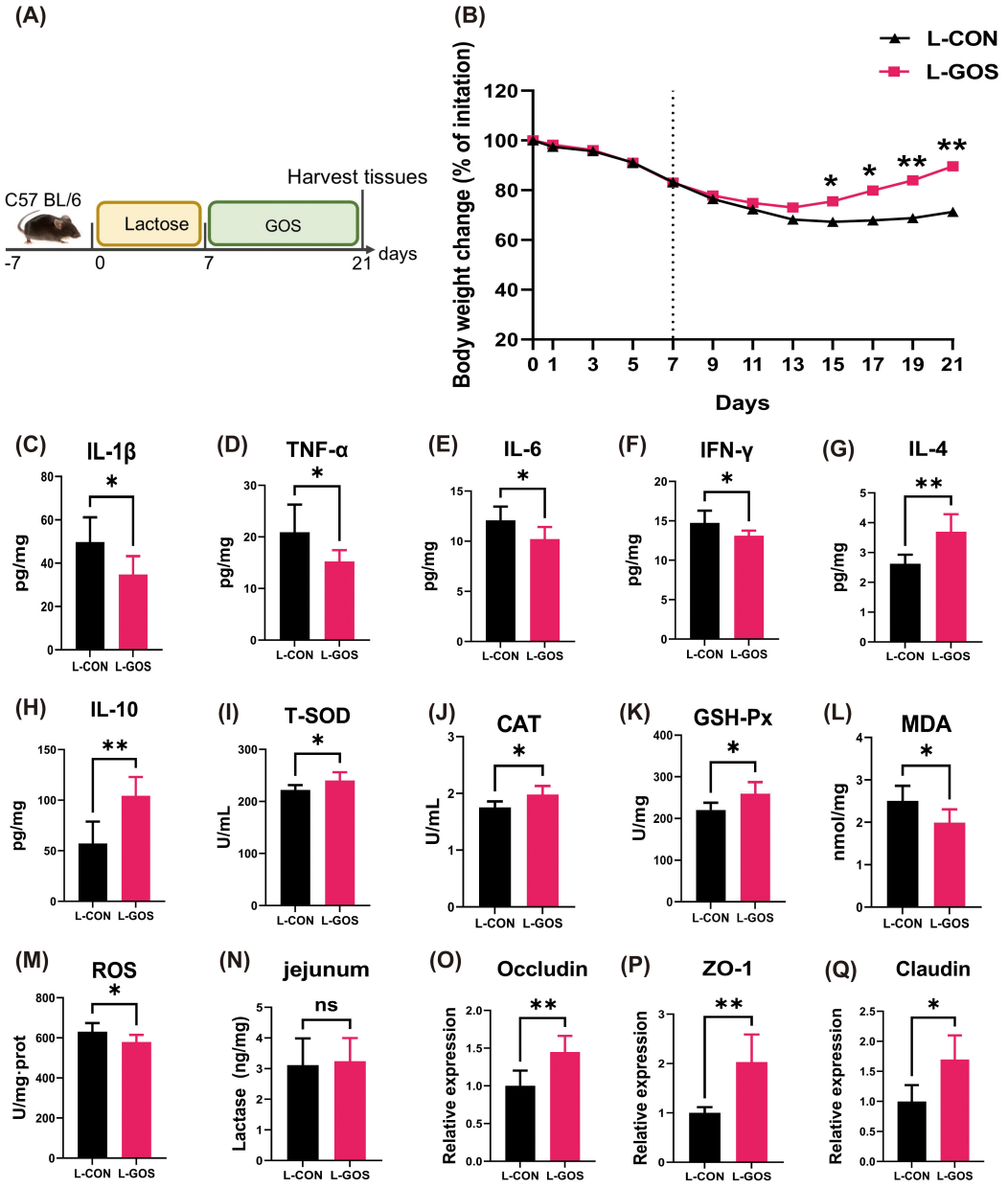

FIGURE 1
GOS alleviated lactose-induced experimental LI. **(A)** Diagram illustrating the mouse model of LI employed in this study. **(B)** Oral normal saline and GOS treatments are indicated. Daily body weight changes throughout the entire duration of the study. **(C–H)** Concentrations of four representative pro-inflammatory cytokines, IL-1β, TNF-α, IL-6, IFN-γ, and anti-inflammatory cytokines, IL-4, IL-10 in the ileum. **(I–M)** GOS attenuated oxidative stress and jejunal damage. Concentrations of T-SOD, CAT, GSH-Px, MDA and ROS in the ileum from each group. **(N)** Concentrations of β-galactosidase in jejunum. **(O–Q)** Relative expression jejunal level of Occludin, ZO-1, Claudin mRNA in mice. Data were presented as means ± SEM (n = 8 per group). Statistical significance was determined using one-way ANOVA, followed by Tukey test. *$P \leq 0.05$, **$P \leq 0.01$.

After one week of acclimatization, male mice were assigned randomly to one of two treatment groups, with 8 mice in each group (Figure 1A). Mice were gavaged orally with lactose for 7 days to build up lactose intolerance, and then daily gavaged with saline (200 μL) or the same volume of saline containing 0.5 g of GOS for 14 days. The treatment groups were as follows: (1) L-CON group: gavaged with lactose for 7 days and followed by saline for 14 days; (2) L-GOS group: gavaged with lactose for 7 days and followed by GOS for 14 days.

Throughout the entire research period, body weight of mice was measured daily. On the 21st day, mice were sacrificed, and cecal chyme samples from all mice were collected aseptically and stored at −80°C for future analysis. The middle segments of the jejunum (2 cm) and ileum (2 cm) were rinsed with physiological saline and rapidly frozen in liquid nitrogen for measurement of inflammatory cytokines, antioxidant indices, barrier injury and lactase.

To investigate the potential preventive effect of GOS in LI mice, Experiment 3 was conducted with a total of 36 mice (n = 6/group). After one week of acclimation, mice were divided randomly into

six groups, with 6 mice in each group (Figure 3A). For three weeks, mice were gavaged orally with saline (200 μL) or the same volume of saline containing GOS daily. Subsequently, mice were gavaged orally for 5 days with saline (200 μL) or the same volume of saline containing lactose daily to induce lactose intolerance. The treatment groups were as follows: (1) CON group: daily gavage with saline for three weeks,; (2) GOS group: daily gavage with saline containing 0.5 g of GOS for three weeks; (3) Gal group: daily gavage with saline containing lactase for three weeks; (4) CON-L group: daily gavage with saline for three weeks, followed by five consecutive days of lactose gavage; (5) GOS-L group: daily gavage with saline containing 0.5 g of GOS for three weeks, followed by five consecutive days of lactose gavage; (6) Gal-L group: daily gavage with saline containing lactose for three weeks, and finally five days of lactose gavage. Thirty minutes before the daily gavage of lactose, lactase was gavaged first. CON, GOS and Gal groups were gavaged with an equal volume of saline at 21–26 days. From day 21 to day 26, body weight was measured daily. All mice were euthanized under anesthesia on the 26th day. Cecal chyme samples from all mice were collected aseptically and stored at −80°C for future analysis. The middle segments of the jejunum and ileum were rinsed with saline and rapidly frozen in liquid nitrogen for measurement of inflammatory cytokines, antioxidant indexes, barrier injury and lactase.

2.3 Quantification of inflammatory cytokines, antioxidant indexes in the ileum and barrier injury in the jejunum

A part of the frozen ileum samples was homogenized with RIPA lysis buffer (Solarbio, Beijing, China) to extract total protein. The homogenate was centrifuged at 12,000 × *g* at 4°C for 15 min. Protein content was quantified using a bicinchoninic acid (BCA) protein assay kit (Solarbio, Beijing, China) in accordance with the manufacturer's instructions. Concentrations of pro-inflammatory cytokines such as IL-1β, IL-6, TNF-α, and IFN-γ, and anti-inflammatory cytokines such as IL-4 and IL-10 in ileal tissue were measured using an enzyme-linked immunosorbent assay (ELISA) (R&D Systems, Minneapolis, MN, USA) as per the manufacturer's recommendations. Concentrations of representative redox enzymes such as total superoxide dismutase (T-SOD), catalase (CAT), glutathione peroxidase (GSH-Px), and concentrations of malondialdehyde (MDA) were quantified using commercial kits (Nanjing Jiancheng Bioengineering Institute, Nanjing, China), and the concentration of reactive oxygen species (ROS) was quantified using the probe method. To assess the effect of GOS on the integrity of the intestinal barrier, mRNA expression levels of tight junction proteins Occludin, ZO-1, and Claudin in the jejunum of mice were measured.

2.4 DNA extraction and 16S rRNA gene sequencing

Total microbial genomic DNA in each sample of cecal chyme was extracted using the E.Z.N.A.® Soil DNA Kit (Omega Bio-Tek, USA). Concentration and integrity of the DNA were evaluated using Agarose 75510019 (Thermo Fisher Scientific, USA) and 1.5% agarose gel electrophoresis, respectively. Subsequently, diluted DNA (1.0 ng/mL) was used to amplify the V3-V4 hypervariable region of the 16S rRNA gene with primers (forward primer 338F: ACTCCTACGGGAGGCAGCAG; reverse primer 806R: GGACTACHVGGGTWTCTAAT). The PCR products were subjected to 2.0% agarose gel electrophoresis, recovered, and purified using the GeneJET Gel Extraction Kit (Thermo Fisher Scientific, USA). The PCR products were quantified using Qubit 4.0 (Thermo Fisher Scientific, USA). According to sequencing requirements for each sample, samples were mixed in the corresponding proportions. The library was constructed using the NEXTFLEX Rapid DNA-Seq Kit and sequenced on the Illumina Miseq PE300 platform (Shanghai Majorbio Biomedical Technology Co., Ltd., Shanghai, China). The microbial sequencing results of Experiments 2 and 3 were deposit to NCBI (BioProject ID: PRJNA1209674 and PRJNA1209660).

2.5 Statistical analysis

All data are presented as the mean ± SEM and analyzed using the GraphPad Prism 9.5 program (GraphPad Software, San Diego, CA, USA). Data from two groups were analyzed using the *t*-test, and data from more than two groups were analyzed using one-way ANOVA followed by Tukey's multiple comparison test. An adjusted $P < 0.05$ was considered statistically significant.

All data analyses were performed on the Majorbio Cloud Platform[1] as follows: The Alpha diversity metrics such as Chao, Sobs and Shannon index were calculated using the mothur (Schloss et al., 2009) software,[2] and the inter-group differences in Alpha diversity were analyzed using the Wilcoxon rank sum test. The PCoA analysis (principal coordinate analysis) based on the Bray-Curtis distance algorithm was used to examine similarity of the microbial community structure among samples, and the PERMANOVA non-parametric test was combined to analyze whether the differences in the microbial community structure among sample groups were significant. Based on a Spearman correlation of $|r| > 0.6$ and $p < 0.05$, species were selected for the correlation network diagram analysis (Barberán et al., 2012).

3 Results

3.1 Successful induction of lactose intolerance model

Obvious changes in intestinal morphology could be observed (Supplementary Figures 1a–d). The tips of the intestinal villi were incomplete, and a large number of white blood cells were aggregated. The levels of intestinal pro-inflammatory cytokines IL-1β and TNF-α significantly increased (Supplementary Figures 1e,f). On the 7th day, 6 h after the lactose challenge, no significant difference in fecal frequency was found between

1 https://cloud.majorbio.com

2 http://www.mothur.org/wiki/calculators

the two groups. Compared with the con group mice, the total fecal weight significantly increased in the lac group (Supplementary Figure 1g). The picture (Supplementary Figure 1h) showed the LI mice intestinal morphology on day 7 of lactose challenge.

3.2 GOS promoted recovery after lactose intolerance in mice

3.2.1 GOS alleviated LI-induced intestinal inflammation

Experiment 1 (Figure 1A). Mice fed with lactose for seven days lost body weight through day 15 of the experiment (Figure 1B). Even after cessation of lactose feeding, the body weight still exhibited a downward trend. Mice treated with GOS demonstrated reduced weight loss, an earlier inflection point for weight recovery, and a faster recovery tendency.

To assess the impact of GOS on the occurrence of inflammation, levels of inflammatory factors in the ileum of mice were measured (Figures 1C–H). GOS significantly decreased the levels of IL-1β, TNF-α, IL-6, and IFN-γ in lactose-intolerant mice, while significantly elevated levels of IL-4 and IL-10. In comparison with the L-CON, L-GOS significantly mitigated the level of intestinal inflammation following the occurrence of lactose intolerance, mainly characterized by a marked decline in the content of intestinal pro-inflammatory factors and a significant increase in the content of anti-inflammatory factors.

3.2.2 GOS alleviated LI-induced intestinal oxidative stress

After GOS supplementation in mice with lactose intolerance, the levels of T-SOD, CAT, and GSH-Px in the ileum of lactose intolerant mice were significantly higher than those in the control group (Figures 1I–M), while the levels of MDA and ROS were significantly lower than those in the control group. The results indicated that GOS intervention significantly mitigates the level of intestinal oxidative stress following the occurrence of lactose intolerance. This mitigation was manifested primarily by a decline in intestinal oxidative stress, an increase in antioxidant enzyme content, and an enhancement in antioxidant capacity.

3.2.3 GOS ameliorated LI-induced intestinal barrier injury

Administration of GOS to LI mice had no statistically significant effect on lactase content of the jejunum (Figure 1N), suggesting that GOS did not affect the expression of intestinal lactase. Presumably, the beneficial role of GOS in alleviating lactose intolerance was not achieved through increasing activity of intestinal lactase.

After administered of GOS, mRNA expression levels of Occludin, ZO-1, and Claudin proteins in the jejunum of lactose intolerant mice (Figures 1O–Q) exhibited significant elevations, which suggests that GOS significantly alleviated intestinal barrier damage caused by the occurrence of lactose intolerance and promoted restoration of intestinal barrier integrity.

3.2.4 GOS regulated the composition of the intestinal microbiota

The α-diversity of intestinal microbiota exhibited a significant decrease in LI mice that supplemented with GOS (Figures 2A–C). Principal co-ordinates analysis (PCoA) based on the Bray-Curtis distance revealed (Figure 2D) that intestinal microbiota populations of the L-CON and the L-GOS mice were significantly different (R = 0.731, P = 0.001). This observation indicates that GOS significantly affected the intestinal microbiota populations of lactose-intolerant mice.

At the phylum level of microbial composition, Bacteroidetes and Firmicutes are the dominant phyla in the cecal microbiota (Figure 2E). Administration of GOS altered the microbial composition, manifested as an increased proportion of Firmicutes, a decreased proportion of Bacteroidetes, and a significantly increased proportion of Actinobacteria. At the genus level, administration of GOS increased *Lactobacillus* (Figure 2F), and decreased *Lachnospiraceae*, and *Alloprevotella*. *Lactobacillus* belongs to the Firmicutes phylum, so the increased abundance of *Lactobacillus* corroborates the increased proportion of Firmicutes. Supplementation of LI mice with GOS, significantly increased the proportion of beneficial bacteria such as *Lactobacillus* and *Enterorhabdus*, and significantly reduced the proportion of *Alloprevotella* and *Colidextribacter* (Figure 2G).

The Spearmen correlation analysis (Figure 2H) indicated that *Lactobacillus* was significantly negatively correlated with IL-1β and TNF-α, and significantly positively correlated with IL-4 and IL-10. Furthermore, *Lactobacillus* was significantly positively correlated with GSH-Px, tended to be correlated positively with T-SOD and tended to be correlated negatively with MDA and ROS. *Enterorhabdus* also exhibited correlations similar to *Lactobacillus*. Correlations among *Alloprevotella* and inflammatory and antioxidant parameters were completely opposite to *Lactobacillus*. In conclusion, these results suggest that the intestinal microbiota may play a crucial role in alleviating lactose intolerance, as well as in anti-inflammatory and antioxidant processes.

3.3 Pre-supplementary GOS prevented lactose intolerance in mice

3.3.1 Prophylactic supplementation of GOS attenuated the inflammatory responses elicited by lactose intolerance

Given that GOS is beneficial in reducing risk of colorectal cancer (Piovani et al., 2019), was conducive to intestinal recovery following lactose intolerance, and had diverse effects on the intestinal microbiota, we explored the prophylactic role of GOS against lactose intolerance (Figure 3A).

Prophylactic supplementation with GOS mitigated lactose intolerance in mice, as demonstrated by a significant reduction in daily weight loss assigned to the GOS-L treatment regimen (Figure 3B). Compared with the CON group, GOS significantly decreased contents of IL-1β, IL-6, IFN-γ, and TNF-α, and significantly increased contents of IL-4 and IL-10 in ileal tissue (Figures 3C–H). Galacto-oligosaccharides significantly reduced levels of pro-inflammatory factors in mice ileum and elevated

10.3389/fmicb.2025.1530156

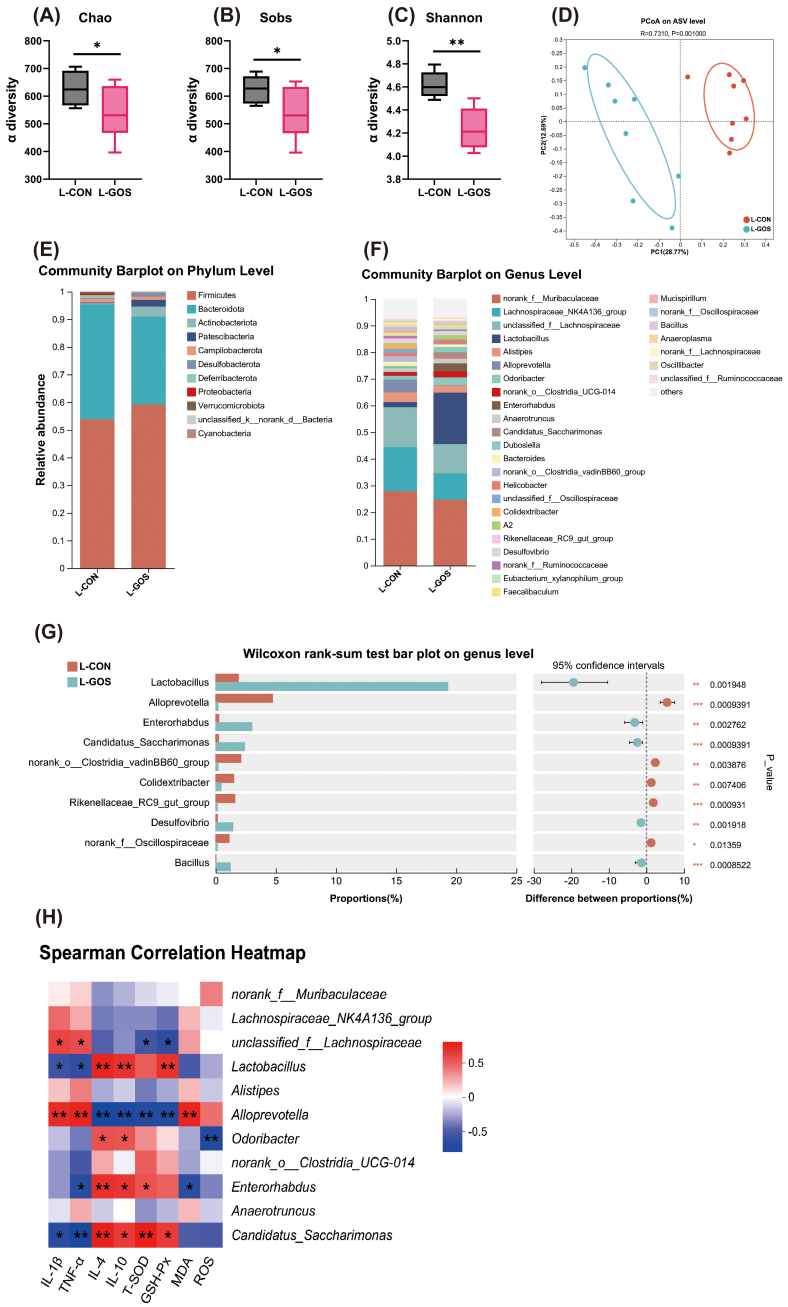

FIGURE 2
GOS regulated the composition and function of intestinal microbiota. **(A–C)** α-diversity upon GOS represented by the Chao, Sobs and Shannon index. **(D)** PCoA plots upon GOS assessed by PERMANOVA. **(E,F)** The relative abundance of colonic contents bacterial phyla and genera presented in 99.5% of the community upon GOS. **(G)** Analysis of differences in the microbial taxa shown by Wilcoxon rank-sum test on genus level upon GOS. **(H)** Spearman correlation between intestinal microbiota and anti-inflammatory or anti-oxidative parameters in two groups. The red color denotes a positive correlation, while blue color denotes a negative correlation. The intensity of the color is proportional to the strength of Spearman correlation. Statistical significance was determined using one-way ANOVA, followed by Tukey test. $^{*}P \leq 0.05$, $^{**}P \leq 0.01$, $^{***}P \leq 0.001$.

the levels of anti-inflammatory factors; whereas prophylactic supplementation of lactase had no significant impact on the levels of inflammatory factors in the ileum. Thess observations suggest that supplementing GOS reduced the intestinal inflammatory response and enhanced immunity. However, supplementing lactase did not alter the inherent inflammatory response of mice. After administering lactose to mice to induce lactose intolerance, levels of IL-1β, IL-6, IFN-γ, and TNF-α increased significantly compared with CON mice and significantly decreased in the contents of IL-4 and IL-10 in the ileum. In the mice supplemented with lactase, there was no obvious change in the levels of inflammatory factors after continuous administration of lactose, suggesting that lactase effectively degraded lactose without causing lactose intolerance. Nevertheless, after prophylactic supplementation of GOS and subsequent exposure to lactose, levels of IL-1β, IL-6, IFN-γ, and TNF-α were significantly lower than those seen in

10.3389/fmicb.2025.1530156

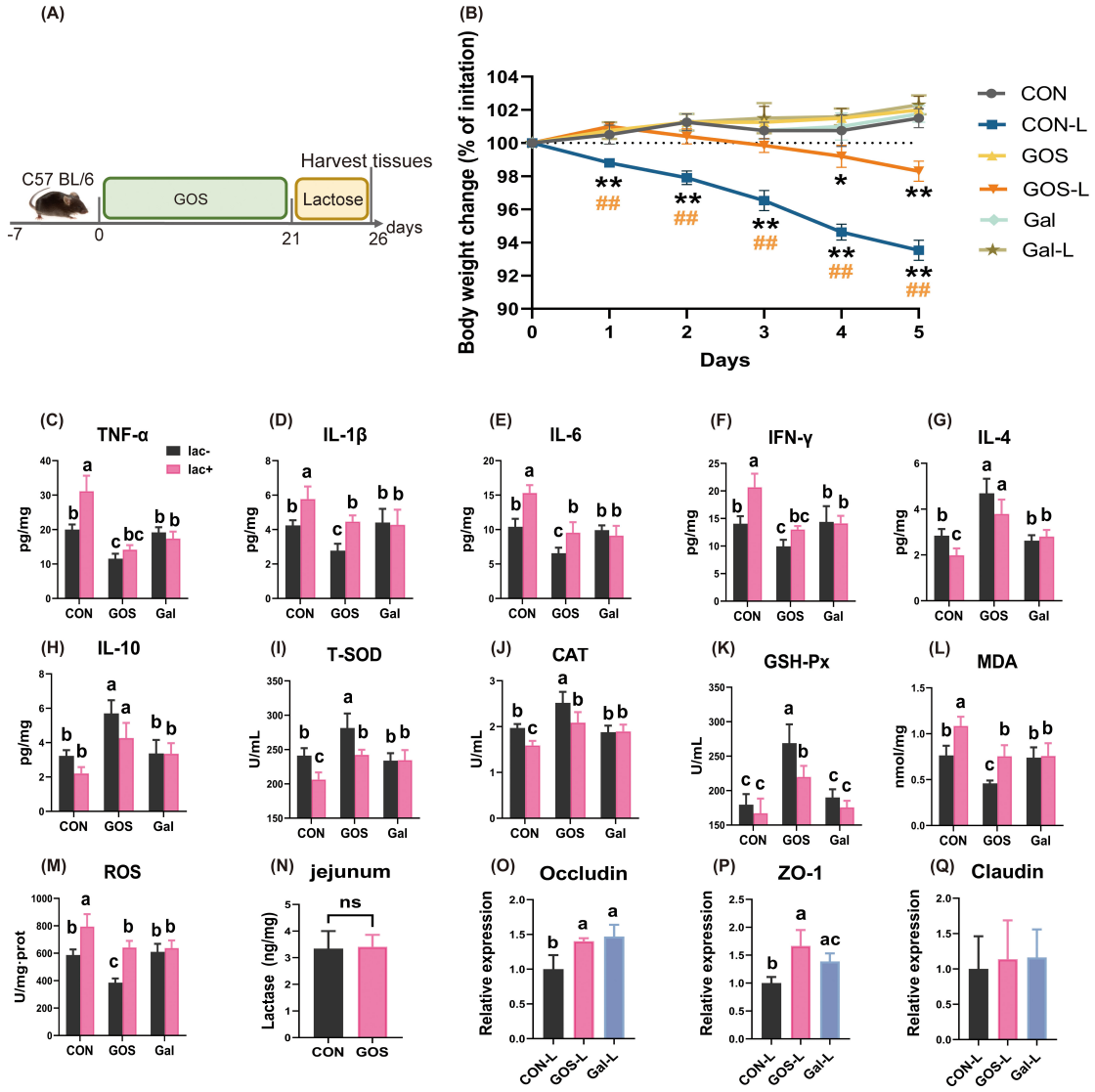

FIGURE 3

Prophylactic GOS attenuated signs of lactose-induced LI. **(A)** Diagram illustrating the experimental design in this study. **(B)** Daily body weight changes following lactose treatment. Statistical significance was determined using one-way ANOVA, followed by Tukey test. $^{*}P \leq 0.05$, $^{**}P \leq 0.01$ relative to CON group; $^{\#\#}P \leq 0.01$ relative to GOS-L group. **(C–H)** Concentrations of four representative pro-inflammatory cytokines, IL-1β, TNF-α, IL-6, IFN-γ, and anti-inflammatory cytokines, IL-4, IL-10 in the ileum. **(I–M)** Prophylactic GOS attenuated oxidative stress and jejunal damage. Concentrations of T-SOD, CAT, GSH-Px, MDA and ROS in the ileum from each group. **(N)** Concentrations of β-galactosidase in jejunum. **(O–Q)** Relative expression jejunal level of Occludin, ZO-1, Claudin mRNA in mice. Data were presented as means ± SEM (n = 6 per group). Statistical significance was determined using one-way ANOVA, followed by Tukey test. $^{*}P \leq 0.05$, $^{**}P \leq 0.01$. $^{a-c}$Dissimilar letters represent significant difference among different treatments ($P < 0.05$).

CON-L mice, and levels of IL-4 and IL-10 were significantly higher. These cytokine concentrations were comparable to the intestinal inflammatory levels in mice supplemented with lactase and then exposed to lactose induction. These results collectively suggest that prophylactic supplementation of GOS significantly suppressed inflammatory responses caused by lactose-induced lactose intolerance, with an effect similar to that of adding lactase.

3.3.2 Prophylactic supplementation of GOS reduced oxidative stress induced by lactose intolerance

Prophylactic supplementation of GOS significantly enhanced the activities of T-SOD, CAT, and GSH-Px (Figures 3I–M), and significantly decreased contents of MDA and ROS in ileum. In contrast, prophylactic supplementation of lactase exerted no significant influence on the oxidative stress level in the ileum of mice. These results suggest that prophylactic supplementation of GOS markedly improved antioxidant capacity of the mouse intestine; but lactase supplementation did not alter the original antioxidant status of mice. In the CON-L group, after administering lactose to mice to induce lactose intolerance, activities of T-SOD, CAT, and GSH-Px decreased significantly, and contents of MDA and ROS increased significantly, indicating that lactose intolerance triggered intense oxidative stress in mice intestine. In the Gal-L group, there was no obvious change in the intestinal oxidative stress level after continuous administration

10.3389/fmicb.2025.1530156

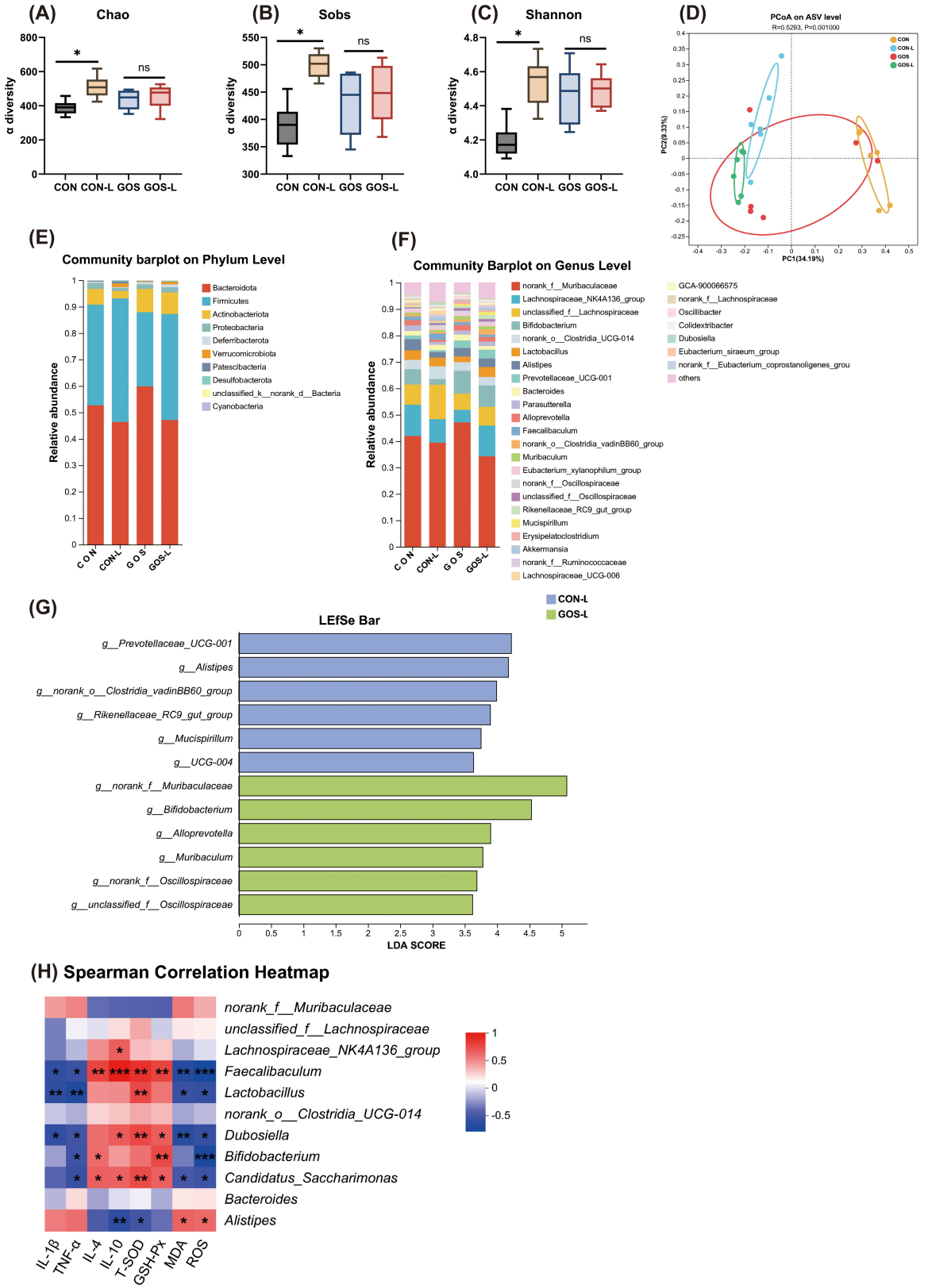

FIGURE 4

Prophylactic GOS regulated the composition and function of intestinal microbiota. **(A–C)** α-diversity represented by the Chao, Sobs and Shannon index. **(D)** PCoA plots assessed by PERMANOVA among the four groups. **(E,F)** The relative abundance of colonic contents bacterial phyla and genera presented in 99.5% of the community in lactose-treated mice with or without receiving GOS. **(G)** Analysis of differences in the microbial taxa shown by using LEfSe (LDA coupled with effect size measurements). **(H)** Spearman correlation between intestinal microbiota and anti-inflammatory or anti-oxidative parameters among the four groups. The red color denotes a positive correlation, while blue color denotes a negative correlation. The intensity of the color is proportional to the strength of Spearman correlation. Statistical significance was determined using one-way ANOVA, followed by Tukey test. $^{*}P \leq 0.05$, $^{**}P \leq 0.01$, $^{***}P \leq 0.001$.

of lactose, suggesting that lactase effectively degraded lactose without causing lactose intolerance. In the GOS-L group, after prophylactic supplementation of GOS and subsequent exposure to lactose challenge, the activities of T-SOD, CAT, and GSH-Px were significantly higher, and the contents of MDA and ROS were significantly lower than those in the CON-L group. In the GOS-L group, antioxidant capacity was slightly higher or comparable to that of mice supplemented with lactase and gavaged with lactose. These results demonstrate that prophylactic supplementation of GOS effectively inhibits intestinal oxidative stress resulting from lactose-induced lactose intolerance. These effects are similar to that of adding lactase.

3.3.3 Prophylactic supplementation of GOS reduced intestinal barrier damage caused by lactose intolerance

Compared with CON, there was no statistically significant difference in the jejunal lactase content of mice with prophylactic supplementation of GOS, indicating that GOS did not affect the expression of intestinal lactase (Figure 3N). The beneficial effects of GOS in alleviating lactose intolerance was not achieved through increasing activity of intestinal lactase. This is consistent with results of Experiment 2.

Prophylactic supplementation of GOS elevated Occludin and ZO-1 in the jejunum in mice (Figures 3O–Q). In the GOS-L group, after receiving prophylactic supplementation of GOS and subsequent lactose induction, mRNA expression levels of Occludin and ZO-1 were significantly higher than those in CON-L mice. Following the lactose challenge, there was no obvious change in levels of mRNA expression for Claudin in jejunum. These results demonstrated that prophylactic supplementation of GOS inhibited damage to the intestinal mucosal barrier caused by lactose intolerance. This response is similar to the response when lactose was supplemented.

3.3.4 Prophylactic supplementation of GOS regulated composition of the intestinal microbiota in lactose-intolerant mice

The alpha diversity of the cecal microbiota was represented by the Chao index, Sobs index, and Shannon index at the ASV level (Figures 4A–C). After mice consumed lactose for five consecutive days, the Chao, Sobs, and Shannon indexes all increased significantly, indicating that the continuous intake of lactose increased the alpha diversity of the cecal microbiota in mice. Compared with GOS mice, the continuous intake of lactose by mice with prophylactic supplementation of GOS did not significantly alter the Chao, Sobs, and Shannon indexes, suggesting that prophylactic supplementation of GOS prevented the change of alpha diversity of the cecal microbiota in mice when consuming lactose-containing foods. Similarly, including lactose with GOS had no effect on microbial diversity in the cecum compared with CON. PCoA based on the Bray-Curtis distance revealed (Figure 4D) that pre-administration of GOS significantly changed structure of the microbial community in mice. Pre-supplementation of mice with GOS led to a significant separation of the intestinal microbial community structure after lactose intake ($R = 0.529$, $P = 0.001$), indicating that the intestinal microbiota structure of mice was significantly affected after pre-supplementation with GOS and subsequent lactose intake.

Cecal microbiota of mice at the phylum level was still mainly composed of Bacteroidetes and Firmicutes (Figure 4E). In mice pre-supplemented with GOS, influence on composition of the cecal microbiota at the phylum level was manifested as an increased proportion of Actinobacteria when exposed to lactose. At the genus level, prophylactic supplementation of GOS significantly increased *Bifidobacterium* (Figure 4F). *Bifidobacterium* belongs to Actinobacteria, and the increased abundance of *Bifidobacterium* corroborated the results of the increased proportion of Actinobacteria. After receiving a lactose challenge, the proportion of *Bifidobacterium* in mice with prophylactic supplementation of GOS remained almost unchanged, and *Lactobacillus* increased slightly. Whether mice were pre-supplemented with GOS or not, changes in the cecal microbiota upon lactose intake were evident through LEfSe analysis. After lactose intake in CON mice, the proportion of *Alistipes* significantly increased (Figure 4G). After lactose intake with prophylactic supplementation of GOS, *Bifidobacterium* was significantly enriched.

To further understand associations between differential microbiota and inflammatory and antioxidant parameters, a Spearman correlation analysis was performed. The Spearman correlation analysis indicated (Figure 4H) that *Faecalibacterium* was negatively correlated with IL-1β and TNF-α, and positively correlated with IL-4 and IL-10. *Lactobacillus* was positively correlated with T-SOD and GSH-Px, and negatively correlated with MDA and ROS. *Lactobacillus*, *Dubosiella*, *Bifidobacterium*, and *Candidatus Saccharimonas* all exhibited trends very similar to those of *Faecalibacterium*. Which suggests they were all associated with reducing inflammation and oxidative stress in the intestine. These organisms simultaneously seemed to enhance anti-inflammatory and antioxidant capabilities. In contrast, *Alisyipes* was correlated negatively with T-SOD and positively with MDA and ROS. *Alisyipes* seemed to be related to increased levels of oxidative stress and inflammation in the intestine. These results suggest that prophylactic supplementation of GOS regulated composition of the intestinal microbiota. By significantly increasing abundance of probiotics such as *Bifidobacterium*, GOS downregulated levels of inflammatory factors and reduced oxidative stress responses, thereby potentially attenuating the microecological imbalance caused by lactose intolerance.

4 Discussion

In humans, LI is usually built up after consuming lactose containing food. There are numerous human reports with varying degree of lactose intolerance (Di Costanzo and Berni Canani, 2018). However, rarely studies using animal model to investigate LI. Here in this study, we developed a mice model by challenging with lactose which demonstrated parallel symptoms of LI as in humans such as higher content of water in stool, bleeding intestines, increased intestinal contents of inflammatory factors and altered intestinal microbiota. The dose of lactose (50 mg/20 g BW) for mice was selected based on the milk content of lactose (25 g/500 mL milk) treated for human (60 kg BW) when measuring

LI (Savaiano et al., 2013), and the ratio of surface area vs. BW of mice (Nair and Jacob, 2016). Our results showed that the mice LI model was successful developed.

Experiment 2 confirmed that GOS reduced intestinal damage in mice with lactose intolerance, and alleviated intestinal inflammation and oxidative stress. Compared to healthy individuals, those with acute diarrhea have reduced absorptive capacity, consumed less food, and consequently experienced continuous weight loss (Nyeko et al., 2010). Expression of pro-inflammatory cytokines which such as IL-1β and TNF-α, in the ileum of mice was significantly decreased, downregulated the inflammatory response. We discovered that GOS increased activity of antioxidant enzymes such as T-SOD and GSH-Px, and reduced the concentration of the lipid oxidation end product, MDA, which alleviated cell damage, and mitigated intestinal oxidative stress induced by lactose intolerance. We also found that GOS elevated mRNA expression of the tight junction proteins, Occludin, ZO-1, and Claudin, in the jejunal mucosa which mitigated damage to barrier integrity induced by lactose intolerance. Xi et al. (2023) has demonstrated that GOS improves intestinal barrier function by mediating the NF-κB pathway. All pathological conditions that cause small intestinal damage result in reduced lactase expression (Di Costanzo and Berni Canani, 2018). We considered whether GOS alleviates lactose intolerance in mice based on enhancing small intestinal lactase activity. We observed that addition of GOS after occurrence of lactose intolerance did not significantly alter lactase activity in the jejunum of mice.

We demonstrated that GOS supplementation alter composition of the intestinal microbiota in lactose-intolerant mice. Changes in composition of the intestinal microbiota modify metabolic characteristics and subsequently influence host health (Sharon et al., 2014). PCoA analysis reveals that GOS has significantly influenced the intestinal microbiota structure in lactose-intolerant mice. GOS supplementation significantly increased abundance of *Lactobacillus*. Krumbeck et al. (2018) also observed that GOS promoted colonization of *Lactobacillus* and improved intestinal barrier function in obese individuals. These observations suggest that the upregulation of mRNA expression of intestinal tight junction proteins in lactose-intolerant mice by GOS might be achieved through increasing abundance of *Lactobacillus*.

Endogenous β-galactosidase expressed by intestinal microbiota facilitates utilization of lactose by humans (Gingold-Belfer et al., 2020). *Lactobacillus* produces β-galactosidase to utilize lactose in the intestine and alleviates lactose intolerance (Masood et al., 2011). Spearman correlation analysis demonstrated that relative abundance of *Lactobacillus* was correlated negatively with pro-inflammatory cytokines and positively with antioxidant enzyme activity. A high abundance of *Lactobacillus* was strongly associated with low levels of the pro-inflammatory cytokines, IL-6 and TNF-α. Simultaneously, a high abundance of *Lactobacillus* was strongly associated with a high abundance of the antioxidant enzymes, T-SOD and GSH-Px. *Lactobacillus* secretes lactose permease to exert anti-inflammatory effects by selectively degrading pro-inflammatory chemokines (Von Schillde et al., 2012). In piglets, early supplementation with GOS also enhanced antioxidant enzyme activity and reduced oxidative stress in the intestine (Tian et al., 2022). This range of observations suggest that increase in *Lactobacillus* abundance was related closely to reduction of inflammation and improvement of antioxidant capacity. Conversely, a high abundance of *Alloprevotella* was inseparable from high levels of inflammatory responses and antioxidant stress. *Alloprevotella* is also an important biomarker associated with gastric cancer, as increased abundance is related to a higher risk of gastric cancer (Liu et al., 2023). These results suggest that the alteration of the intestinal microbiota composition caused by GOS played a crucial role in improvement of lactose intolerance, especially the enrichment of *Lactobacillus*.

Supplementation with lactase before consuming doing products can prevent occurrence of clinical symptoms of lactose intolerance. Endogenous lactase functions in the small intestine, especially in the upper part of the small intestine, such as the duodenum and jejunum. Generally, exogenous lactase supplementation mainly functions in the small intestine as well, hydrolyzing lactose into glucose and galactose, and monosaccharides can be directly absorbed by the small intestine. Different lactase products have different optimal pH ranges. Exogenous lactase supplementation no longer functions in the large intestine because the intestinal microecology environment of the large intestine, such as pH, is not suitable for the activity of lactase (Ibba et al., 2014; Ojetti et al., 2010). To assess the prophylactic effect of GOS on lactose intolerance, a positive control group, Gal-L, was established, where mice were given lactase 30 min before the lactose gavage. Mice in this group did not exhibit signs of lactose intolerance. To eliminate other influences of lactase addition on mice, a 21-day experiment with lactase addition was also conducted.

Similar to therapeutic administration of GOS, prophylactic supplementation of GOS was equally effective in alleviating inflammation in the ileum of lactose-intolerant mice, as manifested by decreased levels of pro-inflammatory cytokines and increased levels of anti-inflammatory cytokines. This response was comparable to the levels of inflammatory factors observed in the Gal-L group which indicates that prophylactic supplementation of GOS can achieve the same effect as adding lactase in reducing intestinal inflammation caused by lactose intolerance. Furthermore, prophylactic administration of GOS increased the activities of antioxidant enzymes such as CAT, T-SOD, and GSH-Px in the ileum, and reduced production of harmful substances associated with oxidative stress, such as MDA and ROS. Collectively, these responses indicated that GOS significantly enhanced the antioxidant status of the intestine, effectively reduced oxidative stress in mice ileum, and the retention of antioxidant enzyme activity could still reach the level of the Gal-L group, suggesting that prophylactic supplementation of GOS enhanced the intestinal antioxidant capacity and achieved the same effect as adding lactase. Prophylactic supplementation of GOS did not increase the activity of lactase in the jejunal mucosa. Similar to results reported by Leforestier et al. (2009). After feeding mice GOS for 4 weeks, activity of lactase did not undergo significant changes (Leforestier et al., 2009), indicating that the beneficial effect of GOS in preventing lactose intolerance was not achieved by increasing the activity of jejunal lactase. Prophylactic supplementation of GOS increased mRNA expression of tight junction proteins in jejunal mucosa, and mRNA expression of Occludin, ZO-1, and Claudin decreased slightly after lactose intake. Prophylactic

supplementation of GOS protected integrity and function of the intestinal barrier after lactose intake, enhanced intestinal tolerance to lactose, and reduced intestinal damage caused by lactose intolerance.

After prophylactic supplementation of GOS, cecal microbial composition of individual mice with lactose intolerance underwent significant changes. The most notable change was the increased the abundance of lactose-metabolizing bacteria. These changes were similar to alterations in the fecal microbiome of lactose-intolerant subjects participating (Azcarate-Peril et al., 2017). In mice receiving prophylactic supplementation of GOS, there was no significant change in community diversity at the ASV level, but results of PCoA analysis indicated a significant alteration in the microbial community structure. Prophylactic supplementation of GOS significantly increased abundance of *Bifidobacterium* and decreased abundance of *Alistipes*. In mice that received prophylactic supplementation of GOS and ingested lactose, the abundance of *Bifidobacterium* did not change significantly, while the abundance of *Lactobacillus* showed a marked increase. These indicated that the changed microbiota played a crucial role in alleviating the development of lactose intolerance. Almeida et al. (2012) found that a 4-week supplementation of *Lactobacillus* and *Bifidobacterium* preparations in lactose-intolerant patients achieved the same effect as supplementing with lactase, and that effect lasted for up to three months. However, there remains no clear conclusions regarding the effective dose and duration of probiotic supplementation. Therefore, more research is needed to evaluate the optimal dose and most suitable supplementation time of combined probiotics to obtain optimal results in improving lactose intolerance. *Bifidobacterium* can metabolize oligosaccharides, inhibit inflammatory responses, and regulate host immunity (Kitaoka, 2012; Chen et al., 2021). *Bifidobacterium* significantly enriched phospho-β-galactosidase and the metabolic pathways for digesting lactose (Caspi et al., 2020). Additional benefits of *Bifidobacterium* as a probiotic on the intestinal tract include protecting the intestinal tract from inflammatory diseases and colorectal cancer, mainly through inhibiting the NF-κB signaling pathway and inflammatory responses (Huang et al., 2017; Celiberto et al., 2017; Paveljšek et al., 2018). Activation of NF-κB is an important pro-inflammatory cellular mediator involved in the occurrence of colon cancer (Han et al., 2016; Huang et al., 2017). *Faecalibacterium* is regarded as an anti-inflammatory genus, because its metabolites can block NF-κB activation. Spearman correlation analysis revealed positive correlations between the abundances of *Bifidobacterium*, *Lactobacillus*, and *Faecalibacterium* with antioxidant capacity and the ability to inhibit inflammatory responses in the intestinal tract of mice. *Dubosiella* enhances immune tolerance of the body (Zhang et al., 2024). *Candidatus Saccharimonas* protects intestinal structure, increases intestinal antioxidant enzymes and activity, and consequently reduces intestinal inflammatory diseases (Cruz et al., 2020). Prophylactic supplementation of GOS decreased abundance of *Alistipes*. *Alistipes* has pathogenic effects on intestinal inflammatory diseases, colorectal cancer, and was associated with mental symptoms of depression (Moschen et al., 2016). Reducing the abundance of *Alistipes* may be associated with a decreased risk of intestinal diseases. In conclusion, the protective effect of prophylactic supplementation of GOS is highly correlated with a significant increase in abundance of *Bifidobacterium*, which possesses anti-inflammatory and anti-tumor properties. Changes in the composition of the intestinal microbiota contribute significantly to enhancing intestinal tolerance to lactose. A recent study by Wu et al. (2024) revealed that GOS enriched *Lactobacillus reuteri* and secondarily promoted with the production of pentadecanoic acid to alleviate intestinal dysfunction. Our results found similar enrichment of *Lactobacillus*. We also measured intestinal pH values which showed slightly lower pH in LI mice than control (data not shown). These findings were consistently with the reported study of Wu et al. (2024).

Our research results indicated that GOS mediated the microbial community. Particularly, the enrichment of *Lactobacillus* and *Bifidobacterium* played a crucial role in alleviating lactose intolerance and enhancing intestinal tolerance to lactose. The increase in microbes mediated by GOS might also be involved in maintaining homeostatic balance in the intestinal tract by improving colonic epithelial integrity and mucosal immunity (Kayama and Takeda, 2020). Eventually, homeostasis of intestinal epithelial cells is strengthened, and tolerance to lactose is concurrently enhanced which reduces the occurrence of lactose intolerance.

In summary, supplementing GOS to mice mitigated their signs of lactose intolerance and favorably altered composition of the intestinal microbiota in mice. Conversely, when lactose-intolerant mice were pre-supplemented with GOS and then exposed to lactose, similar changes occurred in composition of the intestinal microbiota in mice, with an increase in the abundance of probiotics. Spearman correlation analysis implied that enrichment of probiotics following alteration of the intestinal microbiota mediates beneficial effects of anti-inflammation, antioxidation, and maintaining intestinal integrity, thereby achieving the effect of preventing lactose intolerance.

5 Conclusion

We discovered that GOS reduced inflammatory response, enhanced antioxidant capacity, and regulated the composition of the intestinal microbiota, and ultimately alleviated the signs of lactose intolerance. Enriched probiotics such as *Lactobacillus* and *Bifidobacterium* showed a negative correlation with the pro-inflammatory factor TNF-α, promoting intestinal anti-inflammatory and increasing intestinal tolerance to lactose. These findings offer novel insights into using GOS as an alternative to lactase for preventing lactose intolerance and will facilitate development of prevention strategies for lactose intolerance and other intestinal disorders.

Data availability statement

The data presented in the study are deposited in the NCBI repository, accession number: PRJNA1209674, PRJNA1209660.

Ethics statement

The animal study was approved by the Animal Experiment Ethics Committee of the Experimental Animal Center of China Agricultural University. The study was conducted in accordance with the local legislation and institutional requirements.

Author contributions

QL: Conceptualization, Data curation, Formal Analysis, Investigation, Methodology, Project administration, Software, Supervision, Writing – original draft, Writing – review and editing. XW: Data curation, Conceptualization, Writing – review and editing. SG: Data curation, Investigation, Writing – review and editing. TW: Data curation, Conceptualization, Writing – review and editing. HC: Software, Data curation, Writing – review and editing. YC: Supervision, Validation, Writing – review and editing. BD: Conceptualization, Funding acquisition, Methodology, Project administration, Resources, Supervision, Visualization, Writing – review and editing.

Funding

The authors declare that financial support was received for the research and/or publication of this article. This work was supported by the National Key Research and Development Program of China (2023YFD1301103).

Conflict of interest

The authors declare that the research was conducted in the absence of any commercial or financial relationships that could be construed as a potential conflict of interest.

The authors declared that they were an editorial board member of Frontiers, at the time of submission. This had no impact on the peer review process and the final decision.

Generative AI statement

The authors declare that no Generative AI was used in the creation of this manuscript.

Publisher's note

All claims expressed in this article are solely those of the authors and do not necessarily represent those of their affiliated organizations, or those of the publisher, the editors and the reviewers. Any product that may be evaluated in this article, or claim that may be made by its manufacturer, is not guaranteed or endorsed by the publisher.

Supplementary material

The Supplementary Material for this article can be found online at: https://www.frontiersin.org/articles/10.3389/fmicb.2025.1530156/full#supplementary-material

References

Almeida, C. C., Lorena, S. L., Pavan, C. R., Akasaka, H. M., and Mesquita, M. A. (2012). Beneficial effects of long-term consumption of a probiotic combination of Lactobacillus casei Shirota and Bifidobacterium breve Yakult may persist after suspension of therapy in lactose-intolerant patients. *Nutr. Clin. Pract.* 27, 247–251. doi: 10.1177/0884533612440289

Andersen, J. M., Barrangou, R., Abou Hachem, M., Lahtinen, S., Goh, Y. J., Svensson, B., et al. (2011). Transcriptional and functional analysis of galactooligosaccharide uptake by lacS in Lactobacillus acidophilus. *Proc. Natl. Acad. Sci. U S A.* 108, 17785–17790. doi: 10.1073/pnas.1114152108

Azcarate-Peril, M. A., Ritter, A. J., Savaiano, D., Monteagudo-Mera, A., Anderson, C., Magness, S. T., et al. (2017). Impact of short-chain galactooligosaccharides on the gut microbiome of lactose-intolerant individuals. *Proc. Natl. Acad. Sci. U S A.* 114, E367–E375. doi: 10.1073/pnas.1606722113

Azcarate-Peril, M. A., Roach, J., Marsh, A., Chey, W. D., Sandborn, W. J., Ritter, A. J., et al. (2021). A double-blind, 377-subject randomized study identifies Ruminococcus, Coprococcus, Christensenella, and Collinsella as long-term potential key players in the modulation of the gut microbiome of lactose intolerant individuals by galacto-oligosaccharides. *Gut Microbes* 13:1957536. doi: 10.1080/19490976.2021.1957536

Barberán, A., Bates, S. T., Casamayor, E. O., and Fierer, N. (2012). Using network analysis to explore co-occurrence patterns in soil microbial communities. *ISME. J.* 6, 343–351. doi: 10.1038/ismej.2011.119

Caspi, R., Billington, R., Keseler, I. M., Kothari, A., Krummenacker, M., Midford, P. E., et al. (2020). The MetaCyc database of metabolic pathways and enzymes - A 2019 update. *Nucleic Acids Res.* 48, D445–D453. doi: 10.1093/nar/gkz862

Celiberto, L. S., Bedani, R., Dejani, N. N., Ivo de Medeiros, A., and Sampaio Zuanon, J. A., (2017). Effect of a probiotic beverage consumption (Enterococcus faecium CRL 183 and Bifidobacterium longum ATCC 15707) in rats with chemically induced colitis. *PLoS One* 12:e0175935. doi: 10.1371/journal.pone.0175935

Chen, J., Chen, X., and Ho, C. L. (2021). Recent development of probiotic bifidobacteria for treating human diseases. *Front. Bioeng. Biotechnol.* 9:770248. doi: 10.3389/fbioe.2021.770248

Chey, W., Sandborn, W., Ritter, A. J., Foyt, H., Azcarate-Peril, M. A., and Savaiano, D. A. (2020). Galacto-oligosaccharide RP-G28 improves multiple clinica outcomes in lactose intolerant patients. *Nutrients* 12:1058. doi: 10.3390/nu12041058

Cruz, B. C. D. S., Conceição, L. L. D., Mendes, T. A. O., Ferreira, C. L. L. F., Gonçalves, R. V., and Peluzio, M. D. C. G. (2020). Use of the synbiotic VSL#3 and yacon-based concentrate attenuates intestinal damage and reduces the abundance of Candidatus Saccharimonas in a colitis-associated carcinogenesis model. *Food. Res. Int.* 137:109721. doi: 10.1016/j.foodres.2020.109721

Detel, D., Baticic, L., and Varljen, J. (2008). The influence of age on intestinal dipeptidyl peptidase IV (DPP IV/CD26), disaccharidases, and alkaline phosphatase enzyme activity in C57BL/6 mice. *Exp. Aging Res.* 34, 49–62. doi: 10.1080/03610730701761957

Di Costanzo, M., and Berni Canani, R. (2018). Lactose intolerance: Common misunderstandings. *Ann. Nutr. Metab.* 73, 30–37. doi: 10.1159/000493669

Gingold-Belfer, R., Levy, S., Layfer, O., Pakanaev, L., Niv, Y., Dickman, R., et al. (2020). Use of a novel probiotic formulation to alleviate lactose intolerance symptoms-a pilot study. *Probiotics Antimicrob. Proteins* 12, 112–118. doi: 10.1007/s12602-018-9507-7

Han, Y. M., Jeong, M., Park, J. M., Kim, M. Y., Go, E. J., Cha, J. Y., et al. (2016). The ω-3 polyunsaturated fatty acids prevented colitis-associated carcinogenesis through

blocking dissociation of β-catenin complex, inhibiting COX-2 through repressing NF-κB, and inducing 15-prostaglandin dehydrogenase. *Oncotarget* 7, 63583–63595.

Hertzler, S. R., and Savaiano, D. A. (1996). Colonic adaptation to daily lactose feeding in lactose maldigesters reduces lactose intolerance. *Am. J. Clin. Nutr.* 64, 232–236. doi: 10.1093/ajcn/64.2.232

Hertzler, S. R., Savaiano, D. A., and Levitt, M. D. (1997). Fecal hydrogen production and consumption measurements. Response to daily lactose ingestion by lactose maldigesters. *Dig. Dis. Sci.* 42, 348–353. doi: 10.1023/a:1018822103911

Huang, T. H., Wu, S. Y., Huang, Y. J., Wei, P. L., Wu, A. T., and Chao, T. Y. (2017). The identification and validation of Trichosstatin A as a potential inhibitor of colon tumorigenesis and colon cancer stem-like cells. *Am. J. Cancer Res.* 7, 1227–1237.

Ibba, I., Gilli, A., Boi, M. F., and Usai, P. (2014). Effects of exogenous lactase administration on hydrogen breath excretion and intestinal symptoms in patients presenting lactose malabsorption and intolerance. *Biomed. Res. Int.* 2014:680196. doi: 10.1155/2014/680196

Kamada, N., Seo, S. U., Chen, G. Y., and Núñez, G. (2013). Role of the gut microbiota in immunity and inflammatory disease. *Nat. Rev. Immunol.* 13, 321–335. doi: 10.1038/nri3430

Kayama, H., and Takeda, K. (2020). Manipulation of epithelial integrity and mucosal immunity by host and microbiota-derived metabolites. *Eur. J. Immunol.* 50, 921–931. doi: 10.1002/eji.201948478

Kitaoka, M. (2012). Bifidobacterial enzymes involved in the metabolism of human milk oligosaccharides. *Adv. Nutr.* 3, 422S–429S. doi: 10.3945/an.111.001420

Krumbeck, J. A., Rasmussen, H. E., Hutkins, R. W., Clarke, J., Shawron, K., Keshavarzian, A., et al. (2018). Probiotic Bifidobacterium strains and galactooligosaccharides improve intestinal barrier function in obese adults but show no synergism when used together as synbiotics. *Microbiome* 6:121. doi: 10.1186/s40168-018-0494-4

Leforestier, G., Blais, A., Blachier, F., Marsset-Baglieri, A., Davila-Gay, A. M., Perrin, E., et al. (2009). Effects of galacto-oligosaccharide ingestion on the mucosa-associated mucins and sucrase activity in the small intestine of mice. *Eur. J. Nutr.* 48, 457–464. doi: 10.1007/s00394-009-0036-8

Li, J., Zhang, W., Wang, C., Yu, Q., Dai, R., and Pei, X. (2012). Lactococcus lactis expressing food-grade β-galactosidase alleviates lactose intolerance symptoms in post-weaning Balb/c mice. *Appl. Microbiol Biotechnol.* 96, 1499–1506. doi: 10.1007/s00253-012-3977-4

Liu, Y., Wang, H., Jiang, H., Sun, Z., and Sun, A. (2023). Alloprevotella can be considered as a potential oral biomarker in intestinal metaphase of gastric patients. *Stud. Health Technol. Inform.* 308, 155–167. doi: 10.3233/SHTI230836

Luo, K., Chen, G. C., Zhang, Y., Moon, J. Y., Xing, J., Peters, B. A., et al. (2024). Variant of the lactase LCT gene explains association between milk intake and incident type 2 diabetes. *Nat. Metab.* 6, 169–186. doi: 10.1038/s42255-023-00961-1

Masood, M. I., Qadir, M. I., Shirazi, J. H., and Khan, I. U. (2011). Beneficial effects of lactic acid bacteria on human beings. *Crit. Rev. Microbiol.* 37, 91–98. doi: 10.3109/1040841X.2010.536522

Moschen, A. R., Gerner, R. R., Wang, J., Klepsch, V., Adolph, T. E., Reider, S. J., et al. (2016). Lipocalin 2 protects from inflammation and tumorigenesis associated with gut microbiota alterations. *Cell. Host. Microbe* 19, 455–469. doi: 10.1016/j.chom.2016.03.007

Nair, A. B., and Jacob, S. (2016). A simple practice guide for dose conversion between animals and human. *J. Basic Clin. Pharm.* 7, 27–31. doi: 10.4103/0976-0105.177703

Nyeko, R., Kalyesubula, I., Mworozi, E., and Bachou, H. (2010). Lactose intolerance among severely malnourished children with diarrhoea admitted to the nutrition unit, Mulago hospital, Uganda. *BMC Pediatr.* 10:31. doi: 10.1186/1471-2431-10-31

Obermayer-Pietsch, B. M., Bonelli, C. M., Walter, D. E., Kuhn, R. J., Fahrleitner-Pammer, A., Berghold, A., et al. (2004). Genetic predisposition for adult lactose intolerance and relation to diet, bone density, and bone fractures. *J. Bone Miner. Res.* 19, 42–47. doi: 10.1359/JBMR.0301207

Ojetti, V., Gigante, G., Gabrielli, M., Ainora, M. E., Mannocci, A., Lauritano, E. C., et al. (2010). The effect of oral supplementation with Lactobacillus reuteri or tilactase in lactose intolerant patients: Randomized trial. *Eur. Rev. Med. Pharmacol. Sci.* 14, 163–170.

Paveljšek, D., Juvan, P., Košir, R., Rozman, D., Hacin, B., Ivičak-Kocjan, K., et al. (2018). Lactobacillus fermentum L930BB and Bifidobacterium animalis subsp. animalis IM386 initiate signalling pathways involved in intestinal epithelial barrier protection. *Benef. Microbes* 9, 515–525. doi: 10.3920/BM2017.0107

Piovani, D., Danese, S., Peyrin-Biroulet, L., Nikolopoulos, G., Lytras, T., Bonovas, S., et al. (2019). Environmental risk factors for inflammatory bowel diseases: An umbrella review of meta-analyses. *Gastroenterology* 157, 647–659.e4. doi: 10.1053/j.gastro.2019.04.016.

Ross, A. C., Manson, J. E., Abrams, S. A., Aloia, J. F., Brannon, P. M., Clinton, S. K., et al. (2011). The 2011 report on dietary reference intakes for calcium and vitamin D from the institute of medicine: What clinicians need to know. *J. Clin. Endocrinol. Metab.* 96, 53–58. doi: 10.1210/jc.2010-2704

Savaiano, D. A., Ritter, A. J., Klaenhammer, T. R., James, G. M., Longcore, A. T., Chandler, J. R., et al. (2013). Improving lactose digestion and symptoms of lactose intolerance with a novel galacto-oligosaccharide (RP-G28): A randomized, double-blind clinical trial. *Nutr. J.* 12:160. doi: 10.1186/1475-2891-12-160

Schloss, P. D., Westcott, S. L., Ryabin, T., Hall, J. R., Hartmann, M., Hollister, E. B., et al. (2009). Introducing mothur: Open-source, platform-independent, community-supported software for describing and comparing microbial communities. *Appl. Environ. Microbiol.* 75, 7537–7541. doi: 10.1128/AEM.01541-09

Sharon, G., Garg, N., Debelius, J., Knight, R., Dorrestein, P. C., and Mazmanian, S. K. (2014). Specialized metabolites from the microbiome in health and disease. *Cell. Metab.* 20, 719–730. doi: 10.1016/j.cmet.2014.10.016

Szilagyi, A., Shrier, I., Heilpern, D., Je, J., Park, S., Chong, G., et al. (2010). Differential impact of lactose/lactase phenotype on colonic microflora. *Can. J. Gastroenterol.* 24, 373–379. doi: 10.1155/2010/649312

Tian, S., Wang, J., Gao, R., Wang, J., and Zhu, W. (2022). Early-life galacto-oligosaccharides supplementation alleviates the small intestinal oxidative stress and dysfunction of lipopolysaccharide-challenged suckling piglets. *J. Anim. Sci. Biotechnol.* 13:70. doi: 10.1186/s40104-022-00711-5

Toca, M. D. C., Fernández, A., Orsi, M., Tabacco, O., and Vinderola, G. (2022). Lactose intolerance: Myths and facts. An update. *Arch. Argent Pediatr.* 120, 59–66. doi: 10.5546/aap.2022.eng.59

Vandenplas, Y. (2015). Lactose intolerance. *Asia Pac. J. Clin. Nutr.* 24, S9–S13. doi: 10.6133/apjcn.2015.24.s1.02

Von Schillde, M. A., Hörmannsperger, G., Weiher, M., Alpert, C. A., Hahne, H., Bäuerl, C., et al. (2012). Lactocepin secreted by Lactobacillus exerts anti-inflammatory effects by selectively degrading proinflammatory chemokines. *Cell. Host. Microbe* 11, 387–396. doi: 10.1016/j.chom.2012.02.006

Wu, Y., Zhang, X., Liu, X., Zhao, Z., Tao, S., Xu, Q., et al. (2024). Galactooligosaccharides and *Limosilactobacillus reuteri* synergistically alleviate gut inflammation and barrier dysfunction by enriching *Bacteroides acidifaciens* for pentadecanoic acid biosynthesis. *Nat. Commun.* 15:9291. doi: 10.1038/s41467-024-53144-1

Xi, M., Hao, G., Yao, Q., Duan, X., and Ge, W. (2023). Galactooligosaccharide mediates NF-κB pathway to improve intestinal barrier function and intestinal microbiota. *Molecules* 28:7611. doi: 10.3390/molecules28227611

Zhang, P., Liu, J., Xiong, B., Zhang, C., Kang, B., Gao, Y., et al. (2020). Microbiota from alginate oligosaccharide-dosed mice successfully mitigated small intestinal mucositis. *Microbiome* 8:112. doi: 10.1186/s40168-020-00886-x

Zhang, Y., Tu, S., Ji, X., Wu, J., Meng, J., Gao, J., et al. (2024). Dubosiella newyorkensis modulates immune tolerance in colitis via the L-lysine-activated AhR-IDO1-Kyn pathway. *Nat. Commun.* 15:1333. doi: 10.1038/s41467-024-45636-x

frontiers | Frontiers in Microbiology

TYPE Original Research
PUBLISHED 09 April 2025
DOI 10.3389/fmicb.2025.1558588

Check for updates

OPEN ACCESS

EDITED BY
Junling Shi,
Northwestern Polytechnical University, China

REVIEWED BY
Ilias Giannenas,
Aristotle University of Thessaloniki, Greece
Elena Franco Robles,
University of Guanajuato, Mexico
Iftikhar Younis Mallhi,
Minhaj University Lahore, Pakistan
Chuanpi Xiao,
Ludong University, China
Yang Li,
Shandong Agricultural University, China
Eric Auclair,
Phileo Lesaffre Animal Care, France

*CORRESPONDENCE
Wen Chen
✉ cchenwen@henau.edu.cn
Xuemeng Si
✉ sxmswun@126.com

†These authors have contributed equally to this work

RECEIVED 10 January 2025
ACCEPTED 25 March 2025
PUBLISHED 09 April 2025

CITATION
Fan Z, Lei L, Wu X, Xing R, Du P, Wang Z, Zhao H, Huang Y, Chen W and Si X (2025) Dietary fatty acids promote gut health in weaned piglets by regulating gut microbiota and immune function.
Front. Microbiol. 16:1558588.
doi: 10.3389/fmicb.2025.1558588

COPYRIGHT
© 2025 Fan, Lei, Wu, Xing, Du, Wang, Zhao, Huang, Chen and Si. This is an open-access article distributed under the terms of the Creative Commons Attribution License (CC BY). The use, distribution or reproduction in other forums is permitted, provided the original author(s) and the copyright owner(s) are credited and that the original publication in this journal is cited, in accordance with accepted academic practice. No use, distribution or reproduction is permitted which does not comply with these terms.

Dietary fatty acids promote gut health in weaned piglets by regulating gut microbiota and immune function

Zongze Fan[1†], Lei Lei[2†], Xingyue Wu[1], Ronghui Xing[1], Pengfei Du[1], Ziyang Wang[1], Huijuan Zhao[3], Yanqun Huang[1], Wen Chen[1*] and Xuemeng Si[1*]

[1]Institute of Animal Science and Technology, Henan Agricultural University, Zhengzhou, China, [2]Zhengzhou Agricultural Comprehensive Administrative Law Enforcement Detachment, Zhengzhou, China, [3]Delvigent (Hebei) Biotech Co. Ltd., Cangzhou, China

Background: Post-weaning diarrhea in piglets is a common challenge that adversely impacts growth performance and increases mortality, leading to severe economic losses. Medium-chain fatty acids (MCFA) and short-chain fatty acids (SCFA) are frequently used as feed additives due to their bioactive properties. This study evaluated the effects of two different blends of MCFA and SCFA (VSM and VS + VM) as alternatives to zinc oxide (ZnO) on growth performance, nutrient digestibility, oxidative stress, inflammatory, and gut microbiota composition in weaned piglets.

Methods and results: A total of 108 piglets (8.22 ± 0.51 kg) were randomly assigned to three treatments: control (CON, basal diet + ZnO), VSM (basal diet + higher MCFA and lower SCFA content) and VS + VM (basal diet + higher SCFA and lower MCFA content). Results indicated that Both VSM and VS + VM, can replace ZnO to relieve diarrhea of weaned piglets as evidenced by increased average daily gain (ADG) and decreased feed to gain ratio (F/G) in 1–15 days, with no difference in final body weight compared to the CON group. Additionally, dietary MCFA and SCFA supplementation improves anti-oxidative and anti-inflammatory capacity by decreased of malondialdehyde (MDA) activity, and inhibited proinflammatory cytokine tumor necrosis factor α (TNF-α) and interleukin (IL-1β, IL-17A) secretion. Further study showed that the protective effect of MCFA and SCFA were associated with restoring gut barrier, upregulating abundances of *Lactobacillus* and *Roseburia* of piglets.

Interpretation: Collectively, the combination of MCFA and SCFA alleviated oxidative stress, modulated inflammation, and supported gut barrier function in weaned piglets, offering a promising alternative to ZnO, with VSM showing superior effects.

KEYWORDS

medium-chain and short-chain fatty acids, zinc oxide, oxidative stress, inflammatory, *Lactobacillus*, weaned piglets

Introduction

Weaning is widely recognized as the most critical and stressful stage in piglet development. Following weaning, piglets are exposed to a combination of environmental and psychological stressors, often resulting in reduced growth performance, disruption of the gut microbiota, and the onset of diarrhea (Laine et al., 2008). A primary factor contributing to post-weaning diarrhea is oxidative stress, which arises from the imbalance between pro-oxidative forces and antioxidant defenses (Qiao et al., 2023). The imbalance compromises the gut barrier, leading to increased permeability and facilitating pathogen translocation (Feng et al., 2020). The resulting local and systemic inflammation exacerbates diarrhea and further hinders intestinal function, intensifying the negative impacts on piglet health and growth (Campbell et al., 2013). To mitigate the negative effects of post-weaning stress, high doses of zinc oxide (ZnO) have traditionally been included in piglet diets due to their multiple benefits (Long et al., 2017). ZnO supplementation enhances intestinal development, increases digestive enzyme activity and strengthens the intestinal barrier functionality (Liu et al., 2014). Additionally, ZnO demonstrates antimicrobial properties that contribute to modulating gut microbiota composition (Tang et al., 2024). Although ZnO supplementation are effective in reducing diarrhea and supporting growth, their long-term use raises concerns, whereas high levels of ZnO in animal feed have contributed to environmental contamination (Grilli et al., 2015; Jensen et al., 2016; Tan et al., 2023). Thus, the European Union implemented a ban on the inclusion of medicinal doses of ZnO in animal feeds as of June 2022 (Bonetti et al., 2021), thereby reducing environmental concerns and the increasing regulatory restrictions on ZnO usage, alternatives such as organic acids, probiotics, and plant-derived bioactive compounds have gained attention (Abd El-Hack et al., 2022).

Medium-chain and short-chain fatty acids (MCFA/SCFA) have gained popularity as feed additives due to their critical roles in promoting intestinal health and enhancing the growth performance of piglets (Hu et al., 2023). MCFA, consist of fatty acids with 6–12 carbon atoms, are mainly composed of caprylic acid (C8:0), capric acid (C10:0), and lauric acid (C12:0). Compared to conventional organic acids, MCFA possess potent antibacterial activity, particularly against Gram-positive bacteria and *Escherichia coli*, thereby contributing to the regulation of balance of intestinal microbiota (Jiao et al., 2023). Additionally, MCFA can be rapidly absorbed by the organism through the portal vein, and utilized by the liver without requiring the carnitine transport system to enter mitochondria (Nagao and Yanagita, 2010). This enables them to directly supply energy to the intestinal epithelium, thereby promoting the renewal and repair of enterocytes, which is crucial for maintaining intestinal integrity (Zentek et al., 2011). SCFA, on the other hand, are important metabolites produced by intestinal microbiota and serve as the primary energy for colon epithelial cells (den Besten et al., 2013; Nakkarach et al., 2021). SCFA are organic acids containing 1–6 carbon atoms, such as formic acid, acetic acid, and propionic acid, which play a crucial role in maintaining intestinal health (Nakkarach et al., 2021). MCFA and SCFA play an important role in regulating gastrointestinal pH, improving the activity of digestive enzymes, and promoting the growth of acid-tolerant microorganisms, such as lactic acid-producing bacteria (Lauridsen, 2020).

Fatty acids with distinct chain lengths exhibit differential biological properties and mechanisms of action, thereby generating synergistic effects when supplemented in combination (López-Colom et al., 2020). For example, MCFA can disrupt the microbial cell wall, allowing SCFA to enter the bacterial cytoplasm and exert antibacterial effects (Szabó et al., 2023). A study revealed that combined supplementation of capric acid and SCFA in piglets diets resulted in enhanced growth performance compared to SCFA alone (Hanczakowska et al., 2013). Additionally, another study demonstrated that a blend containing MCFA and butyrate supplementation improved antioxidant capacity, optimized intestinal morphology, and reduced diarrhea incidence in weaning piglets (Cai et al., 2024). Despite these promising findings, research on the optimal ratio of MCFA to SCFA remains limited, and further studies are needed to determine the most effective formulation for improving piglet health and performance. In earlier studies, mixtures with higher SCFA than MCFA added to piglet diets were shown to improve growth performance (Kuang et al., 2015). However, our product (VSM) contains a higher MCFA and lower SCFA content, which has been validated in practical production settings to enhance piglet growth performance. To explore the most effective combination, we formulated a VS + VM group, where SCFA levels were higher than MCFA. This allowed us to compare the two fatty acid ratios and determine which formulation yields better growth and gut health outcomes.

The study was conducted to investigate the effects of ZnO substitute MCFA and SCFA supplementation on growth performance, redox homeostasis, and gut microbiota composition of weaned piglets. Specifically, we investigate the protective roles of MCFA and SCFA in mitigating weaning-induced stress and explore potential mechanisms underlying their effects.

Materials and methods

Animal care

All animal procedures were approved by the Institutional Animal Care and Use Committee of Henan Agricultural University (Approval No. HNND20190612) and were conducted in accordance with the Guide for the Care and Use of Laboratory Animals.

Reagents

MCFA and SCFA products were supplied by Delvigent (Hebei) Biotech Co. Ltd., Cangzhou, China. Details of the product composition are as follows:

Phase 1: VSM group: MCFA (caprylic acid, capric acid, and lauric acids) at 1.25 kg/t, SCFA (0.5 kg/t formic acid, 0.19 kg/t acetic acid, and 0.15 kg/t propionic acid). The MCFA:SCFA ratio was approximately 1.5:1. VS + VM group: MCFA at 1.16 kg/t, SCFA (1.24 kg/t formic acid 0.19 kg/t acetic acid), 0.1 kg/t lactic acid. The MCFA:SCFA ratio was approximately 0.8:1.

Phase 2: VSM group: MCFA (caprylic acid, capric acid, and lauric acids) at 1.00 kg/t, SCFA (0.4 kg/t formic acid, 0.15 kg/t acetic acid, and 0.12 kg/t propionic acid), the MCFA:SCFA ratio was

approximately 1.5:1. VS + VM group: MCFA at 0.87 kg/t, SCFA (1.24 kg/t formic acid 0.19 kg/t acetic acid) 0.1 kg/t lactic acid, the MCFA:SCFA ratio was approximately 0.6:1.

The fatty acid products have silica as their carrier, the common organic acids in this study comprise citric acid, benzoic acid, fumaric acid, and lactic acid.

Animals and experiment design

A total of 108 Duroc × Landrace × Large Yorkshire weaned piglets (28 days old, 8.22 ± 0.51 kg) were randomly assigned to one of three diet treatments in a 2-phase feeding trial (nine piglets per replicate, balanced for sex). Dietary treatments were as follows:

In phase 1 (1–15 days), CON (basal diet + 2 kg/t ZnO + 8 kg/t common organic acid), VSM (basal diet + higher MCFA and lower SCFA content, the MCFA/SCFA ratios were 1.5:1) and VS + VM (basal diet + higher SCFA and lower MCFA content, the MCFA/SCFA ratios were 0.8:1). In phase 2 (16–35 days), CON (basal diet + 7 kg/t common organic acid), VSM (basal diet + higher MCFA and lower SCFA content, the MCFA/SCFA ratios were 1.5:1) and VS + VM (basal diet + higher SCFA and lower MCFA content, the MCFA/SCFA ratios were 0.6:1).

The detailed composition and nutritional levels of the experimental diet are presented in Table 1. Each pen was equipped with a slatted

TABLE 1 Ingredient composition and analyzed nutrient concentration of experimental diets (%, as—dry matter basis).

Items	Contents	
	1–15 days	16–35 days
Diet composition		
Broken rice	19	0
Corn	28	52
Puffed corn	12	0
Expanded soybeans	4	10
Fish meal	5	5
Peeled soybean meal	6	12
Fermented soybean meal	8	4
Whey powder	3	6
Lactose	3	0
Sucrose	4	2
Glucose	2	2
Soybean oil	1	2
4% piglet premix	4	4
Nutrient composition		
Digestible energy, Mcal/kg	3.53	3.44
Metabolic energy	3.14	3.08
Crude protein, %	18.01	17.63
Crude fat	4.20	4.07
Crude fiber	2.00	2.03
Coarse ash content	4.20	4.75
Calcium	0.54	0.65
Total phosphorus	0.52	0.55
Non phytic acid phosphorus	0.36	0.39
Lysine	1.60	1.58
Threonine	1.05	1.02
Methionine	0.56	0.57
Cysteine	0.80	0.80
Valine	1.00	0.96
Arginine	1.20	1.10
Isoleucine	0.90	0.85

Provided the vitamin and minerals as following per kilogram of diet: 1,800 IU vitamin A as retinyl acetate; 200 IU vitamin D3 as cholecalciferol; 11 IU vitamin E as DL-a-tocopherol acetate; 0.5 mg vitamin K3 as menadione; 1 mg vitamin B1; 3.5 mg vitamin B2; 10 mg vitamin B5; 1.5 mg of vitamin B6; 17.5 mg vitamin B12; 15 mg niacin; 0.3 mg folic acid; 0.5 mg choline 0.05 mg biotin; 105 mg Fe; 6 mg Cu; 110 mg Zn; 4 mg Mn; 0.30 mg Se; 0.14 mg I.

floor, and environmental conditions were strictly regulated. The temperature inside the pig housing facility was maintained at 22°C–26°C, with a humidity level of 60–70%. Piglets were provided ad libitum access to feed and water throughout the study. Fecal samples were collected on day 35, frozen in liquid nitrogen, and stored at −80°C. Blood samples were collected from the anterior vena cava, and serum was separated and stored at −20°C for subsequent analysis.

Growth performance

Piglets were weighed at the beginning of the experiment and at the end of each phase. Feed intake were recorded daily. Diarrhea was assessed daily using the following scoring system: 0: normal, well-formed feces (solid or in soft strips) without excess moisture or mucus; 1: mild diarrhea, soft, partially formed feces; 2: moderate diarrhea, semi-liquid and mobile feces; 3: severe diarrhea, totally watery feces without any solid content.

$$\text{Diarrhea rate}(\%) = (\text{Total number of diarrhea in each group}) / (\text{Total number of piglets in each group} \times \text{Trial days}) \times 100\%$$

$$\text{Diarrhea index} = \text{Total fecal score} / \text{Total piglets in each group}$$

Nutrient digestibility

Apparent total tract digestibility (ATTD) of nutrients was determined using ash insoluble in hydrochloric acid as an endogenous marker. Fecal samples were thawed, dried at 65°C for 72 h, diets and fecal samples were accurately weighed for AIA analysis [Method 942.05; (AOAC, 2007)]. and analyzed for CP [Method 988.05; (AOAC, 2007)], EE [Method 920.39; (AOAC, 2007)], and ash content. Diets and ingredients were also analyzed for Ca [Method 942.05; (AOAC, 2007)] and P [Method 965.17; (AOAC, 2007)]. ATTD values for EE, CP, Ca, and P were calculated as follows:

$$\text{ATTD}(\%) = 1 - \left([N_f \times A_d] / [N_d \times A_f] \right)$$

where N_f is nutrient concentration in feces, N_d is nutrient concentration in diet, A_d is AIA concentration in diet, and A_f is AIA concentration in feces.

Serum inflammatory cytokines and antioxidant

Serum biochemical indexes, including total protein (TP), albumin (ALB), globulin (GLB), glucose (GLU), triglyceride (TG), total cholesterol (TC), alkaline phosphatase (ALP) and blood urea nitrogen (BUN), were determined using a BK280 Automatic Biochemical Analyzer (Shandong, China). Intestinal permeability indexes, including D-lactate and diamine oxidase (DAO) were determined by their specific assay kits (MM-33732O1, MM-0438O2) Jiangsu Meimian Industrial Co., Ltd., China; serum antioxidant parameters, including total superoxide dismutase (T-SOD), total antioxidant capacity (T-AOC), glutathione peroxidase (GPX), catalase (CAT), malondialdehyde (MDA), hydrogen peroxide (H_2O_2), were determined by their specific assay kits (A001-3-1, A015-2-1, A005-1-2, A007-1-1, A003-1-2, A064-1-1) from Nanjing Jiancheng Bioengineering Institute (Nanjing, China) inflammatory cytokines, including interferon-γ (IFN-γ), transforming growth factor-β (TGF-β), tumor necrosis factor-α (TNF-α), interleukin (IL-1β, IL-4, IL-6, IL-10, and IL-17A) were determined using ELISA kit (MM-0412O2, MM-36525O2, MM-0383O2, MM-0422O2, MM-0419O2, MM-0418O2, MM-0425O2, MM-77840O2) from Jiangsu Meimian Industrial Co. Ltd., China.

Gut microbiota analysis

Microbial genomic DNA was extracted from piglet feces using DNA stool mini kit (Tiangen, Beijing, China) following the manufacturer's instructions. DNA concentration was quantified using a Nanodrop spectrophotometer, and quality was assessed by 1.2% agarose gel electrophoresis. The V3–V4 regions in 16S rDNA genes were amplified by specific primers (338 F and 806 R). The obtained PCR products were purified using the AxyPrep DNA Gel Extraction Kit (Axygen Biosciences, Union City, CA, United States), and sequencing was performed on an Illumina MiSeq platform (Personal Biotechnology Co., Ltd., Shanghai, China).

We performed standardized bioinformatics analyses on the raw data (FASTQ format) generated from Illumina paired-end sequencing to ensure the accuracy and reproducibility of the results. First, the raw FASTQ files were imported into the QIIME 2 (2019.4) platform and converted into a format compatible with QIIME 2 (qza format). Subsequently, the qiime cutadapt trim-paired plugin was used to remove primer sequences from the reads, ensuring the precise removal of primer fragments and filtering out reads that did not match the primer sequences, thereby improving data quality. Next, the qiime dada2 denoise-paired plugin was employed to call DADA2 for denoising. This step applied stringent quality control parameters to filter out low-quality sequences. Chimera sequences were identified and removed using the UCHIME algorithm (v8.1), effectively eliminating potential artifacts that could impact downstream analyses. This process generated high-confidence amplicon sequence variants (ASVs) and their associated abundance tables after chimera removal.

To analyze the microbiota composition, stacked bar plots were generated using the ggplot2 package (version 2.2.1) in R. Correlation network was constructed using the igraph package (version 1.1.2) to visualize relationships between bacterial taxa and host immune markers. Inter-group Venn analysis was conducted with the VennDiagram package (version 1.6.16) to identify overlapping and unique taxa among treatment groups. Given the compositional and non-parametric nature of microbiome data, statistical comparisons of microbial abundance were conducted using Kruskal–Wallis tests followed by *post hoc* Dunn's multiple comparisons to identify significant differences between groups. Additionally, Linear Discriminant Analysis Effect Size (LEfSe) was applied to detect bacterial taxa that were significantly enriched in each treatment group. The alpha-diversity index (Chao1, Observed species, Faith PD, and Goods coverage) and beta-diversity (PCoA analysis based on Bray_curtis) were computed using QIIME2.

Alpha diversity analysis was assessed using the Kruskal-Walli's test. Spearman correlation coefficients of microbial taxa were calculated and visualized using the heatmap package (version 2.3.1) in R software.

Statistical analysis

Data were statistically analyzed by GraphPad Prism 8.0. one-way ANOVA was used to assess differences among treatment groups when data followed a normal distribution. In cases where normality was not met, Kruskal–Wallis tests were applied to ensure robust statistical comparisons. Differences between treatments were determined by Duncan's post hoc tests and $p \leq 0.05$ was taken to indicate statistical significance.

Results

Growth performance

The effects of dietary supplementation of medium and short-chain fatty acids on growth performance of piglets are summarized in Table 2.

Body weight at 15 days and 35 days did not differ among the three groups of piglets. From days 1 to 15, piglets fed the VS + VM diet showed a significantly higher ADG and a lower F/G compared with the CON group ($p < 0.05$), and VSM group showed a trend higher ADG. However, during the second phase (days 16 to 35), the ADG of piglets in the VS + VM group significantly reduced compared to CON ($p < 0.05$).

Nutrient digestibility

As shown in Table 3, the dietary supplementation of medium- and short-chain fatty acids significantly affected nutrient digestibility. Compared with CON group, VSM treatment significantly increased the apparent digestibility of EE in 35 days, and VS + VM treatment significantly improved the apparent digestibility of Ca in 35 days ($p < 0.05$).

Serum biochemical parameters

As shown in Figure 1, the VS + VM group had a significantly higher serum TG concentration than the CON group ($p < 0.05$).

TABLE 2 Effects of MCFA and SCFA on growth performance and diarrhea rate of weaned piglets.

Items	Treatments			*p*-value
	CON	VSM	VS + VM	
Initial BW, kg	8.33 ± 0.52	8.21 ± 0.68	8.12 ± 0.41	0.866
15 days BW, kg	11.83 ± 0.51	12.06 ± 0.92	12.50 ± 0.60	0.429
Final BW, kg	21.96 ± 1.36	21.22 ± 1.50	20.29 ± 0.22	0.114
1 day to 15 days				
ADG (grams/day)	228.50 ± 15.84^{b}	255.75 ± 20.25^{ab}	288.00 ± 35.92^{a}	0.028
ADFI (grams/day)	455.50 ± 48.34	442.25 ± 27.22	435.25 ± 4.57	0.515
F/G	2.03 ± 0.29^{a}	1.75 ± 0.10^{ab}	1.55 ± 0.19^{b}	0.010
Diarrhea rate %	3.70 ± 1.65	2.75 ± 2.08	2.52 ± 1.15	0.592
Diarrhea index	0.84 ± 0.37	0.68 ± 0.55	0.52 ± 0.24	0.587
16 days to 35 days				
ADG (grams/day)	507.00 ± 46.81^{a}	455.00 ± 42.43^{ab}	389.75 ± 32.76^{b}	0.010
ADFI (grams/day)	941.25 ± 78.97	885.50 ± 58.79	834.25 ± 20.02	0.100
F/G	1.85 ± 0.13	1.98 ± 0.10	2.15 ± 0.21	0.059
Diarrhea rate %	3.25 ± 1.46	3.37 ± 0.92	2.56 ± 1.01	0.580
Diarrhea index	1.09 ± 0.49	1.17 ± 0.36	0.83 ± 0.30	0.468
1 day to 35 days				
ADG (grams/day)	386.00 ± 33.32	367.00 ± 29.72	345.50 ± 11.82	0.155
ADFI (grams/day)	731.00 ± 67.01	690.25 ± 43.41	661.50 ± 10.47	0.122
F/G	1.88 ± 0.15	1.90 ± 0.08	1.90 ± 0.12	0.943
Diarrhea rate %	3.44 ± 1.49	3.15 ± 1.14	2.54 ± 0.58	0.538
Diarrhea index	1.92 ± 0.85	1.87 ± 0.72	1.35 ± 0.30	0.439

BW, body weight; ADFI, average daily feed intake; ADG, average daily gain; F/G, feed to gain ratio; CON, basal diet + ZnO/common organic acid; VSM, basal diet + higher MCFA and lower SCFA content; VS + VM, basal diet + higher SCFA and lower MCFA content. Different letters mean statistically significant difference among the groups ($p < 0.05$). The data are presented as the means ± SD.

10.3389/fmicb.2025.1558588

TABLE 3 Effects of MCFA and SCFA on nutrient digestibility of weaned piglet.

Items	Treatments			*p*-value
	CON	VSM	VS + VM	
15 days				
CP %	73.75 ± 9.36	81.00 ± 3.30	75.47 ± 4.57	0.286
EE %	54.26 ± 15.14	67.56 ± 6.98	55.85 ± 8.66	0.221
Ash %	41.83 ± 12.25	57.49 ± 8.50	49.30 ± 5.09	0.102
Ca %	49.33 ± 21.66	70.06 ± 13.70	67.32 ± 7.37	0.174
P %	40.43 ± 14.76	57.83 ± 10.10	53.35 ± 10.45	0.158
35 days				
CP %	75.78 ± 3.49	79.42 ± 2.24	77.20 ± 3.76	0.323
EE %	61.00 ± 4.60^{b}	71.18 ± 3.39^{a}	67.40 ± 4.77^{ab}	0.025
Ash %	41.54 ± 5.85	43.65 ± 1.62	52.96 ± 10.01	0.087
Ca %	35.32 ± 16.55^{b}	31.50 ± 3.05^{b}	63.96 ± 11.43^{a}	0.014
P %	44.63 ± 7.31	51.75 ± 3.14	48.97 ± 12.17	0.508

CP, crude protein; EE, crude fat; ash, crude ash; Ca, calcium; P, phosphorus; CON, basal diet + ZnO/common organic acid; VSM, basal diet + higher MCFA and lower SCFA content; VS + VM, basal diet + higher SCFA and lower MCFA content. Different letters mean statistically significant difference among the groups ($p < 0.05$). The data are presented as the means ± SD ($n = 4$).

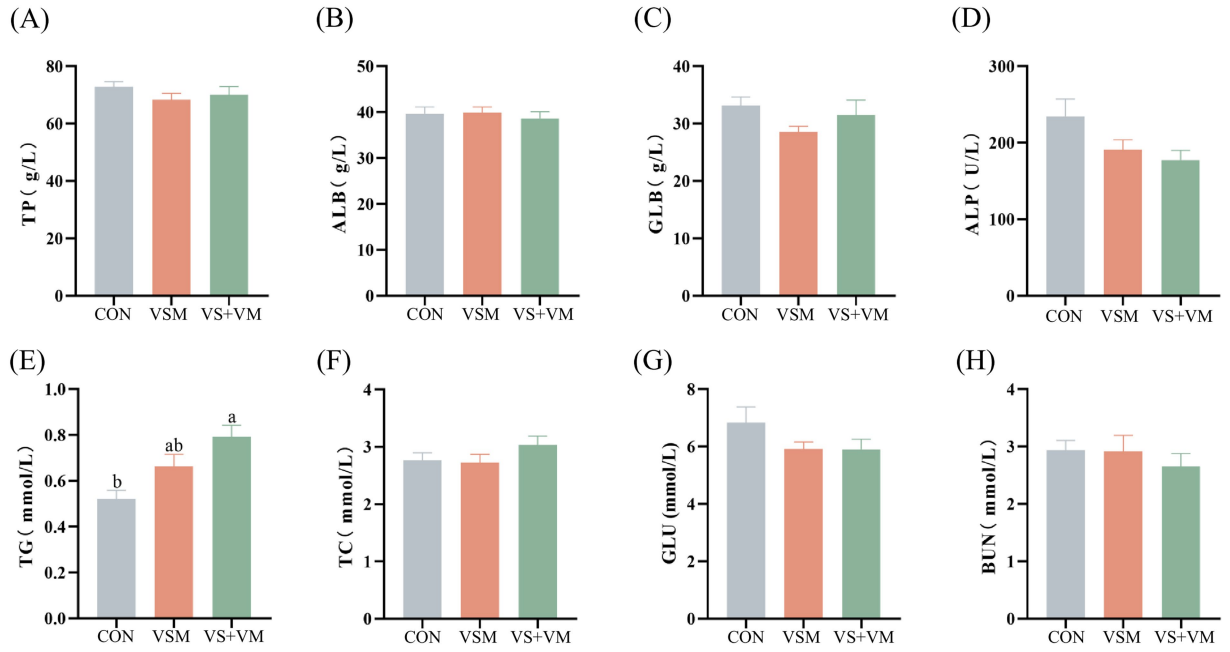

FIGURE 1
The effect of MCFA and SCFA addition on serum biochemical indexes of weaned piglets. **(A)** TP, **(B)** ALB, **(C)** GLB, **(D)** ALP, **(E)** TG, **(F)** TC, **(G)** GLU, and **(H)** BUN. Data were shown as means ± SEM ($n = 8$). TP, total protein; ALB, albumin; GLB, globulin; ALP, alkaline phosphatase; TC, total cholesterol; TG, total glyceride; GLU, glucose; BUN, blood urea nitrogen. CON, basal diet + ZnO/common organic acid; VSM, basal diet + higher MCFA and lower SCFA content; VS + VM, basal diet + higher SCFA and lower MCFA content. Different letters mean statistically significant difference among the groups ($p < 0.05$).

Intestinal permeability

As shown in Figure 2, the intestinal permeability of weaned piglets is reflected by the serum levels of D-lactate and DAO, which are higher in the VSM group and the VS + VM group compared to the CON group ($p < 0.05$).

Antioxidant stress

Antioxidant biochemical parameters in serum are presented in Figure 3. Compared with the CON group, both the VSM and VS + VM groups had significantly higher T-AOC levels in serum, and notably lower MDA concentrations ($p < 0.05$).

10.3389/fmicb.2025.1558588

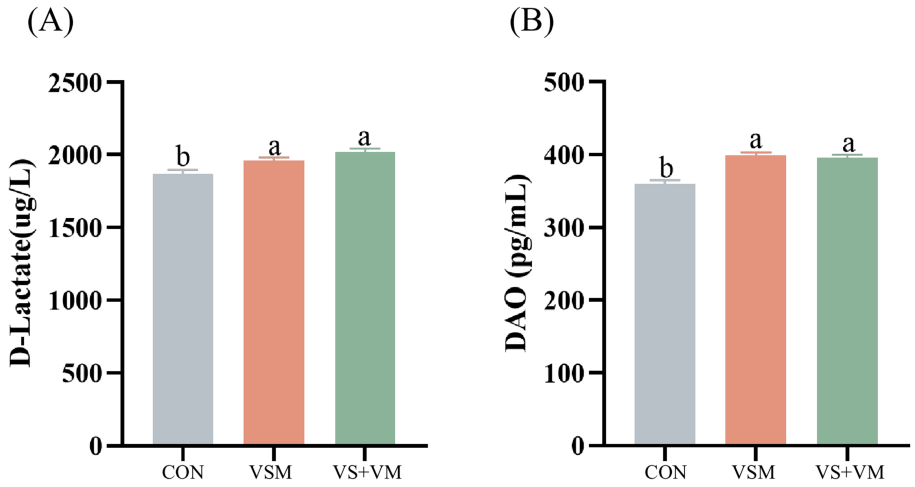

FIGURE 2
The effect of MCFA and SCFA on the concentrations of D-lactate and DAO in serum of weaning piglets. **(A)** D-lactic acid **(B)** DAO (diamine oxidase). CON, basal diet + ZnO/common organic acid; VSM, basal diet + higher MCFA and lower SCFA content; VS + VM, basal diet + higher SCFA and lower MCFA content. Data were shown as means ± SEM (n = 8). Different letters mean statistically significant difference among the groups ($p < 0.05$).

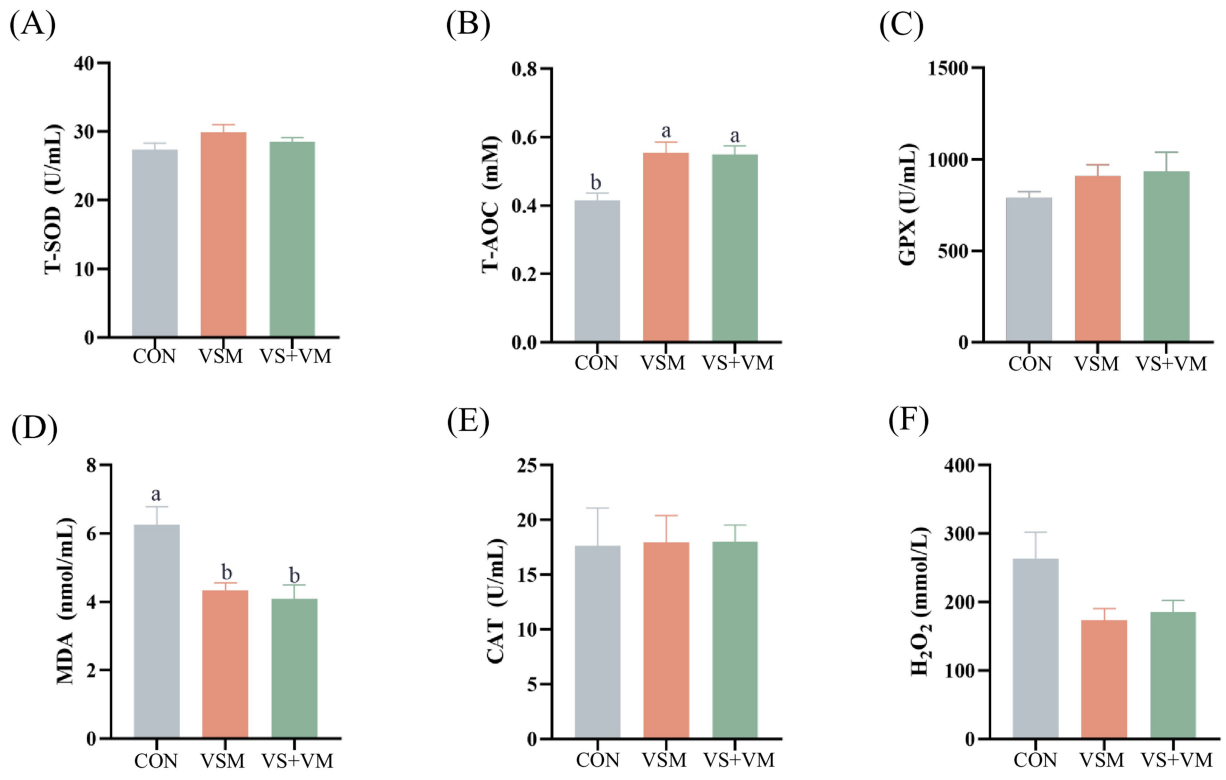

FIGURE 3
The effect of MCFA and SCFA on the serum antioxidant indicators. Serum levels of indicators including **(A)** T-SOD **(B)** T-AOC, **(C)** GPX, **(D)** MDA, **(E)** CAT, and **(F)** H_2O_2, were determined by using respective kits. T-SOD, total superoxide dismutase; T-AOC, total antioxidant capacity; GPX, glutathione peroxidase; CAT, catalase; MDA, malondialdehyde; H_2O_2, hydrogen peroxide CON, basal diet + ZnO/common organic acid; VSM, basal diet + higher MCFA and lower SCFA content; VS + VM, basal diet + higher SCFA and lower MCFA content. Data were shown as means ± SEM (n = 8). Different letters mean statistically significant difference among the groups ($p < 0.05$).

Inflammatory cytokines

The pro-inflammatory and anti-inflammatory cytokine profiles are presented in Figure 4. Compared with CON group, the VSM group notably reduced serum inflammatory cytokines, including IL-1β, TNF-α, IL-17A, IL-4, and IL-10 ($p < 0.05$). Thus, the VS + VM group significantly decreased IL-1β and IL-4, and increased IFN-γ, IL-6 and TGF-β in serum ($p < 0.05$).

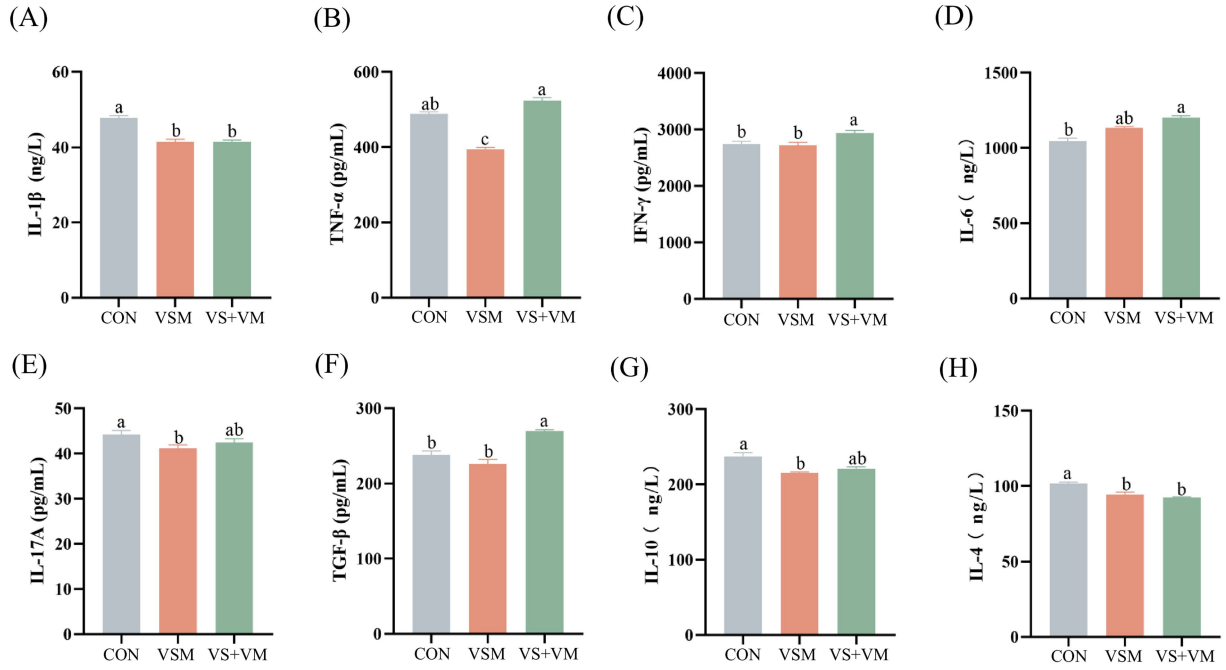

FIGURE 4
The effect of MCFA and SCFA on the production of inflammatory cytokines. Serum levels of **(A)** IL-1β, **(B)** TNF-α, **(C)** IFN-γ, **(D)** IL-6, **(E)** IL-17A **(F)** TGF-β **(G)** IL-10, and **(H)** IL-4 were measured by using ELISA kits. IL-1β, interleukin-1β; TNF-α, tumor necrosis factor-α; IFN-γ, interferon-γ; IL-6, interleukin-6; IL-17A, interleukin-17A; TGF-β, transforming growth factor-β; IL-10, interleukin-10; IL-4, interleukin-4. CON, basal diet + ZnO/common organic acid; VSM, basal diet + higher MCFA and lower SCFA content; VS + VM, basal diet + higher SCFA and lower MCFA content. Data were shown as means ± SEM (n = 8). Different letters mean statistically significant difference among the groups ($p < 0.05$).

Gut microbiota community

Gut microbes play a critical role in intestinal inflammation, we conducted 16S rDNA sequencing analysis of the intestinal bacteria. As shown in Figure 5, compared with the CON group, Chao1, Observed species, and Faith PD indices were significantly increased in the VSM group ($p < 0.05$); both VSM and VS + VM significantly decreased the goods coverage indices compared to the CON group ($p < 0.05$); At the phylum level, compared with the CON group, VS + VM group increased the relative abundance of *Bacteroidetes*, but decreased the relative abundance of *Firmicutes* and the ratio of *Firmicutes* to *Bacteroidetes* ($p < 0.05$) (Figures 6B,C). At the genus level, the abundances of genera *Lactobacillus* and *Butyricicoccus* were upregulated in the VSM group, and the abundance of genus *Butyrivibrio* were downregulated compared to the CON group ($p < 0.05$) (Figures 6D,H,J); further, the abundances of genera *Roseburia* was upregulated in the VS + VM group, and the abundances of genera *SMB53*, *Butyrivibrio* and *Turicibacter* were downregulated compared to the CON group ($p < 0.05$) (Figures 6E,G–I). The microbial composition of fecal samples was further analyzed by Linear discriminant analysis Effect Size (LEfSe) (Figure 6A). Thus, a total of 26 bacterial taxa were identified to be significantly different between the three groups.

Spearman's correlation analysis

The results of Spearman's correlation analysis between gut microbiota and serum immune cytokines are shown in Figure 7. At the phylum level, *Firmicutes* showed negatively correlations with TNF-α and IFN-γ ($p < 0.05$). *Bacteroidota* exhibited a positive correlation with IFN-γ ($p < 0.05$). *Tenericutes* showed negatively correlations with IL-1β, whereas positively correlated with TG ($p < 0.05$). *Proteobacteria* was positively correlated with IL-17A and *WPS-2* was positively correlated with IFN-γ ($p < 0.05$) (Figure 7A). At the genus level, *Megasphaera* was positively correlated with IL-1β, *Roseburia* and *Lachnospira* showed a negative correlation with IL-1β ($p < 0.05$), *SMB53* and *Streptococcus* were negatively correlated with TNF-α ($p < 0.05$), *Oscillospira*, *Phascolarctobacterium* and *p-75-a5* showed positive correlations with IFN-γ ($p < 0.05$), whereas *Lactobacillus* and *Bulleidia* were negatively correlated with IFN-γ ($p < 0.05$), *Lachnospira* was positively correlated with IL-6 ($p < 0.05$), *Megasphaera*, *SMB53*, *Clostridiaceae_Clostridium*, *Butyrivibrio* and *Turicibacter* exhibited a negative correlation with IL-6 ($p < 0.05$); Additionally, *SMB53*, *Bulleidia*, *Streptococcus*, and *Mogibacterium* showed a negative correlation with TGF-β ($p < 0.05$), *Blautia* and *Butyrivibrio* were positively correlated with IL-10, but negatively correlated with TG ($p < 0.05$), *Butyrivibrio* was positively correlated to IL-4 and *Corynebacterium* was positively correlated with T-SOD ($p < 0.05$), *p-75-a5* and *Lachnospira* showed a positive correlation with TG, *Bulleidia* was negatively correlated with TG ($p < 0.05$) (Figure 7B).

Discussion

MCFA and SCFA serve not only as energy sources for intestinal epithelial cells but enhance gut health through their

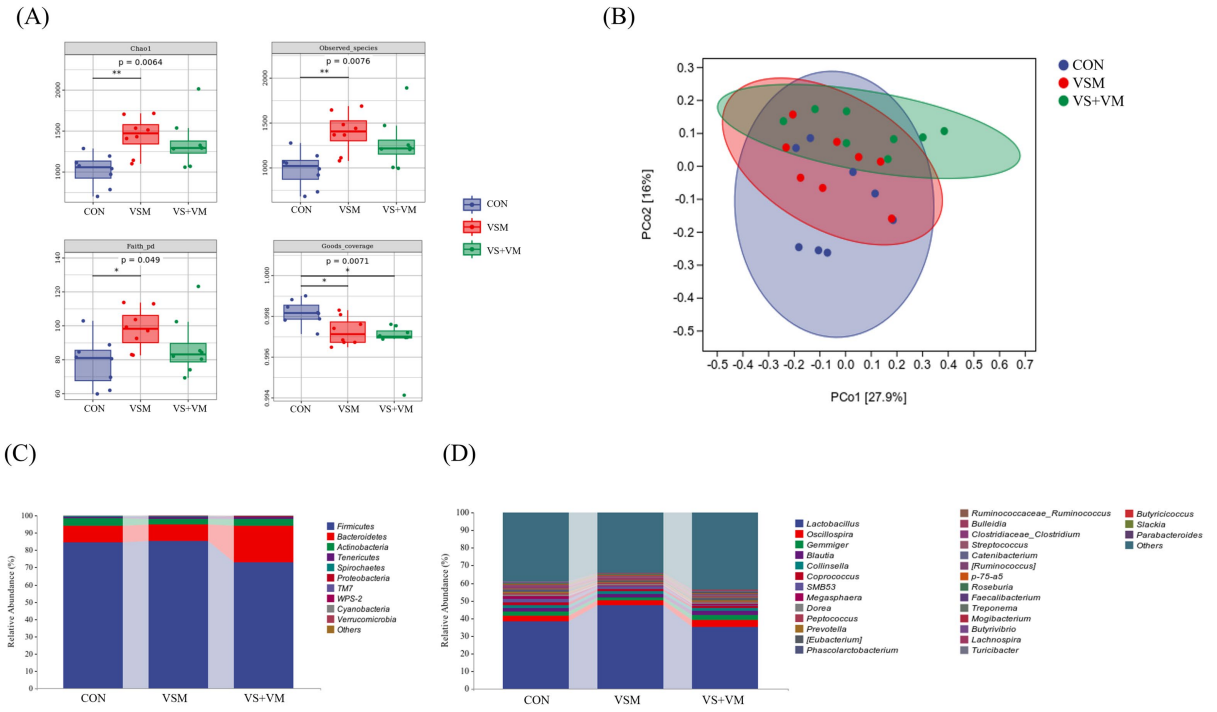

FIGURE 5
The effect of MCFA and SCFA of gut microbiota of piglets (n = 8) **(A)** Comparison of alpha diversity index (Chao1, Observed species, Faith PD, and Goods coverage). **(B)** Principal coordinates analysis (PCoA) based on Bray–Curtis **(C)** Relative abundance of bacterial phylum level. **(D)** Relative abundance of bacterial genus level. CON, basal diet + ZnO/common organic acid; VSM, basal diet + higher MCFA and lower SCFA content; VS + VM, basal diet + higher SCFA and lower MCFA content. Different letters mean statistically significant difference among the groups ($p < 0.05$) (*$p < 0.05$ and **$p < 0.01$).

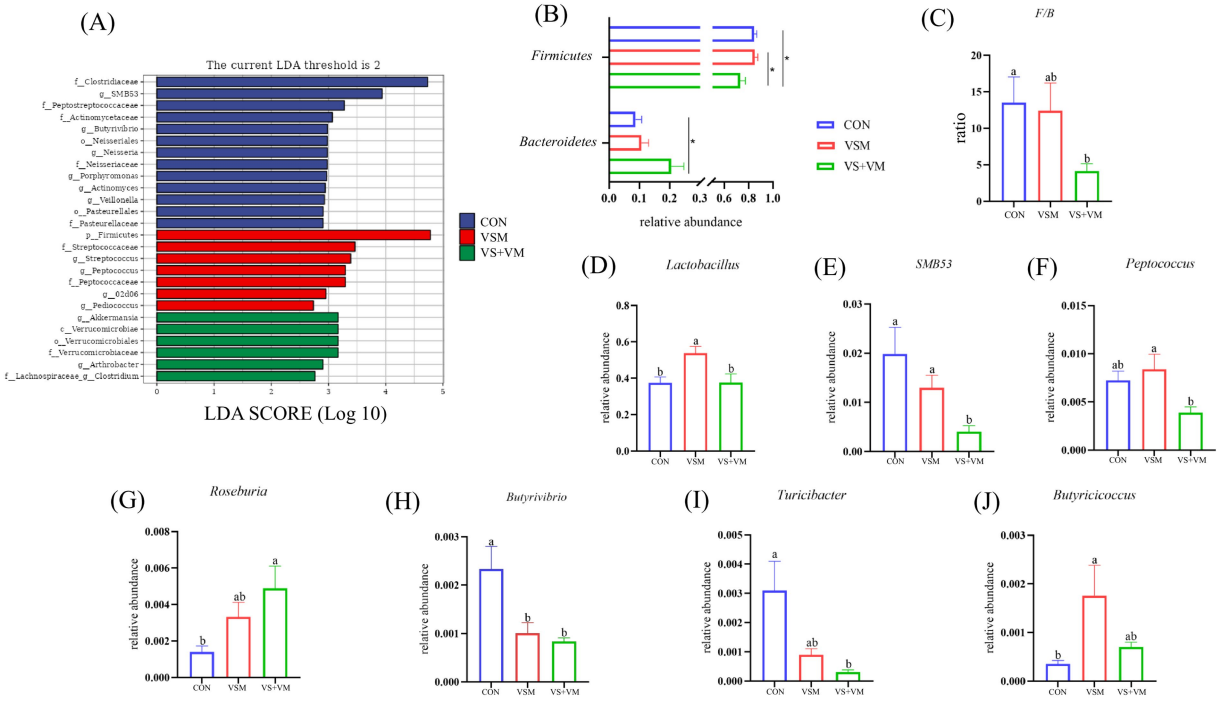

FIGURE 6
Effect of MCFA and SCFA of gut microbiota of piglets (n = 8). **(A)** LEfSe analysis effect size identified the most differentially abundant taxa in the cecal chyme microbiota community of each group, and only taxonomies of LDA score >2 is shown. **(B)** Relative abundance of *Firmicutes* and *Bacteroidetes* among the three groups. **(C)** The ratio of *Firmicutes* and *Bacteroidetes*. **(D–J)** Extended error bar plot showing the bacteria at the genus level that had significant. CON, basal diet + ZnO/common organic acid; VSM, basal diet + higher MCFA and lower SCFA content; VS + VM, basal diet + higher SCFA and lower MCFA content. Different letters mean statistically significant difference among the groups ($p < 0.05$) (*$p < 0.05$ and **$p < 0.01$).

broad-spectrum antibacterial activity (Lauridsen, 2020). By modulating the gastrointestinal microbiota, alleviating oxidative stress, and enhancing growth performance, MCFA and SCFA demonstrate considerable potential as alternatives to ZnO. Previous studies have found that the organic acids and MCFA exert a stronger growth-promoting effect on the weaned piglets than ZnO (Kuang et al., 2015). Additionally, combinations of SCFA and capric acid have been shown to improve production performance in weaned piglets and nursery pigs, likely by enhancing the digestibility of nutrients and supporting the structural integrity of the small intestinal mucosa (Hanczakowska et al., 2013). In this study, two dietary formulations with varied SCFA/MCFA ratio were analyzed, the proportion of MCFA was higher than that of SCFA in the VSM group, whereas the proportion of MCFA was lower than that of SCFA in the VS + VM group. Compared to the ZnO-based diet, both different ratios of MCFA and SCFA increased the ADG of weaned piglets in the first stage and reduced the F/G, aligning with previous findings and supporting the potential of fatty acids as ZnO replacements. However, in the second stage, the growth performance in the VS + VM group declined, suggesting that prolonged feeding of high formic acid levels may adversely affect feed intake, possibly due to changes in palatability. Throughout the entire experimental period, a higher MCFA proportion relative to SCFA appeared to improve the EE digestibility, with a more pronounced positive effect on growth performance.

Serum biochemical parameters reflect the metabolic level and health status of the animal body. In the present study, MCFA and SCFA did not alter TP and BUN content, which was similar to the CP digestibility results, indicating that MCFA and SCFA have no impact on the utilization and metabolism of proteins. Furthermore, serum levels of TG were elevated in the VS + VM group, which was similar to an earlier study (Cera et al., 1989), this phenomenon may be attributed to fatty acids serving as energy substrates to enhance TG synthesis, However, several studies have reported that MCFA can reduce serum TG levels (van de Heijning et al., 2017), and the exact mechanism needs to be further explored.

Oxidative stress is a primary cause of barrier damage and gastrointestinal diseases in piglets, often resulting from an excess of ROS that surpasses exceeding the antioxidant capacity (Lee and Kang, 2017; Qiao et al., 2023). Organic acids help maintain redox homeostasis, and previous studies have indicated that organic acid-based products, such as formic and acetic acid, can alleviate oxidative stress in intestinal epithelial cells (Xu et al., 2022). It is well-known that T-AOC reflects the overall ability of a biological system to counteract oxidative stress by neutralizing free radicals. In contrast, MDA is a byproduct of lipid peroxidation and serves as an indicator of oxidative damage within cells. In the current study, both of MCFA groups showed increased T-AOC level and decreased the MDA levels compared to the ZnO control, consistent with previous study (Long et al., 2018). It was demonstrated that dietary MCFA and SCFA improve antioxidant capacity, suggesting they can alleviate weaning-induced oxidative stress in piglets.

The intestinal barrier selectively facilitates the absorption of nutrients while serving as an important defense mechanism to prevent the translocation of bacteria and toxins from the intestinal lumen to other tissues. Weaning stress compromises the physical barrier, characterized by damage to tight junctions in the intestinal epithelium and increased intestinal permeability (Tang et al., 2022), potentially promoting bacterial translocation and exposing other tissues to pathogenic threats. When intestinal permeability increases, DAO secreted by intestinal mucosal cells and D-lactic

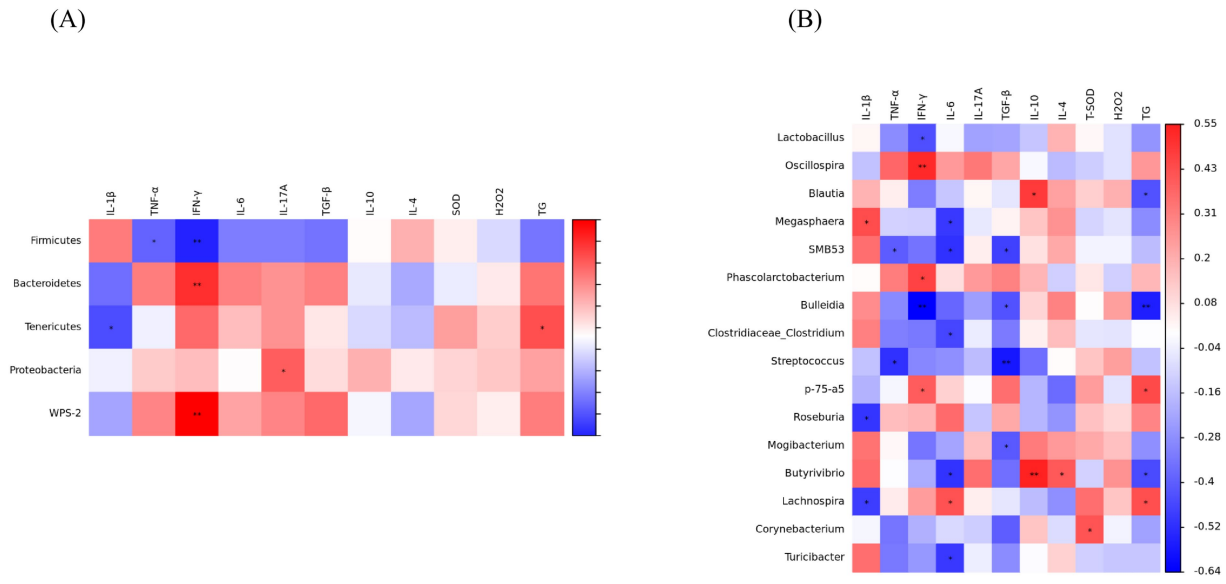

FIGURE 7
Spearman's correlation between antioxidant indicators, inflammatory cytokines and gut microbiota. **(A)** Phylum. **(B)** Genus. IL-1β, interleukin-1β; TNF-α, tumor necrosis factor-α; IFN-γ, interferon-γ; IL-6, interleukin-6; IL-17A, interleukin-17A; TGF-β, transforming growth factor-β; IL-4, interleukin-4; IL-10, interleukin-10; T-SOD, total superoxide dismutase; H_2O_2, hydrogen peroxide; TC, total cholesterol. (Significant correlations were marked by $*p < 0.05$ and $**p < 0.01$).

acid, a product of intestinal bacteria, can enter the bloodstream through the intestinal mucosa. Consequently, these markers are widely used to evaluate intestinal permeability (Song et al., 2013). In the present study, dietary supplementation with MCFA and SCFA resulted in higher serum concentration of DAO and D-lactic acid, suggesting that ZnO may be more effective in reducing intestinal permeability. Previous research showed that ZnO could reduce the serum levels of DAO and D-lactic acid in piglets (Peng et al., 2019). Further investigation is warranted to elucidate the potential of MCFA and SCFA in improving intestinal permeability.

The gut microbiota represents another essential barrier, whose dynamic equilibrium formed by their interdependence and mutual restriction plays a crucial role in maintaining the host's intestinal immune function. In the early stages of weaning, piglets are unable to fully utilize the nutrients in their diet, which provides a source of nutrition for the growth of pathogenic bacteria and may lead to the disruption of the microbial barrier (Su et al., 2022), underscoring the need for nutritional interventions to maintain gut microbiota balance (Lim et al., 2023). MCFA and SCFA exhibit certain antibacterial effects. Undissociated fatty acids penetrate bacterial membranes and dissociate within the alkaline cytoplasm of pathogens such as *Escherichia coli*. Releasing protons that acidify the intracellular environment. This acidification disrupts essential metabolic pathways and ultimately induces bacterial cell death (Gomez-Osorio et al., 2021). *Lactobacillus* and other beneficial bacteria have acid-resistant characteristics. Additionally, an appropriate concentration of acid can serve as a nutritional source for *Lactobacillus* (Hsiao and Siebert, 1999). Previous studies have found that supplementation of sows' diets with a mixture of organic acids and MCFA increases fecal counts of *Lactobacillus* and decreases *Escherichia coli* counts at farrowing and weaning (Lan and Kim, 2018). Our study found that the relative abundance of *Lactobacillus* was significantly higher in the VSM group, in addition, the indices of Chao1 and Observed species were improved in the VSM group. This indicates that a combination with a higher proportion of MCFA than SCFA shows better performance in selectively inhibiting harmful bacteria and promoting the growth of beneficial bacteria.

Dysbiosis in the gut microbiome, characterized by reduced microbial diversity and increased pathogenic bacteria, is closely related to the host inflammatory response (Bäumler and Sperandio, 2016). Dietary supplementation with specific fatty acids, such as MCFA and SCFA, may represent a promising strategy for mitigating intestinal inflammation in piglets (Liu, 2015). Previous studies have found that dietary supplementation with sodium caprylate enhanced immune function by regulating the gut microbiota and increasing the intestinal SCFA concentrations in mice (Zhao et al., 2021). In this study, a higher proportion of MCFA relative to SCFA not only improved microbiota richness and abundance of *Lactobacillus* but also reduced pro-inflammatory cytokine levels, including TNF-α, IL-1β, and IL-17A. These findings suggest that an optimal MCFA-to-SCFA ratio may alleviate inflammatory responses by modulating the gut microbiota. Furthermore, in this study, supplementation with MCFA and SCFA increased the relative abundance of *Roseburia* while decreasing the relative abundance of *Turicibacter*. *Roseburia* has been shown to exert protective effects against gut-dysbiosis-induced mastitis, mucosal inflammation, and systemic inflammation (Zhao et al., 2022). A correlation analusis revealed a negative association between *Roseburia* and IL-1β, a pro-inflammatory factor implicated in intestinal inflammation (Kaminsky et al., 2021), supporting the anti-inflammatory potential of *Roseburia*. Conversely, the pathogenic bacterium *Turicibacter* has been reported to increase in colitis mouse model (Wan et al., 2021). Interestingly, while *Butyrivibrio* bacteria, known for fermenting dietary fibers to produce SCFA like butyrate (Kopečný et al., 2003), decreased in MCFA and SCFA supplementation, this aligns with previous studies attributing the reduction to negative feedback regulation induced by exogenous SCFA supplementation (Zhou et al., 2017). Collectively, these findings indicate that supplementation of MCFA and SCFA positively regulate the intestinal microbiota composition, contributing to the improvement of intestinal health.

Conclusion

In this study, diets with a higher MCFA to SCFA ratio (VSM group) exerted more favorable effects on piglet growth performance and exhibited promise as a potential alternative to zinc oxide. These benefits were associated with improvements in gut microbiota composition, enhanced antioxidant capacity, and reduced inflammatory responses. However, the results for the VS + VM group, where SCFA levels exceeded MCFA, were less conclusive in terms of growth promotion. This may be attributed to the high formic acid content in the SCFA formulation, which could have affected feed palatability and consequently limited nutrient intake. While VS + VM supplementation exhibited some positive effects on gut health and inflammatory modulation, its overall impact on growth performance warrants further investigation.

Data availability statement

The raw data for all 16S rRNA amplicons sequenced in this study have been deposited in NCBI's Sequence Read Archive (SRA) under accession number PRJNA1243349.

Ethics statement

The animal study was approved by Institutional Animal Care and Use Committee of Henan Agricultural University. The study was conducted in accordance with the local legislation and institutional requirements.

Author contributions

ZF: Conceptualization, Methodology, Writing – original draft. LL: Project administration, Methodology, Writing – original draft. XW: Investigation, Validation, Writing – original draft. RX: Data curation, Writing – review & editing. PD: Formal analysis,

Writing – review & editing. ZW: Software, Writing – review & editing. HZ: Investigation, Writing – review & editing. YH: Project administration, Writing – review & editing. WC: Resources, Supervision, Writing – review & editing. XS: Conceptualization, Supervision, Writing – review & editing.

Funding

The author(s) declare that financial support was received for the research and/or publication of this article. This project was supported by Delvigent (Hebei) Biotech Co. Ltd., Cangzhou, China, which is the manufacturer of the MCFA and SCFA product tested within the study.

Conflict of interest

HZ was employed by Delvigent (Hebei) Biotech Co. Ltd., Cangzhou, China.

The remaining authors declare that the research was conducted in the absence of any commercial or financial relationships that could be construed as a potential conflict of interest.

Generative AI statement

The authors declare that no Gen AI was used in the creation of this manuscript.

Publisher's note

All claims expressed in this article are solely those of the authors and do not necessarily represent those of their affiliated organizations, or those of the publisher, the editors and the reviewers. Any product that may be evaluated in this article, or claim that may be made by its manufacturer, is not guaranteed or endorsed by the publisher.

References

Abd El-Hack, M. E., El-Saadony, M. T., Salem, H. M., El-Tahan, A. M., Soliman, M. M., Youssef, G. B. A., et al. (2022). Alternatives to antibiotics for organic poultry production: types, modes of action and impacts on bird's health and production. *Poult. Sci.* 101:101696. doi: 10.1016/j.psj.2022.101696

AOAC (2007) in Official methods of analysis of AOAC international. eds. W. Hortwitz and LatimerG. W. Jr.. *18th* ed (Gaithersburg, MD: AOAC International).

Bäumler, A. J., and Sperandio, V. (2016). Interactions between the microbiota and pathogenic bacteria in the gut. *Nature* 535, 85–93. doi: 10.1038/nature18849

Bonetti, A., Tugnoli, B., Piva, A., and Grilli, E. (2021). Towards zero zinc oxide: feeding strategies to manage post-weaning diarrhea in piglets. *Animals* 11:642. doi: 10.3390/ani11030642

Cai, L., Zhao, Y., Chen, W., Li, Y., Han, Y., Zhang, B., et al. (2024). Effect of an organic acid blend as an antibiotic alternative on growth performance, antioxidant capacity, intestinal barrier function, and fecal microbiota in weaned piglets. *J. Anim. Sci.* 102:skae149. doi: 10.1093/jas/skae149

Campbell, J. M., Crenshaw, J. D., and Polo, J. (2013). The biological stress of early weaned piglets. *J. Anim. Sci. Biotechnol.* 4:19. doi: 10.1186/2049-1891-4-19

Cera, K. R., Mahan, D. C., and Reinhart, G. A. (1989). Postweaning swine performance and serum profile responses to supplemental medium-chain free fatty acids and tallow. *J. Anim. Sci.* 67, 2048–2055. doi: 10.2527/jas1989.6782048x

den Besten, G., van Eunen, K., Groen, A. K., Venema, K., Reijngoud, D. J., and Bakker, B. M. (2013). The role of short-chain fatty acids in the interplay between diet, gut microbiota, and host energy metabolism. *J. Lipid Res.* 54, 2325–2340. doi: 10.1194/jlr.R036012

Feng, Y., An, Z., Chen, H., He, X., Wang, W., Li, X., et al. (2020). Ulva prolifera extract alleviates intestinal oxidative stress via Nrf2 signaling in weaned piglets challenged with hydrogen peroxide. *Front. Immunol.* 11:599735. doi: 10.3389/fimmu.2020.599735

Gomez-Osorio, L. M., Yepes-Medina, V., Ballou, A., Parini, M., and Angel, R. (2021). Short and medium chain fatty acids and their derivatives as a natural strategy in the control of necrotic enteritis and microbial homeostasis in broiler chickens. *Front. Vet. Sci.* 8:773372. doi: 10.3389/fvets.2021.773372

Grilli, E., Tugnoli, B., Vitari, F., Domeneghini, C., Morlacchini, M., Piva, A., et al. (2015). Low doses of microencapsulated zinc oxide improve performance and modulate the ileum architecture, inflammatory cytokines and tight junctions expression of weaned pigs. *Animal* 9, 1760–1768. doi: 10.1017/s1751731115001329

Hanczakowska, E., Szewczyk, A., Swiatkiewicz, M., and Okoń, K. (2013). Short- and medium-chain fatty acids as a feed supplement for weaning and nursery pigs. *Pol. J. Vet. Sci.* 16, 647–654. doi: 10.2478/pjvs-2013-0092

Hsiao, C. P., and Siebert, K. J. (1999). Modeling the inhibitory effects of organic acids on bacteria. *Int. J. Food Microbiol.* 47, 189–201. doi: 10.1016/s0168-1605(99)00012-4

Hu, Z., Liu, L., Guo, F., Huang, J., Qiao, J., Bi, R., et al. (2023). Dietary supplemental coated essential oils and organic acids mixture improves growth performance and gut health along with reduces Salmonella load of broiler chickens infected with *Salmonella enteritidis*. *J. Anim. Sci. Biotechnol.* 14:95. doi: 10.1186/s40104-023-00889-2

Jensen, J., Larsen, M. M., and Bak, J. (2016). National monitoring study in Denmark finds increased and critical levels of copper and zinc in arable soils fertilized with pig slurry. *Environ. Pollut.* 214, 334–340. doi: 10.1016/j.envpol.2016.03.034

Jiao, S., Zheng, Z., Zhuang, Y., Tang, C., and Zhang, N. (2023). Dietary medium-chain fatty acid and Bacillus in combination alleviate weaning stress of piglets by regulating intestinal microbiota and barrier function. *J. Anim. Sci.* 101. doi: 10.1093/jas/skac414

Kaminsky, L. W., Al-Sadi, R., and Ma, T. Y. (2021). IL-1β and the intestinal epithelial tight junction barrier. *Front. Immunol.* 12:767456. doi: 10.3389/fimmu.2021.767456

Kopečný, J., Zorec, M., Mrázek, J., Kobayashi, Y., and Marinšek-Logar, R. (2003). *Butyrivibrio hungatei* sp. nov. and *Pseudobutyrivibrio xylanivorans* sp. nov., butyrate-producing bacteria from the rumen. *Int. J. Syst. Evol. Microbiol.* 53, 201–209. doi: 10.1099/ijs.0.02345-0

Kuang, Y., Wang, Y., Zhang, Y., Song, Y., Zhang, X., Lin, Y., et al. (2015). Effects of dietary combinations of organic acids and medium chain fatty acids as a replacement of zinc oxide on growth, digestibility and immunity of weaned pigs. *Anim. Feed Sci. Technol.* 208, 145–157. doi: 10.1016/j.anifeedsci.2015.07.010

Laine, T. M., Lyytikäinen, T., Yliaho, M., and Anttila, M. (2008). Risk factors for post-weaning diarrhoea on piglet producing farms in Finland. *Acta Vet. Scand.* 50:21. doi: 10.1186/1751-0147-50-21

Lan, R., and Kim, I. (2018). Effects of organic acid and medium chain fatty acid blends on the performance of sows and their piglets. *Anim. Sci. J.* 89, 1673–1679. doi: 10.1111/asj.13111

Lauridsen, C. (2020). Effects of dietary fatty acids on gut health and function of pigs pre- and post-weaning. *J. Anim. Sci.* 98:skaa086. doi: 10.1093/jas/skaa086

Lee, S. I., and Kang, K. S. (2017). Function of capric acid in cyclophosphamide-induced intestinal inflammation, oxidative stress, and barrier function in pigs. *Sci. Rep.* 7:16530. doi: 10.1038/s41598-017-16561-5

Lim, J. A., Cha, J., Choi, S., Kim, J. H., and Kim, D. (2023). Early colonization of the intestinal microbiome of neonatal piglets is influenced by the maternal microbiome. *Animals* 13:3378. doi: 10.3390/ani13213378

Liu, Y. (2015). Fatty acids, inflammation and intestinal health in pigs. *J. Anim. Sci. Biotechnol.* 6:41. doi: 10.1186/s40104-015-0040-1

Liu, P., Pieper, R., Rieger, J., Vahjen, W., Davin, R., Plendl, J., et al. (2014). Effect of dietary zinc oxide on morphological characteristics, mucin composition and gene expression in the colon of weaned piglets. *PLoS One* 9:e91091. doi: 10.1371/journal.pone.0091091

Long, L., Chen, J., Zhang, Y., Liang, X., Ni, H., Zhang, B., et al. (2017). Comparison of porous and nano zinc oxide for replacing high-dose dietary regular zinc oxide in weaning piglets. *PLoS One* 12:e0182550. doi: 10.1371/journal.pone.0182550

Long, S. F., Xu, Y. T., Pan, L., Wang, Q. Q., Wang, C. L., Wu, J. Y., et al. (2018). Mixed organic acids as antibiotic substitutes improve performance, serum immunity, intestinal morphology and microbiota for weaned piglets. *Anim. Feed Sci. Technol.* 235, 23–32. doi: 10.1016/j.anifeedsci.2017.08.018

López-Colom, P., Castillejos, L., Rodríguez-Sorrento, A., Puyalto, M., Mallo, J. J., and Martín-Orúe, S. M. (2020). Impact of in-feed sodium butyrate or sodium heptanoate protected with medium-chain fatty acids on gut health in weaned piglets challenged with *Escherichia coli* F4$^+$. *Arch. Anim. Nutr.* 74, 271–295. doi: 10.1080/1745039x.2020.1726719

Nagao, K., and Yanagita, T. (2010). Medium-chain fatty acids: functional lipids for the prevention and treatment of the metabolic syndrome. *Pharmacol. Res.* 61, 208–212. doi: 10.1016/j.phrs.2009.11.007

Nakkarach, A., Foo, H. L., Song, A. A., Mutalib, N. E. A., Nitisinprasert, S., and Withayagiat, U. (2021). Anti-cancer and anti-inflammatory effects elicited by short chain fatty acids produced by *Escherichia coli* isolated from healthy human gut microbiota. *Microb. Cell Factories* 20:36. doi: 10.1186/s12934-020-01477-z

Peng, P., Chen, J., Yao, K., Yin, Y., Long, L., and Fang, R. (2019). The effects of dietary supplementation with porous zinc oxide on growth performance, intestinal microbiota, morphology, and permeability in weaned piglets. *Anim. Sci. J.* 90, 1220–1228. doi: 10.1111/asj.13228

Qiao, L., Dou, X., Song, X., Chang, J., Yi, H., and Xu, C. (2023). Targeting mitochondria with antioxidant nutrients for the prevention and treatment of postweaning diarrhea in piglets. *Anim. Nutr.* 15, 275–287. doi: 10.1016/j.aninu.2023.09.002

Song, J., Li, Y. L., and Hu, C. H. (2013). Effects of copper-exchanged montmorillonite, as alternative to antibiotic, on diarrhea, intestinal permeability and proinflammatory cytokine of weanling pigs. *Appl. Clay Sci.* 77-78, 52–55. doi: 10.1016/j.clay.2013.01.016

Su, W., Gong, T., Jiang, Z., Lu, Z., and Wang, Y. (2022). The role of probiotics in alleviating postweaning diarrhea in piglets from the perspective of intestinal barriers. *Front. Cell. Infect. Microbiol.* 12:883107. doi: 10.3389/fcimb.2022.883107

Szabó, R. T., Kovács-Weber, M., Zimborán, Á., Kovács, L., and Erdélyi, M. (2023). Effects of short- and medium-chain fatty acids on production, meat quality, and microbial attributes—a review. *Molecules* 28:4956. doi: 10.3390/molecules28134956

Tan, L., Xi, Y., Zhou, C., Xu, Y., Pang, J., Peng, X., et al. (2023). Supplementation with antimicrobial peptides or a tannic acid can effectively replace the pharmacological effects of zinc oxide in the early stages of weaning piglets. *Animals* 13:1797. doi: 10.3390/ani13111797

Tang, X., Xiong, K., Fang, R., and Li, M. (2022). Weaning stress and intestinal health of piglets: a review. *Front. Immunol.* 13:1042778. doi: 10.3389/fimmu.2022.1042778

Tang, X., Xiong, K., Zeng, Y., and Fang, R. (2024). The mechanism of zinc oxide in alleviating diarrhea in piglets after weaning: a review from the perspective of intestinal barrier function. *Int. J. Mol. Sci.* 25:10040. doi: 10.3390/ijms251810040

van de Heijning, B. J. M., Oosting, A., Kegler, D., and van der Beek, E. M. (2017). An increased dietary supply of medium-chain fatty acids during early weaning in rodents prevents excessive fat accumulation in adulthood. *Nutrients* 9:631. doi: 10.3390/nu9060631

Wan, F., Zhong, R., Wang, M., Zhou, Y., Chen, Y., Yi, B., et al. (2021). Caffeic acid supplement alleviates colonic inflammation and oxidative stress potentially through improved gut microbiota community in mice. *Front. Microbiol.* 12:784211. doi: 10.3389/fmicb.2021.784211

Xu, Q., Liu, M., Chao, X., Zhang, C., Yang, H., Chen, J., et al. (2022). Acidifiers attenuate diquat-induced oxidative stress and inflammatory responses by regulating NF-κB/MAPK/COX-2 pathways in IPEC-J2 cells. *Antioxidants* 11:2002. doi: 10.3390/antiox11102002

Zentek, J., Buchheit-Renko, S., Ferrara, F., Vahjen, W., van Kessel, A. G., and Pieper, R. (2011). Nutritional and physiological role of medium-chain triglycerides and medium-chain fatty acids in piglets. *Anim. Health Res. Rev.* 12, 83–93. doi: 10.1017/s1466252311000089

Zhao, C., Bao, L., Qiu, M., Wu, K., Zhao, Y., Feng, L., et al. (2022). Commensal cow *Roseburia* reduces gut-dysbiosis-induced mastitis through inhibiting bacterial translocation by producing butyrate in mice. *Cell Rep.* 41:111681. doi: 10.1016/j.celrep.2022.111681

Zhao, J., Hu, J., and Ma, X. (2021). Sodium caprylate improves intestinal mucosal barrier function and antioxidant capacity by altering gut microbial metabolism. *Food Funct.* 12, 9750–9762. doi: 10.1039/d1fo01975a

Zhou, Z., Nie, K., Huang, Q., Li, K., Sun, Y., Zhou, R., et al. (2017). Changes of cecal microflora in chickens following *Eimeria tenella* challenge and regulating effect of coated sodium butyrate. *Exp. Parasitol.* 177, 73–81. doi: 10.1016/j.exppara.2017.04.007

Glossary

ADFI - Average daily feed intake

ADG - Average daily gain

ALB - Albumin

ALP - Alkaline phosphatase

AIA - Acid-insoluble ash

Ash - Crude ash

ATTD - Apparent total tract digestibility

BUN - Blood urea nitrogen

BW - Body weight

Ca - Calcium

CAT - Catalase

CP - Crude protein

DAO - Diamine oxidase

EE - Crude fat

ELISA - Enzyme-linked immunosorbent assay

F/G - Feed to gain ratio

GLB - Globulin

GLU - Glucose

GPX - Glutathione peroxidase

H_2O_2 - Hydrogen peroxide

IFN-γ - Interferon-γ

IL-1β - Interleukin-1β

IL-4 - Interleukin-4

IL-6 - Interleukin-6

IL-10 - Interleukin-10

IL-17A - Interleukin-17A

MCFA - Medium-chain fatty acid

MDA - Malondialdehyde

P - Phosphorus

ROS - Reactive oxygen species

SCFA - Short-chain fatty acid

T-AOC - Total antioxidant capacity

TC - Total cholesterol

TG - Total glyceride

TGF-β - Transforming growth factor-β

TP - Total protein

T-SOD - Total superoxide dismutase

TNF-α - Tumor necrosis factor-α

ZnO - Zinc oxide

frontiers | Frontiers in Microbiology

TYPE Original Research
PUBLISHED 16 April 2025
DOI 10.3389/fmicb.2025.1556056

Check for updates

OPEN ACCESS

EDITED BY
Yunkyoung Lee,
Jeju National University, Republic of Korea

REVIEWED BY
Wanli Zhao,
Chinese Academy of Sciences, China
Jing Liu,
University of Pennsylvania, United States
Yuting Ke,
Massachusetts Institute of Technology, United States

*CORRESPONDENCE
Lanqing Ma
malanqing@kmmu.edu.cn
Jiangkun Yu
yjk555@ynu.edu.cn

†These authors have contributed equally to this work

RECEIVED 06 January 2025
ACCEPTED 24 March 2025
PUBLISHED 16 April 2025

CITATION
Wang X, Chen H, Yang M, Huang M, Zhang D, Li M, Wang H, Zhou Q, Lu L, Li Y, Yu J and Ma L (2025) Influence of gut microbiota and immune markers in different stages of colorectal adenomas. *Front. Microbiol.* 16:1556056. doi: 10.3389/fmicb.2025.1556056

COPYRIGHT
© 2025 Wang, Chen, Yang, Huang, Zhang, Li, Wang, Zhou, Lu, Li, Yu and Ma. This is an open-access article distributed under the terms of the Creative Commons Attribution License (CC BY). The use, distribution or reproduction in other forums is permitted, provided the original author(s) and the copyright owner(s) are credited and that the original publication in this journal is cited, in accordance with accepted academic practice. No use, distribution or reproduction is permitted which does not comply with these terms.

Influence of gut microbiota and immune markers in different stages of colorectal adenomas

Xianmei Wang[1†], Hang Chen[1†], Meng Yang[1], Minshan Huang[1], Dan Zhang[1], Mingke Li[1], Hui Wang[1], Qingqing Zhou[1], Lihong Lu[1], Yu Li[1], Jiangkun Yu[2]* and Lanqing Ma[1]*

[1]Yunnan Institute of Digestive Disease, The First Affiliated Hospital of Kunming Medical University, Kunming, China, [2]State Key Laboratory for Conservation and Utilization of Bio-Resources in Yunnan, School of Life Sciences, Yunnan University, Kunming, Yunnan, China

Objective: Colorectal adenomas (CRA) are the primary precancerous lesions leading to colorectal cancer (CRC). Early detection and intervention of CRA can significantly reduce the incidence of CRC. We investigated the relationships between the gut microbiome and the expression levels of PD-L1, IL-6, and IFN-γ at different CRA stages.

Methods: Participants were divided into normal, non-advanced adenoma (NAA), and advanced adenoma (AA) groups. PD-L1 expression in collected tissues was analyzed via immunohistochemistry (IHC) and Western blotting. Serum IL-6 and IFN-γ levels were measured using Enzyme-Linked Immunosorbent Assay (ELISA). 16S rRNA gene sequencing was used to examine gut microbiota changes, with correlation analysis to assess microbial influences on CRA progression.

Results: The main differences in bacterial composition among the three groups were found within the Firmicutes and Bacteroidetes phyla. In the normal vs. NAA comparison, *Clostridium sensu stricto, Faecalimonas, Gemmiger, and Ruminococcus* were more abundant in the normal group, while *Solobacterium* was enriched in the NAA group. For the normal vs. AA comparison, the normal group was enriched with *Anaerostipes, Blautia, Clostridium sensu stricto, Intestinibacter, Phocaeicola, and Turicibacter*, whereas *Solobacterium* was more abundant in the AA group. In the NAA vs. AA comparison, the NAA group exhibited higher levels of *Blautia, Faecalimonas, and Turicibacter* relative to the AA group. *Anaerostipes and Blautia* are positively correlated with *taurine and hypotaurine metabolism, propanoate metabolism, and zeatin biosynthesis.* PD-L1 protein levels progressively increase with CRA advancement. Additionally, *Faecalimonas, and Solobacterium* were negatively associated with IFN-γ, while *Gemmiger, and Anaerostipes* were positively associated with IL-6.

Conclusion: This study highlights the dynamic alterations in gut microbiota composition and their potential influence on the regulation of inflammatory cytokines and PD-L1 expression during CRA progression. The enrichment of protective taxa, such as *Anaerostipes* and *Blautia*, in the normal group emphasizes their potential role in mitigating adenoma progression. Dietary modulation to promote the proliferation of these beneficial bacteria could serve as a promising strategy to improve colorectal health. Future research

should further explore the specific relationships between dietary components, gut microbiota, and metabolic pathways, and assess the effects of dietary interventions on gut health.

KEYWORDS

colorectal adenoma, colorectal cancer, microbiota, PD-L1, IL-6, IFN-γ

1 Introduction

Colorectal cancer (CRC) is the third most common malignant tumor globally and the second leading cause of cancer-related death, accounting for approximately 10% of all cancer-related deaths (Sung et al., 2021). In China, CRC has become the third most common malignant tumor (Zheng et al., 2019). Over 85% CRCs originate from colorectal adenomas (CRA), and the causal relationship between the two has been established (Fu et al., 2025). The "normal mucosa-adenoma-cancer" pathway is considered the main route for CRC formation (Mang, 2019). The reported prevalence of CRA in China is approximately 13.3%–18.1%, with the prevalence of advanced adenomas being about 3.5% (Hong et al., 2018; Pan et al., 2020). Advanced adenomas are significant precursors to CRC, with the risk of progression to CRC increasing significantly by approximately 30%–50% (Conteduca et al., 2013). Although much research has focused on the metastatic and therapeutic aspects of advanced CRC, studies on the CRA stage are relatively limited, particularly in the areas of gut microbiota and dietary influences on CRA. Therefore, this study aims to explore the biomarkers and microbiota changes during the CRA stage, combined with dietary interventions, to provide new insights for early diagnosis and intervention of CRA.

Dietary interventions, as a non-pharmacological treatment approach, have been widely applied in the management of various diseases. In the prevention and treatment of CRA and CRC, a well-balanced diet can significantly reduce disease risk and improve patient prognosis. Studies have shown that the intake of dietary fiber can lower the risk of CRC by increasing the abundance of beneficial gut microbiota and reducing carcinogens in the gut (Munteanu and Schwartz, 2024; Song et al., 2018). Therefore, dietary treatment holds great promise as an effective measure for preventing the progression of CRA and the occurrence of CRC.

The "normal mucosa-adenoma-cancer" process is a multifactorial and multistep complex process. The human gut microbiota, primarily composed of bacteria from the Firmicutes, Bacteroidetes, Actinobacteria, and Proteobacteria phyla, is essential for functions such as nutrient absorption and immune regulation (Adak and Khan, 2019). Dysbiosis, or imbalance in this microbiota, can disrupt these functions and contribute to the development of diseases like colorectal tumors. Specifically, dysbiosis is linked to CRA and CRC, potentially by damaging intestinal epithelial cells, altering metabolism, and producing carcinogens (Flemer et al., 2017; Sepich-Poore et al., 2021). This disruption may lead to abnormal crypt foci, promoting the formation of colorectal polyps and eventually cancer (Liang et al., 2020; Zouggar et al., 2020).

In the tumor microenvironment, pro-inflammatory cytokines like IFN-γ and IL-6 can upregulate PD-L1, a protein that helps tumors evade immune detection (Lim et al., 2016). This upregulation allows cancer cells to avoid being targeted by the immune system. The PD-1/PD-L1 pathway, increasingly recognized for its role in CRC, suppresses cytotoxic lymphocyte activity, facilitating immune escape (Chen et al., 2017; Wu et al., 2022). Additionally, changes in the gut microbiota composition and metabolism can contribute to CRC by influencing local inflammation and genotoxic stress (Cao et al., 2022). However, the exact relationship between PD-L1 expression (Freitas et al., 2021; Gatenbee et al., 2022; Miller et al., 2018) and plasma inflammatory cytokines (Huang et al., 2019; Shi et al., 2015) with disease progression remains unclear.

Our study aims to investigate changes in the gut microbiota, IL-6, IFN-γ, and PD-L1 across different stages of CRA. By identifying significant biomarkers associated with these stages, and regulating gut microbiota composition and the production of beneficial metabolic products through dietary interventions.

2 Materials and methods

2.1 Ethics statement

This study was approved by the Ethics Committees of the First Affiliated Hospital of Kunming Medical University (project license number: L-26/2022). It was conducted in accordance with the principles of the Declaration of Helsinki. Written informed consent was obtained from all participants included in the study. Additionally, all research activities were carried out following applicable guidelines and regulations.

2.2 Subjects

The study was conducted between 2022 and 2023 at the First Affiliated Hospital of Kunming Medical University, with a total of 30 participants involved. These individuals were categorized into three groups based on their colorectal health status: normal (n = 10), non-advanced adenoma (NAA, n = 10), and advanced stage adenoma (AA, n = 10). Each participant provided three types of samples: serum samples to measure inflammatory cytokines IL-6 and IFN-γ via Enzyme-Linked Immunosorbent Assay (ELISA), fecal samples for analyzing gut microbiota composition using 16S rRNA gene sequencing, and intestinal tissue samples for assessing PD-L1 protein expression through Western blotting (Figure 1A). According to the 2020 guidelines by the US Multi-Society Task Force on the endoscopic identification and management of malignant colorectal polyps[6], CRA were classified based on their pathological structural characteristics determined by Hematoxylin and Eosin (H&E) staining. These categories included

tubular adenomas (villous component < 25%), villous adenomas (villous component > 75%), and tubulovillous adenomas (villous component between 25 and 75%). For classification purposes, normal samples displayed regular colorectal mucosa, NAA samples exhibited tubular adenomas with a gross specimen length of <10 mm, a villous component <25%, and no high-grade dysplasia, while AA samples showed tubulovillous adenomas with a villous component ranging from 25 to 75% (Figure 1B). Participants were included in the study if they were diagnosed with one of the three groups based on H&E staining (normal, non-advanced adenoma, or advanced stage adenoma). The exclusion criteria consisted of individuals with a history of colorectal polyps or colorectal surgery, a personal or family history of gastrointestinal tumors, inflammatory bowel disease, infectious diseases, metabolic disorders (e.g., diabetes, obesity, and hyperlipidemia), immune system diseases, or severe hepatic or renal conditions.

2.3 Sample collection

All participants provided two samples of normal colonic mucosa or post-operative specimens, with the exact sampling locations detailed in Supplementary Table 1. One sample was stained with H&E, while the other was preserved in liquid nitrogen for subsequent PD-L1 protein expression detection through Western Blot and Immunohistochemistry (IHC). Prior to taking intestinal cleansing agents, fecal samples (5–10 g) were collected using single-use fecal sampling tubes, quickly frozen in liquid nitrogen for 16S rRNA sequencing. Blood samples (5 ml) were drawn from peripheral veins before colonoscopy, processed by centrifugation (3,000 rpm for 10 min at room temperature), and the serum was promptly frozen in liquid nitrogen for subsequent analysis of IL-6 and IFN-γ levels using ELISA.

2.4 Histology

Evaluated the expression of PD-L1 using IHC. Colorectal tissues were processed by embedding in OCT compound and then rapidly frozen in liquid nitrogen. These tissues were then sectioned into 5 μm slices. Tissue sections were baked overnight in an oven, dewaxed progressively with xylene and anhydrous ethanol, subjected to antigen retrieval with sodium citrate, cooled at room temperature, processed for membrane breakage, and blocked with sheep serum for 30 min. The sections were then incubated overnight with primary antibody, rewarmed for 1 h, incubated with secondary antibody, treated with horseradish peroxidase, visualized by DAB, dehydrated, and sealed. Colorectal sections underwent hematoxylin and eosin (H&E) staining for further examination. Image analysis was performed using ImageJ software.

2.5 Examination of inflammatory factors, and PDL1 level

The levels of serum inflammatory factors (IL-6, and IFN-γ) were determined using a commercial ELISA kit (IL-6, EK106/2-96; IFN-γ, EK180-96, Lianke Biotechnology Co., Ltd., Hangzhou, China) following the manufacturer's instructions. Evaluated the protein expression of PD-L1 in colorectal tissue using Western blot. Fresh Colorectal tissues were pulverized under liquid nitrogen, and high-efficiency RIPA lysate (catalog number 89900, Thermo) was utilized for protein extraction. The resultant protein samples were then loaded (20 μg/10 μl per well) and resolved via sodium dodecyl sulfate-polyacrylamide gel electrophoresis (SDS-PAGE) on gels comprised of either 10 or 12.5% acrylamide. Subsequently, the separated proteins were transferred onto polyvinylidene fluoride (PVDF) membranes (catalog number ISEQ00010, Millipore). The membranes were then blocked with 5% skim milk in TBST for 2 h at room temperature. Following blocking, the membranes were incubated with primary antibodies targeted against PDL1 (1:1000) and GAPDH (1:1000). After thorough washing and incubation with appropriate secondary antibodies, the blots were visualized using a ChemiDoc XRS imaging system. The quantification of target proteins was achieved by normalizing their relative intensities in the experimental groups to those in the control group.

2.6 DNA extraction and 16S rRNA gene sequencing

Genomic DNA was extracted from fecal samples and the quality and concentration of purified DNA was measured with NanoDrop 2000. The isolated DNA was stored at −20°C for 16S amplified library preparation or qPCR. The hypervariable V3-V4 region of the 16S rRNA gene in 20 ng of DNA was amplified using gene-specific primers:5′ACTCCTACGGGAGGCAGCAG3′, R:5′ GGACTACHVGGGTWTCTAAT 3′. PCR conditions were 95°C for 3 min, 27 cycles of 95°C for 30 s, 55°C for 30 s and 72°C for 45 s, 72°C for 10 min and holding at 4°C. Two steps of amplification were performed to prepare the sequencing library using TransGen AP221-02. Quantification was performed using the QuantiFluor-ST^{TM} (Promega), followed by paired-end sequencing on an Illumina platform.

2.7 16S rRNA gene amplicon sequencing analysis

Fastq files from the Illumina MiSeq run were processed through the QIIME2 pipeline as shown by Bolyen et al. (2019) using the DADA2 plugin (Callahan et al., 2016) to generate amplicon sequence variants (ASVs). Taxonomic classification was performed using the rdp_16S_v18_classifier database (Hung et al., 2022). While genus-level classifications are robust due to the resolution of the V3-V4 region of the 16S rRNA gene, species-level annotations were inferred based on probabilistic matches in the reference database. We performed multivariate testing between treatment groups and further performed *post hoc* comparisons when significant differences were observed. We determined alpha diversity indices: Pielou's evenness, Shannon diversity and Observed species. Beta diversity was calculated based on the unweighted unifrac distance metric and visualized using principal co-ordinates analysis (PCoA).

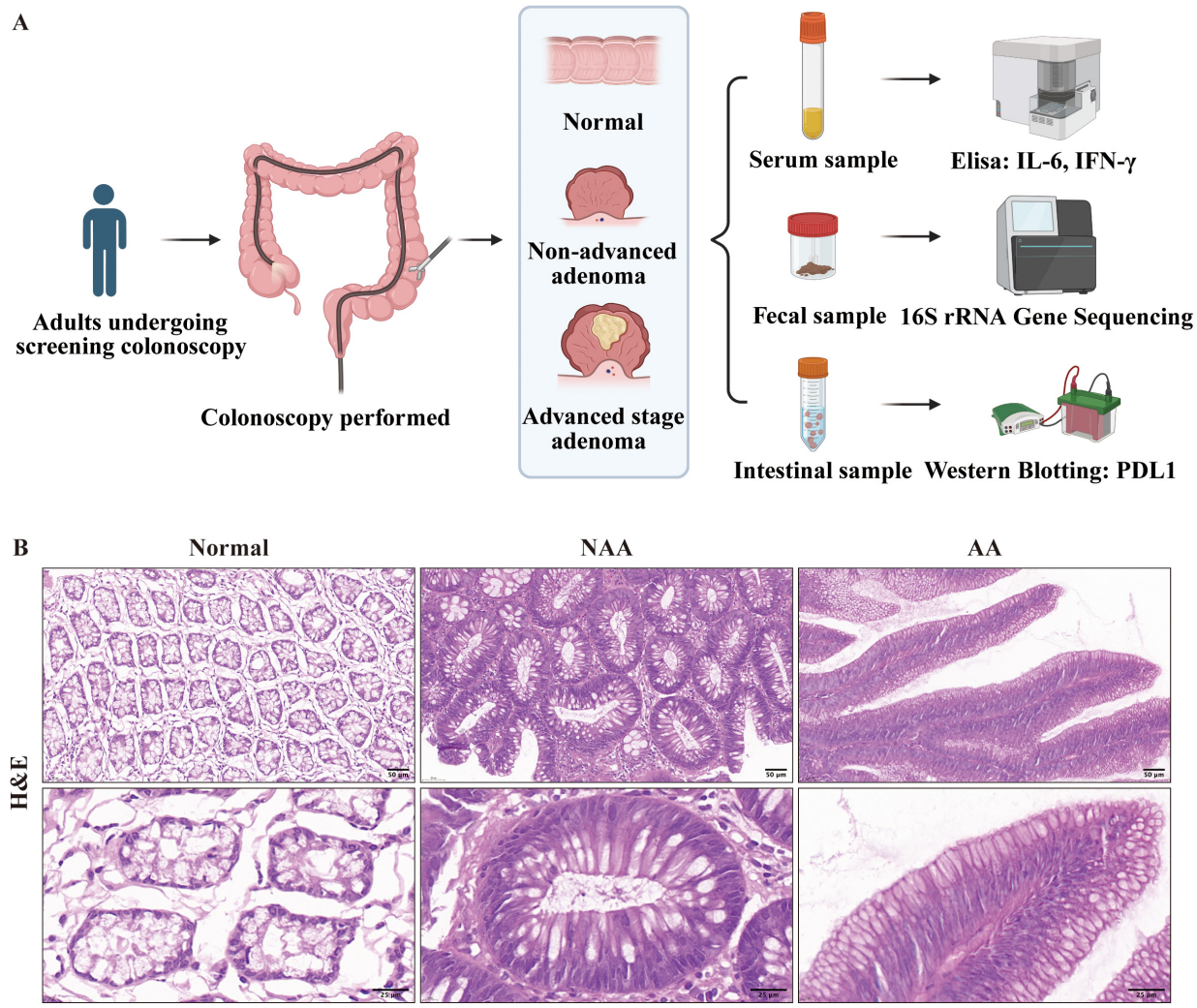

FIGURE 1
Cohort enrollment flowchart and Representative Hematoxylin and Eosin. **(A)** Cohort enrollment flowchart (provided by BioRender.com). **(B)** Representative Hematoxylin and Eosin (H&E) stained sections from each of the normal, NAA, and AA groups (30×, 100× magnification; scale bar: 50, 25 μm). Normal, normal group; NAA, non-advanced adenoma group; AA, advanced stage adenoma group.

2.8 Linear discriminant analysis and function predict

We identified taxa differentiating the normal, NAA, and AA groups using linear discriminant analysis effect size (LEfSe). LEfSe utilizes a non-parametric Kruskal-Wallis rank sum test to assess differential features with significantly different abundances between assigned taxa and performs LDA to estimate the effect size of each sequence variant as reported by Segata et al. (2011). LDA scores ranking differential taxa are displayed on a LEfSe bar chart according to their effect size. For LEfSe analysis data are first converted to log10 before the non-parametric Kruskal-Wallis rank sum test. The cut-off of the LDA score was set to 2, and significant features were considered with *P*-values lower than 0.05. To predict the metabolic pathways, phylogenetic investigation of communities by reconstruction of unobserved states (Picrust2) was performed from sequencing data, as shown before (Douglas et al., 2020). Fastq sequence files for each sample were processed using QIIME2. Representative sequences were used as input files for the Picrust2 analysis pipeline. Metabolic pathways were assigned based on the Kyoto Encyclopedia of Genes and Genomes (KEGG) (Langille et al., 2013).

2.9 Statistical analyses

Statistical evaluations in this study were conducted utilizing GraphPad Prism (ver. 9) and R (ver. 4.3.0). The microbial composition at different levels, KEGG as well as indices of alpha diversity were analyzed using Kruskal-Wallis test. Beta diversity was calculated using unweighted UniFrac distance, and a permutational multivariate analysis of variance (PERMANOVA) (Anderson, 2001) was performed in QIIME2 to confirm significant differences between groups. Spearman's rank correlation method was used to analyze relationships between variables. To ensure consistency, data were preprocessed through normalization and scaling of variables before analysis. The data are presented as

the mean ± standard error of the mean (SEM). Differences were deemed statistically significant at a threshold of $p < 0.05$.

3 Results

3.1 Microbial diversity analysis

3.1.1 Alpha diversity

The study examined changes in α-diversity and β-diversity of the gut microbiota across different stages of CRA using 16S rRNA gene sequencing. For alpha diversity, the observed species showed a slight decrease from the normal group to the NAA group and the AA group, with no statistically significant differences (ns) between the groups, except for a significant reduction ($p < 0.05$) between the normal and AA groups. The Pielou index was significantly higher in the normal group compared to the NAA and AA groups ($p < 0.05$). The NAA group exhibited the lowest Pielou index, while the AA group showed a slightly higher value compared to the NAA group, with no statistically significant difference (ns). The Shannon index progressively decreases from the normal group to the NAA group and further to the AA group, with a significant difference ($p < 0.05$) observed between the normal and AA groups. No statistically significant differences (ns) were observed between the normal and NAA groups or between the NAA and AA groups (Figure 2A).

3.1.2 Beta diversity

Principal co-ordinates analysis was performed at the species level to investigate the gut microbial community structure, revealing significant differences among the normal, NAA, and AA groups (PERMANOVA, $R^2 = 1.524$, P-value = 0.016) (Figure 2B). PCoA1 explained 13.7% of the variation in the microbial community structure, while PCoA2 accounted for 8.1%. These results highlight distinct microbial community profiles across the three groups, with a significant shift from normal to NAA through AA.

3.2 Differential analysis of gut microbiota composition

The LEfSe algorithm was employed to pinpoint the key bacterial taxa responsible for the differences in gut microbiota across the normal, NAA, and AA group phenotypes. Our detailed exploration into the microbial composition at various taxonomic levels, as illustrated in Supplementary Figure 1.

At the family level (Figure 3A), the fecal microbiota primarily comprised three bacterial families: *Clostridiaceae 1, Oscillospiraceae,* and *Turicibacteraceae*. Compared to the NAA and AA groups, the gut microbiota of the normal group was enriched with *Clostridiaceae 1* and *Oscillospiraceae*. Furthermore, compared to the AA group, both the normal and NAA groups exhibited enrichment of *Turicibacteraceae* in the gut microbiome.

At the genus level (Figure 3B), the fecal microbiota primarily comprised bacteria from the following genera: *Anaerostipes, Blautia, Clostridium sensu stricto, Faecalibacterium, Faecalimonas, Gemmiger, Intestinibacter, Phocaeicola, Ruminococcus, Solobacterium,* and *Turicibacter*. Compared to the NAA group, the gut microbiota of the normal group was enriched with *Clostridium sensu stricto, Faecalimonas, Gemmiger,* and *Ruminococcus*. In contrast, the NAA group shows an enrichment of *Solobacterium* when compared to the normal group. Compared to the AA group, the normal group's gut microbiota is enriched with *Anaerostipes, Blautia, Clostridium sensu stricto, Intestinibacter, Phocaeicola,* and *Turicibacter*. Conversely, compared to the normal group, the AA group exhibits an enrichment of *Solobacterium*. Furthermore, compared to the AA group, the NAA group's gut microbiota is enriched with *Blautia, Faecalimonas,* and *Turicibacter*.

At the species level (Figure 3C), the fecal microbiota primarily includes the following species: *Anaerostipes hadrus, Blautia faecis, Faecalimonas umbilicata, Gemmiger formicilis, Intestinibacter bartlettii, Mediterraneibacter lactaris, Phocaeicola vulgatus, Ruminococcus bromii, Solobacterium moorei,* and *Turicibacter bilis*. Compared to the NAA group, the gut microbiota of the normal group is enriched with *Gemmiger formicilis* and *Ruminococcus bromii*. Conversely, compared to the normal group, the NAA group shows an enrichment of *Solobacterium moorei*. Compared to the AA group, the normal group's gut microbiota is enriched with *Anaerostipes hadrus, Intestinibacter bartlettii, Mediterraneibacter lactaris, Phocaeicola vulgatus,* and *Turicibacter bilis*. On the other hand, compared to the normal group, the AA group exhibited an enrichment of *Solobacterium moorei*. Furthermore, compared to the AA group, the NAA group's gut microbiota is enriched with *Blautia faecis, Faecalimonas umbilicata, Mediterraneibacter lactaris,* and *Turicibacter bilis*.

3.3 Predicted KEGG functional pathways in the gut microbiome

In the normal vs. NAA comparison (Figure 4A), 11 KEGG pathways showed significant differences. The NAA group exhibited upregulation in *Nucleocytoplasmic transport, Arginine and proline metabolism, Pentose and glucuronate interconversions,* and *Galactose metabolism*. Downregulated pathways included *Terpenoid backbone biosynthesis, Aminoacyl-tRNA biosynthesis, Protein export, Pyrimidine metabolism, Carbon fixation pathways in prokaryotes, Zeatin biosynthesis, and Protein processing in the endoplasmic reticulum*.

In the normal vs. AA comparison (Figure 4B), three KEGG pathways showed significant differences. The AA group exhibited upregulation in *Taurine and hypotaurine metabolism* and downregulation in *RNA polymerase, Nitrotoluene degradation, and Flagellar assembly*.

In the NAA vs. AA comparison (Figure 4C), 15 KEGG pathways showed significant differences. The AA group exhibited upregulation in *Propanoate metabolism, Zeatin biosynthesis, Terpenoid backbone biosynthesis, DNA replication, Homologous recombination, and Taurine and hypotaurine metabolism*. Downregulated pathways included *Bacterial chemotaxis, Nitrotoluene degradation, ABC transporters, Porphyrin metabolism, Two-component system, Biosynthesis of unsaturated fatty acids, Epithelial cell signaling in Helicobacter pylori infection, N-Glycan biosynthesis, and Nucleocytoplasmic transport*.

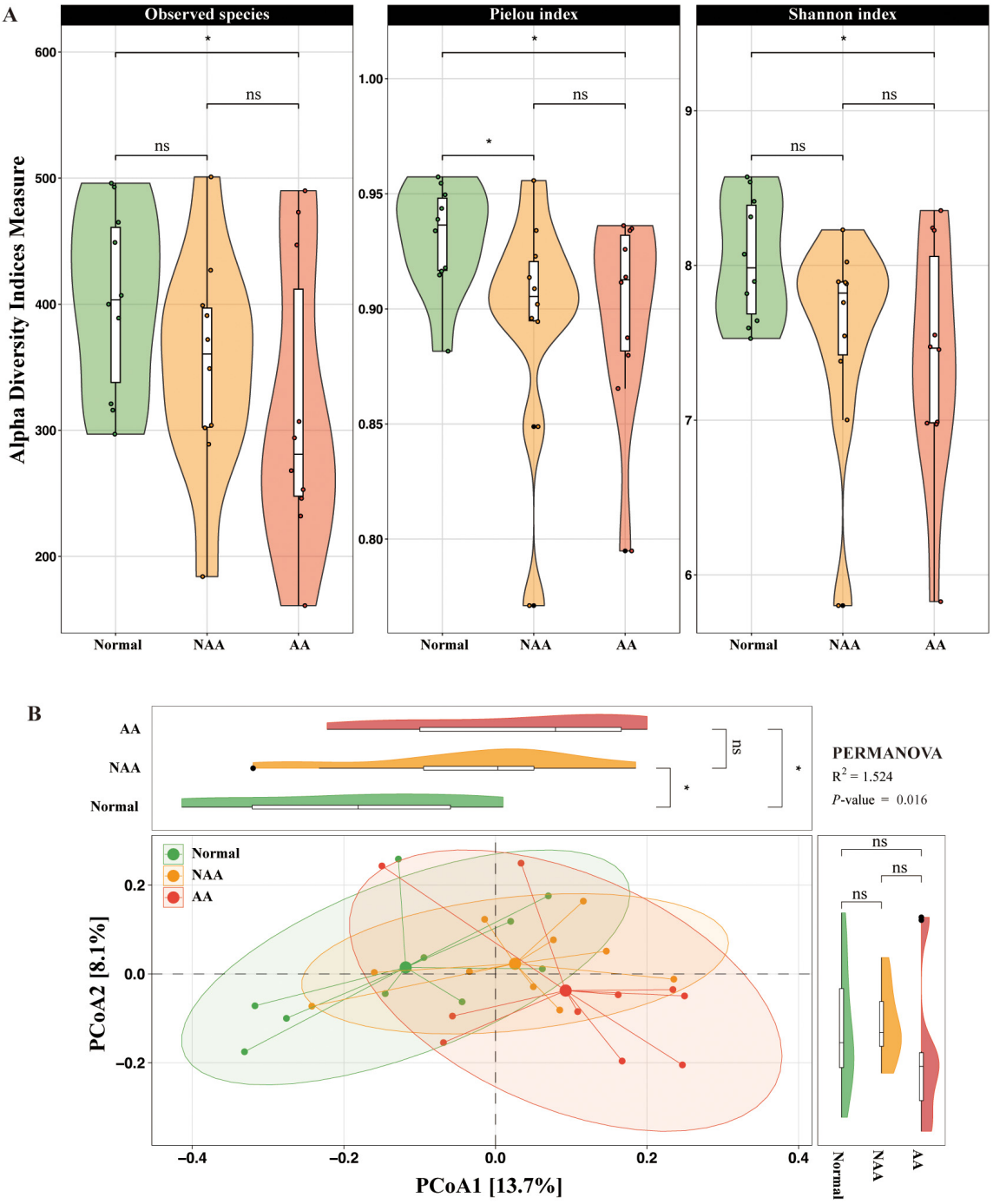

FIGURE 2
Gut microbiota profiling in normal, NAA, and AA groups. **(A)** Alpha diversity of microbial communities in normal, NAA, and AA groups, including observed species, Pielou index and Shannon index. **(B)** Coordination plot of principal co-ordinates analysis (PCoA) of microbial communities among normal, NAA, and AA groups. Normal, normal group; NAA, non-advanced adenoma group; AA, advanced stage adenoma group. The data are presented as means ± SD, $n = 10$. *$P < 0.05$.

3.4 Correlations between the microbial pathways and gut microbes

Figure 5 provides an analysis of the correlations between various bacterial taxa and functional metabolic pathways in the gut microbiota at different stages of CRA (normal, NAA, AA). The heatmap organizes these taxa into two phyla, *Bacillota* and *Bacteroidota*. Significant positive correlations are observed for taxa like *Blautia*, *Blautia faecis*, *Anaerostipes*, and *Anaerostipes hadrus* with metabolic pathways such as Taurine and hypotaurine metabolism, Propanoate metabolism, and Zeatin biosynthesis. On the other hand, taxa such as *Faecalimonas*, *Faecalimonas umbilicata*, *Turicibacteraceae*, *Turicibacter*, and *Turicibacter bilis* are

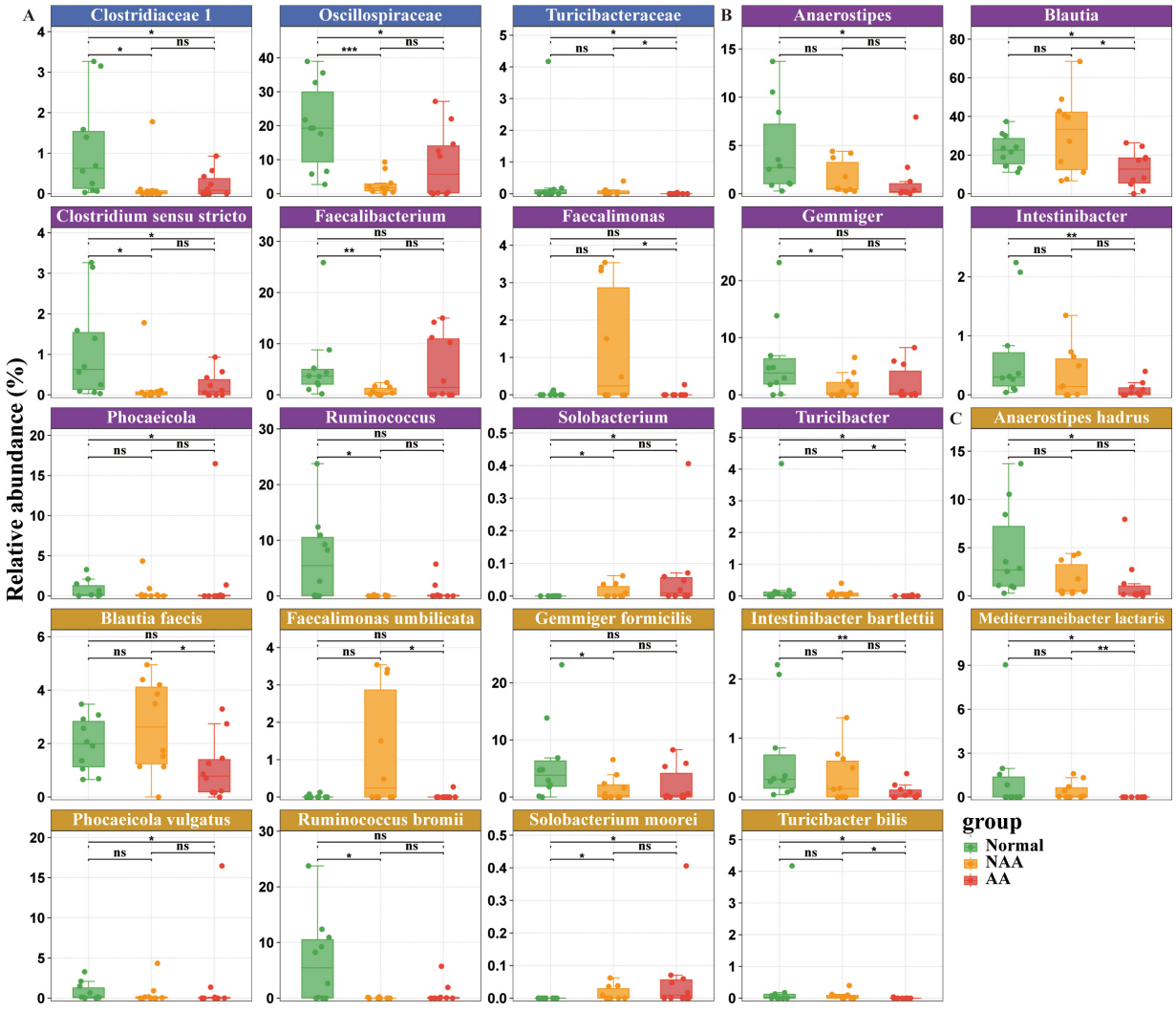

FIGURE 3
Differential gut microbiota composition at family, genus, species level between normal, NAA, and AA groups. **(A)** Family level. **(B)** Genus level. **(C)** Species level. Normal, normal group; NAA, non-advanced adenoma group; AA, advanced stage adenoma group. The data are presented as means ± SD, $n = 10$. *$P < 0.05$; **$P < 0.01$; ***$P < 0.001$.

negatively correlated with pathways including Aminoacyl-tRNA biosynthesis, Terpenoid backbone biosynthesis, and Flagellar assembly.

3.5 PD-L1 expression and correlation of IL-6, IFN-γ, and gut microbes

Immunohistochemistry revealed increasing PD-L1 expression across the groups: normal (+), NAA (++), and AA (+++) (Figure 6A). Western blot analysis confirmed this trend, showing a progressive rise in PD-L1 levels from normal to AA (Figure 6B). Negative correlations were found between IFN-γ and *Faecalimonas, Faecalimonas umbilicata, Solobacterium,* and *Solobacterium moorei* ($p < 0.1$). Positive correlations were identified between IL-6 and *Gemmiger, Gemmiger formicilis, Anaerostipes,* and *Anaerostipes hadrus* ($p < 0.05$ for *Gemmiger* and *Gemmiger formicilis*, $p < 0.1$ for others) (Figure 6C).

4 Discussion

This study adds to the growing body of evidence linking the gut microbiome to CRC, with a specific focus on the precancerous stage of adenomas. By examining tissue PD-L1 protein expression, serum levels of inflammatory cytokines (IL-6, IFN-γ), and fecal gut microbiota composition across various stages of CRA, including normal, NAA, and AA, our research aimed to identify biomarkers indicative of significant changes during adenoma progression. Our research aims to identify biomarkers that signify important changes during adenoma progression and provide scientific support for dietary interventions by elucidating the functional roles of microbial taxa involved.

The observed reduction in α-diversity within the fecal microbiome associated with adenomas aligns with findings from Peters et al. (2016) who reported similar trends. However, contrasting results from Feng et al. (2015) study, which showed

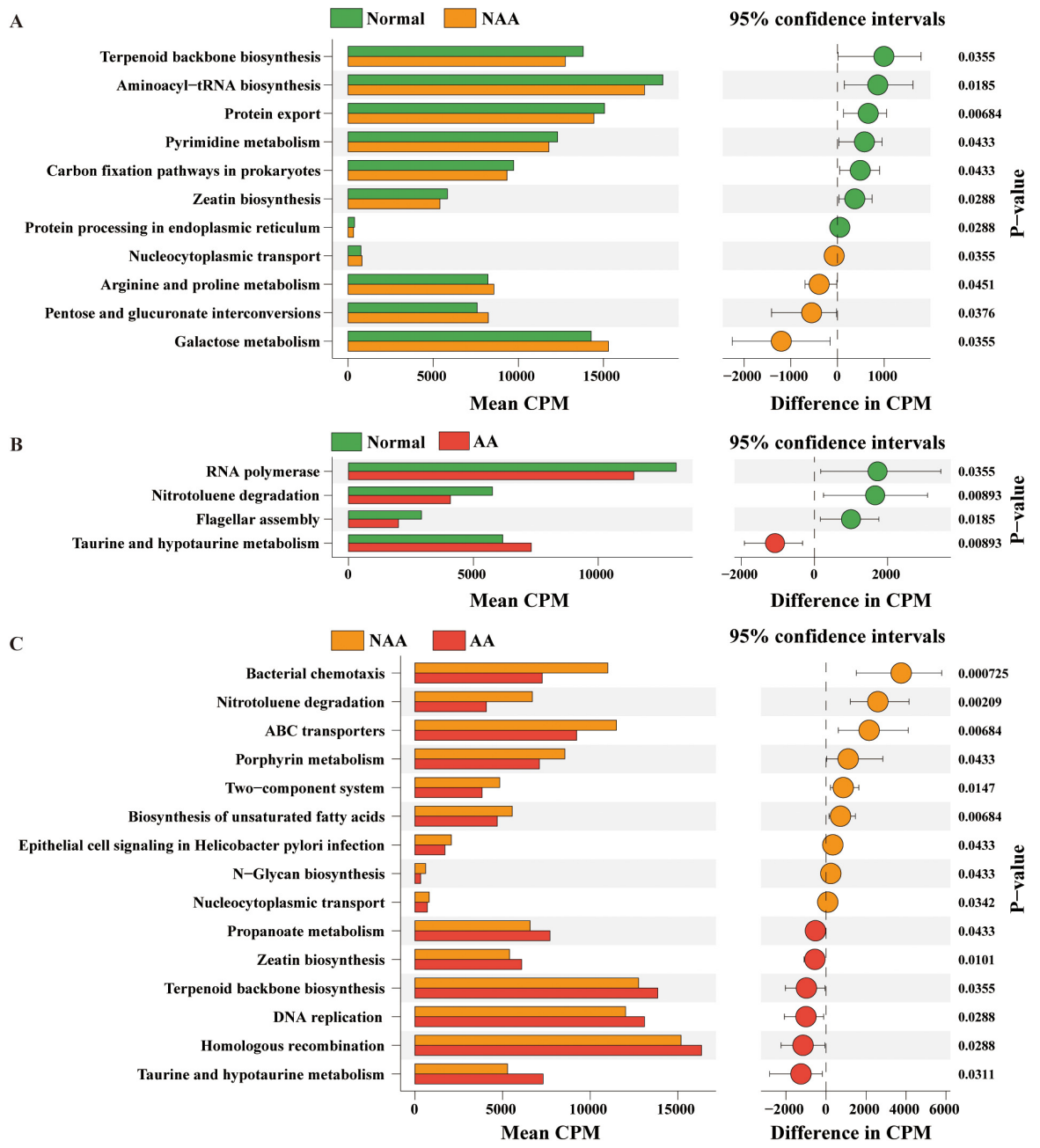

FIGURE 4
Kyoto Encyclopedia of Genes and Genomes (KEGG) functional pathways predicted in the gut microbiome of normal, NAA, and AA groups using Picrust2. **(A)** Linear discriminant analysis of predicted microbial metabolic functions between normal and NAA. **(B)** Linear discriminant analysis of predicted microbial metabolic functions between normal and AA. **(C)** Linear discriminant analysis of predicted microbial metabolic functions between NAA and AA. Selection of discriminative microbial pathways between groups were based on an LDA score cutoff of 3.0 and differences in the relative abundances of pathway (converted to log base 10) were statistically determined based on a Kruskal-Wallis and pairwise Wilcoxon tests. A p-value of <0.05 and a score ≥ 3.0 were considered significant in Kruskal-Wallis and pairwise Wilcoxon tests, respectively, at a significance level of 0.05; $n = 10$. Normal, normal group; NAA, non-advanced adenoma group; AA, advanced stage adenoma group.

higher diversity in pre-tumor and tumor groups, highlight the complex nature of microbiome alterations during adenoma development. This discrepancy suggests that the relationship between microbiota diversity and adenoma progression may be influenced by additional factors, such as genetic predispositions, environmental influences, and lifestyle choices, that warrant further investigation. Specifically, dietary habits are known to play a crucial role in shaping gut microbiota composition. For instance, a high-fiber diet may enhance the diversity of beneficial microbial populations (Yang et al., 2021), while a Western-style diet may lead to an overrepresentation of pro-inflammatory bacteria (Shin et al., 2021). These dietary factors likely contribute to the observed differences in microbiota diversity and may be a key factor in adenoma progression. Notably, participants with the highest dietary fiber intake, particularly from cereals and fruits, had a lower risk of colorectal adenoma and distal colon cancer

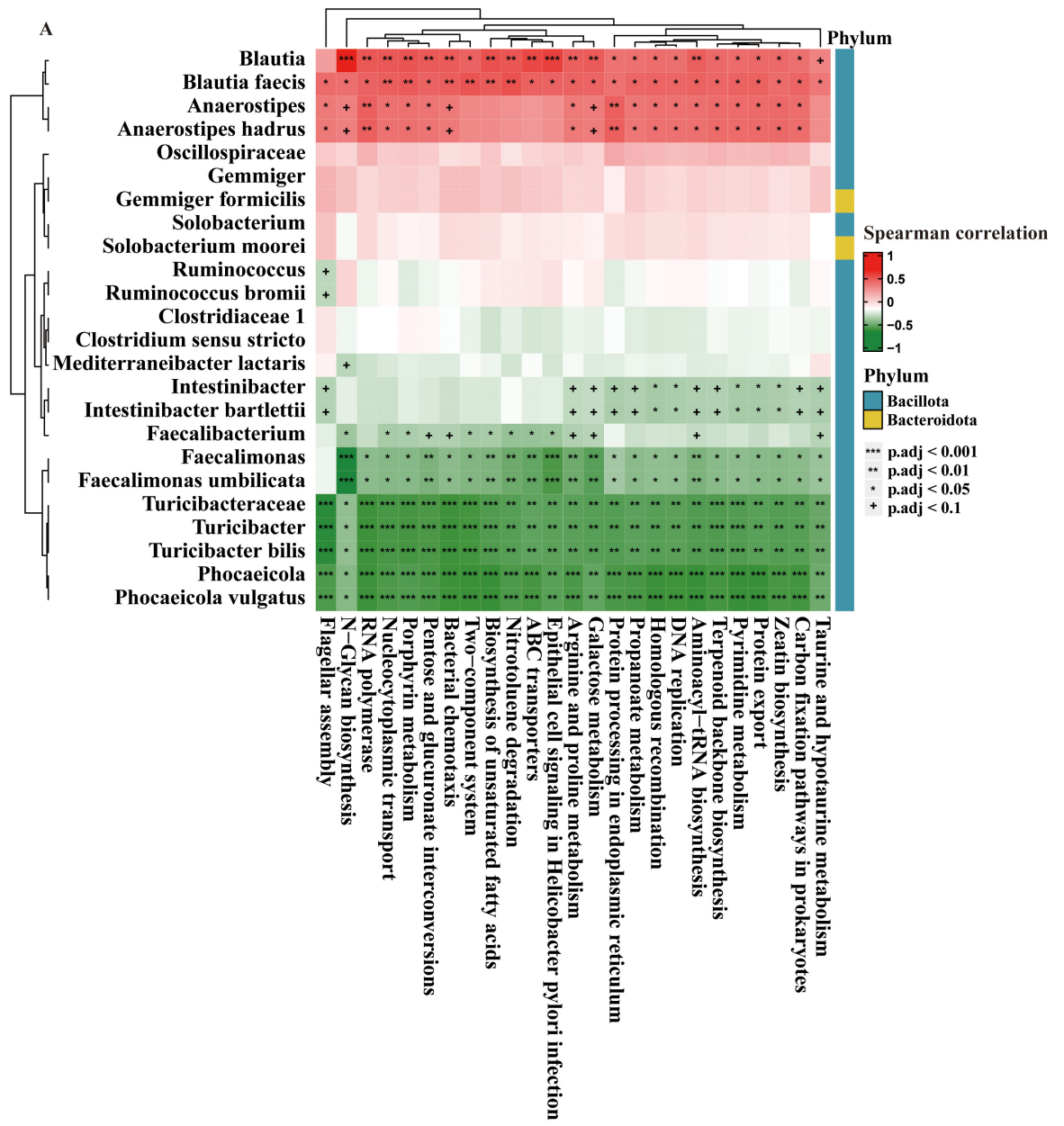

FIGURE 5
Correlation of gut microbes and microbial pathways. The data are presented as means ± SD, $n = 10$. $+P < 0.1$; $*P < 0.05$; $**P < 0.01$; $***P < 0.001$.

(Kunzmann et al., 2015), underscoring its protective role in CRC prevention.

The gut microbiota in the normal group was characterized by the enrichment of *Anaerostipes*, *Blautia*, *Gemmiger*, and *Ruminococcus*. Among them, higher levels of *Gemmiger* are associated with Western dietary patterns, while its reduced abundance in CRC patients exhibiting symptoms like bloody stools suggests a potential influence of diet on its prevalence (Chénard et al., 2020; Hur et al., 2022). Similarly, the positive correlation between dietary fiber intake and the higher population of *Ruminococcus* highlights its role in the fermentation of complex carbohydrates, emphasizing the significant impact of diet on gut microbiota composition and colorectal health. Recent studies have further demonstrated that specific dietary fibers may particularly promote the growth of beneficial bacteria such as *Ruminococcus*, further reinforcing the critical role of diet in CRC prevention (Abell et al., 2008; Abell et al., 2011).

Anaerostipes and Blautia are recognized as key producers of short-chain fatty acids (SCFAs), including acetate and butyrate. Butyrate, as a primary energy source, plays a crucial role in promoting the proliferation and repair of intestinal epithelial cells and exhibits strong anti-inflammatory effects by suppressing the nuclear factor-κB (NF-κB) signaling pathway. These bacteria generate SCFAs through the metabolism of lactate and acetate, as well as the fermentation of sugars and dietary fibers, which are essential for maintaining intestinal barrier integrity and controlling inflammation (Katsaounou et al., 2023; Maki et al., 2022; Song et al., 2023). In addition, *Anaerostipes and Blautia* are positively

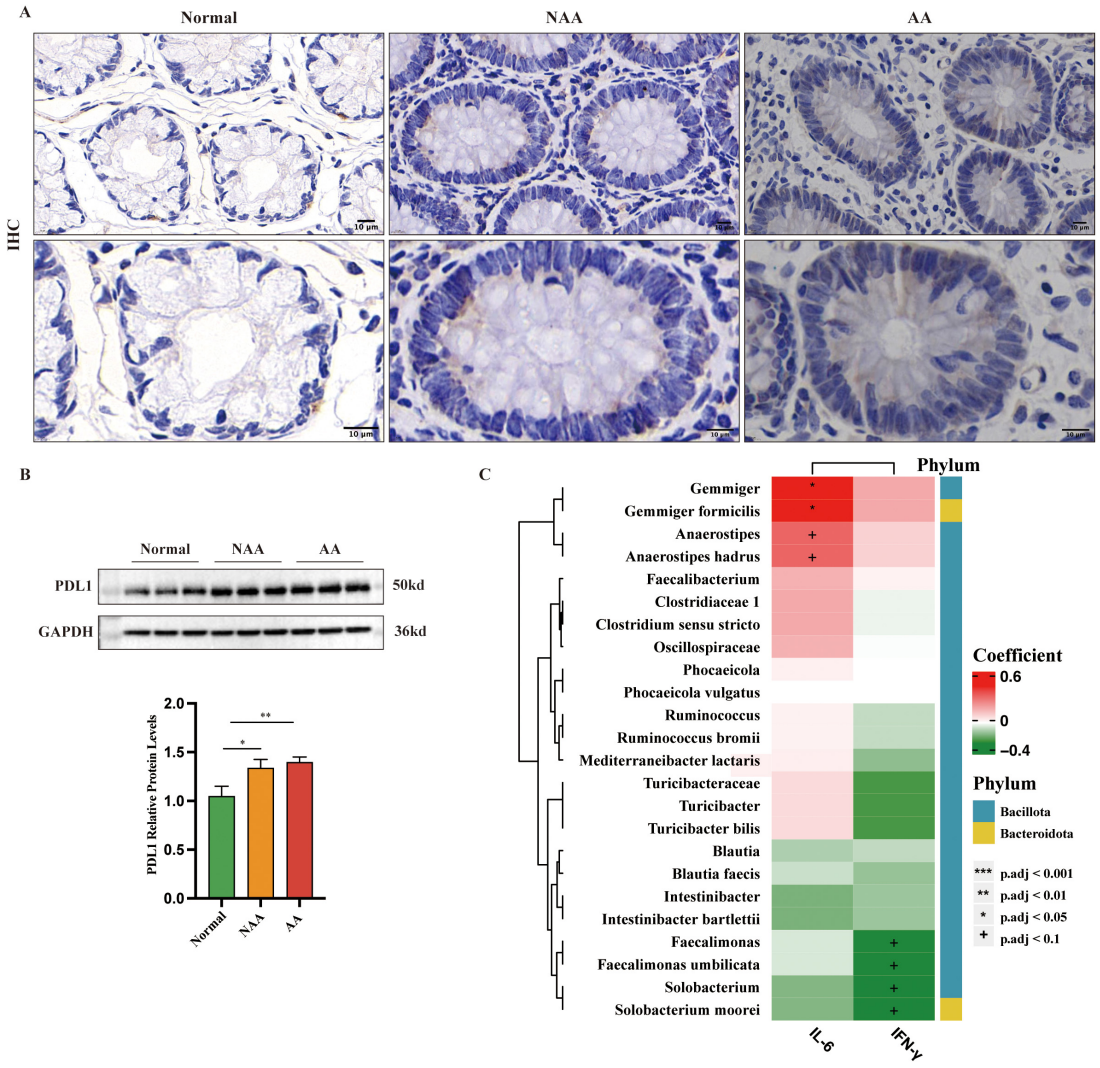

FIGURE 6
Expression of PDL1 as detected by immunohistochemistry (IHC) and western blot and correlations between the abundance of IL-6, IFN-γ and gut microbes. **(A)**. IHC stained sections from each of the normal, NAA, and AA groups. Membranous or cytoplasmic staining in shades of brown or yellow-brown indicates positive PD-L1 expression (100×, 200× magnification; scale bar: 10 μm). **(B)** Protein expression of PDL1 as detected by western blot (n = 5). **(C)** Correlations between the abundance of IL-6, IFN-γ and gut microbes. Normal, normal group; NAA, non-advanced adenoma group; AA, advanced stage adenoma group. Data were analyzed using one-way ANOVA. The data are presented as means ± SD, n = 10. $+P < 0.1$; $*P < 0.05$; $**P < 0.01$; $***P < 0.001$.

correlated with several important metabolic pathways, such as *taurine and hypotaurine metabolism, propanoate metabolism, and zeatin biosynthesis*. Emerging evidence highlights the role of taurine metabolism in regulating bile acid composition and enhancing gut microbiota diversity, which are pivotal in preventing the progression of adenomas (Duszka, 2022; Xu et al., 2021).

The abundance of these bacteria in the normal group decreases significantly during the NAA stage, with *Blautia* initially showing a slight higher before a marked reduction in the AA stage. This pattern indicates a gradual loss of protective bacterial functions and metabolic activities as adenomas progress. Furthermore, recent studies suggest that the metabolic capacity of the gut microbiota may undergo compensatory enhancement during the early stages of adenoma but collapse in later stages due to the intensification of the inflammatory environment and metabolic dysregulation. These findings highlight the importance of early intervention, particularly through dietary modulation, to support the growth of *Anaerostipes and Blautia*. Such interventions may serve as potential strategies for preventing adenoma progression. These findings emphasize the importance of early intervention, particularly through dietary modulation, to promote the growth of *Anaerostipes* and *Blautia*. Such interventions could be effective strategies for preventing adenoma progression.

In contrast, the NAA and AA groups were characterized by an enrichment of *Solobacterium*. This bacterium was more prevalent in the NAA group compared to the normal group. Its elevation in adenomatous polyps and negative correlation with IFN-γ suggest that *Solobacterium* may promote polyp progression via the NF-κB signaling pathway, potentially contributing to chronic inflammation and compromised intestinal barriers (Yu et al., 2024). These findings align with recent studies indicating that *Solobacterium* induces pro-inflammatory responses, making it

a promising target for microbiome-based therapeutic interventions aimed at preventing adenoma progression.

PD-L1, a critical factor in tumor immune escape by inhibiting T-cell function, was assessed across different stages of CRA development. While some studies report elevated PD-L1 in high-grade adenomas and early invasive cancers, others find lower levels in progressive adenomas compared to benign adenomas (Gatenbee et al., 2022; Miller et al., 2018). Our study confirmed that PD-L1 levels higher with adenoma progression, yet the expression dynamics from normal tissue to CRC remain unclear, necessitating further investigation. Additionally, we found negative associations between *Faecalimonas, Faecalimonas umbilicata, Solobacterium,* and *Solobacterium moorei* with IFN-γ, and positive associations of *Gemmiger, Gemmiger formicilis, Anaerostipes,* and *Anaerostipes hadrus* with IL-6. These mixed findings regarding PD-L1 suggest a complex regulatory environment within the tumor microenvironment that warrants further study. Understanding these dynamics could lead to more targeted immunotherapies for CRC, potentially improving patient outcomes.

The modulation of diet to encourage the growth of beneficial bacteria, such as *Anaerostipes* and *Blautia*, is a promising strategy for slowing the progression of CRA and enhancing colorectal health. However, the primary challenge in dietary therapy is determining how to implement effective dietary adjustments, particularly in the early stages. A crucial aspect of this is the development of personalized dietary interventions as part of individualized treatment. A core question in clinical practice is how to use diet to alter the composition of the gut microbiome. Certain dietary components—such as dietary fiber, antioxidants, and fatty acids—may affect different populations in varying ways. For example, dietary fiber promotes the growth of beneficial bacteria and strengthens intestinal barrier function, while antioxidant-rich foods can help reduce inflammation. Despite the evident potential of dietary interventions in preventing CRA and CRC, the clinical application of such therapies faces several challenges. In traditional healthcare systems, dietary therapy is often underappreciated, and there is a lack of comprehensive understanding among clinicians. Additionally, patient compliance presents a significant barrier to the widespread adoption of dietary interventions. Future research should focus on further clarifying the relationships between dietary components, gut microbiota, and metabolic pathways. It should also assess the impact of different dietary strategies on gut health and explore their practical applications in clinical treatment.

This study has several limitations that warrant consideration. First, the relatively small sample size and single-center design may introduce selection bias and restrict the generalizability of the findings. Second, the reliance on 16S rRNA sequencing, particularly the V3-V4 region, constrains the taxonomic resolution to the genus level for most taxa, with species-level identifications being inferred probabilistically rather than determined definitively. The KEGG functional pathway analysis in this study was conducted using PICRUSt2 predictions, which are computational inferences rather than direct measurements. To address these limitations, future studies should include larger, more diverse cohorts and utilize advanced sequencing technologies to improve taxonomic resolution. Additionally, further research should focus on elucidating the mechanistic pathways that link specific microbial taxa to adenoma progression, providing deeper insights into their functional roles.

5 Conclusion

The study emphasizes the critical role of the gut microbiota in colorectal adenoma progression, highlighting key microbial taxa and metabolic pathways as potential biomarkers for early detection and therapeutic intervention. Early dietary modulation to promote beneficial bacteria such as *Anaerostipes and Blautia* could serve as a promising strategy to mitigate adenoma progression and improve colorectal health.

Data availability statement

The original contributions presented in this study are included in this article/Supplementary material, further inquiries can be directed to the corresponding authors. Sequences analyzed in this study are available in GenBank with the accession number PRJNA1107827.

Ethics statement

The studies involving humans were approved by the Ethics Committees of the First Affiliated Hospital of Kunming Medical University. This study was approved by the Ethics Committees of the First Affiliated Hospital of Kunming Medical University (project license number: L-26/2022). The studies were conducted in accordance with the local legislation and institutional requirements. The participants provided their written informed consent to participate in this study.

Author contributions

XW: Writing – original draft, Writing – review and editing. HC: Writing – original draft, Writing – review and editing. MY: Conceptualization, Writing – original draft. MH: Conceptualization, Data curation, Investigation, Writing – original draft. DZ: Methodology, Writing – original draft. ML: Conceptualization, Writing – original draft. HW: Conceptualization, Investigation, Writing – original draft. QZ: Conceptualization, Writing – original draft. LL: Conceptualization, Writing – original draft. YL: Conceptualization, Writing – original draft. JY: Writing – original draft, Writing – review and editing. LM: Writing – original draft, Writing – review and editing.

Funding

The author(s) declare that financial support was received for the research and/or publication of this article. This work was supported by grants from the National Natural Science Foundation of China (Nos. 82160117 and 81760108), Scientific Research Fund Project of Yunnan Education Department (No. 2024Y223), Joint fund of Yunnan Provincial Science and Technology Department

and Kunming Medical University (No. 202401AY070001-009), Kunming Medical University Graduate Student Innovation Fund (No. 2024S045), First-Class Discipline Team of Kunming Medical University (No. 2024XKTDYS02), and Doctoral Service Industry Research and Innovation Cultivation Project (No. FWCY-BSPY2024082).

Acknowledgments

We would like to extend our gratitude to BioRender for providing the tools that significantly aided in the creation of scientific illustrations for this publication.

Conflict of interest

The authors declare that the research was conducted in the absence of any commercial or financial relationships that could be construed as a potential conflict of interest.

Generative AI statement

The authors declare that no Generative AI was used in the creation of this manuscript.

Publisher's note

All claims expressed in this article are solely those of the authors and do not necessarily represent those of their affiliated organizations, or those of the publisher, the editors and the reviewers. Any product that may be evaluated in this article, or claim that may be made by its manufacturer, is not guaranteed or endorsed by the publisher.

Supplementary material

The Supplementary Material for this article can be found online at: https://www.frontiersin.org/articles/10.3389/fmicb.2025.1556056/full#supplementary-material

References

Abell, G., Cooke, C., Bennett, C., Conlon, M., and McOrist, A. (2008). Phylotypes related to Ruminococcus bromii are abundant in the large bowel of humans and increase in response to a diet high in resistant starch. *FEMS Microbiol. Ecol.* 66, 505–515. doi: 10.1111/j.1574-6941.2008.00527.x

Adak, A., and Khan, M. (2019). An insight into gut microbiota and its functionalities. *Cell. Mol. Life Sci.* 76, 473–493. doi: 10.1007/s00018-018-2943-4

Anderson, M. J. (2001). A new method for non-parametric multivariate analysis of variance. *Austral Ecol.* 26, 32–46. doi: 10.1111/j.1442-9993.2001.01070.pp.x

Bolyen, E., Rideout, J., Dillon, M., Bokulich, N., Abnet, C., Al-Ghalith, G., et al. (2019). Reproducible, interactive, scalable and extensible microbiome data science using QIIME 2. *Nat. Biotechnol.* 37, 852–857. doi: 10.1038/s41587-019-0209-9

Callahan, B., McMurdie, P., Rosen, M., Han, A., Johnson, A., and Holmes, S. (2016). DADA2: High-resolution sample inference from Illumina amplicon data. *Nat. Methods* 13, 581–583. doi: 10.1038/nmeth.3869

Cao, Y., Liang, W., Fang, L., Liu, M., Zuo, J., Peng, Y., et al. (2022). PD-L1/PD-L1 signalling promotes colorectal cancer cell migration ability through RAS/MEK/ERK. *Clin. Exp. Pharmacol. Physiol.* 49, 1281–1293. doi: 10.1111/1440-1681.13717

Chen, J., Pitmon, E., and Wang, K. (2017). Microbiome, inflammation and colorectal cancer. *Semin. Immunol.* 32, 43–53. doi: 10.1016/j.smim.2017.09.006

Chénard, T., Malick, M., Dubé, J., and Massé, E. (2020). The influence of blood on the human gut microbiome. *BMC Microbiol.* 20:44. doi: 10.1186/s12866-020-01724-8

Conteduca, V., Sansonno, D., Russi, S., and Dammacco, F. (2013). Precancerous colorectal lesions (Review). *Int. J. Oncol.* 43, 973–984. doi: 10.3892/ijo.2013.2041

Douglas, G., Maffei, V., Zaneveld, J., Yurgel, S., Brown, J., Taylor, C., et al. (2020). PICRUSt2 for prediction of metagenome functions. *Nat. Biotechnol.* 38, 685–688. doi: 10.1038/s41587-020-0548-6

Duszka, K. (2022). Versatile triad alliance: Bile acid, taurine and microbiota. *Cells* 11:2337. doi: 10.3390/cells11152337

Feng, Q., Liang, S., Jia, H., Stadlmayr, A., Tang, L., Lan, Z., et al. (2015). Gut microbiome development along the colorectal adenoma-carcinoma sequence. *Nat. Commun.* 6:6528. doi: 10.1038/ncomms7528

Flemer, B., Lynch, D., Brown, J., Jeffery, I., Ryan, F., Claesson, M., et al. (2017). Tumour-associated and non-tumour-associated microbiota in colorectal cancer. *Gut* 66, 633–643. doi: 10.1136/gutjnl-2015-309595

Freitas, J., Gullo, I., Garcia, D., Miranda, S., Spaans, L., Pinho, L., et al. (2021). The adaptive immune landscape of the colorectal adenoma-carcinoma sequence. *Int. J. Mol. Sci.* 22:9791. doi: 10.3390/ijms22189791

Fu, X., Xu, Y., Han, X., Lin, X., Wang, J., Li, G., et al. (2025). Exploring the mechanism of canmei formula in preventing and treating recurrence of colorectal adenoma based on data mining and algorithm prediction. *Biol. Proced. Online* 27:4. doi: 10.1186/s12575-025-00266-5

Gatenbee, C., Baker, A., Schenck, R., Strobl, M., West, J., Neves, M., et al. (2022). Immunosuppressive niche engineering at the onset of human colorectal cancer. *Nat. Commun.* 13:1798. doi: 10.1038/s41467-022-29027-8

Hong, W., Dong, L., Stock, S., Basharat, Z., Zippi, M., and Zhou, M. (2018). Prevalence and characteristics of colonic adenoma in mainland China. *Cancer Manag. Res.* 10, 2743–2755. doi: 10.2147/CMAR.S166186

Huang, W., Berndt, S., Shiels, M., Katki, H., Chaturvedi, A., Wentzensen, N., et al. (2019). Circulating inflammation markers and colorectal adenoma risk. *Carcinogenesis* 40, 765–770. doi: 10.1093/carcin/bgz027

Hung, Y., Lyu, W., Tsai, M., Liu, C., Lai, L., Tsai, M., et al. (2022). To compare the performance of prokaryotic taxonomy classifiers using curated 16S full-length rRNA sequences. *Comput. Biol. Med.* 145:105416. doi: 10.1016/j.compbiomed.2022.105416

Hur, H., Wu, X., Yang, H., Kim, M., Lee, K., Hong, M., et al. (2022). Beneficial effects of a low-glycemic diet on serum metabolites and gut microbiota in obese women with prevotella and bacteriodes enterotypes: A randomized clinical trial. *Front. Nutr.* 9:861880. doi: 10.3389/fnut.2022.861880

Abell, G. C., Christophersen, C. T., McOrist, A. L., and Clarke, J. M. (2011). Dietary resistant and butyrylated starches have different effects on the faecal bacterial flora of azoxymethane-treated rats. *Br. J. Nutr.* 105, 1480–1485. doi: 10.1017/S0007114510005349

Katsaounou, K., Yiannakou, D., Nikolaou, E., Brown, C., Vogazianos, P., Aristodimou, A., et al. (2023). Fecal microbiota and associated volatile organic compounds distinguishing no-adenoma from high-risk colon adenoma adults. *Metabolites* 13:819. doi: 10.3390/metabo13070819

Kunzmann, A., Coleman, H., Huang, W., Kitahara, C., Cantwell, M., and Berndt, S. (2015). Dietary fiber intake and risk of colorectal cancer and incident and recurrent adenoma in the prostate, lung, colorectal, and ovarian cancer screening trial. *Am. J. Clin. Nutr.* 102, 881–890. doi: 10.3945/ajcn.115.113282

Langille, M., Zaneveld, J., Caporaso, J., McDonald, D., Knights, D., Reyes, J., et al. (2013). Predictive functional profiling of microbial communities using 16S rRNA marker gene sequences. *Nat. Biotechnol.* 31, 814–821. doi: 10.1038/nbt.2676

Liang, J., Li, T., Nakatsu, G., Chen, Y., Yau, T., Chu, E., et al. (2020). A novel faecal Lachnoclostridium marker for the non-invasive diagnosis of colorectal adenoma and cancer. *Gut* 69, 1248–1257. doi: 10.1136/gutjnl-2019-318532

Lim, S., Li, C., Xia, W., Cha, J., Chan, L., Wu, Y., et al. (2016). Deubiquitination and Stabilization of PD-L1 by CSN5. *Cancer Cell.* 30, 925–939. doi: 10.1016/j.ccell.2016.10.010

Maki, J., Lippolis, J., and Looft, T. (2022). Proteomic response of Turicibacter bilis MMM721 to chicken bile and its bile acids. *BMC Res. Notes* 15:236. doi: 10.1186/s13104-022-06127-8

Mang, T. (2019). [Colorectal cancer: Role of imaging in screening]. *Radiologe* 59, 23–34. doi: 10.1007/s00117-018-0479-0

Miller, T., Mccoy, M., Hemmings, C., Iacopetta, B., and Platell, C. (2018). Expression of PD-L1 and SOX2 during rectal tumourigenesis: Potential mechanisms for immune escape and tumour cell invasion. *Oncol. Lett.* 16, 5761–5768. doi: 10.3892/ol.2018.9337

Munteanu, C., and Schwartz, B. (2024). Interactions between dietary antioxidants, dietary fiber and the gut microbiome: Their putative role in inflammation and cancer. *Int. J. Mol. Sci.* 25:8250. doi: 10.3390/ijms25158250

Pan, J., Cen, L., Xu, L., Miao, M., Li, Y., Yu, C., et al. (2020). Prevalence and risk factors for colorectal polyps in a Chinese population: A retrospective study. *Sci. Rep.* 10:6974. doi: 10.1038/s41598-020-63827-6

Peters, B., Dominianni, C., Shapiro, J., Church, T., Wu, J., Miller, G., et al. (2016). The gut microbiota in conventional and serrated precursors of colorectal cancer. *Microbiome* 4:69. doi: 10.1186/s40168-016-0218-6

Segata, N., Izard, J., Waldron, L., Gevers, D., Miropolsky, L., Garrett, W., et al. (2011). Metagenomic biomarker discovery and explanation. *Genome Biol.* 12:R60. doi: 10.1186/gb-2011-12-6-r60

Sepich-Poore, G., Zitvogel, L., Straussman, R., Hasty, J., Wargo, J., and Knight, R. (2021). The microbiome and human cancer. *Science* 371:eabc4552. doi: 10.1126/science.abc4552

Shi, Y., Li, Z., Zheng, W., Liu, X., Sun, C., Laugsand, J., et al. (2015). Changes of immunocytic phenotypes and functions from human colorectal adenomatous stage to cancerous stage: Update. *Immunobiology* 220, 1186–1196. doi: 10.1016/j.imbio.2015.06.003

Shin, J., Ahn, Y., Chung, W., Lim, M., Hong, S., Kim, J., et al. (2021). Effect of saengshik supplementation on the gut microbial composition of healthy korean adults: A single-group pilot study. *Front. Nutr.* 8:743620. doi: 10.3389/fnut.2021.743620

Song, C., Kim, N., Nam, R., Choi, S., Jang, J., Kim, E., et al. (2023). The possible preventative role of lactate- and butyrate-producing bacteria in colorectal carcinogenesis. *Gut Liver* 18, 654–666. doi: 10.5009/gnl230385

Song, M., Wu, K., Meyerhardt, J., Ogino, S., Wang, M., Fuchs, C., et al. (2018). Fiber intake and survival after colorectal cancer diagnosis. *JAMA Oncol.* 4, 71–79. doi: 10.1001/jamaoncol.2017.3684

Sung, H., Ferlay, J., Siegel, R., Laversanne, M., Soerjomataram, I., Jemal, A., et al. (2021). Global cancer statistics 2020: Globocan estimates of incidence and mortality worldwide for 36 cancers in 185 countries. *CA Cancer J. Clin.* 71, 209–249. doi: 10.3322/caac.21660

Wu, M., Huang, Q., Xie, Y., Wu, X., Ma, H., Zhang, Y., et al. (2022). Improvement of the anticancer efficacy of PD-1/PD-L1 blockade via combination therapy and PD-L1 regulation. *J. Hematol. Oncol.* 15:24. doi: 10.1186/s13045-022-01242-2

Xu, J., Yu, X., Ye, H., Gao, S., Deng, N., Lu, Y., et al. (2021). Comparative metabolomics and proteomics reveal vibrio parahaemolyticus targets hypoxia-related signaling pathways of takifugu obscurus. *Front. Immunol.* 12:825358. doi: 10.3389/fimmu.2021.825358

Yang, W., Liu, Y., Yang, G., Meng, B., Yi, Z., Yang, G., et al. (2021). Moderate-intensity physical exercise affects the exercise performance and gut microbiota of mice. *Front. Cell Infect. Microbiol.* 11:712381. doi: 10.3389/fcimb.2021.712381

Yu, S., Wang, X., Li, Z., Jin, D., Yu, M., Li, J., et al. (2024). Solobacterium moorei promotes the progression of adenomatous polyps by causing inflammation and disrupting the intestinal barrier. *J. Transl. Med.* 22:169. doi: 10.1186/s12967-024-04977-3

Zheng, R., Sun, K., Zhang, S., Zeng, H., Zou, X., Chen, R., et al. (2019). [Report of cancer epidemiology in China, 2015]. *Zhonghua Zhong Liu Za Zhi.* 41, 19–28. doi: 10.3760/cma.j.issn.0253-3766.2019.01.005

Zouggar, A., Haebe, J., and Benoit, Y. (2020). Intestinal microbiota influences DNA methylome and susceptibility to colorectal cancer. *Genes (Basel)* 11:808. doi: 10.3390/genes11070808

frontiers | Frontiers in Microbiology

TYPE Original Research
PUBLISHED 23 April 2025
DOI 10.3389/fmicb.2025.1554537

Check for updates

OPEN ACCESS

EDITED BY
Mohammad Altamimi,
An-Najah National University, Palestine

REVIEWED BY
Fengjie Sun,
Georgia Gwinnett College, United States
Xiaokang Ma,
Hunan Agricultural University, China

*CORRESPONDENCE
Xueping Feng
✉ fxp20020605@ymun.edu.cn
Decai Wang
✉ 56023090@ymun.edu.cn

†These authors have contributed equally to this work

RECEIVED 02 January 2025
ACCEPTED 02 April 2025
PUBLISHED 23 April 2025

CITATION
Yang Y, Si J, Mo J, Li J, Pan B, Pan Y, Jiang L, Wang D and Feng X (2025) *Paederia scandens* extract alleviates obesity via modulating the gut microbiota and serum metabolome disorder.
Front. Microbiol. 16:1554537.
doi: 10.3389/fmicb.2025.1554537

COPYRIGHT
© 2025 Yang, Si, Mo, Li, Pan, Pan, Jiang, Wang and Feng. This is an open-access article distributed under the terms of the Creative Commons Attribution License (CC BY). The use, distribution or reproduction in other forums is permitted, provided the original author(s) and the copyright owner(s) are credited and that the original publication in this journal is cited, in accordance with accepted academic practice. No use, distribution or reproduction is permitted which does not comply with these terms.

Paederia scandens extract alleviates obesity via modulating the gut microbiota and serum metabolome disorder

Yuanyuan Yang[1†], Jinglei Si[2†], Jiayuan Mo[3], Jin Li[4], Bin Pan[4], Yi Pan[4], Lihe Jiang[1], Decai Wang[5*] and Xueping Feng[1*]

[1]School of Basic Medicine, Youjiang Medical University for Nationalities, Baise, China, [2]College of Animal Science & Technology, Guangxi University, Nanning, China, [3]College of Animal Science, Anhui Science and Technology University, Chuzhou, China, [4]Laboratory Animal Center, Youjiang Medical University for Nationalities, Baise, China, [5]Library, Youjiang Medical University for Nationalities, Baise, China

Obesity is increasingly becoming a challenge with China's economic development. There is an urgent need to identify more affordable methods to combat this condition. *Paederia scandens* (PS), a cost-effective herbal remedy widely used in China for treating inflammation and pain, shows potential in this regard. To investigate its anti-obesity mechanisms, we established a high-fat diet (HFD)-induced obesity model in mice. The obese mice subsequently received daily oral gavage of PS extract for 21 consecutive days. Upon the completion of the experiment, blood samples were collected to analyze lipid profiles, including total cholesterol (TC), triglycerides (TG), high-density lipoprotein (HDL-C), and low-density lipoprotein (LDL-C). Abdominal adipose tissue was subjected to hematoxylin–eosin (HE) staining for histological analysis, while fecal samples underwent 16S rRNA sequencing to assess gut microbiota composition. Our findings revealed that PS supplementation significantly reduced body weight, lipid metabolism biomarkers, and adipocyte size. PS treatment also restored gut microbial diversity, with 19 specific microbial taxa and 25 KEGG pathways identified as potential mediators of its anti-obesity effects. Notably, PS modulated key obesity-associated gut microbiota, including *Alistipes*, *Lachnoclostridium*, *Odoribacter*, *Prevotellaceae UCG-001*, *Rikenellaceae RC9-gut group*, and *norank_g Bacteroidales S24-7 group*. Serum metabolomics analysis implicated L-ascorbic acid, stevioside, allopurinol, and gingerol, along with amino acid and energy metabolism pathways, in the anti-obesity mechanism of PS. These results provide novel theoretical insights into the therapeutic potential of PS for obesity prevention and treatment.

KEYWORDS

***Paederia scandens*, obesity, high-fat induced, microbes, metabolites**

1 Introduction

Metabolic diseases have emerged as a critical global health challenge (Wu Y. et al., 2024), with obesity representing a central contributor to this epidemic (Zhang et al., 2023). Recent data reveal that 50% of Chinese adults and 25% of children meet the criteria for obesity risk (Wang et al., 2021), a condition projected to incur global economic costs exceeding USD 4.32 trillion annually by 2035 (Mahase, 2023). This escalating crisis has intensified demands for innovative interventions targeting obesity-related mechanisms, including gut microbiota modulation and metabolic regulation (The Lancet Diabetes Endocrinology, 2021).

Paederia scandens (PS), a cost-effective botanical deeply rooted in Chinese traditional medicine, presents unique therapeutic potential (Wang et al., 2014), and is widely consumed as both a medicinal herb and a dietary component in Hainan Province (China). Phytochemical analyses have identified multiple bioactive constituents in PS, including 6'-O-E-feruloylmonotropein (Trung et al., 2023), iridoid glycosides (Xu et al., 2023), and paederosidic acid (Li et al., 2023). Experimental studies demonstrate its multifunctional properties: ameliorating non-alcoholic fatty liver disease through antioxidant enhancement in chickens (Wu et al., 2019), suppressing inflammatory pathways to alleviate diarrhea in mice (Ai et al., 2023), and restoring gut microbial balance in arthritis models (Xiao et al., 2018). These findings collectively position PS as a promising candidate for metabolic regulation, though its anti-obesity mechanisms remain unexplored.

Growing evidence implicates gut microbiota dysbiosis in obesity pathogenesis (Gomes et al., 2018). Specific microbial taxa exhibit distinct roles: *Megamonas rupellensis* promotes lipid absorption (Wu C. et al., 2024), *Fusimonas intestine* and *Lachnospiraceae* facilitate diet-induced obesity (Takeuchi et al., 2023), and *Bacteroidetes* demonstrates anti-obesity correlations (Ley et al., 2006). Therapeutic agents such as spermidine (Ma et al., 2020) and ginsenoside Rg1 (Liu et al., 2023) mitigate obesity via microbiota modulation, suggesting microbial targets for PS intervention. Concurrently, serum metabolomic studies reveal obesity-associated perturbations in glutamate (Liu et al., 2017) and branched-chain amino acids (Wahl et al., 2012), though PS's metabolic regulatory effects remain uncharacterized.

To address these knowledge gaps, we established a high-fat diet-induced murine obesity model to systematically investigate PS's anti-obesity efficacy. PS was orally administered to investigate its effects on body weight, biochemical indicators, and histopathological changes in obese mice. 16S rRNA and metabolomic sequencing were used to determine whether PS supplementation ameliorated fecal microbial dysregulation and serum metabolite disorders in the obesity model. Finally, we identified gut microbes and serum metabolites associated with the underlying protective mechanisms of PS against obesity. This multidisciplinary approach provides critical insights into PS's therapeutic potential while advancing strategies for combating metabolic disorders.

2 Materials and methods

2.1 Animals and groups

In this study, specific pathogen-free (SPF) male C57BL/6 J mice (aged 5 weeks; body weight 19.97 ± 0.93 g) were obtained from RUIYE laboratories (Guangzhou, China; Production License for Experimental Animals: SCXK(YUE)2022–0063; Certificate No.44829700021758). A total of 22 mice were randomly assigned to 3 groups: normal control (NC, $n = 6$), obesity model (OB, $n = 8$), and PS extract treatment (PS, $n = 8$). All animals were housed at the Experimental Animal Center of Youjiang Medical University for Nationalities (Laboratory Animal Use License: SYXK(GUI)2022–0004) under controlled conditions: temperature 22 ± 2°C, relative humidity 55 ± 5%, and 12-h light/dark cycles. The NC group received a standard diet throughout the 13-week experiment, while the OB and PS groups were fed a high-fat diet (HFD) (4.73 kcal/g digestible energy, Charles River Co., Ltd., Jiaxing, China). From weeks 10 to 13, the NC and OB groups were administered normal saline (1 mL/kg/day), whereas the PS group received the PS extraction solution. All animal feeding, management, and experiment procedures strictly comply with the *Regulations on the Management of Experimental Animals* (China National Standard GB/T 35823–2018).

2.2 PS extract preparation

PS extract was prepared by boiling 200 g of dried PS raw material (Zexintang Pharmaceutical Co., Ltd., Bozhou, China) in 1000 mL of double-distilled water. The solution was concentrated to 100 mL under reduced pressure, yielding extract with a final PS concentration of 2 g/mL.

2.3 Physiological, biochemical indexes, and sample collection

The weekly body weight was recorded for all mice. Feces samples were collected at week 13. Following isoflurane anesthesia, blood and abdominal adipose tissue were harvested. Blood samples were centrifuged (3,000 rpm, 15 min, 4°C) to isolate serum. Serum total cholesterol (TC) (A111-1-1), triglycerides (TG) (A110-1-1), high-density lipoprotein cholesterol (HDL-C) (A112-1-1), and low-density lipoprotein cholesterol (LDL-C) (A113-1-1) were quantified using ELISA kits (Jiancheng Bioengineering Institute, Nanjing, China). Abdominal fat was fixed in 4% paraformaldehyde and embedded in paraffin blocks (4 μm thickness). Feces samples were immediately snap-frozen in liquid nitrogen and stored at −80°C for subsequent analysis.

2.4 16s rRNA amplicon sequencing

Fecal microbial genomic DNA was extracted using the MagPure Soil DNA LQ Kit (Magen, Cat. No. D6356-02; Guangzhou, China), following the manufacturer's protocol. DNA quality was verified by NanoDrop 2000 spectrophotometry and 1.5% agarose gel electrophoresis. The V3–V4 region of 16S rRNA was amplified via PCR using barcoded primers 343F (5'-TACGGRAGGCAGCAG-3′) and 798R (5'-AGGGTATCTAATCCT-3′). Libraries were constructed and sequenced on the Illumina MiSeq 6000 platform (OE Biotech, Shanghai, China). The analysis pipeline for 16S rRNA was completed according to a previous study (Mo et al., 2022). Briefly, the raw sequences were analyzed using EasyAmplicon v1.0 with the minimum unique size in the dereplication, and the sintax_cutoff in the removal of plastids and non-bacteria was 12 and 0.1, respectively. After quality control, all the samples were subsampled to 57735 sequences per sample and aligned using the silva_16s_v123 database. Beta diversity was calculated using unweighted UniFrac distances and visualized via principal coordinate analysis (PCoA). The LDA score ≥4 was defined as significant for differential microbes using linear discriminant analysis effect size (Lefse) software. The different KEGG pathways were identified by STAMP software with Bonferroni corrections ($p < 0.05$).

2.5 Serum untargeted metabolomics

After thawing on ice, each serum sample (80 μL) was transferred to 2 mL Eppendorf (EP) tubes containing 400 μL of protein precipitator solvent (ACN:methanol = 1:2, V/V) spiked with internal standards. Samples were sonicated (10 min) and allowed to equilibrate at −40°C overnight. Following centrifugation (12,000 rpm, 20 min, 4°C), 150 μL of supernatant was transferred to sample vials for liquid chromatography-mass spectrometry (LC–MS) analysis at Oebiotech Company (Shanghai, China). LC–MS analysis was performed using an ACQUITY UPLC HSS T3 column (100 mm × 2.1 mm, 1.8 μm, Waters, Milford, MA, USA). Mass spectrometry parameters for positive/negative ion modes are detailed in Table 1. Chromatographic gradients (mobile phase composition) and instrumental parameter profiles are provided in Tables 2, 3, respectively.

Raw LC–MS data were processed through peak filtration, peak extraction, alignment, and retention time correction using XCMS software (v4.5.1). Metabolite annotation was performed by querying the Human Metabolome Database (HMDB), LipidMaps (v2.3), METLIN, and LuMet-Animal 3.0 databases. Then the principal component analysis (PCA), supervised orthogonal partial least squares discriminant analysis (OPLS-DA), permutation test (200 permutations), and Kyoto Encyclopedia of Genes and Genomes (KEGG) analysis were conducted following established protocols (Mo et al., 2021). Metabolites with specific variable importance in projection (VIP) scores (VIP > 2), fold changes (FC) (FC > 4 or FC < 0.25), and p-values ($p < 0.001$) were defined as significantly differential metabolites. Time-series clustering of metabolite profiles was performed using STEM software (see Table 4).

TABLE 1 The MS conditions of position and negative ion model.

Item	ESI+	ESI−
Spray Voltage (V)	3,800	−3,200
Capillary Temperature (°C)	320	320
Aux gas heater temperature (°C)	350	350
Sheath Gas Flow Rate (Arb)	35	35
Aux gas flow rate (Arb)	8	8
S-lens RF level	50	50
Mass range (m/z)	70–1,050	70–1,050
Full ms resolution	60,000	60,000
MS/MS resolution	15,000	15,000
NCE/stepped NCE	10, 20, 40	10, 20, 40

TABLE 2 Instrument operation program of LC–MS analysis.

Item	Parameter
Column temperature	45°C
Flow rate	0.35 mL/min
Sample injection volume	4 μL
Mobile phase A	Water plus 0.1% formic acid
Mobile phase B	Acetonitrile

TABLE 3 Changes of solvents in gradient elution of LC–MS analysis.

Time (min)	A (%)	B (%)
0.0	95.0	5.0
2.0	95.0	5.0
4.0	70.0	30.0
8.0	50.0	50.0
10.0	20.0	80.0
14.0	0.0	100.0
15.0	0.0	100.0
15.1	95.0	5.0
16.0	95.0	5.0

3 Results

3.1 Addition of PS reduced obesity related indices

During the first and second weeks, the mean body weight of mice in the NC, OB, and PS groups showed no significant difference ($p > 0.05$) (Figure 1A). Notably, from weeks 3 to 12, HFD-fed mice (OB and PS groups) showed significantly elevated body weights compared to the NC group ($p < 0.01$) (Figure 1A). By week 13, the body weight in the PS group was significantly higher than in the NC group ($p < 0.05$; Figure 1A). Intriguingly, no significant differences were observed between the OB and PS groups from weeks 1 to 10 ($p > 0.05$; Figure 1A). Following PS administration (weeks 11–13), the PS group exhibited progressive weight reduction, culminating in significantly lower body weight versus the OB group at week 13 ($p < 0.01$; Figure 1A). These findings suggest that PS supplementation ameliorates HFD-induced weight gain. Serum TC, TG, HDL-C, and LDL-C in the OB group were markedly elevated compared to the NC and PS groups ($p < 0.05$; Figure 1B). Similarly, LDL-C levels in the NC group were significantly suppressed relative to the PS group ($p < 0.05$; Figure 1B). Histological analysis of inguinal adipose tissue revealed that the size of fat cells in the OB group was larger than those in the NC and PS groups ($p > 0.05$; Figure 1C). Critically, adipocyte sizes in the PS group did not statistically match those in the NC group ($p > 0.05$), indicating PS-mediated normalization of adipocyte morphology (Figure 1C). Thus, our results show that HFD exacerbates obesity-related metabolic indices and adipocyte hypertrophy, and PS intervention attenuates HFD-induced dyslipidemia and adipose remodeling.

3.2 Addition of PS changes the microbe diversity

The difference in fecal microbiota among the NC, OB, and PS groups was identified using 16S rRNA sequencing. After quality control and dereplication, a total of 1,397,098 reads were obtained, with the number of available sequences ranging from 78,153 to 81,920. The rarefaction curve analysis showed that the data met the requirements for bioinformatics (Figure 2A). A total of 794 amplicon sequence variants (ASVs) were identified, with 169 ASVs (21.3%) shared by all samples and 316 ASVs (39.8%) present in over 90% of

TABLE 4 The restored KEGG pathway by the PS added.

Pathway	NC	OB	PS
Glycosphingolipid biosynthesis - ganglio series	74,172	71,903	86,032
beta-Lactam resistance	14,928	19,423	17,909
Biotin metabolism	79,087	106,166	93,284
Cellular antigens	32,393	44,048	38,634
Cell division	47,207	64,626	55,543
Lipoic acid metabolism	31,208	43,105	37,163
Peroxisome	98,895	137,458	116,658
Folate biosynthesis	181,353	267,903	216,888
Lipopolysaccharide biosynthesis	174,882	260,702	214,077
Penicillin and cephalosporin biosynthesis	14,955	22,689	18,350
Nicotinate and nicotinamide metabolism	173,909	270,089	201,843
Carbon fixation pathways in prokaryotes	431,821	679,188	518,126
Phenylpropanoid biosynthesis	73,053	114,951	101,043
Vitamin B6 metabolism	87,017	137,776	103,411
Chaperones and folding catalysts	417,051	666,043	497,665
Phosphatidylinositol signaling system	35,155	57,206	43,203
Cyanoamino acid metabolism	126,099	209,387	165,213
Glycine, serine and threonine metabolism	332,589	560,344	393,471
Starch and sucrose metabolism	322,937	591,088	421,056
Glycerolipid metabolism	116,271	239,487	137,455
Porphyrin and chlorophyll metabolism	139,159	429,877	199,871
Steroid hormone biosynthesis	2,822	10,111	8,057
Synthesis and degradation of ketone bodies	3,248	16,536	3,296
Prion diseases	965	6,681	1,206
Atrazine degradation	2,389	21,295	3,032

the samples. After normalization to 57,735 sequences per sample, both the ACE and Chao1 indices in the OB group were significantly lower than those in the NC group ($p < 0.05$; Figures 2B,C). However, no significant differences were observed between the PS and NC groups in these indices ($p > 0.05$; Figures 2B,C). β-diversity analysis revealed structure differences in microbiota composition among the three groups (Figure 2D). Principal coordinates (PCo) 1 and 2 accounted for 54.66 and 19.3% of the total variation, respectively (Figure 2D). Notably, the NC group exhibited closer clustering with the PS group than with the OB group (Figure 2D).

3.3 Addition of PS changes the microbe composition

The relative abundances of bacteria are shown at the phylum level (Figure 2E) and the genus level (Figure 2F). A total of 8 phyla, 17 classes, 21 orders, 38 families, and 92 genera were identified in this study. The major bacteria in the phyla were Bacteroidetes, Firmicutes, and Proteobacteria, accounting for over 95.7% of the total in each sample. The relative abundance of Bacteroidetes in the NC, OB, and PS groups was 87.87, 69.22, and 88.89%, respectively. The relative abundance of Firmicutes in the NC, OB, and PS groups was 9.41, 18.23, and 7.14%, respectively. The relative abundance of Proteobacteria in the NC, OB, and PS groups was 1.84, 12.07, and 3.64%, respectively. These results showed that the microbial composition at the phylum level in the PS group was closer to that of the NC group than to that of the OB group. The main bacterial genera in the NC group at the genus level were *Alloprevotella*, *Bacteroides*, *Alistipes*, *Ruminococcaceae UCG-014*, and the *Lachnospiraceae NK4A136 group*. The main bacterial genera in the OB group at the genus level were *Bacteroides*, *Alistipes*, *Lachnospiraceae NK4A136 group*, *Parasutterella*, *Odoribacter*, *Parabacteroides*, and *Lachnoclostridium*. The main bacterial genera in the PS group at the genus level were *Bacteroides*, *Parabacteroides*, *Alistipes*, *Parasutterella*, and *Rikenellaceae RC9-gut group*. These results indicate that the addition of PS changed the dominant microbial composition in feces, and these changes may be related to the protective mechanism of PS against HFD-induced obesity in mice.

3.4 Difference in microbes and pathways between the NC and OB groups

The relative abundances of 19 microbes showed significant differences between the NC and OB groups ($p < 0.05$), including

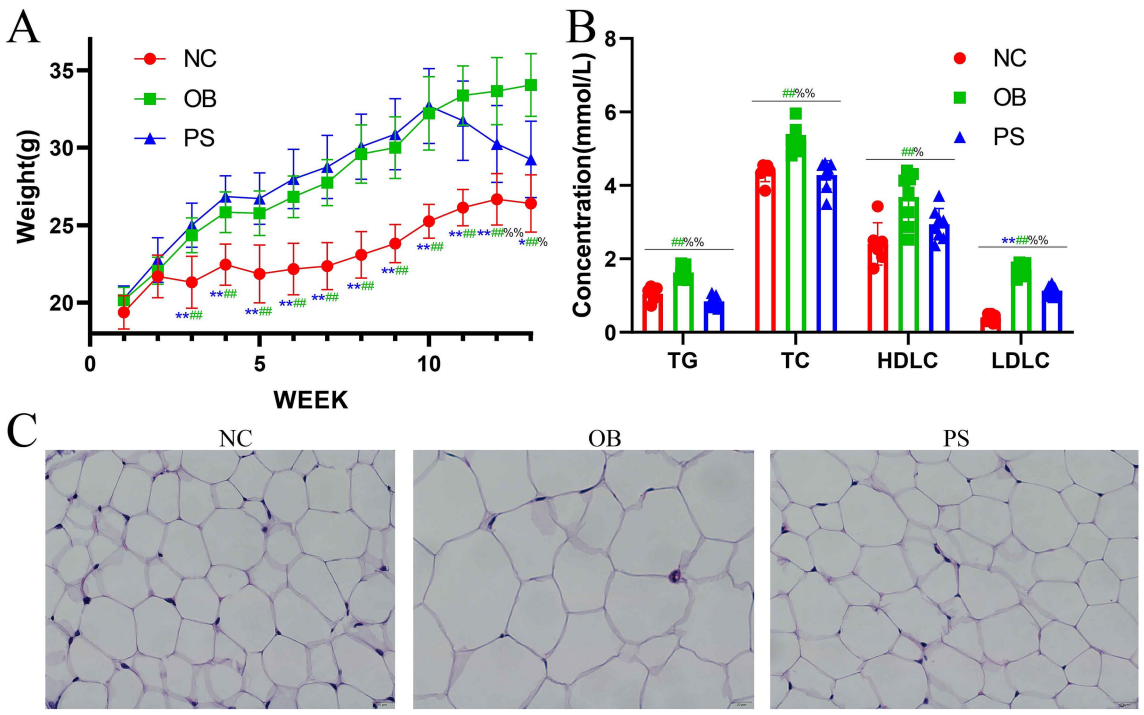

FIGURE 1
Indices and hematoxylin–eosin (HE)-stained sections from obesity. **(A)** body weight; **(B)** TG, TC, HDL-C, and LDL-C concentrations in blood; **(C)** HE-stained section of abdominal fat in three groups. Note: The ** was the extremely significant difference between the NC group and the PS group ($p < 0.01$); the ## was the extremely significant difference between the NC group and the OB group ($p < 0.01$); the %% was the extremely significant difference between the OB group and the PS group ($p < 0.01$); the * was the significant difference between the NC group and the PS group ($p < 0.05$); the # was the significant difference between the NC group and the OB group ($p < 0.05$); and the % was the significant difference between the OB group and the PS group ($p < 0.05$).

Alloprevotella, *norank_g Bacteroidales S24-7 group*, Bacteroidales S24-7 group, Prevotellaceae, Bacteroidales, Bacteroidia, and Bacteroidetes, which were significantly higher in the NC group than in the OB group (Figure 3A). The relative abundance of *Alistipes*, *Bacteroides*, *Lachnoclostridium*, *norank_g Enterobacteriaceae*, Bacteroidaceae, Lachnospiraceae, Porphyromonadaceae, Rikenellaceae, Clostridiales, Clostridia, Firmicutes, and Proteobacteria was significantly lower in the NC group than in the OB group (Figure 3A). The KEGG pathway analysis revealed that 21 KEGG pathways in the NC group were significantly more abundant than those in the OB group, including glycosphingolipid biosynthesis - ganglio series, protein digestion and absorption, biotin metabolism, lipoic acid metabolism, lipopolysaccharide biosynthesis, folate biosynthesis, nicotinate and nicotinamide metabolism, carbon fixation pathways in prokaryotes, vitamin B6 metabolism, and glycine, serine and threonine metabolism pathways, among others (Figure 3B). Additionally, nine KEGG pathways in the NC group were significantly less abundant than those in the OB group, including glycerolipid metabolism, steroid hormone biosynthesis, and synthesis and degradation of ketone bodies pathways, among others (Figure 3B).

3.5 Difference in microbes and pathways between the OB and PS groups

The relative abundances of 18 microbes showed significant differences between the OB and PS groups ($p < 0.05$), including *Alistipes*, *Lachnoclostridium*, *Odoribacter*, Lachnospiraceae, Clostridiales, Clostridia, Firmicutes, and Proteobacteria, which were significantly higher in the OB group than in the PS group (Figure 3C). The relative abundance of *Bacteroides, Prevotellaceae UCG-001, Rikenellaceae RC9-gut group, norank_g Bacteroidales S24-7 group*, Bacteroidaceae, Bacteroidales S24-7 group, Prevotellaceae, Bacteroidales, Bacteroidia, and Bacteroidetes was significantly lower in the OB group than in the PS group (Figure 3C). The KEGG pathway analysis revealed that five KEGG pathways in the OB group were significantly more abundant than those in the PS group, including synthesis and degradation of ketone bodies and glycerolipid metabolism pathways (Figure 3D). Additionally, 22 KEGG pathways in the OB group were significantly less abundant than those in the PS group, including glycine, serine, and threonine metabolism; starch and sucrose metabolism; nicotinate and nicotinamide metabolism; vitamin B6 metabolism; carbon fixation pathways in prokaryotes; folate biosynthesis; lipopolysaccharide biosynthesis; lipoic acid metabolism; biotin metabolism; glycosphingolipid biosynthesis—ganglio series; and protein digestion and absorption pathways, among others (Figure 3D).

3.6 Addition of PS restored the disorder of the feces microbe

Based on microbial differences among the NC, OB, and PS groups, our study identified seven microbial taxa in the OB group with

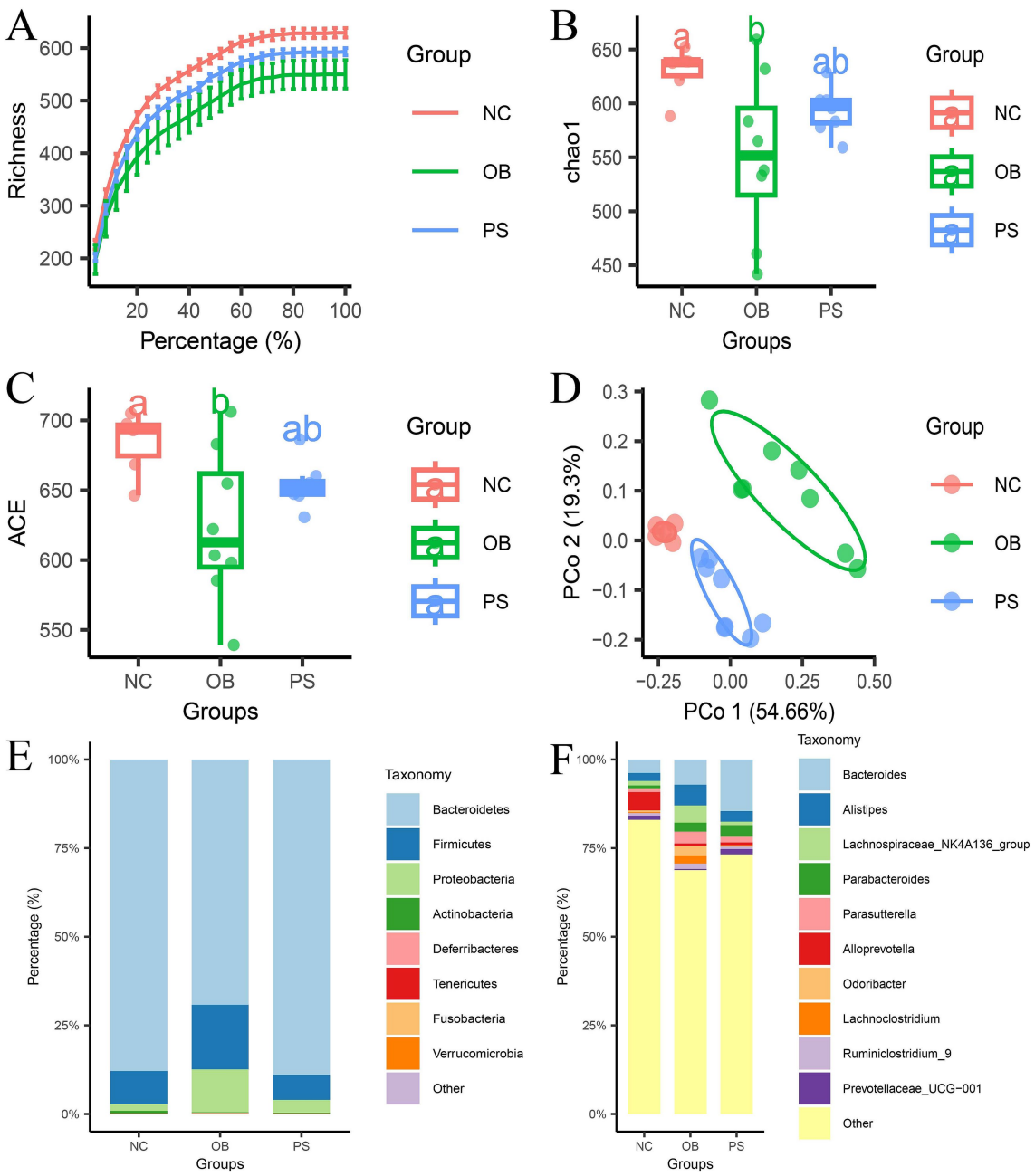

FIGURE 2
Microbial composition analysis. **(A)** the rarefaction curve in three groups; **(B)** the Chao1 index in three groups; **(C)** the ACE index in three groups; **(D)** β-diversity in the three groups; **(E)** the microbial composition at the phylum level; and F: the microbial composition in the genus level.

significantly higher relative abundance than those in both the NC and PS groups, including *Lachnoclostridium*, *Alistipes*, Proteobacteria, Firmicutes, Clostridiales, Lachnospiraceae, and Clostridia ($p < 0.05$). Meanwhile, the relative abundance of these taxa in the PS group was higher than that in the NC group, though not statistically significant ($p > 0.05$). Additionally, the relative abundance of Rikenellaceae was significantly higher in the OB and PS groups compared to the NC group ($p < 0.05$), with the OB group showing a non-significantly higher abundance than the PS group ($p > 0.05$). Thus, eight differential microbial taxa exhibited the highest abundance in the OB group, followed by the PS group, while the NC group showed the lowest levels (Figure 4A).

Three distinct microbial taxa in the OB group exhibited significantly lower relative abundances than those in both the NC and PS groups, including Bacteroidetes, Bacteroidales, and Bacteroidia ($p < 0.05$). Meanwhile, the relative abundance of these taxa in the PS group was higher than that in the NC group, though not statistically significant ($p > 0.05$). Thus, these three taxa showed the highest abundance in the PS group, followed by the NC group, and the lowest in the OB group. Additionally, three differential taxa in the NC group

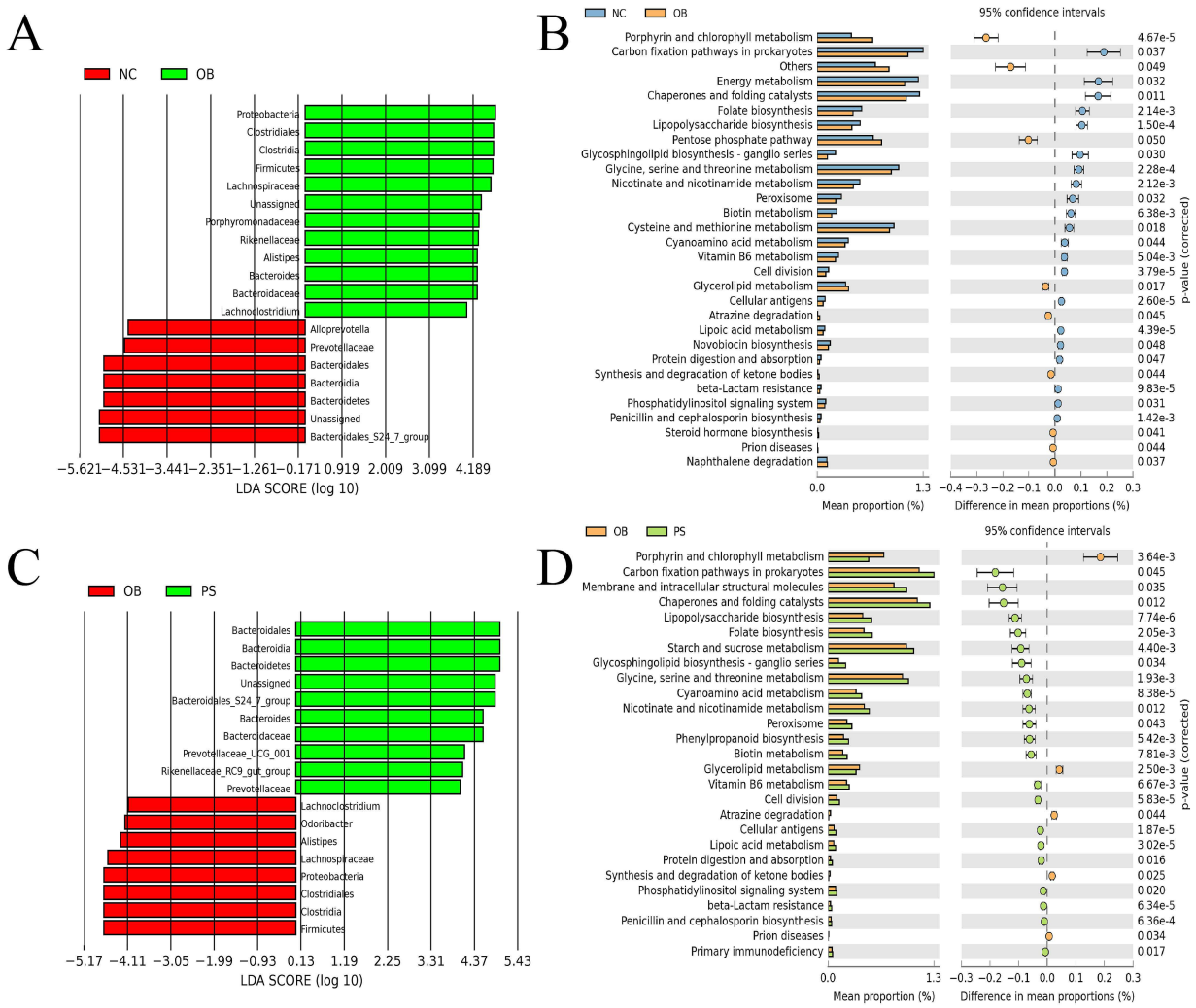

FIGURE 3
Difference in microbes and pathways. **(A)** difference in microbes between the NC and OB groups. **(B)** the difference in pathways between the NC and OB groups. **(C)** difference in microbes between the OB and PS groups. **(D)** difference in pathways between the OB and PS groups.

were significantly more abundant than those in the OB and PS groups ($p < 0.05$), with the PS group also showing significantly higher levels than the OB group ($p < 0.05$), including the Bacteroidales S24-7 group, Prevotellaceae, and *norank_g Bacteroidales S24-7 group*. Therefore, their abundance was highest in the NC group, intermediate in the PS group, and lowest in the OB group (Figure 4A). In summary, PS supplementation alleviated fecal microbial dysbiosis by reducing the abundance of *Lachnoclostridium*, *Alistipes*, Proteobacteria, Firmicutes, Clostridiales, Lachnospiraceae, Rikenellaceae, and Clostridia while enhancing the abundance of Bacteroidetes, Bacteroidales, Bacteroidia, Bacteroidales S24-7 group, Prevotellaceae, and *norank_g Bacteroidales S24-7 group.*

Meanwhile, the dysregulation of 25 significantly altered KEGG pathways was normalized by PS supplementation, such as the decrease of the glycosphingolipid biosynthesis—ganglio series pathway in the OB group was restored by PS intervention (Figure 4B). Additionally, the abnormally elevated levels of biotin metabolism, lipoic acid metabolism, folate biosynthesis, lipopolysaccharide biosynthesis, nicotinate and nicotinamide metabolism, carbon fixation pathways in prokaryotes, vitamin B6 metabolism, glycine, serine and threonine metabolism, starch and sucrose metabolism, glycerolipid metabolism, steroid hormone biosynthesis, and synthesis and degradation of ketone body pathways in the OB group were also restored by PS (Figure 4B). These findings suggest that PS may counteract obesity induced by HFDs by modulating these 25 microbial KEGG pathways.

3.7 Addition of PS changes the serum metabolites profiles

A total of 3,084 metabolites were identified in the serum metabolome, with 1,413 and 1,671 metabolites in the positive and negative ion modes, respectively (Supplementary Table S1). PCA results indicated that the model interpretation rates of X (R^2X) for the positive and negative ion modes were 0.456 and 0.564, respectively. In both PCA score plots, the four quality control (QC) samples clustered tightly, confirming data reproducibility (Figures 4C,D). Notably, the PS group was positioned between the NC and OB groups in both the positive and negative ion modes.

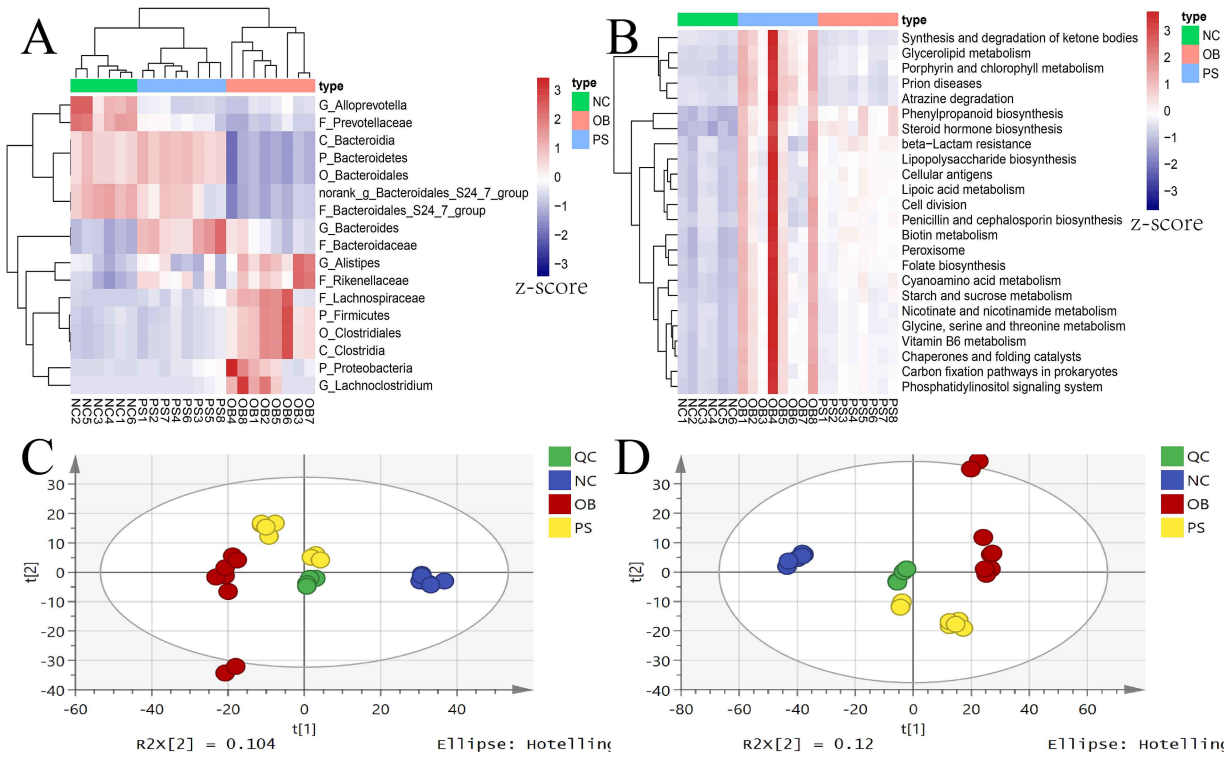

FIGURE 4
Microbial taxa and pathways related to PS anti-obesity and the PCA plot of metabolites. **(A)** the microbial taxa related to PS anti-obesity; **(B)** the microbial pathways related to PS anti-obesity; **(C)** the PCA plot in the positive ion model; and **(D)** the PCA plot in the negative ion model.

3.8 Difference in metabolites and pathways between the NC and OB groups

OPLS-DA analysis revealed a clear separation between the NC and OB groups in both ion modes (Figures 5A,B). The model interpretation rates of Y (R^2Y) in the positive and negative ion modes were 0.662 and 0.761, respectively. The prediction ability (Q^2) in the positive and negative ion modes was over 0.99 in both modes. Permutation test intercepts for both modes were below −0.45, confirming model validity. Among 136 significantly differential metabolites, 56 were upregulated and 80 were downregulated in the NC group compared to the OB group (Supplementary Table S2). MetaboAnalyst 4.0 analysis identified seven enriched metabolic pathways, including D-amino acid metabolism, citrate cycle (TCA cycle), pyruvate metabolism, glycolysis/gluconeogenesis, alanine, aspartate and glutamate metabolism, glyoxylate and dicarboxylate metabolism, and the arachidonic acid metabolism pathway (Figure 5C).

3.9 Difference in metabolites and pathways between the OB and PS groups

OPLS-DA analysis revealed a clear separation between the OB and PS groups in both ion modes (Figures 5D,E). The R^2Y values for the positive and negative ion modes were 0.437 and 0.488, respectively. The Q^2 in both the positive and negative ion modes was over 0.93 in both modes. Permutation test intercepts for both modes were below −0.28, confirming model reliability. Among 60 significantly differential metabolites, 6 were upregulated and 54 downregulated in the OB group compared to the PS group (Supplementary Table S3). MetaboAnalyst 4.0 analyzes eight enriched metabolic pathways, including riboflavin metabolism, purine metabolism, D-amino acid metabolism, citrate cycle (TCA cycle), pyruvate metabolism, glycolysis/gluconeogenesis, alanine, aspartate and glutamate metabolism, and glyoxylate and dicarboxylate metabolism pathway (Figure 5F).

3.10 Addition of PS restored the disorder of serum metabolites

Hierarchical cluster analysis of all significant differential metabolites was performed using the Stem software. From the NC to PS and then OB groups, 189 significant difference metabolites were stratified into three distinct clusters (Figure 6A). Clusters 2, 3, and 11 contained 46, 28, and 18 metabolites, respectively (Supplementary Table S4; Figures 6B–D). Notably, metabolite concentration in clusters 2 and 3 of the PS group was intermediate between the NC and OB groups, suggesting that these 74 metabolites (cluster 2 + 3) may be associated with PS-mediated alleviation of HFD-induced obesity in mice. These metabolites were enriched in seven metabolic pathways, including D-amino acid metabolism, citrate cycle (TCA cycle), pyruvate metabolism, glycolysis/gluconeogenesis, alanine, aspartate and glutamate metabolism, glyoxylate and dicarboxylate metabolism, and the arachidonic acid metabolism pathway (Figure 6E).

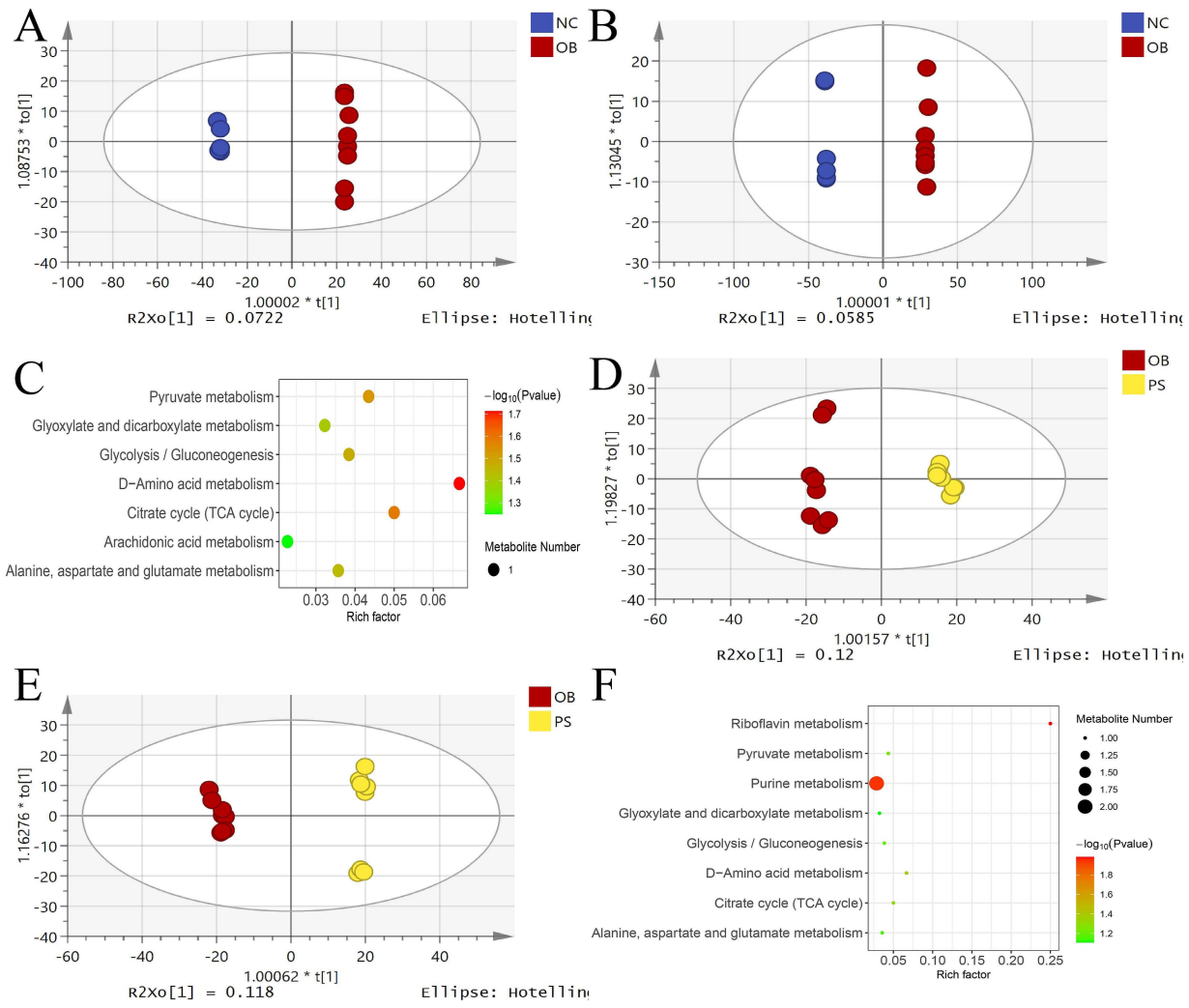

FIGURE 5
OPLS-DA analysis in different groups. **(A)** the OPLS-DA score plot in positive between the NC and OB groups; **(B)** the OPLS-DA score plot in negative between the NC and OB groups; **(C)** the KEGG plot of significantly different metabolites between the NC and OB groups; **(D)** the OPLS-DA score plot in positive between the PS and OB groups; **(E)** the OPLS-DA score plot in negative between the PS and OB groups; and **(F)** the KEGG plot of significantly different metabolites between the PS and OB groups.

4 Discussion

To investigate the protective mechanisms of PS against obesity, we established an HFD-induced obesity model in mice and administered PS via oral gavage to obese subjects. Our study demonstrated that HFD-fed mice exhibited significantly higher body weight than those on a standard diet, consistent with previous findings (Le Roy et al., 2022). Following PS intervention starting at week 10, the body weight of the PS group became lower than the OB group, with statistically significant differences emerging by week 13. These results indicate that PS mitigates high-fat diet-induced weight gain in mice. Similar to the effects of semaglutide (Ren et al., 2022), PS treatment significantly reduced serum lipid levels, including TC, TG, HDL-C, and LDL-C. Notably, TC, TG, and HDL-C levels in the PS group returned to normal ranges compared to the OB group. Additionally, the adipocyte size in the PS group was markedly smaller than in the OB group. Thus, our results showed that the oral administration of PS restored body weight, normalized blood lipid indices, and reduced adipocyte hypertrophy in obese mice. These results confirm that oral PS supplementation is an effective strategy for alleviating obesity in murine models.

Our microbial analysis revealed that HFD decreased α-diversity in mice, while PS intervention restored it to baseline levels. β-diversity metrics demonstrated closer clustering between the NC and PS groups compared to the OB group, indicating PS-mediated restoration of gut microbiota composition in obesity. Differential abundance analysis identified seven microbes that were decreased, and 12 microbes were enhanced in the OB group compared to the NC group. These findings align with prior studies of HFD-induced depletion of *Alloprevotella* and Prevotellaceae, alongside enrichment of *Alistipes* (Kong et al., 2019). Wei et al. (2020) indicated that the HFD decreased the abundance of the Bacteroidales S24-7 group and Bacteroidetes and increased the abundance of Firmicutes and Proteobacteria. Gong et al. (2022) reported that the abundance of *Lachnoclostridium* in the obesity group was enhanced. Duan et al. (2024) found that the abundance of Lachnospiraceae and *Bacteroides* in HFD mice was

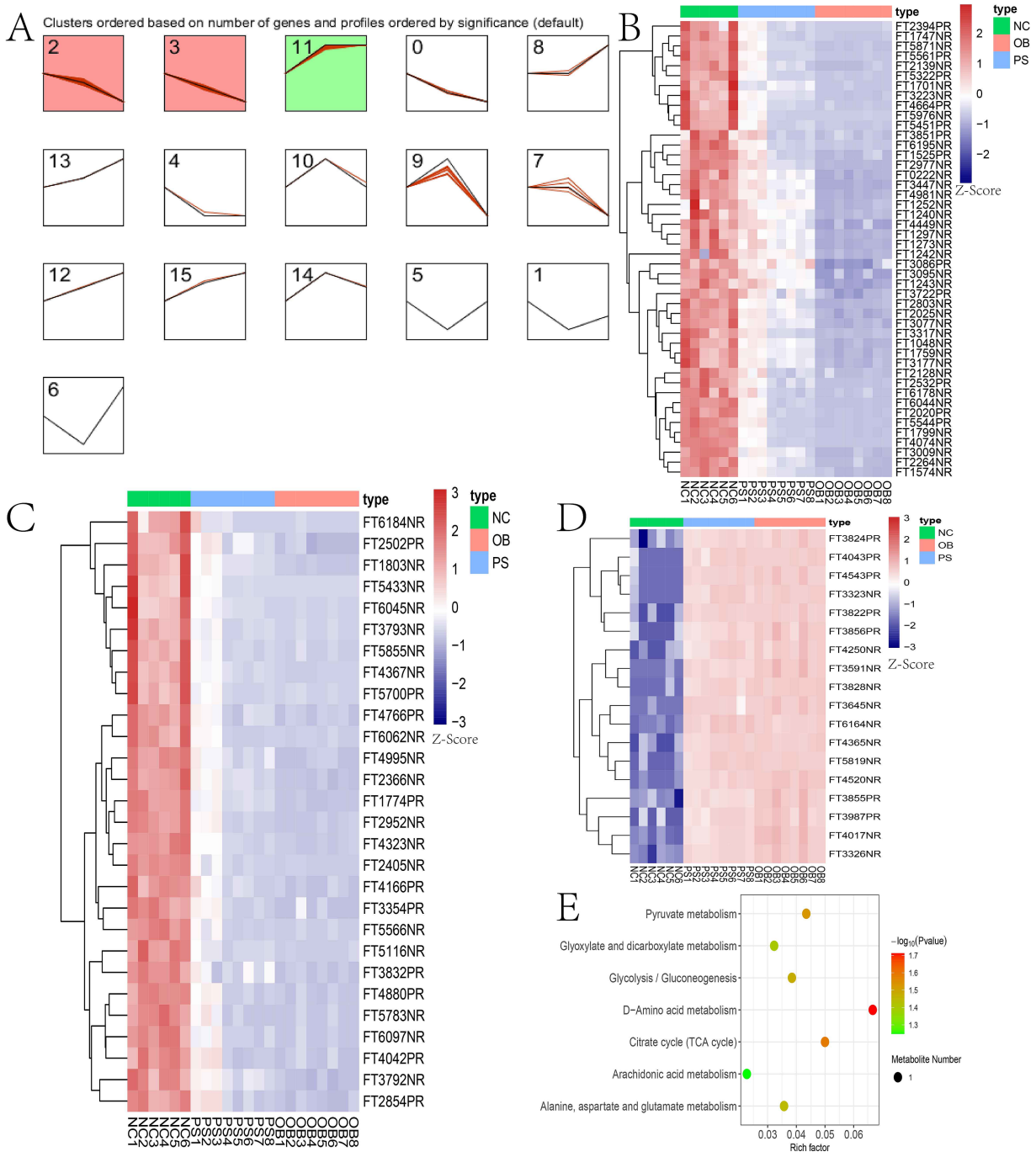

FIGURE 6
Hierarchical cluster analysis results. **(A)** the hierarchical cluster of 189 metabolites; **(B)** the metabolites in cluster 2; **(C)** the metabolites in cluster 3; **(D)** the metabolites in cluster 11; **(E)** the KEGG plot of clusters 2 and 3.

enhanced. Yang et al. (2021) evidenced that the abundance of Porphyromonadaceae in HFD mice was improved, and Daniel et al. (2014) declared that the abundance of Rikenellaceae in HFD mice was enhanced. Notably, PS treatment reversed 14 of 18 OB-associated microbial dysregulations, including eight microbes [*Alistipes* (Kong et al., 2019), *Lachnoclostridium* (Gong et al., 2022), Lachnospiraceae (Duan et al., 2024), Rikenellaceae (Daniel et al., 2014), Clostridiales, Clostridia, Firmicutes, and Proteobacteria] that were decreased by the PS addition, and six microbes (*norank_g Bacteroidales S24-7 group* (Wei et al., 2020), Bacteroidales S24-7 group (Wei et al., 2020), Prevotellaceae (Kong et al., 2019), Bacteroidales, Bacteroidia, and Bacteroidetes) that were increased by the PS addition. Meanwhile, the abundance of *Odoribacter*, *Prevotellaceae UCG-001*, and *Rikenellaceae RC9-gut group* in the PS group was significantly higher than those in the OB group. *Lachnoclostridium* (Dicks, 2024) and *Alistipes* (Chanda and De, 2024) were the short-chain fatty acid (SCFA) producers, and the SCFAs can affect adipose tissue metabolism, lipid oxidation capacity, *β* cell function, and insulin secretion via the SCFA-sensing G

protein-coupled receptors (GPCRs), SCFA transporter (SLC16A and SLC5A), and other SCFA receptor-independent pathways (You et al., 2022). The higher abundances of *Lachnoclostridium* and *Alistipes* in obesity samples in our study and previous studies may be related to the negative feedback mechanism of the body. The *norank_g Bacteroidales S24-7 group* was a butyrate-producing bacterium (Fang et al., 2020), and the butyrate can resist inflammation and obesity (Liu et al., 2018) through GPCR signaling pathways (Saban Güler et al., 2025). The relationship between the *Prevotellaceae UCG-001* and obesity in the body (Han et al., 2024) may be related to the butyrate because the butyrate can enhance the abundance of *Prevotellaceae UCG-001* in the gut (Wang et al., 2024). As a potentially obesity-related biomarker (Liu et al., 2022; Vallianou et al., 2023), the *Odoribacter* improves glucose control and inflammatory profile in obese mice by depleting circulating succinate (Huber-Ruano et al., 2022). A previous study showed that the *Rikenellaceae RC9-gut group* was related to HFD-induced obesity (Fu et al., 2022), and the *Rikenellaceae RC9-gut group* was positively correlated with HFD-induced "harmful indicators" and negatively correlated with "beneficial indicators" (Gao et al., 2020). Thus, PS might alleviate obesity in mice by restoring the abundance at the genus levels of *Alistipes, Lachnoclostridium, Odoribacter*, *Prevotellaceae UCG-001*, *Rikenellaceae RC9-gut group*, and *norank_g Bacteroidales S24-7 group*.

Our metabolomic profiling revealed that the PS group clustered intermediately between the NC and OB groups in both positive and negative ion modes, which was the same as the β-diversity results in the microbe analysis. This spatial distribution suggests the partial restoration of serum metabolite profiles in HFD-induced obese mice by PS intervention. Differential metabolite analysis identified 136 serum metabolites significantly altered by HFD, including cholestanetriol, gingerol, isovaleric acid, and stevioside. Zhu et al. (2021) illustrated that the HFD enhanced the serum cholestanetriol in mice, which was consistent with our study. Same as our study, isovaleric acid was an SCFA in the body and regulated obesity by decreasing lipogenesis (Heimann et al., 2016). Saravanan et al. (2014) reported that the gingerol could decrease the glucose level, body weight, leptin, insulin, amylase, lipase plasma, and tissue lipids in obesity mice. Brahma Naidu et al. (2016) proposed that it might modulate the lipid metabolism through decreasing activity in lipogenesis as well as increasing fatty-acid oxidation, which is contrary to our study. Wang et al. (2012) found that the stevioside may ameliorate insulin resistance in HFD mice by attenuating adipose tissue inflammation and inhibiting the NF-κB pathway. These results may be due to the negative feedback mechanism of the body. The KEGG analysis showed that two amino acid metabolism and three energy metabolism-related pathways were enriched in the different metabolites, which was consistent with the different pathways in the microbe analysis. Thus, the HFD may induce obesity in mice through enhancing the levels of cholestanetriol, gingerol, and stevioside and decreasing the levels of isovaleric acid.

A total of 60 metabolites were identified as significantly different between the PS group and the OB group, including allopurinol, inosine, and L-ascorbic acid. Consistent with our study, allopurinol not only alleviates HFD-induced hypertension and proteinuria (El-Bassossy and Shaltout, 2015) but also ameliorates the HFD-induced hepatic steatosis through modulation of lipid metabolism, inflammation, and the ER stress pathway in mice (Cho et al., 2021). Niemann et al. (2022) demonstrated that inosine can combat obesity by regulating thermogenic fat, which is consistent with our findings. Lee et al. (2019) reported that ascorbic acid suppresses HFD-induced obesity and non-alcoholic fatty liver disease is activation of PPARα. KEGG analysis revealed that two amino acid metabolism and three energy metabolism-related pathways were enriched among the differential metabolites, aligning with the pathways identified in microbial analysis. Cluster analysis indicated that 74 metabolites may be associated with the PS-mediated alleviation of HFD-induced obesity in mice, including allopurinol (El-Bassossy and Shaltout, 2015), cholestanetriol (Zhu et al., 2021), gingerol (Saravanan et al., 2014), inosine (Niemann et al., 2022), L-ascorbic acid (Lee et al., 2019), and stevioside (Wang et al., 2012). Notably, the disrupted concentrations of inosine, L-ascorbic acid, stevioside, allopurinol, and gingerol in the OB group were restored by PS treatment. Furthermore, these 74 metabolites were enriched in two amino acid metabolism and three energy metabolism-related pathways, consistent with the microbial analysis. Collectively, PS might alleviate obesity in mice by restoring serum concentrations of inosine, L-ascorbic acid, stevioside, allopurinol, and gingerol and by regulating amino acid and energy metabolism-related pathways.

However, there were some limitations to our study. For instance, due to the short experimental period, the long-term effect might not be observed; the PS extraction method might have a possible influence on its active ingredients; the number of individuals in each group was small, and the PS administration groups with different doses were absent. We will improve these problems through further study.

5 Conclusion

In this study, an HFD was used to successfully establish a mice obesity model. Oral administration of PS significantly alleviated obesity, as evidenced by reductions in TG, TC, LDL-C, and HDL-C levels, as well as decreased adipocyte size. 16S rRNA sequencing analysis revealed that PS modulated the abundance of 17 microbial taxa associated with obesity mitigation, including *Alistipes, Lachnoclostridium, Odoribacter*, *Prevotellaceae UCG-001*, *Rikenellaceae RC9-gut group*, and *norank_g Bacteroidales S24-7 group*. Metabolomic analysis identified serum metabolites such as L-ascorbic acid, stevioside, allopurinol, and gingerol, along with amino acid metabolism and energy metabolism-related pathways, as key mechanisms underlying the anti-obesity effects of PS. These findings provide novel theoretical and experimental support for the potential application of PS in obesity prevention and treatment.

Data availability statement

The datasets presented in this study can be found in online repositories. The names of the repository/repositories and accession number(s) can be found below: https://ngdc.cncb.ac.cn/, CRA021056.

Ethics statement

The animal study was approved by Youjiang Medical University for Nationalities. The study was conducted in accordance with the local legislation and institutional requirements.

Author contributions

YY: Conceptualization, Data curation, Writing – original draft. JS: Conceptualization, Data curation, Writing – original draft. JM: Methodology, Software, Writing – original draft. JL: Investigation, Supervision, Writing – review & editing. BP: Supervision, Writing – review & editing. YP: Validation, Writing – review & editing. LJ: Visualization, Writing – review & editing. DW: Project administration, Resources, Writing – review & editing. XF: Funding acquisition, Resources, Writing – review & editing.

Funding

The author(s) declare that financial support was received for the research and/or publication of this article. This research was funded by Youjiang Medical University for Nationalities high-level talent research project (grant number RZ2300001266); Baise City science and technology bureau research topic (grant number 20221428).

Acknowledgments

We would like to thank the State Key Laboratory for Conservation and Utilization of Subtropical Agro-bioresources for its instrument support.

Conflict of interest

The authors declare that the research was conducted in the absence of any commercial or financial relationships that could be construed as a potential conflict of interest.

Generative AI statement

The author(s) declare that no Gen AI was used in the creation of this manuscript.

Publisher's note

All claims expressed in this article are solely those of the authors and do not necessarily represent those of their affiliated organizations, or those of the publisher, the editors and the reviewers. Any product that may be evaluated in this article, or claim that may be made by its manufacturer, is not guaranteed or endorsed by the publisher.

Supplementary material

The Supplementary material for this article can be found online at: https://www.frontiersin.org/articles/10.3389/fmicb.2025.1554537/full#supplementary-material

References

Ai, L., Guo, L., Liu, W., Xue, X., Li, L., Sheng, Z., et al. (2023). Determination and mechanism of antidiarrheal chemical constituents of *Paederia scandens* determined by HPLC-ESI-MS integrated with network pharmacology. *ACS Omega* 8, 28834–28845. doi: 10.1021/acsomega.3c03887

Brahma Naidu, P., Uddandrao, V. V. S., Ravindar Naik, R., Suresh, P., Meriga, B., Begum, M. S., et al. (2016). Ameliorative potential of gingerol: promising modulation of inflammatory factors and lipid marker enzymes expressions in HFD induced obesity in rats. *Mol. Cell. Endocrinol.* 419, 139–147. doi: 10.1016/j.mce.2015.10.007

Chanda, D., and De, D. (2024). Meta-analysis reveals obesity associated gut microbial alteration patterns and reproducible contributors of functional shift. *Gut Microbes* 16:2304900. doi: 10.1080/19490976.2024.2304900

Cho, I.-J., Oh, D.-H., Yoo, J., Hwang, Y.-C., Ahn, K. J., Chung, H.-Y., et al. (2021). Allopurinol ameliorates high fructose diet induced hepatic steatosis in diabetic rats through modulation of lipid metabolism, inflammation, and ER stress pathway. *Sci. Rep.* 11:9894. doi: 10.1038/s41598-021-88872-7

Daniel, H., Gholami, A. M., Berry, D., Desmarchelier, C., Hahne, H., Loh, G., et al. (2014). High-fat diet alters gut microbiota physiology in mice. *ISME J.* 8, 295–308. doi: 10.1038/ismej.2013.155

Dicks, L. M. T. (2024). How important are fatty acids in human health and can they be used in treating diseases? *Gut Microbes* 16:2420765. doi: 10.1080/19490976.2024.2420765

Duan, X., Zhang, L., Liao, Y., Lin, Z., Guo, C., Luo, S., et al. (2024). Semaglutide alleviates gut microbiota dysbiosis induced by a high-fat diet. *Eur. J. Pharmacol.* 969:176440. doi: 10.1016/j.ejphar.2024.176440

El-Bassossy, H. M., and Shaltout, H. A. (2015). Allopurinol alleviates hypertension and proteinuria in high fructose, high salt and high fat induced model of metabolic syndrome. *Transl. Res.* 165, 621–630. doi: 10.1016/j.trsl.2014.11.008

Fang, S., Chen, X., Pan, J., Chen, Q., Zhou, L., Wang, C., et al. (2020). Dynamic distribution of gut microbiota in meat rabbits at different growth stages and relationship with average daily gain (ADG). *BMC Microbiol.* 20:116. doi: 10.1186/s12866-020-01797-5

Fu, S., Dang, Y., Xu, H., Li, A., Zhou, X., Gao, X., et al. (2022). *Aloe Vera*-fermented beverage ameliorates obesity and gut dysbiosis in high-fat-diet mice. *Food Secur.* 11:3728. doi: 10.3390/foods11223728

Gao, X., Chang, S., Liu, S., Peng, L., Xie, J., Dong, W., et al. (2020). Correlations between α-linolenic acid-improved multitissue homeostasis and gut microbiota in mice fed a high-fat diet. *mSystems* 5, e00391–e00320. doi: 10.1128/mSystems.00391-20

Gomes, A. C., Hoffmann, C., and Mota, J. F. (2018). The human gut microbiota: metabolism and perspective in obesity. *Gut Microbes* 9, 1–18. doi: 10.1080/19490976.2018.1465157

Gong, J., Shen, Y., Zhang, H., Cao, M., Guo, M., He, J., et al. (2022). Gut microbiota characteristics of people with obesity by Meta-analysis of existing datasets. *Nutrients* 14:2993. doi: 10.3390/nu14142993

Han, Y.-H., Cui, X.-W., Li, Y.-X., Chen, X., Zhang, H., Zhang, Y., et al. (2024). Bacterial cellulose is a desirable biological macromolecule that can prevent obesity via modulating lipid metabolism and gut microbiota. *Int. J. Biol. Macromol.* 283:137522. doi: 10.1016/j.ijbiomac.2024.137522

Heimann, E., Nyman, M., Pålbrink, A.-K., Lindkvist-Petersson, K., and Degerman, E. (2016). Branched short-chain fatty acids modulate glucose and lipid metabolism in primary adipocytes. *Adipocytes* 5, 359–368. doi: 10.1080/21623945.2016.1252011

Huber-Ruano, I., Calvo, E., Mayneris-Perxachs, J., Rodríguez-Peña, M.-M., Ceperuelo-Mallafré, V., Cedó, L., et al. (2022). Orally administered *Odoribacter laneus* improves glucose control and inflammatory profile in obese mice by depleting circulating succinate. *Microbiome* 10:135. doi: 10.1186/s40168-022-01306-y

Kong, C., Gao, R., Yan, X., Huang, L., and Qin, H. (2019). Probiotics improve gut microbiota dysbiosis in obese mice fed a high-fat or high-sucrose diet. *Nutrition* 60, 175–184. doi: 10.1016/j.nut.2018.10.002

Le Roy, T., Moens de Hase, E., Van Hul, M., Paquot, A., Pelicaen, R., Régnier, M., et al. (2022). Dysosmobacter welbionis is a newly isolated human commensal bacterium preventing diet-induced obesity and metabolic disorders in mice. *Gut* 71, 534–543. doi: 10.1136/gutjnl-2020-323778

Lee, H., Ahn, J., Shin, S. S., and Yoon, M. (2019). Ascorbic acid inhibits visceral obesity and nonalcoholic fatty liver disease by activating peroxisome proliferator-activated receptor α in high-fat-diet-fed C57BL/6J mice. *Int. J. Obes.* 43, 1620–1630. doi: 10.1038/s41366-018-0212-0

Ley, R. E., Turnbaugh, P. J., Klein, S., and Gordon, J. I. (2006). Microbial ecology: human gut microbes associated with obesity. *Nature* 444, 1022–1023. doi: 10.1038/4441022a

Li, Y., Li, Y., Zhu, Y., Ji, W., Wang, Y., Dong, X., et al. (2023). Structure-based virtual screening for discovery of paederosidic acid from *Paederia scandens* as novel P2Y14R antagonist. *Phytomedicine* 115:154851. doi: 10.1016/j.phymed.2023.154851

Liu, W., Fang, X., Zhou, Y., Dou, L., and Dou, T. (2022). Machine learning-based investigation of the relationship between gut microbiome and obesity status. *Microbes Infect.* 24:104892. doi: 10.1016/j.micinf.2021.104892

Liu, R., Hong, J., Xu, X., Feng, Q., Zhang, D., Gu, Y., et al. (2017). Gut microbiome and serum metabolome alterations in obesity and after weight-loss intervention. *Nat. Med.* 23, 859–868. doi: 10.1038/nm.4358

Liu, Y., Jin, Z.-Y., Wang, J.-X., Wang, D., Liu, H., Li, D., et al. (2023). Ginsenoside Rg1 activates brown adipose tissue to counteract obesity in high-fat diet-fed mice by regulating gut microbes and bile acid composition. *Food Funct.* 14, 4696–4705. doi: 10.1039/d2fo03142f

Liu, H., Wang, J., He, T., Becker, S., Zhang, G., Li, D., et al. (2018). Butyrate: a double-edged sword for health? *Adv. Nutr.* 9, 21–29. doi: 10.1093/advances/nmx009

Ma, L., Ni, Y., Wang, Z., Tu, W., Ni, L., Zhuge, F., et al. (2020). Spermidine improves gut barrier integrity and gut microbiota function in diet-induced obese mice. *Gut Microbes* 12, 1832857–1832819. doi: 10.1080/19490976.2020.1832857

Mahase, E. (2023). Global cost of overweight and obesity will hit $4.32tn a year by 2035, report warns. *BMJ* 380:523. doi: 10.1136/bmj.p523

Mo, J., Lu, Y., Jiang, S., Yan, G., Xing, T., Xu, D., et al. (2022). Effects of the probiotic, *Lactobacillus delbrueckii* subsp. bulgaricus, as a substitute for antibiotics on the gastrointestinal tract microbiota and metabolomics profile of female growing-finishing pigs. *Animals (Basel)* 12:1778. doi: 10.3390/ani12141778

Mo, J., Sun, L., Cheng, J., Lu, Y., Wei, Y., Qin, G., et al. (2021). Non-targeted metabolomics reveals metabolic characteristics of porcine Atretic follicles. *Front. Vet. Sci.* 8:679947. doi: 10.3389/fvets.2021.679947

Niemann, B., Haufs-Brusberg, S., Puetz, L., Feickert, M., Jaeckstein, M. Y., Hoffmann, A., et al. (2022). Apoptotic brown adipocytes enhance energy expenditure via extracellular inosine. *Nature* 609, 361–368. doi: 10.1038/s41586-022-05041-0

Ren, Q., Chen, S., Chen, X., Niu, S., Yue, L., Pan, X., et al. (2022). An effective glucagon-like Peptide-1 receptor agonists, Semaglutide, improves Sarcopenic obesity in obese mice by modulating skeletal muscle metabolism. *Drug Des. Devel. Ther.* 16, 3723–3735. doi: 10.2147/DDDT.S381546

Saban Güler, M., Arslan, S., Ağagündüz, D., Cerqua, I., Pagano, E., Berni Canani, R., et al. (2025). Butyrate: a potential mediator of obesity and microbiome via different mechanisms of actions. *Food Res. Int.* 199:115420. doi: 10.1016/j.foodres.2024.115420

Saravanan, G., Ponmurugan, P., Deepa, M. A., and Senthilkumar, B. (2014). Anti-obesity action of gingerol: effect on lipid profile, insulin, leptin, amylase and lipase in male obese rats induced by a high-fat diet. *J. Sci. Food Agric.* 94, 2972–2977. doi: 10.1002/jsfa.6642

Takeuchi, T., Kameyama, K., Miyauchi, E., Nakanishi, Y., Kanaya, T., Fujii, T., et al. (2023). Fatty acid overproduction by gut commensal microbiota exacerbates obesity. *Cell Metab.* 35, 361–375.e9. doi: 10.1016/j.cmet.2022.12.013

The Lancet Diabetes Endocrinology (2021). Obesity in China: time to act. *Lancet Diabetes Endocrinol.* 9:407. doi: 10.1016/S2213-8587(21)00150-9

Trung, N. Q., Thu Thanh, N. T., Hoa, N. T., Mechler, A., and Vo, Q. V. (2023). Feruloylmonotropeins: promising natural antioxidants in *Paederia scandens*. *RSC Adv.* 13, 6153–6159. doi: 10.1039/d3ra00458a

Vallianou, N. G., Kounatidis, D., Tsilingiris, D., Panagopoulos, F., Christodoulatos, G. S., Evangelopoulos, A., et al. (2023). The role of next-generation probiotics in obesity and obesity-associated disorders: current knowledge and future perspectives. *Int. J. Mol. Sci.* 24:6755. doi: 10.3390/ijms24076755

Wahl, S., Yu, Z., Kleber, M., Singmann, P., Holzapfel, C., He, Y., et al. (2012). Childhood obesity is associated with changes in the serum metabolite profile. *Obes. Facts* 5, 660–670. doi: 10.1159/000343204

Wang, N., Dilixiati, Y., Xiao, L., Yang, H., and Zhang, Z. (2024). Different short-chain fatty acids unequally modulate intestinal homeostasis and reverse obesity-related symptoms in Lead-exposed high-fat diet mice. *J. Agric. Food Chem.* 72, 18971–18985. doi: 10.1021/acs.jafc.4c04193

Wang, L., Jiang, Y., Han, T., Zheng, C., and Qin, L. (2014). A phytochemical, pharmacological and clinical profile of *Paederia foetida* and *P. scandens*. *Nat. Prod. Commun.* 9, 879–886. doi: 10.1177/1934578X1400900640

Wang, Z., Xue, L., Guo, C., Han, B., Pan, C., Zhao, S., et al. (2012). Stevioside ameliorates high-fat diet-induced insulin resistance and adipose tissue inflammation by downregulating the NF-κB pathway. *Biochem. Biophys. Res. Commun.* 417, 1280–1285. doi: 10.1016/j.bbrc.2011.12.130

Wang, Y., Zhao, L., Gao, L., Pan, A., and Xue, H. (2021). Health policy and public health implications of obesity in China. *Lancet Diabetes Endocrinol.* 9, 446–461. doi: 10.1016/S2213-8587(21)00118-2

Wei, G., Ye, Y., Yan, X., Chao, X., Yang, F., Wang, M., et al. (2020). Effect of banana pulp dietary fibers on metabolic syndrome and gut microbiota diversity in high-fat diet mice. *J. Food Biochem.* 44:e13362. doi: 10.1111/jfbc.13362

Wu, Y., Mo, J., Liang, J., Pu, X., Dong, Y., Zhu, X., et al. (2024). Multiomic study of the protective mechanism of *Persicaria capitata* (Buch.-ham. Ex D.Don) H.Gross against streptozotocin-induced diabetic nephropathy in Guizhou miniature pigs. *Phytomedicine* 128:155499. doi: 10.1016/j.phymed.2024.155499

Wu, Q., Tang, H., and Wang, H. (2019). The anti-oxidation and mechanism of essential oil of *Paederia scandens* in the NAFLD model of chicken. *Animals (Basel)* 9:850. doi: 10.3390/ani9100850

Wu, C., Yang, F., Zhong, H., Hong, J., Lin, H., Zong, M., et al. (2024). Obesity-enriched gut microbe degrades myo-inositol and promotes lipid absorption. *Cell Host Microbe* 32, 1301–1314.e9. doi: 10.1016/j.chom.2024.06.012

Xiao, M., Fu, X., Ni, Y., Chen, J., Jian, S., Wang, L., et al. (2018). Protective effects of *Paederia scandens* extract on rheumatoid arthritis mouse model by modulating gut microbiota. *J. Ethnopharmacol.* 226, 97–104. doi: 10.1016/j.jep.2018.08.012

Xu, Y., Zeng, J., Wang, L., Xu, J., He, X., and Wang, Y. (2023). Anti-inflammatory iridoid glycosides from *Paederia scandens* (Lour.) Merrill. *Phytochemistry* 212:113705. doi: 10.1016/j.phytochem.2023.113705

Yang, Y., Fukui, R., Jia, H., and Kato, H. (2021). Amaranth supplementation improves hepatic lipid dysmetabolism and modulates gut microbiota in mice fed a high-fat diet. *Food Secur.* 10:1259. doi: 10.3390/foods10061259

You, H., Tan, Y., Yu, D., Qiu, S., Bai, Y., He, J., et al. (2022). The therapeutic effect of SCFA-mediated regulation of the intestinal environment on obesity. *Front. Nutr.* 9:886902. doi: 10.3389/fnut.2022.886902

Zhang, X., Ha, S., Lau, H. C.-H., and Yu, J. (2023). Excess body weight: novel insights into its roles in obesity comorbidities. *Semin. Cancer Biol.* 92, 16–27. doi: 10.1016/j.semcancer.2023.03.008

Zhu, T., Zhao, J., Zhuo, S., Hu, Z., Ouyang, S., Wunier, n., et al. (2021). High fat diet and high cholesterol diet reduce hepatic vitamin D-25-hydroxylase expression and serum 25-Hydroxyvitamin D3 level through elevating circulating cholesterol, glucose, and insulin levels. *Mol. Nutr. Food Res.* 65:e2100220. doi: 10.1002/mnfr.202100220

frontiers | Frontiers in Microbiology

TYPE Original Research
PUBLISHED 28 April 2025
DOI 10.3389/fmicb.2025.1560887

Check for updates

OPEN ACCESS

EDITED BY
Mohammad Altamimi,
An-Najah National University, Palestine

REVIEWED BY
Minghui Wang,
Shandong Agricultural University, China
Xinyue Yang,
China Agricultural University, China
Fei Li,
Yangzhou University, China

*CORRESPONDENCE
Xinghua Zhao
✉ dyzhaoxh@hebau.edu.cn
Hailong Liu
✉ Liuhailong423@126.com

RECEIVED 20 January 2025
ACCEPTED 25 March 2025
PUBLISHED 28 April 2025

CITATION
Zhang Y, Ma R, Du X, He X, Zhang Y, Ma N, Liu H and Zhao X (2025) Impact of bacteroides uniformis on fatty liver hemorrhagic syndrome in dawu golden phoenix laying hens: modulation of gut microbiota and arachidonic acid metabolism. *Front. Microbiol.* 16:1560887. doi: 10.3389/fmicb.2025.1560887

COPYRIGHT
© 2025 Zhang, Ma, Du, He, Zhang, Ma, Liu and Zhao. This is an open-access article distributed under the terms of the Creative Commons Attribution License (CC BY). The use, distribution or reproduction in other forums is permitted, provided the original author(s) and the copyright owner(s) are credited and that the original publication in this journal is cited, in accordance with accepted academic practice. No use, distribution or reproduction is permitted which does not comply with these terms.

Impact of bacteroides uniformis on fatty liver hemorrhagic syndrome in dawu golden phoenix laying hens: modulation of gut microbiota and arachidonic acid metabolism

Yu Zhang[1], Rongfei Ma[1], Xicui Du[2], Xin He[1], Yan Zhang[3], Ning Ma[1], Hailong Liu[3]* and Xinghua Zhao[1]*

[1]College of Veterinary Medicine, Hebei Agricultural University, Baoding, China, [2]Hebei Jinkun Animal Pharmaceutical Co. Ltd., Xinji, China, [3]Institute of Animal Science and Veterinary Medicine, Hainan Academy of Agricultural Sciences, Haikou, China

This study explored the impact of *Bacteroides uniformis* (*B. uniformis*) on fatty liver hemorrhagic syndrome (FLHS) induced by a high-energy and low-protein (HELP) diet in laying hens, mainly focusing on hepatic lipid metabolism, gut microbiota, and arachidonic acid (AA) metabolism. A total of 120 Dawu Golden Phoenix laying hens (210-day-old) were randomly divided into four groups. The control group (CON) was fed a standard diet and received a daily gavage of PBS, while the other groups were fed with a HELP diet to induce FLHS and received a daily gavage of PBS (MOD), 1×10^9 CFU/ml *B. uniformis* (BUL), and 1×10^{11} CFU/ml *B. uniformis* (BUH) for 70 days. All hens were administered 1 ml daily by gavage. Each group had 6 replications with 5 hens per replication. The results showed that *B. uniformis* increased the egg production rate and feed conversion ratio and decreased body weight, liver index, and abdominal fat rate ($p < 0.05$). *B. uniformis* treatment reduced liver lipid accumulation by reducing the levels of Triglyceride (TG), Total cholesterol (TC), low-density lipoprotein cholesterol (LDL-C), alanine transaminases (ALT), and aspartate transaminases (AST) in serum and significantly elevated high-density lipoprotein cholesterol (HDL-C) ($p < 0.05$). The results indicated that *B. uniformis* altered the gut microbiota. Specifically, the abundance of *Bacteroides* was higher, and the relative abundances of *Treponema, Helicobacter,* and Spirochaetota were lower than those of the MOD group ($p < 0.05$). Moreover, targeted metabolomic analysis showed that supplementation of *B. uniformis* significantly elevated 6-keto-$PGF_{1\alpha}$ and AA levels, along with significantly reduced levels of thromboxane B_2 (TXB_2), leukotriene D_4 (LTD_4), 8-isoprostaglandin $F_{2\alpha}$ (8-iso-$PGF_{2\alpha}$), 12S-hydroxyeicosatetraenoic acid (12S-HETE), 15S-hydroxyeicosatetraenoic acid (15S-HETE), 9-S-hydroxy-octadecadienoic acid (9S-HODE), and 13-S-hydroxy-octadecadienoic acid (13S-HODE) ($p < 0.05$). In conclusion, the oral intake of *B. uniformis* can improve liver function, gut microbiota, and AA metabolism, thereby helping to ameliorate FLHS in Dawu Golden Phoenix laying hens.

KEYWORDS

fatty liver hemorrhagic syndrome, laying hens, *Bacteroides uniformis*, gut microbiota, arachidonic acid

1 Introduction

The widespread use of cage rearing in the laying hen industry, coupled with restricted movement, increased production pressures, and fluctuating temperatures, adversely affects hepatic lipid metabolism, making laying hens more prone to fatty liver hemorrhagic syndrome (FLHS) (Yadav et al., 2024). In a survey, FLHS accounted for 74% of the total mortality rates in caged laying hens in Queensland (Shini et al., 2018; Anene et al., 2023). The main pathological characteristics of FLHS are hepatic steatosis and, in severe cases, vascular rupture that can lead to sudden death from hemorrhage (Anene et al., 2023). Studies have shown that high-energy and low-protein (HELP) diets are the fundamental pathological contributors to FLHS (Yaqoob et al., 2024). The occurrence of FLHS is first caused by the excessive accumulation of triglycerides (TG) in the liver, inhibition of fatty acid oxidation, and disorders in liver lipid metabolism. Subsequently, insulin resistance, liver oxidative stress, and liver inflammation can further aggravate FLHS (Cheng et al., 2024). Laying hens affected by FLHS closely mimic the conditions seen in humans with non-alcoholic fatty liver disease (NAFLD), given that their livers are a major site for *de novo* lipogenesis (Gao et al., 2021). These findings render them a suitable model for investigating human lipid metabolism disorders. Consequently, using laying hens in research provides a novel and promising avenue for deepening our understanding of NAFLD pathophysiology and exploring potential therapeutic strategies.

Changes to the intestinal microbiota's composition and functionality can significantly influence the development and advancement of FLHS (Li et al., 2020). Due to their low cost and high safety profile, probiotics have emerged as an ideal option for attenuating liver lipid metabolism disorders caused by high-energy diets (Wang et al., 2022). In particular, *B. uniformis* has been extensively used in clinical settings due to its safety and excellent efficacy. It has been reported that *B. uniformis* is inversely associated with serum LDL-cholesterol levels (Yan et al., 2022). Furthermore, *B. uniformis* has been documented to prevent obesity and metabolic disorders (Gómez del Pulgar et al., 2020; Fabersani et al., 2021; Lee et al., 2021; López-Almela et al., 2021). Currently, there is a lack of comprehensive studies on the effects of *B. uniformis* on lipid metabolism in laying hens, particularly regarding the treatment of FLHS induced by high-energy diets. Arachidonic acid (AA), a polyunsaturated fatty acid, is ubiquitous in living organisms (Pereira et al., 2024). It has been confirmed that a disorder in AA metabolism, characterized by reduced levels of AA, is associated with FLHS (Meng et al., 2021). Previous studies have shown that *Bacteroides fragilis* exerts an anti-FLHS effect by modulating oxylipin metabolism and gut microbiota stability, with AA playing a pivotal role (Zhang et al., 2024a, 2024b). Therefore, we hypothesized that *B. uniformis* could effectively relieve FLHS in laying hens by regulating AA metabolism and gut microbiota.

This study aims to elucidate the improvement effect of *B. uniformis* on FLHS by examining liver lipid metabolism, gut microbiota, and AA metabolism and provide a basis for its application in laying hens.

2 Materials and methods

2.1 Materials

The *Bacteroides uniformis* strain was generously provided by Dr. Ma Ning from Hebei Agricultural University (Hebei, China). This bacterial strain was extracted from the cecal contents of healthy laying hens. By aligning its 16S rRNA gene sequence with the NCBI reference database,[1] the strain was confirmed to be *Bacteroides uniformis* strain 19006C (Supplementary Figure S1). All chemicals and solvents were obtained from commercial suppliers and were used as received.

2.2 Bacterial strains and culture conditions

The details of bacterial strains and culture conditions are provided in the Supplementary material.

2.3 Bile acid and simulated gastrointestinal fluid tolerance

The stress resistance of *B. uniformis* is detailed in the Supplementary material.

2.4 Animals and treatment

We acquired 210-day-old 120 Dawu Golden Phoenix laying hens from Hebei Huafeng Farm (Baoding, Hebei, China). The laying hens were housed in wire cages (measuring 100 cm × 70 cm × 60 cm) with five hens per cage. They had free access to clean water and were fed twice daily (7:00 a.m. and 5:00 p.m.). The room temperature was maintained at 25 ± 1°C, with the humidity level of 50 ± 5%. The formulation of the standard diet adhered to the guidelines of the Chinese Feeding Standard of Chickens NPC (1994). The detailed composition and nutritional levels of the standard and HELP diets are presented in Supplementary Table S1. The animal experiment protocol (No. 2022161) was reviewed and approved by the Animal Protection and Ethics Committee of Hebei Agricultural University.

All laying hens were allowed to adapt for 1 week before the experiment and were randomly allocated into four treatment groups, with each group consisting of six replications (five hens per replication). The experimental design was as follows: The control group (CON) was fed a standard diet and given a daily gavage of phosphate-buffered saline (PBS), whereas the other three groups were all fed with a HELP diet to induce FLHS (Zhang et al., 2024a, 2024b). Among the three FLHS groups, one was given a daily gavage of PBS (MOD), and the other groups were treated with 1×10^9 CFU/ml *B. uniformis* (BUL) and 1×10^{11} CFU/ml *B. uniformis* (BUH). All hens were given 1 ml daily by gavage. The experiment lasted for 70 days (Table 1).

1 https://www.NCBI.nlm.nih.gov/

TABLE 1 Experimental treatment.

Groups	Diet	Treament (once daily gavage, 70 days)
CON	Standard diet	1 ml PBS/hen
MOD	HELP diet	1 ml PBS/hen
BUL	HELP diet	1 mL 1 × 10^9 CFU/ml *B. uniformis*/hen
BUH	HELP diet	1 mL 1 × 10^{11} CFU/ml *B. uniformis*/hen

2.5 Measurements and sample collection

The body weights of the laying hens were measured every 2 weeks. Daily feed intake and residual feed were recorded to calculate the average daily feed intake (ADFI). Eggs were collected and weighed daily. The egg-laying rate was calculated based on egg production data on a hen-day basis. The feed conversion ratio (FCR) was determined as grams of feed per gram of egg produced. At the end of the animal experiment, the laying hens underwent a 12-h fasting. Blood samples were collected from the brachial vein and centrifuged (3,500 r/min, 15 min) to obtain serum at 4°C. The serum was then stored at −20°C for further analysis. Subsequently, the laying hens were sacrificed by cervical dislocation and exsanguinated, and the livers and abdominal fat were carefully removed and weighed. A piece of liver tissue was immersed in a 10% formalin solution. The remaining liver tissue and cecal contents were immediately frozen in liquid nitrogen and stored at −80°C until further targeted metabolomic analysis and bacterial DNA extraction.

2.6 Production performance and liver index

At the end of the animal experiment (the 70th day), the egg production rate was calculated according to Equation 1 (Xiong et al., 2024). The ADFI was calculated according to Equation 2 (Taofeek et al., 2022). The FCR was calculated according to Equation 3 (Al-Khalaifah et al., 2024). The liver index was calculated according to Equation 4 (Zhang et al., 2024a, 2024b). The abdominal fat rate was calculated according to Equation 5 (Zhao et al., 2020).

$$\text{Egg production rate}(\%) = \frac{\text{number of eggs laid}}{\text{number of laying hens}} \times 100\% \quad (1)$$

$$\text{ADFI}(\text{g/d}) = \frac{\text{overall feed intake} - \text{overall residual feed}}{\text{days} \times \text{number of laying hens}} \times 100\% \quad (2)$$

$$\text{FCR} = \frac{\text{overall feed intake} - \text{overall residual feed}}{\text{overall weight of eggs}} \times 100\% \quad (3)$$

$$\text{Liver index}(\%) = \frac{\text{weight of the liver}}{\text{body weight}} \times 100\% \quad (4)$$

$$\text{Abdominal fat rate}(\%) = \frac{\text{weight of abdominal fat}}{\text{body weight}} \times 100\% \quad (5)$$

2.7 Biochemistry analysis and liver morphology

Total cholesterol (TC), TG, low-density lipoprotein cholesterol (LDL-C), high-density lipoprotein cholesterol (HDL-C), aspartate transaminases (AST), and alanine transaminases (ALT) were measured in serum following the instructions provided in the kit (Nanjing Jiancheng Institute of Bioengineering, Jiangsu, China). After formalin fixation, the liver tissues were embedded in paraffin and sectioned into 5-μM slices. These sections were subsequently stained with standard hematoxylin and eosin (H & E) for histological examination. Additionally, frozen liver sections were stained with Oil Red O to assess lipid droplet accumulation.

2.8 16S rRNA gene sequencing analysis

The bacterial DNA of the cecal samples was extracted using the Cetyltrimethylammonium Bromide method, following the barcode sequence. The Polymerase Chain Reaction (PCR) amplification primer sequence split the sample data from the offline data, and the forward primer was 515F (5′-CCTAYGGGRBGCASCAG-3′) with reverse primer 806R (5′-GGACTACNNG GGTATCTAAT3′), which amplified the variable region 4 of the microbial 16S rDNA gene. The NEBNext® Ultra™ II FS DNA PCR-free Library Prep Kit (New England Biolabs (Beijing) LTD, Beijing, China) was used to construct the library. The constructed library was quantified using Qubit and qPCR. After the library was qualified, PE 250 on-machine sequencing was performed using a NovaSeq 6000 platform (Illumina Corporation, CA, USA).

Fast Length Adjustment of SHort reads (FLASH Version 1.2.11) was used to assemble the reads of the sample to obtain raw tags, and fastp software (Version 0.23.1) was used for quality control to obtain clean tags. The clean tags remove chimeric sequences by comparing them to the Silva database. Taxonomic annotation and analysis were conducted at both the phylum and genus levels, using the Silva 138.1 database. To assess microbial community diversity, alpha diversity analysis was conducted using Quantitative Insights Into Microbial Ecology 2. Beta diversity analysis utilized the weighted UniFrac distance algorithm and was visualized through principal coordinate analysis (PCoA) plots. The independent T-test was used to analyze inter-group differences in species abundance at various taxonomic levels, focusing on those with statistically significant variations. Linear discriminant analysis effect size (LEfSe) analysis was performed using the microeco package (Linear discriminant analysis (LDA) score > 2). Spearman's correlation analysis was performed to explore the relationships between differential bacteria, serum lipids, and AA metabolites.

2.9 Targeted metabolomics analysis

To determine the changes in AA metabolites in the CON, MOD, and BUL layers, quantitative analysis of AA metabolites in the liver was performed using targeted metabolomics.

The reagents, including methanol, acetonitrile, acetic acid, and isopropanol, were sourced from Merck (NJ, USA). Standard substances and internal standards were procured from Cayman (MI, USA). Liver tissue samples were ground in liquid nitrogen. A total of 20 mg of liver tissue powder was extracted using 200 μl of methanol. The samples were vortexed, and the protein precipitate was allowed to settle at 4°C. Furthermore, 20 μl of an internal standard mixture (1 μM) was added to each sample and vortexed thoroughly. The samples were then centrifuged at 5,000 × *g* for 10 min at 4°C. The extraction process was repeated, and the supernatants from both extractions were combined. Oxylipins were extracted using solid-phase extraction columns. After the concentration and drying of the elution solution, reconstitution was performed using 100 μl of methanol/water (1:1, *v*/*v*) for LC–MS/MS analysis.

The chromatographic conditions were as follows: the samples were separated using an Agilent 1,290 Infinity LC ultra-high-performance liquid chromatography system (Agilent Technologies Inc., CA, USA). The separation of samples was performed on ACQUITY UPLC BEH C18 (1.7 μm, 2.1 mm × 50 mm, Waters, Ireland) at a flow rate of 400 μl/min. Mobile phase A consisted of a 0.1% formic acid aqueous solution, and mobile phase B consisted of a 0.1% formic acid acetonitrile solution. The mobile phase gradient was as follows: 0 to 1 min, 30% B; 1 to 9 min, 30 to 90% B; 9 to 11 min, 90% B; 11 to 11.1 min, 90 to 20%; and 11.1 to 14 min, 20% for equilibration. The injection volume was 20 μl, the column temperature was 35°C, and the autosampler temperature was 4°C.

The mass spectra data were acquired by using a 5,500 QTRAP mass spectrometer (SCIEX, MA, USA) with an ESI source operated in negative mode. The electrospray Ionization parameters were optimized as follows: source temperature, 500°C; Ion Source Gas1, 50; Ion Source Gas2, 50; Curtain gas, 30; IonSapary Voltage Floating, and −4,500 V. The ion pairs to be tested were detected using the multiple reaction monitoring mode.

Multiquant 3.0.2 software (SCIEX, MA, USA) was used to extract chromatographic peak areas and retention times. The standard of the target substance was used to correct the retention time for metabolite identification.

2.10 Statistical analysis

All data were analyzed using SPSS 27.0 software (IBM Inc., NY, USA). Shapiro–Wilk and Levene's tests were used to assess the normal distribution of the data and the homogeneity of variance. One-way analysis of variance (ANOVA) and Tukey's *post hoc* test were employed to determine the significance of mean differences. The results are expressed as mean ± SEM, and a significant difference was set as $p < 0.05$. The data were plotted through Origin software (OriginPro 2021, OriginLab Corporation, USA).

3 Results

3.1 *Bacteroides uniformis* stress resistance

The survival rate of *B. uniformis* in BHI broth at pH 3 was 32.10%. Furthermore, the survival rates of *B. uniformis* in 0.1, 0.3, and 0.5% bile salts were 110.33, 63.04, and 51.16%, respectively. Additionally, the survival rates of *B. uniformis* in simulated gastric juice and intestinal juice were 14.61 and 8.16%, respectively (Table 2).

3.2 Effects of *B. uniformis* on the production performance of FLHS-laying hens

As can be seen from Figure 1A, the body weight of the MOD group was significantly higher than that of other groups from week 2 ($p < 0.05$). A slight improvement in body weight was observed in laying hens of the BUH group, but no statistically significant differences were observed between the CON, BUL, and BUH groups ($p > 0.05$). In terms of average daily feed intake, there was no significant difference between all laying hens in the four groups ($p > 0.05$) (Figure 1B). The egg production rate of the MOD group was significantly lower than that of the other three groups ($p < 0.05$) (Figure 1C). In addition, the egg production rates of the MOD group and BUH group were significantly lower than those of the CON group ($p < 0.05$). Interestingly, the egg production rates of the BUH and BUL groups were significantly higher than those of the MOD groups during the experiment ($p < 0.05$). The egg production rates of the CON, BUL, BUH, and MOD groups were 94.79, 90.48, 88.54, and 75.89%, respectively. The FCR of the BUH and BUL groups was significantly lower than that of the MOD group ($p < 0.05$) (Figure 1D). Upon closer inspection, we also discovered that the FCR of the BUL group was statistically similar to that of the CON group. Details of egg production, egg weight, liver weight, and abdominal fat weight are shown in Supplementary Table S2.

3.3 Effects of *B. uniformis* on liver index and liver morphology in FLHS-laying hens

The liver index and abdominal fat rate of the MOD group were significantly higher than the CON group ($p < 0.05$) (Figures 1E,F). In addition, the liver index and abdominal fat rate were significantly reversed following the administration of *B. uniformis* ($p < 0.05$) (Figures 1E,F). Notably, the reversal effect on the liver index was significantly better in the BUL group than in the BUH group ($p < 0.05$).

The results of pathological examination of the liver staining with H & E and Oil Red O demonstrated a clear and normal liver cell architecture in the CON group. Serious fatty degeneration with lipid droplet accumulation and necrosis was found in laying hens with the

TABLE 2 *B. uniformis* stress resistance.

Treatment		The survival rate (%)
Hydrochloric acid (pH = 3, 3 h)		32.10 ± 1.74
Sodium Taurocholate (12 h)	0.1%	110.33 ± 5.75
	0.3%	63.04 ± 2.37
	0.5%	51.16 ± 4.60
Gasttic juice (4 h)		14.61 ± 0.95
Intestinal juice (4 h)		8.16 ± 1.58

The data was expressed as mean ± SD.

10.3389/fmicb.2025.1560887

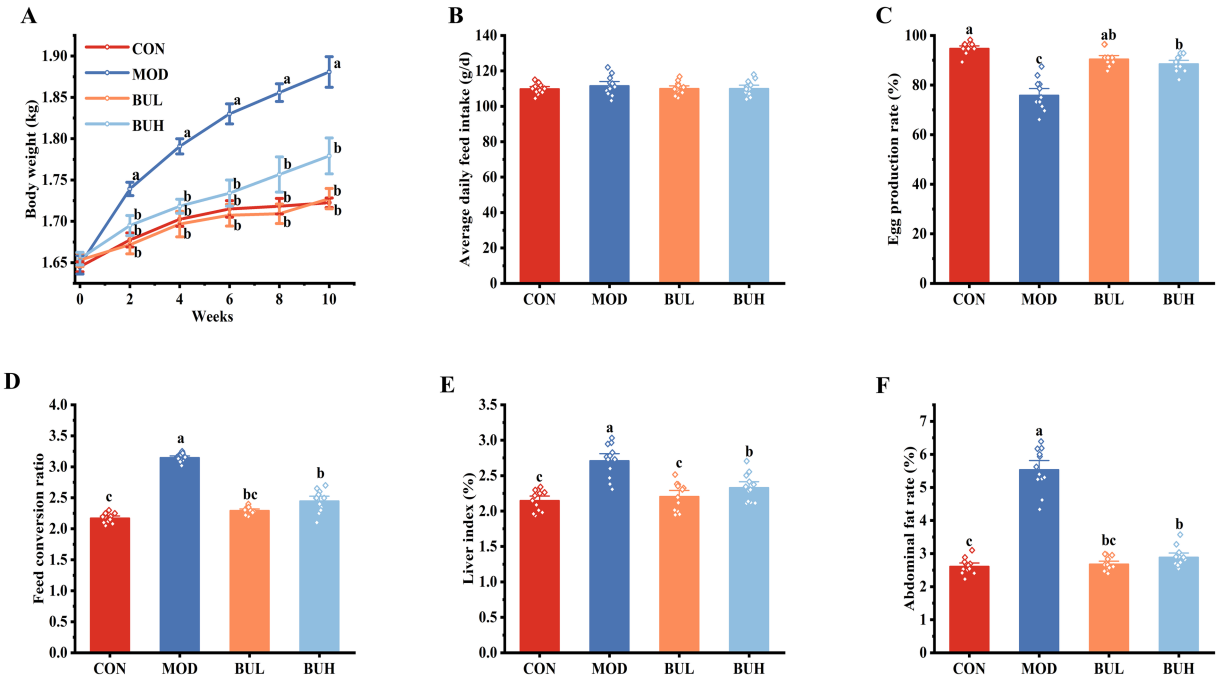

FIGURE 1
Effect of *B. uniformis* on production performance and liver index. **(A)** Body weight. **(B)** Average daily feed intake. **(C)** Egg production rate. **(D)** Feed conversion ratio. **(E)** Liver index. **(F)** Abdominal fat rate. Means with different superscripts differ significantly at a significance level of $p < 0.05$, $n = 12$.

HELP diet in the MOD group. In comparison with the MOD group, HELP diet-induced lipid accumulation in the liver of laying hens with *B. uniformis* treatment was decreased at different degrees, indicating that the fatty degeneration was ameliorated by *B. uniformis* treatment (Figure 2).

3.4 Effects of *B. uniformis* on serum lipid levels in FLHS-laying hens

As shown in Figure 3, the levels of TG, TC, LDL-C, AST, and ALT in the MOD group were significantly increased ($p < 0.05$), whereas HDL-C levels were significantly decreased compared to the CON group ($p < 0.05$). All these indicators were significantly reversed by *B. uniformis* treatment. Notably, the LDL-C, HDL-C, AST, and ALT levels in the BUL group were reversed to a significantly greater extent than those in the BUH group ($p < 0.05$). These results indicated that the reversal effect of BUL was better than that of BUH. Consequently, the BUL group was selected for further experimentation.

3.5 Effects of *B. uniformis* on the gut microbiota of FLHS-laying hens

The goods coverage value was close to 1, indicating that the sequencing depth was likely comprehensive enough to encompass nearly all species within the sample (Figure 4A). The BUL group had the highest observed levels of the Chao1 index and Shannon index, but there was no significant difference ($p > 0.05$) (Figures 4B,C). As shown in Figure 4D, the microbial community structure that could reveal distinct clustering of gut content samples in the MOD group was separated from the CON group, whereas the microbial community structure in the BUL group was obviously altered after *B. uniformis* administration, indicating that *B. uniformis* resisted the dysbiosis of the microbiota community induced by HELP in Dawu Golden Phoenix laying hens. At the phylum level, Bacteroidota, Firmicutes, and Spirochaetota were the dominant phyla, with Bacteroidota being the most abundant (Figure 4E). Supplementation with *B. uniformis* significantly decreased relative abundance of Spirochaetota while significantly increasing relative abundance of Bacteroidota ($p < 0.05$). However, there was no significant difference in the relative abundance of Firmicutes among the groups ($p > 0.05$) (Figures 4F–I). At the genus level, *Bacteroides*, *Rikenellaceae_RC9_gut_group*, *Lactobacillus*, *Treponema*, and *Helicobacter* were the dominant genera (Figure 5A). Supplementation with *B. uniformis* significantly decreased the relative abundances of *Treponema* and *Helicobacter* and significantly increased the relative abundance of *Bacteroides* ($p < 0.05$). However, there was no significant difference in the relative abundance of the *Rikenellaceae_RC9_gut_group* and *Lactobacillus* among the groups ($p > 0.05$) (Figures 5B–F). LEfSe analysis confirmed significant enrichment of Bacteroidales, Bacteroidota, Bacteroidia, *Bacteroides*, *and* Bacteroidaceae in the BUL group, identifying them as signature differential bacteria (Figure 5G). The comparative metastat analysis revealed significant differences in the microbial composition between the MOD and BUL groups. Notably, *Treponema* and *Helicobacter* exhibited a marked decrease in the BUL group compared to the MOD group ($p < 0.05$ or $p < 0.01$). In contrast, *Bacteroides* was more abundant in the BUL group ($p < 0.01$), suggesting a potential increase. These findings underscore the distinct microbial signatures associated with the MOD and BUL groups, highlighting the importance of *Bacteroides* in the BUL group's microbiota profile (Figure 5I).

10.3389/fmicb.2025.1560887

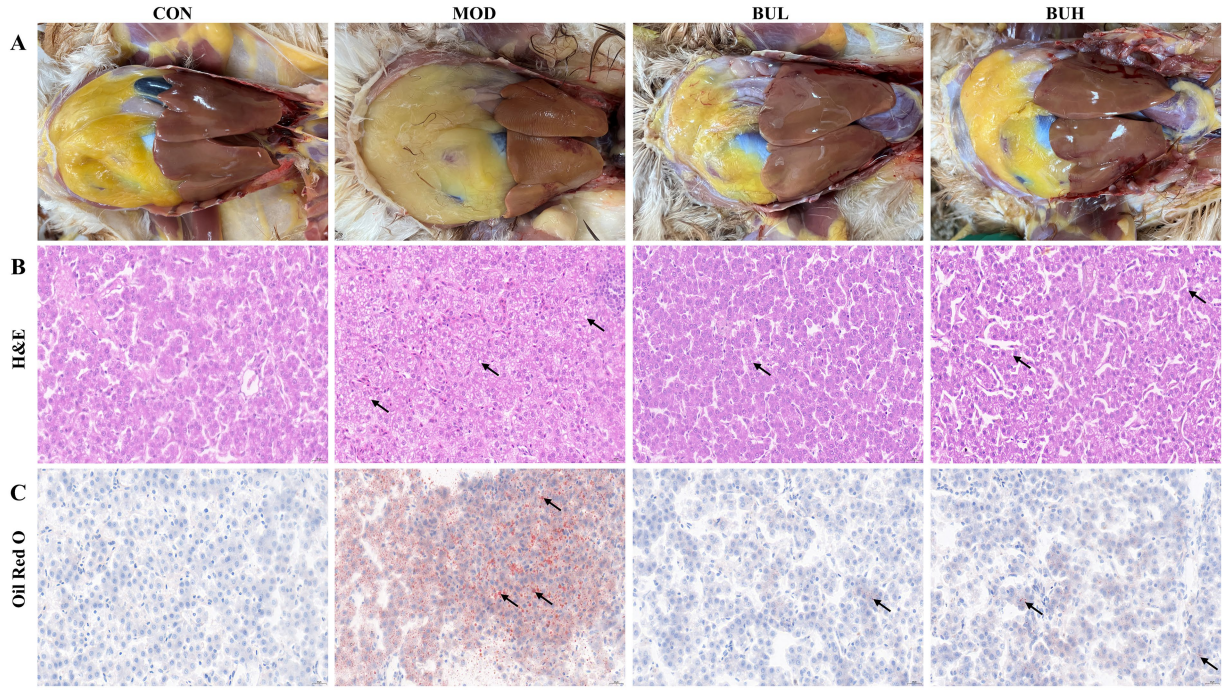

FIGURE 2
Effect of *B. uniformis* on liver morphology of FLHS-laying hens. **(A)** Anatomical map of the liver. **(B)** Liver tissues from the CON, MOD, BUL, and BUH groups were subjected to H&E staining (scale bar: 20 μm). **(C)** Liver tissues from the CON, MOD, BUL, and BUH groups were subjected to Oil Red O staining (scale bar: 20 μm).

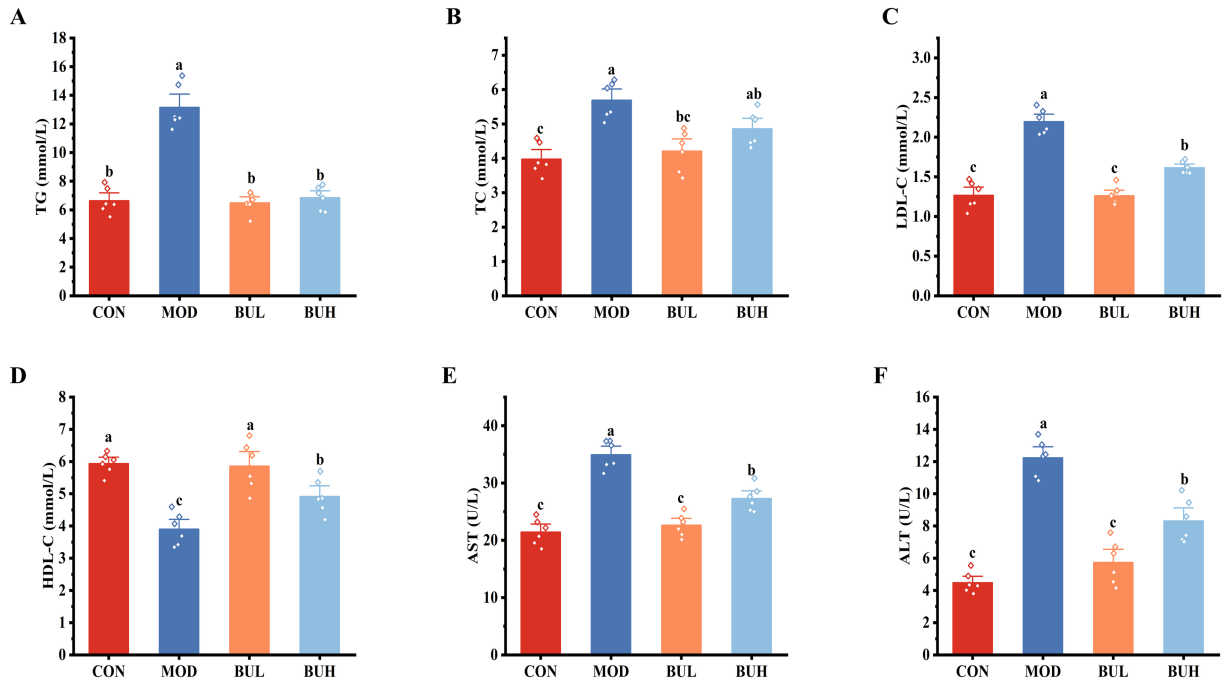

FIGURE 3
Effect of *B. uniformis* on blood lipids and liver function of FLHS-laying hens. **(A–F)** TG, TC, LDL-C, HDL-C, AST, and ALT, respectively. Means with different superscripts differ significantly at a significance level of $p < 0.05$, $n = 6$.

10.3389/fmicb.2025.1560887

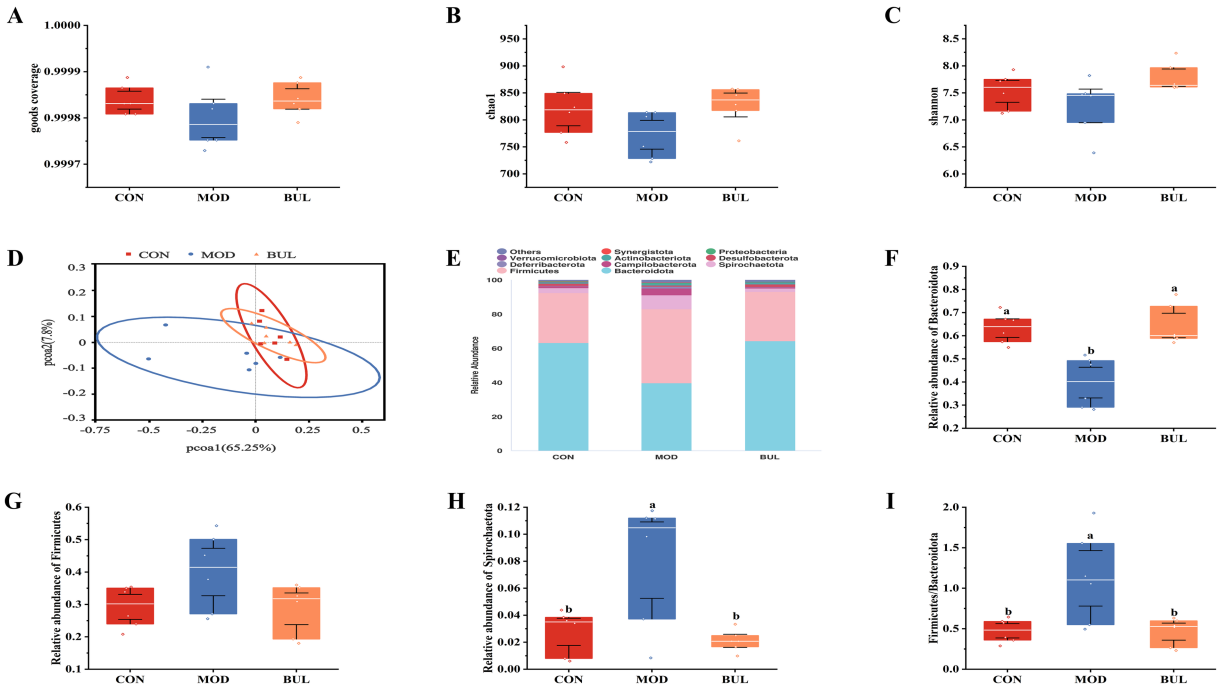

FIGURE 4
Effect of *B. uniformis* on the phylum-level abundance of gut microbiota in FLHS-laying hens. **(A)** Goods coverage index. **(B)** Chao1 index. **(C)** Shannon index. **(D)** PCoA plot based on weighted_unifrac. **(E)** Relative abundance of gut microbiota at the phylum level. **(F)** Relative abundance of Bacteroidota. **(G)** Relative abundance of Firmicutes. **(H)** Relative abundance of Spirochaetota. **(I)** Firmicutes/Bacteroidetes. Means with different superscripts differ significantly at a significance level of $p < 0.05$, $n = 6$.

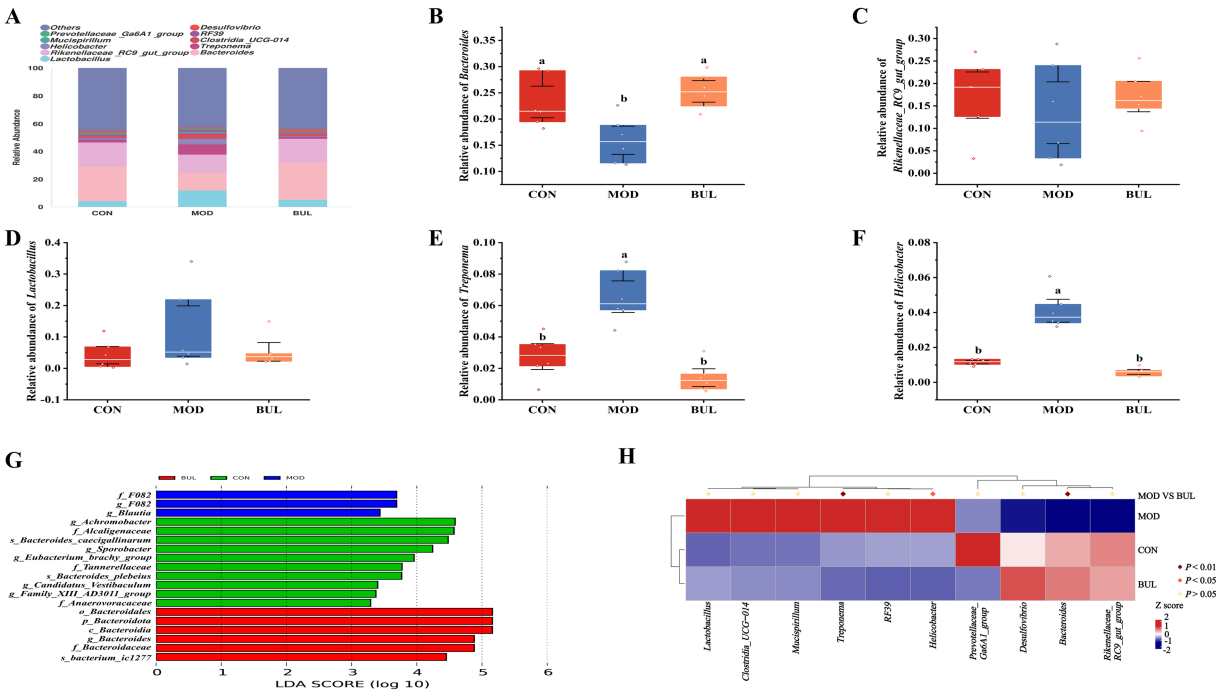

FIGURE 5
Effects of *B. uniformis* on relative abundance of gut microbiota at the genus level in FLHS-laying hens. **(A)** Relative abundance of gut microbiota at genus level. **(B)** Relative abundance of *Bacteroides*. **(C)** Relative abundance of *Rikenellaceae_RC9_gut_group*. **(D)** Relative abundance of *Lactobacillus*. **(E)** Relative abundance of *Treponema*. **(F)** Relative abundance of *Helicobacter*. **(G)** LEfSe analysis. **(H)** Metastat analysis to identify the contribution of differential genus bacteria. Means with different superscripts differ significantly at a significance level of $p < 0.05$, $n = 6$.

3.6 Effect of *B. uniformis* on AA metabolism in FLHS-laying hens

To confirm the relationship between AA metabolism and FLHS and the effect of *B. uniformis* on AA metabolism in Dawu Golden Phoenix laying hens, the composition and content of AA metabolites among the three groups were analyzed using targeted metabolomics. In targeted metabolomics analysis, 14 distinct oxidized lipid metabolites were identified. These included thromboxane B_2 (TXB_2), leukotriene B_4 (LTB_4), leukotriene D_4 (LTD_4), prostaglandin E_2 (PGE_2), 8-isoprostaglandin $F_{2\alpha}$ (8-iso-$PGF_{2\alpha}$), prostaglandin $F_{2\alpha}$ ($PGF_{2\alpha}$), 6-keto-prostaglandin $F_{1\alpha}$ (6-keto-$PGF_{1\alpha}$), prostaglandin D_2 (PGD_2), 12S-hydroxyeicosatetraenoic acid (12S-HETE), 15S-hydroxyeicosatetraenoic acid (15S-HETE), 9-S-hydroxy-octadecadienoic acid (9S-HODE), 13-S-hydroxy-octadecadienoic acid (13S-HODE), AA, and docosahexaenoic acid (DHA). The targeted metabolomics analysis results showed that the levels of 6-keto-$PGF_{1\alpha}$ and AA were significantly decreased ($p < 0.05$), whereas the levels of TXB_2, 8-iso-$PGF_{2\alpha}$, $PGF_{2\alpha}$, 12S-HETE, 15S-HETE, 9S-HODE, and 13S-HODE were significantly increased in the MOD group compared to the CON group ($p < 0.05$), indicating that the HELP diet changed the AA metabolites. The levels of 6-keto-$PGF_{1\alpha}$ and AA were significantly increased ($p < 0.05$), while the levels of TXB_2, LTD_4, 8-iso-$PGF_{2\alpha}$, $PGF_{2\alpha}$, 12S-HETE, 15S-HETE, 9S-HODE, and 13S-HODE were significantly decreased in the BUL group compared to the MOD group ($p < 0.05$), indicating that the changes in AA metabolism induced by the HELP diet were reversed by *B. uniformis*. Notably, the levels of 6-keto-$PGF_{1\alpha}$ and AA were significantly increased ($p < 0.05$), and 15S-HETE was significantly decreased in the BUL group compared to the CON group ($p < 0.05$) (Figures 6A–N).

3.7 Correlations between gut microbiota, serum lipids, and AA metabolites

To further elucidate the relationship between differential bacteria, serum lipids, and AA metabolites, *Bacteroides*, *Treponema*, and *Helicobacter* were selected for Spearman's correlation analysis. The results are shown in Figure 6O. The three differential bacterial genera were significantly correlated with serum lipid levels and AA metabolites. *Bacteroides* was significantly positively correlated with HDL-C, 6-keto-$PGF_{1\alpha}$, and AA ($p < 0.05$). Conversely, it showed a significant negative correlation between TG, TC, LDL-C, ALT, LTD_4, 8-iso-$PGF_{2\alpha}$, $PGF_{2\alpha}$, and 15S-HETE ($p < 0.05$), indicating that *Bacteroides* has beneficial effects on improving FLHS in Dawu Golden Phoenix laying hens. On the other hand, *Treponema* exhibited a significant positive correlation with TG, TC, LDL-C, AST, ALT, TXB_2, LTD_4, PGE_2, 8-iso-$PGF_{2\alpha}$, $PGF_{2\alpha}$, 12S-HETE, 9S-HODE, and 15S-HETE ($p < 0.05$). Conversely, it showed a significant negative correlation between HDL-C, 6-keto-$PGF_{1\alpha}$, and AA ($p < 0.01$). Furthermore, *Helicobacter* exhibited a significant positive correlation between TG, TC, LDL-C, AST, ALT, TXB_2, LTD_4, 8-iso-$PGF_{2\alpha}$, $PGF_{2\alpha}$, 13S-HODE, and 15S-HETE ($p < 0.05$). Conversely, it showed a significant negative correlation between HDL-C, 6-keto-$PGF_{1\alpha}$, and AA ($p < 0.01$). These results indicate that *Treponema and Helicobacter* can aggravate FLHS.

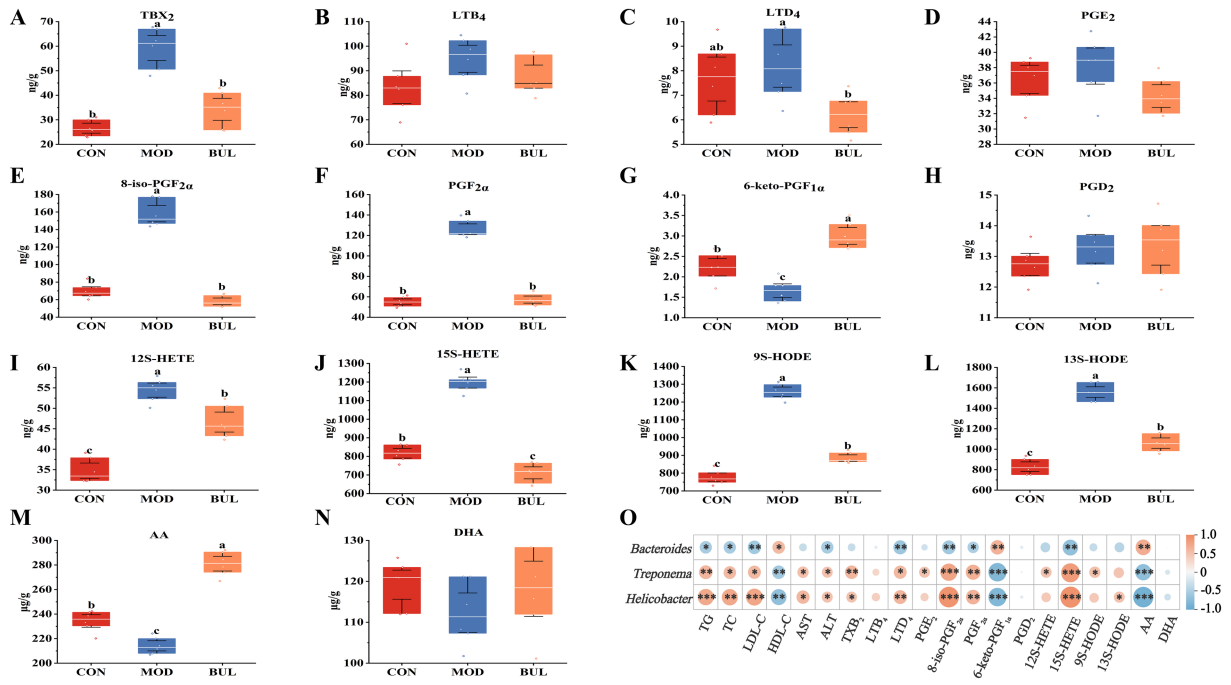

FIGURE 6
Targeted metabolomics analysis and correlation analysis. **(A)** TXB_2. **(B)** LTB_4. **(C)** LTD_4. **(D)** PGE_2. **(E)** 8-iso-$PGF_{2\alpha}$. **(F)** $PGF_{2\alpha}$. **(G)** 6-keto-$PGF_{1\alpha}$. **(H)** PGD_2. **(I)** 12S-HETE. **(J)** 15S-HETE. **(K)** 9S-HODE. **(L)** 13S-HODE. **(M)** AA. **(N)** DHA. **(O)** Correlation analysis. The metabolite units are expressed as ng/g and μg/g liver tissue. Means with different superscripts differ significantly at a significance level of $p < 0.05$, $n = 6$. * indicates $p < 0.05$, ** indicates $p < 0.01$, and *** indicates $p < 0.001$.

4 Discussion

In prior investigations regarding probiotics, especially those focusing on intestinal flora regulation and metabolism improvement, numerous researchers have used comparable dosage levels. Li et al. administered *Lactiplantibacillus plantarum* FRT4 to laying hens at a dosage range of 1×10^9–1×10^{11} CFU/ml. They found that it enhanced laying performance and mitigated FLHS induced by a HELP diet by regulating the gut–liver axis (Li et al., 2024). This provides a valuable reference for selecting *B. uniformis* dosages.

The stress resistance experiment indicated that *B. uniformis* was capable of growing and surviving at low pH and in the presence of bile salts, which demonstrated that *B. uniformis* could tolerate gastrointestinal environmental conditions. The Dawu Golden Phoenix laying hen, autonomously cultivated by China, represents an outstanding breed of high-yielding, red-feathered, pink-shell egg-laying hens. FLHS frequently afflicts commercial caged laying hens, particularly those with high production rates and excessive conditioning, and leads to mortality rates as high as 70% (Shini et al., 2018). *B. uniformis* and *Bacteroides xylanisolvens*, along with other Bacteroides species, have been reported to confer beneficial effects on NAFLD (Qiao et al., 2020; Lee et al., 2021). However, the role of *B. uniformis* in the development of FLHS in poultry is not yet clear. In our study, *B. uniformis* was isolated from the cecum of laying hens and administered to laying hens with FLHS caused by the HELP diet. Furthermore, our findings indicated that *B. uniformis* could ameliorate the adverse effects of FLHS by modulating the hepatic lipid metabolism, regulating gut microbiota, and improving AA metabolism.

The HELP diet is a widely adopted approach for inducing FLHS in chicken models (Miao et al., 2024). Prior studies have established that the HELP diet leads to hepatic lipid overload, thereby inducing lipotoxicity and initiating a cascade of cytotoxic events (Meng et al., 2021). In our experiment, the liver of the MOD group appeared yellowish-brown and greasy, with hemorrhages and bleeding spots. The liver lipid indicators, including TG, TC, LDL-C, ALT, AST, and abdominal fat rate, were significantly increased, which, combined with HDL-C, were significantly reduced in the MOD group. These results confirmed the successful establishment of the FLHS model in laying hens, consistent with existing literature (Li et al., 2024). Notably, the adverse effects observed in the MOD group were significantly reversed by *B. uniformis* treatment. It is worth mentioning that the reversal effect of BUL on the liver index and the levels of LDL-C, HDL-C, ALT, and AST was better than that of BUH. This conclusion has also been confirmed by the macroscopic images and the pathological changes in the liver. These findings were consistent with those of a previous study reporting that *B. uniformis CECT 7771* could reduce serum cholesterol and triglyceride levels in obese mice and alleviate the metabolic and immune disorders caused by high-fat diets (Fabersani et al., 2021).

Impaired intestinal barrier function, increased intestinal permeability, altered bile acid metabolism, and endotoxin-activated hypo-inflammation are all linked to the disrupted intestinal flora, which are involved in the development and progression of FLHS (Dansou et al., 2024). It has been shown that the relative abundance of Bacteroidota is reduced in FLHS-laying hens (Liu et al., 2022). *Bacteroides* has also been demonstrated to promote hepatic glucose storage and influence selective intestinal lipid absorption and serum triglyceride levels (López-Almela et al., 2021). Moreover, rats treated with atorvastatin exhibited a higher abundance of *Bacteroides* in the gut, which led to a reduction in blood lipid levels, including those of TG, TC, and LDL-C. This occurred through the enhancement of propanoate metabolism as well as the metabolism of glycine, serine, and threonine in both feces and plasma, thereby contributing to the overall reduction of blood lipid levels (Li et al., 2022). In our experiments, there was a significant decrease in the relative abundance of Bacteroidota in the MOD group. Supplementing *B. uniformis* increased the relative abundance of *Bacteroides*. *Bacteroides* was significantly negatively correlated with AST, TG, TC, and LDL-C levels (Yang et al., 2023; Zhang et al., 2024a, 2024b). In our experiments, *Bacteroides* was positively correlated with HDL-C and negatively correlated with TG, TC, LDL-C, and ALT. These results were consistent with the previous findings that the increased abundance of *Bacteroides* could reduce the levels of TG, TC, and LDL-C and increase the level of HDL-C in HFD-fed mice (Peng et al., 2023). In addition, our results showed that *Bacteroides* levels also exhibited a positive correlation with 6-keto-PGF1α and AA and a negative correlation with LTD_4, 8-iso-$PGF_{2\alpha}$, $PGF_{2\alpha}$, and 15S-HETE, suggesting that an increase in *Bacteroides* abundance may be linked to the metabolic process of AA.

TXB_2 is a metabolite of thromboxane A_2 (TXA_2). In lipid metabolism, elevated levels of TXA_2/TXB_2 are frequently associated with dyslipidemia and atherosclerosis (DeFilippis et al., 2014; Petrucci et al., 2024). Prostaglandins (PGs) like $PGF_{2\alpha}$ and 8-iso-$PGF_{2\alpha}$ are involved in the inflammatory process, which could disrupt normal lipid-handling mechanisms (Wentzel and Eriksson, 2002; Wang et al., 2021). Leukotrienes, like LTD_4, are also inflammatory mediators. They could exacerbate inflammation in adipose tissue and the liver, potentially interfering with normal lipid metabolism pathways (Ma et al., 2024). Some studies have reported that *Alox15* deficiency, which lowers plasma 15-HETE levels, protects against steatohepatitis, hyperlipidemia, and alcoholic liver disease by reducing reactive oxygen species production, hepatic steatosis, insulin resistance, and inflammatory injury (Yang et al., 2024). 6-keto-$PGF_{1\alpha}$ is a stable metabolite of prostaglandin I_2 (PGI_2) (Griffith et al., 2022). PGI_2 is widely recognized for its vasodilatory and anti-platelet aggregation properties (Rogula et al., 2020). In Cav-1 knockout endothelial cells (Cav-1 KO EC), there is autocrine production of PGI_2. This increase in PGI_2 stimulates the cAMP/PKA pathway, thereby contributing to enhanced lipolysis in Cav-1 KO ECs (Kuo et al., 2017). AA, a crucial omega-6 fatty acid, is a precursor to a suite of PGs and LTB_4. As potent inflammatory mediators, AA plays an important role in inflammation, lipid metabolism, and the regulation of energy balance (Pereira et al., 2024). Our previous research demonstrated that AA levels tend to decrease with the administration of high-fat diets in broilers (Meng et al., 2021). Dietary supplementation with omega-6 polyunsaturated fatty acids, including AA, was shown to favorably affect plasma LDL-C and HDL-C, the AA metabolome, as an important regulator of cholesterol homeostasis (Demetz et al., 2014). AA is activated by the cyclooxygenase (COX) pathway to produce PGG_2, PGH_2, TXB_2, and PGE_2. PGH_2 generates PGF2α and PGI_2 under the catalysis of different enzymes (Xu et al., 2021; Xie et al., 2024). Our study showed that *Bacteroides* could affect the AA metabolism through COX pathways.

In metabolic syndrome, which includes a series of diseases such as obesity, hypertension, and dyslipidemia, the Firmicutes/Bacteroidetes ratio plays an important role in the occurrence and progression of these diseases (Stojanov et al., 2020). A higher ratio of

Firmicutes/Bacteroidota disrupted energy homeostasis, increased lipid synthesis, caused chronic low-grade inflammation, and led to obesity (Ridlon et al., 2006; Zhang et al., 2009; Yun et al., 2017; Cuevas-Sierra et al., 2019). In our experiments, the ratio of Firmicutes/Bacteroidota was significantly increased in the MOD group and reduced after *B. uniformis* treatment. Spirochaeta is known to induce gastrointestinal inflammation (He et al., 2023). Taurine could significantly ameliorate LPS-induced intestinal injury through a decrease in Spirochaetota in the colon (Zhao et al., 2023). In our study, the relative abundance of Spirochaetota in the MOD group was significantly increased and decreased after *B. uniformis* treatment.

Helicobacter was a genus consisting of many pathogenic bacteria associated with gastric inflammation and inflammatory bowel disease (Shibata et al., 2017; Schroeder et al., 2018). A lower relative abundance of *Helicobacter* was considered beneficial for ameliorating metabolic endotoxemia in obese mice (Luo et al., 2022). *Treponema* is a spirochetal bacterium that can colonize a wide range of hosts and tissues, causing different clinical symptoms (Dias et al., 2024). In our study, the supplementation of *B. uniformis* led to a concurrent decrease in the relative abundance of *Treponema and Helicobacter*. Therefore, we speculated that *Treponema* and *Helicobacter* could affect the AA metabolism through the LOX and COX pathways.

In microbial intervention studies, high-dose probiotics are not always more effective than low-dose probiotics, which may be related to multiple factors. The interaction between intestinal microbes and the host immune system is complex. Moderate microbial stimulation helps maintain immune homeostasis, whereas excessive stimulation may cause immune disorders and affect the disease-modifying effects of probiotics (Round and Mazmanian, 2009). In the present study, the high-dose *B. uniformis* (BUH group) induced immune overactivation and interfered with the regulation of liver index and lipid parameters, resulting in less effective treatment. The stability and balance of a microbial community are crucial for its functions. A massive influx of foreign microorganisms may disrupt the original balance (Costello et al., 2009). In the BUH group, the excessively high doses of *B. uniformis* may compete with other microorganisms in the gut for nutrients or living space. Moreover, the metabolic products it produces may also inhibit its growth by itself or other beneficial bacteria, thereby affecting the overall regulatory effect on liver index and blood lipid parameters.

In this study, we found significant correlations among *Bacteroides*, *Treponema*, *Helicobacter*, serum lipids, and AA metabolites. Regarding the limitations of correlation analysis, it is indeed impossible to clearly infer causal relationships solely through Spearman correlation analysis. Fecal microbiota transplantation is a very promising research method. By transplanting a specific microbiota from one individual to another, it is possible to more directly observe the impact of microbiota changes on aspects such as host metabolism and disease development, thus helping to determine the causal relationship between the microbiota and host health (Almeida et al., 2022). We plan to actively adopt this method in subsequent research to deeply explore the potential mechanisms by which *B. uniformis* improves FLHS, make up for the shortcomings of this study in inferring causal relationships, and provide a more in-depth and comprehensive theoretical basis for research in this field.

5 Conclusion

Collectively, the HELP diet resulted in a lower egg production rate and feed conversion ratio and accelerated FLHS formation and development in laying hens. Supplementation of *B. uniformis* significantly increased egg production rate and feed conversion ratio and relieved FLHS with the decline of TG, TC, LDL-C, AST, ALT, and the increase of HDL-C in the liver. Importantly, *B. uniformis* reshaped gut microbiota structure and AA metabolism caused by the HELP diet. In summary, *B. uniformis* mitigated FLHS in laying hens through regulating liver function, gut microbiota, and AA metabolism. Therefore, supplementation of *B. uniformis* could be an effective way to reduce FLHS in laying hens.

Data availability statement

The data presented in the study are deposited in the National Center for Biotechnology Information (NCBI) BioProject database repository, accession number PRJNA1247204.

Ethics statement

The animal study was approved by the Institutional Animal Care and Use Committee of Hebei Agricultural University. The study was conducted in accordance with the local legislation and institutional requirements.

Author contributions

YuZ: Data curation, Formal analysis, Writing – original draft, Writing – review & editing. RM: Investigation, Validation, Writing – review & editing. XD: Data curation, Formal analysis, Writing – review & editing. XH: Project administration, Supervision, Writing – review & editing. YaZ: Data curation, Methodology, Writing – review & editing. NM: Methodology, Writing – review & editing. HL: Conceptualization, Funding acquisition, Writing – review & editing. XZ: Conceptualization, Funding acquisition, Project administration, Supervision, Writing – review & editing.

Funding

The author(s) declare that financial support was received for the research and/or publication of this article. This work was supported by Special Project of Technological Innovation of Hainan Provincial Research Institute (No. SQKY2022-0006) and Central Guidance for Local Projects of Hebei (No. 246Z6603G).

Acknowledgments

The authors thank the Beijing Novogene Co., Ltd.

Conflict of interest

XD was employed by Hebei Jinkun Animal Pharmaceutical Co. Ltd.

The remaining authors declare that the research was conducted in the absence of any commercial or financial relationships that could be construed as a potential conflict of interest.

Generative AI statement

The author(s) declare that no Gen AI was used in the creation of this manuscript.

Publisher's note

All claims expressed in this article are solely those of the authors and do not necessarily represent those of their affiliated organizations, or those of the publisher, the editors and the reviewers. Any product that may be evaluated in this article, or claim that may be made by its manufacturer, is not guaranteed or endorsed by the publisher.

Supplementary material

The Supplementary material for this article can be found online at: https://www.frontiersin.org/articles/10.3389/fmicb.2025.1560887/full#supplementary-material

References

Al-Khalaifah, H. S., Ibrahim, D., Kamel, A. E.-S., Al-Nasser, A., Abdelwarith, A. A., Roushdy, E. M., et al. (2024). Enhancing impact of dietary nano formulated quercetin on laying performance: egg quality, oxidative stability of stored eggs, intestinal immune and antioxidants related genes expression. *BMC Vet. Res.* 20:494. doi: 10.1186/s12917-024-04327-x

Almeida, C., Oliveira, R., Baylina, P., Fernandes, R., Teixeira, F. G., and Barata, P. (2022). Current trends and challenges of fecal microbiota transplantation-an easy method that works for all? *Biomedicines* 10:2742. doi: 10.3390/biomedicines10112742

Anene, D. O., Akter, Y., Groves, P. J., Horadagoda, N., Liu, S. Y., Moss, A., et al. (2023). Association of feed efficiency with organ characteristics and fatty liver haemorrhagic syndrome in laying hens. *Sci. Rep.* 13:5872. doi: 10.1038/s41598-023-30007-1

Cheng, X., Hu, Y., Kuang, J., Guo, X., Cao, H., Wu, H., et al. (2024). Berberine alleviates high-energy and low-protein diet-induced fatty liver hemorrhagic syndrome in laying hens: insights from microbiome and metabolomics. *Poult. Sci.* 103:103968. doi: 10.1016/j.psj.2024.103968

Costello, E. K., Lauber, C. L., Hamady, M., Fierer, N., Gordon, J. I., and Knight, R. (2009). Bacterial community variation in human body habitats across space and time. *Science* 326, 1694–1697. doi: 10.1126/science.1177486

Cuevas-Sierra, A., Ramos-Lopez, O., Riezu-Boj, J. I., Milagro, F. I., and Martinez, J. A. (2019). Diet, gut microbiota, and obesity: links with host genetics and epigenetics and potential applications. *Adv. Nutr.* 10, S17–S30. doi: 10.1093/advances/nmy078

Dansou, D. M., Chen, H., Yu, Y., Yang, Y., Tchana, I. N., Zhao, L., et al. (2024). Enrichment efficiency of lutein in eggs and its function in improving fatty liver hemorrhagic syndrome in aged laying hens. *Poult. Sci.* 103:103286. doi: 10.1016/j.psj.2023.103286

DeFilippis, A. P., Rai, S. N., Cambon, A., Miles, R. J., Jaffe, A. S., Moser, A. B., et al. (2014). Fatty acids and TxA(2) generation, in the absence of platelet-COX-1 activity. *Nutr. Metab. Cardiovasc. Dis.* 24, 428–433. doi: 10.1016/j.numecd.2013.08.012

Demetz, E., Schroll, A., Auer, K., Heim, C., Patsch, J. R., Eller, P., et al. (2014). The arachidonic acid metabolome serves as a conserved regulator of cholesterol metabolism. *Cell Metab.* 20, 787–798. doi: 10.1016/j.cmet.2014.09.004

Dias, A. P., Aguilar, X. F., Buck, J. D., Kutz, S., and Arrazuria, R. (2024). Digital dermatitis-associated Treponema species detection and quantification in migratory tundra caribou (*Rangifer tarandus*). *Res. Vet. Sci.* 171:105210. doi: 10.1016/j.rvsc.2024.105210

Fabersani, E., Portune, K., Campillo, I., López-Almela, I., la Paz, S. M., Romaní-Pérez, M., et al. (2021). *Bacteroides uniformis* CECT 7771 alleviates inflammation within the gut-adipose tissue axis involving TLR5 signaling in obese mice. *Sci. Rep.* 11:11788. doi: 10.1038/s41598-021-90888-y

Gao, G., Xie, Z., Li, E., Yuan, Y., Fu, Y., Wang, P., et al. (2021). Dehydroabietic acid improves nonalcoholic fatty liver disease through activating the Keap1/Nrf2-ARE signaling pathway to reduce ferroptosis. *J. Nat. Med.* 75, 540–552. doi: 10.1007/s11418-021-01491-4

Gómez del Pulgar, E. M., Benítez-Páez, A., and Sanz, Y. (2020). Safety assessment of *Bacteroides Uniformis* CECT 7771, a symbiont of the gut microbiota in infants. *Nutrients* 12:551. doi: 10.3390/nu12020551

Griffith, J. A., Garner, K. L., Bowdridge, E. C., DeVallance, E., Schafner, K. J., Engles, K. J., et al. (2022). Nanomaterial inhalation during pregnancy alters systemic vascular function in a cyclooxygenase-dependent manner. *Toxicol. Sci.* 188, 219–233. doi: 10.1093/toxsci/kfac055

He, Y., Jiang, H., Du, K., Wang, S., Li, M., Ma, C., et al. (2023). Exploring the mechanism of Taohong Siwu decoction on the treatment of blood deficiency and blood stasis syndrome by gut microbiota combined with metabolomics. *Chin. Med.* 18:44. doi: 10.1186/s13020-023-00734-8

Kuo, A., Lee, M. Y., Yang, K., Gross, R. W., and Sessa, W. C. (2017). Caveolin-1 regulates lipid droplet metabolism in endothelial cells via autocrine prostacyclin-stimulated, cAMP-mediated lipolysis. *J. Biol. Chem.* 293, 973–983. doi: 10.1074/jbc.ra117.000980

Lee, H.-B., Do, M.-H., Jhun, H., Ha, S.-K., Song, H.-S., Roh, S.-W., et al. (2021). Amelioration of hepatic steatosis in mice through *Bacteroides uniformis* CBA7346-mediated regulation of high-fat diet-induced insulin resistance and lipogenesis. *Nutrients* 13:2989. doi: 10.3390/nu13092989

Li, D., Cai, H., Liu, G., Han, Y., Qiu, K., Liu, W., et al. (2024). Lactiplantibacillus plantarum FRT4 attenuates high-energy low-protein diet-induced fatty liver hemorrhage syndrome in laying hens through regulating gut-liver axis. *J. Anim. Sci. Biotechnol.* 15:31. doi: 10.1186/s40104-023-00982-6

Li, H., Wang, S., Wang, S., Yu, H., Yu, W., Ma, X., et al. (2022). Atorvastatin Inhibits High-Fat Diet-Induced Lipid Metabolism Disorders in Rats by Inhibiting Bacteroides Reduction and Improving Metabolism. *Drug Design, Development and Therapy* 16, 3805–3816. doi: 10.2147/dddt.s379335

Li, M., Wang, Q., Li, Y., Cao, S., Zhang, Y., Wang, Z., et al. (2020). Apical sodium-dependent bile acid transporter, drug target for bile acid related diseases and delivery target for prodrugs: current and future challenges. *Pharmacol. Ther.* 212:107539. doi: 10.1016/j.pharmthera.2020.107539

Liu, X., Pan, Y., Shen, Y., Liu, H., Zhao, X., Li, J., et al. (2022). Protective effects of Abrus cantoniensis Hance on the fatty liver hemorrhagic syndrome in laying hens based on liver metabolomics and gut microbiota. *Front. Vet. Sci.* 9:862006. doi: 10.3389/fvets.2022.862006

López-Almela, I., Romaní-Pérez, M., Bullich-Vilarrubias, C., Gómez, E. M., Francés, R., Benítez-Páez, A., et al. (2021). *Bacteroides uniformis* combined with fiber amplifies metabolic and immune benefits in obese mice. *Gut Microbes* 13, 1–20. doi: 10.1080/19490976.2020.1865706

Luo, S., He, L., Zhang, H., Li, Z., Liu, C., and Chen, T. (2022). Arabinoxylan from rice bran protects mice against high-fat diet-induced obesity and metabolic inflammation by modulating gut microbiota and short-chain fatty acids. *Food Funct.* 13, 7707–7719. doi: 10.1039/D2FO00569G

Ma, S., He, S., Liu, J., Zhuang, W., Li, H., Lin, C., et al. (2024). Metabolomics unveils the exacerbating role of arachidonic acid metabolism in atherosclerosis. *Front. Mol. Biosci.* 11:1297437. doi: 10.3389/fmolb.2024.1297437

Meng, J., Ma, N., Liu, H., Liu, J., Liu, J., Wang, J., et al. (2021). Untargeted and targeted metabolomics profiling reveals the underlying pathogenesis and abnormal arachidonic acid metabolism in laying hens with fatty liver hemorrhagic syndrome. *Poult. Sci.* 100:101320. doi: 10.1016/j.psj.2021.101320

Miao, S., Mu, T., Li, R., Li, Y., Zhao, W., Li, J., et al. (2024). Coated sodium butyrate ameliorates high-energy and low-protein diet induced hepatic dysfunction via modulating mitochondrial dynamics, autophagy and apoptosis in laying hens. *J. Anim. Sci. Biotechnol.* 15:15. doi: 10.1186/s40104-023-00980-8

Peng, W., He, C.-X., Li, R.-L., Qian, D., Wang, L.-Y., Chen, W.-W., et al. (2023). Zanthoxylum bungeanum amides ameliorates nonalcoholic fatty liver via regulating gut microbiota and activating AMPK/Nrf2 signaling. *J. Ethnopharmacol.* 318:116848. doi: 10.1016/j.jep.2023.116848

Pereira, M., Liang, J., Edwards-Hicks, J., Meadows, A. M., Hinz, C., Liggi, S., et al. (2024). Arachidonic acid inhibition of the NLRP3 inflammasome is a mechanism to explain the anti-inflammatory effects of fasting. *Cell Rep.* 43:113700. doi: 10.1016/j.celrep.2024.113700

Petrucci, G., Buck, G. A., Rocca, B., Parish, S., Baigent, C., Hatem, D., et al. (2024). Thromboxane biosynthesis and future events in diabetes: the ASCEND trial. *Eur. Heart J.* 45, 1355–1367. doi: 10.1093/eurheartj/ehad868

Qiao, S., Bao, L., Wang, K., Sun, S., Liao, M., Liu, C., et al. (2020). Activation of a specific gut Bacteroides-folate-liver Axis benefits for the alleviation of nonalcoholic hepatic steatosis. *Cell Rep.* 32:108005. doi: 10.1016/j.celrep.2020.108005

Ridlon, J. M., Kang, D.-J., and Hylemon, P. B. (2006). Bile salt biotransformations by human intestinal bacteria. *J. Lipid Res.* 47, 241–259. doi: 10.1194/jlr.R500013-JLR200

Rogula, S. P., Mutwil, H. M., Gąsecka, A., Kurzyna, M., and Filipiak, K. J. (2020). Antiplatelet effects of prostacyclin analogues: which one to choose in case of thrombosis or bleeding? *Cardiol. J.* 28, 954–961. doi: 10.5603/cj.a2020.0164

Round, J. L., and Mazmanian, S. K. (2009). The gut microbiota shapes intestinal immune responses during health and disease. *Nat. Rev. Immunol.* 9, 313–323. doi: 10.1038/nri2515

Schroeder, B. O., Birchenough, G. M. H., Ståhlman, M., Arike, L., Johansson, M. E. V., Hansson, G. C., et al. (2018). Bifidobacteria or Fiber protects against diet-induced microbiota-mediated colonic mucus deterioration. *Cell Host Microbe* 23, 27–40.e7. doi: 10.1016/j.chom.2017.11.004

Shibata, W., Sue, S., Tsumura, S., Ishii, Y., Sato, T., Kameta, E., et al. (2017). Helicobacter-induced gastric inflammation alters the properties of gastric tissue stem/progenitor cells. *BMC Gastroenterol.* 17:145. doi: 10.1186/s12876-017-0706-6

Shini, A., Shini, S., and Bryden, W. L. (2018). Fatty liver haemorrhagic syndrome occurrence in laying hens: impact of production system. *Avian Pathol.* 48, 25–34. doi: 10.1080/03079457.2018.1538550

Stojanov, S., Berlec, A., and Štrukelj, B. (2020). The influence of probiotics on the Firmicutes/Bacteroidetes ratio in the treatment of obesity and inflammatory bowel disease. *Microorganisms* 8:1715. doi: 10.3390/microorganisms8111715

Taofeek, N. O., Chimbetete, N., Ceron-Romero, N., Vizcarra, F., Verghese, M., and Vizcarra, J. A. (2022). Systemic infusion of exogenous ghrelin in male broiler chickens (Gallus domesticus). The effect of pulse frequency, doses, and ghrelin forms on feed intake, average daily gain, corticosterone, and growth hormone concentrations. *Poult. Sci.* 101:101945. doi: 10.1016/j.psj.2022.101945

Wang, Y., Ai, Z., Xing, X., Fan, Y., Zhang, Y., Nan, B., et al. (2022). The ameliorative effect of probiotics on diet-induced lipid metabolism disorders: a review. *Crit. Rev. Food Sci. Nutr.* 64, 3556–3572. doi: 10.1080/10408398.2022.2132377

Wang, B., Wu, L., Chen, J., Dong, L., Chen, C., Wen, Z., et al. (2021). Metabolism pathways of arachidonic acids: mechanisms and potential therapeutic targets. *Signal Transduct. Target. Ther.* 6:94. doi: 10.1038/s41392-020-00443-w

Wentzel, P., and Eriksson, U. J. (2002). 8-Iso-PGF(2alpha) administration generates dysmorphogenesis and increased lipid peroxidation in rat embryos in vitro. *Teratology* 66, 164–168. doi: 10.1002/tera.10068

Xie, Y., Xu, H., and Gu, Z. (2024). *Ge-gen* decoction alleviates primary dysmenorrhoea symptoms in a rat model. *J. Obstet. Gynaecol.* 44:2337691. doi: 10.1080/01443615.2024.2337691

Xiong, S., Zhang, K., Wang, J., Bai, S., Zeng, Q., Liu, Y., et al. (2024). Effects of xylo-oligosaccharide supplementation on the production performance, intestinal morphology, cecal short-chain fatty acid levels, and gut microbiota of laying hens. *Poult. Sci.* 103:104371. doi: 10.1016/j.psj.2024.104371

Xu, X., Huang, H., Tu, Y., Sun, J., Xiong, Y., Ma, C., et al. (2021). Celecoxib alleviates radiation-induced brain injury in rats by maintaining the integrity of blood-brain barrier. *Dose-Response* 19:155932582110243. doi: 10.1177/15593258211024393

Yadav, K. K., Boley, P. A., Khatiwada, S., Lee, C. M., Bhandari, M., and Kenney, S. P. (2024). Development of fatty liver disease model using high cholesterol and low choline diet in white leghorn chickens. *Vet. Res. Commun.* 48, 2489–2497. doi: 10.1007/s11259-024-10420-1

Yan, H., Qin, Q., Chen, J.-F., Yan, S., Li, T., Gao, X., et al. (2022). Gut microbiome alterations in patients with visceral obesity based on quantitative computed tomography. *Front. Cell. Infect. Microbiol.* 11:823262. doi: 10.3389/fcimb.2021.823262

Yang, X., Chen, H., Shen, W., Chen, Y., Lin, Z., Zhuo, J., et al. (2024). FGF21 modulates immunometabolic homeostasis via the ALOX15/15-HETE axis in early liver graft injury. *Nat. Commun.* 15:8578. doi: 10.1038/s41467-024-52379-2

Yang, X., Li, D., Zhang, M., Feng, Y., Jin, X., Liu, D., et al. (2023). *Ginkgo biloba* extract alleviates fatty liver hemorrhagic syndrome in laying hens via reshaping gut microbiota. *J. Anim. Sci. Biotechnol.* 14:97. doi: 10.1186/s40104-023-00900-w

Yaqoob, M. U., Qi, Y., Hou, J., Zhe, L., Zhu, X., Wu, P., et al. (2024). Coated cysteamine and choline chloride could be potential feed additives to mitigate the harmful effects of fatty liver hemorrhagic syndrome in laying hens caused by high-energy low-protein diet. *Poult. Sci.* 103:104296. doi: 10.1016/j.psj.2024.104296

Yun, Y., Kim, H.-N., Kim, S. E., Heo, S. G., Chang, Y., Ryu, S., et al. (2017). Comparative analysis of gut microbiota associated with body mass index in a large Korean cohort. *BMC Microbiol.* 17:151. doi: 10.1186/s12866-017-1052-0

Zhang, H., DiBaise, J. K., Zuccolo, A., Kudrna, D., Braidotti, M., Yu, Y., et al. (2009). Human gut microbiota in obesity and after gastric bypass. *Proc. Natl. Acad. Sci. USA* 106, 2365–2370. doi: 10.1073/pnas.0812600106

Zhang, S., Sun, P., Guo, H., Zhang, X., You, M., He, X., et al. (2024a). Alterations of meat quality, lipid composition and flavor in breast meat of laying hens with fatty liver hemorrhagic syndrome. *Poult. Sci.* 103:104360. doi: 10.1016/j.psj.2024.104360

Zhang, S., You, M., Shen, Y., Zhao, X., He, X., Liu, J., et al. (2024b). Improving fatty liver hemorrhagic syndrome in laying hens through gut microbiota and oxylipin metabolism by *Bacteroides fragilis*: a potential involvement of arachidonic acid. *Anim. Nutr.* 20, 182–199. doi: 10.1016/j.aninu.2024.08.008

Zhao, D., Gai, Y., Li, C., Fu, Z., Yin, D.-Q., Xie, M., et al. (2023). Dietary taurine effect on intestinal barrier function, colonic microbiota and metabolites in weanling piglets induced by LPS. *Front. Microbiol.* 14:1259133. doi: 10.3389/fmicb.2023.1259133

Zhao, L., Liu, S., Zhang, Z., Zhang, J., Jin, X., Zhang, J., et al. (2020). Low and high concentrations of butyrate regulate fat accumulation in chicken adipocytes via different mechanisms. *Adipocytes* 9, 120–131. doi: 10.1080/21623945.2020.1738791

frontiers | Frontiers in Microbiology

TYPE Original Research
PUBLISHED 07 May 2025
DOI 10.3389/fmicb.2025.1569592

Check for updates

OPEN ACCESS

EDITED BY
Benoit St-Pierre,
South Dakota State University, United States

REVIEWED BY
Hong Mingsheng,
China West Normal University, China
Sunil Banskar,
University of Arizona, United States

*CORRESPONDENCE
Xianfeng Yi
✉ ympclong@163.com

RECEIVED 01 February 2025
ACCEPTED 18 April 2025
PUBLISHED 07 May 2025

CITATION
Cha M, Wu Y, Man D and Yi X (2025) Associations between gut microbiota and diet composition of three arid-adapted rodent species from the Inner Mongolia grassland. *Front. Microbiol.* 16:1569592. doi: 10.3389/fmicb.2025.1569592

COPYRIGHT
© 2025 Cha, Wu, Man and Yi. This is an open-access article distributed under the terms of the Creative Commons Attribution License (CC BY). The use, distribution or reproduction in other forums is permitted, provided the original author(s) and the copyright owner(s) are credited and that the original publication in this journal is cited, in accordance with accepted academic practice. No use, distribution or reproduction is permitted which does not comply with these terms.

Associations between gut microbiota and diet composition of three arid-adapted rodent species from the Inner Mongolia grassland

Muha Cha[1,2], Yunga Wu[3], Duhu Man[4] and Xianfeng Yi[1]*

[1]College of Life Sciences, Qufu Normal University, Qufu, China, [2]Academy of Agricultural Sciences, Chifeng University, Chifeng, China, [3]Alxa Left Banner Grassland Workstation, Bayanhot, China, [4]College of Agriculture, Hulunbuir University, Hailar, China

Food habits are closely associated with the gut microbiota of herbivorous animals; however, limited knowledge exists regarding the arid-adapted rodents. This study investigates the relationship between gut microbiota and dietary composition to offer a scientific basis for comprehending the ecological adaptation strategies of grassland rodents. Cecal contents of *Spermophilus alashanicus*, *S. dauricus*, and *Meriones unguiculatus* were collected and analyzed by using 16S rRNA amplicon sequencing and DNA metabarcoding techniques to determine the structure of gut microbial communities and dietary composition. The results showed that *S. alashanicus* presented significantly higher gut microbial richness and diversity than *S. dauricus* and *M. unguiculatus*. The dominant gut bacterial genera in *S. alashanicus* and *S. dauricus* were similar, suggesting that their common genetic backgrounds might influence the colonization and symbiosis of gut microbiota. The three species consumed both plant-based and animal-based foods but differed in their dietary preferences. *S. dauricus* displayed a significantly higher diversity of animal-based food consumption compared with the other two species. Correlation analysis between diet and gut microbiota indicated that plant-based foods significantly enhanced the diversity and composition of gut microbiota. In contrast, the consumption of animal-based foods significantly decreased microbial diversity. This finding suggests a potential link between the host's genetic background, dietary composition, and the gut microbiota.

KEYWORDS

rodents, gut microbiota, diet, DNA metabarcoding technology, ecological adaptation strategies

1 Introduction

The intestinal microbiome exerts significant influence over the host's metabolic processes and nutrient uptake, fostering a symbiotic relationship that benefits both parties (Tang et al., 2023; Cao et al., 2024). Through intricate interactions, gut microorganisms dynamically regulate and stabilize their community structure, thereby sustaining a robust microbial environment (Weldon et al., 2015; Lu et al., 2024). In grassland ecosystems, rodents serve dual roles as consumers and secondary producers, acting as pivotal links across various trophic levels by serving as prey for predators higher up in the food chain (Zhao et al. 2024). Their feeding habits are influenced by multiple factors, such as genetic tendencies (Suzuki et al., 2019), the nutritional quality and taste of available vegetation (Petit Bon et al., 2020), environmental conditions (Hufeldt et al., 2010), and seasonal changes (Goldberg et al., 2020).

To cope with these diverse influences, rodents utilize genetic adaptations, physiological modifications, and behavioral tactics, which facilitate efficient and adaptable foraging behaviors (Brown and Kotler, 2004). These adaptive strategies not only maintain stable rodent populations within grassland ecosystems but also enable them to assume varied roles within complex ecological networks. By impacting food web dynamics, rodents significantly contribute to the stability and functionality of the ecosystem.

The structure and activities of gut microbiota are shaped by a multitude of factors, such as dietary habits, the host's environmental conditions, and genetic makeup (Beam et al., 2021; Zhang et al., 2023; Li et al., 2016; Park and Do, 2024). Dietary intake supplies crucial nutrients for gut microbiota and modifies their composition by altering the intestinal microenvironment, including pH levels and concentrations of metabolic products (Cabana et al., 2019; Maurer et al., 2024). The host's living conditions, like temperature, humidity, and altitude, indirectly impact gut microbiota by influencing the host's physiological status or affecting the availability of food resources (Ley et al., 2008). Additionally, genetic elements significantly influence the composition and functionality of gut microbiota. Variations in gut morphology, immune system performance, and gene expression among hosts can substantially affect the colonization potential of specific microbes and the stability of microbial communities (Weinstein et al., 2021). DNA metabarcoding technology, an emerging tool in molecular ecology, has greatly expanded the breadth and accuracy of dietary research (Kowalczyk et al., 2019; Ter Schure et al., 2021). Utilizing high-throughput sequencing to analyze DNA fragments found in gastrointestinal contents or fecal samples, this method facilitates the swift and precise identification of species present in food sources. DNA metabarcoding has seen extensive application in studying the diets of herbivores (Kowalczyk et al., 2019; Ter Schure et al., 2021), carnivores (Wang et al., 2014; Hacker et al., 2021), and omnivores (Xiong et al., 2016; Woo et al., 2022). A comprehensive review of 155 dietary studies published from 2009 to 2020 by Ando et al. (2020) indicated that mammals are the predominant subjects of this technology. This focus is largely attributed to the ease of collecting gut samples from mammals and their significant role as key consumers in ecosystems.

In recent years, studies on the dietary behaviors of rodents have predominantly centered around their food selection tendencies, ecological niche differentiation, coexistence mechanisms among species (Sato et al., 2018; Lopes et al., 2020; Chock et al., 2022), conservation efforts for endangered species (Iwanowicz et al., 2016; Buglione et al., 2018), and the impact of environmental pollutants on their eating patterns and feeding activities (Ozaki et al., 2018). This body of research has become a critical area in rodent ecology and has laid important theoretical groundwork for comprehending adaptive strategies across different environments. The grasslands of Inner Mongolia are home to several rodent species, including *Spermophilus dauricus*, *S. alashanicus*, and *Meriones unguiculatus*. These species are recognized as carriers of plague and play a role in the indirect spread of bacterial and viral pathogens. The *S. dauricus* and the *S. alaschanicus* are closely related species. In the past, the *S. alaschanicus* was classified as a subspecies of the *S. dauricus*, but chromosomal analysis has confirmed it as a distinct species, now listed separately. The *S. alaschanicus* is mainly distributed in the western region of Inner Mongolia, while the *S. dauricus* is primarily found in the central and eastern regions of Inner Mongolia. Both are hibernating species. *S. alaschanicus* feeds on salt-alkali-tolerant plants and underground roots in extremely arid environments, with a narrow but specialized ecological niche. The *S. dauricus* feeds on the roots, stems, leaves, grass seeds, and insects of herbaceous plants, with an increase in animal-based food intake during the breeding season. The *M. unguiculatus* is a representative dominant species of desert grassland rodents, distributed in dry grasslands and agricultural areas, particularly abundant in agro-pastoral zones. It is found in the eastern, western, and central regions of Inner Mongolia, it does not hibernate and breeds year-round. After the autumn harvest, its activity in the fields increases, where it gnaws on crops and stores grains in its burrows. It mainly feeds on drought-resistant Poaceae plants, plant seeds, and crops like sorghum and millet. In wild animal gut microbiome studies, diet and host genetics are core factors shaping the microbiota. This study analyzes the food sources of three rodent species in different habitats to elucidate how food composition drives microbiota functional differentiation. By comparing the microbiota compositions of closely related species, we explore the role of genetics in shaping core microbiota. In this study, we collected and analyzed cecal samples from these three rodent species to examine their gut microbial communities using 16S rRNA amplicon sequencing. Furthermore, their dietary habits were assessed through high-throughput sequencing and DNA metabarcoding techniques. The main goal of this study is to elucidate the connection between gut microbiota and feeding behaviors in these rodents, providing valuable insights into their ecological adaptation strategies and aiding in the prevention of zoonotic disease transmission from wildlife.

2 Materials and methods

2.1 Cecal sample collection

In July 2023, the cecal contents of adult *S. alashanicus* ($n = 8$) were collected in Alxa League, Inner Mongolia (Supplementary Table S1). Additionally, the cecal contents of *S. dauricus* ($n = 16$) were collected in Chifeng and Hulunbuir, Inner Mongolia, while those of *M. unguiculatus* ($n = 12$) were collected in Chifeng, Inner Mongolia (Figure 1). Dissections were performed at the collection site, the contents of the cecum were placed in a freezer container and immediately frozen in liquid nitrogen. Then they were transported to the laboratory and stored in a −80°C refrigerator. The samples were sent to Shanghai Meiji Biomedical Technology Co., Ltd. and were sequenced by high-throughput Illumina PE250 sequencing platform.

2.2 DNA extraction and sequencing

After genomic DNA extraction, the extracted DNA was analyzed using 1% agarose gel electrophoresis. For gut microbiota analysis, primers 338F (5′-ACTCCTACGGGAGGCAGCA-3′) and 806R (5′-GGACTACHVGGGTWTCTAAT-3′) were employed for the PCR amplification of the bacterial 16S rRNA gene V3-V4 region. For plant-based food analysis, primers UniPlantF (5′-TGTGAATTGCARRATYCMG-3′) and UniPlantR (5′-CCCG HYTGAYYTGRGGTCDC-3′) were used, while primers COIF (5′-mlCOlintFGGWACWGGWTGAACWGTWTAYCCYCC-3′) and COIR (5′-jgHCO2198RTANACYTCNGGRTGNCCRAARAA YCA-3′) were utilized for the analysis of animal-based food. To determine the optimal minimum number of PCR cycles, a subset of representative samples was randomly selected for preliminary experiments. This step ensured effective amplification for most samples, producing products at suitable concentrations. PCR

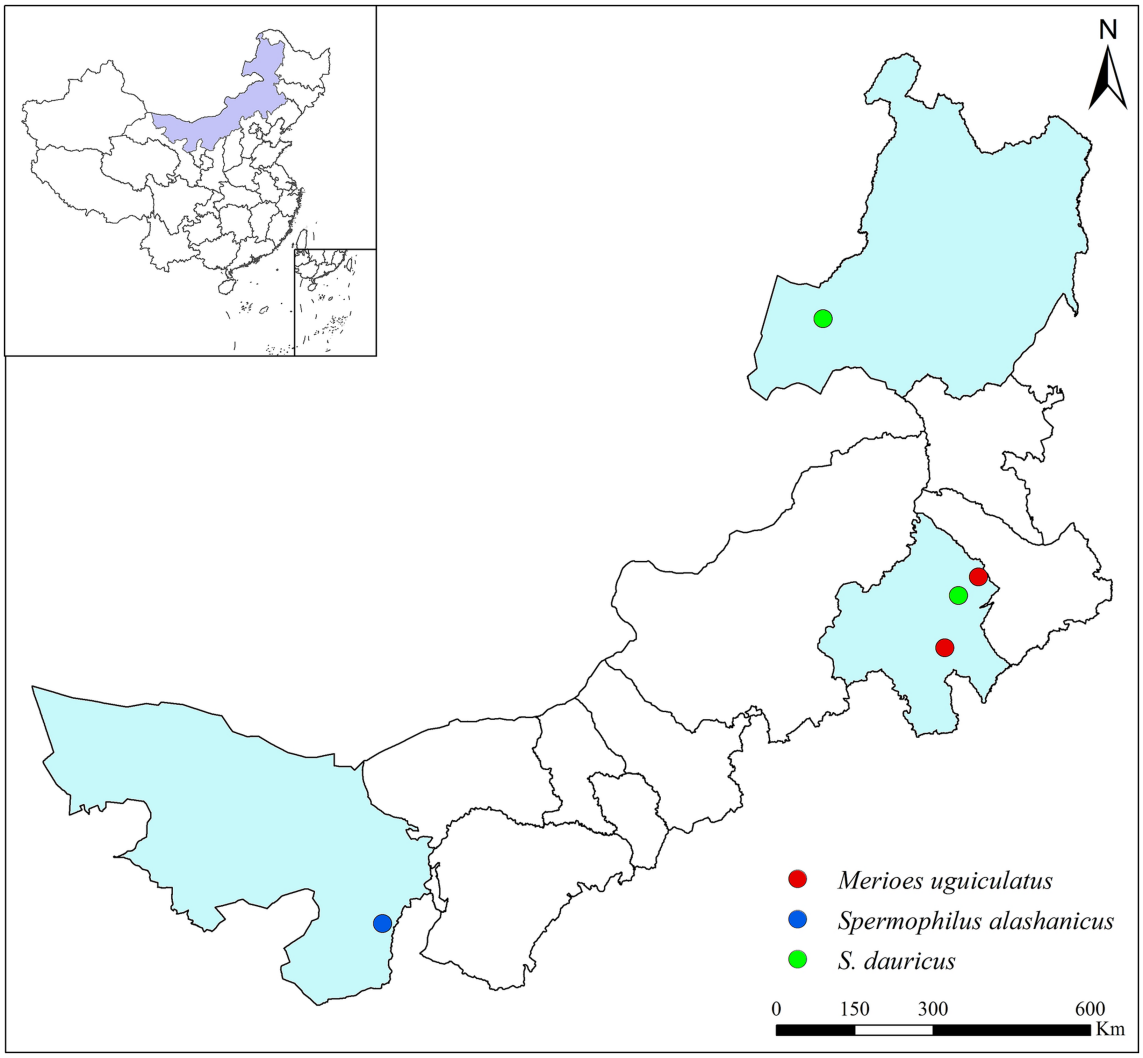

FIGURE 1
Geographical map of the specimen collection areas for the three rodent species.

reactions were performed using TransStart FastPfu DNA Polymerase (TransGen AP221-02) on an ABI GeneAmp® 9700 PCR system. Each sample was amplified in triplicate, and the PCR products from the same sample were pooled. The pooled products were analyzed via 2% agarose gel electrophoresis for quality assessment, recovered using the AxyPrep DNA Gel Extraction Kit (AXYGEN), and eluted with Tris–HCl buffer. For fluorescence quantification, PCR products were measured using the QuantiFluor™-ST blue fluorescence quantification system (Promega), guided by preliminary quantification results from gel electrophoresis. Products were then combined according to sequencing requirements. Illumina adapter sequences were added to the target regions through PCR, and the resulting products were recovered by gel extraction and eluted with Tris–HCl buffer. The final products were analyzed via 2% agarose gel electrophoresis. Single-stranded DNA fragments were generated through denaturation with sodium hydroxide. During Illumina sequencing, one end of the single-stranded DNA hybridized with a complementary primer sequence fixed on the chip. Using the single strand as a template, PCR synthesis was conducted on the chip based on the fixed primer sequences. DNA clusters were generated through bridge PCR, and sequences were read via stepwise fluorescent labeling, resulting in the complete sequence of the target DNA fragments.

2.3 Bioinformatics analysis process

The paired-end (PE) reads obtained from Illumina sequencing were first assembled based on overlap relationships, with sequence quality controlled and filtered. The 16S rRNA genomic fragments were generated from the paired-end reads using the QIIME software (version 1.9.1). Following sample differentiation, operational taxonomic unit (OTU) clustering and taxonomic classification were performed. The OTU clustering was performed using Uparse (version 11), with a similarity threshold of 97% for clustering. OTU-based analyses enabled the evaluation of various diversity indices and the assessment of sequencing depth. Additionally, statistical analyses of community structure were conducted across multiple taxonomic levels using the taxonomic information.

2.4 Statistical analysis

Statistical analyses and visualizations based on the relative abundance tables of genes, species, and functions were performed using R language tools. Data clustering and abundance analyses were conducted with the vegan package in R, and the results were visualized using heatmaps. The richness and diversity of gut microbial communities were assessed using the α diversity Shannon index and Chao index. The Kruskal-Wallis H test was performed to detect significant differences between the indices of each pair of groups, and box plots were created to illustrate the differences in diversity indices among different species. Principal Coordinate Analysis (PCoA) based on the unweighted UniFrac distance matrix was utilized to evaluate differences between groups at the species, gene, and functional levels, with PCoA plots generated for visualization. In addition, non-metric multidimensional scaling (NMDS) based on based on the unweighted UniFrac metrics was applied with Analysis of similarities (ANOSIM) to analyze the difference in microbial composition among subjects and test the significance of the difference. PERMANOVA analysis, conducted using QIIME software, decomposed total variance based on Bray-Curtis distances. The non-weighted Unifrac distance was calculated by QIIME to characterize the differences in microbial communities among the samples. A linear model was applied to assess the explanatory power of different grouping factors on sample variability, and permutation tests were used to determine statistical significance. The Kruskal-Wallis rank-sum test was employed to analyze abundance differences in species and functions among groups, while the Mann–Whitney U test was applied to evaluate significant diversity differences between two groups. Spearman correlation analysis was performed to investigate the relationship between dominant gut microbiota and dietary habits. All p-values from statistical tests were adjusted for multiple comparisons, with significance defined as ($p < 0.05$).

3 Results

3.1 Sequencing results

A total of 36 gut microbiota samples were analyzed, comprising 8 samples from *S. alashanicus*, 16 from *S. dauricus*, and 12 from *M. unguiculatus*. Sequences were grouped into operational taxonomic units (OTUs) at 97% sequence similarity, resulting in 2,992,093 sequences and a total of 1,232,190,167 bases, with an average sequence length of 411 bp. These sequences were then clustered into 8,590 OTUs, which were taxonomically annotated into 1 domain, 1 kingdom, 17 phyla, 37 classes, 95 orders, 164 families, 333 genera, and 646 species. As sequencing depth increased, rarefaction curves for all samples approached a plateau, indicating that the sequencing depth was sufficient to capture the microbial diversity. The analysis of unique and shared OTUs among the gut microbiota of the three rodent species (Figure 2A) identified 820 shared OTUs across all species. Additionally, 2,377 OTUs were shared between *S. alashanicus* and *S. dauricus*, 1,103 between *S. dauricus* and *M. unguiculatus*, and 911 between *S. alashanicus* and *M. unguiculatus*. The highest number of shared OTUs was observed between *S. dauricus* and *S. alashanicus*.

3.2 Comparison of α and β diversity in the gut microbiota of the three rodent species

The gut microbiota α-diversity among the three rodent species differed significantly (Figures 2B,C). The Kruskal-Wallis H test showed significant differences in the Chao and Shannon indices among the three species ($p < 0.05$). The Chao index of *S. alashanicus* and *S. dauricus* was significantly higher than that of *Meriones unguiculatus*, while pairwise comparisons of the Shannon index revealed no significant differences among the species. To further investigate the relationship between the host and gut microbial composition, the β-diversity of the gut microbiota in *S. alashanicus*, *S. dauricus*, and *M. unguiculatus* was analyzed using principal coordinate analysis (PCoA) (Figure 2D). The PCoA based on OTU levels showed that significant differences between the groups ($R = 0.7935$, $p = 0.001$). The NMDS based on OTU levels (Figure 2E) showed that the gut bacterial samples of *S. dauricus*, *S. alaschanicus* and *M. unguiculatus* exhibited intra-group clustering but inter-group separation (Stress = 0.129; $R = 0.7895$, $p = 0.001$).

3.3 Analysis of gut microbiota composition

The gut microbial community composition of *S. alashanicus*, *S. dauricus*, and *M. unguiculatus* was predominantly represented by five phyla with the highest average relative abundances: Bacillota (67.97%), Bacteroidota (16.68%), Desulfobacterota (4.79%), Actinobacteriota (4.28%), and Verrucomicrobiota (2.74%). A total of seven phyla had an average relative abundance exceeding 1%. At the genus level, the relatively abundant bacteria noted include Alistipes, Desulfovibrio, Lactobacillus. At the phylum level (Figure 3A), the dominant phyla in *S. alashanicus* were Bacillota (78.48%), Bacteroidetes (13.75%), Verrucomicrobiota (5.44%), and Actinobacteriota (1.31%). In *S. dauricus*, the primary dominant phyla were Bacillota (65.72%), Bacteroidetes (24.05%), Actinobacteriota (4.98%), and Verrucomicrobiota (1.92%). For *M. unguiculatus*, the dominant phyla included Bacillota (59.70%), Desulfobacterota (13.76%), Bacteroidota (12.22%), and Actinobacteriota (6.57%). Across all three species, Bacillota displayed the highest relative abundance, followed by Bacteroidota and Desulfobacterota. Notably, the top four dominant phyla in *S. alashanicus* and *S. dauricus* were the same, although their relative proportions differed.

At the genus level (Figure 3B), the dominant genus in *S. alashanicus* was *Alistipes* (8.61%), and in *S. dauricus*, the dominant genus was also *Alistipes* (7.47%), belonging to the phylum Bacteroidota. The primary dominant genera in *M. unguiculatus* were *Desulfovibrio* (13.63%) and *Lactobacillus* (10.29%). *Alistipes* was the shared dominant genus in both *S. alashanicus* and *S. dauricus*, while *Desulfovibrio* was the dominant genus in *M. unguiculatus*, differing from the dominant genera in the other two species.

3.4 The α and β diversity of plant-based and animal-based foods and the diet composition of three rodent species

The Kruskal-Wallis H test for the α-diversity of plant-based food among the three rodent species (Figures 4A,B) revealed no significant

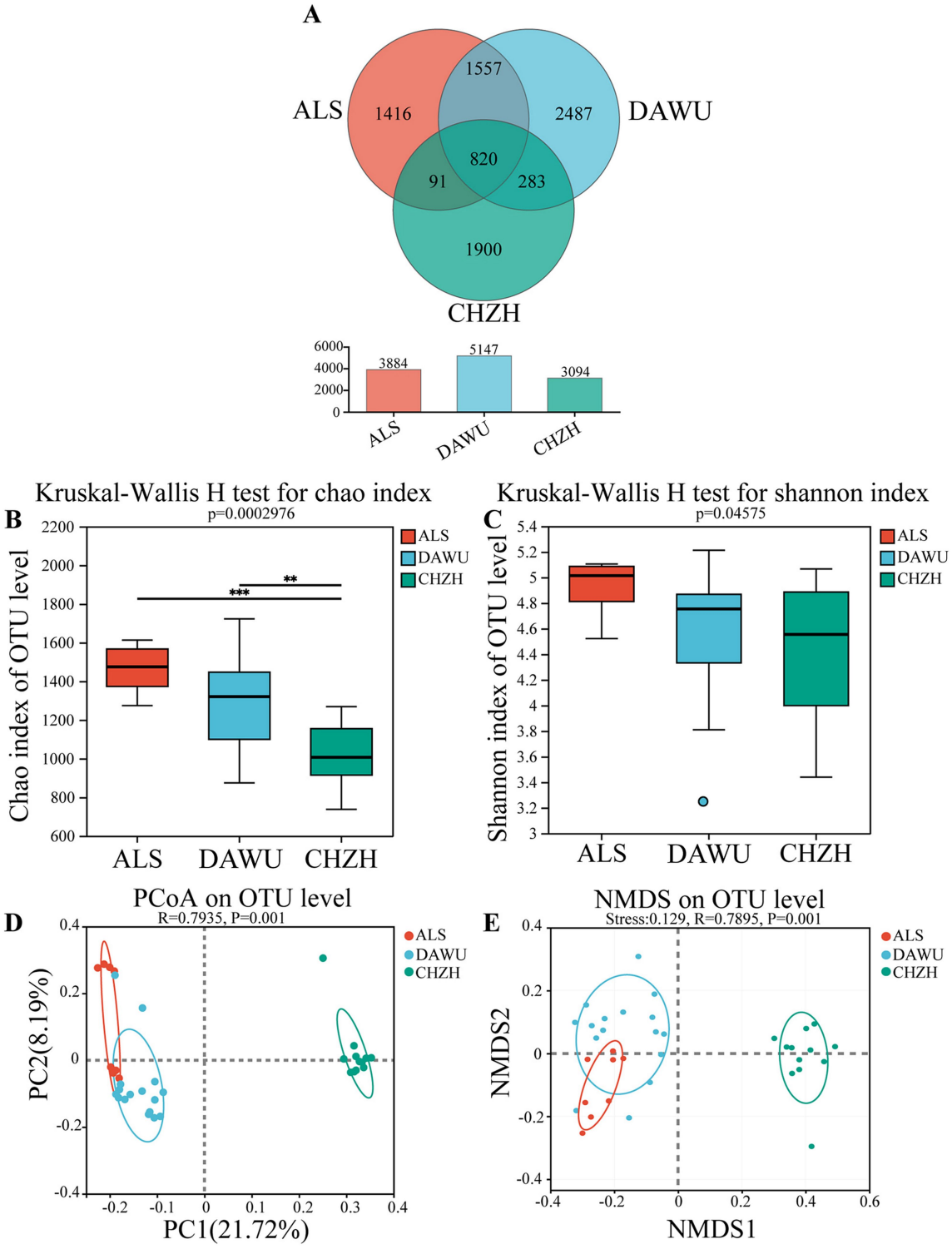

FIGURE 2
Gut microbiota diversity in the three rodent species (ALS, DAWU, and CHZH refer to *S. alashanicus*, *S. dauricus*, and *M. unguiculatus*, respectively). **(A)** Venn diagram shows shared OTUs between the gut microbiota. **(B,C)** Indicates α diversity. **(D,E)** Represent β diversity. **, and *** stand for statistically significant at $p < 0.01$, and 0.001, respectively.

differences in the Chao and Shannon indices ($p > 0.05$). The PCoA based on OTU levels (Figure 4C) showed that significant differences between the groups ($R = 0.3444$, $p = 0.001$). The NMDS based on OTU levels (Figure 4D) showed that the *S. dauricus*, *S. alaschanicus* and *M. unguiculatus* group samples exhibited intra-group clustering but inter-group separation (Stress = 0.181; $R = 0.3514$, $p = 0.001$).

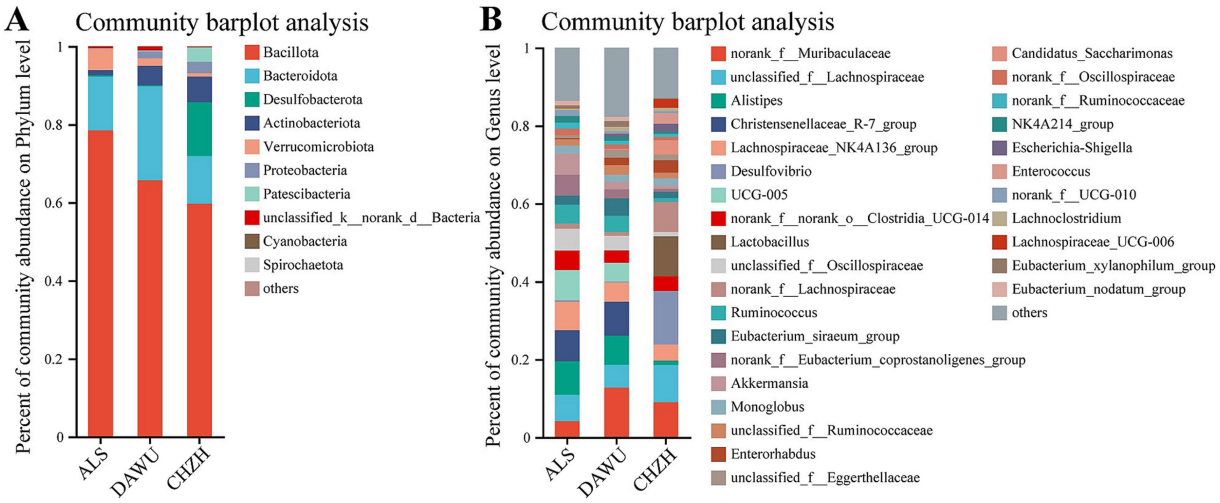

FIGURE 3
Composition of the gut microbiota at the phylum and genus level **(A,B)** (ALS, DAWU, and CHZH refer to *S. alashanicus*, *S. dauricus*, and *M. unguiculatus*, respectively).

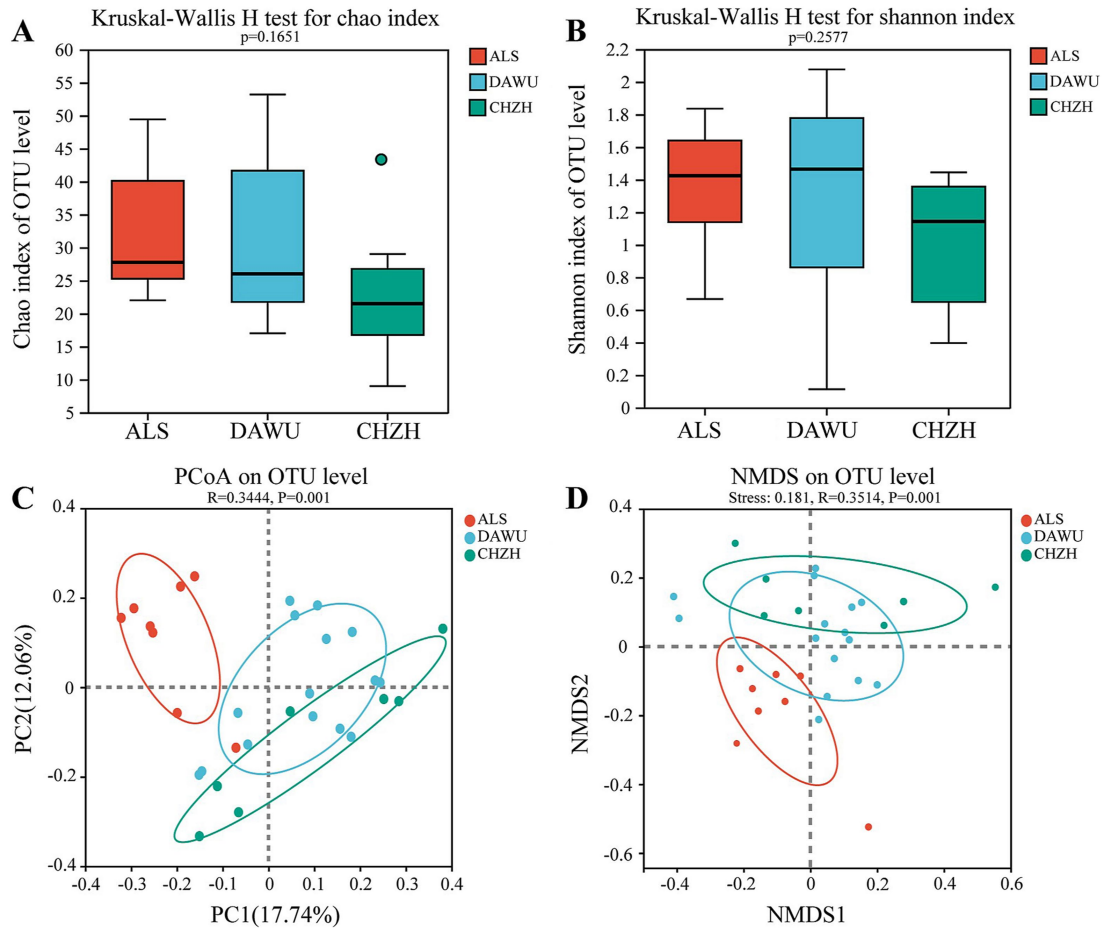

FIGURE 4
The α and β diversity index of plant-based diet composition in three rodent species (ALS, DAWU, and CHZH refer to *S. alashanicus*, *S. dauricus*, and *M. unguiculatus*, respectively). **(A,B)** Indicates α diversity. **(C,D)** Represent β diversity.

For the α-diversity of animal-based food, the Kruskal-Wallis H test (Figures 5A,B) revealed that the Chao index for *S. dauricus* was significantly higher than that for *S. alashanicus* and *M. unguiculatus* ($p < 0.05$), while the Shannon index for *M. unguiculatus* was significantly higher than that for *S. dauricus* and *S. alashanicus* ($p < 0.05$). The PCoA based on OTU levels (Figure 5C) showed that significant differences between the groups ($R = 0.3536$, $p = 0.001$). The NMDS based on OTU levels (Figure 5D) showed that the *S. dauricus*, *S. alaschanicus* and *M. unguiculatus* group samples exhibited intra-group clustering but inter-group separation (Stress = 0.002; $R = 0.1625$, $p = 0.001$).

The plant-based food of the three rodent species belonged to the phylum Streptophyta and the class Magnoliopsida. At the order and genus levels, 10 orders and 27 genera exhibited relative abundances greater than 1% (Figures 6A,B). At the order level, the most abundant taxa included Asterales, Poales, Fabales, and Solanales. Among these, the plant-based food of *S. alashanicus* was dominated by Solanales (33.52%), *S. dauricus* by Asterales (43.13%), and *M. unguiculatus* by Poales (39.03%). At the genus level, the most abundant taxa in *S. alashanicus* were *Convolvulus* (33.52%), *Neopallasia* (17.08%), and *Artemisia* (10.52%). In *S. dauricus*, the most abundant taxa were *Ixeris* (32.57%), unclassified_f__Amaranthaceae (9.52%), and *Panicum* (9.81%). In *M. unguiculatus*, the most abundant genera were *Chloris* (26.08%), *Neopallasia* (17.78%), and *Melilotus* (11.86%).

The animal-based food of *S. alashanicus*, *S. dauricus*, and *M. unguiculatus* was predominantly composed of invertebrates from the phylum Arthropoda (Figures 6C,D). The diet of *S. alashanicus* consisted entirely of arthropods (Arthropoda, 100%), while the diet of *S. dauricus* included Arthropoda (94.70%), unclassified_k__Metazoa (2.48%), and Cnidaria (1.69%). For *M. unguiculatus*, the animal-based food consisted of Arthropoda (77.27%) and Annelida (22.72%). At the order level, the animal-based food of all three species was dominated by Diptera, Lepidoptera, Coleoptera, Thysanoptera, Collembola, and Tubicola. At the genus level, the most abundant taxa in *S. alashanicus* were unclassified_f__Tachinidae (48.39%), *Chromatomyia* (19.35%), and *Kakothrips* (12.90%). In *S. dauricus*, the dominant genera were *Nephrotoma* (16.80%), unclassified_f__Bourletiellidae (14.09%), and *Agrotis* (13.42%). For *M. unguiculatus*, the most abundant taxa were *Mimeoma* (38.18%), *Dasybranchus* (22.72%), and *Protoschinia* (20.91%).

3.5 The association between diet and gut microbiota

The spearman correlation analysis of plant-based food composition and Bacillota and Bacteroidota (Figure 7A) revealed that *Convolvulus*, *Linum*, *Elymus*, and *Agropyron* were significantly

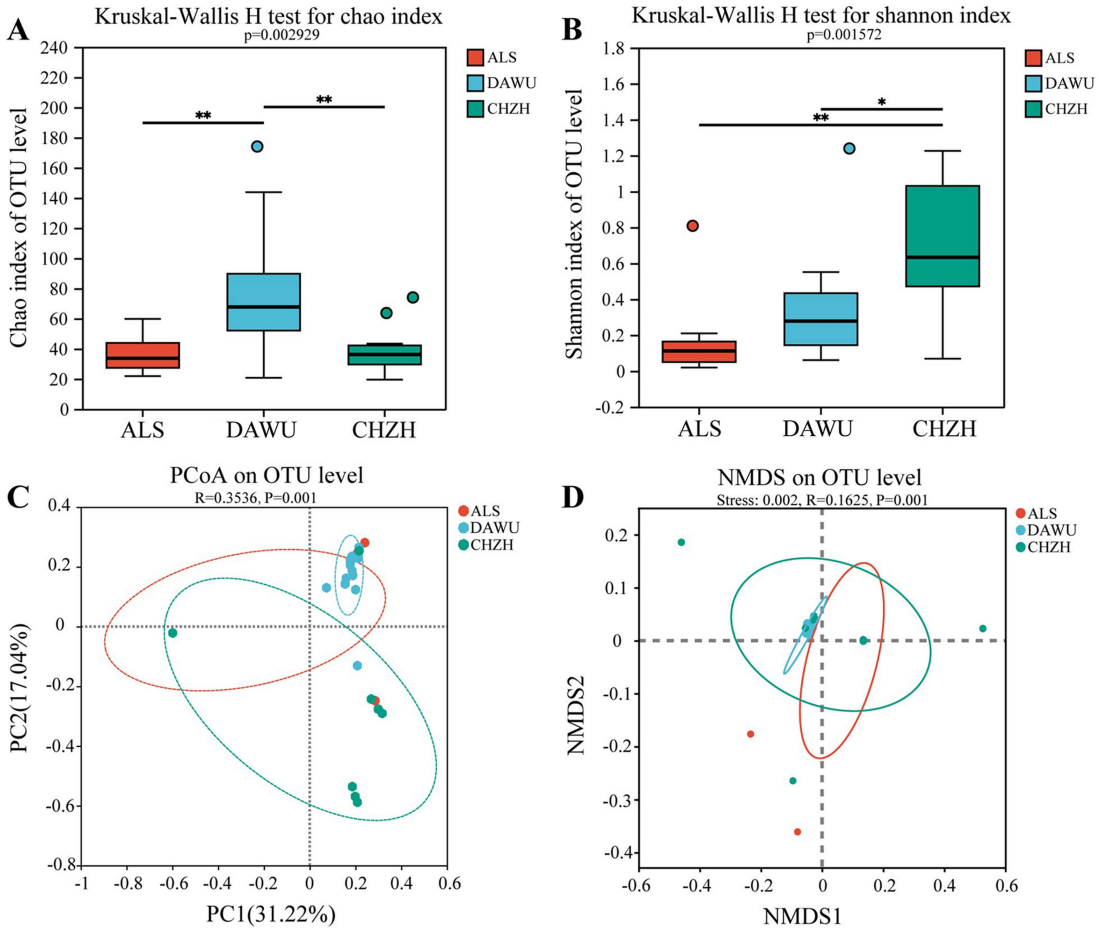

FIGURE 5
The α and β diversity index of animal-based diet composition in three rodent species (ALS, DAWU, and CHZH refer to *S. alashanicus*, *S. dauricus*, and *M. unguiculatus*, respectively). **(A,B)** Indicates α diversity. **(C,D)** Represent β diversity. *, and ** stand for statistically significant at $p < 0.05$, and 0.01, respectively.

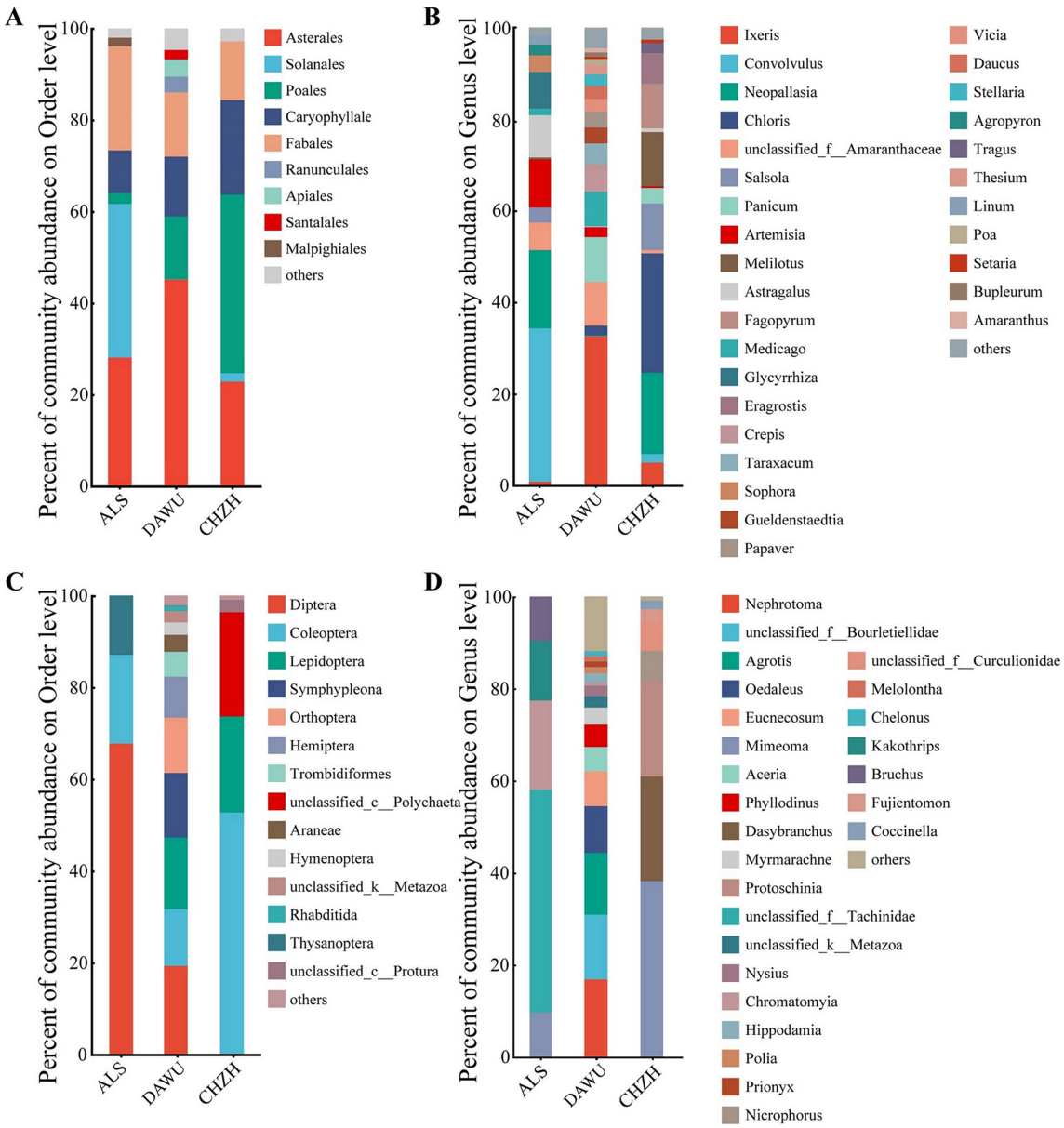

FIGURE 6
The dietary composition of the three rodent species (ALS, DAWU, and CHZH refer to *S. alashanicus*, *S. dauricus*, and *M. unguiculatus*, respectively). **(A,B)** Refer to plant-based diet composition at the order and genus level, respectively; **(C,D)** refer to animal-based diet composition at the order and genus level, respectively.

positively correlated with Bacillota, whereas *Vicia*, *Papaver*, and *Bupleurum* showed significant negative correlations. For Bacteroidota, significant positive correlations were observed with *Taraxacum*, *Papaver*, *Vicia*, *Helianthus*, and *Chenopodium*, while *Lespedeza*, and *Pinus* displayed significant negative correlations. The spearman correlation analysis of animal-based food composition and Bacillota and Bacteroidota (Figure 7B) indicated that *Eucnecosum*, unclassified_k__Metazoa, *Obelia*, *Aphis*, and *Zanclea* were significantly correlated with Bacteroidota, while no significant correlations were observed with Bacillota.

The spearman correlation analysis of plant-based food composition and gut microbiota diversity (Figure 8A) demonstrated that *Thesium*, *Silene*, *Sanguisorba*, and *Hieracium* were significantly positively correlated with the Shannon, Ace, and Chao indices, but significantly negatively correlated with the Simpson and Coverage indices. In contrast, *Chloris*, *Gueldenstaedtia*, and *Euphorbia* showed significant negative correlations with the Shannon index, while exhibiting significant positive correlations with the Simpson index. The spearman correlation analysis of animal-based food composition and gut microbiota diversity (Figure 8B) revealed that *Agrotis*, *Aceria*, *Hippodamia*, and *Liriomyza* were significantly negatively correlated with the Shannon index. Meanwhile, *Mimeoma* showed significant negative correlations with the Ace and Chao indices.

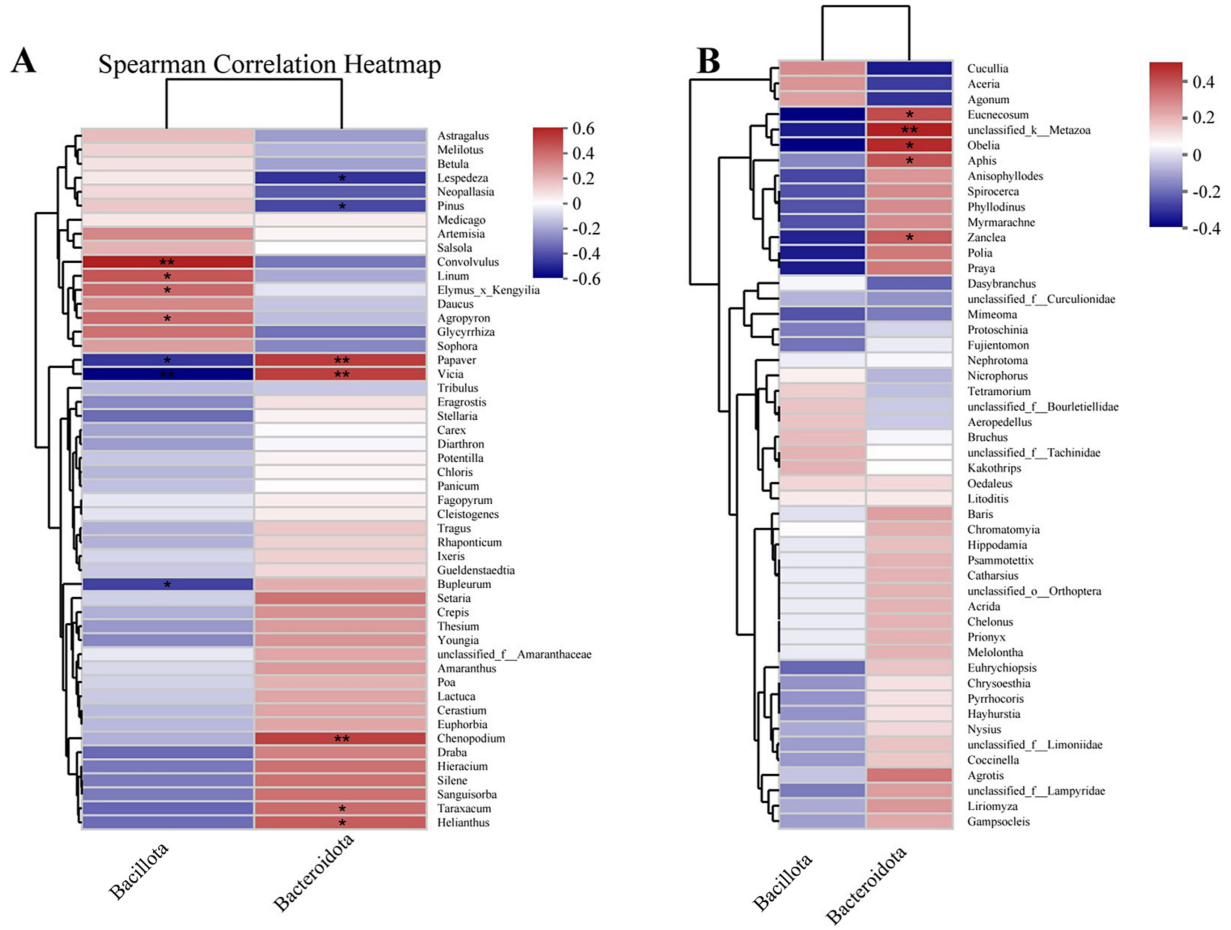

FIGURE 7
Associations between gut microbiota and diet composition of three rodent specie. **(A)** Correlation between the abundance of microbial phylum (Bacillota and Bacteroidota) and plant-based diet genera. **(B)** Correlation between the abundance of microbial phylum (Bacillota and Bacteroidota) and animal-based diet genera. *, and ** stand for statistically significant at $p < 0.05$, and 0.01, respectively.

4 Discussion

This study examined the cecal contents of three rodent species from the Inner Mongolia grasslands: *S. alashanicus*, *S. dauricus*, and *M. unguiculatus*. Through 16S rRNA amplicon sequencing, it was found that the gut microbiota of *S. alashanicus* and *S. dauricus* was primarily composed of the phyla Bacillota, Bacteroidetes, Thermodesulfobacteria, and Actinobacteria. In contrast, the gut microbiota of *M. unguiculatus* was mainly characterized by the presence of Bacillota, Verrucomicrobia, Bacteroidetes, and Actinobacteria. Ley et al. (2008) conducted an analysis of the gut microbiota across 60 mammalian species, identifying the six most prevalent phyla as Bacillota, Bacteroidetes, Proteobacteria, Actinobacteria, Verrucomicrobia, and Fusobacteria. Similarly, studies on the gut microbiota of *Marmota himalayana* and *Ictidomys tridecemlineatus* revealed distinct compositions. The gut microbiota of *Marmota himalayana* was predominantly dominated by Proteobacteria, Bacillota, Bacteroidetes, and Actinobacteria (Xu et al., 2021), while that of *Ictidomys tridecemlineatus* was mainly comprised of Bacteroidetes, Bacillota, and Verrucomicrobia (Carey et al., 2013). The gut microbiota composition observed in this study for the three rodent species shows some similarities with previous findings, although notable interspecies differences were evident. Specifically, Bacillota exhibited the highest relative abundance across all three species. The core gut microbiota of rodents is jointly regulated by the host's genetic background and external environmental factors, with diet serving as a key environmental variable. By providing substrate selection pressure and regulating metabolic products, diet plays a decisive role in the structural stability and functional adaptability of microbial communities (Fu et al., 2021; Weinstein et al., 2021).

These findings underscore the significance of integrating both genetic and environmental factors when investigating the gut microbiota of various rodent species. Alpha diversity serves as an indicator of microbial richness and diversity within a community. Specifically, the Chao index assess microbial richness, while the Shannon index measures diversity. Among the studied species, *S. alashanicus* and *S. dauricus* exhibits significantly higher Chao indices compared to *M. unguiculatus*. The habitats and dietary patterns of *S. alashanicus* and *S. dauricus* appear to foster richer and more diverse gut microbiota. Both habitat-specific food resources and host genetics play crucial roles in shaping gut microbiota composition (Sanders et al., 2014; Moran et al., 2019), with specific dietary nutrients promoting the enrichment of certain bacterial groups. Notably, *S. alashanicus*, which inhabit the arid desert regions of Inner Mongolia

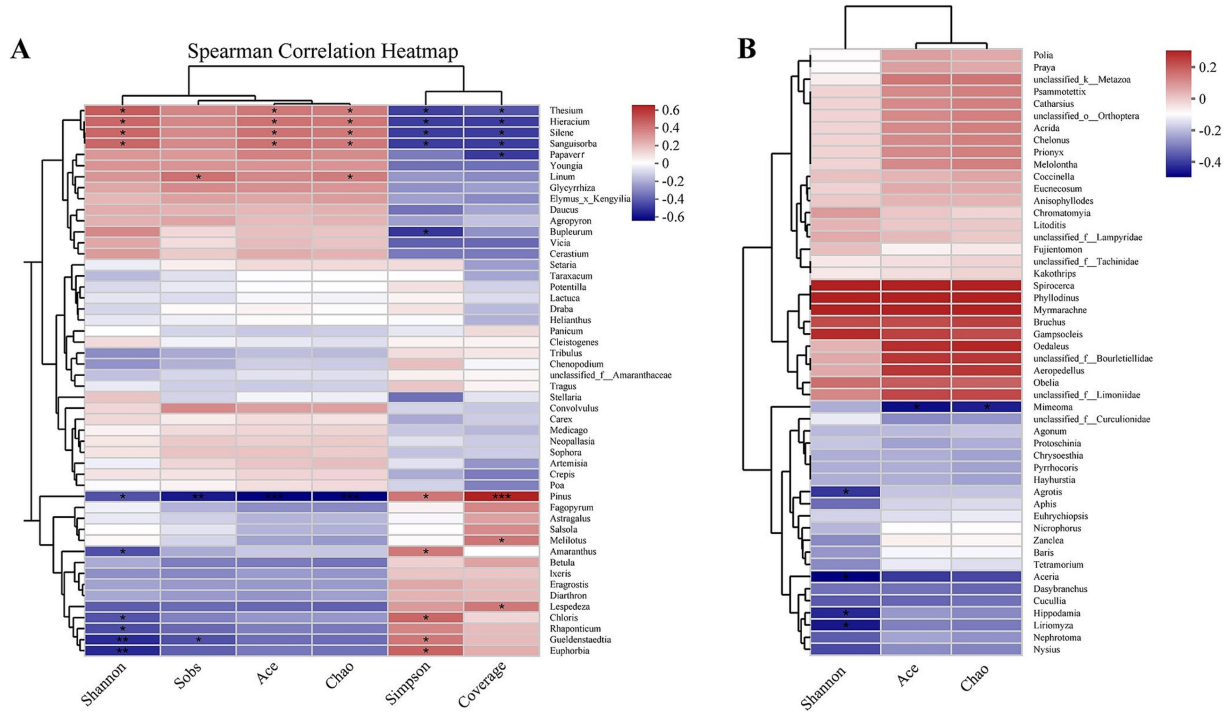

FIGURE 8
Associations between gut microbiota α diversity and diet composition of three rodent species. **(A)** Correlation between the gut microbiota α diversity and plant-based diet genera. **(B)** Correlation between the gut microbiota α diversity and animal-based diet genera. *, **, *** stand for statistically significant at $p < 0.05$, 0.01, and 0.001, respectively.

with relatively limited plant resources, exhibit higher alpha diversity indices compared to the other two species. This increased gut microbial diversity likely enhances the host's adaptability to environmental changes. Moreover, the gut microbiota of wild mice differs substantially from that of laboratory mice, with wild mice harboring microbial communities that promote host health and improve disease resistance (Rosshart et al., 2017). Animals with specialized diets host unique microbial profiles in their guts, facilitating adaptation to specific environments and dietary conditions. In summary, these results highlight the interplay between environmental factors and host genetics in shaping gut microbial communities, emphasizing the importance of considering both elements in ecological and evolutionary studies of rodents.

Despite being collected from sites 1,500 km apart, *S. alashanicus* and *S. dauricus* both belong to the *Sciuridae* family's *Spermophilus* genus. Their phylogenetic relationship leads to notable similarities in their gut microbiota composition, with *Alistipes* being dominant genera in both species. This contrasts sharply with *M. unguiculatus*, where Desulfovibrio is the dominant genus. The shared gut microbial characteristics between *S. alashanicus* and *S. dauricus*, despite the considerable geographical distance, suggest that host genetics play a pivotal role in shaping gut microbiota (Amato et al., 2019). From the standpoint of microbial colonization, the genetic background of the host may influence the selection of microbes during the early stages of gut colonization. Specific physiological traits of the gut can favor the adhesion and proliferation of certain microbes. Over time, the host's genetically determined immune system facilitates the recognition and response to gut microbes, supporting the stable presence and functionality of beneficial microorganisms. For example, *Alistipes* are known for their ability to continuously metabolize dietary fiber, produce short-chain fatty acids, and modulate immunity (Parker et al., 2020; Ma et al., 2022). In terms of long-term functional co-evolution, these two closely related *Spermophilus* species have likely undergone co-evolution between host digestive system-related genes and gut microbiota, particularly concerning digestive functions. This co-evolution enables certain microbes to assist the host in enhancing nutrient acquisition efficiency, thereby occupying a dominant position in the gut. This strongly supports the critical influence of host genetic factors on gut microbiota composition, colonization, and the maintenance of symbiotic relationships. These findings provide important evidence for a deeper understanding of the mutual relationship between hosts and their gut microbial communities. They highlight how host genetics and environmental factors jointly shape the gut microbiota, influencing both its composition and function. This interplay underscores the importance of considering both genetic and ecological factors when studying the gut microbiota of different rodent species.

The dietary composition of three rodent species—*S. alashanicus*, *S. dauricus*, and *M. unguiculatus*—was analyzed using DNA metabarcoding technology. The results indicated that all three species consume both plant and animal matter. At the order level, the plant-based diet of *S. alashanicus* was predominantly composed of Solanales, while *S. dauricus* favored Asterales, and *M. unguiculatus* preferred Poales. For animal-based components, *S. alashanicus* primarily consumed arthropods, *S. dauricus* included unclassified arthropods within k__Metazoa and members of the phylum Nematoda, and

M. unguiculatus fed on arthropods and annelids. Compared to traditional dietary analysis methods, DNA metabarcoding significantly enhances species resolution and accuracy in identifying animal-based food components, while also providing a more comprehensive analysis of plant-based dietary elements. Most plant species identified in the rodents' diets were present across their sampling sites, further validating the reliability of the study's findings. DNA metabarcoding has emerged as a crucial tool for analyzing dietary composition in animals (Buglione et al., 2018; Zhang et al., 2022; Pinho et al., 2022). Traditional methods often underestimate dietary diversity. For instance, Soininen et al. (2014) used high-throughput sequencing of the chloroplast gene trnL to analyze the stomach contents of *Myodes rufocanus* and *Microtus oeconomus*. Their findings revealed that traditional microscopic methods identified mosses as the primary food source, whereas metabarcoding uncovered a much more diverse diet. Similarly, Iwanowicz et al. (2016) employed DNA metabarcoding to investigate the diet of the endangered Pacific pocket mouse. Due to its nocturnal behavior, the dietary characteristics of this species were previously poorly understood. By sequencing DNA from fecal samples, they identified multiple plant genera within individual samples. Regarding animal-based food composition, the Chao index for *S. dauricus* was significantly higher than those for *S. alashanicus* and *M. unguiculatus*, indicating greater diversity in the animal-based diet of *S. dauricus*. This diversity is likely influenced by its habitat, foraging behavior, or population structure (Zhong et al., 2016). In contrast, the Coverage indices for *M. unguiculatus* and *S. alashanicus* were significantly higher than those for *S. dauricus*, suggesting more thorough utilization of animal-based food resources. No significant differences were observed in the plant-based food diversity indices among the three species, implying similar breadth and evenness in their use of plant-based resources. Despite being collected from different habitats, these three rodent species have evolved similar digestive physiological mechanisms and foraging strategies over time, leading to convergent patterns in their utilization of plant-based foods (Kartzinel et al., 2019). This convergence highlights the adaptability and flexibility of these species in response to varying environmental conditions.

The *S. alaschanicus* relies on salt-alkali tolerant plants, such as *Convolvulus* (Convolvulaceae) and *Artemisia* (Asteraceae), in extremely arid environments. High salt, high fiber, and secondary metabolites promote the growth of Bacillota, a phylum with strong tolerance, and functional bacterial genera like Alistipes. Alistipes breaks down complex carbohydrates to support host energy acquisition; synthesizes SCFAs to regulate metabolism and immunity; degrades toxins and adapts to stress, enhancing the host's environmental adaptability. The intestinal microbiota composition of the *S. dauricus* is highly synchronized with its omnivorous dietary habits. Its plant-based diet primarily consists of Asteraceae (e.g., Ixeris), which is rich in soluble fiber and may promote the proliferation of Bacillota. This fermentation generates short-chain fatty acids (SCFAs), enhancing the host's energy metabolism efficiency. The animal-based diet, primarily consisting of arthropods, provides protein and drives the Bacteroidetes (e.g., Bacteroides) to degrade nitrogen-containing polysaccharides. Compared to the *M. unguiculatus*, whose diet is mainly composed of Poaceae, the *S. dauricus*'s preference for Asteraceae has shaped a more efficient fiber-degrading microbiota, while animal-based food strengthens the metabolic flexibility of its gut microbiota. The intestinal microbiota composition of the *M. unguiculatus* is closely associated with its omnivorous diet, which is centered around Poales. Its plant-based food mainly consists of grasses like Chloris and Neopallasia, which are rich in complex cellulose. This may drive the enrichment of fiber-degrading microbiota (e.g., Spirillaceae or Fibrobacter), enhancing the host's metabolic capacity for structural polysaccharides. The animal-based diet, consisting mainly of arthropods and annelids, with high intake of chitin and protein, may promote the expression of chitinase in Bacteroidetes (e.g., Mimeoma) and protein degradation functions in Proteobacteria (e.g., Protoschinia). The Poales-based diet of the *M. unguiculatus* shapes a microbiota structure better suited for high-fiber degradation.

Plant-based food is strongly and significantly associated with the gut microbiota of rodents, playing a crucial role in shaping both the abundance and diversity of gut microbial communities. The composition of different plant genera exhibits distinct correlations with specific gut microbiota phyla, underscoring the complexity and critical importance of plant-based food in regulating gut microbial ecology (Wang et al., 2022). Studies on the relationship between diet and gut microbiota in grassland rodents have also highlighted the significance of animal-based food. The composition of animal-based food showed a significant positive correlation with the abundance of Bacteroidota but no significant correlation with Bacillota, indicating its unique influence on gut microbiota structure. Furthermore, animal-based food intake was significantly negatively correlated with gut microbiota diversity indices, suggesting that its consumption reduces microbial diversity. This phenomenon may reflect an adaptive strategy, as rodents in resource-limited grassland environments likely rely on energy-dense animal-based food to supplement their diets during periods of food scarcity. Previous research on the diets of grassland rodents has predominantly focused on plant-based food, often overlooking the role of animal-based food. However, the findings of this study underscore the need to reassess the dietary composition of grassland rodents and its impact on gut microbiota. These results provide a more comprehensive understanding of the ecological adaptation strategies of grassland rodents and the intricate interactions between their diets and gut microbiota. This study offers a new perspective and key research direction for exploring the survival mechanisms and ecological roles of grassland rodents within their ecosystems. By considering both plant-based and animal-based food components, we gain deeper insights into how these rodents adapt to their environments and maintain their health through complex gut microbiota interactions. This holistic approach enhances our understanding of the ecological dynamics and survival strategies of grassland rodents.

Data availability statement

The original contributions presented in the study are included in the article/Supplementary material, further inquiries can be directed to the corresponding author.

Ethics statement

The animal study was approved by the Ethics Committee of Chifeng University. The study was conducted in accordance with the local legislation and institutional requirements.

Author contributions

MC: Data curation, Writing – original draft, Writing – review & editing. YW: Data curation, Investigation, Writing – original draft. DM: Data curation, Investigation, Writing – original draft. XY: Data curation, Writing – original draft, Writing – review & editing.

Funding

The author(s) declare that financial support was received for the research and/or publication of this article. This work was supported by the Natural Science Foundation of Shandong Province (ZR2024MC092).

Conflict of interest

The authors declare that the research was conducted in the absence of any commercial or financial relationships that could be construed as a potential conflict of interest.

Generative AI statement

The authors declare that no Gen AI was used in the creation of this manuscript.

Publisher's note

All claims expressed in this article are solely those of the authors and do not necessarily represent those of their affiliated organizations, or those of the publisher, the editors and the reviewers. Any product that may be evaluated in this article, or claim that may be made by its manufacturer, is not guaranteed or endorsed by the publisher.

Supplementary material

The Supplementary material for this article can be found online at: https://www.frontiersin.org/articles/10.3389/fmicb.2025.1569592/full#supplementary-material

References

Amato, K. R., Sanders, J. G., Song, S. J., Nute, M., Metcalf, J. L., Thompson, L. R., et al. (2019). Evolutionary trends in host physiology outweigh dietary niche in structuring primate gut microbiomes. *ISME J.* 13, 576–587. doi: 10.1038/s41396-018-0175-0

Ando, H., Mukai, H., Komura, T., Dewi, T., Ando, M., and Isagi, Y. (2020). Methodological trends and perspectives of animal dietary studies by noninvasive fecal DNA metabarcoding. *Environ. DNA* 2, 391–406. doi: 10.1002/edn3.117

Beam, A., Clinger, E., and Hao, L. (2021). Effect of diet and dietary components on the composition of the gut microbiota. *Nutrients* 13:2795. doi: 10.3390/nu13082795

Brown, J., and Kotler, B. (2004). Hazardous duty pay and the foraging cost of predation. *Ecol. Lett.* 7, 999–1014. doi: 10.1111/j.1461-0248.2004.00661.x

Buglione, M., Maselli, V., Rippa, D., de Filippo, G., Trapanese, M., and Fulgione, D. (2018). A pilot study on the application of DNA metabarcoding for non-invasive diet analysis in the Italian hare. *Mamm. Biol.* 88, 31–42. doi: 10.1016/j.mambio.2017.10.010

Cabana, F., Clayton, J. B., Nekaris, K. A. I., Wirdateti, W., Knights, D., and Seedorf, H. (2019). Nutrient-based diet modifications impact on the gut microbiome of the Javan slow loris (*Nycticebus javanicus*). *Sci. Rep.* 9:4078. doi: 10.1038/s41598-019-40911-0

Cao, H., Shi, Y., Wang, J., Niu, Z., Wei, L., and John, N. (2024). The intestinal microbiota and metabolic profiles of Strauchbufo raddei underwent adaptive changes during hibernation. *Integr. Zool.* 19, 612–630. doi: 10.1111/1749-4877.12749

Carey, H. V., Walters, W. A., and Knight, R. (2013). Seasonal restructuring of the ground squirrel gut microbiota over the annual hibernation cycle. *Am. J. Physiol. Regul. Integr. Comp. Physiol.* 304, R33–R42. doi: 10.1152/ajpregu.00387.2012

Chock, R. Y., Shier, D. M., and Grether, G. F. (2022). Niche partitioning in an assemblage of granivorous rodents, and the challenge of community-level conservation. *Oecologia* 198, 553–565. doi: 10.1007/s00442-021-05104-5

Fu, H., Zhang, L., Fan, C., Liu, C., Li, W., Cheng, Q., et al. (2021). Environment and host species identity shape gut microbiota diversity in sympatric herbivorous mammals. *Microb. Biotechnol.* 14, 1300–1315. doi: 10.1111/1751-7915.13687

Goldberg, A. R., Conway, C. J., Tank, D. C., Andrews, K. R., Gour, D. S., and Waits, L. P. (2020). Diet of a rare herbivore based on DNA metabarcoding of feces: selection, seasonality, and survival. *Ecol. Evol.* 10, 7627–7643. doi: 10.1002/ece3.6488

Hacker, C. E., Jevit, M., Hussain, S., Muhammad, G., Munkhtsog, B., Munkhtsog, B., et al. (2021). Regional comparison of snow leopard (*Panthera uncia*) diet using DNA metabarcoding. *Microb. Biotechnol.* 30, 797–817. doi: 10.1007/s10531-020-02062-7

Hufeldt, M. R., Nielsen, D. S., Vogensen, F. K., Midtvedt, T., and Hansen, A. K. (2010). Variation in the gut microbiota of laboratory mice is related to both genetic and environmental factors. *Comp. Med.* 60, 336–347. doi: 10.31236/osf.io/5j7ek

Iwanowicz, D. D., Vandergast, A. G., Cornman, R. S., Adams, C. R., Kohn, J. R., Fisher, R. N., et al. (2016). Metabarcoding of fecal samples to determine herbivore diets: a case study of the endangered Pacific pocket mouse. *PLoS One* 11:e0165366. doi: 10.1371/journal.pone.0165366

Kartzinel, T. R., Hsing, J. C., Musili, P. M., Brown, B. R., and Pringle, R. M. (2019). Covariation of diet and gut microbiome in African megafauna. *Proc. Natl. Acad. Sci.* 116, 23588–23593. doi: 10.1073/pnas.1905666116

Kowalczyk, R., Wójcik, J. M., Taberlet, P., Kamiński, T., Miquel, C., Valentini, A., et al. (2019). Foraging plasticity allows a large herbivore to persist in a sheltering forest habitat: DNA metabarcoding diet analysis of the European bison. *Forest Ecol. Manag.* 449:117474. doi: 10.1016/j.foreco.2019.117474

Ley, R. E., Hamady, M., Lozupone, C., Turnbaugh, P. J., Ramey, R. R., Bircher, J. S., et al. (2008). Evolution of mammals and their gut microbes. *Science* 320, 1647–1651. doi: 10.1126/science.1155725

Li, H., Li, T., Beasley, D. E., Heděnec, P., Xiao, Z., Zhang, S., et al. (2016). Diet diversity is associated with beta but not alpha diversity of pika gut microbiota. *Front. Microbiol.* 7:1169. doi: 10.3389/fmicb.2016.01169

Lopes, C. M., De Barba, M., Boyer, F., Mercier, C., Galiano, D., Kubiak, B. B., et al. (2020). Ecological specialization and niche overlap of subterranean rodents inferred from DNA metabarcoding diet analysis. *Mol. Ecol.* 29, 3143–3153. doi: 10.1111/mec.15549

Lu, Y., Zhang, L., Liu, X., Lan, Y., Wu, L., Wang, J., et al (2024). Red pandas with different diets and environments exhibit different gut microbial functional composition and capacity. *Integr. Zool.* 19, 662–682. doi: 10.1111/1749-4877.12813

Ma, Y., Deng, X., Yang, X., Wang, J., Li, T., Hua, G., et al. (2022). Characteristics of bacterial microbiota in different intestinal segments of Aohan fine-wool sheep. *Front. Microbiol.* 13:874536. doi: 10.3389/fmicb.2022.874536

Maurer, M. L., Goyco-Blas, J. F., and Kohl, K. D. (2024). Dietary tannins alter growth, behavior, and the gut microbiome of larval amphibians. *Integr. Zool.* 19, 585–595. doi: 10.1111/1749-4877.12758

Moran, N. A., Ochman, H., and Hammer, T. J. (2019). Evolutionary and ecological consequences of gut microbial communities. *Annu. Rev. Ecol. Evol. Syst.* 50, 451–475. doi: 10.1146/annurev-ecolsys-110617-062453

Ozaki, S., Fritsch, C., Valot, B., Mora, F., Cornier, T., Scheifler, R., et al. (2018). Does pollution influence small mammal diet in the field? A metabarcoding approach in a generalist consumer. *Mol. Ecol.* 27, 3700–3713. doi: 10.1111/mec.14823

Park, J. K., and Do, Y. (2024). The difference and variation of gut bacterial community and host physiology can support adaptation during and after overwintering in frog population. *Integr. Zool.* 19, 631–645. doi: 10.1111/1749-4877.12798

Parker, B. J., Wearsch, P. A., Veloo, A. C., and Rodriguez-Palacios, A. (2020). The genus Alistipes: gut bacteria with emerging implications to inflammation, cancer, and mental health. *Front. Immunol.* 11:906. doi: 10.3389/fimmu.2020.00906

Petit Bon, M., Gunnarsdotter Inga, K., Jónsdóttir, I. S., Utsi, T. A., Soininen, E. M., and Bråthen, K. A. (2020). Interactions between winter and summer herbivory affect spatial and temporal plant nutrient dynamics in tundra grassland communities. *Oikos* 129, 1229–1242. doi: 10.1111/oik.07074

Pinho, C. J., Lopes, E. P., Paupério, J., Gomes, I., Romeiras, M. M., and Vasconcelos, R. (2022). Trust your guts? The effect of gut section on diet composition and impact of *Mus musculus* on islands using metabarcoding. *Ecol. Evol.* 12:e8638. doi: 10.1002/ece3.8638

Rosshart, S. P., Vassallo, B. G., Angeletti, D., Hutchinson, D. S., Morgan, A. P., Takeda, K., et al. (2017). Wild mouse gut microbiota promotes host fitness and improves disease resistance. *Cell* 171, 1015–1028.e13. doi: 10.1016/j.cell.2017.09.016

Sanders, J. G., Powell, S., Kronauer, D. J., Vasconcelos, H. L., Frederickson, M. E., and Pierce, N. E. (2014). Stability and phylogenetic correlation in gut microbiota: lessons from ants and apes. *Mol. Ecol.* 23, 1268–1283. doi: 10.1111/mec.12611

Sato, J. J., Shimada, T., Kyogoku, D., Komura, T., Uemura, S., Saitoh, T., et al. (2018). Dietary niche partitioning between sympatric wood mouse species (Muridae: Apodemus) revealed by DNA meta-barcoding analysis. *J. Mammal.* 99, 952–964. doi: 10.1093/jmammal/gyy063

Soininen, E. M., Ehrich, D., Lecomte, N., Yoccoz, N. G., Tarroux, A., Berteaux, D., et al. (2014). Sources of variation in small rodent trophic niche: new insights from DNA metabarcoding and stable isotope analysis. *Isot. Environ. Health Stud.* 50, 361–381. doi: 10.1080/10256016.2014.915824

Suzuki, T. A., Phifer-Rixey, M., Mack, K. L., Sheehan, M. J., Lin, D., Bi, K., et al. (2019). Host genetic determinants of the gut microbiota of wild mice. *Mol. Ecol.* 28, 3197–3207. doi: 10.1111/mec.15139

Tang, L., Yan, L., Jia, H., Xiong, Y., Ma, X., Chu, H., et al. (2023). Gut microbial community structure and function of Przewalski' horses varied across reintroduced sites in China. *Integr. Zool.* 18, 1027–1040. doi: 10.1111/1749-4877.12699

Ter Schure, A. T., Pillai, A. A., Thorbek, L., Bhavani Shankar, M., Puri, R., Ravikanth, G., et al. (2021). eDNA metabarcoding reveals dietary niche overlap among herbivores in an Indian wildlife sanctuary. *Environ. DNA* 3, 214–230. doi: 10.1002/edn3.161

Wang, J., Laguardia, A., Damerell, P. J., Riordan, P., and Shi, K. (2014). Dietary overlap of snow leopard and other carnivores in the Pamirs of northwestern China. *Chin. Sci. Bull.* 59, 3162–3168. doi: 10.1007/s11434-014-0370-y

Wang, Z., Zhang, C., Li, G., and Yi, X. (2022). The influence of species identity and geographic locations on gut microbiota of small rodents. *Front. Microbiol.* 13:983660. doi: 10.3389/fmicb.2022.983660

Weinstein, S. B., Martínez-Mota, R., Stapleton, T. E., Klure, D. M., Greenhalgh, R., Orr, T. J., et al. (2021). Microbiome stability and structure is governed by host phylogeny over diet and geography in woodrats (*Neotoma spp.*). *Proc. Natl. Acad. Sci.* 118:e2108787118. doi: 10.1073/pnas.2108787118

Weldon, L., Abolins, S., Lenzi, L., Bourne, C., Riley, E. M., and Viney, M. (2015). The gut microbiota of wild mice. *PLoS One* 10:e0134643. doi: 10.1371/journal.pone.0134643

Woo, C., Kumari, P., Eo, K. Y., Lee, W. S., Kimura, J., and Yamamoto, N. (2022). Using DNA metabarcoding and a novel canid-specific blocking oligonucleotide to investigate the composition of animal diets of raccoon dogs (*Nyctereutes procyonoides*) inhabiting the waterside area in Korea. *PLoS One* 17:e0271118. doi: 10.1371/journal.pone.0271118

Xiong, M., Shao, X., Long, Y., Bu, H., Zhang, D., Wang, D., et al. (2016). Molecular analysis of vertebrates and plants in scats of leopard cats (*Prionailurus bengalensis*) in Southwest China. *J. Mammal.* 97, 1054–1064. doi: 10.1093/jmammal/gyw061

Xu, P., Zhang, X. F., and Ma, Y. (2021). Using 16S rDNA to study the diversity of the intestinalflora of the Oinghai Himalayan marmot. *Chin. J. Zoonoses* 37, 773–782. doi: 10.3969/j.issn.1001-6980.2021.09.004

Zhang, X. Y., Khakisahneh, S., Liu, W., Zhang, X., Zhai, W., Cheng, J., et al. (2023). Phylogenetic signal in gut microbial community rather than in rodent metabolic traits. *Nat. Sci. Rev.* 10:nwad209. doi: 10.1093/nsr/nwad209

Zhang, X., Zou, Y., Zou, X., Xu, Z., Nan, X., and Han, C. (2022). DNA metabarcoding uncovers the diet of subterranean rodents in China. *PLoS One* 17:e0258078. doi: 10.1371/journal.pone.0258078

Zhao, J., Feng, T., An, X., Chen, X., Han, N., Wang, J., et al. (2024). Livestock grazing is associated with the gut microbiota and antibiotic resistance genes in sympatric plateau pika (Ochotona curzoniae). *Integr. Zool.* 19, 646–661. doi: 10.1111/1749-4877.12778

Zhong, W., Wang, G., Zhou, Q., Ma, L., Wan, X., and Liu, W. (2016). Spatial niche partitioning of coexisting small mammals in sand dunes. *Ital. J. Zool.* 83, 248–254. doi: 10.1080/11250003.2016.1139636

frontiers | Frontiers in Microbiology

TYPE Original Research
PUBLISHED 09 May 2025
DOI 10.3389/fmicb.2025.1580847

Check for updates

OPEN ACCESS

EDITED BY
Junling Shi,
Northwestern Polytechnical University, China

REVIEWED BY
Yang Liu,
Fudan University, China
Changkun Li,
Shanghai Jiao Tong University, China

*CORRESPONDENCE
Haipeng Sun
✉ sun.haipeng@tmu.edu.cn
Wenyan Niu
✉ wniu@tmu.edu.cn

†These authors have contributed equally to this work and share first authorship

RECEIVED 24 February 2025
ACCEPTED 14 April 2025
PUBLISHED 09 May 2025

CITATION
Zhang X, Li Z, Cao J, Sun H and Niu W (2025) *Clostridium Butyricum 337279* shapes the gut microbiota to attenuate metabolic disorder in diet-induced obese mice.
Front. Microbiol. 16:1580847.
doi: 10.3389/fmicb.2025.1580847

COPYRIGHT
© 2025 Zhang, Li, Cao, Sun and Niu. This is an open-access article distributed under the terms of the Creative Commons Attribution License (CC BY). The use, distribution or reproduction in other forums is permitted, provided the original author(s) and the copyright owner(s) are credited and that the original publication in this journal is cited, in accordance with accepted academic practice. No use, distribution or reproduction is permitted which does not comply with these terms.

Clostridium Butyricum 337279 shapes the gut microbiota to attenuate metabolic disorder in diet-induced obese mice

Xuejiao Zhang†, Zhiyu Li†, Junjun Cao, Haipeng Sun* and Wenyan Niu*

Key Laboratory of Immune Microenvironment and Disease of the Educational Ministry of China, NHC Key Lab of Hormones and Development and Tianjin Key Lab of Metabolic Diseases,Tianjin Medical University Chu Hsien-I Memorial Hospital and Institute of Endocrinology, Tianjin, China

Aims: Obesity is one of the important challenges to public health worldwide. Dysbiotic intestinal microbiota is a key factor in the onset and progression of obesity and related diseases. Short chain fatty acids (SCFAs) derived from *butyricogenic bacteria* has beneficial effects on obesity. *Clostridium Butyricum 337279* (*C.B*), one of the SCFA producing bacteria, has been used to treat inflammatory bowel disease. The effect of *C.B* on obese mice remains unclear.

Methods: A high fat diet (HFD)-induced mouse model of obesity was constructed, and the mice were treated with *C.B* to examine their role on obesity and related metabolic disorder. RT-qPCR, Western blotting, immunohistochemical staining, and 16S rRNA gene sequencing were performed to investigate the role and mechanism of *C.B*. Plasma levels of BCAA and BCKA were detected by Shimadzu LC-20 AD liquid chromatography (LC) system.

Results: Here we demonstrated that oral administration of *C.B* effectively alleviated HFD-induced obesity and associated metabolic disorders, including glucose intolerance and hyperlipidemia, as well as systemic inflammation, as evidenced by reduced levels of LPS, TNF-α, and IL-1β. *C.B* alleviated intestinal flora imbalance and modulated the composition of gut microbiota and their metabolites in HFD-induced obese mice. It also significantly ameliorated intestinal barrier disorders by increasing protein level of tight junction proteins ZO-1 and occludin. Importantly, dietary *C.B* potentially suppressed bacterial biosynthesis of branched-chain amino acids (BCAA) and reduced the excessive accumulation of BCAA in plasma, suggesting its role in restoring BCAA metabolism of mice.

Conclusion: *C.B* intervention significantly ameliorated gut microbiota imbalance in obese mice and alleviated obesity-related metabolic disorders by upregulating the expression of tight junction proteins (ZO-1 and occludin), attenuating endotoxemia and systemic inflammation and reducing microbial-derived BCAA production.

KEYWORDS

gut microbiota, systemic inflammation, branched-chain amino acids, metabolic disorder, insulin resistance

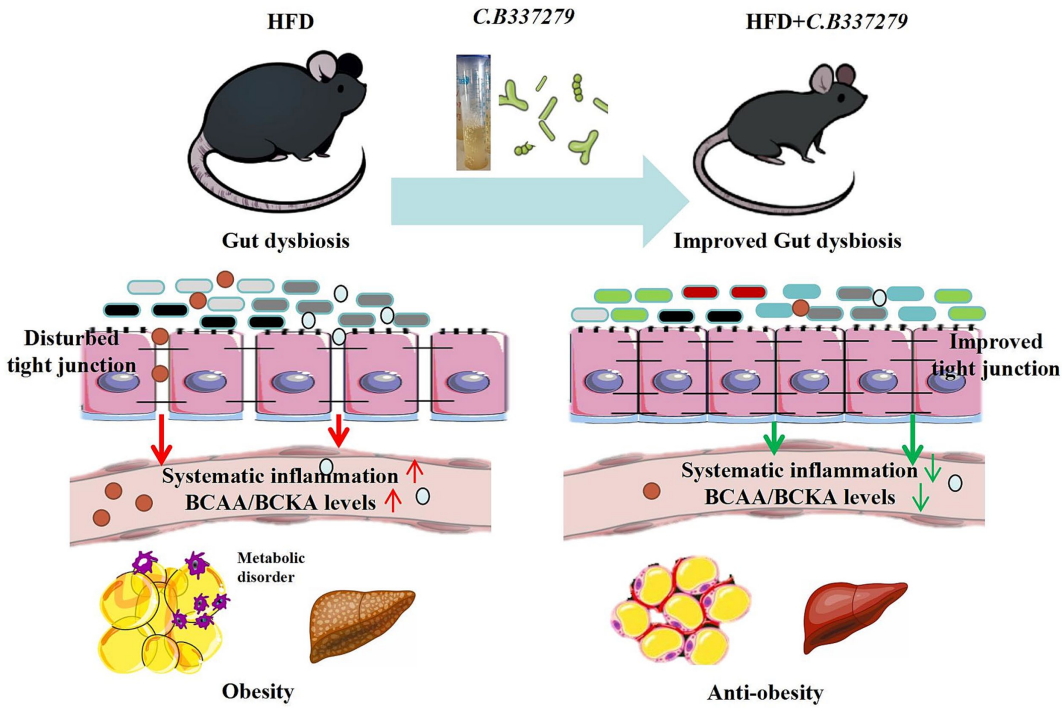

Introduction

Metabolic syndrome (MetS), a clinical constellation encompassing obesity, hyperlipidemia, insulin resistance (IR), and metabolic dysfunction-associated steatotic liver disease (MASLD) (Lemieux and Després, 2020), is intricately linked to gut microbial dysbiosis (Dabke et al., 2019). Emerging evidence highlights microbial metabolites-particularly short-chain fatty acids (SCFAs; acetate, propionate, and butyrate)-as pivotal mediators of host-microbiome crosstalk that modulate obesity progression (Mann et al., 2024). SCFAs are predominantly produced by *Clostridium* species. They are primarily absorbed by intestinal epithelial cells, and directly activate G-coupled-receptors, inhibit histone deacetylases, and serve as energy substrates (Wong et al., 2006; Cresci et al., 2017; Koh et al., 2016). Beyond their role in mucosal protection, SCFAs regulate systemic energy homeostasis and mitigate metabolic inflammation (Yao et al., 2022). Notably, HFD-induced intestinal barrier dysfunction contributes to the development of metabolic disorders and colitis, both of which can be effectively alleviated by prebiotic interventions (Kang et al., 2022; Lee et al., 2022). Orally administered probiotic *Clostridium butyricum* produces large amounts of SCFAs in intestinal tracts (Cassir et al., 2016). However, the potential therapeutic effects of *Clostridium butyricum* on metabolic syndrome remain unclear, and its application as a therapeutic intervention faces significant challenges.

The intestinal barrier of obese mice is compromised, allowing microbiota-derived metabolites to translocate from the gut lumen into systemic circulation (Riedel et al., 2021). These microbial metabolites subsequently infiltrate key metabolic organs, including the liver and adipose tissue, thereby inducing systemic inflammation and contributing to the pathogenesis of MetS (Tilg et al., 2020; Winer et al., 2016). Extensive research has demonstrated that HFD-induced gut microbiota dysbiosis (GMD) generates pathogenic metabolites and compromises intestinal barrier integrity, ultimately resulting in enhanced intestinal permeability. This may facilitate toxin translocation into the systemic circulation to induce metabolic diseases. Studies have revealed the relationship between dietary BCAA and gut microbiota (Karusheva et al., 2019; Wang et al., 2023; Li et al., 2022). BCAA (valine, leucine, isoleucine) are essential amino acids. Elevated BCAAs levels are associated with metabolic diseases such as obesity and diabetes (Zhou et al., 2019), which are often accompanied by microbiome disorders. Evidence showed that gut microbiota play a role in BCAA metabolism (Ridaura et al., 2013; Pedersen et al., 2016; Oh et al., 2021). Several gut microbiome were identified as the most abundant amino acid biosynthesis bacteria (Neis et al., 2015). Given the well-established association between disrupted gut microbiota and obesity (Mitev and Taleski, 2019), the potential relationship between GDM and elevated BCAA levels, remains to be elucidated.

Here we showed that *Clostridium butyricum 337279* (*C.B 337279*), a butyrate-producing strain, counteracts HFD-induced gut dysbiosis, intestinal hyperpermeability, and metabolic inflammation. Concurrently, it restored gut barrier integrity via upregulation of tight junction proteins (ZO-1, occludin), reducing systemic endotoxemia and proinflammatory cytokines (IL-6, TNF-α). Metagenomic analysis revealed that *C.B 337279* selectively suppressed BCAA-producing pathobionts (*Proteobacteria*, *Desulfovibrionaceae*). This microbial shift correlated with decreased plasma levels of BCAAs and BCKAs, which are established drivers of IR. These results establish *C.B 337279* as a microbiota-modulating therapeutic agent for metabolic disorders and redefine BCAA homeostasis as a mechanistic target for microbiome-based interventions.

10.3389/fmicb.2025.1580847

Methods

In vitro C.B 337279 culture

Clostridium Butyricum 337279 (BNCC *337279*) was purchased from the Beijing Beina Innovation Alliance Institute of Biotechnology (BNCC). *C.B 337279* was cultured in Reinforced Clostridial Medium (RCM) that contained 10 g/L peptone, 5 g/L yeast extract, 3 g/L glucose, 5 g/L NaCl, and 1 g/L soluble starch, adjusted to pH 6.8. *C.B 337279* was cultured at 37°C for 48 h and the bacterial suspension was centrifuged at 8000 rpm for 20 min, the cultured bacterial cells were resuspended in normal saline for gavage. Oral administration of *C.B* ($1–5 \times 10^8$ CFU for each mouse) was performed every other day for 8 weeks.

Animals and treatment

Six-week-old wild type C57BL/6 male mice were purchased from Huafukang Institute of Experimental Animal Research, Beijing, China (Table 1). After 7 days antibioticmixture (Abx) treatment, mice were randomly divided into two groups fed normal control diet (ND) or 60% HFD for 20 weeks, respectively. Each group mice were further divided into saline groups and *C.B* groups (ND + Saline, ND + *C.B*, HFD + Saline, HFD + *C.B*) for the last 8 weeks (Figure 1A). Following an 8-week intervention period, mice were fasted for 6 h, anesthetized with 3% isoflurane, and euthanized via cervical dislocation. Content and mucosa of the small intestine, cecum and colon were collected following immediately frozen, and stored at −80°C. All animal procedures were approved by the Animal Care and Use Committee of Tianjin Medical University and were conducted in accordance with the Guide for the Care and Use of Laboratory.

TABLE 1 Diets used in this study.

Product #	D12450B (10%fat)		D12451 (45%fat)	
%	gm	*kcal*	gm	*kcal*
Protein	19	20	24	20
Carbohydrate	67	70	41	35
Fat	4	10	24	45
Total		100		
kcal/gm	3.8		4.7	

Ingredient	gm	*kcal*	gm	*kcal*
Casein	200	800	200	800
L-Cystine	3	12	3	12
Corn starch	315	1,260	72.8	291
Maltodextrin 10	35	140	100	400
Sucrose	350	1,400	172.8	691
Cellulose, Bw200	50	0	50	0
Soybean oil	25	225	25	225
Lard	20	180	177.5	1,598
Mineral MixS10026	10	0	10	0
Dicalcium phosphate	13	0	13	0
Calcium carbonate	5.5	0	5.5	0
Potassium citrate.1 H20	16.5	0	16.5	0
Vitamin MixV10001	10	40	10	40
Choline bitartrate	2	0	2	0
FD&C Yellow Dye #5	0.05	0	0	0
FD&C Red Dye #40	0	0	0.05	0
FD&C Blue Dye #1	0	0	0	0
Total	**1055.1**	**4,057**	**858.15**	**4,057**

Measurements of metabolic indices and serum cytokines

Liver tissues (30 mg) were homogenized in ice-cold chloroform:methanol extraction buffer (2:1 v/v; Sigma-Aldrich C2432/M1775). Following 16-h solvent extraction at 4°C, samples were phase-separated by adding 300 µL deionized water and centrifuged at 12,000 × g for 10 min (4°C). Lipid-containing organic phases were vacuum-dried (CentriVap Concentrator, Labconco) and reconstituted in 200 µL 5% Triton X-100 (Sigma-Aldrich T9284). Hepatic triglyceride (TG) and total cholesterol (TC) levels were quantified using enzymatic assay kits (Zhongsheng Beikong, #ZS-1011-TG/#ZS-1012-TC). The serum cytokines including IL-1β, IL-6, lipopolysaccharide-binding protein (LBP), lipopolysaccharide (LBS) and TNFα were detected with commercial kits according to the manufacturer's introduction.

Oil Red O staining, histological analyses and immunohistochemistry

Fresh liver specimens were embedded in optimal cutting temperature compound (OCT; Sakura #4583) and snap-frozen in liquid nitrogen-cooled isopentane. Cryoblocks were sectioned at 7 µm thickness using a cryostat (Leica CM1950), and fixed in 10% neutral buffered formalin for 10 min. Sections were deparaffinized and rehydrated following with Hematoxylin and eosin staining or incubating with anti-ZO-1(D6L1E) antibody (Cell Signaling Technology, #13663), anti-Occludin-1(E6B4R) antibody (Cell Signaling Technology, #91131) at 4°C for overnight, respectively. Then the sections were incubated with secondary antibody for 30 min. Images were acquired under a Leica microscope.

RNA extraction and real-time PCR

Total RNA from frozen livers or white adipose tissue were isolated with TRlzol reagent (15596026, Invitrogen) and subjected to complementary DNA synthesis by reverse-transcription with random primers. The mRNA expression of different genes was normalized to that of β-actin. The quantitative PCR procedure followed the Minimum Information for Publication of Quantitative Real-Time Polymerase Chain Reaction Experiments guidelines. Sequences of primers for quantitative PCR are shown in Table 2.

16S rRNA analysis

Total genomic DNA was extracted from the digestive tract of the colon using the QIAamp DNA Stool Mini Kit (Qiagen GmbH, Hilden, Germany) according to the manufacturer's instructions. The

10.3389/fmicb.2025.1580847

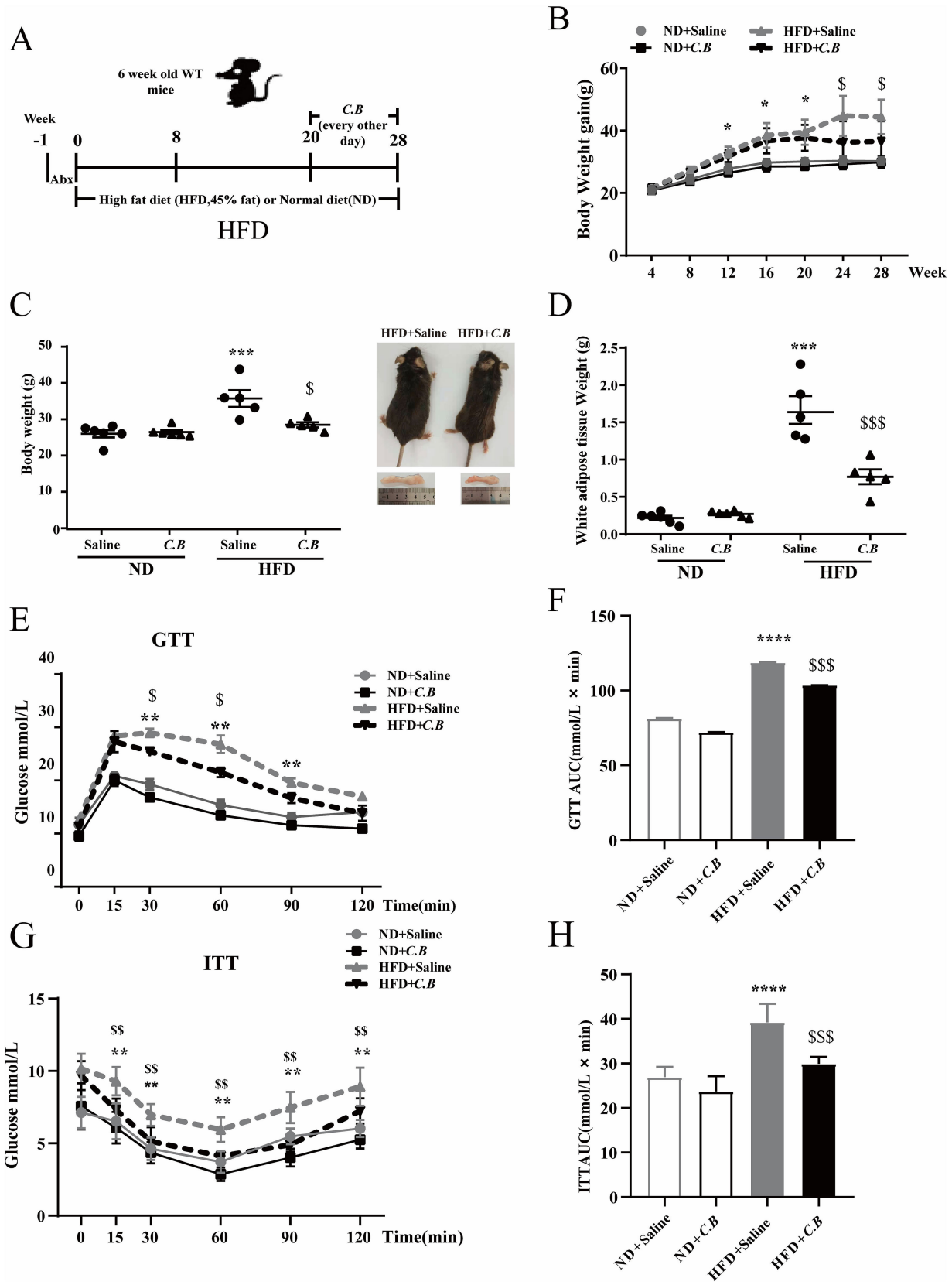

FIGURE 1
Dietary *C.B* alleviated IR in obese mice. **(A)** Schematic diagram showing the study design for *C.B* administration in HFD mice. **(B)** Time series of body weights. **(C)** Body weight and representative mice from the HFD and HFD + *C.B* groups. **(D)** The weight of WAT from different group. **(E,F)** Effect of *C.B* on glucose tolerance measured by oral glucose tolerance test (OGTT). Right: Area under the curve (AUC). **(G,H)** Effect of *C.B* on percentage of initial blood glucose level during insulin tolerance test (ITT). Right: AUC. Statistical significance was determined by two-way ANOVA with Tukey tests for multiple-group comparisons, (n = 5–7). * $p < 0.05$, ** $p < 0.01$ vs. ND + Saline, and $^{\$}$ $p < 0.05$, $^{\$\$}$ $p < 0.01$ vs. HFD + Saline.

TABLE 2 List of the gene-specific primer sequences used in this study.

Gene	Species	Stand	Sequence
β-actin	Mouse	Forward primer	CCTCTATGCCAACACAGTGC
		Reverse primer	CCTGCTTGCTGATCCACATC
cd36	Mouse	Forward primer	TGGTCAAGCCAGCTAGAAA
		Reverse primer	CCCAGTCTCATTTAGCCAC
IL-1β	Mouse	Forward primer	GCCCATCCTCTGTGACTCAT
		Reverse primer	AGGCCACAGGTATTTTGTCG
tnf-α	Mouse	Forward primer	CCAGACCCTCACACTCAGATC
		Reverse primer	CACTTGGTGGTTTGCTACGAC
Mcp-1	Mouse	Forward primer	TGGCTCAGCCAGATGCAGT
		Reverse primer	CCAGCCTACTCATTGGGATCA

concentration of genomic DNA were measured and purified. The integrity of extracted genomic DNA was determined by electrophoresis on 1% (w/v) agarose gel. Primer sequencing and bioinformatics analysis were conducted by Novogene (Beijing, China) using paired end sequencing on the Illumina HiSeq platform. The V3–V4 region of the bacterial 16S rRNA gene was amplified by PCR using bacterial universal primers to fully define bacterial composition and abundance. Use Uparse (Uparse v7.0.1001) to cluster the obtained sequences into operational taxonomic units (OTUs) with 97% sequence identity for α diversity and β diversity analysis.

BCAA measurement

The plasma levels of BCAA and BCKA were detected by multiple reaction monitoring (MRM) in positive and negative electrospray ionization mode, respectively. Chromatographic separation was achieved on an Agilent ZORBAX SB-C18 (150 × 3 mm, 5 μm) column, and temperature controlled at 50°C. The standards and samples were separated using a mobile phase consisting of methanol/water (20:80, v/v) with 0.1% formic acid (eluent A) and acetonitrile (eluent B). The mobile was 0% B initially, which held for 1.5 min and then increased to 90% over 0.5 min. The mobile phase was held at 90% B for 5 min and then re-equilibrated to 0% B and held for 6 min. The flow rate was 0.9 mL/min. An aliquot of 10 μL plasma was spiked with 110 μL methanol/acetonitrile/water (50:50:10, v/v/v) containing stable-isotope-labeled internal standards (48 ng [D3] Leucine, 24 ng [13C4, D3] KIV sodium salt, and 16 ng [D3] KIC sodium salt) and remained on ice for 10 min before being centrifuged at 14000 g at 4°C for 10 min. The supernatant was collected and dried with a stream of nitrogen. Following this, the samples were reconstituted in 100 μL of methanol/water (20:80, v/v) for analysis. The injection volume was 10 μL. Data acquisition and quantitation were performed with Analyst 1.7 and MultiQuant 3.0 software, respectively.

Glucose and insulin tolerance tests

For the glucose tolerance test (GTT), mice were fasted for 9 h and subsequently administered an intraperitoneal injection of glucose (2 g/kg body weight). Blood glucose levels were measured using a handheld glucometer (Accu-CHEK; Roche, Mannheim, Germany) from tail vein blood samples collected at 0, 15, 30, 60, 90, and 120 min. For the insulin tolerance test (ITT), mice fasted for 9 h received an intraperitoneal bolus injection of insulin (1.5 U/kg body weight). Glucose was measured as described above.

Statistical analysis

Statistical analyses were performed using GraphPad Prism 8.0.1.[1] Significant differences were evaluated using two-way analysis of variance (ANOVA) with Tukey tests for multiple-group comparisons. All values are expressed as mean ± SEM. $p < 0.05$ was considered significant.

Results

C.B attenuated HFD-induced obesity and alleviated obesity associated-IR

We initially investigated whether *C.B* exerts any effects on MetS in mice with HFD-induced obesity. Mice fed with HFD for 20 weeks showed significant increases in body weight, white adipose tissue weight, and impaired glucose tolerance test compared to mice fed with chow diet (Figures 1B–F). Notably, oral administration of *C.B* ($1–5 \times 10^8$ CFU) administered every other day for 8 weeks effectively attenuated HFD-induced body weight gain (Figures 1B,C). This effect was not associated with food intake (Supplementary Figure S1). Liver weight was not changed (data is not shown), while the weight of white adipose tissue was significantly reduced by *C.B* (Figure 1D). In addition, *C.B* significantly improved glucose tolerance (Figure 1E) and insulin sensitivity (Figure 1G). Furthermore, *C.B* administration significantly reduced the area under the curve (AUC) of GTT (Figure 1F, $p < 0.05$) and improved insulin tolerance, as evidenced by the percentage change in ITT at both 30- and 60-min time points (Figure 1H, $p < 0.05$). These findings collectively demonstrate that *C.B* treatment not only attenuated body weight gain but also enhanced insulin sensitivity in diet-induced obese mice.

C.B ameliorated HFD-induced hyperlipemia and ectopic lipid deposition

Prolonged HFD feeding has been consistently associated with progressive hepatic alterations, including steatosis, fibrosis, and

1 https://www.graphpad.com/

inflammatory responses. To investigate the therapeutic potential of *C.B* intervention, we subsequently evaluated its effects on the progression of MASLD in the HFD-induced mouse model. As shown in Figure 2A, *C.B* treatment significantly ameliorated hepatic lipid accumulation and fibrogenesis compared to the HFD-fed control group. Consistent with the histological observations, quantitative analysis demonstrated a substantial reduction in hepatic lipid content, with triglyceride (TG) levels showing a particularly significant decrease of 33.3% ($p < 0.05$) in *C.B*-treated mice relative to HFD controls (Figures 2B,C). Furthermore, *C.B* administration led to a significant improvement in serum lipid profiles, as indicated by pronounced reductions in both TG and total cholesterol (CHOL) levels (Figures 2D,E). Taken together, these findings demonstrate that *C.B* treatment effectively ameliorates systemic lipid metabolic disorders, particularly in both circulating and hepatic lipid homeostasis.

C.B reduced systemic inflammatory in obese mice

SCFAs have been well-documented to exert immunomodulatory effects on systemic inflammatory responses. Based on this established mechanism, we subsequently investigated whether *C.B* administration could ameliorate metabolic dysfunction through the attenuation of systemic inflammation. The immunophenotypic characterization of peripheral blood mononuclear cell (PBMC) subpopulations was performed using flow cytometry. As shown in Figure 3A, the proportion of $CD11b^{+}Ly6C^{hi}Ly6G^{-}$ cells in HFD group was higher than that in ND group (3.62% vs. 6.03%, $p < 0.01$). After *C.B* administration, the proportion of monocytic cells in HFD group reduced significantly, which was in accordance with the reduced proportion of $CD11b^{+}Ly6C^{-}Ly6G^{hi}$ cells (Figure 3B). Consistent with the above findings, serum analysis demonstrated significantly elevated levels of pro-inflammatory cytokines, including TNF-α, IL-1β, and IL-6, in HFD-fed mice compared to ND controls ($p < 0.01$). Notably, oral administration of *C.B* effectively attenuated these inflammatory responses, as evidenced by significant reductions in cytokine levels (Figures 3C–E, $p < 0.05$). In line with these observations, *C.B* treatment significantly reduced the infiltration of $F4/80^{+}$ macrophages in both hepatic and WAT compartments of HFD-fed mice (Figure 3F). Most notably, *C.B* administration markedly downregulated the expression of pro-inflammatory markers in HFD-fed mice, with particularly pronounced effects observed in WAT ($p < 0.01$, Figures 3G,H). Collectively, these findings demonstrate that *C.B* possesses potent anti-inflammatory properties that effectively ameliorate obesity-associated inflammation in multiple metabolic tissues.

C.B reduced HFD-induced intestinal permeability

A growing body of works suggests that early changes in the gastrointestinal (GI) barrier may contribute to both local, within the GI lining, and systemic inflammation in obesity (Acciarino et al., 2024; Nascimento et al., 2021). We next examined the effects of *C.B* on intestinal integrity. As the immunofluorescence data shown in Figures 4A,B, the tight junction proteins zonula occludens-1 (ZO-1) and occludin in HFD group were decreased, which was significantly reversed after *C.B* treatment. We also evaluated the integrity of the intestinal barrier. The mRNA levels of tight junction-related (TJ) gens in the intestinal tissue, including ZO-1 and occludin were higher in HFD + *C.B* group than that in HFD group (Figures 4C,D, $p < 0.01$). In comparison, claudin-2 in HFD + *C.B* group was lower than that in HFD group (Figure 4E, $p < 0.05$). In a line with these results, *C.B* treatment significantly decreased the circulation levels of LBP and LBS caused by HFD (Figures 4F,G), indicating a potential role of *C.B* in modulating intestinal permeability, which may contribute to the alleviation of systemic inflammation.

C.B regulates the microbiota composition of the HFD fed mice

The above data showed that *C.B* is crucial for mediating the intestinal permeability. We speculated that *C.B* may act as a gut microbiota-modulator to inhibit inflammation and improve dyslipidemia via remodeling the microbiota. To elucidate the impact of dietary *C.B* intervention on gut microbial ecology, we performed comprehensive 16S rRNA gene sequencing analysis to characterize alterations in intestinal microbiota composition. Microbial α-diversity was quantitatively assessed using established ecological indices, including observed operational taxonomic units (OTUs), Chao1 richness estimator, Shannon diversity index, and Simpson diversity index, across three experimental groups (ND + Saline, HFD + Saline, HFD + *C.B*). As illustrated in Figures 5A–C, Shannon's diversity index was lower in the HFD group than ND group. This was restored by *C.B*. Moreover, the Simpson index and Chao1 index showed the same trend among three groups. Principal coordinates analysis (PCoA) of the fecal microbiota based on weighted_unifrac was used to measure overall structure difference among different groups. As demonstrated in Figure 5D, distinct clustering patterns were observed, indicating differential microbial community structures in response to *C.B* interventions. These results revealed that HFD feeding significantly reduced gut microbial richness, as evidenced by decreased observed species counts, while *C.B* intervention effectively restored bacterial diversity and induced structural reorganization of the gut microbiota community.

To identify differentially abundant microbial taxa across experimental groups, we performed linear discriminant analysis effect size (LEfSe) analysis. As illustrated in Figures 5E,F, the analysis revealed distinct microbial signatures with significant differences in taxonomic abundance spanning multiple phylogenetic levels, from phylum to species. LEfSe analysis identified several significantly enriched bacterial taxa in the HFD group, including *S_Mucispirillum_schaedleri* (species), *o_Deferribacterales* (order), *p_Deferribacteres* (phylum), *g_Mucispirillum* (genus), *f_Deferribacteraceae* (family), *p_Proteobacteria* (phylum), *f_Desulfovibrionaceae* (family), and *o_Desulfovibrionales* (order). Notably, comparative analysis revealed distinct microbial signatures in the *C.B*-treated group, demonstrating significant alterations in dominant bacterial populations compared to HFD controls. These findings suggest that *C.B* intervention induces substantial remodeling of the gut microbial community structure in HFD-fed mice.

10.3389/fmicb.2025.1580847

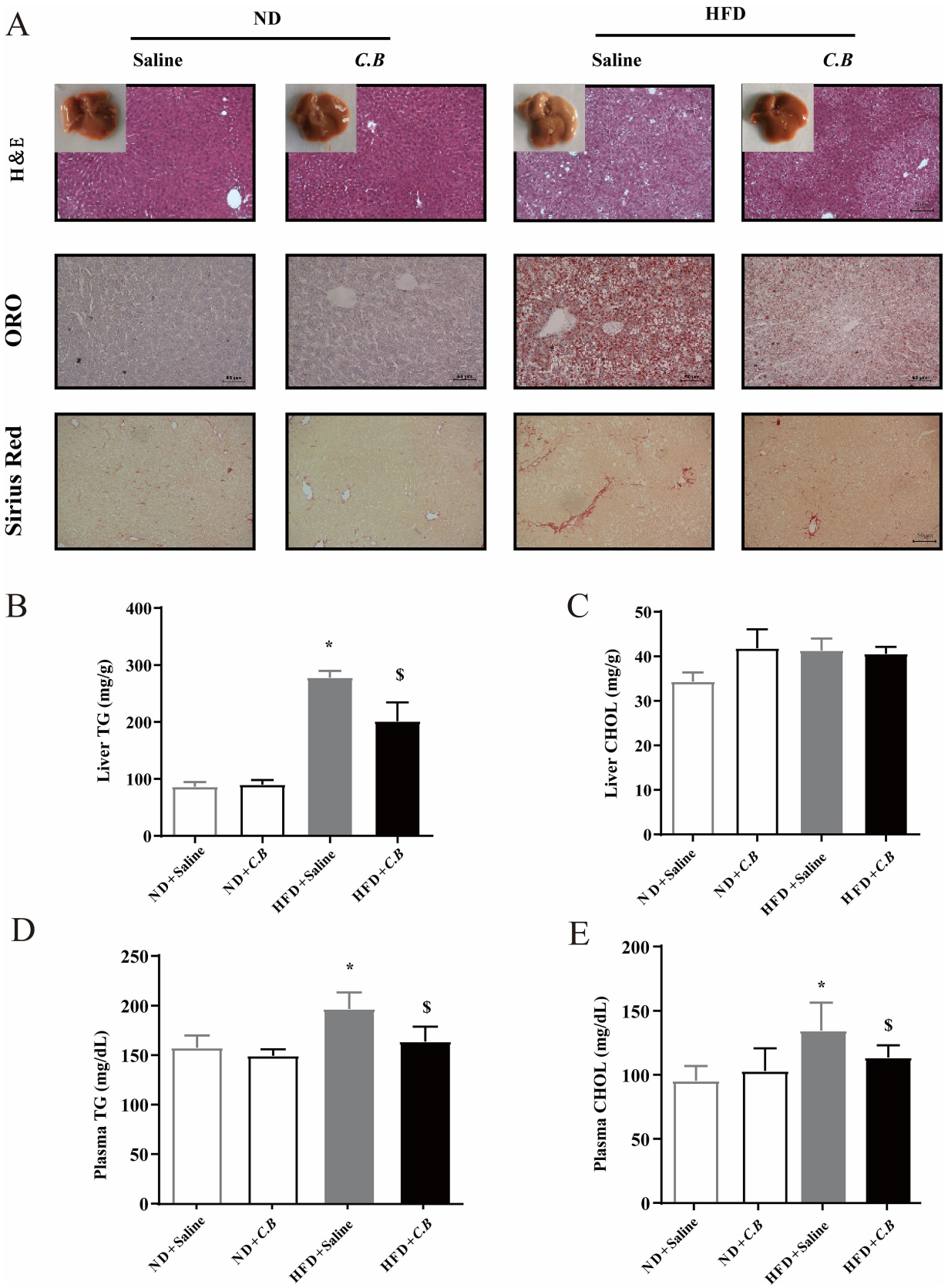

FIGURE 2
C.B ameliorated hyperlipemia and ectopic lipid deposition of obese mice. **(A)** Representative images of liver sections stained with H&E, Oil Red O, and Sirius Red (scale bars, 50 μm). **(B,C)** Quantification of hepatic triglycerides and cholesterol. **(D,E)** Serum levels of triglycerol and cholesterol. Statistical significance was determined by two-way ANOVA with Tukey tests for multiple-group comparisons, data are expressed as mean ± SEM, (n = 5–7). * $p < 0.05$ vs. ND + Saline, $^{\$}$ $p < 0.05$ vs. HFD + Saline.

10.3389/fmicb.2025.1580847

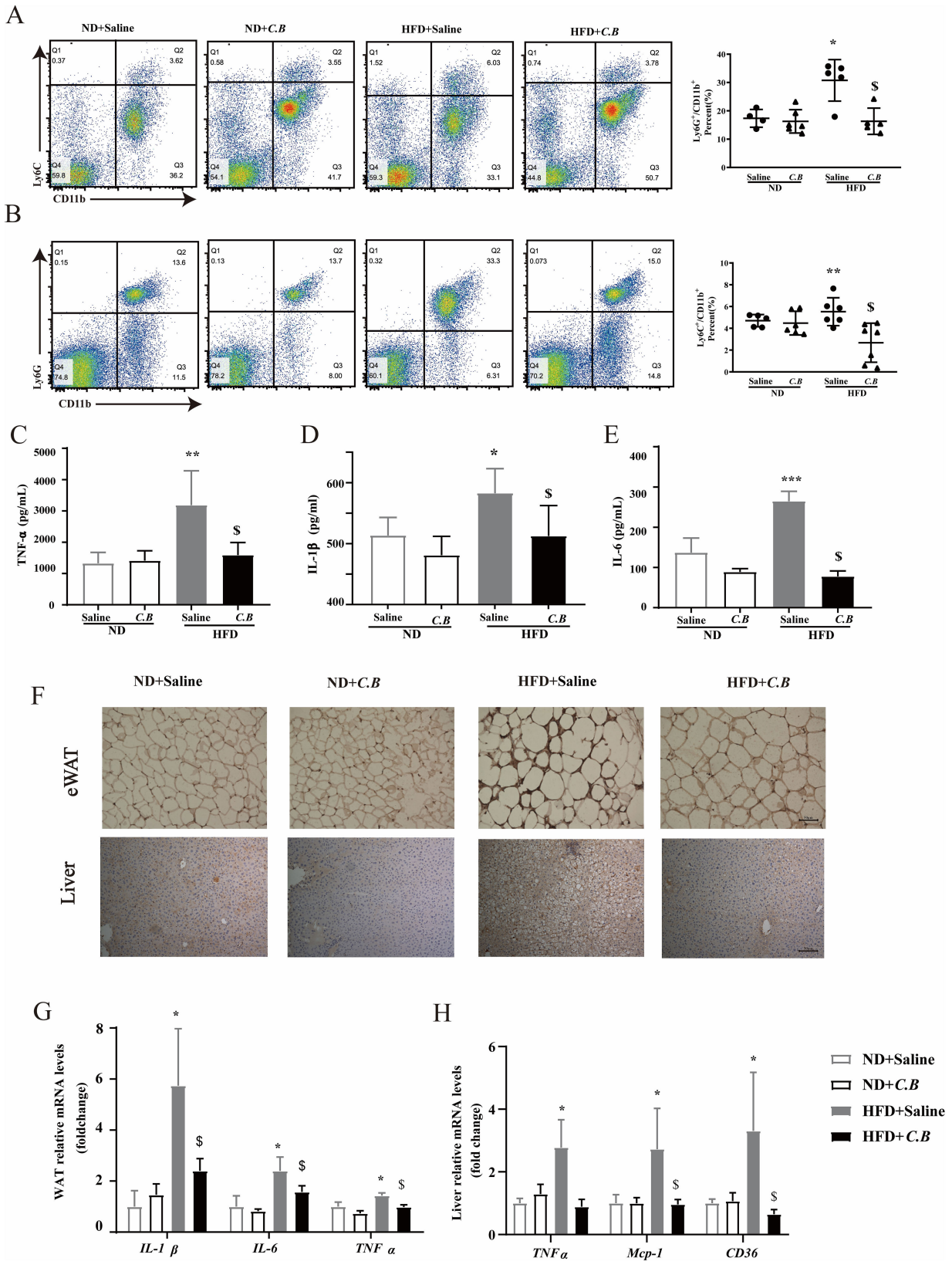

FIGURE 3
C.B protects systemic inflammation of obese mice. **(A)** Fluorescence-activated cell sorting (FACS) analysis of $CD11b^{+}Ly6C^{hi}Ly6G^{-}$ in PBMC. **(B)** FACS analysis of $CD11b^{+}Ly6C^{hi}Ly6G^{+}$. **(C–E)** Serum levels of IL-6, IL-1b and TNF-α were detected by ELISA. **(F)** Representative images for immunostaining of F4/80 in adipose tissues and liver section from four groups (scale bars, 50 μm). **(G,H)** qPCR results of pro-inflammatory genes expression in adipose and liver tissue from four groups. Statistical significance was determined by two-way ANOVA with Tukey tests for multiple-group comparisons. Data are mean ± SEM, (n = 5–7). * $p < 0.05$ vs. ND + Saline, $^{\$}$ $p < 0.05$ vs. HFD + Saline.

10.3389/fmicb.2025.1580847

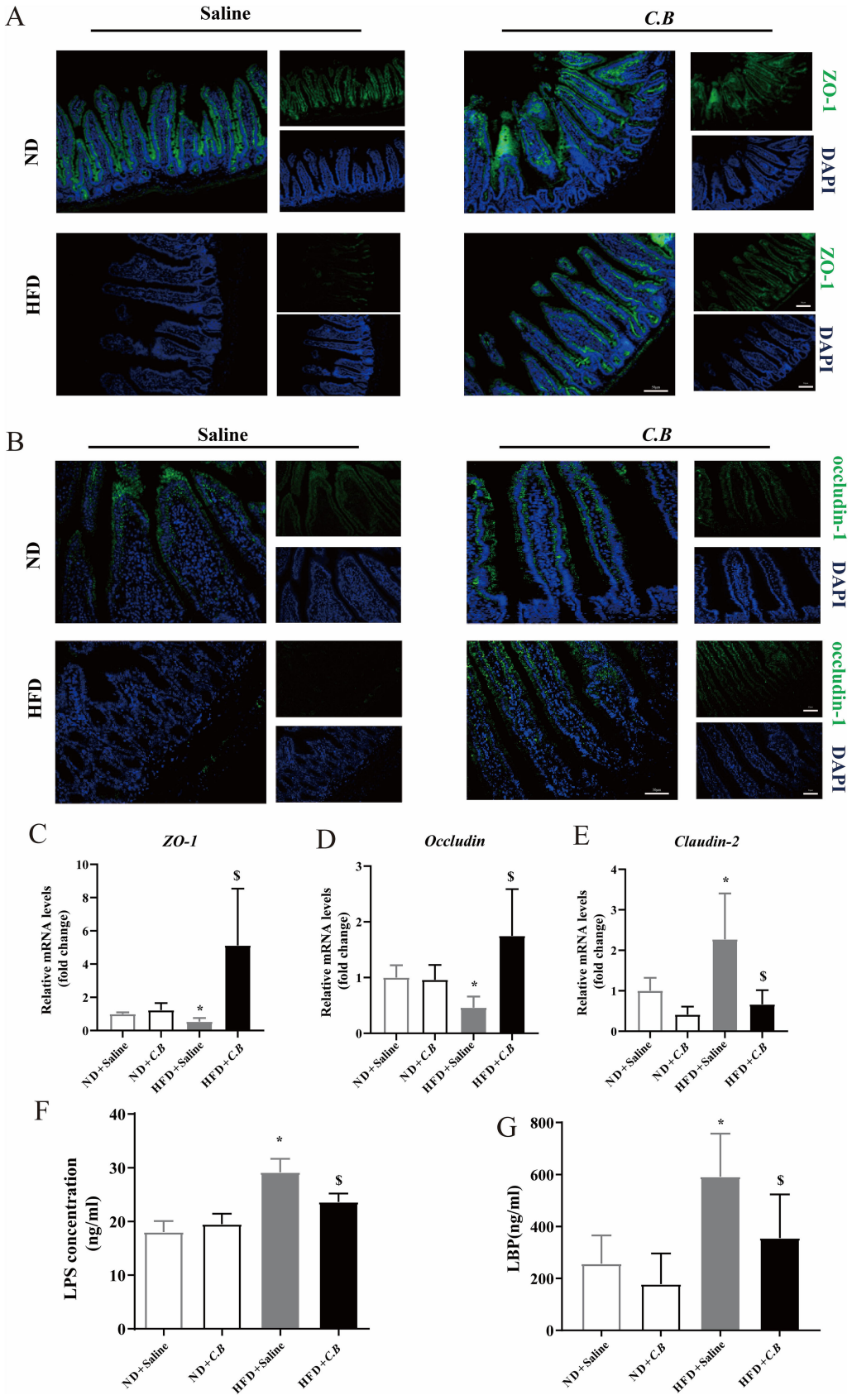

FIGURE 4
C.B protects the disturb of intestinal barrier in obese mice. **(A,B)** Immunohistochemistry of ZO-1 and occludin, (scale bars, 50 μm). **(C–E)** The expression of the zo-1, Occludin and Claudin-2 genes in the intestinal. **(F,G)** Serum LPS and LBP concentration. Statistical significance was determined by two-way ANOVA with Tukey tests for multiple-group comparisons. Results were shown as mean ± SEM (n = 6). * $p < 0.05$ vs. ND + Saline group, $^{\$}$ $p < 0.05$ vs. HFD + Saline group.

10.3389/fmicb.2025.1580847

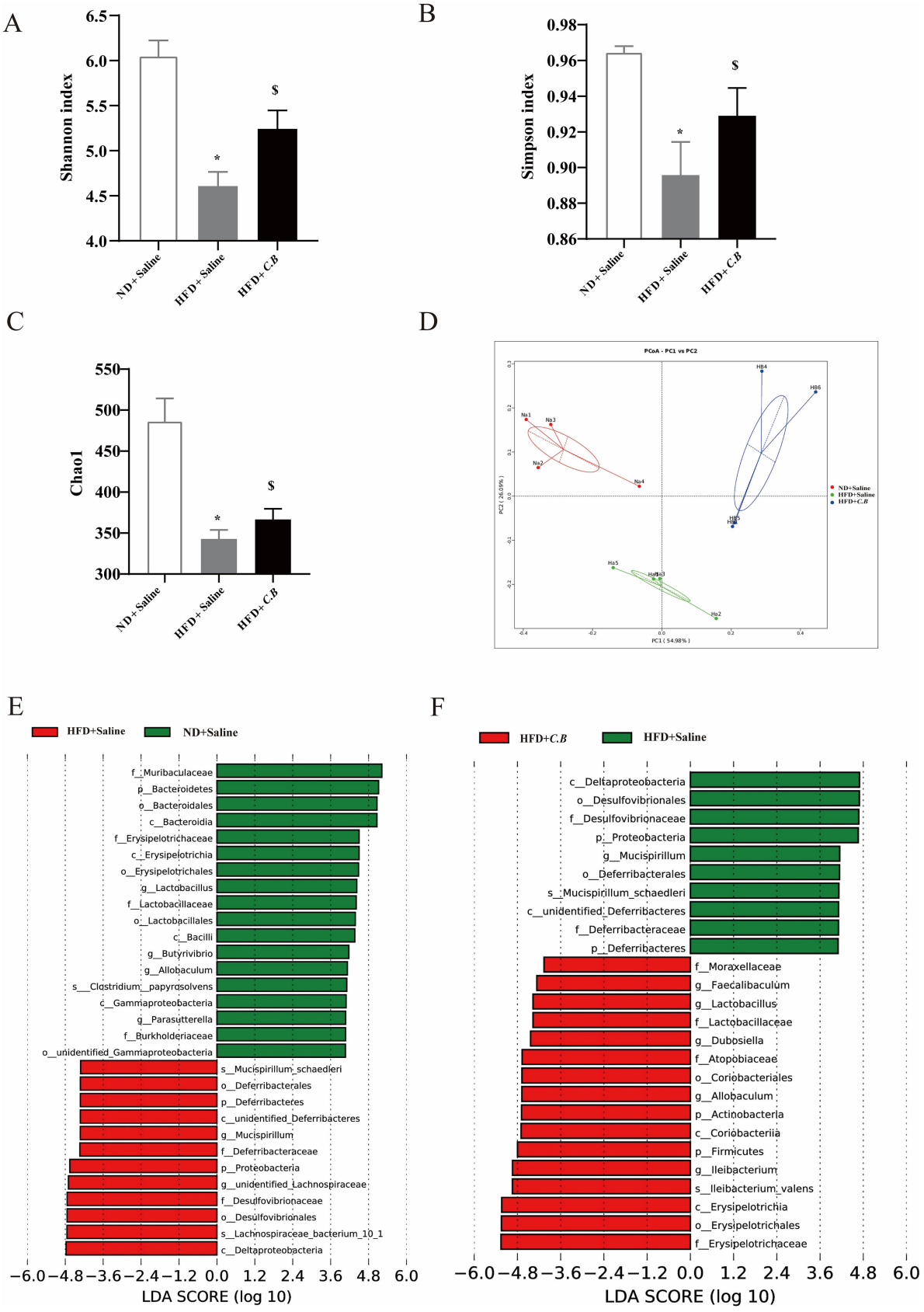

FIGURE 5
C.B protects gut microbiota dysbiosis in obese mice. **(A–C)** Alpha diversity between the chow and HFD groups: Shannon index **(A)**, Simpson index **(B)** and Chao1 index **(C)**. Statistical significance was determined by two-way ANOVA with Tukey tests for multiple-group comparisons. **(D)** The *β*-

(Continued)

FIGURE 5 (Continued)
diversity of gut microbiota was determined by principal coordinate analysis based on the unweighted unique fraction metric distance. **(E,F)** LEfSe analysis shows the species that best explain differences between **(E)** the ND and HFD groups and **(F)** the HFD and HFD + *C.B* groups. The taxonomic levels were indicated as "s" = species; "g" = genus; "f" = family; "o" = order. LDA, linear discriminant analysis; PCoA, principal coordinates analysis. Results were shown as mean ± SEM (n = 4). * $p < 0.05$ vs. ND + Saline group, $^{\$}$ $p < 0.05$ vs. HFD + Saline group.

C.B act as a gut microbiota-modulator keeping the balance between dominant and inferior flora

To further clarify the role of *C.B* as a gut microbiota-modulator, we compared the relative abundances of the predominant phyla and species in the three groups, especially taxa whose abundances were altered in response to *C.B* administration. At the phylum level, taxonomic profiling revealed a significant increase in the relative abundance of *Proteobacteria* and a concurrent decrease in *Actinobacteria* in HFD-fed mice compared to ND controls. Remarkably, *C.B* intervention effectively normalized these HFD-induced phylum-level alterations, restoring the relative abundances of both *Proteobacteria* and *Actinobacteria* to levels comparable to those observed in ND mice (Figure 6A). At the family level, microbial analysis revealed that HFD-fed mice exhibited a significant increase in the abundance of *Desulfovibrionaceae*, a bacterial family associated with LPS production, coupled with a marked reduction in *Erysipelotrichaceae*, known for its protective role against hepatic steatosis. Importantly, *C.B* intervention effectively counteracted these HFD-induced alterations (Figure 6B), demonstrating its capacity to restore a beneficial microbial profile. Notably, at the genus level, *C.B* administration significantly enhanced the abundance of *Allobaculum*, a well-characterized butyrate-producing genus known for its role in SCFA biosynthesis and maintenance of gut epithelial integrity (Figure 6C). Furthermore, *C.B* intervention markedly increased the relative abundance of *Lactobacillus reuteri*, a well-established probiotic species with demonstrated beneficial effects on host metabolism and intestinal barrier function (Figure 6D).

Next, Tax4Fun2 was applied to predict functional profiles (KEGG pathways) from 16S rRNA data, and significant differences in metabolic pathways between the HFD and HFD + *C.B* groups were analyzed. Notably, cecal microbiota from HFD-fed mice demonstrated marked upregulation of key metabolic pathways, particularly those involved in lipid metabolism, carbohydrate processing, and glycan biosynthesis and metabolism (Figure 6E). Importantly, *C.B* administration demonstrated remarkable efficacy in modulating key metabolic processes, as evidenced by the significant downregulation of lipid biosynthesis pathways, BCAA biosynthesis, and systemic inflammatory signaling cascades (Figure 6E). It has been established that the circulating BCAA levels are associated with the risk of type 2 diabetes (Zhou et al., 2019; White et al., 2018). The serum metabolome of insulin-resistant individuals is characterized by increased levels of BCAA and BCKA (Wang et al., 2011). Surprisingly, we observed that *C.B* decreased the BCAA and BCKA levels of HFD-fed mice (Figure 6F).

Correlation analysis of physical and chemical indicators with intestinal flora

To elucidate the potential functional relationships between the six most abundant OTUs and systemic metabolic parameters in HFD-fed mice, we performed comprehensive correlation analysis using Spearman's rank correlation coefficient to assess associations with serum biochemical markers and obesity-related metabolic indices. *Proteobacteria* and *Desulfovibrionaceae* exhibited significant positive correlations with pro-inflammatory markers (TNF-α and IL-6), glucose intolerance (GTT AUC), and branched-chain keto acid (BCKA) levels (Figure 6G). Furthermore, beneficial microbial taxa, including *Actinobacteria*, *Erysipelotrichaceae*, *Allobaculum*, and *Lactobacillus reuteri*, showed significant inverse relationships with key metabolic indicators, particularly the circulating BCAA/BCKA and LPS concentrations. These findings suggest that *C.B*-induced modulation of these bacterial populations may play a crucial role in ameliorating obesity-associated metabolic dysregulation by simultaneously regulating metabolite profiles of intestinal flora.

Discussion

Accumulating evidence suggests that HFD-induced GMD represents a pivotal factor in the disruption of energy homeostasis, impairment of intestinal barrier integrity, and development of systemic low-grade inflammation (Fan et al., 2022; Ren et al., 2023; Potrykus et al., 2021). It is urgent to find strategies to alleviate the intestinal barrier and inflammation. Previous clinical studies have demonstrated that *Clostridium butyricum* effectively ameliorates dextran sulfate sodium (DSS)-induced intestinal pathologies, including fibrosis, inflammation, and barrier dysfunction in pediatric patients (Ma et al., 2022; Stoeva et al., 2021). However, the therapeutic potential of *Clostridium butyricum* in addressing obesity-associated intestinal complications remains largely unexplored. In this study, we demonstrated that *C.B 337279* effectively ameliorates HFD-induced metabolic disorders through gut microbiota remodeling and modulation of microbial metabolites in obese mice. Our findings reveal that administration of *C.B* during the final phase of HFD feeding significantly enhanced microbial α-diversity, as evidenced by increased Shannon and Simpson indices. Furthermore, PCoA of β-diversity revealed distinct clustering patterns and significant alterations in microbial community structure between *C.B*-treated and HFD control groups.

The gut microbiota plays a pivotal role in the pathogenesis of diet-associated metabolic disorders, with substantial evidence demonstrating its involvement in the development of intestinal barrier dysfunction (leaky gut syndrome) and obesity-related systemic metabolic complications (Wang et al., 2022; Xu et al., 2022). Consistent with previous findings, our analysis revealed that HFD decreased the richness and diversity of gut microbes. Notably, *C.B* functioned as a gut microbiota-modulator effectively and restored gut microbial diversity and enhanced bacterial richness, demonstrating its capacity to ameliorate HFD-induced dysbiosis. Specifically, *C.B*-treated HFD mice exhibited significant enrichment of beneficial butyrate-producing bacterial taxa, including *Faecalibaculum* (genus), *Factobacillus* (genus) *and*

10.3389/fmicb.2025.1580847

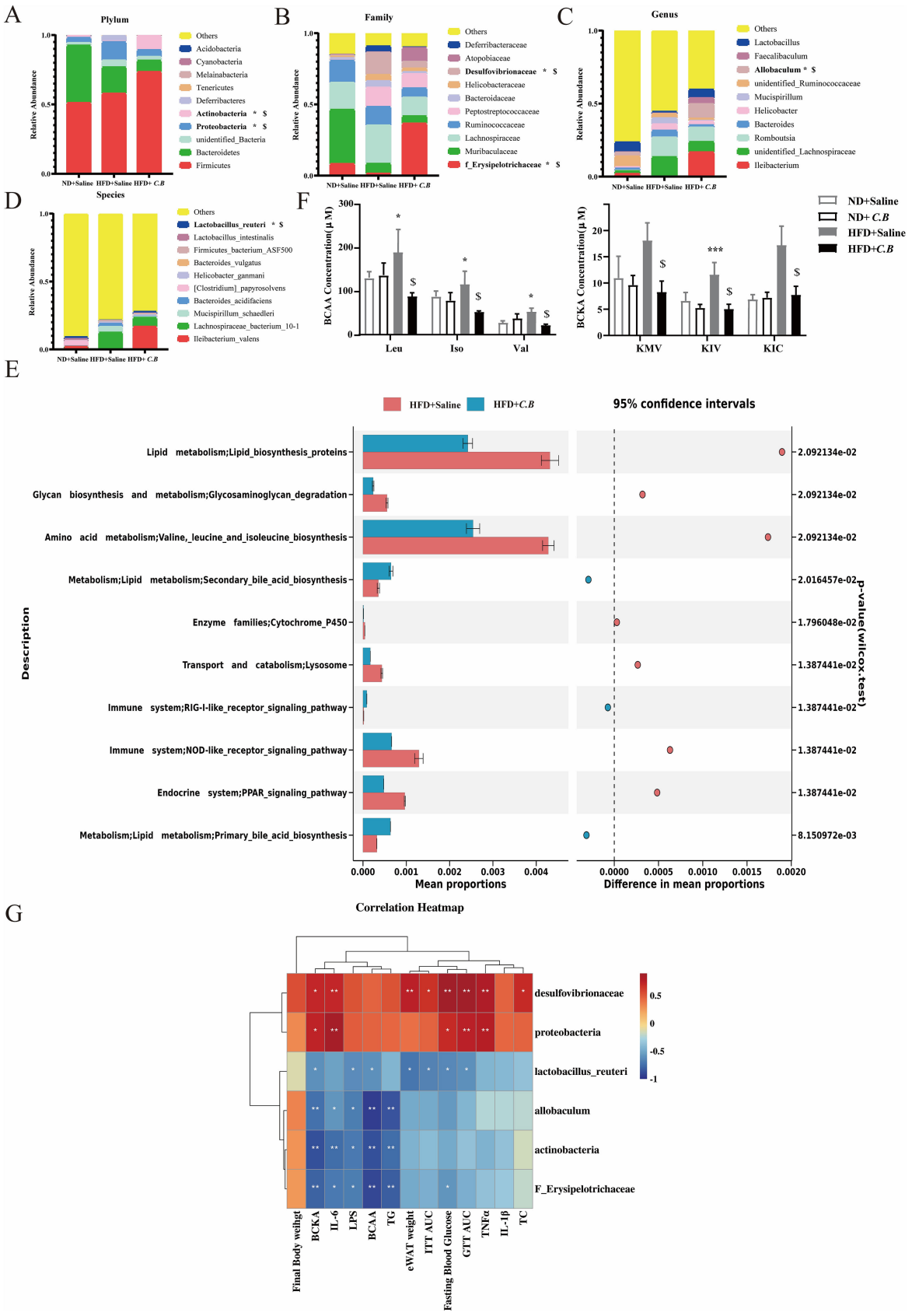

FIGURE 6
C.B act as a gut microbiota-modulator remodeling the abundance of flora related with BCAA biosynthesis and systematic inflammation. **(A–D)** Relative abundance of the gut microbiota at the plylums **(A)**, family **(B)**, genus **(C)**, and specie level **(D)**. Results were shown as mean ± SEM (n = 4).* $p < 0.05$ vs.

(Continued)

FIGURE 6 (Continued)
ND + Saline group, $^{\$}$ $p < 0.05$ vs. HFD + Saline group. **(E)** Function prediction of the functional gene composition between the HFD group and HFD + *C.B* group based on Tax4Fun. The middle shows the difference ratio of functional abundance within the 95% confidence interval. **(F)** Plasma levels of BCAAs and BCKAs ($n = 8$). **(G)** Partial Spearman's correlation analyses between significant metabolites and gut microbiota. All values are expressed as the mean ± SEM ($n = 4$). * $p < 0.05$, *** $p < 0.001$ vs. ND + Saline group, $^{\$}$ $p < 0.05$ vs. HFD + Saline group.

Erysipelotrichaceae (family) (Figure 6). These SCFA-producing bacteria play a crucial role in maintaining intestinal epithelial barrier function through the production of SCFAs, attenuating systemic inflammatory responses and promoting metabolic homeostasis (Wang et al., 2023). Members of the *Lactobacillaceae* family have emerged as promising probiotic candidates with significant potential in promoting host metabolic health (Chuandong et al., 2024). Furthermore, *Erysipelotrichaceae* has been increasingly recognized for its anti-obesity properties and beneficial metabolic effects (Zeng et al., 2023; Tong et al., 2021). Furthermore, *C.B* intervention significantly reduced the relative abundance of *Desulfovibrionaceae*, a bacterial family associated with LPS production and pro-inflammatory responses (Zhao et al., 2020). Notably, *C.B* administration also attenuated the expansion of *Proteobacteria*, a well-established microbial marker of gut dysbiosis and intestinal barrier dysfunction (Shin et al., 2015). Importantly, some studies described that the gut microbiota of obese animals and humans exhibits a higher *Firmicutes*/*Bacteroidetes* ratio, proposing this ratio as an eventual biomarker. In the current study, HFD indeed significantly enhanced the ratio of *p_Firmicutes*/*p_Bacteroidetes*, while *C.B* administration had no effect on this ratio.

GDM is a major determinant of low-grade inflammation by disrupting the function of the intestinal barrier scaffold. Evidences showed GDM has strong association with metabolic disorder (Violi et al., 2023). Orally administered *C.B* spores germinate and grow in intestinal tracts, and produce large amounts of SCFAs (Sato and Tanaka, 1997). Several animal studies showed that LPS induced systematic inflammation and increased serum FFA level (Cani et al., 2008). Our findings demonstrate that *C.B* administration significantly reduced the abundance of LPS-producing *Desulfovibrionaceae*. Furthermore, the observed upregulation of tight junction protein-encoding genes, coupled with a marked decrease in circulating LPS levels, provides compelling evidence that *C.B* intervention effectively enhances intestinal barrier integrity and reduces endotoxemia. Importantly, *C.B* supplementation decreased the gut microbiota related to lipogenesis and increased the gut microbiota related to secondary bile acid biosynthesis (Figure 6E). These results were further supported by the decreased lipid content in plasma and in liver, however, the mechanism underlying this finding need further study.

Circulating levels of BCAA are related with IR and postulated as predictive biomarkers of T2DM (Zhou et al., 2019; White and Newgard, 2019; Ramzan et al., 2022). Our previous studies showed that BCAA supplementation elevated the plasma level of BCAA and counteracted exercise-attenuated IR in obese mice (Cao et al., 2024). These results prompted the importance of regulation the serum BCAA within a normal range. Bacteria are capable of numerous biochemical processes, including digestion of proteins or peptides that escaped absorption in the upper part of the digestive tract (Wang et al., 2022). It has been reported that gut bacterial proteins encompass a higher ratio of BCAA to other amino acids compared with the mammalian organism (Dai et al., 2011). Notably, the abundance of *B. stercoris* in human participants was positively correlate with BCAA (statistically significant for valine) and promotes NAFLD (Ni et al., 2023). Here, we found the top 10 KEGG pathways were enriched based on microbiota function. The up-regulated pathways of cecal microbiota in obese mice included lipid metabolism, glycan biosynthesis and metabolism and BCAA biosynthesis were significantly down regulated after 2-month *C.B* intervention. This was consistent with the decreases of serum BCAA/BCKA. It is widely accepted that some gut metabolites may leak into circulation, which may have directly impact on host metabolism (Stoeva et al., 2021; Wang et al., 2022). Therefore, we speculate the decreased serum levels of BCAA may partly result from the more tight junction in *C.B* treated HFD group mice. Altogether, the above results suggested that *C.B* can alleviate metabolic disorder of obese mice, at least partially through inhibition of LPS and BCAA biosynthesis.

BCAA levels in mouse blood are determined by the ingested food, tissue metabolism of BCAAs, and gut microbe (Kannaiyan et al., 2025). Gut bacteria possess autonomous BCAA biosynthesis capacity, and the entire BCAA biosynthetic pathway is induced in the gut microbiota of obese compared to lean humans (Ridaura et al., 2013). Meanwhile, it has been shown that the colonization of *Bacteroides* in obese mice enhances gut BCAA degradation efficiency, reducing microbial production of BCAA, ultimately leading to decreased circulating BCAA levels in the host (Yoshida et al., 2021). Another research found that increased BCAA biosynthesis and depletion for genes encoding the transport system for bacterial BCAA uptake (referred to as inward BCAA transport) in the gut microbiome of insulin-resistant individuals contribute to an increased BCAA pool (Pedersen et al., 2016). Therefore, it is possible that *C.B* affects the BCAA biosynthesis, degradation, and uptake by gut microbe. On the other hand, *C.B* may affect tissue BCAA metabolism in host. BCAAs cannot be synthesized *de novo* in mammalian cells. The plasma BCAA levels can be affected by BCAA uptake, catabolism, or release by tissue cells, which possibly affected by *C.B* through unknown mechanism. Nevertheless, the potential mechanisms by which *C.B* may influence BCAA levels guarantee further exploration.

In conclusion, our study revealed that orally administration of *Clostridium butyricum 337279* reversed obese mice metabolic disorder mainly by altering gut microbiota composition and functionality, which lowered circulating BCAA/BCKA, LPS levels, alleviate key obesity indexes (body weight, WAT, plasma TG/TC) and systematic inflammation. These results indicated a novel mechanism of *C.B* for obesity that improve metabolic disorder at least partially through decreasing LPS and BCAA production of intestinal flora. Our findings might contribute to further understanding of obesity and the development of innovative microbiome-based therapeutics.

Data availability statement

The datasets presented in this study can be found in online repositories. The names of the repository/repositories and accession number(s) can be found in the article/Supplementary material.

Ethics statement

The animal study was approved by the Experimental Animal Ethics Committee of Chu Hsien-I Memorial Hospital, Tianjin Medical University/Wenjun Qi. The study was conducted in accordance with the local legislation and institutional requirements.

Author contributions

XZ: Data curation, Investigation, Methodology, Writing – original draft. ZL: Data curation, Formal analysis, Writing – original draft. JC: Formal analysis, Methodology, Writing – original draft. HS: Conceptualization, Supervision, Writing – original draft, Writing – review & editing. WN: Resources, Supervision, Writing – original draft, Writing – review & editing.

Funding

The author(s) declare that financial support was received for the research and/or publication of this article. This work was supported by the National Natural Science Foundation of China (No. 81870547, 82270856, 32200965),Tianjin Municipal Science and Technology Commission (No. 22JCQNJC01330), and Tianjin Key Medical Discipline (Specialty) Construction Project (TJYXZDXK-032A).

Conflict of interest

The authors declare that the research was conducted in the absence of any commercial or financial relationships that could be construed as a potential conflict of interest.

Generative AI statement

The authors declare that no Gen AI was used in the creation of this manuscript.

Publisher's note

All claims expressed in this article are solely those of the authors and do not necessarily represent those of their affiliated organizations, or those of the publisher, the editors and the reviewers. Any product that may be evaluated in this article, or claim that may be made by its manufacturer, is not guaranteed or endorsed by the publisher.

Supplementary material

The Supplementary material for this article can be found online at: https://www.frontiersin.org/articles/10.3389/fmicb.2025.1580847/full#supplementary-material

References

Acciarino, A., Diwakarla, S., Handreck, J., Bergola, C., Sahakian, L., and McQuade, R. M. (2024). The role of the gastrointestinal barrier in obesity-associated systemic inflammation. *Obes. Rev.* 25:e13673. doi: 10.1111/obr.13673

Cani, P. D., Bibiloni, R., Knauf, C., Waget, A., Neyrinck, A. M., Delzenne, N. M., et al. (2008). Changes in gut microbiota control metabolic endotoxemia-induced inflammation in high-fat diet-induced obesity and diabetes in mice. *Diabetes* 57, 1470–1481. doi: 10.2337/db07-1403

Cao, W., Liu, Y., Wei, H., Dong, Y., Sun, H., Zhang, X., et al. (2024). Aerobic exercise attenuates insulin resistance via restoring branched chain amino acids homeostasis in obese mice. *Front. Nutr.* 11:1451429. doi: 10.3389/fnut.2024.1451429

Cassir, N., Benamar, S., and La Scola, B. (2016). Clostridium butyricum: from beneficial to a new emerging pathogen. *Clin. Microbiol. Infect.* 22, 37–45. doi: 10.1016/j.cmi.2015.10.014

Chuandong, Z., Hu, J., Li, J., Wu, Y., Wu, C., Lai, G., et al. (2024). Distribution and roles of Ligilactobacillus murinus in hosts. *Microbiol. Res.* 282:127648. doi: 10.1016/j.micres.2024.127648

Cresci, G. A., Glueck, B., McMullen, M. R., Xin, W., Allende, D., and Nagy, L. E. (2017). Prophylactic tributyrin treatment mitigates chronic-binge ethanol-induced intestinal barrier and liver injury. *J. Gastroenterol. Hepatol.* 32, 1587–1597. doi: 10.1111/jgh.13731

Dabke, K., Hendrick, G., and Devkota, S. (2019). The gut microbiome and metabolic syndrome. *J. Clin. Invest.* 129, 4050–4057. doi: 10.1172/JCI129194

Dai, Z. L., Wu, G., and Zhu, W. Y. (2011). Amino acid metabolism in intestinal bacteria: links between gut ecology and host health. *Front Biosci (Landmark Ed)* 16, 1768–1786. doi: 10.2741/3820

Fan, Z., Zhang, X., Shang, Y., Zou, M., Zhou, M., Qiukai, E., et al. (2022). Intestinal Flora changes induced by a high-fat diet promote activation of primordial follicles through macrophage infiltration and inflammatory factor secretion in mouse ovaries. *Int. J. Mol. Sci.* 23:4797. doi: 10.3390/ijms23094797

Kang, Y., Kang, X., Yang, H., Liu, H., Yang, X., Liu, Q., et al. (2022). Lactobacillus acidophilus ameliorates obesity in mice through modulation of gut microbiota dysbiosis and intestinal permeability. *Pharmacol. Res.* 175:106020. doi: 10.1016/j.phrs.2021.106020

Kannaiyan, S. P., Prasanna, A., Chaganti, S., Perin, M., Dinakar, S., Khedekar, S., et al. (2025). Branched-chain amino acids in obesity and diabetes: implications and insights. *Int J Med Biochem* 8, 139–150. doi: 10.14744/ijmb.2025.16779

Karusheva, Y., Koessler, T., Strassburger, K., Markgraf, D., Mastrototaro, L., Jelenik, T., et al. (2019). Short-term dietary reduction of branched-chain amino acids reduces meal-induced insulin secretion and modifies microbiome composition in type 2 diabetes: a randomized controlled crossover trial. *Am. J. Clin. Nutr.* 110, 1098–1107. doi: 10.1093/ajcn/nqz191

Koh, A., de Vadder, F., Kovatcheva-Datchary, P., and Bäckhed, F. (2016). From dietary Fiber to host physiology: short-chain fatty acids as key bacterial metabolites. *Cell* 165, 1332–1345. doi: 10.1016/j.cell.2016.05.041

Lee, H., An, J., Kim, J., Choi, D., Song, Y., Lee, C. K., et al. (2022). A novel bacterium, Butyricimonas virosa, preventing HFD-induced diabetes and metabolic disorders in mice via GLP-1 receptor. *Front. Microbiol.* 13:858192. doi: 10.3389/fmicb.2022.858192

Lemieux, I., and Després, J. P. (2020). Metabolic syndrome: past, present and future. *Nutrients* 12:3501. doi: 10.3390/nu12113501

Li, Z., Zhang, R., Mu, H., Zhang, W., Zeng, J., Li, H., et al. (2022). Oral Administration of Branched-Chain Amino Acids Attenuates Atherosclerosis by inhibiting the inflammatory response and regulating the gut microbiota in ApoE-deficient mice. *Nutrients* 14:5065. doi: 10.3390/nu14235065

Ma, L., Shen, Q., Lyu, W., lv, L., Wang, W., Yu, M., et al. (2022). Clostridium butyricum and its derived extracellular vesicles modulate gut homeostasis and ameliorate acute experimental colitis. *Microbiol Spectr* 10:e0136822. doi: 10.1128/spectrum.01368-22

Mann, E. R., Lam, Y. K., and Uhlig, H. H. (2024). Short-chain fatty acids: linking diet, the microbiome and immunity. *Nat. Rev. Immunol.* 24, 577–595. doi: 10.1038/s41577-024-01014-8

Mitev, K., and Taleski, V. (2019). Association between the gut microbiota and obesity. *Open Access Maced. J. Med. Sci.* 7, 2050–2056. doi: 10.3889/oamjms.2019.586

Nascimento, J. C., Matheus, V. A., Oliveira, R. B., Tada, S. F. S., and Collares-Buzato, C. B. (2021). High-fat diet induces disruption of the tight junction-mediated Paracellular barrier in the proximal small intestine before the onset of type 2 diabetes and Endotoxemia. *Dig. Dis. Sci.* 66, 3359–3374. doi: 10.1007/s10620-020-06664-x

Neis, E. P., Dejong, C. H., and Rensen, S. S. (2015). The role of microbial amino acid metabolism in host metabolism. *Nutrients* 7, 2930–2946. doi: 10.3390/nu7042930

Ni, Y., Qian, L., Siliceo, S. L., Long, X., Nychas, E., Liu, Y., et al. (2023). Resistant starch decreases intrahepatic triglycerides in patients with NAFLD via gut microbiome alterations. *Cell Metab.* 35, 1530–1547.e8. doi: 10.1016/j.cmet.2023.08.002

Oh, S. F., Praveena, T., Song, H., Yoo, J. S., Jung, D. J., Erturk-Hasdemir, D., et al. (2021). Host immunomodulatory lipids created by symbionts from dietary amino acids. *Nature* 600, 302–307. doi: 10.1038/s41586-021-04083-0

Pedersen, H. K., Gudmundsdottir, V., Nielsen, H. B., Hyotylainen, T., Nielsen, T., Jensen, B. A., et al. (2016). Human gut microbes impact host serum metabolome and insulin sensitivity. *Nature* 535, 376–381. doi: 10.1038/nature18646

Potrykus, M., Czaja-Stolc, S., Stankiewicz, M., Kaska, Ł., and Małgorzewicz, S. (2021). Intestinal microbiota as a contributor to chronic inflammation and its potential modifications. *Nutrients* 13:3839. doi: 10.3390/nu13113839

Ramzan, I., Ardavani, A., Vanweert, F., Mellett, A., Atherton, P. J., and Idris, I. (2022). The association between circulating branched chain amino acids and the temporal risk of developing type 2 diabetes mellitus: a Systematic Review & Meta-Analysis. *Nutrients* 14:4411. doi: 10.3390/nu14204411

Ren, X., Xu, J., Xu, Y., Wang, Q., Huang, K., and He, X. (2023). Artemether attenuates gut barrier dysfunction and intestinal Flora imbalance in high-fat and high-fructose diet-fed mice. *Nutrients* 15:4860. doi: 10.3390/nu15234860

Ridaura, V. K., Faith, J. J., Rey, F. E., Cheng, J., Duncan, A. E., Kau, A. L., et al. (2013). Gut microbiota from twins discordant for obesity modulate metabolism in mice. *Science* 341:1241214. doi: 10.1126/science.1241214

Riedel, S., Pheiffer, C., Johnson, R., Louw, J., and Muller, C. J. (2021). Intestinal barrier function and immune homeostasis are missing links in obesity and type 2 diabetes development. *Front Endocrinol (Lausanne)* 12:833544. doi: 10.3389/fendo.2021.833544

Sato, R., and Tanaka, M. (1997). Intestinal distribution and intraluminal localization of orally administered Clostridium butyricum in rats. *Microbiol. Immunol.* 41, 665–671. doi: 10.1111/j.1348-0421.1997.tb01909.x

Shin, N. R., Whon, T. W., and Bae, J. W. (2015). Proteobacteria: microbial signature of dysbiosis in gut microbiota. *Trends Biotechnol.* 33, 496–503. doi: 10.1016/j.tibtech.2015.06.011

Stoeva, M. K., Garcia-So, J., Justice, N., Myers, J., Tyagi, S., Nemchek, M., et al. (2021). Butyrate-producing human gut symbiont, Clostridium butyricum, and its role in health and disease. *Gut Microbes* 13, 1–28. doi: 10.1080/19490976.2021.1907272

Tilg, H., Zmora, N., Adolph, T. E., and Elinav, E. (2020). The intestinal microbiota fuelling metabolic inflammation. *Nat. Rev. Immunol.* 20, 40–54. doi: 10.1038/s41577-019-0198-4

Tong, L. T., Xiao, T., Wang, L., Lu, C., Liu, L., Zhou, X., et al. (2021). Plant protein reduces serum cholesterol levels in hypercholesterolemia hamsters by modulating the compositions of gut microbiota and metabolites. *iScience* 24:103435. doi: 10.1016/j.isci.2021.103435

Violi, F., Cammisotto, V., Bartimoccia, S., Pignatelli, P., Carnevale, R., and Nocella, C. (2023). Gut-derived low-grade endotoxaemia, atherothrombosis and cardiovascular disease. *Nat. Rev. Cardiol.* 20, 24–37. doi: 10.1038/s41569-022-00737-2

Wang, T. J., Larson, M. G., Vasan, R. S., Cheng, S., Rhee, E. P., McCabe, E., et al. (2011). Metabolite profiles and the risk of developing diabetes. *Nat. Med.* 17, 448–453. doi: 10.1038/nm.2307

Wang, S., Li, M., Lin, H., Wang, G., Xu, Y., Zhao, X., et al. (2022). Amino acids, microbiota-related metabolites, and the risk of incident diabetes among normoglycemic Chinese adults: findings from the 4C study. *Cell Rep Med* 3:100727. doi: 10.1016/j.xcrm.2022.100727

Wang, G., Liu, J., Zhang, Y., Xie, J., Chen, S., Shi, Y., et al. (2023). Ginsenoside Rg3 enriches SCFA-producing commensal bacteria to confer protection against enteric viral infection via the cGAS-STING-type I IFN axis. *ISME J.* 17, 2426–2440. doi: 10.1038/s41396-023-01541-7

Wang, D., Wang, L., Han, L., Wang, B., Shi, R., Ye, J., et al. (2023). Leucine-restricted diet ameliorates obesity-linked cognitive deficits: involvement of the microbiota-gut-brain Axis. *J. Agric. Food Chem.* 71, 9404–9418. doi: 10.1021/acs.jafc.3c01524

Wang, L., Zhang, P., Li, C., Xu, F., and Chen, J. (2022). A polysaccharide from Rosa roxburghii Tratt fruit attenuates high-fat diet-induced intestinal barrier dysfunction and inflammation in mice by modulating the gut microbiota. *Food Funct.* 13, 530–547. doi: 10.1039/D1FO03190B

White, P. J., McGarrah, R. W., Grimsrud, P. A., Tso, S. C., Yang, W. H., Haldeman, J. M., et al. (2018). The BCKDH kinase and phosphatase integrate BCAA and lipid metabolism via regulation of ATP-citrate Lyase. *Cell Metab.* 27, 1281–1293.e7. doi: 10.1016/j.cmet.2018.04.015

White, P. J., and Newgard, C. B. (2019). Branched-chain amino acids in disease. *Science* 363, 582–583. doi: 10.1126/science.aav0558

Winer, D. A., Luck, H., Tsai, S., and Winer, S. (2016). The intestinal immune system in obesity and insulin resistance. *Cell Metab.* 23, 413–426. doi: 10.1016/j.cmet.2016.01.003

Wong, J. M., de Souza, R., Kendall, C. W., Emam, A., and Jenkins, D. J. (2006). Colonic health: fermentation and short chain fatty acids. *J. Clin. Gastroenterol.* 40, 235–243. doi: 10.1097/00004836-200603000-00015

Xu, Z., Jiang, W., Huang, W., Lin, Y., Chan, F. K., and Ng, S. C. (2022). Gut microbiota in patients with obesity and metabolic disorders – a systematic review. *Genes Nutr.* 17:2. doi: 10.1186/s12263-021-00703-6

Yao, Y., Cai, X., Fei, W., Ye, Y., Zhao, M., and Zheng, C. (2022). The role of short-chain fatty acids in immunity, inflammation and metabolism. *Crit. Rev. Food Sci. Nutr.* 62, 1–12. doi: 10.1080/10408398.2020.1854675

Yoshida, N., Yamashita, T., Osone, T., Hosooka, T., Shinohara, M., Kitahama, S., et al. (2021). Bacteroides spp. promotes branched-chain amino acid catabolism in brown fat and inhibits obesity. *iScience* 24:103342. doi: 10.1016/j.isci.2021.103342

Zeng, H., He, S., Xiong, Z., Su, J., Wang, Y., Zheng, B., et al. (2023). Gut microbiota-metabolic axis insight into the hyperlipidemic effect of lotus seed resistant starch in hyperlipidemic mice. *Carbohydr. Polym.* 314:120939. doi: 10.1016/j.carbpol.2023.120939

Zhao, Z., Chen, L., Zhao, Y., Wang, C., Duan, C., Yang, G., et al. (2020). Lactobacillus plantarum NA136 ameliorates nonalcoholic fatty liver disease by modulating gut microbiota, improving intestinal barrier integrity, and attenuating inflammation. *Appl. Microbiol. Biotechnol.* 104, 5273–5282. doi: 10.1007/s00253-020-10633-9

Zhou, M., Shao, J., Wu, C. Y., Shu, L., Dong, W., Liu, Y., et al. (2019). Targeting BCAA catabolism to treat obesity-associated insulin resistance. *Diabetes* 68, 1730–1746. doi: 10.2337/db18-0927

frontiers | Frontiers in Microbiology

TYPE Original Research
PUBLISHED 15 May 2025
DOI 10.3389/fmicb.2025.1531131

Check for updates

OPEN ACCESS

EDITED BY
Mohammad Altamimi,
An-Najah National University, Palestine

REVIEWED BY
Maria Gazouli,
National and Kapodistrian University of Athens, Greece
Ana Maria Calderon De La Barca,
National Council of Science and Technology (CONACYT), Mexico

*CORRESPONDENCE
Joy Scaria
✉ joy.scaria@okstate.edu

RECEIVED 19 November 2024
ACCEPTED 02 April 2025
PUBLISHED 15 May 2025

CITATION
Kidangathazhe A, Amponsah T, Maji A, Adams S, Chettoor M, Wang X and Scaria J (2025) Synthetic vs. non-synthetic sweeteners: their differential effects on gut microbiome diversity and function. *Front. Microbiol.* 16:1531131. doi: 10.3389/fmicb.2025.1531131

COPYRIGHT
© 2025 Kidangathazhe, Amponsah, Maji, Adams, Chettoor, Wang and Scaria. This is an open-access article distributed under the terms of the Creative Commons Attribution License (CC BY). The use, distribution or reproduction in other forums is permitted, provided the original author(s) and the copyright owner(s) are credited and that the original publication in this journal is cited, in accordance with accepted academic practice. No use, distribution or reproduction is permitted which does not comply with these terms.

Synthetic vs. non-synthetic sweeteners: their differential effects on gut microbiome diversity and function

Alex Kidangathazhe[1], Theresah Amponsah[2], Abhijit Maji[1], Seidu Adams[1], Maria Chettoor[1], Xiuqing Wang[2] and Joy Scaria[1,3]*

[1]Department of Veterinary and Biomedical Sciences, South Dakota State University, Brookings, SD, United States, [2]Department of Biology and Microbiology, South Dakota State University, Brookings, SD, United States, [3]Department of Veterinary Pathobiology, Oklahoma State University, Stillwater, OK, United States

The rising use of artificial sweeteners, favored for their zero-calorie content and superior sweetness, necessitates understanding their impact on the gut microbiome. This study examines the effects of five common artificial sweeteners—Acesulfame K, Rebaudioside A, Saccharin, Sucralose, and Xylitol—on gut microbiome diversity using minibioreactor arrays. Fecal samples from three healthy individuals were used to inoculate bioreactors that were subsequently supplemented with each sweetener. Over 35 days, microbial diversity and network composition were analyzed. Results revealed synthetic sweeteners like Sucralose and Saccharin significantly reduced microbial diversity, while non-synthetic sweeteners, particularly Rebaudioside A and Xylitol, were less disruptive. Acesulfame K increased diversity but disrupted network structure, suggesting potential long-term negative impacts on microbiome resilience. Sucralose enriched pathogenic families such as Enterobacteriaceae, whereas natural sweeteners promoted beneficial taxa like Lachnospiraceae. Random Matrix Theory (RMT) based analysis highlighted distinct microbial interaction patterns, with Acesulfame K causing persistent structural changes. Findings suggest non-synthetic sweeteners may be more favorable for gut health than synthetic ones, emphasizing cautious use, particularly for those with gut health concerns. This study enhances our understanding of artificial sweeteners' effects on the gut microbiome, highlighting the need for further research into their long-term health implications.

KEYWORDS

artificial sweetener, gut microbiome, bioreactor, acesulfame K, rebaudioside A, saccharin, sucralose, xylitol

Introduction

As larger portions of the population become aware of the adverse effects of overconsuming natural sugar, many now turn towards zero-calorie alternative sweeteners. These alternative sweeteners can be both synthetic or artificial, but all are non-nutritive; that is, they have negligible caloric content yet are usually sweeter than natural sugar (Radenkovic, 2023; Kossiva et al., 2024). They are substituted in place of sugar in various foods, sometimes becoming even more prevalent than normal sugar. Such alternative sweeteners are added to foods such as desserts, sodas, cereals, dairy products, powdered drink mixes, baked goods, candy, chocolates, puddings, canned foods, jams and jellies, and confectionery chewing gums.

All mainstream sweeteners, including acesulfame K, aspartame, neotame, advantame, saccharin, and sucralose (with the exception of cyclamate, which has not yet been

approved by the FDA) (Sun and Xu, 2025), have been approved for human consumption, given that the allowable daily intake (ADI) is followed (Feng et al., 2024). Since humans cannot metabolize these sweeteners, there are very few direct effects resulting from their consumption. However, previous literature has shown that although the human digestive system cannot directly interact with such sweeteners, another equally important part of the human body, i.e., gut microbiome can and is impacted by it (Lee et al., 2024; Gauthier et al., 2024; Conz et al., 2023; Angelin et al., 2024).

The human gut microbiome is affected by all things that enter the gut, and because of its importance in maintaining homeostasis, any change in the gut can affect the overall health of the human. Previous literature has shown that there are definite interactions between zero-calorie alternative sugars and the gut microbiome (Liu et al., 2024). These interactions have been studied in rats, mice, piglets, hamsters, and humans themselves (Gauthier et al., 2024; Suez et al., 2022; Cyphert et al., 2024). However, there has been a great disparity in the results of such studies, with different sweeteners producing both positive and negative effects on overall health (Conz et al., 2023; Shil et al., 2024).

In this context, bioreactors offer a simple model system for determining the effect of food additives such as artificial sweeteners. Bioreactors offer several key advantages as a model system for studying the gut microbiome compared to animal models (Auchtung et al., 2015; Auchtung et al., 2016). They allow for precise control and reproducibility of environmental factors, enabling the isolation and study of specific variables. Bioreactors facilitate real-time monitoring and sampling, providing insights into dynamic changes over time. For example, bioreactor model has been used to monitor the real-time dynamics of the gut microbiome in response to antibiotic treatment, revealing the rapid shifts in microbial composition and the subsequent recovery process (Guzman-Rodriguez et al., 2018). This real-time monitoring capability allows for a deeper understanding of the temporal dynamics of the gut microbiome, which is more challenging to achieve in animal models. Moreover, bioreactors are cost-effective, ethically advantageous, and offer flexibility and high throughput compared to animal models. Furthermore, bioreactor systems has the potential as an alternative to animal models for studying the gut microbiome, reducing cost, increasing throughput, and the ability to test multiple conditions simultaneously (Agrinier et al., 2024). The use of bioreactors also reduces the need for animal testing, aligning with the principles of the 3Rs (Replacement, Reduction, and Refinement) in animal research (Russell and Burch, 1959). Additionally, bioreactors can be inoculated with human-derived gut microbiota, increasing the relevance of findings to human health. We have previously used minibioreactor arrays to study the modulation of human gut microbiome by dietary fiber and flavonoids (Ghimire et al., 2021). This human-derived inoculation approach enhances the translatability of bioreactor findings to human gut health and disease.

In this study, using minibioreactors arrays, we analyzed the impact of five major artificial sweeteners, i.e., Acesulfame K, Rebaudioside A, Saccharin, Sucralose, and Xylitol on human gut microbiome. Our results show that although all artificial sweeteners tested caused changes to gut microbial diversity indices and network composition, non-synthetic sweeteners were less disruptive when compared to synthetic sweeteners.

Methods

Selection of artificial sweeteners and bioreactor experiments

To ensure that our results would be broadly relevant across human populations, we chose five of the most commonly used artificial sweeteners in food: sucralose, saccharin, rebaudioside A, xylitol, and acesulfame K. We used a minibioreactor array as the model system to determine the impact of these artificial sweeteners on the gut microbiome. Fecal samples were donated by three individuals who had not taken antibiotics in the previous year and did not have any known health issues (e.g., obesity or diarrhea), serving as the source microbiome inoculum in the minibioreactor array. The fecal samples were collected following approval from South Dakota State University Institutional Review Board and were processed in an anaerobic chamber following procedures we published previously (Ghimire et al., 2021). We used modified Brain Heart Infusion Broth (BHI) as it has been shown to support the growth of a broad range of gut bacteria (Fenske et al., 2020; Ghimire et al., 2020). All media and solutions used were pre-reduced in advance. The mini-bioreactors were sterilized, assembled with minor modifications according to previous literature, and placed in a Coy anaerobic chamber maintained at 37°C. Modified BHI media was used as the control, while treatment groups received the sweeteners dissolved in the media. The final experimental groups consisted of modified BHI with the addition of sucralose (96.88 mg/L), acesulfame K (290.6 mg/L), rebaudioside A (232.5 mg/L), xylitol (968.8 mg/L), and saccharin (96.88 mg/L). The input and output of the Watson Marlow pumps were set at 1 and 2 rpm, respectively, and the rotating magnetic stirrer was set at 130 rpm. The media were allowed to flow continuously for 24 h each in 4 replicates. Three hundred microliters of the inoculum was introduced into all replicates with a retention time of 16 h. The minibioreactors were then operated for up to 35 days post-inoculation. The sweeteners were introduced to the media and allowed to run continuously from day 7 to day 21. After treatment with the sweeteners, a run with media lacking artificial sweeteners was continued until the last day of the experiment (day 35). Five hundred microliters of the media was collected for optical density (OD) and pH estimation, as well as sequencing, at days 2, 7, 14, 21, and 35, and directly frozen at −80°C. OD and pH of the samples were estimated using a biophotometer (Eppendorf) and an Orion Star A211 pH meter (Thermo Scientific), respectively.

Microbial community sequencing and bioinformatics analysis of the data

DNA isolation was performed on 144 samples. The DNA was extracted from 500 µL of each sample using a Powersoil DNA isolation kit (MoBio Laboratories Inc., CA) following the manufacturer's instructions. After extraction, the quality of DNA was measured using NanoDrop™ One (Thermo Fisher Scientific, DE) and quantified using a Qubit Fluorometer 3.0 (Invitrogen, CA). The DNA samples were stored at −20°C until further use. To analyze the variation in microbial composition over time, all samples were amplicon sequenced using an Illumina MiSeq platform with 300 base paired-end V3 chemistry. The library was prepared using an Illumina Nextera XT library preparation kit (Illumina Inc., CA) targeting the V3-V4 regions of the 16S rRNA gene. The libraries were bead normalized and multiplexed before

loading into the sequencer. We used QIIME (Bolyen et al., 2019) for Operational Taxonomic Unit (OTU) assignment and taxonomic classification. DADA2 (Callahan et al., 2016) was used as the classifier with the GreenGenes database for taxonomy (DeSantis et al., 2006), and QIIME was otherwise run with default settings. The resulting table was filtered to remove low-abundance species, which may have been anomalies, and then combined with the taxonomic output. Data was further analyzed using R packages such as superheat for the heatmap. The networks were created by grouping the combined OTU and taxonomic data into periods 7–21 (treatment) and periods 28–35 (withdrawal). For the Random Matrix Theory (RMT) based network analysis of the community, these datasets were then independently imported into the program MENA (Deng et al., 2012), where the networks were created and then exported to Cytoscape (Cline et al., 2007; Smoot et al., 2011). Modularity was calculated using the short random walks methodology, and MENA calculated node degree and node centrality. Cytoscape was used to format and correspond network statistics and the visual layout of the network.

Results

Artificial sweeteners induce differential alterations in microbiome diversity and enrich some taxa, particularly members of *Bacillaceae*

To comprehensively understand the impact of the tested artificial sweeteners on the microbial community in the bioreactors, we calculated multiple diversity indices (Figure 1). All indices showed clear and consistent changes in alpha diversity. Three treatments—acesulfame K, rebaudioside A, and xylitol—appeared to slightly increase diversity across all indices. The Observed, Chao1, and ACE indices clearly indicated that acesulfame K provided the greatest increase in diversity. The Shannon, Simpson, and J indices showed a nearly equal increase from both acesulfame K and xylitol, with rebaudioside A being marginally lower or comparable. In contrast, saccharin and sucralose decreased diversity across all indices. However, while saccharin caused only a marginal decrease, sucralose led to a much larger and more significant reduction in diversity. These results highlight the differential effects of artificial sweeteners on microbial community diversity, with some sweeteners promoting diversity while others have detrimental impacts.

Next, we examined the microbiome community compositional changes at the family level. Our experimental approach included a one-week stabilization phase (days 1–7), followed by a two-week artificial sweetener supplementation period (days 7–21) and a 2-week no supplementation phase (days 21–35). The supplementation phase aimed to determine which taxa were enriched or depleted, while the no supplementation phase was intended to assess whether the microbiota could revert to its original composition after the intervention ceased. This analysis (Figure 2) revealed that all treatments exhibited varying levels of change compared to the control. Sucralose was the most divergent from the control, enriching members of *Veillonellaceae*, *Bifidobacteriaceae*, and Enterobacteriaceae while suppressing others to less than 10% of the total community. Interestingly, all

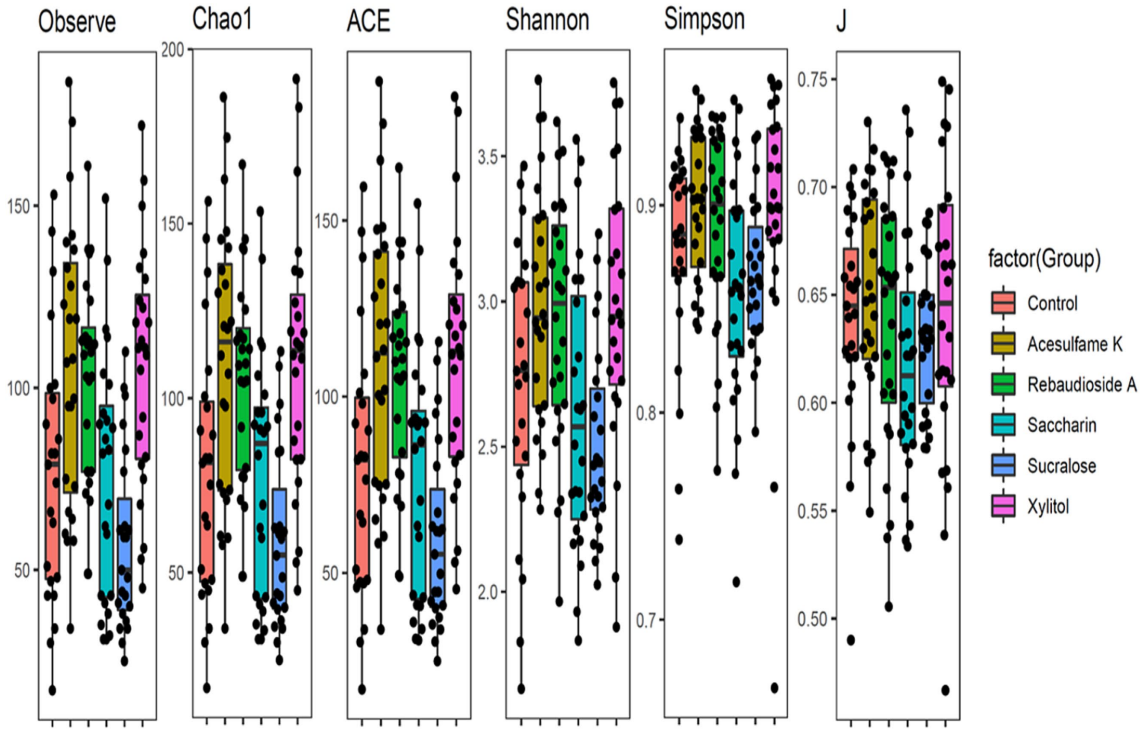

FIGURE 1
Box plots showing diversity metrics of gut microbiota across different artificial sweetener Treatments- The black dots represent individual data points within each group.

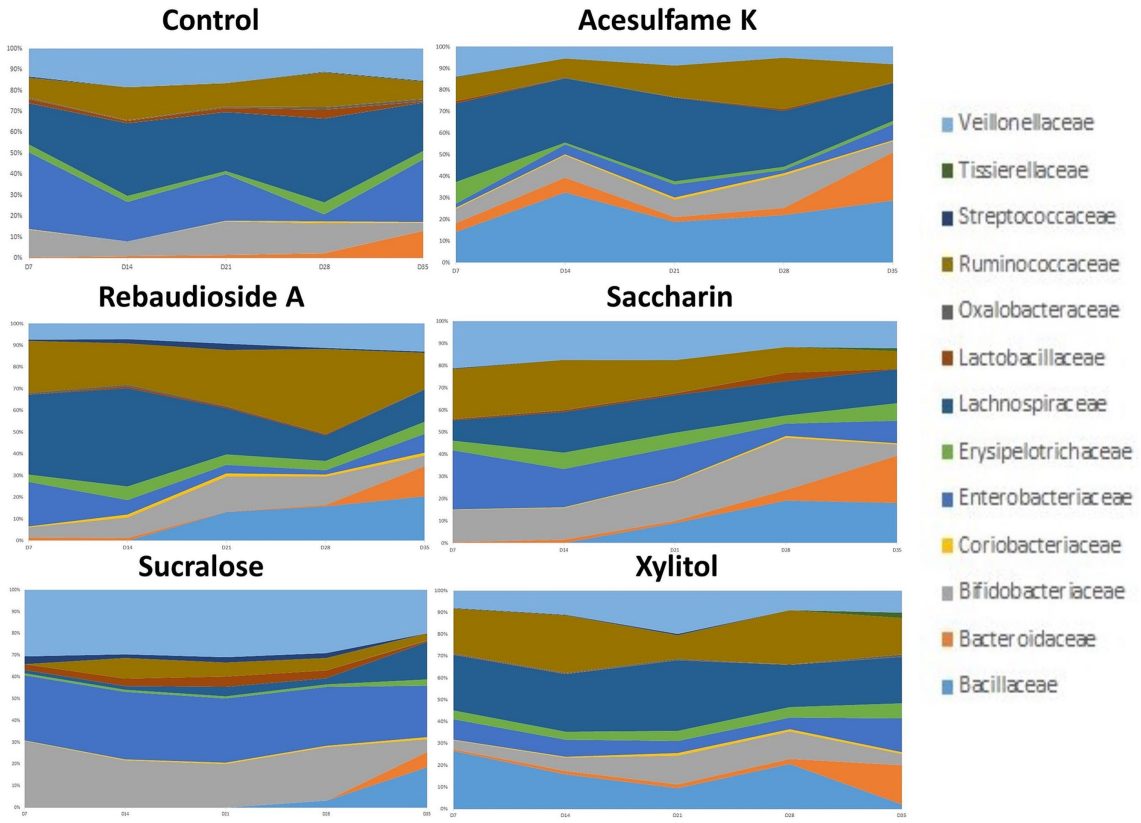

FIGURE 2
Compositional changes of microbiome at family level. The most abundant 13 bacterial taxa at day 7, 14, 21, 28, and 35 are shown. Days 7–21 are artificial sweetener supplementation period. Days 22–35 are withdrawal period.

sweeteners enriched *Bacillaceae*, although this family was not detected in the control group. Among the sweeteners, acesulfame K consistently showed the strongest enrichment of *Bacillaceae*. After the treatment was withdrawn, all the sweetener treated groups began trending towards a composition similar to the control. However, none of them fully reverted to the original community composition by the end of the 14-day withdrawal period.

Motivated by the enrichment of specific families in the treated groups, we further investigated the microbiome composition at the genus level. Figure 3 presents the top 19 genera found in each treatment group. While all treatments enriched multiple genera, sucralose uniquely enriched *Bifidobacterium*, a genus not observed in any other treatment. *Lactobacillus* and *Ruminococcus* were also enriched, consistent with the family-level analysis. *Succinispira* and *Streptococcus* exhibited large variations in abundance depending on the treatment administered; however, rebaudioside A was the only sweetener that enriched both genera. Other notably enriched genera included *Selenomonas* by sucralose and saccharin. Interestingly, *Pediococcus* was eliminated in all treatments except sucralose. These findings underscore the persistent and differential impact of artificial sweeteners on the gut microbiome composition, highlighting the need for further research to understand the long-term consequences of these changes on host health and well-being.

Random matrix theory (RMT) based network analysis reveals distinct impacts of artificial sweeteners on microbiome community structure and interactions

To gain deeper insights into the impact of the treatments on the microbiome, we employed Random Matrix Theory (RMT) based network analysis of the treated community. RMT analysis is a powerful approach that uncovers complex interactions and relationships among microbial taxa and identifies distinct microbial modules that are influenced by a given treatment. Figure 4 presents the network of the microbial communities during treatment (days 14–21). Structurally, it is evident that even on days 14–21, some stabilization of the bioreactor is yet to occur, as demonstrated by the large imbalance in node degree and centrality in all treatments, excluding acesulfame K. In the case of acesulfame K, although it increases diversity, it significantly alters the overall community structure by reducing its centrality and interconnectedness. Acesulfame K is the only treatment with three modules, and these modules are far less interconnected and centrally located compared to all other treatments. It is also important to note that every species in the acesulfame K treatment possesses the same node degree, indicating that the average number of connections between bacteria is quite low but uniform across the entire community. This suggests that a general island-forming phenomenon has occurred. Regarding the other treatments, most structurally resemble

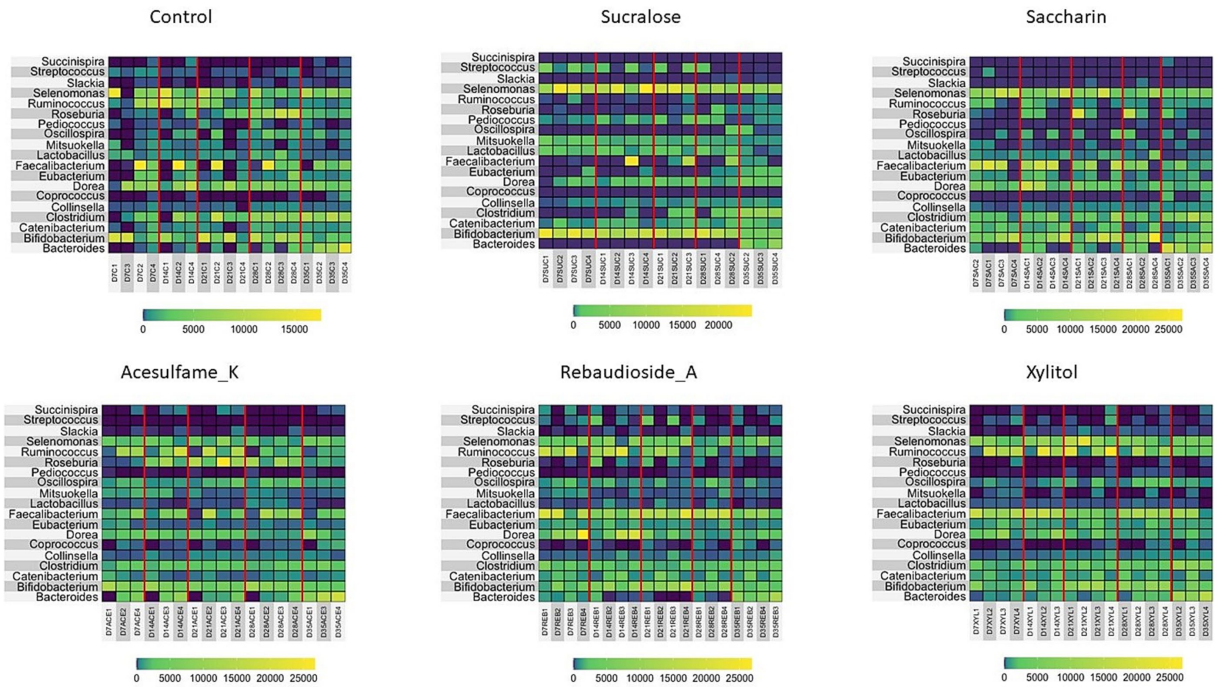

FIGURE 3
Compositional changes of microbiome at genus level. Heatmap showing the most abundant 13 bacterial taxa at day 7, 14, 21, 28, and 35 are shown. Days 7–21 are artificial sweetener supplementation period. Days 22–35 are withdrawal period.

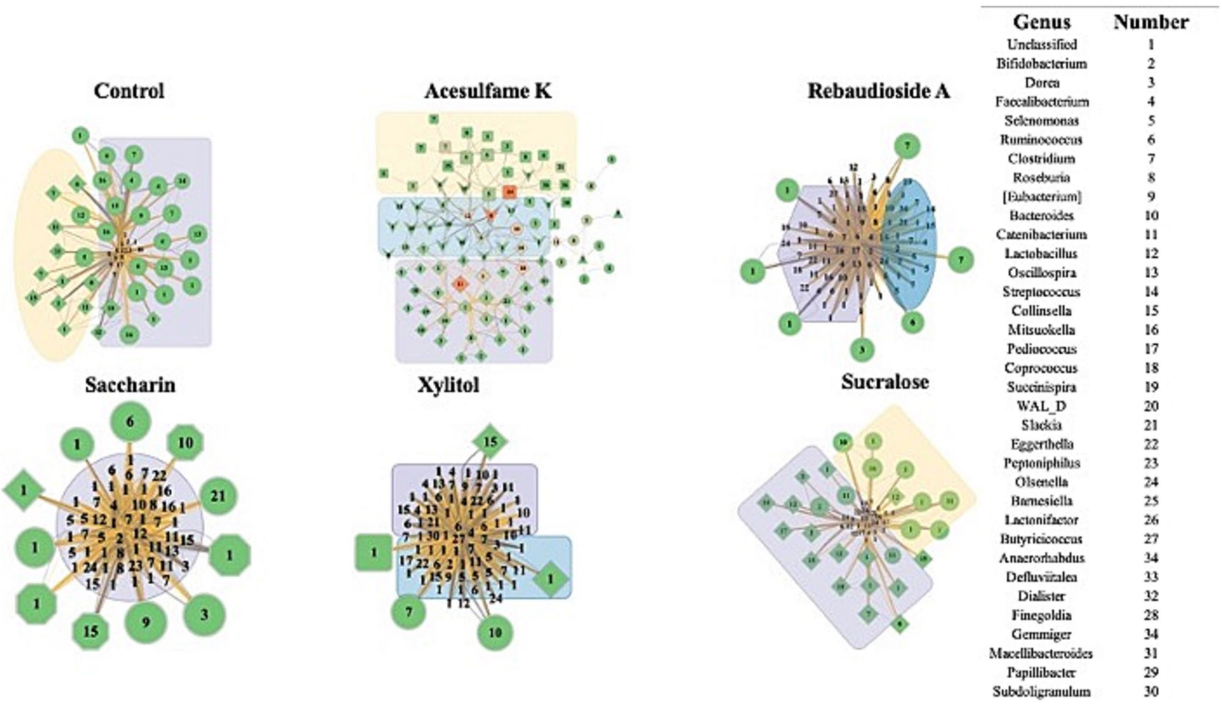

FIGURE 4
Impact of artificial sweeteners on the community composition during treatment period. RMT based Network created in MENAP with the samples from days 14–21 separated by treatment. Node size is node-degree and node color represents a gradient of node centrality. The edge color represents positive and negative connections between nodes. The shape of the node represents the module it is part of. The colored annotations are the top 3 modules by number of nodes going from Purple (1), Yellow (2), and Blue (3) however there will be no annotation if there are less than 20 nodes in a module.

the control, with a significant portion of the bacterial species having extremely low node degrees surrounded by several highly important bacteria. Although this may be entirely due to the lack of full community stabilization, the similarity persists. The impacts on diversity are clearly visible, with sucralose having the fewest number of species and rebaudioside A having a multitude of equally insignificant species. Saccharin and xylitol are intermediate in terms of the quantity of bacterial species and are similar to the control but have a greatly diminished number of key species.

Figure 5 shows the results of the network analysis during the withdrawal period (days 21–35). The most immediately notable observation is the similarity between all treatments and the control, with the exception of acesulfame K. After being treatment-free for 2 weeks, these treatments exhibit a far more balanced and natural network structure. Acesulfame K is the only treatment that has become less structurally defined. Even after the treatment has been fully withdrawn for 2 weeks, all modularity has disappeared. Furthermore, several completely isolated islands have split from the main network, which has decreased in both centrality and degree. Rebaudioside A, sucralose, and xylitol have all become extremely similar in structure to the control, albeit with fewer nodes in some cases. In the case of saccharin, significant structural recovery has been made; however, several bacteria remain heavily suppressed in the center of the network. Although these bacteria remain connected to the main network, they are in contrast to the isolated islands observed in the acesulfame K treatment. These findings suggest that while most artificial sweeteners allow the microbiome community to recover its structure after the withdrawal period, acesulfame K has a more lasting impact on the network properties and interactions.

Discussion

When discussing artificial sweeteners and their impact on the gut microbiome, it is crucial to consider their origin and manufacturing process. Two of the sweeteners in the study can be considered natural: rebaudioside A and xylitol. Rebaudioside A is the sweetening component in Stevia (a plant) (Gardana et al., 2003; Peteliuk et al., 2021), whereas xylitol, although found in most plants, is usually produced industrially through chemical means (Umai et al., 2022). It is also important to note that sucralose is a chlorinated sugar substitute, meaning that in its manufacturing process, sucrose has three of its hydroxyl groups replaced with chlorine atoms (Hellwig, 2024). Saccharin and acesulfame K are also fully synthetic but have no notable components that would explain their effects (Wang and Lin, 2025).

While previous research generally suggests that artificial sweeteners negatively impact diversity (Castañeda-Monsalve et al., 2024; Shou et al., 2024), our study finds that acesulfame K, rebaudioside A, and xylitol increased diversity. Rebaudioside A and xylitol are both natural sweeteners, leading us to believe that naturally derived sugar substitutes may be more beneficial for diversity compared to their synthetic counterparts. This aligns with previous studies suggesting that natural sweeteners have less disruptive effects

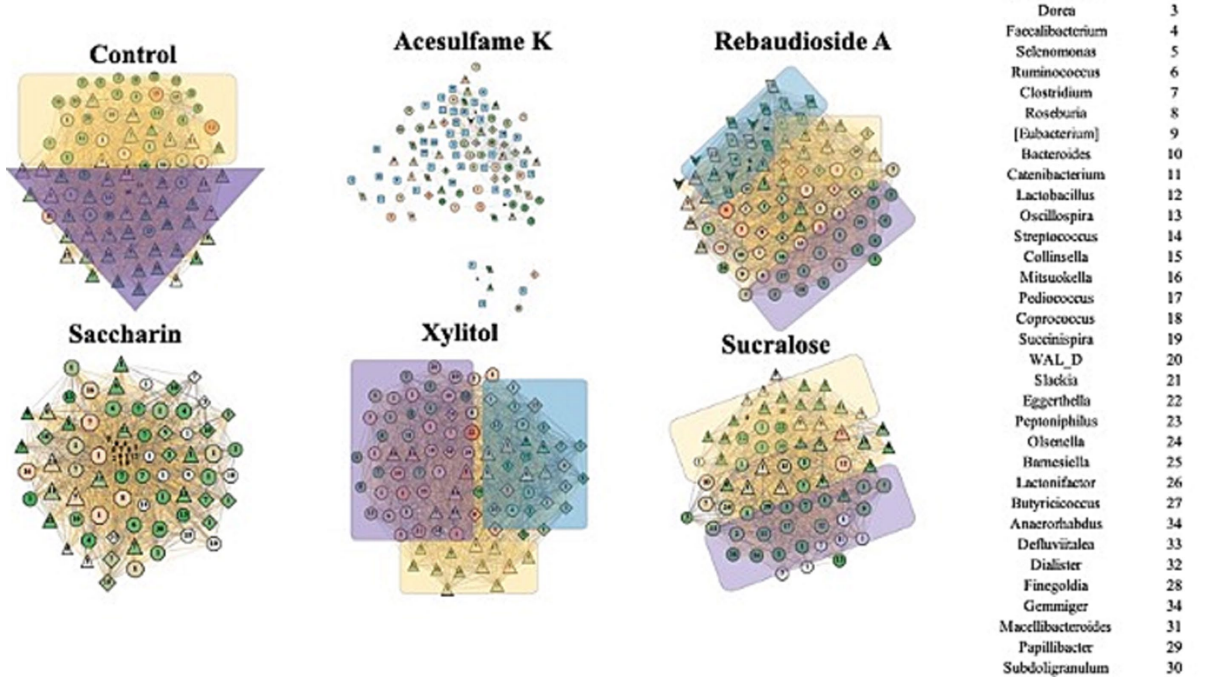

FIGURE 5
Impact of artificial sweeteners on the community composition during withdrawal period. RMT Network created in MENAP with the samples from days 28–35 separated by treatment. Node size is node-degree and node color is gradient of node-centrality. The edge color represents positive and negative connections between nodes. The shape of the node represents the module it is part of. The colored annotations are the top 3 modules by number of nodes going from Purple (1), Yellow (2), and Blue (3) however there will be no annotation if there are less than 20 nodes in a module.

on the gut microbiota (Serrano et al., 2021). We also hypothesize that the significant drop in diversity observed with sucralose could be due to the presence of chlorine in its manufacturing process, as chlorine is antibacterial (Jani, 2019).

Our analysis at the family level shows that while all sweeteners induce change, sucralose induced severe alterations, enriching potentially harmful families like Enterobacteriaceae, which includes pathogenic genera such as Escherichia and Citrobacter. This can be potentially detrimental to human health as these bacteria are often associated with gut inflammation and dysbiosis. In contrast, rebaudioside A and xylitol, which are naturally based, promoted beneficial families such as Lachnospiraceae and Ruminococcaceae, which are important for the production of short-chain fatty acids (SCFAs) like butyrate, essential for gut health. These trends are also observed at the genus level. Although sucralose significantly enriched Bifidobacterium and Lactobacillus, typically considered beneficial (Oerlemans et al., 2021; Xiao et al., 2021; Zoghi et al., 2021; Zacarchenco et al., 2022), this came at the cost of overall diversity, indicating a selective pressure that may not be entirely beneficial in the long term. Rebaudioside A and xylitol promoted the genus Ruminococcus (Ze et al., 2012; Reichardt et al., 2014), which plays a critical role in digesting complex carbohydrates and SCFA production, despite their treatment not having a large prevalence of complex carbohydrates. The presence of SCFAs like butyrate and propionate is crucial for maintaining intestinal barrier integrity and reducing inflammation (Ghimire et al., 2021; Rios-Covian et al., 2015; Seekatz et al., 2018).

RMT-based network analysis was key in understanding how artificial sweeteners structurally alter the community. Acesulfame K stood out in its lack of centrality and modularity, which can lead to a less resilient microbiome, making it more susceptible to external stressors and less capable of recovering from perturbations. It was also the only sweetener that did not begin to trend towards the control structurally after treatment was withdrawn, implying that the structural harm caused by acesulfame K is more pervasive and longer-lasting than that caused by other sweeteners. While all other sweeteners had similar structures after treatment was withdrawn, saccharin still heavily suppressed several species. During treatment, the suppression of a large percentage of the community was observed, suggesting that the community would be more susceptible to external stressors and less capable of recovering from perturbations.

While these findings contribute to our understanding of the complex interactions between artificial sweeteners and the gut microbiome, there are some limitations to our study. First, our results are based on testing fecal microbiota samples from a small number of donors. It is well known that the composition of the human gut microbiota can vary substantially among individuals and across populations (Mancabelli et al., 2024; Joos et al., 2025). Therefore, testing a larger cohort of donor samples will be needed to determine whether our results hold true on a broader population scale. Second, our study examined the effect of five common artificial sweeteners over a relatively short period, which may not capture the potential longer-term effects of these compounds. The onset of conditions such as type 2 diabetes, metabolic syndrome, and obesity—linked to artificial sweetener consumption—often requires prolonged exposure. Many studies have reported a link between artificial sweetener intake and an increased risk of type 2 diabetes mellitus, potentially driven by changes in gut microbiota composition, higher glucose absorption, and insulin insensitivity (Okoro and Markus, 2025; Zhang et al., 2024). Although artificial sweeteners are frequently marketed as weight-management aids, long-term use has been associated in some research with weight gain, metabolic syndrome (a cluster of conditions including high blood pressure and abnormal cholesterol levels), and obesity (Khalil et al., 2024; Jiang et al., 2024). Consequently, our short-term findings may not be fully applicable to these conditions. Finally, the functional consequences of taxa enrichment, such as that of Enterobacteriaceae, need further validation in animal models, for example, in mice.

Data availability statement

Raw sequence data from this study is deposited in NCBI SRA under Bioproject ID: PRJNA1125406.

Ethics statement

The studies involving humans were approved by South Dakota State University Institutional Review Board. The studies were conducted in accordance with the local legislation and institutional requirements. The participants provided their written informed consent to participate in this study.

Author contributions

AK: Data curation, Formal analysis, Investigation, Methodology, Visualization, Writing – original draft. TA: Investigation, Writing – review & editing. AM: Methodology, Writing – review & editing. SA: Methodology, Writing – review & editing. MC: Formal analysis, Writing – review & editing. XW: Resources, Supervision, Writing – review & editing. JS: Conceptualization, Funding acquisition, Project administration, Resources, Supervision, Validation, Visualization, Writing – review & editing.

Funding

The author(s) declare that financial support was received for the research and/or publication of this article. This work was supported in part by USDA grant numbers SD00H702–20, SD00R646–20 and the Walter R. Sitlington Endowment awarded to JS.

Acknowledgments

Authors thank Julia Nelson, Animal Disease Research and Diagnostic Laboratory (ADRDL), South Dakota State University, Brookings SD for the assistance with Illumina sequencing of the microbiome samples. Computations supporting this project were performed using the High-Performance Computing systems at

South Dakota State University and the OU Supercomputing Center for Education & Research (OSCER) at the University of Oklahoma (OU).

Conflict of interest

The authors declare that the research was conducted in the absence of any commercial or financial relationships that could be construed as a potential conflict of interest.

The author(s) declared that they were an editorial board member of Frontiers, at the time of submission. This had no impact on the peer review process and the final decision.

Generative AI statement

The author(s) declare that no Gen AI was used in the creation of this manuscript.

Publisher's note

All claims expressed in this article are solely those of the authors and do not necessarily represent those of their affiliated organizations, or those of the publisher, the editors and the reviewers. Any product that may be evaluated in this article, or claim that may be made by its manufacturer, is not guaranteed or endorsed by the publisher.

References

Agrinier, A. L., Pilon, G., and Marette, A. (2024). A low-cost, easy-to-use prototype bioreactor model for the investigation of human gut microbiota: validation using a prebiotic treatment. *Front. Microbiol.* 15:1250366. doi: 10.3389/fmicb.2024.1250366

Angelin, M., Kumar, J., Vajravelu, L. K., Satheesan, A., Chaithanya, V., and Murugesan, R. (2024). Artificial sweeteners and their implications in diabetes: a review. *Front. Nutr.* 11:1411560. doi: 10.3389/fnut.2024.1411560

Auchtung, J. M., Robinson, C. D., and Britton, R. A. (2015). Cultivation of stable, reproducible microbial communities from different fecal donors using minibioreactor arrays (MBRAs). *Microbiome* 3:42. doi: 10.1186/s40168-015-0106-5

Auchtung, J. M., Robinson, C. D., Farrell, K., and Britton, R. A. (2016). MiniBioReactor arrays (MBRAs) as a tool for Studying *C. difficile* physiology in the presence of a complex community. *Methods Mol. Biol.* 1476, 235–258. doi: 10.1007/978-1-4939-6361-4_18

Bolyen, E., Rideout, J. R., Dillon, M. R., Bokulich, N. A., Abnet, C. C., Al-Ghalith, G. A., et al. (2019). Reproducible, interactive, scalable and extensible microbiome data science using QIIME 2. *Nat. Biotechnol.* 37, 852–857. doi: 10.1038/s41587-019-0209-9

Callahan, B. J., McMurdie, P. J., Rosen, M. J., Han, A. W., Johnson, A. J. A., and Holmes, S. P. (2016). DADA2: high-resolution sample inference from Illumina amplicon data. *Nat. Methods* 13, 581–583. doi: 10.1038/nmeth.3869

Castañeda-Monsalve, V., Fröhlich, L.-F., Haange, S.-B., Homsi, M. N., Rolle-Kampczyk, U., Fu, Q., et al. (2024). High-throughput screening of the effects of 90 xenobiotics on the simplified human gut microbiota model (SIHUMIx): a metaproteomic and metabolomic study. *Front. Microbiol.* 15:1349367. doi: 10.3389/fmicb.2024.1349367

Cline, M. S., Smoot, M., Cerami, E., Kuchinsky, A., Landys, N., Workman, C., et al. (2007). Integration of biological networks and gene expression data using Cytoscape. *Nat. Protoc.* 2, 2366–2382. doi: 10.1038/nprot.2007.324

Conz, A., Salmona, M., and Diomede, L. (2023). Effect of non-nutritive sweeteners on the gut microbiota. *Nutrients* 15:1869. doi: 10.3390/nu15081869

Cyphert, E. L., Liu, C., Morales, A. L., Nixon, J. C., Blackford, E., Garcia, M., et al. (2024). Effects of high dose aspartame-based sweetener on the gut microbiota and bone strength in young and aged mice. *JBMR Plus* 8:ziae082. doi: 10.1093/jbmrpl/ziae082

Deng, Y., Jiang, Y.-H., Yang, Y., He, Z., Luo, F., and Zhou, J. (2012). Molecular ecological network analyses. *BMC bioinformatics* 13:113. doi: 10.1186/1471-2105-13-113

DeSantis, T. Z., Hugenholtz, P., Larsen, N., Rojas, M., Brodie, E. L., Keller, K., et al. (2006). Greengenes, a chimera-checked 16S rRNA gene database and workbench compatible with ARB. *Appl. Environ. Microbiol.* 72, 5069–5072. doi: 10.1128/AEM.03006-05

Feng, J., Peng, J., Hsiao, Y. C., Liu, C. W., Yang, Y., Zhao, H., et al. (2024). Non/low-caloric artificial sweeteners and gut microbiome: from perturbed species to mechanisms. *Meta* 14:544. doi: 10.3390/metabo14100544

Fenske, G. J., Ghimire, S., Antony, L., Christopher-Hennings, J., and Scaria, J. (2020). Integration of culture-dependent and independent methods provides a more coherent picture of the pig gut microbiome. *FEMS Microbiol. Ecol.* 96:fiaa022. doi: 10.1093/femsec/fiaa022

Gardana, C., Simonetti, P., Canzi, E., Zanchi, R., and Pietta, P. (2003). Metabolism of stevioside and rebaudioside a from *Stevia rebaudiana* extracts by human microflora. *J. Agric. Food Chem.* 51, 6618–6622. doi: 10.1021/jf0303619

Gauthier, E., Milagro, F. I., and Navas-Carretero, S. (2024). Effect of low-and non-calorie sweeteners on the gut microbiota: a review of clinical trials and cross-sectional studies. *Nutrition* 117:112237. doi: 10.1016/j.nut.2023.112237

Ghimire, S., Roy, C., Wongkuna, S., Antony, L., Maji, A., Keena, M. C., et al. (2020). Identification of Clostridioides difficile-inhibiting gut commensals using Culturomics, phenotyping, and combinatorial community assembly. *mSystems* 5:e00620-19. doi: 10.1128/mSystems.00620-19

Ghimire, S., Wongkuna, S., Sankaranarayanan, R., Ryan, E. P., Bhat, G. J., and Scaria, J. (2021). Positive synergistic effects of quercetin and Rice bran on human gut microbiota reduces Enterobacteriaceae Family abundance and elevates propionate in a bioreactor model. *Front. Microbiol.* 12:751225. doi: 10.3389/fmicb.2021.751225

Guzman-Rodriguez, M., McDonald, J. A. K., Hyde, R., Allen-Vercoe, E., Claud, E. C., Sheth, P. M., et al. (2018). Using bioreactors to study the effects of drugs on the human microbiota. *Methods* 149, 31–41. doi: 10.1016/j.ymeth.2018.08.003

Hellwig, M. (2024). Formation of chlorinated carbohydrate degradation products and amino acids during heating of sucralose in model systems and food. *J. Agric. Food Chem.* 72, 26441–26450. doi: 10.1021/acs.jafc.4c08059

Jani, M. (2019). Modification and characterization of chloro-sugar derivatives as anti-bacterial agents. Theses and Dissertations. 2692. Available at: https://rdw.rowan.edu/etd/2692

Jiang, L., Yu, Z., Zhao, Y., and Yin, D. (2024). Obesogenic potentials of environmental artificial sweeteners with disturbances on both lipid metabolism and neural responses. *Sci. Total Environ.* 919:170755. doi: 10.1016/j.scitotenv.2024.170755

Joos, R., Boucher, K., Lavelle, A., Arumugam, M., Blaser, M. J., Claesson, M. J., et al. (2025). Examining the healthy human microbiome concept. *Nat. Rev. Microbiol.* 23, 192–205. doi: 10.1038/s41579-024-01107-0

Khalil, S., Haikal, Y., and Aoun, A. (2024). Non-nutritive sweeteners: weight loss or weight gain? *Endocr. Metab. Immune Disord. Drug Targets* 24, 749–757. doi: 10.2174/0118715303245646230926054352

Kossiva, L., Kakleas, K., Christodouli, F., Soldatou, A., Karanasios, S., and Karavanaki, K. (2024). Chronic use of artificial sweeteners: pros and cons. *Nutrients* 16:3162. doi: 10.3390/nu16183162

Lee, C. Y., So, Y. S., Yoo, S. H., Lee, B. H., and Seo, D. H. (2024). Impact of artificial sweeteners and rare sugars on the gut microbiome. *Food Sci. Biotechnol.* 33, 2047–2064. doi: 10.1007/s10068-024-01597-x

Liu, Q., Wang, M., Hou, Y., Chen, R., Liu, H., Han, T., et al. (2024). Deciphering the multifaceted effects of artificial sweeteners on body health and metabolic functions: a comprehensive review and future perspectives. *Crit. Rev. Food Sci. Nutr.* 1–23. doi: 10.1080/10408398.2024.2411410

Mancabelli, L., Milani, C., Biase, R. D., Bocchio, F., Fontana, F., Lugli, G. A., et al. (2024). Taxonomic and metabolic development of the human gut microbiome across life stages: a worldwide metagenomic investigation. *mSystems* 9, e01294–e01223. doi: 10.1128/msystems.01294-23

Oerlemans, M. M., Akkerman, R., Ferrari, M., Walvoort, M. T., and de Vos, P. (2021). Benefits of bacteria-derived exopolysaccharides on gastrointestinal microbiota, immunity and health. *J. Funct. Foods* 76:104289. doi: 10.1016/j.foodres.2022.111445

Okoro, F. O., and Markus, V. (2025). Artificial sweeteners and type 2 diabetes mellitus: a review of current developments and future research directions. *J. Diabetes Complicat.* 39:108954. doi: 10.1016/j.jdiacomp.2025.108954

Peteliuk, V., Rybchuk, L., Bayliak, M., Storey, K. B., and Lushchak, O. (2021). Natural sweetener *Stevia rebaudiana*: functionalities, health benefits and potential risks. *EXCLI J.* 20, 1412–1430. doi: 10.17179/excli2021-4211

Radenkovic, S. (2023). Investigating the effects of artificial sweeteners. *Nat. Rev. Endocrinol.* 19:442. doi: 10.1038/s41574-023-00860-1

Reichardt, N., Duncan, S. H., Young, P., Belenguer, A., McWilliam Leitch, C., Scott, K. P., et al. (2014). Phylogenetic distribution of three pathways for propionate production within the human gut microbiota. *ISME J.* 8, 1323–1335. doi: 10.1038/ismej.2014.14

Rios-Covian, D., Gueimonde, M., Duncan, S. H., Flint, H. J., and de los Reyes-Gavilan, C. G. (2015). Enhanced butyrate formation by cross-feeding between

Faecalibacterium prausnitzii and *Bifidobacterium adolescentis*. *FEMS Microbiol. Lett.* 362:fnv176. doi: 10.1093/femsle/fnv176

Russell, WMS, and Burch, RL. (1959). The principles of humane experimental technique.

Seekatz, A. M., Theriot, C. M., Rao, K., Chang, Y. M., Freeman, A. E., Kao, J. Y., et al. (2018). Restoration of short chain fatty acid and bile acid metabolism following fecal microbiota transplantation in patients with recurrent *Clostridium difficile* infection. *Anaerobe* 53, 64–73. doi: 10.1016/j.anaerobe.2018.04.001

Serrano, J., Smith, K. R., Crouch, A. L., Sharma, V., Yi, F., Vargova, V., et al. (2021). High-dose saccharin supplementation does not induce gut microbiota changes or glucose intolerance in healthy humans and mice. *Microbiome* 9:11. doi: 10.1186/s40168-020-00976-w

Shil, A., Ladeira Faria, L. M., Walker, C. A., and Chichger, H. (2024). The artificial sweetener neotame negatively regulates the intestinal epithelium directly through T1R3-signaling and indirectly through pathogenic changes to model gut bacteria. *Front. Nutr.* 11:1366409. doi: 10.3389/fnut.2024.1366409

Shou, N., Rensing, C., Lin, Q., Xu, W., Fu, K., Yuan, X., et al. (2024). Acesulfame potassium induces hepatic inflammation and fatty acids accumulation via disturbance of carnitine metabolism and gut microbiota. *Food Biosci.* 62:105101. doi: 10.1016/j.fbio.2024.105101

Smoot, M. E., Ono, K., Ruscheinski, J., Wang, P. L., and Ideker, T. (2011). Cytoscape 2.8: new features for data integration and network visualization. *Bioinformatics* 27, 431–432. doi: 10.1093/bioinformatics/btq675

Suez, J., Cohen, Y., Valdés-Mas, R., Mor, U., Dori-Bachash, M., Federici, S., et al. (2022). Personalized microbiome-driven effects of non-nutritive sweeteners on human glucose tolerance. *Cell* 185, 3307–3328.e19. doi: 10.1016/j.cell.2022.07.016

Sun, Y., and Xu, B. (2025). A critical review on effects of artificial sweeteners on gut microbiota and gastrointestinal health. *J. Sci. Food Agric.* 105, 2737–2747. doi: 10.1002/jsfa.14148

Umai, D., Kayalvizhi, R., Kumar, V., and Jacob, S. (2022). Xylitol: bioproduction and applications-a review. *Front. Sustain.* 3:826190. doi: 10.3389/frsus.2022.826190

Wang, Y., and Lin, L. (2025). Naturally occurring and artificial nonnutritive sweeteners: potential impacts on metabolic diseases. *eFood* 6:e70028.

Xiao, Y., Zhai, Q., Zhang, H., Chen, W., and Hill, C. (2021). Gut colonization mechanisms of Lactobacillus and Bifidobacterium: an argument for personalized designs. *Annu. Rev. Food Sci. Technol.* 12, 213–233. doi: 10.1146/annurev-food-061120-014739

Zacarchenco, P. B., Pimentel, T. C., ATS, A., Spadoti, L. M., Esmerino, E. A., Silva, M. C., et al. (2022). Chapter 16 - Health benefits of probiotics: an overview. Editor(s): J. Singh, A. Vyas, Advances in Dairy Microbial Products, Woodhead Publishing. 235–245. doi: 10.1016/B978-0-323-85793-2.00015-1

Ze, X., Duncan, S. H., Louis, P., and Flint, H. J. (2012). *Ruminococcus bromii* is a keystone species for the degradation of resistant starch in the human colon. *ISME J.* 6, 1535–1543. doi: 10.1038/ismej.2012.4

Zhang, Y., Tang, Z., Shi, Y., and Li, L. (2024). Associations between artificial sweetener intake from cereals, coffee, and tea and the risk of type 2 diabetes mellitus: a genetic correlation, mediation, and mendelian randomization analysis. *PLoS One* 19:e0287496. doi: 10.1371/journal.pone.0287496

Zoghi, A., Massoud, R., Todorov, S. D., Chikindas, M. L., Popov, I., Smith, S., et al. (2021). Role of the lactobacilli in food bio-decontamination: friends with benefits. *Enzym. Microb. Technol.* 150:109861. doi: 10.1016/j.enzmictec.2021.109861

frontiers | Frontiers in Microbiology

TYPE Review
PUBLISHED 04 June 2025
DOI 10.3389/fmicb.2025.1564902

Check for updates

OPEN ACCESS

EDITED BY
Mohammad Altamimi,
An-Najah National University, Palestine

REVIEWED BY
Doureradjou Peroumal,
University of Pittsburgh, United States
Huoxiang Zhou,
Zhengzhou University, China

*CORRESPONDENCE
Lei Zhang
✉ zhanglei7@sdu.edu.cn
Ning Li
✉ 754520623@qq.com
Qinghua Wang
✉ chm_wangqh@ujn.edu.cn

†These authors have contributed equally to this work

RECEIVED 22 January 2025
ACCEPTED 19 May 2025
PUBLISHED 04 June 2025

CITATION
Wu N, Ning K, Liu Y, Wang Q, Li N and Zhang L (2025) Relationship between high-fat diet, gut microbiota, and precocious puberty: mechanisms and implications.
Front. Microbiol. 16:1564902.
doi: 10.3389/fmicb.2025.1564902

COPYRIGHT
© 2025 Wu, Ning, Liu, Wang, Li and Zhang. This is an open-access article distributed under the terms of the Creative Commons Attribution License (CC BY). The use, distribution or reproduction in other forums is permitted, provided the original author(s) and the copyright owner(s) are credited and that the original publication in this journal is cited, in accordance with accepted academic practice. No use, distribution or reproduction is permitted which does not comply with these terms.

Relationship between high-fat diet, gut microbiota, and precocious puberty: mechanisms and implications

Nan Wu[1†], Ke Ning[1†], Yanan Liu[2†], Qinghua Wang[3*], Ning Li[2*] and Lei Zhang[1*]

[1]Microbiome-X, School of Public Health, Cheeloo College of Medicine, Shandong University, Jinan, China, [2]Jinan Institute of Child Health Care, Children's Hospital Affiliated to Shandong University (Jinan Children's Hospital), Jinan, China, [3]School of Biological Science and Technology, University of Jinan, Jinan, China

Precocious puberty (PP) is the second most common pediatric endocrine disorder globally and poses a growing public health concern, particularly among girls. While the exact biological mechanisms underlying PP remain unclear, unhealthy dietary patterns, particularly the consumption of a high-fat diet (HFD), are recognized as significant modifiable risk factors. The gut microbiota (GM) is an environmental factor that is disrupted by HFD and may modulate the onset and progression of PP. This review explored the intricate relationship between HFD, GM, and PP, and elucidated the potential mechanisms by which HFD may promote PP development by summarizing evidence from preclinical to clinical research, focusing on the role of GM and its derived metabolites, including short-chain fatty acids, bile acids, lipopolysaccharides, and neurotransmitters. Mechanistic exploration provides novel insights for developing microbiota-targeted therapeutic strategies, such as dietary and lifestyle interventions, fecal microbiota transplantation, probiotics, and traditional Chinese medicine, paving the way for promising approaches to prevent and manage PP.

KEYWORDS

high-fat diet, gut microbiota, precocious puberty, probiotics, gut metabolites

1 Introduction

Precocious puberty (PP) is characterized by the premature emergence of secondary sexual characteristics—before age 8 in girls and 9 in boys (Alghamdi and Alghamdi, 2023). PP can be classified into two main categories considering the underlying pathogenetic mechanism: central PP (CPP) and peripheral PP (PPP). CPP is caused by early activation of the hypothalamic–pituitary–gonadal (HPG) axis, leading to the development of both primary and secondary sexual characteristics. This form accounts for approximately 80% of PP cases. In contrast, PPP results from factors that elevate steroid hormone levels to those typical of puberty, independent of gonadotropin secretion (For detailed discussions on the etiology, diagnosis, and treatment of both subtypes, see the review; Cheuiche et al., 2021). Notably, the incidence of PP in girls is markedly higher than in boys, with a rate 15 to 20 times greater, and its global prevalence continues to rise (Shim et al., 2021; Park et al., 2021). The onset of PP results from a complex interaction of genetic, dietary, environmental, and lifestyle factors. Among these, a high-fat diet (HFD) has emerged as a modifiable risk factor that has garnered significant attention.

With advancements in microbiomics, the gut microbiota (GM) and its derived metabolites have been increasingly recognized as important molecules in the gut-organ crosstalk, exerting either beneficial or detrimental effects on various extra-intestinal organs. Mounting evidence indicates various perturbations in GM associated with PP. Notably, excessive fat consumption in HFD results in consequences such as gut dysbiosis, gut barrier dysfunction, emphasizing GM's potential mediating role in the pathogenesis of PP induced by HFD. In this review, we summarized studies exploring the relationship between HFD, GM, and PP and specifically discussed the direct effects of HFD on PP and its indirect effects mediated by GM and its metabolites. Finally, we reviewed the potential of GM regulation as a strategy to mitigate or manage PP, offering valuable insights for future research and therapeutic interventions.

2 HFD promotes PP

HFD significantly disrupts neuroendocrine and metabolic homeostasis, serving as a critical environmental determinant in the pathogenesis of PP. Robust epidemiological studies have revealed differential effects of HFD components on pubertal timing (Supplementary Table 1; Chen et al., 2024; Gu et al., 2024; Günther et al., 2010; Xiong et al., 2022; Du et al., 2024; Cheng et al., 2021b; Xu et al., 2022; Cheng et al., 2021a; Shahatah et al., 2021; Nguyen et al., 2020; Jansen et al., 2016; Mueller et al., 2015; Carwile et al., 2015; Mervish et al., 2013; Wiley, 2011; Rogers et al., 2010; Koo et al., 2002; Berkey et al., 2000; Maclure et al., 1991; Merzenich et al., 1993; Szamreta et al., 2020). Animal protein intake is consistently associated with accelerated pubertal development, manifesting as premature onset of thelarche, enhanced growth velocity, and earlier menarche (Gu et al., 2024; Günther et al., 2010; Cheng et al., 2021b; Rogers et al., 2010; Berkey et al., 2000). Conversely, milk's effects remain controversial, with studies reporting negative (Du et al., 2024; Wiley, 2011), positive (Wiley, 2011), or no significant associations (Carwile et al., 2015) with early pubertal onset, potentially due to genetic backgrounds, study design, dietary intake assessment, and temporal context. These inconsistencies highlight the need for future studies to control confounding variables more rigorously to derive precise conclusions.

Regarding dietary lipids, polyunsaturated fatty acids (PUFAs)—essential steroidogenesis precursors—exhibited a dose-dependent positive correlation with earlier pubertal onset and menarche in girls (Xu et al., 2022; Cheng et al., 2021a; Nguyen et al., 2020; Rogers et al., 2010), whereas monounsaturated fatty acids (MUFAs) demonstrated inhibitory effects (Nguyen et al., 2020). Additionally, plant-derived components such as flavonoids, soy, and dietary fiber were associated with delayed pubertal timing (Xiong et al., 2022; Nguyen et al., 2020; Mervish et al., 2013), suggesting potential preventive strategies through reduced animal protein/dietary fat consumption and increased plant-based diet intake.

Human studies primarily provided observational evidence, but preclinical research established direct causality, demonstrating that maternal or female offspring exposure to HFD significantly accelerated vaginal opening (VO), a key marker of puberty onset, and gonadal maturation (Bo et al., 2022; Wang et al., 2020). The underlying mechanisms are illustrated in Figure 1.

2.1 Hypothalamic microglial cells

Microglial cells play a critical role in the context of PP and exhibit heightened sensitivity to fatty acids, particularly long-chain saturated fatty acids, which further enhance their activation (Wang et al., 2012; Gupta et al., 2012). Activated hypothalamic microglia release prostaglandins, acting as neurotrophic factors that stimulate GnRH neurons and subsequently hasten puberty (Sheremeta et al., 2024; Fujioka et al., 2013). Additionally, sustained HFD exposure further activates microglial cells to secrete pro-inflammatory cytokines, including interleukin-1β, interleukin-6, nitric oxide (NO), tumor necrosis factor-α, and reactive oxygen species, which collectively induce hypothalamic inflammation and exacerbate the aberrant activation of GnRH neurons (Tzounakou et al., 2024; Chen et al., 2022). This mechanism has been thoroughly reviewed by Stathori et al., whose comprehensive analysis elucidates the potential pathways through which HFD-induced neuroinflammation affects the activity of HPG axis (Stathori et al., 2025). Intriguingly, evidence suggests that HFD Short-term HFD induces triggers microglial activation beyond the effects of obesity, suggesting that HFD introduces unique stressors to the central nervous system, amplifying microglial activation (Gao et al., 2014).

2.2 Phoenixin

Phoenixin, a reproductive peptide crucial for regulating the estrous cycle, is elevated in response to fatty acids such as palmitate and oleate (Mcilwraith et al., 2018), thereby accelerating puberty through GnRH activation mediated by kisspeptin (Stein et al., 2016; Gozukara et al., 2016; Dhillo et al., 2005; Clarke and Dhillo, 2016). In addition, research studies have demonstrated that Phoenixin not only impairs the HPG axis but also adversely affects the follicular development and function. Nguyen et al. were the first to identify Phoenixin, along with its receptor G-protein coupled receptor (GPR) 173, in the ovarian follicles of women post-cervical cancer surgery. *In vitro* studies further verified Phoenixin's capacity to promote follicular growth and increase ovulated oocyte numbers, as well as enhance estradiol (E2) secretion in a dose-responsive manner (Nguyen et al., 2019; Clarke and Dhillo, 2019). Overall, these findings establish Phoenixin serves as a key mediator of HFD-induced PP by integrating metabolic signals with the neuroendocrine system and ovarian development.

2.3 Transcription factor p53

The transcription factor p53, a well-known tumor suppressor, has also been found to regulate the genetic pathways governing puberty onset (Chen et al., 2020). In the HFD-induced PP model, hypothalamic p53 expression positively correlated with pubertal onset timing, where p53 overexpression significantly accelerated puberty progression, providing causal evidence for p53 in the development of PP (Chen et al., 2021). Mechanistically, p53 exerts dual regulatory effects through the Lin28/let-7 system: centrally, it activates the Kiss1/GPR54 and phosphatidylinositol 3-kinase (PI3K)-mammalian target of rapamycin (mTOR) signaling pathways to stimulate GnRH secretion (Chen et al., 2021; Xie et al., 2025); gonadally, it directly promotes

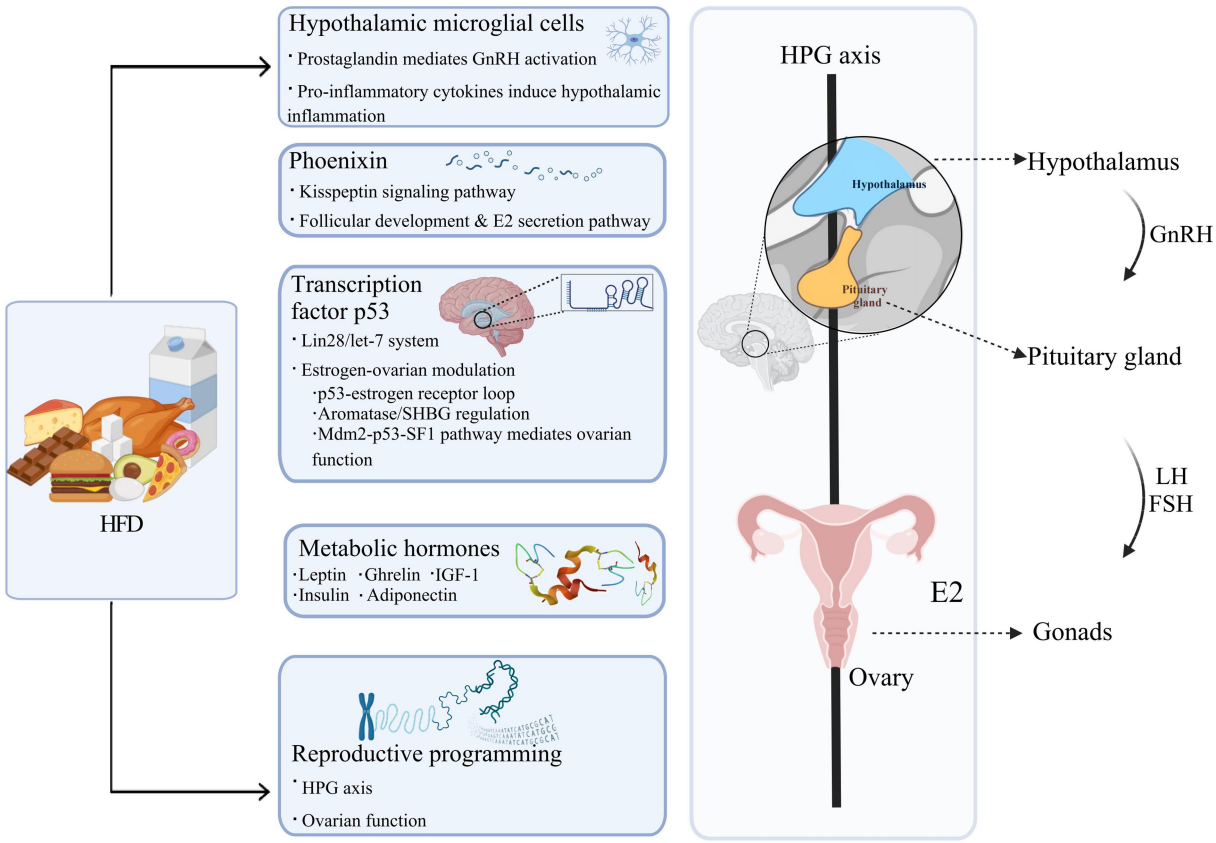

FIGURE 1
The pathways through which HFD contributes to PP. HFD, a high-fat diet; GnRH, gonadotropin-releasing hormone; LH, luteinizing hormone; FSH, follicle-stimulating hormone; HPG axis, hypothalamic–pituitary-gonadal axis; E2, estradiol; SHBG, sex hormone-binding globulin; Mdm2, mouse double minute 2 homolog; SF1, steroidogenic factor 1; IGF-1, insulin-like growth factor-1. Figure created with BioRender.com.

ovarian granulosa cells proliferation and E2 synthesis (Sui et al., 2023). In addition, p53 orchestrates estrogen signaling and ovarian function through multiple mechanisms: forming a bidirectional regulatory loop with estrogen receptor α (ERα) that enables mutual transcriptional control through promoter binding and estrogen response element-mediated transactivation (Shirley et al., 2009; Berger et al., 2012); modulating estrogen levels and bioactivity by regulating the expression of aromatase (the rate-limiting enzyme in estrogen synthesis) and sex hormone-binding globulin (SHBG; Charni-Natan et al., 2019); and participating in ovarian function regulation via the mouse double minute 2 homolog (Mdm2)-p53-steroidogenic factor 1(SF1) signaling pathway in granulosa cells (Zanjirband et al., 2023). While our understanding of the mechanisms and regulation of p53 in HFD-induced PP is gradually improving, the upstream mechanisms by which HFD upregulates p53 expression are not completely understood. However, emerging evidence suggests that ketone bodies, particularly β-hydroxybutyrate, may play a potential role in this regulatory process (Roberts et al., 2017).

2.4 Metabolic hormones

Long-term HFD consumption disrupts the regulation of key metabolic hormones, which regulate both energy homeostasis and the pathogenesis of PP. Clinical observations reveal that girls with PP exhibit characteristic endocrine alterations, including elevated leptin (Zurita-Cruz et al., 2021), insulin (Zhang et al., 2025), and insulin-like growth factor-1 (IGF-1; Zhang et al., 2025) levels alongside reduced adiponectin (APN; Zurita-Cruz et al., 2021; Sitticharoon et al., 2017), while ghrelin changes remain inconsistent (Tarçin et al., 2024; Zhu et al., 2008). Mechanistic investigations have elucidated distinct neuroendocrine pathways through which metabolic hormones coordinate pubertal timing. Leptin accelerates sexual maturation through dual mechanisms, including central activation of hypothalamic Kisspeptin-GnRH neurons and direct stimulation of ovarian granulosa cell function (Childs et al., 2021). APN, conversely, exerts inhibitory control by suppressing GnRH neuronal activity through adenosine-monophosphate-activated protein kinase (AMPK)-mediated pathway (Mathew et al., 2018). Ghrelin activates GnRH neurons via growth hormone secretagogue receptors (GHSR) or kisspeptin-dependent pathways, and potentially modulates the HPG axis through adrenocorticotropic hormone (ACTH; Farkas et al., 2013; Shi et al., 2022). Insulin enhances leptin synthesis to exert synergistic effects, while IGF-1 likely regulates pubertal progression through multiple mechanisms involving IGF-binding proteins, GnRH neurons, Kisspeptin neurons, and gonadotropins (Salvi et al., 2006).

Collectively, these hormones act on both the hypothalamus and ovarian tissues to regulate pubertal progression, with leptin, insulin, and IGF-1 primarily exerting stimulatory effects while APN and ghrelin mainly demonstrate inhibitory actions.

2.5 Reproductive programming

Reproductive system development begins around the fifth week of gestation and continues until after birth, during which newborns experience a temporary surge in gonadotropin levels, triggering a phenomenon known as "mini-puberty." Following this transient activation, the HPG axis becomes dormant through a combination of gonadal and non-gonadal inhibitory mechanisms (Yao et al., 2021). These physiological changes highlight how adverse environmental conditions during pregnancy and the early postnatal period can significantly affect the development and function of the reproductive system.

Maternal overnutrition or obesity during pregnancy and lactation substantially accelerates reproductive maturation in offspring have been demonstrated. A large-scale cohort study found that daughters of mothers who gained more than 40 pounds during pregnancy were 30% more likely to experience menarche before age 11 (Boynton-Jarrett et al., 2011). Similarly, female offspring of maternal mice fed HFD during pregnancy and lactation also exhibited earlier puberty onset, with increased E2 levels and decreased luteinizing hormone (LH) levels. Interestingly, supplementation with conjugated linoleic acid during these stages effectively reversed early-onset puberty in offspring (Reynolds et al., 2015). Collectively, maternal HFD during pregnancy and lactation promotes early puberty and reproductive system abnormalities in offspring by disrupting the developmental programming of the HPG axis and ovarian function, with dietary fatty acids potentially influencing this process.

3 HFD disrupts the balance of the GM

The GM exhibits high sensitivity to dietary shifts and changes in the physiological state of the digestive system, with effects observable within 24 h (Qin et al., 2020). Short-term HFD exposure induces dysbiosis characterized by an elevated Firmicutes/Bacteroidetes ratio (Shang et al., 2017), concomitant with increased abundance of bile-resistant genera (e.g., *Alistipes*, *Bacteroides*) and decreased populations of plant polysaccharide-degrading Firmicutes (e.g., *Roseburia*, *Ruminococcus bromii*; Bisanz et al., 2019; David et al., 2014). Importantly, while short-term HFD induces transient microbial shifts, long-term dietary patterns exert more profound effects: European children consuming a long-term HFD, rich in animal proteins and fats, exhibited a gut microbiome predominantly composed of *Bacteroides* enterotypes, contrasting sharply with the microbial profiles of Burkinabe children maintained on traditional carbohydrate-rich, low-protein diets (De Filippo et al., 2010; Daniel et al., 2014; Wu et al., 2011).

The types of fatty acids prevalent in HFD also have important consequences for both GM and health. Elevated n-6 PUFA levels promote the proliferation of pro-inflammatory species, such as *Mucispirillum schaedleri* and *Lactobacillus murinus* (Selmin et al., 2021), establishing a pro-inflammatory intestinal milieu that exacerbates metabolic endotoxemia and harms health. Furthermore, increased intake of saturated fatty acids, another key component of HFD, facilitates the entry of Gram-negative bacterial lipopolysaccharides (LPS) into the bloodstream, triggering the release of pro-inflammatory cytokines and activating the toll-like receptor 4 signaling pathway, contributing to insulin resistance and inflammation (Hu et al., 2022).

4 Gut microbial imbalance promotes PP

Evidence that antibiotic exposure may elevate the risk of PP in children points toward a role of gut microbiome dysbiosis in PP pathogenesis (Hu et al., 2022). Multiple 16S rRNA gene sequencing studies have revealed global perturbations in the GM of girls with PP compared to healthy controls (Supplementary Table 2; Bo et al., 2022; Wang et al., 2020; Wang Y. et al., 2024; Wang L. et al., 2024; Huang et al., 2023; Huang et al., 2022; Li et al., 2021b; Dong et al., 2020; Qian et al., 2024; Yi et al., 2024; Nguyen et al., 2024; Yuan et al., 2023; Wang et al., 2022), characterized by altered abundances of key taxa (such as *Ruminococcus*; Wang Y. et al., 2024; Huang et al., 2022; Dong et al., 2020), *Bifidobacterium* (Wang L. et al., 2024; Huang et al., 2023; Qian et al., 2024), and *Bacteroides* (Wang Y. et al., 2024; Wang L. et al., 2024; Huang et al., 2022; Qian et al., 2024), along with increased butyrate-producing bacteria (Wang Y. et al., 2024; Huang et al., 2022), and enhanced metabolic potential for neuroendocrine and oxidative stress-related pathways (Wang Y. et al., 2024; Huang et al., 2023; Li et al., 2021b). These findings were further validated in PP animal models (Bo et al., 2022; Yi et al., 2024). Integrating evidence on microbiota-derived metabolites such as short-chain fatty acids (SCFAs) and bile acids (BAs; detailed in Section 5.2), these observations suggest a role for GM and their metabolites in PP development.

However, cross-sectional studies cannot distinguish whether microbial alterations represent causative "driver" microorganisms or secondary "passenger" species proliferating in the PP microenvironment. To address this limitation, recent animal experiments utilizing fecal microbiota transplantation (FMT) from PP donors (either human patients or PP model rats) to recipient female rats demonstrated accelerated puberty onset, accompanied by elevated serum levels of LH, follicle-stimulating hormone (FSH), and E2, as well as upregulated hypothalamic *Kiss1* and *Gnrh* gene expression (Bo et al., 2022; Qian et al., 2024). These findings provided compelling evidence that GM can promote PP through modulation of the HPG axis, although the precise molecular mechanisms by which specific microbial taxa and their metabolic products regulate pubertal timing remain to be elucidated.

5 HFD promotes PP development through changes in GM

From a physiological standpoint, a pivotal connection between a HFD and PP lies in the GM, which acts as a "virtual endocrine organ" with endocrine function, and the bioactive metabolites it produces influence the host's physiological processes. Figure 2 illustrates the interaction mechanisms through which HFD promotes PP by the modulation of GM and its metabolic products, including SCFAs, BAs, LPS, and neurotransmitters such as γ-aminobutyric acid (GABA), dopamine (DA), and serotonin (5-HT), which are further detailed in subsequent sections.

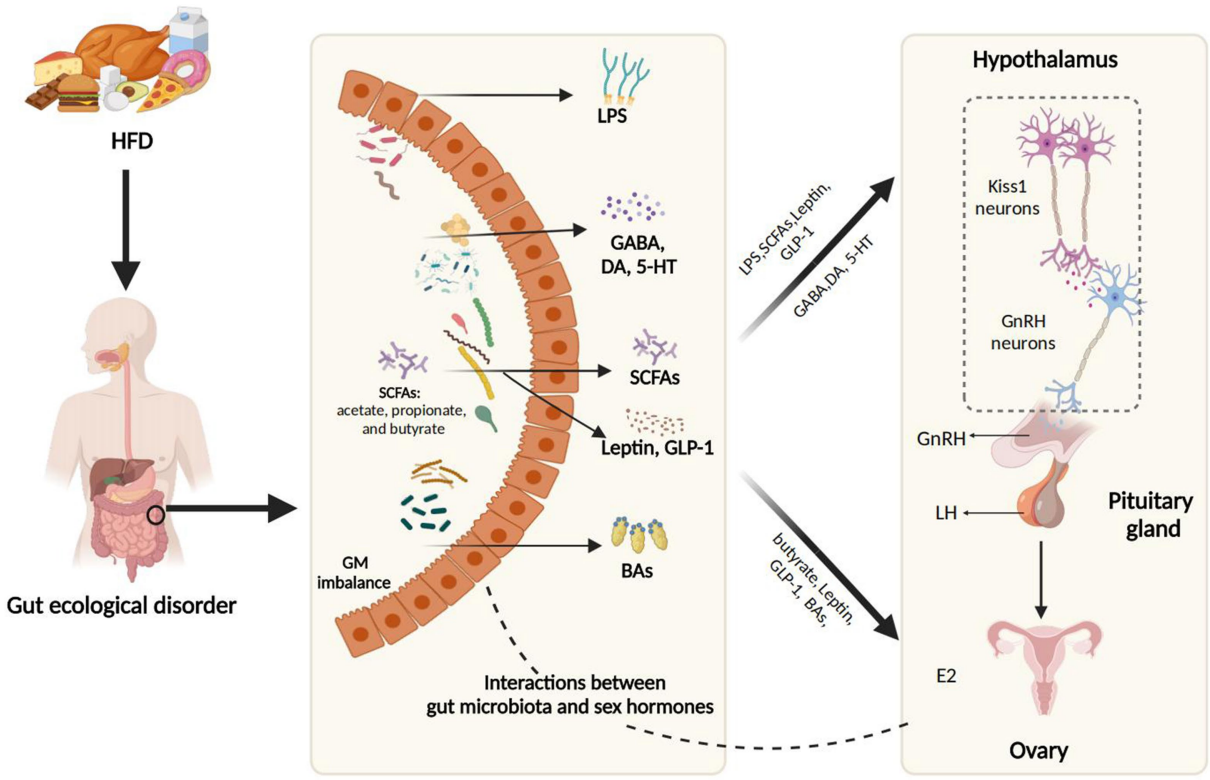

FIGURE 2
The interaction mechanisms through which HFD promotes PP by modulation of GM and its metabolic products. HFD, a high-fat diet; SCFAs, short-chain fatty acids; LPS, lipopolysaccharide; GABA, Gamma-aminobutyric acid; DA, dopamine; 5-HT, 5-hydroxytryptamine; GLP-1, glucagon-like peptide-1; BAs, bile acids; E2, estradiol; iNOS, inducible nitric oxide synthase; NO, nitric oxide; GnRH, gonadotropin-releasing hormone; LH, luteinizing hormone. Figure created with BioRender.com.

5.1 Interaction between GM and sex hormones in HFD

Mutual interactions between GM and sex hormones have been reported, particularly in the context of HFD. The GM can directly modulate sex hormone levels. For example, β-glucuronidase, an enzyme secreted by *Clostridium* species prevalent in HFD, activates estrogen by deconjugation, thereby enhancing its bioavailability and absorption in the gut and peripheral tissues (Zengul, 2019). Conversely, sex hormone levels can also shape GM composition and diversity. Mueller et al. noted that premenopausal healthy women had lower *Bacteroides* and *Prevotella* abundances than age-matched men, a difference absent in postmenopausal women (Mueller et al., 2006). A parallel sexual dimorphism in the composition of rodent GM emerged concomitantly with pubertal onset and was subsequently abolished after castration (Org et al., 2016). Additionally, direct evidence of the influence of sex hormones on the GM was provided in E2-induced PP mice, where an increase in *Dubosiella*, *Faecalibaculum*, and *Bifidobacterium* was noted in response to E2 (Bo et al., 2022; For a more detailed discussion on the bidirectional interactions between GM and sex hormones, refer to the review; Calcaterra et al., 2022)

A deeper exploration of this complex interplay between GM and sex hormones will advance both mechanistic understanding of PP pathogenesis and development of microbiota-targeted therapies.

5.2 HFD promotes PP through metabolic intermediates

5.2.1 SCFAs

SCFAs are fatty acids with fewer than six carbon atoms, primarily produced in the colon through the fermentation of dietary fibers by GM. The most common SCFAs, including acetate, propionate, and butyrate, play crucial roles in gut health and overall metabolism. HFD typically suppresses the proliferation of SCFA-producing gut bacteria while fostering pathogenic bacteria growth (Onishi et al., 2017). The link between SCFAs and PP is long established, with a metabolomic study revealing negative correlations between fecal butyrate, isovalerate, and caproate levels and early puberty onset (Yuan et al., 2023). Notably, a 2022 animal study provided the first experimental evidence that SCFAs exert protective effects against HFD-induced PP by reversing pubertal symptoms through the Kiss1-GPR54-protein kinase C (PKC)-extracellular-regulated kinase 1/2 (ERK1/2) signaling pathway (Wang et al., 2022). This suggests a promising non-invasive therapeutic strategy for preventing and ameliorating PP.

Despite these promising results, the role of SCFAs in PP is incompletely understood as 16S rRNA gene sequencing studies paradoxically revealed increased SCFA-producing bacteria in PP girls (Wang Y. et al., 2024; Huang et al., 2022; Dong et al., 2020). This discrepancy may reflect fundamental differences between experimental and physiological conditions. First, animal studies

utilizing supraphysiological SCFA doses through direct administration may not accurately mirror the complex gut-brain communication mediated by microbial metabolites in humans. Second, cross-sectional human studies are unable to distinguish whether increased SCFA producers are drivers or passengers in PP. Third, physiological barriers—including intestinal absorption, hepatic metabolism, and blood–brain barrier permeability—may weaken SCFAs' effects (Parker et al., 2020), explaining why higher SCFA-producing bacterial abundance does not necessarily prevent PP. Consequently, the dysbiosis induced by HFD, leading to altered SCFA profiles, necessitates further research within the PP context.

5.2.2 BAs

BAs are vital for fat metabolism, aiding in the emulsification and absorption of dietary fats and fat-soluble vitamins in the intestine. HFD significantly boosts bile acid (BA) synthesis and secretion—particularly of hydrophobic secondary BAs—with certain gut bacteria (such as *Clostridium* and Ruminococcaceae families; Araki et al., 2005; Stenman et al., 2013; Chen et al., 2023; Jiao et al., 2017) catalyzing this process via 7α-dehydroxylation reactions (Li et al., 2021a). The relationship between BAs and puberty was first noted by Bergmann et al. in 1986, who found elevated BA saturation during female puberty, positively correlating with estrogen levels (Bergmann et al., 1986). Recent integrated 16S rRNA gene sequencing and metabolomic analyses revealed notably decreased metabolites involved in primary BA biosynthesis (such as glycocholate, cholic acid, and taurochenodeoxycholic acid) in CPP, with glycocholate potentially enhancing sex hormone absorption (Huang et al., 2023). Mechanistically, HFD-induced female PP rats showed significantly reduced GDCA levels, with glycodeoxycholic acid (GDCA) supplementation ameliorating PP symptoms through the modulation of the hypothalamic *Sirt1*/*Kiss1* signaling pathway (Wu et al., 2025). BAs may also exert diverse biological effects via receptors, such as takeda G-protein-coupled receptor 5 (TGR5) and farnesoid X receptor (FXR). As Vanden Brink et al. showed, hypothalamic TGR5 receptor activation accelerated puberty in normal female rats through kisspeptin receptor-dependent GnRH secretion (Vanden Brink et al., 2024). This 'paradox' may be attributable to factors such as genetic background variations, context-dependent effects (HFD versus normal diet), and non-native forms of GDCA that mediate hypothalamic signaling. Importantly, significant species differences in BA metabolism—particularly the abundance of rodent-specific hydrophilic and 6α-hydroxylated BAs—underscore the need for clinical validation when translating these animal findings to human applications (Straniero et al., 2020).

5.2.3 LPS

LPS, a major component of the outer membrane of Gram-negative bacteria, acts as an endotoxin that triggers strong inflammatory responses in host organisms. Mounting evidence indicates that HFD increases the prevalence of LPS-producing bacteria (such as those in the S24-7 family, Enterobacteriaceae, and Desulfovibrionaceae), and exacerbate intestinal permeability, leading to elevated intestinal LPS levels entering the bloodstream (Stenman et al., 2013; Moreira et al., 2012; Kang et al., 2017). LPS activates toll-like receptor 4 receptors on glial cells in the brain, inducing the release of inflammatory mediators and promoting potentiates oxidative stress, which may be accentuated during puberty (Iwasa et al., 2015; Zhao et al., 2019; Schoeler and Caesar, 2019).

Additionally, LPS stimulates the expression of inducible NO synthase in various cells, increasing NO levels that are involved in regulating female reproduction. A research group found that the NO synthesis pathway is more active in girls with CPP compared to healthy controls. Further mechanistic studies showed that NO not only stimulates GnRH secretion (Araki et al., 2005; Zhao et al., 2019), but may also promote follicular development through the PI3K/protein kinase B (AKT)/FoxO3a pathway, thereby accelerating puberty onset (Han G. et al., 2022; Luo et al., 2021; Li et al., 2020).

5.2.4 Neurotransmitters

Most neurotransmitters closely associated with PP are produced by the GM. HFD disrupts the intestinal microbial balance, diminishing populations of *Lactobacillus* and *Bifidobacterium*, both known to produce GABA through glutamate decarboxylase activity (Chen et al., 2023; Strandwitz, 2018). Genome-wide association studies have identified several alleles associated with the GABA signaling pathway that correlate with the age of menarche (Perry et al., 2014). GABA acts as a critical inhibitory modulator of hypothalamic GnRH neurons by engaging GABA receptors, thereby suppressing GnRH secretion (Watanabe et al., 2014). Further experiments in prepubertal rhesus monkeys demonstrated that GABA inhibits the upstream gene *Kiss1* and its expression, contributing to the delay in puberty onset (Kurian et al., 2012). Additionally, GABA reduces NO production in the hypothalamus, diminishing the stimulation of the HPG axis and the promotion of follicular development (Yang et al., 2020).

In parallel, HFD also augments gut bacteria linked to intestinal inflammation (e.g., *Bilophila*, *Desulfovibrio*, and *Escherichia*), which synthesize neurotransmitters like dopamine and 5-HT, both of which are critical regulators during puberty (Chen et al., 2023; Wang M. et al., 2024). DA activates GnRH through a cAMP-mediated mechanism, enhancing the amplitude and duration of GnRH pulses to promote the onset of puberty (Winters et al., 2014). In contrast, 5-HT exerts a biphasic effect on GnRH neurons: rapid inhibition via 5-HT1A receptors, followed by slow excitation through 5-HT2A receptors (Bhattarai et al., 2014). Despite these insights, the exact mechanisms and causal relationships between neurotransmitters and PP require more detailed exploration.

6 Targeting GM modulation for PP

6.1 Dietary and lifestyle interventions

Recent advancements in dietary interventions have demonstrated their effectiveness as a supplemental strategy for managing PP by influencing GM composition and biological activity, thereby modulating the host's sexual development. Diets rich in vegetables and proteins have shown effectiveness in mitigating the onset and progression of PP (Gu et al., 2024). Specifically, plant-based high-fiber diets may diminish estrogen levels by inhibiting the dissociation of estrogen-binding proteins and facilitating increased estrogen excretion via feces. This reduction in circulating estrogen may delay puberty onset and slow sexual maturation (Cheng et al., 2012).

In addition to dietary modifications, clinical trials have highlighted the efficacy of certain supplements in delaying sexual

development. For instance, a combination of GnRHa and pomegranate extract has proven more effective than GnRHa alone in managing idiopathic CPP (Liu and Tang, 2017). Treatment with decaffeinated green tea polyphenol in prepubertal obese girls not only improved obesity but also delayed puberty onset (Xie et al., 2021). Lifestyle interventions like intermittent fasting have yielded positive outcomes in PP management (Yu et al., 2021). Taken together, while these dietary and lifestyle interventions show promise in alleviating symptoms of PP, further research is required to identify and establish the most effective and evidence-based approaches for managing this condition.

6.2 Probiotics

Probiotics are live microorganisms that confer health benefits to the host when administered in adequate amounts (Sanders et al., 2019). While direct clinical studies on the effects of probiotics in children with PP are lacking, emerging animal researches evaluate potential advantages. Specific gut microbial combinations, such as a regimen predominantly containing *Bifidobacterium longum* or a blend of *Lactobacillus rhamnosus* and *Lactobacillus helveticus*, have demonstrated the potential in delaying puberty onset in female mice with PP (Yuan et al., 2023; Cowan and Richardson, 2019). Future research should prioritize large-scale, randomized controlled trials to confirm the efficacy and safety of these interventions.

6.3 FMT

FMT is an innovative therapeutic option in treating conditions such as *Clostridium difficile* infection (Cheng Y. W. et al., 2021), diabetes (De Groot et al., 2021), metabolic syndrome (Li et al., 2016), and autism (Kang et al., 2020). This procedure involves transplanting fecal material from a healthy donor into the patient's gastrointestinal tract to reestablish microbial balance (Hamamah et al., 2022). There are currently only two animal experimental studies that have been reported FMT could play a critical role in puberty regulation. In both studies, researchers transplanted fecal microbiota from HFD-induced PP rats and from PP girls, and observed an accelerated puberty onset in healthy rats (Bo et al., 2022). In summary, FMT could serve as a viable future treatment for PP, although more studies are needed to fully elucidate the underlying mechanisms and safety in children (Yue and Zhang, 2024).

6.4 Traditional Chinese medicine (TCM)

TCM has been effectively utilized for centuries to treat various health issues, including Alzheimer's disease (Ding et al., 2022), Parkinson's disease (Muhammad et al., 2022), rheumatoid arthritis (Jakobsson et al., 2022), and PP (Han X. X. et al., 2022). Several TCM herbs, such as Anemarrhena (Yan et al., 2021), Phellodendron (Su et al., 2021), Berberine (Yang et al., 2022), and Poria (Shan-Shan et al., 2019), show efficacy in modulating the dysregulation of the gut microbial ecosystem. Currently, commonly prescribed formulations for PP in clinical practice include Zhibai Dihuang Wan, Dabu Yin Wan, and Shugan Zhi Yin Jiao Huo Fang. A meta-analysis also revealed integrating TCM with GnRHa therapy improved treatment outcomes compared to GnRHa alone (Lee et al., 2020). Despite these advantages, integrated treatment approaches should be approached cautiously, with careful consideration to ensure that TCM complements rather than interferes with conventional therapies.

7 Discussion

Given the contribution already made by the study described above, we believe that future research should focus on the following key areas:

7.1 The relationship between HFD, GM, and PP

Extensive observational studies have established that HFD (particularly PUFAs and animal proteins) represents a significant risk factor for PP in girls (Chen et al., 2024; Gu et al., 2024; Günther et al., 2010; Xiong et al., 2022; Du et al., 2024; Cheng et al., 2021b; Xu et al., 2022; Cheng et al., 2021a; Shahatah et al., 2021; Nguyen et al., 2020; Jansen et al., 2016; Mueller et al., 2015; Carwile et al., 2015; Mervish et al., 2013; Wiley, 2011; Rogers et al., 2010; Koo et al., 2002; Berkey et al., 2000; Maclure et al., 1991; Merzenich et al., 1993; Szamreta et al., 2020). Preclinical investigations further revealed that maternal or prepubertal HFD exposure induces PP in rodent models (Bo et al., 2022; Wang et al., 2020), with the reported potential mechanisms involving two distinct yet interconnected pathways: microbiota-independent mechanisms (detailed in Section 2), including hypothalamic microglial activation, p53 upregulation, metabolic hormone dysregulation, and others, all of which have been elucidated in multiple reviews as contributing to the activation of the HPG axis (Stathori et al., 2025; Calcaterra et al., 2023; Valsamakis et al., 2021); and microbiota-dependent pathways, whereby HFD-induced gut dysbiosis directly interferes with sex hormone metabolism while modulating key metabolic mediators (such as SCFAs, BAs, and LPS) through microbial enzymatic activities. The latter pathway highlights the mediating role of gut microbiota and their metabolites in HFD-induced PP.

Although 16S rRNA gene sequencing and metabolomics from clinical and preclinical studies have identified characteristic microbial and metabolic signatures in PP, these cross-sectional approaches cannot establish causal relationships with HFD-induced PP (Bo et al., 2022; Wang et al., 2020; Wang Y. et al., 2024; Wang L. et al., 2024; Huang et al., 2023; Huang et al., 2022; Li et al., 2021b; Dong et al., 2020; Qian et al., 2024; Yi et al., 2024; Nguyen et al., 2024; Yuan et al., 2023; Wang et al., 2022). Intervention studies employing FMT and targeted metabolite administration have confirmed that GM influences HFD-induced PP by regulating the hypothalamic Kiss1-GnRH system, with specific metabolites like SCFAs and GDCA exerting ameliorative effects through this pathway (Bo et al., 2022; Wang et al., 2022; Wu et al., 2025). GDCA upregulated *Sirt1* expression to suppress the *Kiss1* gene. Intriguingly, SCFAs (Jiao et al., 2020; Caetano-Silva et al., 2023; Lin et al., 2022) and specific BAs (Shihabudeen et al., 2015; Yanguas-Casás et al., 2017; Paluschinski et al., 2019; such as tauroursodeoxycholic acid, glycochenodeoxycholic acid, chenodeoxycholic acid, and others) may inhibit multiple key

nodes in microbiota-independent pathways, including attenuating p53 expression, reducing microglial activation, and modulating metabolic hormone dysregulation. Leptin, in turn, has been reported to modulate gut microbial metabolic function by enhancing duodenal sympathetic tone and to regulate systemic BA metabolism (Wen et al., 2021; Toledo et al., 2025). However, critical issues still remain: first, the discordance between increased SCFA-producing bacteria and their biological effects in PP may stem from multiple factors, such as pharmacologic versus physiologic concentration disparities, cross-sectional study limitations, and distinct mechanisms of direct interventions versus microbial-mediated actions; second, species-specific variations in BA metabolism constrain clinical translation to humans (Straniero et al., 2020); third, it remains unclear the specific microbial sources of bioactive metabolites and how GM and metabolites regulate hypothalamic gene expression via the microbiota-gut-brain (MGB), potentially through vagal or circulatory pathways (detailed in Section 7.2).

Additionally, key neuromodulators (GABA, DA, 5-HT) and LPS are promising metabolites warranting further investigation, though their precise roles and concentration changes in HFD-induced PP remain to be elucidated. Collectively, HFD impacts pubertal timing through both microbiota-dependent and microbiota-independent pathways that exhibit cross-regulation, providing a conceptual framework for understanding PP pathogenesis and developing targeted interventions.

7.2 Evidence between the gut-brain axis and PP

Mounting evidence linking the GM to hypothalamic dysfunction in the context of PP has underscored the bidirectional communication between the GM and the brain via the MGB axis. MGB axis is theorized to occur through various systems, including the autonomic and enteric nervous systems, neuroendocrine pathways, and the immune system (Cryan et al., 2019). Nowadays, understanding of the mechanisms of PP through the MGB axis focuses on several pathways.

First, GM may modulate brain function through vagal nerve activation, the most extensively studied pathway. Clinical evidence shows cardiac autonomic dysfunction in girls with idiopathic PP, mainly manifested as a decrease in vagal nerve tension (Yi et al., 2017). Animal experiments further demonstrate that prepubertal vagotomy could lead to ovarian dysfunction, confirming its crucial role in the development of puberty (Morales-Ledesma et al., 2004). Mechanistically, as the main conduction pathway connecting the enteric nervous system and the central nervous system, the vagus nerve expresses receptors for a variety of bioactive compounds on its surface (such as GLP-1 receptor, cholecystokinin 1 receptor, neuropeptide Y receptor Y2, GPR35, and GPR119), enabling direct recognition of signaling molecules from GM and their metabolites, such as LPS-producing bacteria (Ma et al., 2024), acetate-producing bacteria and acetate (Zheng et al., 2021), kynurenic acid (Fan et al., 2023b), indole (Jaglin et al., 2018) and others. While cross-disease studies provide experimental support for vagus nerve–mediated microbiota-brain communication, critical gaps persist in understanding its specific regulatory mechanisms in PP pathogenesis—particularly how distinct microbial metabolites modulate HPG axis activity via the vagus nerve.

Second, under pathological conditions, harmful gut microbes and their metabolites in the bloodstream can also disrupt hypothalamus function. Given its anatomical proximity to the blood–brain barrier (BBB), the hypothalamus is particularly vulnerable to the detrimental effects of BBB dysfunction and leakage (Thaler et al., 2012). Developmental studies have shown that sex hormones in the neonatal period can significantly regulate the development of cerebral blood vessels and the integrity of the BBB. This critical period coincides with the early activation peak of the HPG axis, providing important clues for understanding the association between PP and abnormal BBB function (Collignon et al., 2024). In addition, a study demonstrated a causal relationship between microbial alterations and gut barrier dysfunction, as alterations were observed in gut barrier permeability and in tight junction protein occludin in both the frontal cortex and hippocampus in germ-free adult mice, and these alterations were shown to recover following treatment with SCFA-producing bacterial strains or sodium butyrate (Braniste et al., 2014). These findings provide direct evidence for the regulation of neuroendocrine function by the MGB axis, suggesting that the GM may play a crucial role in the pathogenesis of PP by affecting the integrity of the BBB. However, direct animal and clinical data on the specific regulatory mechanisms of the MGB axis in PP are remain lacking, underscoring the urgent need for future research in this field.

Although there is growing discussion about the role of the MGB axis in regulating neurological and metabolic disorders, direct animal and clinical evidence in the context of PP remains lacking. Future research in this area is urgently needed.

7.3 The role of HFD and obesity

The relationship between HFD, obesity, and PP has been a subject of ongoing debate. Emerging evidence confirms that HFD can indeed trigger PP through obesity-independent pathways: first, animal studies demonstrate that both HFD-induced and kisspeptin-induced PP occur independently of weight changes, with short-term HFD exposure sufficient to elevate gonadotropins without altering body fat or leptin levels (Ullah et al., 2019; Frisch et al., 1977; Sahin et al., 2015); second, gut microbes specifically enriched in female rats with PP (such as *Bilophila*; Kimura et al., 2013; Kimura et al., 2011), *Lachnoclostridium* (Zhao et al., 2021), *Lactobacillus* (Henning et al., 2018), *Lactobacillus murinus* (Li et al., 2024), *Lactobacillus reuteri* (Zhang et al., 2022) are negatively correlated with obesity, indicating differences between the microbial communities regulating pubertal development and the microbiota associated with obesity; third, the conventional paradigm recognizes obesity as a significant risk factor for PP through its induction of metabolic hormone dysregulation, a well-established mechanism extensively documented in reviews (Shi et al., 2022; Calcaterra et al., 2023). However, HFD serves as the primary instigator of both metabolic hormone imbalance and subsequent obesity development (Chakraborty et al., 2016; Fan et al., 2023a). Under HFD conditions, metabolic hormone dysregulation and obesity exhibit complex bidirectional interactions, with obesity serving as an exacerbating factor rather than a prerequisite for metabolic dysfunction. This is evidenced by findings that long-term

HFD-fed mice exhibit increased GLP-1 secretion and insulin resistance independent of obesity and body weight (Wang et al., 2015; Clegg et al., 2011), and girls with CPP show high serum leptin levels uncorrelated with body mass index (BMI; Zurita-Cruz et al., 2021; Kang et al., 2018). Collectively, these findings confirm that HFD induces PP not only through the traditional "obesity-metabolic hormone" pathway but also via obesity-independent mechanisms.

7.4 Integrated omics technologies and population research

Intestinal microbes and their metabolic byproducts provide new biological insights into the link between HFD and PP. However, existing research still has significant limitations. Firstly, the current evidence primarily relies on cross-sectional designs and the low-resolution 16S rRNA gene sequencing technology, which limits the comprehensive revelation of dynamic evolution of GM and lacks precision at the species level. To break through this bottleneck, future research should prioritize conducting longitudinal cohort studies combined with high-throughput technologies such as metagenomic sequencing for multi-omics integration analysis (including metabolomics, epigenomics, and proteomics). Such research can dynamically capture the key biological processes in the occurrence and development of PP, identify reliable biomarker prediction models through machine learning algorithms, and deeply analyze the "microorganisms-metabolites-hosts" interaction network. The feasibility of this methodological approach has been well established in prior research. For example, Huang et al. developed a diagnostic classifier to differentiate CPP from healthy controls using integrated microbiome-metabolome analysis, identifying potential therapeutic biomarkers (Huang et al., 2023). In addition, complementary animal studies using combined transcriptomic-epigenomic profiling elucidated critical regulatory genes and pathway networks in PP pathogenesis (Mohamed et al., 2022). Secondly, most mechanistic data on PP is largely based on animal experiments and lacks sufficient clinical evidence to definitively support its role in humans. Given the complexity and specificity of the disease, large-scale clinical studies are likely to provide more valuable insights into its pathophysiology than animal models.

In conclusion, HFD-induced PP arises from the overlapping effects of GM dysbiosis and high-fat intake, involving multiple mechanisms. Fortunately, advances in omics research and breakthroughs in mechanistic studies using animal models are rapidly enhancing our understanding of the causal mechanisms between HFD, GM, and PP. These advancements also reveal the potential therapeutic effects of key bacterial species or taxa, paving the way for optimizing microbiota-based therapeutic strategies and developing innovative, non-invasive treatment options for children with PP.

Author contributions

NW: Visualization, Writing – original draft. KN: Visualization, Writing – original draft. YL: Visualization, Writing – original draft. QW: Conceptualization, Funding acquisition, Writing – review & editing. NL: Conceptualization, Funding acquisition, Writing – review & editing. LZ: Conceptualization, Funding acquisition, Writing – review & editing.

Funding

The author(s) declare that financial support was received for the research and/or publication of this article. This research was funded by the National Natural Science Foundation of China (82370785 and 82172320); Shandong Provincial Natural Science Foundation (ZR2024MH220); Shandong University Outstanding Young Scholars Program, and National Center for Women and Children's Health, China CDC "Maternal and Infants Nutrition and Health Research Programs" (2022FYH008); Key R&D Program (Innovation Capacity Improvement Project for Science and Technology-based Small and Medium-sized Enterprises) of Shandong Province, China (2024TSGC0372).

Acknowledgments

Thanks for the support of Children's Hospital Affiliated to Shandong University (Jinan Children's Hospital). Thanks to all the participants for this study.

Conflict of interest

The authors declare that the research was conducted in the absence of any commercial or financial relationships that could be construed as a potential conflict of interest.

Generative AI statement

The author(s) declare that no Gen AI was used in the creation of this manuscript.

Publisher's note

All claims expressed in this article are solely those of the authors and do not necessarily represent those of their affiliated organizations, or those of the publisher, the editors and the reviewers. Any product that may be evaluated in this article, or claim that may be made by its manufacturer, is not guaranteed or endorsed by the publisher.

Supplementary material

The Supplementary material for this article can be found online at: https://www.frontiersin.org/articles/10.3389/fmicb.2025.1564902/full#supplementary-material

References

Alghamdi, A., and Alghamdi, A. H. (2023). Precocious puberty: types, pathogenesis and updated management. *Cureus* 15:e47485. doi: 10.7759/cureus.47485

Araki, Y., Katoh, T., Ogawa, A., Bamba, S., Andoh, A., Koyama, S., et al. (2005). Bile acid modulates transepithelial permeability via the generation of reactive oxygen species in the Caco-2 cell line. *Free Radic. Biol. Med.* 39, 769–780. doi: 10.1016/j.freeradbiomed.2005.04.026

Berger, C. E., Qian, Y., Liu, G., Chen, H., and Chen, X. (2012). p53, a target of estrogen receptor (Er) α, modulates Dna damage-induced growth suppression in Er-positive breast cancer cells. *J. Biol. Chem.* 287, 30117–30127. doi: 10.1074/jbc.M112.367326

Bergmann, K. V., Becker, M., and Leiss, O. (1986). Biliary cholesterol saturation in non-obese women and non-obese men before and after puberty. *Eur. J. Clin. Investig.* 16, 531–535.

Berkey, C. S., Gardner, J. D., and Lindsay Frazier, A. (2000). Relation of childhood diet and body size to menarche and adolescent growth in girls. *Am. J. Epidemiol.* 152, 446–452.

Bhattarai, J. P., Roa, J., Herbison, A. E., and Han, S. K. (2014). Serotonin acts through 5-Ht1 and 5-Ht2 receptors to exert biphasic actions on Gnrh neuron excitability in the mouse. *Endocrinology* 155, 513–524. doi: 10.1210/en.2013-1692

Bisanz, J. E., Upadhyay, V., and Turnbaugh, J. A. (2019). Meta-analysis reveals reproducible gut microbiome alterations in response to a high-fat diet. *Cell Host Microbe* 26, 265–272. doi: 10.1016/j.chom.2019.06.013

Bo, T., Liu, M., Tang, L., Lv, J., Wen, J., and Wang, D. (2022). Effects of high-fat diet during childhood on precocious puberty and gut microbiota in mice. *Front. Microbiol.* 13:930747. doi: 10.3389/fmicb.2022.930747

Boynton-Jarrett, R., Rich-Edwards, J., Fredman, L., Hibert, E. L., Michels, K. B., Forman, M. R., et al. (2011). Gestational weight gain and daughter's age at menarche. *J. Women's Health* 20, 1193–1200. doi: 10.1089/jwh.2010.2517

Braniste, V., Al-Asmakh, M., and Kowal, C. (2014). The gut microbiota influences blood-brain barrier permeability in mice. *Sci. Transl. Med.* 6:263ra158. doi: 10.1126/scitranslmed.3009759

Caetano-Silva, M. E., Rund, L., Hutchinson, N. T., Woods, J. A., Steelman, A. J., and Johnson, R. W. (2023). Inhibition of inflammatory microglia by dietary fiber and short-chain fatty acids. *Sci. Rep.* 13:2819. doi: 10.1038/s41598-022-27086-x

Calcaterra, V., Magenes, V. C., Hruby, C., Siccardo, F., Mari, A., Cordaro, E., et al. (2023). Links between childhood obesity, high-fat diet, and central precocious puberty. *Child. Aust.* 10:241. doi: 10.3390/children10020241

Calcaterra, V., Rossi, V., Massini, G., Regalbuto, C., Hruby, C., Panelli, S., et al. (2022). Precocious puberty and microbiota: the role of the sex hormone–gut microbiome axis. *Front. Endocrinol.* 13:1000919. doi: 10.3389/fendo.2022.1000919

Carwile, J. L., Willett, W. C., Wang, M., Rich-Edwards, J., Frazier, A. L., and Michels, K. B. (2015). Milk consumption after age 9 years does not predict age at menarche. *J. Nutr.* 145, 1900–1908. doi: 10.3945/jn.115.214270

Chakraborty, T. R., Donthireddy, L., Adhikary, D., and Chakraborty, S. (2016). Long-term high fat diet has a profound effect on body weight, hormone levels, and estrous cycle in mice. *Medical Sci. Monitor: Int. Medical J. Experimental Clin. Res.* 22, 1601–1608. doi: 10.12659/MSM.897628

Charni-Natan, M., Aloni-Grinstein, R., Osher, E., and Rotter, V. (2019). Liver and steroid hormones—can a touch of p53 make a difference? *Front. Endocrinol.* 10:374. doi: 10.3389/fendo.2019.00374

Chen, T., Chen, C., Wu, H., Chen, X., Xie, R., Wang, F., et al. (2021). Overexpression of p53 accelerates puberty in high-fat diet–fed mice through Lin28/let-7 system. *Exp. Biol. Med.* 246, 66–71. doi: 10.1177/1535370220961320

Chen, X., Fu, S., Chen, C., Yuan, Y., Dai, Z., Chen, A., et al. (2024). Association of Traditional dietary pattern with early and precocious puberty: a population-based cross-sectional study. *Pediatr. Res.* 96, 245–252. doi: 10.1038/s41390-024-03110-w

Chen, X., Huang, L., Cui, L., Xiao, Z., Xiong, X., and Chen, C. (2022). Sodium–glucose cotransporter 2 inhibitor ameliorates high fat diet-induced hypothalamic–pituitary–ovarian axis disorders. *J. Physiol.* 600, 4549–4568. doi: 10.1113/JP283259

Chen, T., Wu, H., Chen, X., Xie, R., Wang, F., Sun, H., et al. (2020). p53 mediates Gnrh secretion via Lin28/let-7 system in Gt1-7 cells. *Diabetes, Metabolic Syndrome Obesity* 13, 4681–4688. doi: 10.2147/DMSO.S279901

Chen, J., Xiao, Y., Li, D., Zhang, S., Wu, Y., Zhang, Q., et al. (2023). New insights into the mechanisms of high-fat diet mediated gut microbiota in chronic diseases. *iMeta* 2:e69. doi: 10.1002/imt2.69

Cheng, Y.-W., Alhaffar, D., Saha, S., Khanna, S., Bohm, M., Phelps, E., et al. (2021). Fecal microbiota transplantation is safe and effective in patients with Clostridioides difficile infection and cirrhosis. *Clin. Gastroenterol. Hepatol.* 19, 1627–1634. doi: 10.1016/j.cgh.2020.06.051

Cheng, G., Buyken, A. E., Shi, L., Karaolis-Danckert, N., Kroke, A., Wudy, S. A., et al. (2012). Beyond overweight: nutrition as an important lifestyle factor influencing timing of puberty. *Nutr. Rev.* 70, 133–152. doi: 10.1111/j.1753-4887.2011.00461.x

Cheng, T. S., Day, F. R., and Perry, J. R. (2021a). Prepubertal dietary and plasma phospholipid fatty acids related to puberty timing: longitudinal cohort and Mendelian randomization analyses. *Nutrients* 13:1868. doi: 10.3390/nu13061868

Cheng, T. S., Sharp, S. J., and Brage, S. (2021b). Longitudinal associations between prepubertal childhood total energy and macronutrient intakes and subsequent puberty timing in UK boys and girls. *Eur. J. Nutr.* 61, 1–11. doi: 10.1007/s00394-021-02629-6

Cheuiche, A. V., Da Silveira, L. G., and De Paula, L. C. P. (2021). Diagnosis and management of precocious sexual maturation: an updated review. *Eur. J. Pediatr.* 180, 3073–3087. doi: 10.1007/s00431-021-04022-1

Childs, G. V., Odle, A. K., and Macnicol, M. C. (2021). The importance of leptin to reproduction. *Endocrinology* 162:bqaa204. doi: 10.1210/endocr/bqaa204

Clarke, S. A., and Dhillo, W. S. (2016). Kisspeptin across the human lifespan: evidence from animal studies and beyond. *J. Endocrinol.* 229, R83–R98. doi: 10.1530/JOE-15-0538

Clarke, S A, and Dhillo, W S. "Phoenixin and its role in reproductive hormone release"; *Proceedings of the seminars in reproductive medicine*, (2019). Thieme Medical Publishers.

Clegg, D. J., Gotoh, K., Kemp, C., Wortman, M. D., Benoit, S. C., Brown, L. M., et al. (2011). Consumption of a high-fat diet induces central insulin resistance independent of adiposity. *Physiol. Behav.* 103, 10–16. doi: 10.1016/j.physbeh.2011.01.010

Collignon, A., Dion-Albert, L., Ménard, C., and Coelho-Santos, V. (2024). Sex, hormones and cerebrovascular function: from development to disorder. *Fluids Barriers CNS* 21:2. doi: 10.1186/s12987-023-00496-3

Cowan, C. S., and Richardson, R. (2019). Early-life stress leads to sex-dependent changes in pubertal timing in rats that are reversed by a probiotic formulation. *Dev. Psychobiol.* 61, 679–687. doi: 10.1002/dev.21765

Cryan, J. F., O'Riordan, K. J., and Cowan, C. S. M., Sandhu, K. V., Bastiaanssen, T. F. S., Boehme, M., et al. (2019). The Microbiota-Gut-Brain Axis. *Physiol Rev.* 99, 1877–2013. doi: 10.1152/physrev.00018.2018

Daniel, H., Gholami, A. M., Berry, D., Desmarchelier, C., Hahne, H., Loh, G., et al. (2014). High-fat diet alters gut microbiota physiology in mice. *ISME J.* 8, 295–308. doi: 10.1038/ismej.2013.155

David, L. A., Maurice, C. F., Carmody, R. N., Gootenberg, D. B., Button, J. E., Wolfe, B. E., et al. (2014). Diet rapidly and reproducibly alters the human gut microbiome. *Nature* 505, 559–563. doi: 10.1038/nature12820

De Filippo, C., Cavalieri, D., and Di Paola, M. (2010). Impact of diet in shaping gut microbiota revealed by a comparative study in children from Europe and rural Africa. *Proc. Natl. Acad. Sci.* 107, 14691–14696. doi: 10.1073/pnas.1005963107

De Groot, P., Nikolic, T., and Pellegrini, S. (2021). Faecal microbiota transplantation halts progression of human new-onset type 1 diabetes in a randomised controlled trial. *Gut* 70, 92–105. doi: 10.1136/gutjnl-2020-322630

Dhillo, W. S., Chaudhri, O. B., Patterson, M., Thompson, E. L., Murphy, K. G., Badman, M. K., et al. (2005). Kisspeptin-54 stimulates the hypothalamic-pituitary gonadal axis in human males. *J. Clin. Endocrinol. Metab.* 90, 6609–6615. doi: 10.1210/jc.2005-1468

Ding, M.-R., Qu, Y.-J., Hu, B., and An, H. M. (2022). Signal pathways in the treatment of Alzheimer's disease with traditional Chinese medicine. *Biomed. Pharmacother.* 152:113208. doi: 10.1016/j.biopha.2022.113208

Dong, G., Zhang, J., Yang, Z., Feng, X., Li, J., Li, D., et al. (2020). The association of gut microbiota with idiopathic central precocious puberty in girls. *Front. Endocrinol.* 10:941. doi: 10.3389/fendo.2019.00941

Du, Y., Yan, W., Bigambo, F. M., Zhou, Q., Ma, C., Gu, W., et al. (2024). Association between dietary behavior and puberty in girls. *BMC Pediatr.* 24:349. doi: 10.1186/s12887-024-04840-w

Fan, S., Chen, S., and Lin, L. (2023a). Research progress of gut microbiota and obesity caused by high-fat diet. *Front. Cell. Infect. Microbiol.* 13:1139800. doi: 10.3389/fcimb.2023.1139800

Fan, S., Guo, W., and Xiao, D. (2023b). Microbiota-gut-brain axis drives overeating disorders. *Cell Metab.* 35, 2011–2027. doi: 10.1016/j.cmet.2023.09.005

Farkas, I., Vastagh, C., Sárvári, M., and Liposits, Z. (2013). Ghrelin decreases firing activity of gonadotropin-releasing hormone (Gnrh) neurons in an estrous cycle and endocannabinoid signaling dependent manner. *PLoS One* 8:e78178. doi: 10.1371/journal.pone.0078178

Frisch, R., Hegsted, D., and Yoshinaga, K. (1977). Carcass components at first estrus of rats on high-fat and low-fat diets: body water, protein, and fat. *Proc. Natl. Acad. Sci. USA* 74, 379–383.

Fujioka, H., Kakehashi, C., Funabashi, T., and Akema, T. (2013). Immunohistochemical evidence for the relationship between microglia and Gnrh neurons in the preoptic area of ovariectomized rats with and without steroid replacement. *Endocr. J.* 60, 191–196. doi: 10.1507/endocrj.EJ12-0280

Gao, Y., Ottaway, N., Schriever, S. C., Legutko, B., García-Cáceres, C., de la Fuente, E., et al. (2014). Hormones and diet, but not body weight, control hypothalamic microglial activity. *Glia* 62, 17–25. doi: 10.1002/glia.22580

Gozukara, I., Dokuyucu, R., Özgür, T., Özcan, O., Pınar, N., Kurt, R. K., et al. (2016). Histopathologic and metabolic effect of ursodeoxycholic acid treatment on Pcos rat model. *Gynecol. Endocrinol.* 32, 492–497. doi: 10.3109/09513590.2015.1134478

Gu, Q., Wu, Y., Feng, Z., Chai, Y., Hou, S., Yu, Z., et al. (2024). Dietary pattern and precocious puberty risk in Chinese girls: a case-control study. *Nutr. J.* 23:14. doi: 10.1186/s12937-024-00916-6

Günther, A. L., Karaolis-Danckert, N., Kroke, A., Remer, T., and Buyken, A. E. (2010). Dietary protein intake throughout childhood is associated with the timing of puberty. *J. Nutr.* 140, 565–571. doi: 10.3945/jn.109.114934

Gupta, S., Knight, A. G., Gupta, S., Keller, J. N., and Bruce-Keller, A. J. (2012). Saturated long-chain fatty acids activate inflammatory signaling in astrocytes. *J. Neurochem.* 120, 1060–1071. doi: 10.1111/j.1471-4159.2012.07660.x

Hamamah, S., Gheorghita, R., Lobiuc, A., Sirbu, I. O., and Covasa, M. (2022). Fecal microbiota transplantation in non-communicable diseases: recent advances and protocols. *Front. Med.* 9:1060581. doi: 10.3389/fmed.2022.1060581

Han, G., Xuanyuan, S., and Zhang, B. (2022). Activation of Pi3K/Akt prevents hypoxia/reoxygenation-induced Gnrh decline via Foxo3a. *Physiol. Res.* 71:509. doi: 10.33549/physiolres.934861

Han, X. X., Zhao, F.-Y., Gu, K.-R., Wang, G. P., Zhang, J., Tao, R., et al. (2022). Development of precocious puberty in children: surmised medicinal plant treatment. *Biomed. Pharmacother.* 156:113907. doi: 10.1016/j.biopha.2022.113907

Henning, S. M., Yang, J., Hsu, M., Lee, R.-P., Grojean, E. M., Ly, A., et al. (2018). Decaffeinated green and black tea polyphenols decrease weight gain and alter microbiome populations and function in diet-induced obese mice. *Eur. J. Nutr.* 57, 2759–2769. doi: 10.1007/s00394-017-1542-8

Hu, Y., Li, J., Yuan, T., Yu, T., Chen, Y., Kong, H., et al. (2022). Exposure to antibiotics and precocious puberty in children: a school-based cross-sectional study in China. *Environ. Res.* 212:113365. doi: 10.1016/j.envres.2022.113365

Huang, X., Chen, J., Zou, H., Huang, P., Luo, H., Li, H., et al. (2023). Gut microbiome combined with metabolomics reveals biomarkers and pathways in central precocious puberty. *J. Transl. Med.* 21:316. doi: 10.1186/s12967-023-04169-5

Huang, C., Liu, H., Yang, W., Li, Y., Wu, B., Chen, J., et al. (2022). Distinct gut microbiota structure and function of children with idiopathic central and peripheral precocious puberty. *Int. J. Endocrinol.* 2022, 1–11. doi: 10.1155/2022/7175250

Iwasa, T., Matsuzaki, T., Tungalagsuvd, A., Munkhzaya, M., Kawami, T., Yamasaki, M., et al. (2015). Developmental changes in hypothalamic toll-like-receptor 4 mrna expression and the effects of lipopolysaccharide on such changes in female rats. *Int. J. Dev. Neurosci.* 40, 12–14. doi: 10.1016/j.ijdevneu.2014.10.002

Jaglin, M., Rhimi, M., Philippe, C., Pons, N., Bruneau, A., Goustard, B., et al. (2018). Indole, a signaling molecule produced by the gut microbiota, negatively impacts emotional behaviors in rats. *Front. Neurosci.* 12:216. doi: 10.3389/fnins.2018.00216

Jakobsson, P. J., Robertson, L., Welzel, J., Zhang, M., Zhihua, Y., Kaixin, G., et al. (2022). Where traditional Chinese medicine meets Western medicine in the prevention of rheumatoid arthritis. *J. Intern. Med.* 292, 745–763. doi: 10.1111/joim.13537

Jansen, E. C., Marín, C., Mora-Plazas, M., and Villamor, E. (2016). Higher childhood red meat intake frequency is associated with earlier age at menarche. *J. Nutr.* 146, 792–798. doi: 10.3945/jn.115.226456

Jiao, S., Cao, H., Dai, Y., Wu, J., Lv, J., du, R., et al. (2017). Effect of high-fat diet and growth stage on the diversity and composition of intestinal microbiota in healthy bovine livestock. *J. Sci. Food Agric.* 97, 5004–5013. doi: 10.1002/jsfa.8380

Jiao, A., Yu, B., He, J., Yu, J., Zheng, P., Luo, Y., et al. (2020). Short chain fatty acids could prevent fat deposition in pigs via regulating related hormones and genes. *Food Funct.* 11, 1845–1855. doi: 10.1039/C9FO02585E

Kang, D.-W., Adams, J. B., Vargason, T., Santiago, M., Hahn, J., and Krajmalnik-Brown, R. (2020). Distinct fecal and plasma metabolites in children with autism spectrum disorders and their modulation after microbiota transfer therapy. *Msphere* 5:e00314-20. doi: 10.1128/msphere.00314-20

Kang, M. J., Oh, Y. J., Shim, Y. S., Baek, J. W., Yang, S., and Hwang, I. T. (2018). The usefulness of circulating levels of leptin, kisspeptin, and neurokinin B in obese girls with precocious puberty. *Gynecol. Endocrinol.* 34, 627–630. doi: 10.1080/09513590.2017.1423467

Kang, C., Wang, B., Kaliannan, K., Wang, X., Lang, H., Hui, S., et al. (2017). Gut microbiota mediates the protective effects of dietary capsaicin against chronic low-grade inflammation and associated obesity induced by high-fat diet. *MBio* 8:e00470-17. doi: 10.1128/mbio.00470-17

Kimura, I., Inoue, D., Maeda, T., Hara, T., Ichimura, A., Miyauchi, S., et al. (2011). Short-chain fatty acids and ketones directly regulate sympathetic nervous system via G protein-coupled receptor 41 (Gpr41). *Proc. Natl. Acad. Sci. USA* 108, 8030–8035. doi: 10.1073/pnas.1016088108

Kimura, I., Ozawa, K., Inoue, D., Imamura, T., Kimura, K., Maeda, T., et al. (2013). The gut microbiota suppresses insulin-mediated fat accumulation via the short-chain fatty acid receptor Gpr43. *Nat. Commun.* 4:1829. doi: 10.1038/ncomms2852

Koo, M. M., Rohan, T. E., Jain, M., McLaughlin, J. R., and Corey, P. N. (2002). A cohort study of dietary fibre intake and menarche. *Public Health Nutr.* 5, 353–360. doi: 10.1079/PHN2002261

Kurian, J. R., Keen, K. L., Guerriero, K. A., and Terasawa, E. (2012). Tonic control of kisspeptin release in prepubertal monkeys: implications to the mechanism of puberty onset. *Endocrinology* 153, 3331–3336. doi: 10.1210/en.2012-1221

Lee, Y. B., Lee, J. A., and Lee, H. L. (2020). Herbal medicine for idiopathic central precocious puberty: a systematic review and meta-analysis. *J. Altern. Complement. Med.* 26, 976–999. doi: 10.1089/acm.2019.0312

Li, Y., Hou, H., Wang, X., Dai, X., Zhang, W., Tang, Q., et al. (2021a). Diammonium glycyrrhizinate ameliorates obesity through modulation of gut microbiota-conjugated bas-Fxr signaling. *Front. Pharmacol.* 12:796590. doi: 10.3389/fphar.2021.796590

Li, Y., Shen, L., Huang, C., Li, X., Chen, J., Li, S. C., et al. (2021b). Altered nitric oxide induced by gut microbiota reveals the connection between central precocious puberty and obesity. *Clin. Transl. Med.* 11:e299. doi: 10.1002/ctm2.299

Li, X., Yang, J., Zhou, X., Dai, C., Kong, M., Xie, L., et al. (2024). Ketogenic diet-induced bile acids protect against obesity through reduced calorie absorption. *Nat. Metab.* 6, 1397–1414. doi: 10.1038/s42255-024-01072-1

Li, J., Zhang, W., Zhu, S., and Shi, F. (2020). Nitric oxide synthase is involved in follicular development via the Pi3K/Akt/FoxO3a pathway in neonatal and immature rats. *Animals* 10:248. doi: 10.3390/ani10020248

Li, S. S., Zhu, A., Benes, V., Costea, P. I., Hercog, R., Hildebrand, F., et al. (2016). Durable coexistence of donor and recipient strains after fecal microbiota transplantation. *Science* 352, 586–589. doi: 10.1126/science.aad8852

Lin, T., Yang, W.-Q., Luo, W.-W., Zhang, L. L., Mai, Y. Q., Li, Z. Q., et al. (2022). Disturbance of fatty acid metabolism promoted vascular endothelial cell senescence via acetyl-CoA-induced protein acetylation modification. *Oxidative Med. Cell. Longev.* 2022, 1–24. doi: 10.1155/2022/1198607

Liu, J., and Tang, J. (2017). Effects of pomegranate extract in supplementing gonadotropin-releasing hormone therapy on idiopathic central precocious puberty in Chinese girls: a randomized, placebo-controlled, double-blind clinical trial. *Food Funct.* 8, 695–700. doi: 10.1039/C6FO01616B

Luo, Y., Zhu, Y., Basang, W., Wang, X., Li, C., and Zhou, X. (2021). Roles of nitric oxide in the regulation of reproduction: a review. *Front. Endocrinol.* 12:752410. doi: 10.3389/fendo.2021.752410

Ma, X., Kim, J.-K., Shin, Y.-J., Park, H. S., Lee, D. Y., Yim, S. V., et al. (2024). Lipopolysaccharide-producing Veillonella infantium and *Escherichia fergusonii* cause vagus nerve-mediated cognitive impairment in mice. *Brain Behav. Immun.* 118, 136–148. doi: 10.1016/j.bbi.2024.02.031

Maclure, M., Travis, L. B., Willett, W., and MacMahon, B. (1991). A prospective cohort study of nutrient intake and age at menarche. *Am. J. Clin. Nutr.* 54, 649–656.

Mathew, H., Castracane, V. D., and Mantzoros, C. (2018). Adipose tissue and reproductive health. *Metab. Clin. Exp.* 86, 18–32. doi: 10.1016/j.metabol.2017.11.006

Mcilwraith, E. K., Loganathan, N., and Belsham, D. D. (2018). Phoenixin expression is regulated by the fatty acids palmitate, docosahexaenoic acid and oleate, and the endocrine disrupting chemical bisphenol a in immortalized hypothalamic neurons. *Front. Neurosci.* 12:838. doi: 10.3389/fnins.2018.00838

Mervish, N. A., Gardiner, E. W., Galvez, M. P., Kushi, L. H., Windham, G. C., Biro, F. M., et al. (2013). Dietary flavonol intake is associated with age of puberty in a longitudinal cohort of girls. *Nutr. Res.* 33, 534–542. doi: 10.1016/j.nutres.2013.04.005

Merzenich, H., Boeing, H., and Wahrendorf, J. (1993). Dietary fat and sports activity as determinants for age at menarche. *Am. J. Epidemiol.* 138, 217–224.

Mohamed, A. R., Naval-Sanchez, M., Menzies, M., Evans, B., King, H., Reverter, A., et al. (2022). Leveraging transcriptome and epigenome landscapes to infer regulatory networks during the onset of sexual maturation. *BMC Genomics* 23:413. doi: 10.1186/s12864-022-08514-8

Morales-Ledesma, L., Betanzos-García, R. O., and Domínguez-Casalá, R. (2004). Unilateral or bilateral vagotomy performed on prepubertal rats at puberty onset of female rat deregulates ovarian function. *Arch. Med. Res.* 35, 279–283. doi: 10.1016/j.arcmed.2004.03.007

Moreira, A. P. B., Texeira, T. F. S., Ferreira, A. B., do Carmo Gouveia Peluzio, M., and de Cássia Gonçalves Alfenas, R. (2012). Influence of a high-fat diet on gut microbiota, intestinal permeability and metabolic endotoxaemia. *Br. J. Nutr.* 108, 801–809. doi: 10.1017/S0007114512001213

Mueller, N. T., Jacobs, D. R. Jr., and Maclehose, R. F. (2015). Consumption of caffeinated and artificially sweetened soft drinks is associated with risk of early menarche. *Am. J. Clin. Nutr.* 102, 648–654. doi: 10.3945/ajcn.114.100958

Mueller, S., Saunier, K., Hanisch, C., Norin, E., Alm, L., Midtvedt, T., et al. (2006). Differences in fecal microbiota in different European study populations in relation to age, gender, and country: a cross-sectional study. *Appl. Environ. Microbiol.* 72, 1027–1033. doi: 10.1128/AEM.72.2.1027-1033.2006

Muhammad, F., Liu, Y., Zhou, Y., Yang, H., and Li, H. (2022). Antioxidative role of traditional Chinese medicine in Parkinson's disease. *J. Ethnopharmacol.* 285:114821. doi: 10.1016/j.jep.2021.114821

Nguyen, N. T. K., Fan, H.-Y., Tsai, M.-C., Tung, T. H., Huynh, Q. T. V., Huang, S. Y., et al. (2020). Nutrient intake through childhood and early menarche onset in girls: systematic review and meta-analysis. *Nutrients* 12:2544. doi: 10.3390/nu12092544

Nguyen, N. N., Lin, C.-Y., Tsai, W.-L., Huang, H. Y., Chen, C. M., Tung, Y. T., et al. (2024). Natural sweetener glycyrrhizin protects against precocious puberty by modulating the gut microbiome. *Life Sci.* 350:122789. doi: 10.1016/j.lfs.2024.122789

Nguyen, X. P., Nakamura, T., Osuka, S., Bayasula, B., Nakanishi, N., Kasahara, Y., et al. (2019). Effect of the neuropeptide phoenixin and its receptor Gpr173 during folliculogenesis. *Reproduction* 158, 25–34. doi: 10.1530/REP-19-0025

Onishi, J. C., Campbell, S., Moreau, M., Patel, F., Brooks, A. I., Zhou, Y. X., et al. (2017). Bacterial communities in the small intestine respond differently to those in the caecum and colon in mice fed low-and high-fat diets. *Microbiology* 163, 1189–1197. doi: 10.1099/mic.0.000496

Org, E., Mehrabian, M., Parks, B. W., Shipkova, P., Liu, X., Drake, T. A., et al. (2016). Sex differences and hormonal effects on gut microbiota composition in mice. *Gut Microbes* 7, 313–322. doi: 10.1080/19490976.2016.1203502

Paluschinski, M., Castoldi, M., Schöler, D., Bardeck, N., Oenarto, J., Görg, B., et al. (2019). Tauroursodeoxycholate protects from glycochenodeoxycholate-induced gene expression changes in perfused rat liver. *Biol. Chem.* 400, 1551–1565. doi: 10.1515/hsz-2019-0204

Park, S., Lee, S., Kim, Y., Lee, Y., Kang, M. W., Kim, K., et al. (2021). Causal effects of relative fat, protein, and carbohydrate intake on chronic kidney disease: a Mendelian randomization study. *Am. J. Clin. Nutr.* 113, 1023–1031. doi: 10.1093/ajcn/nqaa379

Parker, A., Fonseca, S., and Carding, S. R. (2020). Gut microbes and metabolites as modulators of blood-brain barrier integrity and brain health. *Gut Microbes* 11, 135–157. doi: 10.1080/19490976.2019.1638722

Perry, J. R., Day, F., Elks, C. E., Sulem, P., Thompson, D. J., Ferreira, T., et al. (2014). Parent-of-origin-specific allelic associations among 106 genomic loci for age at menarche. *Nature* 514, 92–97. doi: 10.1038/nature13545

Qian, Y., Fang, X., Chen, Y., Ding, M., and Gong, M. (2024). Gut flora influences the hypothalamic-gonadal axis to regulate the pathogenesis of obesity-associated precocious puberty. *Sci. Rep.* 14:28844. doi: 10.1038/s41598-024-80140-8

Qin, N., Song, G., Ren, X., Zhang, L., Gao, J., Xia, X., et al. (2020). Fish oil extracted from *Coregonus peled* improves obese phenotype and changes gut microbiota in a high-fat diet-induced mouse model of recurrent obesity. *Food Funct.* 11, 6158–6169. doi: 10.1039/d0fo00911c

Reynolds, C. M., Segovia, S. A., and Zhang, X. D. (2015). Conjugated linoleic acid supplementation during pregnancy and lactation reduces maternal high-fat-diet-induced programming of early-onset puberty and hyperlipidemia in female rat offspring. *Biol. Reprod.* 92, 1–10. doi: 10.1095/biolreprod.114.125047

Roberts, M. N., Wallace, M. A., Tomilov, A. A., Zhou, Z., Marcotte, G. R., Tran, D., et al. (2017). A ketogenic diet extends longevity and healthspan in adult mice. *Cell Metab.* 26, 539–546.e5. doi: 10.1016/j.cmet.2017.08.005

Rogers, I. S., Northstone, K., Dunger, D. B., Cooper, A. R., Ness, A. R., and Emmett, P. M. (2010). Diet throughout childhood and age at menarche in a contemporary cohort of British girls. *Public Health Nutr.* 13, 2052–2063. doi: 10.1017/S1368980010001461

Sahin, Z., Canpolat, S., Ozcan, M., Ozgocer, T., and Kelestimur, H. (2015). Kisspeptin antagonist prevents Rf9-induced reproductive changes in female rats. *Reproduction* 149, 465–473. doi: 10.1530/REP-14-0683

Salvi, R., Castillo, E., Voirol, M.-J., Glauser, M., Rey, J. P., Gaillard, R. C., et al. (2006). Gonadotropin-releasing hormone-expressing neurons immortalized conditionally are activated by insulin: implication of the mitogen-activated protein kinase pathway. *Endocrinology* 147, 816–826. doi: 10.1210/en.2005-0728

Sanders, M. E., Merenstein, D. J., Reid, G., Gibson, G. R., and Rastall, R. A. (2019). Probiotics and prebiotics in intestinal health and disease: from biology to the clinic. *Nat. Rev. Gastroenterol. Hepatol.* 16, 605–616. doi: 10.1038/s41575-019-0173-3

Schoeler, M., and Caesar, R. (2019). Dietary lipids, gut microbiota and lipid metabolism. *Rev. Endocr. Metab. Disord.* 20, 461–472. doi: 10.1007/s11154-019-09512-0

Selmin, O. I., Papoutsis, A. J., Hazan, S., Smith, C., Greenfield, N., Donovan, M. G., et al. (2021). N-6 high fat diet induces gut microbiome dysbiosis and colonic inflammation. *Int. J. Mol. Sci.* 22:6919. doi: 10.3390/ijms22136919

Shahatah, M. A., Jadkarim, A. M., Banjar, R. Z., Kabli, Y. O., Milyani, A. A., and al-Agha, A. E. (2021). The relationship between body weight and dietary habits with respect to the timing of puberty among Saudi children and adolescents. *Ann. Afr. Med.* 20, 193–197. doi: 10.4103/aam.aam_41_20

Shang, Y., Khafipour, E., Derakhshani, H., Sarna, L. K., Woo, C. W., Siow, Y. L., et al. (2017). Short term high fat diet induces obesity-enhancing changes in mouse gut microbiota that are partially reversed by cessation of the high fat diet. *Lipids* 52, 499–511. doi: 10.1007/s11745-017-4253-2

Shan-Shan, S., Kai, W., Ke, M., Bao, L., and Liu, H.-W. (2019). An insoluble polysaccharide from the sclerotium of Poria cocos improves hyperglycemia, hyperlipidemia and hepatic steatosis in Ob/Ob mice via modulation of gut microbiota. *Chin. J. Nat. Med.* 17, 3–14. doi: 10.1016/S1875-53641930003-2

Sheremeta, C.-L., Yarlagadda, S., Smythe, M. L., and Noakes, P. G. (2024). Prostaglandins in the inflamed central nervous system: potential therapeutic targets. *Curr. Drug Targets* 25, 885–908. doi: 10.2174/0113894501323980240815113851

Shi, L., Jiang, Z., and Zhang, L. (2022). Childhood obesity and central precocious puberty. *Front. Endocrinol.* 13:1056871. doi: 10.3389/fendo.2022.1056871

Shihabudeen, M. S., Roy, D., James, J., and Thirumurugan, K. (2015). Chenodeoxycholic acid, an endogenous Fxr ligand alters adipokines and reverses insulin resistance. *Mol. Cell. Endocrinol.* 414, 19–28. doi: 10.1016/j.mce.2015.07.012

Shim, Y. S., Lee, H. S., and Hwang, J. S. (2021). Genetic factors in precocious puberty. *Clin. Exp. Pediatr.* 65:172. doi: 10.3345/cep.2021.00521

Shirley, S. H., Rundhaug, J. E., Tian, J., Cullinan-Ammann, N., Lambertz, I., Conti, C. J., et al. (2009). Transcriptional regulation of estrogen receptor-α by p53 in human breast cancer cells. *Cancer Res.* 69, 3405–3414. doi: 10.1158/0008-5472.CAN-08-3628

Sitticharoon, C., Sukharomana, M., Likitmaskul, S., Churintaraphan, M., and Maikaew, P. (2017). Increased high molecular weight adiponectin, but decreased total adiponectin and kisspeptin, in central precocious puberty compared with aged-matched prepubertal girls. *Reprod. Fertil. Dev.* 29, 2466–2478. doi: 10.1071/RD16282

Stathori, G., Tzounakou, A.-M., Vlahos, N. F., Charmandari, E., and Valsamakis, G. (2025). Unveiling the link: obesity, diet, hypothalamic inflammation and central precocious puberty-recent insights and implications. *Horm. Res. Paediatr.*, 1–17. doi: 10.1159/000544837

Stein, L. M., Tullock, C. W., Mathews, S. K., Garcia-Galiano, D., Elias, C. F., Samson, W. K., et al. (2016). Hypothalamic action of phoenixin to control reproductive hormone secretion in females: importance of the orphan G protein-coupled receptor Gpr173. *Am. J. Phys. Regul. Integr. Comp. Phys.* 311, R489–R496. doi: 10.1152/ajpregu.00191.2016

Stenman, L. K., Holma, R., Eggert, A., and Korpela, R. (2013). A novel mechanism for gut barrier dysfunction by dietary fat: epithelial disruption by hydrophobic bile acids. *American J. Physiol. Gastrointestinal Liver Physiol.* 304, G227–G234. doi: 10.1152/ajpgi.00267.2012

Strandwitz, P. (2018). Neurotransmitter modulation by the gut microbiota. *Brain Res.* 1693, 128–133. doi: 10.1016/j.brainres.2018.03.015

Straniero, S., Laskar, A., Savva, C., Härdfeldt, J., Angelin, B., and Rudling, M. (2020). Of mice and men: murine bile acids explain species differences in the regulation of bile acid and cholesterol metabolism. *J. Lipid Res.* 61, 480–491. doi: 10.1194/jlr.RA119000307

Su, S., Wang, X., Xi, X., Zhu, L., Chen, Q., Zhang, H., et al. (2021). Phellodendrine promotes autophagy by regulating the Ampk/mtor pathway and treats ulcerative colitis. *J. Cell. Mol. Med.* 25, 5707–5720. doi: 10.1111/jcmm.16587

Sui, Z., Zhang, Y., Zhang, Z., Wang, C., Li, X., and Xing, F. (2023). Lin28B overexpression decreases let-7b and let-7g levels and increases proliferation and estrogen secretion in Dolang sheep ovarian granulosa cells. *Archives Animal Breed.* 66, 217–224. doi: 10.5194/aab-66-217-2023

Szamreta, E. A., Qin, B., Rivera-Núñez, Z., Parekh, N., Barrett, E. S., Ferrante, J., et al. (2020). Greater adherence to a Mediterranean-like diet is associated with later breast development and menarche in peripubertal girls. *Public Health Nutr.* 23, 1020–1030. doi: 10.1017/S1368980019002349

Tarçin, G., Bayramoğlu, E., and Güneş Kaya, D. (2024). The role of body composition and appetite-regulating hormones in idiopathic central precocious puberty and their changes during Gnrh analog therapy. *J. Endocrinol. Investig.* 48, 1–8. doi: 10.1007/s40618-024-02413-3

Thaler, J. P., Yi, C.-X., Schur, E. A., Guyenet, S. J., Hwang, B. H., Dietrich, M. O., et al. (2012). Obesity is associated with hypothalamic injury in rodents and humans. *J. Clin. Invest.* 122, 153–162. doi: 10.1172/JCI59660

Toledo, M., Martínez-Martínez, S., and Van Hul, M. (2025). Rapid modulation of gut microbiota composition by hypothalamic circuits in mice. *Nat. Metab.*, 1–13. doi: 10.1038/s42255-025-01280-3

Tzounakou, A.-M., Stathori, G., Paltoglou, G., Valsamakis, G., Mastorakos, G., Vlahos, N. F., et al. (2024). Childhood obesity, hypothalamic inflammation, and the onset of puberty: a narrative review. *Nutrients* 16:1720. doi: 10.3390/nu16111720

Ullah, R., Raza, A., Rauf, N., Shen, Y., Zhou, Y. D., and Fu, J. (2019). Postnatal feeding with a fat rich diet induces precocious puberty independent of body weight, body fat, and leptin levels in female mice. *Front. Endocrinol.* 10:758. doi: 10.3389/fendo.2019.00758

Valsamakis, G., Arapaki, A., Balafoutas, D., Charmandari, E., and Vlahos, N. F. (2021). Diet-induced hypothalamic inflammation, phoenixin, and subsequent precocious puberty. *Nutrients* 13:3460. doi: 10.3390/nu13103460

Vanden Brink, H., Vandeputte, D., and Brito, I. L. (2024). Changes in the bile acid pool and timing of female puberty: potential novel role of hypothalamic Tgr5. *Endocrinology* 165:bqae098. doi: 10.1210/endocr/bqae098

Wang, Y., Jin, C., Li, H., Liang, X., Zhao, C., Wu, N., et al. (2024). Gut microbiota-metabolite interactions mediate the effect of dietary patterns on precocious puberty. *Iscience* 27:109887. doi: 10.1016/j.isci.2024.109887

Wang, Z., Liu, D., Wang, F., Liu, S., Zhao, S., Ling, E. A., et al. (2012). Saturated fatty acids activate microglia via toll-like receptor 4/Nf-κB signalling. *Br. J. Nutr.* 107, 229–241. doi: 10.1017/S0007114511002868

Wang, M., Sun, P., Chai, X., Liu, Y. X., Li, L., Zheng, W., et al. (2024). Reconstituting gut microbiota-colonocyte interactions reverses diet-induced cognitive deficits: the beneficial of eucommiae cortex polysaccharides. *Theranostics* 14, 4622–4642. doi: 10.7150/thno.99468

Wang, L., Xu, H., Tan, B., Yi, Q., Liu, H., Deng, H., et al. (2022). Gut microbiota and its derived Scfas regulate the Hpga to reverse obesity-induced precocious puberty in female rats. *Front. Endocrinol.* 13:1051797. doi: 10.3389/fendo.2022.1051797

Wang, L., Yi, Q., Xu, H., Liu, H., Tan, B., Deng, H., et al. (2024). Alterations in the gut microbiota community are associated with childhood obesity and precocious puberty. *BMC Microbiol.* 24:311. doi: 10.1186/s12866-024-03461-8

Wang, F., Yoder, S. M., Yang, Q., Kohan, A. B., Kindel, T. L., Wang, J., et al. (2015). Chronic high-fat feeding increases Gip and Glp-1 secretion without altering body weight. *American J. Physiol. Gastrointestinal Liver Physiol.* 309, G807–G815. doi: 10.1152/ajpgi.00351.2013

Wang, M., Zhang, Y., Miller, D., Rehman, N. O., Cheng, X., Yeo, J. Y., et al. (2020). Microbial reconstitution reverses early female puberty induced by maternal high-fat diet during lactation. *Endocrinology* 161:bqz041. doi: 10.1210/endocr/bqz041

Watanabe, M., Fukuda, A., and Nabekura, J. (2014). The role of GABA in the regulation of Gnrh neurons. *Front. Neurosci.* 8:387. doi: 10.3389/fnins.2014.00387

Wen, J., Jiang, Y., Lei, Z., He, J., Ye, M., and Fu, W. (2021). Leptin influence cholelithiasis formation by regulating bile acid metabolism. *Turk J Gastroenterol* 32, 97–105. doi: 10.5152/tjg.2020.19594

Wiley, A. S. (2011). Milk intake and total dairy consumption: associations with early menarche in Nhanes 1999-2004. *PLoS One* 6:e14685. doi: 10.1371/journal.pone.0014685

Winters, S. J., Ghooray, D. T., Yang, R. Q., Holmes, J. B., O'Brien, A. R. W., Morgan, J., et al. (2014). Dopamine-2 receptor activation suppresses Pacap expression in gonadotrophs. *Endocrinology* 155, 2647–2657. doi: 10.1210/en.2013-2147

Wu, G. D., Chen, J., Hoffmann, C., Bittinger, K., Chen, Y. Y., Keilbaugh, S. A., et al. (2011). Linking long-term dietary patterns with gut microbial enterotypes. *Science* 334, 105–108. doi: 10.1126/science.1208344

Wu, N., Jiang, X., Liu, Y., Zhang, M., Yue, M., Chen, F., et al. (2025). Glycodeoxycholic acid alleviates central precocious puberty by modulating gut microbiota and metabolites in high-fat diet-fed female rats. *Cell. Mol. Life Sci.* 82, 1–14. doi: 10.1007/s00018-025-05680-2

Xie, Y., Li, X., Wang, M., Chu, M., and Cao, G. (2025). Lin28b-let-7 modulates mrna expression of Gnrh1 through multiple signaling pathways related to glycolysis in Gt1-7 cells. *Animals* 15:120. doi: 10.3390/ani15020120

Xie, L., Tang, Q., Yao, D., Gu, Q., Zheng, H., Wang, X., et al. (2021). Effect of decaffeinated green tea polyphenols on body fat and precocious puberty in obese girls: a randomized controlled trial. *Front. Endocrinol.* 12:736724. doi: 10.3389/fendo.2021.736724

Xiong, J., Xu, Y., Liu, X., Wang, X., Shan, S., Crabbe, M. J. C., et al. (2022). Prospective association of dietary soy and fibre intake with puberty timing: a cohort study among Chinese children. *BMC Med.* 20:145. doi: 10.1186/s12916-022-02320-5

Xu, Y., Xiong, J., Gao, W., Wang, X., Shan, S., Zhao, L., et al. (2022). Dietary fat and polyunsaturated fatty acid intakes during childhood are prospectively associated with puberty timing independent of dietary protein. *Nutrients* 14:275. doi: 10.3390/nu14020275

Yan, D., Fan, P., Sun, W., Ding, Q., Zheng, W., Xiao, W., et al. (2021). Anemarrhena asphodeloides modulates gut microbiota and restores pancreatic function in diabetic rats. *Biomed. Pharmacother.* 133:110954. doi: 10.1016/j.biopha.2020.110954

Yang, Y., Cao, S., Xu, W., Zang, C., Zhang, F., Xie, Y., et al. (2022). Dual modulation of gut bacteria and fungi manifests the gut-based anti-hyperlipidemic effect of Coptidis Rhizoma. *Biomed. Pharmacother.* 153:113542. doi: 10.1016/j.biopha.2022.113542

Yang, X., Tan, J., Xu, X., Yang, H., Wu, F., Xu, B., et al. (2020). Prepubertal overexposure to manganese induce precocious puberty through Gabaa receptor/nitric oxide pathway in immature female rats. *Ecotoxicol. Environ. Saf.* 188:109898. doi: 10.1016/j.ecoenv.2019.109898

Yanguas-Casás, N., Barreda-Manso, M. A., Nieto-Sampedro, M., and Romero-Ramírez, L. (2017). Tudca: An agonist of the bile acid receptor Gpbar1/Tgr5 with anti-inflammatory effects in microglial cells. *J. Cell. Physiol.* 232, 2231–2245. doi: 10.1002/jcp.25742

Yao, S., Lopez-Tello, J., and Sferruzzi-Perri, A. N. (2021). Developmental programming of the female reproductive system—a review. *Biol. Reprod.* 104, 745–770. doi: 10.1093/biolre/ioaa232

Yi, L.-F., Wen, H.-X., and Qiu, M. (2017). An analysis of cardiac autonomic nerve function in girls with idiopathic central precocious puberty. *Zhongguo Dang Dai Er Ke Za Zhi = Chin. J. Contemp. Pediatr.* 19, 1239–1242. doi: 10.7499/j.issn.1008-8830.2017.12.003

Yi, C., Zou, H., Lin, X., Liu, S., Wang, J., Tian, Y., et al. (2024). Zhibai dihuang pill (Zbdh) exhibits therapeutic effects on idiopathic central sexual precocity in rats by modulating the gut microflora. *Heliyon* 10:e29723. doi: 10.1016/j.heliyon.2024.e29723

Yu, Z., Zhan, Q., Chen, A., Han, J., Zheng, Y., Gong, Y., et al. (2021). Intermittent fasting ameliorates di-(2-ethylhexyl) phthalate-induced precocious puberty in female rats: a study of the hypothalamic–pituitary–gonadal axis. *Reprod. Biol.* 21:100513. doi: 10.1016/j.repbio.2021.100513

Yuan, X., Shangguan, H., Zhang, Y., Lin, X., and Chen, R. (2023). Intervention effect of probiotics on the early onset of puberty induced by Daidzein in female mice. *Mol. Nutr. Food Res.* 67:e2200501. doi: 10.1002/mnfr.202200501

Yue, M., and Zhang, L. (2024). Exploring the mechanistic interplay between gut microbiota and precocious puberty: a narrative review. *Microorganisms* 12:323. doi: 10.3390/microorganisms12020323

Zanjirband, M., Hodayi, R., Safaeinejad, Z., Nasr-Esfahani, M. H., and Ghaedi-Heydari, R. (2023). Evaluation of the p53 pathway in polycystic ovarian syndrome pathogenesis and apoptosis enhancement in human granulosa cells through transcriptome data analysis. *Sci. Rep.* 13:11648. doi: 10.1038/s41598-023-38340-1

Zengul, A. G. (2019). Exploring the link between dietary fiber, the gut microbiota and estrogen metabolism among women with breast cancer. Birmingham: the University of Alabama.

Zhang, C., Fang, R., Lu, X., Zhang, Y., Yang, M., Su, Y., et al. (2022). *Lactobacillus reuteri* J1 prevents obesity by altering the gut microbiota and regulating bile acid metabolism in obese mice. *Food Funct.* 13, 6688–6701. doi: 10.1039/D1FO04387K

Zhang, H.-R., Xiao, Y., and Jiang, S.-Q. (2025). Diagnostic value of fasting insulin and insulin-like growth factor-1 levels in girls with central precocious puberty. *J. Pediatr. Endocrinol. Metab.* 38, 240–247. doi: 10.1515/jpem-2024-0479

Zhao, J., Bi, W., Xiao, S., Lan, X., Cheng, X., Zhang, J., et al. (2019). Neuroinflammation induced by lipopolysaccharide causes cognitive impairment in mice. *Sci. Rep.* 9:5790. doi: 10.1038/s41598-019-42286-8

Zhao, Q., Hou, D., Fu, Y., Xue, Y., Guan, X., and Shen, Q. (2021). Adzuki bean alleviates obesity and insulin resistance induced by a high-fat diet and modulates gut microbiota in mice. *Nutrients* 13:3240. doi: 10.3390/nu13093240

Zheng, H., Xu, P., Jiang, Q., Xu, Q., Zheng, Y., Yan, J., et al. (2021). Depletion of acetate-producing bacteria from the gut microbiota facilitates cognitive impairment through the gut-brain neural mechanism in diabetic mice. *Microbiome* 9:145. doi: 10.1186/s40168-021-01088-9

Zhu, H., Chen, L., and Jiang, Y.-J. (2008). Relationship of plasma ghrelin and adenohypophyseal hormone levels in female precocious puberty. *Zhejiang Da Xue Xue Bao Yi Xue Ban = J. Zhejiang Univ. Med. Sci.* 37, 506–510. doi: 10.3785/j.issn.1008-9292.2008.05.015

Zurita-Cruz, J. N., Villasís-Keever, M. A., Manuel-Apolinar, L., Damasio-Santana, L., Gutierrez-Gonzalez, A., Wakida-Kusunoki, G., et al. (2021). Altered cardiometabolic profile in girls with central precocious puberty and adipokines: a propensity score matching analysis. *Cytokine* 148:155660. doi: 10.1016/j.cyto.2021.155660

Glossary

PP - precocious puberty

HFD - a high-fat diet

GM - gut microbiota

CPP - central precocious puberty

PPP - peripheral precocious puberty

HPG - hypothalamic–pituitary-gonadal

NO - nitric oxide

E2 - estradiol

LPS - lipopolysaccharides

SCFAs - short-chain fatty acids

SCFA - short-chain fatty acid

BA - bile acid

BAs - bile acids

GABA - γ-aminobutyric acid

5-HT - serotonin

DA - dopamine

GLP-1 - glucagon-like peptide-1

GPR - G-protein coupled receptor

FMT - Fecal Microbiota Transplantation

TCM - Traditional Chinese medicine

MGB - microbiota-gut-brain

BBB - blood–brain barrier

GDCA - glycodeoxycholic acid

BMI - body mass index

PKC - protein kinase C

ERK1/2 - extracellular signal-regulated kinase1/2

LH - luteinizing hormone

FSH - follicle-stimulating hormone

APN - adiponectin

IGF-1 - insulin-like growth factor-1

PI3K - phosphatidylinositol-3-kinase

MUFAs - monounsaturated fatty acids

PUFAs - polyunsaturated fatty acids

TGR5 - takeda G-protein-coupled receptor 5

FXR - farnesoid X receptor

mTOR - mammalian target of rapamycin

SF1 - steroidogenic factor 1

Mdm2 - mouse double minute 2 homolog

AMPK - adenosine-monophosphate-activated protein kinase

ACTH - adrenocorticotropic hormone

ERα - estrogen receptor α

GHSR - growth hormone secretagogue receptors

AKT - protein kinase B

frontiers | Frontiers in Microbiomes

TYPE Original Research
PUBLISHED 06 June 2025
DOI 10.3389/frmbi.2025.1589484

Check for updates

OPEN ACCESS

EDITED BY
Guiguo Zhang,
Shandong Agricultural University, China

REVIEWED BY
Zhigang Zhang,
Northeast Agricultural University, China
Muyang Li,
Heilongjiang Bayi Agricultural University, China

*CORRESPONDENCE
Youji Ma
yjma@gsau.edu.cn

RECEIVED 07 March 2025
ACCEPTED 30 April 2025
PUBLISHED 06 June 2025

CITATION
Zhao Q, Li W, Liu Z, Li Q and Ma Y (2025) Dietary *Codonopsis pilosula* polysaccharides promote gut health and enhance immunity in Hu sheep.
Front. Microbiomes 4:1589484.
doi: 10.3389/frmbi.2025.1589484

COPYRIGHT
© 2025 Zhao, Li, Liu, Li and Ma. This is an open-access article distributed under the terms of the Creative Commons Attribution License (CC BY). The use, distribution or reproduction in other forums is permitted, provided the original author(s) and the copyright owner(s) are credited and that the original publication in this journal is cited, in accordance with accepted academic practice. No use, distribution or reproduction is permitted which does not comply with these terms.

Dietary *Codonopsis pilosula* polysaccharides promote gut health and enhance immunity in Hu sheep

Qing Zhao, Wanning Li, Zilong Liu, Qiao Li and Youji Ma*

College of Animal Science and Technology, Gansu Agricultural University, Lanzhou, China

In recent years, there has been a growing emphasis on the use of plant polysaccharides in animal husbandry, attracting attention for their distinctive benefits and roles. These natural and eco-friendly feed additives not only enhanced livestock performance but also promoted intestinal health and strengthen immunity. This study utilized 16S rRNA high-throughput sequencing to investigate the effects of dietary *Codonopsis pilosula* polysaccharides on the gut microbiota of Hu sheep. Eighteen 3-month-old Hu sheep with similar body weight (19.60 ± 1.63 kg) and good body condition, were randomly allocated into three groups: a control group (CK) receiving a standard diet, and two trial groups: T1 (supplemented with 0.15% *Codonopsis pilosula* polysaccharides) and T2 (supplemented with 0.3% *Codonopsis pilosula* polysaccharides), with six animals in each group. The pre-trial period lasted for 7 days, followed by an experimental period of 90 days. Results demonstrated that incorporating *Codonopsis pilosula* polysaccharides into the diet markedly increased the acetic acid levels in the ileum. This incorporation was found to enhance the diversity of intestinal flora and influence the species composition and richness of the intestinal microbiota. LEfSe analysis revealed that the genus enriched in the three intestinal segments were primarily *Candidatus_Saccharimonas*, *Christensenellaceae*_R_7_group, *Romboutsia*, and *UCG_005*. The relative expression levels of *Claudin*, *Occludin*, and *ZO-1* mRNA in the T1 group were found to be elevated compared to the CK and T2 groups across all three intestinal segments. In conclusion, these findings indicate that dietary supplementation with *Codonopsis pilosula* polysaccharides not only regulate the intestinal microbial composition of Hu sheep but also enhance their immune capacity by increasing the presence of specific beneficial bacteria, thus fostering the intestinal health of Hu sheep.

KEYWORDS

***Codonopsis pilosula* polysaccharides, immunity, gut microbiota, sheep, practical production**

1 Introduction

In recent years the large-scale development of the breeding industry has led to the widespread use of feed additives (Li et al., 2025; Yu and Li, 2025). However, many of these additives consist of antibiotics, hormones, and other synthetic drugs that, while enhancing the quality of livestock products, pose several issues, including impaired livestock function, reduced immunity, and the development of drug resistance. Additionally, they contribute to environmental pollution (Manyi-Loh et al., 2018) and pose risks to human health (Cheng et al., 2018; Kuppusamy et al., 2018). Therefore, it is been gradually developed to add plant feed ingredients instead of chemical additives, such as flavonoids, polysaccharides and so on (Du et al., 2022; Zhao et al., 2025). In contrast, *Codonopsis pilosula* polysaccharides, primarily derived from Chinese herbs and produced through specialized technology, represent a non-polluting, green alternative. Unlike chemically synthesized drugs, *Codonopsis pilosula* polysaccharides are less likely to induce drug resistance and typically exhibit low toxicity and minimal residue, while preserving their natural structure and biological activity (Alem, 2024). *Codonopsis pilosula* belongs to Chinese herbal plants. These herbal additives not only prevent and treat diseases but also enhance animal performance (Cao et al., 2015). *Codonopsis pilosula*, sourced from nature, can regulate physiological functions and provide multiple benefits, including disease prevention, treatment, immune system enhancement and rich in pharmacological effects (Guo et al., 2024a). As both a therapeutic agent and a green product, *Codonopsis pilosula* is rich in active substances. Its complex and diverse composition contributes to its high efficiency, low toxicity, minimal drug residues, and abundant resource supply (Gao et al., 2018). The primary effects of *Codonopsis pilosula* polysaccharides encompass antimicrobial properties, promotion of growth (Guo et al., 2024b), reduction of inflammation (Chu et al., 2016), enhancement of immune response (Xia et al., 2025), and maintenance of intestinal health (Cao et al., 2022; Zhou et al., 2025). Research indicates that plant-based feed additives have been recognized as effective supplements for non-ruminants (Biswas et al., 2024). This supplementation aids in optimizing and balancing the formulation of livestock and poultry feed, thereby enhancing the nutritional value and utilization efficiency of the feed. The modernization of *Codonopsis pilosula* has led to significant advancements in their application. Numerous studies indicate that these additives enhance growth performance, boost immunity, and improve meat quality, among other benefits. *Codonopsis pilosula* polysaccharides mainly improve the body's immunity, unlike other bioactive ingredients, such as astragalus polysaccharides, which improves skeletal muscle development and regeneration (Su et al., 2023). Lycium barbarum polysaccharide inhibit lipid oxidation and protein degradation in mutton (Jiangyong et al., 2022), and flavonoids mainly affect the growth of bacteria and play an antibacterial role (Donadio et al., 2021). In the poultry sector, research has demonstrated the positive impacts of *Codonopsis pilosula* polysaccharides on the production performance of laying hens, particularly in enhancing their antioxidant capacity, immunity, and intestinal health (Liu et al., 2021, 2023; Liu and Xie, 2024). Currently, the application of *Codonopsis pilosula* polysaccharides in poultry farming has transitioned from traditional crude usage to a more scientific approach involving precise formulation and standardized production. These natural, eco-friendly feed additives not only effectively enhance the production performance of livestock and poultry but also improve intestinal health and bolster immunity. Considering the global emphasis on green and sustainable development, the integration of *Codonopsis pilosula* polysaccharides in organic farming is expected to emerge as a significant growth area, playing a crucial role in the sustainable advancement of the global livestock industry. Ongoing scientific research and technological innovation are anticipated to expand the applications of *Codonopsis pilosula* in the future, thereby significantly contributing to human health and the sustainable development of animal husbandry.

Gut microorganisms are essential for maintaining the intestinal barrier and play a crucial role in regulating host metabolism (Krishnan et al., 2015), intestinal nutrient digestion, the development and maturation of the immune system (Sanos et al., 2009; Honda and Littman, 2016), and maintaining body homeostasis, thereby significantly contributing to intestinal health (Xiang et al., 2020). Research indicates that *Codonopsis pilosula* polysaccharides can modulate the intestinal flora of lactating piglets, enhancing the population of beneficial intestinal bacteria (Liao, 2024). While numerous studies have investigated the effects of *Codonopsis pilosula* polysaccharides on the rumen of Hu sheep, there is a relative lack of research focusing on their impact on intestinal microorganisms. Therefore, this study aims to analyze the changes and functions of intestinal flora through 16S rRNA sequencing to explore the effects of *Codonopsis pilosula* polysaccharides on the intestinal microbial composition of Hu sheep. The objective is to validate the efficacy of *Codonopsis pilosula* polysaccharides as non-conventional feed options and to provide a theoretical foundation for their practical applications in production.

2 Materials and methods

2.1 Ethics statement

All animal management and experiments were approved by the Animal Committee of Gansu Agricultural University (GSAU-AEW-2020-0057).

2.2 Animals and experimental design

Eighteen 3-month-old Hu sheep, with comparable body weight (19.60 ± 1.63 kg) and in good body condition, were randomly divided into three groups of six sheep each: the CK group (control group, fed a basal diet), the T1 group (trial group I, supplemented with *Codonopsis pilosula* polysaccharides at 0.15% of the basal diet), and the T2 group (trial group II, supplemented with *Codonopsis pilosula* polysaccharides at 0.3% of the basal diet). The pre-test period lasted for seven days, followed by a positive test period of 90 days. Prior to the commencement of the test, the pen was thoroughly sterilized, sheep ear tags were numbered and registered, and the lambs were weighed and assigned to their respective pens. They were fed twice daily at 08:00 and 16:00. The daily *Codonopsis pilosula* polysaccharides were evenly mixed into the concentrate supplement, and water was made available ad libitum. Throughout the feeding phase, all groups were subjected to identical feeding and management protocols.

2.3 Preparation of test materials

Extraction of *Codonopsis pilosula* polysaccharides was carried out with reference to the literature (Xu, 2006; Nan et al., 2008). These additives were administered to Hu sheep at rates of 0.15% and 0.3% of the concentrate supplement, respectively. The base ration complied with the nutritional requirements outlined in China's Meat Sheep Feeding Standard (NY/T 861-2004), with its composition and nutritional levels detailed in Tables 1.

2.4 Sample collection

At the conclusion of the experiment, the test sheep were euthanized. The duodenum, ileum, and cecum were ligated, excised, and rinsed; subsequently, the intestinal contents were scraped, and the tissues were removed using a sterile scalpel. The intestinal tissue was then cleaned with phosphate-buffered saline (PBS) and stored in cryopreservation tubes. These tubes underwent rapid freezing in liquid nitrogen before being immediately placed in liquid nitrogen. Finally, they were transferred to ultra-low-temperature freezers maintained at −80°C for long-term storage.

TABLE 1 Composition and nutrient levels of basal diet (dry matter basis).

Ingredients	Content/%	Nutrient levels	Content/%
Corn	40.00	ME/(MJ/Kg)[2]	8.57
Wheat bran	9.00	CP	14.51
Peanut seedling	29.00	EE	2.21
Cottonseed meal	5.50	NDF	30.11
Soybean meal	12.50	ADF	19.58
CaHPO4	0.50	Ca	1.01
Vitamin–mineral mix[1]	1.00	P	0.47
Limestone	1.50		
Nacl	1.00		
Total	100.00		

[1]The premix provided the following per kg of diets: Fe (as ferrous sulfate) 75 mg, Cu (as copper sulfate) 14 mg, Zn (as zinc sulfate) 80 mg, Se (as sodium selenite) 0.25 mg, I (as potassium iodide) 0.25 mg, Co 0.30 mg, Mn (as manganese sulfate) 400 mg, VA 3000 IU, VD 500 IU, VE 200 IU.
[2]ME was a calculated value, while the others were measured values.

2.5 Determination of ileal VFAs

The concentration of volatile fatty acids (VFA) was determined using gas chromatography, following the method described by Kristensen et al (Kristensen and Harmon, 2004).

2.6 16S rRNA sequencing and qRT-PCR

DNA was extracted from the contents of the duodenum, ileum and cecum using a commercial kit. The concentration of DNA was assessed via agarose gel electrophoresis, while DNA quality was evaluated using UV spectrophotometry. Specific primers were employed to purify the PCR products, which were subsequently utilized to generate sequencing libraries. The 16S rRNA sequencing was performed by Biomarker Technologies (Beijing, China).

Total RNA was extracted from the duodenum, ileum, and cecum tissues using Trizol reagent. The concentration and purity of the extracted RNA were assessed with an ultra-micro spectrophotometer. Subsequently, first-strand cDNA was synthesized following the protocol provided with the reverse transcription kit. The mRNA sequences for sheep *ZO-1* and *β-actin* were retrieved from the NCBI database, and primers were designed using Oligo 6.0 software and the NCBI online platform (https://www.ncbi.nlm.nih.gov/). The primers were synthesized by Xi'an Kengke Biotechnology Co., Ltd., with the sequences listed in Table 2. The qRT-PCR amplification system comprised a total volume of 20 μL, which included 0.5 μL of each upstream and downstream primer (10 μmol/L), 2× Fast qPCR Master Mixture (Green), and 10 μL of cDNA. The two-step reaction program included an initial denaturation at 95 °C for 2 minutes, followed by 40 cycles of denaturation at 95 °C for 15 seconds and annealing at 60 °C for 30 seconds. The results of the qRT-PCR were analyzed using the $2^{-\Delta\Delta Ct}$ method.

2.7 Data processing and analysis

The Biomarker Technologies Cloud platform facilitates the processing and analysis of sequencing data, which includes species taxonomic analysis, diversity analysis, significance analysis, and association analysis. We primarily employed Venn diagrams to illustrate the number of unique and shared features across the three intestinal segments. β-diversity analysis was utilized to compare species diversity among samples, focusing on the top 10

TABLE 2 Primer sequence information.

Genes	Product length	Tm/°C	Primer sequence (5′–3′)
β-actin	147 bp	Forward: 58.94	Forward: AGTACCCCATTGAACACGGT
		Revers: 59.04	Revers: CTCTGTTGGCTTTGGGGTTC
Claudin	143 bp	Forward: 58.70	Forward: GGTGAAGAAGATGCGGATGG
		Revers: 58.88	Revers: TCTGGTGTTAACGGGTGTGA
Occludin	139 bp	Forward: 55.00	Forward: TCCTCATCGTCATCCTGCTC
		Revers: 55.00	Revers: TTCTTCACCCACTCCTCCAC
ZO-1	146 bp	Forward: 58.93	Forward: GAAGAGAGCACAGAACGCAG
		Revers: 58.97	Revers: CACTTGTGGCAAGCTGAAGT

colonies at both the phylum and genus levels. Additionally, correlation analysis was conducted to examine the relationship between immune indices and the top 10 colonies at the genus level. The experimental data were analyzed using a one-way ANOVA test with SPSS 27.0 statistical software, and multiple comparisons were performed using Duncan's method. Results are presented as "mean ± standard deviation" (mean ± SD). Finally, the *P*-value was calculated, with a significance threshold set at $P < 0.05$, indicating that $P < 0.05$ denotes a statistically significant difference, while $P > 0.05$ indicates a lack of significance.

3 Results

3.1 Variations in volatile fatty acids levels in the ileum of Hu sheep

The concentrations of acetic acid, propionic acid, isobutyric acid, and butyric acid were measured in the ileum of Hu sheep, and the differences in volatile fatty acid content were compared among the groups, as presented in Table 3. In the ileum, the concentration of acetic acid was significantly higher in the T1 and T2 groups compared to the CK group ($P < 0.05$). However, the concentrations of propionic acid, isobutyric acid and butyric acid did not exhibit statistically significant differences ($P > 0.05$).

3.2 OTU cluster analysis of intestinal microorganisms

OTU cluster analysis was conducted to quantify the number of operational taxonomic units (OTUs) present in each group. A Venn diagram illustrates the number of OTUs that are common to or unique among the three groups. In the duodenal samples, the unique

TABLE 3 Differences in the content of volatile fatty acids in the ileum of Hu sheep.

Item	Group [1]			*P*-value
	CK	T1	T2	
Acetic acid, mmol/L	5.91 ± 2.49^{c}	10.86 ± 0.61^{b}	15.26 ± 0.18^{a}	0.005
Propionic acid, mmol/L	6.64 ± 0.24	4.49 ± 0.02	6.31 ± 0.73	0.057
Isobutyric acid, mmol/L	0.21 ± 0.03	2.99 ± 2.28	1.85 ± 1.29	0.602
Butyric acid, mmol/L	1.13 ± 0.03	0.74 ± 0.37	1.74 ± 0.18	0.102

[1]CK, basal diet; T1, supplemented with *Codonopsis pilosula* polysaccharides according to the basal diet 0.15%; T2, supplemented with *Codonopsis pilosula* polysaccharides according to the basal diet 0.3%.
^{a,b,c}Means within a row with different superscript letters are significantly different ($P < 0.05$).

OTUs for the CK group, T1 group, and T2 group were 310, 406, and 276, respectively (Figure 1A). For the ileum samples, the unique OTUs for the CK group, T1 group, and T2 group were 230, 272, and 288, respectively (Figure 1B). In the cecum samples, the unique OTUs for the CK group, T1 group, and T2 group were 254, 203, and 430, respectively (Figure 1C). These results indicate that dietary supplementation with *Codonopsis pilosula* polysaccharides can significantly influence the gut microbiota of Hu sheep.

3.3 Analysis of the alpha diversity of intestinal microorganisms

As shown in Table 4, in the duodenum, the differences in the ACE, Chao1, and Simpson indices between the T1 and T2 groups were not significant compared to the CK group ($P > 0.05$). However, the differences in the Shannon index were significant ($P < 0.05$). In the ileum, no significant differences were observed among the groups for the Shannon, Simpson, ACE and Chao1 indices ($P > 0.05$). In the cecum, when compared to the CK group, the differences in the ACE, Shannon, and Simpson indices between the T1 and T2 groups were not significant ($P > 0.05$), whereas the differences in the Chao1 index were significant ($P < 0.05$).

3.4 Analysis of the β-diversity of intestinal microorganisms

The analysis of β-diversity in intestinal microorganisms was performed using Partial Least Squares Discriminant Analysis (PLS-DA), which is based on the classical partial least squares regression model. This analysis effectively highlights the differences in microbial community structures among samples from various groups. In the three intestinal segments examined, the distribution of intestinal microorganisms among the CK, T1, and T2 groups exhibited a clear separation between the upper and lower parts segments of the groups, with significant aggregation observed within each group ($P < 0.05$). These findings suggest that the

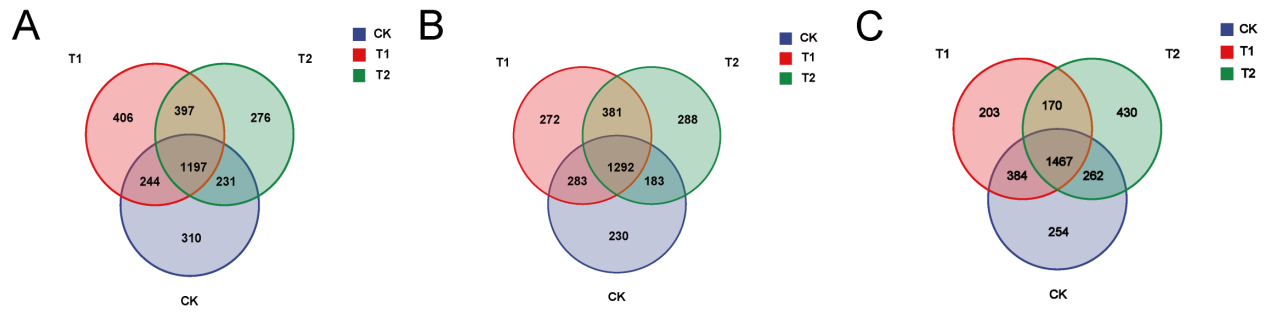

FIGURE 1
Cluster analysis **(A)** Venn diagram of the three groups in the duodenum. **(B)** Venn diagram of the three groups in the ileum. **(C)** Venn diagram of the three groups in the cecum.

microbial community structures of the three groups are distinct, and that the incorporation of *Codonopsis pilosula* polysaccharides into the diet may influence the composition of gut microorganisms in Hu sheep (Table 4; Figure 2).

3.5 Effect of *Codonopsis pilosula* polysaccharides on microbial phylum levels in three intestinal segment of Hu sheep

The top ten species in terms of total abundance were analyzed in depth at the phylum level through species annotation and statistical counting of valid sequences obtained at various taxonomic levels. Firmicutes were identified as the dominant bacteria across all groups within the duodenum of Hu sheep. The relative abundance of Bacteroidota exhibited a gradual increase with higher levels of additives (Figure 3A). In the ileum of Hu sheep, Firmicutes continued to dominate across all groups, with a similar trend observed for Bacteroidota, which increased in relative abundance alongside the amount of additive administered (Figure 3B). In the cecum, the predominant phyla among all groups of Hu sheep included Firmicutes, Patescibacteria, Bacteroidota, and Actinobacteriota (Figure 3C). The genus with the highest relative abundance in the duodenum of the CK group was *Romboutsia*, while *uncultured_rumen_bacterium* was the most abundant in the T1 and T2 groups. The relative abundance of *Christensenellaceae*_R_7_ group and *UCG-005* progressively increased with higher additive levels (Figure 3D). At the ileal microbial genus level, *uncultured_rumen_bacterium* and *Christensenellaceae*_R_7_group emerged as the dominant genera, followed by *[Eubacterium]_hallii_group* and *Lachnospiraceae_NK3A20_group*. Notably, the genera *Romboutsia*, *Paeniclostridium* and *Solibacillus* were

TABLE 4 Effects of *Codonopsis pilosula* polysaccharides on α-diversity index of three intestinal segments of Hu sheep.

Item	Diversity index	Group [1]			*P*-value
		CK	T1	T2	
Duodenum	ACE	1273.03 ± 113.89	1296.54 ± 98.15	1150.39 ± 58.32	0.11
	Chao1	1143.85 ± 162.27	1271.76 ± 189.88	1169.28 ± 67.81	0.52
	Simpson	0.97 ± 0.25	0.97 ± 0.17	0.98 ± 0.01	0.24
	Shannon	5.80 ± 0.44[b]	7.27 ± 0.96[a]	7.76 ± 0.45[a]	0.01
Ileum	ACE	1166.55 ± 162.81	1233.93 ± 468.37	1319.82 ± 75.82	0.76
	Chao1	1177.59 ± 180.71	1240.25 ± 462.87	1208.89 ± 205.21	0.97
	Simpson	0.97 ± 0.02	0.99 ± 0.01	0.97 ± 0.03	0.43
	Shannon	7.14 ± 0.74	8.08 ± 1.02	7.05 ± 1.17	0.35
Cecum	ACE	1471.12 ± 111.31	1414.73 ± 88.55	1345.72 ± 81.05	0.30
	Chao1	1494.87 ± 110.79[a]	1445.04 ± 83.46[a]	1243.93 ± 93.80[b]	0.02
	Simpson	0.98 ± 0.02	0.98 ± 0.01	0.97 ± 0.03	0.30
	Shannon	8.09 ± 0.62	8.14 ± 0.12	7.98 ± 0.08	0.90

[1]CK, basal diet; T1, supplemented with *Codonopsis pilosula* polysaccharides according to the basal diet 0.15%; T2, supplemented with *Codonopsis pilosula* polysaccharides according to the basal diet 0.3%.
[a,b]Means within a row with different superscript letters are significantly different ($P < 0.05$).

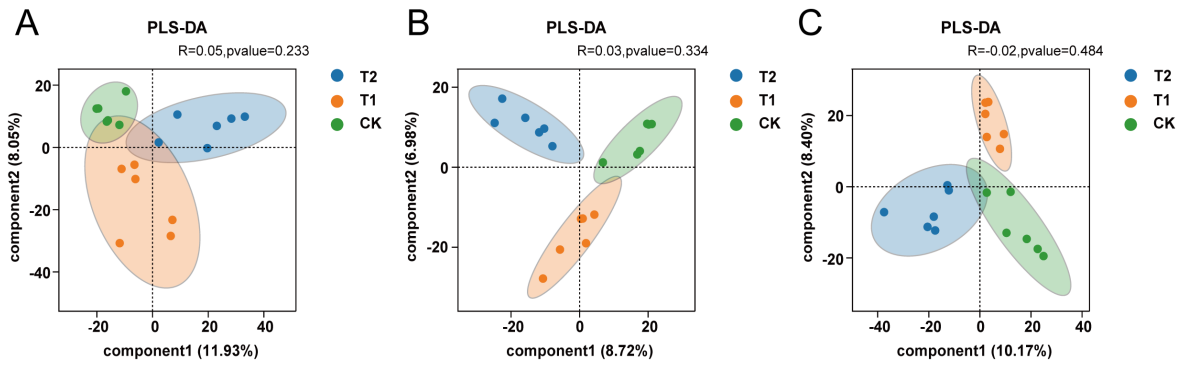

FIGURE 2
Analysis of diversity **(A)** β-diversity analysis of the three groups in the duodenum. **(B)** β-diversity analysis of the three groups in the ileum. **(C)** β-diversity analysis of the three groups in the cecum.

significantly elevated ($P<0.05$) in the T2 group (Figure 3E). In the cecum, the dominant genus in the CK group included *uncultured_rumen_bacterium*, *Christensenellaceae*_R_7_group, and *UCG_005*, whereas in the T1 and T2 groups, the dominant genera consisted of *uncultured_rumen_bacterium*, *Candidatus_Saccharimonas* and *Christensenellaceae*_R_7_group (Figure 3F).

3.6 LEfSe analysis

Significantly altered gut microorganisms were identified through LEfSe analysis, focusing on those with an LDA score greater than 2 (LDA > 2) at the genus level. In the duodenum, three, one, and six groups were enriched in the CK, T1, and T2 groups, respectively, with the highest LDA score impacts attributed to *g_Anaerosporobacter*, *g_Vibrio*, and *g_Christensenellaceae_R_7_group* (Figures 4A, B). In the ileum, two, two, and four groups were enriched in the CK, T1, and T2 groups, respectively, with the highest LDA score impacts associated with *g_uncultured_rumen_bacterium*, *g_Faecalibaculum*, and *g_Clostridium_sensu_stricto_1* (Figures 4C, D). In the cecum, three, six, and two groups were enriched in the CK, T1, and T2 groups, respectively, with the highest LDA score impacts linked to *g_Corynebacterium*, *g_Anaerorhabdus_furcosa_group*, and *g_Saccharofermentans* (Figures 4E, F).

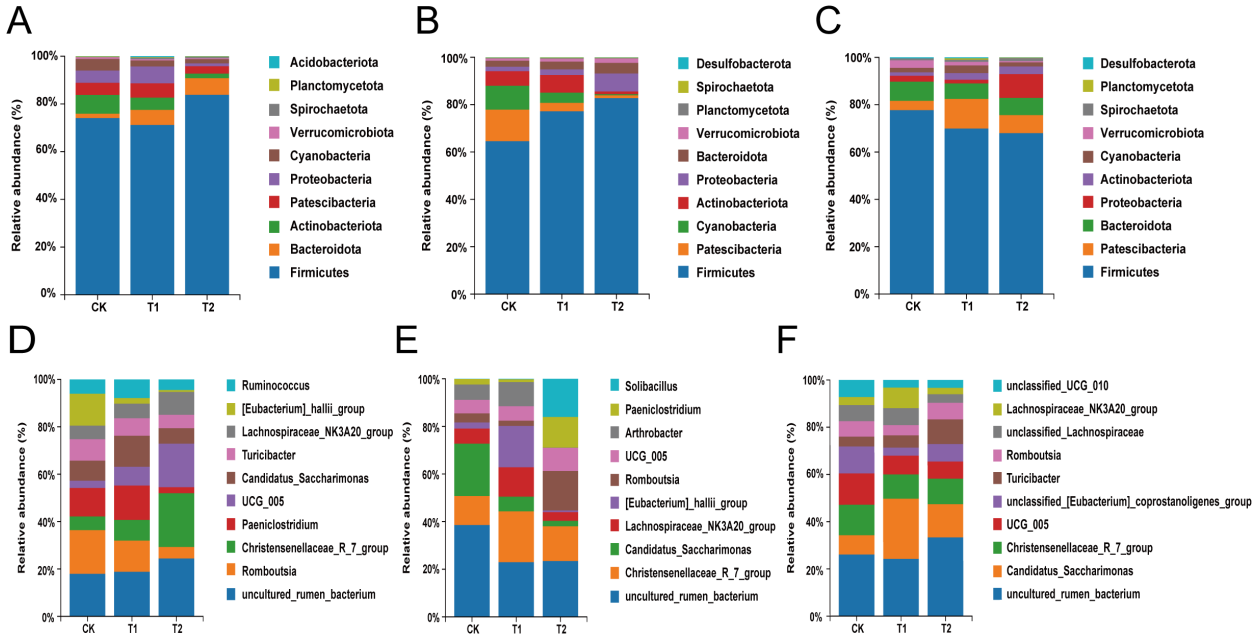

FIGURE 3
Analysis of differences in species composition of intestinal flora. **(A)** Composition of the duodenum at the phylum level. **(B)** Composition of the ileum at the phylum level. **(C)** Composition of the cecum at the phylum level. **(D)** Composition of the duodenum at the genus level. **(E)** Composition of the ileum at the genus level. **(F)** Composition of the cecum at the genus level.

10.3389/frmbi.2025.1589484

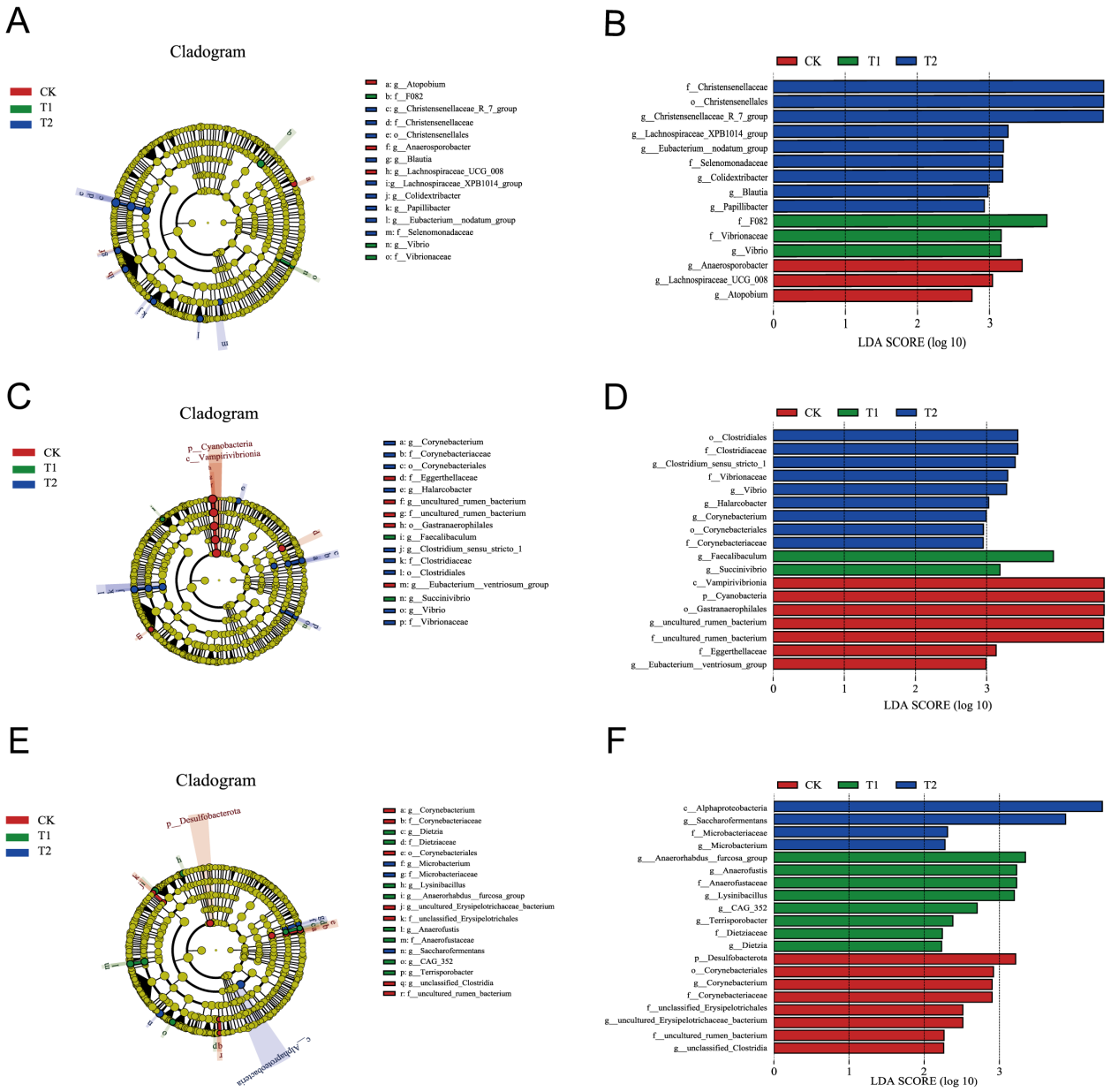

FIGURE 4
Significance analysis of differences between the three groups. **(A)** LEfSe analysis of duodenum. **(B)** LDA score chart of the duodenum. **(C)** LEfSe analysis of ileum. **(D)** LDA score chart of the ileum. **(E)** LEfSe analysis of cecum. **(F)** LDA score chart of the cecum.

3.7 Effects on the intestinal mucosal barrier of intestinal tissues in Hu sheep

In the duodenum, the *Claudin* mRNA expression levels were considerably increased in the T1 group compared to both the CK and T2 groups. Additionally, the mRNA expression of *Occludin* showed a significant rise in the T1 group relative to the T2 group, although no notable difference was noted in comparison to the CK group. Furthermore, the relative expression of *ZO-1* mRNA was significantly greater in the T1 group than in both the CK and T2 groups (Figure 5). In the ileum, both *Claudin* and *Occludin* mRNA levels were notably elevated in the T1 group in comparison to the CK and T2 groups. Moreover, the *ZO-1* mRNA expression was significantly greater in the T1 group when assessed against both the CK and T2 groups (Figure 6).

4 Discussion

In ruminants, volatile fatty acids are primarily produced in the rumen and intestine (Svartström et al., 2017). The duodenum is vital for absorbing digestive products from sugars, fats, and proteins, while the production and absorption of volatile fatty acids mainly occur in the posterior part of the intestine (Song

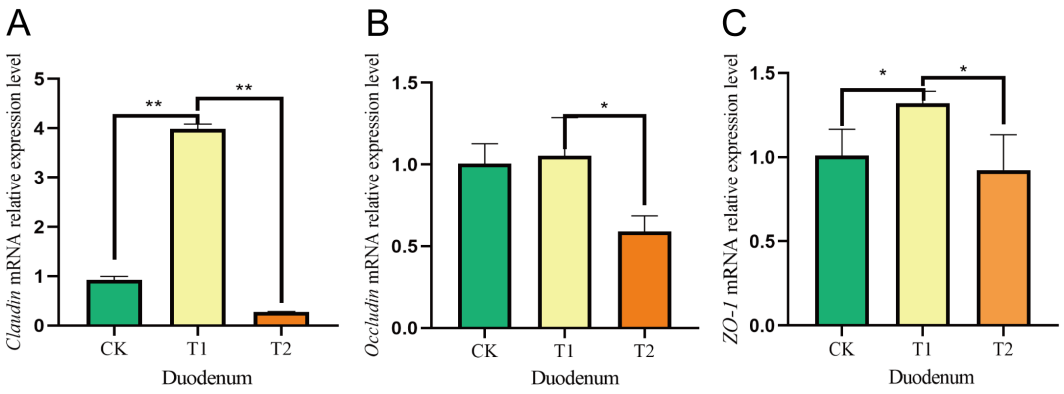

FIGURE 5
Effects of adding *Codonopsis pilosula* polysaccharides to diets on the expression of intestinal barrier related genes in Hu sheep. **(A)** Effect of *Claudin* mRNA expression in duodenum. **(B)** Effect of *Occludin* mRNA expression in duodenum. **(C)** Effect of *ZO-1* mRNA expression in duodenum. * represents significant difference ;** represents extremely significant difference.

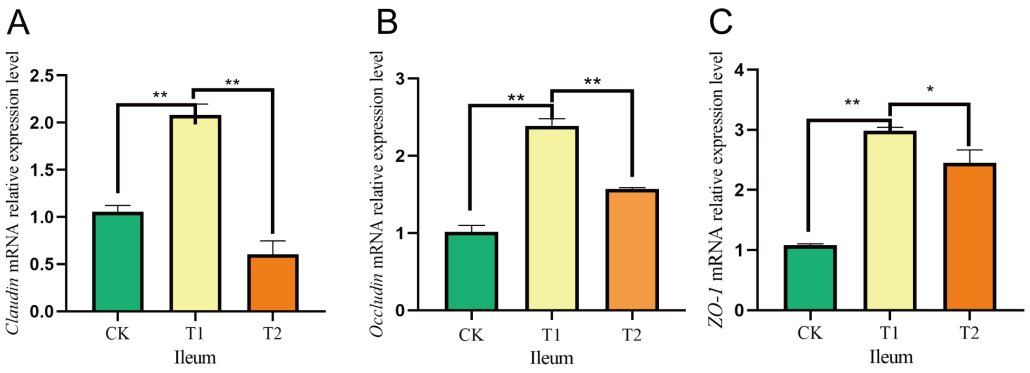

FIGURE 6
Effects of adding *Codonopsis pilosula* polysaccharides to diets on the expression of intestinal barrier related genes in Hu sheep. **(A)** Effect of *Claudin* mRNA expression in ileum. **(B)** Effect of *Occludin* mRNA expression in ileum. **(C)** Effect of *ZO-1* mRNA expression in ileum. * represents significant difference ;** represents extremely significant difference.

et al., 2021). In our study, we measured the volatile fatty acid content in the ileum to investigate the effects of *Codonopsis pilosula* polysaccharides on the intestinal tract. The results demonstrated that the acetic acid content was significantly higher in the T1 and T2 groups compared to the CK group. Acetic acid, a short-chain fatty acid (SCFA), is produced by the bacterial fermentation of indigestible carbohydrates and influences lipid, carbohydrate and protein metabolism (Frampton et al., 2020). SCFAs are essential for maintaining intestinal microflora and are necessary substances for balancing the intestinal internal environment (Van Hoek and Merks, 2012). Prior research has clearly shown that SCFAs could significantly contribute to the prevention and management of intestinal disorders (Blouin et al., 2011). Therefore, we hypothesized that the addition of *Codonopsis pilosula* polysaccharides to the ration could enhance the digestive capacity of the intestinal tract in Hu sheep.

Alpha diversity is primarily employed to assess species richness and evenness within a specific region, utilizing metrics such as the Chao1, ACE, Shannon, and Simpson indexes. Elevated values of the Chao1 and ACE indexes indicate greater species richness, whereas higher values of the Shannon index reflect increased community diversity. In contrast, lower values of the Simpson index suggest a higher level of community diversity (Hughes et al., 2001; Kim et al., 2017). It has been established that the diversity of the gut microbial community is essential for the health of the host organism and plays a significant role in immunization (Yadav and Jha, 2019). In this study, we observed that the α-diversity Shannon index of the duodenum and the α-diversity Chao1 index of the cecum were significantly higher ($P < 0.05$) in Hu sheep that received *Codonopsis pilosula* polysaccharides compared to the CK group. The β-diversity analysis revealed a clear separation of microorganisms between groups, accompanied by aggregation within groups. This finding indicates that the inclusion of *Codonopsis pilosula* polysaccharides in the diet may alter the intestinal microbial composition of Hu sheep and enhance the diversity of microbial communities in the duodenum and cecum, thereby fostering the development of immunity-related microbial communities in the intestinal tract and ultimately improving the immune capacity of the Hu sheep.

Significant difference analysis at the phylum level revealed that Firmicutes was the predominant flora across all three intestinal segments. This finding aligns with the observations of Zhong et al. (2022), who identified Firmicutes as the primary dominant flora in the intestinal tract of sheep. Additionally, Zhang et al. (2018) utilized high-throughput sequencing technology to demonstrate that Firmicutes was the dominant flora in the cecum of small-tailed cold sheep. Members of Firmicutes actively contribute to the host immune system by stimulating immune responses and influencing the activity of immune cells (Ross et al., 2024). They efficiently break down polysaccharides by secreting various enzymes (Gharechahi et al., 2023), degrading fibers and cellulose (Thoetkiattikul et al., 2013) and fermenting polysaccharides to produce short-chain fatty acids(SCFAs). These SCFAs are crucial for maintaining normal intestinal function, supporting intestinal health, regulating host metabolism, and facilitating nutrient digestion and absorption (Wang et al., 2019; Hu et al., 2023). The results also indicated that the relative abundance of Bacteroidetes were higher in each group. Bacteriophages are beneficial bacteria capable of metabolizing polysaccharides and oligosaccharides, thereby providing nutrients to the host (Zafar and Saier, 2021). The incorporation of LBP into the diets of weaned piglet, as a substitute for antibiotics, has been demonstrated to enhance antioxidant capacity, bolster immunity, and modulate the gut microbial composition of these animals (Yin et al., 2021). Furthermore, Zhang et al. (2024) found that the addition of shiitake mushroom polysaccharides to milk replacer powder elevated serum levels of IgA, IgG, and IgM in calves, thereby improving their immune function. In the present study, as the content of *Codonopsis pilosula* polysaccharides gradually increased, was associated with a gradual increase in the relative abundance of Firmicutes in the ileum, corresponding to the increased quantity of *Codonopsis pilosula* polysaccharides. This finding suggests that *Codonopsis pilosula* polysaccharides have influenced the relative abundance of Firmicutes, subsequently impacting intestinal fermentation. Such alterations have not only enhanced the digestion and absorption of rations in Hu sheep but also improved their immune response.

In this experiment, the analysis of significant differences at the genus level revealed that the dominant genera in the three intestinal segments were *Romboutsia*, *UCG_005*, and *Christensenellaceae*_R_7_group. This finding aligns with the results reported by Ma et al (Ma et al., 2022), which indicated that the dominant genera in the hindgut (ileum and cecum) of sheep are *UCG_005* and *Christensenellaceae*_R_7_group. By LEfSe analysis, in the ileum, *g_Faecalibaculum* and *g_Clostridium_sensu_stricto_1* were significantly enriched in the T1 and T2 groups compared to the CK group. *g_Faecalibaculum* possesses anti-inflammatory properties and is a key producer of butyric acid, which plays a crucial protects the digestive system and maintains intestinal health (Sokol et al., 2008). *g _Clostridium_sensu_stricto_1* is an anaerobic bacterium that has been associated with the integrity of the intestinal barrier (Kasahara et al., 2018). Additionally, in the cecum, both *g_Anaerorhabdus_furcosa_group* and *g_Saccharofermentans* were significantly enriched in T1 and T2 groups compared to the CK group. The *g_Anaerorhabdus_furcosa_group*, which belongs to the phylum Bacteroidota, is known for producing substantial amounts of acetic acid, thereby promoting intestinal health. *g_Saccharofermentans*, a member of the phylum Firmicutes, plays a role in enhancing gut microbiota diversity. *Romboutsia* is primarily involved in regulating of lipid metabolism, as well as fat digestion and absorption, and is classified as a probiotic bacterium. In our study, the relative abundance of *Romboutsia* in the ileum and cecum was significantly higher in the T2 group compared to the CK group, suggesting that *Codonopsis pilosula* polysaccharides enhanced the population of beneficial intestinal bacteria in Hu sheep. *UCG-005*, which belongs to the family Ruminalococcaceae, includes members that play a critical role in the degradation and digestion of cellulose and starch in animals (Chassard et al., 2012; Cann et al., 2016; Huang et al., 2022). Consequently, the family Ruminalococcaceae is regarded as potentially beneficial bacteria capable of regulating the gut's internal environment and may be linked to immune modulation (Cheng et al., 2023). The genus *Christensenellaceae*_R_7_group part of the family Christensenellaceae, is often recognized for its positive effects on maintaining intestinal health and plays an important role in the degradation of cellulose and hemicellulose (Xin et al., 2019). Research has shown that *Christensenellaceae*_R_7_group is associated with feed efficiency and may participate in host metabolic processes, with significant implications for gut health and host energy balance (Pang et al., 2022). The Christensenellaceae family can use a variety of sugars, the most important fermentation end products are acetic acid and butyric acid (Morotomi et al., 2012). The analysis of differences at the genus level revealed a gradual increase in the relative abundance of *UCG-005* and *Christensenellaceae*_R_7_group in both the duodenum and ileum. This finding suggests that the incorporation of *Codonopsis pilosula* polysaccharides into the diet enhances the relative abundance of beneficial gut bacteria, thereby influencing gut flora composition, increasing gut flora biodiversity, and supporting intestinal health.

In ruminants, gut microbes significantly influence gut barrier function by regulating host–microbe relationships (Lyte et al., 2018). The tight junction proteins *Occludin*, *Claudin* and *ZO-1* family are critical components of the barrier (Zhang et al., 2022; Li et al., 2024). Given that the small intestine serves as the primary digestive organ alongside the tumor, and later in our researches we found that the major phylum and genus level microorganisms were immunologically relevant, we investigated the relative gene expression of *Occludin*, *Claudin* and *ZO-1* following the incorporation of *Codonopsis pilosula* polysaccharides into the diet. Our results indicated that the relative expression levels of *Occludin*, *Claudin* and *ZO-1* in the duodenum and ileum were higher in the T1 group compared to the CK and T2 groups. Research indicates that feeding mice an appropriate amount of *Codonopsis pilosula* polysaccharides can boost T lymphocytes and beneficially regulate intestinal mucosal immunity. Conversely, high doses may inhibit these cells (Wang et al., 2024). This is similar to our research findings, where the gene expression in the T1 group was higher than that in the T2 group, possibly because high doses of *Codonopsis pilosula* polysaccharides may cause overactivation of the immune system, leading to abnormal immune responses and gastrointestinal dysfunction. We hypothesize that the inclusion of *Codonopsis pilosula* polysaccharides in the diet may enhance the

intestinal barrier, however, the specific mechanisms underlying this effect require further investigation.

5 Conclusions

The results of this study indicated that *Codonopsis pilosula* polysaccharides significantly increase the levels of acetic acid in the ileum. Additionally, *Codonopsis pilosula* polysaccharides influence the diversity of intestinal microorganisms in the duodenum and cecum of Hu sheep. At the phylum level, Firmicutes were the dominant bacteria across all groups in the three intestinal segments. At the genus level, the predominant genera across the three intestinal segments included *Romboutsia*, *UCG-005*, and *Christensenellaceae*_R_7_group. Ultimately, this study concluded that the addition of *Codonopsis pilosula* polysaccharides to the diet might modulate the intestinal microbial composition of Hu sheep, improve intestinal barrier function, and enhance their immune competence by increasing the abundance of specific dominant flora. Therefore, the appropriate amount of *Codonopsis pilosula* polysaccharides can be used as a green feed additive, which is helpful to promote the development of animal husbandry to a more ecological, environmental protection and sustainable direction, in line with the modern green agricultural concept.

Data availability statement

The original contributions presented in the study are publicly available. This data can be found here: NCBI, accession PRJNA1202939.

Ethics statement

All animal management and experiments were approved by the Animal Committee of Gansu Agricultural University (GSAU-AEW-2020-0057). The study was conducted in accordance with the local legislation and institutional requirements.

Author contributions

QZ: Conceptualization, Data curation, Formal Analysis, Methodology, Writing – original draft, Writing – review & editing. WL: Software, Validation, Writing – review & editing. ZL: Investigation, Resources, Visualization, Writing – review & editing. QL: Investigation, Supervision, Visualization, Writing – review & editing. YM: Funding acquisition, Project administration, Writing – review & editing.

Funding

The author(s) declare that financial support was received for the research and/or publication of this article. This research was funded by the Technology Integration Technology Project of Linxia Beef and Sheep Industry Development Research Institute (KJJC-LX-2023-05) and Discipline Team Project of Gansu Agricultural University (GAU-XKTD-2022-20).

Acknowledgments

We extend our gratitude to all members who participated in this study for their invaluable support.

Conflict of interest

The authors declare that the research was conducted in the absence of any commercial or financial relationships that could be construed as a potential conflict of interest.

Generative AI statement

The author(s) declare that no Generative AI was used in the creation of this manuscript.

Publisher's note

All claims expressed in this article are solely those of the authors and do not necessarily represent those of their affiliated organizations, or those of the publisher, the editors and the reviewers. Any product that may be evaluated in this article, or claim that may be made by its manufacturer, is not guaranteed or endorsed by the publisher.

References

Alem, W. T. (2024). Effect of herbal extracts in animal nutrition as feed additives. *Heliyon* 10, e24973. doi: 10.1016/j.heliyon.2024.e24973

Biswas, S., Ahn, J. M., and Kim, I. H. (2024). Assessing the potential of phytogenic feed additives: A comprehensive review on their effectiveness as a potent dietary enhancement for nonruminant in swine and poultry. *J. Anim. Physiol. Anim. Nutr. (Berl)* 108, 711–723. doi: 10.1111/jpn.13922

Blouin, J.-M., Penot, G., Collinet, M., Nacfer, M., Forest, C., Laurent-Puig, P., et al. (2011). Butyrate elicits a metabolic switch in human colon cancer cells by targeting the pyruvate dehydrogenase complex. *Int. J. Cancer* 128, 2591–2601. doi: 10.1002/ijc.25599

Cann, I., Bernardi, R. C., and Mackie, R. I. (2016). Cellulose degradation in the human gut: Ruminococcus champanellensis expands the cellulosome paradigm. *Environ. Microbiol.* 18, 307–310. doi: 10.1111/1462-2920.13152

Cao, L., Du, C., Zhai, X., Li, J., Meng, J., Shao, Y., et al. (2022). *Codonopsis pilosula* polysaccharide improved spleen deficiency in mice by modulating gut microbiota and energy related metabolisms. *Front. Pharmacol.* 13. doi: 10.3389/fphar.2022.862763

Cao, H., Zhang, A., Zhang, H., Sun, H., and Wang, X. (2015). The application of metabolomics in traditional Chinese medicine opens up a dialogue between Chinese and Western medicine. *Phytother. Res.* 29, 159–166. doi: 10.1002/ptr.5240

Chassard, C., Delmas, E., Robert, C., Lawson, P. A., and Bernalier-Donadille, A. (2012). Ruminococcus Champanellensis sp. nov., a cellulose-degrading bacterium from human gut microbiota. *Int. J. Syst. Evol. Microbiol.* 62, 138–143. doi: 10.1099/ijs.0.027375-0

Cheng, X., Du, X., Liang, Y., Degen, A. A., Wu, X., Ji, K., et al. (2023). Effect of grape pomace supplement on growth performance, gastrointestinal microbiota, and methane production in Tan lambs. *Front. Microbiol.* 14. doi: 10.3389/fmicb.2023.1264840

Cheng, D. L., Ngo, H. H., Guo, W. S., Liu, Y. W., Zhou, J. L., Chang, S. W., et al. (2018). Bioprocessing for elimination antibiotics and hormones from swine wastewater. *Sci. Total Environ.* 621, 1664–1682. doi: 10.1016/j.scitotenv.2017.10.059

Chu, X., Liu, X. J., Qiu, J. M., Zeng, X. L., Bao, H. R., and Shu, J. (2016). Effects of Astragalus and *Codonopsis pilosula* polysaccharides on alveolar macrophage phagocytosis and inflammation in chronic obstructive pulmonary disease mice exposed to PM2.5. *Environ. Toxicol. Pharmacol.* 48, 76–84. doi: 10.1016/j.etap.2016.10.006

Donadio, G., Mensitieri, F., Santoro, V., Parisi, V., Bellone, M. L., De Tommasi, N., et al. (2021). Interactions with microbial proteins driving the antibacterial activity of flavonoids. *Pharmaceutics* 13, 660. doi: 10.3390/pharmaceutics13050660

Du, J. H., Xu, M. Y., Wang, Y., Lei, Z., Yu, Z., and Li, M. Y. (2022). Evaluation of Taraxacum mongolicum flavonoids in diets for Channa argus based on growth performance, immune responses, apoptosis and antioxidant defense system under lipopolysaccharide stress. *Fish Shellfish Immunol.* 131, 1224–1233. doi: 10.1016/j.fsi.2022.11.034

Frampton, J., Murphy, K. G., Frost, G., and Chambers, E. S. (2020). Short-chain fatty acids as potential regulators of skeletal muscle metabolism and function. *Nat. Metab.* 2, 840–848. doi: 10.1038/s42255-020-0188-7

Gao, S. M., Liu, J. S., Wang, M., Cao, T. T., Qi, Y. D., Zhang, B. G., et al. (2018). Traditional uses, phytochemistry, pharmacology and toxicology of Codonopsis: A review. *J. Ethnopharmacol* 219, 50–70. doi: 10.1016/j.jep.2018.02.039

Gharechahi, J., Vahidi, M. F., Sharifi, G., Ariaeenejad, S., Ding, X. Z., Han, J. L., et al. (2023). Lignocellulose degradation by rumen bacterial communities: New insights from metagenome analyses. *Environ. Res.* 229, 115925. doi: 10.1016/j.envres.2023.115925

Guo, H., Lou, Y., Hou, X., Han, Q., Guo, Y., Li, Z., et al. (2024a). A systematic review of the mechanism of action and potential medicinal value of *Codonopsis pilosula* in diseases. *Front. Pharmacol.* 15. doi: 10.3389/fphar.2024.1415147

Guo, R., Zhang, H., Jiang, C., Niu, C., Chen, B., Yuan, Z., et al. (2024b). The impact of *Codonopsis Pilosulae* and *Astragalus Membranaceus* extract on growth performance, immunity function, antioxidant capacity and intestinal development of weaned piglets. *Front. Vet. Sci.* 11. doi: 10.3389/fvets.2024.1470158

Honda, K., and Littman, D. R. (2016). The microbiota in adaptive immune homeostasis and disease. *Nature* 535, 75–84. doi: 10.1038/nature18848

Hu, R., Li, S., Diao, H., Huang, C., Yan, J., Wei, X., et al. (2023). The interaction between dietary fiber and gut microbiota, and its effect on pig intestinal health. *Front. Immunol.* 14. doi: 10.3389/fimmu.2023.1095740

Huang, S., Zheng, G., Men, H., Wang, W., and Li, S. (2022). The response of fecal microbiota and host metabolome in dairy cows following rumen fluid transplantation. *Front. Microbiol.* 13. doi: 10.3389/fmicb.2022.940158

Hughes, J. B., Hellmann, J. J., Ricketts, T. H., and Bohannan, B. J. (2001). Counting the uncountable: statistical approaches to estimating microbial diversity. *Appl. Environ. Microbiol.* 67, 4399–4406. doi: 10.1128/AEM.67.10.4399-4406.2001

Jiangyong, Y., Minyi, G., Guishan, L., Jingjing, Z., Naiyun, F., Xiaorui, L., et al. (2022). Lycium barbarum Polysaccharide Inhibits Lipid Oxidation and Protein Degradation in Tan Sheep Meatballs during Frozen Storage. *Food Sci. Anim. Resources.* 10, 5851. doi: 10.5851/kosfa.2022.e23

Kasahara, K., Krautkramer, K. A., Org, E., Romano, K. A., Kerby, R. L., Vivas, E. I., et al. (2018). Interactions between Roseburia intestinalis and diet modulate atherogenesis in a murine model. *Nat. Microbiol.* 3, 1461–1471. doi: 10.1038/s41564-018-0272-x

Kim, B. R., Shin, J., Guevarra, R., Lee, J. H., Kim, D. W., Seol, K. H., et al. (2017). Deciphering diversity indices for a better understanding of microbial communities. *J. Microbiol. Biotechnol.* 27, 2089–2093. doi: 10.4014/jmb.1709.09027

Krishnan, S., Alden, N., and Lee, K. (2015). Pathways and functions of gut microbiota metabolism impacting host physiology. *Curr. Opin. Biotechnol.* 36, 137–145. doi: 10.1016/j.copbio.2015.08.015

Kristensen, N. B., and Harmon, D. L. (2004). Effect of increasing ruminal butyrate absorption on splanchnic metabolism of volatile fatty acids absorbed from the washed reticulorumen of steers. *J. Anim. Sci.* 82, 3549–3559. doi: 10.2527/2004.82123549x

Kuppusamy, S., Kakarla, D., Venkateswarlu, K., Megharaj, M., Yoon, Y.-E., and Lee, Y. B. (2018). Veterinary antibiotics (VAs) contamination as a global agro-ecological issue: A critical view. *Agriculture Ecosyst. Environ.* 257, 47–59. doi: 10.1016/j.agee.2018.01.026

Li, M.-Y., Liu, Y.-Z., Chen, X.-M., Niu, X.-T., Chen, L., Zhao, L., et al. (2025). Astaxanthin ameliorates high-carbohydrate diet-induced ER stress, immunosuppression and hepatic glucose metabolism through AMPK/autophagy pathway in Channa argus. *Aquaculture* 598, 742010. doi: 10.1016/j.aquaculture.2024.742010

Li, M. Y., Shi, Y. C., Xu, W. X., Zhao, L., and Zhang, A. Z. (2024). Exploring Cr(VI)-induced blood-brain barrier injury and neurotoxicity in zebrafish and snakehead fish, and inhibiting toxic effects of astaxanthin. *Environ. pollut.* 355, 124280. doi: 10.1016/j.envpol.2024.124280

Liao, W. L. (2024). Effects of extract from *Codonopsis pilosula* on the growth performance, biochemical indexes in serum, and intestinal health of weaned piglets. *Anim. Breed. Feed* 23, 10–16. doi: 10.13300/j.cnki.cn42-1648/s.2024.09.003

Liu, S., Xiao, G., Wang, Q., Tian, J., Feng, X., Zhang, Q., et al. (2023). Effects of dietary Astragalus membranaceus and *Codonopsis pilosula* extracts on growth performance, antioxidant capacity, immune status, and intestinal health in broilers. *Front. Vet. Sci.* 10. doi: 10.3389/fvets.2023.1302801

Liu, K. H., and Xie, S. H. (2024). Study on antioxidant activity of Codonopsis polysaccharides and their effects on serum immunity and antioxidant function in laying hens. *Feed Res.* 47, 56–60. doi: 10.13557/j.cnki.issn1002-2813.2024.06.011

Liu, K. H., Xie, S. H., Li, T., Wang, B. Z., Zhang, H. Y., Zhu, G. S., et al. (2021). Study on *Codonopsis pilosula* polysaccharides in enhancing chicken immune activity. *Heilongjiang Anim. Sci. Veterinary Med.* 116-119. doi: 10.13881/j.cnki.hljxmsy.2020.09.0215

Lyte, M., Villageliú, D. N., Crooker, B. A., and Brown, D. R. (2018). Symposium review: Microbial endocrinology-Why the integration of microbes, epithelial cells, and neurochemical signals in the digestive tract matters to ruminant health. *J. Dairy Sci.* 101, 5619–5628. doi: 10.3168/jds.2017-13589

Ma, Y., Deng, X., Yang, X., Wang, J., Li, T., Hua, G., et al. (2022). Characteristics of bacterial microbiota in different intestinal segments of Aohan fine-wool sheep. *Front. Microbiol.* 13. doi: 10.3389/fmicb.2022.874536

Manyi-Loh, C., Mamphweli, S., Meyer, E., and Okoh, A. (2018). Antibiotic use in agriculture and its consequential resistance in environmental sources: potential public health implications. *Molecules* 23, 795. doi: 10.3390/molecules23040795

Morotomi, M., Nagai, F., and Watanabe, Y. (2012). Description of Christensenella minuta gen. nov., sp. nov., isolated from human faeces, which forms a distinct branch in the order Clostridiales, and proposal of Christensenellaceae fam. nov. *Int. J. Syst. Evol. Microbiol.* 62, 144–149. doi: 10.1099/ijs.0.026989-0

Nan, H. J., Qin, X. M., Wu, B., Li, Y., Zhang, L. Z., and Guo, X. Q. (2008). Ultrasonic extraction and content determination of polysaccharide in Codonopsis. *J. Shanxi Med. Univ.*, 641–643.

Pang, K., Dai, D., Yang, Y., Wang, X., Liu, S., Huang, W., et al. (2022). Effects of high concentrate rations on ruminal fermentation and microbiota of yaks. *Front. Microbiol.* 13. doi: 10.3389/fmicb.2022.957152

Ross, F. C., Patangia, D., Grimaud, G., Lavelle, A., Dempsey, E. M., Ross, R. P., et al. (2024). The interplay between diet and the gut microbiome: implications for health and disease. *Nat. Rev. Microbiol.* 22, 671–686. doi: 10.1038/s41579-024-01068-4

Sanos, S. L., Bui, V. L., Mortha, A., Oberle, K., Heners, C., Johner, C., et al. (2009). RORγt and commensal microflora are required for the differentiation of mucosal interleukin 22–producing NKp46+ cells. *Nat. Immunol.* 10, 83–91. doi: 10.1038/ni.1684

Sokol, H., Pigneur, B., Watterlot, L., Lakhdari, O., Bermúdez-Humarán, L. G., Gratadoux, J. J., et al. (2008). Faecalibacterium prausnitzii is an anti-inflammatory commensal bacterium identified by gut microbiota analysis of Crohn disease patients. *Proc. Natl. Acad. Sci. U.S.A.* 105, 16731–16736. doi: 10.1073/pnas.0804812105

Song, X., Pi, S., Gao, Y., Zhou, F., Yan, S., Chen, Y., et al. (2021). The role of vasoactive intestinal peptide and mast cells in the regulatory effect of Lactobacillus casei ATCC 393 on intestinal mucosal immune barrier. *Front. Immunol.* 12. doi: 10.3389/fimmu.2021.723173

Su, Y., Gao, X., Wang, Y., Li, X., Zhang, W., and Zhao, J. (2023). Astragalus polysaccharide promotes sheep satellite cell differentiation by regulating miR-133a through the MAPK/ERK signaling pathway. *Int. J. Biol. Macromolecules* 239, 124351. doi: 10.1016/j.ijbiomac.2023.124351

Svartström, O., Alneberg, J., Terrapon, N., Lombard, V., De Bruijn, I., Malmsten, J., et al. (2017). Ninety-nine *de novo* assembled genomes from the moose (Alces alces) rumen microbiome provide new insights into microbial plant biomass degradation. *Isme J.* 11, 2538–2551. doi: 10.1038/ismej.2017.108

Thoetkiattikul, H., Mhuantong, W., Laothanachareon, T., Tangphatsornruang, S., Pattarajinda, V., Eurwilaichitr, L., et al. (2013). Comparative analysis of microbial profiles in cow rumen fed with different dietary fiber by tagged 16S rRNA gene pyrosequencing. *Curr. Microbiol.* 67, 130–137. doi: 10.1007/s00284-013-0336-3

Van Hoek, M. J., and Merks, R. M. (2012). Redox balance is key to explaining full vs. partial switching to low-yield metabolism. *BMC Syst. Biol.* 6, 22. doi: 10.1186/1752-0509-6-22

Wang, M., Wichienchot, S., He, X., Fu, X., Huang, Q., and Zhang, B. (2019). *In vitro* colonic fermentation of dietary fibers: Fermentation rate, short-chain fatty acid production and changes in microbiota. *Trends Food Sci. Technol.* 88, 1–9. doi: 10.1016/j.tifs.2019.03.005

Wang, J. R., Zhang, H. Q., Sun, J. Y., and Xu, X. H. (2024). Effects of baitiao dangshen polysaccharide on the immune function of the intestinal mucosa in mice. *Western J. Traditional Chin. Med.* 37, 10–14.

Xia, Z., Li, G., Zhai, Y., Tong, L., Ru, Y., Wu, M., et al. (2025). Immunomodulatory effects and multi-omics analysis of *Codonopsis Pilosula* Extract in septic rats. *J. Ethnopharmacol* 337, 118847. doi: 10.1016/j.jep.2024.118847

Xiang, Q., Wu, X., Pan, Y., Wang, L., Cui, C., Guo, Y., et al. (2020). Early-life intervention using fecal microbiota combined with probiotics promotes gut microbiota maturation, regulates immune system development, and alleviates weaning stress in piglets. *Int. J. Mol. Sci.* 21, 503. doi: 10.3390/ijms21020503

Xin, J., Chai, Z., Zhang, C., Zhang, Q., Zhu, Y., Cao, H., et al. (2019). Comparing the microbial community in four stomach of dairy cattle, yellow cattle and three yak herds in Qinghai-Tibetan plateau. *Front. Microbiol.* 10. doi: 10.3389/fmicb.2019.01547

Xu, Y. Y. (2006). Extraction methods and techniques of polysaccharides. *J. Fisheries Researc*, 32–36. doi: 10.14012/j.cnki.fjsc.2006.03.009

Yadav, S., and Jha, R. (2019). Strategies to modulate the intestinal microbiota and their effects on nutrient utilization, performance, and health of poultry. *J. Anim. Sci. Biotechnol.* 10, 2. doi: 10.1186/s40104-018-0310-9

Yin, Y., Wang, F., Yang, M., Tan, B., Yin, Y., Chen, J., et al. (2021). Lycium barbarum polysaccharides as antibiotic substitutes improve growth performance, serum immunity, antioxidant status, and intestinal health for weaned piglets. *Front. Microbiol.* 12. doi: 10.3389/fmicb.2021.819993

Yu, Z., and Li, M. (2025). Application of nutrition interventions strategy to enhance fish flesh quality. *J. Food Composition Anal.* 138, 107010. doi: 10.1016/j.jfca.2024.107010

Zafar, H., and Saier, J. M. H. (2021). Gut Bacteroides species in health and disease. *Gut Microbes* 13, 1848158. doi: 10.1080/19490976.2020.1848158

Zhang, H., Shao, M., Huang, H., Wang, S., Ma, L., Wang, H., et al. (2018). The dynamic distribution of small-tail han sheep microbiota across different intestinal segments. *Front. Microbiol.* 9. doi: 10.3389/fmicb.2018.00032

Zhang, Y., Wang, Q. R., Shi, X. C., He, X., Zhang, T., and Zhao, X. H. (2024). Effects of lentinan polysaccharides on growth performance, intestinal microbiota diversity, serum antioxidant capacity and immune function of calves. *Heilongjiang Anim. Sci. Veterinary Med.*, 85–90 + 97 + 112. doi: 10.13881/j.cnki.hljxmsy.2023.11.0092

Zhang, K., Xu, Y., Yang, Y., Guo, M., Zhang, T., Zong, B., et al. (2022). Gut microbiota-derived metabolites contribute negatively to hindgut barrier function development at the early weaning goat model. *Anim. Nutr.* 10, 111–123. doi: 10.1016/j.aninu.2022.04.004

Zhao, L., Yu, J., Liu, Y., Liu, Y., Zhao, Y., and Li, M.-Y. (2025). The major roles of intestinal microbiota and TRAF6/NF-κB signaling pathway in acute intestinal inflammation in mice, and the improvement effect by Hippophae rhamnoides polysaccharide. *Int. J. Biol. Macromolecules* 296, 139710. doi: 10.1016/j.ijbiomac.2025.139710

Zhong, T., Wang, Y., Wang, X., Freitas-De-Melo, A., Li, H., Zhan, S., et al. (2022). Diarrhea in suckling lambs is associated with changes in gut microbiota, serum immunological and biochemical parameters in an intensive production system. *Front. Microbiol.* 13. doi: 10.3389/fmicb.2022.1020657

Zhou, J., Yang, Q., Wei, W., Huo, J., and Wang, W. (2025). *Codonopsis pilosula* polysaccharide alleviates ulcerative colitis by modulating gut microbiota and SCFA/GPR/NLRP3 pathway. *J. Ethnopharmacol* 337, 118928. doi: 10.1016/j.jep.2024.118928

frontiers | Frontiers in Microbiology

TYPE Original Research
PUBLISHED 13 June 2025
DOI 10.3389/fmicb.2025.1590400

Check for updates

OPEN ACCESS

EDITED BY
Mohammad Altamimi,
An-Najah National University, Palestine

REVIEWED BY
Chaichana Suriyapha,
Khon Kaen University, Thailand
Xuan Ma,
Ningxia University, China

*CORRESPONDENCE
Youji Ma
✉ myj1124@163.com

RECEIVED 09 March 2025
ACCEPTED 21 May 2025
PUBLISHED 13 June 2025

CITATION
Li X, Li D, Wang C, Li Q, Nie Y, Zhang L, Xu J and Ma Y (2025) Metagenomic insights into the effects of Chive seed flavonoid on intestinal fermentation, morphology, and microbiota composition in sheep. *Front. Microbiol.* 16:1590400. doi: 10.3389/fmicb.2025.1590400

COPYRIGHT
© 2025 Li, Li, Wang, Li, Nie, Zhang, Xu and Ma. This is an open-access article distributed under the terms of the Creative Commons Attribution License (CC BY). The use, distribution or reproduction in other forums is permitted, provided the original author(s) and the copyright owner(s) are credited and that the original publication in this journal is cited, in accordance with accepted academic practice. No use, distribution or reproduction is permitted which does not comply with these terms.

Metagenomic insights into the effects of Chive seed flavonoid on intestinal fermentation, morphology, and microbiota composition in sheep

Xujie Li[1,2], Dengpan Li[1,2], Chunhui Wang[1,2], Qiao Li[1,2], Yajing Nie[1,2], Liming Zhang[1,2], Jin Xu[1,2] and Youji Ma[1,2]*

[1]College of Animal Science and Technology, Gansu Agricultural University, Lanzhou, China, [2]Gansu Key Laboratory of Animal Generational Physiology and Reproductive Regulation, Lanzhou, China

Chive seed flavonoid (CSF) exhibits antioxidant, digestive, and immunomodulatory properties, yet their effects on ruminant intestinal development and microbial ecosystems remain underexplored. This study systematically evaluated CSF supplementation (0.25% of concentrate) on intestinal morphology, volatile fatty acids (VFAs) dynamics, and microbiota composition in 16 weaned Hu lambs (3 months; 19.57 ± 1.56 kg initial weight) using histomorphometry, VFA quantification, and full-length 16S rRNA sequencing. Animals were randomly allocated to a control (basal diet) or CSF-supplemented group (T), following a 7-day adaptation and 90-day experimental protocol. Key findings revealed: (1) The T group demonstrated increased jejunal and ileal villus length ($p < 0.05$), elevated villus height-to-crypt depth ratio (V/C; $p < 0.05$), thickened muscular layers ($p < 0.05$), and reduced crypt depth ($p < 0.05$). (2) CSF supplementation significantly elevated acetate, propionate, butyrate, and total VFAs ($p < 0.05$) in ileum, cecum, colon, and rectum, with notable jejunal propionate and total VFAs increases ($p < 0.05$). (3) Upregulated expression of ileal and cecal genes (*IGF1*, *CD81*, *CTNNBL1*, *SLC39A8*) linked to tissue morphogenesis and VFAs absorption was observed in the T group ($p < 0.01$). (4) Full-length 16S analysis demonstrated CSF-enhanced microbial diversity and selective enrichment of *Cyanobacteriota*, *Bacillus*, *Acetobacterium*, and *Streptomyces* [Linear Discriminant Analysis Effect Size (LEfSe) analysis]. Regional microbial shifts included *Bacteroidota* proliferation in the small intestine and rectum, *Actinomycetota* dominance in duodenum/cecum/colon, and ileal enrichment of *Bacillota*, *Clostridium*, and *Streptomyces*. KEGG pathway analysis confirmed CSF-driven enhancements in carbohydrate/energy metabolism, immune regulation, and intestinal barrier pathways ($p < 0.05$). In conclusion, dietary supplementation with 0.25% CSF improved intestinal morphology, increased the production of VFAs, and optimized microbial composition, thereby promoting intestinal health in sheep. This study provides a theoretical basis for the application of CSF in promoting healthy production in sheep.

KEYWORDS

Chive seed flavonoid, intestinal morphology, VFAs, gut microbiota, sheep

1 Introduction

The global demand for food safety and the rapid development of the livestock industry have led to the widespread use of antibiotics. However, the long-term administration of antibiotics has resulted in antimicrobial residues and the emergence of antimicrobial resistance, posing significant threats to human health and animal productivity. As a result, there is an urgent need to restrict or ban the use of antibiotics in agriculture (Li et al., 2024). Traditional livestock farming practices are increasingly unable to meet modern demands, driving the sector toward high-quality and sustainable development. To ensure sustainable development, food safety, and public health, the development of alternative feed resources has become a critical area of research (van Dijk et al., 2018). With advancements in biotechnology, multi-omics technologies, particularly microbiome and genomics, have entered the field of animal production. The rise of microbiome research has further promoted sustainable development in animal husbandry, not only improving animal production performance and health but also reducing environmental pollution and enhancing economic efficiency (Liu et al., 2024).

Against this backdrop, Chive seed has garnered attention as a promising agricultural by-product. It contains a wide array of bioactive compounds, including amino acids, flavonoids, and saponins (Sang et al., 2000). Flavonoids, as secondary metabolites widely present in plants, have attracted significant interest in animal nutrition and health due to their notable antioxidant, antimicrobial, anti-inflammatory, and growth-promoting properties (Muqier et al., 2017). Accumulating evidence highlights the diverse benefits of flavonoids in animal health. For instance, soy isoflavones have been found to enhance animal growth while exhibiting anti-obesity and anti-diabetic effects in humans (Nakai and Kamei, 2020). Additionally, flavonoids have been shown to enhance immune function, improve milk and egg production (Amanzadeh et al., 2019), and mitigate conditions such as necrotic enteritis in broilers (Buiatte et al., 2024). Furthermore, these compounds can maintain gut barrier integrity, regulate gut hormone secretion, and modulate the composition and function of gut microbiota (Oteiza et al., 2018). Mulberry leaf flavonoid, for example, have been reported to improve nutrient digestibility and energy utilization in sheep while reducing methane emissions (Chen et al., 2015). CSF, a well-known plant-derived extract, are rich in various phytochemicals, including quercetin, kaempferol, kaempferol glycosides, naringenin, naringenin glycosides, hesperetin, and epicatechin. The total flavonoids present in Allium cepa exhibit strong antioxidant, anti-aging, and antimicrobial effects. These flavonoid compounds are stable in nature, resistant to degradation, and capable of inhibiting food oxidation and suppressing harmful bacteria in food products (de Freitas et al., 2020).

Current research on CSF has primarily focused on their antioxidant, antiviral, and antibacterial effects in humans and mice, with limited studies conducted in ruminants. Ruminant gut microbiota comprise four major phyla: bacteria, fungi, archaea, and protists (Zhang et al., 2024), which play pivotal roles in maintaining gut barriers, enhancing immunity, and promoting metabolism (Hooper and Macpherson, 2010; Zhang et al., 2022). The sheep gut, as a natural barrier, maintains intestinal homeostasis, protects the host against pathogens, and is essential for digestion and metabolism (Lee and Hase, 2014; Li D. et al., 2023; Zhang et al., 2024). A well-functioning gut barrier not only enhances the host's ability to absorb nutrients but also defends against pathogenic microbial invasions. Based on this background, this study posits that CSF may exert their beneficial effects through their antimicrobial and probiotic properties, modulating gut microbiota composition by significantly increasing the abundance of beneficial bacteria while suppressing the growth of potentially harmful pathogens. This modulation could lead to elevated VFAs levels and improved intestinal pH balance, thereby maintaining gut fermentation homeostasis. Additionally, CSF may enhance gut barrier function and improve intestinal morphological traits, including villus height, muscular layer thickness, and crypt depth optimization, ultimately improving nutrient absorption efficiency. To explore these hypotheses, this study investigates the effects of dietary supplementation with 0.25% CSF on gut tissue morphology, microbial composition, and fermentation parameters in sheep. These findings aim to provide theoretical support for the application of CFS in ruminant nutrition.

2 Materials and methods

2.1 Ethic statement

All experimental procedures were conducted in accordance with the guidelines of the Ministry of Science and Technology of the People's Republic of China (Approval No. 2006-398) and approved by the Animal Ethics and Welfare Committee of Gansu Agricultural University (GSAU-AEW-2020-0057).

2.2 Animals, feeding management and experimental design

This experiment adopted a completely randomized single-factor design. Sixteen Hu lambs (3-month-old; initial body weight: 19.56 ± 1.59 kg) with homogeneous genetic backgrounds and comparable health status were selected as experimental subjects. The lambs, sourced from Shengyuan Agricultural and Animal Husbandry Technology Co., Ltd. (Linxia Hui Autonomous Prefecture, Gansu Province, China), were randomly allocated into two groups (8 lambs/group): a control group (CK) fed a basal diet and an experimental group (T) receiving the basal diet supplemented with 0.25% CSF in the concentrate portion. The trial included a 7-day adaptation period and a 90-day experimental period. The basal diet was formulated in accordance with the Chinese agricultural standard *Nutrient Requirements of Meat-Type Sheep and Goats* (NY/T 816-2021), with detailed compositions and nutritional levels provided in Table 1, while CSF's nutritional and bioactive profiles are presented in Table 2. All lambs were housed individually in pens within a disinfected facility. Prior to the trial, animals were ear-tagged for identification and acclimatized to the environment. Daily feeding occurred at 07:00 and 18:00 h, with *ad libitum* access to feed and water. Pens were cleaned daily to

TABLE 1 Composition and nutritional levels of the basal diet (dry matter basis).

Diet ingredient	Content/%
Corn	33.00
Corn germ meal	6.00
Soybean meal	12.00
Cottonseed meal	6.00
Whole corn silage	22.00
Alfalfa hay	14.00
Wheat bran	4.00
Sodium bicarbonate	0.90
Limestone	1.20
Salt	0.60
Premix1	0.30
Total	100.00
Nutritional levels	
Metabolic energy (MJ/kg)	11.52
Crude protein (%)	17.23
Crude fat (%)	3.14
NDF (%)	25.60
ADF (%)	16.14
Ga (%)	0.83
P (%)	0.42
Dry matter (%)	89.2

NDF, neutral detergent fiber; ADF, acid detergent fiber. The same as the table below. The premix provided per kg of diet: Fe 100 mg, Cu 8.5 mg, Zn 65 mg, Se 0.25 mg, I 0.5 mg, Co 0.30 mg, Mn.40 mg, VA 10,000 IU, VD 5,000 IU, VE 150 IU. ME was a calculated value, while the others were measured values.

remove feces and urine, and routine disinfection was performed to maintain hygienic conditions.

2.3 Sample collection

At the conclusion of the trial, all sheep underwent a 12-h fasting period followed by 2 h of water deprivation. Five lambs per group were randomly selected and euthanized via intravenous injection 30 mL of 20% pentobarbital sodium solution. Immediately post-euthanasia, the abdominal cavity was opened, and junctions between intestinal segments (duodenum, jejunum, ileum, cecum, colon, rectum) were ligated to prevent cross-contamination of luminal contents. Luminal contents from the mid-sections of each segment were filtered through four-layer gauze into pre-labeled beakers for pH measurement. Aliquots of the solid-liquid mixtures were transferred into 5 mL cryotubes, flash-frozen in liquid nitrogen, and transported to the laboratory within 1 hour for storage at −80°C pending VFAs and microbial community analyses. Concurrently, two 1 cm^2 tissue samples were excised from the mid-portions of the duodenum, jejunum, and ileum. These tissues were rinsed three times with sterile phosphate-buffered saline (PBS; pH 7.4) to remove residual luminal contents, one of the rinsed samples

TABLE 2 Composition and nutritional levels of Chive seed flavonoid (dry matter basis).

Items	Content/%	Items	Content/%
Crude protein	16.82	Ca	0.52
Crude fat	14.62	P	0.68
NDF	35.70	Dry matter	92.01
ADF	24.55	Total flavonoids	0.5

followed by immersion fixation in 4% paraformaldehyde (4°C, 24–48 h) to preserve histological integrity, and the other was placed in a cryopreservation tube and filled with liquid nitrogen for subsequent quantitative analysis.

2.4 Morphological indicators of small intestinal tissue

Intestinal tissues fixed in a 4% paraformaldehyde solution were subjected to dehydration, clearing, and embedding processes to create paraffin sections with a thickness of 6 μm. These sections were stained with hematoxylin-eosin (HE) and examined under a microscope at 10x magnification. A digital slide scanner (Pannoramic DESK, Hungary) was utilized to scan the sections, and the Slide Viewer 2.6 image analysis system was employed to analyze three discontinuous sections per sample. Measurements of villus height, crypt depth, and muscle layer thickness in the duodenum, jejunum, and ileum were conducted, with at least five fields of view measured per section. The average values were subsequently calculated to provide the final measurement data.

2.5 Determination of fermentation parameters in intestinal contents

The pH levels of the contents in each intestinal segment were measured using a portable pH meter (LC23020970, Shanghai, China). The VFAs present in the contents of each intestinal segment were quantified following the gas chromatography method outlined in previous studies (Shi et al., 2023). Briefly, the contents of each intestinal segment were thawed in a refrigerator at 4°C, and 1 g of cecal, colonic, and jejunal contents was dissolved in 2 mL of pure water. Subsequently, the contents from all six intestinal segments were transferred into a 5 mL centrifuge tube and centrifuged at 5,400 rpm for 10 minutes at 4°C. After centrifugation, 1 mL of the supernatant was transferred into a 1.5 mL centrifuge tube, to which 0.2 mL of a 25% metaphosphoric acid deproteinization solution (containing 2 g/L of the internal standard 2EB) was added. The mixture was thoroughly mixed and incubated on ice for 30 min. Following this, it was centrifuged at 10,000 rpm for 10 min at 4°C. The supernatant was then drawn using a disposable syringe, filtered through a 0.22 μm membrane into a 2 mL brown sample vial, and the VFAs were measured using a gas chromatograph (HP6890N, Agilent, United States) equipped with an HP19091N-213 capillary column (Agilent, United States).

2.6 16S rRNA Full-length sequencing of intestinal microbiota

2.6.1 DNA extraction and quality control

Total genomic DNA samples were extracted using the OMEGA Soil DNA Kit M5635-02 (Omega Bio-Tek, Norcross, GA, United States) following the manufacturer's instructions and stored at −20°C prior to further analysis. The quantity and quality of the extracted DNA were assessed using the NanoDrop NC 2000 spectrophotometer (Thermo Fisher Scientific, Waltham, MA, United States) and agarose gel electrophoresis, respectively.

2.6.2 PCR amplification and library construction

Following DNA extraction, PCR amplification of the full-length 16S rRNA gene, which encompasses the V1-V9 regions of bacteria, was conducted using standard bacterial 16S full-length primer sequences (27F: AGRGTTYGATYMTGGCTCAG, 1492R: RGYTACCTTGTTACGACT). All PCR amplification products were purified with Amplecourt AMPure Beads (Beckman Coulter, Indianapolis, IN) and subsequently quantified using the PicoGreen dsDNA Assay Kit (Invitrogen, Carlsbad, CA, United States). Library construction was performed utilizing the TruSeq Nano DNA LT Library Prep Kit (SMRT technology) from Illumina (San Diego, CA, United States). After rigorous quality control, the qualified libraries were dispatched to Personal Biotechnology Co., Ltd. (Shanghai, China) for sequencing on the PacBio Sequel II platform.

2.7 Sequencing data analysis

The raw sequencing data obtained from high-throughput sequencing undergoes an initial screening based on sequence quality, with problematic samples being subjected to re-sequencing or supplementary sequencing. The raw sequences that pass this initial quality screening are then assigned to libraries and samples according to their Index and Barcode information, followed by the removal of barcode sequences. Subsequently, in accordance with the methodology (Bolyen et al., 2019), the sequences undergo quality filtering, denoising, operational taxonomic unit (OUT) clustering, merging, and chimera removal using the dada 2 plugin of the QIIME 2 software. The sequence data analysis is primarily conducted using QIIME 2 and the R package (v3.2.0). Based on the distribution of ASV/OTU across different samples, the Alpha diversity levels of each sample are evaluated, and the adequacy of the sequencing depth is assessed through the rarefaction curve. Further evaluation of Alpha diversity indices such as Chao 1, Observed-species, Faith-pd, Goods-coverage, Shannon, and Simpson is performed. By plotting the rank abundance curves at the ASV level, the richness and evenness of ASVs across different samples are compared. At the ASV/OTU level, R software (v3.2.0) is utilized to generate Principal Coordinate Analysis PCoA and Non-metric Multidimensional Scaling NMDS plots, combined with statistical test methods (such as ANOSIM) to quantify the differences in Beta diversity between different groups and assess their significance. Finally, statistical analysis is conducted on the feature table after the removal of singletons, allowing for the visualization of the compositional distribution of each sample at the phylum and genus taxonomic levels, with the analysis results presented in bar charts Utilize LEfSe to identify differentially abundant taxa among various groups, and represent significantly enriched species along with their importance levels within each group through a bar graph illustrating the distribution of LDA values for these significant species. Conduct functional predictions by analyzing 16S rRNA gene sequences in the KEGG database using PICRUSt 2, and employ STAMP v2.1.3 software to visualize differences in gene enrichment across metabolic pathways among distinct samples or groups.

2.8 Quantitative real-time PCR

To elucidate the potential causal relationships between microbiota-host interactions identified through 16S rRNA full-length sequencing data, this study focused on the ileum and cecum segments of sheep, which showed the most pronounced responses to CSF intervention, as evidenced by significant changes in intestinal histomorphology and fermentation parameters. Based on prior microbiota analysis suggesting their relevance to host-microbe crosstalk, mucosal epithelial tissues from these segments were subjected to quantitative real-time PCR (qPCR) analysis of six candidate genes (*IGF1*, *CD81*, *CTNNBL1*, *MGST1*, *GPX4*, *SLC39A8*) implicated in histomorphological development and VFAs sorption. Total RNA in intestinal tissues was extracted using TRIzol reagent (Beijing Quanshijin Biotechnology Co., Ltd., China), the concentration and purity of total RNA were detected using an ultramicro spectrophotometer (Implen, Germany), and then according to the Evo-MLV RT kit (Accurate Biotechnology, Hunan) Reverse transcribe cDNA from the isolated total RNA in China, followed by qPCR amplification with the SYBR Green qPCR Kit from the same manufacturer. Each experiment included at least four independent biological replicates. Primer sequences are detailed in Table 3. Gene expression levels were normalized to the β-actin reference gene and quantified using the 2-ΔΔCt method.

2.9 Statistical analysis

The experimental data were initially organized using Excel 2024 software, and the differences in the data were analyzed using SPSS 25.0 (version 25.0, SPSS Inc., Chicago, IL, United States). Independent sample *t*-tests were conducted to analyze the pH and VFAs content across different intestinal segments of the two groups of lambs, with results presented as means and standard errors of the mean (SEM). $0.05 \leq p < 0.1$ was considered indicative of a trend, $p < 0.05$ was deemed a significant difference, and $p < 0.01$ was classified as a highly significant difference, all of which are statistically meaningful. Furthermore, Spearman's correlation test was employed to analyze the correlation between intestinal microbiota and fermentation parameters; $r < 0$ means negative correlation, $r > 0$ means positive correlation.

TABLE 3 Primer sequence information.

Gene	Primer sequence(5′–3′)	Length	Annealing temperature	Accession number
β-Actin	F:AGCCTTCCTTCCTGGGCATGGA R:GGACAGCACCGTGTTGGCGTAGA	113 bp	60°C	NM_001009784.3
IGF1	F:AGGAATCGTGGATGAGTGCTG R:ACTCCCTCTGCTTGTGTTCTTC	169 bp	60°C	XM_060411609.1
CD81	F:ATGACCCACAGACCACCAAC R:ACTCCCTCTGCTTGTGTTCTTC	127 bp	60°C	NM_001127281.1
CTNNBL1	F:CCCTGGTGAAGATGCTTGGT R:CGCACTGCCATTTTAGCTCC	106 bp	60°C	NM_001308590.1
MGSTI	F:CCTTTGCCTCTTACACGACG R:CACCCTGTCATCTGTCCGAA	164 bp	60°C	XM_004006818.5
GPX4	F:AAGAACGGCTGTGTGGTGAAG R:AGGGTGAGGGACGACTTTTCC	106 bp	60°C	XM_060416444.1
SLC39A8	F:TCGCCTGGATGATAACGCTC R:TGTCGAGTGCTCATTCCTGC	184 bp	60°C	XM_060416847.1

3 Results

3.1 Effects of Chive seed flavonoid on intestinal fermentation parameters, intestinal barrier function and small intestinal tissue morphology in sheep

The CK group exhibited significantly elevated pH values and total TVFAs concentrations in the duodenum and jejunum compared to the T group ($p < 0.05$), as detailed in Table 4. Conversely, the butyric acid content in the T group was highly significant that in the CK group ($p < 0.01$). In the ileum, colon, and rectum segments (Tables 4, 5), the pH value, acetic acid, propionic acid, butyric acid, and TVFAs content in the T group were significantly higher than those in the CK group ($p < 0.05$). Notably, in the cecum, the T group exhibited significantly greater concentrations of acetic acid, propionic acid, and TVFAs compared to the CK group ($p < 0.01$). As illustrated in Table 6), the villus length and muscularis thickness in the jejunum and ileum of the T group were significantly higher than those of the CK group ($p < 0.01$). The crypt depth in the CK group was significantly higher than that in the T group in the jejunum ($p < 0.05$) and highly significantly higher in the duodenum and ileum ($p < 0.01$). Additionally, the villus length in the duodenum of the CK group was significantly higher than that of the T group ($p < 0.01$), while V/C ratio in the jejunum and ileum of the T group was significantly higher than that of the CK group ($p < 0.01$), with no significant difference between the two groups in the duodenum ($p > 0.05$). In the cecum, the T group exhibited significantly greater concentrations of acetic acid, propionic acid, and TVFAs compared to the CK group ($p < 0.01$).

Quantitative analysis of six candidate genes potentially involved in tissue morphogenesis regulation and VFAs absorption (Figure 1) revealed distinct expression patterns between ileum and cecum epithelia. In the ileum, epithelial barrier-associated genes *IGF1*, *CD81*, *CTNNBL1*, and *SLC39A8* exhibited differential expression, with highly significant relative expression levels in T group versus CK group ($p < 0.01$). While *MGST1* and *GPX4* showed an upward trend in T group compared to CK, these differences lacked statistical significance ($p > 0.05$). In contrast, cecum analysis demonstrated markedly elevated relative expression levels of *IGF1*, *CD81*, *CTNNB2*, *MGST1*, *GPX4*, and *SLC39A8* in T group relative to CK group ($p < 0.01$).

3.2 Effects of Chive seed flavonoid on the whole of intestine microbiota in sheep

This study utilized the Vsearch software to match the upstream and downstream primers for the full-length 16S rRNA V1-V9 region sequencing raw data, resulting in a total of 3,996,732 sequences. After denoising and clustering, chimeras were removed, yielding 3,103,668 high-quality sequences. Subsequently, the FrameBot functional gene project was employed for correction, and singletons were excluded, ultimately producing 2,333,782 sequences, with an average of 38,896 sequences per sample (Supplementary Table 1). Using the Venn Diagram software for clustering and reading data, we analyzed the number of features between the two groups and found that the total number of features in the CK group in the sheep intestine was 32,178, while the T group had 34,428 features, with 5,490 OTUs shared between them (Figure 2A). The Rarefaction Curve indicated that the curves for the 60 samples tended to flatten as the number of sequences increased, suggesting that the sequencing results adequately reflected the diversity of the current samples, and further increasing the sequencing depth would not uncover a significant number of previously undiscovered new ASVs/OTUs (Figure 2B).

This study conducted an Alpha diversity analysis of the intestinal microbiota in two groups of sheep, with results presented in Figures 2C,D and Table 7. Specifically, the Chao1 index, Observed-species index, Faith-pd index, Shannon index, and Simpson index were all higher in the T group compared to the CK group; however, these differences did not reach statistical significance ($p > 0.05$). Additionally, the Goods-coverage index showed no significant difference between the two groups ($p > 0.05$). To further investigate the distribution differences in microbial communities between the sample groups, we employed NMDS and PCoA for Beta diversity analysis. PCoA is an analytical method

10.3389/fmicb.2025.1590400

TABLE 4 Effects of Chive seed flavonoid on small intestinal fermentation parameters in sheep.

Region	Items	Group		SEM	*P*-value
		CK	*T*		
Duodenum	pH	6.56[a]	6.49[b]	0.017	0.028
	Acetate (mmol/L)	15.91	14.77	0.325	0.066
	Propionate (mmol/L)	4.13	3.64	0.153	0.110
	Butyrate (mmol/L)	3.17	2.84	0.124	0.212
	Acetate/propionate	3.86	4.08	0.126	0.437
	TVFAs (mmol/L)	26.14[a]	23.69[b]	0.626	0.022
Jejunum	pH	6.85[a]	6.13[b]	0.162	<0.001
	Acetate (mmol/L)	15.53	14.44	0.369	0.153
	Propionate (mmol/L)	3.68[b]	3.78[a]	0.268	0.028
	Butyrate (mmol/L)	2.79[a]	1.61[b]	0.268	<0.001
	Acetate/propionate	4.22	3.86	0.180	0.150
	TVFAs (mmol/L)	26.39[a]	21.53[b]	1.132	0.002
Ileum	pH	6.88[b]	7.04[a]	0.038	<0.001
	Acetate (mmol/L)	23.56[b]	26.82[a]	0.758	0.002
	Propionate (mmol/L)	5.27[b]	6.55[a]	0.317	0.013
	Butyrate (mmol/L)	1.49[b]	4.04[a]	0.573	<0.001
	Acetate/propionate	4.48	4.10	0.107	0.54
	TVFAs (mmol/L)	31.44[b]	41.78[a]	2.371	0.001

CK, the control group; T, the experimental group; SEM, standard error of the mean; TVFAs, total volatile fatty acids. The two groups were compared; Numerical superscripts without letters indicate no significant difference, while different letters indicate significant difference. The same as the table below.

TABLE 5 Effects of Chive seed flavonoid on large intestinal fermentation parametersin in sheep.

Region	Items	Group		SEM	*P*-value
		CK	*T*		
Cecum	pH	7.00	7.02	0.011	0.602
	Acetate (mmol/L)	53.08[b]	64.76[a]	2.648	<0.001
	Propionate (mmol/L)	11.51[b]	16.59[a]	1.206	0.006
	Butyrate (mmol/L)	3.59	4.26	0.246	0.202
	Acetate/propionate	4.16[a]	3.92[b]	0.180	0.029
	TVFAs (mmol/L)	70.11[b]	87.82[a]	4.088	0.001
Colon	pH	7.09[b]	7.19[a]	0.025	0.013
	Acetate (mmol/L)	24.38[b]	39.21[a]	3.318	<0.001
	Propionate (mmol/L)	5.70[b]	8.41[a]	0.691	0.022
	Butyrate (mmol/L)	2.41[b]	3.37[a]	0.246	0.023
	Acetate/propionate	4.46	4.66	0.180	0.755
	TVFAs (mmol/L)	33.72[b]	52.75[a]	4.280	<0.001
Rectum	pH	7.11	7.15	0.009	0.035
	Acetate (mmol/L)	10.97[b]	22.87[a]	2.676	<0.001
	Propionate (mmol/L)	2.76[b]	5.29[a]	0.564	<0.001
	Butyrate (mmol/L)	1.04[b]	1.70[a]	0.161	0.010
	Acetate/propionate	3.98[b]	4.33[a]	0.090	0.016
	TVFAs (mmol/L)	15.88[b]	33.96[a]	4.059	<0.001

10.3389/fmicb.2025.1590400

TABLE 6 Effects of Chive seed flavonoid on small intestinal histomorphology in sheep.

Region	Items	Group		SEM	*P*-value
		CK	*T*		
Duodenum	Villus height/μM	535.51[a]	435.18[b]	16.470	<0.001
	Crypt depth/μM	381.88[a]	261.23[b]	22.247	0.001
	Muscular layer thickness/μM	130.56	132.96	3.243	0.729
	V/C	1.42	1.69	0.074	0.066
Jejunum	Villus height/μM	418.44[b]	467.27[a]	9.866	0.005
	Crypt depth/μM	338.26[a]	300.85[b]	9.425	0.04
	Muscular layer thickness/μM	112.36[b]	157.39[a]	6.944	<0.001
	V/C	1.24[b]	1.56[a]	0.024	0.007
Ileum	Villus height/μM	373.10[b]	551.10[a]	27.510	<0.001
	Crypt depth/μM	315.10[a]	232.27[b]	28.116	<0.001
	Muscular layer thickness/μM	101.13[b]	185.73[a]	13.319	<0.001
	V/C	1.18[b]	2.37[a]	0.057	0.005

V/C, Villus height/Crypt depth.

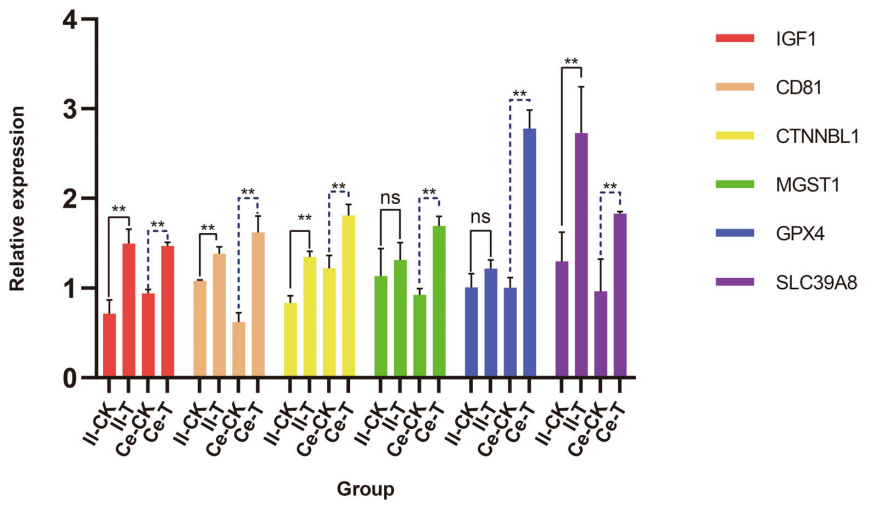

FIGURE 1
Quantitative analysis of genes associated with the regulation of tissue morphogenesis and VFAs absorption in the ileum and cecum. Data are expressed as mean ± SD. Significance levels: $^{**}p < 0.01$; ns, not significant. The letters Il and Ce represent ileum and cecum.

based on a linear model, while NMDS employs a non-linear model. The results of the NMDS analysis (Figure 2E) indicate no significant differences in microbial communities among samples within groups ($p > 0.05$), while significant distributional differences were observed between samples across groups ($p < 0.05$). Furthermore, the PCoA results (Figure 2F) reveal that the distances between samples within groups are relatively close, indicating significant differences between groups ($p < 0.05$).

3.3 Effects of Chive seed flavonoid on the composition of intestine microbiota in sheep

The visualization results revealed that at the phylum level (Figure 3A), six groups—Bacteroidota, Pseudomonadota, Cyanobacteriota, Spirochaetota, Planctomycetota, and Acidobacteriota—were dominant in the T group, with their proportions being 64.17, 3.39, 0.93, 0.73, 0.56, and 0.23%, respectively, all of which were higher than those in the CK group. In contrast, four groups—Bacillota, Actinomycetota, Mycoplasmatota, and Chloroflexota—dominated in the CK group, accounting for 65.83, 19.07, 0.42, and 0.21%, respectively, all of which were higher than those in the T group. At the genus level (Figure 3B), among the top 10 bacterial genera in the gut microbiota, five genera—*Clostridium, Myceligenerans, Mageeibacillus, Tepidibacter* and *Bacillus*—were the dominant microbiota in the T group, with proportions of 21.25, 4.72, 4.23, 3.61, and 2.34%, respectively, all of which were higher than those in the CK group. The genera *Blautia, Bifidobacterium, Paenibacillus, Solobacterium* and *Bacteroides* were dominant in the CK group, with proportions of 12.66, 11.09, 8.14, 5.92, and 4.96%, respectively, all of which were higher than those in the T group. Based on cluster analysis, we conducted LEfSe analysis (LDA > 3), which revealed

10.3389/fmicb.2025.1590400

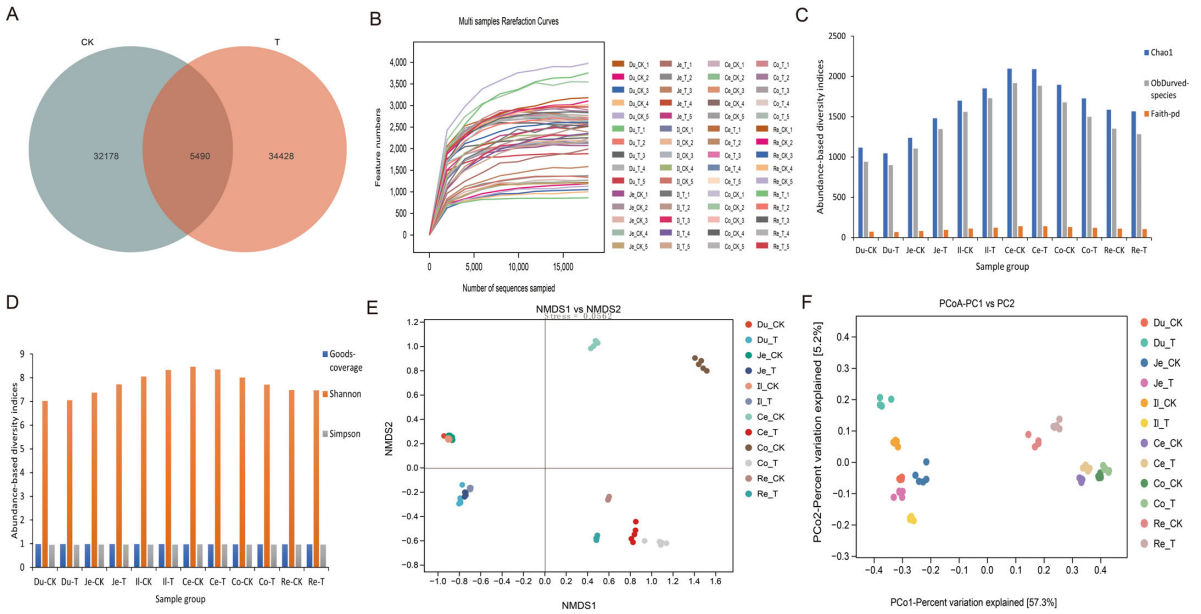

FIGURE 2
Effects of Chive seed flavonoid on Gut Microbial Diversity in Sheep. **(A)** OTU distribution. **(B)** Rarefaction curves. **(C,D)** Alpha diversity indices (Chao1, observed species, Faith-pd, Goods-coverage, Shannon, Simpson). **(E)** NMDS analysis of beta diversity. **(F)** PCoA analysis of beta diversity. The letters Du, Je, Il, Ce, Co, and Re represent the duodenum, jejunum, ileum, cecum, colon, and rectum, respectively. The same applies to the figure below.

TABLE 7 Differences in alpha diversity indices of gut microbiota between CK and T groups.

Items	Group		SEM	*P*-value
	CK	T		
Chao1	2235.745	2429.182	88.803	0.225
Observed-species	1946.547	2090.293	80.040	0.374
Faith-pd	123.835	135.481	3.685	0.115
Goods-coverage	0.973	0.970	0.001	0.389
Shannon	8.697	9.075	0.150	0.210
Simpson	0.980	0.988	0.002	0.051

a total of 17 statistically significant biomarkers. These biomarkers are distributed across various taxonomic levels: 1 at the phylum level, 1 at the class level, 3 at the order level, 6 at the family level, and 6 at the genus level. In the T group, 12 biomarkers, including Cyanobacteriota, *Bacillus, Halobacillus*, *Acetobacterium* and *Streptomyces*, were identified. In contrast, the CK group yielded 5 biomarkers, such as *Paenibacillus*, *Paenibacillaceae*, and *Corynebacterium*, as illustrated in Figure 3C.

3.4 Effect of Chive seed flavonoid on the intestinal microbiota of sheep small intestine

Analysis of the small intestine microbiota revealed notable differences in microbial composition between the CK and T groups. A total of 245 shared OTUs were identified across both groups. In the duodenum and jejunum, the T group exhibited a higher number of microbial features compared to the CK group. However, in the ileum, the CK group exhibited a higher number of microbial features. Overall, the total number of microbial features across the small intestine segments followed the order: ileum > jejunum > duodenum (Figure 4A). At the phylum level (Figure 4B), Bacillota and Actinomycetota were the dominant phyla in both groups across all intestinal segments, accounting for more than 80% of the total composition. Other phyla, such as Pseudomonadota and Bacteroidota, were also present in relatively high proportions. A detailed comparison revealed that in the duodenum, only Bacillota (63.94% in CK vs. 49.80% in T) and Actinomycetota (32.61% in CK vs. 30.82% in T) were less abundant in the T group compared to the CK group. Notably, Pseudomonadota exhibited the largest difference between the two groups (9.91% in T vs. 1.84% in CK). In the jejunum, only Actinomycetota (31.54% in T vs. 30.15% in CK), Bacteroidota (1.24% in T vs. 1.03% in CK) and Cyanobacteriota (0.94% in T vs. 0.37% in CK) were more abundant in the T group compared to the CK group. In the ileum, only Bacillota (73.91% in T vs. 57.94% in CK) and Cyanobacteriota (1.75% in T vs. 0.32% in CK) were more abundant in the T group compared to the CK group. At the genus level (Figure 4C), *Bifidobacterium* and *Blautia* were the most

10.3389/fmicb.2025.1590400

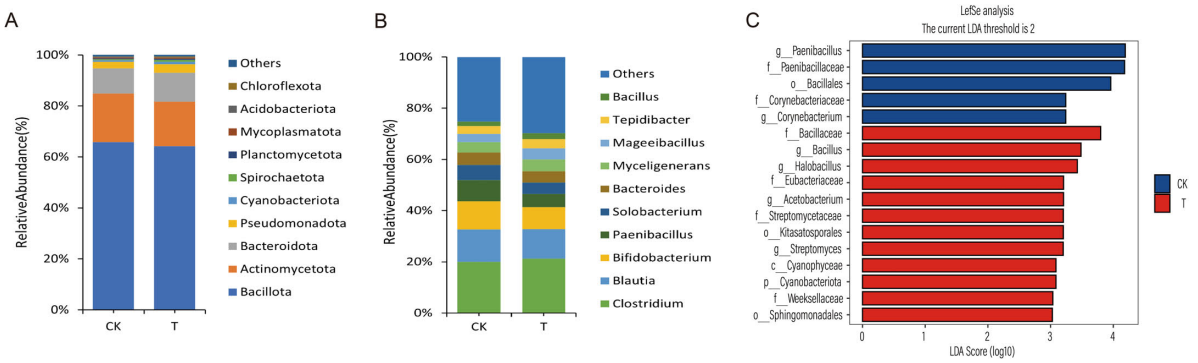

FIGURE 3
Analysis of differences in gut microbiota composition in sheep influenced by Chive seed flavonoid. **(A)** Phylum-level composition of gut microbiota between CK and T groups. **(B)** Genus-level composition of gut microbiota between CK and T groups. **(C)** LEfSe analysis showing LDA values for differentially abundant biomarkers.

abundant genera in both groups, accounting for more than 20% of the total composition. In the duodenum, *Clostridium* (9.29% in T vs. 8.83% in CK) and *Kandleria* (3.94% in T vs. 1.78% in CK) exhibited higher relative abundances in the T group compared to the CK group. In the jejunum, *Blautia* (15.39% in T vs. 13.28% in CK), *Clostridium* (14% in T vs. 9.68% in CK), *Myceligenerans* (8.15% in T vs. 5.53% in CK), *Tepidibacter* (6.12% in T vs. 4.02% in CK), *Kandleria* (1.76% in T vs. 1.54% in CK) and *Streptomyces* (1.91% in T vs. 1.14% in CK) were significantly more abundant in the T group compared to the CK group. In the ileum, *Clostridium* (12.64% in T vs. 7.90% in CK), *Paenibacillus* (10.57% in T vs. 10% in CK), *Mageeibacillus* (14.19% in T vs. 2.67% in CK), *Myceligenerans* (6.59% in T vs. 6.51% in CK), *Tepidibacter* (7.33% in T vs. 4.84% in CK) and *Streptomyces* (2.44% in T vs. 1.83% in CK) exhibited higher relative abundances in the T group compared to the CK group.

To further explore differences between groups, LEfSe analysis (LDA > 4) was performed. In the duodenum, 18 differential biomarkers were identified (Figure 4D), in the T group, *Bacteroidota*, *Gammaproteobacteria* and Bacillaceae were significantly enriched, while in the CK group, Bacillota, Eubacteriales, Clostridia and Blautia were significantly enriched. In the jejunum, 20 differential biomarkers were identified (Figure 4E), in the T group, *Clostridium*, *Myceligenerans and Tepidibacter* were significantly enriched, while in the CK group, *Paenibacillus*, *Solobacterium* and *Mageeibacillus* were significantly enriched. In the ileum, 20 differential biomarkers were identified (Figure 4F), in the T group, Bacillota, *Mageeibacillus, Clostridium* and *Tepidibacter* were significantly enriched, while in the CK group, Actinomycetota, *Bifidobacterium* and *Blautia* were significantly enriched. These findings demonstrate that the addition of CSF significantly altered the structure of the small intestinal microbiota.

3.5 Effect of Chive seed flavonoid on the intestinal microbiota of sheep large intestine

The gut microbiota composition of sheep was analyzed using 16S rRNA amplicon sequencing to investigate the effects of CSF. After quality control, the unique OTUs and shared OTUs across blind sac, colon, and rectum habitats were identified. The CK group exhibited 7,513 unique OTUs in the blind sac, 7,461 in the colon, and 5,424 in the rectum. In contrast, the T group had 6,322 unique OTUs in the blind sac, 6,092 in the colon, and 6,314 in the rectum. Notably, the CK group had higher unique OTU counts in the blind sac and colon compared to the T group, but lower unique OTU counts in the rectum. The shared OTUs among all groups totaled 123, as shown in the UpSet plot (Figure 5A). This analysis further confirmed that CSF significantly influenced the gut microbiota structure in sheep. Statistical analysis of the filtered OTU table revealed significant microbiota diversity changes at the phylum level (Figure 5B). Bacillota and Bacteroidota were the most abundant phyla in the sheep gut microbiota, collectively accounting for over 80% of the community. Actinomycetota, Pseudomonadota, and Spirochaetota followed, collectively exceeding 4%. Compared to the CK group, the T group exhibited higher relative abundances of Bacteroidota (19.17% vs. 18.82%) and Actinomycetota (5.54% vs. 3.36%). Additionally, Pseudomonadota and Spirochaetota abundances were higher in the CK group in the blind sac but higher in the T group in the colon and rectum. Cyanobacteriota, Mycoplasmatota, and Planctomycetota abundances were higher in the T group in the blind sac but lower in the colon and rectum. At the genus level (Figure 5C), significant differences in microbial abundances were observed across groups. *Clostridium* dominated the gut microbiota, comprising over 25% of the community. *Blautia, Bacteroides* and *Paenibacillus* followed, collectively exceeding 20%. Compared to the CK group, the T group showed higher abundances of *Blautia* in the colon and Bacteroides in the rectum. Additionally, *Phocaeicola, Myceligenerans* and *Riemerella* abundances were higher in the T group's blind sac and rectum compared to the CK group, while *Ercella, Bacillus and Shouchella* were more abundant in the T group's blind sac and colon.

Further analysis using LEfSe revealed significant differences in microbial biomarkers (LDA > 4) between groups. In the blind sac, six discriminant species were identified, with *Bacillaceae* being the only taxon at the family level with higher abundance in the T group (Figure 5D). In the colon, seven discriminant species

10.3389/fmicb.2025.1590400

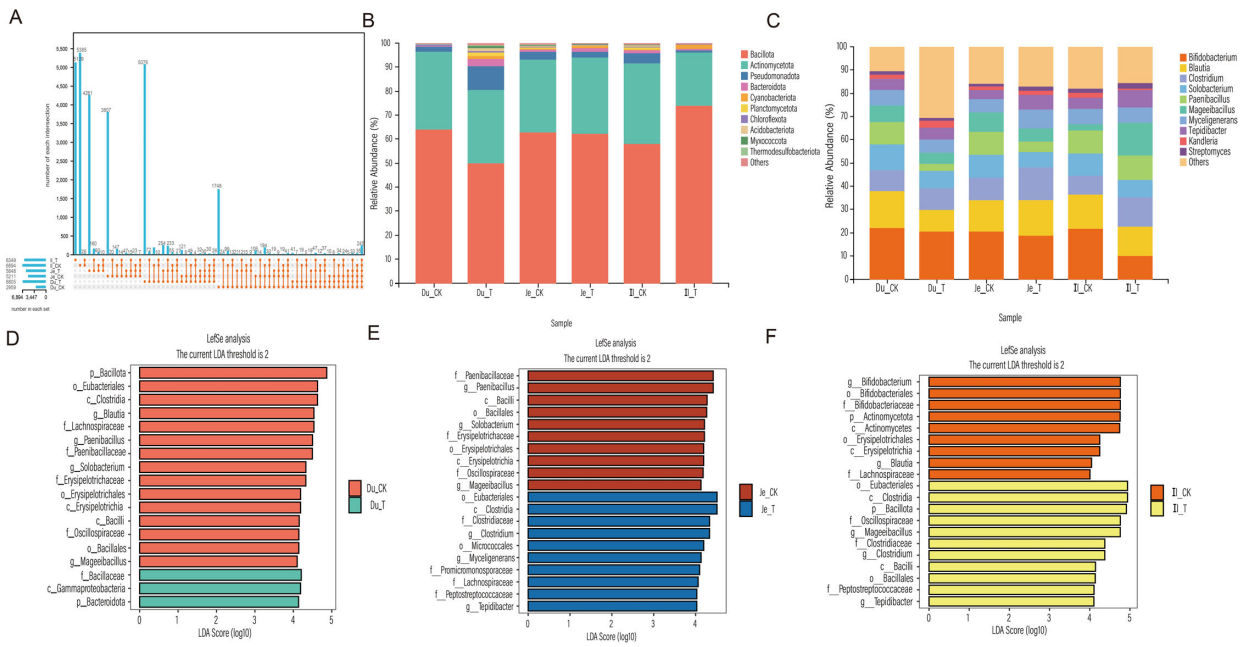

FIGURE 4
Analysis of the small intestinal microbial community in sheep. **(A)** UpSet plot showing the number of microbial features. **(B)** Relative abundance of microbial phyla. **(C)** Genus-level relative abundance. **(D)** LDA distribution histogram of OTUs in the duodenum. **(E)** LDA distribution histogram of OTUs in the jejunum. **(F)** LDA distribution histogram of OTUs in the ileum.

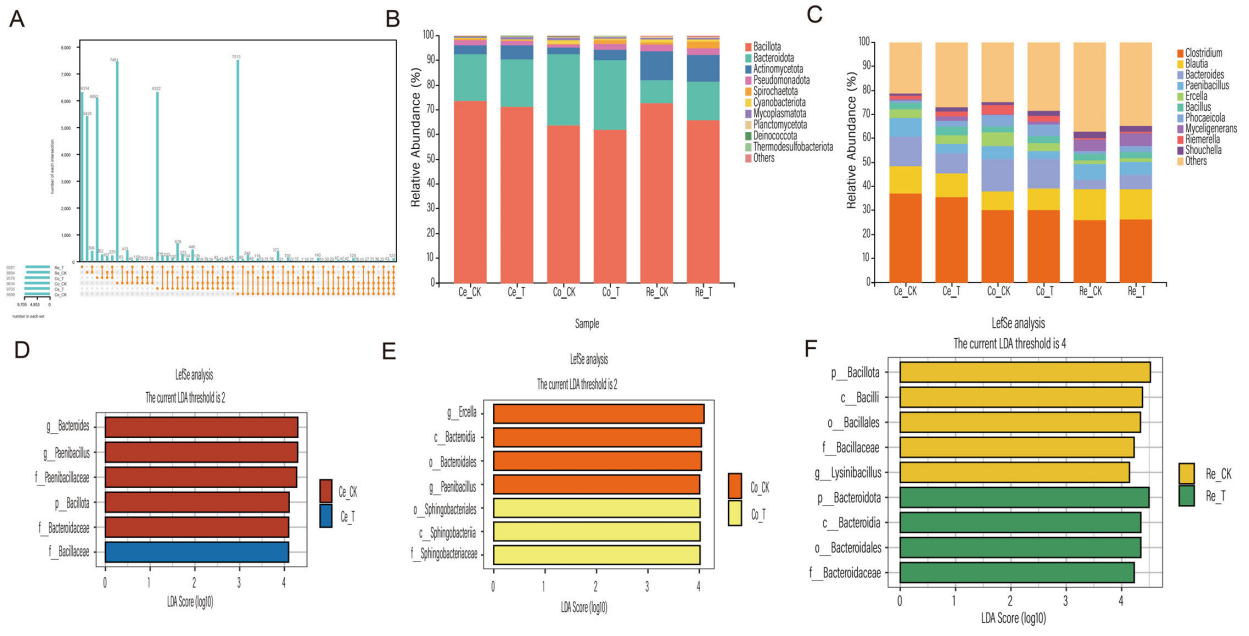

FIGURE 5
Analysis of the large intestinal microbial community in sheep. **(A)** UpSet plot showing the number of microbial features. **(B)** Relative abundance of microbial phyla. **(C)** Genus-level relative abundance. **(D)** LDA distribution histogram of OTUs in the blind sac. **(E)** LDA distribution histogram of OTUs in the colon. **(F)** LDA distribution histogram of OTUs in the rectum.

were identified, including *Sphingobacteriales*, *Sphingobacteriia*, and *Sphingobacteriaceae* at the order, class, and family levels, which were more abundant in the T group. *Ercella* and *Paenibacillus* were identified as abundant species at the genus level in the CK group (Figure 5E). In the rectum, nine discriminant species were identified, with *Bacteroidota* being the abundant phylum in the T group and Bacillota dominating in the CK group (Figure 5F). These findings demonstrate that the addition of CSF significantly improved the gut microbiota community structure in sheep.

3.6 Intestinal microbial gene functional prediction, metagenomic analysis of microbial community, fermentation parameters, and intestinal tissue morphology correlation

3.6.1 Prediction of small intestinal microbial gene functional profiles, metagenomic analysis of microbial community, fermentation parameters, and intestinal tissue morphology correlation

To predict the functional profiles of microbial genes, we employed the PICRUSt 2 software (based on 16S rRNA full-length sequencing) to infer gene functions from the microbial community. A total of 57 KEGG Orthology families were identified, encompassing pathways related to elements, amino acids, secondary metabolite biosynthesis, nucleic acids, lipids, vitamins, and protein transport. In the duodenum, 8 KEGG pathways exhibited significant differences ($p < 0.05$) (Figure 6A). Compared to the CK group, the addition of CSF significantly enriched the butirosin and neomycin biosynthesis pathways ($p < 0.01$). In the jejunum, 12 KEGG pathways showed significant differences ($p < 0.05$) (Figure 6B). These included porphyrin and chlorophyll metabolism, riboflavin metabolism, sphingolipid metabolism, and other glycan degradation pathways, which were significantly enriched in the T group compared to the CK group ($p < 0.05$). Conversely, the CK group exhibited significantly higher enrichment of selenium-containing compound metabolism and chloroalkane and chloroalkene degradation pathways compared to the T group ($p < 0.05$). In the ileum, 37 KEGG pathways were detected (Figure 6C). Among these, 29 pathways (e.g., biosynthesis of vancomycin group antibiotics, streptomycin biosynthesis, fatty acid biosynthesis, and D-Alanine metabolism) exhibited significantly higher enrichment in the T group compared to the CK group ($p < 0.05$). Overall, the KEGG pathways significantly associated with the predicted gene profiles were primarily enriched in metabolic pathways, immune regulation, and energy supply-related physiological responses.

To investigate the correlation between gut microbiota, fermentation parameters, and gut tissue morphology, we selected the 20 most abundant microbial communities at the phylum and genus levels using the Spearman correlation analysis method. We then analyzed their relationships with fermentation parameters and gut tissue morphology. After excluding undetected species, we found that at the phylum level (Figure 6D), only Bacillota showed a significant positive correlation with butyrate, villus length, crypt depth, and muscular layer thickness ($p < 0.05$). In contrast, Planctomycetota, Acidobacteriota, and Myxococcota exhibited significant negative correlations with certain fermentation parameters and tissue morphology indices ($p < 0.05$). At the genus level (Figure 6E), *Clostridium* and *Tepidibacter* displayed significant positive correlations with villus length, muscular layer thickness, and crypt depth ($p < 0.05$). *Paenibacillus* demonstrated a highly significant positive correlation with pH, acetate, propionate, and TVFAs ($p < 0.01$), along with a significant positive correlation with crypt depth ($p < 0.05$). *Mageeibacillus* showed an extremely significant positive correlation with butyrate, crypt depth, villus length, and muscular layer thickness ($p < 0.01$), as well as a highly significant positive correlation with pH ($p < 0.01$) and significant positive correlations with propionate and butyrate ($p < 0.05$). *Kandleria*, *Rhodococcus*, and *Phocaeicola* exhibited significant negative correlations with pH, propionate, butyrate, and villus length ($p < 0.05$) or extremely significant negative correlations ($p < 0.01$). These findings indicate that Bacillota, *Clostridium, Tepidibacter, Paenibacillus*, *Mageeibacillus*, and *Ercella* demonstrate strong positive correlations with fermentation parameters and various gut tissue morphology indices.

3.6.2 Prediction of gut microbial gene function and correlation analysis between microbial community and fermentation parameters

As described in section 2.6.1, the microbial gene sequences were functionally predicted using PICRUSt 2 software, resulting in the identification of 47 KEGG gene families in the colon. Among these, 29 pathways exhibited significant differences ($p < 0.05$) between the T group and the CK group in the cecum. Specifically, 19 pathways, including other glycan degradation, Glycosaminoglycan degradation, Galactose metabolism, Secondary bile acid biosynthesis, Amino sugar and nucleotide sugar metabolism, Streptomycin biosynthesis, Protein export, and Starch and sucrose metabolism, demonstrated higher proportions in the T group (Figure 7A). In both the colon and rectum, 9 pathways each showed significant differences ($p < 0.05$). In the colon, two pathways, Bacterial chemotaxis and Flagellar assembly, exhibited higher proportions in the T group compared to the CK group (Figure 7B). In the rectum, six pathways, including other glycan degradation, Glycosaminoglycan degradation, Protein digestion and absorption, Sphingolipid metabolism, C5-Branched dibasic acid metabolism, and Vitamin B6 metabolism, displayed higher proportions in the T group (Figure 7C). These results suggest that CSF may play significant roles in carbohydrate metabolism, lipid and nitrogen metabolism, energy metabolism, immune regulation, and bacterial motility mechanisms within the colon microbiota of sheep.

Spearman correlation analysis indicated that, at the phylum level (Figure 7D), Spirochaetota exhibited a significant positive correlation with pH ($p < 0.01$). Conversely, Actinomycetota, Cyanobacteriota, and Chloroflexota demonstrated significant negative correlations with various fermentation parameters ($p < 0.05$). At the genus level (Figure 7E), *Clostridium, Bacillus, Streptomyces,* and *Microbacterium* were significantly positively correlated with Acetate, Propionate, Butyrate, and TVFAs ($p < 0.01$); Additionally, *Schouchella* and *Rhodococcus* showed a significant positive correlation with pH but exhibited significant negative correlations with Acetate, Propionate, and other indices ($p < 0.05$). Meanwhile, *Streptococcus* displayed significant negative correlations with fermentation parameter indices ($p < 0.01$). Overall, Spirochaetota, *Clostridium*, *Bacillus, Streptomyces* and *Microbacterium* were found to have strong positive correlations with fermentation parameters.

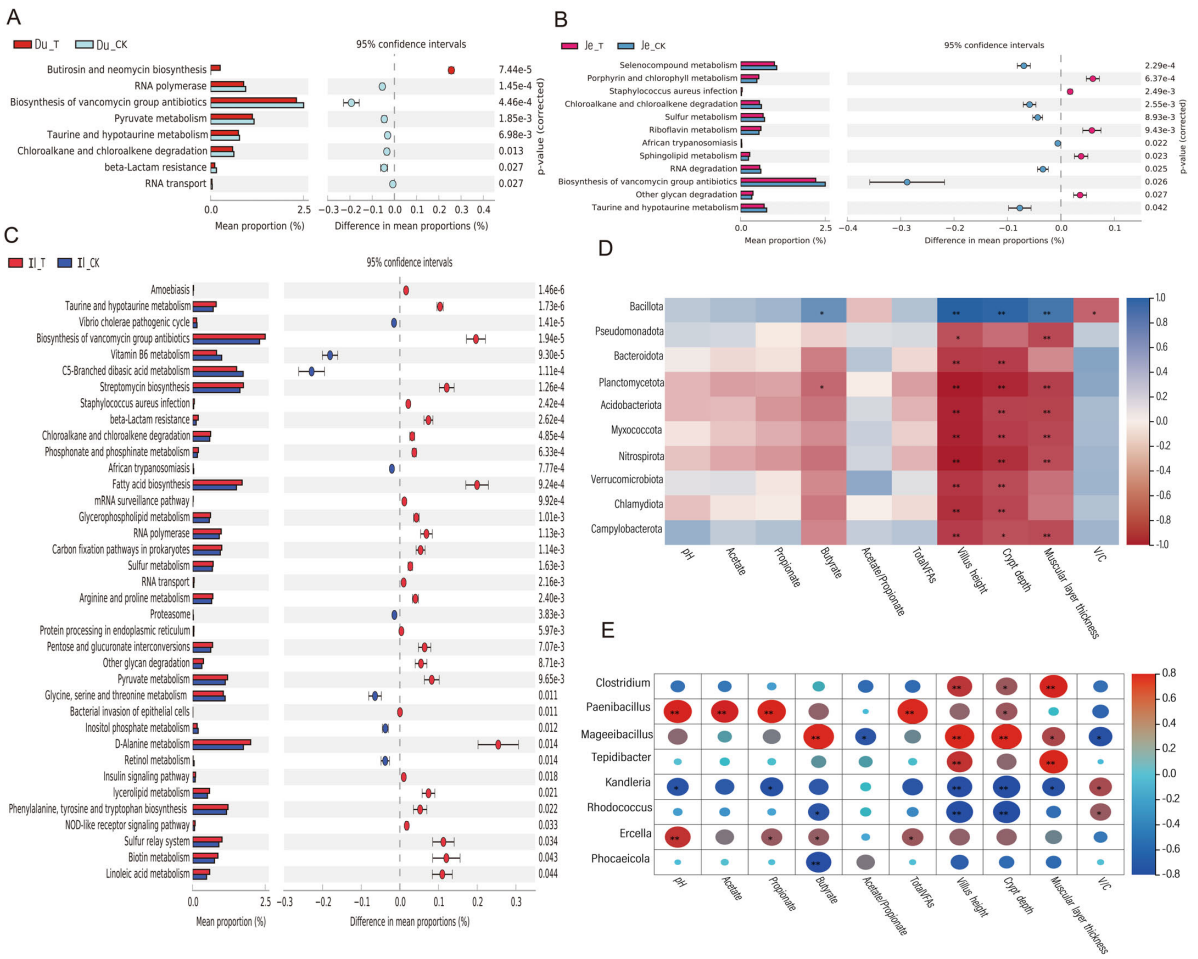

FIGURE 6
KEGG Pathway and Interaction Correlation Heatmap. **(A)** KEGG functional prediction analysis of microbial communities in the duodenum. **(B)** KEGG functional prediction analysis of microbial communities in the colon. **(C)** KEGG functional prediction analysis of microbial communities in the jejunum. **(D)** Correlation heatmap between small intestinal microbiota and fermentation parameters/organ morphology (top 20 genus-level microbial communities). **(E)** Correlation heatmap between small intestinal microbiota and fermentation parameters/organ morphology (top 20 phylum-level microbial communities). Adjusted $^{*}p$-value < 0.05 and $^{**}p < 0.01$ by Student's *t*-test.

4 Discussion

4.1 Effects of Chive seed flavonoid on intestinal fermentation parameters and histomorphology in sheep

The intestine is a critical site for nutrient absorption, metabolic regulation, and further digestion in ruminants. Among factors influencing intestinal health, pH serves as a key indicator of internal environmental stability, reflecting microbial activity and digestive efficiency. In the present study, dietary supplementation with 0.25% CSF reduced duodenal and jejunal pH but elevated pH in the ileum and colon. These site-specific pH shifts may stem from CSF's modulation of gut microbiota composition and fermentation patterns. Notably, VFAs—primarily acetate, propionate, and butyrate—are central microbial metabolites in ruminants, providing 70–80% of the host's metabolic energy (Ma et al., 2021). Beyond their energetic role, VFAs enhance nutrient absorption (lipids and proteins) in the small intestine and serve as critical substrates for epithelial cells in the ileum and colon (Dalile et al., 2019; Yao et al., 2022). The results of this study indicate that the addition of 0.25% CSF to the diet increased the concentrations of acetate, propionate, butyrate, and TVFAs in the ileum, cecum, colon, and rectum. Previous studies pointed out that flavonoid supplementation can enhance gastrointestinal fermentation parameters and alleviate symptoms of ruminal acidosis (Balcells et al., 2012). Furthermore, *in vitro* fermentation studies have demonstrated that certain flavonoids can increase the levels of ammonia-nitrogen and SCFAs in the gut (Pan et al., 2023). This is similar to the results of previous studies. Furthermore, it also increased propionate and total VFAs in the jejunum. The supplementation with flavonoids (luteolin and quercetin) has been shown to enhance TVFAs production in sheep fecal microbiota (Pan et al., 2023), suggesting that the observed elevation of intestinal TVFAs levels in ruminants may be attributed to specific bioactive constituents within these phytochemical compounds.

Intestinal histomorphology is a critical metric for assessing gut health and function, with key indicators including villus

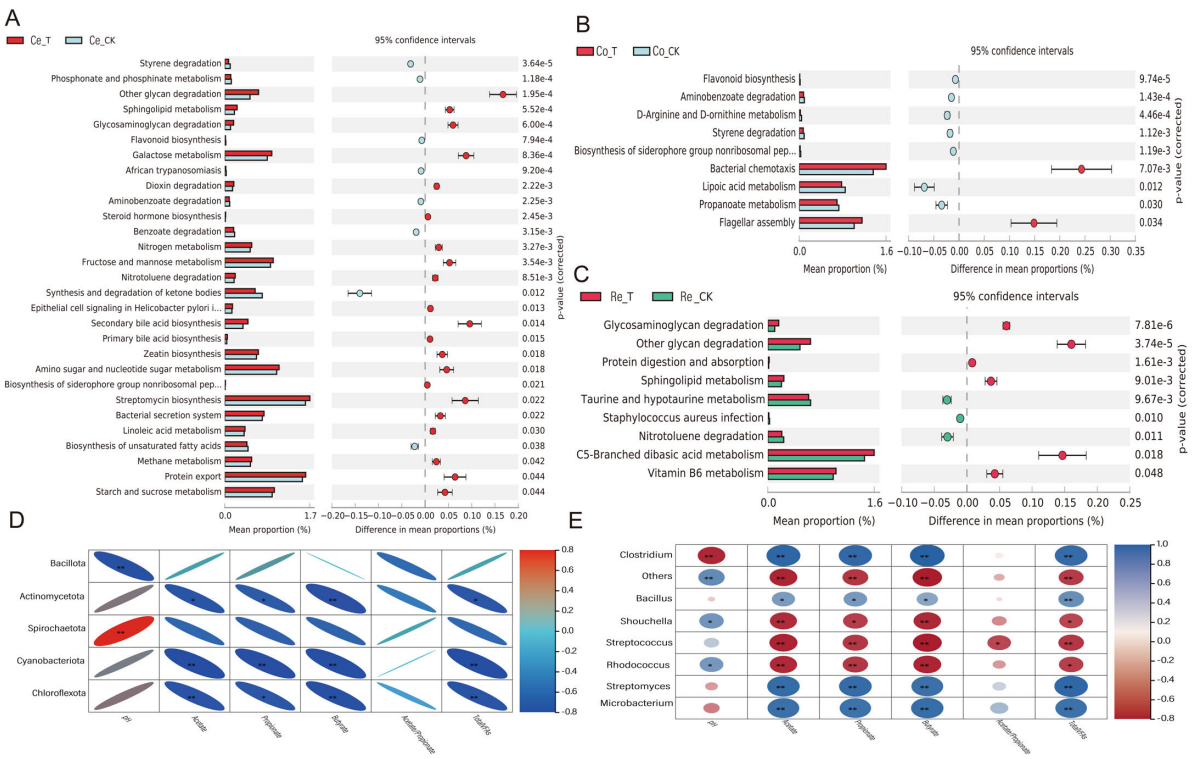

FIGURE 7
KEGG pathway predictions and interaction correlation heatmaps. **(A)** KEGG functional prediction analysis between cecal microbes. **(B)** KEGG functional prediction analysis between colonic microbes. **(C)** KEGG functional prediction analysis between rectal microbes. **(D)** Correlation heatmap between colon microbiota and fermentation parameters (top 20 genera with the highest relative abundance). **(E)** Correlation heatmap between colon microbiota and fermentation parameters (top 20 phyla with the highest relative abundance). Adjusted $^{*}p < 0.05$ and $^{**}p < 0.01$ by Student's *t*-test.

length, crypt depth, muscle layer thickness, and the V/C ratio (Liao and Nyachoti, 2017). Increased villus length expands the intestinal epithelium's absorptive surface area, directly enhancing nutrient uptake (Casas et al., 2020; Munoz et al., 2023). Conversely, reduced crypt depth reflects accelerated epithelial cell maturation, which improves nutrient absorption efficiency (Rubin and Levin, 2016). Muscle layer thickness correlates with intestinal contractile strength, facilitating nutrient transport, while a higher V/C ratio signifies structural integrity of the mucosa and improved digestive capacity. In this study, the addition of 0.25% CSF to the diet improved villus length, muscle layer thickness, and V/C ratio in the jejunum and ileum, while reducing crypt depth in the small intestine. These findings align with reports that dietary fiber enhances ileal V/C ratios in weaned piglets (Ellner et al., 2021) and that fatty acids modulate jejunal morphology in poultry (Palomar et al., 2023), suggesting CSF may act through analogous nutrient-driven pathways. Quantitative functional gene analysis revealed upregulated expression levels of *IGF1*, *CD81*, *CTNNBL1*, *MGST1*, *GPX4*, and *SLC39A8* in the ileum and cecum epithelium of T group. *IGF1* was observed to suppress cellular autophagy and enhance myocyte proliferation via the mTOR and FoxO signaling pathways (Weeks et al., 2017), suggesting potential associations between increased small intestinal muscularis thickness and *IGF1*-mediated regulation. These findings imply that CSF may improve intestinal morphogenesis through enhanced epithelial gene expression and elevated fatty acid content, potentially potentiating the absorptive and transport capacities of enterocytes. However, systematic investigations are required to elucidate the precise mechanisms underlying these phenotypic improvements and their nutritional implications.

4.2 Effects of Chive seed flavonoid on the whole intestinal microbiota of sheep

Full-length bacterial 16S rRNA sequencing, performed using the PacBio Revio platform, is a third-generation sequencing method that enables high-resolution analysis of microbiome diversity by capturing near-complete rRNA gene sequences (Wagner et al., 2016). This approach improves taxonomic annotation accuracy and offers deeper insights into microbial community dynamics. Host-microbe interactions, often symbiotic, are mediated by microbial metabolites that regulate host physiology (Liu et al., 2020; Ren et al., 2018). Alpha diversity, measured through statistical indices such as Shannon and Chao1, quantifies species richness and evenness within a community. Elevated gut microbial alpha diversity is strongly associated with intestinal homeostasis and systemic health, as it enhances resistance to pathogen colonization, supports immune function, and optimizes nutrient metabolism (Li D. et al., 2023). In this study, dietary supplementation with CSF showed a trend toward increased alpha diversity indices, suggesting a potential improvement in microbial

community resilience. Beta diversity analyses (PCoA and NMDS) further revealed distinct clustering of gut microbiota between the CSF-treated (T) and control (CK) groups, indicating significant compositional differences. In most mammals, the gut microbiota is dominated by the phyla Firmicutes (recently reclassified as Bacillota) and Bacteroidetes, which collectively comprise over 98% of the community (Benson et al., 2010; Ley et al., 2008; Ley et al., 2006). However, in sheep from this study, the dominant phyla were Bacillota (formerly Firmicutes), Actinobacteriota, and Bacteroidota, with Bacillota being the most abundant. This divergence may reflect species-specific adaptations, age-related shifts, or environmental influences. LEfSe analysis identified significant CSF-induced alterations in microbial abundance, with the T group harboring a greater number of differential biomarkers than the CK group. Notably, Cyanobacteria (phylum level) and *Bacillus* (genus level) were enriched in the T group. While Cyanobacteria are atypical in gut microbiomes, their presence could indicate dietary influence or ecological niche specialization. The prominence of *Bacillus*, a genus known for metabolic versatility, aligns with CSF's potential to modulate nutrient-processing taxa. These structural shifts suggest CSF enhances gut microbiota functionality, possibly synergizing with its previously reported effects on volatile fatty acid production and intestinal morphogenesis.

4.2.1 Effect of Chive seed flavonoid on the intestinal microbiota of sheep small intestine

The small intestine, particularly the jejunum and ileum, plays a pivotal role in nutrient absorption and digestion. As the primary site for nutrient uptake, a healthy jejunum is critical for animal growth and overall health. The ileum, positioned downstream of the jejunum, further contributes to digestion and absorption processes (Godoy-Vitorino et al., 2012). To evaluate the impact of CSF on gut microbiota, the study analyzed microbial communities across intestinal segments. This study results revealed distinct compositional differences between the large and small intestines. At the phylum level, Firmicutes and Bacteroidetes were identified as the most abundant microbial communities in the small intestine of sheep. The abundance of Clostridia increased significantly in the ileum, which aligns with its beneficial effects, such as inhibiting the proliferation of harmful bacteria, promoting the growth of beneficial bacteria, enhancing villus height and the V/C ratio, restoring intestinal permeability, and improving nutrient absorption. The observed improvements in ileal villus length, muscle layer thickness, and V/C ratio in this study can be attributed to the promotion of Clostridia abundance by CSF, which, in turn, fosters intestinal development. Additionally, the abundance of Bacteroidetes increased significantly in the duodenum, consistent with previous reports indicating that the duodenum and jejunum are primarily composed of Firmicutes and Bacteroidetes (Di Rienzi et al., 2013), Firmicutes and Bacteroidetes, the most diverse microbial communities in nature, exhibit exceptional metabolic capabilities and play a key role in immune regulation, particularly in the production of antibiotics (Barka et al., 2016; van Bergeijk et al., 2020). Bacteroides and Cyanobacteria exhibited significant increases throughout the small intestine. Previous studies have demonstrated that Bacteroides are particularly effective at degrading carbohydrates and polysaccharides, metabolizing these compounds into VFAs (Fan et al., 2024). Cyanobacteria, as key components of the sheep gut microbiome, perform a variety of functions, including the synthesis of vitamin B, anaerobic fermentation, oxygen-dependent hydrogen production, nitrogen fixation, and the degradation of hemicellulose and pectin, as well as methane reduction (Huo et al., 2014). At the genus level, *Clostridium* (phylum Firmicutes) was highly abundant in the small intestine, with increased levels in the jejunum and ileum. This genus enhances host energy absorption and immune regulation (Reuss et al., 2016) and produces butyrate, a short-chain fatty acid critical for gut health and diarrhea prevention (Benson et al., 2010). Similarly, *Streptomyces* (phylum Actinobacteria) surged in the ileum. Known for metabolic diversity, *Streptomyces* synthesizes bioactive metabolites that strengthen the intestinal barrier by blocking pathogens (Odchimar et al., 2024). Both genera degrade dietary fiber into VFAs, aligning with elevated VFA levels in CSF-supplemented sheep. LEfSe analysis revealed that the small intestinal microbial community enriched by CSF in sheep belonged to the phyla Firmicutes, Bacteroidetes, Bacteroides, and Clostridia, with *Lachnospiraceae* and *Micrococcales* (both belonging to Firmicutes) serving as specific biomarkers for the jejunum. These bacteria are potentially beneficial, as *Lachnospiraceae* are involved in the metabolism of various carbohydrates (Zhang et al., 2023) and *Micrococcales* contribute to metabolic activities in the intestine, thereby maintaining the stability of the sheep gut barrier. Functional pathway enrichment analysis indicated that the number of microbial gene pathways enriched in the small intestine was highest in the ileum, followed by the jejunum and duodenum. These pathways are implicated in multiple physiological and biochemical processes, with significantly enriched pathways in the treatment group primarily focusing on protein synthesis and processing, immune responses, amino acid metabolism, signal transduction, energy metabolism, and the transmission and expression of genetic information (e.g., glycan degradation, fatty acid biosynthesis, protein processing in the endoplasmic reticulum, and mRNA surveillance pathways). These pathways correlate with upregulated genes (*IGF1*, *CD81*, *CTNNBL1*), which enhance antioxidant and immune functions (Shahsavari et al., 2023; Xiao et al., 2021), suggesting CSF boosts immunocompetence via microbiota-host crosstalk. The ileum's role in the gut-liver axis and amino acid absorption underscores its importance in nutrient metabolism, consistent with CSF's effects on ileal morphology and VFA production (Liu et al., 2024). Additionally, gut microbiota may amplify CSF's benefits by metabolizing flavonoids (Li Z. et al., 2023). Further emphasizing the essential role of the ileum in nutrient digestion and absorption in the small intestine, consistent with our findings.

Correlation heatmap analysis revealed Firmicutes (phylum) positively correlated with butyrate levels, villus length, crypt depth, and muscle layer thickness. This aligns with its known role in enhancing intestinal structural integrity (Fan et al., 2024). In contrast, Bacteroidetes and Actinobacteria showed negative correlations with villus length and crypt depth. While Actinobacteria maintain mucosal barriers via antibiotic production and Bacteroidetes regulate polysaccharide uptake and metabolic health (White et al., 2023), their limited direct impact on mucosal growth may explain these inverse trends. At the genus level, Clostridium, *Tepidibacter*, *Mageeibacillus*, *Paenibacillus*, and

Ercella correlated positively with fermentation metrics and histomorphology. *Clostridium*, a beneficial symbiont, modulates microbiota, produces nutrients, and enhances immunity (Guo et al., 2020). *Mageeibacillus* (thermophilic fermenter) and *Paenibacillus* degrade carbohydrates/proteins into metabolites like acetate, while *Ercella* produces SCFAs for barrier integrity. Notably, *Paenibacillus* may reduce methane by competing with methanogens (Justine et al., 2025), Although *Mageeibacillus*'s role in butyrate synthesis and mucosal development remains understudied (Austin et al., 2015), its correlation with histomorphological improvements highlights its potential as a probiotic target.

4.2.2 Effect of Chive seed flavonoid on the intestinal microbiota of sheep large intestine

The large intestine, particularly the cecum, is a key site for microbial fermentation in herbivores, hosting diverse microbiota critical for digestion and health (Ballout and Diener, 2021). Unlike the rumen, the cecum specializes in breaking down recalcitrant polymers like lignin and starch (Godoy-Vitorino et al., 2012). Cecal fermentation produces 12% of TVFAs and contributes 17% of cellulose digestion (Dixon and Nolan, 1982), aligning with our finding of elevated VFAs levels in the cecum. Downstream, the colon houses carbohydrate-degrading microbiota that supply energy (Lin et al., 2021) and modulate immune-linked diseases (O'Keefe, 2016; Yan et al., 2017). The rectum, the terminal segment, ensures waste expulsion and homeostasis by preventing toxin accumulation. Microbial richness and diversity were higher in the large intestine than the small intestine. Bacillota (formerly Firmicutes) and Bacteroidota (formerly Bacteroidetes) dominated, with CSF increasing Actinobacteriota abundance in the cecum and colon. Actinobacteriota regulates gut permeability, immunity, and the gut-brain axis, offering therapeutic potential (Binda et al., 2018). Accumulating evidence indicates that dietary flavonoids suppress inflammatory cascades, modulate immune cell functionality, and preserve intestinal barrier integrity through microbiota-dependent pathways (Wang et al., 2024). Notably, CSF elevated Bacteroidota in the rectum, possibly stabilizing gut metabolism, though reduced Bacteroidota in other segments suggests niche-specific ecological shifts (Lin et al., 2021). These findings suggest that CSF enhances Bacteroidota abundance to stabilize gut health-related metabolic processes. At the genus level, *Clostridium* was the most abundant bacterium in the large intestine, though CSF minimally affected its abundance. Increased *Clostridium* in the small intestine may stem from environmental variations there. *Blautia* and *Bacteroides* were less abundant than *Clostridium*, consistent with prior studies (Ye et al., 2022). *Bacteroides* aids complex carbohydrate digestion (Spence et al., 2006), while *Blautia* influences metabolism and inflammation (Liu et al., 2021). Additionally, *Shouchella* exhibited increased abundance in the cecum and colon, suggesting its potential as a beneficial probiotic with protective gut functions. LEfSe analysis showed CSF shifted cecal dominance to Bacillaceae (phylum Bacillota), key for nutrient degradation (Gebeyew et al., 2021). In the colon, discriminatory taxa included *Sphingobacteriia* (class), *Sphingobacteriales* (order), and *Sphingobacteriaceae* (family) (phylum Bacteroidetes), reflecting microbiota instability (Smoliński et al., 2021). Rectal biomarkers aligned with Bacteroidetes dominance (Zhang et al., 2018). KEGG analysis highlighted cecal dominance in pathways like energy, lipid, and toxin metabolism. CSF enriched cecal genes in carbohydrate/galactose metabolism and protein turnover—critical for growth and adaptation (González and Cullen, 2022). Lipid metabolism dysregulation links to disease (Petrenko et al., 2023). In the colon, pathways such as bacterial chemotaxis and flagellar assembly exhibited significantly increased microbial gene enrichment. Bacterial chemotaxis is a strategy employed by bacteria to enhance nutrient and energy uptake (Keegstra et al., 2022), while bacterial flagella are large protein machines essential for motility and biofilm formation, processes critical for bacterial survival and pathogenesis (Takekawa et al., 2020). In the rectum, pathways associated with glycan metabolism, vitamin B6 metabolism, and protein digestion exhibited significantly increased microbial gene enrichment. Crucially, intestinal microorganisms engage in mutualistic symbiosis with flavonoid compounds, wherein microbial metabolism enhances flavonoid bioactivity while these phytochemicals reciprocally shape microbial community structure to sustain gut homeostasis (Williamson et al., 2018), supporting CSF as a phytogenic additive with microbiota-modulating potential.

Correlation analysis between microbiota and fermentation parameters revealed that Spiraeochnusella is positively correlated with pH, playing a significant role in regulating gut microecological balance and serving as a primary degrader of lignocellulose (Lin et al., 2018). Genera such as *Clostridium, Bacillus, Streptococcus* and *Microbacterium* showed positive correlations with acetate, propionate, butyrate, and TVFAs. *Clostridiu*, a member of Firmicutes, facilitates the degradation of fibers and polysaccharides, thereby promoting growth and development. *Bacillus* and *Streptococcus* can utilize sugar-based substrates and exhibit strong hydrolytic capacities for starch and proteins (Sánchez-Moya et al., 2017), while *Microbacterium*, an aerobic bacterium, likely possesses the ability to degrade complex carbohydrates and enhance nutrient absorption and utilization based on the correlation heatmap findings.

In summary, CSF enhances the abundance of beneficial gut bacteria, thereby promoting effective fermentation and utilization of feed, as well as carbohydrate and lipid metabolism, immune regulation, and the maintenance of gut barrier stability through multiple mechanisms. These effects positively influence the health and growth of sheep.

5 Conclusion

Dietary supplementation with 0.25% CSF enhanced intestinal development and microbiota in sheep. CSF increased jejunal and ileal villus length, V/C ratio, and muscle layer thickness, while reducing crypt depth. It elevated acetate, propionate, butyrate, and TVFAs in the ileum, cecum, colon, and rectum, and boosted propionate and TVFAs in the jejunum. Notably, the addition of CSF significantly optimized the structure of beneficial bacteria in the gut. T group also upregulated the expression of ileum and cecum epithelial genes (*IGF1*, *CD81*, *CTNNBL1*, *MGST1*, *GPX4*, *SLC39A8*) associated with the regulation of tissue morphogenesis and VFAs absorption. Specifically, the abundances of Bacteroidota and Cyanobacteriota were elevated throughout the small intestine,

while Actinobacteria abundance increased in the duodenum. In the jejunum, the abundance of Clostridia increased, and in the ileum, the abundances of both *Clostridium* and *Streptomyces* were elevated. Additionally, Actinobacteria abundances were increased in both the cecum and colon, and Bacteroidota abundance rose in the rectum. Functional predictions suggested that CSF may promote carbohydrate metabolism, energy metabolism, immune regulation, and maintenance of the intestinal barrier. Therefore, these findings suggest that CSF may enhance VFAs biosynthesis by modulating the composition and metabolic functions of the intestinal microbiota in sheep. Concurrently, VFAs serve as critical energy substrates for intestinal epithelial cells, activating gene expression associated with tissue morphogenesis and development. This process drives intestinal villi hyperplasia and crypt structure maturation, thereby improving VFAs absorption capacity and establishing a synergistic regulatory mechanism of "microbial metabolism-morphological development-nutrient absorption." This evidence confirms the feasibility of utilizing CSF as botanical feed additives, providing a theoretical foundation for advancing nutritional regulation strategies in ruminant husbandry.

Data availability statement

The original contributions presented in the study are publicly available. This data can be found at: https://www.ncbi.nlm.nih.gov/, accession number: PRJNA1225640.

Ethics statement

All experimental procedures were conducted in accordance with the guidelines of the Ministry of Science and Technology of the People's Republic of China (Approval No. 2006-398) and approved by the Animal Ethics and Welfare Committee of Gansu Agricultural University (GSAU-AEW-2020-0057). The studies were conducted in accordance with the local legislation and institutional requirements. Written informed consent was obtained from the owners for the participation of their animals in this study.

Author contributions

XL: Writing – original draft, Writing – review & editing. DL: Formal Analysis, Writing – review & editing. CW: Software, Writing – review & editing. QL: Software, Writing – review & editing. YN: Software, Writing – review & editing. LZ: Software, Writing – review & editing. JX: Software, Writing – review & editing. YM: Funding acquisition, Supervision, Writing – original draft, Writing – review & editing.

Funding

The author(s) declare that financial support was received for the research and/or publication of this article. This research was funded by the Technology Integration Technology Project of Linxia Beef and Sheep Industry Development Research Institute (KJJC-LX-2023-05); and Discipline Team Project of Gansu Agricultural University (GAU-XKTD-2022-20).

Acknowledgments

We extend our heartfelt gratitude to all the authors and reviewers who have contributed to this research topic.

Conflict of interest

The authors declare that the research was conducted in the absence of any commercial or financial relationships that could be construed as a potential conflict of interest.

Generative AI statement

The authors declare that no Generative AI was used in the creation of this manuscript.

Publisher's note

All claims expressed in this article are solely those of the authors and do not necessarily represent those of their affiliated organizations, or those of the publisher, the editors and the reviewers. Any product that may be evaluated in this article, or claim that may be made by its manufacturer, is not guaranteed or endorsed by the publisher.

Supplementary material

The Supplementary Material for this article can be found online at: https://www.frontiersin.org/articles/10.3389/fmicb.2025.1590400/full#supplementary-material

References

Amanzadeh, E., Esmaeili, A., Rahgozar, S., and Nourbakhshnia, M. (2019). Application of quercetin in neurological disorders: From nutrition to nanomedicine. *Rev. Neurosci.* 30, 555–572. doi: 10.1515/revneuro-2018-0080

Austin, M. N., Rabe, L. K., Srinivasan, S., Fredricks, D. N., Wiesenfeld, H. C., and Hillier, S. L. (2015). *Mageeibacillus indolicus* gen. nov., sp. nov.: A novel bacterium isolated from the female genital tract. *Anaerobe* 32, 37–42. doi: 10.1016/j.anaerobe.2014.12.003

Balcells, J., Aris, A., Serrano, A., Seradj, A. R., Crespo, J., and Devant, M. (2012). Effects of an extract of plant flavonoids (Bioflavex) on rumen fermentation and performance in heifers fed

high-concentrate diets. *J. Anim. Sci.* 90, 4975–4984. doi: 10.2527/jas.2011-4955

Ballout, J., and Diener, M. (2021). The role of HCO(3)(-) in propionate-induced anion secretion across rat caecal epithelium. *Pflugers Arch.* 473, 937–951. doi: 10.1007/s00424-021-02565-8

Barka, E. A., Vatsa, P., Sanchez, L., Gaveau-Vaillant, N., Jacquard, C., Meier-Kolthoff, J. P., et al. (2016). Taxonomy, physiology, and natural products of actinobacteria. *Microbiol. Mol. Biol. Rev.* 80, 1–43. doi: 10.1128/mmbr.00019-15

Benson, A. K., Kelly, S. A., Legge, R., Ma, F., Low, S. J., Kim, J., et al. (2010). Individuality in gut microbiota composition is a complex polygenic trait shaped by multiple environmental and host genetic factors. *Proc. Natl. Acad. Sci. U.S.A.* 107, 18933–18938. doi: 10.1073/pnas.1007028107

Binda, C., Lopetuso, L. R., Rizzatti, G., Gibiino, G., Cennamo, V., and Gasbarrini, A. (2018). Actinobacteria: A relevant minority for the maintenance of gut homeostasis. *Dig. Liver Dis.* 50, 421–428. doi: 10.1016/j.dld.2018.02.012

Bolyen, E., Rideout, J. R., Dillon, M. R., Bokulich, N. A., Abnet, C. C., Al-Ghalith, G. A., et al. (2019). Author Correction: Reproducible, interactive, scalable and extensible microbiome data science using QIIME 2. *Nat. Biotechnol.* 37:1091. doi: 10.1038/s41587-019-0252-6

Buiatte, V., Proszkowiec-Weglarz, M., Miska, K., Dominguez, D., Mahmoud, M., Lesko, T., et al. (2024). The effects of a high-flavonoid corn cultivar on the gastrointestinal tract microbiota in chickens undergoing necrotic enteritis. *PLoS One* 19:e0307333. doi: 10.1371/journal.pone.0307333

Casas, G. A., Blavi, L., Cross, T. L., Lee, A. H., Swanson, K. S., and Stein, H. H. (2020). Inclusion of the direct-fed microbial Clostridium butyricum in diets for weanling pigs increases growth performance and tends to increase villus height and crypt depth, but does not change intestinal microbial abundance. *J. Anim. Sci.* 98:skz372. doi: 10.1093/jas/skz372

Chen, D., Chen, X., Tu, Y., Wang, B., Lou, C., Ma, T., et al. (2015). Effects of mulberry leaf flavonoid and resveratrol on methane emission and nutrient digestion in sheep. *Anim. Nutr.* 1, 362–367. doi: 10.1016/j.aninu.2015.12.008

Dalile, B., Van Oudenhove, L., Vervliet, B., and Verbeke, K. (2019). The role of short-chain fatty acids in microbiota-gut-brain communication. *Nat. Rev. Gastroenterol. Hepatol.* 16, 461–478. doi: 10.1038/s41575-019-0157-3

de Freitas, K. S., Squarisi, I. S., Acésio, N. O., Nicolella, H. D., Ozelin, S. D., Reis Santos, et al. (2020). Licochalcone A, a licorice flavonoid: antioxidant, cytotoxic, genotoxic, and chemopreventive potential. *J. Toxicol. Environ. Health A* 83, 673–686. doi: 10.1080/15287394.2020.1813228

Di Rienzi, S. C., Sharon, I., Wrighton, K. C., Koren, O., Hug, L. A., Thomas, B. C., et al. (2013). The human gut and groundwater harbor non-photosynthetic bacteria belonging to a new candidate phylum sibling to Cyanobacteria. *Elife* 2:e01102. doi: 10.7554/eLife.01102

Dixon, R. M., and Nolan, J. V. (1982). Studies of the large intestine of sheep. 1. Fermentation and absorption in sections of the large intestine. *Br. J. Nutr.* 47, 289–300. doi: 10.1079/bjn19820038

Ellner, C., Martínez-Vallespín, B., Saliu, E. M., Zentek, J., and Röhe, I. (2021). Effects of cereal and protein source on performance, apparent ileal protein digestibility and intestinal characteristics in weaner piglets. *Arch. Anim. Nutr.* 75, 263–277. doi: 10.1080/1745039x.2021.1958647

Fan, D., Fu, Y., Zhang, J., Bi, Y., Ma, T., Diao, Q., et al. (2024). Sheep-derived butyrate-producing *Clostridium beijerinckii* R8 alleviates diarrhea by shaping the gut microbiota of goat kids. *Anim. Nutr.* 19, 13–24. doi: 10.1016/j.aninu.2024.06.004

Gebeyew, K., Chen, K., Wassie, T., Azad, M. A. K., He, J., Jiang, W., et al. (2021). Dietary amylose/amylopectin ratio modulates cecal microbiota and metabolites in weaned goats. *Front. Nutr.* 8:774766. doi: 10.3389/fnut.2021.774766

Godoy-Vitorino, F., Goldfarb, K. C., Karaoz, U., Leal, S., Garcia-Amado, M. A., Hugenholtz, P., et al. (2012). Comparative analyses of foregut and hindgut bacterial communities in hoatzins and cows. *ISME J.* 6, 531–541. doi: 10.1038/ismej.2011.131

González, B., and Cullen, P. J. (2022). Regulation of Cdc42 protein turnover modulates the filamentous growth MAPK pathway. *J. Cell Biol.* 221:e202112100. doi: 10.1083/jcb.202112100

Guo, P., Zhang, K., Ma, X., and He, P. (2020). Clostridium species as probiotics: Potentials and challenges. *J. Anim. Sci. Biotechnol.* 11:24. doi: 10.1186/s40104-019-0402-1

Hooper, L. V., and Macpherson, A. J. (2010). Immune adaptations that maintain homeostasis with the intestinal microbiota. *Nat. Rev. Immunol.* 10, 159–169. doi: 10.1038/nri2710

Huo, W., Zhu, W., and Mao, S. (2014). Impact of subacute ruminal acidosis on the diversity of liquid and solid-associated bacteria in the rumen of goats. *World J. Microbiol. Biotechnol.* 30, 669–680. doi: 10.1007/s11274-013-1489-8

Justine, E. E., Lee, H. J., Jung, K. H., Lee, Y. S., and Kim, Y. J. (2025). Methane emission mitigation of *Paenibacillus yonginensis* DCY84(T) incorporated with silicate on paddy rice (*Oryzae sativa* L.) plantation revealed in soil microbiome profiling. *Sci. Total Environ.* 958:177996. doi: 10.1016/j.scitotenv.2024.177996

Keegstra, J. M., Carrara, F., and Stocker, R. (2022). The ecological roles of bacterial chemotaxis. *Nat. Rev. Microbiol.* 20, 491–504. doi: 10.1038/s41579-022-00709-w

Lee, W. J., and Hase, K. (2014). Gut microbiota-generated metabolites in animal health and disease. *Nat. Chem. Biol.* 10, 416–424. doi: 10.1038/nchembio.1535

Ley, R. E., Hamady, M., Lozupone, C., Turnbaugh, P. J., Ramey, R. R., Bircher, J. S., et al. (2008). Evolution of mammals and their gut microbes. *Science* 320, 1647–1651. doi: 10.1126/science.1155725

Ley, R. E., Turnbaugh, P. J., Klein, S., and Gordon, J. I. (2006). Microbial ecology: Human gut microbes associated with obesity. *Nature* 444, 1022–1023. doi: 10.1038/4441022a

Li, D., Yang, H., Li, Q., Ma, K., Wang, H., Wang, C., et al. (2023). Prickly Ash Seeds improve immunity of Hu sheep by changing the diversity and structure of gut microbiota. *Front. Microbiol.* 14:1273714. doi: 10.3389/fmicb.2023.1273714

Li, Q., Wu, Y., Qi, X., Liu, Z., Wang, C., Ma, X., et al. (2024). Effects of prickly ash seed dietary supplementation on meat quality, antioxidative capability, and metabolite characteristics of hu lambs. *Foods* 13:3415. doi: 10.3390/foods13213415

Li, Z., Ren, Z., Zhao, L., Chen, L., Yu, Y., Wang, D., et al. (2023). Unique roles in health promotion of dietary flavonoids through gut microbiota regulation: Current understanding and future perspectives. *Food Chem.* 399:133959. doi: 10.1016/j.foodchem.2022.133959

Liao, S. F., and Nyachoti, M. (2017). Using probiotics to improve swine gut health and nutrient utilization. *Anim. Nutr.* 3, 331–343. doi: 10.1016/j.aninu.2017.06.007

Lin, L., Trabi, E. B., Xie, F., and Mao, S. (2021). Comparison of the fermentation and bacterial community in the colon of Hu sheep fed a low-grain, non-pelleted, or pelleted high-grain diet. *Appl. Microbiol. Biotechnol.* 105, 2071–2080. doi: 10.1007/s00253-021-11158-5

Lin, X., Wang, J., Hou, Q., Wang, Y., Hu, Z., Shi, K., et al. (2018). Effect of hay supplementation timing on rumen microbiota in suckling calves. *Microbiologyopen* 7:e00430. doi: 10.1002/mbo3.430

Liu, X., Mao, B., Gu, J., Wu, J., Cui, S., Wang, G., et al. (2021). Blautia-a new functional genus with potential probiotic properties? *Gut Microbes* 13, 1–21. doi: 10.1080/19490976.2021.1875796

Liu, X., Sha, Y., Dingkao, R., Zhang, W., Lv, W., Wei, H., et al. (2020). Interactions between rumen microbes, VFAs, and host genes regulate nutrient absorption and epithelial barrier function during cold season nutritional stress in tibetan sheep. *Front. Microbiol.* 11:593062. doi: 10.3389/fmicb.2020.593062

Liu, Z., Wang, H., Ma, K., Li, Q., Wu, Y., Qi, X., et al. (2024). Supplementation with Chinese herbal preparations protect the gut-liver axis of Hu sheep, promotes gut-liver circulation, regulates intestinal flora and immunity. *Front. Immunol.* 15:1454334. doi: 10.3389/fimmu.2024.1454334

Ma, J., Wang, C., Wang, Z., Cao, G., Hu, R., Wang, X., et al. (2021). Active dry yeast supplementation improves the growth performance, rumen fermentation, and immune response of weaned beef calves. *Anim. Nutr.* 7, 1352–1359. doi: 10.1016/j.aninu.2021.06.006

Munoz, L. R., Bailey, M. A., Krehling, J. T., Bourassa, D. V., Hauck, R., Pacheco, W. J., et al. (2023). Effects of dietary yeast cell wall supplementation on growth performance, intestinal *Campylobacter jejuni* colonization, innate immune response, villus height, crypt depth, and slaughter characteristics of broiler chickens inoculated with *Campylobacter jejuni* at d 21. *Poult. Sci.* 102:102609. doi: 10.1016/j.psj.2023.102609

Muqier, Qi, S., Wang, T., Chen, R., Wang, C., and Ao, C. (2017). Effects of flavonoids from *Allium mongolicum* Regel on growth performance and growth-related hormones in meat sheep. *Anim. Nutr.* 3, 33–38. doi: 10.1016/j.aninu.2017.01.003

Nakai, S., and Kamei, Y. (2020). Health promotion effects of soy isoflavones. *J. Nutr. Sci. Vitaminol. (Tokyo)* 66, 502–507. doi: 10.3177/jnsv.66.502

Odchimar, N. M. O., Macalalad, M. A. B., and Orosco, F. L. (2024). From antibiotic to antiviral: Computational screening reveals a multi-targeting antibiotic from *Streptomyces* spp. against Nipah virus fusion proteins. *Mol. Divers.* 29, 1541–1555. doi: 10.1007/s11030-024-10932-7

O'Keefe, S. J. (2016). Diet, microorganisms and their metabolites, and colon cancer. *Nat. Rev. Gastroenterol. Hepatol.* 13, 691–706. doi: 10.1038/nrgastro.2016.165

Oteiza, P. I., Fraga, C. G., Mills, D. A., and Taft, D. H. (2018). Flavonoids and the gastrointestinal tract: Local and systemic effects. *Mol. Aspects Med.* 61, 41–49. doi: 10.1016/j.mam.2018.01.001

Palomar, M., Garcés-Narro, C., Piquer, O., Sala, R., Tres, A., García-Bautista, J. A., et al. (2023). Influence of free fatty acid content and degree of fat saturation on production performance, nutrient digestibility, and intestinal morphology of laying hens. *Anim. Nutr.* 13, 313–323. doi: 10.1016/j.aninu.2023.03.002

Pan, L., Ye, H., Pi, X., Liu, W., Wang, Z., Zhang, Y., et al. (2023). Effects of several flavonoids on human gut microbiota and its metabolism by in vitro simulated fermentation. *Front. Microbiol.* 14:1092729. doi: 10.3389/fmicb.2023.1092729

Petrenko, V., Sinturel, F., Riezman, H., and Dibner, C. (2023). Lipid metabolism around the body clocks. *Prog. Lipid Res.* 91:101235. doi: 10.1016/j.plipres.2023.101235

Ren, W., Wang, P., Yan, J., Liu, G., Zeng, B., Hussain, T., et al. (2018). Melatonin alleviates weanling stress in mice: Involvement of intestinal microbiota. *J. Pineal Res.* 64:e12448. doi: 10.1111/jpi.12448

Reuss, B., Asif, A. R., Almamy, A., Schwerk, C., Schroten, H., Ishikawa, H., et al. (2016). Antisera against *Neisseria gonorrhoeae* cross-react with specific brain proteins of the common marmoset monkey and other nonhuman primate species. *Brain Res.* 1653, 23–38. doi: 10.1016/j.brainres.2016.10.012

Rubin, D. C., and Levin, M. S. (2016). Mechanisms of intestinal adaptation. *Best Pract. Res. Clin. Gastroenterol.* 30, 237–248. doi: 10.1016/j.bpg.2016.03.007

Sánchez-Moya, T., López-Nicolás, R., Planes, D., González-Bermúdez, C. A., Ros-Berruezo, G., and Frontela-Saseta, C. (2017). In vitro modulation of gut microbiota by whey protein to preserve intestinal health. *Food Funct.* 8, 3053–3063. doi: 10.1039/c7fo00197e

Sang, S. M., Xia, Z. H., Mao, S. L., Lao, A. N., and Chen, Z. L. (2000). [Studies on chemical constitutents in seeds of *Allium tuberosum* Rottl]. *Zhongguo Zhong Yao Za Zhi* 25, 286–288. doi: 10.1186/s12906-019-2542-4

Shahsavari, M., Mohammadabadi, M., Khezri, A., Asadi Fozi, M., Babenko, O., Kalashnyk, O., et al. (2023). Correlation between insulin-like growth factor 1 gene expression and fennel (*Foeniculum vulgare*) seed powder consumption in muscle of sheep. *Anim. Biotechnol.* 34, 882–892. doi: 10.1080/10495398.2021.2000997

Shi, J., Lei, Y., Wu, J., Li, Z., Zhang, X., Jia, L., et al. (2023). Antimicrobial peptides act on the rumen microbiome and metabolome affecting the performance of castrated bulls. *J. Anim. Sci. Biotechnol.* 14:31. doi: 10.1186/s40104-023-00832-5

Smoliński, J., Szeligowska, N., Cholewińska, P., Czyż, K., and Janczak, M. (2021). Levels of main bacterial phyla in the gastrointestinal tract of sheep depending on parity and age. *Animals (Basel)* 11:2203. doi: 10.3390/ani11082203

Spence, C., Wells, W. G., and Smith, C. J. (2006). Characterization of the primary starch utilization operon in the obligate anaerobe *Bacteroides fragilis*: Regulation by carbon source and oxygen. *J. Bacteriol.* 188, 4663–4672. doi: 10.1128/jb.00125-06

Takekawa, N., Imada, K., and Homma, M. (2020). Structure and energy-conversion mechanism of the bacterial Na(+)-driven flagellar motor. *Trends Microbiol.* 28, 719–731. doi: 10.1016/j.tim.2020.03.010

van Bergeijk, D. A., Terlouw, B. R., Medema, M. H., and van Wezel, G. P. (2020). Ecology and genomics of Actinobacteria: New concepts for natural product discovery. *Nat. Rev. Microbiol.* 18, 546–558. doi: 10.1038/s41579-020-0379-y

van Dijk, A., Hedegaard, C. J., Haagsman, H. P., and Heegaard, P. M. H. (2018). The potential for immunoglobulins and host defense peptides (HDPs) to reduce the use of antibiotics in animal production. *Vet. Res.* 49:68. doi: 10.1186/s13567-018-0558-2

Wagner, J., Coupland, P., Browne, H. P., Lawley, T. D., Francis, S. C., and Parkhill, J. (2016). Evaluation of PacBio sequencing for full-length bacterial 16S rRNA gene classification. *BMC Microbiol.* 16:274. doi: 10.1186/s12866-016-0891-4

Wang, L., Li, M., Gu, Y., Shi, J., Yan, J., Wang, X., et al. (2024). Dietary flavonoids-microbiota crosstalk in intestinal inflammation and carcinogenesis. *J. Nutr. Biochem.* 125:109494. doi: 10.1016/j.jnutbio.2023.109494

Weeks, K. L., Bernardo, B. C., Ooi, J. Y. Y., Patterson, N. L., and McMullen, J. R. (2017). The IGF1-PI3K-Akt signaling pathway in mediating exercise-induced cardiac hypertrophy and protection. *Adv. Exp. Med. Biol.* 1000, 187–210. doi: 10.1007/978-981-10-4304-8_12

White, J. B. R., Silale, A., Feasey, M., Heunis, T., Zhu, Y., Zheng, H., et al. (2023). Outer membrane utilisomes mediate glycan uptake in gut Bacteroidetes. *Nature* 618, 583–589. doi: 10.1038/s41586-023-06146-w

Williamson, G., Kay, C. D., and Crozier, A. (2018). The bioavailability, transport, and bioactivity of dietary flavonoids: A review from a historical perspective. *Compr. Rev. Food Sci. Food Saf.* 17, 1054–1112. doi: 10.1111/1541-4337.12351

Xiao, C., Jin, H. G., Zhang, L. C., Liu, J. Q., He, M., Ma, H. H., et al. (2021). Effects of SPARCL1 on the proliferation and differentiation of sheep preadipocytes. *Adipocyte* 10, 658–669. doi: 10.1080/21623945.2021.2010901

Yan, S., Zhu, C., Yu, T., Huang, W., Huang, J., Kong, Q., et al. (2017). Studying the differences of bacterial metabolome and microbiome in the colon between landrace and meihua piglets. *Front. Microbiol.* 8:1812. doi: 10.3389/fmicb.2017.01812

Yao, Y., Cai, X., Fei, W., Ye, Y., Zhao, M., and Zheng, C. (2022). The role of short-chain fatty acids in immunity, inflammation and metabolism. *Crit. Rev Food Sci. Nutr.* 62, 1–12. doi: 10.1080/10408398.2020.1854675

Ye, M., Hou, M., Peng, Q., Jia, S., Peng, B., Yin, F., et al. (2022). The microbiota and cytokines correlation between the jejunum and colon in altay sheep. *Animals (Basel)* 12:1564. doi: 10.3390/ani12121564

Zhang, H., Shao, M., Huang, H., Wang, S., Ma, L., Wang, H., et al. (2018). The dynamic distribution of small-tail han sheep microbiota across different intestinal segments. *Front Microbiol* 9:32. doi: 10.3389/fmicb.2018.00032

Zhang, H., Zha, X., Zhang, B., Zheng, Y., Elsabagh, M., Wang, H., et al. (2024). Gut microbiota contributes to bisphenol A-induced maternal intestinal and placental apoptosis, oxidative stress, and fetal growth restriction in pregnant ewe model by regulating gut-placental axis. *Microbiome* 12:28. doi: 10.1186/s40168-024-01749-5

Zhang, T., Sun, P., Geng, Q., Fan, H., Gong, Y., Hu, Y., et al. (2022). Disrupted spermatogenesis in a metabolic syndrome model: The role of vitamin A metabolism in the gut-testis axis. *Gut* 71, 78–87. doi: 10.1136/gutjnl-2020-323347

Zhang, X., Yu, D., Wu, D., Gao, X., Shao, F., Zhao, M., et al. (2023). Tissue-resident *Lachnospiraceae* family bacteria protect against colorectal carcinogenesis by promoting tumor immune surveillance. *Cell Host Microbe* 31:418–432.e418. doi: 10.1016/j.chom.2023.01.013

frontiers | Frontiers in Microbiology

TYPE Review
PUBLISHED 23 June 2025
DOI 10.3389/fmicb.2025.1549160

Check for updates

OPEN ACCESS

EDITED BY
Guiguo Zhang,
Shandong Agricultural University, China

REVIEWED BY
Catherine M. T. Sherwin,
University of Western Australia, Australia
Hao Tian,
Chengdu University of Traditional Chinese Medicine, China

*CORRESPONDENCE
Xianqiong Feng
✉ fengxianqiong66@126.com

RECEIVED 20 December 2024
ACCEPTED 09 June 2025
PUBLISHED 23 June 2025

CITATION
Zeng Q, Feng X, Hu Y and Su S (2025) The human gut microbiota is associated with host lifestyle: a comprehensive narrative review. *Front. Microbiol.* 16:1549160. doi: 10.3389/fmicb.2025.1549160

COPYRIGHT
© 2025 Zeng, Feng, Hu and Su. This is an open-access article distributed under the terms of the Creative Commons Attribution License (CC BY). The use, distribution or reproduction in other forums is permitted, provided the original author(s) and the copyright owner(s) are credited and that the original publication in this journal is cited, in accordance with accepted academic practice. No use, distribution or reproduction is permitted which does not comply with these terms.

The human gut microbiota is associated with host lifestyle: a comprehensive narrative review

Qin Zeng[1,2], Xianqiong Feng[3,4]*, Yanling Hu[1,2] and Shaoyu Su[1,2]

[1]Department of Pediatrics Nursing, West China Second University Hospital, Sichuan University, Chengdu, China, [2]Key Laboratory of Birth Defects and Related Diseases of Women and Children (Sichuan University), Ministry of Education, Chengdu, China, [3]Department of Nursing, West China Hospital, Sichuan University, Chengdu, China, [4]Nursing Key Laboratory of Sichuan Province, West China School of Nursing, Sichuan University, Chengdu, China

Background: The gut microbiota serves as a critical interface between lifestyle factors and host physiology. Despite extensive research on individual domains including diet, sleep, and exercise, an integrated understanding of their synergistic effects on microbial communities remains incomplete. This knowledge gap limits our ability to develop targeted microbiome-based interventions for metabolic and immune-related disorders.

Methods: To address this gap, we conducted a comprehensive evaluation of peer-reviewed literature from 2000 to present, identified through systematic searches of PubMed, Web of Science, and Scopus using key terms related to gut microbiota and lifestyle interventions. Our analysis focused on studies incorporating microbiome profiling techniques, controlled lifestyle interventions, and multi-omics data integration. The review prioritized mechanistic insights from both clinical and preclinical investigations while critically assessing methodological approaches across the field.

Results: High-fiber dietary patterns consistently promoted the abundance of beneficial, short-chain fatty acid-producing bacteria, though with notable inter-individual variation. Circadian rhythm disruption was associated with reduced microbial diversity and expansion of pro-inflammatory bacterial taxa, paralleling increases in systemic inflammation markers. Athletic populations demonstrated unique microbial signatures characterized by enhanced metabolic potential, with distinct taxonomic profiles emerging across different sport disciplines.

Conclusion: This work synthesizes current evidence into a novel framework for understanding lifestyle-microbiota interactions, while identifying key challenges in study design and data interpretation. We propose standardized methodological approaches for future investigations and outline translational strategies for personalized microbiota modulation. These insights advance the potential for targeted microbial interventions to optimize metabolic and immune health outcomes.

KEYWORDS

gut microbiome, precision nutrition, circadian biology, exercise immunology, metabolic health

1 Introduction

The human gut microbiota constitutes a complex, dynamic ecosystem comprising bacteria, archaea, fungi, viruses, and eukaryotes that collectively encode >3 million genes—150-fold more than the human genome (Qin et al., 2010). This "second genome" plays pivotal roles in nutrient metabolism (Sonnenburg and Bäckhed, 2016), immune system maturation (Zheng et al., 2020), and neuroendocrine signaling through the gut-brain axis (Cryan et al., 2019). Mounting evidence from large-scale initiatives like the Human Microbiome Project (Qin et al., 2010) and MetaHIT (Arumugam et al., 2011) highlights the role of gut microbial dysbiosis in human health. This imbalance has been linked to the pathogenesis of various conditions, from metabolic disorders such as obesity and T2DM (Wu et al., 2021) to neurological diseases like Parkinson's and autism spectrum disorders (Lynch and Pedersen, 2016). Particularly compelling are recent findings showing that gut microbiota composition can predict individualized glycemic responses to foods (Ben-Yacov et al., 2023), suggesting its potential as a therapeutic target. Furthermore, recent studies have highlighted the significant impact of diet, exercise, and other lifestyle factors (e.g., sleep) on gut bacterial composition. According to a 2023 review by Pedroza Matute and Iyavoo (2023), adjustments to these lifestyle elements hold potential as effective avenues for personalized interventions aimed at enhancing gut health and overall well-being. However, the precise mechanisms by which modifiable lifestyle factors influence microbial community structure and function remain incompletely characterized, creating an urgent need for systematic synthesis of current evidence. While psychological stress, alcohol consumption, and medication use also modulate gut microbiota, this review focuses on diet, sleep, and exercise due to their direct modifiability and robust evidence base.

To address this gap, we systematically evaluated peer-reviewed English-language literature (2000–present). Our searches in PubMed, Web of Science, and Scopus employed Boolean logic targeting: ("gut microbiota" OR "gut microbiome") AND ("diet" OR "nutrition"), ("circadian rhythm" AND "microbiota"), and ("exercise" AND "microbial diversity"). Excluded studies primarily focused on non-modifiable factors (e.g., genetics) or lacked microbial profiling data. Our analysis prioritized: (i) Randomized controlled trials (RCTs) with microbial profiling (16S rRNA sequencing, metagenomics); (ii) Longitudinal cohort studies incorporating multi-omics data; (iii) Mechanistic animal studies employing germ-free or gnotobiotic models; (iv) Seminal reviews and meta-analyses to synthesize evolving theoretical frameworks. Key foundational works (David et al., 2014; Turnbaugh et al., 2009) were considered alongside cutting-edge research [e.g., fecal microbiota transplantation studies (Ianiro et al., 2022)] to provide both historical context and contemporary perspectives.

This review makes three novel contributions to the field. First, we present a critical appraisal of how distinct dietary patterns (Mediterranean, plant-based, Western) differentially modulate microbial diversity and functional capacity, with particular attention to the role of microbiota-accessible carbohydrates (Deehan et al., 2020). Second, we synthesize emerging evidence for circadian misalignment-induced dysbiosis and its metabolic consequences (Cheng et al., 2021), proposing testable hypotheses about the gut microbiota's role in sleep disorder pathophysiology. Finally, we evaluate dose-dependent effects of exercise on microbial short-chain fatty acids (SCFAs) production (Mailing et al., 2019) and identify promising avenues for athlete microbiota optimization. By integrating findings across these domains, we highlight understudied interactions between lifestyle factors and propose a framework for personalized microbiota modulation strategies.

2 Gut microbiota in systemic diseases

In the cardiovascular system, a multitude of diseases are associated with gut microbiota. Recent studies have established a strong link between gut microbiota dysbiosis and hypertension pathogenesis. Clinical observations reveal that hypertensive patients consistently show reduced gut microbial diversity, characterized by significant depletion of beneficial bacteria such as *Akkermansia muciniphila* and *Faecalibacterium prausnitzii* (Li et al., 2017). This causal relationship is further supported by experimental evidence demonstrating that fecal microbiota transplantation from hypertensive donors to germ-free mice can directly elevate blood pressure (Yan et al., 2020). Mechanistic investigations indicate that gut dysbiosis promotes increased intestinal permeability and subsequent lipopolysaccharide (LPS) translocation, which triggers systemic inflammation and contributes to vascular stiffness (Luo et al., 2023). Deficiency of short-chain fatty acids, particularly butyrate, has been shown to impair baroreceptor sensitivity and disrupt blood pressure regulation (Muralitharan et al., 2025). Additionally, emerging evidence highlights the critical role of gut microbiota-derived trimethylamine-N-oxide (TMAO) in atherosclerosis pathogenesis (Ma et al., 2022).

Furthermore, within the digestive system, the gut microbiota plays a pivotal role in maintaining gastrointestinal homeostasis, with dysbiosis implicated in various digestive disorders. In inflammatory bowel disease (IBD), patients exhibit reduced microbial diversity, with depletion of anti-inflammatory bacteria like *Faecalibacterium prausnitzii* and overgrowth of pro-inflammatory *Escherichia coli* strains (Sharma et al., 2025). Fecal microbiota transplantation (FMT) has shown remarkable efficacy in *Clostridioides difficile* infection by restoring microbial balance (Baunwall et al., 2020). Mechanistically, gut dysbiosis disrupts mucosal barrier function through altered tight junction proteins (occludin, ZO-1), while microbial metabolites like butyrate regulate intestinal immunity via HDAC inhibition and Treg cell induction (Di Vincenzo et al., 2024). Emerging evidence also links specific microbial signatures (e.g., *Fusobacterium nucleatum* enrichment) to colorectal carcinogenesis through Wnt/β-catenin pathway activation, highlighting the microbiota's dual role in digestive health and disease pathogenesis (Mondal et al., 2025).

Additionally, in the Nervous system, emerging evidence demonstrates a bidirectional communication between the gut microbiota and the central nervous system, termed the gut-brain axis, which plays a pivotal role in neurological health (Figure 1). In Parkinson's disease (PD), patients exhibit decreased *Prevotella* and increased Enterobacteriaceae abundance, correlating with motor symptom severity (Bi et al., 2022; Blommer et al., 2023). Notably, fecal microbiota transplantation from PD patients to mice induces α-synuclein aggregation and motor deficits (Munoz-Pinto et al., 2024; Sampson et al., 2016). Mechanistically, gut dysbiosis promotes neuroinflammation via microglial activation through LPS-TLR4 signaling (Niño et al., 2018), while microbial metabolites like SCFAs modulate blood–brain barrier integrity (Parker et al., 2020). Similarly, in Alzheimer's disease (AD), reduced microbial diversity and elevated *Escherichia/Shigella* are associated with amyloid-β deposition (Li et al., 2019).

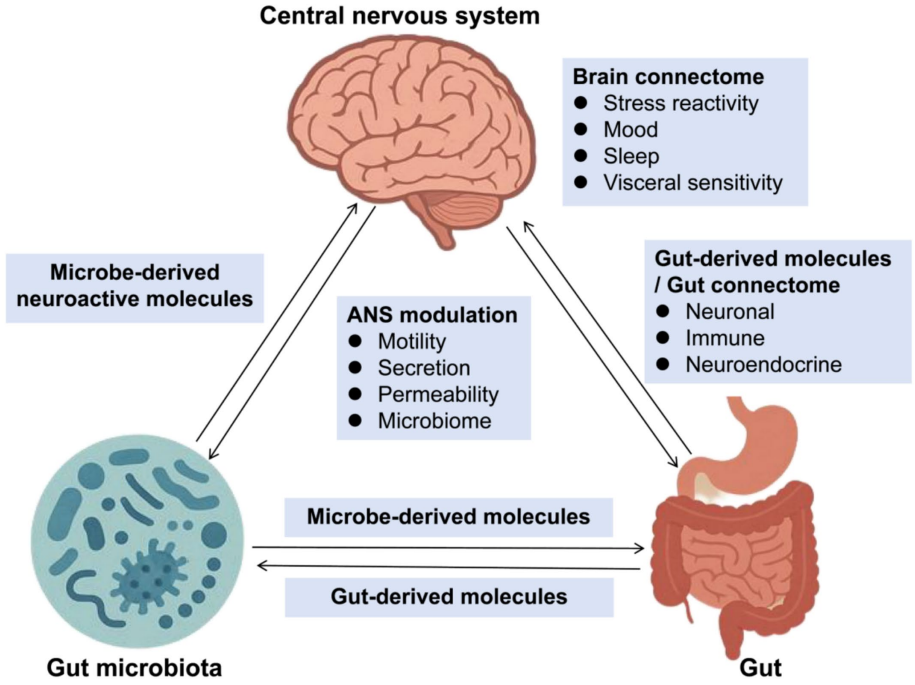

FIGURE 1
Gut-brain-microbiota axis. ANS, Autonomic Nervous System. This diagram illustrates the complex interactions between the gut microbiota, gut-derived molecules, and the central nervous system (CNS), highlighting the role of the brain connectome and ANS modulation. The gut-brain-microbiota axis plays a crucial role in maintaining homeostasis and influencing various physiological and psychological functions.

Moreover, in the musculoskeletal system, emerging evidence highlights the critical role of gut microbiota in musculoskeletal health. In sarcopenia, elderly patients exhibit reduced gut microbial diversity, particularly with depletion of *Bifidobacterium* and *Faecalibacterium prausnitzii* (Rashidah et al., 2022). Notably, fecal microbiota transplantation from young donors to aged mice restores muscle mass and strength (Kim et al., 2022), demonstrating a causal link between gut microbiota and sarcopenia. Mechanistically, gut dysbiosis drives systemic inflammation (elevated IL-6/TNF-α) and accelerates muscle protein degradation (Mancin et al., 2023). Conversely, butyrate-producing taxa (e.g., *Roseburia*, *Eubacterium*) enhance mitochondrial function through AMPK activation (Kundu et al., 2019). Similarly, in osteoporosis, postmenopausal women show decreased *Lactobacillus* abundance correlated with lower bone mineral density (Jansson et al., 2019). The gut microbiota-disease relationships across major physiological systems are summarized in Table 1 and Figure 2.

In addition to being associated with various system diseases in the human body, the gut microbiota is also linked to the host's lifestyle factors, such as diet, sleep, and exercise.

3 The correlation between gut microbiota and host lifestyle

3.1 Diet and gut microbiota interactions

3.1.1 Dietary patterns

Dietary habits profoundly shape gut microbiota composition, with distinct microbial signatures emerging across major dietary regimes. Contemporary research highlights three predominant patterns—the Western diet, plant-based diets, and the Mediterranean diet—each exhibiting unique impacts on microbial ecology and host health. The Western diet, characterized by excessive intake of processed foods, saturated animal fats, and refined sugars coupled with low fiber consumption, drives gut dysbiosis through multifactorial mechanisms. Clinical evidence demonstrates significant reductions in microbial diversity and depletion of beneficial SCFA-producing taxa such as *Faecalibacterium prausnitzii*, alongside expansion of pro-inflammatory Enterobacteriaceae and pathobionts like *Clostridium difficile* (Du et al., 2025; Zeng et al., 2022). This dietary pattern elevates circulating TMAO levels by 2.5-fold through microbial choline metabolism, correlating with atherosclerotic plaque formation (Ma et al., 2022), while concurrently decreasing colonic butyrate production by 40–60% compared to fiber-rich diets, thereby impairing epithelial barrier integrity (Sánchez-Tapia et al., 2020). Recent metabolomics analyses further reveal that diet-induced depletion of *Faecalibacterium* decreases colonic butyrate synthesis by 58%, directly impairing mitochondrial β-oxidation in enterocytes (Benjamin et al., 2022). However, the metabolomics analysis in 2025 further revealed that the decrease in *Faecalibacterium prausnitzii* caused by diet would lead to a 58% reduction in colonic butyrate synthesis, directly impairing the mitochondrial beta-oxidation function of intestinal epithelial cells (Münte and Hartmann, 2025). Animal models further reveal that high-fat components selectively enrich bile acid-transforming *Bilophila wadsworthia*, exacerbating colitis via TH17-mediated inflammation (Reynolds et al., 2017), and downregulate tight junction proteins facilitating lipopolysaccharide (LPS) translocation and systemic endotoxemia (Thaiss et al., 2016).

In contrast, plant-based and Mediterranean diets enhance microbial diversity and metabolic homeostasis. High-fiber plant-based

TABLE 1 Gut microbiota-disease associations across physiological systems.

System/disease	Key microbial alterations	Mechanistic pathways	Clinical/experimental evidence
Cardiovascular	↓ *Akkermansia muciniphila*	• LPS-induced inflammation	FMT transfers hypertension phenotype
• Hypertension	↓ *Faecalibacterium prausnitzii*	• Butyrate deficiency	
		• TMAO production	
Digestive	↓ *Faecalibacterium prausnitzii*	• Tight junction disruption	FMT efficacy in *C. difficile* infection
• IBD	↑ *Escherichia coli*	• Wnt/β-catenin activation	
• Colorectal cancer	↑ *Fusobacterium nucleatum*		
Nervous	↓ *Prevotella*	• LPS-TLR4 microglial activation	FMT induces α-synuclein pathology
• Parkinson's disease	↑ Enterobacteriaceae	• SCFA-mediated BBB regulation	
• Alzheimer's disease	↑ *Escherichia/Shigella*		
Musculoskeletal	↓ *Bifidobacterium*	• IL-6/TNF-α elevation	FMT restores muscle mass in aged mice
• Sarcopenia	↓ *Faecalibacterium prausnitzii*	• AMPK pathway modulation	
• Osteoporosis	↓ *Lactobacillus*		

↑ indicates increase, ↓ indicates decrease; TMAO, trimethylamine N-oxide; SCFA, short-chain fatty acids; FMT, fecal microbiota transplantation.

regimens enrich *Prevotella-dominant* enterotypes and fiber-degrading specialists such as *Xylanibacter*, driving SCFA production through cross-feeding networks (De Filippo et al., 2010; Portincasa et al., 2022). Within high-fiber plant-based regimens, resistant starch further induces strain-level specialization in *Bifidobacterium adolescentis*, enhancing amylolytic activity while competitively excluding *Clostridium perfringens* (Wang et al., 2025; Zhao et al., 2024; Zhao et al., 2025). The Mediterranean diet synergizes olive oil polyphenols (e.g., hydroxytyrosol) with complex carbohydrates, elevating *Bifidobacterium* abundance and reducing inflammatory markers such as C-reactive protein and interleukin-6 (Haskey et al., 2023; Perrone and D'Angelo, 2025). Long-term adherence to this diet increases fecal butyrate concentrations by 25–30% through *Roseburia-mediated* fermentation, correlating with improved insulin sensitivity (D'Archivio et al., 2022). These findings collectively underscore the critical role of dietary patterns in modulating gut microbial ecosystems, with profound implications for metabolic and inflammatory health outcomes.

3.1.2 Specific dietary components

Key dietary constituents differentially modulate microbial communities through targeted mechanisms. Non-digestible carbohydrates, particularly soluble fiber, serve as keystone substrates for saccharolytic taxa, with soluble fiber-derived butyrate upregulating claudin-1 expression and suppressing NF-κB activation via histone deacetylase (HDAC) inhibition (Cuevas-Sierra et al., 2024). In contrast, insoluble fiber accelerates intestinal transit, reducing pathogenic overgrowth through mechanical clearance (De Filippo et al., 2010; Portincasa et al., 2022). Saturated fats induce *Bilophila*-dominated dysbiosis, activating NLRP3 inflammasomes and increasing inflammatory bowel disease risk, while concurrently reducing *Lactobacillus* abundance and impairing secondary bile acid metabolism (Cani et al., 2007; Henao-Mejia et al., 2012; Sánchez-Tapia et al., 2020). Among micronutrients, olive oil phenolics such as oleuropein inhibit *Fusobacterium nucleatum* biofilm formation and downregulate Wnt/β-catenin signaling in colorectal carcinogenesis (D'Archivio et al., 2022). Similarly, vitamin D insufficiency correlates with *Lactobacillus* depletion and compromised IgA-mediated mucosal immunity (Zeevi et al., 2015). These findings collectively illustrate how specific dietary components orchestrate microbial dynamics, with profound implications for gut homeostasis and disease susceptibility. The impacts of various dietary patterns on gut microbial composition and functional outcomes are summarized in Table 2.

3.1.3 Controversies and emerging frontiers

Despite robust evidence linking dietary patterns to microbial alterations, significant controversies persist. While plant-based diets are consistently associated with *Prevotella* enrichment, methodological limitations challenge interpretability, including small sample sizes [e.g., Garcia-Mantrana et al., $n = 27$ (Garcia-Mantrana et al., 2018)] that limit generalizability, cross-sectional designs unable to establish causality, and conflicting outcomes across studies. For instance, high-animal-protein diets variably correlate with Firmicutes abundance (de Wit et al., 2012; Du et al., 2025), and Mediterranean diets show inconsistent effects on α-diversity despite *Bifidobacterium* enrichment (De Filippis et al., 2016; Nagpal et al., 2018). These discrepancies likely stem from methodological heterogeneity, such as divergent dietary assessment tools (e.g., food frequency questionnaires vs. controlled feeding studies) and sequencing platforms (e.g., 16S rRNA vs. shotgun metagenomics) (Armet et al., 2022; Ross et al., 2024; Wilson et al., 2020). Additionally, host-specific confounders, including baseline microbiota composition, genetic polymorphisms, and unmeasured lifestyle factors, contribute to these inconsistencies (Baldi et al., 2024; Diacova et al., 2025). To address these gaps, future studies should prioritize longitudinal designs, standardized protocols, and multi-omics integration (metagenomics, metabolomics, proteomics).

Emerging research extends diet-microbiota interactions to circadian regulation, with SCFAs such as butyrate modulating core clock genes (e.g., Bmal1, Per2) in intestinal epithelial cells, thereby synchronizing host metabolic rhythms and glucose homeostasis (Cheng et al., 2021; Choi et al., 2021). This intersection of dietary habits, microbial ecology, and chronobiology illuminates novel pathways for metabolic disease pathogenesis. Additionally, a bidirectional relationship exists between sleep architecture and gut microbiota: chronic sleep disruption reduces *Faecalibacterium* abundance while elevating pro-inflammatory taxa like Enterobacteriaceae, whereas microbial metabolites (e.g., serotonin

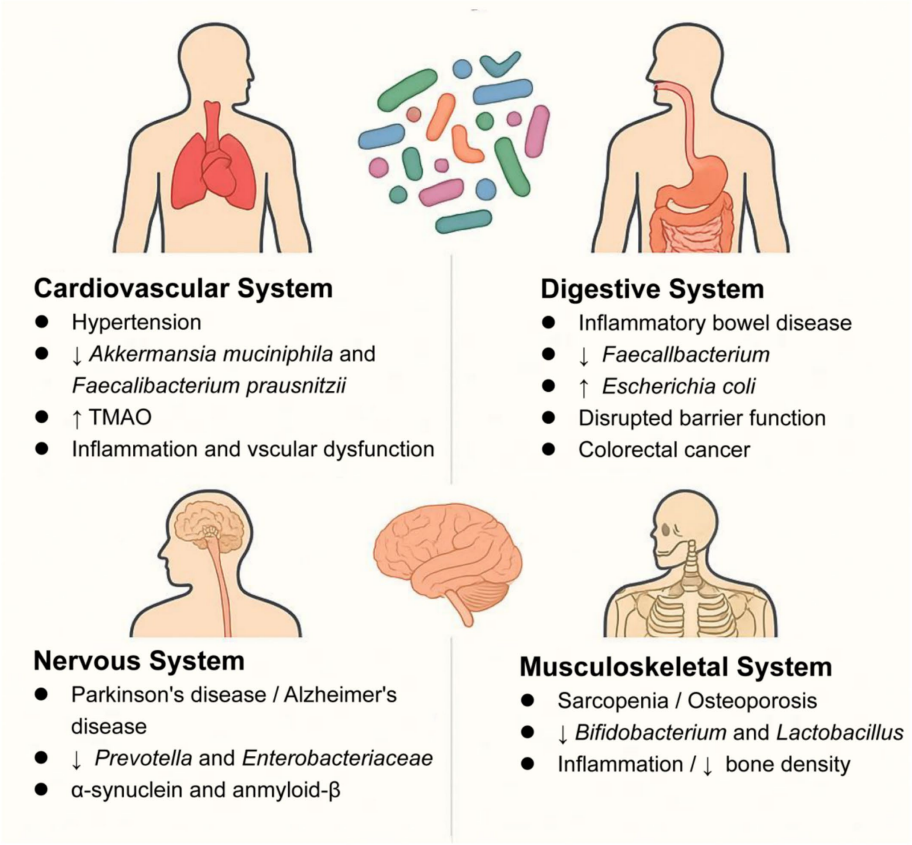

FIGURE 2
Key microbiota alterations in systemic diseases: ↓ beneficial taxa (*Akkermansia*), ↑ pathogens (*Escherichia coli*). ↑ indicates increase, ↓ indicates decrease; TMAO, trimethylamine N-oxide.

TABLE 2 Effects of dietary patterns on gut microbiota composition and functional outcomes.

Diet type	Key microbial changes	Mechanisms/health implications
High-animal-protein	↑Firmicutes, Enterobacteriaceae, Proteus ↓*Bacteroides*, *Lactobacillus*, *Rosebacillus*	↑Inflammation, metabolic dysfunction, LPS, Chronic low-grade inflammation, Metabolic disorders ↓SCFAs levels
Plant-based	↑*Prevotella*, *Xylanibacter*, *Prevotella*	↑Anti-inflammatory, Insulin sensitivity, SCFAs levels
Mediterranean	↑Firmicutes, *Prevotella*, *Bifidobacterium*	↑Anti-inflammatory, SCFAs levels

↑ indicates increase, ↓ indicates decrease; SCFA, short-chain fatty acids.

precursors) reciprocally regulate sleep quality—a dynamic interplay explored in subsequent sections.

3.2 Sleep and gut microbiota interactions

Growing evidence demonstrates a bidirectional relationship between gut microbiota imbalance and sleep disturbances, though current findings indicate correlation rather than causation (Nagpal et al., 2018). The host's circadian rhythm and gut microbiota exhibit reciprocal regulation, where chronic sleep disruption alters microbial composition and function (Choi et al., 2021; Segers and Depoortere, 2021; Triplett et al., 2020).

Clinical studies consistently report that insomnia patients display characteristic gut microbiota changes, including elevated Bacteroidetes, reduced Firmicutes and Proteobacteria, and decreased Firmicutes-to-Bacteroidetes ratios compared to healthy individuals (Adak and Khan, 2019; Nagpal et al., 2018; Zhou et al., 2022). Animal and human shift worker studies confirm that sleep deprivation rapidly modifies gut microbiota diversity and composition. For example, Thaiss et al. (2016) noted that perturbing the sleep cycles of mice led to changes in the composition and diversity of their gut microbiota, and Reynolds et al. (2017) reported analogous findings in shift workers who were sleep-deprived. These alterations may influence sleep through several mechanisms: (1) microbial metabolites (tryptophan)

supporting serotonin/melatonin synthesis; (2) SCFAs regulating blood–brain barrier function and clock genes; (3) LPS-induced neuroinflammation via TLR4/NF-κB signaling (Matenchuk et al., 2020; Wang et al., 2021).

Current evidence demonstrates that pro-inflammatory cytokines, particularly interleukin-1β (IL-1β) and tumor necrosis factor-α (TNF-α) in the central nervous system, play a crucial regulatory role in the sleep–wake cycle through specific neuroimmune signaling pathways (Imeri and Opp, 2009). Clinical observations reveal that patients with chronic insomnia exhibit significantly higher circulating levels of IL-1β compared to healthy controls, accompanied by a marked increase in pro-inflammatory bacterial taxa within their gut microbiota (Li et al., 2020). Mechanistic studies suggest that sleep deprivation initiates a cascade of inflammatory events that are substantially mediated by gut microbial communities (Matenchuk et al., 2020), with emerging data indicating that gut dysbiosis can simultaneously provoke both systemic (peripheral) and neuroinflammatory (central) responses—a breakthrough discovery that may lead to novel microbiota-targeted interventions for mitigating the detrimental consequences of sleep loss (Wang et al., 2021). In a separate study, Bowers et al. (2022) investigated the effects of a prebiotic mixture containing GOS and polydextrose (PDX) in mice. Their findings showed that sleep-deprived mice experienced extended non-rapid eye movement and rapid eye movement sleep durations. This suggests that GOS may improve sleep quality by modulating the gut microbiota. Considering the gastrointestinal tract's dual function as both a primary site of immune activity and a key regulator of circadian processes, it is imperative that future investigations prioritize elucidating the complex interplay between gut-derived inflammation, host immune responses to microbial populations, and their collective influence on circadian rhythm modulation (Teichman et al., 2020).

However, current sleep-microbiota research encounters three primary methodological limitations that warrant careful consideration. First, the predominant reliance on subjective sleep assessments (e.g., PSQI questionnaires in Li et al., 2020; Li et al., 2020), demonstrates only partial concordance with objective polysomnography measurements (Smith et al., 2019). Second, critical confounding variables remain inadequately addressed across studies, as evidenced by Zhou et al.'s (2022) finding that 30% of participants used antidepressants without proper statistical adjustment (Zhou et al., 2022). Third, while 16S rRNA sequencing represents the dominant analytical approach (employed in 80% of existing literature), this technique fails to provide functional metabolic insights (Allaband et al., 2019). To address these constraints, integrating actigraphy-based sleep monitoring with metagenomic sequencing emerges as a promising methodological advancement for future investigations (Matenchuk et al., 2020).

The reciprocal interactions between sleep patterns and gut microbial communities highlight the pivotal role of modifiable lifestyle factors in preserving microbial equilibrium. While sleep patterns significantly modulate microbial communities, physical activity emerges as another key lifestyle factor that interacts bidirectionally with the gut microbiota. Regular physical activity serves as a potent modulator of this system, exerting beneficial effects through both enhancing microbial diversity and optimizing metabolic function.

3.3 Exercise and gut microbiota interactions

A growing body of evidence from human and animal studies demonstrates a complex bidirectional relationship between physical activity and gut microbial composition, mediated through multiple physiological pathways. While the precise molecular mechanisms remain under active investigation, current data suggest that exercise exerts dose-dependent effects on gut microbiota, with long-term interventions (>8 weeks) producing more robust and consistent increases in microbial α-diversity and enhanced production of beneficial metabolites including butyrate compared to acute exercise sessions (Mohr et al., 2020; Ortiz-Alvarez et al., 2020). Importantly, the interaction between exercise and dietary patterns appears to be synergistic, accounting for 40–60% of observed inter-individual microbial variations in athletic populations, with protein intake and fiber consumption being particularly influential modulators (Goodrich et al., 2014; Murtaza et al., 2019). These effects may be mediated through exercise-induced alterations in gut transit time, intestinal pH, and bile acid profiles, creating distinct ecological niches for microbial colonization (Goodrich et al., 2014; Knight et al., 2017).

Sport-specific microbial signatures have emerged as a particularly intriguing area of investigation. Endurance athletes (e.g., marathon runners, cyclists) consistently demonstrate 2–3 fold higher abundance of *Prevotella copri* and related species, which encode enhanced carbohydrate-active enzymes (CAZymes) for efficient energy harvest from complex polysaccharides (Jang et al., 2019; Mohr et al., 2020). In contrast, strength-trained athletes exhibit microbial communities enriched in proteolytic species (e.g., *Bacteroides* spp.) with upregulated peptidase activity (Jang et al., 2019). Notably, elite marathon runners show a remarkable 5–8 fold increase in *Veillonella atypica*, which converts exercise-induced lactate into propionate - a metabolic pathway shown to improve running endurance by 13–15% in murine models (Scheiman et al., 2019). Studies have demonstrated that high-intensity interval training (HIIT) more significantly improves peak VO_2 and alters microbial metabolites associated with insulin sensitivity compared to moderate-intensity continuous training (MICT) (Jiang et al., 2024; Kasperek et al., 2023). Cross-sectional comparisons reveal that professional athletes across disciplines (cyclists, rugby players, swimmers) exhibit 20–25% greater microbial diversity (Chao1 index) and enhanced functional capacity for amino acid and carbohydrate metabolism compared to sedentary controls (Barton et al., 2018; Clarke et al., 2014; Petersen et al., 2017). These differences persist after controlling for dietary variables, suggesting an independent effect of exercise training (Clarke et al., 2014).

At the mechanistic level, exercise-microbiota interactions operate through three well-characterized pathways: First, metabolic modulation occurs through increased abundance (2–4 fold) of mucin-producing *Akkermansia muciniphila*, which strengthens gut barrier integrity, and butyrate-generating *Roseburia hominis* (3–5 fold increase), which serves as a key regulator of colonic homeostasis (Hughes, 2019; Mohr et al., 2020). Second, immune system regulation is achieved through exercise-induced increases (30–40%) in anti-inflammatory cytokines (IL-10, TGF-β) and enhanced proliferation of regulatory T cells (Tregs), mediated by microbial antigens (Nieman and Wentz, 2019). Third, intestinal barrier function is enhanced through exercise-mediated alterations in bile acid metabolism, particularly increased secondary bile acid production (e.g.,

deoxycholic acid) which inhibits FXR signaling and reduces endotoxin translocation by 40–50% (Goodrich et al., 2014; Knight et al., 2017). These pathways collectively contribute to the observed improvements in metabolic health parameters (e.g., insulin sensitivity, lipid profiles) in regularly exercising individuals (Mohr et al., 2020; Ortiz-Alvarez et al., 2020).

Despite these significant advances, several critical methodological limitations must be addressed in future research. Current studies frequently conflate acute exercise effects (e.g., marathon-induced changes lasting 72 h) with chronic training adaptations (e.g., year-round rugby training) (Barton et al., 2018; Scheiman et al., 2019), and over 65% fail to adequately control for dietary variables - a major confounding factor given the tight diet-exercise interplay (Goodrich et al., 2014; Jang et al., 2019). Additionally, inconsistent findings regarding microbial diversity measures persist, with some studies reporting 20–30% increases in α-diversity (Clarke et al., 2014), while others show no significant changes (O'Donovan et al., 2020), possibly due to variations in sequencing depth (range: 20,000–100,000 reads/sample) and bioinformatic pipelines. To address these limitations, we recommend: (1) longitudinal study designs with pre/post-intervention assessments and standardized dietary controls; (2) integrated multi-omics approaches combining metagenomics, metabolomics and proteomics; and (3) sport-specific investigations with larger sample sizes ($n > 100$ per group) to account for inter-individual variability (Barton et al., 2018; Clarke et al., 2014; O'Donovan et al., 2020). Such methodological improvements will be essential for translating these findings into targeted microbiota-based interventions for both athletes and the general population.

Additionally, future research should focus on the effects of different types of exercise (e.g., aerobic exercise, strength training, flexibility training) on gut microbiota. Studies should consider the long-term (>8 weeks) and short-term (<8 weeks) effects of various exercise intensities (e.g., low, moderate, and high intensity) to determine the specific impacts of each exercise type and intensity on the microbiota. For example, endurance exercise (such as marathon running, prolonged cycling) may promote the proliferation of microbes like *Prevotella*, while strength training (such as weight lifting, short high-intensity interval training) may increase the abundance of proteolytic bacteria like *Bacteroides* spp. Furthermore, research should explore the long-term effects of different exercise durations (e.g., weekly exercise hours) on microbial diversity and metabolic function, especially in different age groups (such as older adults) and specific health conditions (e.g., obesity, diabetes). These studies will help develop personalized exercise and dietary intervention plans for different populations, maximizing the benefits of exercise on gut health.

4 Current research gaps and future directions

The field of lifestyle-microbiota interactions faces three fundamental challenges that hinder translational applications. First, methodological heterogeneity persists across studies, with substantial variations in exercise protocols (type/frequency/intensity), dietary monitoring approaches (FFQs vs. controlled feeding), and sequencing techniques (16S rRNA vs. metagenomics) - exemplified by 5-fold differences in reported Prevotella enrichment among endurance athletes due to sequencing depth disparities (20,000–100,000 reads/sample). Second, uncontrolled confounders (e.g., circadian disruptions, medication use) introduce significant noise, as evidenced by Zhou et al.'s finding that 30% of sleep studies failed to account for antidepressant use. Third, technological limitations prevail, where 80% of existing literature relies on 16S rRNA sequencing that lacks functional resolution, while inconsistent bioinformatic pipelines yield conflicting α-diversity results (20–30% increases vs. null effects). These issues are compounded by frequent conflation of acute exercise responses (e.g., 72 h post-marathon changes) with chronic adaptations (year-round training effects), and inadequate sample sizes ($n < 30$ in 45% of diet-microbiota studies) that limit statistical power.

To overcome these barriers, we propose a tripartite roadmap for next-generation research: (1) Standardized protocols incorporating ISO-certified exercise regimens, validated dietary tracking tools (ASA24), and unified multi-omics workflows (prioritizing metagenomics for functional insights); (2) Large-scale longitudinal randomized controlled trials (RCTs) (n > 100/group) with stringent control of host variables (age, BMI, medication) and integrated actigraphy-microbiota monitoring to disentangle circadian effects; (3) Mechanistic synergy studies employing germ-free models and fecal microbiota transplantation to investigate how diet-exercise-sleep combinations (e.g., high-fiber diets + endurance training) modulate specific microbial functions (e.g., *Roseburia*-mediated butyrate production). Such approaches should be complemented by cross-validation of sequencing platforms (Illumina vs. Nanopore) and establishment of microbial "responder" thresholds (e.g., >10% *Faecalibacterium* increase) to enhance reproducibility.

Critical knowledge gaps demanding urgent attention include: (1) Exercise-type specificity- resolving how resistance training preferentially enriches proteolytic *Bacteroides* versus aerobic exercise-induced *Prevotella* through microbial lactate metabolism; (2) Population-tailored dynamics - determining optimal lifestyle prescriptions for elderly (probiotics + protein supplementation) versus metabolic syndrome patients (high-fiber diets + moderate exercise) to counteract age- or disease-related dysbiosis; (3) Circadian-microbiota crosstalk - elucidating how microbial metabolites (SCFAs, tryptophan) regulate clock genes in shift workers. As highlighted in Table 3, addressing these priorities through concerted multidisciplinary efforts will enable development of precision microbiota interventions targeting immune-metabolic disorders, bridging the current gap between mechanistic insights and clinical applications. Future studies should particularly focus on longitudinal monitoring of athlete cohorts and high-risk populations (T2DM, elderly) to establish causal timelines for microbial changes and their functional health impacts.

5 Summary and translational perspectives

Collectively, the interplay of dietary habits, sleep architecture, and exercise regimens shapes gut microbial ecosystems in distinct yet interconnected ways, ultimately influencing host health outcomes. Having addressed the key research gaps and methodological challenges, this comprehensive synthesis establishes the gut microbiota as a pivotal mediator linking modifiable lifestyle factors (diet, sleep, and exercise) to host physiology and disease susceptibility. Our analysis demonstrates that targeted lifestyle interventions can reshape

TABLE 3 Critical appraisal of microbiota research limitations and future directions across lifestyle domains.

Domain	Major limitations	Conflicting findings	Proposed solutions	Priority research gaps
Diet	1. Small sample sizes 2. Cross-sectional designs 3. Inconsistent findings	1. Firmicutes: Bacteroidetes ratio changes inconsistent (↑ in 60% vs. ↔ in 40% of high-protein diet studies) 2. Mediterranean diet effects on α-diversity (↑ in 65% vs. ↔ in 35% of trials)	1. Standardized 7-day weighed food records + biomarkers 2. Longitudinal RCTs with multi-omics 3. Baseline microbiota stratification	1. MACs-microbiome dose–response 2. Host genetics-microbiota interactions3.Personalized nutrition algorithms
Sleep	1. Overreliance on subjective sleep measures (PSQI) 2. 30% studies fail to control antidepressant use 3. 80% studies use 16S rRNA without functional data	1. 55% vs. 45% studies report microbial diversity changes in insomnia 2. Bidirectional causality debates (microbiota→sleep vs. sleep→microbiota)	1. Actigraphy + polysomnography integration 2. Medication-naïve cohort studies 3. Metagenomics + metabolomics pairing	1. Microbial circadian rhythms 2. LPS-neuroinflammation axis 3. FMT timing effects
Exercise	1. Diet-exercise confounding (65% of studies) 2. Intensity quantification lacking (70% of trials) 3. Homogeneous populations (85% young athletes)	Inconsistent reports on microbial diversity: some show 20–30% ↑ α-diversity, others find no change, possibly due to sequencing depth (20,000–100,000 reads/sample) or bioinformatics differences	1. Longitudinal designs + standardized diet control 2. Multi-omics integration (metagenomics, metabolomics, proteomics) 3. Sport-specific studies with larger cohorts (n > 100/group)	1. Compare exercise types (aerobic/strength/flexibility) on microbiota 2. Dose–response: intensity (low/moderate/high) and duration (short- < 8w, long- > 8w) 3. Population-specific effects (age, obesity/diabetes) 4. Mechanisms: e.g., endurance→↑*Prevotella*; strength→↑*Bacteroides*

↑ indicates increase; RCTs, randomized controlled trials; MACs, microbiota-accessible carbohydrates; PSQI, Pittsburgh sleep quality index; LPS, lipopolysaccharide; FMT, fecal microbiota transplantation.

microbial communities to favor beneficial taxa (e.g., fiber-fermenting *Roseburia* and *Faecalibacterium*) while suppressing pro-inflammatory species, with measurable impacts on metabolic, immune, and neurological health outcomes. The accumulated evidence positions microbiota modulation as a promising strategy for chronic disease prevention and management, particularly for conditions like metabolic syndrome, IBD, and neurodegenerative disorders where dysbiosis plays an established pathogenic role.

Moving forward, the field must transition from observational correlations to mechanistic, causal understandings through: (1) standardized multi-omics protocols that resolve functional pathways beyond taxonomic profiling; (2) large-scale longitudinal interventions controlling for key confounders (genetics, medications, circadian rhythms); and (3) personalized approaches accounting for interindividual microbial variability. The integration of these strategies with emerging technologies - including AI-driven microbiota analysis and wearable monitoring devices - will accelerate the development of precision microbiota medicine. These advances promise to transform public health paradigms by enabling evidence-based, microbiota-conscious lifestyle recommendations tailored to individual risk profiles and health statuses.

Author contributions

QZ: Conceptualization, Methodology, Investigation, Writing – original draft, Writing – review & editing. XF: Supervision, Project administration, Writing – review & editing. YH: Data curation, Formal analysis, Visualization, Writing – review & editing. SS: Software, Validation, Resources, Writing – review & editing.

Funding

The author(s) declare that no financial support was received for the research and/or publication of this article.

Acknowledgments

The authors gratefully acknowledge all researchers whose work was cited in this review.

Conflict of interest

The authors declare that the research was conducted in the absence of any commercial or financial relationships that could be construed as a potential conflict of interest.

Generative AI statement

The authors declare that no Gen AI was used in the creation of this manuscript.

Publisher's note

All claims expressed in this article are solely those of the authors and do not necessarily represent those of their affiliated organizations, or those of the publisher, the editors and the reviewers. Any product that may be evaluated in this article, or claim that may be made by its manufacturer, is not guaranteed or endorsed by the publisher.

References

Adak, A., and Khan, M. R. (2019). An insight into gut microbiota and its functionalities. *Cell. Mol. Life Sci.* 76, 473–493. doi: 10.1007/s00018-018-2943-4

Allaband, C., McDonald, D., Vázquez-Baeza, Y., Minich, J. J., Tripathi, A., Brenner, D. A., et al. (2019). Microbiome 101: studying, analyzing, and interpreting gut microbiome data for clinicians. *Clin. Gastroenterol. Hepatol.* 17, 218–230. doi: 10.1016/j.cgh.2018.09.017

Armet, A. M., Deehan, E. C., O'Sullivan, A. F., Mota, J. F., Field, C. J., Prado, C. M., et al. (2022). Rethinking healthy eating in light of the gut microbiome. *Cell Host Microbe* 30, 764–785. doi: 10.1016/j.chom.2022.04.016

Arumugam, M., Raes, J., Pelletier, E., Le Paslier, D., Yamada, T., Mende, D. R., et al. (2011). Enterotypes of the human gut microbiome. *Nature* 473, 174–180. doi: 10.1038/nature09944

Baldi, A., Braat, S., Hasan, M. I., Bennett, C., Barrios, M., Jones, N., et al. (2024). Effects of iron supplements and iron-containing micronutrient powders on the gut microbiome in Bangladeshi infants: a randomized controlled trial. *Nat. Commun.* 15:8640. doi: 10.1038/s41467-024-53013-x

Barton, W., Penney, N. C., Cronin, O., Garcia-Perez, I., Molloy, M. G., Holmes, E., et al. (2018). The microbiome of professional athletes differs from that of more sedentary subjects in composition and particularly at the functional metabolic level. *Gut* 67, 625–633. doi: 10.1136/gutjnl-2016-313627

Baunwall, S. M. D., Lee, M. M., Eriksen, M. K., Mullish, B. H., Marchesi, J. R., Dahlerup, J. F., et al. (2020). Faecal microbiota transplantation for recurrent Clostridioides difficile infection: an updated systematic review and meta-analysis. *EClinicalMedicine* 29-30:100642. doi: 10.1016/j.eclinm.2020.100642

Benjamin, D. I., Both, P., Benjamin, J. S., Nutter, C. W., Tan, J. H., Kang, J., et al. (2022). Fasting induces a highly resilient deep quiescent state in muscle stem cells via ketone body signaling. *Cell Metab.* 34, 902–918.e6. doi: 10.1016/j.cmet.2022.04.012

Ben-Yacov, O., Godneva, A., Rein, M., Shilo, S., Lotan-Pompan, M., Weinberger, A., et al. (2023). Gut microbiome modulates the effects of a personalised postprandial-targeting (PPT) diet on cardiometabolic markers: a diet intervention in pre-diabetes. *Gut* 72, 1486–1496. doi: 10.1136/gutjnl-2022-329201

Bi, M., Feng, L., He, J., Liu, C., Wang, Y., Jiang, H., et al. (2022). Emerging insights between gut microbiome dysbiosis and Parkinson's disease: pathogenic and clinical relevance. *Ageing Res. Rev.* 82:101759. doi: 10.1016/j.arr.2022.101759

Blommer, J., Pitcher, T., Mustapic, M., Eren, E., Yao, P. J., Vreones, M. P., et al. (2023). Extracellular vesicle biomarkers for cognitive impairment in Parkinson's disease. *Brain* 146, 195–208. doi: 10.1093/brain/awac258

Bowers, S. J., Summa, K. C., Thompson, R. S., González, A., Vargas, F., Olker, C., et al. (2022). A prebiotic diet alters the fecal microbiome and improves sleep in response to sleep disruption in rats. *Front. Neurosci.* 16:889211. doi: 10.3389/fnins.2022.889211

Cani, P. D., Amar, J., Iglesias, M. A., Poggi, M., Knauf, C., Bastelica, D., et al. (2007). Metabolic endotoxemia initiates obesity and insulin resistance. *Diabetes* 56, 1761–1772. doi: 10.2337/db06-1491

Cheng, W.-Y., Lam, K.-L., Li, X., Kong, A. P.-S., and Cheung, P. C.-K. (2021). Circadian disruption-induced metabolic syndrome in mice is ameliorated by oat β-glucan mediated by gut microbiota. *Carbohydr. Polym.* 267:118216. doi: 10.1016/j.carbpol.2021.118216

Choi, H., Rao, M. C., and Chang, E. B. (2021). Gut microbiota as a transducer of dietary cues to regulate host circadian rhythms and metabolism. *Nat. Rev. Gastroenterol. Hepatol.* 18, 679–689. doi: 10.1038/s41575-021-00452-2

Clarke, S. F., Murphy, E. F., O'Sullivan, O., Lucey, A. J., Humphreys, M., Hogan, A., et al. (2014). Exercise and associated dietary extremes impact on gut microbial diversity. *Gut* 63, 1913–1920. doi: 10.1136/gutjnl-2013-306541

Cryan, J. F., O'Riordan, K. J., Cowan, C. S. M., Sandhu, K. V., Bastiaanssen, T. F. S., Boehme, M., et al. (2019). The microbiota-gut-brain Axis. *Physiol. Rev.* 99, 1877–2013. doi: 10.1152/physrev.00018.2018

Cuevas-Sierra, A., Chero-Sandoval, L., Higuera-Gómez, A., Vargas, J. A., Martínez-Urbistondo, M., Castejón, R., et al. (2024). Modulatory role of Faecalibacterium on insulin resistance and coagulation in patients with post-viral long haulers depending on adiposity. *IScience* 27:110450. doi: 10.1016/j.isci.2024.110450

D'Archivio, M., Santangelo, C., Silenzi, A., Scazzocchio, B., Varì, R., and Masella, R. (2022). Dietary EVOO polyphenols and gut microbiota interaction: are there any sex/gender influences? *Antioxidants* 11:1744. doi: 10.3390/antiox11091744

David, L. A., Maurice, C. F., Carmody, R. N., Gootenberg, D. B., Button, J. E., Wolfe, B. E., et al. (2014). Diet rapidly and reproducibly alters the human gut microbiome. *Nature* 505, 559–563. doi: 10.1038/nature12820

De Filippis, F., Pellegrini, N., Vannini, L., Jeffery, I. B., La Storia, A., Laghi, L., et al. (2016). High-level adherence to a Mediterranean diet beneficially impacts the gut microbiota and associated metabolome. *Gut* 65, 1812–1821. doi: 10.1136/gutjnl-2015-309957

De Filippo, C., Cavalieri, D., Di Paola, M., Ramazzotti, M., Poullet, J. B., Massart, S., et al. (2010). Impact of diet in shaping gut microbiota revealed by a comparative study in children from Europe and rural Africa. *Proc. Natl. Acad. Sci. USA* 107, 14691–14696. doi: 10.1073/pnas.1005963107

de Wit, N., Derrien, M., Bosch-Vermeulen, H., Oosterink, E., Keshtkar, S., Duval, C., et al. (2012). Saturated fat stimulates obesity and hepatic steatosis and affects gut microbiota composition by an enhanced overflow of dietary fat to the distal intestine. *Am. J. Physiol. Gastrointest. Liver Physiol.* 303, G589–G599. doi: 10.1152/ajpgi.00488.2011

Deehan, E. C., Yang, C., Perez-Muñoz, M. E., Nguyen, N. K., Cheng, C. C., Triador, L., et al. (2020). Precision microbiome modulation with discrete dietary Fiber structures directs Short-chain fatty acid production. *Cell Host Microbe* 27, 389–404.e6. doi: 10.1016/j.chom.2020.01.006

Di Vincenzo, F., Del Gaudio, A., Petito, V., Lopetuso, L. R., and Scaldaferri, F. (2024). Gut microbiota, intestinal permeability, and systemic inflammation: a narrative review. *Intern. Emerg. Med.* 19, 275–293. doi: 10.1007/s11739-023-03374-w

Diacova, T., Cifelli, C. J., Davis, C. D., Holscher, H. D., Kable, M. E., Lampe, J. W., et al. (2025). Best practices and considerations for conducting research on diet-gut microbiome interactions and their impact on health in adult populations: an umbrella review. *Adv. Nutr. (Bethesda, Md.)* 16:100419. doi: 10.1016/j.advnut.2025.100419

Du, W., Zou, Z.-P., Ye, B.-C., and Zhou, Y. (2025). Gut microbiota and associated metabolites: key players in high-fat diet-induced chronic diseases. *Gut Microbes* 17:2494703. doi: 10.1080/19490976.2025.2494703

Garcia-Mantrana, I., Selma-Royo, M., Alcantara, C., and Collado, M. C. (2018). Shifts on gut microbiota associated to Mediterranean diet adherence and specific dietary intakes on general adult population. *Front. Microbiol.* 9:890. doi: 10.3389/fmicb.2018.00890

Goodrich, J. K., Di Rienzi, S. C., Poole, A. C., Koren, O., Walters, W. A., Caporaso, J. G., et al. (2014). Conducting a microbiome study. *Cell* 158, 250–262. doi: 10.1016/j.cell.2014.06.037

Haskey, N., Estaki, M., Ye, J., Shim, R. K., Singh, S., Dieleman, L. A., et al. (2023). A Mediterranean diet pattern improves intestinal inflammation concomitant with reshaping of the Bacteriome in ulcerative colitis: a randomised controlled trial. *J. Crohns Colitis* 17, 1569–1578. doi: 10.1093/ecco-jcc/jjad073

Henao-Mejia, J., Elinav, E., Jin, C., Hao, L., Mehal, W. Z., Strowig, T., et al. (2012). Inflammasome-mediated dysbiosis regulates progression of NAFLD and obesity. *Nature* 482, 179–185. doi: 10.1038/nature10809

Hughes, R. L. (2019). A review of the role of the gut microbiome in personalized sports nutrition. *Front. Nutr.* 6:191. doi: 10.3389/fnut.2019.00191

Ianiro, G., Punčochář, M., Karcher, N., Porcari, S., Armanini, F., Asnicar, F., et al. (2022). Variability of strain engraftment and predictability of microbiome composition after fecal microbiota transplantation across different diseases. *Nat. Med.* 28, 1913–1923. doi: 10.1038/s41591-022-01964-3

Imeri, L., and Opp, M. R. (2009). How (and why) the immune system makes us sleep. *Nat. Rev. Neurosci.* 10, 199–210. doi: 10.1038/nrn2576

Jang, L.-G., Choi, G., Kim, S.-W., Kim, B.-Y., Lee, S., and Park, H. (2019). The combination of sport and sport-specific diet is associated with characteristics of gut microbiota: an observational study. *J. Int. Soc. Sports Nutr.* 16:21. doi: 10.1186/s12970-019-0290-y

Jansson, P.-A., Curiac, D., Lazou Ahrén, I., Hansson, F., Martinsson Niskanen, T., Sjögren, K., et al. (2019). Probiotic treatment using a mix of three *Lactobacillus* strains for lumbar spine bone loss in postmenopausal women: a randomised, double-blind, placebo-controlled, multicentre trial. *Lancet Rheumatol.* 1, e154–e162. doi: 10.1016/S2665-9913(19)30068-2

Jiang, L., Liu, P., Wang, M., Deng, Q., Wang, J., Jiang, Y., et al. (2024). Effect of high-intensity intermittent rehabilitation training on physical function, gut microbiome and metabolite after percutaneous coronary intervention in patients with coronary heart disease. *Front. Cardiovasc. Med.* 11:1508456. doi: 10.3389/fcvm.2024.1508456

Kasperek, M. C., Mailing, L., Piccolo, B. D., Moody, B., Lan, R., Gao, X., et al. (2023). Exercise training modifies xenometabolites in gut and circulation of lean and obese adults. *Physiol. Rep.* 11:e15638. doi: 10.14814/phy2.15638

Kim, K. H., Chung, Y., Huh, J.-W., Park, D. J., Cho, Y., Oh, Y., et al. (2022). Gut microbiota of the young ameliorates physical fitness of the aged in mice. *Microbiome* 10:238. doi: 10.1186/s40168-022-01386-w

Knight, R., Callewaert, C., Marotz, C., Hyde, E. R., Debelius, J. W., McDonald, D., et al. (2017). The microbiome and human biology. *Annu. Rev. Genomics Hum. Genet.* 18, 65–86. doi: 10.1146/annurev-genom-083115-022438

Kundu, P., Lee, H. U., Garcia-Perez, I., Tay, E. X. Y., Kim, H., Faylon, L. E., et al. (2019). Neurogenesis and prolongevity signaling in young germ-free mice transplanted with the gut microbiota of old mice. *Sci. Transl. Med.* 11:eaau4760. doi: 10.1126/scitranslmed.aau4760

Li, B., He, Y., Ma, J., Huang, P., Du, J., Cao, L., et al. (2019). Mild cognitive impairment has similar alterations as Alzheimer's disease in gut microbiota. *Alzheimers Dement.* 15, 1357–1366. doi: 10.1016/j.jalz.2019.07.002

Li, Y., Zhang, B., Zhou, Y., Wang, D., Liu, X., Li, L., et al. (2020). Gut microbiota changes and their relationship with inflammation in patients with acute and chronic insomnia. *Nat. Sci. Sleep* 12, 895–905. doi: 10.2147/NSS.S271927

Li, J., Zhao, F., Wang, Y., Chen, J., Tao, J., Tian, G., et al. (2017). Gut microbiota dysbiosis contributes to the development of hypertension. *Microbiome* 5:14. doi: 10.1186/s40168-016-0222-x

Luo, S., Zhao, Y., Zhu, S., Liu, L., Cheng, K., Ye, B., et al. (2023). *Flavonifractor plautii* protects against elevated arterial stiffness. *Circ. Res.* 132, 167–181. doi: 10.1161/CIRCRESAHA.122.321975

Lynch, S. V., and Pedersen, O. (2016). The human intestinal microbiome in health and disease. *N. Engl. J. Med.* 375, 2369–2379. doi: 10.1056/NEJMra1600266

Ma, S.-R., Tong, Q., Lin, Y., Pan, L.-B., Fu, J., Peng, R., et al. (2022). Berberine treats atherosclerosis via a vitamine-like effect down-regulating choline-TMA-TMAO production pathway in gut microbiota. *Signal Transduct. Target. Ther.* 7:207. doi: 10.1038/s41392-022-01027-6

Mailing, L. J., Allen, J. M., Buford, T. W., Fields, C. J., and Woods, J. A. (2019). Exercise and the gut microbiome: a review of the evidence, potential mechanisms, and implications for human health. *Exerc. Sport Sci. Rev.* 47, 75–85. doi: 10.1249/JES.0000000000000183

Mancin, L., Wu, G. D., and Paoli, A. (2023). Gut microbiota-bile acid-skeletal muscle axis. *Trends Microbiol.* 31, 254–269. doi: 10.1016/j.tim.2022.10.003

Matenchuk, B. A., Mandhane, P. J., and Kozyrskyj, A. L. (2020). Sleep, circadian rhythm, and gut microbiota. *Sleep Med. Rev.* 53:101340. doi: 10.1016/j.smrv.2020.101340

Mohr, A. E., Jäger, R., Carpenter, K. C., Kerksick, C. M., Purpura, M., Townsend, J. R., et al. (2020). The athletic gut microbiota. *J. Int. Soc. Sports Nutr.* 17:24. doi: 10.1186/s12970-020-00353-w

Mondal, T., Chattopadhyay, D., Saha Mondal, P., Das, S., Mondal, A., Das, A., et al. (2025). *Fusobacterium nucleatum* modulates the Wnt/β-catenin pathway in colorectal cancer development. *Int. J. Biol. Macromol.* 299:140196. doi: 10.1016/j.ijbiomac.2025.140196

Munoz-Pinto, M. F., Candeias, E., Melo-Marques, I., Esteves, A. R., Maranha, A., Magalhães, J. D., et al. (2024). Gut-first Parkinson's disease is encoded by gut dysbiome. *Mol. Neurodegener.* 19:78. doi: 10.1186/s13024-024-00766-0

Münte, E., and Hartmann, P. (2025). The role of Short-chain fatty acids in metabolic dysfunction-associated Steatotic liver disease and other metabolic diseases. *Biomol. Ther.* 15:469. doi: 10.3390/biom15040469

Muralitharan, R., Zheng, T., Dinakis, E., Xie, L., Barbaro-Wahl, A., Jama, H. A., et al. (2025). Gut microbiota metabolites sensed by host GPR41/43 protect against hypertension. *Circ. Res.* 136, e20–e33. doi: 10.1161/CIRCRESAHA.124.325770

Murtaza, N., Burke, L. M., Vlahovich, N., Charlesson, B., O'Neill, H. M., Ross, M. L., et al. (2019). Analysis of the effects of dietary pattern on the oral microbiome of elite endurance athletes. *Nutrients* 11:614. doi: 10.3390/nu11030614

Nagpal, R., Shively, C. A., Appt, S. A., Register, T. C., Michalson, K. T., Vitolins, M. Z., et al. (2018). Gut microbiome composition in non-human primates consuming a western or Mediterranean diet. *Front. Nutr.* 5:28. doi: 10.3389/fnut.2018.00028

Nieman, D. C., and Wentz, L. M. (2019). The compelling link between physical activity and the body's defense system. *J. Sport Health Sci.* 8, 201–217. doi: 10.1016/j.jshs.2018.09.009

Niño, D. F., Zhou, Q., Yamaguchi, Y., Martin, L. Y., Wang, S., Fulton, W. B., et al. (2018). Cognitive impairments induced by necrotizing enterocolitis can be prevented by inhibiting microglial activation in mouse brain. *Sci. Transl. Med.* 10:eaan0237. doi: 10.1126/scitranslmed.aan0237

O'Donovan, C. M., Madigan, S. M., Garcia-Perez, I., Rankin, A., O' Sullivan, O., and Cotter, P. D. (2020). Distinct microbiome composition and metabolome exists across subgroups of elite Irish athletes. *J. Sci. Med. Sport* 23, 63–68. doi: 10.1016/j.jsams.2019.08.290

Ortiz-Alvarez, L., Xu, H., and Martinez-Tellez, B. (2020). Influence of exercise on the human gut microbiota of healthy adults: a systematic review. *Clin. Transl. Gastroenterol.* 11:e00126. doi: 10.14309/ctg.0000000000000126

Parker, A., Fonseca, S., and Carding, S. R. (2020). Gut microbes and metabolites as modulators of blood-brain barrier integrity and brain health. *Gut Microbes* 11, 135–157. doi: 10.1080/19490976.2019.1638722

Pedroza Matute, S., and Iyavoo, S. (2023). Exploring the gut microbiota: lifestyle choices, disease associations, and personal genomics. *Front. Nutr.* 10:1225120. doi: 10.3389/fnut.2023.1225120

Perrone, P., and D'Angelo, S. (2025). Gut microbiota modulation through Mediterranean diet foods: implications for human health. *Nutrients* 17:948. doi: 10.3390/nu17060948

Petersen, L. M., Bautista, E. J., Nguyen, H., Hanson, B. M., Chen, L., Lek, S. H., et al. (2017). Community characteristics of the gut microbiomes of competitive cyclists. *Microbiome* 5:98. doi: 10.1186/s40168-017-0320-4

Portincasa, P., Bonfrate, L., Vacca, M., De Angelis, M., Farella, I., Lanza, E., et al. (2022). Gut microbiota and Short chain fatty acids: implications in glucose homeostasis. *Int. J. Mol. Sci.* 23:1105. doi: 10.3390/ijms23031105

Qin, J., Li, R., Raes, J., Arumugam, M., Burgdorf, K. S., Manichanh, C., et al. (2010). A human gut microbial gene catalogue established by metagenomic sequencing. *Nature* 464, 59–65. doi: 10.1038/nature08821

Rashidah, N. H., Lim, S. M., Neoh, C. F., Majeed, A. B. A., Tan, M. P., Khor, H. M., et al. (2022). Differential gut microbiota and intestinal permeability between frail and healthy older adults: a systematic review. *Ageing Res. Rev.* 82:101744. doi: 10.1016/j.arr.2022.101744

Reynolds, A. C., Paterson, J. L., Ferguson, S. A., Stanley, D., Wright, K. P., and Dawson, D. (2017). The shift work and health research agenda: considering changes in gut microbiota as a pathway linking shift work, sleep loss and circadian misalignment, and metabolic disease. *Sleep Med. Rev.* 34, 3–9. doi: 10.1016/j.smrv.2016.06.009

Ross, F. C., Patangia, D., Grimaud, G., Lavelle, A., Dempsey, E. M., Ross, R. P., et al. (2024). The interplay between diet and the gut microbiome: implications for health and disease. *Nat. Rev. Microbiol.* 22, 671–686. doi: 10.1038/s41579-024-01068-4

Sampson, T. R., Debelius, J. W., Thron, T., Janssen, S., Shastri, G. G., Ilhan, Z. E., et al. (2016). Gut microbiota regulate motor deficits and Neuroinflammation in a model of Parkinson's disease. *Cell* 167, 1469–1480.e12. doi: 10.1016/j.cell.2016.11.018

Sánchez-Tapia, M., Miller, A. W., Granados-Portillo, O., Tovar, A. R., and Torres, N. (2020). The development of metabolic endotoxemia is dependent on the type of sweetener and the presence of saturated fat in the diet. *Gut Microbes* 12:1801301. doi: 10.1080/19490976.2020.1801301

Scheiman, J., Luber, J. M., Chavkin, T. A., MacDonald, T., Tung, A., Pham, L.-D., et al. (2019). Meta-omics analysis of elite athletes identifies a performance-enhancing microbe that functions via lactate metabolism. *Nat. Med.* 25, 1104–1109. doi: 10.1038/s41591-019-0485-4

Segers, A., and Depoortere, I. (2021). Circadian clocks in the digestive system. *Nat. Rev. Gastroenterol. Hepatol.* 18, 239–251. doi: 10.1038/s41575-020-00401-5

Sharma, B., Agriantonis, G., Twelker, K., Ebelle, D., Kiernan, S., Siddiqui, M., et al. (2025). Gut microbiota serves as a crucial independent biomarker in inflammatory bowel disease (IBD). *Int. J. Mol. Sci.* 26:2503. doi: 10.3390/ijms26062503

Smith, R. P., Easson, C., Lyle, S. M., Kapoor, R., Donnelly, C. P., Davidson, E. J., et al. (2019). Gut microbiome diversity is associated with sleep physiology in humans. *PLoS One* 14:e0222394. doi: 10.1371/journal.pone.0222394

Sonnenburg, J. L., and Bäckhed, F. (2016). Diet-microbiota interactions as moderators of human metabolism. *Nature* 535, 56–64. doi: 10.1038/nature18846

Teichman, E. M., O'Riordan, K. J., Gahan, C. G. M., Dinan, T. G., and Cryan, J. F. (2020). When rhythms meet the blues: circadian interactions with the microbiota-gut-brain axis. *Cell Metab.* 31, 448–471. doi: 10.1016/j.cmet.2020.02.008

Thaiss, C. A., Levy, M., Korem, T., Dohnalová, L., Shapiro, H., Jaitin, D. A., et al. (2016). Microbiota diurnal rhythmicity programs host transcriptome oscillations. *Cell* 167, 1495–1510.e12. doi: 10.1016/j.cell.2016.11.003

Triplett, J., Ellis, D., Braddock, A., Roberts, E., Ingram, K., Perez, E., et al. (2020). Temporal and region-specific effects of sleep fragmentation on gut microbiota and intestinal morphology in Sprague Dawley rats. *Gut Microbes* 11, 706–720. doi: 10.1080/19490976.2019.1701352

Turnbaugh, P. J., Hamady, M., Yatsunenko, T., Cantarel, B. L., Duncan, A., Ley, R. E., et al. (2009). A core gut microbiome in obese and lean twins. *Nature* 457, 480–484. doi: 10.1038/nature07540

Wang, Z., Chen, W.-H., Li, S.-X., He, Z.-M., Zhu, W.-L., Ji, Y.-B., et al. (2021). Gut microbiota modulates the inflammatory response and cognitive impairment induced by sleep deprivation. *Mol. Psychiatry* 26, 6277–6292. doi: 10.1038/s41380-021-01113-1

Wang, X., Jia, R., Chen, W., Zheng, B., and Guo, Z. (2025). Structural characteristics of lotus seed starch-chlorogenic acid complexes during dynamic *in vitro* digestion and prebiotic activities. *Food Chem.* 467:142329. doi: 10.1016/j.foodchem.2024.142329

Wilson, A. S., Koller, K. R., Ramaboli, M. C., Nesengani, L. T., Ocvirk, S., Chen, C., et al. (2020). Diet and the human gut microbiome: an international review. *Dig. Dis. Sci.* 65, 723–740. doi: 10.1007/s10620-020-06112-w

Wu, J., Wang, K., Wang, X., Pang, Y., and Jiang, C. (2021). The role of the gut microbiome and its metabolites in metabolic diseases. *Protein Cell* 12, 360–373. doi: 10.1007/s13238-020-00814-7

Yan, X., Jin, J., Su, X., Yin, X., Gao, J., Wang, X., et al. (2020). Intestinal Flora modulates blood pressure by regulating the synthesis of intestinal-derived corticosterone in high salt-induced hypertension. *Circ. Res.* 126, 839–853. doi: 10.1161/CIRCRESAHA.119.316394

Zeevi, D., Korem, T., Zmora, N., Israeli, D., Rothschild, D., Weinberger, A., et al. (2015). Personalized nutrition by prediction of glycemic responses. *Cell* 163, 1079–1094. doi: 10.1016/j.cell.2015.11.001

Zeng, X., Xing, X., Gupta, M., Keber, F. C., Lopez, J. G., Lee, Y.-C. J., et al. (2022). Gut bacterial nutrient preferences quantified *in vivo*. *Cell* 185, 3441–3456.e19. doi: 10.1016/j.cell.2022.07.020

Zhao, X., Jia, S., Zhao, H., Liu, P., Wu, Z., Tao, H., et al. (2025). The interaction between maize resistant starch III and *Bifidobacterium adolescentis* during *in vitro* fermentation. *Food Chem.* 463:140968. doi: 10.1016/j.foodchem.2024.140968

Zhao, M., Lu, C., Hu, X., and Ma, Z. (2024). Evolution of multi-scale structure and microbiota metabolism of lentil resistant starch during the dynamic fermentation *in vitro*. *Food Chem.* 461:140914. doi: 10.1016/j.foodchem.2024.140914

Zheng, D., Liwinski, T., and Elinav, E. (2020). Interaction between microbiota and immunity in health and disease. *Cell Res.* 30, 492–506. doi: 10.1038/s41422-020-0332-7

Zhou, J., Wu, X., Li, Z., Zou, Z., Dou, S., Li, G., et al. (2022). Alterations in gut microbiota are correlated with serum metabolites in patients with insomnia disorder. *Front. Cell. Infect. Microbiol.* 12:722662. doi: 10.3389/fcimb.2022.722662

frontiers | Frontiers in Microbiology

TYPE Original Research
PUBLISHED 25 June 2025
DOI 10.3389/fmicb.2025.1606437

Check for updates

OPEN ACCESS

EDITED BY
Shyam Sundar Paul,
ICAR, India

REVIEWED BY
Feed Research Institute (CAAS),
Chinese Academy of Agricultural Sciences,
China
Wenchao Cai,
Shihezi University, China
Yafei Duan,
South China Sea Fisheries Research Institute,
China
Muhammad Zahid Farooq,
University of Veterinary and Animal Sciences,
Pakistan

*CORRESPONDENCE
Kailun Yang
✉ yangkailun2002@aliyun.com
Guodong Zhao
✉ zhaogd2021@163.com

RECEIVED 07 April 2025
ACCEPTED 30 May 2025
PUBLISHED 25 June 2025
CORRECTED 26 June 2025

CITATION
Liu R, Li P, Fan C, Wang S, Liu Z, Zhao G and Yang K (2025) Effect of supplementation with *L*-Citrulline on rumen microbiota structure, plasma metabolites, reproductive hormones, and antioxidant capacity of Hu ewes. *Front. Microbiol.* 16:1606437. doi: 10.3389/fmicb.2025.1606437

COPYRIGHT
© 2025 Liu, Li, Fan, Wang, Liu, Zhao and Yang. This is an open-access article distributed under the terms of the Creative Commons Attribution License (CC BY). The use, distribution or reproduction in other forums is permitted, provided the original author(s) and the copyright owner(s) are credited and that the original publication in this journal is cited, in accordance with accepted academic practice. No use, distribution or reproduction is permitted which does not comply with these terms.

Effect of supplementation with *L*-Citrulline on rumen microbiota structure, plasma metabolites, reproductive hormones, and antioxidant capacity of Hu ewes

Renping Liu[1], Peiyao Li[1], Chen Fan[1], Shanshan Wang[1], Zhiqiang Liu[2], Guodong Zhao[1]* and Kailun Yang[1]*

[1]College of Animal Science, Xinjiang Agricultural University, Urumqi, China, [2]Xinjiang Shangpin Meiyang Technology Co., Ltd., Changji, China

L-Citrulline (*L*-Cit), a non-essential amino acid, is characterized by its unique extrahepatic metabolism, which significantly enhances the bioavailability of arginine metabolism in tissues. This study investigated the impact of *L*-Cit supplementation on ruminal microbiota composition, plasma metabolites, reproductive hormones, and antioxidant capacity in Hu ewes. Sixty non-pregnant Hu ewes, similar in age and parity, with an average body weight of 47 ± 5.05 kg, were randomly assigned to either a Control group or Experimental group. The Control group received a basal diet, while the Experimental group was supplemented with 10 g/d of *L*-Cit in addition to the basal diet for 65 days. Compared to the Control group, the Experimental group exhibited a significantly higher estrus rate. Plasma estradiol (E_2) levels were significantly reduced ($p < 0.01$), while luteinizing hormone (LH) and follicle-stimulating hormone (FSH) concentrations showed significant increases ($p < 0.05$). Testosterone (T) content was also significantly elevated ($p < 0.01$). Plasma levels of superoxide dismutase (SOD), malondialdehyde (MDA), glutathione peroxidase (GSH-PX), catalase (CAT), and total antioxidant capacity (T-AOC) were significantly higher in the experimental group, with highly significant differences ($p < 0.01$). The 16S rRNA sequencing analysis revealed that at the phylum level, the relative abundance of Bacteroidetes was decreased, while that of Firmicutes was increased in the experimental group. At the family level, the relative abundance of norank_o__Clostridia_UCG-014 was significantly increased. At the genus level, the relative abundance of Prevotellaceae_UCG-003 was significantly decreased. The main enriched pathways in the CON group were identified as Lipoic acid metabolism and Nicotinate and nicotinamide metabolism. The main enriched pathways in the experimental group were identified as Prion diseases, Chlorocyclohexane and chlorobenzene degradation, Chloroalkane and chloroalkene degradation, Biofilm formation-*Escherichia coli*, and Phosphotransferase system (PTS). LC–MS analysis indicated significant upregulation of pathways such as drug metabolism by other enzymes, folate biosynthesis, and valine, leucine, and isoleucine biosynthesis, whereas oxidative phosphorylation and propanoate metabolism were significantly downregulated. These results demonstrate that *L*-Cit supplementation in the diet modulates the ruminal microbiota of Hu ewes, optimizing volatile fatty acid (VFA) proportions, enhancing carbohydrate metabolism, improving xenobiotic degradation capacity, stimulating the synthesis and release of reproductive hormones. Ultimately, these coordinated effects led to a synergistic increase in estrus and conception rates.

KEYWORDS

L-Citrulline, rumen microbiota, untargeted metabolomics, volatile fatty acids, reproductive hormones, antioxidant capacity

1 Introduction

L-Citrulline (*L*-Cit), a non-essential amino acid, plays a pivotal role in nitric oxide (NO) synthesis and systemic metabolism via two primary pathways: arginine metabolism and NO production, which contribute to the generation of NO and polyamines (Ma et al., 2019). It has been demonstrated in studies that plasma arginine levels are increased, NO synthesis is enhanced, and vascular relaxation and exercise performance are improved through supplementation with L-citrulline (Schwedhelm et al., 2008). In addition, the urea cycle is promoted, blood ammonia levels following exercise are reduced, and the onset of fatigue is delayed through L-citrulline supplementation (Suzuki et al., 2015). Arginine serves as a key substrate for protein synthesis and the production of nitrogen-containing metabolites, supporting numerous cellular metabolic functions (Wu et al., 2018). Studies have shown that arginine availability is largely dependent on hepatic uptake (Cynober et al., 1995; Curis et al., 2005; Schwedhelm et al., 2008). In contrast, *L*-Cit, due to its distinct extrahepatic metabolic properties, significantly enhances the bioavailability of arginine in tissues (Gilbreath et al., 2020). Our previous research demonstrated that *L*-Cit supplementation (at optimal levels of 10–15 g/d per ewe) markedly improved plasma reproductive hormone levels, antioxidant capacity, and reproductive performance in Hu sheep ewes (An, 2022; Ma et al., 2023). Similar improvements were observed in rams, including enhanced blood reproductive hormone levels and antioxidant capacity (Liu, 2021; Zhao et al., 2022b). While the effects of *L*-Cit on gut microbiota restructuring in rodents have been established (Li Xiabin et al., 2019). However, the impact of L-citrulline on the rumen microbiota of Hu sheep remains unelucidated, and the dynamic alterations in the blood metabolome induced by its ingestion have not been systematically characterized. The rumen of ruminants represents a complex microbial fermentation system, where the microbiota structure and host metabolism are intricately linked. To address this gap, the current study utilized Hu sheep ewes as a model, analyzing plasma metabolomic changes through liquid chromatography-mass spectrometry (LC–MS) and characterizing the rumen microbial community using 16S rRNA high-throughput sequencing. This research aims to elucidate the impact of *L*-Cit supplementation on host metabolic regulation and ruminal microecology, thereby providing a theoretical foundation for the application of *L*-Cit in the nutritional management of ruminants.

2 Materials and methods

2.1 Experimental materials

L-Cit (Purity≥99.9%) was obtained from Shandong Pingju Biotechnology Co., Ltd., and cloprostenol sodium (Prostaglandin, PG) was sourced from Ningbo Second Hormone Factory.

2.2 Experimental design and grouping

The experiment was conducted from September to December 2024 at Xinjiang Shangpin Meiyang Technology Co., Ltd. (longitude 87.136291, latitude 44.359568). A total of sixty multiparous Hu sheep ewes, with an average body weight of 47 ± 5.05 kg and similar age and parity, were selected for the study. The ewes were randomly assigned to either a Control group (C) or an Experimental group (T), and a 65-day supplementation trial was carried out (Table 1). Day 0 was recorded as the start of formal supplementation. To induce rapid luteolysis and ensure uniform physiological status, the experimental ewes were administered intramuscular injections of PG using a two-batch method at a dose of 1.5 mL per ewe on days −7 and −3 of the trial. The Control group (C) received only the basal diet, while the Experimental group (T) was supplemented with 10 g/d of *L*-Cit per animal in addition to the basal diet, Refeed in two batches for 5 g/per ewe each time, with the dosage being determined based on previous studies (Ma et al., 2023). *L*-Cit was fully mixed with 100 g bran and a small amount of water was added to ensure that it was fed after adsorption with bran. The control group was fed 100 g bran, and TMR diet was fed after the drug was completely eaten. Supplementation ceased on day 10 of the trial. A 7-day heat detection period was conducted from days 15 to 21, and estrus rates were calculated upon completion of the detection. Pregnancy diagnosis was performed on day 30 after mating, and pregnancy rates were recorded (Supplementary Table S1).

TABLE 1 Composition and nutrient levels of TMR diet (DM basis %).

Ingredients	Content %	Nutrient levels	Content %
Whole corn silage	47.42	Organic compound	92.12
Alfalfa hay	18.58	Crude protein	11.32
Wheat straw	19.59	Neutral detergent fiber	53.35
Concentrate supplement	14.41	Acidic detergent fiber	32.28
Total	100	Ca P	0.65 0.33

Composition of the concentrate supplement: Crude Protein ≥18%; Crude Fiber ≤15%; Crude Ash ≤15%; Calcium: 0.5–2.5%; Sodium Chloride: 0.5–2.0%; Sulfur-Containing Amino Acids ≥0.4%; Moisture ≤14%; Total Phosphorus ≥0.4%.
The above values are estimate.

2.3 Feeding management

Throughout the experiment, the ewes in each group were housed in separate pens, with each pen subdivided into six smaller pens containing 10 ewes each. All experimental ewes were managed under identical feeding conditions, provided with a total mixed ration (TMR) diet of consistent nutritional quality, supplied by Xinjiang Shangpin Meiyang Technology Co., Ltd. The TMR diet was administered in two daily batches at 09:00 and 16:00, the ewes were allowed free access to feed and water, with a daily dry matter intake of approximately 1.65 kg per ewe (Table 1).

2.4 Sample collection and measurement

2.4.1 Collection of blood samples

The official supplementation period commenced on day 0 of the experiment. On days −7 and −3, two doses of PG treatment were administered. Blood samples were collected from the jugular vein of the ewes on Day 10 (under the morning fasting state and 3 h post-feeding). During blood collection, the ewe was restrained with its neck extended upward, and pressure was applied to the jugular vein until it became prominent. A blood collection needle was inserted at a 45-degree angle towards the head, and once blood return was observed, the needle was placed into a heparin sodium blood collection tube. Approximately 10 mL of blood was collected into two tubes. The collected blood was centrifuged at 3500 rpm for 15 min in a high-speed centrifuge to prepare plasma. The plasma was then aliquoted into 1.8 mL cryovials, labeled according to group, and stored at −20°C for subsequent analysis.

2.4.2 Determination of plasma biochemical parameters and metabolites

Plasma levels of gonadotropin-releasing hormone (GnRH), follicle-stimulating hormone (FSH), luteinizing hormone (LH), testosterone (T), and estradiol (E_2) were measured. Antioxidant markers, including superoxide dismutase (SOD), malondialdehyde (MDA), glutathione peroxidase (GSH-PX), catalase (CAT), nitric oxide (NO), and total antioxidant capacity (T-AOC), were also assessed. Plasma LC–MS detection followed the method outlined by Xian et al. (2022). All samples were sent to Shanghai Majorbio Bio-pharm Technology Co., Ltd. for testing.

2.4.3 Rumen fluid collection

On day 11 of the experiment, 100 mL of rumen fluid was collected via the oral cavity using a negative pressure extraction device, 3 h after morning feeding. To avoid saliva contamination, the first 50 mL of rumen fluid was discarded. The pH of the rumen fluid was then measured using a portable pH meter (Supplementary Table S2). The rumen fluid was subsequently filtered through four layers of medical gauze, aliquoted, and stored at −80°C.

2.4.4 Measurement of rumen fluid parameters

16S rRNA sequencing was outsourced to Shanghai Majorbio Bio-pharm Technology Co., Ltd. Universal bacterial primers (338F: 5'-ACTCCTACGGGAGGCAGCAG-3′ and 806R: 5'-GGACTACHV GGGTWTCTAAT-3′) were used to amplify the V3-V4 region of the bacterial 16S rRNA via PCR. PCR products were electrophoresed on a 2% agarose gel. PCR reaction parameters were as follows: (a) 1 × (3 min at 95°C), (b) Number of cycles × (30 s at 95°C; 30 s at the annealing temperature; 45 s at 72°C), (c) 10 min at 72°C, followed by 10°C until halted by the user. The raw data has been uploaded to NCBI: https://www.ncbi.nlm.nih.gov/sra/PRJNA1231430.

2.5 Data analysis

Data on estrus rate, conception rate, reproductive hormones, and antioxidant markers in plasma were initially organized using Microsoft Excel 2021. Independent samples *t*-tests for reproductive hormones and antioxidant indicators were performed using IBM SPSS Statistics 27 software. Statistical analysis and graphing were carried out using GraphPad Prism 10. Analysis of rumen fluid samples and untargeted metabolomics data was performed on the cloud platform of Shanghai Majorbio Bio-pharm Technology Co., Ltd.

3 Results

3.1 Effects of *L*-Citrulline supplementation on the rumen microbial community in Hu sheep ewes

3.1.1 Alpha diversity analysis

As presented in Supplementary Supplementary Table S3, no significant differences were observed between the control and experimental groups across various indices. These results suggest that dietary supplementation with *L*-Cit did not significantly alter the diversity of the rumen microbial community. Additionally, the species coverage for all groups reached 99.9%, confirming that the sequencing depth adequately captured the true composition of the microbial community in the rumen fluid samples.

3.1.2 Principal component analysis

Figure 1 illustrates that the first principal component explains 12.25% of the sample variation, while the second principal component accounts for 10.34%. The CON and experimental groups form distinct species clusters, with the CON group displaying a relatively compact microbial composition, indicating smaller differences in bacterial communities. In contrast, the experimental group shows greater dispersion, suggesting a higher degree of variability in its microbial community.

3.1.3 Effects of *L*-Citrulline supplementation on rumen microbiota (phylum level) in Hu sheep ewes

As shown in Supplementary Figure S1A, Bacteroidota and Firmicutes were predominantly represented among the top 10 phyla in rumen microbiota relative abundance at the phylum level, being identified as the dominant phyla in both the Control group and the Experimental group. A higher relative abundance of Bacteroidota was observed in the Control group (49.46%) compared to the Experimental group, while Firmicutes was found

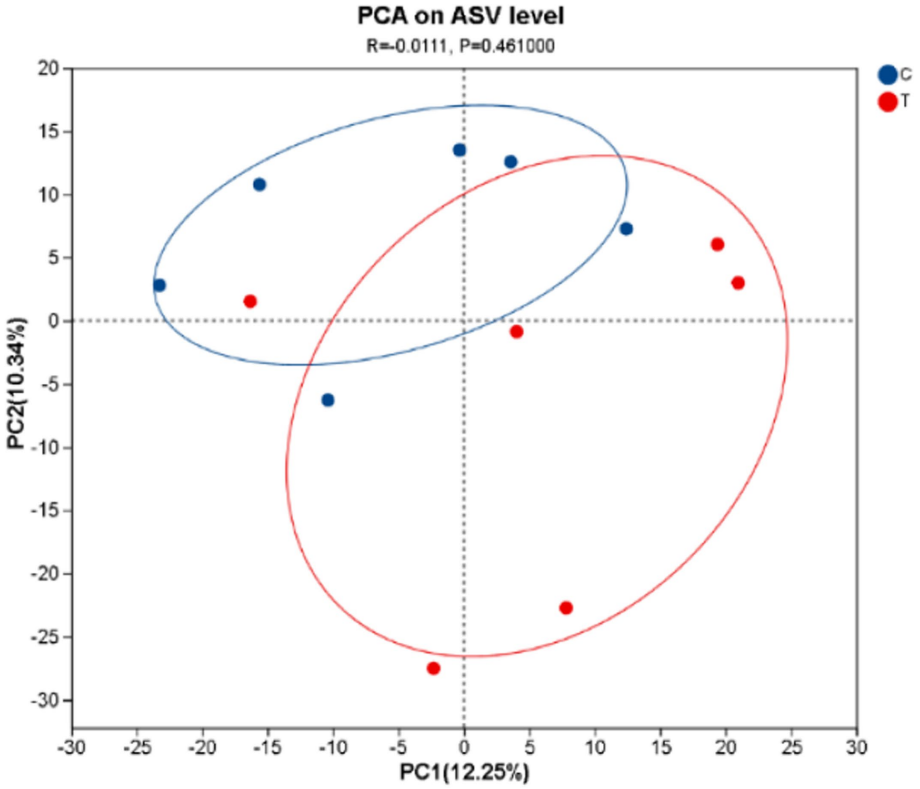

FIGURE 1
The PCA plot was generated. C denotes the control group; T represents the experimental group.

to be more predominant in the Experimental group (50.43%) than in the Control group.

3.1.4 Effects of *L*-Citrulline supplementation on rumen microbiota (family level) in Hu sheep ewes

As shown in Supplementary Figure S1B, Prevotellaceae, Ruminococcaceae, and Lachnospiraceae were predominantly represented among the top 10 families in rumen microbiota relative abundance at the family level, being identified as the dominant families in both the Control group and the Experimental group. A higher relative abundance of Prevotellaceae was observed in the Control group (30.12%) compared to the Experimental group. Higher relative abundances of Ruminococcaceae and Lachnospiraceae were observed in the Experimental group (13.41 and 13.84%, respectively) compared to the Control group. Furthermore, a significantly higher relative abundance of norank_o__Clostridia_UCG-014 was observed in the Experimental group compared to the Control group.

3.1.5 Effects of *L*-Citrulline supplementation on rumen microbiota (genus level) in Hu sheep ewes

As shown in Supplementary Figure S1C, Prevotella and Ruminococcus were predominantly represented among the top 10 genera in rumen microbiota relative abundance at the genus level, being identified as the dominant genera in both the Control group and the Experimental group. A higher relative abundance of Prevotella was observed in the Control group (23.42%) compared to the experimental group, while Ruminococcus was found to be more predominant in the Experimental group (12.61%) than in the Control group. A significantly higher relative abundance of Prevotellaceae_UCG-003 was observed in the Control group compared to the Experimental group, with a statistically significant difference.

3.1.6 Comparative analysis of differential microbial species in rumen microbiota

Figure 2 highlights 19 microbial taxa with significant differences between the Control group and Experimental group, including 1 class, 4 orders, 4 families, and 10 genera. In the Control group, the species Prevotellaceae_UCG-003, Mycoplasmataceae, Mycoplasmatales, Mycoplasma, Prevotellaceae_UCG-004, Rickettsiales, Roseburia, Prevotellaceae_Ga6A1_group, and V9D2013_group are prevalent. The Experimental group is dominated by the species norank_o__Clostridia_UCG-014, Clostridia_UCG-014, norank_o__Clostridia_UCG-014, Negativicutes, norank_f__Eubacterium_coprostanoligenes_group, Eubacterium_coprostanoligenes_group, Acidaminococcales, Succiniclasticum, Acidaminococcaceae, and Lachnospiraceae_XPB1014_group.

3.1.7 Functional prediction

Figure 3 presents the identification of 7 differential metabolic pathways between the Control group and Experimental groups. The primary enriched pathways in the Control group are Lipoic acid metabolism and Nicotinate and nicotinamide metabolism, whereas the Experimental group shows significant enrichment in Prion diseases, Chlorocyclohexane and chlorobenzene degradation, Chloroalkane and chloroalkene degradation, *Biofilm formation – *Escherichia coli*, and Phosphotransferase system (PTS).

10.3389/fmicb.2025.1606437

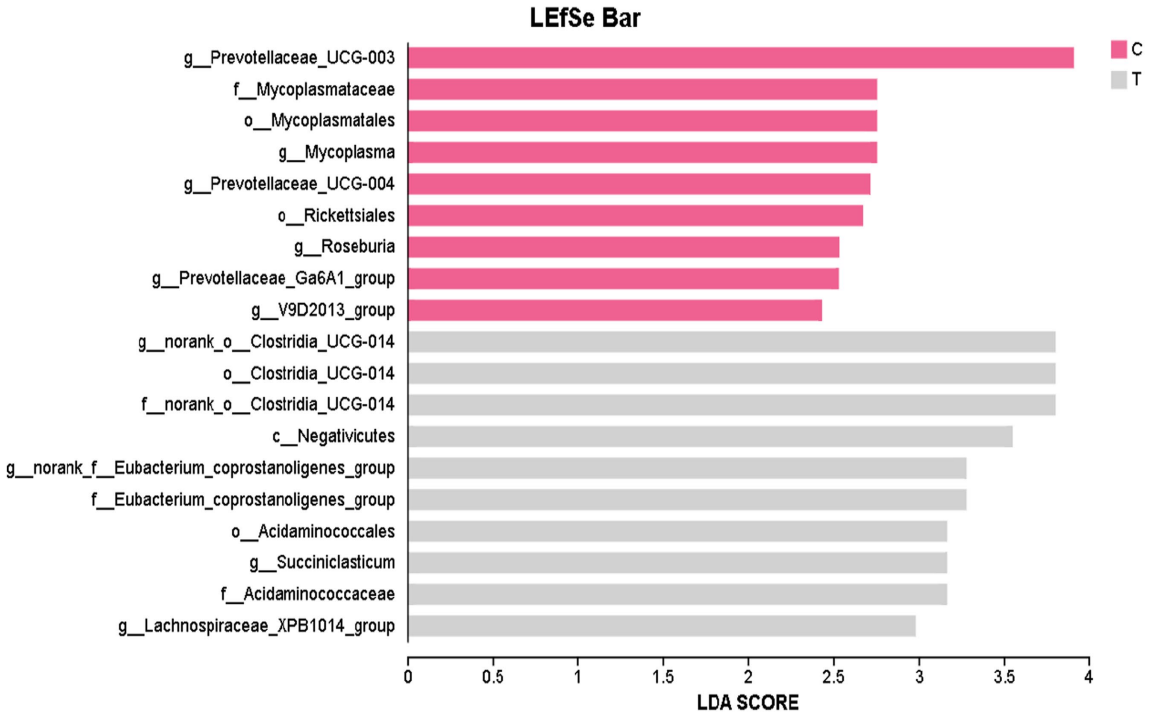

FIGURE 2
The LefSe LDA bar plot was generated to display discriminative features. The LDA discriminant bar chart statistically represents microbial taxa with significant effects across multiple groups. The LDA score, obtained through LDA analysis (linear regression analysis), indicates that the higher the LDA score, the greater the impact of species abundance on the differential effect. C denotes the control group; T represents the experimental group.

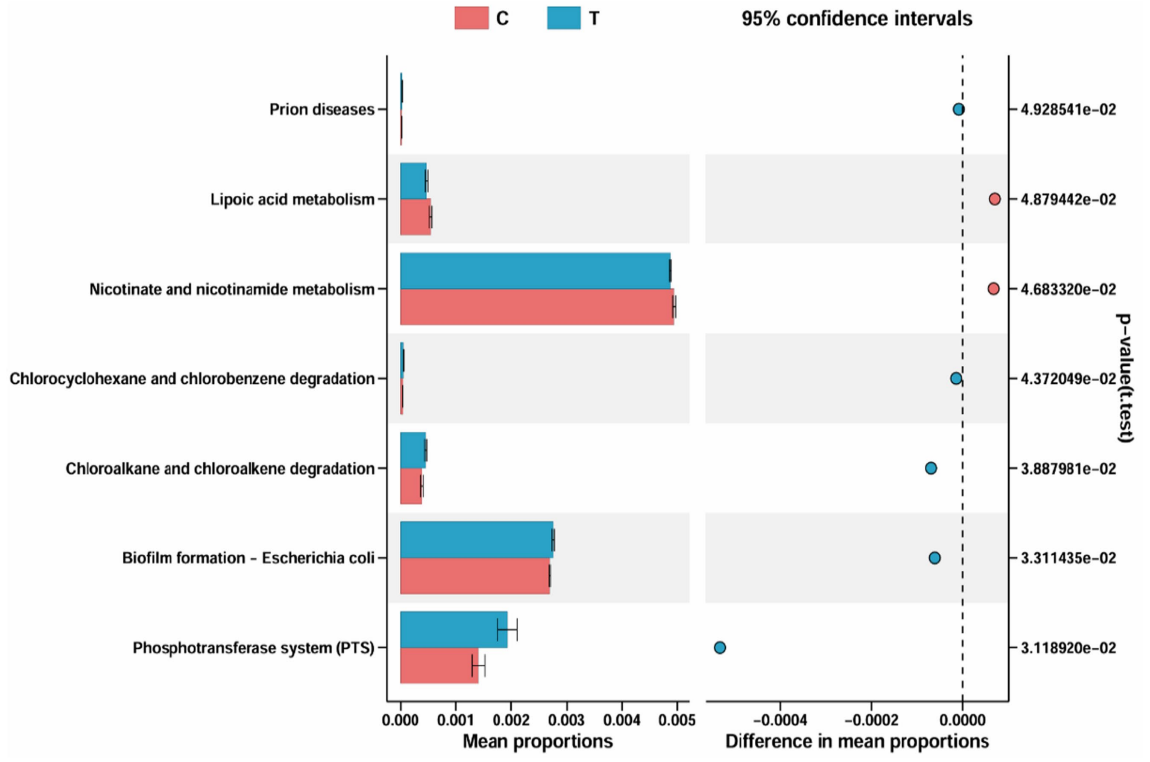

FIGURE 3
Metabolic pathway differences diagram. C denotes the control group; T represents the experimental group.

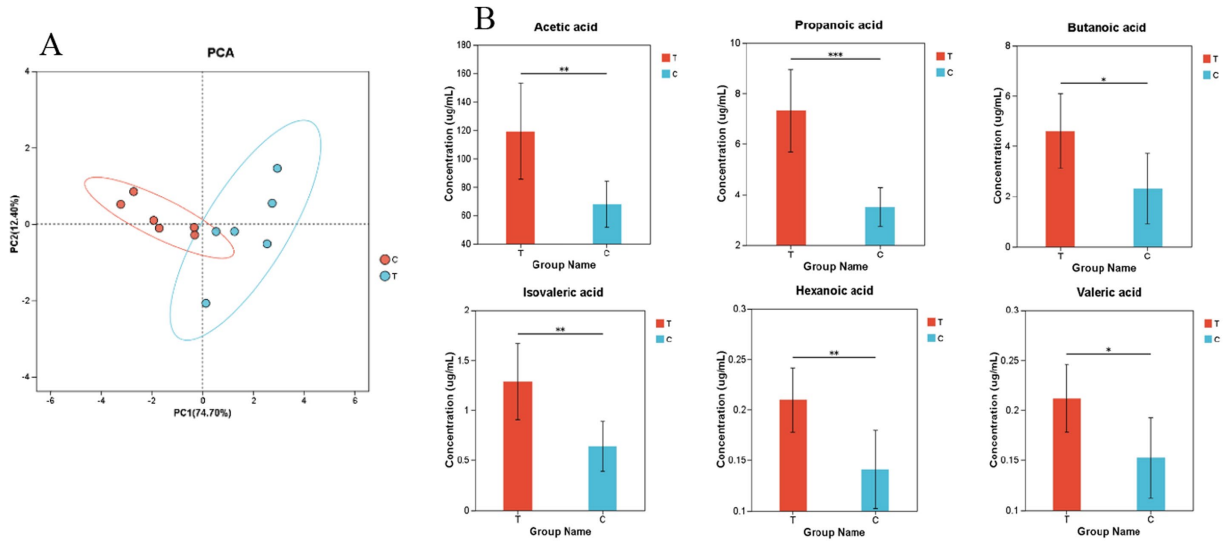

FIGURE 4
(A) Principal Component Analysis **(B)** Bar Chart of Relative Abundance of Volatile Fatty Acids. **(B)** The bar chart represents the relative expression abundance of metabolites in each group. The horizontal axis denotes the different groups, while the vertical axis represents the mass spectrometry intensity values (preprocessed mass spectrometry intensity). The error bars indicate the mean ± standard deviation. Significant differences are marked with asterisks (*$0.01 < p \leq 0.05$, **$0.001 < p \leq 0.01$, ***$p \leq 0.001$). **(A,B)** C denotes the control group; T represents the experimental group.

3.2 Effects of *L*-Citrulline supplementation on volatile fatty acid profiles in the rumen of Hu sheep ewes

As shown in Figure 4A, the first principal component accounts for 74.70% of the sample variation, while the second principal component accounts for 12.40%. The Experimental group exhibits a more dispersed structure and greater variability compared to the Control group.

Figure 4B demonstrates that the relative abundances of acetic acid, propanoic acid, isovaleric acid, and hexanoic acid are significantly higher in the Experimental group than in the Control group. Additionally, the relative abundances of butanoic acid and valeric acid are also significantly elevated in the Experimental group compared to the Control group.

It was found through calculations that the rumen fermentation types of both the control and experimental groups were acetate-type (Supplementary Table S4).

3.3 Impact of *L*-Citrulline supplementation on plasma metabolites in Hu sheep ewes

3.3.1 Partial least squares discriminant analysis

As presented in Figure 5, the PLS-DA score plot effectively visualizes the classification performance of the model. Greater separation between the two sample groups indicates a more significant classification effect. The first principal component explains 16.60% of the variance, while the second principal component accounts for 13.10%.

3.3.2 Screening of differential plasma metabolites

Figure 6 highlights a total of 152 differential metabolites identified in both anion and cation modes, with 70 upregulated and 82 downregulated metabolites. The OPLS-DA model, using VIP values > 1 and $p < 0.05$ as the criteria for significant differential metabolites, revealed a total of 50 metabolites in cation mode, 29 of which exhibited an upward trend. In anion mode, 13 metabolites were identified, with 4 showing an upward trend (Supplementary Tables S4, S5).

3.3.3 KEGG pathway enrichment analysis

As presented in Figure 7A, among the top 20 key enriched pathways, 8 metabolic pathways exhibited significant differences ($p < 0.05$), including Propanoate metabolism, Pyruvate metabolism, Drug metabolism – other enzymes, Arginine and proline metabolism, D-Amino acid metabolism, Alanine, aspartate and glutamate metabolism, Sulfur metabolism, and Cysteine and methionine metabolism. These results indicate that a large portion of the identified differential metabolites are closely associated with the biological functions of these 8 metabolic pathways.

3.3.4 Differential abundance in KEGG pathways

Figure 7B identifies 12 metabolic pathways that tend to be upregulated, including Aminoacyl-tRNA biosynthesis, Biosynthesis of cofactors, Antifolate resistance, Starch and sucrose metabolism, Folate biosynthesis, Central carbon metabolism in cancer, Valine, leucine, and isoleucine biosynthesis, Mineral absorption, ABC transporters, D-Amino acid metabolism, Arginine and proline metabolism, and Drug metabolism – other enzymes. The upregulation trends in pathways such as Starch and sucrose metabolism, Antifolate resistance, and Drug metabolism – other enzymes are significantly more pronounced compared to other pathways. Conversely, 3 metabolic pathways exhibited downregulation, namely Oxidative phosphorylation, Alanine, aspartate, and glutamate metabolism, and Propanoate metabolism.

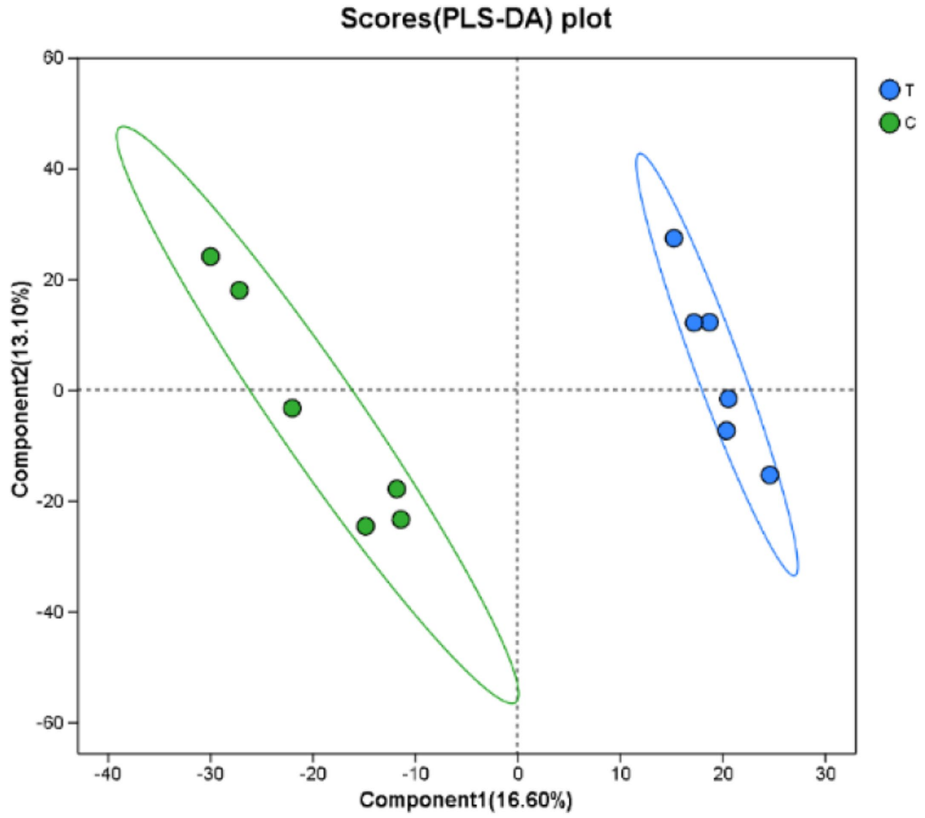

FIGURE 5
PLS-DA score chart. C denotes the control group; T represents the experimental group.

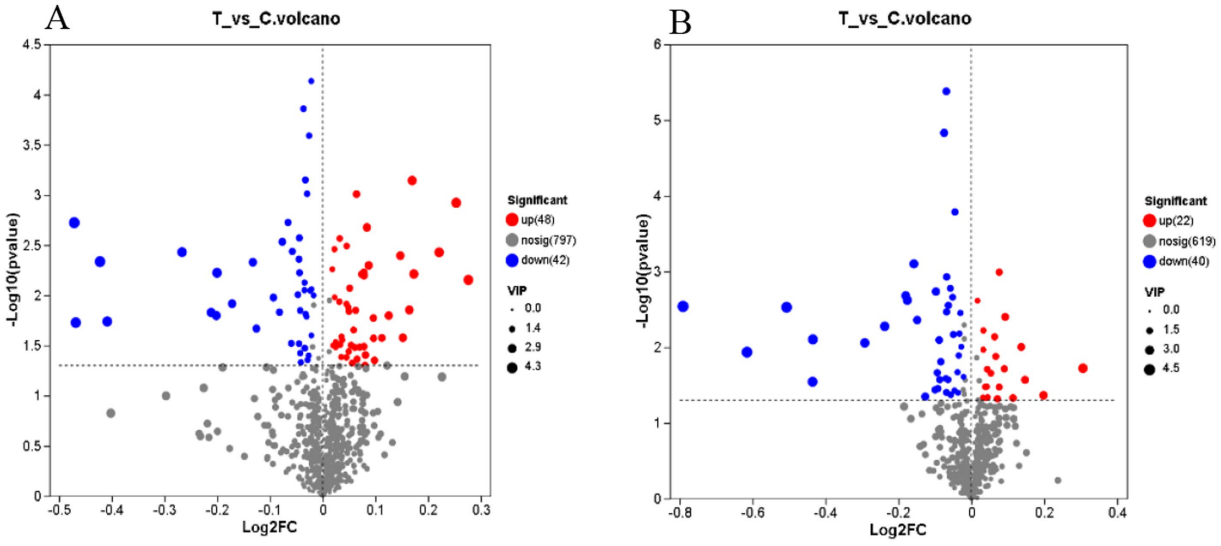

FIGURE 6
Volcanic diagram of differences in the merging of anions and cations. **(A)** Cation mode **(B)** Anion mode. The horizontal axis represents the fold change in metabolite expression between the two groups, i.e., log2FC, while the vertical axis represents the statistical test value of the difference in metabolite expression levels, i.e., −log10 (*p*_value). Higher values indicate more significant expression differences, and both axes are logarithmically transformed. Each point in the graph represents a specific metabolite, with the size of the point indicating the VIP value. By default, red points denote significantly upregulated metabolites, blue points denote significantly downregulated metabolites, and gray points represent non-significant differences. **(A,B)** C denotes the control group; T represents the experimental group.

10.3389/fmicb.2025.1606437

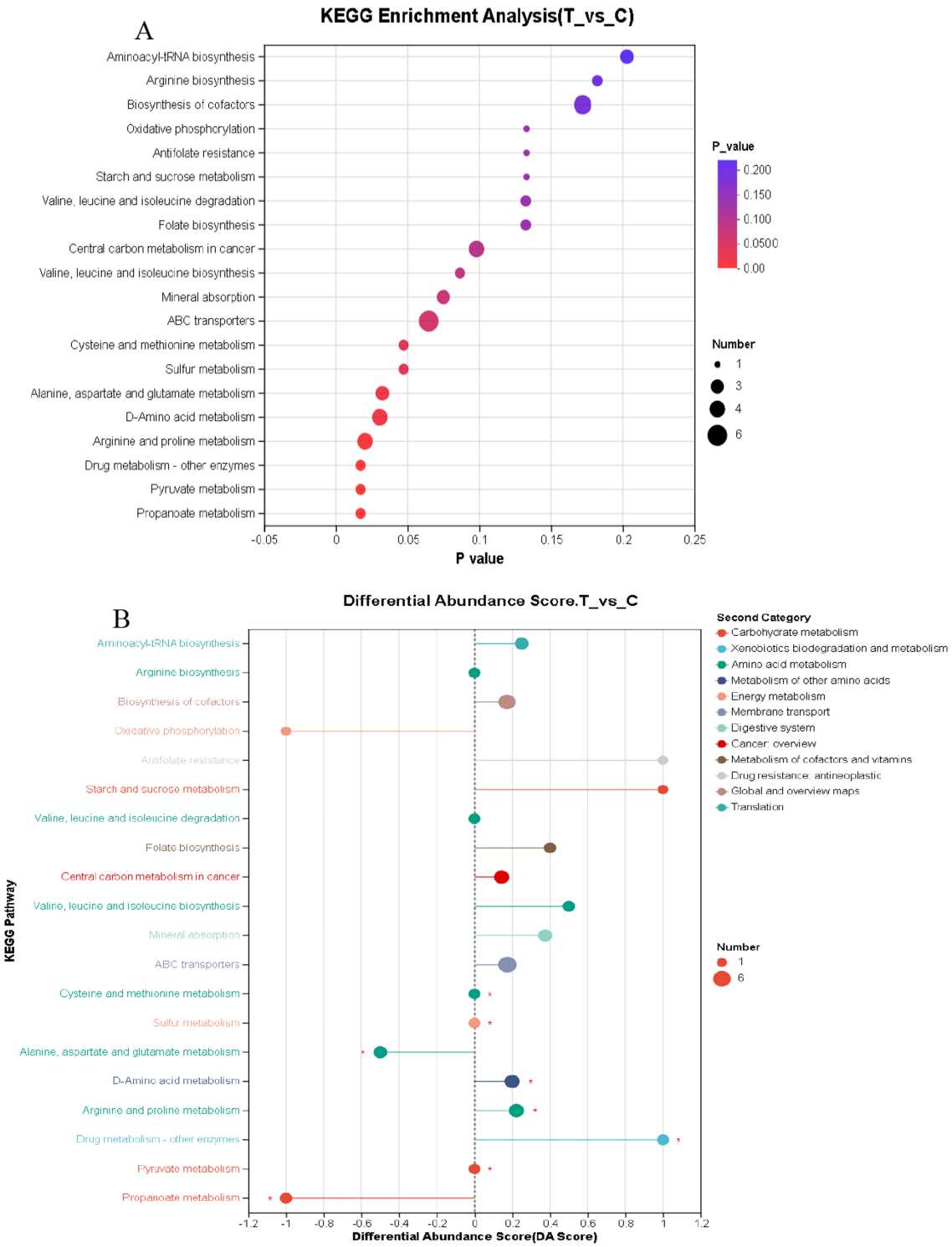

FIGURE 7
(A) KEGG enrichment analysis bubble chart **(B)** KEGG pathway differential abundance score chart. **(A,B)** C denotes the control group; T represents the experimental group. **(A)** The horizontal axis represents the enrichment significance *p*-value; the smaller the p-value, the more statistically significant it is, with a *p*-value less than 0.05 generally considered as a significant enrichment item. The vertical axis represents the KEGG pathways. The size of the bubbles in the graph indicates the number of metabolites enriched in the metabolic set within that pathway. **(B)** In the graph, the horizontal axis represents the Differential Abundance Score (DA Score), while the vertical axis lists the names of the KEGG metabolic pathways. The DA Score reflects the overall changes in all metabolites within a metabolic pathway, with a score of 1 indicating an upward trend in the expression of all annotated differential metabolites in the pathway, and –1 indicating a downward trend. The length of the line segment represents the absolute value of the DA Score. The size of the dots indicates the number of annotated differential metabolites in the pathway, with larger dots representing a greater number of differential metabolites. Dots located to the right of the central axis with longer line segments suggest that the overall expression of the pathway tends to be upregulated; conversely, dots to the left of the central axis with longer line segments indicate a tendency towards downregulation in the pathway's overall expression.

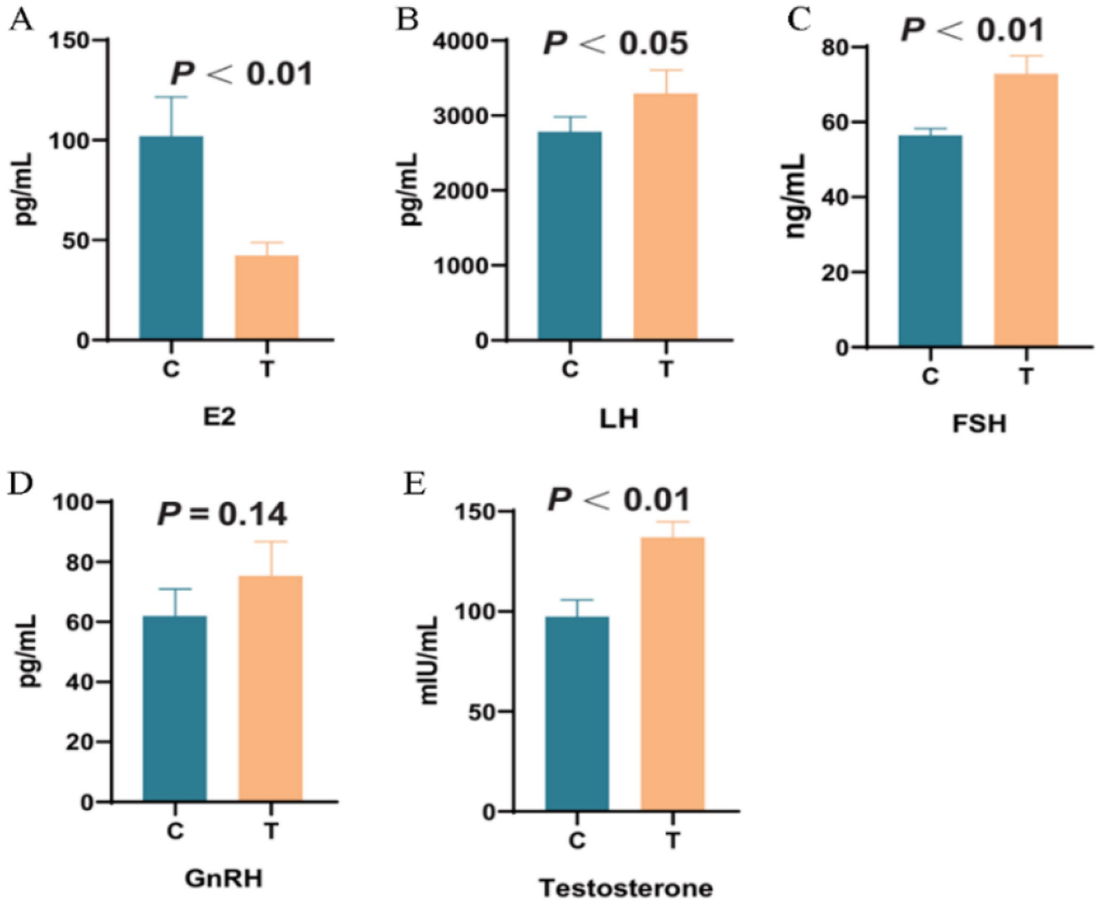

FIGURE 8
The effect of supplementing *L*-Cit on plasma reproductive hormones. Note: C denotes the control group; T represents the experimental group. **(A)**: Estradiol; **(B)**: Luteinizing hormone; **(C)**: Follicle-stimulating hormone; **(D)**: Gonadotropin-releasing hormone; **(E)**: Testosterone.

3.4 Effects of *L*-Citrulline supplementation on reproductive hormone levels in plasma of Hu sheep ewes

As shown in Figure 8, compared with the control group, the plasma E2 level in the experimental group in Figure 8A was significantly reduced by 54.67% ($p < 0.01$). The LH level in Figure 8B was increased by 22.42% ($p < 0.05$), the FSH level in Figure 8C was increased by 16.70% ($p < 0.05$), and the Testosterone level in Figure 8E was increased by 30.02% ($p < 0.01$). No significant change was observed in the GnRH level in Figure 8D.

3.5 Effects of *L*-Citrulline supplementation on plasma antioxidant capacity in Hu sheep ewes

Figure 9 demonstrates that, compared to the Control group, the Experimental group showed significant increases in antioxidant activity: SOD activity increased by 48.30% ($p < 0.01$), MDA levels increased by 23.36% ($p < 0.01$), GSH-PX activity increased by 26.50% ($p < 0.01$), CAT activity increased by 18.49% ($p < 0.01$), and T-AOC increased by 21.43% ($p < 0.01$). However, no significant change in NO levels was observed between the two groups.

3.6 Effects of *L*-Citrulline supplementation on estrus rate and conception rate in Hu sheep ewes

On the 30th day after mating, B-ultrasound detection was conducted. After restraining the ewe, the probe was slowly inserted obliquely upwards into the reproductive tract. Upon reaching the uterine position, the probe was aligned vertically and tightly with the coupling agent-coated skin. As the probe moved, the screen image was monitored. Once pregnancy was confirmed, the ewe's ear tag number was recorded, and the conception rate was calculated. The estrus and conception rates are summarized in Table 2.

4 Correlation analysis

4.1 Correlation analysis of rumen microbial Flora with plasma reproductive hormones and antioxidant capacity

4.1.1 Correlation analysis between rumen microflora (phylum level) and plasma reproductive hormones and antioxidant capacity

The correlation heatmap visualizes the relationships between species and environmental factors, offering a clear representation

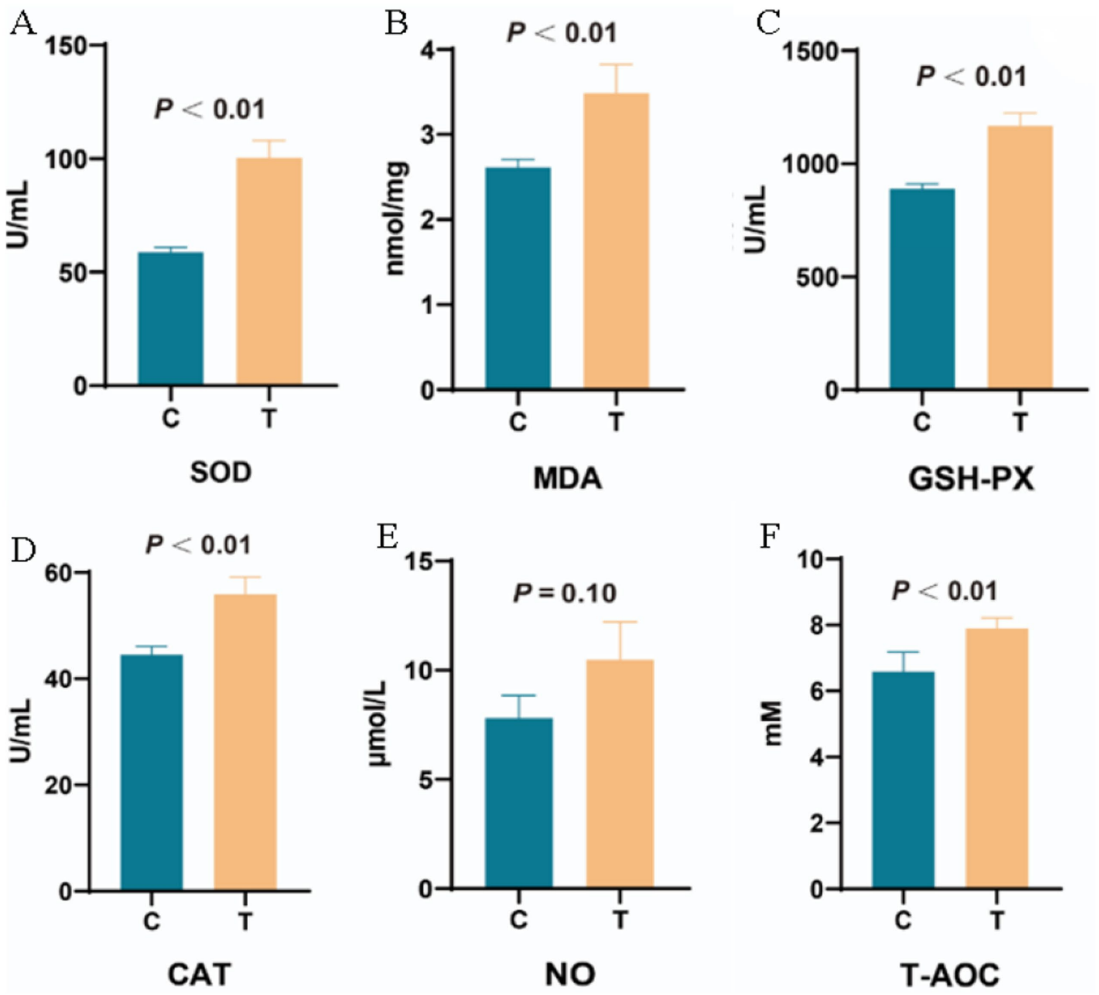

FIGURE 9
The effect of supplementing *L*-Cit on plasma antioxidant capacity. **(A)** Superoxide Dismutase; **(B)** Malondialdehyde; **(C)** Glutathione Peroxidase; **(D)** Catalase; **(E)** Nitric Oxide; **(F)** Total Antioxidant Capacity. Note: C denotes the control group; T represents the experimental group.

TABLE 2 The effect of *L*-Citrulline on estrus rate and conception rate of Hu ewes (%).

Item	Control group (C) group	Experimental group (T) group	*P*-value
Estrus rate	50.00^{b}%(15/30)	93.00^{a}%(28/30)	<0.01
Conception rate	73.00%(11/15)	82.00%(23/28)	-

of correlation magnitudes among various environmental factors and species. It also reveals whether these correlations exhibit significant differences. As illustrated in Figure 10A, correlation analysis of the rumen microbiota of Hu sheep ewes at the phylum level and plasma reproductive hormones identified a significant negative correlation between E_2 levels and Chloroflexi abundance ($0.01 < p \leq 0.05$). LH levels were significantly positively correlated with the abundances of Fusobacteriota, SAR324_cladeMarine_group_B, and Armatimonadota ($0.01 < p \leq 0.05$), while negatively correlated with Bacteroidota abundance ($0.01 < p \leq 0.05$). GnRH content showed a highly significant negative correlation with Proteobacteria ($0.001 < p \leq 0.01$). T concentration was positively correlated with Firmicutes abundance ($0.01 < p \leq 0.05$).

As shown in Figure 10A, a correlation analysis of the rumen microbiota at the phylum level and antioxidant capacity revealed that SOD activity was significantly positively correlated with the abundances of Patescibacteria, Cyanobacteria, and Elusimicrobiota ($0.01 < p \leq 0.05$), while negatively correlated with Bacteroidota ($0.01 < p \leq 0.05$). MDA levels were negatively correlated with Bacteroidota ($0.01 < p \leq 0.05$). CAT activity showed a highly significant positive correlation with Synergistota abundance ($0.001 < p \leq 0.01$). NO concentration was positively correlated with Armatimonadota abundance ($0.01 < p \leq 0.05$). T-AOC concentration was highly positively correlated with the abundance of Elusimicrobiota and Cyanobacteria ($p \leq 0.001$; $0.001 < p \leq 0.01$).

10.3389/fmicb.2025.1606437

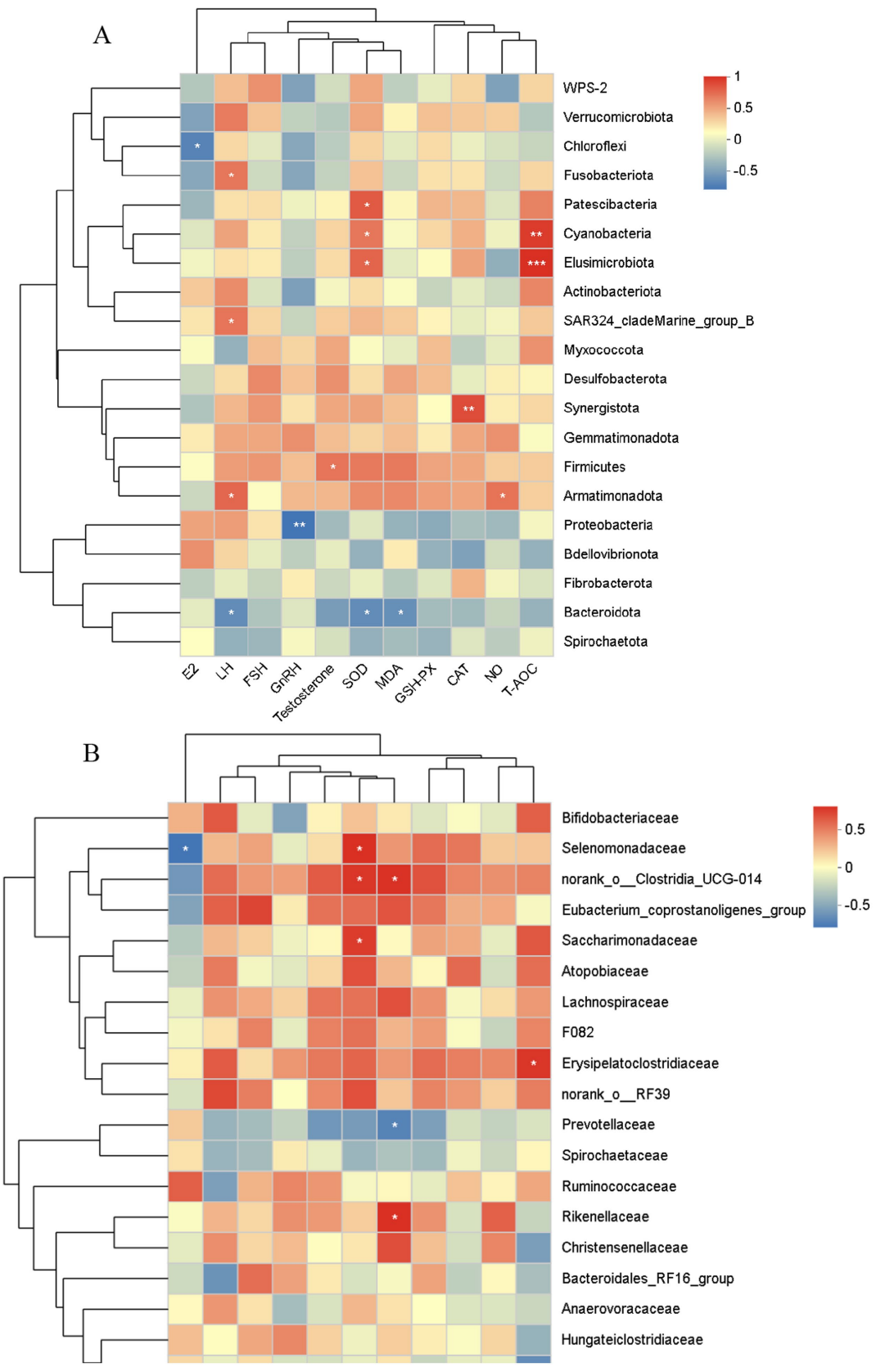

FIGURE 10 (Continued)

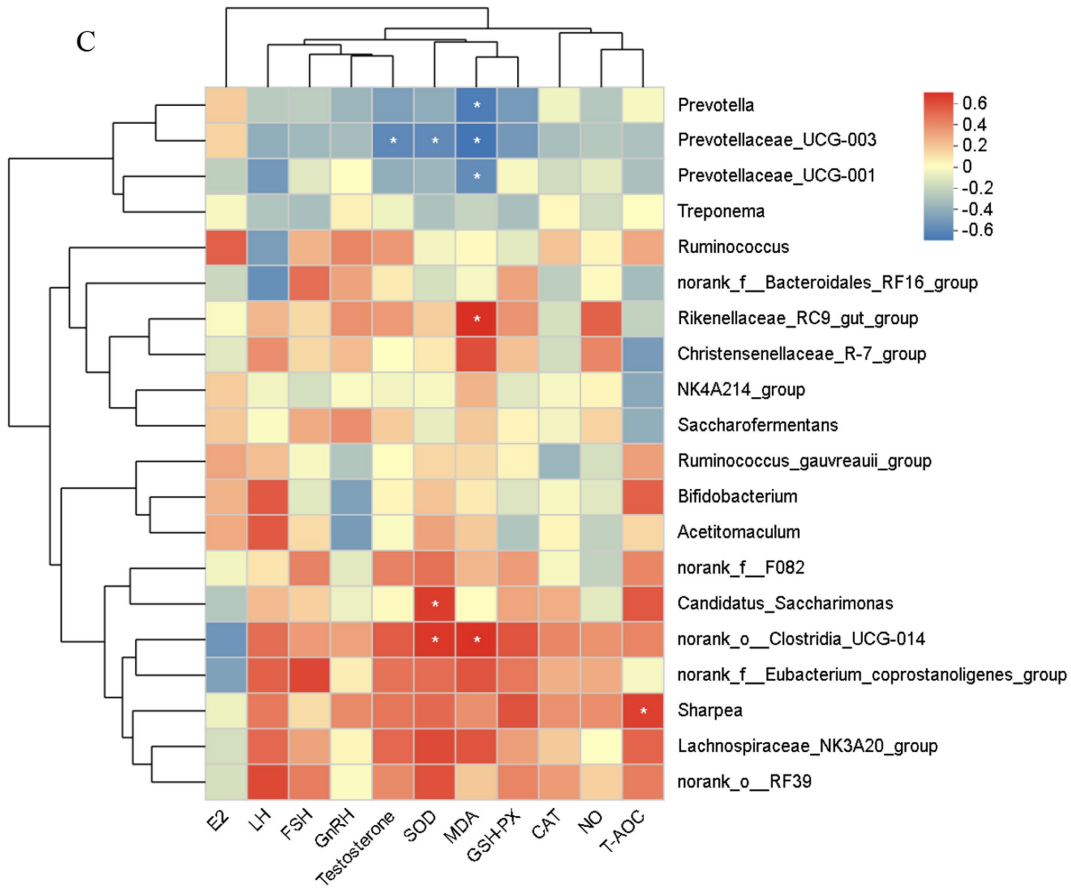

FIGURE 10
Correlation analysis of rumen microbiota with reproductive hormones and antioxidant markers across different levels. **(A)** Phylum level, **(B)** Family level, **(C)** Genus level. The X-axis and Y-axis represent environmental factors and species, respectively. The *R*-value and *p*-value are calculated. The R-value is displayed in different colors in the graph, and if the p-value is less than 0.05, it is marked with an asterisk (*). The legend on the right shows the color range for different *R*-values. *$0.01 < p \leq 0.05$, **$0.001 < p \leq 0.01$, ***$p \leq 0.001$.

4.1.2 Correlation analysis between rumen microflora (family level) and plasma reproductive hormones and antioxidant capacity

Figure 10B depicts the correlation analysis of rumen microbiota at the family level and plasma reproductive hormones, revealing a significant negative correlation between E_2 levels and Selenomonadaceae abundance ($0.01 < p \leq 0.05$). MDA content was significantly positively correlated with the abundance of norank_o__Clostridia_UCG-014 and Rikenellaceae ($0.01 < p \leq 0.05$), but negatively correlated with Prevotellaceae abundance ($0.01 < p \leq 0.05$). T-AOC concentration was significantly positively correlated with Erysipelatoclostridiaceae abundance ($0.01 < p \leq 0.05$), while negatively correlated with Oscillospiraceae abundance ($0.01 < p \leq 0.05$).

4.1.3 Correlation analysis between rumen microflora (genus level) and plasma reproductive hormones and antioxidant capacity

As depicted in Figure 10C, correlation analysis of rumen microbiota at the family level and plasma reproductive hormones in Hu sheep ewes revealed a significant negative correlation between T content and Prevotellaceae_UCG-003 abundance ($0.01 < p \leq 0.05$). Additionally, as shown in Figure 10C, a correlation analysis of rumen microbiota at the phylum level and antioxidant capacity indicated that SOD activity was significantly positively correlated with Candidatus_Saccharimonas and norank_o__Clostridia_UCG-014 abundance ($0.01 < p \leq 0.05$), but significantly negatively correlated with Prevotellaceae_UCG-003 abundance ($0.01 < p \leq 0.05$). MDA content was significantly positively correlated with norank_o__Clostridia_UCG-014 abundance ($0.01 < p \leq 0.05$) and significantly negatively correlated with the abundance of Prevotellaceae_UCG-001, Prevotella, and Prevotellaceae_UCG-003 ($0.01 < p \leq 0.05$). T-AOC concentration was significantly positively correlated with Sharpea abundance ($0.01 < p \leq 0.05$).

4.2 Correlation analysis between rumen microbiota and volatile fatty acids

4.2.1 Correlation analysis between rumen microbiota (phylum level) and volatile fatty acids

As shown in Figure 11A, correlation analysis of rumen microbiota at the phylum level and volatile fatty acids (VFAs) in Hu sheep ewes revealed that the relative abundance of acetic acid was significantly positively correlated with Elusimicrobiota and Cyanobacteria ($0.001 < p \leq 0.01$), as well as with Patescibacteria ($0.01 < p \leq 0.05$), and significantly negatively correlated with Bacteroidota

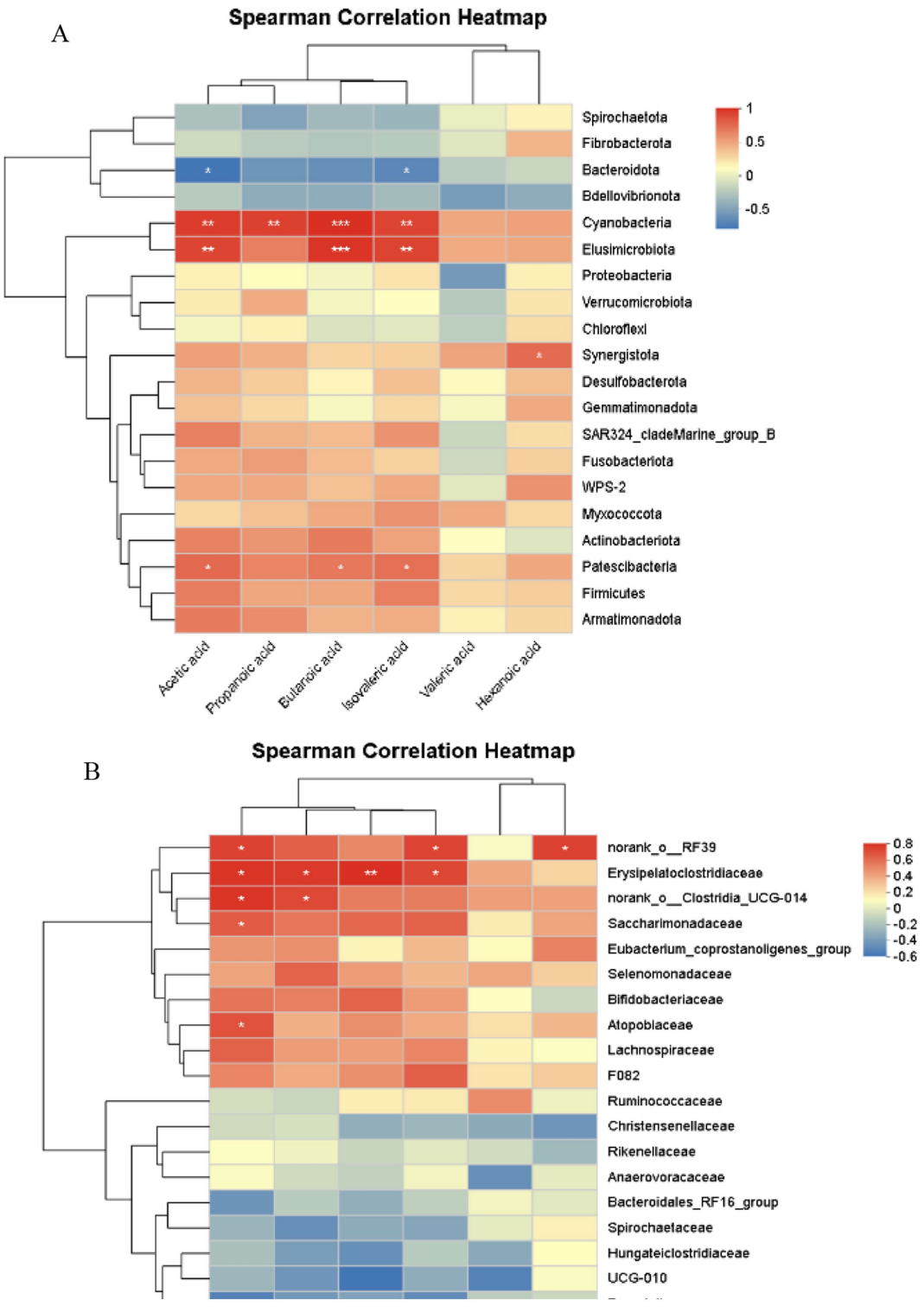

FIGURE 11 (Continued)

($0.01 < p \leq 0.05$). Propanoic acid abundance showed a significant positive correlation with Cyanobacteria ($0.01 < p \leq 0.05$). Butanoic acid was significantly positively correlated with Elusimicrobiota and Cyanobacteria ($0.001 < p \leq 0.01$), and Patescibacteria ($0.01 < p \leq 0.05$). Isovaleric acid was significantly positively correlated with Elusimicrobiota and Cyanobacteria ($0.001 < p \leq 0.01$) as well as with Patescibacteria ($0.01 < p \leq 0.05$), and negatively correlated with Bacteroidota ($0.01 < p \leq 0.05$). Hexanoic acid abundance showed a significant positive correlation with Synergistota ($0.01 < p \leq 0.05$).

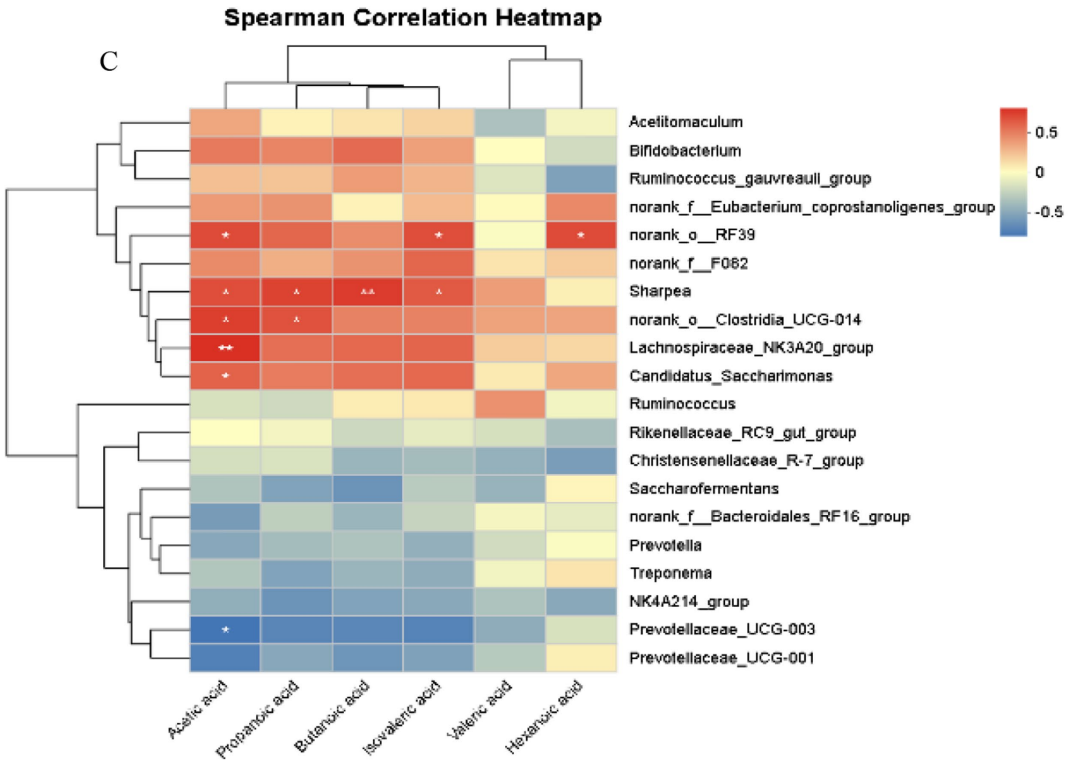

FIGURE 11
Correlation analysis of rumen microbiota and volatile fatty acids (VFAs) across different levels. **(A)** Phylum level, **(B)** Family level, **(C)** Genus level. The X-axis and Y-axis represent environmental factors and species, respectively. The *R*-value and *p*-value are calculated. The *R*-value is displayed in different colors in the graph, and if the *p*-value is less than 0.05, it is marked with an asterisk (*). The legend on the right shows the color range for different *R*-values. *$0.01 < p \leq 0.05$, **$0.001 < p \leq 0.01$, ***$p \leq 0.001$.

4.2.2 Correlation analysis between rumen microbiota (family level) and volatile fatty acids

As shown in Figure 11B, correlation analysis of rumen microbiota at the family level and VFAs in Hu sheep ewes demonstrated that acetic acid was significantly positively correlated with norank_o__RF39, Erysipelatoclostridiaceae, norank_o__Clostridia_UCG-014, Saccharimonadaceae, and Atopobiaceae ($0.01 < p \leq 0.05$). Propanoic acid abundance was significantly positively correlated with Erysipelatoclostridiaceae and norank_o__Clostridia_UCG-014 ($0.01 < p \leq 0.05$). Butanoic acid was significantly positively correlated with Erysipelatoclostridiaceae ($0.001 < p \leq 0.01$). Isovaleric acid was significantly positively correlated with norank_o__RF39 and Erysipelatoclostridiaceae ($0.01 < p \leq 0.05$). Hexanoic acid abundance showed a significant positive correlation with norank_o__RF39 ($0.01 < p \leq 0.05$).

4.2.3 Correlation analysis between rumen microbiota (genus level) and volatile fatty acids

As shown in Figure 11C, correlation analysis of rumen microbiota at the genus level and VFAs in Hu sheep ewes revealed that the relative abundance of acetic acid was significantly positively correlated with Lachnospiraceae_NK3A20_group ($0.001 < p \leq 0.01$), and with norank_o_RF39, Sharpea, norank_o_Clostridia_UCG-014, and Candidatus_Saccharimonas ($0.01 < p \leq 0.05$). It was significantly negatively correlated with the abundance of Prevotellaceae_UCG-003 ($0.01 < p \leq 0.05$). Propanoic acid abundance was significantly positively correlated with Sharpea and norank_o_Clostridia_UCG-014 ($0.01 < p \leq 0.05$). Butanoic acid was significantly positively correlated with Sharpea ($0.001 < p \leq 0.01$). Isovaleric acid abundance was significantly positively correlated with norank_o_RF39 and Sharpea ($0.01 < p \leq 0.05$). Hexanoic acid abundance was significantly positively correlated with norank_o_RF39 ($0.01 < p \leq 0.05$).

4.3 Correlation analysis of plasma metabolites with reproductive hormones and antioxidant capacity

As shown in Figure 12A, correlation analysis of plasma differential metabolites (top 20) and plasma reproductive hormones in Hu sheep ewes revealed that E_2 levels were positively correlated with 2-Methyl-6-{[(5-Phenyl-2-Thienyl)Carbonyl]Amino} Benzoic Acid, Armillaramide, 2,8-Quinolinediol 2-Sulfate, and 3-Indole Carboxylic Acid Glucuronide ($p \leq 0.001$, $0.001 < p \leq 0.01$, $0.01 < p \leq 0.05$), and negatively correlated with *L*-Methionine, *L*-Valine, Gpcho (16:0/22:6), Gpcho (20:5/20:4), Propionylcarnitine, and (+/−)-Propionylcarnitine ($0.001 < p \leq 0.01$, $0.01 < p \leq 0.05$). LH levels were positively correlated with Coixinden B ($0.01 < p \leq 0.05$). FSH levels were negatively correlated with Formycin B, N-[(4E,8Z)-1,3-Dihydroxyoctadeca-4,8-Dien-2-Yl] Hexadecanamide 1-Glucoside, 2-Methyl-6-{[(5-Phenyl-2-Thienyl)Carbonyl]Amino} Benzoic Acid, and 3-Indole Carboxylic Acid Glucuronide ($0.01 < p \leq 0.05$). T levels were positively correlated

10.3389/fmicb.2025.1606437

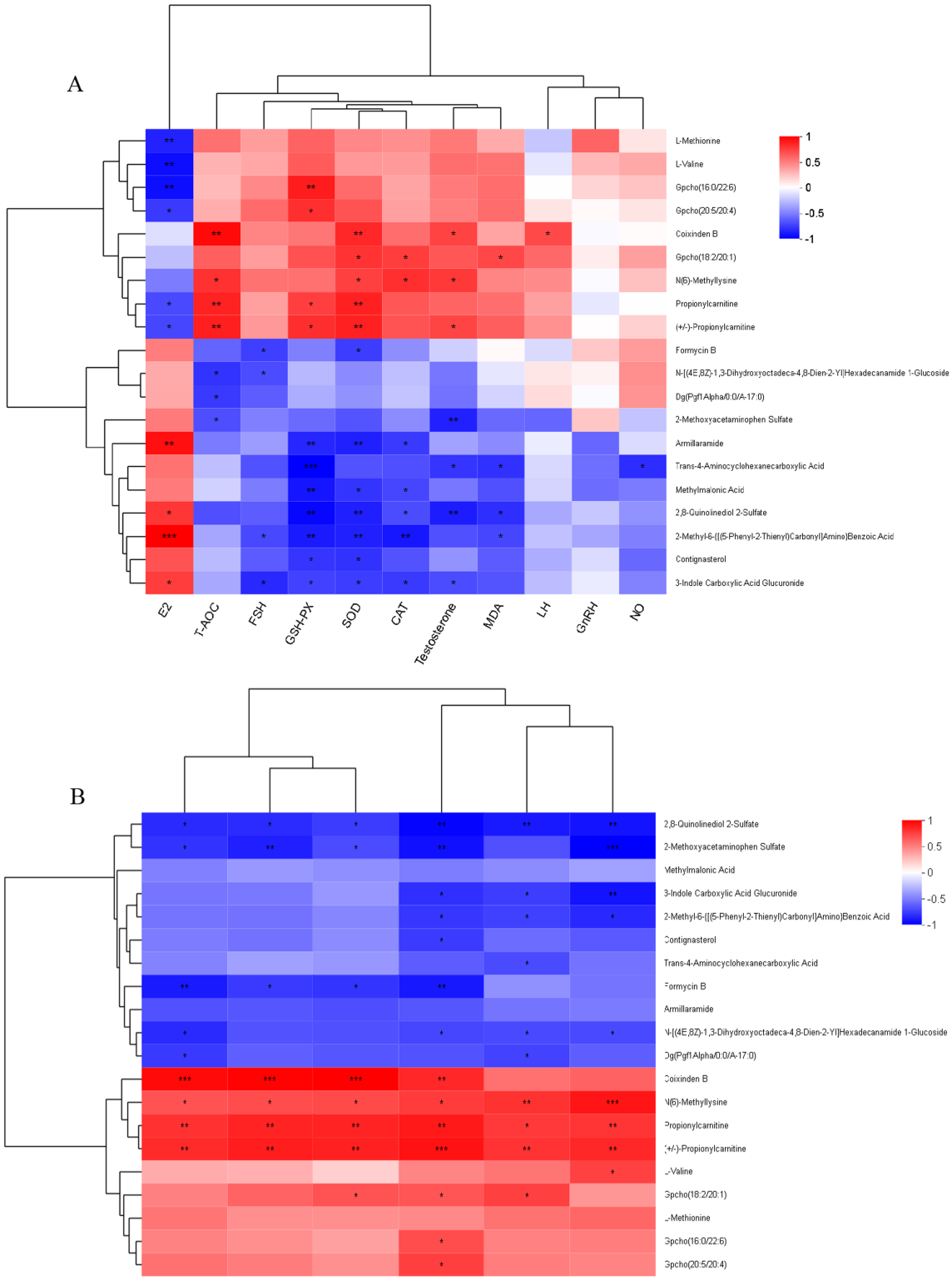

FIGURE 12
(A) Correlation network: plasma metabolites vs. reproductive hormones and antioxidant markers. **(B)** Correlation analysis plot of plasma differential metabolites and volatile fatty acids. The right side of the graph displays the names of metabolites, while the bottom lists the names of associated data. Each cell in the graph represents the correlation between two attributes (metabolites and associated features), with different colors indicating the magnitude of the correlation coefficient between the attributes. Asterisks denote the significance level of the p-value: *$0.01 < p \leq 0.05$, **$0.001 < p \leq 0.01$, ***$p \leq 0.001$.

with Coixinden B, N (6)-Methyllysine, and (+/−)-Propionylcarnitine ($0.01 < p \leq 0.05$), and negatively correlated with 2-Methoxyacetaminophen Sulfate, 2,8-Quinolinediol 2-Sulfate, Trans-4-Aminocyclohexanecarboxylic Acid, and 3-Indole Carboxylic Acid Glucuronide ($0.001 < p \leq 0.01$, $0.01 < p \leq 0.05$).

As shown in Figure 12A, correlation analysis of plasma differential metabolites (top 20) and antioxidant indicators in Hu sheep ewes revealed that SOD activity was significantly positively correlated with Coixinden B, Propionylcarnitine, and (+/−)-Propionylcarnitine ($0.001 < p \leq 0.01$), and with Gpcho (18:2/20:1) and N (6)-Methyllysine ($0.01 < p \leq 0.05$). It was significantly negatively correlated with Armillaramide, 2,8-Quinolinediol 2-Sulfate, and 2-Methyl-6-{[(5-Phenyl-2-Thienyl)Carbonyl]Amino} Benzoic Acid ($0.001 < p \leq 0.01$), as well as with Formycin B, Methylmalonic Acid, Contignasterol, and 3-Indole Carboxylic Acid Glucuronide ($0.01 < p \leq 0.05$).

MDA content exhibited a significant positive correlation with Gpcho (18:2/20:1) ($0.01 < p \leq 0.05$) and a significant negative correlation with Trans-4-Aminocyclohexanecarboxylic Acid, 2,8-Quinolinediol 2-Sulfate, and 2-Methyl-6-{[(5-Phenyl-2-Thienyl) Carbonyl]Amino} Benzoic Acid ($0.01 < p \leq 0.05$).

GSH-PX was significantly positively correlated with Gpcho (16:0/22:6) ($0.001 < p \leq 0.01$); Gpcho (20:5/20:4), Propionylcarnitine, and (+/−)-Propionylcarnitine ($0.01 < p \leq 0.05$); and significantly negatively correlated with Trans-4-Aminocyclohexanecarboxylic Acid ($p \leq 0.001$), Armillaramide, Methylmalonic Acid, 2,8-Quinolinediol 2-Sulfate, and 2-Methyl-6-{[(5-Phenyl-2-Thienyl)Carbonyl]Amino} Benzoic Acid ($0.001 < p \leq 0.01$). Additionally, it exhibited significant negative correlations with Contignasterol and 3-Indole Carboxylic Acid Glucuronide ($0.01 < p \leq 0.05$).

CAT showed a significant positive correlation with Gpcho (18:2/20:1) and N (6)-Methyllysine ($0.01 < p \leq 0.05$), and a significant negative correlation with 2-Methyl-6-{[(5-Phenyl-2-Thienyl) Carbonyl]Amino} Benzoic Acid ($0.001 < p \leq 0.01$), Armillaramide, Methylmalonic Acid, 2,8-Quinolinediol 2-Sulfate, and 3-Indole Carboxylic Acid Glucuronide ($0.01 < p \leq 0.05$). NO displayed a significant negative correlation with Trans-4-Aminocyclohexanecarboxylic Acid ($0.01 < p \leq 0.05$).

T-AOC was extremely positively correlated with Coixinden B, Propionylcarnitine, and (+/−)-Propionylcarnitine ($0.001 < p \leq 0.01$), positively correlated with N (6)-Methyllysine ($0.01 < p \leq 0.05$), and negatively correlated with N-[(4E,8Z)-1,3-Dihydroxyoctadeca-4,8-Dien-2-Yl] Hexadecanamide 1-Glucoside, Dg (Pgf1Alpha/0:0/A-17:0), and 2-Methoxyacetaminophen Sulfate ($0.01 < p \leq 0.05$).

4.4 Correlation analysis between plasma metabolites and volatile fatty acids

Figure 12B illustrates the correlation analysis of plasma differential metabolites (top 20) and VFAs in Hu sheep ewes, revealing that the relative abundance of acetic acid was significantly positively correlated with Coixinden B ($p \leq 0.001$), Propionylcarnitine, and (+/−)-Propionylcarnitine ($0.001 < p \leq 0.01$), positively correlated with N(6)-Methyllysine ($0.01 < p \leq 0.05$), and negatively correlated with 2-Methoxyacetaminophen Sulfate ($0.001 < p \leq 0.01$). Additionally, it showed a significant negative correlation with 2,8-Quinolinediol 2-Sulfate and Formycin B ($0.01 < p \leq 0.05$).

Propanoic acid demonstrated a significant positive correlation with (+/−)-Propionylcarnitine ($p \leq 0.001$), Coixinden B, and Propionylcarnitine ($0.001 < p \leq 0.01$), positively correlated with Gpcho(18:2/20:1), Gpcho(16:0/22:6), and Gpcho(20:5/20:4) ($0.01 < p \leq 0.05$), and negatively correlated with 2,8-Quinolinediol 2-Sulfate, 2-Methoxyacetaminophen Sulfate, and Formycin B ($0.001 < p \leq 0.01$). It also exhibited significant negative correlations with 3-Indole Carboxylic Acid Glucuronide, 2-Methyl-6-{[(5-Phenyl-2-Thienyl)Carbonyl]Amino}Benzoic Acid, Contignasterol, and N-[(4E,8Z)-1,3-Dihydroxyoctadeca-4,8-Dien-2-Yl]Hexadecanamide 1-Glucoside ($0.01 < p \leq 0.05$).

The relative abundance of butanoic acid was significantly positively correlated with Coixinden B ($p \leq 0.001$), Propionylcarnitine, and (+/−)-Propionylcarnitine ($0.001 < p \leq 0.01$), as well as with N(6)-Methyllysine and Gpcho(18:2/20:1) ($0.01 < p \leq 0.05$). It was significantly negatively correlated with 2,8-Quinolinediol 2-Sulfate, 2-Methoxyacetaminophen Sulfate, and Formycin B ($0.01 < p \leq 0.05$).

Isovaleric acid showed a significant positive correlation with Coixinden B ($p \leq 0.001$), Propionylcarnitine, and (+/−)-Propionylcarnitine ($0.001 < p \leq 0.01$), as well as with N(6)-Methyllysine ($0.01 < p \leq 0.05$). It exhibited significant negative correlations with Formycin B ($0.001 < p \leq 0.01$), 2,8-Quinolinediol 2-Sulfate, 2-Methoxyacetaminophen Sulfate, N-[(4E,8Z)-1,3-Dihydroxyoctadeca-4,8-Dien-2-Yl]Hexadecanamide 1-Glucoside, and Dg(Pgf1Alpha/0:0/A-17:0) ($0.01 < p \leq 0.05$).

Valeric acid was significantly positively correlated with N(6)-Methyllysine and (+/−)-Propionylcarnitine ($0.001 < p \leq 0.01$), Propionylcarnitine, and Gpcho(18:2/20:1) ($0.01 < p \leq 0.05$). It showed a significant negative correlation with 2,8-Quinolinediol 2-Sulfate ($0.001 < p \leq 0.01$) and with 3-Indole Carboxylic Acid Glucuronide, 2-Methyl-6-{[(5-Phenyl-2-Thienyl)Carbonyl]Amino}Benzoic Acid, Trans-4-Aminocyclohexanecarboxylic Acid, N-[(4E,8Z)-1,3-Dihydroxyoctadeca-4,8-Dien-2-Yl]Hexadecanamide 1-Glucoside, and Dg(Pgf1Alpha/0:0/A-17:0) ($0.01 < p \leq 0.05$).

Hexanoic acid displayed a significant positive correlation with N(6)-Methyllysine ($p \leq 0.001$), Propionylcarnitine, and (+/−)-Propionylcarnitine ($0.001 < p \leq 0.01$), as well as with Gpcho(18:2/20:1) ($0.01 < p \leq 0.05$). It was significantly negatively correlated with 2-Methoxyacetaminophen Sulfate ($p \leq 0.001$), 2,8-Quinolinediol 2-Sulfate, and 3-Indole Carboxylic Acid Glucuronide ($0.001 < p \leq 0.01$), and with 2-Methyl-6-{[(5-Phenyl-2-Thienyl)Carbonyl]Amino}Benzoic Acid and N-[(4E,8Z)-1,3-Dihydroxyoctadeca-4,8-Dien-2-Yl]Hexadecanamide 1-Glucoside ($0.01 < p \leq 0.05$).

5 Discussion

The rumen of ruminants, a highly intricate micro-ecosystem, harbors a diverse array of microorganisms, including bacteria, archaea, fungi, and protozoa (Indugu et al., 2017). These microorganisms are essential for maintaining rumen homeostasis, promoting fiber degradation, and regulating nutrient metabolism through a dynamic balance of community structure and relative abundance (Stewart et al., 2018). Specifically, plant cell wall polysaccharides are broken down by rumen microbes, releasing VFA, microbial proteins, vitamins, and other nutrients via the secretion of hydrolytic enzymes such as cellulases and hemicellulases. This process

provides approximately 70% of the host's energy requirements (Wirth et al., 2018). Microbial composition analysis reveals that the phyla Firmicutes and Bacteroidetes dominate the rumen microbiome, accounting for over 80% of the microbial community. Core functional genera, including Prevotella, Ruminococcus, and Succinivibrio, collaborate in the cascade of fiber degradation through synergistic interactions (Calabrò, 2015). The metabolic pathways involved include the depolymerization of cellulose into oligosaccharides by primary degraders, followed by conversion into intermediates like succinate and lactate by secondary degraders. These intermediates are subsequently converted into VFAs (acetate:propionate:butyrate ≈ 70:20:10) by acetate-producing and methane-producing bacteria (Stevens and Hume, 1998). In this study, *L*-Cit supplementation significantly altered the rumen microbial community structure. At the phylum level, the relative abundance of Firmicutes increased significantly ($p < 0.05$), while Bacteroidetes and Proteobacteria abundances significantly decreased ($p < 0.05$). Notably, the reduction in Bacteroidetes, which play a pivotal role in soluble polysaccharide metabolism, may be linked to *L*-Cit's regulation of carbohydrate-active enzyme expression (Thomas et al., 2011). Concurrently, the upregulation of genes involved in butyrate synthesis within the Firmicutes phylum may explain the observed increase in butyrate proportion among the VFAs. At the genus level, an increase in Ruminococcus and a decrease in Prevotella abundance were detected in the Experimental group. Additionally, the reduced abundance of Proteobacteria may reflect the inhibition of opportunistic pathogens by *L*-Cit through modulation of redox status (Moon et al., 2018). Alpha diversity analysis revealed higher Sobs, Chao1, and Ace indices in the Experimental group compared to the control group, suggesting that *L*-Cit enhances microbial community diversity. This increase in diversity could be attributed to *L*-Cit's role as an arginine precursor, facilitating nitrogen metabolism within the microbial community (Gilbreath et al., 2020).

This study conducted a systematic analysis of the correlations between the rumen microbiota of Hu sheep ewes and plasma reproductive hormones as well as antioxidant capacity indicators at the phylum, family, and genus levels, uncovering potential links between microbial composition and host physiological functions. The key findings at each taxonomic level are as follows: at the phylum level, the significant negative correlation between Chloroflexi and E_2 suggests that this phylum may inhibit estrogen activity through metabolic or signaling pathways, although the exact mechanisms warrant further investigation. The positive correlations between Fusobacteriota and Armatimonadota with LH may be linked to their role in VFA metabolism. Additionally, the positive correlation between Firmicutes and T could be attributed to the influence of this phylum on steroid hormone synthesis via bile acid metabolism (Lee et al., 2022). In terms of antioxidant capacity, the positive correlations of Cyanobacteria and Elusimicrobiota with SOD activity and T-AOC may reflect their secretion of antioxidant enzymes or the antioxidant properties of their metabolites. The negative correlations between Bacteroidota and both SOD activity and MDA suggest that this phylum might affect oxidative balance by promoting oxidative stress or inhibiting host antioxidant enzyme activity. At the family level, Selenomonadaceae was negatively correlated with E_2 but positively correlated with SOD activity, indicating that this family of microorganisms might influence hormone metabolism and redox balance through distinct mechanisms. At the genus level, Prevotellaceae_UCG-003 showed negative correlations with T and SOD activity, possibly reflecting the inhibitory effects of its fermentation metabolites on hormone synthesis or oxidative stress. Additionally, the positive correlation between norank_o__Clostridia_UCG-014 and MDA suggests that it may exacerbate oxidative damage via lipid peroxidation pathways. This study identified highly significant correlations, such as the association between CAT activity and Synergistota ($p \leq 0.001$), highlighting the reliability of these results and suggesting potent interactions between the microbiota and host. The functional predictions presented in the manuscript are inherently constrained by the absence of experimental validation, resulting in defined limitations within this section. In conclusion, significant associations were found between the rumen microbiota of Hu sheep and reproductive hormones as well as antioxidant capacity across multiple taxonomic levels, suggesting that the microbiota may regulate reproductive endocrinology and oxidative homeostasis through metabolites or host–microbe interactions.

Rumen VFAs, as essential signaling molecules in rumen microbial metabolism, are intimately linked to the physiological functions of the rumen in ruminants, with changes in their composition being of significant importance (Song et al., 2025). As the end products of carbohydrate and amino acid fermentation, VFAs provide 70–80% of the energy requirements for ruminants, contributing to approximately two-thirds of the body's metabolic carbon flux (Zhao et al., 2022a), while also regulating rumen environmental homeostasis through concentration gradients. In this study, rumen pH in both the *L*-Cit supplemented Experimental group and the Control group remained within the physiological range (5.5–7.5), with no significant differences observed between the groups ($p > 0.05$), indicating that *L*-Cit supplementation did not negatively impact rumen fermentation in Hu sheep ewes. Analysis of VFA composition revealed specific metabolic changes in the Experimental group: the relative abundances of butyrate ($p < 0.05$) and valerate ($p < 0.05$) were significantly increased, while acetate, propionate, isovalerate, and caproate showed highly significant increases ($p < 0.01$). These alterations were closely associated with changes in the rumen microbial community structure: the relative abundance of Firmicutes (the primary group of fiber-degrading bacteria) increased, whereas the abundance of Bacteroidetes (dominant polysaccharide-degrading bacteria) decreased. Notably, the non-dominant phyla Cyanobacteria and Elusimicrobiota were significantly enriched in the Experimental group ($p < 0.05$) and were extremely significantly positively correlated with acetic acid, butyric acid, and isovaleric acid ($p < 0.01$), suggesting their potential synergistic role in VFA synthesis. Functional analysis indicated that changes in VFA concentrations induced by *L*-Cit have several physiological implications: the increase in butyric acid enhances the energy supply to ruminal epithelial cells (Fu et al., 2022), while the accumulation of isovaleric acid improves microbial protein efficiency by promoting the synthesis of branched-chain amino acids (Zhang et al., 2022). More importantly, the elevated VFA concentrations activated the host's immune regulatory network: intestinal mucosal dendritic cells and macrophages were stimulated via the GPCR pathway (Shi et al., 2017), leading to the promotion of anti-inflammatory cytokine secretion. Simultaneously, the chemotactic activity of neutrophils was enhanced (Dahlstrand Rudin et al., 2021; Miller et al., 2023), thereby establishing a positive regulation of the "microbiota-metabolite-immunity" axis.

This study analyzed the associations between ruminal microbiota and VFAs in Hu sheep ewes supplemented with *L*-Cit, uncovering the complex relationships between microbial community structure at different taxonomic levels (phylum, family, genus) and VFA production. At the phylum level, Elusimicrobiota and Cyanobacteria were significantly positively correlated with the abundances of VFAs such as acetic acid, butyric acid, and isovaleric acid ($p \leq 0.01$), suggesting that these bacterial groups play a pivotal role in VFA synthesis. Additionally, the negative correlation between Bacteroidota and acetic acid as well as isovaleric acid ($p \leq 0.05$) indicates that this phylum may inhibit VFA metabolic pathways. At the family and genus levels, microbial groups such as Erysipelatoclostridiaceae, Sharpea, and norank_o_RF39 were significantly positively correlated with multiple VFAs, suggesting that these families and genera directly contribute to VFA synthesis. The significant positive correlation between Lachnospiraceae_NK3A20_group and acetic acid ($p \leq 0.01$) further highlights the important role of Firmicutes members in acetic acid production. In conclusion, the associations between ruminal microbiota and VFAs in Hu sheep ewes were taxonomically specific and potentially regulated by *L*-Cit intervention.

Using non-targeted metabolomics technology, the effects of *L*-Cit supplementation on plasma metabolites in Hu sheep ewes were systematically analyzed, revealing potential metabolic regulatory mechanisms. PLS-DA modeling showed a clear separation between the Control group and the Experimental group, indicating that *L*-Cit intervention significantly influenced plasma metabolite profiles. This finding aligns with the strengths of non-targeted metabolomics in detecting dynamic metabolic changes (Ribbenstedt et al., 2018) and provides reliable evidence for the identification of functional metabolites. A total of 152 significantly differential metabolites were identified (50 in the positive ion mode and 13 in the negative ion mode), with 70 metabolites up-regulated and 82 down-regulated. These results suggest that the biological effects of *L*-Cit are mediated through bidirectional regulation of the metabolic network. Notably, the significant enrichment of arginine and proline metabolic pathways (VIP > 1, $p < 0.05$) is likely linked to their roles in nitrogen metabolism, immune regulation, and muscle synthesis (Majumdar et al., 2016). The significant upregulation of drug metabolic pathways, including the "drug metabolism - other enzymes" pathway, suggests that *L*-Cit may indirectly regulate the metabolic efficiency of exogenous substances by influencing the activity of drug-metabolizing enzymes. This finding could provide a valuable reference for future nutritional interventions combined with drug therapies (Fukami et al., 2022). Differential abundance analysis of KEGG pathways revealed that 12 pathways, such as aminoacyl-tRNA biosynthesis and starch and sucrose metabolism, were significantly upregulated, while 3 pathways, including oxidative phosphorylation, were significantly downregulated. The upregulation of aminoacyl-tRNA biosynthesis suggests enhanced protein translation efficiency, thereby supporting anabolic metabolism in the body (Yoon et al., 2024). Conversely, the downregulation of oxidative phosphorylation may indicate a shift in energy metabolism towards glycolysis (Wilson, 2017).

These findings align with the hypothesis that *L*-Cit, as an NO precursor, may regulate mitochondrial function and redox balance (Dawoud and Malinski, 2020). Notably, the bidirectional changes in D-amino acid metabolism pathways, observed in both enrichment and differential abundance analyses, suggest a complex role in host–microbe interactions, warranting further investigation.

The study also explored the regulatory mechanism of *L*-Cit on reproductive hormones in Hu sheep ewes through the NO metabolic pathway. As an arginine precursor for NO synthesis, *L*-Cit influences NO metabolism in macrophages by regulating the activities of arginase and inducible nitric oxide synthase (iNOS)(Romero et al., 2006). Notably, the NO signaling pathway can act on the hypothalamic–pituitary-gonadal (HPG) axis, regulating the pulsatile secretion of GnRH and the release of FSH and LH from the pituitary, ultimately modulating ovarian steroid hormone synthesis (Wu et al., 2005; Zhang, 2011). The experimental results indicated that *L*-Cit supplementation significantly increased the plasma levels of LH, FSH, and T in Hu sheep ewes ($p < 0.05$), while E_2 concentration was extremely significantly decreased ($p < 0.01$). These findings align with those reported by Zhao et al. (2022b) in rams but contrast with the results of Ma et al. (2023). The discrepancy may be attributed to factors such as the method of *L*-Cit administration, the timing of intervention, seasonal influences on the endocrine system, and differences in the pretreatment physiological state of the experimental animals. From a mechanistic perspective, the decrease in E_2 levels may be due to the dual regulatory role of NO: on one hand, NO could reduce gonadotropin release by inhibiting GnRH secretion (Wu et al., 2005), and on the other, it may directly inhibit the activity of aromatase in ovarian granulosa cells (Zhang, 2011). The study also found a significant increase in the estrus rate in the Experimental group, suggesting that *L*-Cit may enhance follicle development and ovulation by optimizing the signaling efficiency of the hypothalamic–pituitary-ovarian axis.

Reactive oxygen species (ROS) are highly reactive chemical species derived from oxygen-containing molecules. They are characterized by the presence of unpaired electrons or unstable chemical bonds and primarily include hydrogen peroxide (H_2O_2), superoxide anion (O_2^-), hydroxyl radical (-OH), and peroxyl radicals (Shields et al., 2021). These molecules can damage biological macromolecules such as lipids, proteins, carbohydrates, and nucleic acids through oxidative stress. To maintain redox homeostasis, animal organisms rely on an antioxidant defense system, which includes enzymes like SOD, CAT, and GSH-Px. In this study, plasma antioxidant indices in Hu sheep ewes revealed that *L*-Cit supplementation significantly increased the activities of SOD, GSH-Px, and CAT ($p < 0.01$), while the levels of MDA and T-AOC were also significantly higher ($p < 0.01$). Notably, while NO levels showed an increasing trend, the differences in NO levels between groups were not statistically significant. These findings contradict the reported decreases in MDA levels observed in studies by Liu (2021) and Li et al. (2024), suggesting that oxidative stress processes may be regulated by *L*-Cit through specific mechanisms. Nitric oxide (NO) exhibits a marked concentration-dependent biphasic effect in biological systems: antioxidative protection is mediated through free radical scavenging at low concentrations, while peroxynitrite ($ONOO^-$), a potent oxidant, is generated via reaction with superoxide anion (O_2^-) at elevated concentrations, leading to oxidative damage such as lipid peroxidation (He et al., 2010). This dual mechanism is manifested through two distinct pathways by which cellular functions are modulated: biological macromolecules are modified either through direct oxidative reactions mediated by $ONOO^-$, or cellular structures are disrupted via free radical-mediated indirect mechanisms. Consequently, signal fine-tuning is achieved under physiological conditions, while severe oxidative stress is induced

during pathological states (Pacher et al., 2007). As central mediators in inflammatory regulation, immune responses are coordinated through a cascade signaling network by inflammatory cytokines. Attenuated inflammatory reactions are directly associated with reduced expression levels of these cytokines (Hunter and Jones, 2015). Specifically, bovine mammary tissue damage is demonstrated to be alleviated and milk production performance is significantly enhanced through inhibition of key factors such as IL-1β (Alnakip et al., 2014). Under heat stress conditions, the upregulation of IL-1β and IL-6 expression is effectively suppressed through supplementation with antioxidants such as vitamin E, resulting in dairy cow production performance being consequently improved (Molinari et al., 2023). Notably, in the weaned calf model, a reduction in diarrhea incidence and a 23% enhancement in daily weight gain are achieved through downregulation of inflammatory cytokines (Hulbert and Moisá, 2016). Such precise regulation is mediated by a dynamic equilibrium network composed of cytokines, their inhibitory factors, and soluble receptors, where spatiotemporal modulation of inflammatory progression is achieved through multi-target synergy (Vebr et al., 2023).

In this study, while no significant differences in plasma NO levels were observed, it is hypothesized that *L*-Cit supplementation may cross the pro-oxidative threshold of NO concentration in the local microenvironment, as suggested by the dose-effect characteristics of iNOS activation. This could explain the observed increase in MDA levels. A significant negative correlation was found between MDA content and the abundance of Bacteroidetes ($p \leq 0.05$). Specifically, compared to the CON group, the relative abundance of Bacteroidetes was decreased in the experimental group, with the abundance of Prevotellaceae_UCG-003, a genus under Bacteroidetes, significantly downregulated ($p = 0.04$). Furthermore, a significant negative correlation was observed with MDA content ($p \leq 0.05$), suggesting that specific Bacteroidetes microbiota may influence oxidative stress by modulating host metabolism. Further plasma metabolomic analysis revealed a significant negative correlation between MDA content and three downregulated metabolites: trans-4-aminocyclohexanecarboxylic acid, 2,8-quinolinediol-2-sulfate, and 2-methyl-6-{[(5-phenyl-2-thienyl)carbonylamino] benzoic acid} ($p \leq 0.05$). These metabolites may indirectly influence lipid peroxidation through their involvement in antioxidant defense or signal transduction pathways (Figure 13).

6 Conclusion

Under the experimental conditions of this study, the following conclusions can be drawn: (Ma et al., 2019) Supplementation with L-citrulline was found to alter the rumen microbiota structure in Hu sheep ewes, resulting in an increased relative abundance of Firmicutes along with decreased relative abundances of Bacteroidetes and Proteobacteria.(Wu et al., 2018) *L*-Citrulline supplementation was demonstrated to significantly increase ($p < 0.01$) the ruminal concentrations of acetate, propionate, isovalerate, and caproate, while significantly elevating ($p < 0.05$) butyrate and valerate levels in Hu sheep ewes.(Cynober et al., 1995) L-citrulline supplementation was shown to enhance glucose metabolic efficiency and xenobiotic degradation capacity in the blood of Hu sheep ewes.(Curis et al., 2005) L-citrulline supplementation significantly improved reproductive hormone levels, estrus rate, and conception rate in Hu sheep ewes.

Therefore, the rumen microbiota structure in Hu sheep ewes is modified through supplemental feeding of L-citrulline, leading to an increase in ruminal volatile fatty acid content. This modification promotes the efficiency of blood glucose metabolism and the

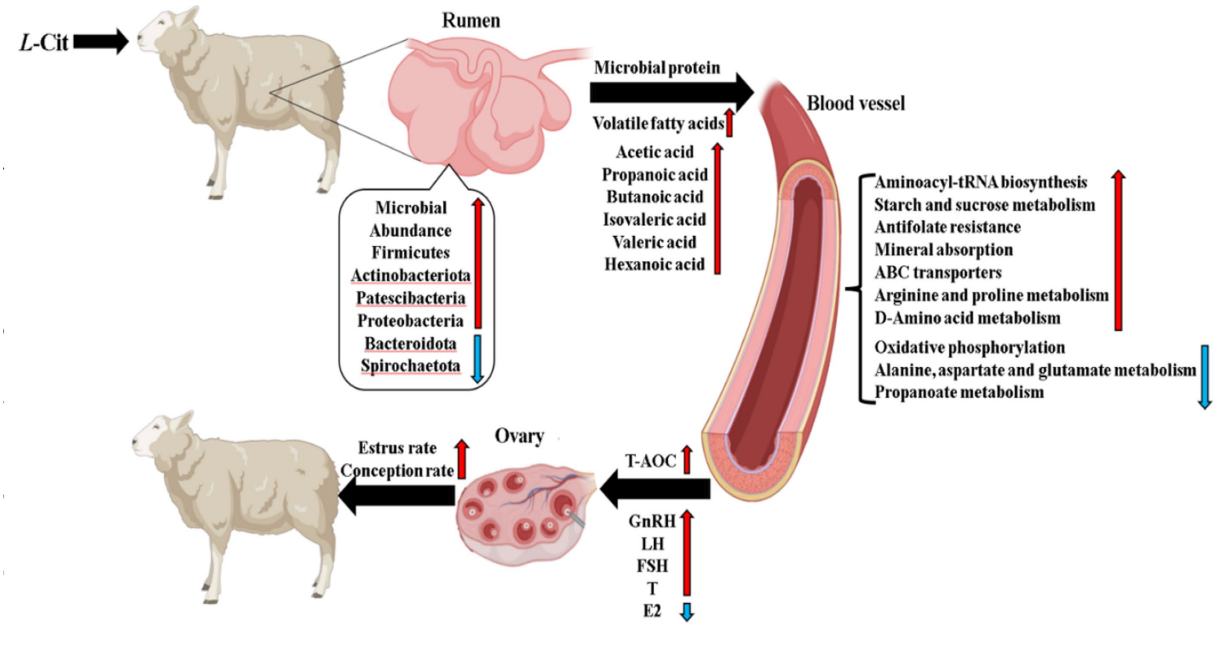

FIGURE 13
Synthesis figure of conclusions.

degradation capacity of exogenous substances in the organism, while relevant reproductive hormone levels are elevated. Consequently, both the estrus rate and conception rate are enhanced through these mechanisms.

Data availability statement

The datasets presented in this study can be found in online repositories. The names of the repository/repositories and accession number(s) can be found in the article/Supplementary material.

Ethics statement

The animal studies were approved by the Animal Experiment Ethics Committee of Xinjiang Agricultural University. The studies were conducted in accordance with the local legislation and institutional requirements. Written informed consent was obtained from the owners for the participation of their animals in this study.

Author contributions

RL: Formal analysis, Visualization, Validation, Conceptualization, Data curation, Writing – original draft, Software, Investigation, Writing – review & editing. PL: Writing – review & editing, Formal analysis, Investigation, Visualization, Validation. CF: Visualization, Writing – review & editing, Investigation, Validation, Formal Analysis. SW: Writing – review & editing, Investigation. ZL: Methodology, Validation, Investigation, Writing – review & editing, Supervision. GZ: Visualization, Formal analysis, Validation, Writing – review & editing, Methodology, Supervision. KY: Validation, Conceptualization, Methodology, Project administration, Supervision, Resources, Funding acquisition, Writing – review & editing, Formal analysis, Visualization.

Funding

The author(s) declare that financial support was received for the research and/or publication of this article. This research was financed by the R&D and integrated demonstration of key technologies for healthy and efficient breeding of local meat sheep in South Xinjiang Uygur Autonomous Region (grant number: 2021YFD1600702-2).

Conflict of interest

ZL was employed by the Xinjiang Shangpin Meiyang Technology Co., Ltd.

The remaining authors declare that the research was conducted in the absence of any commercial or financial relationships that could be construed as a potential conflict of interest.

Generative AI statement

The authors declare that no Gen AI was used in the creation of this manuscript.

Correction note

This article has been corrected with minor changes. These changes do not impact the scientific content of the article.

Publisher's note

All claims expressed in this article are solely those of the authors and do not necessarily represent those of their affiliated organizations, or those of the publisher, the editors and the reviewers. Any product that may be evaluated in this article, or claim that may be made by its manufacturer, is not guaranteed or endorsed by the publisher.

Supplementary material

The Supplementary material for this article can be found online at: https://www.frontiersin.org/articles/10.3389/fmicb.2025.1606437/full#supplementary-material

References

Alnakip, M. E., Quintela-Baluja, M., Böhme, K., Fernández-No, I., Caamaño-Antelo, S., Calo-Mata, P., et al. (2014). The immunology of mammary gland of dairy ruminants between healthy and inflammatory conditions. *J. Vet. Med.*:659801. doi: 10.1155/2014/659801

An, M. (2022). Effects of dietary L-citrulline supplementation on reproductive performance, lactation performance, and lamb growth in Hu ewes, thesis, Xinjiang Agricultural University, Urumqi

Calabrò, S. (2015). "Plant secondary metabolites" in Rumen microbiology: From evolution to revolution. eds. A. Puniya, R. Singh and D. Kamra (New Delhi: Springer), 153–159.

Curis, E., Nicolis, I., Moinard, C., Osowska, S., Zerrouk, N. I. M., Bénazeth, S., et al. (2005). Almost all about citrulline in mammals. *Amino Acids* 29, 177–205. doi: 10.1007/s00726-005-0235-4

Cynober, L., Le Boucher, J., and Vasson, M. P. (1995). Arginine metabolism in mammals. *J. Nutr. Biochem.* 6, 402–413. doi: 10.1016/0955-2863(95)00066-9

Dahlstrand Rudin, A., Khamzeh, A., Venkatakrishnan, V., Basic, A., Christenson, K., and Bylund, J. (2021). Short chain fatty acids released by *Fusobacterium nucleatum* are neutrophil chemoattractants acting via free fatty acid receptor 2 (FFAR2). *Cell. Microbiol.* 23:e13348. doi: 10.1111/cmi.13348

Dawoud, H., and Malinski, T. (2020). Vitamin D3, L-arginine, L-citrulline, and antioxidant supplementation enhances nitric oxide bioavailability and reduces oxidative stress in the vascular endothelium--clinical implications for cardiovascular system. *Pharm. Res.* 12, 17–23. doi: 10.4103/pr.pr_79_19

Fu, Y. Z., Jiao, S., and Zhang, N. F. (2022). Research progress of acidogenic mechanism of butyrate-producing bacteria and its regulation on intestinal health. *Acta Vet. Zootech. Sin.* 53, 4148–4158. doi: 10.11843/j.issn.0366-6964.2022.12.003

Fukami, T., Yokoi, T., and Nakajima, M. (2022). Non-P450 drug-metabolizing enzymes: contribution to drug disposition, toxicity, and development. *Annu. Rev. Pharmacol. Toxicol.* 62, 405–425. doi: 10.1146/annurev-pharmtox-052220-105907

Gilbreath, K. R., Bazer, F. W., Satterfield, M. C., Cleere, J. J., and Wu, G. (2020). Ruminal microbes of adult sheep do not degrade extracellular l-citrulline. *J. Anim. Sci.* 98:skaa164. doi: 10.1093/jas/skaa164

He, J., Chen, M., Liu, X. Y., Wang, Y. P., and Liu, L. B. (2010). Effects of oxidative stress on NF-κB, iNOS and NO in endothelial cells. *J. Fujian Med. Univ.* 44, 186–189. doi: 10.3969/j.issn.1672-4194.2010.03.007

Hulbert, L. E., and Moisá, S. J. (2016). Stress, immunity, and the management of calves. *J. Dairy Sci.* 99, 3199–3216. doi: 10.3168/jds.2015-10198

Hunter, C. A., and Jones, S. A. (2015). IL-6 as a keystone cytokine in health and disease. *Nat. Immunol.* 16, 448–457. doi: 10.1038/ni.3153

Indugu, N., Vecchiarelli, B., Baker, L. D., Ferguson, J. D., Vanamala, J. K., and Pitta, D. W. (2017). Comparison of rumen bacterial communities in dairy herds of different production. *BMC Microbiol.* 17:190. doi: 10.1186/s12866-017-1098-z

Lee, J. W., Cowley, E. S., Wolf, P. G., Doden, H. L., Murai, T., Caicedo, K. Y. O., et al. (2022). Formation of secondary Allo-bile acids by novel enzymes from gut Firmicutes. *Gut Microbes* 14:2132903. doi: 10.1080/19490976.2022.2132903

Li, P., Sun, S., Zhang, W., Ouyang, W., Li, X., and Yang, K. (2024). The Effects of L-citrulline supplementation on the athletic performance, physiological and biochemical parameters, antioxidant capacity, and blood amino acid and polyamine levels in speed-racing Yili Horses. *Animals* 14:2438. doi: 10.3390/ani14162438

Li Xiabin, L. X., Zhao Guodong, Z. G., Qiu Haori, Q. H., Abudukahaer, A., Aizezi, M., and Ai, L. (2019). Effects of L-citrulline on body weight and intestinal flora diversity of mice. *Chin. J. Anim. Nutr.* 31, 4235–4241. doi: 10.3969/j.issn.1006-267x.2019.09.037

Liu, Z. Q. (2021). Effects of different dosages of L-citrulline on reproductive hormones and antioxidant capacity in Turpan black rams, thesis, Xinjiang Agricultural University, Urumqi

Ma, Y., Zeng, Z., Kong, L., Chen, Y., and He, P. (2019). Determination of N-carbamylglutamate in feeds and animal products by high performance liquid chromatography tandem mass spectrometry. *Molecules* 24, 3172–3176. doi: 10.3390/molecules24173172

Ma, Y., Zhao, G., Wang, C., An, M., Ma, C., Liu, Z., et al. (2023). Effects of supplementation with different concentrations of L-citrulline on the plasma amino acid concentration, reproductive hormone concentrations, antioxidant capacity, and reproductive performance of Hu ewes. *Anim. Prod. Sci.* 63, 853–861. doi: 10.1071/AN22290

Majumdar, R., Barchi, B., Turlapati, S. A., Gagne, M., Minocha, R., Long, S., et al. (2016). Glutamate, ornithine, arginine, proline, and polyamine metabolic interactions: the pathway is regulated at the post-transcriptional level. *Front. Plant Sci.* 7, 1–17. doi: 10.3389/fpls.2016.00078

Miller, A., Fantone, K. M., Tucker, S. L., Gokanapudi, N., Goldberg, J. B., and Rada, B. (2023). Short chain fatty acids reduce the respiratory burst of human neutrophils in response to cystic fibrosis isolates of *staphylococcus aureus*. *J. Cyst. Fibros.* 22, 756–762. doi: 10.1016/j.jcf.2023.04.022

Molinari, P. C., Davidson, B. D., Laporta, J., Dahl, G. E., Sheldon, I. M., and Bromfield, J. J. (2023). Prepartum heat stress in dairy cows increases postpartum inflammatory responses in blood of lactating dairy cows. *J. Dairy Sci.* 106, 1464–1474. doi: 10.3168/jds.2022-22405

Moon, C. D., Young, W., Maclean, P. H., Cookson, A. L., and Bermingham, E. N. (2018). Metagenomic insights into the roles of Proteobacteria in the gastrointestinal microbiomes of healthy dogs and cats. *Microbiology* 7:e00677. doi: 10.1002/mbo3.677

Pacher, P., Beckman, J. S., and Liaudet, L. (2007). Nitric oxide and peroxynitrite in health and disease. *Physiol. Rev.* 87, 315–424. doi: 10.1152/physrev.00029.2006

Ribbenstedt, A., Ziarrusta, H., and Benskin, J. P. (2018). Development, characterization and comparisons of targeted and non-targeted metabolomics methods. *PLoS One* 13:e0207082. doi: 10.1371/journal.pone.0207082

Romero, M. J., Platt, D. H., Caldwell, R. B., and Caldwell, R. W. (2006). Therapeutic use of citrulline in cardiovascular disease. *Cardiovasc. Drug Rev.* 24, 275–290. doi: 10.1111/j.1527-3466.2006.00275.x

Schwedhelm, E., Maas, R., Freese, R., Jung, D., Lukacs, Z., Jambrecina, A., et al. (2008). Pharmacokinetic and pharmacodynamic properties of oral L-citrulline and L-arginine: impact on nitric oxide metabolism. *Br. J. Clin. Pharmacol.* 65, 51–59. doi: 10.1111/j.1365-2125.2007.02990.x

Shi, N., Li, N., Duan, X., and Niu, H. (2017). Interaction between the gut microbiome and mucosal immune system. *Mil. Med. Res.* 4, 1–7. doi: 10.1186/s40779-017-0122-9

Shields, H. J., Traa, A., and Van Raamsdonk, J. M. (2021). Beneficial and detrimental effects of reactive oxygen species on lifespan: a comprehensive review of comparative and experimental studies. *Front. Cell Dev. Biol.* 9:628157. doi: 10.3389/fcell.2021.628157

Song, L., Zhao, X. W., Qi, Y. J., and Zhang, Y. D. (2025). Research advances on the effects of short-chain fatty acids on the rumen microbial community in dairy cows. *Acta Veterin. Zootech. Sin.* 56, 2082–2092. doi: 10.11843/j.issn.0366-6964.2025.05.009

Stevens, C. E., and Hume, I. D. (1998). Contributions of microbes in vertebrate gastrointestinal tract to production and conservation of nutrients. *Physiol. Rev.* 78, 393–427. doi: 10.1152/physrev.1998.78.2.393

Stewart, R. D., Auffret, M. D., Warr, A., Wiser, A. H., Press, M. O., Langford, K. W., et al. (2018). Assembly of 913 microbial genomes from metagenomic sequencing of the cow rumen. *Nat. Commun.* 9:870. doi: 10.1038/s41467-018-03317-6

Suzuki, T., Morita, M., Kobayashi, Y., and Kamimura, A. (2015). Oral L-citrulline supplementation enhances cycling time trial performance in healthy well-trained males. *J. Int. Soc. Sports Nutr.* 12:P52. doi: 10.1186/1550-2783-12-S1-P52

Thomas, F., Hehemann, J. H., Rebuffet, E., Czjzek, M., and Michel, G. (2011). Environmental and gut bacteroidetes: the food connection. *Front. Microbiol.* 2:93. doi: 10.3389/fmicb.2011.00093

Vebr, M., Pomahačová, R., Sýkora, J., and Schwarz, J. (2023). A narrative review of cytokine networks: pathophysiological and therapeutic implications for inflammatory bowel disease pathogenesis. *Biomedicines* 11:3229. doi: 10.3390/biomedicines11123229

Wilson, D. F. (2017). Oxidative phosphorylation: regulation and role in cellular and tissue metabolism. *J. Physiol.* 595, 7023–7038. doi: 10.1113/JP273839

Wirth, R., Kádár, G., Kakuk, B., Maróti, G., Bagi, Z., Szilágyi, Á., et al. (2018). The planktonic core microbiome and core functions in the cattle rumen by next generation sequencing. *Front. Microbiol.* 9:2285. doi: 10.3389/fmicb.2018.02285

Wu, G., Bazer, F. W., Johnson, G. A., and Hou, Y. (2018). BOARD-INVITED REVIEW: arginine nutrition and metabolism in growing, gestating, and lactating swine. *J. Anim. Sci.* 96, 5035–5051. doi: 10.1093/jas/sky377

Wu, X. F., Sang, R. Z., Zhang, Z. L., Zhang, G. L., and Zhang, Y. (2005). Physiological regulation of nitric oxide on the hypothalamic-pituitary-ovarian axis. *Prog. Vet. Med.* 26, 4–7. doi: 10.16437/j.cnki.1007-5038.2005.07.002

Xian, M., Shen, L., Zhan, S., Chen, S., Lin, H., Cai, J., et al. (2022). Integrated 16S rRNA gene sequencing and LC/MS-based metabolomics ascertained synergistic influences of the combination of acupuncture and NaoMaiTong on ischemic stroke. *J. Ethnopharmacol.* 293:115281.

Yoon, I., Kim, U., Choi, J., and Kim, S. (2024). Disease association and therapeutic routes of aminoacyl-tRNA synthetases. *Trends Mol. Med.* 30, 89–105. doi: 10.1016/j.molmed.2023.10.006

Zhang, Y. (2011). Study on the dual regulatory effects of gnrh analogues on ovarian cancer and ovarian function, thesis, Fudan University, Shanghai

Zhang, Z. W., Zhu, M. X., and Wang, C. F. (2022). Effects of isoacids on ruminal metabolism and performance in rumiants: a review. *Chin. J. Anim. Nutr.* 34, 1408–1415. doi: 10.3969/j.issn.1006.267x.2022.03.005

Zhao, Y., Zhang, Y., Khas, E., Ao, C., and Bai, C. (2022a). Effects of Allium mongolicum regel ethanol extract on three flavor-related rumen branched-chain fatty acids, rumen fermentation and rumen bacteria in lambs. *Front. Microbiol.* 13:978057. doi: 10.3389/fmicb.2022.978057

Zhao, G., Zhao, X., Song, Y., Haire, A., Dilixiati, A., Liu, Z., et al. (2022b). Effect of L-citrulline supplementation on sperm characteristics and hormonal and antioxidant levels in blood and seminal plasma of rams. *Reprod. Domest. Anim.* 57, 722–733. doi: 10.1111/rda.14111

frontiers | Frontiers in Microbiology

TYPE Review
PUBLISHED 09 July 2025
DOI 10.3389/fmicb.2025.1566267

Check for updates

OPEN ACCESS

EDITED BY
Mohammad Altamimi,
An-Najah National University, Palestine

REVIEWED BY
Luana De Mendonça Oliveira,
University of São Paulo, Brazil
Muhammad Zohaib Aslam,
Tuskegee University, United States

*CORRESPONDENCE
Chuanjian Yuan
✉ 18340077693@163.com
Junling Zhang
✉ zhangjunlingtj@126.com

RECEIVED 24 January 2025
ACCEPTED 27 June 2025
PUBLISHED 09 July 2025

CITATION
Yuan C, Liu L, Zeng D, Yuan J, Guo L and Zhang J (2025) Exploring the influence of gut microbiota metabolites on vitiligo through the gut-skin axis.
Front. Microbiol. 16:1566267.
doi: 10.3389/fmicb.2025.1566267

COPYRIGHT
© 2025 Yuan, Liu, Zeng, Yuan, Guo and Zhang. This is an open-access article distributed under the terms of the Creative Commons Attribution License (CC BY). The use, distribution or reproduction in other forums is permitted, provided the original author(s) and the copyright owner(s) are credited and that the original publication in this journal is cited, in accordance with accepted academic practice. No use, distribution or reproduction is permitted which does not comply with these terms.

Exploring the influence of gut microbiota metabolites on vitiligo through the gut-skin axis

Chuanjian Yuan[1]*, Lyuye Liu[1], Duorong Zeng[1], Jinxiang Yuan[1], Liyuan Guo[2] and Junling Zhang[2]*

[1]Graduate School, Tianjin University of Traditional Chinese Medicine, Tianjin, China, [2]Department of Dermatology, Affiliated Hospital of Tianjin Academy of Traditional Chinese Medicine, Tianjin, China

Vitiligo is an autoimmune skin disease with a complex pathogenesis closely linked to immune imbalance and oxidative stress. Currently, comprehensive curative treatments and effective relapse prevention strategies are lacking. Recently, the "gut-skin axis" hypothesis has offered new insights into the pathological mechanisms of vitiligo. Studies indicate that gut microbiota and their metabolic products significantly affect disease progression by regulating immune homeostasis and inflammatory responses in the host. This review systematically examines the effects of short-chain fatty acids, secondary bile acids, and tryptophan metabolites on the human immune system and the inflammatory milieu, and their direct impact on melanocytes. Furthermore, considering the reduced diversity of gut microbiota in individuals with vitiligo, this article also evaluates methods including probiotic intervention, the Mediterranean diet, and fecal microbiota transplantation, which may emerge as potential therapeutic strategies for vitiligo by restoring microbiota balance. Future multidimensional therapeutic strategies that target gut microbiota metabolites show promise for pioneering innovative approaches in vitiligo management.

KEYWORDS

vitiligo, gut microbiota, short-chain fatty acids, secondary bile acids, tryptophan

1 Introduction

Vitiligo is an autoimmune disorder characterized by the progressive loss of melanocytes (MCs) and resulting skin depigmentation (Utama et al., 2024). Damage to MCs is influenced by various factors, such as genetic susceptibility, autoimmunity, and oxidative stress (Iwanowski et al., 2023). Immune responses in MCs can be triggered by endogenous or exogenous factors, including damage-associated molecular patterns (DAMPs) (Migayron et al., 2020). Current treatments for vitiligo (including topical agents, phototherapy, and immunosuppressants) primarily aim to suppress immune responses or promote localized repigmentation, yet they generally fail to completely halt disease progression or prevent recurrence. Notably, some patients may experience even more extensive depigmentation following treatment discontinuation. Furthermore, long-term use of corticosteroids or immunosuppressive agents may lead to adverse effects such as cutaneous atrophy and increased infection risks, while surgical interventions like autologous epidermal transplantation present traumatic risks and prove unsuitable for patients with extensive lesions. Collectively, these therapeutic approaches demonstrate unstable efficacy due to their insufficient targeting of vitiligo's underlying pathogenic mechanisms. The intractable nature and high recurrence rate of vitiligo reflect the delicate balance of immune system homeostasis in affected individuals. The gut

microenvironment is essential for immune system homeostasis, with the gut microbiota influencing skin health through strain transfer, metabolite exchange, and immune regulation (Sinha et al., 2021; Gao et al., 2023). Recent studies based on the "gut-skin axis" hypothesis suggest that gut microbiota and their metabolites, including short-chain fatty acids (SCFAs), tryptophan(Trp), and secondary bile acids (SBAs), play a vital role in regulating immune responses, inflammation, and metabolism (Mostafavi Abdolmaleky and Zhou, 2024; Xiao et al., 2023). The gut microbiota and its metabolites effectively maintain the intestinal barrier and regulate disease progression in skin disorders like psoriasis and atopic dermatitis (Li et al., 2024; Zhang et al., 2024; Pessôa et al., 2023). However, there is a current lack of a comprehensive review concerning the impact of gut microbiota and its metabolites on vitiligo. Consequently, this review examines the influence of gut microbiota and its metabolites on the host's immune system and inflammation via the gut-skin axis, to identify novel therapeutic strategies for the clinical management of vitiligo.

The gut and skin both possess extensive neural and vascular networks that perform immunoregulatory and neuroendocrine functions. Sharing a common embryonic origin (the endoderm), both the gut and skin host diverse symbiotic microbial communities with significant functional correlations (Salem et al., 2018). Numerous studies provided evidence for a profound bidirectional link between gastrointestinal health and skin homeostasis through modification of the immune system (De Pessemier et al., 2021). Imbalances in the gut microbiota can disrupt mucosal immune tolerance, adversely affecting skin health (Chen et al., 2024). Similarly, skin damage can disrupt gut homeostasis and alter its microbiome (Dokoshi et al., 2024). The high comorbidity of inflammatory bowel diseases in patients with clinical vitiligo underscores the significant correlation between gut and skin health (Hadi et al., 2020). Studies have revealed significant differences in the gut microbial community's structure and function between vitiligo patients and healthy individuals (Luan et al., 2023; Bzioueche et al., 2021; Wu et al., 2023; Ganju et al., 2016; Ni et al., 2020). Research using vitiligo mouse models suggests that antibiotics may reduce Clostridium populations in the gut, leading to the loss of skin melanocytes (Dellacecca et al., 2020). The mechanism by which the gut-skin axis influences vitiligo is closely related to gut microbial metabolites' actions (Zhang et al., 2024). Extensive crosstalk between gut microorganisms and host-microbiota co-metabolism allows metabolite measurements to directly reflect the host-microbiota system (Krautkramer et al., 2021). These metabolites, especially SCFAs, SBAs, and Trp, regulate immune system homeostasis and the physiological functions of various organs (Gasaly et al., 2021). However, the influence of gut metabolites on vitiligo pathogenesis is not fully understood.

This article explores the synthesis, function, and signaling mechanisms of gut microbiota metabolic products, with a focus on their impact on the immune system and inflammatory processes through the gut-skin axis, particularly the relationship between major metabolites and vitiligo. The aim is to elucidate the mechanisms by which gut microbiota metabolic products influence vitiligo, and to establish a theoretical basis for their application in the clinical management of the disease.

1.1 The main pathophysiological mechanisms of vitiligo

In vitiligo, oxidative stress and immune dysregulation are significant contributors to disease onset in genetically predisposed individuals. Oxidative stress, characterized by an excessive production of reactive molecules such as reactive oxygen species (ROS) and hydrogen peroxide (H_2O_2), creates a pro-inflammatory microenvironment in affected tissues (Białczyk et al., 2023). This pro-inflammatory environment may activate innate immune cells, including dendritic cells (DCs) and natural killer (NKs) cells. These cells play a central role in the inflammatory response by releasing pro-inflammatory cytokines such as heat shock protein 70 (HSP70i), interleukins (e.g., IL-6, IL-17, IL-23, IL-27), and tumor necrosis factor-alpha (TNF-α), thereby exacerbating inflammation (Seneschal et al., 2021; Xie et al., 2023; Mukhatayev and Le Poole, 2024; Hayran et al., 2024; De et al., 2023; Ahmed et al., 2022). Subsequently, these chemokines and cytokines stimulate damaged melanocytes (MCs) to release their antigens, which are subsequently engulfed by antigen-presenting cells, such as dendritic cells, and presented to CD8 + T cells through MHC class I molecules (Song et al., 2024). This leads to the recruitment of melanocyte-specific CD8 + T cells that secrete interferon-gamma (IFN-γ), establishing a positive feedback loop. This cascade ultimately results in the targeted attack of autoantibodies on melanocytes, increased infiltration and cytotoxicity of CD8 + T cells, and upregulation of immune regulatory factors, such as IL-15-mediated activation of the JAK–STAT signaling pathway. Consequently, an adaptive immune response develops in the epidermis of vitiligo patients. Consequently, MCs dysfunction and apoptosis ensue. The unrestrained attack on MCs is attributed to compromised regulatory T cell (Tregs) activity. Memory T cells (TRMs) establish residence in lesional skin, impeding repigmentation and promoting disease relapses (Riding and Harris, 2019). The inflammatory cytokine IFN-γplays a pivotal role in this pathological process. Although IFN-γmay alter the composition and function of the gut microbiome (Yue et al., 2021), its effects are not yet fully understood. (The pathogenesis of vitiligo is shown in Figure 1).

2 The main metabolic products of the gut microbiota and their targets of action

2.1 Changes in gut microbial communities in patients with vitiligo

Metabolomic analyses of vitiligo patients have uncovered alterations in the diversity within their gut microbial communities. A trend toward diminished alpha diversity was observed in vitiligo patients, coupled with an elevated Firmicutes-to-Bacteroidetes ratio (Luan et al., 2023; Bzioueche et al., 2021). However, there is also a study that indicates a higher alpha diversity among patients with vitiligo (Ni et al., 2020), which may be attributed to the relatively small sample size of individuals included in these studies. In these studies, it was found that the proportion of Actinobacteria and Pseudomonadales increased among patients with vitiligo. This can be partially explained by the protective role of Pseudomonadales

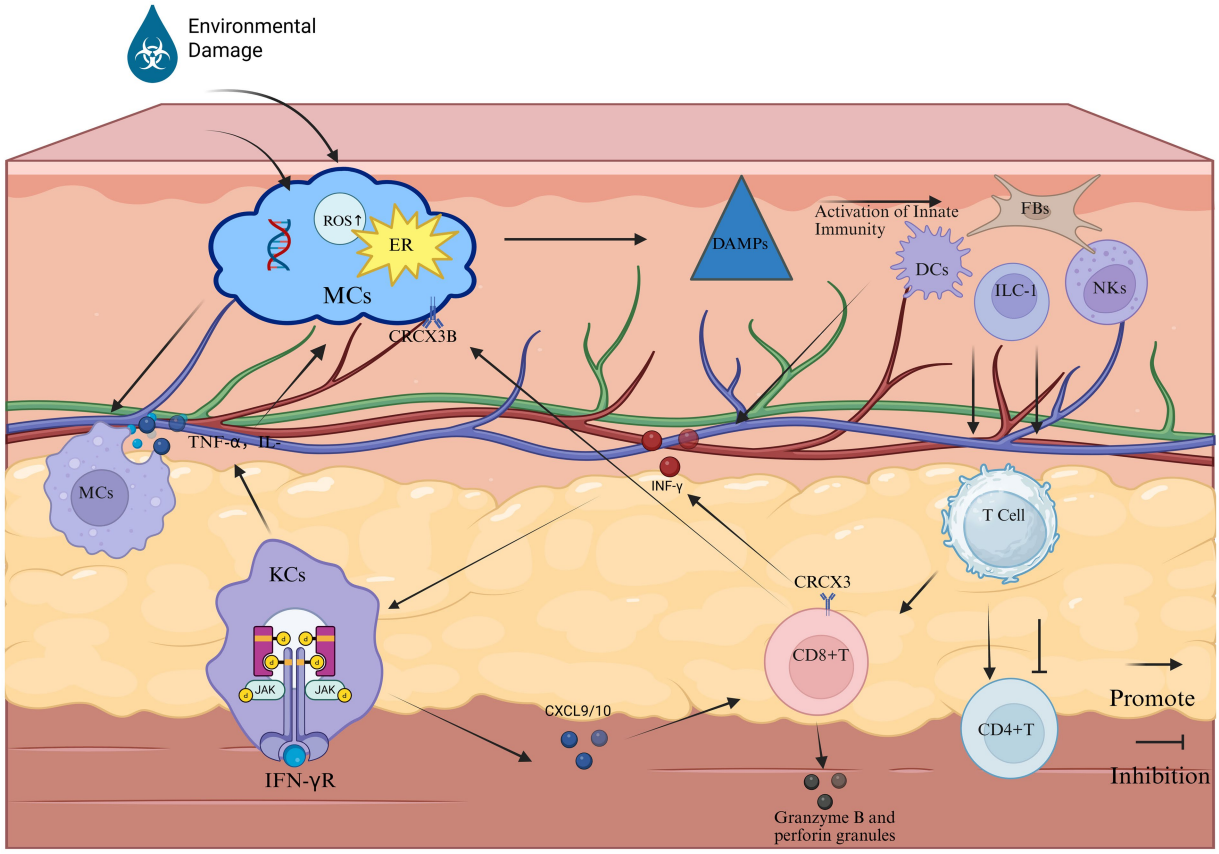

FIGURE 1
The primary pathological process of vitiligo (Created in https://BioRender.com). Phase 1: Melanocyte stress response: Stressed melanocytes manifest pathophysiological alterations characterized by endoplasmic reticulum (ER) stress, elevated ROS, and DNA damage. These cellular distress signals are recognized by cutaneous innate immune sentinels—DCs, NKs cells, ILC1s, and FBs—which subsequently undergo activation through pattern recognition receptor signaling. Phase 2: Innate immune activation: This immunogenic cascade triggers the JAK–STAT signaling axis, inducing keratinocytes to overexpress chemokines CXCL9 and CXCL10. These IFN-γ-inducible chemokines mediate CD8 + T cell recruitment to the dermo-epidermal junction via CXCR3 receptor ligation. Phase 3: Adaptive Immune Execution: Cytotoxic Mechanisms: Infiltrating CD8 + T lymphocytes release IFN-γ and cytolytic mediators (perforin, granzyme B), directly inducing melanocyte apoptosis. IFN-γ amplifies MHC class I expression on residual melanocytes, enhancing autoimmune targeting. Macrophage-Mediated Inflammation: Tissue-resident macrophages phagocytize apoptotic melanocytes, subsequently secreting pro-inflammatory cytokines (TNF-α, IL-6, IL-1β). These cytokines perpetuate local inflammation, disrupt melanocyte stem cell niches, and inhibit pigment regeneration. Pathogenic Feedback Loop: Sustained cytokine release (particularly IFN-γ and TNF-α) reactivates keratinocyte JAK–STAT signaling, establishing a self-reinforcing inflammatory circuit that drives progressive depigmentation.

against the loss of skin pigmentation. After the application of antibiotics, there was an increase in the levels of Pseudomonadales species and a decrease in the level of depigmentation compared to mice that were not exposed (Dellacecca et al., 2020).

2.2 Major metabolites of gut microbiota

SCFAs primarily comprise acetate (C2), propionate (C3), and butyrate (C4, 35). Specific subsets of anaerobic bacteria, in particular members of the Clostridium, Eubacterium and Butyrivibrio genera, produce SCFAs at high levels in the intestine (Singh et al., 2023). SCFAs can be transported from the gut to the skin via the bloodstream, and their concentration in the blood is sufficient to affect immune cells in distant organs, thereby modulating systemic immune responses (Liu et al., 2023). SBAs consist of deoxycholic acid (DCA), lithocholic acid (LCA), ursodeoxycholic acid, and related derivatives (Guzior and Quinn, 2021). SBAs are primarily transformed by bacterial genera including Clostridium, Enterococcus, Bifidobacterium, Lactobacillus, and Bacteroides (Cai et al., 2022). These bile acids are initially synthesized in the liver and transported to the intestine, where they undergo transformation mediated by the gut microbiota (Shapiro et al., 2018). Trp is an essential amino acid for humans and serves as an excellent substrate for various metabolic transformations within the body (Alkhalaf and Ryan, 2015). Tryptophan is primarily synthesized and metabolized through the action of various bacteria including Clostridium, Peptostreptococcus, Lactobacillus, *Escherichia coli* (*E. coli*), and Bifidobacterium (Roager and Licht, 2018). Trp is metabolized by gut microbiota through various pathways, including the kynurenine (KYN) pathway, the serotonin pathway (primarily 5-hydroxytryptamine (5-HT)), and the pathway involving indole and its derivatives. Metabolomic evidence suggests that vitiligo patients experience Trp depletion and enhanced KYN pathway metabolism, resulting in systemic accumulation of kynurenic acid (KYNA) and diminished synthesis of 5-HT and indoles (Singh et al.,

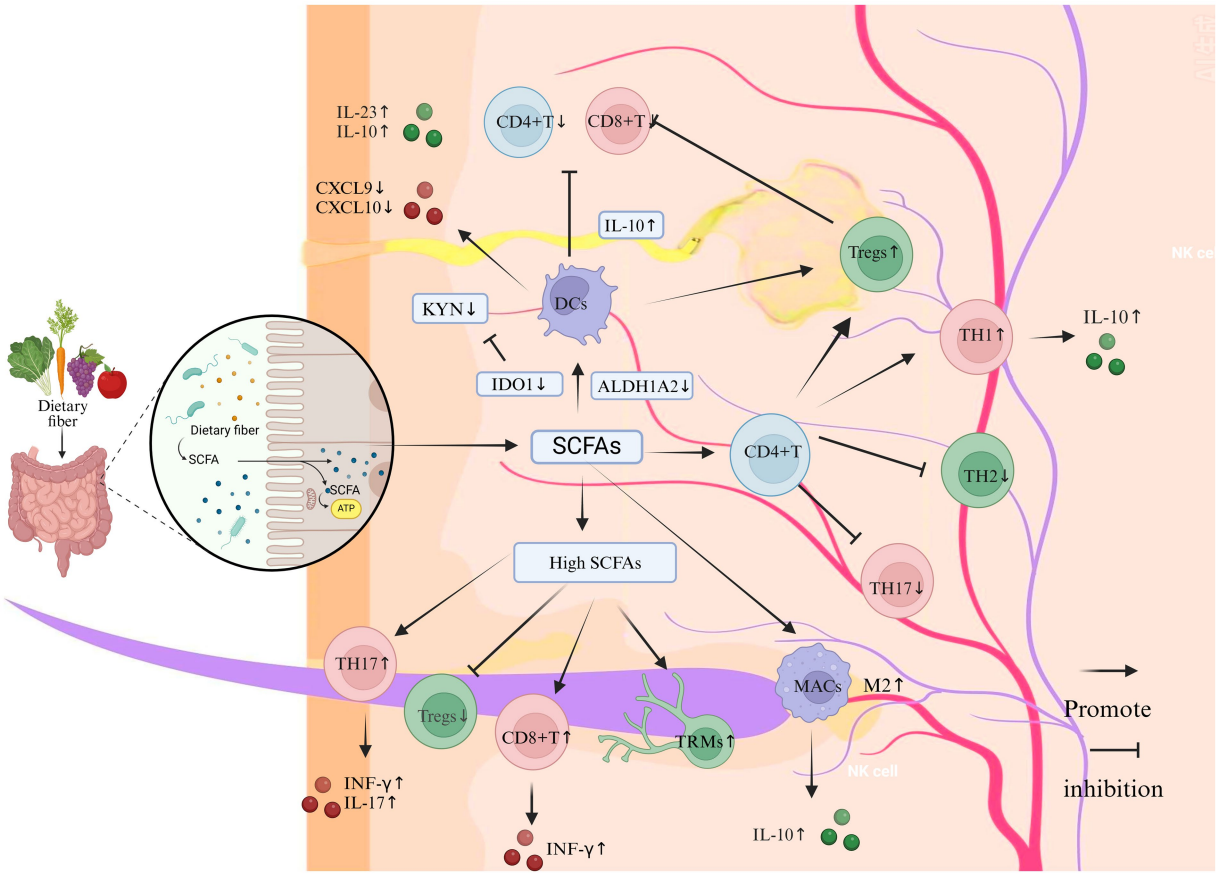

FIGURE 2
The impact of SCFAs on the immune system and inflammation in vitiligo (Created in https://BioRender.com). Dietary fiber-derived SCFAs (e.g., acetate, propionate, butyrate), generated through gut microbial fermentation, modulate cutaneous immune homeostasis via the gut-skin axis. At physiological concentrations, SCFAs enhance Tregs proliferation and potentiate their immunosuppressive capacity to restrain CD8 + T cell cytotoxicity and Th17-mediated inflammation. Mechanistically, SCFA-primed Tregs upregulate anti-inflammatory IL-10 secretion, which suppresses pro-inflammatory cytokines including IFN-γ and IL-17. Concurrently, SCFAs inhibit DCs maturation and downregulate the production of T cell-recruiting chemokines CXCL9 and CXCL10. Furthermore, SCFAs promote M2 macrophage polarization with concomitant IL-10 release, thereby facilitating tissue repair while suppressing inflammatory cascades. In contrast, supraphysiological SCFA levels exhibit paradoxical immunostimulatory effects: Th1/Th17 Polarization: Augment differentiation of Th1 and Th17 cells, elevating IFN-γ and IL-17 production. Keratinocyte Activation: Stimulate keratinocytes to release pro-inflammatory chemokines (CXCL9/CXCL10). CD8 + T Cell Recruitment: Enhance cutaneous infiltration of cytotoxic CD8 + T lymphocytes. Tissue-resident memory T cell maintenance: Sustain survival of autoreactive Trm cells in lesional skin.

2017). The potential influence of these metabolic products on vitiligo pathogenesis is depicted in Figures 2–4.

2.3 Targets of action of major metabolites of gut microbiota

SCFAs, such as acetate, propionate, and butyrate, signal through surface-expressed free fatty acid receptors and G protein-coupled receptors (GPCRs), including GPR41, GPR43, and GPR109A. These receptors are found on epithelial cells, adipose tissue, and various immune cells, including neutrophils, dendritic cells, macrophages, and lymphocytes, such as T cells (Sun et al., 2017). The differential expression of these GPCRs across various tissues, along with their unique affinities for specific SCFAs, could explain the differences in immune and inflammatory responses mediated by different SCFAs. In humans, GPR43 has the strongest affinity for acetate and propionate, followed by butyrate, while GPR109a has the strongest affinity for butyrate (He et al., 2020). Additionally, butyrate and propionate modulate gene expression by inhibiting histone deacetylase (HDAC) activity (Mann et al., 2024). Modulation of the immune system occurs primarily through the gut microbiota. However, commensal skin microbiota are essential for the maintenance of the skin immune homeostasis (Belkaid and Tamoutounour, 2016). In the skin, SCFAs such as propionate stimulate the production of pro-inflammatory cytokines following TLR activation (Sanford et al., 2016), which drives dendritic cell maturation and T cell proliferation (Sawada et al., 2021). Notably, butyrate exhibits an anti-inflammatory effect in the skin by reducing contact hypersensitivity and promoting the expansion of Tregs (Schwarz et al., 2017), highlighting the necessity of distinguishing between individual SCFAs. SBAs interact with a variety of receptors, including nuclear receptors—farnesoid X receptor (FXR), liver-X-receptor (LXR), pregnane X receptor (PXR), vitamin D receptor (VDR), retinoid-related orphan receptor (RORγt), and constitutive androstane receptor (CAR)—as well as membrane receptors such as G-protein bile acid receptor 1 (GPBAR1 or TGR5),

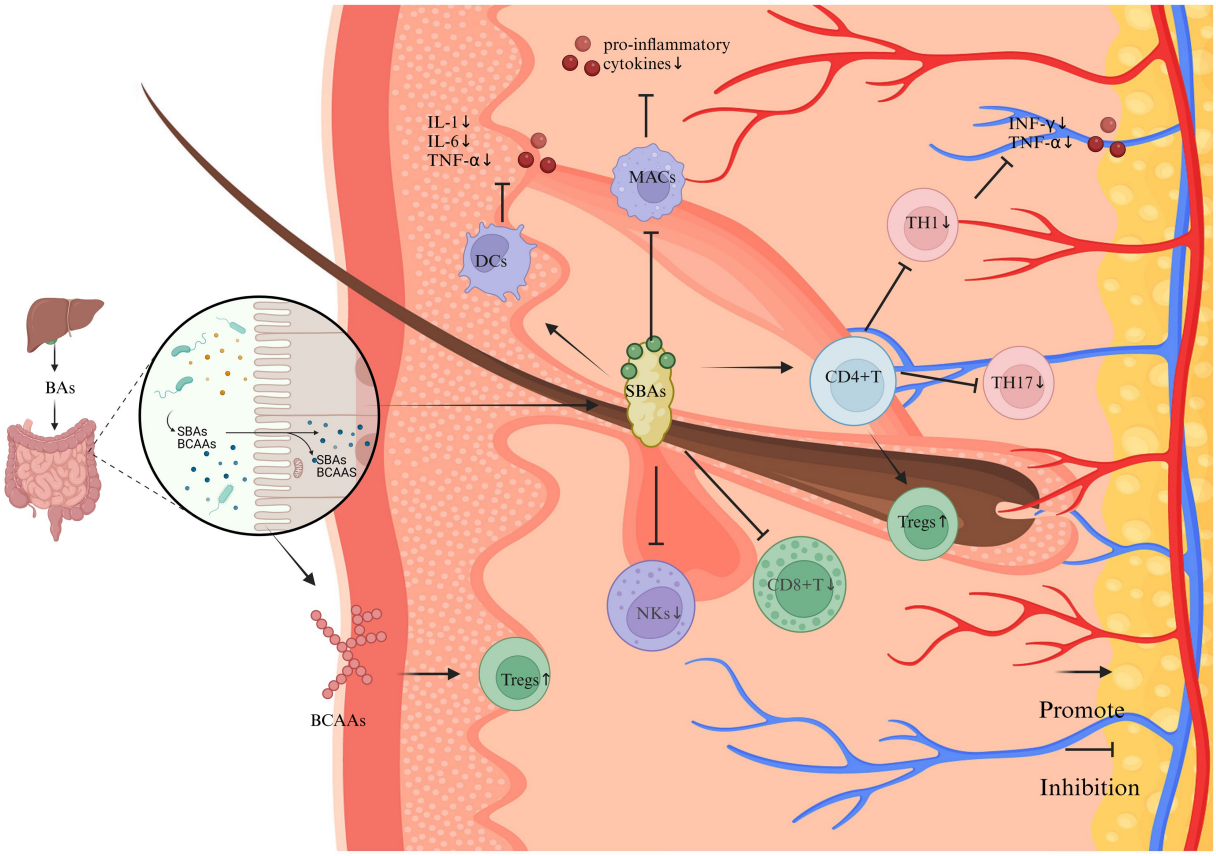

FIGURE 3
The impact of SBAs and BCAAs on the immune system and inflammation in vitiligo (Created in https://BioRender.com). SBAs, synthesized through microbial metabolism of hepatically derived primary bile acids, exhibit predominant anti-inflammatory properties through multifaceted immunomodulatory mechanisms. Key regulatory pathways include: T Cell Homeostasis: SBAs enhance Tregs differentiation via the gut-immune axis, while suppressing the polarization of pro-inflammatory Th17 and Th1 lineages. This Tregs/Th17 imbalance attenuates IFN-γ-mediated immune responses and downregulates TNF-α expression. Cytotoxic Cell Suppression: SBAs signaling inhibits the cytotoxic activity of CD8 + T lymphocytes and natural killer (NK) cells, thereby reducing melanocyte targeting. Innate Immune Regulation: Dendritic cells: Suppress pro-inflammatory cytokine secretion. Macrophages: Downregulate IL-1β, IL-6, and TNF-α production through a TGR5-dependent mechanism. Synergistically ameliorates inflammatory microenvironments in cutaneous tissues. BCAAs demonstrate complementary immunoregulatory effects, potentially augmenting Treg populations through analogous gut-immune crosstalk.

sphingosine-1-phosphate receptor 2 (S1PR2), muscarinic cholinergic receptors 2 and 3 (CHRM2 and CHRM3), and MAS-related G-protein-coupled receptor family member X4 (MRGPRX4) (Biagioli et al., 2021). The aryl hydrocarbon receptor (AHR) binds to several key metabolites of Trp metabolism (Seo and Kwon, 2023). Abnormal Trp metabolism, leading to immune imbalance, is thought to be linked to AHR dysregulation (Fang et al., 2022; Zhuang et al., 2023). Reduced expression of the AHR has been associated with the progression of unstable vitiligo (Liu et al., 2021). IAId, a Trp metabolite derived from skin microbiota, has been shown to suppress skin inflammation in AD patients, underscoring the significant role of skin microbiota in the development of skin diseases (Yu et al., 2019).

3 The impact on T cells

3.1 The impact on CD4 + T cells

Upon activation, naive CD4 + T cells differentiate into various effector subsets, including Tregs, T helper 1 (Th1) cells, and T helper 2 (Th2) cells, and T helper 17 (Th17) cells (Yang et al., 2020). Th1 cells produce cytokines such as IFN-γ and tumor necrosis factor-alpha (TNF-α), which enhance the functionality of antigen-presenting DCs. Th2 cells contribute primarily to humoral immunity by producing cytokines such as IL-4, IL-5, IL-10, and IL-13 (Cenerenti et al., 2022). Th17 cells release cytokines including IL-6, IL-17, IL-21, IL-22, and TNF-α (Belpaire et al., 2022). Elevated levels of IL-17 and IL-23 in the peripheral blood of vitiligo patients implicate Th17 cells in the disease's pathogenesis (Singh et al., 2016; Bhardwaj et al., 2020). Tregs are crucial in maintaining immune homeostasis and preventing excessive immune responses and autoimmune diseases (Mukhatayev et al., 2020). In vitiligo patients, Tregs are functionally impaired, and the Th1-skewed inflammatory microenvironment in the serum is implicated in the generation of Th1-like Tregs (Chen et al., 2022). These Th1-like Tregs exhibit a markedly diminished inhibitory effect on the proliferation and activation of CD8 + T cells. Enhanced activity of Tregs suppresses inflammation in the depigmented regions of vitiligo and inhibits CD8 + T cell-mediated attacks on melanocytes (Jin et al., 2024). Overall, a significant increase in CD4 + and CD8 + T cells, along with a marked reduction in Forkhead box P3

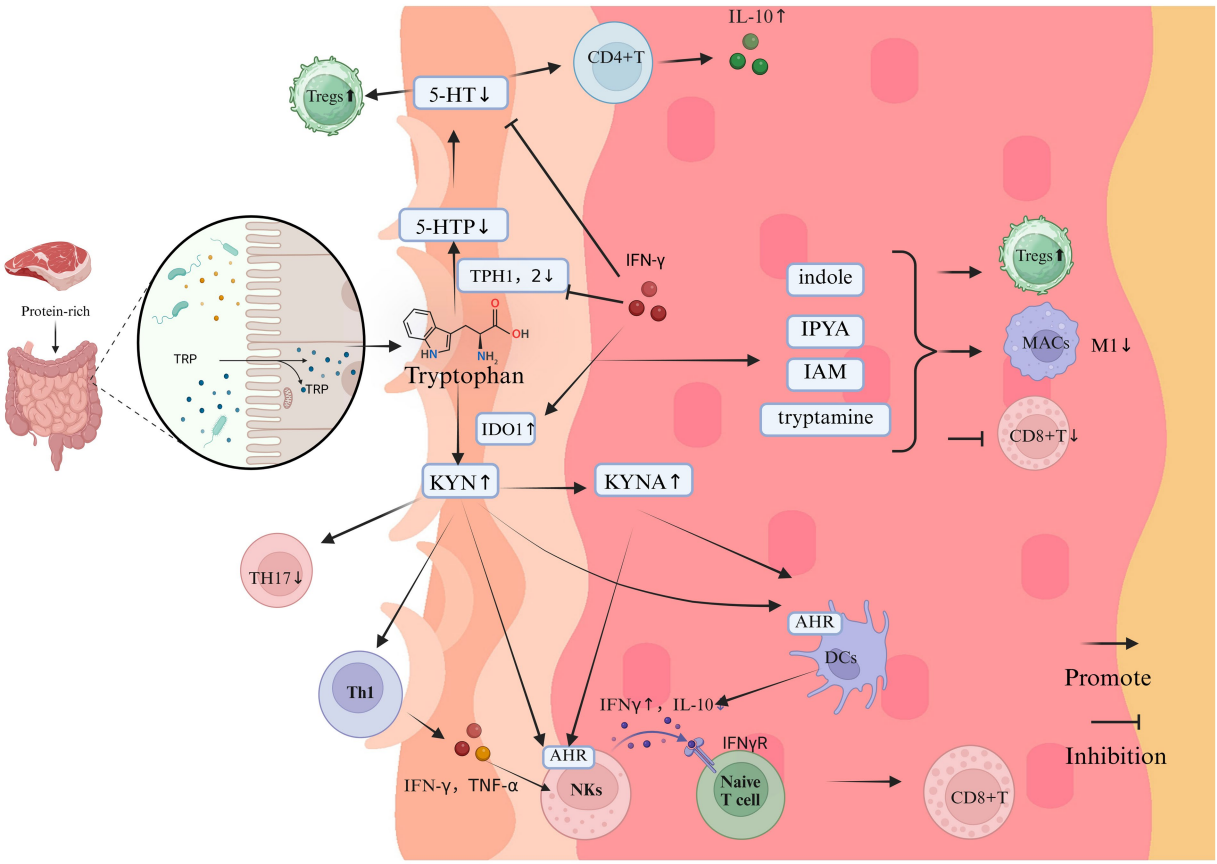

FIGURE 4
The impact of Trp on the immune system and inflammation in vitiligo (Created in https://BioRender.com). Tryptophan, derived from protein-rich diets, undergoes gut microbiota-mediated metabolism primarily through three pathways: the KYN axis, 5-HT pathway, and indole derivative biosynthesis. In vitiligo pathogenesis, dysregulation of these metabolic cascades manifests as:1. KYN Pathway Hyperactivation: Pathological Accumulation: Elevated KYN and its derivatives; Immunopathological Mechanisms: AhR Signaling: KYN activates AhR signaling in keratinocytes, triggering CXCL10 overexpression that recruits cytotoxic CD8 + T cells to melanocyte-rich areas; IFN-γ Feedback Loop: KYN-stimulated NKs release IFN-γ, which further amplifies KYN biosynthesis and melanocyte destruction via IDO1 upregulation; Anti-Inflammatory Suppression: KYNA accumulation inhibits IL-10 production, exacerbating pro-inflammatory polarization. 2. 5-HT pathway disruption. Enzymatic Inhibition: IFN-γ downregulates TPH isoforms TPH1/TPH2, reducing cutaneous 5-HT bioavailability. Melanogenic Dysregulation: Depleted 5-HT disrupts its dual modulation of melanogenesis through 5-HT1A/1B and 5-HT7 receptor signaling. 3. indole metabolite depletion. immunological consequences: Reduced microbiota-derived indoles (e.g., indole-3-aldehyde, indoleacetic acid) impair their native anti-inflammatory functions; Promotes CD8 + T cell hyperactivation and M1 macrophage polarization; Suppresses Treg differentiation via PPAR-γ/STAT3 signaling axis dysregulation.

(Foxp3)-expressing Tregs, was observed in the marginal skin of both stable and active vitiligo cases (Abdallah et al., 2014).

TH1 cells secrete the cytokine IFN-γ, activating the JAK/STAT pathway, which induces keratinocytes to produce the chemokines CXCL9 and CXCL10 and promotes autoimmune destruction of melanocytes. Thus, targeting TH1 cell activity may offer a therapeutic strategy for vitiligo. Butyrate enhances Th1 cell development via upregulation of IFN-γ and T-bet expression, while it concurrently inhibits Th17 cell development by downregulating IL-17, Rorα, and Rorγt expression (Chen et al., 2019). Butyrate's influence on TH1 cell differentiation is mediated by HDAC inhibition, independent of GPR43 signaling. Butyrate's influence on TH1 cell differentiation is mediated by HDAC inhibition, independent of GPR43 signaling. However, research also indicates that butyrate markedly decreases TH1 cell proliferation in a dose-dependent fashion (Kibbie et al., 2021). Butyrate can increase IL-10 production in TH1 cells (Sun et al., 2018). IL-10, an immunosuppressive cytokine, helps modulate TH1 cell-mediated immunity, preventing excessive inflammation and contributing to immune homeostasis. Reduced IL-10 levels, along with increased IFN-γ, perforin, and granzyme B secretion from tissue-resident memory T cells (TRMs), lead to impaired regulatory Tregs that cannot adequately suppress TRM cytotoxicity and proliferation (Shah et al., 2024). Collectively, existing studies affirm the anti-inflammatory effects of butyrates. Physiological levels of LCA suppress human and mouse Th1 cell activation, consequently reducing TNF-α and INF-γ production (Pols et al., 2017). Excessive KYN accumulation triggers AhR overactivation, which stimulates IFN-γ production by Th1 and NK cells and upregulates indoleamine 2,3-dioxygenase 1 (IDO1) expression (Shiu et al., 2022), thereby increasing Trp consumption and the accumulation of KYN pathway metabolites (Singh et al., 2017). IFN-γ not only activates the JAK–STAT pathway but also impedes melanin synthesis in response to 5-HT. Through IFNGR1/IFNGR2, IFN-γ downregulates 5-HT receptor expression, directly influencing 5-HT-induced melanin production (Cai et al., 2019).

SCFAs promote the initial differentiation of T cells into Th17 cells in a dose-dependent manner by inducing the transcription of IL-17A, IL-17F, and IFN-γ genes, and concurrently inhibit the differentiation of Tregs (Park et al., 2015). Research indicates that oral dietary fiber can enrich key gut microbiota associated with the Th17/Treg balance to alleviate inflammation, including Ligilactobacillus, Lactobacillus, Bacteroides, and Akkermansia. Concurrently, levels of microbial metabolites such as SCFAs and BAs are significantly increased (Yuan et al., 2024; Kim, 2021). Pentanoateis also a type of short-chain fatty acid that can effectively inhibit the proliferation of Th17 lymphocytes and the production of IL-17A (Luu et al., 2019). Secondary bile acids, 3-oxoLCA and isoLCA, are products of gut bacterial metabolism of lithocholic acid and exert a considerable influence on T cell differentiation and function. These metabolites inhibit TH17 cell differentiation by antagonizing the retinoic acid receptor-related orphan nuclear receptor gamma t (RORγt), a pivotal transcription factor in the promotion of TH17 cells (Hang et al., 2020; Paik et al., 2022). Kynurenine inhibits the activity of RORyt, which promotes the differentiation of pro-inflammatory Th17 cells (Riaz et al., 2022).

The investigation, a meta-analysis of 1,223 individuals with vitiligo and 1,109 control participants, revealed a significantly lower prevalence of Treg cells in the vitiligo cohort. Additionally, FOXP3 was markedly decreased in both the blood and skin tissues of patients with vitiligo (Giri et al., 2022). The reduction of proteins such as FOXP3 has been proven to be closely related to the progression of vitiligo (Abdallah et al., 2014; Giri et al., 2020). SCFAs promote the differentiation and function of Tregs by activating GPCRs and inhibiting the activity of HDAC. The enrichment of the TGF-*β*-based protocol with butyrate or propionate potentiated the *in vitro* differentiation of human naïve CD4 non-Tregs towards iTregs and augmented the suppressive capacity of the latter (Hu et al., 2022). Additionally, treatment of naive T cells with butyrate under Treg-cell-polarizing conditions enhanced histone H3 acetylation in the promoter and conserved non-coding sequence regions of the Foxp3 locus (Papaccio et al., 2024). The administration of 3-oxoLCA and isoalloLCA to mice reduced TH17 cell differentiation and increased Treg cell differentiation, respectively (Hang et al., 2020; Paik et al., 2022). SBAs induce RORγ+ Tregs generation via the vitamin D receptor, essential for immune homeostasis 5-HT favors the expansion of FoxP3 Tregs and increased IL-10 production by CD4 T cells (Sacramento et al., 2018).

3.2 The impact on CD8 + T cells

CD8 + T cells are involved in the cytotoxicity against MCs (Fukuda, 2022), and the presence of CD8 + tissue-resident memory T cells may play a crucial role in disease recurrence (Shah et al., 2021). In individuals with vitiligo, the chemokines CXCL9 and CXCL10, predominantly secreted by keratinocytes, mediate the recruitment of CD8 + T cells to the sites of lesions. CD8 + T cells in vitiligo lesions display a hyperactive phenotype. The IFN-γ they secrete activates the JAK–STAT signaling pathway in keratinocytes, leading to the expression of chemokines CXCL9 and CXCL10. This chemokine production subsequently recruits additional CD8 + T cells to the skin, thereby establishing a positive feedback loop (Frisoli et al., 2020). Interestingly, under normal conditions, SCFAs favor IL-10-mediated immune tolerance. However, during active immune responses, SCFAs help generate the effector T cells required to clear pathogens. This can also be applied to CD8 + T cells. Specifically, SCFAs at low concentrations induce Treg differentiation, whereas at higher concentrations, they enhance CD8 + T cell recruitment and IFN-*γ* expression in a dose-dependent manner (Luu et al., 2018). Following bacterial infection, increased peripheral blood acetate enhances glycolysis-driven rapid recall responses in memory CD8 + T cells (Balmer et al., 2016). Moreover, butyrate enhances the memory T-cell response upon antigen re-encounter (Bachem et al., 2019). DCA targets plasma membrane Ca2 + ATPase to inhibit the activated T cell signaling pathway (Cong et al., 2024). Bovine bile acid diminishes the number and impairs the function of CD8 + T cells and NK cell, and impairs their effector functions (Xun et al., 2021). In patients with vitiligo, excessive accumulation of KYNA may induce the expression of CXCL10 in keratinocytes through activation of the AhR pathway, which contributes to the recruitment of CD8 + T cells at the site of lesions (Chen et al., 2024). In summary, physiological levels of SCFAs are essential for maintaining immune homeostasis. Elevated SCFAs concentrations, however, enhance the recruitment of CD8 + T cells. Previous discussions suggest that individuals with vitiligo may experience a deficiency in SCFAs, which may have led to the absence of the anti-inflammatory effects of SCFAs. And SBAs inhibit CD8 + T cell activity. Additionally, the abnormal accumulation of KYN observed in vitiligo patients facilitates CD8 + T cell recruitment, further exacerbating the condition.

4 The impact on dendritic cells

Dendritic cells, the primary antigen-presenting cells in the skin, play a pivotal role in mediating the interaction between innate and adaptive immune responses (Singh et al., 2021). DCs are implicated in the pathogenesis of vitiligo via antigen presentation, immune system activation, and pro-inflammatory cytokine production (Migayron et al., 2020; Srivastava et al., 2021; Singh et al., 2021). Butyrate can affect the differentiation of DCs generated from human monocytes and can inhibit T cell proliferation. Butyrate substantially down-regulates the expression of CD80, CD83, and MHC class II molecules; increases endocytic capability; reduces allostimulatory abilities; promotes IL-10 production; and inhibits IL-12 and IFN-*γ* production (Liu et al., 2012). Propionate and butyrate strongly modulated gene expression in both immature and mature human monocyte-derived DCs and diminished the production of specific DCs chemokines, such as CXCL9 and CXCL10 (Nastasi et al., 2015). Research found that DCs exposed to acetate express the immunosuppressive enzymes IDO1 and aldehyde dehydrogenase 1A2 (Aldh1A2), promote conversion of naive T-cells into immunosuppressive FoxP3(+) Tregs and suppress conversion of naive T-cells into pro-inflammatory IFN-γ-producing cells (Gurav et al., 2015). IDO1, the rate-limiting enzyme in the kynurenine pathway, the excessive activation of the KYN pathway can diminish tyrosinase activity in vitiligo-affected areas, inhibit tyrosinase expression in MCs and KCs co-cultures, and reduce melanosome numbers in the 3D human skin reconstruct model (Ferreira Branquinho et al., 2022). This complexity suggests a multifaceted interplay between gut microbiota-derived metabolites and vitiligo. DCA suppresses the expression of pro-inflammatory cytokines IL-1, IL-6, and TNF-αin bacterial lipopolysaccharide-stimulated DCs (Hu et al., 2021). Additionally, isoDCA constrains FXR activity in DCs, conferring an anti-inflammatory phenotype (Campbell et al., 2020). In summary, SCFAs

attenuate the induction of autoimmunity and diminish the secretion of pro-inflammatory cytokines in DCs. Similarly, SBAs inhibit the release of pro-inflammatory cytokines from DCs. Furthermore, the deficiency of acetate may contribute to the upregulation of IDO1 in the skin, leading to an increased local depletion of trp.

5 The impact on macrophages

Macrophages and the macrophage migration inhibitory Factor (MIF) they secrete are associated with the severity of vitiligo. Downregulation of MIF can inhibit the activation and proliferation of CD8 + T cells in the lymph nodes of mice with vitiligo, and this effect extends to the CD8 T cells in the peripheral blood mononuclear cells of patients with vitiligo (Chen et al., 2023). Inflammatory macrophages (M1) predominantly participate in proinflammatory responses, while tissue-resident macrophages (M2) are primarily engaged in immunosuppressive activities. During active vitiligo, there is a notable increase in the infiltration of M1 macrophages in the bloodstream, which triggers a T-helper 1 (Th1) or T-helper 17 (Th17)-mediated immune response. This response exacerbates the destruction of melanocytes and leads to increased depigmentation. Conversely, the proportion of M2 macrophages remains comparable to that found in healthy tissue (Sain et al., 2024). SCFAs inhibit pro-inflammatory cytokines through HDAC activity suppression and also promote anti-inflammatory IL-10 expression in macrophages (Liu et al., 2012). Butyrate exerts anti-inflammatory effects by enhancing STAT6 signaling and inhibiting HDAC1, thereby promoting M2 macrophage polarization (Ji et al., 2016). SBAs inhibit the release of pro-inflammatory factors in macrophages induced by bacterial lipopolysaccharides in a TGR5-dependent manner (Haselow et al., 2013). Reduced Trp intake promotes M1-type macrophage polarization and facilitates CD8 + T cell accumulation, whereas restoring Trp intake reverses this effect (Jiang et al., 2024). GPR35$^+$ macrophages constitute a pro-inflammatory subset found in the small intestine. These cells facilitate the Th17 immune response through the KYNA-GPR35 signaling pathway and are involved in the pathogenesis of autoimmune diseases. KYNA modulates the recruitment and aggregation of GPR35$^+$ macrophages (Miyamoto et al., 2023). While the exact mechanisms through which gut microbiota-derived metabolites influence macrophages in vitiligo remain to be fully elucidated, the modulation of macrophage polarization represents a potential mechanism for ameliorating vitiligo lesions.

6 The direct effects of gut microbiota metabolites on vitiligo and melanocytes

Research observed a reduction in the abundance of bacterial taxa typically associated with a healthy gut microbiome, as well as a decrease in SCFAs-producing taxa in individuals with vitiligo (Kumar et al., 2024). Butyrate plays a crucial role in maintaining the integrity of the intestinal barrier and exhibits anti-inflammatory and immune-regulatory properties in autoimmune diseases. However, its efficacy can be affected by factors such as concentration, site of action, and the physiological status of the host (Kumar et al., 2024; Gerunova et al., 2024). Studies on neonatal melanocytes have shown that butyrate is cytotoxic to primary melanocytes at concentrations above 1 mM (Du et al., 2022). At lower, non-toxic concentrations (0.5 and 1 mM), however, butyrate significantly enhances melanocyte differentiation, resulting in melanosome formation and increased pigment deposition (Goenka, 2024). Topical application of butyrate, either alone or in combination with *S. epidermidis* and glycerol, significantly reduced UVB-induced IL-6 production (Keshari et al., 2019). Propionate effectively reduces melanin content in melanocytes, and treatment with 4 mM propionate significantly inhibits tyrosinase activity without affecting cell proliferation, indicating that propionate's suppression of melanogenesis occurs via downregulation of tyrosinase gene expression (Kao et al., 2021). Although the aforementioned studies appear to contradict the anti-inflammatory activity of SCFAs, it is important to note that SCFA levels may be reduced in vitiligo patients, potentially diminishing their anti-inflammatory and high-dose cytotoxic effects. Additionally, differential GPCRs expression in tissues and their specific affinity for SCFAs must be considered. This evidence collectively suggests that SCFAs likely exert pleiotropic physiological roles through multiple pathways, with their net effects potentially modulated by concentration gradients, tissue-specific distribution, and host metabolic status.

Research indicates that Ursodeoxycholic Acid (UDCA, a secondary bile acid generated by the gut microbiota through modifications such as hydroxylation of primary bile acids) mitigates the cellular impact of UV light exposure on human skin by diminishing intracellular oxidative stress and cutaneous inflammation. In this experiment, UDCA has been shown to reduce melanin content in normal human melanocytes (Moon et al., 2021). However, this study was based on experiments constructed using an aging skin model, which is not consistent with the pathogenesis of vitiligo. Moreover, UCDA has demonstrated anti-inflammatory and antioxidant effects. Therefore, the role of UCDA in vitiligo requires further exploration.

At a concentration of 5 mM, KYN significantly inhibited DNA synthesis in melanocytes (Walczak et al., 2020). Further research has shown that KYN, originating from sources such as microbial metabolism and fibroblast production, inhibits DNA synthesis and significantly reduces metabolic activity in primary human melanocytes (Walczak et al., 2023). Excessive accumulation of kynurenine can also impair tyrosinase activity in vitiligo-affected areas, downregulate tyrosinase expression in melanocyte and keratinocyte co-cultures, and decrease melanosomes in 3D human skin models (Ferreira Branquinho et al., 2022). As previously mentioned, vitiligo patients exhibit elevated blood levels of kynurenine aminotransferase, leading to kynurenine pathway deviation and systemic accumulation of KYNA (Singh et al., 2017). Consequently, excessive KYN accumulation in vitiligo patients may damage melanocytes and contribute to the pathophysiology of the disease. Oxidative stress can deplete epidermal Trp, leading to lower serotonin and melatonin levels (Schallreuter et al., 2012). *In vitro* studies show that melanophores in lower vertebrates exhibit dose-dependent pigmentation in response to 5-HT1 and 5-HT2 receptor agonists, while 5-HT3 and 5-HT4 receptor agonists induce dose-dependent pigment aggregation (Ali et al., 2012; Yue et al., 2022; Wu et al., 2014). The serotonin/5-HT7 receptor mediates an adaptive response that enhances pigmentation under environmental stress through various signaling pathways, including cAMP-PKA-MAPK, Rab27a/RhoA, and PI3K/AKT (Tang et al., 2023). Emotional stress can reduce skin serotonin levels, thereby affecting melanin production (Liao et al., 2017). Consequently, fluoxetine, a serotonin reuptake

inhibitor, has been shown to effectively treat pigment loss disorders (Slominski et al., 2012). Indole derivatives, as endogenous ligands of the AHR, activate AHR signaling and alleviate psoriasis and certain dermatitis conditions (Uberoi et al., 2021; Furue et al., 2019). However, direct evidence of their effect on vitiligo is currently lacking. The details of the above study can be found in Table 1.

7 Treatment based on gut microbiota metabolites

Diet emerges as a pivotal determinant of gut microbiota community structure and function (Zmora et al., 2019; De Angelis et al., 2019). The effects of diet on host metabolism and physiology can be mediated through the gut microbiota (Guan and Liu, 2023). Specific nutrients present in the diet can be metabolized into bacterial metabolites, thereby influencing the composition of gut microbiota. Secondly, ingestion can introduce probiotic or pathogenic bacteria from diet into the intestinal microenvironment, leading to alterations in the resident gut microbiota population and composition (Hills et al., 2019; Wilson et al., 2020). Thirdly, consuming certain diets may alter the physical environment within the gut, including the pH level, thereby potentially changing the composition of the gut microbiota. In this context, dietary intervention through the use of probiotics, prebiotics and antioxidant foods can be considered a contribution to the modulation of vitiligo (Ferreira et al., 2022).

7.1 The impact of diet on gut microbiota

The Mediterranean diet (Med) has been demonstrated to elevate levels of Bacteroidetes and Prevotellaceae families, thereby increasing the concentration of SCFAs (Gutiérrez-Díaz et al., 2016). In a preliminary four-day study, Indole-3-acetic acid (IAA), Indole-3-propionic acid(IPA), and Indole-3-lactic acid (ILA) were significantly increased after the Mediterranean diet and decreased after the fast-food diet (FF), whereasTrp, indole-6-carboxaldehyde, and 4-(1-piperazinyl)-1H-indole increased after FF and decreased after Med. The ratio of kynurenine to Trp was significantly decreased after FF and increased after Med, and no change in bile acids was observed in this study (Zhu et al., 2020). Currently, there is a lack of research on the Mediterranean diet as a potential adjunctive therapy for individuals with vitiligo. This gap in the literature warrants future investigation into its therapeutic efficacy.

7.2 The application of probiotics and prebiotics

Probiotics are live microorganisms that, when consumed in adequate amounts, confer a health benefit on the host. They are commonly found in fermented foods such as yogurt, kefir, and pickles, as well as in dietary supplements. Prebiotics, on the other hand, are indigestible food components that stimulate the growth and activity of beneficial bacteria in the gut, and are typically present in fiber-rich foods such as fruits, vegetables, and whole grains. In the past ten years, the number of commercially available topical probiotics has dramatically increased (Lee et al., 2019), and probiotics have been applied topically and orally to treat various skin disorders, such as acne, atopic dermatitis, and rosacea (França, 2021). Prebiotics or symbiotics have been demonstrated to significantly improve skin health by improving the gut microbiota and its metabolites (Al-Smadi et al., 2023).

7.3 Fecal microbiota transplantation

Fecal Microbiota Transplantation (FMT) entails the transfer of gut microbiota from healthy donors to patients. FMT, which is primarily used to treat intestinal diseases by reshaping and balancing the gut microbiota, also appears to be a viable approach for managing skin inflammatory diseases (Wu et al., 2024). Moreover, the application of FMT in various autoimmune disorders has demonstrated promising safety and efficacy, which lays a theoretical foundation for its potential use in the treatment of vitiligo. Patients undergoing FMT have exhibited increased diversity in gut microbiota, especially in SCFAs-producing bacteria, resulting in a significant elevation in fecal SCFAs concentration (Huang et al., 2022). Patients with alopecia areata have shown improvement after undergoing FMT therapy (Rebello et al., 2017; Xie et al., 2019), and since the pathogenesis of alopecia areata and vitiligo shares commonalities, targeting the microbiome through methods such as fecal FMT is an emerging and promising strategy. However, the precise effects and potential mechanisms of FMT in the treatment of vitiligo require further clinical research to be confirmed.

7.4 Other potential dietary management strategies

Additionally, a growing body of evidence suggests the role of herbal bioactive compounds and nutritional supplements in vitiligo, including *Ginkgo Biloba*, Polypodium leucotomos, Capsaicin, Curcumin, *Phyllanthus emblica* fruit extract, carotenoids, Canthaxanthin, *Nigella sativa* seed oil, Picrorhiza kurroa, and Khellin (Shakhbazova et al., 2021). A research finds that the total-fat content of the diet had a more impressive role than the specific subclasses of fats on the incidence risk of vitiligo (Derakhshandeh-Rishehri et al., 2019). Therefore, reducing fat intake may be an effective strategy for preventing the recurrence of vitiligo. Based on a mendelian randomization study, vitiligo patients are advised to avoid excessive alcohol consumption. However, moderate intake of wine, cider, beer and champagne may be acceptable. In addition, vitiligo patients should limit their intake of tea and bread. And consuming high-fibre and probiotic-rich foods may help vitiligo patients regulate their gut microbiota overall (Zhang et al., 2024).

The complexity of the pathogenesis of vitiligo and its tendency to relapse highlight the fragile immune homeostasis in patients with the condition. The gut microbiota and its metabolic byproducts have a profound and distinct impact on the host's immune balance and inflammatory stability. While dietary interventions cannot be thought of as a standalone therapy, they still make a case for being used as adjuncts (Hadi et al., 2024). In the future, it is worth further exploration to manage vitiligo by utilizing the gut-skin axis and regulating the metabolic products of the gut microbiota.

TABLE 1 The direct effects of gut microbiota metabolites on vitiligo and melanocytes.

Years	Metabolites	Research models or objects	Research results	Author
2024	Butyrate	Primary human MCS	1. Butyrate shows cytotoxicity at high concentrations (>1 mM) and promotes differentiation at low concentrations. 2. It does not affect MITF levels but stimulates tyrosinase synthesis while inhibiting its activity, with no impact on melanin. 3. Butyrate also induces IL-6 without affecting oxidative stress.	Shilpi Goenka
2019	Butyrate	Dorsal skin of mice	1. UVB exposure on mice skin increased IL-6 production. 2. Butyric acid or *S. epidermidis* with glycerol reduced UVB-induced IL-6. Knocking down FFAR2 in mouse skin blocked this probiotic effect.	Keshari S
2021	Propionate	DOPA-positive MCs AND mice ear skin tissue	1. Propionate from Pluronic F68 fermentation of Cutibacterium acnes was the most abundant fatty acid and reduced DOPA-positive melanocytes by inhibiting tyrosinase activity via FFAR2 binding. 2. Propionate at 4 mM did not affect melanocyte proliferation, making it a safe and effective treatment for hyperpigmentation.	Kao H. J.
2021	UCDA	Senescent skin	1. UDCA reduced UV-induced ROS, SASP, and pro-inflammatory cytokines. 2. UDCA decreased melanogenesis in human melanocytes co-cultured with skin cells.	Moon I. J.
2020	KYN	MCs and melanoma A375	1. KYN, KYNA and FICZ in higher concentrations inhibited the protein level of AhR but did not affect the gene expression.	Walczak K.
2023	KYN	MCs	1. KYN inhibited MCs cell metabolism by reducing cyclin D1 and CDK4 levels via the AhR pathway.	Walczak K.
2012	5-HT	Amphibian pigment cells	1. In vitro studies show that melanophores in lower vertebrates exhibit dose-dependent pigmentation in response to 5-HT1 and 5-HT2 receptor agonists, while 5-HT3 and 5-HT4 receptor agonists induce dose-dependent pigment aggregatio	Ali S. A.
2022	5-HT2R	Mouse melanoma cell line B16F10, human skin, and zebrafish embryos	1. HTR2A antagonists reduced serotonin-induced melanogenesis in mouse melanoma cells and zebrafish embryos. 2. HTR2A agonists increased melanin synthesis and transfer in B16F10 cells, human skin tissue, and zebrafish embryos.	Yue Y.
2014	5-HT1A/1B	C57BL/6 mouse skin	1. The serotoninergic system plays an important role in the regulation of stress-induced depigmentation, which can be mediated by 5-HT1A/1B receptors	Wu H. L.
2023	5-HT7R	Human skin cells, human tissue, mice, and zebrafish models	1.5-HT7R selective agonist, LP-12, had been demonstrated to enhance melanin production, dendrite growth, and chemotactic motility in B16F10 cells, normal human melanocytes, and zebrafish.	Tang H. H.
2017	5-HT	Mouse skin	1. Stress altered hippocampal morphology, reduced brain and skin 5-HT levels, and downregulated 5-HT1A receptors in the hippocampal CA1 region and skin. 2. Stress caused melanocyte damage and inhibited keratinocyte proliferation in hair follicles, leading to pigment loss.	Liao S.

10.3389/fmicb.2025.1566267

8 Discussion

This review is grounded in the "gut-skin axis" theory and systematically examines the regulatory effects of gut microbiota-derived metabolites on immune dysregulation and melanocyte dysfunction in vitiligo. Current evidence indicates that microbial metabolites, including SCFAs, SBAs, and Trp catabolites, significantly influence disease progression through modulation of immune cell differentiation (particularly Th17/Treg balance and CD8 + T cell cytotoxicity) and inflammatory cytokine networks. Notably, the concentration-dependent biological effects of these metabolites (e.g., low-dose butyrate promotes tissue repair while high concentrations exacerbate inflammatory responses) reveal complex microbiota-immune microenvironment interactions. Clinical observations demonstrate that vitiligo patients exhibit reduced gut microbial diversity and accumulated pro-inflammatory metabolites, which correlate with disrupted immune homeostasis, suggesting microbial metabolic dysbiosis as a potential pathogenic driver. However, discrepancies in research outcomes, particularly regarding the directionality of α-diversity alterations in gut microbiota, may stem from sample heterogeneity or individual variations in host-microbiota crosstalk. Furthermore, caution is warranted when extrapolating *in vitro* findings to physiological microenvironments. These mechanistic insights provide a theoretical foundation for developing novel metabolic-immunological therapeutic strategies, highlighting the potential clinical value of restoring immune equilibrium through targeted modulation of gut microbiota and their metabolic networks.

In summary, this review is based on the gut-skin axis theory and investigates the impact of gut microbiota metabolic products on vitiligo. We hope that this research will stimulate a comprehensive discussion on the interaction mechanisms between the gut microbiota and vitiligo. Future explorations are warranted to examine the potential of using dietary fiber supplementation or probiotics as intervention measures to regulate the immune dysregulation in vitiligo and promote repigmentation in the depigmented areas.

8.1 Future challenges

1. According to our current research, a change has been observed in the gut microbiota composition of patients with vitiligo, a phenomenon that has garnered our significant attention. Additionally, we have discovered a reduction in the production of microbial metabolic products such as SCFAs, 5-HT, and indole compounds, which may have adverse effects on the health of patients. Conversely, the accumulation of KYN is excessive and this alteration cannot be overlooked. These factors seem to collectively influence the progression of vitiligo in patients, yet to date, no comprehensive study has been able to fully explain this issue, warranting further research in the future.
2. It remains uncertain whether there is a difference in the gut microbiota between patients with stable vitiligo and those with rapidly progressing disease, which is a question that requires in-depth exploration. At the same time, we are also considering whether the dysregulation of gut microbiota metabolic products plays an important role in the onset of vitiligo during rapid progression, which is equally a direction worthy of future study.
3. Furthermore, it is worth investigating whether targeted dietary interventions, such as the supplementation of dietary fiber, could improve the clinical manifestation of vitiligo patients. This is a potential therapeutic approach that may bring new hope to those suffering from vitiligo.

Author contributions

CJY: Conceptualization, Investigation, Writing – original draft, Writing – review & editing. LYL: Investigation, Writing – original draft, Writing – review & editing. DRZ: Investigation, Writing – original draft, Writing – review & editing. JXY: Investigation, Writing – original draft, Writing – review & editing. LYG: Investigation, Writing – original draft, Writing – review & editing. JLZ: Conceptualization, Investigation, Writing – original draft, Writing – review & editing.

Funding

The author(s) declare that no financial support was received for the research and/or publication of this article.

Conflict of interest

The authors declare that the research was conducted in the absence of any commercial or financial relationships that could be construed as a potential conflict of interest.

Generative AI statement

The authors declare that no Gen AI was used in the creation of this manuscript.

Publisher's note

All claims expressed in this article are solely those of the authors and do not necessarily represent those of their affiliated organizations, or those of the publisher, the editors and the reviewers. Any product that may be evaluated in this article, or claim that may be made by its manufacturer, is not guaranteed or endorsed by the publisher.

References

Abdallah, M., Lotfi, R., Othman, W., and Galal, R. (2014). Assessment of tissue FoxP3+, CD4+ and CD8+ T-cells in active and stable nonsegmental vitiligo. *Int. J. Dermatol.* 53, 940–946. doi: 10.1111/ijd.12160

Ahmed, A. A. E., Mikhael, N. W., Elfallah, A. A., and Hamed, A. M. (2022). Unraveling the relation between vitiligo, interleukin 17, and serum amyloid a. *J. Cosmet. Dermatol.* 21, 6428–6433. doi: 10.1111/jocd.15329

Ali, S. A., Salim, S., Sahni, T., Peter, J., and Ali, A. S. (2012). 5-HT receptors as novel targets for optimizing pigmentary responses in dorsal skin melanophores of frog, *Hoplobatrachus tigerinus*. *Br. J. Pharmacol.* 165, 1515–1525. doi: 10.1111/j.1476-5381.2011.01630.x

Alkhalaf, L. M., and Ryan, K. S. (2015). Biosynthetic manipulation of tryptophan in bacteria: pathways and mechanisms. *Chem. Biol.* 22, 317–328. doi: 10.1016/j.chembiol.2015.02.005

Al-Smadi, K., Leite-Silva, V. R., Filho, N. A., Lopes, P. S., and Mohammed, Y. (2023). Innovative approaches for maintaining and enhancing skin health and managing skin diseases through microbiome-targeted strategies. *Antibiotics (Basel).* 12:1698. doi: 10.3390/antibiotics12121698

Bachem, A., Makhlouf, C., Binger, K. J., de Souza, D. P., Tull, D., Hochheiser, K., et al. (2019). Microbiota-derived short-chain fatty acids promote the memory potential of antigen-activated CD8 T cells. *Immunity* 51, 285–297e5. doi: 10.1016/j.immuni.2019.06.002

Balmer, M. L., Ma, E. H., Bantug, G. R., Grählert, J., Pfister, S., Glatter, T., et al. (2016). Memory CD8(+) T cells require increased concentrations of acetate induced by stress for optimal function. *Immunity* 44, 1312–1324. doi: 10.1016/j.immuni.2016.03.016

Belkaid, Y., and Tamoutounour, S. (2016). The influence of skin microorganisms on cutaneous immunity. *Nat. Rev. Immunol.* 16, 353–366. doi: 10.1038/nri.2016.48

Belpaire, A., van Geel, N., and Speeckaert, R. (2022). From IL-17 to IFN-γ in inflammatory skin disorders: is transdifferentiation a potential treatment target? *Front. Immunol.* 13:932265. doi: 10.3389/fimmu.2022.932265

Bhardwaj, S., Rani, S., Kumaran, M. S., Bhatia, A., and Parsad, D. (2020). Expression of Th17- and Treg-specific transcription factors in vitiligo patients. *Int. J. Dermatol.* 59, 474–481. doi: 10.1111/ijd.14766

Biagioli, M., Marchianò, S., Carino, A., di Giorgio, C., Santucci, L., Distrutti, E., et al. (2021). Bile acids activated receptors in inflammatory bowel disease. *Cells* 10:1281. doi: 10.3390/cells10061281

Białczyk, A., Wełniak, A., Kamińska, B., and Czajkowski, R. (2023). Oxidative stress and potential antioxidant therapies in vitiligo: a narrative review. *Mol. Diagn. Ther.* 27, 723–739. doi: 10.1007/s40291-023-00672-z Y

Bzioueche, H., Simonyté Sjödin, K., West, C. E., Khemis, A., Rocchi, S., Passeron, T., et al. (2021). Analysis of matched skin and gut microbiome of patients with vitiligo reveals deep skin Dysbiosis: link with mitochondrial and immune changes. *J. Invest. Dermatol.* 141, 2280–2290. doi: 10.1016/j.jid.2021.01.036

Cai, J., Sun, L., and Gonzalez, F. J. (2022). Gut microbiota-derived bile acids in intestinal immunity, inflammation, and tumorigenesis. *Cell Host Microbe* 30, 289–300. doi: 10.1016/j.chom.2022.02.004

Cai, M., Zhou, L., Liao, J., Huang, Q., Xia, Z., and Shang, J. (2019). IFN-γ inhibits 5-HT-induced melanin biosynthesis via downregulation of 5-HT receptors in vivo/in vitro. *J. Pharmacol. Sci.* 141, 1–8. doi: 10.1016/j.jphs.2019.05.005

Campbell, C., McKenney, P. T., Konstantinovsky, D., Isaeva, O. I., Schizas, M., Verter, J., et al. (2020). Bacterial metabolism of bile acids promotes generation of peripheral regulatory T cells. *Nature* 581, 475–479. doi: 10.1038/s41586-020-2193-0

Cenerenti, M., Saillard, M., Romero, P., and Jandus, C. (2022). The era of cytotoxic CD4 T cells. *Front. Immunol.* 13:867189. Published 2022 Apr 27. doi: 10.3389/fimmu.2022.867189

Chen, J., Guo, W., Du, P., et al. (2023). MIF inhibition alleviates vitiligo progression by suppressing CD8 T cell activation and proliferation. *J. Pathol.* 260, 84–96. doi: 10.1002/path.6073+

Chen, Z., Li, Y., Tan, X., Nie, S., Chen, B., Mei, X., et al. (2024). Dysregulated tryptophan metabolism and AhR pathway contributed to CXCL10 upregulation in stable non-segmental vitiligo. *J. Dermatol. Sci.* 115, 33–41. doi: 10.1016/j.jdermsci.2024.06.003

Chen, L., Sun, M., Wu, W., Yang, W., Huang, X., Xiao, Y., et al. (2019). Microbiota metabolite butyrate differentially regulates Th1 and Th17 cells' differentiation and function in induction of colitis. *Inflamm. Bowel Dis.* 25, 1450–1461. doi: 10.1093/ibd/izz046

Chen, J., Wang, X., Cui, T., Ni, Q., Zhang, Q., Zou, D., et al. (2022). Th1-like Treg in vitiligo: An incompetent regulator in immune tolerance. *J. Autoimmun.* 131:102859. doi: 10.1016/j.jaut.2022.102859

Chen, M., Wang, R., and Wang, T. (2024). Gut microbiota and skin pathologies: mechanism of the gut-skin axis in atopic dermatitis and psoriasis. *Int. Immunopharmacol.* 141:112658. doi: 10.1016/j.intimp.2024.112658

Cong, J., Liu, P., Han, Z., Ying, W., Li, C., Yang, Y., et al. (2024). Bile acids modified by the intestinal microbiota promote colorectal cancer growth by suppressing CD8+ T cell effector functions. *Immunity* 57, 876–889.e11. doi: 10.1016/j.immuni.2024.02.014

De Angelis, M., Garruti, G., Minervini, F., Bonfrate, L., Portincasa, P., and Gobbetti, M. (2019). The food-gut human Axis: the effects of diet on gut microbiota and metabolome. *Curr. Med. Chem.* 26, 3567–3583. doi: 10.2174/0929867324666170428103848

De, A., Choudhary, N., Sil, A., Sarda, A., and Hasanoor Raja, A. H. (2023). A Cross-sectional study of the levels of cytokines IL-6, TNF-α, and IFN-γ in blood and skin (Lesional and uninvolved) of vitiligo patients and their possible role as biomarkers. *Indian J. Dermatol.* 68, 67–72. doi: 10.4103/ijd.ijd_27_22

De Pessemier, B., Grine, L., Debaere, M., Maes, A., Paetzold, B., and Callewaert, C. (2021). Gut-skin Axis: current knowledge of the interrelationship between microbial Dysbiosis and skin conditions. *Microorganisms* 9:353. doi: 10.3390/microorganisms9020353

Dellacecca, E. R., Cosgrove, C., Mukhatayev, Z., Akhtar, S., Engelhard, V. H., Rademaker, A. W., et al. (2020). Antibiotics drive microbial imbalance and vitiligo development in mice. *J. Invest. Dermatol.* 140, 676–687.e6. doi: 10.1016/j.jid.2019.08.435

Derakhshandeh-Rishehri, S. M., Heidari-Beni, M., Jaffary, F., Askari, G., Nilfroshzade, M., and Adibi, N. (2019). Role of fatty acids intake in generalized vitiligo. *Int. J. Prev. Med.* 10:52. doi: 10.4103/ijpvm.IJPVM_47_17

Dokoshi, T., Chen, Y., Cavagnero, K. J., Rahman, G., Hakim, D., Brinton, S., et al. (2024). Dermal injury drives a skin to gut axis that disrupts the intestinal microbiome and intestinal immune homeostasis in mice. *Nat. Commun.* 15:3009. doi: 10.1038/s41467-024-47072-3

Du, Y., Li, X., An, Y., Song, Y., and Lu, Y. (2022). Association of gut microbiota with sort-chain fatty acids and inflammatory cytokines in diabetic patients with cognitive impairment: a cross-sectional, non-controlled study. *Front. Nutr.* 9:930626. doi: 10.3389/fnut.2022.930626

Fang, Z., Pan, T., Li, L., Wang, H., Zhu, J., Zhang, H., et al. (2022). *Bifidobacterium longum* mediated tryptophan metabolism to improve atopic dermatitis via the gut-skin axis. *Gut Microbes* 14:2044723. doi: 10.1080/19490976.2022.2044723

Ferreira Branquinho, M. S., Silva, M. B. B., Castilho, G. A., Cavalcante, J., Barros, S. B. M., Clara, R. O., et al. (2022). Kynurenine inhibits melanogenesis in human melanocyte-keratinocyte co-cultures and in a reconstructed 3D skin model. *Exp. Dermatol.* 31, 427–432. doi: 10.1111/exd.14486

Ferreira, R. D. S., Mendonça, L. A. B. M., Ribeiro, C. F. A., Calças, N. C., Guimarães, R. C. A., Nascimento, V. A. D., et al. (2022). Relationship between intestinal microbiota, diet and biological systems: an integrated view. *Crit. Rev. Food Sci. Nutr.* 62, 1166–1186. doi: 10.1080/10408398.2020.1836605

França, K. (2021). Topical probiotics in dermatological therapy and skincare: a concise review. *Dermatol Ther* 11, 71–77. doi: 10.1007/s13555-020-00476-7

Frisoli, M. L., Essien, K., and Harris, J. E. (2020). Vitiligo: mechanisms of pathogenesis and treatment. *Annu. Rev. Immunol.* 38, 621–648. doi: 10.1146/annurev-immunol-100919-023531

Fukuda, K. (2022). Networks of CD8+ T cell response activation in melanoma and vitiligo. *Front. Immunol.* 13:866703. doi: 10.3389/fimmu.2022.866703

Furue, M., Hashimoto-Hachiya, A., and Tsuji, G. (2019). Aryl hydrocarbon receptor in atopic dermatitis and psoriasis. *Int. J. Mol. Sci.* 20:5424. doi: 10.3390/ijms20215424

Ganju, P., Nagpal, S., Mohammed, M. H., Nishal Kumar, P., Pandey, R., Natarajan, V. T., et al. (2016). Microbial community profiling shows dysbiosis in the lesional skin of vitiligo subjects. *Sci. Rep.* 6:18761. Published 2016 Jan 13. doi: 10.1038/srep18761

Gao, T., Wang, X., Li, Y., and Ren, F. (2023). The role of probiotics in skin health and related gut-skin Axis: a review. *Nutrients* 15:3123. doi: 10.3390/nu15143123

Gasaly, N., de Vos, P., and Hermoso, M. A. (2021). Impact of bacterial metabolites on gut barrier function and host immunity: a focus on bacterial metabolism and its relevance for intestinal inflammation. *Front. Immunol.* 12:658354. Published 2021 May 26. doi: 10.3389/fimmu.2021.658354

Gerunova, L. K., Gerunov, T. V., P'yanova, L. G., Lavrenov, A. V., Sedanova, A. V., Delyagina, M. S., et al. (2024). Butyric acid and prospects for creation of new medicines based on its derivatives: a literature review. *J. Vet. Sci.* 25:e23. doi: 10.4142/jvs.23230

Giri, P. S., Dwivedi, M., and Begum, R. (2020). Decreased suppression of CD8+ and CD4+ T cells by peripheral regulatory T cells in generalized vitiligo due to reduced NFATC1 and FOXP3 proteins. *Exp. Dermatol.* 29, 759–775. doi: 10.1111/exd.14157

Giri, P. S., Mistry, J., and Dwivedi, M. (2022). Meta-analysis of alterations in regulatory T cells' frequency and suppressive capacity in patients with vitiligo. *J Immunol Res* 2022:6952299. doi: 10.1155/2022/6952299

Goenka, S. (2024). Exploring the effect of butyric acid, a metabolite from periodontopathic bacteria, on primary human melanocytes: An in vitro study. *J. Oral Biosci.* 66, 253–259. doi: 10.1016/j.job.2024.01.002

Guan, L., and Liu, R. (2023). The role of diet and gut microbiota interactions in metabolic homeostasis. *Adv. Biol.* 7:e2300100. doi: 10.1002/adbi.202300100

Gurav, A., Sivaprakasam, S., Bhutia, Y. D., Boettger, T., Singh, N., and Ganapathy, V. (2015). Slc5a8, a Na+−coupled high-affinity transporter for short-chain fatty acids, is a conditional tumour suppressor in colon that protects against colitis and colon cancer under low-fibre dietary conditions. *Biochem. J.* 469, 267–278. doi: 10.1042/BJ20150242

Gutiérrez-Díaz, I., Fernández-Navarro, T., Sánchez, B., Margolles, A., and González, S. (2016). Mediterranean diet and faecal microbiota: a transversal study. *Food Funct.* 7, 2347–2356. doi: 10.1039/c6fo00105j

Guzior, D. V., and Quinn, R. A. (2021). Review: microbial transformations of human bile acids. *Microbiome* 9:140. doi: 10.1186/s40168-021-01101-1

Hadi, Z., Kaur, R., Parekh, Z., Khanna, S., Khalil, A. B. B., Abbasi, H. Q., et al. (2024). Exploring the impact of diet and nutrition on vitiligo: a systematic review of dietary factors and nutritional interventions. *J. Cosmet. Dermatol.* 23, 2320–2327. doi: 10.1111/jocd.16277

Hadi, A., Wang, J. F., Uppal, P., Penn, L. A., and Elbuluk, N. (2020). Comorbid diseases of vitiligo: a 10-year cross-sectional retrospective study of an urban US population. *J. Am. Acad. Dermatol.* 82, 628–633. doi: 10.1016/j.jaad.2019.07.036

Hang, S., Paik, D., Yao, L., Kim, E., Trinath, J., Lu, J., et al. (2020). Bile acid metabolites control TH17 and Treg cell differentiation. *Nature* 579:143–148. doi: 10.1038/s41586-020-2030-5

Haselow, K., Bode, J. G., Wammers, M., Ehlting, C., Keitel, V., Kleinebrecht, L., et al. (2013). Bile acids PKA-dependently induce a switch of the IL-10/IL-12 ratio and reduce proinflammatory capability of human macrophages. *J. Leukoc. Biol.* 94, 1253–1264. doi: 10.1189/jlb.0812396

Hayran, Y., Yücel, Ç., Oğuz, E. F., Eren, F., Turhan, T., and Yalçın, B. (2024). Serum levels of IL-35, one of the newest members of interleukin-12 family of cytokines, in patients with vitiligo. *Dermatol. Pract. Concept.* 14:e2024069. doi: 10.5826/dpc.1402a69

He, J., Zhang, P., Shen, L., Niu, L., Tan, Y., Chen, L., et al. (2020). Short-chain fatty acids and their association with Signalling pathways in inflammation, glucose and lipid metabolism. *Int. J. Mol. Sci.* 21:6356. doi: 10.3390/ijms21176356

Hills, R. D. Jr., Pontefract, B. A., Mishcon, H. R., Black, C. A., Sutton, S. C., and Theberge, C. R. (2019). Gut microbiome: profound implications for diet and disease. *Nutrients* 11:1613. doi: 10.3390/nu11071613

Hu, M., Alashkar Alhamwe, B., Santner-Nanan, B., Miethe, S., Harb, H., Renz, H., et al. (2022). Short-chain fatty acids augment differentiation and function of human induced regulatory T cells. *Int. J. Mol. Sci.* 23:5740. doi: 10.3390/ijms23105740

Hu, J., Wang, C., Huang, X., Yi, S., Pan, S., Zhang, Y., et al. (2021). Gut microbiota-mediated secondary bile acids regulate dendritic cells to attenuate autoimmune uveitis through TGR5 signaling. *Cell Rep.* 36:109726. doi: 10.1016/j.celrep.2021.109726

Huang, C., Yi, P., Zhu, M., Zhou, W., Zhang, B., Yi, X., et al. (2022). Safety and efficacy of fecal microbiota transplantation for treatment of systemic lupus erythematosus: an EXPLORER trial. *J. Autoimmun.* 130:102844. doi: 10.1016/j.jaut.2022.102844

Iwanowski, T., Kołkowski, K., Nowicki, R. J., and Sokołowska-Wojdyło, M. (2023). Etiopathogenesis and emerging methods for treatment of vitiligo. *Int. J. Mol. Sci.* 24:9749. doi: 10.3390/ijms24119749

Ji, J., Shu, D., Zheng, M., Wang, J., Luo, C., Wang, Y., et al. (2016). Microbial metabolite butyrate facilitates M2 macrophage polarization and function. *Sci. Rep.* 6:24838. doi: 10.1038/srep24838

Jiang, L., Hao, Y., Han, D., Dong, W., Yang, A., Sun, Z., et al. (2024). Gut microbiota dysbiosis deteriorates immunoregulatory effects of tryptophan via colonic indole and LBP/HTR2B-mediated macrophage function. *ISME J.* 18:wrae166. doi: 10.1093/ismejo/wrae166

Jin, S., Wan, S., Xiong, R., Li, Y., Dong, T., and Guan, C. (2024). The role of regulatory T cells in vitiligo and therapeutic advances: a mini-review. *Inflamm. Res.* 73, 1311–1332. doi: 10.1007/s00011-024-01900-w

Kao, H. J., Wang, Y. H., Keshari, S., Yang, J. J., Simbolon, S., Chen, C. C., et al. (2021). Propionic acid produced by Cutibacterium acnes fermentation ameliorates ultraviolet B-induced melanin synthesis. *Sci. Rep.* 11:11980. doi: 10.1038/s41598-021-91386-x

Keshari, S., Balasubramaniam, A., Myagmardoloonjin, B., Herr, D. R., Negari, I. P., and Huang, C. M. (2019). Butyric acid from probiotic *Staphylococcus epidermidis* in the skin microbiome Down-regulates the ultraviolet-induced pro-inflammatory IL-6 cytokine via short-chain fatty acid receptor. *Int. J. Mol. Sci.* 20:4477. doi: 10.3390/ijms20184477

Kibbie, J. J., Dillon, S. M., Thompson, T. A., Purba, C. M., McCarter, M. D., and Wilson, C. C. (2021). Butyrate directly decreases human gut lamina propria CD4 T cell function through histone deacetylase (HDAC) inhibition and GPR43 signaling. *Immunobiology* 226:152126. doi: 10.1016/j.imbio.2021.152126

Kim, C. H. (2021). Control of lymphocyte functions by gut microbiota-derived short-chain fatty acids. *Cell. Mol. Immunol.* 18, 1161–1171. doi: 10.1038/s41423-020-00625-0

Krautkramer, K. A., Fan, J., and Bäckhed, F. (2021). Gut microbial metabolites as multi-kingdom intermediates. *Nat. Rev. Microbiol.* 19, 77–94. doi: 10.1038/s41579-020-0438-4

Kumar, S., Mahajan, S., Kale, D., Chourasia, N., Khan, A., Asati, D., et al. (2024). Insights into the gut microbiome of vitiligo patients from India. *BMC Microbiol.* 24:440 2024 Oct 28. doi: 10.1186/s12866-024-03529-5

Lee, G. R., Maarouf, M., Hendricks, A. J., Lee, D. E., and Shi, V. Y. (2019). Topical probiotics: the unknowns behind their rising popularity. *Dermatol. Online J.* 25:13030. doi: 10.5070/D3255044062

Li, C., Zhai, S., Duan, M., Cao, L., Zhang, J., Wang, Y., et al. (2024). Weizmannia coagulans BC99 enhances intestinal barrier function by modulating butyrate formation to alleviate acute alcohol intoxication in rats. *Nutrients* 16:4142. doi: 10.3390/nu16234142

Liao, S., Lv, J., Zhou, J., Kalavagunta, P. K., and Shang, J. (2017). Effects of two chronic stresses on mental state and hair follicle melanogenesis in mice. *Exp. Dermatol.* 26, 1083–1090. doi: 10.1111/exd.13380

Liu, T., Li, J., Liu, Y., Xiao, N., Suo, H., Xie, K., et al. (2012). Short-chain fatty acids suppress lipopolysaccharide-induced production of nitric oxide and proinflammatory cytokines through inhibition of NF-κB pathway in RAW264.7 cells. *Inflammation* 35, 1676–1684. doi: 10.1007/s10753-012-9484-z

Liu, L., Li, L., Min, J., Wang, J., Wu, H., Zeng, Y., et al. (2012). Butyrate interferes with the differentiation and function of human monocyte-derived dendritic cells. *Cell. Immunol.* 277, 66–73. doi: 10.1016/j.cellimm.2012.05.011

Liu, X. F., Shao, J. H., Liao, Y. T., Wang, L. N., Jia, Y., Dong, P. J., et al. (2023). Regulation of short-chain fatty acids in the immune system. *Front. Immunol.* 14:1186892. doi: 10.3389/fimmu.2023.1186892

Liu, B., Xie, Y., Mei, X., Sun, Y., Shi, W., and Wu, Z. (2021). Reciprocal regulation of interleukin-17A and interleukin-22 secretion through aryl hydrocarbon receptor activation in CD4+ T cells of patients with vitiligo. *Exp. Ther. Med.* 21:158. doi: 10.3892/etm.2020.9589

Luan, M., Niu, M., Yang, P., Han, D., Zhang, Y., Li, W., et al. (2023). Metagenomic sequencing reveals altered gut microbial compositions and gene functions in patients with non-segmental vitiligo. *BMC Microbiol.* 23:265. doi: 10.1186/s12866-023-03020-7

Luu, M., Pautz, S., Kohl, V., Singh, R., Romero, R., Lucas, S., et al. (2019). The short-chain fatty acid pentanoate suppresses autoimmunity by modulating the metabolic-epigenetic crosstalk in lymphocytes. *Nat. Commun.* 10:760. doi: 10.1038/s41467-019-08711-2

Luu, M., Weigand, K., Wedi, F., Breidenbend, C., Leister, H., Pautz, S., et al. (2018). Regulation of the effector function of CD8+ T cells by gut microbiota-derived metabolite butyrate. *Sci. Rep.* 8:14430. doi: 10.1038/s41598-018-32860-x

Mann, E. R., Lam, Y. K., and Uhlig, H. H. (2024). Short-chain fatty acids: linking diet, the microbiome and immunity. *Nat. Rev. Immunol.* 24, 577–595. doi: 10.1038/s41577-024-01014-8

Migayron, L., Boniface, K., and Seneschal, J. (2020). Vitiligo, from physiopathology to emerging treatments: a review. *Dermatol Ther* 10, 1185–1198. doi: 10.1007/s13555-020-00447-y

Miyamoto, K., Sujino, T., Harada, Y., Ashida, H., Yoshimatsu, Y., Yonemoto, Y., et al. (2023). The gut microbiota-induced kynurenic acid recruits GPR35-positive macrophages to promote experimental encephalitis. *Cell Rep.* 42:113005. doi: 10.1016/j.celrep.2023.113005

Moon, I. J., Yoo, H., Paik, S. H., Kim, H. T., Kim, S. Y., Song, Y., et al. (2021). Ursodeoxycholic acid may inhibit environmental aging-associated hyperpigmentation. *Antioxidants* 10:267. doi: 10.3390/antiox10020267

Mostafavi Abdolmaleky, H., and Zhou, J. R. (2024). Gut microbiota Dysbiosis, oxidative stress, inflammation, and epigenetic alterations in metabolic diseases. *Antioxidants* 13:985. doi: 10.3390/antiox13080985

Mukhatayev, Z., Dellacecca, E. R., Cosgrove, C., Shivde, R., Jaishankar, D., Pontarolo-Maag, K., et al. (2020). Antigen specificity enhances disease control by Tregs in vitiligo. *Front. Immunol.* 11:581433. Published 2020 Dec 1. doi: 10.3389/fimmu.2020.581433

Mukhatayev, Z., and Le Poole, I. C. (2024). Vitiligo: advances in pathophysiology research and treatment development. *Trends Mol. Med.* 30, 844–862. doi: 10.1016/j.molmed.2024.04.009

Nastasi, C., Candela, M., Bonefeld, C. M., Geisler, C., Hansen, M., Krejsgaard, T., et al. (2015). The effect of short-chain fatty acids on human monocyte-derived dendritic cells. *Sci. Rep.* 5:16148. doi: 10.1038/srep16148

Ni, Q., Ye, Z., Wang, Y., Chen, J., Zhang, W., Ma, C., et al. (2020). Gut microbial Dysbiosis and plasma metabolic profile in individuals with vitiligo. *Front. Microbiol.* 11:592248. Published 2020. doi: 10.3389/fmicb.2020.592248

Paik, D., Yao, L., Zhang, Y., Bae, S., D'Agostino, G. D., Zhang, M., et al. (2022). Human gut bacteria produce TH17-modulating bile acid metabolites. *Nature* 603, 907–912. doi: 10.1038/s41586-022-04480-z

Papaccio, F., Ottaviani, M., Truglio, M., D'Arino, A., Caputo, S., Pacifico, A., et al. (2024). Markers of metabolic abnormalities in vitiligo patients. *Int. J. Mol. Sci.* 25:10201. doi: 10.3390/ijms251810201

Park, J., Kim, M., Kang, S. G., Jannasch, A. H., Cooper, B., Patterson, J., et al. (2015). Short-chain fatty acids induce both effector and regulatory T cells by suppression of histone deacetylases and regulation of the mTOR-S6K pathway. *Mucosal Immunol.* 8, 80–93. doi: 10.1038/mi.2014.44

Pessôa, R., Clissa, P. B., and Sanabani, S. S. (2023). The interaction between the host genome, epigenome, and the gut-skin Axis microbiome in atopic dermatitis. *Int. J. Mol. Sci.* 24:14322. doi: 10.3390/ijms241814322

Pols, T. W. H., Puchner, T., Korkmaz, H. I., Vos, M., Soeters, M. R., and de Vries, C. J. M. (2017). Lithocholic acid controls adaptive immune responses by inhibition of Th1 activation through the vitamin D receptor. *PLoS One* 12:e0176715. doi: 10.1371/journal.pone.0176715

Rebello, D., Wang, E., Yen, E., Lio, P. A., and Kelly, C. R. (2017). Hair growth in two alopecia patients after fecal microbiota transplant. *ACG Case Rep J.* 4:e107. Published 2017 Sep 13. doi: 10.14309/crj.2017.107

Riaz, F., Wei, P., and Pan, F. (2022). Fine-tuning of regulatory T cells is indispensable for the metabolic steatosis-related hepatocellular carcinoma: a review. *Front. Cell Dev. Biol.* 10:949603 2022 Jul 15. doi: 10.3389/fcell.2022.949603

Riding, R. L., and Harris, J. E. (2019). The role of memory CD8+ T cells in vitiligo. *J. Immunol.* 203, 11–19. doi: 10.4049/jimmunol.1900027

Roager, H. M., and Licht, T. R. (2018). Microbial tryptophan catabolites in health and disease. *Nat. Commun.* 9:3294. doi: 10.1038/s41467-018-05470-4

Sacramento, P. M., Monteiro, C., Dias, A. S. O., Kasahara, T. M., Ferreira, T. B., Hygino, J., et al. (2018). Serotonin decreases the production of Th1/Th17 cytokines and elevates the frequency of regulatory CD4+ T-cell subsets in multiple sclerosis patients. *Eur. J. Immunol.* 48, 1376–1388. doi: 10.1002/eji.201847525

Sain, N., Hooda, V., Singh, A., Gupta, S., Arava, S., and Sharma, A. (2024). Macrophage inhibitory factor alters the functionality of macrophages and their involvement in disease pathogenesis of active generalized vitiligo patients. *Cytokine* 176:156516. doi: 10.1016/j.cyto.2024.156516

Salem, I., Ramser, A., Isham, N., and Ghannoum, M. A. (2018). The gut microbiome as a major regulator of the gut-skin Axis. *Front. Microbiol.* 9:1459. doi: 10.3389/fmicb.2018.01459

Sanford, J. A., Zhang, L. J., Williams, M. R., Gangoiti, J. A., Huang, C. M., and Gallo, R. L. (2016). Inhibition of HDAC8 and HDAC9 by microbial short-chain fatty acids breaks immune tolerance of the epidermis to TLR ligands. *Sci Immunol.* 1:eaah4609. doi: 10.1126/sciimmunol.aah4609

Sawada, Y., Nakatsuji, T., Dokoshi, T., Kulkarni, N. N., Liggins, M. C., Sen, G., et al. (2021). Cutaneous innate immune tolerance is mediated by epigenetic control of MAP2K3 by HDAC8/9. *Sci Immunol.* 6:eabe1935. doi: 10.1126/sciimmunol.abe1935

Schallreuter, K. U., Salem, M. A., Gibbons, N. C., Martinez, A., Slominski, R., Lüdemann, J., et al. (2012). Blunted epidermal L-tryptophan metabolism in vitiligo affects immune response and ROS scavenging by Fenton chemistry, part 1: epidermal H2O2/ONOO(−)-mediated stress abrogates tryptophan hydroxylase and dopa decarboxylase activities, leading to low serotonin and melatonin levels. *FASEB J.* 26, 2457–2470. doi: 10.1096/fj.11-197137

Schwarz, A., Bruhs, A., and Schwarz, T. (2017). The short-chain fatty acid sodium butyrate functions as a regulator of the skin immune system. *J. Invest. Dermatol.* 137, 855–864. doi: 10.1016/j.jid.2016.11.014

Seneschal, J., Boniface, K., D'Arino, A., and Picardo, M. (2021). An update on vitiligo pathogenesis. *Pigment Cell Melanoma Res.* 34, 236–243. doi: 10.1111/pcmr.12949

Seo, S. K., and Kwon, B. (2023). Immune regulation through tryptophan metabolism. *Exp. Mol. Med.* 55, 1371–1379. doi: 10.1038/s12276-023-01028-7

Shah, F., Giri, P. S., Bharti, A. H., and Dwivedi, M. (2024). Compromised melanocyte survival due to decreased suppression of CD4+ & CD8+ resident memory T cells by impaired TRM-regulatory T cells in generalized vitiligo patients. *Exp. Dermatol.* 33:e14982. doi: 10.1111/exd.14982

Shah, F., Patel, S., Begum, R., and Dwivedi, M. (2021). Emerging role of tissue resident memory T cells in vitiligo: from pathogenesis to therapeutics. *Autoimmun. Rev.* 20:102868. doi: 10.1016/j.autrev.2021.102868

Shakhbazova, A., Wu, H., Chambers, C. J., and Sivamani, R. K. (2021). A systematic review of nutrition, supplement, and herbal-based adjunctive therapies for vitiligo. *J. Altern. Complement. Med.* 27, 294–311. doi: 10.1089/acm.2020.0292

Shapiro, H., Kolodziejczyk, A. A., Halstuch, D., and Elinav, E. (2018). Bile acids in glucose metabolism in health and disease. *J. Exp. Med.* 215, 383–396. doi: 10.1084/jem.20171965

Shiu, J., Zhang, L., Lentsch, G., Flesher, J. L., Jin, S., Polleys, C., et al. (2022). Multimodal analyses of vitiligo skin identify tissue characteristics of stable disease. *JCI Insight* 7:e154585. doi: 10.1172/jci.insight.154585

Singh, A., Das, D., Kurra, S., Arava, S., Gupta, S., and Sharma, A. (2021). Dendritic cells and their associated pro-inflammatory cytokines augment to the inflammatory milieu in vitiligo skin. *Cytokine* 148:155598. doi: 10.1016/j.cyto.2021.155598

Singh, A., Gotherwal, V., Junni, P., Vijayan, V., Tiwari, M., Ganju, P., et al. (2017). Mapping architectural and transcriptional alterations in non-lesional and lesional epidermis in vitiligo. *Sci. Rep.* 7:9860. doi: 10.1038/s41598-017-10253-w

Singh, V., Lee, G., Son, H., Koh, H., Kim, E. S., Unno, T., et al. (2023). Butyrate producers, "the sentinel of gut": their intestinal significance with and beyond butyrate, and prospective use as microbial therapeutics. *Front. Microbiol.* 13:1103836. doi: 10.3389/fmicb.2022.1103836

Singh, R. K., Lee, K. M., Vujkovic-Cvijin, I., Ucmak, D., Farahnik, B., Abrouk, M., et al. (2016). The role of IL-17 in vitiligo: a review. *Autoimmun. Rev.* 15, 397–404. doi: 10.1016/j.autrev.2016.01.004

Sinha, S., Lin, G., and Ferenczi, K. (2021). The skin microbiome and the gut-skin axis. *Clin. Dermatol.* 39, 829–839. doi: 10.1016/j.clindermatol.2021.08.021

Slominski, A. T., Zmijewski, M. A., Skobowiat, C., Zbytek, B., Slominski, R. M., and Steketee, J. D. (2012). Sensing the environment: regulation of local and global homeostasis by the skin's neuroendocrine system. *Adv. Anat. Embryol. Cell Biol.* 212, v–115. doi: 10.1007/978-3-642-19683-6_1

Song, P., Zhang, W., Guo, S., Wang, G., Gao, T., Li, C., et al. (2024). Membranal expression of Calreticulin induced by unfolded protein response in melanocytes: a mechanism underlying oxidative stress-induced autoimmunity in vitiligo. *J. Invest. Dermatol.* 144, 1622–1632.e5. doi: 10.1016/j.jid.2024.01.007

Srivastava, N., Bishnoi, A., Parsad, D., Kumaran, M. S., Vinay, K., and Gupta, S. (2021). Dendritic cells sub-sets are associated with inflammatory cytokine production in progressive vitiligo disease. *Arch. Dermatol. Res.* 313, 759–767. doi: 10.1007/s00403-020-02168-w

Sun, M., Wu, W., Chen, L., Yang, W., Huang, X., Ma, C., et al. (2018). Microbiota-derived short-chain fatty acids promote Th1 cell IL-10 production to maintain intestinal homeostasis. *Nat. Commun.* 9:3555. doi: 10.1038/s41467-018-05901-2

Sun, M., Wu, W., Liu, Z., and Cong, Y. (2017). Microbiota metabolite short chain fatty acids, GPCR, and inflammatory bowel diseases. *J. Gastroenterol.* 52, 1–8. doi: 10.1007/s00535-016-1242-9

Tang, H. H., Zhang, Y. F., Yang, L. L., Hong, C., Chen, K. X., Li, Y. M., et al. (2023). Serotonin/5-HT7 receptor provides an adaptive signal to enhance pigmentation response to environmental stressors through cAMP-PKA-MAPK, Rab27a/RhoA, and PI3K/AKT signaling pathways. *FASEB J.* 37:e22893. doi: 10.1096/fj.202201352RR

Uberoi, A., Bartow-McKenney, C., Zheng, Q., Flowers, L., Campbell, A., Knight, S. A. B., et al. (2021). Commensal microbiota regulates skin barrier function and repair via signaling through the aryl hydrocarbon receptor. *Cell Host Microbe* 29, 1235–1248.e8. doi: 10.1016/j.chom.2021.05.011

Utama, A., Wijesinghe, R., and Thng, S. (2024). Janus kinase inhibitors and the changing landscape of vitiligo management: a scoping review. *Int. J. Dermatol.* 63, 1020–1035. doi: 10.1111/ijd.17157

Walczak, K., Langner, E., Makuch-Kocka, A., Szelest, M., Szalast, K., Marciniak, S., et al. (2020). Effect of tryptophan-derived AhR ligands, kynurenine, Kynurenic acid and FICZ, on proliferation, cell cycle regulation and cell death of melanoma cells-in vitro studies. *Int. J. Mol. Sci.* 21:7946. doi: 10.3390/ijms21217946

Walczak, K., Szalast, K., and Krasowska, D. (2023). The biological interactions between kynurenine and AhR in melanocytes: in vitro studies. *Amino Acids* 55, 947–954. doi: 10.1007/s00726-023-03279-0

Wilson, A. S., Koller, K. R., Ramaboli, M. C., Nesengani, L. T., Ocvirk, S., Chen, C., et al. (2020). Diet and the human gut microbiome: An international review. *Dig. Dis. Sci.* 65, 723–740. doi: 10.1007/s10620-020-06112-w

Wu, M., Chen, X., Lu, Q., and Yao, X. (2024). Fecal microbiota transplantation for the treatment of chronic inflammatory skin diseases. *Heliyon* 10:e37432. Published 2024 Sep 7. doi: 10.1016/j.heliyon.2024.e37432

Wu, Q., Cheng, P., Shao, T., Li, Z., Ji, Q., Wang, L., et al. (2023). Alterations of gut microbiota and gut metabolites in the young-adult vitiligo patients. *J. Eur. Acad. Dermatol. Venereol.* 37, e904–e907. doi: 10.1111/jdv.19012

Wu, H. L., Pang, S. L., Liu, Q. Z., Wang, Q., Cai, M. X., and Shang, J. (2014). 5-HT1A/1B receptors as targets for optimizing pigmentary responses in C57BL/6 mouse skin to stress. *PLoS One* 9:e89663. doi: 10.1371/journal.pone.0089663

Xiao, X., Hu, X., Yao, J., Cao, W., Zou, Z., Wang, L., et al. (2023). The role of short-chain fatty acids in inflammatory skin diseases. *Front. Microbiol.* 13:1083432. doi: 10.3389/fmicb.2022.1083432

Xie, W. R., Yang, X. Y., Xia, H. H., Wu, L. H., and He, X. X. (2019). Hair regrowth following fecal microbiota transplantation in an elderly patient with alopecia areata: a case report and review of the literature. *World J. Clin. Cases* 7, 3074–3081. doi: 10.12998/wjcc.v7.i19.3074

Xie, B., Zhu, Y., Shen, Y., Xu, W., and Song, X. (2023). Treatment update for vitiligo based on autoimmune inhibition and melanocyte protection. *Expert Opin. Ther. Targets* 27, 189–206. doi: 10.1080/14728222.2023.2193329

Xun, Z., Lin, J., Yu, Q., Liu, C., Huang, J., Shang, H., et al. (2021). Taurocholic acid inhibits the response to interferon-α therapy in patients with HBeAg-positive chronic hepatitis B by impairing CD8 T and NK cell function. *Cell. Mol. Immunol.* 18, 461–471. doi: 10.1038/s41423-020-00601-8

Yang, W., Chen, X., and Hu, H. (2020). CD4+ T-cell differentiation in vitro. *Methods Mol. Biol.* 2111, 91–99. doi: 10.1007/978-1-0716-0266-9_8

Yu, J., Luo, Y., Zhu, Z., Zhou, Y., Sun, L., Gao, J., et al. (2019). A tryptophan metabolite of the skin microbiota attenuates inflammation in patients with atopic dermatitis through the aryl hydrocarbon receptor. *J. Allergy Clin. Immunol.* 143, 2108–2119.e12. doi: 10.1016/j.jaci.2018.11.036

Yuan, M., Chang, L., Gao, P., Li, J., Lu, X., Hua, M., et al. (2024). Synbiotics containing sea buckthorn polysaccharides ameliorate DSS-induced colitis in mice via regulating Th17/Treg homeostasis through intestinal microbiota and their production of BA metabolites and SCFAs. *Int. J. Biol. Macromol.* 276:133794. doi: 10.1016/j.ijbiomac.2024.133794

Yue, R., Wei, X., Zhao, J., Zhou, Z., and Zhong, W. (2021). Essential role of IFN-γ in regulating gut antimicrobial peptides and microbiota to protect against alcohol-induced bacterial translocation and hepatic inflammation in mice. *Front. Physiol.* 11:629141. doi: 10.3389/fphys.2020.629141

Yue, Y., Zhong, M., An, X., Feng, Q., Lai, Y., Yu, M., et al. (2022). Serotonin (5-HT) 2A receptor involvement in melanin synthesis and transfer via activating the PKA/CREB signaling pathway. *Int. J. Mol. Sci.* 23:6111. doi: 10.3390/ijms23116111

Zhang, K., Jiang, L., Fu, C., Huang, J., Wen, Y., Zhou, S., et al. (2024). Identification of dietary factors that impact the gut microbiota associated with vitiligo: a Mendelian randomization study and meta-analysis. *Exp. Dermatol.* 33:e15176. doi: 10.1111/exd.15176

Zhang, Q., Zhao, L., Li, Y., Wang, S., Lu, G., and Wang, H. (2024). Advances in the mechanism of action of short-chain fatty acids in psoriasis. *Int. Immunopharmacol.* 141:112928. doi: 10.1016/j.intimp.2024.112928

Zhu, C., Sawrey-Kubicek, L., Beals, E., Rhodes, C. H., Houts, H. E., Sacchi, R., et al. (2020). Human gut microbiome composition and tryptophan metabolites were changed differently by fast food and Mediterranean diet in 4 days: a pilot study. *Nutr. Res.* 77, 62–72. doi: 10.1016/j.nutres.2020.03.005

Zhuang, H., Ren, X., Jiang, F., and Zhou, P. (2023). Indole-3-propionic acid alleviates chondrocytes inflammation and osteoarthritis via the AhR/NF-κB axis. *Mol. Med.* 29:17. doi: 10.1186/s10020-023-00614-9

Zmora, N., Suez, J., and Elinav, E. (2019). You are what you eat: diet, health and the gut microbiota. *Nat. Rev. Gastroenterol. Hepatol.* 16, 35–56. doi: 10.1038/s41575-018-0061-2

frontiers | Frontiers in Microbiology

TYPE Original Research
PUBLISHED 16 July 2025
DOI 10.3389/fmicb.2025.1610170

Check for updates

OPEN ACCESS

EDITED BY
Mohammad Altamimi,
An-Najah National University, Palestine

REVIEWED BY
Jian Li,
Tulane University, United States
Muawuz Ijaz,
University of Veterinary and Animal Sciences, Pakistan

*CORRESPONDENCE
Francesca Turroni
francesca.turroni@unipr.it

RECEIVED 11 April 2025
ACCEPTED 30 June 2025
PUBLISHED 16 July 2025

CITATION
Mancabelli L, Tarracchini C, Longhi G, Alessandri G, Ventura M and Turroni F (2025) Dissecting the molecular interactions between botanical extracts and the human gut microbiota. *Front. Microbiol.* 16:1610170. doi: 10.3389/fmicb.2025.1610170

COPYRIGHT
© 2025 Mancabelli, Tarracchini, Longhi, Alessandri, Ventura and Turroni. This is an open-access article distributed under the terms of the Creative Commons Attribution License (CC BY). The use, distribution or reproduction in other forums is permitted, provided the original author(s) and the copyright owner(s) are credited and that the original publication in this journal is cited, in accordance with accepted academic practice. No use, distribution or reproduction is permitted which does not comply with these terms.

Dissecting the molecular interactions between botanical extracts and the human gut microbiota

Leonardo Mancabelli[1,2], Chiara Tarracchini[3], Giulia Longhi[3], Giulia Alessandri[3], Marco Ventura[2,3] and Francesca Turroni[2,3]*

[1]Department of Medicine and Surgery, University of Parma, Parma, Italy, [2]Microbiome Research Hub, University of Parma, Parma, Italy, [3]Laboratory of Probiogenomics, Department of Chemistry, Life Sciences, and Environmental Sustainability, University of Parma, Parma, Italy

Over millions of years, humans and their gut microbes have developed a symbiotic relationship that benefits both organisms. Many plants and herbs consumed as food by humans, such as aloe vera gel and dandelion root extracts, contain bioactive compounds with recognized therapeutic or preventive effects. However, the impact of these botanicals on the composition and functionality of the human gut microbiota is not yet understood. In this study, the molecular impact of these botanicals on reconstructed human gut microbiota was assessed by *in-vitro* bioreactor experiments followed by metagenomics and transcriptomic approaches, highlighting both taxonomic and functional changes in the human gut microbiome. Furthermore, cross-feeding activities established by common human gut microbial taxa like *Bacteroides* spp. when cultivated on these extracts were assessed. In conclusion, the results show that botanicals affect intestinal populations that are highly dependent on the microbial taxa present and that trophic interactions are established in few key gut members.

KEYWORDS

gut microbiota, microbiome, dandelion root, aloe vera gel, bifidobacteria

1 Introduction

The human intestine hosts one of the most complex, diverse, and intricate microbial communities in the biosphere, known as the gut microbiota, which includes bacteria, Archaea, viruses, fungi, and protozoa (Ursell et al., 2012; Matijasic et al., 2020; Sudheer et al., 2022). Millions of years of co-evolution between the human host and its gut microbial ecosystem have led to the establishment of a binary symbiotic relationship from which both organisms benefit (Pickard et al., 2017; Takiishi et al., 2017; Alessandri et al., 2019). Indeed, the host guarantees a wide variety of nutrients and a perfect environment for the proliferation of gut microbes, while the gut microbiota, in turn, offers the host a plethora of metabolic and physiological activities that play a crucial role in influencing host health (Pickard et al., 2017; Takiishi et al., 2017; Afzaal et al., 2022; Lee et al., 2024). In addition to its ability to metabolize indigestible food compounds, it can provide nutrition for enterocytes and produce a wide variety of bioactive metabolites, including short-chain fatty acids (SCFAs), vitamins, neuroactive molecules, tryptophan derivatives, and indole lactic acids (Rahman et al., 2023; Tarracchini et al., 2024). The intestinal microbiota is also involved in a continuous molecular dialogue with the host immune system, influencing immune responses as well as bowel homeostasis and functionality (Levy et al., 2017; Rahman et al., 2023; Donkers et al., 2024; Tarracchini et al., 2024). Furthermore, it is

widely recognized that the gut microbiota is important in limiting pathogen colonization and promoting the maintenance of intestinal barrier integrity (Moens and Veldhoen, 2012; Pickard et al., 2017; Sanchez et al., 2017; Van Hul et al., 2024). However, despite these multiple beneficial activities exploited by gut microbes, the intestinal microbiota can also be responsible for adverse health effects. Indeed, when a disruption of the climax and dynamic balance, also known as homeostasis, among the bacterial species of the gut microbiota occurs, a dysbiosis condition can be established with consequent stimulation and exacerbation of the host's health disturbances (DeGruttola et al., 2016). This imbalance contributes to the onset of several chronic pathological conditions, including intestine-related pathologies such as inflammatory bowel disease, irritable bowel syndrome, or colorectal cancer, but also extra-intestinal diseases, ranging from diabetes and obesity to cardiovascular, kidney, liver, and even neurological disorders (Belizario and Faintuch, 2018; Wilkins et al., 2019; Dixit et al., 2021; Lee et al., 2024; Manske, 2024).

In this context, in recent decades, several efforts have been placed to identify strategies that can be adopted to maintain intestinal homeostasis or prevent/restore intestinal dysbiosis. Among many different approaches, functional and/or therapeutic foods are valid ways to prevent gut dysbiosis (Medina-Vera et al., 2019; Perez-Burillo et al., 2020; Banerjee et al., 2023). These foods may contain bioactive compounds such as tannins, polyphenols, flavonoids, terpenoids, and complex polysaccharides, which can have functional effects on our health (Thumann et al., 2019; Sudheer et al., 2022; Banerjee et al., 2023; Jacquier et al., 2024). Within botanicals with possible effects on the human gut microbiota, aloe vera gel and dandelion root extracts have been used for centuries as herbal medicines due to their therapeutic benefits (Le Phan et al., 2021; Cuvas-Limon et al., 2022; Li et al., 2022; Maiuolo et al., 2022; Li et al., 2024; Yan and Dong, 2024). Specifically, dandelion root (DR) extracts have renowned beneficial effects on the gastrointestinal tract, reducing the expression of reactive proteins and oxidative stress and regulating gut microbiota through their antioxidant and anti-inflammatory properties (Kaur et al., 2021; Li et al., 2022; Yan and Dong, 2024). In parallel, aloe vera gel (AVG), which is currently included in several beverages with functional potential, is used for its countless beneficial effects on human health, encompassing immunomodulatory, anti-obesity, antiviral, anti-diabetic, and antibacterial properties (Holscher et al., 2015; Cuvas-Limon et al., 2022; Maiuolo et al., 2022). At the same time, certain studies demonstrated the role of these medicinal plant extracts in regulating gut dysbiosis (Fu et al., 2022; Maiuolo et al., 2022; Yan et al., 2023; Yan and Dong, 2024). However, despite the multiple beneficial properties of AVG and dandelion root extracts, these botanicals' effect on the taxonomic composition and functional potential of the human gut microbiota is still far from being thoroughly dissected.

Here, an *in-vitro* growth experiment involving 10 artificial gut microbiota was performed to investigate whether AVG and dandelion root extracts could have a role in modulating both the taxonomic and functional profile of the human intestinal ecosystem through the combination of metagenomic approaches with flow cytometry. In addition, specific cross-feeding activities of the two botanicals on the most impacted gut microbes were evaluated.

2 Materials and methods

2.1 *In-vitro* gut microbiota cultivation in the presence of aloe vera gel or dandelion root extracts

To evaluate whether AVG or dandelion root can modulate the taxonomic composition of the human gut microbiota, 10 artificial gut microbiota (AGM) communities were cultivated in the presence of two botanical extracts. Specifically, the AGMs were obtained in the framework of another study (Alessandri et al., 2024). Briefly, the bacterial community of each collected fecal sample was immobilized on 1–2 mm gellan-xanthan gel beads and inoculated in a bioreactor-based colonic fermentation system (Solaris Biotech Solutions, Italy). AGM cultivation was performed by using a human gut environment-simulating growth medium, which has been previously described (Alessandri et al., 2022), with a temperature set at 37°C, continuous stirring at 200 rpm, while the pH was maintained at 6.8 by the addition of 2.5 M NaOH. The cultivation was run for 15 days in a continuous mode (Alessandri et al., 2024). After the gut microbiota stabilization, an aliquot of the obtained AGMs was withdrawn from the bioreactor system and used as inoculum for subsequent experiments. Specifically, each AGM was individually cultivated in the presence of aloe vera gel or dandelion root extracts or without the addition of any botanicals as a control sample. AGMs were inoculated at a final inoculum concentration of 2% (v/v) in 2 mL of the same culture medium used to stabilize fecal samples (Alessandri et al., 2022), while botanical dry extracts, after filter-based sterilization, were added to the culture medium to a final concentration of 0.1% (w/v). Cultivations were performed following the MiPro model protocol (Li et al., 2019), i.e., 96-deep well plates were covered with a silicone gel mat with a vent hole on each well created with a sterile syringe needle to facilitate gas exchange. Plates were incubated under anaerobic conditions at 37°C and shaken at 5,000 rpm. After 24 h, cultures were collected and stored at −80°C until they were processed for DNA extraction and flow cytometry-based total bacterial cell count. Each experiment was carried out in triplicates.

2.2 DNA extraction and shallow shotgun sequencing

After growth assays in the presence of AVG or dandelion root extracts, every obtained replicate, including the control samples, was subjected to total bacterial DNA extraction using the QIAmp DNA Stool Mini Kit (Qiagen, Germany), following the manufacturer's instructions. Then, the extracted DNA was prepared using the Illumina Nextera XT DNA Library Preparation Kit, following the Illumina Nextera XT protocol. Specifically, DNA samples were enzymatically fragmented, barcoded, and purified using magnetic beads. Subsequently, the prepared samples were quantified using a fluorometric Qubit quantification system (Life Technologies, USA), loaded on a TapeStation Instrument (Agilent Technologies, USA), and normalized to 4 nM. Paired-end

sequencing was performed using an Illumina NextSeq sequencer (Illumina Inc., San Diego, USA) with the NextSeq reagent Kit v3 and a 1% PhiX control library spike-in.

2.3 Shallow shotgun metagenomic dataset analysis

The obtained raw data in.fastq format were submitted to a filtering step to remove reads with a quality of <25 as well as sequencing corresponding to human DNA by mapping the reads on the *Homo sapiens* genome, while reads with a length of >149 bp were retained. As previously reported, quality-filtered data was used for further analysis with METAnnotatorX2 for taxonomic profile reconstruction (Milani et al., 2021). Retained sequences were used as input to perform a MegaBLAST local alignment of reads to a pre-processed database, including available genomes of eukaryotes (Fungi and Protists), viruses, archaea, and bacteria, following the METAnnotatorX2 protocol (Milani et al., 2021). Reads showing a nucleotide identity of >94% to the genomes included in the database were classified at the species level, while they were classified at the genus level as undefined species when a lower percentage was detected. Taxonomic profiles of each sample were exploited to calculate the Shannon index and species richness to assess α-diversity. Species richness represented the number of bacterial species detected for each metagenomic sample. Bray-Curtis dissimilarity matrices based on species abundance, calculated through the Rstudios software, were used to evaluate similarities between samples (β-diversity). The similarity range was calculated as a value between 0 and 1. Principal coordinate analysis (PCoA) was used to represent β-diversity through Emperor. In the PCoA, each sphere represents a single sample distributed in tridimensional space according to its specific taxonomic profile. Functional profiling of the sequenced reads was performed with the METAnnotatorX2 bioinformatics platform (Milani et al., 2021). Functional classification of reads was carried out to identify metabolic pathways based on the MetaCyc database (release 24.1; Caspi et al., 2016) through RAPSearch2 software (Ye et al., 2011; Zhao et al., 2012).

2.4 Evaluation of bacterial cell density through flow cytometry

Each replicate underwent a total bacterial cell count through flow cytometry. Specifically, replicates were 10,000 diluted in Phosphate Buffered Saline (PBS) solution, and 1 mL of the bacterial dilution was stained with 1 µL of SYBR Green I (Thermo Fisher Scientific, USA; 1:100 diluted in DMSO; Merk, Germany), vortex-mixed, and incubated in the dark for at least 15 min before measurement. Count assays were performed using the Attune NxT flow cytometer (Thermo Fisher Scientific, USA) equipped with a blue laser set at 50 mW and an excitation wavelength of 488 nm. Multiparametric analyses were carried out on both scattering signals, including forward and side scatter, while SYBR Green I fluorescence was detected on the BL1 530/30 nm channel. Cell debris were excluded from the acquisition analysis by setting a BL1 threshold. In addition, the gated fluorescence events were evaluated on the forward-sideways density plot to exclude background events and to obtain an accurate microbial cell count, as previously described (Vandeputte et al., 2017).

2.5 Growth assays using co-culture duet system

To investigate the interactions among co-culture members and validate the proof of concept, we employed a Cerillo co-culture duet system (Cerillo, USA). In this system, the wells are separated by a semi-permeable membrane divider filter with a porosity of 0.2 µm, allowing for the monitoring individual strain cell numbers by flow cytometry within the co-culture. The experiment was performed in triplicate.

2.6 RNA extraction and sequencing

Total RNA was isolated as previously described (Turroni et al., 2010). Briefly,1 mL of QIAZOL (Qiagen, United Kingdom) and 0.8 g of glass beads (diameter, 106 µm; Sigma) were used to resuspend cell pellets for lysis. Specifically, this was obtained by alternating 2 min of stirring on a bead beater with 2 min of static cooling on ice. RNA was recovered from the upper phase after centrifugation at 12,000 rpm for 15 min and after purification using an RNeasy minikit (Qiagen, Germany) following the manufacturer's guidelines. The RNA concentration and purity were evaluated using a spectrophotometer (Eppendorf, Germany). For RNA-Seq, from 100 ng to 1 µg of extracted RNA was depleted from rRNA by employing QIAseq FastSelect−5S/16S/23S according to the producer's guide (Qiagen, Germany). mRNA yield was checked using a Tape station 2200 (Agilent Technologies, USA). Then, the TruSeq Standard mRNA preparation kit (Illumina, San Diego, CA) was used to prepare the sequencing library. The samples were run into a NextSeq 2000 high output v2.5 kit (150 cycles, single end; Illumina). Low-quality reads (minimum mean quality, 20; minimum length, 150 bp) and any residual ribosomal locus-encompassing reads were removed using the METAnnotatorX2 (Milani et al., 2021). Bowtie2 software (Langdon, 2015) was used to align the reads with respect to the reference genome of each *Bacteroides* strain used. Htseq-counts script of HTSeq software in "union" mode was employed to quantify reads mapped to individual transcripts (Anders et al., 2015). Raw data were then normalized utilizing CPM (mapped reads) for filtering genes with low counts (CPM < 1) and trimmed mean of *M* values (TMM) for statistically robust differential gene expression analysis through the EdgeR package (Robinson et al., 2010). Genes showing a fold-change in transcription of ≥2 ($Log_2FC > 1$; up-regulated) and a fold-change in transcription of ≤2 ($Log_2FC < 1$; down-regulated), in combination with a *p*-value of ≤0.05 calculated through correction for multiple comparisons using the False Discovery Rate (FDR) procedure, were considered as significantly differentially transcribed between the bi-associations when compared to mono-associations.

2.7 Statistical analyses

All statistical analyses were performed using SPSS software, except for beta-diversity comparisons. Before group comparisons, the Shapiro-Wilk test was applied to assess the normality of the distribution for each variable, including bacterial species abundances, alpha-diversity indices, and enzyme-coding gene counts, within each sample. Based on the normality test results, parametric or non-parametric tests were selected accordingly. Specifically, ANOVA was used for normally distributed data, while the Kruskal-Wallis test was applied for non-normally distributed data. *Post-hoc* pairwise comparisons between treatment groups were performed using the Bonferroni correction to control for multiple testing. These tests evaluated alpha-diversity differences, bacterial taxa's relative abundances, and functional genes across experimental conditions. Differences in beta-diversity between groups were assessed using PERMANOVA (Permutational Multivariate Analysis of Variance), based on Bray–Curtis dissimilarity matrices, computed with QIIME2 (Bolyen et al., 2019) using 999 permutations. Moreover, MaAsLin2 software (Mallick et al., 2021) was used to perform multivariable association analysis to evaluate the impact of botanical treatments (AVG and DR) on microbial taxonomic profiles while accounting for inter-individual variability. In detail, a linear mixed-effects model was applied, specifying treatment (AVG, DR) as a fixed effect and sample identity (AGM1–AGM10) as a random effect. The CTRL group was set as the reference condition. The Benjamini–Hochberg false discovery rate (FDR) correction adjusted *P*-values for multiple testing.

3 Results

3.1 Assessing the influence of aloe vera gel and dandelion root extract on gut microbiota composition

To investigate whether AVG or DR extracts may exploit a role in modulating the human intestinal ecosystem, 10 AGMs were cultured in the presence of each botanical extract as well as in their absence as control samples in a 96-deep well plate, as previously described (Li et al., 2019; Alessandri et al., 2022; Figure 1A). The AGMs were obtained in the framework of another study through a continuous cultivation system, starting from fecal samples of healthy adult human individuals as inoculum, allowing them to stabilize both dominant and accessory bacterial species of 10 different subjects (Alessandri et al., 2024). Specifically, except for AGM1 and AGM2, which resulted in being dominated by *Escherichia coli*, for the other eight AGMs, a predominance of the genus *Bacteroides*, i.e., one of the most abundant and prevalent bacterial taxa of the human gut microbiota (Arumugam et al., 2011; Mancabelli et al., 2017; Costea et al., 2018; Alessandri et al., 2024; Shin et al., 2024). In addition, other main microbial players of the human gut microbiota, including *Akkermansia muciniphila*, *Anaerotignum faecicola*, *Collinsella aerofaciens*, *Faecalibacterium prausnitzii*, *Parabacteroides distasonis*, *Parabacteroides merdae*, *Phocaeicola dorei*, and *Ruminococcus gnavus*, recently reclassified as *Mediterraneibacter gnavus* (Togo et al., 2018) were also stabilized.

Cultivations of AGMs in presence of botanicals were carried out in triplicate by exploiting the identical human gut environment-simulating culture medium used for the stabilization of the AGMs (Alessandri et al., 2022, 2024). After 24 h of growth under anaerobic conditions, AGMs cultures were subjected to DNA extraction and shallow shotgun sequencing (Figure 1A). The latter produced 5,661,100 quality-filtered reads with an average of 62,901 filtered reads per sample (Supplementary Table S1).

The generated species-level taxonomic profiles were used to explore the α-diversity among samples. Specifically, an overall species richness analysis did not reveal any significant difference in the number of detected bacterial species among the three groups, i.e., control and AVG- or DR-treated samples (ANOVA Bonferroni p-value > 0.05 in all cases), as also confirmed by the calculation of the Shannon index (Figure 1B). Thus, this suggests that these botanicals do not induce drastic/major shifts in the bacterial complexity of the gut microbiota. A desirable outcome since a radical alteration of gut bacterial species number is generally associated with dysbiosis status (Scher et al., 2015; Chandrasekaran et al., 2023; Hajj Hussein et al., 2023; Jauregui-Amezaga and Smet, 2024). However, the same species richness analysis performed for each AGM highlighted some significant variations (Figure 1B). Indeed, both AGM3 and AGM7 showed a meaningful enhancement of the bacterial complexity when AGMs were exposed to AVG with respect to the control (ANOVA Bonferroni p-value of 0.036 and 0.029, respectively; Figure 1B). For AGM9, a significant decrease in bacterial taxa was recorded in the presence of both AVG and DR when compared to the control (ANOVA Bonferroni p-value of 0.035 and 0.027, respectively; Figure 1B). Similarly, the Shannon index calculation highlighted an important reduction of the α-diversity for AGM1, AGM4, and AGM7 when exposed to DR (ANOVA Bonferroni p-value < 0.05 in all cases), as well as in AGM10 when cultivated in the presence of both AVG and DR when compared to the controls (ANOVA Bonferroni p-value of 0.021 and 0.017, respectively; Figure 1B). This suggests that, in certain circumstances (in 35% of cases), AVG and DR may exert a role in modulating the bacterial complexity of the human gut microbiota through specific microbial taxa.

Interestingly, no significant compositional differences were observed among the three different groups within each sample (pairwise PERMANOVA p-value > 0.05 in all cases) using a β-diversity analysis based on a Bray-Curtis dissimilarity matrix (Figure 1C). Indeed, no treatment-associated clustering of samples was observed. Thus, suggesting that neither AVG nor DR significantly modify the overall abundance ratios among bacterial species composing the human gut microbiota.

3.2 Aloe vera gel or dandelion root extract-driven modifications of the gut microbiota taxonomic composition

To evaluate whether AVG or DR extracts may have a role in modulating the abundance of the various bacterial taxa constituting the human gut microbiota, any significant

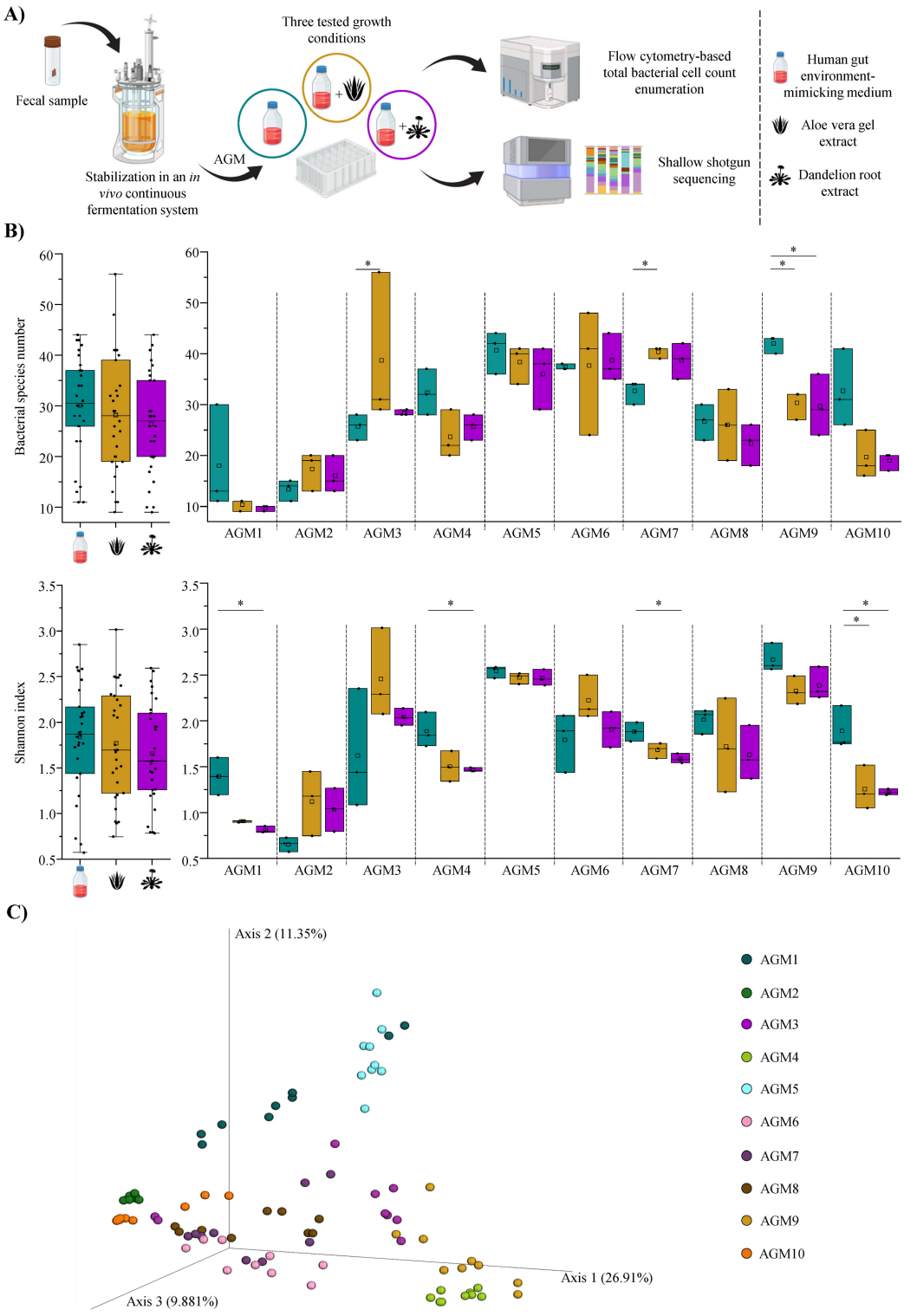

FIGURE 1
Plant extracts-driven modulation of the human gut microbiota biodiversity. **(A)** Schematically depicts the workflow used to assess the modulatory effects of AVG and DR extracts on the human gut microbiota. **(B)** Shows the box and whiskers plots of the alpha-diversity evaluated through a species richness analysis (at the top) and the Shannon index calculation (at the bottom). In both cases, the graphs on the left report the overall species richness or Shannon index average for each group, i.e., control samples and AVG- and DR-treated samples, while the graphs on the right display the two alpha-diversity indices calculated as the average of the obtained triplicates for each AGM and condition. In all cases, boxes are determined by the 25th and 75th percentiles, while the maximum and minimum values determine the whiskers and correspond to the box's extreme values. Lines inside the boxes represent the average, while squares correspond to the median. **(C)** Depicts the three-dimensional Bray-Curtis dissimilarity index-based PCoA of each sample divided per AGMs. *$p < 0.05$.

differences were investigated for each sample among the three groups. In this context, a total of 40 bacterial species showed key changes in their relative abundance, suggesting that these botanicals may have an effective role in influencing the abundance ratios among the bacterial taxa of the intestinal microbiota (Figure 2A and Supplementary Table S2). In-depth insights into the bacterial species whose abundance significantly differed among the conditions tested revealed that the relative load of *Akkermansia muciniphila* underwent a significant increase in AGM6 when in the presence of both AVG and DR with respect to the reference conditions (ANOVA Bonferroni *p*-value of 0.047 and 0.003, respectively; Figure 2A and Supplementary Table S2). This microorganism has recently been proposed as a novel promising probiotic bacterium due to its ability to attenuate certain inflammatory conditions, including acute and chronic colitis, or improve metabolic disorders, while its absence has been demonstrated to be associated with a plethora of diseases such as diabetes, obesity, or cancer (Bian et al., 2019; van der Lugt et al., 2019; Segers and de Vos, 2023; Calvo et al., 2024; Jiang et al., 2024; Panzetta and Valdivia, 2024). Therefore, since AVG and DR stimulate the abundance of *A. muciniphila* in AGM6, it can be argued that these botanicals may exert a potential beneficial effect on the intestinal microbiota, contributing to improving the abundance of this positive bacterium and, therefore, the overall host health. However, in the other sample containing this bacterial species, i.e., AGM5, *A. muciniphila* underwent no significant change (Supplementary Table S2). Therefore, this suggests that the ability of these botanicals to promote an increase in the relative abundance of these beneficial bacterial species may depend on cross-feeding interactions that originate in every AGM. It is plausible that some strains may possess genetic traits that encode enzymes that degrade these two plant extracts, allowing for energy recovery and the release of simpler compounds usable by other species (e.g., *A. muciniphila*) with which they share the ecological environment (Belzer et al., 2017; Wu et al., 2024).

In addition, members of another bacterial taxon known to exploit multiple beneficial effects upon its host, i.e., the genus *Bifidobacterium* (Bottacini et al., 2017; Hidalgo-Cantabrana et al., 2017; Alessandri et al., 2019; Martin et al., 2023), underwent significant shifts in their relative abundance when exposed to the two botanical extracts. Specifically, *Bifidobacterium adolescentis* exposed to DR in AGM1 (Kruskall-Wallis *p*-value of 0.034) and *Bifidobacterium pseudocatenulatum* cultivated in AVG for AGM2 (ANOVA Bonferroni *p*-value of 0.049) displayed a significant reduction in their relative abundances when compared to the control (Figure 2A and Supplementary Table S2). Conversely, *Bifidobacterium longum* loads significantly increased in AGM7 in the presence of both botanicals compared to the reference condition (ANOVA Bonferroni *p*-value < 0.05 in both cases; Figure 2A and Supplementary Table S2). Therefore, while for some bifidobacterial species, the two botanicals seemed to have a bacteriostatic/growth inhibitory effect, for other species, they may act as a selective substrate for their growth, as previously observed for other plant extracts (Duda-Chodak, 2012; Firrman et al., 2016; Santhiravel et al., 2022). Thus, it suggests that both AVG and DR can be exploited for the selective growth of particular bifidobacterial species with positive effects on the host health, given the renowned bifidobacterial anti-inflammatory properties (Martorell et al., 2021; Choi et al., 2022; Lueschow et al., 2022; Gavzy et al., 2023; Leser and Baker, 2023; Martin et al., 2023).

Beyond these potentially beneficial bacteria that generally represent only a small portion of the more complex and intricate human gut microbiota (Lay et al., 2005; Derrien et al., 2008; O'Callaghan and van Sinderen, 2016; Si et al., 2022), the analysis of the species-level taxonomic profiles revealed that AVG and DR also significantly influenced the relative abundance of species belonging to one of the most abundant and prevalent bacterial genera of the human gut microbiota, i.e., the genus *Bacteroides* (Arumugam et al., 2011; Mancabelli et al., 2017; Costea et al., 2018; Mancabelli et al., 2024). Specifically, *Bacteroides caccae* in AGM8 and *Bacteroides nordii* in AGM6, both treated with DR (ANOVA Bonferroni *p*-value of 0.02 and Kruskall-Wallis *p*-value of 0.02, respectively), showed a significant decrement in their relative abundance compared to the control. A similar reduction was observed for *Bacteroides faecis* in AGM7, also treated with both DR and AVG (ANOVA Bonferroni *p*-value < 0.05 in both cases). Conversely, *Bacteroides cellulosilyticus* in AGM3, treated with DR, displayed an opposite trend (ANOVA Bonferroni *p*-value of 0.03; Figure 2A and Supplementary Table S2). For three other *Bacteroides* species, instead, a significant change in their relative abundance with alterations varying according to the AGM they belong to was recorded (Figure 2A and Supplementary Table S2). Specifically, *Bacteroides ovatus* levels significantly increased in AGM3 with DR (ANOVA Bonferroni *p*-value of 0.04) and AGM9 with both AVG and DR (ANOVA Bonferroni *p*-value < 0.05 in both cases). At the same time, the species showed a significant reduction in AGM6 with DR (ANOVA Bonferroni *p*-value of 0.04) and AGM7 with AVG (Kruskall-Wallis *p*-value of 0.04) when compared to the reference condition (Figure 2A and Supplementary Table S2). Similarly, AGM3-associated *Bacteroides thetaiotaomicron* increased its relative abundance when cultured in DR (ANOVA Bonferroni *p*-value of 0.03), while the levels of this species significantly decreased in AGM4 and AGM10 in the presence of both AVG and DR when compared to the control (ANOVA Bonferroni *p*-value < 0.05 in all cases; Figure 2A and Supplementary Table S2). Finally, *Bacteroides xylanisolvens* relative abundance significantly increased in AGM2 after DR and AVG exposure (ANOVA Bonferroni *p*-value < 0.05 in both cases). At the same time, it decreased in AGM4 (ANOVA Bonferroni *p*-value < 0.05 in both cases) and AGM7 (Kruskall-Wallis *p*-value of 0.04 when compared to CTRL and DR; Figure 2A and Supplementary Table S2). Thus, suggesting not only that these two botanical extracts have a role in modulating the abundance of some of the most abundant and prevalent species of the human gut microbiota but also reinforcing the notion that these modifications in the abundance may be either strain-dependent or dependent on cross-feeding events closely associated with the gut microbiota composition.

Similar to *Bacteroides*, a different trend was observed for certain members of the genus *Enterococcus*, depending on the species. Indeed, *Enterococcus casseliflavus*, as well as *Enterococcus gallinarum*, and *Enterococcus* spp. significantly increased their load in AGM8 (Kruskall-Wallis *p*-value of 0.02, ANOVA Bonferroni *p*-value of 0.008 and 0.0008, respectively), while *Enterococcus faecium*

10.3389/fmicb.2025.1610170

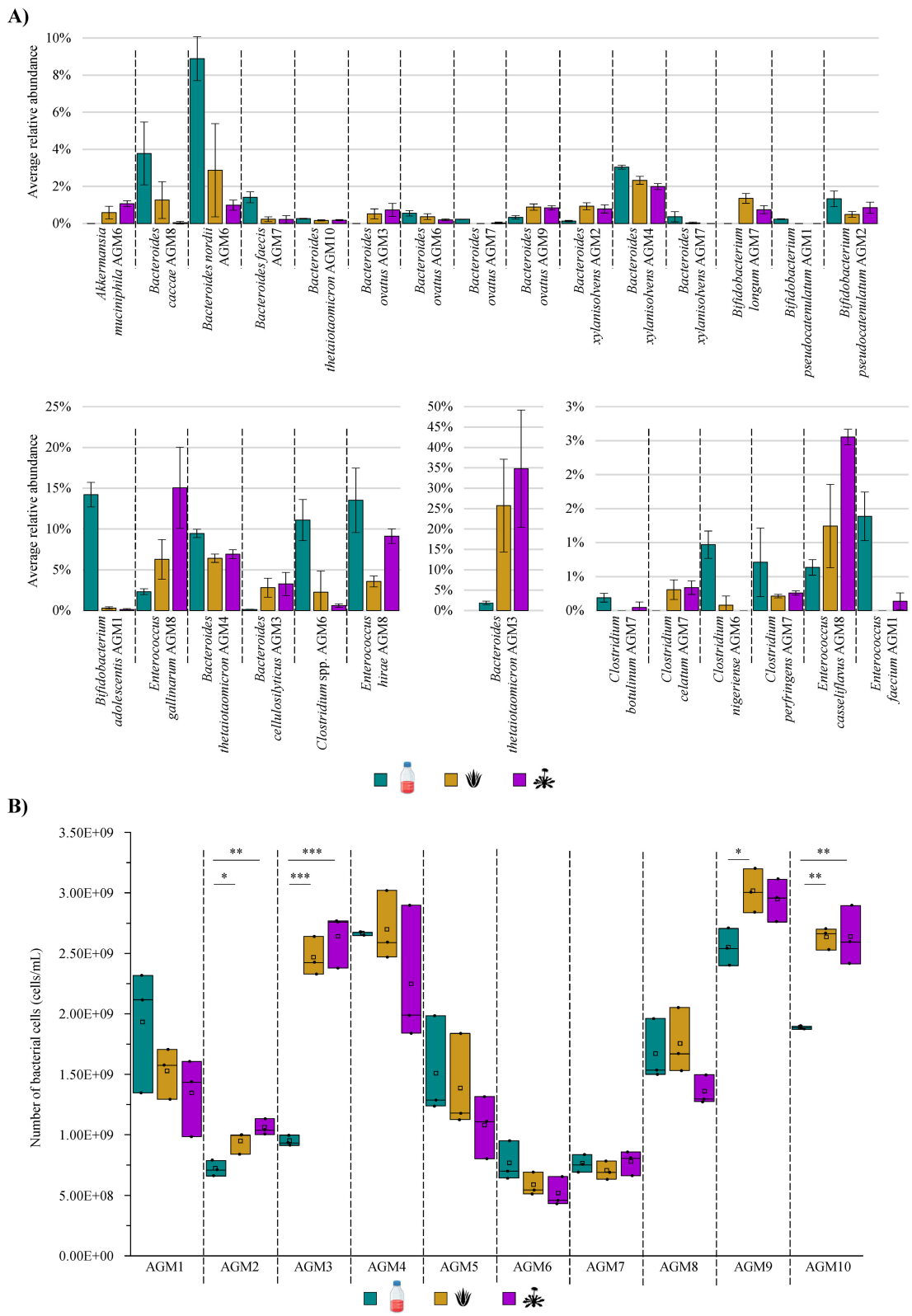

FIGURE 2
Modulation of gut microbiota taxonomic composition and growth performances in the presence of AVG and DR. **(A)** Reports the average relative abundance of the bacterial species that significantly differ among the three tested growth conditions per AGM. **(B)** Displays the box and whiskers plot associated with the total bacterial cell enumeration of each AGM in tested growth conditions. In the plot, boxes are determined by the 25th and 75th percentiles, while the whiskers are determined by the maximum and minimum values and correspond to the box extreme values. The lines inside the boxes represent the average, while the squares correspond to the median. *$p < 0.05$; **$p < 0.01$; ***$p < 0.001$.

and *Enterococcus hirae* average relative abundance decreased in AGM1 (Kruskall-Wallis p-value of 0.03) and AGM8 (ANOVA Bonferroni p-value of 0.007), respectively, when cultivated in the presence of one of the two botanicals with respect to the control (Figure 2A and Supplementary Table S2). On the other side, several species of the genus *Clostridium*, except for *Clostridium celatum*, showed a significant decrease in their relative abundance in the presence of at least one of the two botanicals (Figure 2A and Supplementary Table S2). In this context, since members of the genus *Clostridium* have been described as potential pathogens positively associated with gastrointestinal cancers, the AVG- and/or DR-driven decrease of these species can be considered a positive effect induced by these two botanicals (Yu et al., 2023; Cao et al., 2024; Garvey, 2024). These results show not only that the two botanicals are able to modulate the abundance ratios among species of the human intestinal microbiota, but they also appear to have a beneficial impact on the host health by promoting the growth of particular species with health-promoting activity and, at the same time, limiting/reducing the proliferation of other potentially pathogenic bacterial taxa.

To better understand the overall impact of botanical treatments on gut microbiota composition, a global statistical approach was implemented to evaluate treatment-driven effects while controlling for individual variability. Specifically, a linear mixed-effects model was applied using MaAsLin2, where treatments, i.e., AVG and DR, were included as fixed effects and sample identity was set as a random effect. This approach allowed the estimation of treatment effects across all samples, using the CTRL group as the reference condition.

At a significance threshold of $p < 0.05$, a total of 53 taxa showed treatment-associated changes in relative abundance (Supplementary Table S3). However, after correction for multiple tests using the Benjamini–Hochberg procedure ($q < 0.05$), only seven taxa remained significant (Supplementary Table S3). Each microbial taxon was counted only once, even when significantly affected by both treatments. Specifically, six bacterial taxa were significantly associated with AVG exposure and five with DR, all displaying negative coefficients. This observation suggests that both botanical extracts may selectively reduce the abundance of specific microbial taxa without inducing broad-scale shifts in overall community diversity.

This pattern aligns with the absence of significant changes in alpha-diversity, supporting the hypothesis that these botanicals exert targeted effects on particular taxa rather than altering the overall richness or evenness of the gut microbiota.

3.3 Impact of AVG and DR on gut microbiota growth performances

In addition to the fact that AVG- and/or DR-induced significant changes in the relative abundance of bacterial species composing the human gut microbiota, it was also assessed whether the two considered botanical extracts could have a role in modulating the growth performances of this complex microbial ecosystem. In this context, to obtain a comprehensive biological interpretation of AVG and DR effects on gut microbiota, a quantitative microbiome profiling assay was performed through flow cytometry to enumerate bacterial cells of each biological replicate and culture condition after 24 h of cultivation in a 96-deep well plate. Notably, considering the three macro-groups, no significant differences in the number of bacterial cells were observed among groups (Kruskal-Wallis p-value of 0.624), with a recorded average bacterial cell count of 1.54E+09 cells/mL, 1.77E+09 cells/mL, and 1.66E+09 cells/mL for the control, AVG- and DR-treated samples, respectively (Figure 2B). These data confirmed that the two botanicals produce no crucial effects either in stimulating or inhibiting the overall bacterial growth of the human intestinal microbiota. However, a thorough analysis of the statistical data obtained for each AGM revealed some significant differences in the growth performances of certain stabilized microbiota in the presence of AVG and/or DR compared to the control (Figure 2B). In detail, the number of bacterial cells was significantly higher after 24 h of cultivation in AGM2, AGM3, and AGM10 in the presence of either AVG or DR when compared to the control (ANOVA Bonferroni p-value < 0.05 for all cases; Figure 2B). In addition, the exposure to AVG extract induced a significant bacterial cell number increment in AGM9 with respect to the control (ANOVA Bonferroni p-value $= 0.047$; Figure 2B). This notion suggests that, depending on the taxonomic composition of the intestinal microbiota, the two plant extracts may have a role in influencing the growth performances of (some) bacterial species composing the human gut microbiota.

3.4 Cross-feeding activity on *Bacteroides* species

The *Bacteroides* species, representing the dominant taxa of 8 of the 10 AGMs, appears to be significantly impacted by botanicals, i.e., seven different species significantly increase/decrease their cell numbers (Figure 2A). To corroborate whether bi-associations of *Bacteroides* species could engage cross-feeding interactions on AVG and DR extract, respectively, *in-vitro* duets co-culture assays were established in triplicates. Specifically, the number of bacterial cells of the couple *Bacteroides cellulosilyticus* 55F-*Bacteroides xylanisolvens* 220F, *Bacteroides cellulosilyticus* 55F-*Bacteroides uniformis* 176F and *Bacteroides ovatus* 39F-*Bacteroides xylanisolvens* 220F were enumerated by flow cytometry. Growth analyses showed that the presence of botanicals has an impact in all the bi-associations except only for *B. xylanisolvens* 220F on DR, which appears to be unaltered (Figure 3A). On the contrary, *B. ovatus* 39F cells showed a significant enhancement when co-cultivated with *B. uniformis* 176F (p-value < 0.0001) both in the presence of AVG and DR, respectively (Figure 3B). The same behavior was depicted for *B. uniformis* 176F when grown in the presence of *B. cellulosilyticus* 55F (p-value equals 0.0001) in the presence of AVG and DR, respectively (Figure 3C). This data reinforces the assumption highlighted in previous experiments that the gut microbiota responds to botanicals differently, strongly dependent on the original composition of the complex microbial communities. Furthermore, the impact on gene expression of these *Bacteroides* strains grown in bi-association, which were highly affected by the presence of botanicals compared to single

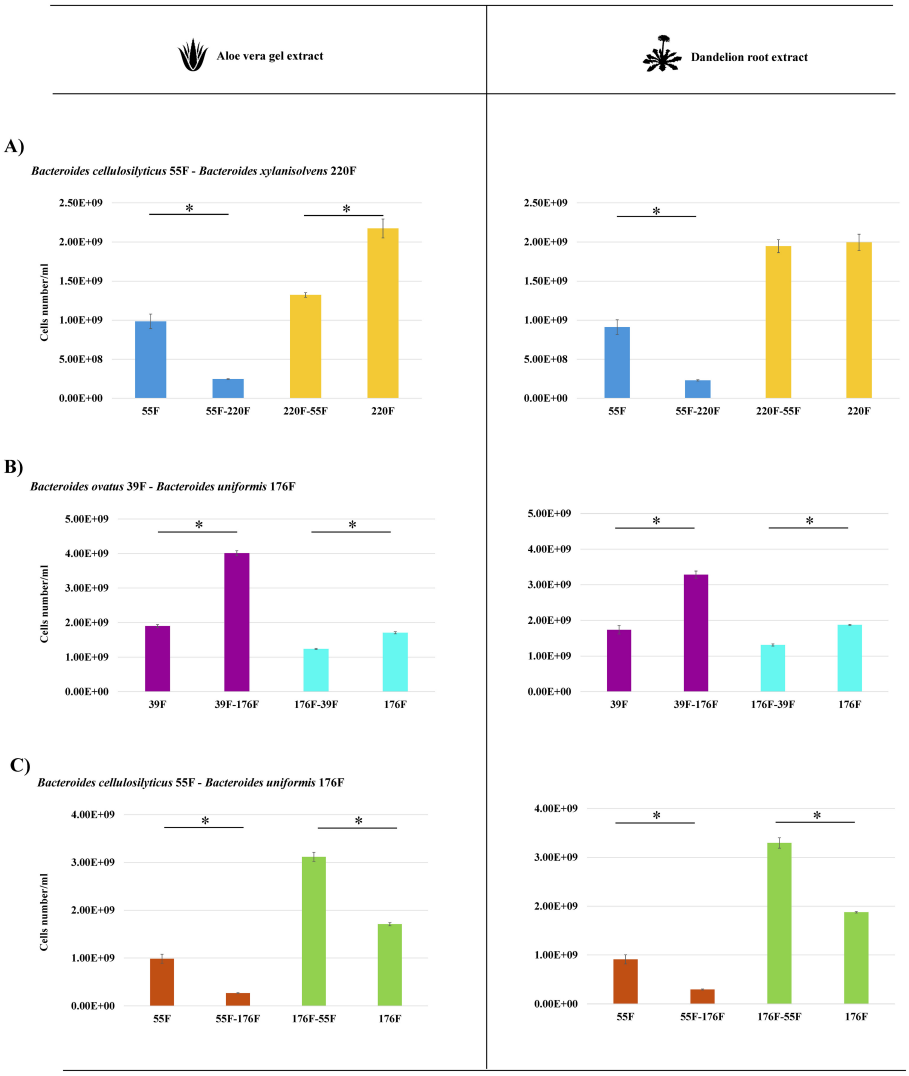

FIGURE 3
Quantification of the cell numbers of *Bacteroides* species in bi-association experiments. **(A)** depicts the cell number evaluation of the *Bacteroides cellulosilyticus* 55F and *Bacteroides xylanisolvens* 220F growth in mono and bi-association on AVG on the left and DR on the right. **(B)** Displays the cell number evaluation of the *Bacteroides ovatus* 39F-*Bacteroides uniformis* 176F growth in mono and bi-association on AVG on the left and DR extract on the right. In **(C)** the cell number quantification of the *Bacteroides cellulosilyticus* 55F and *Bacteroides uniformis* 176F growth in mono and bi-association on AVG on the left and DR extract on the right were shown. The flow cytometry quantification results are represented by bars in which the *y*-axis is the number/ml of bacterial cells, and the *x*-axis shows the names of the strains involved in mono-and bi-associations. Asterisks indicate that the presented data display a significant (*$p < 0.0003$) deviation from the obtained values of the mono-association.

cultivation, was evaluated through RNA sequencing. The latter generated 238474 quality-filtered reads, averaging 9936 reads per sample (Supplementary Table S4). In this context, only genes showing a fold-change in the transcription of ≥ 2 ($Log_2FC > 1$) in combination with a *p*-value of ≤ 0.05 calculated through correction for multiple comparisons using the False Discovery Rate (FDR) procedure were considered as significantly differentially transcribed between the bi-associations when compared to mono-associations. Interestingly, strains grown in bi-association were found to have an increase in gene expression ranging from 7.79 to 18.36% compared to growth alone, suggesting different cross-feeding interactions (Figure 4A). According to the Cluster of Orthologous Genes (COGs) categorization, the most impacted genes are involved in replication/recombination/repair (L), cell wall/membrane/envelope biogenesis (M), and carbohydrate transport and metabolism (G) in addition to the function unknown (S) (Figure 4B). These data clearly show that the strains are metabolically more active in bi-association and that the external structures involved in the uptake and metabolism of carbon sources are highly expressed in such conditions. There are several genes encoding glycoside hydrolases, glycan-binding surface proteins, sugar transferases, ABC and MFS transporters, cell surface proteins, and secretion systems that are up-regulated when bacteria are co-cultivated on these botanicals respect when they are grown alone (Figure 4A and Supplementary Tables S5–S8). In addition, several TonB-dependent receptors are expressed when the strains are growing in bi-association, with respect to the mono-association, ranging from 18 to 47 genes. TonB-dependent

A)

	176F-39F in AVG		176F-39F in DR	
	176F	**39F**	**176F**	**39F**
% genes up-regulated	15.63	7.79	18.36	18.17
% genes down-regulated	17.36	8.34	17.09	9.26
n° of TonB-dependent receptors encoding genes	23	18	24	47
n° of transporters encoding genes	13	7	17	10
n° of glycosyl hydrolases encoding genes	28	14	18	23
n° of extracellular structures encoding genes	7	14	8	15

B)

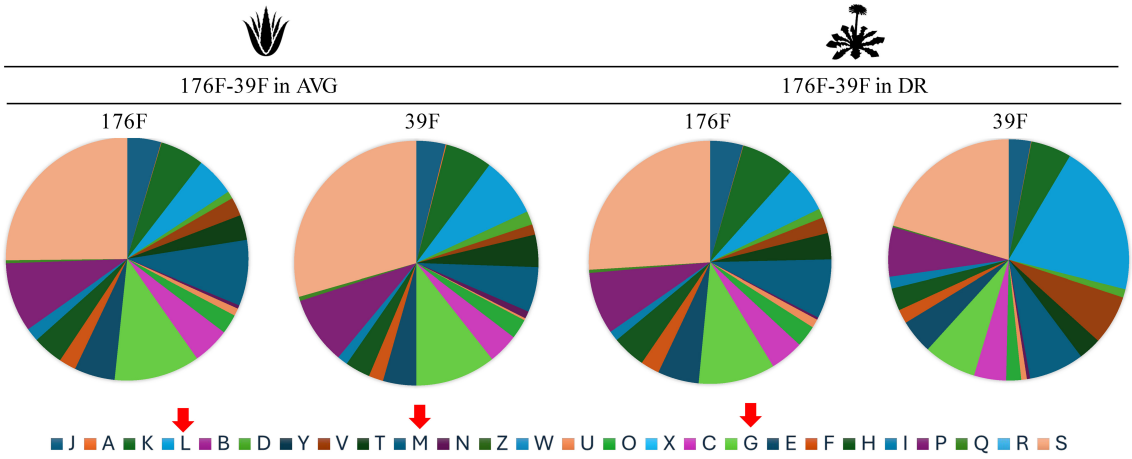

FIGURE 4
Effects of AVG and DR on *Bacteroides* transcriptomes after cross-feeding experiments. **(A)** displays the percentage of genes up and down-regulated of the two strains *Bacteroides ovatus* 39F and *Bacteroides uniformis* 176F, during their bi-association in AVG on the left and DR on the right. **(B)** depicts cakes diagram of the statistically significant impacted genes (up- and down-regulated) of the two strains' growth in bi-association subdivided following the Cluster of Orthologue Genes (COG) classification. The red arrows indicate the most represented classes.

receptors comprise outer membrane transport systems that could be involved in the transport of several substrates, such as proteins, inorganic substances (e.g., iron), vitamins, starch, and lignin-derived aromatic compounds (Noinaj et al., 2010; Fujita et al., 2019). All these data reinforce the notion that during bi-association, a cross-talk occurs between the involved strains in the presence of botanicals.

3.5 Prediction of AVG- and/or DR-driven functional changes in the human gut microbiome

Shotgun sequencing data allowed us to assess whether taxonomic changes were also conveyed by significant alterations in the functional potential of the human gut microbiota in terms of enzymatic profiles based on the MetaCyc database and Enzymatic Commission classification. Interestingly, a variable number of enzyme-encoding genes whose abundance significantly differed among the three tested groups per AGM was observed, ranging from 6 in AGM5 to 47 in AGM10 (Supplementary Table S9). Thus, this confirms that the taxonomic botanical-induced changes are also associated with metabolic modifications and suggests that the latter are, as expected, gut microbiota taxonomic composition-dependent.

Furthermore, in-depth insights into the microbiome data, whose abundance varied significantly between control samples and those exposed to botanical extracts, revealed that, in most cases, they corresponded to genes encoding enzymes involved in vitamin and carbohydrate metabolism, as well as even if to a less extent, in pathways associated with the production of SCFA, antibiotics,

amino acid or butanoate metabolism (Supplementary Table S9 and Supplementary text). Thus, it leads to the notion that plant extracts influence the taxonomic composition of the gut microbiota by mostly favoring changes in the abundance of genes involved in these specific metabolic pathways. However, a unique modification pattern in the abundance of genes participating in the same metabolic pathway was not observed among AGMs, corroborating the data about AVG and DR's effects on the gut microbiota composition.

4 Discussion

The human gut harbors a diverse microbial community that supports overall health by aiding digestion, generating essential metabolites, and regulating the immune system. However, disruptions to this microbial balance can contribute to various health problems, including gastrointestinal diseases and metabolic disorders. Functional vegetables rich in bioactive compounds such as polyphenols and flavonoids have positively affected gut health and may help mitigate dysbiosis. Among these, AVG and DR stand out due to their traditional medicinal use for their antioxidant and anti-inflammatory properties. Nonetheless, their specific effects on the gut microbiota's taxonomic composition and functional capabilities remain insufficiently understood.

In this study, the growth of 10 artificial gut microbiota (AGM) communities cultivated in a bioreactor, exposed to the botanical extracts and not as controls, showed no drastic changes among the three groups, i.e., control and AVG- or DR-treated samples, if we consider the 10 AGMs as biological replicates. However, a more detailed analysis of each sample revealed significant changes in the relative abundance of 40 bacterial species, suggesting that these botanicals may substantially impact modulating the composition of the intestinal microbiota. Some of these microbial genera are associated with good gut balance, i.e., *Bifidobacterium*, *Akkermansia,* and *Bacteroides*, highlighting a possible positive impact on consumer health. The effect could be due to the growth/reduction of some microorganisms that, in turn, influence others, like the network in a mesh, highlighting how each microorganism in a complex microbiota has an impact on all the others, which appears to be dependent on the taxonomic composition of the intestinal microbiota exposed to the two botanicals. This behavior is confirmed by specific cross-feeding experiments carried out on some species of the *Bacteroides* genus, which resulted statistically impacted in their growth. This observation reinforces that such botanicals exploit a molecular effect on the human gut microbiota members, indirectly influencing human health. This is in line with what the World Health Organization already emphasizes in preferring a healthy diet, that is to favor plant-based foods rather than simple sugars, salt, and fats (https://www.who.int/news-room/fact-sheets/detail/healthy-diet). Indeed, further investigation into how the presence of botanicals impacts the specific microbial taxa observed in this study would help to understand and explain the dynamics observed in our complex microbiota experiments.

Data availability statement

Raw shallow shotgun sequences and RNAseq data are accessible through the Sequence Read Archive (SRA) under the BioProject accession number PRJNA1247491.

Author contributions

LM: Formal analysis, Methodology, Writing – review & editing, Validation. CT: Methodology, Formal analysis, Writing – review & editing. GL: Formal analysis, Methodology, Writing – review & editing. GA: Writing – review & editing, Methodology, Investigation. MV: Writing – review & editing, Supervision. FT: Conceptualization, Supervision, Writing – original draft, Funding acquisition.

Funding

The author(s) declare that financial support was received for the research and/or publication of this article. FT is founded by Piano di Sviluppo e Coesione of the Italian Ministry of Health 2014–2020 (Grant Number T5-AN-11). MV and CT are funded by the European Union, NextGeneration EU, PNRR-M4C2-I1.1, PRIN 2022—Project Code 20229LEB99—CUP Code D53D23014150006, Project title: Disentangling the molecular interplay between the gut microbiota and the host in the first stages of life (I-MAP). MV and GL are funded under the National Recovery and Resilience Plan (NRRP), Mission 4 Component 2 Investment 1.3—Call for tender No. 341 of 15 March 2022 of Italian Ministry of University and Research funded by the European Union—NextGenerationEU; Award Number: Project code PE00000003, Project title "ON Foods - Research and innovation network on food and nutrition Sustainability, Safety and Security – Working ON Foods."

Acknowledgments

We thank GenProbio srl for the financial support of the Probiogenomics laboratory. Part of this research was conducted using the High Performance Computing (HPC) facility at the University of Parma. Part of Figure 1 was generated with Biorender.com.

Conflict of interest

The authors declare that the research was conducted in the absence of any commercial or financial relationships that could be construed as a potential conflict of interest.

The author(s) declared that they were an editorial board member of Frontiers, at the time of submission. This had no impact on the peer review process and the final decision.

Generative AI statement

The author(s) declare that no Gen AI was used in the creation of this manuscript.

Publisher's note

All claims expressed in this article are solely those of the authors and do not necessarily represent those of their affiliated organizations, or those of the publisher, the editors and the reviewers. Any product that may be evaluated in this article, or claim that may be made by its manufacturer, is not guaranteed or endorsed by the publisher.

Supplementary material

The Supplementary Material for this article can be found online at: https://www.frontiersin.org/articles/10.3389/fmicb.2025.1610170/full#supplementary-material

References

Afzaal, M., Saeed, F., Shah, Y. A., Hussain, M., Rabail, R., Socol, C. T., et al. (2022). Human gut microbiota in health and disease: unveiling the relationship. *Front. Microbiol.* 13:999001. doi: 10.3389/fmicb.2022.999001

Alessandri, G., Fontana, F., Mancabelli, L., Lugli, G. A., Tarracchini, C., Argentini, C., et al. (2022). Exploring species-level infant gut bacterial biodiversity by meta-analysis and formulation of an optimized cultivation medium. *NPJ Biofilms Microbiomes* 8:88. doi: 10.1038/s41522-022-00349-1

Alessandri, G., Ossiprandi, M. C., MacSharry, J., van Sinderen, D., and Ventura, M. (2019). Bifidobacterial dialogue with its human host and consequent modulation of the immune system. *Front. Immunol.* 10:2348. doi: 10.3389/fimmu.2019.02348

Alessandri, G., Rizzo, S. M., Mancabelli, L., Fontana, F., Longhi, G., Turroni, F., et al. (2024). Impact of cryoprotective agents on human gut microbes and *in vitro* stabilized artificial gut microbiota communities. *Microb. Biotechnol.* 17:e14509. doi: 10.1111/1751-7915.14509

Anders, S., Pyl, P. T., and Huber, W. (2015). HTSeq–a Python framework to work with high-throughput sequencing data. *Bioinformatics* 31, 166–169. doi: 10.1093/bioinformatics/btu638

Arumugam, M., Raes, J., Pelletier, E., Le Paslier, D., Yamada, T., Mende, D. R., et al. (2011). Enterotypes of the human gut microbiome. *Nature* 473, 174–180. doi: 10.1038/nature09944

Banerjee, A., Somasundaram, I., Das, D., Jain Manoj, S., Banu, H., Mitta Suresh, P., et al. (2023). Functional foods: a promising strategy for restoring gut microbiota diversity impacted by SARS-CoV-2 variants. *Nutrients* 15:2631. doi: 10.3390/nu15112631

Belizario, J. E., and Faintuch, J. (2018). Microbiome and gut dysbiosis. *Exp. Suppl.* 109, 459–476. doi: 10.1007/978-3-319-74932-7_13

Belzer, C., Chia, L. W., Aalvink, S., Chamlagain, B., Piironen, V., Knol, J., et al. (2017). Microbial metabolic networks at the mucus layer lead to diet-independent butyrate and vitamin B(12) production by intestinal symbionts. *MBio* 8:e00770-17. doi: 10.1128/mBio.00770-17

Bian, X., Wu, W., Yang, L., Lv, L., Wang, Q., Li, Y., et al. (2019). Administration of *Akkermansia muciniphila* ameliorates dextran sulfate sodium-induced ulcerative colitis in mice. *Front. Microbiol.* 10:2259. doi: 10.3389/fmicb.2019.02259

Bolyen, E., Rideout, J. R., Dillon, M. R., Bokulich, N. A., Abnet, C. C., Al-Ghalith, G. A., et al. (2019). Reproducible, interactive, scalable and extensible microbiome data science using QIIME 2. *Nat. Biotechnol.* 37, 852–857. doi: 10.1038/s41587-019-0209-9

Bottacini, F., van Sinderen, D., and Ventura, M. (2017). Omics of bifidobacteria: research and insights into their health-promoting activities. *Biochem. J.* 474, 4137–4152. doi: 10.1042/BCJ20160756

Calvo, A., Pastor, Y., Rosas-Val, P., and Gamazo, C. (2024). Unveiling the immunomodulatory effect of the novel probiotic *Akkermansia muciniphila* and its protective effect *in vitro*. *Microbiol Res.* 283:127677. doi: 10.1016/j.micres.2024.127677

Cao, C., Yue, S., Lu, A., and Liang, C. (2024). Host-gut microbiota metabolic interactions and their role in precision diagnosis and treatment of gastrointestinal cancers. *Pharmacol. Res.* 207:107321. doi: 10.1016/j.phrs.2024.107321

Caspi, R., Billington, R., Ferrer, L., Foerster, H., Fulcher, C. A., Keseler, I. M., et al. (2016). The MetaCyc database of metabolic pathways and enzymes and the BioCyc collection of pathway/genome databases. *Nucleic Acids Res.* 44, D471–480. doi: 10.1093/nar/gkv1164

Chandrasekaran, P., Han, Y., Zerbe, C. S., Heller, T., DeRavin, S. S., Kreuzberg, S. A., et al. (2023). Intestinal microbiome and metabolome signatures in patients with chronic granulomatous disease. *J. Allergy Clin. Immunol.* 152, 1619–1633.e1611. doi: 10.1016/j.jaci.2023.07.022

Choi, Y. J., Shin, S. H., and Shin, H. S. (2022). Immunomodulatory effects of *Bifidobacterium* spp. and Use of *Bifidobacterium breve* and *Bifidobacterium longum* on acute diarrhea in children. *J. Microbiol. Biotechnol.* 32, 1186–1194. doi: 10.4014/jmb.2206.06023

Costea, P. I., Hildebrand, F., Arumugam, M., Backhed, F., Blaser, M. J., Bushman, F. D., et al. (2018). Enterotypes in the landscape of gut microbial community composition. *Nat. Microbiol.* 3, 8–16. doi: 10.1038/s41564-017-0072-8

Cuvas-Limon, R. B., Ferreira-Santos, P., Cruz, M., Teixeira, J. A., Belmares, R., and Nobre, C. (2022). Novel bio-functional aloe vera beverages fermented by probiotic *Enterococcus faecium* and *Lactobacillus lactis*. *Molecules* 27:2473. doi: 10.3390/molecules27082473

DeGruttola, A. K., Low, D., Mizoguchi, A., and Mizoguchi, E. (2016). Current understanding of dysbiosis in disease in human and animal models. *Inflamm. Bowel Dis.* 22, 1137–1150. doi: 10.1097/MIB.0000000000000750

Derrien, M., Collado, M. C., Ben-Amor, K., Salminen, S., and de Vos, W. M. (2008). The Mucin degrader *Akkermansia muciniphila* is an abundant resident of the human intestinal tract. *Appl. Environ. Microbiol.* 74, 1646–1648. doi: 10.1128/AEM.01226-07

Dixit, K., Chaudhari, D., Dhotre, D., Shouche, Y., and Saroj, S. (2021). Restoration of dysbiotic human gut microbiome for homeostasis. *Life Sci.* 278:119622. doi: 10.1016/j.lfs.2021.119622

Donkers, J. M., Wiese, M., van den Broek, T. J., Wierenga, E., Agamennone, V., Schuren, F., et al. (2024). A host-microbial metabolite interaction gut-on-a-chip model of the adult human intestine demonstrates beneficial effects upon inulin treatment of gut microbiome. *Microbiome Res. Rep.* 3:18. doi: 10.20517/mrr.2023.79

Duda-Chodak, A. (2012). The inhibitory effect of polyphenols on human gut microbiota. *J. Physiol. Pharmacol.* 63, 497–503.

Firrman, J., Liu, L., Zhang, L., Arango Argoty, G., Wang, M., Tomasula, P., et al. (2016). The effect of quercetin on genetic expression of the commensal gut microbes *Bifidobacterium catenulatum*, *Enterococcus caccae* and *Ruminococcus gauvreauii*. *Anaerobe* 42, 130–141. doi: 10.1016/j.anaerobe.2016.10.004

Fu, S., Dang, Y., Xu, H., Li, A., Zhou, X., Gao, X., et al. (2022). Aloe vera-fermented beverage ameliorates obesity and gut dysbiosis in high-fat-diet mice. *Foods* 11:3728. doi: 10.3390/foods11223728

Fujita, M., Mori, K., Hara, H., Hishiyama, S., Kamimura, N., and Masai, E. (2019). A TonB-dependent receptor constitutes the outer membrane transport system for a lignin-derived aromatic compound. *Commun. Biol.* 2:432. doi: 10.1038/s42003-019-0676-z

Garvey, M. (2024). Intestinal dysbiosis: microbial imbalance impacts on colorectal cancer initiation, progression and disease mitigation. *Biomedicines* 12:740. doi: 10.3390/biomedicines12040740

Gavzy, S. J., Kensiski, A., Lee, Z. L., Mongodin, E. F., Ma, B., and Bromberg, J. S. (2023). Bifidobacterium mechanisms of immune modulation and tolerance. *Gut Microbes* 15:2291164. doi: 10.1080/19490976.2023.2291164

Hajj Hussein, I., Dosh, L., Al Qassab, M., Jurjus, R., El Masri, J., Abi Nader, C., et al. (2023). Highlights on two decades with microbiota and inflammatory bowel disease from etiology to therapy. *Transpl. Immunol.* 78:101835. doi: 10.1016/j.trim.2023.101835

Hidalgo-Cantabrana, C., Delgado, S., Ruiz, L., Ruas-Madiedo, P., Sanchez, B., and Margolles, A. (2017). Bifidobacteria and their health-promoting effects. *Microbiol. Spectr.* 5, 73–98. doi: 10.1128/microbiolspec.BAD-0010-2016

Holscher, H. D., Caporaso, J. G., Hooda, S., Brulc, J. M., Fahey, G. C. Jr., and Swanson, K. S. (2015). Fiber supplementation influences phylogenetic structure and functional capacity of the human intestinal microbiome: follow-up of a randomized controlled trial. *Am. J. Clin. Nutr.* 101, 55–64. doi: 10.3945/ajcn.114.092064

Jacquier, E. F., van de Wouw, M., Nekrasov, E., Contractor, N., Kassis, A., and Marcu, D. (2024). Local and systemic effects of bioactive food ingredients: is there a role for functional foods to prime the gut for resilience? *Foods* 13:739. doi: 10.3390/foods13050739

Jauregui-Amezaga, A., and Smet, A. (2024). The microbiome in inflammatory bowel disease. *J. Clin. Med.* 13:4622. doi: 10.3390/jcm13164622

Jiang, P., Ji, S., Su, D., Zhao, Y., Goncalves, V. B. E., Xu, G., et al. (2024). The biofunction of *Akkermansia muciniphila* in intestinal-related diseases. *Microbiome Res. Rep.* 3:47. doi: 10.20517/mrr.2024.12

Kaur, A. P., Bhardwaj, S., Dhanjal, D. S., Nepovimova, E., Cruz-Martins, N., Kuca, K., et al. (2021). Plant prebiotics and their role in the amelioration of diseases. *Biomolecules* 11:440. doi: 10.3390/biom11030440

Langdon, W. B. (2015). Performance of genetic programming optimised Bowtie2 on genome comparison and analytic testing (GCAT) benchmarks. *BioData Min.* 8, 1–7. doi: 10.1186/s13040-014-0034-0

Lay, C., Rigottier-Gois, L., Holmstrom, K., Rajilic, M., Vaughan, E. E., de Vos, W. M., et al. (2005). Colonic microbiota signatures across five northern European countries. *Appl. Environ. Microbiol.* 71, 4153–4155. doi: 10.1128/AEM.71.7.4153-4155.2005

Le Phan, T. H., Park, S. Y., Jung, H. J., Kim, M. W., Cho, E., Shim, K. S., et al. (2021). The role of processed aloe vera gel in intestinal tight junction: an *in vivo* and *in vitro* study. *Int. J. Mol. Sci.* 22:6515. doi: 10.3390/ijms22126515

Lee, J. Y., Bays, D. J., Savage, H. P., and Baumler, A. J. (2024). The human gut microbiome in health and disease: time for a new chapter? *Infect. Immun.* 92:e0030224. doi: 10.1128/iai.00302-24

Leser, T., and Baker, A. (2023). Bifidobacterium adolescentis - a beneficial microbe. *Benef. Microbes* 14, 525–551. doi: 10.1163/18762891-20230030

Levy, M., Blacher, E., and Elinav, E. (2017). Microbiome, metabolites and host immunity. *Curr. Opin. Microbiol.* 35, 8–15. doi: 10.1016/j.mib.2016.10.003

Li, L., Abou-Samra, E., Ning, Z., Zhang, X., Mayne, J., Wang, J., et al. (2019). An *in vitro* model maintaining taxon-specific functional activities of the gut microbiome. *Nat. Commun.* 10:4146. doi: 10.1038/s41467-019-12087-8

Li, Y., Chen, Y., and Sun-Waterhouse, D. (2022). The potential of dandelion in the fight against gastrointestinal diseases: a review. *J. Ethnopharmacol.* 293:115272. doi: 10.1016/j.jep.2022.115272

Li, Z., Li, X., Shi, P., Li, P., Fu, Y., Tan, G., et al. (2024). Modulation of acute intestinal inflammation by Dandelion polysaccharides: an in-depth analysis of antioxidative, anti-inflammatory effects and gut microbiota regulation. *Int. J. Mol. Sci.* 25:1429. doi: 10.3390/ijms25031429

Lueschow, S. R., Boly, T. J., Frese, S. A., Casaburi, G., Mitchell, R. D., Henrick, B. M., et al. (2022). *Bifidobacterium longum* subspecies infantis strain EVC001 decreases neonatal murine necrotizing enterocolitis. *Nutrients* 14:495. doi: 10.3390/nu14030495

Maiuolo, J., Musolino, V., Gliozzi, M., Carresi, C., Scarano, F., Nucera, S., et al. (2022). Involvement of the intestinal microbiota in the appearance of multiple sclerosis: aloe vera and *Citrus bergamia* as potential candidates for intestinal health. *Nutrients* 14:2711. doi: 10.3390/nu14132711

Mallick, H., Rahnavard, A., McIver, L. J., Ma, S., Zhang, Y., Nguyen, L. H., et al. (2021). Multivariable association discovery in population-scale meta-omics studies. *PLoS Comput. Biol.* 17:e1009442. doi: 10.1371/journal.pcbi.1009442

Mancabelli, L., Milani, C., De Biase, R., Bocchio, F., Fontana, F., Lugli, G. A., et al. (2024). Taxonomic and metabolic development of the human gut microbiome across life stages: a worldwide metagenomic investigation. *mSystems* 9:e0129423. doi: 10.1128/msystems.01294-23

Mancabelli, L., Milani, C., Lugli, G. A., Turroni, F., Ferrario, C., van Sinderen, D., et al. (2017). Meta-analysis of the human gut microbiome from urbanized and pre-agricultural populations. *Environ. Microbiol.* 19, 1379–1390. doi: 10.1111/1462-2920.13692

Manske, S. (2024). The microbiome: a foundation for integrative medicine. *Integr. Med. (Encinitas)* 23, 28–31.

Martin, A. J. M., Serebrinsky-Duek, K., Riquelme, E., Saa, P. A., and Garrido, D. (2023). Microbial interactions and the homeostasis of the gut microbiome: the role of Bifidobacterium. *Microbiome Res. Rep.* 2:17. doi: 10.20517/mrr.2023.10

Martorell, P., Alvarez, B., Llopis, S., Navarro, V., Ortiz, P., Gonzalez, N., et al. (2021). Heat-Treated *Bifidobacterium longum* CECT-7347: a whole-cell postbiotic with antioxidant, anti-inflammatory, and gut-barrier protection properties. *Antioxidants* 10:536. doi: 10.3390/antiox10040536

Matijasic, M., Mestrovic, T., Paljetak, H. C., Peric, M., Baresic, A., and Verbanac, D. (2020). Gut microbiota beyond bacteria-mycobiome, virome, archaeome, and eukaryotic parasites in IBD. *Int. J. Mol. Sci.* 21:2668. doi: 10.3390/ijms21082668

Medina-Vera, I., Sanchez-Tapia, M., Noriega-Lopez, L., Granados-Portillo, O., Guevara-Cruz, M., Flores-Lopez, A., et al. (2019). A dietary intervention with functional foods reduces metabolic endotoxaemia and attenuates biochemical abnormalities by modifying faecal microbiota in people with type 2 diabetes. *Diabetes Metab.* 45, 122–131. doi: 10.1016/j.diabet.2018.09.004

Milani, C., Lugli, G. A., Fontana, F., Mancabelli, L., Alessandri, G., Longhi, G., et al. (2021). METAnnotatorX2: a comprehensive tool for deep and shallow metagenomic data set analyses. *mSystems* 6:e0058321. doi: 10.1128/mSystems.00583-21

Moens, E., and Veldhoen, M. (2012). Epithelial barrier biology: good fences make good neighbours. *Immunology* 135, 1–8. doi: 10.1111/j.1365-2567.2011.03506.x

Noinaj, N., Guillier, M., Barnard, T. J., and Buchanan, S. K. (2010). TonB-dependent transporters: regulation, structure, and function. *Annu. Rev. Microbiol.* 64, 43–60. doi: 10.1146/annurev.micro.112408.134247

O'Callaghan, A., and van Sinderen, D. (2016). Bifidobacteria and their role as members of the human gut microbiota. *Front. Microbiol.* 7:925. doi: 10.3389/fmicb.2016.00925

Panzetta, M. E., and Valdivia, R. H. (2024). Akkermansia in the gastrointestinal tract as a modifier of human health. *Gut Microbes* 16:2406379. doi: 10.1080/19490976.2024.2406379

Perez-Burillo, S., Hinojosa-Nogueira, D., Pastoriza, S., and Rufian-Henares, J. A. (2020). Plant extracts as natural modulators of gut microbiota community structure and functionality. *Heliyon* 6:e05474. doi: 10.1016/j.heliyon.2020.e05474

Pickard, J. M., Zeng, M. Y., Caruso, R., and Nunez, G. (2017). Gut microbiota: role in pathogen colonization, immune responses, and inflammatory disease. *Immunol. Rev.* 279, 70–89. doi: 10.1111/imr.12567

Rahman, S., O'Connor, A. L., Becker, S. L., Patel, R. K., Martindale, R. G., and Tsikitis, V. L. (2023). Gut microbial metabolites and its impact on human health. *Ann. Gastroenterol.* 36, 360–368. doi: 10.20524/aog.2023.0809

Robinson, M. D., McCarthy, D. J., and Smyth, G. K. (2010). edgeR: a bioconductor package for differential expression analysis of digital gene expression data. *Bioinformatics* 26, 139–140. doi: 10.1093/bioinformatics/btp616

Sanchez, B., Delgado, S., Blanco-Miguez, A., Lourenco, A., Gueimonde, M., and Margolles, A. (2017). Probiotics, gut microbiota, and their influence on host health and disease. *Mol. Nutr. Food Res.* 61:1600240. doi: 10.1002/mnfr.201600240

Santhiravel, S., Bekhit, A. E. A., Mendis, E., Jacobs, J. L., Dunshea, F. R., Rajapakse, N., et al. (2022). The impact of plant phytochemicals on the gut microbiota of humans for a balanced life. *Int. J. Mol. Sci.* 23:8124. doi: 10.3390/ijms23158124

Scher, J. U., Ubeda, C., Artacho, A., Attur, M., Isaac, S., Reddy, S. M., et al. (2015). Decreased bacterial diversity characterizes the altered gut microbiota in patients with psoriatic arthritis, resembling dysbiosis in inflammatory bowel disease. *Arthritis Rheumatol.* 67, 128–139. doi: 10.1002/art.38892

Segers, A., and de Vos, W. M. (2023). Mode of action of *Akkermansia muciniphila* in the intestinal dialogue: role of extracellular proteins, metabolites and cell envelope components. *Microbiome Res. Rep.* 2:6. doi: 10.20517/mrr.2023.05

Shin, J. H., Tillotson, G., MacKenzie, T. N., Warren, C. A., Wexler, H. M., and Goldstein, E. J. C. (2024). Bacteroides and related species: the keystone taxa of the human gut microbiota. *Anaerobe* 85:102819. doi: 10.1016/j.anaerobe.2024.102819

Si, J., Kang, H., You, H. J., and Ko, G. (2022). Revisiting the role of *Akkermansia muciniphila* as a therapeutic bacterium. *Gut Microbes* 14:2078619. doi: 10.1080/19490976.2022.2078619

Sudheer, S., Gangwar, P., Usmani, Z., Sharma, M., Sharma, V. K., Sana, S. S., et al. (2022). Shaping the gut microbiota by bioactive phytochemicals: an emerging approach for the prevention and treatment of human diseases. *Biochimie* 193, 38–63. doi: 10.1016/j.biochi.2021.10.010

Takiishi, T., Fenero, C. I. M., and Camara, N. O. S. (2017). Intestinal barrier and gut microbiota: shaping our immune responses throughout life. *Tissue Barriers* 5:e1373208. doi: 10.1080/21688370.2017.1373208

Tarracchini, C., Lugli, G. A., Mancabelli, L., van Sinderen, D., Turroni, F., Ventura, M., et al. (2024). Exploring the vitamin biosynthesis landscape of the human gut microbiota. *mSystems* 9:e0092924. doi: 10.1128/msystems.00929-24

Thumann, T. A., Pferschy-Wenzig, E. M., Moissl-Eichinger, C., and Bauer, R. (2019). The role of gut microbiota for the activity of medicinal plants traditionally used in the European Union for gastrointestinal disorders. *J. Ethnopharmacol.* 245:112153. doi: 10.1016/j.jep.2019.112153

Togo, A. H., Diop, A., Bittar, F., Maraninchi, M., Valero, R., Armstrong, N., et al. (2018). Description of Mediterraneibacter massiliensis, gen. nov., sp. nov., a new genus isolated from the gut microbiota of an obese patient and reclassification of *Ruminococcus faecis*, *Ruminococcus lactaris*, *Ruminococcus torques*, *Ruminococcus gnavus* and *Clostridium glycyrrhizinilyticum* as *Mediterraneibacter faecis* comb. nov., *Mediterraneibacter lactaris* comb. nov., *Mediterraneibacter torques* comb. nov., *Mediterraneibacter gnavus* comb. nov. and *Mediterraneibacter glycyrrhizinilyticus* comb. nov. *Antonie Van Leeuwenhoek* 111, 2107–2128. doi: 10.1007/s10482-018-1104-y

Turroni, F., Foroni, E., O'Connell Motherway, M., Bottacini, F., Giubellini, V., Zomer, A., et al. (2010). Characterization of the serpin-encoding gene of *Bifidobacterium breve* 210B. *Appl. Environ. Microbiol.* 76, 3206–3219. doi: 10.1128/AEM.02938-09

Ursell, L. K., Metcalf, J. L., Parfrey, L. W., and Knight, R. (2012). Defining the human microbiome. *Nutr. Rev.* 70(Suppl 1), S38–44. doi: 10.1111/j.1753-4887.2012.00493.x

van der Lugt, B., van Beek, A. A., Aalvink, S., Meijer, B., Sovran, B., Vermeij, W. P., et al. (2019). *Akkermansia muciniphila* ameliorates the age-related decline in colonic mucus thickness and attenuates immune activation in accelerated aging Ercc1 (-/Delta7) mice. *Immun. Ageing* 16:6. doi: 10.1186/s12979-019-0145-z

Van Hul, M., Cani, P. D., Petitfils, C., De Vos, W. M., Tilg, H., and El-Omar, E. M. (2024). What defines a healthy gut microbiome? *Gut* 73, 1893–1908. doi: 10.1136/gutjnl-2024-333378

Vandeputte, D., Kathagen, G., D'Hoe, K., Vieira-Silva, S., Valles-Colomer, M., Sabino, J., et al. (2017). Quantitative microbiome profiling links gut community variation to microbial load. *Nature* 551, 507–511. doi: 10.1038/nature24460

Wilkins, L. J., Monga, M., and Miller, A. W. (2019). Defining dysbiosis for a cluster of chronic diseases. *Sci. Rep.* 9:12918. doi: 10.1038/s41598-019-49452-y

Wu, H., Qi, S., Yang, R., Pan, Q., Lu, Y., Yao, C., et al. (2024). Strategies for high cell density cultivation of *Akkermansia muciniphila* and its potential metabolism. *Microbiol. Spectr.* 12:e0238623. doi: 10.1128/spectrum.02386-23

Yan, S., and Dong, R. (2024). Integrated microbiome-metabolomics analysis reveals the potential mechanism of dandelion root polysaccharides to ameliorate ulcerative colitis. *Metabolites* 14:351. doi: 10.3390/metabo14070351

Yan, S., Yin, L., and Dong, R. (2023). Inhibition of IEC-6 cell proliferation and the mechanism of ulcerative colitis in C57BL/6 mice by dandelion root polysaccharides. *Foods* 12:3800. doi: 10.3390/foods12203800

Ye, Y., Choi, J. H., and Tang, H. (2011). RAPSearch: a fast protein similarity search tool for short reads. *BMC Bioinformatics* 12:159. doi: 10.1186/1471-2105-12-159

Yu, H., Li, X. X., Han, X., Chen, B. X., Zhang, X. H., Gao, S., et al. (2023). Fecal microbiota transplantation inhibits colorectal cancer progression: reversing intestinal microbial dysbiosis to enhance anti-cancer immune responses. *Front. Microbiol.* 14:1126808. doi: 10.3389/fmicb.2023.1126808

Zhao, Y., Tang, H., and Ye, Y. (2012). RAPSearch2: a fast and memory-efficient protein similarity search tool for next-generation sequencing data. *Bioinformatics* 28, 125–126. doi: 10.1093/bioinformatics/btr595

frontiers | Frontiers in Microbiology

TYPE Original Research
PUBLISHED 22 July 2025
DOI 10.3389/fmicb.2025.1597774

Check for updates

OPEN ACCESS

EDITED BY
Guiguo Zhang,
Shandong Agricultural University, China

REVIEWED BY
Hengjia Ni,
Institute of Subtropical Agriculture (CAS), China
Ankit Kumar Dubey,
Indian Institute of Technology Madras, India

*CORRESPONDENCE
Gang Liu
✉ gangle.liu@gmail.com
Chenmei Xia
✉ xia_chenmei@163.com

RECEIVED 24 March 2025
ACCEPTED 03 July 2025
PUBLISHED 22 July 2025

CITATION
Hu X, Han X, Liu G, Guan G and Xia C (2025) Ferulic acid and N-Feruloylserotonin ameliorate LPS-induced intestinal inflammation via modulation of gut microbiota, metabolome, and transcriptome. *Front. Microbiol.* 16:1597774. doi: 10.3389/fmicb.2025.1597774

COPYRIGHT
© 2025 Hu, Han, Liu, Guan and Xia. This is an open-access article distributed under the terms of the Creative Commons Attribution License (CC BY). The use, distribution or reproduction in other forums is permitted, provided the original author(s) and the copyright owner(s) are credited and that the original publication in this journal is cited, in accordance with accepted academic practice. No use, distribution or reproduction is permitted which does not comply with these terms.

Ferulic acid and N-Feruloylserotonin ameliorate LPS-induced intestinal inflammation via modulation of gut microbiota, metabolome, and transcriptome

Xiangdong Hu[1,2,3], Xuebing Han[2,4], Gang Liu[2]*, Guiping Guan[2] and Chenmei Xia[1]*

[1]Department of Gastroenterology, The First People's Hospital of Wenling, Wenling, China, [2]Hunan Provincial Engineering Research Center of Applied Microbial Resources Development for Livestock and Poultry, College of Bioscience and Biotechnology, Hunan Agricultural University, Changsha, China, [3]State Key Laboratory of Subtropical Silviculture, Zhejiang A&F University, Hangzhou, China, [4]Bamboo Diseases and Pests Control and Resources Development Key Laboratory of Sichuan Province, College of Life Science, Leshan Normal University, Leshan, China

Intestinal homeostasis depends critically on the dynamic interplay between gut microbiota, epithelial barriers, and host immunity, dysregulation of this triad can initiate inflammatory cascades. Ferulic acid and its derivative N-Feruloylserotonin demonstrate significant anti-inflammatory activity, though their intestinal protective effects and mechanisms require further elucidation. Therefore, this study examined how these compounds mitigate lipopolysaccharide (LPS)-induced acute inflammation through integrated modulation of the gut microbiome, serum metabolome, and transcriptional networks. Our findings reveal that both compounds, attenuated LPS-induced intestinal pathology in murine models, suppressed pro-inflammatory cytokine expression, elevated beneficial metabolites including 1-naphthalenesulfonic acid, enriched probiotic taxa (Ruminococcaceae, Muribaculaceae, Lachnospiraceae, Bifidobacteriaceae, Prevotellaceae, Roseburia, Blautia, and Butyricicoccus), and suppressed pathobionts (Proteobacteria, Gammaproteobacteria, Enterobacterales, and Bacillus). Transcriptomic profiling further implicated modulation of antigen processing and presentation, NF-κB signal pathway, MAPK signal pathway, and PI3K-Akt signal pathway. Key regulatory targets identified include: Pik3cd, H2-DMb1, H2-Oa, Kdr, Fgfr3, Il1r2, Rac, Irak4, Traf6, Ticam1, Rip1, and Rip3. This work establishes a mechanistic foundation for deploying ferulic acid and N-Feruloylserotonin in intestinal health preservation and inflammatory disease prevention, while providing novel insights into microbiota-homeostasis crosstalk.

KEYWORDS

ferulic acid, N-Feruloylserotonin, LPS, intestinal microorganisms, metabolites, transcriptome

1 Introduction

The intestine constitutes the body's largest immune organ, functioning not only in nutrient absorption but also as a critical physicochemical barrier against diverse pathogenic insults (Funk et al., 2020). Its innate immune system serves as the primary defense against enteric pathogens (Roh et al., 2021), with 70% of systemic immune cells residing in the gut mucosa to combat environmental toxins. Homeostasis is maintained through dynamic interactions

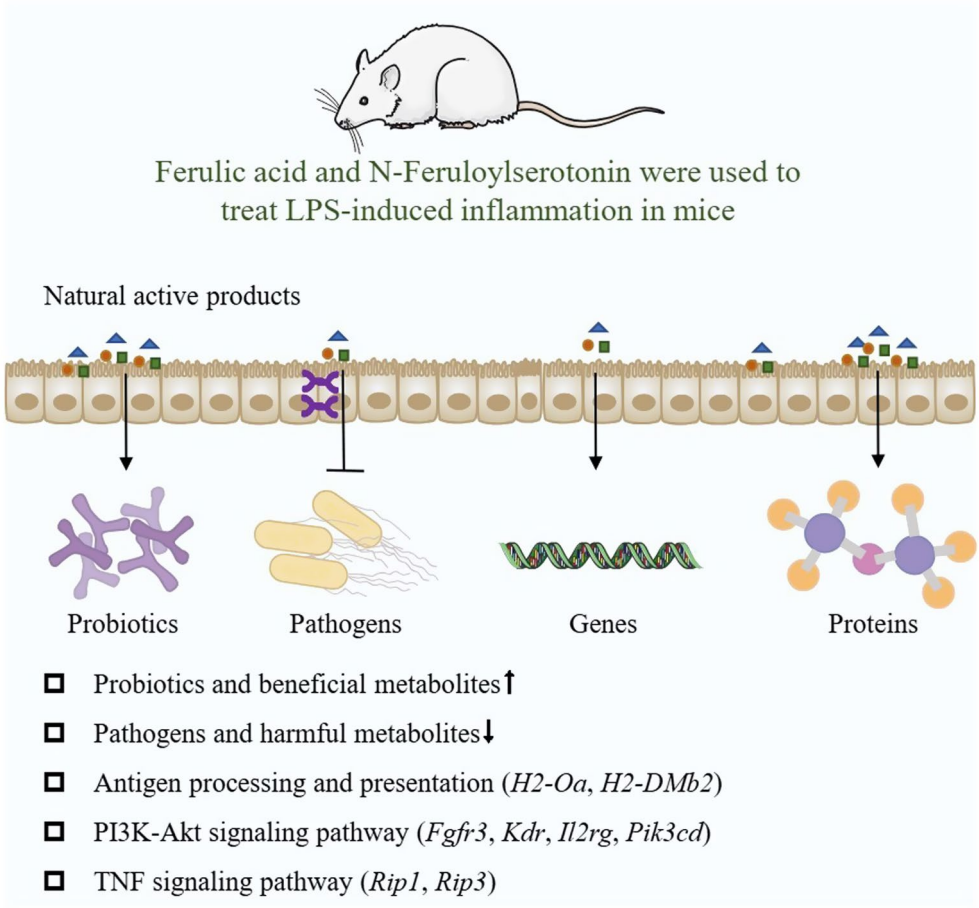

GRAPHICAL ABSTRACT

between the gut microbiota and intestinal barrier, a balance essential for gastrointestinal health (Veiga-Fernandes and Pachnis, 2017). This crosstalk establishes an immunoregulatory microenvironment where immune cells coordinate with commensal flora to sustain mucosal immunity (Wang et al., 2023). Disruption of this equilibrium triggers systemic inflammation and predisposes to multiple pathologies, including neurodegenerative disorders (Loh et al., 2024), colorectal cancer (Li et al., 2024), and inflammatory bowel disease (Danne et al., 2024). Consequently, intestinal integrity is fundamental to metabolic regulation, immune competence, and pathogen resistance.

Natural products, bioactive compounds derived from living organisms, demonstrate anticancer, anti-inflammatory, antioxidant, and neuroprotective properties, offering therapeutic potential for disease prevention and management (Chopra and Dhingra, 2021). Their structural complexity and prolonged intestinal residence facilitate bidirectional interactions: they modulate microbial diversity while gut microbiota metabolize them into physiologically active compounds inaccessible to host biosynthesis (Zhao et al., 2022). Ferulic acid is a phenolic substance that is usually present in cereal seeds, grapes, parsley, whole grains, rhubarb, and spinach. It exhibits many biological activities, such as clearing excess ROS, free radicals, and enzymes that produce free radicals, thereby resisting oxidative damage and reducing inflammatory reactions (Li et al., 2021). In addition, ferulic acid also exerts anti-inflammatory effects by regulating PPAR γ, NF-κB, and MAPK signaling pathways, which has a protective effect on various diseases (Li et al., 2021). Previous studies have documented the protective effects of ferulic acid on the intestinal tract (Hwang et al., 2022; Tian et al., 2022); however, a comprehensive assessment of its mechanism of action, impact on gut microbiota, and associated metabolomic alterations remains lacking. N-Feruloylserotonin is an amide formed by 5-hydroxytryptamine and ferulic acid, which is a derivative of ferulic acid and widely present in many plants (Carola et al., 2021). N-Feruloylserotonin has many anti-inflammatory functions similar to ferulic acid, which can significantly reduce the production of reactive oxygen species, nitric oxide and prostaglandin E2 induced by LPS, and inhibit NF-κB signal pathway (Park et al., 2023). However, the intestinal protective effects of N-Feruloylserotonin and their underlying mechanisms remain unknown.

This study employed LPS-induced mouse acute intestinal injury to investigate both compounds. We assessed the structural protection via jejunal histopathology, microbial shifts through 16S rRNA sequencing, metabolic reprogramming via untargeted metabolomics and mechanistic pathways by transcriptomic profiling. Our findings elucidate how ferulic acid and N-Feruloylserotonin ameliorate intestinal inflammation, establishing a theoretical framework for their therapeutic application in gut health maintenance and inflammatory disease prevention. Furthermore, we provide novel insights into microbiota-homeostasis dynamics.

2 Methods

2.1 Animals

All experimental protocols received prior approval from the Biomedical Research Ethics Committee of Hunan Agricultural University (Approval No. 2023-51). Thirty-two 8-week-old male ICR mice were acclimatized in specific pathogen-free (SPF) environmental chambers maintained at 25 ± 3°C with 50 ± 5% relative humidity under standardized photoperiodic conditions (12-h light/dark cycle). Following a 7-day acclimatization period, mice were randomly allocated to four experimental groups (n = 8/group): vehicle group (CTRL); LPS-only group (LPS); LPS and ferulic acid treatment group (FA); LPS and N-Feruloylserotonin treatment group (NFS). Dietary composition and nutritional profiles are detailed in Supplementary Tables S1, S2. All experimental groups received the standard diet throughout the study. The acclimatization endpoint was designated as Day 0. Commencing on Day 1, the FA group received dietary supplementation of 200 mg/kg ferulic acid. From Day 22 onward, the NFS group was administered 5 mg/kg N-Feruloylserotonin via dietary incorporation. On the 27th day, the mice in the LPS, FA and NFS groups were intraperitoneally injected with 10 mg/kg LPS (from *E. coli* O55: B5, dissolved in water to prepare a stock solution of 10 mg/mL), and mice in the CTRL group were injected with the same volume of normal saline. Cervical dislocation was performed to euthanize the mice 24 h later. During the procedure, the operator grasped the base of the mouse's tail firmly with the right hand and elevated the animal. The mouse was then positioned on a cage lid or other textured surface. The operator applied firm downward pressure to the head and cervical region using the thumb and index finger of the left hand. Concurrently, the tail base was grasped with the right hand and pulled sharply upward and backward. This action resulted in cervical dislocation, severing the connection between the spinal cord and the brainstem, leading to instantaneous death of the animal.

2.2 HE staining

First, the jejunal intestinal slices were harvested immediately post-euthanasia, rinsed in ice-cold saline, and processed fixed in 4% formaldehyde for HE staining. Then, the fixed slices were subjected to gradient dehydration with ethanol. Next, the dehydrated slices were embedded with paraffin. After hematoxylin and eosin staining, the tissue damage of mice in the four groups was observed and analyzed by microscope. Specific methods can refer to previous study (Han et al., 2023).

2.3 qPCR

The colon tissue was a separate aliquot was snap-frozen in liquid nitrogen and cryopreserved at −80°C for RNA extraction. The expression of tight junction protein genes, inflammatory cytokines, and specific marker molecules was detected by qPCR. After extracting RNA from mouse colon tissue, the concentration was measured using a spectrophotometer. Supplementary Table S3 is a list of primers (Gene-specific primer pairs for qPCR analysis were designed using NCBI, and synthesized commercially by Sangon Biotech). The reaction system includes "2 × SYBR Green Master Mix 10 μL, 0.5 μL of forward and reverse primers, 2 μL of cDNA template, ddH_2O supplemented to 20 μL," and the reaction conditions are "pre-denaturation at 95°C for 3 min, followed by 40 cycles of 95°C for 15 s, 60°C for 30 s ". The specific methods and calculation formulas were referred to previous studies (Ren et al., 2014; Ma et al., 2019).

2.4 Intestinal microbial sequencing

After collecting the colonic contents of mice, the microbial DNA was isolated, and its concentration and purity were tested. Then, the V3-V4 region of 16S rRNA was amplified by primers F (5′-ACTCCTACGGGAGGCAGCA-3′) and R (5′-GGACTACHVGGGTWTCTAAT-3′). High throughput sequencing was carried out on Illumina platform after the purification of PCR products. Using SILVA as the reference database, the Naive Bayes Classifier was used to classify the feature sequences. Then, the data is filtered, with the filtering condition is set to base greater than 50% and mass greater than 20. The clean tags are clustered into OTUs with similarity greater than 97%. In order to detect the composition of community and α diversity of microorganisms, RDP classifier (v.2.2) and mothur (version 1.33.3) were used, respectively. α diversity metrics is primarily evaluated using indices such as Shannon index, Simpson index, Chao1 index, ACE index, and PD-whole-tree index. LEfSe was used to identify the species with different abundances.

2.5 Serum metabolites analysis

Blood samples were collected from the orbital sinus of mice using sterile technique. Ophthalmic forceps were employed to apply gentle pressure to the globe, facilitating the natural efflux of blood. The exudate was collected directly into pre-chilled EDTA-coated collection tubes. The blood samples were centrifuged for 10 min at the condition of 3,500 rpm, 4°C to collect the serum of mice. Then, LC–MS was performed in positive ion and negative ion modes respectively, and the raw data were obtained. This study employed a NMR platform. SIMCA14.1 (Umetrics, Umea, Sweden) was used to perform data statistics, with the serum metabolites were determined by comparing peak with metabolites in Human Metabolome Database. Pathway analysis, encompassing both enrichment analysis and topological analysis, was performed by integrating differential metabolites via the MetaboAnalyst 3.0 platform.

2.6 Transcriptome analysis

The purity, concentration and integrity of total RNA extracted from mice colonic tissue were detected. And the library was constructed as follows: The mRNA was randomly interrupted using a fragmentation buffer after the enrichment of mRNA. Then, the first cDNA chain and second strand were synthesized using mRNA as template. The purified double stranded cDNA was subjected to end repair, A-tail addition, and sequencing adapter connection, followed by fragment size selection using AMPure XP beads. Finally, the cDNA library was obtained by PCR enrichment. After the construction of the

library, the Qsep400 high-throughput analysis system was used to detect the insert fragments of the library. In order to ensure the library quality, q-PCR was used to accurately quantify the effective concentration (>2 nM). After that, the sequencing was performed through Illumina NovaSeq6000 sequencing platform. After filtering to get clean data, the mapped data was obtained by sequence alignment with a specified reference genome. Finally, library quality evaluation, structure level analysis, differential expression analysis, gene function annotation and function enrichment were carried out. Finally, the library quality evaluation, differential expression analysis, gene function annotation and function enrichment were performed through BMKCloud (www.biocloud.net). Differentially expressed genes (DEGs) were analyzed by DESeq2 software. DEGs with |fold change| > 2 and Q value (adjusted *p*-value) < 0.05 were considered to be significantly different expressed genes.

2.7 Data analysis

The software SPSS 21 (SPSS, Inc., Chicago, United States), R and GraphPad were used to compare the differences among groups through one-way ANOVA with a Tukey HSD. The data were expressed as mean value ± standard deviation (mean ± SD). When $p < 0.05$, the difference between the groups was statistically significant.

3 Results

3.1 The effects of ferulic acid and N-Feruloylserotonin on intestinal injury and barrier of mice

Histopathological analysis of jejunal tissue revealed intact mucosal architecture with tightly arranged villi in control (CTRL) mice. In contrast, LPS-challenged mice exhibited significant intestinal damage characterized by villous atrophy and epithelial denudation. Notably, both ferulic acid (FA) and N-Feruloylserotonin (NFS) treatments ameliorated these structural alterations (Figure 1A). Expression profiles of tight junction proteins differed significantly across groups (Figures 1B–D). LPS administration markedly suppressed *Claudin 1*, *Occludin* and *ZO-1* expression when compared with the CTRL group ($p < 0.05$). FA treatment partially restored expression levels, whereas NFS administration induced significant upregulation of all three genes ($p < 0.05$).

Pro-inflammatory cytokine *IL-1β* was significantly elevated in the LPS group ($p < 0.05$). Both compounds reduced *IL-1β* expression, though not statistically significantly (Figure 1E). Concurrently, LPS-induced *iNOS* expression, a downstream effector of proinflammatory signaling, was significantly attenuated by FA and NFS treatments (Figure 1F, $p < 0.05$). While *CD206* expression showed a non-significant reduction following LPS exposure, both compounds demonstrated restorative trends (Figure 1G). *Arg-1* expression was significantly suppressed in LPS-treated mice ($p < 0.05$), with both interventions normalizing expression to CTRL levels (Figure 1H).

Necroptosis-related gene expression in murine colonic tissue was assessed (Figures 1I–K). LPS challenge significantly upregulated *Rip3* and *Mlkl* expression ($p < 0.05$), with a concomitant non-significant increase in *Rip1*. Both ferulic acid and N-Feruloylserotonin interventions significantly downregulated *Mlkl* expression ($p < 0.05$), and reduced expression trends for *Rip1* and *Rip3*.

3.2 The effects of ferulic acid and N-Feruloylserotonin on intestinal microbiota in mice

Intestinal microbial diversity was quantified across experimental groups using α diversity metrics. As shown in Figure 2A, the LPS group exhibited significant reductions in Shannon index, Simpson index, Chao1 index, ACE index, and PD-whole-tree index ($p < 0.05$), whereas FA and NFS interventions significantly elevated these diversity parameters ($p < 0.05$).

Taxonomic profiling at the phylum levelrevealed marked alterations (Figure 2B). Bacteroidetes was inhibited significantly in the LPS group, and it was promoted significantly in the FA and NFS groups ($p < 0.05$). Proteobacteria and Firmicutes in the four groups showed an opposite trend to that of Bacteroidetes, which were significantly promoted by LPS and significantly inhibited by ferulic acid and N-Feruloylserotonin ($p < 0.05$). Many microorganisms have changed in different groups at the class level. Among them, the abundance of Bacteroidia in LPS group was significantly decreased, and the abundance of Gammaproteobacteria was significantly increased when compared with the CTRL group (Figure 2C, $p < 0.05$). Ferulic acid and N-Feruloylserotonin restored them to the similar level with CTRL group. As for the order level (Figure 2D), Bacteroidales in the LPS group was significantly inhibited, the abundance of Saccharimonadales decreased slightly, while Enterobacterales was promoted significantly ($p < 0.05$). After treatment with ferulic acid, Bacteroidales and Saccharimonadales showed significant increases in abundance, and Enterobacterales was inhibited significantly ($p < 0.05$). After N-Feruloylserotonin treatment, the abundance of Bacteroidales increased significantly, and Enterobacterales was also inhibited significantly ($p < 0.05$). At family level, the abundance of Lachnospiraceae, Prevotellaceae and Ruminococcaceae in LPS group decreased significantly, and they were significantly promoted by N-Feruloylserotonin, with Prevotellaceae was also promoted significantly by ferulic acid (Figure 2E, $p < 0.05$). Moreover, Muribaculaceae, Bacteroidaceae, and Bifidobacteriaceae were slightly decreased in LPS group, while ferulic acid significantly promoted the growth of Muribaculaceae and Bifidobacteriaceae, and N-Feruloylserotonin significantly promoted the growth of Bacteroidaceae and Bifidobacteriaceae ($p < 0.05$). *Butyricicoccus* at the genus level was inhibited significantly in the LPS group and promoted significantly in the NFS group (Figure 2F, $p < 0.05$). Moreover, the abundance of *Akkermansia, Roseburia*, and *Blautia* in the LPS group also tended to decrease, while N-Feruloylserotonin significantly increased that of *Blautia* and *Akkermansia* ($p < 0.05$). The abundance of *Bacillus* and *Escherichia Shigella* in LPS group increased significantly, while ferulic acid and N-Feruloylserotonin significantly reduced their abundance ($p < 0.05$).

LEfSe analysis identified taxonomic biomarkers characteristic of each group (Figure 3A). The family Prevotellaceae, and Rikenellaceae, genus *Alloprevotella* and *Alistipes* were species with high abundance in the CTRL group. The phylum Firmicute and Proteobacteria, genus

10.3389/fmicb.2025.1597774

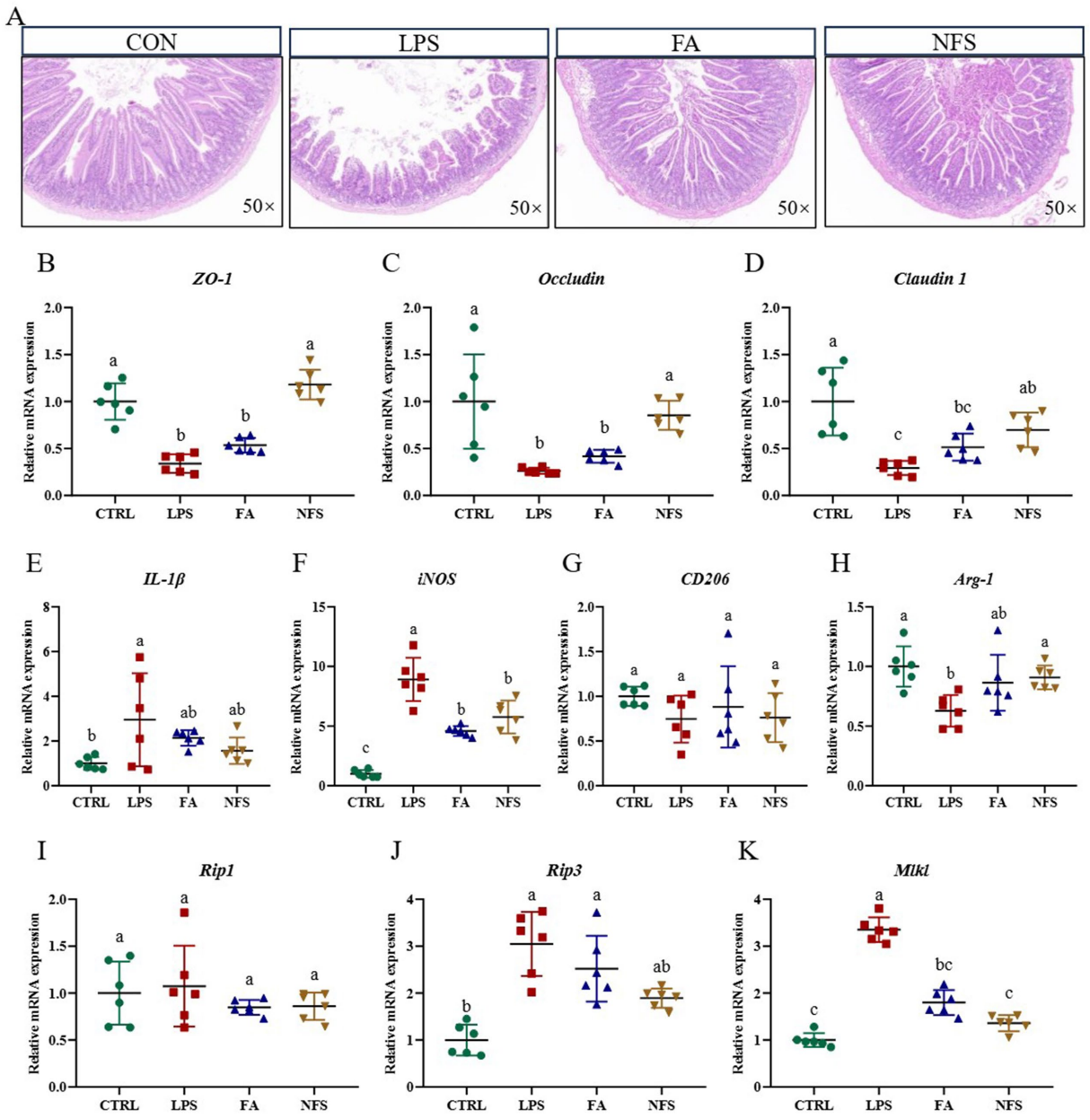

FIGURE 1
The effect of ferulic acid and N-Feruloylserotonin on the intestinal structure and barrier of mice. The images of jejunal tissue **(A)** and relative expression of *ZO-1* **(B)**, *Occludin* **(C)**, *Claudin 1* **(D)**, *IL-1β* **(E)**, *iNOS* **(F)**, *CD206* **(G)**, *Arg-1* **(H)**, *Rip1* **(I)**, *Rip3* **(J)**, and *Mlkl* **(K)**. Data are mean ± SD (n = 6). The absence of the same letter mark indicating significant differences ($p < 0.05$).

Escherichia Shigella were species with high abundance in the LPS group. The phylum Bacteroidetes, class Bacteroidia and Saccharimonadia, genus *Parasutterella* were species with high abundance in the FA group. The phylum Desulfobacterota, order Lachnospirales, genus *Bacteroides* were species with high abundance in the NFS group.

Functional gene enrichment analysis of colonic microbiomes revealed distinct pathway signatures (Figures 3B–D). The LPS *vs* CTRL comparison identified 9 significantly altered pathways, including microbial metabolism in diverse environments, biosynthesis of secondary metabolites, biosynthesis of antibiotics, two-component system, biosynthesis of amino acids, metabolic pathways, ABC transporters, purine metabolism, and ribosome. The significant differential enrichment pathways between FA and LPS groups were two-component system, microbial metabolism in diverse environments, biosynthesis of amino acids, metabolic pathways, biosynthesis of secondary metabolites, ribosome, biosynthesis of antibiotics, purine metabolism, ABC transporters, and carbon metabolism. The significant differential enrichment pathways between NFS and LPS groups were biosynthesis of secondary metabolites, biosynthesis of amino acids, metabolic pathways, biosynthesis of antibiotics, purine metabolism, ABC transporters, microbial metabolism in diverse environments, two-component system, ribosome, and carbon metabolism.

10.3389/fmicb.2025.1597774

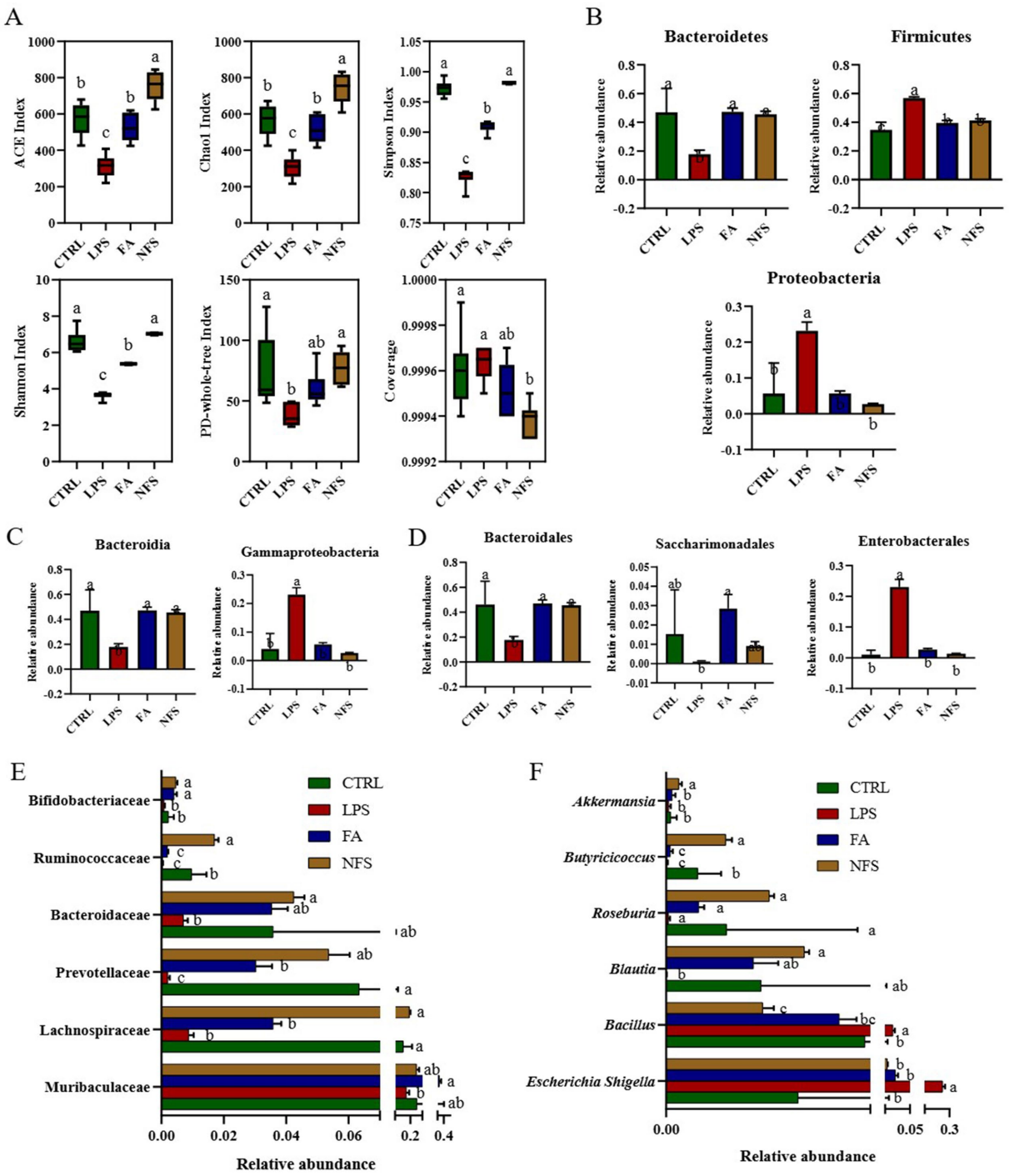

FIGURE 2
The effects of ferulic acid and N-Feruloylserotonin on intestinal microbiota in mice. The microbial α diversity of mice **(A)** and abundance of gut microbe phyla **(B)**, gut microbe classes **(C)**, gut microbe orders **(D)**, gut microbe families **(E)**, and gut microbe genera **(F)**. Data are mean ± SD (n = 6). The absence of the same letter mark indicating significant differences ($p < 0.05$).

3.3 The effects of ferulic acid and N-Feruloylserotonin on serum metabolites in mice

Orthogonal partial least squares discriminant analysis (OPLS-DA) was employed to evaluate metabolic profiles across four experimental groups under both positive and negative ionization modes (Figure 4). The OPLS-DA score plots demonstrated complete separation of sample clusters between distinct groups, indicating statistically significant intergroup metabolic disparities, while intragroup sample aggregation reflected high metabolic homogeneity within each cohort.

Volcano plot visualization was utilized to identify differentially abundant metabolites in three comparative analyses: CTRL *vs* LPS, FA

10.3389/fmicb.2025.1597774

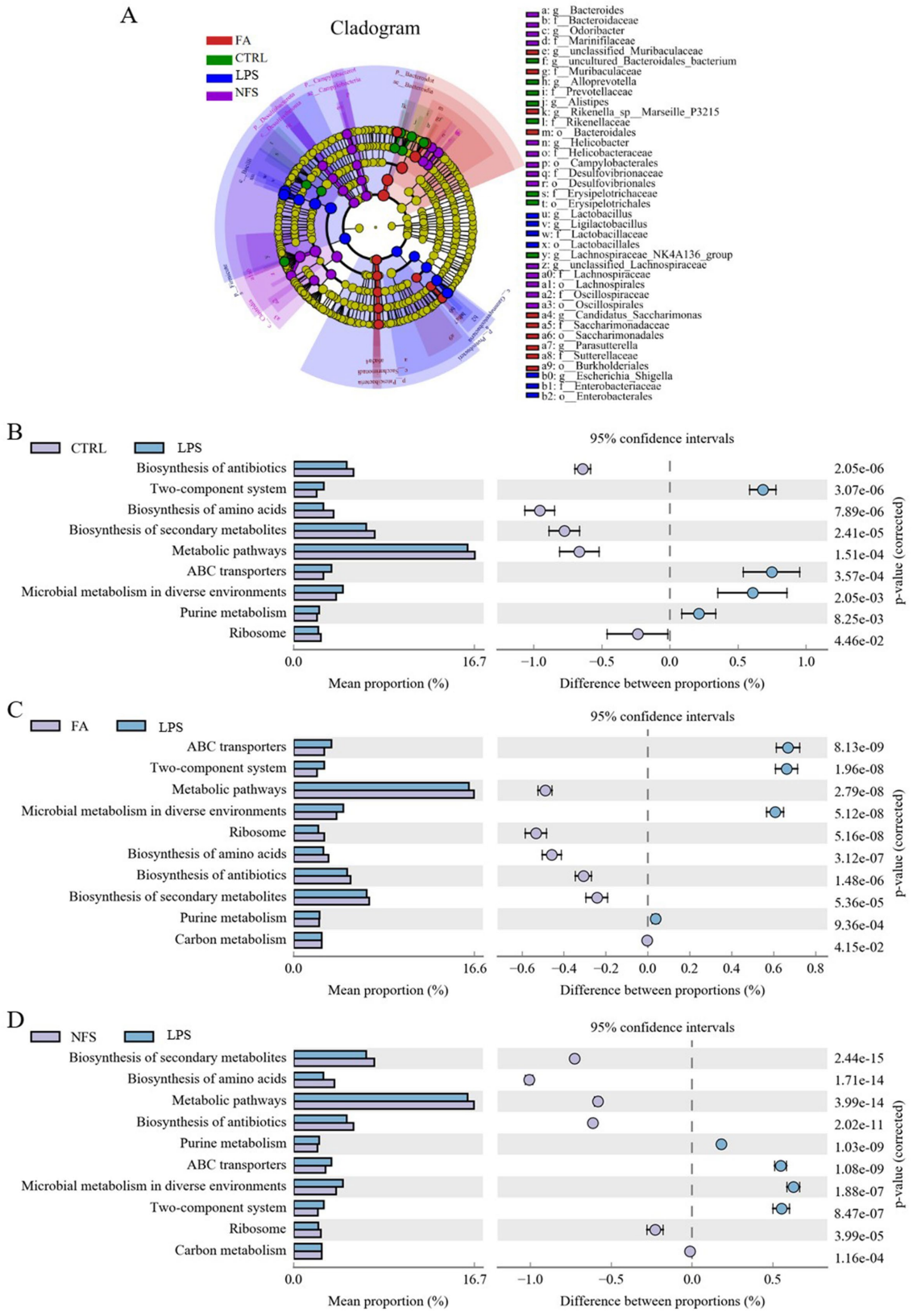

FIGURE 3
Changes in the composition and function of gut microorganisms. LEfSe **(A)** and significant differences in KEGG enrichment pathways in CTRL *vs* LPS groups **(B)**, FA *vs* LPS groups **(C)**, and NFS *vs* LPS groups **(D)**.

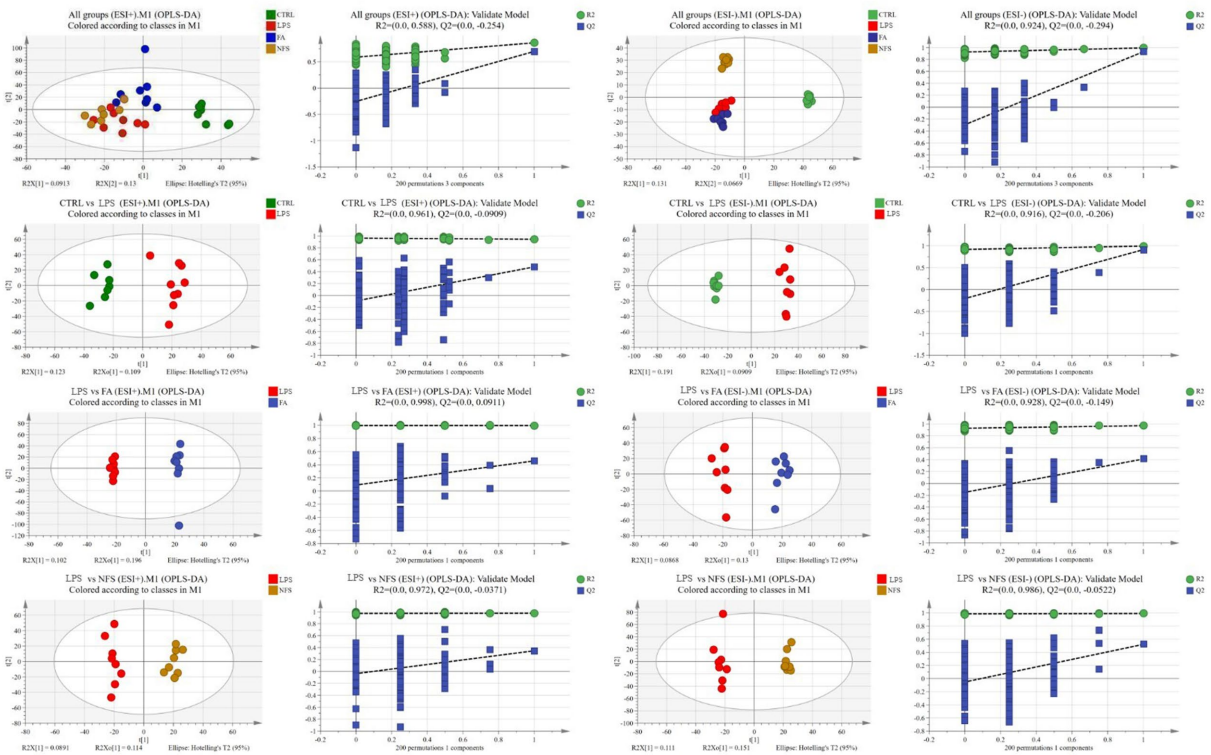

FIGURE 4
Multivariable statistical comparison plots of metabolites in groups.

vs LPS, and NFS *vs* LPS (Figures 5A–C). Pathway enrichment analysis of significant metabolic alterations revealed conserved and group-specific perturbations. In CTRL *vs* LPS comparisons, alpha-linolenic acid metabolism, steroid hormone biosynthesis, linoleic acid metabolism, and glycerophospholipid metabolism constituted the primary enriched pathways (Figure 5D). The FA *vs* LPS comparison yielded identical pathway signatures (alpha-linolenic acid, glycerophospholipid, steroid hormone, and linoleic acid metabolism) (Figure 5E). Notably, the NFS *vs* LPS analysis expanded the pathway repertoire to include vitamin B6 metabolism and sphingolipid metabolism in addition to the conserved pathways (Figure 5F).

A hierarchical clustering heatmap was constructed to visualize metabolites exhibiting significant differential expression (Figure 5G). Compared with the CTRL group, PE(22:1(11Z)/22:1(11Z)), DG(14:0/19:0/0:0), PG(12:0/12:0), Siroheme, Idebenone, Aliskiren, PG(P-16:0/12:0), Cer(d14:1(4E)/20:0(2OH)), Phylloquinone, CerP(d18:1/26:1(17Z)), and 1-Naphthalenesulfonic acid were decreased significantly in the LPS group ($p < 0.05$). In the FA group, the content of PE(22:1(11Z)/22:1(11Z)), PG(12:0/12:0), Siroheme, Aliskiren, PG(P-16:0/12:0), and Cer(d14:1(4E)/20:0(2OH)) increased significantly ($p < 0.05$). PE(20:0/22:1(13Z)) was also slightly decreased in the LPS group, and upregulated by ferulic acid. Compared with the CTRL group, 1-Naphthalenesulfonic acid and Solasodine were significantly down-regulated in the LPS group ($p < 0.05$). In the NFS group, the content of 1-Naphthalenesulfonic acid increased significantly ($p < 0.05$), with the content of Solasodine also increased slightly. In addition, (24R)-24-fluoro-1,25-dihydroxyvitamin D2 and PE(22:4(7Z,10Z,13Z,16Z)/17:0) also showed a downward trend in the LPS group and were slightly up-regulated by N-Feruloylserotonin.

3.4 The effects of ferulic acid and N-Feruloylserotonin on colonic transcriptome in mice

Volcano plots were generated to visualize DEGs across experimental comparisons (Figures 6A–C). A total of 6,324 DEGs were identified in the CTRL *vs* LPS comparison, 3,517 DEGs in the FA *vs* LPS comparison, and 248 DEGs in the NFS *vs* LPS comparison. Pathway enrichment analysis of these DEGs revealed distinct functional signatures (Figures 6D–F). In the CTRL *vs* LPS groups, the DEGs were mainly enriched in the TNF signaling pathway, MAPK signaling pathway, focal adhesion, and MicroRNAs in cancer. The main differential enrichment pathways of FA *vs* LPS groups included MAPK signaling pathway, glycerolipid metabolism, fatty acid degradation, tight junction, and VEGF signaling pathway. As for the differentially expressed genes in the NFS and LPS groups, they were mainly enriched in TNF signaling pathway, insulin resistance, Toll and Imd signaling pathway, focal adhesion, and HIF-1 signaling pathway.

Cross-comparison analysis identified 123 DEGs co-regulated in both CTRL *vs* LPS and FA *vs* LPS comparisons ($|\log_2 FC| > 2$), comprising 80 genes upregulated in LPS but downregulated with FA treatment, and 43 genes exhibiting reciprocal regulation patterns (Supplementary Table S5). Among these co-regulated genes, *Pik3cd*, *Prkca*, *Prkcb*, *Ccnd1*, *Cdkn1a*, *Plcg2*, *Rac2*, *H2-Oa*, *H2-DMb2*, *Tgfa*, *Cxcr4*, *Cxcl12*, *Il2rg*, *Pdgfc*, *Fgfr3*, *Ticam1*, *Irak4*, *Traf6*, and *Lat*, which involved in antigen processing and presentation, PI3K-Akt signaling pathway, Rap1 signaling pathway, Ras signaling pathway, Th17 cell differentiation, chemokine signaling pathway, VEGF signaling pathway, ErbB signaling pathway, MAPK signaling pathway, NF-kappa B

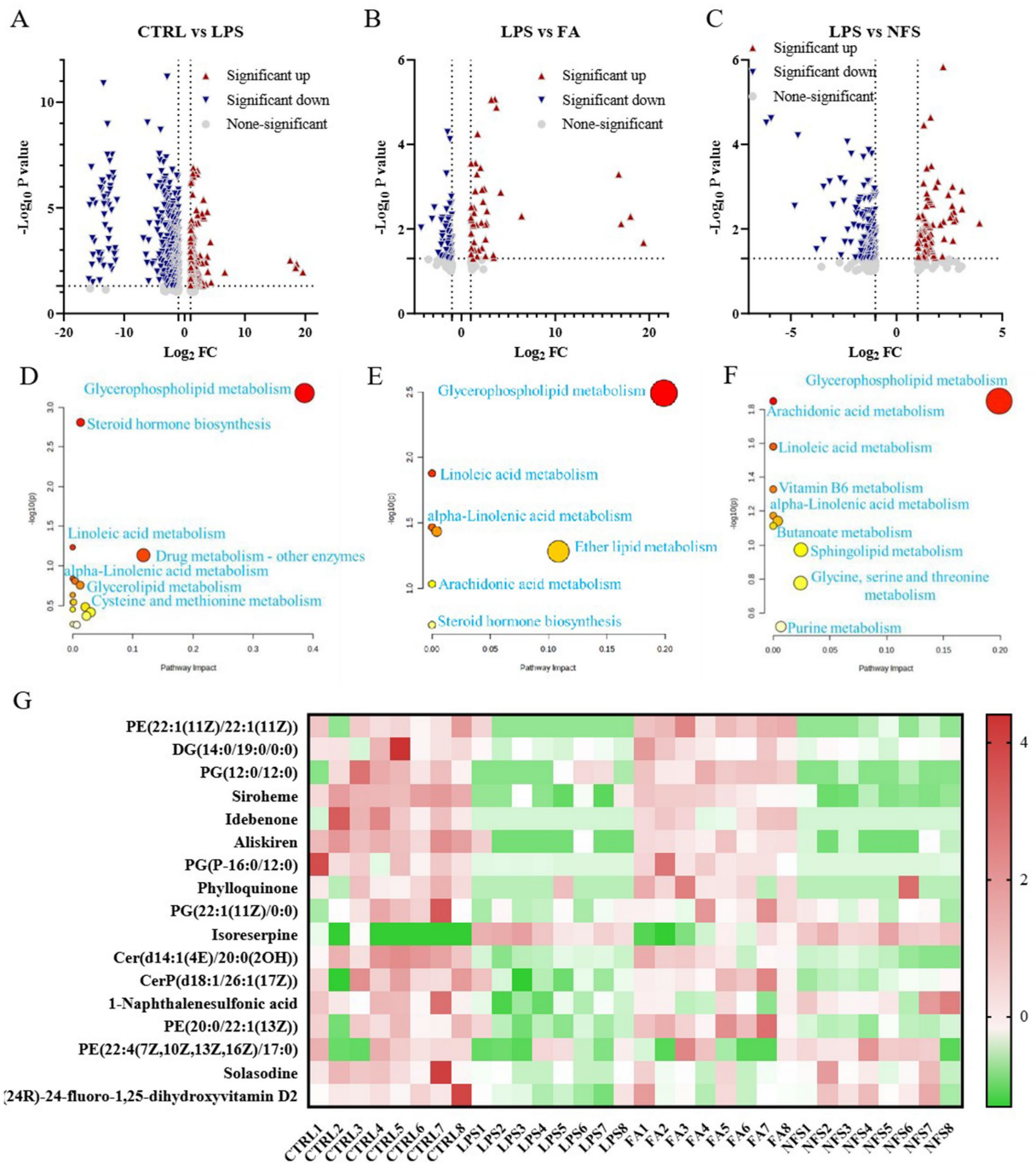

FIGURE 5
The effects of ferulic acid and N-Feruloylserotonin on serum metabolites in mice. Volcano maps of differential metabolites in CTRL *vs* LPS groups **(A)**, FA *vs* LPS groups **(B)**, and NFS *vs* LPS groups **(C)**; The enrichment pathway of differential metabolites in CTRL *vs* LPS groups **(D)**, LPS *vs* FA groups **(E)**, and LPS *vs* NFS groups **(F)**; Content of metabolites in different groups **(G)**.

signaling pathway, intestinal immune network for IgA production, and cytokine-cytokine receptor interaction, may be the potential targets for ferulic acid to regulate intestinal inflammation (Figure 7).

A parallel analysis of CTRL *vs* LPS and NFS *vs* LPS comparisons yielded 38 co-regulated DEGs, with 29 genes exhibiting LPS-induced upregulation reversed by NFS treatment, and 9 genes demonstrating reciprocal regulation (Supplementary Table S6). Among these co-regulated genes, *Cxcl10*, *Kdr*, *Areg*, *Cxcl9*, *Reln*, and *Ccl8*, which involved in cytokine-cytokine receptor interaction, PI3K-Akt signaling pathway, focal adhesion, and MAPK signaling pathway, may be the potential targets for N-Feruloylserotonin to regulate intestinal inflammation (Figure 8).

Heatmaps were constructed to visualize expression patterns of shared co-regulated genes (Figure 9). Among them, *Sprr1a*, *Trim15*, *Gm4841*, *Prr5l*, and *Ccl8* were up-regulated in LPS group and down-regulated in FA and NFS groups. *Hbb-bs*, *Hbb-bt*, *Hba-a1*, *Cbx2*, *Reln*,

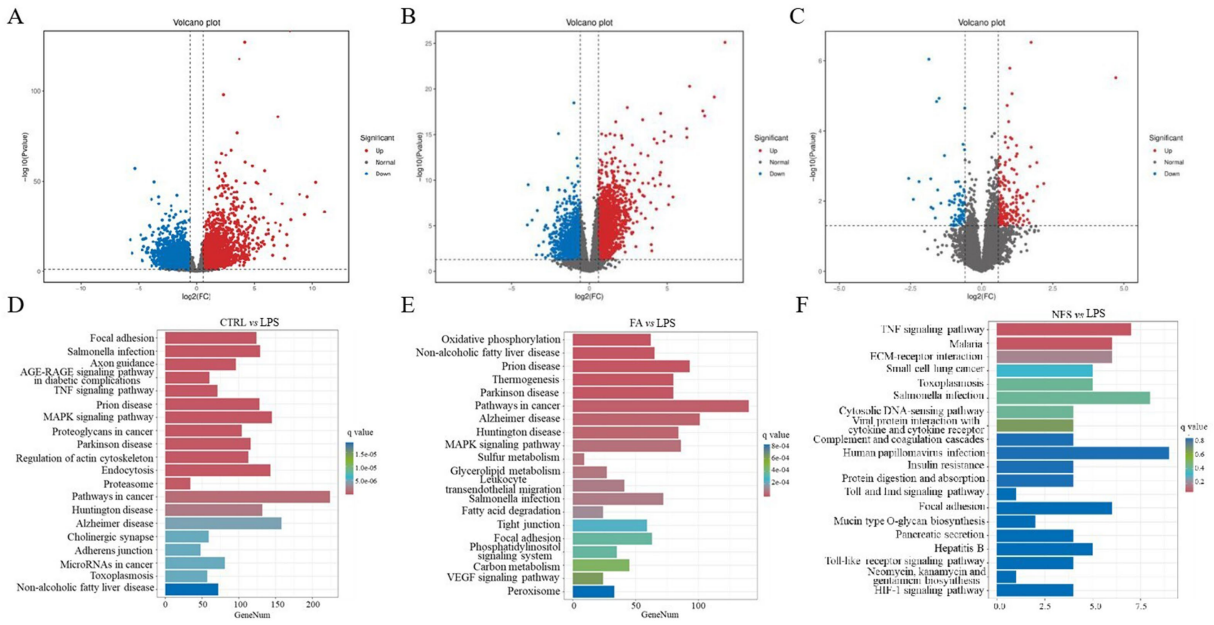

FIGURE 6
The effects of ferulic acid and N-Feruloylserotonin on colonic transcriptome in mice. Volcano maps of differentially expressed genes in CTRL *vs* LPS groups **(A)**, FA *vs* LPS groups **(B)**, and NFS *vs* LPS groups **(C)**; The enrichment pathway of differentially expressed genes in CTRL *vs* LPS groups **(D)**, LPS *vs* FA groups **(E)**, and LPS *vs* NFS groups **(F)**.

Rps2, and *Kdr* were down-regulated in LPS group and up-regulated in FA and NFS groups.

4 Discussion

The effects of ferulic acid and N-Feruloylserotonin on LPS-induced intestinal inflammation were investigated in this study. The results showed that ferulic acid and N-Feruloylserotonin reduced the levels of inflammatory factors and necroptosis pathway genes, increased the expression of genes encoding tight junction proteins, and alleviated the intestinal structural damage caused by LPS. According to the microbial sequencing, ferulic acid and N-Feruloylserotonin promoted the growth of probiotics such as Ruminococcaceae, Akkermansia, Lachnospiraceae, Bifidobacteriaceae, Prevotellaceae and *Roseburia*, and inhibited that of Proteobacteria, Gammaproteobacteria, Enterobacterales and *Bacillus*. Serum metabolites in different groups also changed significantly. LPS reduced metabolites including 1-Naphthalenesulfonic acid, while ferulic acid and N-Feruloylserotonin increased their content. The results of transcriptome sequencing showed that *Sprr1a*, *Trim15*, *Gm4841*, *Prr5l*, and *Ccl8* were up-regulated in LPS group and down-regulated in FA and NFS groups, while *Hbb-bs*, *Hbb-bt*, *Hba-a1*, *Cbx2*, *Reln*, *Rps2*, and *Kdr* were down-regulated in LPS group and up-regulated in FA and NFS groups.

Intestinal epithelial cells construct a barrier that supports nutrient absorption and prevent pathogen invasion. Tight junctions in paracellular spaces are maintained by complex protein–protein interaction networks, and tight junction dysfunction can lead to a variety of local and systemic diseases (Buckley and Turner, 2018). Studies have shown that LPS can increase intestinal permeability and induce the significant down-regulation of *ZO-1* and *Occludin* in cells (He et al., 2022; Liu et al., 2023). In this study, LPS reduced *Claudin 1*, *Occludin*, and *ZO-1* expression, while ferulic acid and N-Feruloylserotonin increased their expression, indicating that they can effectively reduce intestinal permeability, support intestinal nutrient absorption, and prevent pathogen invasion. *iNOS*, a pro-inflammatory mediator that affects immune system, is mainly expressed by immune cells, including T cells, macrophages, and mature CDs (Xue et al., 2018). It regulates the differentiation and function of immune cells by nitrating key molecules involved in transcription or signaling pathways (Mao et al., 2013). IRF5 is a significant marker for the activation of M1 macrophages, and *iNOS* expressed by macrophages can regulate the balance between M1 and M2 macrophages by modifying it (Ischiropoulos and Gow, 2005). In contrast, CD206 and Arg-1 are specific markers of M2 macrophages, which can defend against pathogens, eliminate apoptotic cells, reduce inflammation and promote wound healing (Rőszer, 2015). According to this study, LPS induced the expression of *iNOS* and reduced that of *CD206* and *Arg-1*, while ferulic acid and N-Feruloylserotonin reversed their expression, indicating that LPS aggravated inflammation, and these two natural active substances effectively alleviated inflammation.

A variety of bacterial communities are colonized in the gut, which affect the functions of the host. The diversity of gut microbiome is an indispensable part of its resilience, the diversified microbiome can resist the invasion of pathogens and ensure the stability of intestinal microecology (Cullen et al., 2023). In this study, LPS significantly reduced Shannon index, Simpson index, Chao1 index, ACE index, and PD-whole-tree index of mice, while ferulic acid and N-Feruloylserotonin significantly increased the α diversity of colonic microorganisms in mice, which contributed to the stability of intestinal microecology in mice. The intestinal

10.3389/fmicb.2025.1597774

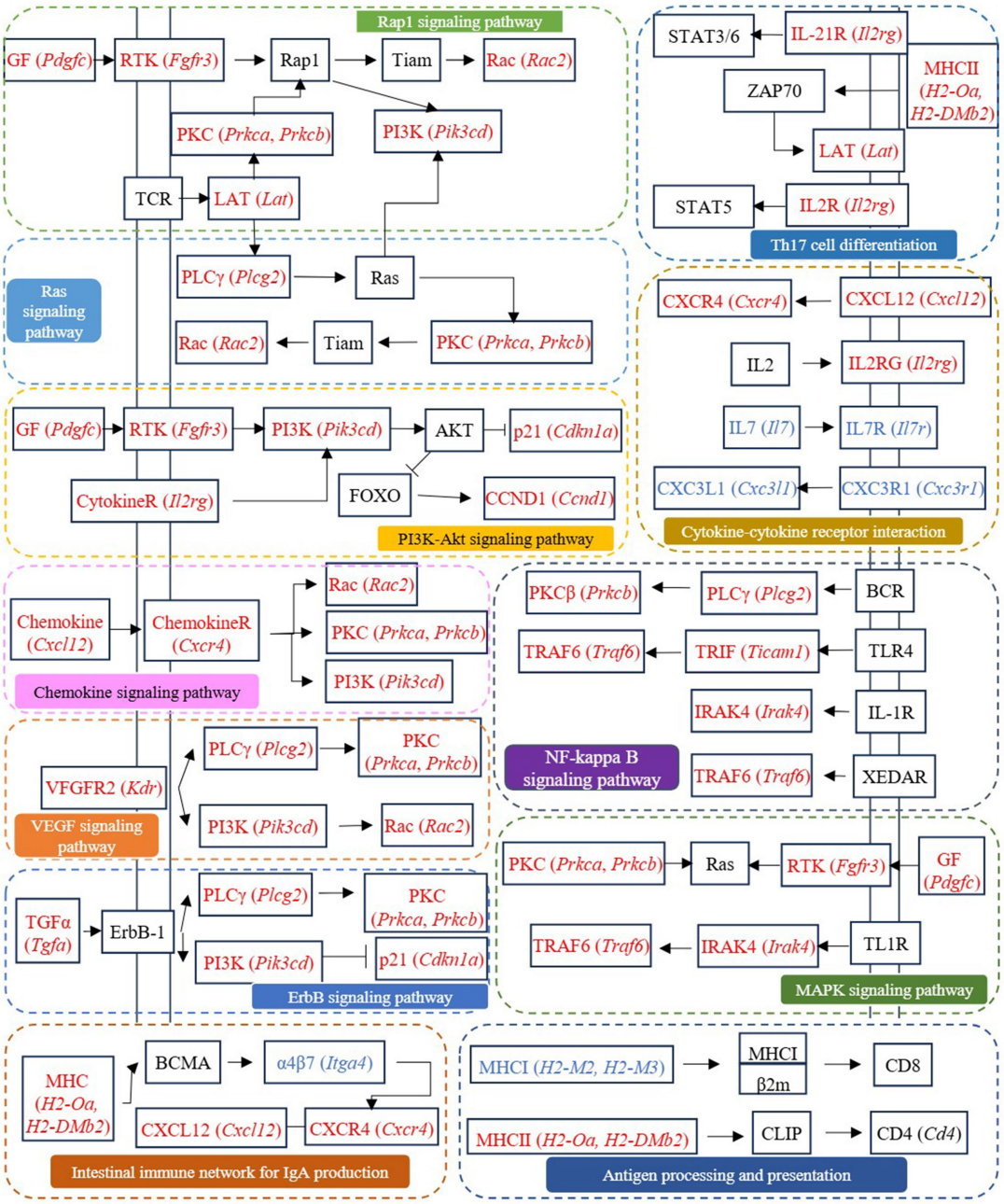

FIGURE 7
The signaling pathways involved in differentially expressed genes co-regulated by CTRL *vs* LPS and FA *vs* LPS groups.

microbiota maintains the host mucosal immune system and regulates intestinal homeostasis by interacting with the intestinal mucosa. Typical intestinal bacteria found in healthy individuals include Bacteroidaceae, Clostridiaceae, Prevotellaceae, Eubacteriaceae, Ruminococcaceae, Bifidobacteriaceae, Lactobacillaceae, Saccharomycetaceae, and Methanobacteriaceae (Jackson and Theiss, 2020). Among them, Bacteroidaceae, Prevotellaceae, Ruminococcaceae and Bifidobacteriaceae were significantly up-regulated by Ferulic acid and N-Feruloylserotonin in this study. The members of Bacteroidaceae are the main members of the intestinal bacteria, which can not only degrade complex polysaccharides to provide energy for the colon, but also participate in a variety of important metabolic activities of the body (Zafar and Saier, 2021). Prevotellaceae and Ruminococcaceae are potential probiotics, which are closely related to metabolism and health, and have the function of relieving inflammation (Ortega-Santos and Whisner, 2019; Feng et al., 2022). Bifidobacteriaceae contributes to the absorption of sugar, minerals and nutrients, as well as the synthesis of vitamins. It exerts anti-inflammatory properties by affecting essential fatty acids, and the reduction in its abundance will negatively affect the intestinal epithelial barrier function (Hanifi et al., 2021). Microbial metabolites, the messengers of colonic epithelial cells and immune cells, can affect metabolism, epigenetic modification and gene expression. SCFAs are the most studied

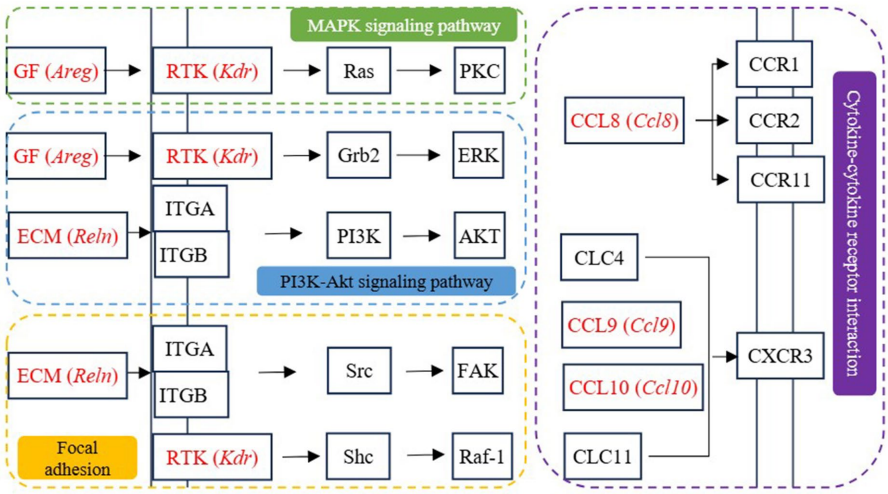

FIGURE 8
The signaling pathways involved in differentially expressed genes co-regulated by CTRL *vs* LPS and NFS *vs* LPS groups.

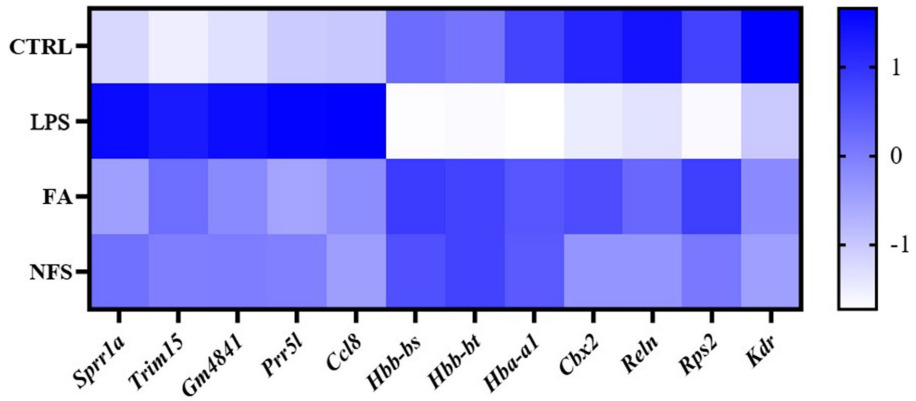

FIGURE 9
Heatmap of differentially expressed genes.

microbial metabolites, which provide energy to colonic epithelial cells and contribute to maintain colonic homeostasis (He et al., 2024). In this study, Ruminococcaceae, Muribaculaceae, Akkermansia, Lachnospiraceae, Bifidobacteriaceae, Prevotellaceae, *Roseburia*, *Blautia*, and *Butyricicoccus*, which can produce SCFAs, were significantly increased in the FA and NFS groups. Proteobacteria contains many pathogenic bacteria, and the increase of its abundance will lead to imbalance among different bacterial species, increase of intestinal permeability and disorder of intestinal microbial community, leading to aggravation of inflammation (Cuesta et al., 2022). Gammaproteobacteria, Enterobacterales and *Escherichia Shigella* belong to Proteobacteria, which were increased significantly in the LPS group and down-regulated significantly by ferulic acid and N-Feruloylserotonin. The above results showed that ferulic acid and N-Feruloylserotonin can alleviate intestinal inflammation by regulating the intestinal flora of mice, they can increase the abundance of beneficial bacteria and reduce that of pathogenic bacteria.

According to the serum metabolomics, some metabolites beneficial to the health of the body were down-regulated in the LPS group. For example, Idebenone is an antioxidant that can effectively inhibit lipid peroxidation in brain tissue and protect cells from oxidative damage (Yan et al., 2018). Phylloquinone belongs to vitamin K, and its most well-known function is to act as a cofactor that activates vitamin K-dependent coagulation factors. (24R)-24-fluoro-1,25-dihydroxyvitamin D2 is a metabolite of vitamin D2. Vitamin D is the precursor of hormones, which plays a key role in regulating calcium and phosphate metabolism, thereby maintaining normal function of bone (Wilson et al., 2017). PE(22:1(11Z)/22:1(11Z)), PE(20:0/22:1(13Z)) and PE(22:4(7Z,10Z,13Z,16Z)/17:0) are phosphatidylethanolamines, which are the second most abundant phospholipids in mammalian cells with strong biological activity. They can act as lipid chaperones to help certain membrane proteins fold, contribute to the initiation of autophagy, and act as receptors for host defense peptides to promote their antibacterial activity (Pohl and Jovanovic, 2019).

DG(14:0/19:0/0:0), which belongs to diacylglycerol, is a lipid second messenger that affects the proliferation, survival and intracellular signal transduction of mammalian cells, and exerts many biological functions through protein kinase C, other effector isozymes, and small GTPase regulatory proteins (Cooke and Kazanietz, 2022). PG(12:0/12:0), PG(P-16:0/12:0), and PG(22:1(11Z)/0:0) are phosphatidylglycerols, which can regulate the function of keratinocytes and inhibit the occurrence and development of inflammation (Xie et al., 2018). The promotion of these metabolites by ferulic acid and N-Feruloylserotonin indicated the potential role of these two substances in maintaining body health. In addition, the increase of some harmful substances will have a negative impact on the health of mice. For example, Isoreserpine belongs to alkaloids, which induce endothelial injury and pulmonary hypertension by targeting extracellular calcium-sensitive receptors, as well as acute cerebrovascular disease, astrocytic proliferation and neuronal degeneration associated with behavioral changes in rats (Silva et al., 2023). The increase of Isoreserpine in LPS group indicated the aggravation of intestinal inflammation in mice, while its down-regulation in FA and NFS groups indicated the protective effect of ferulic acid and N-Feruloylserotonin on the health of mice.

LPS is the main structural component of the outer membrane of most Gram-negative bacteria, which can stimulate the immune system and induce a series of pathological states in the body (Kell and Pretorius, 2015). LPS-induced signal transduction processes include intracellular signal transduction directly activated by TLR4 receptor complex and continuous induction of indirect autocrine and paracrine signal transduction events (Bode et al., 2012). Liu et al. used LPS to induce mastitis in dairy cows, and the results found that the DEGs between the CON group and the LPS-treated group were mainly enriched in NF-κB signaling pathway, IL-17 signaling pathway, and cytokine-cytokine receptor interaction, which was consistent with the results of this study (Liu et al., 2024). NF-κB and MAPK signaling pathway are involved in LPS-mediated TNF-α secretion. There is also evidence that the crosstalk between MAPK pathway and signal transduction mediated by STAT 3 forms a critical axis continuously activated by LPS, which is critical for the induction and spread of inflammatory macrophage responses (Bode et al., 2012). As an important intracellular signaling pathway, PI3K/Akt regulates many cellular processes, including cancer progression, cell proliferation, metabolism and survival (Li et al., 2008). PI3K phosphorylation activates Akt, which has a variety of biological functions and activates downstream protein molecules (Xie et al., 2019). Antigen processing and presentation are the basis of adaptive immunity. The major histocompatibility complex (MHC) molecules responsible for antigen presentation are MHCI and MHCII molecules, which present antigen peptides to CD8 T cells and CD4 T cells, respectively (Pishesha et al., 2022). Cytokines play a biological role by binding to the corresponding cytokine receptors on the cell surface. LPS induces the production of cytokines in immune cells, including TNF, IL-1β, IFN-γ and chemokines (Cavaillon, 2018). The combination of cytokines and their receptors initiates complex intracellular molecular interactions, which ultimately lead to changes in cell gene transcription and coordinate the immune response. Moreover, the Ras and Rap1 signaling pathway are also important signaling mechanisms in cells and are involved in many biological processes, such as cell growth, differentiation, apoptosis and metabolism (Kosuru and Chrzanowska, 2020; Sadeghi Shaker et al., 2023). Therefore, according to the results of transcriptome sequencing, genes involved in the above pathways and regulated by ferulic acid, including *Pik3cd*, *Prkca*, *Prkcb*, *Ccnd1*, *Cdkn1a*, *Plcg2*, *Rac2*, *H2-Oa*, *H2-DMb2*, *Tgfa*, *Cxcr4*, *Cxcl12*, *Il2rg*, *Pdgfc*, *Fgfr3*, *Ticam1*, *Irak4*, *Traf6*, and *Lat*, may be potential targets for ferulic acid to alleviate intestinal inflammation. And *Cxcl10*, *Kdr*, *Areg*, *Cxcl9*, *Reln*, and *Ccl8* may be potential targets for N-Feruloylserotonin to alleviate intestinal inflammation.

In addition, some genes shared by the co-regulated genes may also be potential targets for two substances to alleviate intestinal inflammation in mice. Among them, *Sprr1a* encodes small proline rich protein 1A. The knockout of *Sprr1a* in mice can improve cardiac dysfunction after myocardial infarction (Kawaguchi et al., 2023), and the expression of *Sprr1a* in colorectal cancer tissues is significantly increased, which may be used as a potential biomarker for the prognosis of colon cancer (Deng et al., 2020). Hemoglobin is considered to be an iron-containing protein essential for oxygen transport in mammalian blood (Gell, 2018). *Hbb-bs*, *Hbb-bt* and *Hba-al* are genes encoding hemoglobin, which are up-regulated by ferulic acid and N-Feruloylserotonin, helping to maintain the normal functioning of life. Vascular endothelial growth factor (VEGF) is the main growth factor of endothelial cells. The elevated gene *Kdr* in the FA and NFS groups encodes a receptor for VEGF, which is called a kinase insert domain receptor, a key regulator of angiogenesis, and the major mediator of VEGF-induced endothelial proliferation, survival and migration (Boyer, 2002). Notably, the expression of key genes in necroptosis, including *Rip1*, *Rip3*, and *Mlkl*, were also detected in this study. RIP1/RIP3/MLKL pathway is a classical regulatory pathway of necroptosis (Vandenabeele et al., 2010). Under the stimulation of ischemia/reperfusion, inflammation and oxidative stress, RIP1 and RIP3 form a complex through the RIP terminal interaction motif, which then induce the activation and translocation of MLKL, and finally lead to cell lysis (Liu et al., 2019). The activation of caspase-1 and NLRP3 mediated by MLKL, and the secretion of pro-inflammatory cytokine IL-1β are the main determinants of necroptosis-derived inflammatory signals (Conos et al., 2017). The assembly of NLRP3 inflammasome leads to the activation of caspase-1, the release of IL-1β and IL-18, and the cleavage of gasdermin D, thereby promoting cell death and aggravating the occurrence and development of inflammatory diseases (Xu and Núñez, 2023). In this study, LPS increased the expression of *Rip1*, *Rip3*, *Mlkl*, and *IL-1β*, indicating the activation of necroptosis pathway, while ferulic acid and N-Feruloylserotonin inhibited the activation of necroptosis and alleviated intestinal inflammation in mice. Therefore, ferulic acid and N-Feruloylserotonin may alleviate inflammation and maintain health by inhibiting necroptosis.

5 Conclusion

Natural active products can mitigate LPS-induced intestinal injury in mice, they may alleviate the intestinal inflammation by regulating antigen processing and presentation, NF-κB signal pathway, MAPK signal pathway and PI3K-Akt signal pathway, among which *Pik3cd*, *H2-DMb1*, *H2-Oa*, *Kdr*, *Fgfr3*, *Il1r2*, *Rac*,

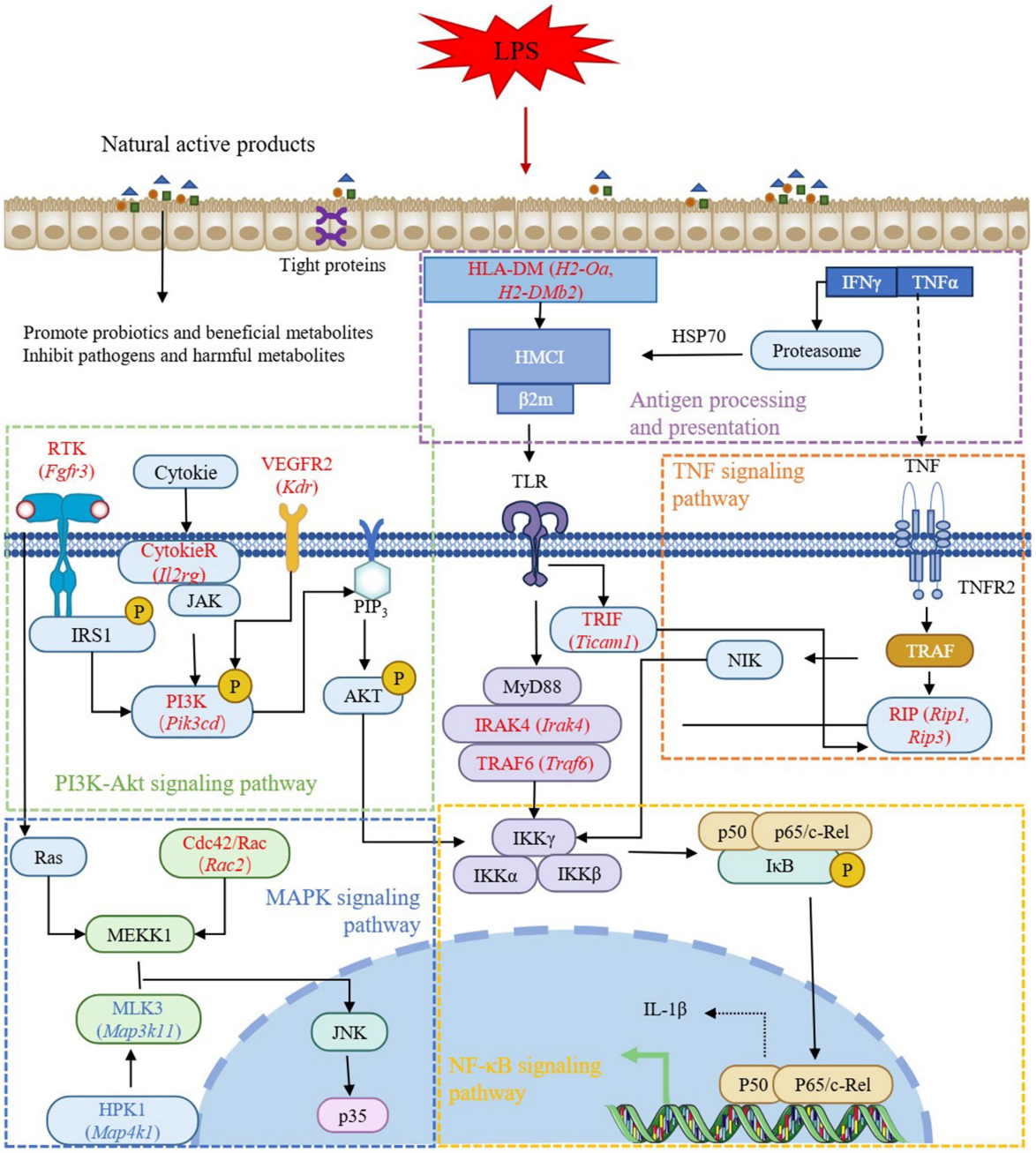

FIGURE 10
Potential mechanisms of natural active products regulating intestinal inflammation.

Irak4, *Traf6*, *Ticam1*, *Rip1*, and *Rip3* are potential targets (Figure 10).

Data availability statement

The data supporting this article have been included as part of the Supplementary material. The 16S rRNA gene raw sequence data and RNA-seq raw sequence data were deposited into the NCBI Sequence Read Archive (SRA) database under the accession numbers PRJNA1237577 and PRJNA1240033, respectively.

Ethics statement

The animal study was approved by Animal Care Committee of Hunan Agricultural University. The study was conducted in accordance with the local legislation and institutional requirements.

Author contributions

XiH: Formal analysis, Data curation, Investigation, Writing – original draft. XuH: Writing – review & editing, Formal analysis, Data

curation, Investigation. GL: Investigation, Writing – review & editing, Supervision. GG: Funding acquisition, Writing – review & editing, Supervision. CX: Writing – review & editing, Project administration.

Funding

The author(s) declare that financial support was received for the research and/or publication of this article. This study was supported by the National Natural Science Foundation of China (32472930 and 31772642), the Scientific Research Fund of Hunan Provincial Education Department (22A0154), Zhejiang Provincial Medical and Health Plan (2023XY234), Hunan Provincial Science and Technology Department (2019TP2004 and 2016TP2005).

Conflict of interest

The authors declare that the research was conducted in the absence of any commercial or financial relationships that could be construed as a potential conflict of interest.

Generative AI statement

The authors declare that no Gen AI was used in the creation of this manuscript.

Publisher's note

All claims expressed in this article are solely those of the authors and do not necessarily represent those of their affiliated organizations, or those of the publisher, the editors and the reviewers. Any product that may be evaluated in this article, or claim that may be made by its manufacturer, is not guaranteed or endorsed by the publisher.

Supplementary material

The Supplementary material for this article can be found online at: https://www.frontiersin.org/articles/10.3389/fmicb.2025.1597774/full#supplementary-material

References

Bode, J. G., Ehlting, C., and Häussinger, D. (2012). The macrophage response towards LPS and its control through the p38(MAPK)-STAT3 axis. *Cell. Signal.* 24, 1185–1194. doi: 10.1016/j.cellsig.2012.01.018

Boyer, S. J. (2002). Small molecule inhibitors of KDR (VEGFR-2) kinase: an overview of structure activity relationships. *Curr. Top. Med. Chem.* 2, 973–1000. doi: 10.2174/1568026023393273

Buckley, A., and Turner, J. R. (2018). Cell biology of tight junction barrier regulation and mucosal disease. *Cold Spring Harb. Perspect. Biol.* 10:a029314. doi: 10.1101/cshperspect.a029314

Carola, C., Salazar, A., Rakers, C., Himbert, F., Do, Q. T., Bernard, P., et al. (2021). A cornflower extract containing *N*-feruloylserotonin reduces inflammation in human skin by neutralizing CCL17 and CCL22 and inhibiting COX-2 and 5-LOX. *Mediat. Inflamm.* 2021:6652791. doi: 10.1155/2021/6652791

Cavaillon, J. M. (2018). Exotoxins and endotoxins: inducers of inflammatory cytokines. *Toxicon* 149, 45–53. doi: 10.1016/j.toxicon.2017.10.016

Chopra, B., and Dhingra, A. K. (2021). Natural products: a lead for drug discovery and development. *Phytother. Res.* 35, 4660–4702. doi: 10.1002/ptr.7099

Conos, S. A., Chen, K. W., De Nardo, D., Hara, H., Whitehead, L., Núñez, G., et al. (2017). Active MLKL triggers the NLRP3 inflammasome in a cell-intrinsic manner. *Proc. Natl. Acad. Sci. USA* 114, e961–e969. doi: 10.1073/pnas.1613305114

Cooke, M., and Kazanietz, M. G. (2022). Overarching roles of diacylglycerol signaling in cancer development and antitumor immunity. *Sci. Signal.* 15:eabo0264. doi: 10.1126/scisignal.abo0264

Cuesta, S., Burdisso, P., Segev, A., Kourrich, S., and Sperandio, V. (2022). Gut colonization by Proteobacteria alters host metabolism and modulates cocaine neurobehavioral responses. *Cell Host Microbe* 30, 1615–1629.e5. doi: 10.1016/j.chom.2022.09.014

Cullen, J. M. A., Shahzad, S., and Dhillon, J. (2023). A systematic review on the effects of exercise on gut microbial diversity, taxonomic composition, and microbial metabolites: identifying research gaps and future directions. *Front. Physiol.* 14:1292673. doi: 10.3389/fphys.2023.1292673

Danne, C., Skerniskyte, J., Marteyn, B., and Sokol, H. (2024). Neutrophils: from IBD to the gut microbiota. *Nat. Rev. Gastroenterol. Hepatol.* 21, 184–197. doi: 10.1038/s41575-023-00871-3

Deng, Y., Zheng, X., Zhang, Y., Xu, M., Ye, C., Lin, M., et al. (2020). High SPRR1A expression is associated with poor survival in patients with colon cancer. *Oncol. Lett.* 19, 3417–3424. doi: 10.3892/ol.2020.11453

Feng, J., Ma, H., Huang, Y., Li, J., and Li, W. (2022). Ruminococcaceae_UCG-013 promotes obesity resistance in mice. *Biomedicines* 10:3272. doi: 10.3390/biomedicines10123272

Funk, M. C., Zhou, J., and Boutros, M. (2020). Ageing, metabolism and the intestine. *EMBO Rep.* 21:e50047. doi: 10.15252/embr.202050047

Gell, D. A. (2018). Structure and function of haemoglobins. *Blood Cells Mol. Dis.* 70, 13–42. doi: 10.1016/j.bcmd.2017.10.006

Han, X., Fu, Y., Wang, K., Li, S., Jiang, C., Wang, S., et al. (2023). Epigallocatechin gallate alleviates osteoporosis by regulating the gut microbiota and serum metabolites in rats. *Food Funct.* 14, 10564–10580. doi: 10.1039/d3fo03233g

Hanifi, G. R., Samadi Kafil, H., Tayebi Khosroshahi, H., Shapouri, R., and Asgharzadeh, M. (2021). Bifidobacteriaceae family diversity in gut microbiota of patients with renal failure. *Arch. Razi Inst.* 76, 521–528. doi: 10.22092/ari.2020.352271.1557

He, Y., Li, Z., Xu, T., Luo, D., Chi, Q., Zhang, Y., et al. (2022). Polystyrene nanoplastics deteriorate LPS-modulated duodenal permeability and inflammation in mice via ROS drived-NF-κB/NLRP3 pathway. *Chemosphere* 307:135662. doi: 10.1016/j.chemosphere.2022.135662

He, M., Wei, W., Zhang, Y., Xiang, Z., Peng, D., Kasimumali, A., et al. (2024). Gut microbial metabolites SCFAs and chronic kidney disease. *J. Transl. Med.* 22:172. doi: 10.1186/s12967-024-04974-6

Hwang, H. J., Lee, S. R., Yoon, J. G., Moon, H. R., Zhang, J., Park, E., et al. (2022). Ferulic acid as a protective antioxidant of human intestinal epithelial cells. *Antioxidants (Basel)* 11:1448. doi: 10.3390/antiox11081448

Ischiropoulos, H., and Gow, A. (2005). Pathophysiological functions of nitric oxide-mediated protein modifications. *Toxicology* 208, 299–303. doi: 10.1016/j.tox.2004.11.018

Jackson, D. N., and Theiss, A. L. (2020). Gut bacteria signaling to mitochondria in intestinal inflammation and cancer. *Gut Microbes* 11, 285–304. doi: 10.1080/19490976.2019.1592421

Kawaguchi, S., Moukette, B., Sepúlveda, M. N., Hayasaka, T., Aonuma, T., Haskell, A. K., et al. (2023). SPRR1A is a key downstream effector of MiR-150 during both maladaptive cardiac remodeling in mice and human cardiac fibroblast activation. *Cell Death Dis.* 14:446. doi: 10.1038/s41419-023-05982-y

Kell, D. B., and Pretorius, E. (2015). On the translocation of bacteria and their lipopolysaccharides between blood and peripheral locations in chronic, inflammatory diseases: the central roles of LPS and LPS-induced cell death. *Integr. Biol. (Camb.)* 7, 1339–1377. doi: 10.1039/c5ib00158g

Kosuru, R., and Chrzanowska, M. (2020). Integration of Rap1 and calcium signaling. *Int. J. Mol. Sci.* 21:1616. doi: 10.3390/ijms21051616

Li, J., Chen, Z., Wang, Q., Du, L., Yang, Y., Guo, F., et al. (2024). Microbial and metabolic profiles unveil mutualistic microbe-microbe interaction in obesity-related colorectal cancer. *Cell Rep. Med.* 5:101429. doi: 10.1016/j.xcrm.2024.101429

Li, L., Qu, Y., Mao, M., Xiong, Y., and Mu, D. (2008). The involvement of phosphoinositid 3-kinase/Akt pathway in the activation of hypoxia-inducible factor-1alpha in the developing rat brain after hypoxia-ischemia. *Brain Res.* 1197, 152–158. doi: 10.1016/j.brainres.2007.12.059

Li, D., Rui, Y. X., Guo, S. D., Luan, F., Liu, R., and Zeng, N. (2021). Ferulic acid: a review of its pharmacology, pharmacokinetics and derivatives. *Life Sci.* 284:119921. doi: 10.1016/j.lfs.2021.119921

Liu, J., Gao, Y., Zhang, X., Hao, Z., Zhang, H., Gui, R., et al. (2024). Transcriptome sequencing analysis of bovine mammary epithelial cells induced by lipopolysaccharide. *Anim. Biotechnol.* 35:2290527. doi: 10.1080/10495398.2023.2290527

Liu, Y., Liu, T., Lei, T., Zhang, D., Du, S., Girani, L., et al. (2019). RIP1/RIP3-regulated necroptosis as a target for multifaceted disease therapy (review). *Int. J. Mol. Med.* 44, 771–786. doi: 10.3892/ijmm.2019.4244

Liu, H., Wang, S., Gong, L., Shen, Y., Xu, F., Wang, Y., et al. (2023). SIRT6 ameliorates LPS-induced apoptosis and tight junction injury in ARDS through the ERK1/2 pathway and autophagy. *Int. J. Med. Sci.* 20, 581–594. doi: 10.7150/ijms.80920

Loh, J. S., Mak, W. Q., Tan, L. K. S., Ng, C. X., Chan, H. H., Yeow, S. H., et al. (2024). Microbiota-gut-brain axis and its therapeutic applications in neurodegenerative diseases. *Signal Transduct. Target. Ther.* 9:37. doi: 10.1038/s41392-024-01743-1

Ma, Y., Jiang, H., Fang, J., and Liu, G. (2019). IRW and IQW reduce colitis-associated cancer risk by alleviating DSS-induced colonic inflammation. *Biomed. Res. Int.* 2019:6429845. doi: 10.1155/2019/6429845

Mao, K., Chen, S., Chen, M., Ma, Y., Wang, Y., Huang, B., et al. (2013). Nitric oxide suppresses NLRP3 inflammasome activation and protects against LPS-induced septic shock. *Cell Res.* 23, 201–212. doi: 10.1038/cr.2013.6

Ortega-Santos, C. P., and Whisner, C. M. (2019). The key to successful weight loss on a high-fiber diet may be in gut microbiome prevotella abundance. *J. Nutr.* 149, 2083–2084. doi: 10.1093/jn/nxz248

Park, C. H., Han, S. W., Seong, S. H., Choi, J. S., Jeon, J. P., and Yokozawa, T. (2023). N-feruloylserotonin inhibits lipopolysaccharide-induced inflammation via SIRT1-stimulated FOXO1 and NF-κB signaling pathways in RAW 264.7 cells. *Cell. Mol. Biol. (Noisy-le-Grand)* 69, 109–115. doi: 10.14715/cmb/2023.69.11.17

Pishesha, N., Harmand, T. J., and Ploegh, H. L. (2022). A guide to antigen processing and presentation. *Nat. Rev. Immunol.* 22, 751–764. doi: 10.1038/s41577-022-00707-2

Pohl, E. E., and Jovanovic, O. (2019). The role of phosphatidylethanolamine adducts in modification of the activity of membrane proteins under oxidative stress. *Molecules* 24:4545. doi: 10.3390/molecules24244545

Ren, W., Yin, J., Wu, M., Liu, G., Yang, G., Xion, Y., et al. (2014). Serum amino acids profile and the beneficial effects of L-arginine or L-glutamine supplementation in dextran sulfate sodium colitis. *PLoS One* 9:e88335. doi: 10.1371/journal.pone.0088335

Roh, T. T., Chen, Y., Rudolph, S., Gee, M., and Kaplan, D. L. (2021). *In vitro* models of intestine innate immunity. *Trends Biotechnol.* 39, 274–285. doi: 10.1016/j.tibtech.2020.07.009

Rőszer, T. (2015). Understanding the mysterious M2 macrophage through activation markers and effector mechanisms. *Mediat. Inflamm.* 2015:816460. doi: 10.1155/2015/816460

Sadeghi Shaker, M., Rokni, M., Mahmoudi, M., and Farhadi, E. (2023). Ras family signaling pathway in immunopathogenesis of inflammatory rheumatic diseases. *Front. Immunol.* 14:1151246. doi: 10.3389/fimmu.2023.1151246

Silva, A. L., Oliveira, J. L., do Nascimento, R. P., Santos, L. O., de Araújo, F. M., Dos Santos, B. L., et al. (2023). Monocrotaline induces acutely cerebrovascular lesions, astrogliosis and neuronal degeneration associated with behavior changes in rats: a model of vascular damage in perspective. *Neurotoxicology* 94, 59–70. doi: 10.1016/j.neuro.2022.10.017

Tian, B., Geng, Y., Wang, P., Cai, M., Neng, J., Hu, J., et al. (2022). Ferulic acid improves intestinal barrier function through altering gut microbiota composition in high-fat diet-induced mice. *Eur. J. Nutr.* 61, 3767–3783. doi: 10.1007/s00394-022-02927-7

Vandenabeele, P., Galluzzi, L., Vanden Berghe, T., and Kroemer, G. (2010). Molecular mechanisms of necroptosis: an ordered cellular explosion. *Nat. Rev. Mol. Cell Biol.* 11, 700–714. doi: 10.1038/nrm2970

Veiga-Fernandes, H., and Pachnis, V. (2017). Neuroimmune regulation during intestinal development and homeostasis. *Nat. Immunol.* 18, 116–122. doi: 10.1038/ni.3634

Wang, Q., Lu, Q., Jia, S., and Zhao, M. (2023). Gut immune microenvironment and autoimmunity. *Int. Immunopharmacol.* 124:110842. doi: 10.1016/j.intimp.2023.110842

Wilson, L. R., Tripkovic, L., Hart, K. H., and Lanham-New, S. A. (2017). Vitamin D deficiency as a public health issue: using vitamin D2 or vitamin D3 in future fortification strategies. *Proc. Nutr. Soc.* 76, 392–399. doi: 10.1017/s0029665117000349

Xie, D., Choudhary, V., Seremwe, M., Edwards, J. G., Wang, A., Emmons, A. C., et al. (2018). Soy phosphatidylglycerol reduces inflammation in a contact irritant ear edema mouse model *in vivo*. *J. Pharmacol. Exp. Ther.* 366, 1–8. doi: 10.1124/jpet.117.244756

Xie, Y., Shi, X., Sheng, K., Han, G., Li, W., Zhao, Q., et al. (2019). PI3K/Akt signaling transduction pathway, erythropoiesis and glycolysis in hypoxia (review). *Mol. Med. Rep.* 19, 783–791. doi: 10.3892/mmr.2018.9713

Xu, J., and Núñez, G. (2023). The NLRP3 inflammasome: activation and regulation. *Trends Biochem. Sci.* 48, 331–344. doi: 10.1016/j.tibs.2022.10.002

Xue, Q., Yan, Y., Zhang, R., and Xiong, H. (2018). Regulation of iNOS on immune cells and its role in diseases. *Int. J. Mol. Sci.* 19:3805. doi: 10.3390/ijms19123805

Yan, A., Liu, Z., Song, L., Wang, X., Zhang, Y., Wu, N., et al. (2018). Idebenone alleviates neuroinflammation and modulates microglial polarization in LPS-stimulated BV2 cells and mptp-induced Parkinson's disease mice. *Front. Cell. Neurosci.* 12:529. doi: 10.3389/fncel.2018.00529

Zafar, H., and Saier, M. H. Jr. (2021). Gut *Bacteroides* species in health and disease. *Gut Microbes* 13, 1–20. doi: 10.1080/19490976.2020.1848158

Zhao, Y., Zhong, X., Yan, J., Sun, C., Zhao, X., and Wang, X. (2022). Potential roles of gut microbes in biotransformation of natural products: an overview. *Front. Microbiol.* 13:956378. doi: 10.3389/fmicb.2022.956378

frontiers | Frontiers in Microbiology

TYPE Original Research
PUBLISHED 23 July 2025
DOI 10.3389/fmicb.2025.1616720

Check for updates

OPEN ACCESS

EDITED BY
Junling Shi,
Northwestern Polytechnical University, China

REVIEWED BY
Rishi Drolia,
Old Dominion University, United States
Carolina Matto,
Ministerio de Ganadería, Agricultura y Pesca, Uruguay

*CORRESPONDENCE
Ok Kyung Koo
okoo@cnu.ac.kr

RECEIVED 23 April 2025
ACCEPTED 03 July 2025
PUBLISHED 23 July 2025

CITATION
Kim DW, Singh S, Kim UI, An SH, Je HJ, Lee DY, Yun EJ and Koo OK (2025) Exploring the fate of *Listeria monocytogenes* in an *in vitro* digestion and fecal fermentation model: insights into survival during digestion and interaction with gut microbiota. *Front. Microbiol.* 16:1616720. doi: 10.3389/fmicb.2025.1616720

COPYRIGHT
© 2025 Kim, Singh, Kim, An, Je, Lee, Yun and Koo. This is an open-access article distributed under the terms of the Creative Commons Attribution License (CC BY). The use, distribution or reproduction in other forums is permitted, provided the original author(s) and the copyright owner(s) are credited and that the original publication in this journal is cited, in accordance with accepted academic practice. No use, distribution or reproduction is permitted which does not comply with these terms.

Exploring the fate of *Listeria monocytogenes* in an *in vitro* digestion and fecal fermentation model: insights into survival during digestion and interaction with gut microbiota

Dong Woo Kim[1], Saloni Singh[1], Ui In Kim[1], So Hyeon An[1], Hyeon Ji Je[1], Dong Young Lee[2], Eun Ju Yun[2] and Ok Kyung Koo[1]*

[1]Department of Food Science & Technology, Chungnam National University, Daejeon, Republic of Korea, [2]Department of Biotechnology, The Catholic University of Korea, Bucheon, Republic of Korea

Listeria monocytogenes is a foodborne pathogen that causes listeriosis, a disease with a mortality rate of 20 ~ 30%. This bacterium enters the human body through contaminated food or ingredients and encounters primary innate defense systems, including gastric acid, bile salts, and gut microbiota. These systems play a critical role in preventing pathogen colonization and infection. However, interactions with pathogens can also alter the gut microbiota profile. This study aimed to investigate the host's defense mechanisms against *L. monocytogenes* and the changes in the gut microbiota profile following infection. *L. monocytogenes* ATCC 7644 showed the greatest reduction (7.6 log CFU), followed by ATCC 19111 (5.71 log), F2365 (5.02 log), ATCC 19113 (3.96 log), and NCCP 14714 (3.38 log), while the pooled cocktail exhibited a 3.49 log CFU reduction. Notably, the clinical isolates NCCP 14714 and F2365 exhibited greater resistance to the simulated digestive process compared to the food isolate ATCC 7644. *L. monocytogenes* infection induced notable shifts in specific bacterial groups, including *Bacteroides*, *Bifidobacterium*, and the *Mediterraneibacter gnavus* group, as well as an increase in ethanol levels. These alterations may contribute to gut barrier disruption and the upregulation of immune responses, ultimately promoting the pathogenesis of *L. monocytogenes* infection. The findings from this study provide valuable insights into the interaction between *L. monocytogenes* and the human gut microbiota, offering a comparative reference for the interpretation of future research.

KEYWORDS

***Listeria monocytogenes*, gut microbiota, *in vitro* digestion, fecal fermentation, microbial interactions**

1 Introduction

Listeria monocytogenes is a Gram-positive, foodborne pathogen renowned for its capacity to cause severe infections, termed listeriosis (Osek et al., 2022). Listeriosis is recognized as one of the top five foodborne illnesses, with a mortality rate of 20 ~ 30% (Koopmans et al., 2023; Osek et al., 2022). The illness primarily occurs in pregnant women, newborns, elderly, and immunocompromised individuals, with pregnant women being over 100 times more likely to

develop the infection compared to women with reproductive capability (Centers for Disease Control and Prevention, 2024; Koopmans et al., 2023). The incidence of foodborne outbreaks caused by *L. monocytogenes* has decreased through the implementation of regulations, practices, and screening methods such as HACCP (Koopmans et al., 2023). However, the costs associated with listeriosis still reached up to 22 billion dollars in North America, serving as a significant public health concern worldwide (Koopmans et al., 2023).

Listeria monocytogenes can primarily be transmitted through contaminated food ingredients or food products, such as meat, fish, ready-to-eat products, sliced vegetables, juice, and salad (Buchanan et al., 2017; Je et al., 2024). *L. monocytogenes* is introduced into the digestive system along with these contaminated foods, where it encounters primary defense mechanisms in the human body: gastric acid and bile salts (Koopmans et al., 2023). These harsh conditions of the digestive system can structurally damage the bacterial surface, increasing surface irregularities and potentially causing dissolution during passage through the gastrointestinal tract (Zou et al., 2024). Bile hinders microbial growth, and its toxicity against bacteria leads to heightened DNA damage, formation of secondary RNA structures, and instability in cellular membranes (Dowd et al., 2011). However, some *L. monocytogenes* can overcome acidic and enzymatic stress through the glutamate decarboxylase system, acid tolerance response, bile acid deconjugation, and the upregulation of multidrug efflux pumps (Koopmans et al., 2023; Zou et al., 2024). The σ^B operon is also considered a critical genetic element in adapting to acidic stress and surviving in the gastrointestinal tract (Gahan and Hill, 2014; Guerreiro et al., 2022). *L. monocytogenes*, which survives the digestive process, reaches the intestine, where it adheres to or invades the intestinal epithelium, leading to infection in the host (Koopmans et al., 2023).

Gut microbiota, comprising Bacteroidota (formerly Bacteroidetes), Bacillota (formerly Firmicutes), Pseudomonadota (formerly Proteobacteria), and Actinomycetota (formerly Actinobacteria), colonize the human intestine and play a crucial role in maintaining homeostasis (Park and Im, 2020). They are resistant against pathogens by competing with limited resources, altering the gut environment, and secreting antimicrobial substances such as short-chain fatty acids (SCFAs) and bacteriocins (Kamada et al., 2013). Some *Bacteroides* and lactic acid bacteria exhibit direct colonization resistance and infection resistance against pathogens such as *Citrobacter rodentium*, *Escherichia coli*, *Clostridium difficile,* and *Salmonella* (Buffie and Pamer, 2013). SCFAs decrease pH-sensitive pathogens, such as *Enterobacteriaceae* and Clostridia, and reduce the pathogenicity of *Campylobacter jejuni* and *Staphylococcus aureus* (Alva-Murillo et al., 2012; Sittipo et al., 2019; Van Deun et al., 2008). Pathogens can also lead to the death of anaerobic microbes and modify the gut microbiota profile by inducing secretion of antibacterial compounds, such as reactive oxygen species and reactive nitrogen species (Bäumler and Sperandio, 2016; Rogers et al., 2021). These imbalances reduce the diversity of gut microbiota and metabolite production, which aid pathogens in evading the microbial defense mechanisms (Rogers et al., 2021).

Various studies have explored pathogenic susceptibility, survival rates, and dynamics of intestinal bacteria in animal models (Becattini et al., 2017; Las Heras et al., 2019; Wolter et al., 2021). However, significant biological differences in intestinal structures, immune systems, and particularly in gut microbiota profiles between animals and humans can lead to results that may not accurately reflect human conditions (Park and Im, 2020). An *in vitro* fecal fermentation model, which utilizes human fecal inoculation and maintains a stable gut microbiota composition over extended periods, offers a more relevant platform for studying bacteria-to-bacteria interactions between human gut microbiota and *L. monocytogenes* (Li et al., 2019). Additionally, *in vitro* studies offer several advantages, including speed, cost-effectiveness, reduced labor demands, the ability to process multiple samples simultaneously, and no ethical concerns (Li et al., 2019; Minekus et al., 2014).

The aim of this study was to investigate the host's defense strategy against *L. monocytogenes* and the modulation of the gut microbiota profile following listerial infection. The survival of *L. monocytogenes* during digestion was assessed *in vitro*, and the changes in gut microbiota and their metabolites induced by the pathogen were explored using a fecal fermentation model (Li et al., 2019; Minekus et al., 2014). Ultimately, understanding the interactions between *L. monocytogenes* and the gut microbiota is crucial for developing effective strategies to enhance the host's defense mechanisms. Insights from this study may enhance our understanding of the interactions between gut microbiota and *L. monocytogenes*, aiming to mitigate the impact of *L. monocytogenes* infection and thereby promoting overall gut health and food safety.

2 Materials and methods

2.1 Selection of *L. monocytogenes* strains and growth conditions

Five *L. monocytogenes* strains [*L. monocytogenes* F2365 (4b), ATCC 19111 (1/2a), ATCC 19113 (3a), ATCC 7644 (1/2c), and NCCP 14714 (1/2b)] were selected from the culture collection at the Food Safety Lab of Chungnam National University, South Korea. These strains were chosen to represent a diverse range of serotypes commonly associated with foodborne outbreaks and environmental isolates (Koopmans et al., 2023). All strains were stored at −80°C. For each experiment, the strains were incubated on brain heart infusion (BHI; Kisan Bio, Seoul, South Korea) agar at 37°C for 24 h. Subsequently, a single colony of each *L. monocytogenes* was inoculated into BHI broth and cultured overnight at 37°C. A pooled *L. monocytogenes* culture was prepared by combining equal proportions of each strain incubated in broth.

2.2 *In vitro* digestion model

The survival of *L. monocytogenes* during gastrointestinal transit was assessed using an *in vitro* digestion model, with modifications based on the protocol of Pettersen et al. (2019). The five *L. monocytogenes* strains described above were tested with pooled cocktail to represent the genetic and phenotypic diversity in nature and compared the result with each single-strain. Overnight cultures of *L. monocytogenes* strains were centrifuged, and the pellets were resuspended in 0.1% peptone water (Kisan Bio). The bacterial suspension was exposed to simulated gastric fluid (SGF) containing porcine pepsin (2,000 U/mL; Sigma-Aldrich, St. Louis, MO, United States) in a 1:1 ratio. The SGF composition included 6.9 mM KCl (Junsei, Tokyo, Japan), 0.9 mM KH_2PO_4 (Sigma-Aldrich), 25 mM

$NaHCO_3$ (Daejung, Siheung, South Korea), 47.2 mM NaCl (Daejung), 0.1 mM $MgCl_2{\cdot}7H_2O$ (Daejung), 0.5 mM $(NH_4)_2{\cdot}CO_3$ (Junsei), and 0.15 mM $CaCl_2{\cdot}2H_2O$ (Daejung). The pH was adjusted to either 2.0 or 5.5 using 1 M HCl (Daejung) to mimic fasted or fed states (AquaSearcher AB23PH; Ohaus Corporation, Parsippany, NJ, United States). The gastric mixtures were incubated at 37°C in a shaking water bath (Maxturdy-18, Daihan Scientific, South Korea) at 100 rpm for 40 min. For the intestinal phase, the gastric mixture was combined with a simulated intestinal fluid (SIF), supplemented with 10 mM bovine bile (Sigma-Aldrich), and 100 U/mL porcine pancreatin (Sigma-Aldrich) at a 1:1 ratio. The SIF composition included 6.8 mM KCl, 0.8 mM KH_2PO_4, 85 mM $NaHCO_3$, 38.4 mM NaCl, 0.33 mM $MgCl_2{\cdot}6H_2O$, and 0.6 mM $CaCl_2{\cdot}2H_2O$. The pH was adjusted to 7.0 using 1 M NaOH (Daejung) and incubated at 37°C in a shaking water bath at 100 rpm for 2 h. At each step, *L. monocytogenes* was enumerated by serial dilution in 0.1% peptone water and plating onto Oxford agar (Kisan Bio).

2.3 Fecal sample collection

Fecal samples (~5 g) were collected from three healthy donors using stool containers (SPL Life Sciences, Pocheon, South Korea). The samples were stored at 4°C and processed within 6 h. The donors were selected based on the absence of congenital or chronic diseases, no medication, and no antibiotic treatment within 4 weeks prior to collection. The ethical approval for fecal sample collection was obtained from the Institutional Review Board (IRB, 202209-BR-125-01).

2.4 *In vitro* fecal fermentation model

An *in vitro* fecal fermentation was conducted, based on Li et al. (2019) with slight modifications. Fresh fecal samples (2 g) were homogenized using a vortexer in 20 mL of sterile phosphate-buffered saline (PBS; Gibco BRL, Paisley, Scotland, UK) with 0.5% (w/v) L-cysteine hydrochloride (Junsei). The homogenized fecal mixture was filtered through sterile gauze. All experiments were conducted in a Coy Anaerobic Vinyl chamber (Coy Laboratory Product, MI, United States) under an anaerobic atmosphere (5% H_2, 5% CO_2, and 90% N_2) at 37°C.

MiPro medium was prepared with the following components: 2.0 g/L peptone water, 2.0 g/L yeast extract (Kisan Bio), 0.5 g/L L-cysteine hydrochloride, 2 mL/L Tween 80 (Daejung), 5 mg/L hemin bovine (Sigma-Aldrich), 10 µL/L vitamin K1 (Sigma-Aldrich), 0.4 g/L K_2HPO_4 (Sigma-Aldrich), 0.4 g/L KH_2PO_4, 0.1 g/L $MgSO_4{\cdot}7H_2O$, 0.1 g/L $CaCl_2{\cdot}2H_2O$, 4.0 g/L $NaHCO_3$, 4.0 g/L porcine gastric mucin (Sigma-Aldrich), and 0.5 g/L bile salts (Merck, Darmstadt, Germany) (Li et al., 2019). The sterile medium was placed in the anaerobic chamber a day prior to the experiment to ensure anaerobic conditions. Overnight cultures of *L. monocytogenes* were centrifuged and resuspended in fresh MiPro medium. The *L. monocytogenes* cocktail and the gut microbiota inocula were adjusted to reach approximately 8 log gene copies (GC)/mL. Fermentation was conducted in 96-deep well plates (Eppendorf, Hamburg, Germany) covered with silicone mats punctured for sampling, and incubated at 37°C. The samples were collected at 6 h, 12 h, and 24 h, and pH was measured at each time point. The survival of *L. monocytogenes* was verified by plating onto Oxford agar. The pellets were collected via centrifugation at 8,000 rpm for 10 min and stored at −80°C for subsequent analysis. The supernatants were filtered using a 0.22 µm syringe filter (13 mm; polytetrafluoroethylene) (Advantec, Tokyo, Japan) and stored at −80°C for SCFA analysis.

2.5 Quantitative PCR, and 16S rRNA amplicon sequencing

DNA was extracted using a NucleoSpin DNA Stool kit (Macherey-Nagel, Duren, Germany). Quantitative PCR (qPCR) was conducted on a CFX Connect Real-Time System (Bio-Rad, Hercules, CA, United States), using iQ SYBR-Green supermix (Bio-Rad) with 0.5 µM forward and reverse primers and template DNA. Universal primers targeting the 16S rRNA gene (forward: 5`-GTG STG CAY GGY YGT CGT CA-3`; reverse: 5`-ACG TCR TCC MCN CCT TCC TC-3`) were used following cycling conditions: 95°C for 3 min followed by 40 cycles of 95°C for 5 s, and 60°C for 30 s (Fuller et al., 2007; Reichardt et al., 2018). The 16S rRNA gene of *Bifidobacterium miconisargentati* 82T25 (accession ID: NR_181805.1, 148 bp) was used as the standard with concentrations ranging from 10^4 to 10^9 GC/ng (Macrogen Co. Ltd., Seoul, South Korea).

The 16S rRNA amplicon sequencing of the gut microbiota was conducted by Sanigen Co. Ltd. (Anyang, South Korea). In short, PCR was conducted with 341F and 806R primers to amplify the V3-V4 region of bacterial 16S rRNA genes. Then, the amplicon purification was carried out employing AMPure XP beads (Beckman Coulter, CA, United States). Library preparation for sequencing was carried out using the Nextera XT library prep kit (Illumina, San Diego, CA, United States). Sequencing was performed on the Illumina MiSeq platform (Illumina), generating 2 × 300 bp paired-end reads. Sequence processing, including trimming of low-quality reads, error correction of noisy reads, and elimination of chimeric sequences, was performed with Trimmomatic v0.39 (Bolger et al., 2014) and DADA2-QIIME2 (Callahan et al., 2016). Taxonomic classification was conducted using the SILVA 138 reference database (Quast et al., 2012), and diversity analyses were performed with QIIME2 (Bolyen et al., 2019). Metadata from this study is publicly available through the NCBI Sequence Read Archive under BioProject accession number PRJNA1254141, with associated BioSample accessions SAMN48096620 to SAMN48096647. To clearly understand the effects of *L. monocytogenes* infection, the OTU value of *L. monocytogenes* was excluded prior to analyzing diversity and profile abundance.

2.6 Quantitative analysis of SCFAs

Short-chain fatty acids concentrations in the fermentation supernatants were determined using the Nexera series high-performance liquid chromatography (HPLC) system (Shimadzu, Kyoto, Japan) installed with a RID-20A detector (Shimadzu) and an Aminex HPX-87H column (300 × 7.8 mm; Bio-Rad). The mobile phase consisted of 0.008 N sulfuric acid (Sigma-Aldrich), maintained at a constant flow rate of 0.6 mL/min at 35°C. Sample 20 µL was injected, and the analytes were detected over a 25 min run time. All samples were treated under the same conditions.

2.7 Statistical analysis

All experiments were conducted in triplicate to ensure data reproducibility and reliability. Statistical analysis was performed using one-way analysis of variance (ANOVA), followed by Tukey's multiple comparisons test. A p-value of <0.05 was considered statistically significant for all analyses.

3 Results

3.1 Survival of *L. monocytogenes* during digestion

Five individual *L. monocytogenes* strains and their cocktail were subjected to an *in vitro* digestion model. During the gastric phase at pH 2.0, the five individual strains exhibited an average reduction of 5.13 log CFU, while the pooled *L. monocytogenes* cocktail demonstrated a 3.49 log CFU reduction (Figure 1A). Log reduction rates varied across individual strains, ranging from 3.38 to 7.6. *L. monocytogenes* ATCC 7644 showed the highest reduction at 7.6 log, followed by ATCC 19111 with 5.71 log, F2365 with 5.02 log, ATCC 19113 with 3.96 log, and ATCC 14714 with 3.38 log reduction. In the gastric phase at pH 5.5, all strains showed no significant differences in survival (Figure 1B). In the subsequent intestinal phase, regardless of initial pH, survival of all strains remained consistent within a ± 1 log range, indicating stable resistance throughout this phase (Figure 1).

3.2 Survival of gut microbiota and *L. monocytogenes* during fecal fermentation

Gut microbiota in the *L. monocytogenes*-infected and non-infected samples reached 10.62 and 10.25 log GC/mL at 6 h, respectively (Supplementary Figure S1). The levels further increased to 11.39 and 11.46 log GC/mL at 12 h, then stabilized at 11.61 and 11.65 log GC/mL at 24 h. The *L. monocytogenes* cocktail, 7.34 log CFU/mL, increased to 8.58 log CFU/mL at 6 h, stabilized at 8.55 log CFU/mL at 12 h, and slightly declined to 8.17 log CFU/mL by 24 h. When cultured in MiPro medium alone, *L. monocytogenes* reached 8.41 log CFU/mL at 6 h, rose to 8.61 log CFU/mL at 12 h, and decreased slightly to 8.47 log CFU/mL by 24 h. Initial pH was 7.6, which decreased to 6.98 at 6 h, remained steady until 12 h, and then slightly increased to 7.2 by 24 h.

3.3 Dynamics of gut microbiota profile

At 0 h, the dominant phyla in fecal samples were Bacillota (51.98%), Bacteroidota (38.21%), Pseudomonadota (6.89%), and Fusobacteriota (0.11%) comprising over 95% of the microbial community (Figure 2). At 6 h, there was a significant shift in the microbial composition: Pseudomonadota and Fusobacteriota increased to 49.72 and 4.47%, respectively, while Bacteroidota and Bacillota decreased to 28.43 and 16.46%, respectively. Pseudomonadota reduced by 22.12% at 12 h and by 16.40% at 24 h, while Bacteroidota and Bacillota recovered to 35.90 and 25.26% at 12 h, respectively, with further stabilization at 24 h. Fusobacteriota increased to 15.39% at 12 h and remained relatively stable at 12.66% at 24 h. Notably, the abundance of Fusobacteriota in single feces 3 (SF3) decreased to below 0.05% after 12 h.

Alpha and beta diversity analyses indicated that infection with *L. monocytogenes* reduced richness while increased evenness, though the changes were not statistically significant (Figures 3A,B). The diversity was significantly decreased at 6 h, recovered at 12 h, with richness and evenness continuing to increase through 24 h (Figures 3C,D). Weighted distance analysis displayed clustering differences based on infection conditions, with incubation time exerting a stronger influence on cluster patterns (Figure 3E). Notably, 0 h samples were distinct from latter time points, while 12 h and 24 h samples exhibited greater

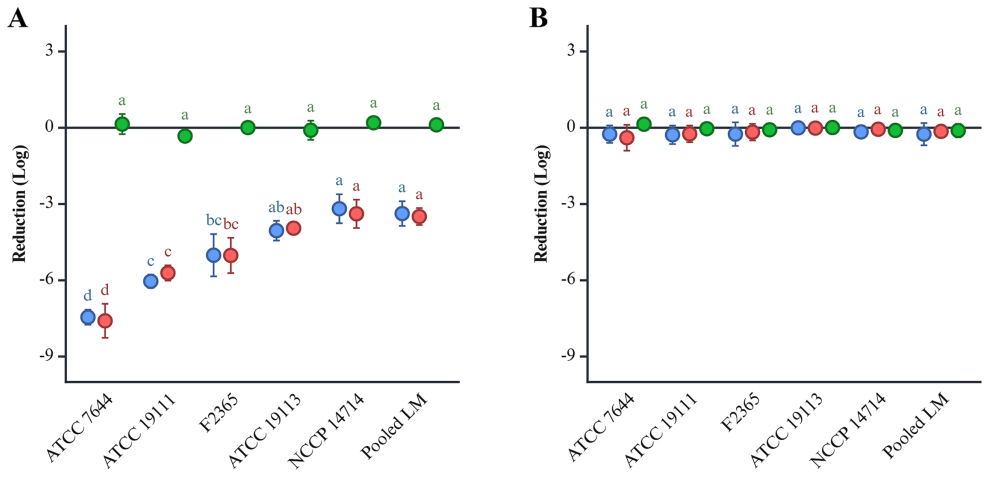

FIGURE 1
The reduction of *L. monocytogenes* at pH 2.0 **(A)** and 5.5 **(B)** during *in vitro* gastric digestion. *L. monocytogenes* was inoculated at a final concentration of 9 log CFU/mL. Gastric and intestinal digestions are indicated in red and green, respectively. The overall reduction is shown in blue. Significant differences ($p < 0.05$) are indicated by alphabets.

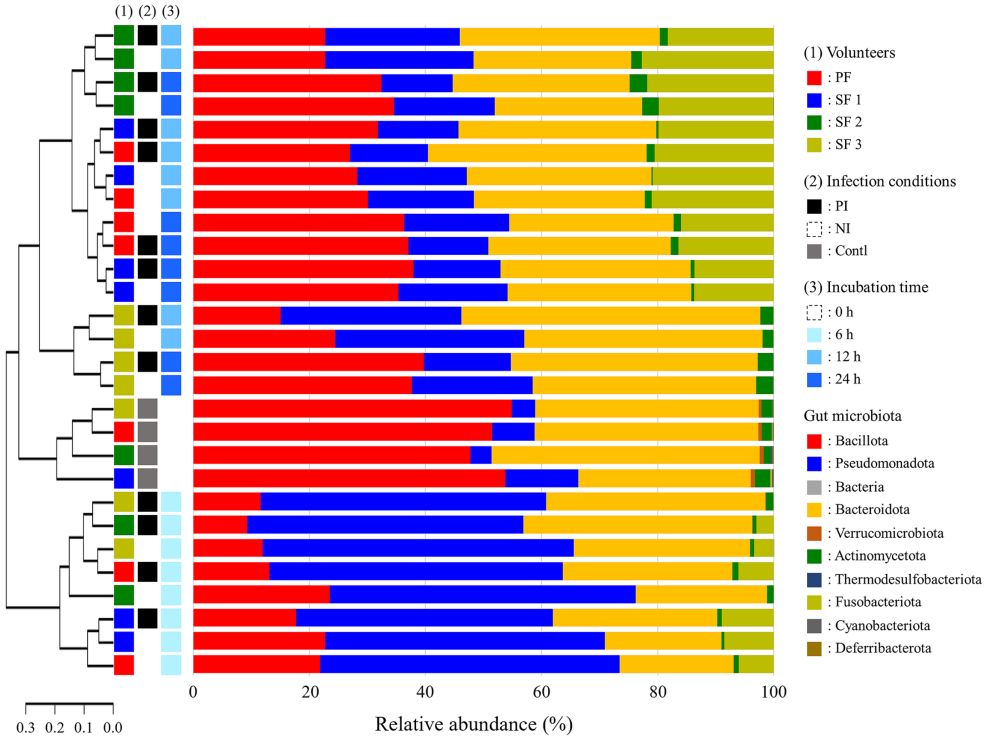

FIGURE 2
Phylogenetic tree and relative abundance of gut microbiota at the phylum level after *L. monocytogenes* infection during fecal fermentation, categorized by (1) volunteers, (2) *in vitro* infection conditions, and (3) incubation time. The phylogenetic analysis was performed using weighted distance values of gut microbiota. PF, pooled feces; SF, single feces; PI, post-infected; NI, non-infected; Contl, control.

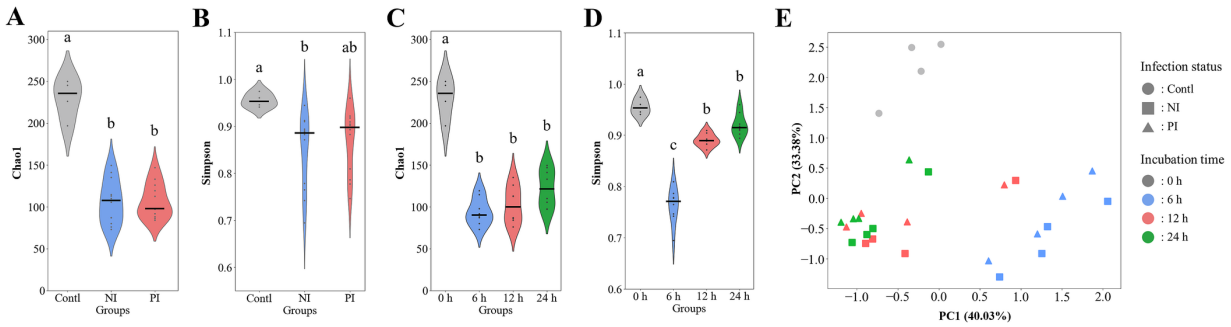

FIGURE 3
Violin plots and principal coordinate analysis (PCA) comparing the alpha and beta diversity of gut microbiota during fecal fermentation based on infection status **(A,B)** and incubation time **(C,D)**. The plots include the species richness as measured by the chao1 index **(A,C)** as well as the species evenness as measured by the Simpson diversity index **(B,D)**. PCA is presented by weighted Bray–Curtis distances **(E)**. Significant differences ($p < 0.05$) are indicated by alphabets. Contl, control; NI, non-infected; PI, post-infected.

proximity, clustering more closely together, which aligns with phylogenetic results (Figure 2).

3.4 Gut microbiota profile in the phylum, family, and genus level

Pseudomonadota was more dominant in the non-infected (NI) group (18.77 ~ 51.54%) than post-infected (PI) groups (14.03 ~ 47.90%), while Bacteroidota was more abundant in PI (33.69 ~ 39.43%) compared to NI (23.17 ~ 32.37%) groups (Figure 4). This pattern remained consistent across all fecal samples and time points. Bacillota showed higher levels in NI (20.00%) than PI (12.93%) at 6 h, with similar levels thereafter. *L. monocytogenes* infection delayed the recovery of Bacillota at 6 h in the pooled feces (PF) group and SF1 and 2 groups and 12 h in the SF3 group (data not shown). At the family level, PI groups consistently exhibited lower *Erysipelotrichaceae* but higher *Bacteroidaceae*, *Lachnospiraceae*, and *Bifidobacteriaceae* abundances than NI at all time points (Supplementary Figure S2). Notably, both *Bacteroidaceae* and

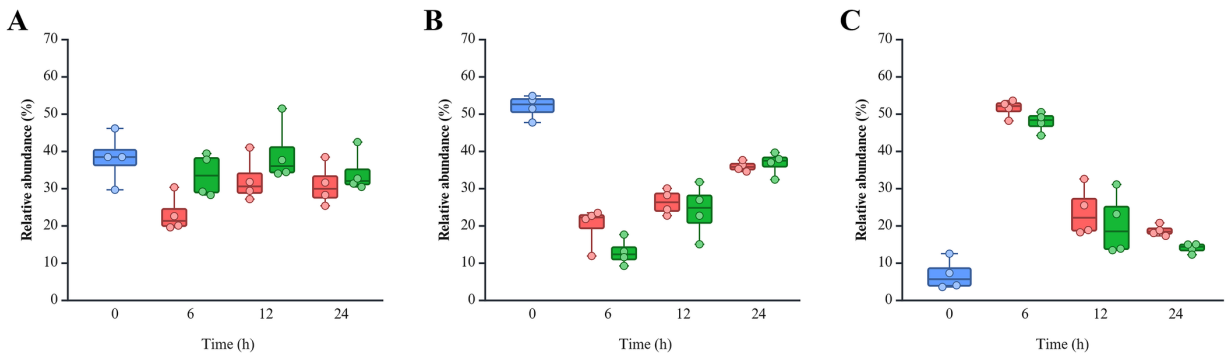

FIGURE 4
Relative abundance of three phyla of interest: **(A)** Bacteroidota, **(B)** Bacillota, and **(C)** Pseudomonadota. The color of each bar chart represents different infection conditions: control (blue), non-infected (red), and post-infected (green). Each dot represents the value for each sample.

Lachnospiraceae showed a marked increase in response to *L. monocytogenes* infection across all fecal groups (data not shown). Eight genera within these families exhibited abundance patterns consistent with trends observed at the family level (Figure 5). *Bacteroides* (*Bacteroidaceae*) and *Bifidobacterium* (*Bifidobacteriaceae*) were more abundant in PI (30.55 ~ 34.90% and 0.10 ~ 0.74%) than NI (20.80 ~ 28.74% and 0.12 ~ 0.61%). *Faecalitalea*, belonging to *Erysipelotrichaceae*, was more prevalent in NI (7.77 ~ 12.72%) than PI (4.12 ~ 11.19%). *Blautia* and *Mediterraneibacter gnavus* group of *Lachnospiraceae* exhibited higher abundances in PI (0.14 ~ 1.17% and 1.04 ~ 3.41%) than NI (0.14 ~ 0.94% and 0.83 ~ 3.32%).

3.5 Changes in SCFAs and ethanol

Acetate and propionate concentrations were comparable between the NI and PI groups, with acetate ranging from 0 to 30.14 mM in NI and 0 to 30.47 mM in PI, and propionate ranging from 0 to 11.74 mM in NI and 0 to 11.88 mM in PI (Figure 6). Butyrate levels were slightly higher in NI (0 ~ 15.55 mM) compared to PI (0 ~ 14.87 mM). In contrast, ethanol production was elevated in the PI group, ranging from 39.07 to 63.82 mM, compared to 27.78 to 55.13 mM in the NI group. Over time, the concentration of both SCFAs and ethanol increased progressively throughout the incubation period.

4 Discussion

Listeria monocytogenes is a significant public health and food safety concern because of its virulence and resistance against various environmental stresses (Muchaamba et al., 2022). Its infectious dose can be influenced by the human innate immune system, which plays a crucial role in determining the severity of infection (Guo et al., 2023; Koopmans et al., 2023). During the gastrointestinal passage, *L. monocytogenes* must endure the stressful environment, with its survival capability varying by strain, isolate origin, and serotype (Ramalheira et al., 2010; Zou et al., 2024). Survived *L. monocytogenes* that bypass host's defense systems must encounter gut microbiota, which competes for energy sources and secretes antibacterial compounds (Kamada et al., 2013). In immunocompromised individuals, *L. monocytogenes* can establish prolonged colonization in the cecum and colon, thereby altering the gut microbiota profile (Koopmans et al., 2023). Although several studies have explored the changes in gut microbiota due to *L. monocytogenes* infection, specific interactions between bacteria remain poorly understood (Becattini et al., 2017; Guo et al., 2023; Wolter et al., 2021). In this study, we aimed to investigate the survival of *L. monocytogenes* during digestion, assess its pathogenic risk, and determine its impact on gut microbiota and metabolite profiles.

Among the 14 serotypes of *L. monocytogenes*, 92 ~ 95% of the clinical isolates belong to serotypes 4b, 1/2a, and 1/2b (Koopmans et al., 2023). Serotypes 4b and 1/2a exhibit higher resistance to environmental stresses, including acidity, than serotypes 4a and 1/2c (Chakravarty et al., 2021; Jiang et al., 2010; Zou et al., 2024). Additionally, clinical isolates exhibited greater resistance to acidic and bile stresses compared to food isolates (Ramalheira et al., 2010). *L. monocytogenes* F2365 (serotype 4b) and NCCP 14714 (serotype 1/2b) were clinical isolates, while ATCC 7644 (serotype 1/2c) was isolated from food (Koopmans et al., 2023). *L. monocytogenes* F2365 and NCCP 14714 showed significantly higher resistance in the simulated gastric phase (pH 2.0) than ATCC 7644. Acidic stress adaption is regulated by the stress response factor σ^B, encoded by the *rsbRSTUVWX* and *sigB* genes (Gahan and Hill, 2014; Guerreiro et al., 2022). The *rsbS* gene plays a critical role in stress signaling, as it mediates the phosphorylation and activation of the stressosome (Guerreiro et al., 2022). Notably, a *ΔrsbS* mutant strain exhibited reduced acid tolerance, falling below detection limits after just 15 min of exposure to pH 5.0 (Guerreiro et al., 2022). *L. monocytogenes* ATCC 7644 has an adenine deletion in the *rsbS* gene with a premature stop codon, resulting in reduced survival under acidic conditions. This characteristic suggests the need for further research to explore the mechanisms underlying this phenomenon. Previous studies have documented the presence of multiple *L. monocytogenes* strains in a single food sample, as well as multi-strain involvement in listeriosis outbreaks (Zilelidou and Skandamis, 2018). In addition to the individual strains, a five-strain cocktail was evaluated to reflect potential real-world contamination scenarios involving multiple serotypes. The cocktail exhibited greater resistance than the more acid-sensitive individual strains, such as ATCC 7644, but showed lower resistance than F2365 and NCCP 14714. Although inter-strain interactions among *L. monocytogenes*, such as quorum sensing, bacteriocin production, or biofilm cooperation, may enhance

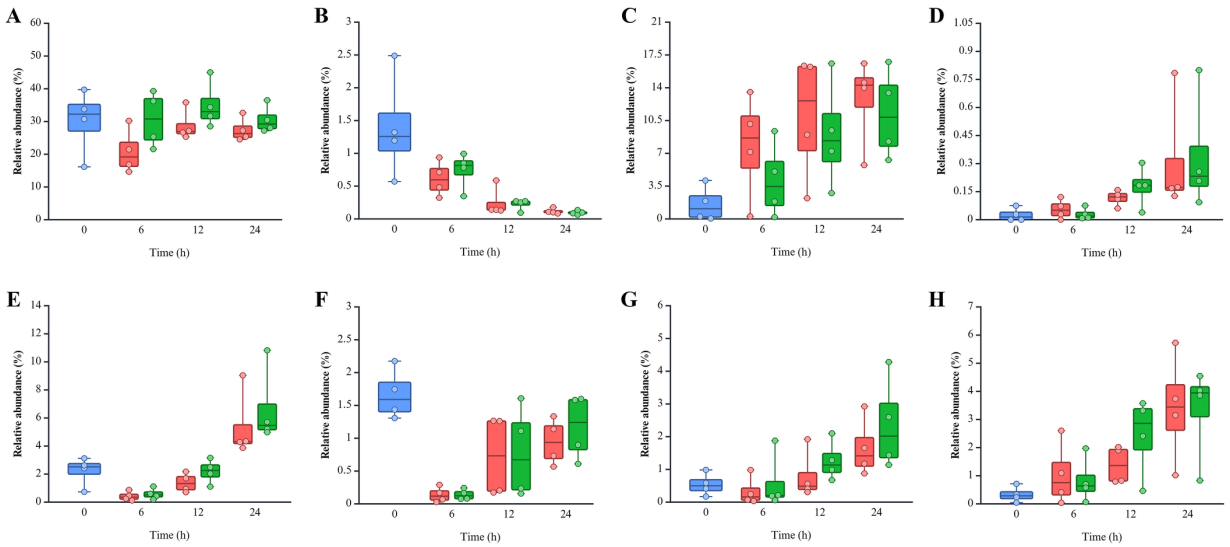

FIGURE 5
Relative abundance of eight genera belonging to *Bacteroidaceae*, *Bifidobacteriaceae*, *Erysipelotrichaceae*, and *Lachnospiraceae*: **(A)** *Bacteroides*, **(B)** *Bifidobacterium*, **(C)** *Faecalitalea*, **(D)** *Clostridium innocuum* group, **(E)** *Lachnoclostridium*, **(F)** *Blautia*, **(G)** *Ruminococcus torques* group, and **(H)** *Mediterraneibacter gnavus* group. The color of each bar chart represents different infection conditions: control (blue), non-infected (red), and post-infected (green). Each dot represents the value for each sample.

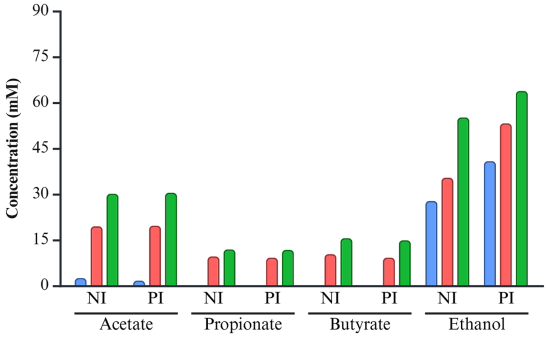

FIGURE 6
The concentration of short-chain fatty acids and ethanol of *L. monocytogenes* infected and non-infected pooled fecal samples during fermentation. The color of each bar chart represents the different incubation times: 6 h (blue), 12 h (red), and 24 h (green). NI, non-infected; PI, post-infected.

virulence or survival, the overall survival observed in the cocktail can be attributed primarily to the intrinsic resistance of the more tolerant strains (Zilelidou and Skandamis, 2018).

The human colon contains nearly 11 to 12 log CFU/g of bacteria, comprising 500 to 1,000 species (Rizzatti et al., 2017). Factors such as diet, illness, and antibiotic treatment can significantly impact microbial diversity and often result in gut dysbiosis (Rogers et al., 2021). In the present work, alpha and beta diversity of the gut microbiota showed three distinct phases regardless of infection status. A significant decline in the diversity was observed within the first 6 h, followed by a gradual recovery, highlighting a rebalance within the microbial ecosystem and the resilience of the gut microbiota after exposure to stress. A decline can be attributed to dysbiosis induced by the initial fecal processing step, resulting in unfavorable conditions (Rogers et al., 2021). Pseudomonadota decreased over time, which includes various human pathogens, such as *Shigella*, *Escherichia*, *Salmonella*, *Yersinia*, and *Helicobacter* (Rizzatti et al., 2017). Conversely, Fusobacteriota showed a continuous increase, suggesting that the gut microbiota had reached an alternate stable state which was different from its baseline status.

Gut dysbiosis can increase susceptibility to *L. monocytogenes* infection. Once established, listerial infections may exacerbate the condition by further disrupting the microbial community structure (Bäumler and Sperandio, 2016; Becattini et al., 2017). In C57BL/6 mice, *L. monocytogenes* significantly decreased Chao1 and Shannon indices, indicating a reduction in microbial diversity (Alam et al., 2021; Keane et al., 2023). Similarly, a decrease in evenness was found in the macaque monkey, although the difference was insignificant (Hugon et al., 2023). In this study, *L. monocytogenes* infection resulted in decreased richness and increased evenness, consistent with a reduction in specific taxa and the reorganization of community structure. Furthermore, PCA analysis of weighted distances also revealed distinct clustering between non-infected and infected groups, highlighting differences in the microbial community composition. The observed differences in gut microbiota diversity can be, in part, attributed to bacteriocins produced by *L. monocytogenes*, such as listeriolysin S (LLS) and Lmo2776 (Lee, 2020). *L. monocytogenes* ATCC 7644 and F2365 have the Lmo2776 synthesis operon and Lmo2776 expressed under *in vitro* conditions (Rolhion et al., 2019). Lmo2776 specifically targeted *Prevotella* spp. and *Segatella copri* (formerly *Prevotella copri*) (Rolhion et al., 2019). *L. monocytogenes* NCCP 14714 and F2365 contain the LLS synthesis cluster. LLS is expressed in gastrointestinal tracts *in vivo* and decreases the abundance of *Allobaculum* and *Alloprevotella* in mice (Quereda et al., 2016; Quereda et al., 2017). The antimicrobial activities of these *L. monocytogenes*-derived bacteriocins may suppress the richness of specific microbial taxa. Conversely, the absence of such bacteriocins

could facilitate the proliferation of other microbial species by relieving competitive pressures within the gut environment.

In this study, *L. monocytogenes* infection led to a decrease in Bacillota, while Bacteroidota was increased, consistent with the findings from the BALB/c mice study by Guo et al. (2023), though opposite results were reported in C57BL/6 mice model (Alam et al., 2021). Bacteroidota has been linked to inflammation, suggesting that *L. monocytogenes* can modulate inflammation by altering the gut microbial composition (Guo et al., 2023; Rogers et al., 2021). The reduction and delayed recovery of Bacillota may weaken gut barrier function and impair immune regulation, heightening susceptibility to pathogens and promoting inflammation (Rogers et al., 2021). *L. monocytogenes* infection led to an increase in Pseudomonadota in the BALB/c mice, which contradicts the findings of this study (Guo et al., 2023). Elevated levels of Pseudomonadota was reported in pregnant individuals, who are at the highest risk for listeriosis (Becattini et al., 2017; Koopmans et al., 2023). However, little research has been conducted on the specific relationship between Pseudomonadota and *L. monocytogenes*.

Several bacterial groups known for their protective roles against intestinal pathogens showed increased abundance following *L. monocytogenes* infection in this study. *Bacteroides* spp. contribute to intestinal homeostasis by degrading mucin and supporting nutrient availability for other microbes (Zafar and Saier Jr, 2021). They also interact with the host immune system and compete with pathogens (Wexler, 2007; Zafar and Saier Jr, 2021). In murine models, *L. monocytogenes* infection altered *Bacteroides* populations: *B. caccae* increased while *B. ovatus* decreased in BALB/c mice, and in C57BL/6 mice, *B. uniformis* and *Bacteroidaceae* decreased while *B. acidifaciens* increased (Alam et al., 2021; Guo et al., 2023; Las Heras et al., 2019; Wolter et al., 2021). The observed increase in *Bacteroides* may have contributed to the reduction of Pseudomonadota in our study, potentially through colonization resistance mechanisms. In particular, *B. thetaiotaomicron* has been shown to directly inhibit the colonization of *E. coli* and *Salmonella*, both members of Pseudomonadota, supporting the proposed role of *Bacteroides* in colonization resistance (Buffie and Pamer, 2013). *Bifidobacterium* spp. also play a well-established role in inhibiting pathogen colonization. They improve host outcomes in infections by *E. coli* O157: H7 and *Clostridium perfringens*, and can inhibit *L. monocytogenes* EGDe invasion by 60–90% through secreted proteinaceous factors (Corr et al., 2007; O'Callaghan and Van Sinderen, 2016). The increased abundance of *Bifidobacterium* following listerial infection may be related to *L. monocytogenes* mitigating oxidative stress on *B. bifidum* through neutralization of reactive oxygen species (Yu et al., 2020). *Lachnospiraceae*, also known as *Clostridium* cluster XIVa, are fiber-degrading bacteria that produce SCFAs and help maintain gut barrier function (Vacca et al., 2020). Within this family, *Blautia producta* has demonstrated anti-listerial activity by inhibiting *L. monocytogenes* propagation (Becattini et al., 2017). Increased abundance of *Lachnospiraceae* has been observed in infected C57BL/6 mice fed a high-fat diet and in aged C57BL/6 mice (Alam et al., 2021; Las Heras et al., 2019), and a positive correlation ($\rho = 0.33$) was reported between *Lachnospiraceae* and *L. monocytogenes* abundance in human listeriosis patients (Hafner et al., 2021). These findings align with our observation of elevated *Lachnospiraceae* following infection. The increased abundance of *Bacteroides*, *Bifidobacterium*, and *Lachnospiraceae*, which are known to protect against *L. monocytogenes*, following infection may reflect an intrinsic compensatory mechanism of the human gut microbiota to restore microbial balance in response to pathogenic challenge (Becattini et al., 2017; Buffie and Pamer, 2013; Corr et al., 2007). This observation supports the hypothesis that individuals with a diverse and resilient gut microbiota are better protected against listeriosis (Guo et al., 2023; Hafner et al., 2021; Wolter et al., 2021).

The direct impact of SCFA on *L. monocytogenes* has been unknown, however, SCFAs can regulate the host's immune system and enhance gut barrier function by strengthening tight junctions (Becattini et al., 2017; Rogers et al., 2021). Acetate and propionate exhibited a synergistic effect with nisin, produced by *Lactococcus lactis*, potentially contributing to shifts in the bacterial profile (Rodpan et al., 2022). SCFAs produced by beneficial microbes such as *Bifidobacterium* could lower intestinal pH, thereby creating an unfavorable environment for opportunistic pathogens (O'Callaghan and Van Sinderen, 2016). The pH in this study decreased to 6.98 due to the buffering capacity of MiPro medium, limiting the ability to assess microbial changes directly related to pH fluctuations.

Acetate, propionate, and butyrate are detected in the human colon and stool at a 3:1:1 ratio, with total SCFA concentrations ranging from 20 to 70 mM in the distal colon (Den Besten et al., 2013). Comparable levels were observed in this study, with ~30.14 mM acetate, ~11.88 mM propionate, and ~15.55 mM butyrate. Although aformentioned bacteria such as *Bacteroides*, *Bifidobacterium*, and *Lachnospiraceae* are known contributors to SCFA production, no significant differences in SCFA levels were observed between infected and non-infected groups (O'Callaghan and Van Sinderen, 2016; Vacca et al., 2020). *Listeria* infection increased ethanol levels, a primary metabolite associated with bacteria such as *B. thetaiotaomicron*, *Bifidobacterium*, and *M. gnavus* group (Crost et al., 2018; Elshaghabee et al., 2016; Yamaguchi et al., 2018). Although many gut microbiota are capable of producing ethanol, its elevated levels during the infected state are linked to an increased abundance of these bacteria. Ethanol can disrupt epithelial cells and weaken tight junctions. This "leaky gut" condition allows harmful substances, such as endotoxins, to penetrate the bloodstream, triggering systemic inflammation and potentially exacerbating *Listeria* infection (Chen et al., 2022). Since most gut microbiota cannot metabolize ethanol, it is predominantly converted to acetate through host metabolic pathways (Martino et al., 2022). Ethanol consumption increases Bacteroidetes more through elevated acetate levels, an ethanol metabolite, than through ethanol itself (Martino et al., 2022). As this *in vitro* model excludes host interactions, predicting acetate accumulation from ethanol metabolism and its impact on the gut microbiota remains challenging. Therefore, the observed increase in Bacteroidetes cannot be solely attributed to ethanol.

This study highlights the intricate interactions between *L. monocytogenes* and the gut microbiota, emphasizing the pathogen's ability to survive and adapt within the gastrointestinal environment. Our study demonstrates that clinical *L. monocytogenes* strains exhibit greater resistance to the human digestive process than food-derived strains. *L. monocytogenes* was observed to cause minimal to no significant changes in the gut microbiota diversity, consistent with previous studies (Becattini et al., 2017; Hugon et al.,

2023; Keane et al., 2023; Las Heras et al., 2019; Li et al., 2019). Hugon et al. (2023) reported that *L. monocytogenes* alone did not induce dysbiosis; however, listeriosis may contribute to gut microbiota alterations under specific conditions, such as pregnancy. Comparative studies using macaque monkeys, BALB/c mice, and C57BL/6 mice have reported varying results, highlighting discrepancies between animal models and human microbiome data (Alam et al., 2021; Guo et al., 2023; Hafner et al., 2021; Hugon et al., 2023). These differences may stem from defense mechanisms against pathogens and variations in the host's immune system. The administration of *Akkermansia muciniphila* to mice has been shown to decrease susceptibility to *L. monocytogenes* (Keane et al., 2023). This protective effect was not directly attributed to changes in gut microbiota composition or the bacterium itself but rather through interactions with the host's immune system, indicating that the inhibition of *L. monocytogenes* by gut microbiota may be more intricate than previously understood (Keane et al., 2023). LLS expressed by *L. monocytogenes* has been found to have no effect on human eukaryotic cells but exhibits antimicrobial activity against prokaryotes, suggesting that *Listeria* can directly influence gut microbiota composition (Quereda et al., 2017). This study primarily focused on the interplay between human gut microbiota and *Listeria* and did not account for the potential involvement of the immune system. The findings provide valuable insights into understanding complex mechanisms underlying gut microbiota-pathogen interactions. Notably, *Listeria* infection was associated with an increased abundance of bacteria such as *Bacteroides*, *Bifidobacterium*, and the *M. gnavus* group, which are known ethanol producers. Elevated ethanol levels may compromise epithelial barrier integrity to a leaky gut that facilitates the translocation of harmful substances, exacerbates inflammatory responses, and further complicates conditions like listeriosis. Although ethanol has not been previously recognized as a metabolic biomarker in *Listeria* infection studies, the unexpected increase observed in this study highlights the need for further investigation into its role in gut function and host health. Due to the use of pooled samples, correlation analyses between specific taxa and ethanol production were not feasible, limiting direct functional inference. Future studies with larger sample sizes and individual-level measurements will be required to validate these observations.

Data availability statement

The datasets presented in this study can be found in online repositories. The names of the repository/repositories and accession number(s) can be found: https://www.ncbi.nlm.nih.gov/, PRJNA1254141.

Ethics statement

The studies involving humans were approved by Chungnam National University Institutional Review Board. The studies were conducted in accordance with the local legislation and institutional requirements. The participants provided their written informed consent to participate in this study.

Author contributions

DK: Data curation, Visualization, Validation, Investigation, Writing – review & editing, Formal analysis, Writing – original draft. SS: Writing – review & editing, Investigation, Validation. UK: Writing – review & editing, Investigation. SA: Writing – review & editing, Investigation. HJ: Writing – review & editing. DL: Validation, Investigation, Writing – review & editing. EY: Methodology, Supervision, Resources, Writing – review & editing. OK: Supervision, Conceptualization, Writing – review & editing, Resources, Project administration, Funding acquisition.

Funding

The author(s) declare that financial support was received for the research and/or publication of this article. This research was supported by the National Research Foundation of Korea (RS-2023-00242749 and RS-2024-00396978).

Conflict of interest

The authors declare that the research was conducted in the absence of any commercial or financial relationships that could be construed as a potential conflict of interest.

Generative AI statement

The authors declare that no Gen AI was used in the creation of this manuscript.

Publisher's note

All claims expressed in this article are solely those of the authors and do not necessarily represent those of their affiliated organizations, or those of the publisher, the editors and the reviewers. Any product that may be evaluated in this article, or claim that may be made by its manufacturer, is not guaranteed or endorsed by the publisher.

Supplementary material

The Supplementary material for this article can be found online at: https://www.frontiersin.org/articles/10.3389/fmicb.2025.1616720/full#supplementary-material

References

Alam, M. S., Gangiredla, J., Hasan, N. A., Barnaba, T., and Tartera, C. (2021). Aging-induced dysbiosis of gut microbiota as a risk factor for increased *Listeria monocytogenes* infection. *Front. Immunol.* 12:672353. doi: 10.3389/fimmu.2021.672353

Alva-Murillo, N., Ochoa-Zarzosa, A., and López-Meza, J. E. (2012). Short chain fatty acids (propionic and hexanoic) decrease *Staphylococcus aureus* internalization into bovine mammary epithelial cells and modulate antimicrobial peptide expression. *Vet. Microbiol.* 155, 324–331. doi: 10.1016/j.vetmic.2011.08.025

Bäumler, A. J., and Sperandio, V. (2016). Interactions between the microbiota and pathogenic bacteria in the gut. *Nature* 535, 85–93. doi: 10.1038/nature18849

Becattini, S., Littmann, E. R., Carter, R. A., Kim, S. G., Morjaria, S. M., Ling, L., et al. (2017). Commensal microbes provide first line defense against *Listeria monocytogenes* infection. *J. Exp. Med.* 214, 1973–1989. doi: 10.1084/jem.20170495

Bolger, A. M., Lohse, M., and Usadel, B. (2014). Trimmomatic: a flexible trimmer for Illumina sequence data. *Bioinformatics* 30, 2114–2120. doi: 10.1093/bioinformatics/btu170

Bolyen, E., Rideout, J. R., Dillon, M. R., Bokulich, N. A., Abnet, C. C., Al-Ghalith, G. A., et al. (2019). Reproducible, interactive, scalable and extensible microbiome data science using QIIME 2. *Nat. Biotechnol.* 37, 852–857. doi: 10.1038/s41587-019-0209-9

Buchanan, R. L., Gorris, L. G., Hayman, M. M., Jackson, T. C., and Whiting, R. C. (2017). A review of *Listeria monocytogenes*: an update on outbreaks, virulence, dose-response, ecology, and risk assessments. *Food Control* 75, 1–13. doi: 10.1016/j.foodcont.2016.12.016

Buffie, C. G., and Pamer, E. G. (2013). Microbiota-mediated colonization resistance against intestinal pathogens. *Nat. Rev. Immunol.* 13, 790–801. doi: 10.1038/nri3535

Callahan, B. J., McMurdie, P. J., Rosen, M. J., Han, A. W., Johnson, A. J. A., and Holmes, S. P. (2016). DADA2: high-resolution sample inference from Illumina amplicon data. *Nat. Methods* 13, 581–583. doi: 10.1038/nMeth.3869

Centers for Disease Control and Prevention. (2024). *Listeria* infection (listeriosis). Available online at: https://www.cdc.gov/ (accessed April 10, 2025)

Chakravarty, D., Sahukhal, G., Arick, M., Davis, M. L., and Donaldson, J. R. (2021). Transcriptomic analysis of *Listeria monocytogenes* in response to bile under aerobic and anaerobic conditions. *Front. Microbiol.* 12:754748. doi: 10.3389/fmicb.2021.754748

Chen, G., Shi, F., Yin, W., Guo, Y., Liu, A., Shuai, J., et al. (2022). Gut microbiota dysbiosis: the potential mechanisms by which alcohol disrupts gut and brain functions. *Front. Microbiol.* 13:916765. doi: 10.3389/fmicb.2022.916765

Corr, S. C., Gahan, C. G., and Hill, C. (2007). Impact of selected *Lactobacillus* and *Bifidobacterium* species on *Listeria monocytogenes* infection and the mucosal immune response. *FEMS Immunol. Med. Microbiol.* 50, 380–388. doi: 10.1111/j.1574-695X.2007.00264.x

Crost, E. H., Le Gall, G., Laverde-Gomez, J. A., Mukhopadhya, I., Flint, H. J., and Juge, N. (2018). Mechanistic insights into the cross-feeding of *Ruminococcus gnavus* and *Ruminococcus bromii* on host and dietary carbohydrates. *Front. Microbiol.* 9:2558. doi: 10.3389/fmicb.2018.02558

Den Besten, G., Van Eunen, K., Groen, A. K., Venema, K., Reijngoud, D. J., and Bakker, B. M. (2013). The role of short-chain fatty acids in the interplay between diet, gut microbiota, and host energy metabolism. *J. Lipid Res.* 54, 2325–2340. doi: 10.1194/jlr.R036012

Dowd, G. C., Joyce, S. A., Hill, C., and Gahan, C. G. (2011). Investigation of the mechanisms by which *Listeria monocytogenes* grows in porcine gallbladder bile. *Infect. Immun.* 79, 369–379. doi: 10.1128/IAI.00330-10

Elshaghabee, F. M., Bockelmann, W., Meske, D., De Vrese, M., Walte, H. G., Schrezenmeir, J., et al. (2016). Ethanol production by selected intestinal microorganisms and lactic acid bacteria growing under different nutritional conditions. *Front. Microbiol.* 7:47. doi: 10.3389/fmicb.2016.00047

Fuller, Z., Louis, P., Mihajlovski, A., Rungapamestry, V., Ratcliffe, B., and Duncan, A. J. (2007). Influence of cabbage processing methods and prebiotic manipulationof colonic microflora on glucosinolate breakdown in man. *Br. J. Nutr.* 98, 364–372. doi: 10.1017/S0007114507709091

Gahan, C. G., and Hill, C. (2014). *Listeria monocytogenes*: survival and adaptation in the gastrointestinal tract. *Front. Cell. Infect. Microbiol.* 4:9. doi: 10.3389/fcimb.2014.00009

Guerreiro, D. N., Pucciarelli, M. G., Tiensuu, T., Gudynaite, D., Boyd, A., Johansson, J., et al. (2022). Acid stress signals are integrated into the σ^B-dependent general stress response pathway via the stressosome in the food-borne pathogen *Listeria monocytogenes*. *PLoS Pathog.* 18:e1010213. doi: 10.1371/journal.ppat.1010213

Guo, L., Yin, X., and Liu, Q. (2023). Fecal microbiota transplantation reduces mouse mortality from *Listeria monocytogenes* infection. *Microb. Pathog.* 178:106036. doi: 10.1016/j.micpath.2023.106036

Hafner, L., Pichon, M., Burucoa, C., Nusser, S. H., Moura, A., Garcia-Garcera, M., et al. (2021). *Listeria monocytogenes* faecal carriage is common and depends on the gut microbiota. *Nat. Commun.* 12:6826. doi: 10.1038/s41467-021-27069-y

Hugon, A. M., Deblois, C. L., Simmons, H. A., Mejia, A., Schotzo, M. L., Czuprynski, C. J., et al. (2023). *Listeria monocytogenes* infection in pregnant macaques alters the maternal gut microbiome. *Biol. Reprod.* 109, 618–634. doi: 10.1093/biolre/ioad104

Je, H. J., Kim, U. I., and Koo, O. K. (2024). A comprehensive systematic review and meta-analysis of *Listeria monocytogenes* prevalence in food products in South Korea. *Int. J. Food Microbiol.* 415:110655. doi: 10.1016/j.ijfoodmicro.2024.110655

Jiang, L., Olesen, I., Andersen, T., Fang, W., and Jespersen, L. (2010). Survival of *Listeria monocytogenes* in simulated gastrointestinal system and transcriptional profiling of stress- and adhesion-related genes. *Foodborne Pathog. Dis.* 7, 267–274. doi: 10.1089/fpd.2009.0361

Kamada, N., Chen, G. Y., Inohara, N., and Núñez, G. (2013). Control of pathogens and pathobionts by the gut microbiota. *Nat. Immunol.* 14, 685–690. doi: 10.1038/ni.2608

Keane, J. M., Las Heras, V., Pinheiro, J., FitzGerald, J. A., Núñez-Sánchez, M. A., Hueston, C. M., et al. (2023). *Akkermansia muciniphila* reduces susceptibility to *Listeria monocytogenes* infection in mice fed a high-fat diet. *Gut Microbes* 15:2229948. doi: 10.1080/19490976.2023.2229948

Koopmans, M. M., Brouwer, M. C., Vázquez-Boland, J. A., and van de Beek, D. (2023). Human listeriosis. *Clin. Microbiol. Rev.* 36, e0006019–e0000019. doi: 10.1128/cmr.00060-19

Las Heras, V., Clooney, A. G., Ryan, F. J., Cabrera-Rubio, R., Casey, P. G., Hueston, C. M., et al. (2019). Short-term consumption of a high-fat diet increases host susceptibility to *Listeria monocytogenes* infection. *Microbiome* 7, 7–12. doi: 10.1186/s40168-019-0621-x

Lee, S. (2020). Bacteriocins of *Listeria monocytogenes* and their potential as a virulence factor. *Toxins* 12:103. doi: 10.3390/toxins12020103

Li, L., Abou-Samra, E., Ning, Z., Zhang, X., Mayne, J., Wang, J., et al. (2019). An *in vitro* model maintaining taxon-specific functional activities of the gut microbiome. *Nat. Commun.* 10:4146. doi: 10.1038/s41467-019-12087-8

Martino, C., Zaramela, L. S., Gao, B., Embree, M., Tarasova, J., Parker, S. J., et al. (2022). Acetate reprograms gut microbiota during alcohol consumption. *Nat. Commun.* 13:4630. doi: 10.1038/s41467-022-31973-2

Minekus, M., Alminger, M., Alvito, P., Ballance, S., Bohn, T., Bourlieu, C., et al. (2014). A standardised static in vitro digestion method suitable for food–an international consensus. *Food Funct.* 5, 1113–1124. doi: 10.1039/c3fo60702j

Muchaamba, F., Eshwar, A. K., Stevens, M. J., Stephan, R., and Tasara, T. (2022). Different shades of *Listeria monocytogenes*: strain, serotype, and lineage-based variability in virulence and stress tolerance profiles. *Front. Microbiol.* 12:792162. doi: 10.3389/fmicb.2021.792162

O'Callaghan, A., and Van Sinderen, D. (2016). Bifidobacteria and their role as members of the human gut microbiota. *Front. Microbiol.* 7:206360. doi: 10.3389/fmicb.2016.00925

Osek, J., Lachtara, B., and Wieczorek, K. (2022). *Listeria monocytogenes*–how this pathogen survives in food-production environments? *Front. Microbiol.* 13:866462. doi: 10.3389/fmicb.2022.866462

Park, J. C., and Im, S. H. (2020). Of men in mice: the development and application of a humanized gnotobiotic mouse model for microbiome therapeutics. *Exp. Mol. Med.* 52, 1383–1396. doi: 10.1038/s12276-020-0473-2

Pettersen, K. S., Skjerdal, T., Wasteson, Y., Lindbäck, T., Vegarud, G., Comi, I., et al. (2019). Survival of *Listeria monocytogenes* during *in vitro* gastrointestinal digestion after exposure to 5 and 0.5% sodium chloride. *Food Microbiol.* 77, 78–84. doi: 10.1016/j.fm.2018.08.010

Quast, C., Pruesse, E., Yilmaz, P., Gerken, J., Schweer, T., Yarza, P., et al. (2012). The SILVA ribosomal RNA gene database project: improved data processing and web-based tools. *Nucleic Acids Res.* 41, D590–D596. doi: 10.1093/nar/gks1219

Quereda, J. J., Dussurget, O., Nahori, M. A., Ghozlane, A., Volant, S., Dillies, M. A., et al. (2016). Bacteriocin from epidemic *Listeria* strains alters the host intestinal microbiota to favor infection. *Proc. Natl. Acad. Sci.* 113, 5706–5711. doi: 10.1073/pnas.1523899113

Quereda, J. J., Nahori, M. A., Meza-Torres, J., Sachse, M., Titos-Jiménez, P., Gomez-Laguna, J., et al. (2017). Listeriolysin S is a streptolysin S-like virulence factor that targets exclusively prokaryotic cells *in vivo*. *MBio* 8:10-1128. doi: 10.1128/mbio.00259-17

Ramalheira, R., Almeida, M., Azeredo, J., Brandao, T. R., Almeida, G., Silva, J., et al. (2010). Survival of clinical and food isolates of *Listeria monocytogenes* through simulated gastrointestinal tract conditions. *Foodborne Pathog. Dis.* 7, 121–128. doi: 10.1089/fpd.2009.0319

Reichardt, N., Vollmer, M., Holtrop, G., Farquharson, F. M., Wefers, D., Bunzel, M., et al. (2018). Specific substrate-driven changes in human faecal microbiota composition contrast with functional redundancy in short-chain fatty acid production. *ISME J.* 12, 610–622. doi: 10.1038/ismej.2017.196

Rizzatti, G., Lopetuso, L., Gibiino, G., Binda, C., and Gasbarrini, A. (2017). Proteobacteria: a common factor in human diseases. *Biomed. Res. Int.* 2017:9351507. doi: 10.1155/2017/9351507

Rodpan, S., Usman, J. N., Koga, Y., and Jongruja, N. (2022). Synergistic effect of nisin with acetic and propionic acids inactivates *Bacillus subtilis* on meat and potato. *Biocatal. Agric. Biotechnol.* 41:102317. doi: 10.1016/j.bcab.2022.102317

Rogers, A. W., Tsolis, R. M., and Bäumler, A. J. (2021). *Salmonella* versus the microbiome. *Microbiol. Mol. Biol. Rev.* 85, 10–1128. doi: 10.1128/MMBR.00027-19

Rolhion, N., Chassaing, B., Nahori, M. A., De Bodt, J., Moura, A., Lecuit, M., et al. (2019). A *Listeria monocytogenes* bacteriocin can target the commensal *Prevotella copri* and modulate intestinal infection. *Cell Host Microbe* 26, 691–701.e5. doi: 10.1016/j.chom.2019.10.016

Sittipo, P., Shim, J. W., and Lee, Y. K. (2019). Microbial metabolites determine host health and the status of some diseases. *Int. J. Mol. Sci.* 20:5296. doi: 10.3390/ijms20215296

Vacca, M., Celano, G., Calabrese, F. M., Portincasa, P., Gobbetti, M., and De Angelis, M. (2020). The controversial role of human gut lachnospiraceae. *Microorganisms* 8:573. doi: 10.3390/microorganisms8040573

Van Deun, K., Pasmans, F., Van Immerseel, F., Ducatelle, R., and Haesebrouck, F. (2008). Butyrate protects Caco-2 cells from *Campylobacter jejuni* invasion and translocation. *Br. J. Nutr.* 100, 480–484. doi: 10.1017/S0007114508921693

Wexler, H. M. (2007). *Bacteroides*: the good, the bad, and the nitty-gritty. *Clin. Microbiol. Rev.* 20, 593–621. doi: 10.1128/CMR.00008-07

Wolter, M., Steimle, A., Parrish, A., Zimmer, J., and Desai, M. S. (2021). Dietary modulation alters susceptibility to *Listeria monocytogenes* and *Salmonella typhimurium* with or without a gut microbiota. *mSystems* 6:e00717-00721. doi: 10.1128/mSystems.00717-21

Yamaguchi, M., Yang, Y., Ando, M., Kumrungsee, T., Kato, N., and Okazaki, Y. (2018). Increased intestinal ethanol following consumption of fructooligosaccharides in rats. *Biomed. Rep.* 9, 427–432. doi: 10.3892/br.2018.1150

Yu, X., Wu, X., Shah, N. P., and Xu, F. (2020). Interaction between *Bifidobacterium bifidum* and *Listeria monocytogenes* enhances antioxidant activity through oxidoreductase system. *LWT* 127:109209. doi: 10.1016/j.lwt.2020.109209

Zafar, H., and Saier, M. H. Jr. (2021). Gut *Bacteroides* species in health and disease. *Gut Microbes* 13, 1–20. doi: 10.1080/19490976.2020.1848158

Zilelidou, E. A., and Skandamis, P. N. (2018). Growth, detection and virulence of *Listeria monocytogenes* in the presence of other microorganisms: microbial interactions from species to strain level. *Int. J. Food Microbiol.* 277, 10–25. doi: 10.1016/j.ijfoodmicro.2018.04.011

Zou, Y., Zhou, C., Chang, X., Zhao, F., and Ye, K. (2024). Differential mechanism between *Listeria monocytogenes* strains with different virulence contaminating ready-to-eat sausages during the simulated gastrointestinal tract. *Food Res. Int.* 186:114312. doi: 10.1016/j.foodres.2024.114312

frontiers | Frontiers in Microbiology

TYPE Original Research
PUBLISHED 25 July 2025
DOI 10.3389/fmicb.2025.1607918

Check for updates

OPEN ACCESS

EDITED BY
Mohammad Altamimi,
An-Najah National University, Palestine

REVIEWED BY
Bing Yan,
China Academy of Chinese Medical Sciences, China
Andrea Garcia Contreras,
University of Guadalajara, Mexico

*CORRESPONDENCE
Shinji Fukuda
✉ sfukuda@metagen.co.jp

RECEIVED 08 April 2025
ACCEPTED 08 July 2025
PUBLISHED 25 July 2025

CITATION
Sasaki H, Masutomi H, Yamauchi Y, Ishihara K and Fukuda S (2025) Effectiveness of personalized granola tailored to the gut microbiota for improving gut environment and mood states.
Front. Microbiol. 16:1607918.
doi: 10.3389/fmicb.2025.1607918

COPYRIGHT
© 2025 Sasaki, Masutomi, Yamauchi, Ishihara and Fukuda. This is an open-access article distributed under the terms of the Creative Commons Attribution License (CC BY). The use, distribution or reproduction in other forums is permitted, provided the original author(s) and the copyright owner(s) are credited and that the original publication in this journal is cited, in accordance with accepted academic practice. No use, distribution or reproduction is permitted which does not comply with these terms.

Effectiveness of personalized granola tailored to the gut microbiota for improving gut environment and mood states

Hiroyuki Sasaki[1], Hirofumi Masutomi[1], Yohsuke Yamauchi[2], Katsuyuki Ishihara[1] and Shinji Fukuda[2,3,4,5,6]*

[1]Research & Development Division, Calbee, Inc., Utsunomiya, Japan, [2]Metagen, Inc., Tsuruoka, Japan, [3]Institute for Advanced Biosciences Keio University, Tsuruoka, Japan, [4]Gut Environmental Design Group, Kanagawa Institute of Industrial Science and Technology, Kawasaki, Japan, [5]Transborder Medical Research Center, University of Tsukuba, Tsukuba, Japan, [6]Innovative Microbiome Therapy Research Center, Juntendo University Graduate School of Medicine, Bunkyō, Japan

The gut microbiota plays a critical role in host metabolism, immunity, and mental health. Short-chain fatty acids (SCFAs), produced through the gut microbial fermentation of dietary fibers, are essential metabolites influencing host physiology. Previous studies have suggested that dietary interventions impact SCFA production, but individual responses vary owing to gut microbiota composition. This study sought to investigate whether personalized granola, formulated based on an individual's gut microbiota, enhances SCFA production and improves metabolic and mental health outcomes. A single-arm, single-blind, before-and-after study was conducted on 99 participants. Personalized granola (BodyGranola®, Calbee, Inc.) was tailored to the gut microbiota composition of each individual by incorporating three prebiotic ingredients selected from six options. Participants consumed 50 g of granola daily for 8 weeks. Fecal samples were collected at baseline, week 4, and week 8 for gut microbiota and intestinal metabolite analysis via 16S rRNA gene sequencing and gas chromatography–mass spectrometry. Mood and defecation were assessed using the Profile of Mood States Second Edition (POMS2), Athens Insomnia Scale (AIS), and defecation questionnaires. Personalized granola consumption tended to increase SCFAs, including acetic acid and caproic acid. The relative abundance of *Bifidobacterium* also increased. POMS2 assessments indicated improvements in vitality and total mood disturbance scores. Stool volume increased, but bloating and gas accumulation worsened. Microbiota-type-specific variations in metabolite production were observed. Personalized granola enhances SCFA production and improves mood, suggesting that dietary interventions tailored to gut microbiota composition may optimize health outcomes. Future studies should explore gut microbiota-based precision nutrition in larger, controlled trials.

KEYWORDS

precision nutrition, short-chain fatty acids, gut microbiota, prebiotics, granola

1 Introduction

Approximately 40 trillion gut bacteria reside in the intestines of mammals, collectively referred to as the gut microbiota. In recent years, research has demonstrated that the gut microbiota plays a crucial role in various physiological processes, including host immunity, nutrient absorption, and metabolism (Marchesi et al., 2016). Among the metabolites produced by the gut microbiota, short-chain fatty acids (SCFAs) play a critical role in regulating host physiological functions. SCFAs contribute to a range of processes, such as intestinal immunity,

metabolic regulation, endocrine signaling, and neural function. A reduction in SCFA production has been associated with the development of several diseases, including obesity, hypertension, and central nervous system disorders (Chambers et al., 2018; Silva et al., 2020; Overby and Ferguson, 2021; Lange et al., 2023).

SCFAs are produced when the gut microbiota ferments and breaks down indigestible dietary components, such as dietary fiber and resistant oligosaccharides (Koh et al., 2016). When dietary fiber reaches the large intestine, it is hydrolyzed into monosaccharides by gut bacteria-specific enzymes. Most of these monosaccharides are subsequently converted into pyruvate via the glycolytic pathway, and SCFAs are subsequently synthesized from pyruvate through distinct microbial metabolic pathways (Koh et al., 2016). As is evident from this process, indigestible nutrients play a critical role in SCFA production. In particular, prebiotics—indigestible compounds that selectively stimulate beneficial gut bacteria—have been shown to significantly influence gut microbiota composition and SCFA production (David et al., 2014). For instance, inulin, a well-characterized prebiotic, has been reported to alter gut microbiota composition and promote the growth of butyrate-producing bacteria, which generate a key SCFA, butyrate (Valcheva et al., 2015; Barber et al., 2022). Moreover, reduced SCFA levels have been implicated in the development of major depressive disorder and schizophrenia (Yu et al., 2024). Animal studies have demonstrated that butyrate administration can alleviate depressive-like behavior and manic states in models of depression and bipolar disorder (Resende et al., 2013; Wei et al., 2014).

Granola is a food made from a mixture of oats, rye, and other grains and is rich in dietary fiber (Yamauchi et al., 2023). Owing to its high fiber content, granola is believed to influence gut microbiota composition. In fact, studies have reported that consuming granola for breakfast promotes bowel movements in both adult women and elementary school children (Kyo et al., 2017; Matsumoto et al., 2023). Furthermore, in patients undergoing hemodialysis, granola consumption has been shown to alter gut microbiota composition, reduce blood pressure, and lower the serum levels of the uremic toxin indoxyl sulfate (Nagasawa et al., 2021; Nagasawa et al., 2024). Recent studies have reported that consuming granola containing multiple prebiotic ingredients can alter the gut microbiota, including an increase in *Bifidobacterium*. These changes have been associated with reduced perceived stress, improved mood, and a decrease in subjective feelings of sleepiness (Sasaki et al., 2025). Based on the above findings, granola consumption has the potential to promote SCFA production. However, when we measured SCFA levels and various other metabolites in individuals who consumed granola, we found no significant increase in SCFA levels (Yamauchi et al., 2023). One possible explanation for this lack of increase is the presence of substantial interindividual variability—while some individuals exhibited increased SCFA production, others did not. However, a positive correlation was observed between changes in SCFA levels and the abundance of *Prevotella 9*. In other words, the greater the abundance of *Prevotella 9* in the gut, the more granola consumption-promoted SCFA production was observed (Yamauchi et al., 2023). Individuals who exhibit a response to dietary interventions are referred to as responders, while those who do not are classified as non-responders. It is believed that these differences between responders and non-responders are primarily determined by an individual's gut microbiota composition (Korpela et al., 2014).

Previous studies have shown that individuals can be classified as responders or non-responders in response to prebiotics. For example, barley consumption has been associated with improved glucose metabolism and enhanced blood glucose regulation. However, this effect is primarily observed in responders—individuals with a high abundance of *Prevotella* in their gut microbiota exhibit greater improvements in glucose metabolism (Kovatcheva-Datchary et al., 2015). In addition, studies have identified distinct groups based on their gut microbiota response to inulin consumption. One group exhibited significant changes in microbiota composition, while another exhibited no substantial increase in SCFA levels. Notably, the former group tended to consume a high-fiber diet regularly and harbored a greater abundance of *Bifidobacterium* in the gut (Healey et al., 2018).

As described above, the composition of the gut microbiota varies among individuals, making it challenging to identify a single diet that is optimal for everyone. In recent years, the importance of personalized and precision nutrition—approaches that integrate gut microbiota data to tailor dietary recommendations for individuals—has been increasingly recognized (Kolodziejczyk et al., 2019; Agrawal et al., 2024). Additionally, a narrative review reported that personalizing dietary interventions based on factors such as gut microbiota, metabolic profiles, and genetic variations may help improve risk factors for obesity and type 2 diabetes (Antwi, 2023). Therefore, in the case of prebiotics, it is considered important to account for an individual's gut microbiota composition and provide prebiotics tailored to enhance the production of metabolites, including SCFAs. However, only a few studies have implemented interventions involving the administration of prebiotics tailored to an individual's gut microbiota. Therefore, based on previous research, we identified gut bacteria that actively metabolize specific prebiotics and promote SCFA production. Using this information, we developed personalized granola designed to match an individual's gut microbiota by optimizing the combination of prebiotics and gut bacteria. The aim of this study was to evaluate the effectiveness of personalized granola, hypothesizing that it would significantly enhance the production of metabolites, including SCFAs. In addition to metabolite production, we also aimed to evaluate whether personalized granola improves stool frequency and mental health indicators such as stress levels, given their reported associations with gut microbiota and SCFA levels.

2 Materials and methods

2.1 Formulation of personalized granola tailored to the gut microbiota

In this study, we developed personalized granola (BodyGranola®, Calbee, Inc., Tokyo, Japan) tailored to each individual's gut microbiota using the following method. Based on a 640 g batch of granola, three out of six prebiotic toppings were selected according to the individual's gut microbiota composition. Each selected topping (120 g) was added to the base granola and thoroughly mixed, with daily consumption set at 50 g. The six prebiotic toppings included inulin, barley, fructo-oligosaccharide, resistant starch, galacto-oligosaccharide, and Hi-Cacao (high-cacao chocolate). Drawing from previous research, we identified gut bacterial species that actively metabolize each prebiotic and contribute to SCFA production. The combinations of prebiotic toppings and their corresponding gut bacterial species are presented in Table 1.

For the personalization process, we focused on six specific gut bacterial genera. After measuring each participant's gut microbiota composition, we identified the top three genera (by relative abundance) among the six, and selected the corresponding prebiotic toppings to create a customized granola formulation. The matching between prebiotics and bacterial genera was based on literature reports that linked specific prebiotics to the growth or metabolic activation of particular gut bacteria involved in SCFA production. This strategy was designed to target the most dominant genera in each individual's gut to potentially maximize metabolic response. However, we acknowledge that this genus–prebiotic matching was based on indirect evidence, and no direct functional validation was performed in this study. The nutritional composition of the base granola and prebiotic toppings is provided in Table 2, while the ingredient details for each granola formulation and prebiotic topping are listed in Supplementary Table 1. We selected the top three genera (based on relative abundance) out of six candidate genera to simplify the formulation process and ensure palatability, as the number of prebiotic toppings was limited to three per granola batch. This approach was also intended to maximize the potential response by targeting the most dominant bacterial genera. However, we acknowledge that this selection criterion was somewhat arbitrary and have discussed its limitations and the need for refinement in the Discussion section.

2.2 Participants

The study flow, from participant selection to intervention and analysis, is illustrated in Figure 1. Participants were recruited through the physical management app "Calomama," and a total of 652 men and women aged 20–65 years were enrolled. The inclusion criteria were as follows: (1) men and women aged between 20 and 65 years at the time of consent; (2) registered users of the "Calomama" app; (3) individuals with a habit of eating breakfast and who were able to replace their regular breakfast with the test food during the intervention period; (4) individuals capable of collecting a fecal sample at home and mailing it to a designated laboratory; and (5) individuals who received a full explanation of the study, understood its content, and provided written informed consent. From this pool, 300 participants were selected based on predefined exclusion criteria. The exclusion criteria were as follows: (1) individuals who had taken or planned to take laxatives, antibiotics, or intestinal medications within 1 month prior to the start of the study; (2) individuals who had undergone an appendectomy; (3) individuals who had undergone surgery within the past 6 months that could potentially influence the study results (e.g., colonoscopy, gallbladder removal, gallstone removal, gastric bypass surgery); (4) individuals currently participating in, or planning to participate in, a clinical trial for another pharmaceutical product or health food; (5) individuals with highly irregular dietary habits; (6) heavy drinkers; (7) individuals living with another study participant; (8) individuals whose lifestyle would change significantly during the trial period, such as shift workers or those being transferred; (9) individuals unable to consume milk; (10) individuals with a history of serious heart, liver, kidney, gastrointestinal (including constipation, diarrhea, inflammatory bowel disease, or colitis), or other diseases, or those currently diagnosed with such conditions; (11) pregnant, breastfeeding, or those planning to become pregnant; (12) individuals with lactose intolerance; and (13) individuals with food allergies. These conditions were assessed using a self-administered pre-screening questionnaire, which asked participants to report any history or current treatment for gastrointestinal or systemic diseases. In addition, participants reported their typical defecation frequency and stool consistency, as part of the baseline data collection.

Next, a fecal collection kit (Mykinso, Cykinso, Inc., Tokyo, Japan) was mailed to the 300 selected participants, and their gut microbiota was analyzed to classify microbiota types. Based on previous research (Watanabe et al., 2021; Yoshida et al., 2022), and the method used to select the three gut bacterial species as mentioned earlier, it has been established that 80% of the Japanese population can be categorized into the following five gut microbiota types: (1) BaBiBl type: high relative abundance of *Bacteroides*, *Bifidobacterium*, and *Blautia*; (2) BaBiF type: high relative abundance of *Bacteroides*, *Bifidobacterium*, and *Faecalibacterium*; (3) BaFBl type: high relative abundance of *Bacteroides*, *Faecalibacterium*, and *Blautia*; (4) BaPF type: high relative abundance of *Bacteroides*, *Prevotella*, and *Faecalibacterium*; and (5) BaRF type: high relative abundance of *Bacteroides*, *Ruminococcus*, and *Faecalibacterium*. Among the 295 participants who returned their fecal samples, the distribution of gut microbiota types was as follows: 83 participants had the BaBiBl type; 50 had the BaBiF type; 32, the BaFBl type; 29, the BaPF type; 19, the BaRF type; and 82 belonged to other microbiota types. The following participants were excluded from the five gut microbiota types, and 20 individuals from each type were selected to receive the intervention according to the following groups: (1) individuals who consume cereal at least 3 days per week; (2) individuals who consume cereal at least 5 days per week; (3) individuals who eat mushrooms at least five-to-six times per week; (4) individuals who consume oligosaccharides at least five-to-six times per week; (5) individuals who drink lactic acid bacteria beverages or take probiotic supplements daily; (6) individuals who consume kimchi or natto at least 5 days per week; and (7) individuals who take Chinese herbal medicine or vitamin supplements daily. The physical characteristics of the selected participants are presented in Table 3.

This study was conducted in accordance with the principles of the Declaration of Helsinki and was approved by the Ethics Review

TABLE 1 Combination of prebiotic-toppings and corresponding gut bacteria.

Prebiotic-toppings	Gut bacteria	Main metabolites	References
Inulin	*Bacteroides*	Propionic acid	Aoki et al. (2021) and Chambers et al. (2019)
Barley	*Prevotella*	Succinic acid	Kovatcheva-Datchary et al. (2015) and Fehlbaum et al. (2018)
FOS	*Faecalibacterium*	Butyric acid	Tochio et al. (2018) and Scott et al. (2014)
RS	*Ruminococcus*	Acetic acid	Ze et al. (2012) and Abell et al. (2008)
GOS	*Bifidobacterium*	Acetic acid	Liu et al. (2017) and Fehlbaum et al. (2018)
Hi-Cacao	*Blautia*	Acetic acid	Shin et al. (2022) and Tzounis et al. (2008)

FOS, fructooligosaccharide; RS, resistant starch; GOS, galactooligosaccharide; Hi-Cacao, high cacao chocolate.

10.3389/fmicb.2025.1607918

TABLE 2 Nutritional composition of fruit granola and each prebiotic-toppings (/100 g).

Nutritional component	Fruit granola	Inulin	Barley	FOS	RS	GOS	Hi-Cacao
Energy (kcal)	443.8	366.7	383.3	366.7	416.7	350	433.3
Protein (g)	6.9	6.7	6.7	6.7	5	6.7	10
Fat (g)	15.9	5	5	5	11.7	3.3	11.7
Carbohydrate (g)	72.5	83.4	83.3	83.3	80	86.6	73.4
Sugar (g)	63.4	61.7	73.3	60	66.7	63.3	66.7
Fiber (g)	9.1	21.7	10	23.3	13.3	23.3	6.7
Sodium content (g)	0.6	0.5	0.5	0.7	0.7	0.3	0.7

FOS, fructooligosaccharide; RS, resistant starch; GOS, galactooligosaccharide; Hi-Cacao, high cacao chocolate.

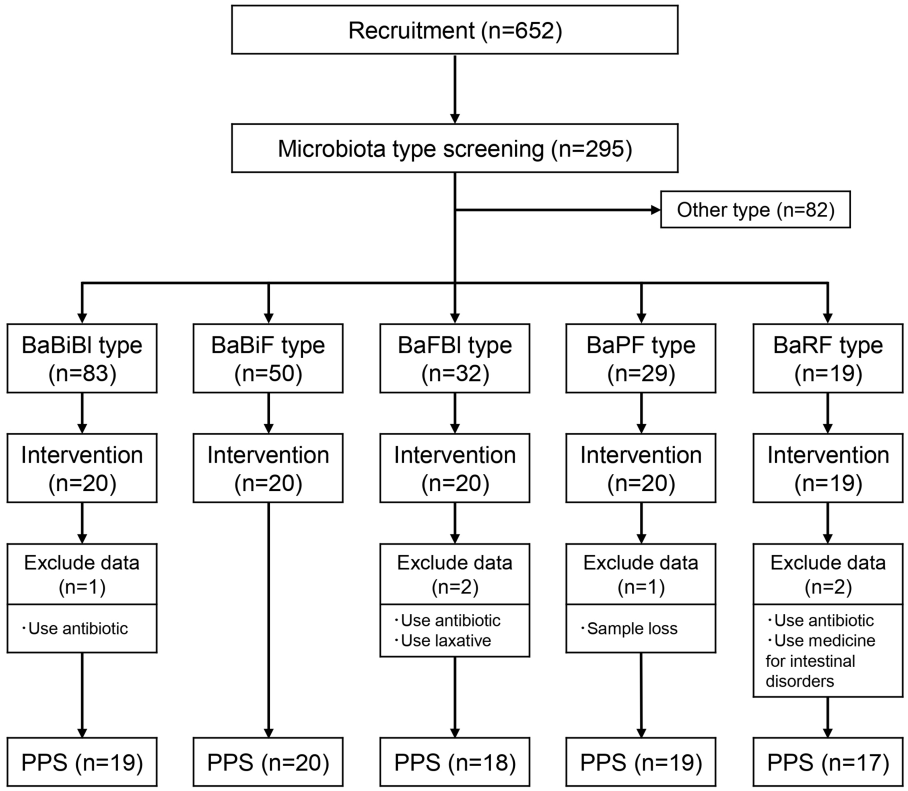

FIGURE 1
Flow diagram of this trial. Number of participants classified into each gut microbiota type and number of participants who underwent the intervention. PPS, per protocol set; BaBiBl type, gut microbiota type with a high relative abundance of *Bacteroides*, *Bifidobacterium*, and *Blautia*; BaBiF type, gut microbiota type with a high relative abundance of *Bacteroides*, *Bifidobacterium*, and *Faecalibacterium*; BaFBl type, gut microbiota type with a high relative abundance of *Bacteroides*, *Faecalibacterium*, and *Blautia*; BaPF type, gut microbiota type with a high relative abundance of *Bacteroides*, *Prevotella*, and *Faecalibacterium*; BaRF type, gut microbiota type with a high relative abundance of *Bacteroides*, *Ruminococcus*, and *Faecalibacterium*.

Committee of the Chiyoda Paramedical Care Clinic (Approval Number: 15000088). Informed consent was obtained from all participants prior to enrollment. This clinical trial is registered with the institutional ethics committee of the Japanese University Hospital Medical Information Network (Clinical Trial Reference Number: UMIN000053204).

2.3 Study design and procedure

The study was conducted between December 2023 and June 2024 as a single-arm, non-targeted, single-blind, before-and-after comparison study. All 99 participants were instructed to consume 50 g of personalized granola (test meal) with 200 mL of milk for breakfast daily for 8 weeks and record their lifestyle data in the "Calomama" app. Participants collected fecal samples using a fecal collection kit at the following time points: week 0 (from 4 days before to 1 day before consuming the test meal), week 4 (from day 24 to day 28 after starting test meal consumption), and week 8 (from day 52 to day 56 after starting test meal consumption). The samples were then mailed for analysis. Additionally, participants completed a questionnaire on defecation status, which included the following items: (1) defecation frequency (number of bowel movements per week); (2) stool volume, assessed using an egg-based equivalency scale; and (3) stool consistency, evaluated using the Bristol Stool Scale (BSS). Furthermore, participants responded to the Athens Insomnia Scale (AIS) and Profile of Mood States 2 (POMS2) questionnaire (Figure 2). During the study period, 93 participants were included in the per protocol

TABLE 3 Physical characteristics.

Type	Number of subjects		Age	Height	Weight
	Male	Female			
BaBiBl	8	11	43.00 ± 2.28	164.7 ± 2.46	63.4 ± 4.56
BaBiF	6	14	48.05 ± 1.69	163.5 ± 1.72	61.4 ± 2.24
BaFBl	6	12	47.83 ± 2.39	163.0 ± 1.66	60.4 ± 2.67
BaPF	6	13	44.35 ± 1.81	163.8 ± 1.77	62.3 ± 2.84
BaRF	6	11	52.88 ± 1.81	160.9 ± 1.52	57.8 ± 2.32
Total	32	61	47.71 ± 0.94	163.3 ± 0.83	61.2 ± 1.36

Values are means ± SEM.

set (PPS) analysis, after excluding five participants who used antibiotics, laxatives, or intestinal medications, and one participant who lost their sample. Although participants' diets were not strictly controlled, they were instructed to maintain their habitual dietary patterns and avoid major dietary changes during the study period, particularly regarding alcohol and probiotic or prebiotic supplement intake. Dietary intake was monitored using the "Calomama" app, which allows users to log their daily meals. However, not all participants recorded their meals consistently, and the calculated values for energy and nutrient intake were found to be unreliable due to underreporting and input variability. Therefore, precise dietary intake data could not be included in the analysis. Nevertheless, the consumption of fermented foods commonly found in the Japanese diet, such as natto, was assessed through a pre-study questionnaire. This information was used as part of the participant selection and screening process. The AIS, POMS2, and questionnaire on defecation were self-administered and completed individually at home, without the influence of study personnel. To enhance neutrality and reduce potential bias, a third-party organization (CPCC Co., Ltd.) was contracted to manage conducting test, the participants and the distribution, collection, and aggregation of questionnaire data. Participants were informed that their responses would be treated confidentially and used solely for research purposes, which helped minimize social desirability bias. Furthermore, the use of validated and widely adopted instruments, such as the AIS and POMS2 (Soldatos et al., 2000, 2003; McNair et al., 2012), supports the robustness of the data.

2.4 Organic acid level measurements

Metabolites were extracted from fecal samples collected using MG kit (Metagen, Inc. Japan) as previously described (Hashimoto et al., 2023). Dried fecal samples were mechanically disrupted by shaking with 3.0 mm zirconia beads at 1,500 × g for 10 min using a Shake Master (Biomedical Science, Tokyo, Japan). A 10 mg fecal sample was suspended in 100 µL of purified water containing 500 µM crotonic acid as an internal standard. Thereafter, 50 µL of hydrochloric acid and 200 µL of diethyl ether were added. The mixture was shaken at 1,500 × g for 10 min using the Shake Master and then centrifuged at 10,000 × g for 10 min. After centrifugation, 80 µL of the upper ether layer was collected, and 16 µL of derivatization reagent (MTBSTFA: N-tert-butyldimethylsilyl N-methyltrifluoroacetamide) was added. The mixture was transferred to an Agilent crimp-cap vial, which was sealed and incubated at 80°C for 20 min. The sample was then left at room temperature overnight for derivatization. A 2 µL aliquot of the derivatized sample was injected into a 7,890 series GC-MS system (Agilent Technologies, CA, United States) equipped with a DB-5 ms column (0.25 mm × 30 m × 0.25 µm, Agilent Technologies). Helium was used as the carrier gas at a flow rate of 1.2 mL/min. The head pressure was set to 10.5 psi with a 100:1 split ratio. The injector, ion source, quadrupole mass analyzer, and transfer line temperatures were set to 250°C, 230°C, 150°C, and 260°C, respectively. Measurements were conducted using the Agilent MassHunter Workstation Data Acquisition software (version 10.0, Agilent Technologies), and data were analyzed using the Agilent MassHunter Quantitative Analysis software (version 10.1, Agilent Technologies).

2.5 DNA extraction from fecal sample

Fecal samples were collected using a fecal collection kit containing guanidine thiocyanate solution. The collected samples were shipped at room temperature and stored at 4°C upon arrival. DNA extraction was performed using an automated DNA extractor (GENE PREP STAR PI-480; Kurabo Industries Ltd., Osaka, Japan) according to the manufacturer's protocol.

2.6 16S rRNA gene sequencing and analysis

The V1–V2 region of the 16S rRNA gene was amplified from extracted DNA using the following primers and KAPA HiFi HotStart ReadyMix (Roche, Basel, Switzerland):

Forward primer: 16S 27Fmod = TCG TCG GCA GCG TCA GAT GTG TAT AAG AGA CAG AGR GTT TGA TYM TGG CTC AG.
Reverse primer: 16S 338R = GTC TCG TGG GCT CGG AGA TGT GTA TAA GAG ACA GTG CTG CCT CCC GTA GGA GT.

Library preparation was performed according to the Illumina 16S library preparation protocol (Illumina, San Diego, CA, United States) as follows. Using the Nextera XT Index Kit (Illumina, San Diego, CA, United States), libraries were prepared with dual index adapters. Each library was diluted to 5 ng/µL, and equal amounts were pooled to a final concentration of 4 nM. The DNA concentration of the libraries was quantified by qPCR using KAPA SYBR FAST qPCR Master Mix (KK4601, KAPA Biosystems).

Sequencing was performed using the MiSeq Reagent Kit V2 (500 cycles), generating 250 bp paired-end reads. Paired-end reads were analyzed for gut microbiota composition using QIIME2 (version 2024.2) (Bolyen et al., 2019). First, DADA2 was applied to denoise and low-quality reads were filtered, generating amplicon sequence variants (ASVs) (Callahan et al., 2016). Taxonomic classification of ASVs was performed using the Silva SSU Ref Nr 99 (version 132) classifier (Quast et al., 2013). Additionally, alpha diversity was calculated for the ASVs using three indices: Chao1, Shannon, and Simpson.

2.7 AIS

Sleep disturbances, particularly insomnia, were assessed using the AIS. The AIS is a questionnaire consisting of eight items (Soldatos et al., 2000, 2003), each rated on a four-point scale: (0 = no problem at all, 1 = slight problem, 2 = significant problem, 3 = very significant problem).

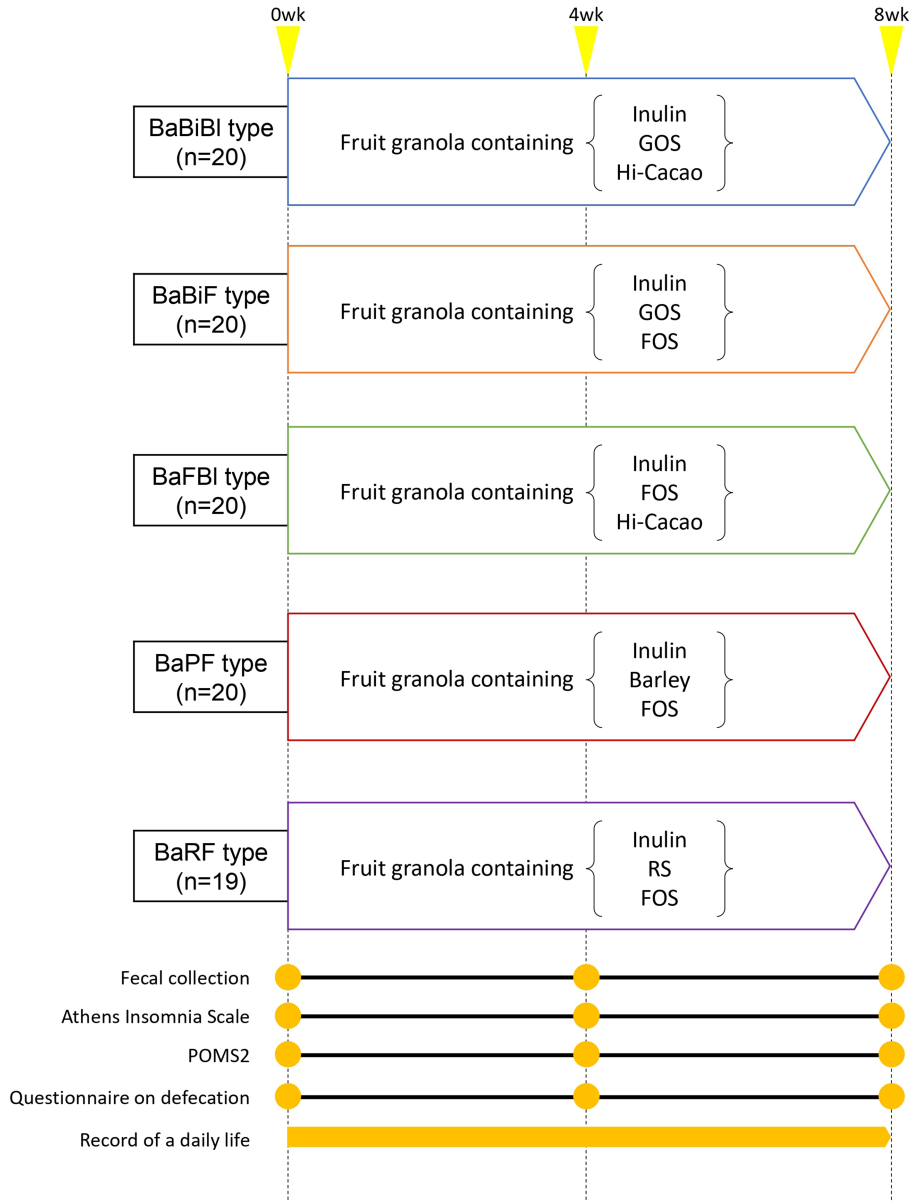

FIGURE 2
Intervention diagram. Participants consumed personalized granola (fruit granola with three prebiotic toppings) for 8 weeks, depending on their gut microbiota type. Questionnaires and fecal samples were collected at weeks 0, 4 and, 8 (yellow circle points). A daily life diary was recorded throughout the study period.

The questionnaire evaluates the following aspects of sleep: (1) difficulty falling asleep, (2) nighttime awakenings, (3) early morning awakenings, (4) total sleep duration, (5) overall sleep quality, (6) daytime mood state, (7) daytime mental and physical functioning, and (8) daytime sleepiness. The total score of these eight items constitutes the AIS score. A cutoff score >6 is used to identify insomnia (Soldatos et al., 2003).

2.8 POMS2

The Japanese version of POMS2 was used to assess mood states (McNair et al., 2012). The questionnaire consists of seven mood scales: (1) anger–hostility (AH), (2) confusion–bewilderment (CB), (3) depression–dejection (DD), (4) fatigue–inertia (FI), (5) tension–anxiety (TA), (6) vigor–activity (VA), and (7) friendship (F). Additionally, the total mood disturbance (TMD) score was calculated as an overall measure of mood state. To reduce participant burden, a shortened version of POMS2 was used in this study. Participants completed 35 questions, rating their current emotional state on a 5-point scale from "not at all" (0 points) to "very much" (4 points). The TMD score was calculated by summing the total scores of AH, CB, DD, FI, and TA, and then subtracting the total score of VA. The POMS2 raw scores were converted into standardized T-scores, which were used for mood state evaluation.

2.9 Questionnaire on defecation

The following six items were assessed in relation to defecation:

1. Defecation frequency: evaluated based on the number of bowel movements per day.
2. Stool volume: assessed using an equivalency scale based on the number of chicken egg-sized stool units.
3. Stool consistency: rated on a 7-point scale [1 = very hard, 2 = hard, 3 = somewhat hard, 4 = normal, 5 = somewhat soft, 6 = soft (muddy), 7 = very soft (watery)].
4. Feeling of incomplete evacuation: rated on a 4-point scale (1 = persistent discomfort after defecation; 2 = slight feeling of incomplete evacuation; 3 = almost no feeling of incomplete evacuation; somewhat refreshed; and 4 = no feeling of incomplete evacuation; completely refreshed).
5. Bloating severity: rated on a 6-point scale (1 = very strong, 2 = strong, 3 = normal, 4 = weak, 5 = very weak, 6 = not particularly strong).
6. Gas build-up severity: rated on a 6-point scale (1 = very strong, 2 = strong, 3 = normal, 4 = weak, 5 = very weak, 6 = not particularly strong).

2.10 Statistical analysis

Statistical analyses were conducted using GraphPad Prism (version 9.5.1, GraphPad Software Inc., United States). All data are presented as mean ± SEM. Statistical comparisons were performed between weeks 0, 4, and 8, while comparisons between gut microbiota types were not conducted. For each variable, normality was assessed using the D'Agostino–Pearson test, followed by variance testing using Bartlett's test. If the data were normally distributed and had equal variances, a one-way repeated measures ANOVA was applied, with Tukey's multiple comparison test used as a *post-hoc* test. If the data were non-normally distributed or had unequal variances, the Friedman test (a non-parametric alternative) was performed, followed by Dunn's multiple comparison test for *post-hoc* analysis. For correlation analysis, Spearman's correlation coefficient was calculated. *p*-values were computed for each test, and $p < 0.05$ was considered statistically significant.

3 Results

3.1 Personalized granola consumption increased SCFAs

First, we analyzed the effects of consuming personalized granola tailored to each individual's gut microbiota on the gut environment in 93 participants, examining overall changes regardless of gut microbiota type. Among the organic acids produced as metabolic byproducts, SCFAs such as acetic acid and butyric acid were measured. The results are presented in Figure 3. Acetic acid levels were tended to increase from week 0 to week 8 following the consumption of personalized granola (Figure 3A). Caproic acid levels exhibited significant differences between week 0 and week 4, as well as between week 0 and week 8 (Figure 3G).

In addition to SCFAs, other organic acids were also analyzed (Figure 4). Formic acid levels decreased significantly from week 0 to week 8 (Figure 4A). Lactic acid levels exhibited an increasing trend from week 0 to week 8, while succinic acid levels increased significantly between week 0 and week 4, week 0 and week 8, as well as between week 4 and week 8 (Figures 4B,D,E). Total organic acid levels, excluding the main SCFAs, increased significantly from week 0 to week 8 (Figure 4G).

These findings indicate that consuming personalized granola leads to an overall increase in organic acids, which are key metabolic substances in the gut, regardless of gut microbiota type.

3.2 Relative abundance of *Bifidobacterium* increased with the consumption of personalized granola

The consumption of personalized granola led to an increase in organic acid levels, which are key metabolic substances in the gut. However, we further investigated whether the composition of the gut microbiota responsible for producing these metabolites was altered.

First, we examined overall gut microbiota composition using beta diversity analysis (Supplementary Figure 1 and Supplementary Table 2). The results indicated that while gut microbiota composition varied significantly based on microbiota type, no significant changes were observed within the same microbiota type over the study period. In other words, these findings suggest that consuming personalized granola does not significantly alter the overall gut microbiota composition.

Therefore, rather than analyzing the gut microbiota as a whole, we specifically examined the relative abundance of the six bacterial genera used to define personalized granola (Figure 5). As a result, we observed a significant increase in the relative abundance of *Bifidobacterium* among these six bacterial genera following personalized granola consumption (Figure 5C).

Additionally, analysis of the alpha diversity revealed that the Chao1 and Shannon diversity indices significantly decreased after personalized granola consumption (Supplementary Figure 2).

3.3 Personalized granola consumption improved overall mood disturbance

Thus far, we have confirmed that personalized granola consumption increases metabolite levels, regardless of gut microbiota type, and enhances the relative abundance of *Bifidobacterium*. Considering that gut microbiota-derived metabolites contribute to the regulation of host physiological functions, we hypothesized that this increase in metabolites could influence the host's mental and physical well-being. To explore this, we analyzed the results of the POMS2, AIS, and defecation questionnaires (Figures 6, 7).

In the POMS2 assessment, a significant improvement was observed in vitality (VA) between week 0 and week 4 (Figure 6F). Additionally, the total TMD score decreased significantly from week 0 to week 8 (Figure 6H), suggesting that consuming personalized granola may contribute to overall mood improvement. However, no significant changes were observed in the AIS (Figure 6I). From the defecation questionnaire, it was found that stool volume increased significantly following personalized granola consumption (Figure 7B). However, the scores for bloating and gas accumulation worsened (Figures 7E,F).

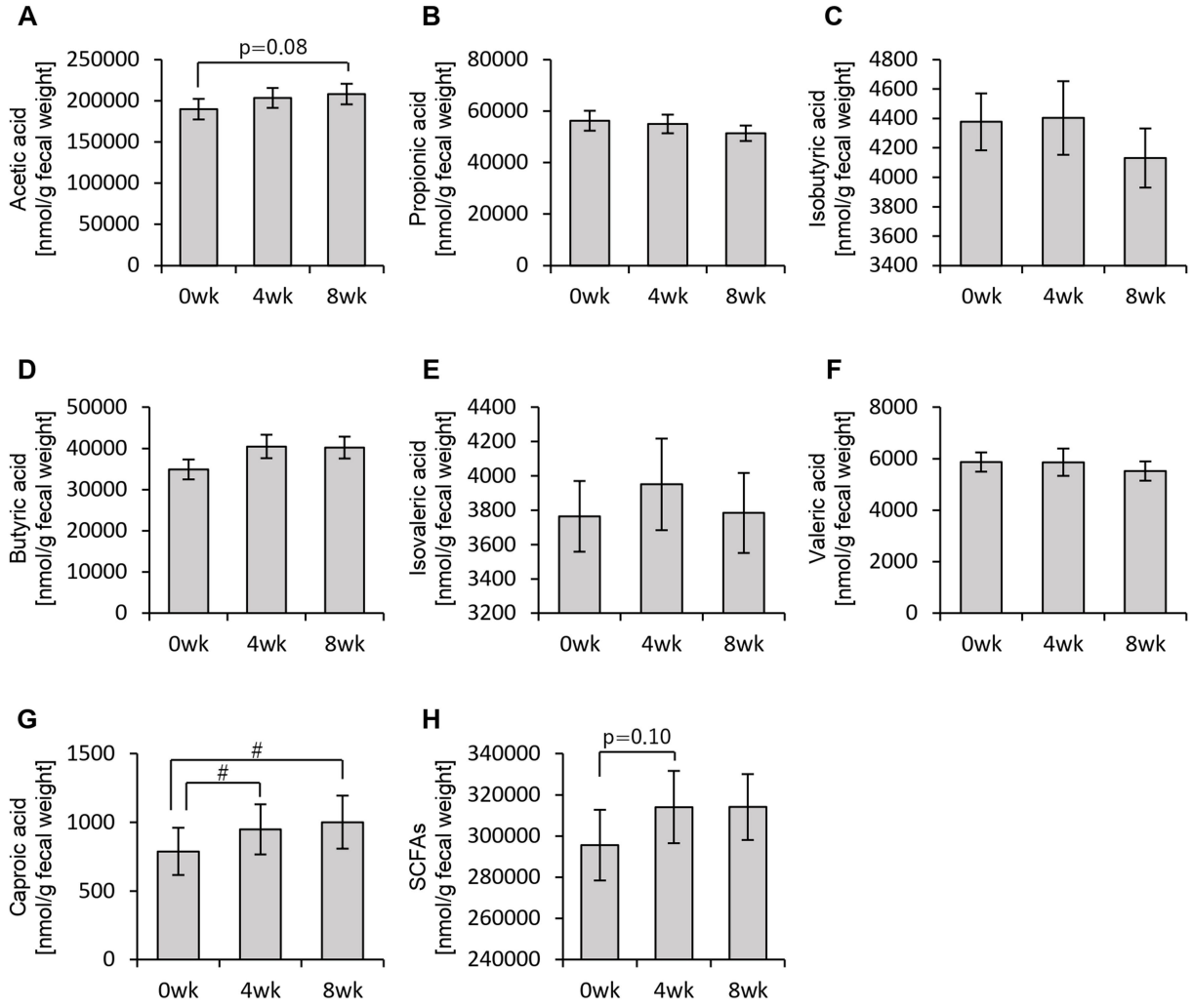

FIGURE 3
Personalized granola consumption increases short-chain fatty acid production regardless of gut microbiota type. Short-chain fatty acid (SCFA) production in all subjects: **(A)** acetic acid, **(B)** propionic acid, **(C)** isobutyric acid, **(D)** butyric acid, **(E)** isovaleric acid, **(F)** valeric acid, **(G)** caproic acid, and **(H)** SCFAs [the sum of **(A)** through **(G)**]. All values are represented as mean ± SEM (n = 93). $^{\#}p < 0.05$, evaluated using the Friedman test with Dunn's *post-hoc* test.

These findings indicate that personalized granola consumption improves mood and increases stool volume, regardless of gut microbiota type. However, it may also lead to side effects including increased bloating and gas accumulation.

3.4 Increase in organic acids in different gut microbiota types

We examined the overall effects of personalized granola consumption on the gut microbiota, irrespective of microbiota type. Next, we analyzed the impact of personalized granola consumption on each specific gut microbiota type to determine whether the effects varied by gut microbiota composition.

First, we examined the metabolites produced by the gut microbiota in each microbiota type (Figures 8, 9). In the BaBiBl type, caproic acid, lactic acid, and succinic acid increased significantly (Figures 8G, 9B,D), while 2-methylvaleric acid decreased (Figure 9E). In the BaBiF type, butyric acid exhibited an upward trend at week 4 (Figure 8D); in addition, caproic acid and 2-methylvaleric acid increased (Figures 8G, 9E). In the BaFBl type, caproic acid exhibited an increasing trend from week 0 to week 8 (Figure 8G), and 2-methylvaleric acid increased significantly (Figure 9E). In the BaPF type, formic acid decreased significantly from week 0 to week 8 (Figure 9A), while malonic acid and 2-methylvaleric acid increased significantly (Figures 9C,E). Succinic acid also exhibited increasing trend between week 0 and week 4 in this type (Figure 9D). The total amount of organic acids (excluding SCFAs) tended to increase between week 0 and week 4 (Figure 9G). In the BaRF type, acetic acid and butyric acid increased from week 0 to week 8 (Figures 8A,D). While the total SCFA levels increased in this type (Figure 8H), other organic acids also exhibited an increasing trend, with a significant rise in 2-methylvaleric acid levels (Figures 9B,E).

These findings suggest that the types of organic acids produced in response to personalized granola consumption vary depending on gut microbiota type, highlighting distinct metabolic responses across different microbiota compositions.

Next, we examined the relative abundances of the six bacterial genera that were used to define personalized granola.

10.3389/fmicb.2025.1607918

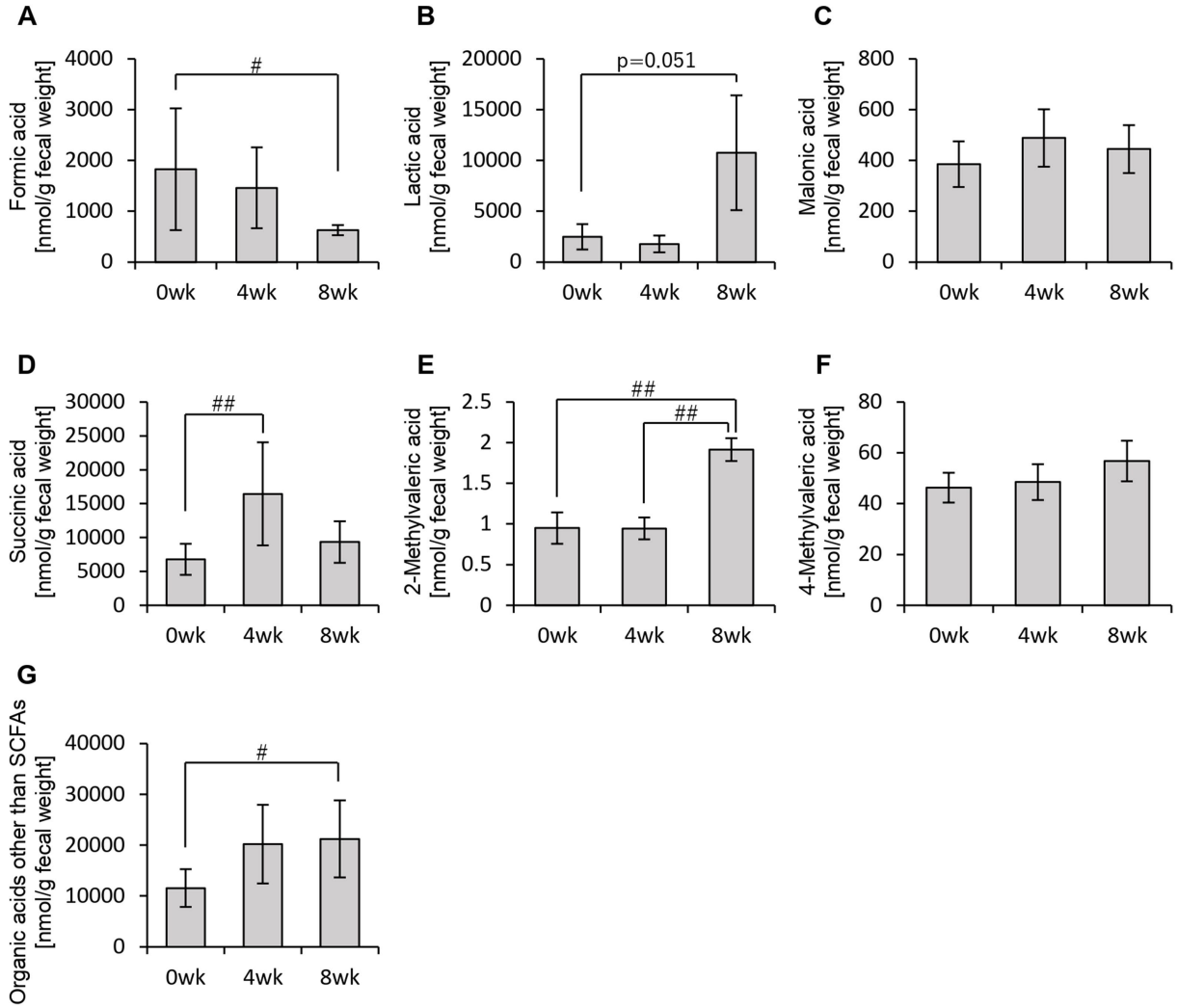

FIGURE 4
Personalized granola consumption increases organic acids other than SCFA production regardless of gut microbiota type. Organic acid production in all subjects: **(A)** formic acid, **(B)** lactic acid, **(C)** malonic acid, **(D)** succinic acid, **(E)** 2-methylvaleric acid, **(F)** 4-methylvaleric acid, and **(G)** organic acids other than SCFAs [the sum of **(A)** through **(F)**]. All values are represented as mean ± SEM (n = 93). $^{\#\#}p < 0.01$ and $^{\#}p < 0.05$, evaluated using the Friedman test with Dunn's *post-hoc* test.

The relative abundance of *Bifidobacterium* increased between week 0 and week 4 or between week 0 and week 8 in all gut microbiota types except for the BaFBl type (Figure 10C). Notably, *Bifidobacterium* exhibited significant increases, even in microbiota types where it was not among the top three most abundant bacterial species, such as the BaPF and BaRF types. Furthermore, no significant changes were observed in other bacterial genera, such as *Bacteroides* and *Blautia* (Figures 10A,B,D–F).

Analysis of the alpha diversity revealed a significant decrease or a decreasing trend in the Chao1 index across all gut microbiota types (Supplementary Figure 3A).

3.5 Disturbances in physical and mental states vary based on gut microbiota type

We previously confirmed that different gut microbiota types exhibited distinct metabolic responses to personalized granola consumption. Next, we sought to examine how these variations affected physical and mental states by analyzing data from the POMS2, AIS, and defecation status questionnaires for each microbiota type (Figures 11, 12).

In the BaBiBl type, VA (POMS2) significantly improved from week 0 to week 4 (Figure 11F) while insomnia disturbance (AIS) significantly improved from week 0 to week 8 (Figure 11I). In the BaBiF type, AH (POMS2) significantly improved from week 0 to week 4 (Figure 11A). In the BaFBl type: VA (POMS2) significantly improved from week 0 to week 8 (Figure 11F). In the BaPF type, TA (POMS2) significantly improved from week 0 to week 4, while the TMD scores significantly improved between week 0 and week 4 as well as between week 0 and week 8. In the BaRF type, FI (POMS2) significantly worsened from week 0 to week 4. These findings indicate that specific POMS2 and AIS items were affected differently depending on the gut microbiota type. A significant increase in stool volume was observed in all microbiota types except BaPF (Figure 12B). A significant increase in gas accumulation was observed in all microbiota types except BaBiBl (Figure 12F).

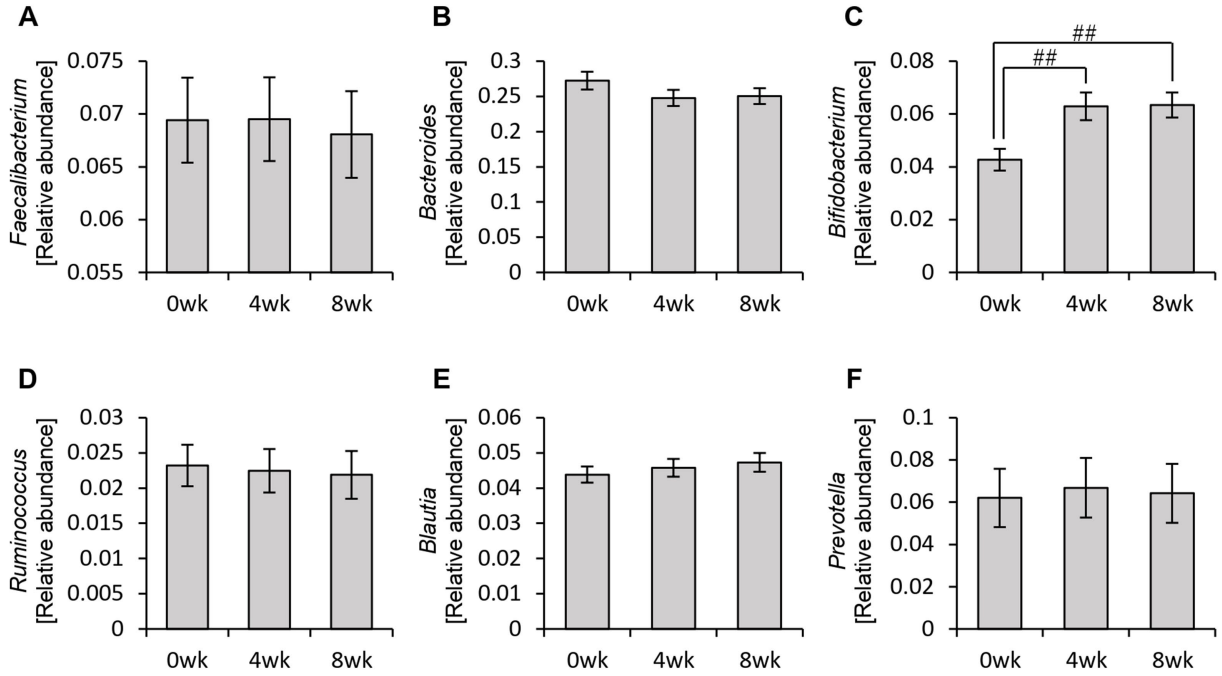

FIGURE 5
Changes in the six bacterial genera considered when formulating personalized granola. The relative abundance of six bacteria at the genus level in all participants: **(A)** *Faecalibacterium*, **(B)** *Bacteroides*, **(C)** *Bifidobacterium*, **(D)** *Ruminococcus*, **(E)** *Blautia*, and **(F)** *Prevotella*. All values are represented as mean ± SEM (n = 93). $^{\#\#}p < 0.01$, evaluated using the Friedman test with Dunn's *post-hoc* test.

These results suggest that the physical and mental effects of personalized granola consumption vary across gut microbiota types, with common effects on defecation and gut microbiota-dependent effects on mood disturbances.

4 Discussion

In this study, we demonstrated that personalized granola, designed to match each individual's gut microbiota composition, significantly increased metabolites, including SCFAs, and contributed to mood improvement. Furthermore, the specific metabolites that increased following personalized granola consumption varied among the gut microbiota types defined in this study. In a previous study examining intestinal metabolites in 33 healthy men and women who consumed the same fruit granola used as the base for this study, we found that granola intake increased medium-chain fatty acids (having a carbon number of eight or more). However, no significant increase in SCFAs was observed (Yamauchi et al., 2023). In contrast, in the personalized granola experiment, an overall analysis of 93 participants revealed an increasing trend of acetic acid and a significant increase in caproic acid. Additionally, the levels of lactic acid and succinic acid, which are involved in SCFA production, also increased. Furthermore, in a subset analysis of <20 participants, a significant increase in acetic acid, butyric acid, and caproic acid was observed across the different gut microbiota types. Although direct comparisons with previous studies are challenging owing to differences in sample size and consumption duration, the results of this study suggest that personalized granola may be more effective in promoting SCFA production than standard granola.

Additionally, we observed a significant decrease in alpha diversity (Shannon index) when all participants were analyzed together, but no significant changes were detected when participants were stratified by gut microbiota type (Supplementary Figures 2, 3). One likely explanation is the reduced sample size in each microbiota-type subgroup (approximately 20 participants), which may have resulted in insufficient statistical power to detect within-group changes. Moreover, while the overall participants included a broad range of microbial compositions, participants within the same microbiota type likely had more similar baseline microbiota structures, resulting in less variation in alpha diversity metrics over time. These factors combined may explain the discrepancy between the overall and subgroup-level results.

Additionally, questionnaire results from this study indicated a significant increase in stool volume following personalized granola consumption. In contrast, previous studies on granola consumption have primarily reported increased stool frequency rather than stool volume (Yamauchi et al., 2023). Some studies have reported improvements in constipation symptoms among healthy Japanese women and patients undergoing hemodialysis (Higgins and Johanson, 2004). Given that increased dietary fiber intake can lead to both greater stool volume and higher defecation frequency and may help alleviate constipation (Park and Jhon, 2009; Watanabe et al., 2018), the increase in stool volume observed in this study following personalized granola consumption may serve as a potential intervention for constipation relief, similar to previous studies on granola consumption. However, personalized granola consumption was also associated with increased bloating and gas accumulation. Specifically, 56.99% (53 out of 93 participants) reported abdominal bloating, and 68.81% (64 out of 93 participants) reported a sensation of gas

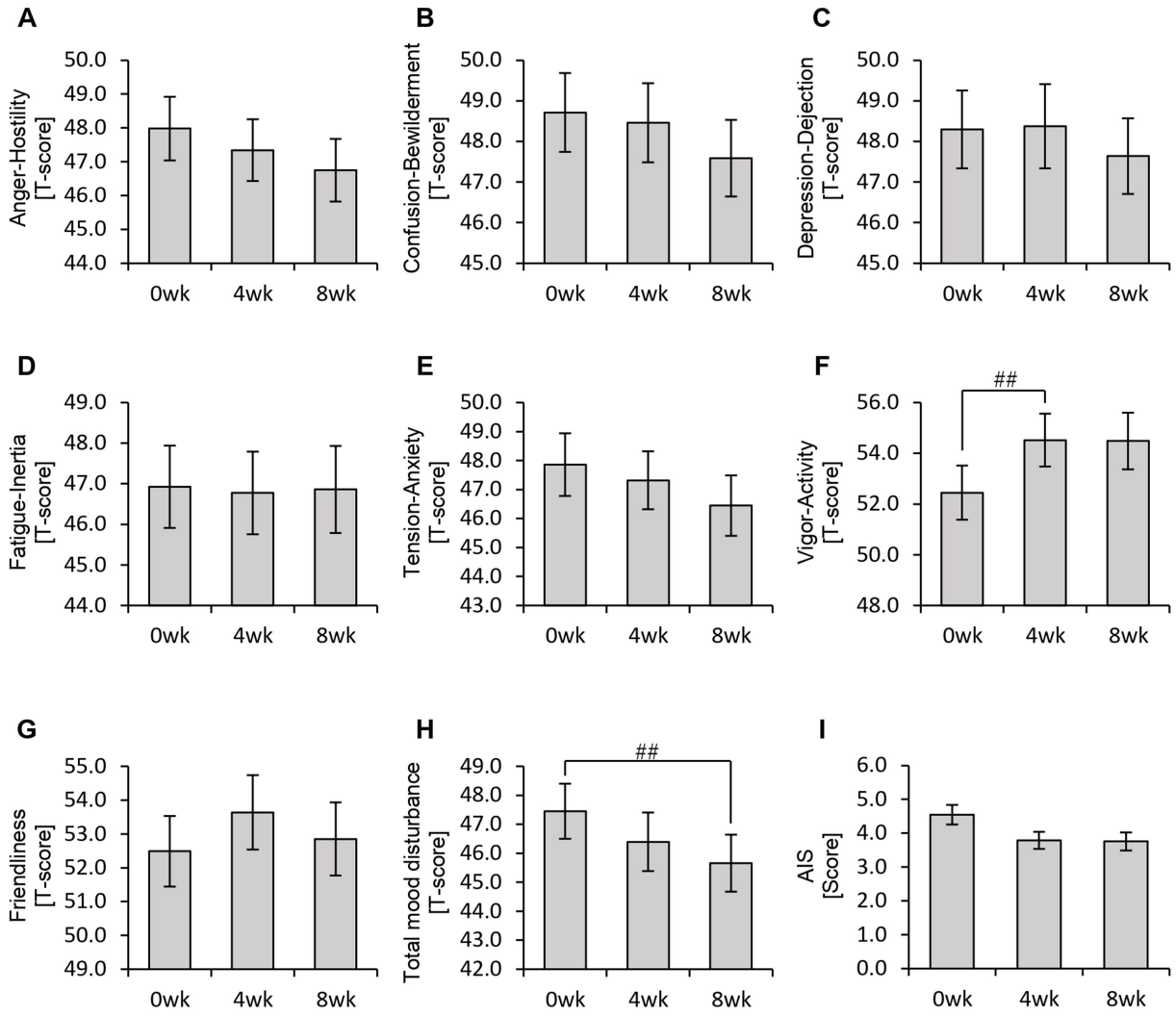

FIGURE 6
Personalized granola consumption may improve total mood disturbances. Summary of scores obtained from answers to each questionnaire in all participants: **(A–H)** POMS2 [Profile of Mood States 2nd edition **(A)** Anger–Hostility scale, **(B)** Confusion–Bewilderment scale, **(C)** Depression–Dejection scale, **(D)** Fatigue–Inertia scale, **(E)** Tension–Anxiety scale, **(F)** Vigor–Activity scale, **(G)** Friendliness scale, and **(H)** Total mood disturbance]. **(I)** AIS (Athens Insomnia Scale). All values are represented as mean ± SEM (n = 93). $^{\#\#}p < 0.01$, evaluated using the Friedman test with Dunn's *post-hoc* test.

accumulation during the intervention period. While indigestible nutrients, such as dietary fiber, can aid in constipation relief, excessive intake has been reported to cause abdominal bloating and gas accumulation (Zhang et al., 2020; Mysonhimer and Holscher, 2022). Most of the prebiotic toppings used in personalized granola contain higher amounts of dietary fiber per gram than standard granola, suggesting that personalized granola may have a greater overall dietary fiber content. Additionally, dietary fiber that is rapidly fermented in the large intestine is sometimes classified as a fermentable dietary fiber (Delcour et al., 2016). Inulin, a common ingredient in personalized granola, is one such fermentable dietary fiber, and *in vitro* studies have shown that inulin fermentation produces more gas compared with that of β-glucan, which is found in oat bran and barley (Carlson et al., 2017). This suggests that the increased fermentation of inulin in the large intestine may contribute to the sensation of abdominal distension. According to the 2023 National Health and Nutrition Survey, the average dietary fiber intake among Japanese individuals was 17.8 g, which falls below the 2025 recommendation of 25 g (Ministry of Health, 2024, 2025). While it remains unclear whether the dietary fiber intake from personalized granola was excessive, it is likely that the increase in fiber consumption contributed to bloating and gas accumulation.

Regarding POMS2, the overall analysis indicated that personalized granola consumption led to an improvement in TMD. Additionally, when examined based on gut microbiota type, improvements were observed across various POMS2 scales. Previous studies have reported that healthy adults with low prebiotic food intake exhibited improvements in TMD scores on POMS2 after an 8-week intervention with high-prebiotic foods (Freijy et al., 2022). These findings align closely with the results of the present study. SCFAs are considered potential role-players through which prebiotics, such as those used in this study, influence mood disturbances. Specifically, butyric acid and propionic acid are believed to act directly on the afferent vagus nerve system, transmitting neural signals to the brain and contributing to

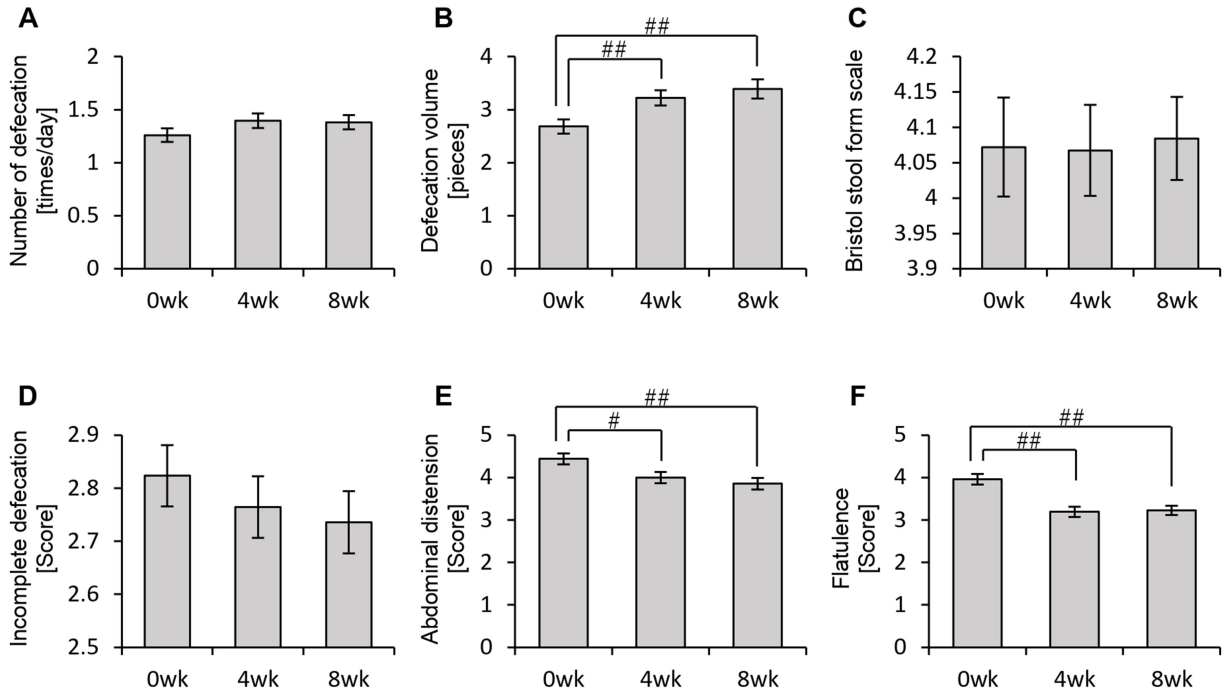

FIGURE 7
Personalized granola consumption can change defecation conditions. The summary of the results of the questionnaire on defecation condition in all participants: **(A)** number of stools per day; **(B)** defecation volume when converted to the number of eggs; **(C)** Bristol stool form scale; **(D)** incomplete defecation; **(E)** abdominal distension; and **(F)** flatulence. All values are represented as mean ± SEM (n = 93). $^{\#\#}p < 0.01$ and $^{\#}p < 0.05$, evaluated using the Friedman test with Dunn's *post-hoc* test.

stress relief (Goswami et al., 2018; Dalile et al., 2019; La Torre et al., 2021). Moreover, SCFAs have been shown to modulate the reactivity of the hypothalamic-pituitary-adrenal (HPA) axis, attenuating the cortisol response to psychosocial stress (Dalile et al., 2020). Additionally, a meta-analysis investigating the effects of dietary interventions on mental health beyond TMD reported that dietary fiber-rich interventions improved depressive symptoms (Firth et al., 2019). However, despite these findings, research on prebiotic interventions remains limited. Recent systematic reviews indicate insufficient evidence supporting the effectiveness of inulin and galacto-oligosaccharides in improving mental health conditions such as depression, bipolar disorder, and schizophrenia (Ribera et al., 2024). Therefore, further investigation is needed to determine whether prebiotic-containing foods, such as those examined in this study, have a beneficial impact on mood states and mental health disorders.

When analyzing the metabolites produced by each gut microbiota type, we observed that different metabolites increased depending on the gut microbiota type. This variation is considered reasonable, as each microbiota type is characterized by distinct dominant bacterial species, and the metabolites produced vary accordingly. However, one common feature among all microbiota types examined in this study was the presence of *Bacteroides* as a dominant bacterial genus. Previous studies have identified propionate as the main metabolic product of *Bacteroides* (Chambers et al., 2019; Aoki et al., 2021), suggesting that propionate levels should have increased across all microbiota types. Contrary to this expectation, no significant increase in propionate was observed. One possible explanation for this finding is that SCFAs produced in the gut are rapidly absorbed into the bloodstream (Kaji et al., 2015). Additionally, cross-feeding interactions between gut bacteria may play a role. Cross-feeding refers to a symbiotic relationship in which metabolites produced by one bacterial species serve as nutrients for another (Culp and Goodman, 2023). Among SCFAs, acetic acid, butyric acid, and propionic acid are often considered as the final metabolic products (Culp and Goodman, 2023). However, acetic acid can also serve as a precursor, stimulating the growth of butyrate-producing bacteria, thereby promoting butyrate production (Barcenilla et al., 2000; Duncan et al., 2004). Additionally, acetic acid and propionic acid produced by *Veillonella* may be utilized by other symbiotic bacteria to support their growth (Zhang et al., 2024). These findings suggest that increases in specific bacterial species are not solely dictated by direct associations with specific metabolite production. Instead, gut microbiota composition and metabolic output are influenced by complex cross-feeding interactions. Although *Bacteroides* was present in all microbiota types in this study, the metabolites produced varied, likely depending on the presence of other bacterial genera, such as *Blautia*, *Faecalibacterium*, and *Bifidobacterium*. Owing to the highly complex nature of microbial interactions, further studies should focus on a broader range of bacterial species, beyond the six genera used in this study to define personalized granola composition, to better elucidate these relationships. Despite the complexity of metabolite production, an increase in *Bifidobacterium* abundance was observed in most microbiota types examined in this study. Indeed, previous studies have reported that inulin, a prebiotic associated with *Bacteroides* as defined in this study, promotes the growth of *Bifidobacterium* (Costabile et al., 2010; Petry et al., 2012; Birkeland et al., 2020). However, no clear explanation for the discrepancy between bacterial abundance and metabolite production currently exists, that is, while the relative

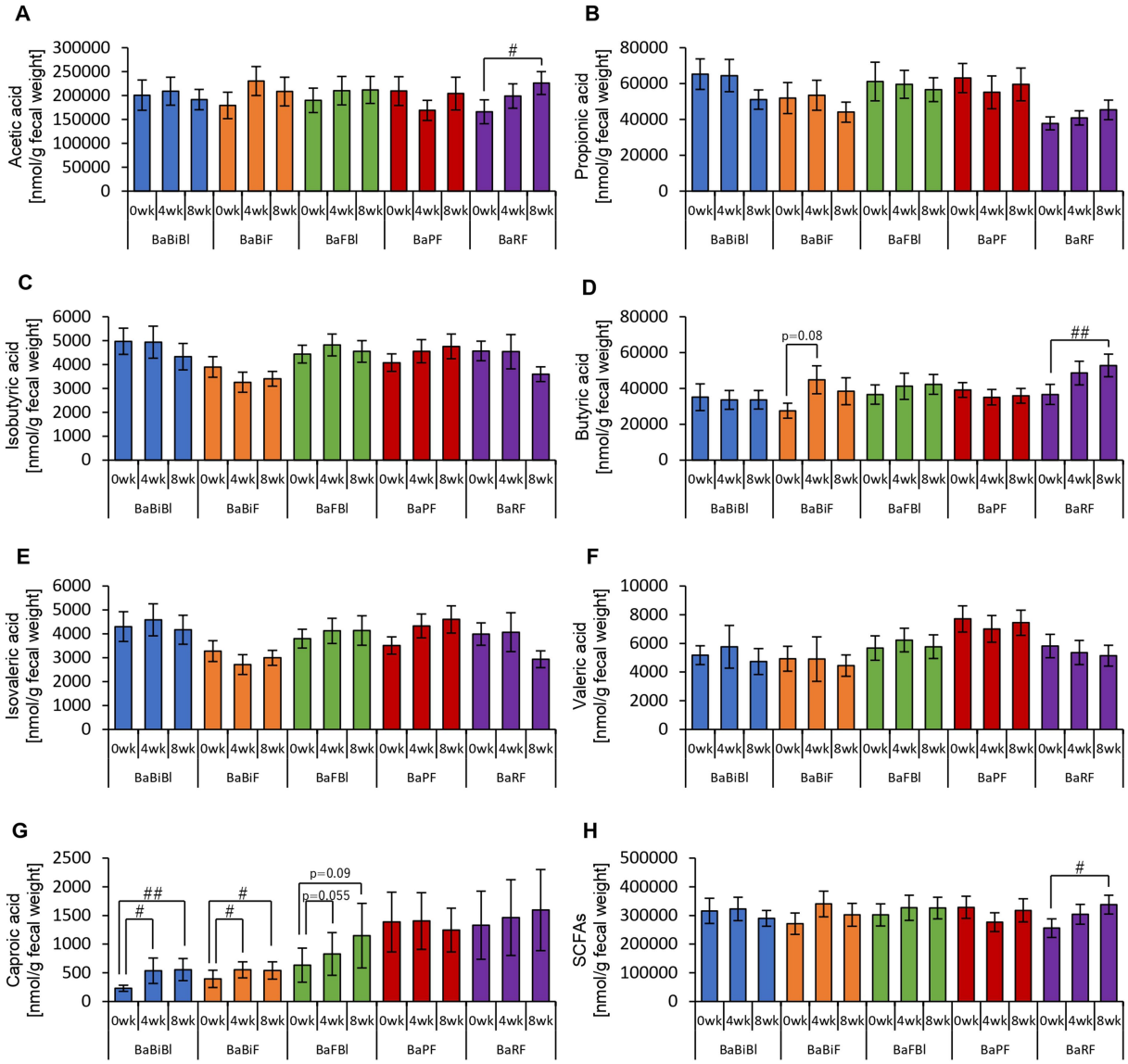

FIGURE 8
Personalized granola intake increases SCFAs that differ depending on the type of gut microbiota. SCFA production by each type of gut microbiota: **(A)** acetic acid, **(B)** propionic acid, **(C)** isobutyric acid, **(D)** butyric acid, **(E)** isovaleric acid, **(F)** valeric acid, **(G)** caproic acid, and **(H)** SCFAs [the sum of **(A)** through **(G)**]. All values are represented as mean ± SEM (BaBiBl type: n = 19, BaBiF type: n = 20, BaFBl type: n = 18, BaPF type: n = 19, and BaRF type: n = 17). $^{\#\#}p < 0.01$ and $^{\#}p < 0.05$, evaluated using the Friedman test with Dunn's *post-hoc* test to compare between weeks within the gut microbiota type.

abundance of certain bacterial genera increases, the expected concomitant increase in specific metabolites is not consistently observed.

In this study, we observed a tendency for *Bacteroides* and *Faecalibacterium* to decrease following the intervention (Figures 5A,B). While the exact mechanisms remain unclear, one possible explanation is that the bacterial abundance was expressed in relative terms, and the significant increase in *Bifidobacterium* may have led to an apparent decrease in other genera. In compositional data analysis, such changes do not necessarily indicate an actual decline in bacterial load but rather a shift in the proportion of different taxa within the microbial community. Future studies incorporating absolute quantification methods (e.g., qPCR) are warranted to clarify whether these shifts reflect true reductions or relative effects due to the expansion of other bacterial taxa. Additionally, a previous study has reported that dietary intake of prebiotic-containing granola significantly decreased *Bacteroides* abundance (Sasaki et al., 2025), suggesting that certain prebiotic components in our formulation might have contributed to the observed reduction.

This study has certain limitations. The first limitation concerns the definition used to create personalized granola. In this study, we selected six bacterial genera and their corresponding prebiotic toppings based on previous research. However, the relationship between gut bacteria and prebiotics is not strictly one-to-one. In other words, a single prebiotic topping may stimulate metabolic activity in multiple bacterial species, leading to increased metabolite production. For instance, as discussed earlier, inulin not only increases the relative abundance of *Bifidobacterium* but also affects *Bacteroides* and may

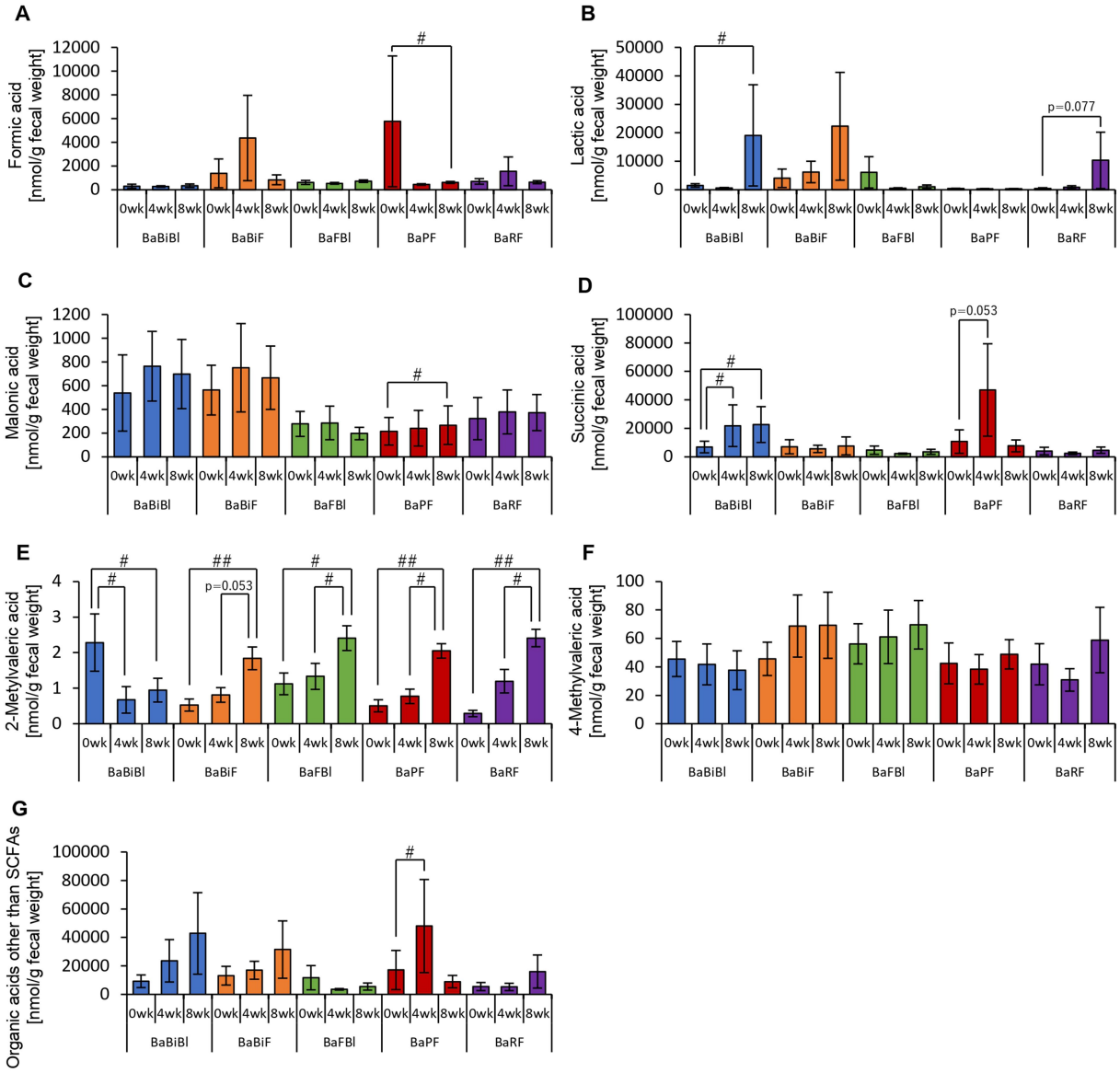

FIGURE 9
Personalized granola consumption increases organic acids other than SCFAs that differ depending on the type of gut microbiota. Organic acid production based on each type of gut microbiota in all subjects. **(A)** Formic acid, **(B)** lactic acid, **(C)** malonic acid, **(D)** succinic acid, **(E)** 2-methylvaleric acid, **(F)** 4-methylvaleric acid, **(G)** organic acids other than SCFAs [the sum of **(A)** through **(F)**]. All values are represented as mean ± SEM (BaBiBl type: n = 19, BaBiF type: n = 20, BaFBl type: n = 18, BaPF type: n = 19, BaRF type: n = 17). $^{\#\#}p < 0.01$ and $^{\#}p < 0.05$, evaluated using the Friedman test with Dunn's *post-hoc* test to compare between weeks within the gut microbiota type.

contribute to SCFA production (Birkeland et al., 2020). Additionally, in this study, prebiotic toppings were selected based on their compatibility with the granola formulation. However, to further optimize precision nutrition, it may be necessary to explore a broader range of ingredients. In this study, the gut microbiota type was determined based on the top three bacterial genera out of six candidate genera. However, there is no clear rationale for selecting only the top three. Future studies should explore alternative methods for defining gut microbiota types, potentially considering a broader range of bacterial species or different classification criteria. Furthermore, the selection of prebiotic toppings based on genus-level abundance assumes that the identified bacteria will actively metabolize the assigned prebiotic *in vivo*. While this assumption was grounded in prior *in vitro* and *in vivo* studies, the actual functionality and response may vary between individuals. Future studies should consider incorporating functional validation (e.g., metabolite response testing or *in vitro* fermentation assays) to confirm the appropriateness of personalized combinations. Additionally, baseline SCFA levels at the start of the experiment may also play a crucial role. In this study, when analyzing the correlation between initial metabolite levels (week 0) and changes in those metabolites over time (week 8 vs. week 0), a significant negative correlation was observed for most metabolic substances (Supplementary Figure 4). In other words, individuals with higher baseline metabolite levels tended to experience greater increases in metabolite production after consuming granola. Given this finding, pre-experiment metabolite measurement and

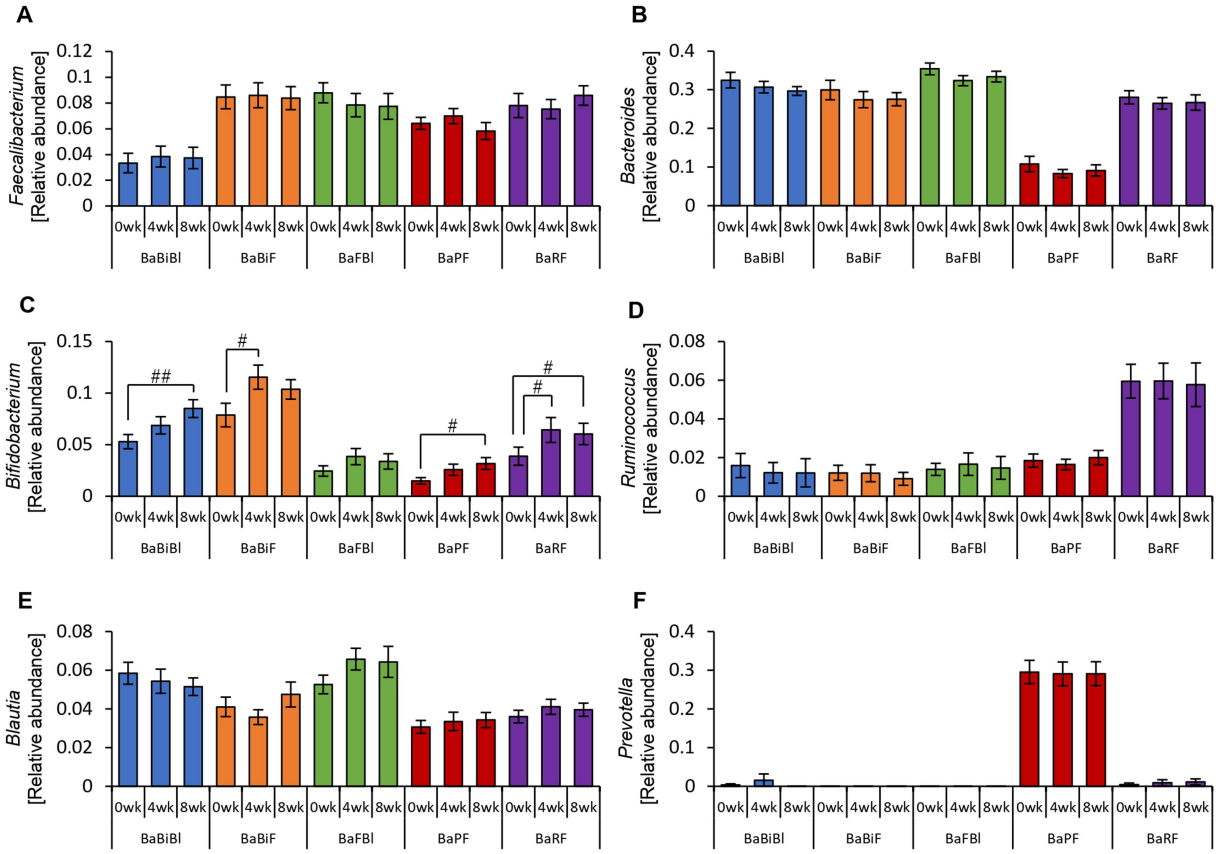

FIGURE 10
Bifidobacterium was altered in most gut microbiota types based on the consumption of personalized granola. The relative abundance of six bacteria at the genus level according to gut microbiota types: **(A)** *Faecalibacterium*, **(B)** *Bacteroides*, **(C)** *Bifidobacterium*, **(D)** *Ruminococcus*, **(E)** *Blautia*, and **(F)** *Prevotella*. All values are represented as mean ± SEM (BaBiBl type: $n = 19$, BaBiF type: $n = 20$, BaFBl type: $n = 18$, BaPF type: $n = 19$, and BaRF type: $n = 17$). $^{\#\#}p < 0.01$ and $^{\#}p < 0.05$, evaluated using the Friedman test with Dunn's *post-hoc* test to compare between weeks within the gut microbiota type.

classification may be necessary. Establishing specific criteria for baseline metabolite levels and stratifying participants accordingly could allow the formulation of tailored granola interventions based on individual metabolic profiles. Moving forward, gut microbiota classification should not rely solely on bacterial composition but should incorporate multiple perspectives, including metabolic activity and other host factors, to refine precision nutrition strategies. The second limitation concerns the study design. This study employed a single-group before-and-after comparison, which has the advantage of minimizing individual differences by comparing participants to themselves. However, this design does not fully account for potential placebo effects and psychological expectations. To address this limitation, future research should implement a randomized, double-blind study with two groups: an intervention group consuming granola containing three prebiotic toppings tailored to their gut microbiota type and a control group consuming granola with three prebiotic toppings that do not match their gut microbiota type. Such a study design would allow for a more rigorous evaluation of whether matching dietary interventions to gut microbiota type is essential for optimizing health outcomes. Furthermore, this study did not include a control group consuming the base granola without any prebiotic toppings. As a result, it is not possible to distinguish whether the observed effects were due to the base granola itself or to the addition of specific prebiotics. Although we previously conducted a separate study in which participants consumed the same base granola without prebiotic toppings, and observed that individuals with a high abundance of *Prevotella 9* showed an increase in SCFA levels (Yamauchi et al., 2023), that study did not allow for the direct comparison between base granola and personalized prebiotic formulations. Therefore, future studies should consider including both a base granola-only control group and a personalized prebiotic group to more rigorously isolate the independent and combined effects of base granola and prebiotic additions on gut microbiota and metabolic outcomes. The third limitation is that dietary intake was not fully controlled. Participants were instructed not to increase their alcohol or probiotic supplement intake beyond their usual levels and to avoid making major dietary changes during the study period. However, their overall diet was not standardized, meaning that individual dietary habits may have influenced the results. In addition, although dietary intake was monitored using the "Calomama" app, participants did not consistently log all meals, and the recorded data showed signs of underreporting. As a result, the calculated values for energy and nutrient intake were considered unreliable and were not included in the final analysis. This lack of accurate dietary data limits our ability to adjust for potential dietary confounders in interpreting the study results. Additionally, 38 out of 93 participants reported consuming

10.3389/fmicb.2025.1607918

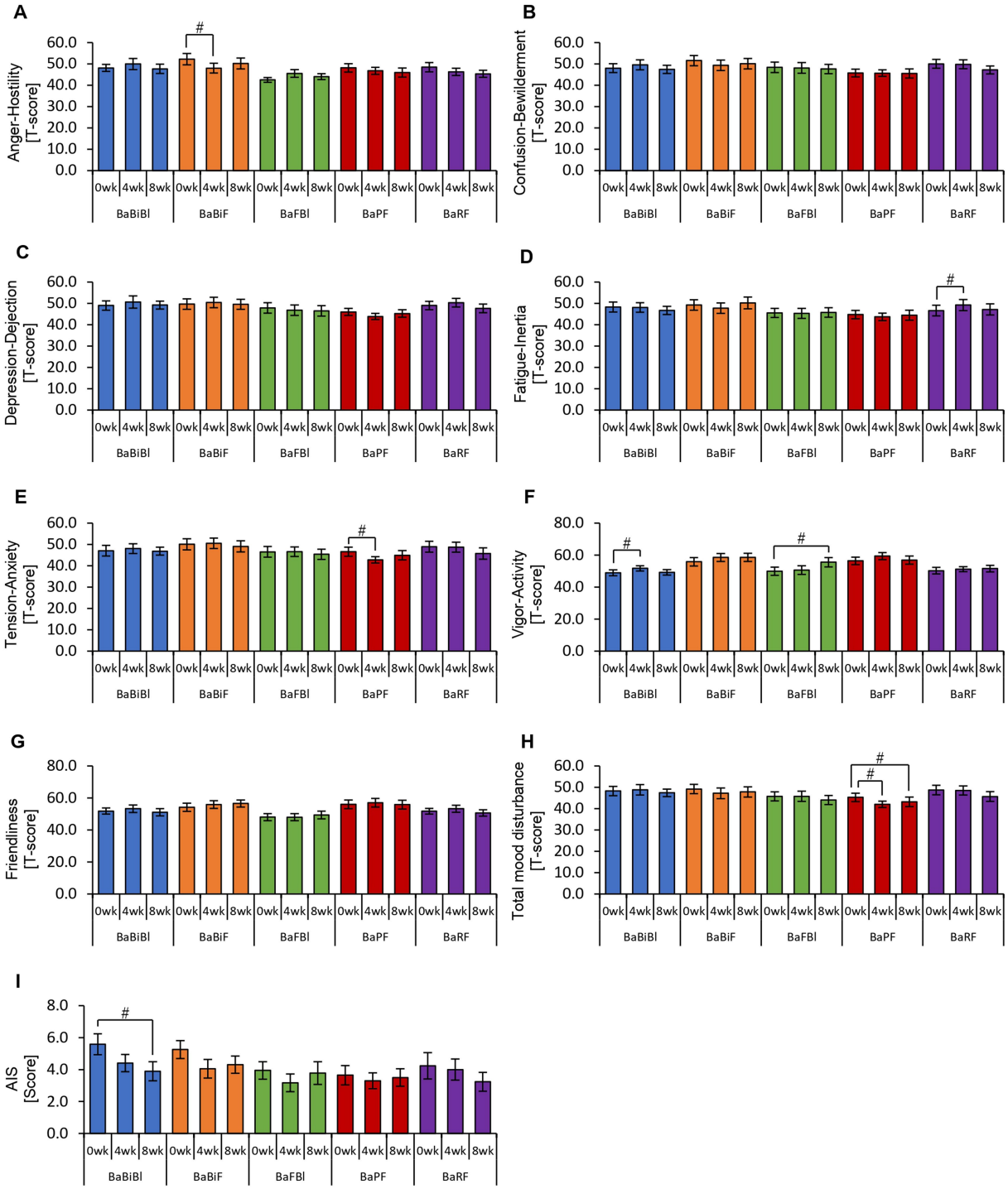

FIGURE 11
Personalized granola consumption causes changes in mood states that differ depending on the type of gut microbiota. Summary of scores obtained from answers to each questionnaire according to gut microbiota types: **(A–H)** POMS2 [Profile of Mood States 2nd edition **(A)** Anger–Hostility scale, **(B)** Confusion–Bewilderment scale, **(C)** Depression–Dejection scale, **(D)** Fatigue–Inertia scale, **(E)** Tension–Anxiety scale, **(F)** Vigor–Activity scale, **(G)** Friendliness scale, and **(H)** Total mood disturbance]. **(I)** AIS (Athens Insomnia Scale). All values are represented as mean ± SEM (BaBiBl type: n = 19, BaBiF type: n = 20, BaFBl type: n = 18, BaPF type: n = 19, and BaRF type: n = 17). $^{\#\#}p < 0.01$ and $^{\#}p < 0.05$, evaluated using the Friedman test with Dunn's *post-hoc* test to compare between weeks within the gut microbiota type.

probiotic-containing foods (such as yogurt, fermented milk beverages, cheese, and natto) during the study period. Although we did not restrict probiotic food intake, participants were instructed to maintain their usual consumption habits and avoid major dietary changes. Therefore, while the influence of probiotic intake on gut microbiota cannot be entirely ruled out, we believe its impact was limited, especially since baseline microbiota compositions were measured and used as the reference for each participant's outcome evaluation. To

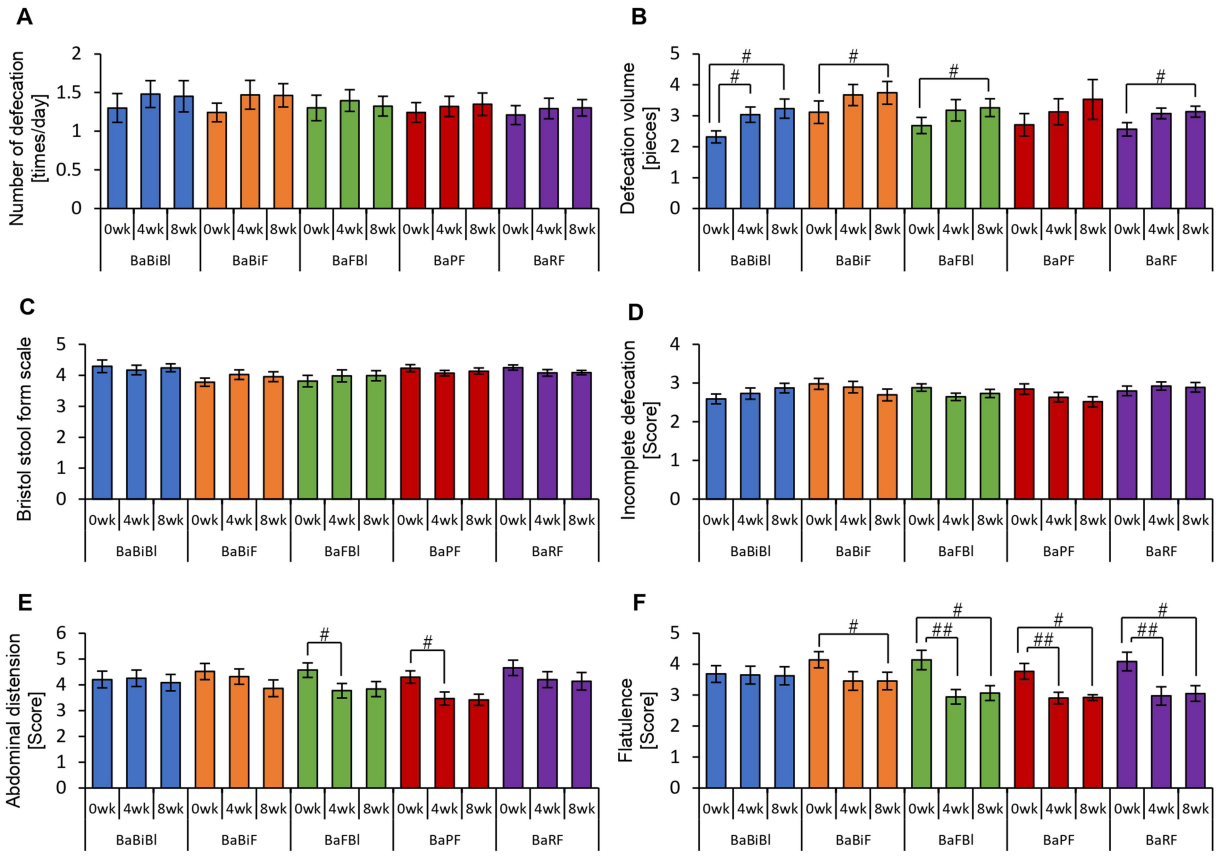

FIGURE 12
Consumption of personalized granola may increase the defecation volume in any gut microbiota type. The summary of the results of a questionnaire on defecation condition according to gut microbiota types: **(A)** number of stools per day; **(B)** defecation volume when converted to the number of eggs; **(C)** Bristol stool form scale; **(D)** incomplete defecation; **(E)** abdominal distension; and **(F)** flatulence. All values are represented as mean ± SEM (BaBiBl type: $n = 19$, BaBiF type: $n = 20$, BaFBl type: $n = 18$, BaPF type: $n = 19$, and BaRF type: $n = 17$). $^{\#\#}p < 0.01$ and $^{\#}p < 0.05$, evaluated using the Friedman test with Dunn's *post-hoc* test to compare between weeks within the gut microbiota type.

further evaluate the influence of probiotic-containing foods on the increase in *Bifidobacterium*, we conducted a subgroup analysis comparing participants who consumed probiotics during the intervention period ($n = 38$) and those who did not ($n = 55$). As shown in Supplementary Figure 5, a significant increase in *Bifidobacterium* was observed in both groups, indicating that the personalized granola itself likely played a dominant role in promoting *Bifidobacterium* growth. Therefore, while we cannot fully rule out the potential confounding effects of probiotics, these results suggest that their influence was limited in this study. Additionally, while participants were asked to maintain a consistent meal timing, the exact time of food intake was not strictly controlled. Previous studies have shown that the gut microbiota follows a circadian rhythm, which is influenced by meal timing and fasting duration (Thaiss et al., 2014; Sasaki et al., 2019). Thus, a later-than-usual dinner or a shorter fasting period before breakfast could potentially affect gut microbiota composition and SCFA production. Next, unmeasured and uncontrolled confounding factors may have impacted the study outcomes. Gut microbiota composition and SCFA production are influenced by multiple variables, including exercise, sleep, and social factors such as work-related stress and marital status. These factors should be taken into account when interpreting the results, as they may introduce potential biases. Finally, we note that psychological and bowel-related outcomes were assessed using self-administered questionnaires, including the AIS and POMS2. Although these instruments are validated, self-reported data are inherently subject to potential biases such as recall bias, reporting inaccuracy, or social desirability bias. While participants were instructed to respond as truthfully as possible and were assured of confidentiality, these biases cannot be entirely ruled out and should be considered when interpreting the results.

In this study, gut microbiota types were classified based on gut microbiota composition, and participants consumed personalized granola containing prebiotics tailored to their bacterial type. As a result, different microbiota types exhibited distinct metabolite production patterns, and a significant increase in *Bifidobacterium* abundance was observed. Additionally, participants reported a significant increase in stool volume, and total mood disturbance (TMD) scores from the POMS2 questionnaire significantly improved, indicating beneficial effects on both bowel function and mental health. In terms of microbial metabolites, levels of caproic acid and formic acid showed significant changes over the eight-week intervention. These findings suggest that personalized granola, formulated according to individual gut microbiota types, can effectively promote beneficial bacterial growth, enhance metabolite production, and improve physiological and psychological outcomes.

Data availability statement

The datasets presented in this study can be found in the Figshare repository at the following link: https://dx.doi.org/10.6084/m9.figshare.29554772.

Ethics statement

The studies involving humans were conducted in accordance with the principles of the Declaration of Helsinki and approved by the Ethics Review Committee of the Chiyoda Paramedical Care Clinic (Approval Number: 15000088). The studies were conducted in accordance with the local legislation and institutional requirements. The participants provided their written informed consent to participate in this study.

Author contributions

HS: Formal analysis, Investigation, Visualization, Writing – original draft. HM: Conceptualization, Formal analysis, Investigation, Writing – review & editing. YY: Data curation, Formal analysis, Investigation, Writing – review & editing. KI: Conceptualization, Writing – review & editing. SF: Conceptualization, Writing – review & editing.

Funding

The author(s) declare that financial support was received for the research and/or publication of this article. This research was funded by Calbee Inc.

Acknowledgments

The authors would like to express their appreciation to the subjects who participated in the study.

Conflict of interest

The authors declare that this study received funding from Calbee Inc. The funder had the following involvement in the study: data analysis, interpretation of data, writing of this article.

HS, HM, and KI were employed by Calbee, Inc. YY and SF were employed by Metagen, Inc.

Generative AI statement

The authors declare that no Gen AI was used in the creation of this manuscript.

Publisher's note

All claims expressed in this article are solely those of the authors and do not necessarily represent those of their affiliated organizations, or those of the publisher, the editors and the reviewers. Any product that may be evaluated in this article, or claim that may be made by its manufacturer, is not guaranteed or endorsed by the publisher.

Supplementary material

The Supplementary material for this article can be found online at: https://www.frontiersin.org/articles/10.3389/fmicb.2025.1607918/full#supplementary-material

References

Abell, G. C., Cooke, C. M., Bennett, C. N., Conlon, M. A., and Mcorist, A. L. (2008). Phylotypes related to *Ruminococcus bromii* are abundant in the large bowel of humans and increase in response to a diet high in resistant starch. *FEMS Microbiol. Ecol.* 66, 505–515. doi: 10.1111/j.1574-6941.2008.00527.x

Agrawal, P., Kaur, J., Singh, J., Rasane, P., Sharma, K., Bhadariya, V., et al. (2024). Genetics, nutrition, and health: a new frontier in disease prevention. *J. Am. Nutr. Assoc.* 43, 326–338. doi: 10.1080/27697061.2023.2284997

Antwi, J. (2023). Precision nutrition to improve risk factors of obesity and type 2 diabetes. *Curr. Nutr. Rep.* 12, 679–694. doi: 10.1007/s13668-023-00491-y

Aoki, R., Onuki, M., Hattori, K., Ito, M., Yamada, T., Kamikado, K., et al. (2021). Commensal microbe-derived acetate suppresses NAFLD/NASH development via hepatic FFAR2 signalling in mice. *Microbiome* 9:188. doi: 10.1186/s40168-021-01125-7

Barber, C., Sabater, C., Ávila-Gálvez, M., Vallejo, F., Bendezu, R. A., Guérin-Deremaux, L., et al. (2022). Effect of resistant dextrin on intestinal gas homeostasis and microbiota. *Nutrients* 14:4611. doi: 10.3390/nu14214611

Barcenilla, A., Pryde, S. E., Martin, J. C., Duncan, S. H., Stewart, C. S., Henderson, C., et al. (2000). Phylogenetic relationships of butyrate-producing bacteria from the human gut. *Appl. Environ. Microbiol.* 66, 1654–1661. doi: 10.1128/AEM.66.4.1654-1661.2000

Birkeland, E., Gharagozlian, S., Birkeland, K. I., Valeur, J., Måge, I., Rud, I., et al. (2020). Prebiotic effect of inulin-type fructans on faecal microbiota and short-chain fatty acids in type 2 diabetes: a randomised controlled trial. *Eur. J. Nutr.* 59, 3325–3338. doi: 10.1007/s00394-020-02282-5

Bolyen, E., Rideout, J. R., Dillon, M. R., Bokulich, N. A., Abnet, C. C., Al-Ghalith, G. A., et al. (2019). Reproducible, interactive, scalable and extensible microbiome data science using QIIME 2. *Nat. Biotechnol.* 37, 852–857. doi: 10.1038/s41587-019-0209-9

Callahan, B. J., Mcmurdie, P. J., Rosen, M. J., Han, A. W., Johnson, A. J., and Holmes, S. P. (2016). DADA2: high-resolution sample inference from Illumina amplicon data. *Nat. Methods* 13, 581–583. doi: 10.1038/nmeth.3869

Carlson, J. L., Erickson, J. M., Hess, J. M., Gould, T. J., and Slavin, J. L. (2017). Prebiotic dietary fiber and gut health: comparing the *in vitro* fermentations of beta-glucan, inulin and xylooligosaccharide. *Nutrients* 9:1361. doi: 10.3390/nu9121361

Chambers, E. S., Byrne, C. S., Morrison, D. J., Murphy, K. G., Preston, T., Tedford, C., et al. (2019). Dietary supplementation with inulin-propionate ester or inulin improves insulin sensitivity in adults with overweight and obesity with distinct effects on the gut microbiota, plasma metabolome and systemic inflammatory responses: a randomised cross-over trial. *Gut* 68, 1430–1438. doi: 10.1136/gutjnl-2019-318424

Chambers, E. S., Preston, T., Frost, G., and Morrison, D. J. (2018). Role of gut microbiota-generated short-chain fatty acids in metabolic and cardiovascular health. *Curr. Nutr. Rep.* 7, 198–206. doi: 10.1007/s13668-018-0248-8

Costabile, A., Kolida, S., Klinder, A., Gietl, E., Bäuerlein, M., Frohberg, C., et al. (2010). A double-blind, placebo-controlled, cross-over study to establish the bifidogenic effect of a very-long-chain inulin extracted from globe artichoke (*Cynara scolymus*) in healthy human subjects. *Br. J. Nutr.* 104, 1007–1017. doi: 10.1017/S0007114510001571

Culp, E. J., and Goodman, A. L. (2023). Cross-feeding in the gut microbiome: ecology and mechanisms. *Cell Host Microbe* 31, 485–499. doi: 10.1016/j.chom.2023.03.016

Dalile, B., Van Oudenhove, L., Vervliet, B., and Verbeke, K. (2019). The role of short-chain fatty acids in microbiota-gut-brain communication. *Nat. Rev. Gastroenterol. Hepatol.* 16, 461–478. doi: 10.1038/s41575-019-0157-3

Dalile, B., Vervliet, B., Bergonzelli, G., Verbeke, K., and Van Oudenhove, L. (2020). Colon-delivered short-chain fatty acids attenuate the cortisol response to psychosocial stress in healthy men: a randomized, placebo-controlled trial. *Neuropsychopharmacology* 45, 2257–2266. doi: 10.1038/s41386-020-0732-x

David, L. A., Materna, A. C., Friedman, J., Campos-Baptista, M. I., Blackburn, M. C., Perrotta, A., et al. (2014). Host lifestyle affects human microbiota on daily timescales. *Genome Biol.* 15:R89. doi: 10.1186/gb-2014-15-7-r89

Delcour, J. A., Aman, P., Courtin, C. M., Hamaker, B. R., and Verbeke, K. (2016). Prebiotics, fermentable dietary fiber, and health claims. *Adv. Nutr.* 7, 1–4. doi: 10.3945/an.115.010546

Duncan, S. H., Holtrop, G., Lobley, G. E., Calder, A. G., Stewart, C. S., and Flint, H. J. (2004). Contribution of acetate to butyrate formation by human faecal bacteria. *Br. J. Nutr.* 91, 915–923. doi: 10.1079/BJN20041150

Fehlbaum, S., Prudence, K., Kieboom, J., Heerikhuisen, M., van den Broek, T., Schuren, F. H. J., et al. (2018). *In vitro* fermentation of selected prebiotics and their effects on the composition and activity of the adult gut microbiota. *Int. J. Mol. Sci.* 19:3097. doi: 10.3390/ijms19103097

Firth, J., Marx, W., Dash, S., Carney, R., Teasdale, S. B., Solmi, M., et al. (2019). The effects of dietary improvement on symptoms of depression and anxiety: a meta-analysis of randomized controlled trials. *Psychosom. Med.* 81, 265–280. doi: 10.1097/PSY.0000000000000673

Freijy, T. M., Cribb, L., Oliver, G., Metri, N. J., Opie, R. S., Jacka, F. N., et al. (2022). Effects of a high-prebiotic diet versus probiotic supplements versus synbiotics on adult mental health: the "gut feelings" randomised controlled trial. *Front. Neurosci.* 16:1097278. doi: 10.3389/fnins.2022.1097278

Goswami, C., Iwasaki, Y., and Yada, T. (2018). Short-chain fatty acids suppress food intake by activating vagal afferent neurons. *J. Nutr. Biochem.* 57, 130–135. doi: 10.1016/j.jnutbio.2018.03.009

Hashimoto, A., Kawamura, N., Tarusawa, E., Takeda, I., Aoyama, Y., Ohno, N., et al. (2023). Microglia enable cross-modal plasticity by removing inhibitory synapses. *Cell Rep.* 42:112383. doi: 10.1016/j.celrep.2023.112383

Healey, G., Murphy, R., Butts, C., Brough, L., Whelan, K., and Coad, J. (2018). Habitual dietary fibre intake influences gut microbiota response to an inulin-type fructan prebiotic: a randomised, double-blind, placebo-controlled, cross-over, human intervention study. *Br. J. Nutr.* 119, 176–189. doi: 10.1017/S0007114517003440

Higgins, P. D., and Johanson, J. F. (2004). Epidemiology of constipation in North America: a systematic review. *Am. J. Gastroenterol.* 99, 750–759. doi: 10.1111/j.1572-0241.2004.04114.x

Kaji, I., Iwanaga, T., Watanabe, M., Guth, P. H., Engel, E., Kaunitz, J. D., et al. (2015). SCFA transport in rat duodenum. *Am. J. Physiol. Gastrointest. Liver Physiol.* 308, G188–G197. doi: 10.1152/ajpgi.00298.2014

Koh, A., De Vadder, F., Kovatcheva-Datchary, P., and Bäckhed, F. (2016). From dietary fiber to host physiology: short-chain fatty acids as key bacterial metabolites. *Cell* 165, 1332–1345. doi: 10.1016/j.cell.2016.05.041

Kolodziejczyk, A. A., Zheng, D., and Elinav, E. (2019). Diet-microbiota interactions and personalized nutrition. *Nat. Rev. Microbiol.* 17, 742–753. doi: 10.1038/s41579-019-0256-8

Korpela, K., Flint, H. J., Johnstone, A. M., Lappi, J., Poutanen, K., Dewulf, E., et al. (2014). Gut microbiota signatures predict host and microbiota responses to dietary interventions in obese individuals. *PLoS One* 9:e90702. doi: 10.1371/journal.pone.0090702

Kovatcheva-Datchary, P., Nilsson, A., Akrami, R., Lee, Y. S., De Vadder, F., Arora, T., et al. (2015). Dietary fiber-induced improvement in glucose metabolism is associated with increased abundance of *Prevotella*. *Cell Metab.* 22, 971–982. doi: 10.1016/j.cmet.2015.10.001

Kyo, H., Hasebe, H., Ishihara, K., Ito, M., Uebaba, K., and Suzuki, N. (2017). Effects of the intake of fruits granola on defecation and quality of life. *Jpn. J. Complement. Altern. Med.* 14, 23–26. doi: 10.1625/jcam.14.23

La Torre, D., Verbeke, K., and Dalile, B. (2021). Dietary fibre and the gut-brain axis: microbiota-dependent and independent mechanisms of action. *Gut Microbiome* 2:e3. doi: 10.1017/gmb.2021.3

Lange, O., Proczko-Stepaniak, M., and Mika, A. (2023). Short-chain fatty acids-a product of the microbiome and its participation in two-way communication on the microbiome-host mammal line. *Curr. Obes. Rep.* 12, 108–126. doi: 10.1007/s13679-023-00503-6

Liu, F., Li, P., Chen, M., Luo, Y., Prabhakar, M., Zheng, H., et al. (2017). Fructooligosaccharide (FOS) and galactooligosaccharide (GOS) increase *Bifidobacterium* but reduce butyrate producing bacteria with adverse glycemic metabolism in healthy young population. *Sci. Rep.* 7:11789. doi: 10.1038/s41598-017-10722-2

Marchesi, J. R., Adams, D. H., Fava, F., Hermes, G. D., Hirschfield, G. M., Hold, G., et al. (2016). The gut microbiota and host health: a new clinical frontier. *Gut* 65, 330–339. doi: 10.1136/gutjnl-2015-309990

Matsumoto, Y., Sasaki, H., Masutomi, H., Ishihara, K., Shibata, S., Hirao, K., et al. (2023). Effects of additional granola in children's breakfast on nutritional balance, sleep and defecation: an open-label randomized cross-over trial. *Children* 10:779. doi: 10.3390/children10050779

Mcnair, D. M., and Heuchert, J. P. (2012). Profile of mood states, POMS2. North Tonawanda, N.Y: Multi-Health Systems Inc.

Ministry of Health. (2024). The National Health and Nutrition Survey in Japan, 2023. Available at: https://www.mhlw.go.jp/stf/seisakunitsuite/bunya/kenkou_iryou/kenkou/eiyou/r5-houkoku_00001.html (Accessed June 17, 2025)

Ministry of Health. (2025). Dietary Reference Intakes for Japanese, 2025. Available at: https://www.mhlw.go.jp/stf/newpage_44138.html (Accessed June 17, 2025)

Mysonhimer, A. R., and Holscher, H. D. (2022). Gastrointestinal effects and tolerance of nondigestible carbohydrate consumption. *Adv. Nutr.* 13, 2237–2276. doi: 10.1093/advances/nmac094

Nagasawa, H., Suzuki, S., Kobayashi, T., Otsuka, T., Okuma, T., Matsushita, S., et al. (2024). Effect of fruits granola (Frugra®) consumption on blood pressure reduction and intestinal microbiome in patients undergoing hemodialysis. *Hypertens. Res.* 47, 3214–3224. doi: 10.1038/s41440-024-01895-1

Nagasawa, H., Ueda, S., Otsuka, T., Kaifu, K., Ono, S., Okuma, T., et al. (2021). Safety and efficacy of using cereal food (Frugra®) to improve blood pressure and bowel health in patients undergoing chronic hemodialysis: a pilot study. *J. Pharmacol. Sci.* 147, 132–137. doi: 10.1016/j.jphs.2021.06.007

Overby, H. B., and Ferguson, J. F. (2021). Gut microbiota-derived short-chain fatty acids facilitate microbiota:host cross talk and modulate obesity and hypertension. *Curr. Hypertens. Rep.* 23:8. doi: 10.1007/s11906-020-01125-2

Park, E. J., and Jhon, D. Y. (2009). Effects of bamboo shoot consumption on lipid profiles and bowel function in healthy young women. *Nutrition* 25, 723–728. doi: 10.1016/j.nut.2009.01.007

Petry, N., Egli, I., Chassard, C., Lacroix, C., and Hurrell, R. (2012). Inulin modifies the bifidobacteria population, fecal lactate concentration, and fecal pH but does not influence iron absorption in women with low iron status. *Am. J. Clin. Nutr.* 96, 325–331. doi: 10.3945/ajcn.112.035717

Quast, C., Pruesse, E., Yilmaz, P., Gerken, J., Schweer, T., Yarza, P., et al. (2013). The SILVA ribosomal RNA gene database project: improved data processing and web-based tools. *Nucleic Acids Res.* 41, D590–D596. doi: 10.1093/nar/gks1219

Resende, W. R., Valvassori, S. S., Réus, G. Z., Varela, R. B., Arent, C. O., Ribeiro, K. F., et al. (2013). Effects of sodium butyrate in animal models of mania and depression: implications as a new mood stabilizer. *Behav. Pharmacol.* 24, 569–579. doi: 10.1097/FBP.0b013e32836546fc

Ribera, C., Sánchez-Ortí, J. V., Clarke, G., Marx, W., Mörkl, S., and Balanzá-Martínez, V. (2024). Probiotic, prebiotic, synbiotic and fermented food supplementation in psychiatric disorders: a systematic review of clinical trials. *Neurosci. Biobehav. Rev.* 158:105561. doi: 10.1016/j.neubiorev.2024.105561

Sasaki, H., Masutomi, H., Nakamura, S., Tanigawa, C., Cui, Y., Ishihara, K., et al. (2025). Granola consumption with multiple prebiotics in Japanese participants increases *Bifidobacterium* abundance and improves stress and subjective sleepiness. *Front. Nutr.* 12:1551313. doi: 10.3389/fnut.2025.1551313

Sasaki, H., Miyakawa, H., Watanabe, A., Nakayama, Y., Lyu, Y., Hama, K., et al. (2019). Mice microbiota composition changes by inulin feeding with a long fasting period under a two-meals-per-day schedule. *Nutrients* 11:2802. doi: 10.3390/nu11112802

Scott, K. P., Martin, J. C., Duncan, S. H., and Flint, H. J. (2014). Prebiotic stimulation of human colonic butyrate-producing bacteria and bifidobacteria, *in vitro*. *FEMS Microbiol. Ecol.* 87, 30–40. doi: 10.1111/1574-6941.12186

Shin, J. H., Kim, C. S., Cha, J., Kim, S., Lee, S., Chae, S., et al. (2022). Consumption of 85% cocoa dark chocolate improves mood in association with gut microbial changes in healthy adults: a randomized controlled trial. *J. Nutr. Biochem.* 99:108854. doi: 10.1016/j.jnutbio.2021.108854

Silva, Y. P., Bernardi, A., and Frozza, R. L. (2020). The role of short-chain fatty acids from gut microbiota in gut-brain communication. *Front. Endocrinol.* 11:25. doi: 10.3389/fendo.2020.00025

Soldatos, C. R., Dikeos, D. G., and Paparrigopoulos, T. J. (2000). Athens Insomnia Scale: validation of an instrument based on ICD-10 criteria. *J. Psychosom. Res.* 48, 555–560. doi: 10.1016/S0022-3999(00)00095-7

Soldatos, C. R., Dikeos, D. G., and Paparrigopoulos, T. J. (2003). The diagnostic validity of the Athens Insomnia Scale. *J. Psychosom. Res.* 55, 263–267. doi: 10.1016/S0022-3999(02)00604-9

Thaiss, C. A., Zeevi, D., Levy, M., Zilberman-Schapira, G., Suez, J., Tengeler, A. C., et al. (2014). Transkingdom control of microbiota diurnal oscillations promotes metabolic homeostasis. *Cell* 159, 514–529. doi: 10.1016/j.cell.2014.09.048

Tochio, T., Kadota, Y., Tanaka, T., and Koga, Y. (2018). 1-Kestose, the smallest fructooligosaccharide component, which efficiently stimulates *Faecalibacterium prausnitzii* as well as bifidobacteria in humans. *Foods* 7:140. doi: 10.3390/foods7090140

Tzounis, X., Vulevic, J., Kuhnle, G. G., George, T., Leonczak, J., Gibson, G. R., et al. (2008). Flavanol monomer-induced changes to the human faecal microflora. *Br. J. Nutr.* 99, 782–792. doi: 10.1017/S0007114507853384

Valcheva, R., Hotte, N., Gillevet, P., Sikaroodi, M., Thiessen, A., and Madsen, K. L. (2015). Soluble dextrin fibers alter the intestinal microbiota and reduce proinflammatory cytokine secretion in male IL-10-deficient mice. *J. Nutr.* 145, 2060–2066. doi: 10.3945/jn.114.207738

Watanabe, S., Kameoka, S., Shinozaki, N. O., Kubo, R., Nishida, A., Kuriyama, M., et al. (2021). A cross-sectional analysis from the Mykinso Cohort Study: establishing reference ranges for Japanese gut microbial indices. *Biosci. Microbiota Food Health* 40, 123–134. doi: 10.12938/bmfh.2020-038

Watanabe, N., Suzuki, M., Yamaguchi, Y., and Egashira, Y. (2018). Effects of resistant maltodextrin on bowel movements: a systematic review and meta-analysis. *Clin. Exp. Gastroenterol.* 11, 85–96. doi: 10.2147/CEG.S153924

Wei, Y., Melas, P. A., Wegener, G., Mathé, A. A., and Lavebratt, C. (2014). Antidepressant-like effect of sodium butyrate is associated with an increase in TET1 and in 5-hydroxymethylation levels in the Bdnf gene. *Int. J. Neuropsychopharmacol.* 18:pyu032. doi: 10.1093/ijnp/pyu032

Yamauchi, Y., Masutomi, H., Ishihara, K., Hartanto, T., Lee, C. G., and Fukuda, S. (2023). The differential effect of two cereal foods on gut environment: a randomized, controlled, double-blind, parallel-group study. *Front. Nutr.* 10:1254712. doi: 10.3389/fnut.2023.1254712

Yoshida, N., Watanabe, S., Yamasaki, H., Sakuma, H., Takeda, A. K., Yamashita, T., et al. (2022). Average gut flora in healthy Japanese subjects stratified by age and body mass index. *Biosci. Microbiota Food Health* 41, 45–53. doi: 10.12938/bmfh.2021-056

Yu, H., Li, R., Liang, X. J., Yang, W. M., Guo, L., Liu, L., et al. (2024). A cross-section study of the comparison of plasma inflammatory cytokines and short-chain fatty acid in patients with depression and schizophrenia. *BMC Psychiatry* 24:834. doi: 10.1186/s12888-024-06277-y

Ze, X., Duncan, S. H., Louis, P., and Flint, H. J. (2012). *Ruminococcus bromii* is a keystone species for the degradation of resistant starch in the human colon. *ISME J.* 6, 1535–1543. doi: 10.1038/ismej.2012.4

Zhang, S. M., Hung, J. H., Yen, T. N., and Huang, S. L. (2024). Mutualistic interactions of lactate-producing lactobacilli and lactate-utilizing *Veillonella dispar*: lactate and glutamate cross-feeding for the enhanced growth and short-chain fatty acid production. *Microb. Biotechnol.* 17:e14484. doi: 10.1111/1751-7915.14484

Zhang, M., Juraschek, S. P., Appel, L. J., Pasricha, P. J., Miller, E. R. 3rd, and Mueller, N. T. (2020). Effects of high-fiber diets and macronutrient substitution on bloating: findings from the OmniHeart trial. *Clin. Transl. Gastroenterol.* 11:e00122. doi: 10.14309/ctg.0000000000000122

frontiers | Frontiers in Microbiology

TYPE Original Research
PUBLISHED 30 July 2025
DOI 10.3389/fmicb.2025.1622488

Check for updates

OPEN ACCESS

EDITED BY
Junling Shi,
Northwestern Polytechnical University, China

REVIEWED BY
Giovanni Tarantino,
University of Naples Federico II, Italy
Brigitte Le Magueresse-Battistoni,
INSERM U1060 Laboratoire de Recherche en Cardiovasculaire, Métabolisme, diabétologie et Nutrition, France
Wang Meng,
Heilongjiang University of Chinese Medicine, China

*CORRESPONDENCE
Jianlong Yan
jianlong.yan@szhospital.com
Xinli Pang
Pangxinli2024@163.com
Da Yin
szyinda@hotmail.com
Xin Sun
sunxinflying@163.com
Weixiang Luo
luo.weixiang@szhospital.com

†These authors have contributed equally to this work

RECEIVED 06 May 2025
ACCEPTED 30 June 2025
PUBLISHED 30 July 2025

CITATION
Yan J, Pan Y, Liu H, Yuan J, Chen J, Gao Y, Lin C, Lin F, Wang R, He Y, Wang C, Xu C, Li T, Zhang P, Lan Y, Shao W, Pang X, Yin D, Sun X and Luo W (2025) Bisphenol F exposure induced vascular toxicity through intestinal microbiota imbalance.
Front. Microbiol. 16:1622488.
doi: 10.3389/fmicb.2025.1622488

COPYRIGHT
© 2025 Yan, Pan, Liu, Yuan, Chen, Gao, Lin, Lin, Wang, He, Wang, Xu, Li, Zhang, Lan, Shao, Pang, Yin, Sun and Luo. This is an open-access article distributed under the terms of the Creative Commons Attribution License (CC BY). The use, distribution or reproduction in other forums is permitted, provided the original author(s) and the copyright owner(s) are credited and that the original publication in this journal is cited, in accordance with accepted academic practice. No use, distribution or reproduction is permitted which does not comply with these terms.

Bisphenol F exposure induced vascular toxicity through intestinal microbiota imbalance

Jianlong Yan[1*†], Yanbin Pan[2†], Huadong Liu[1], Jie Yuan[1], Jie Chen[1], Yannan Gao[1], Chaolan Lin[1], Feng Lin[1], Rongning Wang[1], Yaqiong He[1], Caiping Wang[1], Cong Xu[1], Tangzhiming Li[1], Peng Zhang[1], Yu Lan[1], Wenming Shao[3], Xinli Pang[1*], Da Yin[1*], Xin Sun[1*] and Weixiang Luo[4*]

[1]Department of Cardiology, Shenzhen Cardiovascular Minimally Invasive Medical Engineering Technology Research and Development Center, Shenzhen People's Hospital (The Second Clinical Medical College, Jinan University; The First Affiliated Hospital, Southern University of Science and Technology), Shenzhen, Guangdong, China, [2]Department of Health Management Center, Shenzhen People's Hospital (The Second Clinical Medical College, Jinan University; The First Affiliated Hospital, Southern University of Science and Technology), Shenzhen, Guangdong, China, [3]Department of Emergency, The First Affiliated Hospital of Jinan University, Guangzhou, Guangdong, China, [4]Nursing Department, Shenzhen People's Hospital (The Second Clinical Medical College, Jinan University; The First Affiliated Hospital, Southern University of Science and Technology), Shenzhen, Guangdong, China

Introduction: Bisphenol F (BPF), a common substitute for bisphenol A (BPA), has documented toxicity in multiple organs, but its vascular effects remain unclear. This study investigated BPF's role in vascular calcification (VC) and underlying mechanisms.

Methods: Differences in the intestinal microbiota were analyzed by 16S ribosomal RNA gene sequencing. Metabolites were analyzed using liquid chromatography-mass spectrometry. Faecal microbiota transplantation and antibiotic treatment experiments were performed to evaluate the functions of the intestinal microbiota in VC.

Results: We enrolled consecutively 57 patients. Patients were assigned to a calcification group (30 patients) and a non-calcification group (27 patients) based on the presence or absence of calcification in the thoracic aorta wall. The results showed that patients with vascular calcification (VC) had higher levels of bisphenol F (BPF), bisphenol S (BPS) and bisphenol A (BPA) in the fecal samples than patients without VC. The thoracic aortic calcification score was significantly positively correlated with the BPF (Spearman $r = 0.4935$, $p < 0.001$), BPA (Spearman $r = 0.2860$, $p < 0.05$) and BPS (Spearman $r = 0.2650$, $p < 0.05$). We then explored the effects of BPF exposure on normal and vitamin D3 + nicotine (VDN)-treated rats. BPF exposure induced mild VC in normal rats and aggravated VC in VDN-treated rats. BPF exposure disturbed the gut microbiota and promoted inflammatory responses.

Conclusion: The results here elucidate the mechanism underlying BPF-triggered or BPF-aggravated VC through the gut–vascular axis and provide a theoretical basis for cardiovascular disease risk assessment in humans.

KEYWORDS

bisphenol F, faecal microbiota transplantation, gut microbiota, inflammation, short-chain fatty acids, vascular calcification

1 Introduction

Although bisphenol A (BPA) remains the most extensively studied bisphenol, growing recognition of its health risks has prompted regulatory restrictions and replacement with alternatives in consumer products. BPF has emerged as a prevalent industrial substitute for BPA and widely used in various areas of life and industry, such as construction materials (industrial floors, coatings, and electrical varnishes) (Rochester and Bolden, 2015; Czarny-Krzymińska et al., 2023), consumer products (water pipes, plastics, food packaging, and dental sealants) (Rochester and Bolden, 2015), and paper products (currencies, tickets, and airplane boarding passes) (Liao and Kannan, 2014). However, due to incomplete polymerization during product manufacture as well as the aging and degradation of the product as it is used over time, bisphenols may migrate from the container into food (Kang et al., 2006). In addition, the random discarding and unreasonable recycling of plastic products and thermal paper can cause bisphenols to diffuse into environmental media, such as water, soil, river sediment, atmosphere, and indoor dust (Liao et al., 2012; Yang et al., 2014; Lambré et al., 2023). In daily life, the bisphenols in food, necessities and various environmental media can enter the human body through the digestive tract, skin, or respiratory tract, extensively exposing the human body to bisphenols (Zhang et al., 2018). Currently, BPF can be detected in biological samples from different populations, such as infants (Zheng et al., 2024), pregnant women (Hu et al., 2019), children (Chen et al., 2018), adults (Li et al., 2023), and elderly individuals (Gao et al., 2021). After BPF enters the human body, it can potentially harm multiple human systems.

BPA has been reported to cause a variety of adverse biological effects in the body. For example, zebrafish larvae exposed to BPF displayed disruptions in the regulatory functions of the hypothalamus–pituitary–thyroid axis, with the main manifestation being thyroid endocrine toxicity (Huang et al., 2016). After exposure to an environmentally relevant concentration of BPF (0.0005 mg/L), zebrafish embryos display activated astrocyte- and microglia-mediated neuroinflammation, induced central nervous system cell apoptosis, and inhibited neural development (Yuan et al., 2019). In addition, some studies have shown that exposure to BPF can cause neuronal loss in the zebrafish brain, impairing cognitive ability (Mu et al., 2022a,b). Moreover, exposure to BPF could affect the antioxidant defense system and destroy the metabolic function of the liver (Meng et al., 2019). Intestinal microbial community disorders, oxidative damage and inflammation can be caused by BPF exposure in the zebrafish intestine (Wang et al., 2021). Furthermore, exposing zebrafish to BPF could disrupt the regulatory functions of the hypothalamus–pituitary–gonadal axis and inhibit their pawning capacity, while parental BPF exposure affects the development of the offspring, which mainly manifests as a decreased heart rate, reduced body length, and the inhibition of spontaneous movement (Mu et al., 2022a,b). BPF can also inhibit angiogenesis in zebrafish by increasing oxidative stress (Ji et al., 2022). Moreover, BPF induced bradycardia in zebrafish embryos and potentiated the cardiotoxicity of calcium channel blockers (Arrokhman et al., 2023). Another study showed that cardiotoxicity was induced in mice exposed to BPF for 14 weeks, which mainly manifested as myocardial hypertrophy and cardiac dysfunction (Cheng et al., 2023). Although studies of the toxic effects of BPF have focused on animal experiments, there is growing concern about the potential toxic effects of BPF to humans.

Cardiovascular disease (CVD) is the leading cause of death worldwide (Mahmood et al., 2014). The pathogenesis and development of CVDs are influenced by many factors, including genetics and the environment (Lu et al., 2022). However, after continued in-depth study of the causes and mechanisms of CVDs, it has been found that genetic variations account for only a small portion (<20%) of CVD risk (Ripatti et al., 2010; Ardissino et al., 2011). Therefore, environmental factors play decisive roles in the pathogenesis of CVD, among which exposure to environmental pollution is a critical factor (Münzel et al., 2023). As an environmental pollutant, BPF affects the cardiovascular system, but its effect and mechanism on vascular calcification (VC) are still poorly understood. VC is a common pathological phenomenon in which hydroxyapatite crystals are deposited in the extracellular matrix and between the endarterium and adventitia. VC is the common basis of cardiovascular and cerebrovascular diseases and can lead to arterial stiffness, reduced plasticity, and increased pulse wave velocity, predisposing individuals to CVD events such as heart failure, myocardial infarction, cerebral infarction, and peripheral vascular disease. However, to date, the effect of BPF on vascular toxicity, particularly VC, remains unclear (Dias et al., 2022; Ji et al., 2022; Kang et al., 2023). This underscores a significant knowledge gap in environmental toxicology. Therefore, it is necessary to investigate the effect of BPF on VC.

In this study, we aimed to determine whether there are differences in urine BPF between individuals with VC and those without VC and to investigate the effects of BPF on VC, which provides a new understanding of the effect of BPF on blood vessels and provides a theoretical basis for the risk assessment of BPF-induced cardiovascular disease.

2 Materials and methods

2.1 Study participants

Fifty-seven consecutive patients with chest pain, including 30 patients with VC and 27 patients without VC, were included in this study. The inclusion criterion was completion of diagnostic thoracic computed tomography imaging. Exclusion criteria were defined as follows: (I) history of gastrointestinal surgery within 12 months, (II) active gastrointestinal disorders (including but not limited to diarrhea, constipation, or bleeding) within 3 months preceding enrollment, (III) comorbid malignancy, autoimmune disease, active infection, or severe renal impairment (serum creatinine >267 μmol/L), (IV) antibiotic, probiotic, or prebiotic use exceeding 3 consecutive days during the 3-month pre-enrollment period, (V) non-compliance with study protocols or withdrawal of informed consent, and (VI) incomplete baseline datasets or missing biological specimens. This observational study was registered under trial NCT04864457. All selected participants provided informed consent, and the research protocol was approved by the Ethics Committee of Shenzhen People's Hospital. The VC scores were calculated in a manner similar to the calculation of the Agatston calcification score (Agatston et al., 1990); that is, the sum of the calcification scores for the ascending aorta, the aortic arch and the thoracic aorta (from the root of the ascending aorta to the diaphragm) were used as the aortic calcification score (Pedrosa et al., 2019). In addition, basic clinical information of the participants, including age, sex, medical history, etc., was collected.

2.2 BPF treatment

The animal experimental protocols complied with the requirements of the Animal Management Committee of Shenzhen People's Hospital for experimental animal operation and animal welfare. Seven- to eight-week-old male Sprague–Dawley rats were purchased from the Guangdong Medical Experimental Animal Center. The rats were housed in the specific pathogen-free animal room of the Innovation Collaborative Center of Shenzhen People's Hospital. The rearing conditions were as follows: the animal rooms were alternately light and dark for 12 h each, the relative humidity was 50–70%, and the room temperature was 25 ± 1°C. Each group contained 5 rats housed in two cages (3 and 2 rats per cage, respectively), and they were given free access to food and water. The animals were allowed to adapt to the environment for 1 week, after which the experiment began.

We constructed a VC model according to methods described in previous literature, with slight modifications (Yan et al., 2022). In brief, on the first day, the rats received vitamin D3 (300,000 IU/kg) via intramuscular injection and nicotine (25 mg/kg) via gavage, followed by an additional gavage of nicotine 9 h later. To assess the effect of BPF in normal rats and rats with vitamin D3 + nicotine (VDN)-induced VC, we established four experimental groups, as follows: (i) wild-type rats exposed to olive oil as the normal group (normal group), (ii) rats with VDN-induced VC exposed to olive oil as a VC model (VC group), (iii) wild-type rats exposed to BPF (1 mg/kg body weight/day) (normal + BPF group), and (iv) rats with VDN-induced VC exposed to BPF (1 mg/kg body weight/day) (VC + BPF group). BPF was dissolved in olive oil to prepare a 1 mg/mL solution, which was administered daily at a dose of 1 mg/kg body weight. The exact volume administered to each rat was calculated based on its individual body weight. Following 120 days of BPF exposure, all rats were anesthetized using gas inhalation (3–4% isoflurane with 1–2 L/min oxygen flow during induction, followed by 1.5–2.5% isoflurane at 1 L/min oxygen flow for maintenance) and subsequently euthanized. Rat feces and plasma were collected, and the aortas were fixed in 4% paraformaldehyde, and the remaining tissues were stored at −80°C for future use.

Previous studies have employed varying BPF dosages (0.01–200 mg/kg body weight/day) (Castro et al., 2015; Ullah et al., 2018; Zhao et al., 2018; Ullah et al., 2019; Lee et al., 2022). The lowest observed adverse effect level (LOAEL) for BPF is established at 20 mg/kg, a dose associated with acute hepatorenal dysfunction (Rochester and Bolden, 2015; Zhao et al., 2018). In the present study, we administered 1 mg/kg/day BPF – a dosage substantially below this toxicological threshold (5% of LOAEL). Consequently, adverse effects at this exposure level were significantly milder relative to established toxicity benchmarks.

2.3 Fecal microbiota transplantation (FMT)

To determine the changes induced by BPF in the gut microbiota in animals with VC, the feces of the rats in the VC + BPF group (donors) were collected to prepare a fecal bacteria solution. The fecal bacteria solution was prepared according to methods described in previous literature (Staley et al., 2017; Zheng et al., 2021). In brief, fresh feces from donor rats were collected and immediately mixed with sterile PBS (1×) at a ratio of 1:10 (m:v) and vortexed vigorously for 40 s using a benchtop vortex. The mixture was then centrifuged at 1,000 × g for 3 min at 4°C, the collected supernatant was further centrifuged at 6,000 × *g* for 15 min at 4°C after which this supernatant was discarded, and the pellet was resuspended in sterile PBS (1×) to obtain the fresh fecal bacteria solution. The rats in the VC group (recipients) received gavage of the fecal microbial solution once a day based on body weight (a dose of 5 mL/kg) for 14 consecutive days. The group of recipient rats that received the fecal bacteria solution from the rats in the VC + BPF group were named the VC + FMT group.

2.4 Depletion of the gut bacteria with the antibiotic cocktail

To study the key role of the gut microbiota in VC, the rats in the VC + BPF group were intragastrically administered antibiotics (ABX) to deplete the gut microbiota, which consisted of 1 mg/mL ampicillin, 1 mg/mL neomycin sulfate, 1 mg/mL metronidazole, 0.5 mg/mL vancomycin hydrochloride, and 1 mg/mL gentamicin dissolved in 0.9% sodium chloride solution (Zhao et al., 2020). The rats were gavaged with Abx at a dosage of 10 μL/g body weight/day once each week, and each gavage was performed continuously for 7 days. Rats in the control group were given the same 0.9% sodium chloride solution without ABX.

2.5 Determination of calcification

Samples were fixed in 4% paraformaldehyde, dehydrated, cleared, soaked in paraffin, embedded, sectioned (5 μm), baked, dewaxed, and stained with 2% alizarin red solution (pH = 4.2) for 5 min before being observed under a light microscope (Nikon Eclipse 80i, Tokyo, Japan) and photographed. Image analysis was performed using Image-Pro Plus software (Version 6.0; Media Cybernetics, Rockville, MD, United States).

2.6 Biochemical parameters

The serum concentrations of lipopolysaccharide (LPS), diamine oxidase (DAO), interleukin-1β (IL-1β), interleukin-6 (IL-6), and tumor necrosis factor-α (TNF-α) were assessed using enzyme-linked immunosorbent assay (ELISA) kits obtained from Jianglai Biotech, Shanghai, China. All biochemical parameters were analyzed following the manufacturers' protocols.

2.7 DNA sequencing of the microbiota

Total DNA extraction was completed by the cetyltrimethylammonium bromide (CTAB) method (Yan et al., 2022). The concentration and purity of the extracted DNA were determined via 1% agarose gels. PCR amplification was carried out for the V3-V4 variable regions in the 16S rRNA genes of bacteria using the primers 341F (5'-CCTAYGGGRBGCASCAG-3′) and 806R (5′- GGACTACNNGGGTATCTAAT-3′). The amplification procedure was as follows: predenaturation at 98°C for 1 min;

30 cycles of denaturation at 98°C for 10 s followed by annealing at 50°C for 30 s and extension at 72°C for 30 s; and a final extension at 72°C for 5 min (PCR instrument: T100PCR, Bio-Rad, United States). Then, 2% agarose gel electrophoresis was performed to detect the PCR products, and a Qiagen Gel Extraction Kit (Qiagen, Germany) was utilized for purification. Finally, a TruSeq® DNA PCR-Free Sample Preparation Kit (Illumina, United States) was used to construct a library, and sequencing was conducted on an Illumina NovaSeq 6,000 PE250 (Novogene, Tianjin, China).

2.8 Bioinformatic analysis

In this study, the analytical processes used were consistent with those described in our previously publication (Yan et al., 2022). First, the raw sequence data were processed using Quantitative Insights into Microbial Ecology 2 (QIIME2, version 2020.2) software. This included application of the dada2 plugin QIIME2 to perform quality control, truncation, denoising, connection, and chimera removal to generate the final representative sequence list. Subsequently, using the feature classifier plugin QIIME2, the representative amplicon sequence variants (ASVs) were matched to the Silva database to identify the corresponding taxa and determine their abundance. To identify potential biomarkers in the microbial communities, we used the linear discriminant analysis effect size (LEfSe) method for difference analysis. In addition, we used the observed ASVs and the Shannon index to measure the microbial diversity (α diversity) in the samples. Finally, the differences between different community structures were explored by principal coordinate analysis (PCoA) and permutation multivariate analysis of variance (PERMANOVA) ($^{*}p < 0.05$, $^{**}p < 0.01$, $^{***}p < 0.001$, $^{****}p < 0.0001$).

2.9 Plasma sample pretreatment

First, 100 μL of serum was aliquoted into individual 1.5 mL polypropylene extraction tubes. Methanol was then added at a 1:4 (v/v) ratio and the mixture was vortexed thoroughly. Following centrifugation at 20,000 rpm for 20 min (4°C), the supernatant was carefully collected. Subsequently, 300 μL of ethyl acetate and 10 μL of 0.5% formic acid were added to the supernatant. The mixture was vortex-mixed for 30 s and centrifuged at 20,000 rpm for 3 min (4°C) to separate the ethyl acetate layer. This extraction procedure was repeated twice more with fresh ethyl acetate. All ethyl acetate fractions were pooled for derivatization (Zhu et al., 2016; Zheng et al., 2018).

2.10 Fecal sample pretreatment for extracting SCFAs

A stool sample (150–200 mg) was placed in a polypropylene extraction tube, and 1.0 mL of acetonitrile (CAN) was added. Next, the mixture was vortexed for 3 min. Afterward, centrifugation was performed at 20,000 rpm for 3 min at 4°C, and the supernatant was carefully collected. This centrifugation step was repeated three times, and the supernatant was carefully collected each time and retained for subsequent derivatization experiments (Yuan et al., 2018).

2.11 Fecal sample pretreatment for extracting bisphenols

Accurately weighed fecal samples (2–3 g) were transferred into conical flasks. Then, 20 mL of 50% (v/v) methanol was added for extraction, followed by incubation for 2.0 h at room temperature. After extraction, 10 mL of supernatant was transferred to a pre-conditioned Oasis HLB solid-phase extraction (SPE) cartridge (pre-activated sequentially with 5 mL methanol and 5 mL pure water). The initial eluate was discarded, and the cartridge was washed successively with 5 mL pure water and 8 mL methanol–water (1:1, v/v). Target analytes were eluted with 6 mL pure methanol at a controlled flow rate of 1 mL/min. The eluate was concentrated to near-dryness under a gentle nitrogen stream. The residue was reconstituted in 1 mL methanol–water (1:1, v/v) and filtered through a 0.22 μm membrane prior to instrumental analysis.

2.12 Derivatization

A total of 30 μL (20 μmol/mL) of triethylamine (TEA) and 15 μL (20 μmol/mL) of 2-chloro-1-methylpyridinium iodide (CMPI) were added to the above sample, followed by homogeneous mixing using a vortex mixer. The mixture was incubated at 40°C for 5 min. Next, 30 μL (20 μmol/mL) N, N-Dimethylethylenediamine (DMED) was added, and incubation continued at 40°C for 60 min. After that, the sample was dried under a nitrogen flow, and 100 μL of Acetonitrile (ACN) can was added (Zhu et al., 2016; Yuan et al., 2018; Zheng et al., 2018).

2.13 Liquid chromatography–mass spectrometry analysis for SCFAs

This study used a method similar to that described in our previously published study (Yan et al., 2022). In brief, the LC conditions were as follows: the column used was an ACQUITY UPLC HSS T3 column (100 Å, 1.8 μm, 2.1 mm × 100 mm) (Waters, Milford, MA, United States); and mobile phase A consisted of water (containing 0.1% formic acid) and mobile phase B consisted of ACN (containing 0.1% formic acid). Gradient elution was performed as follows: 0 ~ 5 min, 2–10% B; 5 ~ 13 min, 10% ~ 100% B; 13 ~ 15 min, 100% B; 15 ~ 16 min, 100% ~ 2% B; and 16 ~ 20 min, 2% B. The flow rate was 0.2 mL/min, the temperature of the sample chamber was 10°C, the column temperature was 25°C, and the injection volume was 2 μL. MS conditions: The Q Exactive Focus system (Thermo Fisher Scientific, Santa Clara, CA, United States) was operated in positive ion mode with electrospray ionization: Orbitrap; ion source: HESI; scan type: full MS; heater temperature, 350°C; capillary temperature, 320°C; sheath gas flow, 40 arbitrary units; auxiliary gas flow, 10 arbitrary units; spray voltage, 3.8 kV; capillary voltage, 35 V; S-lens RF level, 50%; maximum injection time, 100 ms; scan range: m/z 70–1,050; and resolution: 70,000 FWHM.

2.14 Liquid chromatography–mass spectrometry analysis for bisphenols

Liquid chromatography conditions: The chromatographic column was an Agilent Eclipseplus C18 (100 Å, 1.8 μm, 2.1 mm × 100 mm),

column temperature: 40°C; flow rate: 0.3 mL/min; injection volume: 2 μL; mobile phase: water (A) – methanol (B); gradient elution: 0–0.5 min, 95% A; 0.5–2.5 min, 95–40% A; 2.5–6.0 min, 40–5% A; 6.0–7.5 min, 5% A; 7.5–7.51 min, 95 A%; 7.51–12 min, 95 A%. Mass spectrometry conditions: The analysis was performed using an Agilent 6465B Triple Quadrupole LC–MS system (Agilent Technologies, Santa Clara, CA, United States); Ionization mode: electrospray ionization (ESI-); Scan mode: multiple reaction monitoring mode; Dryer temperature: 350°C; Dryer flow rate: 7 L/min; Nebulizer pressure: 30 psi; Sheath gas temperature: 300°C; Sheath gas flow rate: 11 L/min; Capillary voltage: 2000 V.

2.15 Statistical analysis

Statistical analyses were performed using EmpowerStats[1], R[2], and GraphPad Prism 8.0. Data are expressed as mean ± standard deviation (SD) for normally distributed variables (analyzed by two-tailed Student's *t*-test after confirming equal variance via *F*-test) or median with interquartile range (P25, P75) for non-normally distributed variables (analyzed by Kruskal–Wallis rank sum test). Categorical variables are presented as frequencies/percentages and compared using chi-square tests. Correlation analyses were conducted using Spearman's rho non-parametric correlation. PERMANOVA was performed using OmicShare tools for data[3]. A two-sided $p < 0.05$ defined statistical significance.

3 Results

3.1 Characteristics of the participants

A total of 57 participants were consecutively enrolled in this study. The results showed that compared with those in the Non-VC group, the participants in the VC group were older, had a lower eGFR, and had higher rates of smoking ($p < 0.05$). There were no significant differences in sex, BMI, total cholesterol, triglyceride, HDL-C, LDL-C, uric acid, serum calcium, serum phosphorus, creatinine, drinking, hypertension, diabetes mellitus ($p > 0.05$). The basic demographic and clinical characteristics of all study subjects are shown in Table 1.

TABLE 1 Characteristics of the participants at baseline.

Characteristics	Non-VC (*n* = 27)	VC (*n* = 30)	*P*-value
Score	0.0 (0.0–0.0)	291.5 (149.1–768.0)	<0.001
Age, (years)	54.0 ± 7.0	60.9 ± 7.3	<0.001
Male, *n* (%)	15 (55.6)	16 (53.3)	0.866
BMI, kg/m^2	25.4 ± 3.2	24.7 ± 3.0	0.401
Total cholesterol, mmol/L	5.45 ± 1.05	5.33 ± 1.22	0.694
Triglyceride, mmol/L	1.26 (1.14–1.74)	1.31 (1.06–1.98)	0.765
HDL-C, mmol/L	1.48 ± 0.39	1.44 ± 0.39	0.708
LDL-C, mmol/L	3.00 ± 0.80	2.93 ± 0.94	0.761
Uric acid, mmol/L	406.0 ± 102.1	417.4 ± 92.1	0.660
Serum calcium, mmol/L	2.42 ± 0.08	2.39 ± 0.09	0.221
Serum phosphorus, mmol/L	1.14 ± 0.14	1.12 ± 0.17	0.681
Creatinine, μmol/L	69.0 ± 15.3	73.5 ± 13.1	0.236
eGFR (mL/min/1.73 m^2)	97.0 ± 12.2	87.5 ± 13.4	0.008
Smoking, *n* (%)	4 (14.8)	12 (40.0)	0.035
Drinking, *n* (%)	6 (22.2)	7 (23.3)	0.920
Hypertension, *n* (%)	14 (51.9)	16 (53.3)	0.911
Diabetes mellitus, *n* (%)	6 (22.2)	6 (20.0)	0.837
Bisphenol S, (μg/g)	0.008 (0.003–0.013)	0.014 (0.007–0.024)	0.003
Bisphenol F, (μg/g)	0.012 (0.007–0.020)	0.027 (0.015–0.040)	<0.001
Bisphenol A, (μg/g)	0.019 (0.014–0.026)	0.028 (0.018–0.047)	0.006

Data are presented as mean ± standard deviation (SD), median (interquartile range [IQR]) or *n* (%). *P*-value < 0.05 was considered statistically significant. BMI, Body mass index; EGFR, estimated glomerular filtration rate; HDL-C, high density lipoprotein cholesterol; LDL-C, low density lipoprotein cholesterol.

3.2 Fecal bisphenols in patients with VC

Patients with VC had significantly higher levels of BPS, BPF and BPA in the fecal samples than Non-VC patients (Figure 1A). To further reveal the relationship between bisphenols exposure and VC severity, we conducted a correlation analysis between the levels of bisphenols and the VC score. The results indicated that the VC scores were positively correlated with the levels of BPF (Spearman $r = 0.4935$, $p < 0.001$) (Figure 1B), BPA (Spearman $r = 0.2860$, $p < 0.05$) (Figure 1C) and BPS (Spearman $r = 0.2650$, $p < 0.05$) (Figure 1D). In addition, receiver operating characteristic (ROC) curves were plotted to calculate the area under the curve (AUC) to assess the predictive role of bisphenols for VC. It was discovered that the largest AUC was generated by BPF, followed by BPS, and BPA had the lowest AUC (Figure 1E).

3.3 Association between fecal bisphenols and gut microbiota in patients with VC

To reveal the structure and abundance of the intestinal microbiota in vascular calcification patients with higher bisphenols in the fecal samples, we used 16S rRNA gene sequencing to analyze the structure and abundance of the gut microbiota. Principal coordinate analysis (PCoA) at the bacterial phylum level indicated that there were structural differences in the intestinal microbiota between the two groups ($R^2 = 0.0923$, $p = 0.009$) (Figure 2A), despite non-significant changes in α-diversity (Figures 2B,C). Furthermore, linear discriminant analysis (LDA) effect size (LEfSe) indicated that VC were enriched in *Escherichia_Shigella*, *Anaerovibrio*, *Prevotella*, *Bacteroides*, etc. (LDA > 3.5) (Figure 2D). Furthermore, spearman correlation analysis demonstrated that the abundances of *Escherichia_Shigella*,

1 http://www.empowerstats.com
2 http://www.R-project.org
3 www.com.analyses/tools

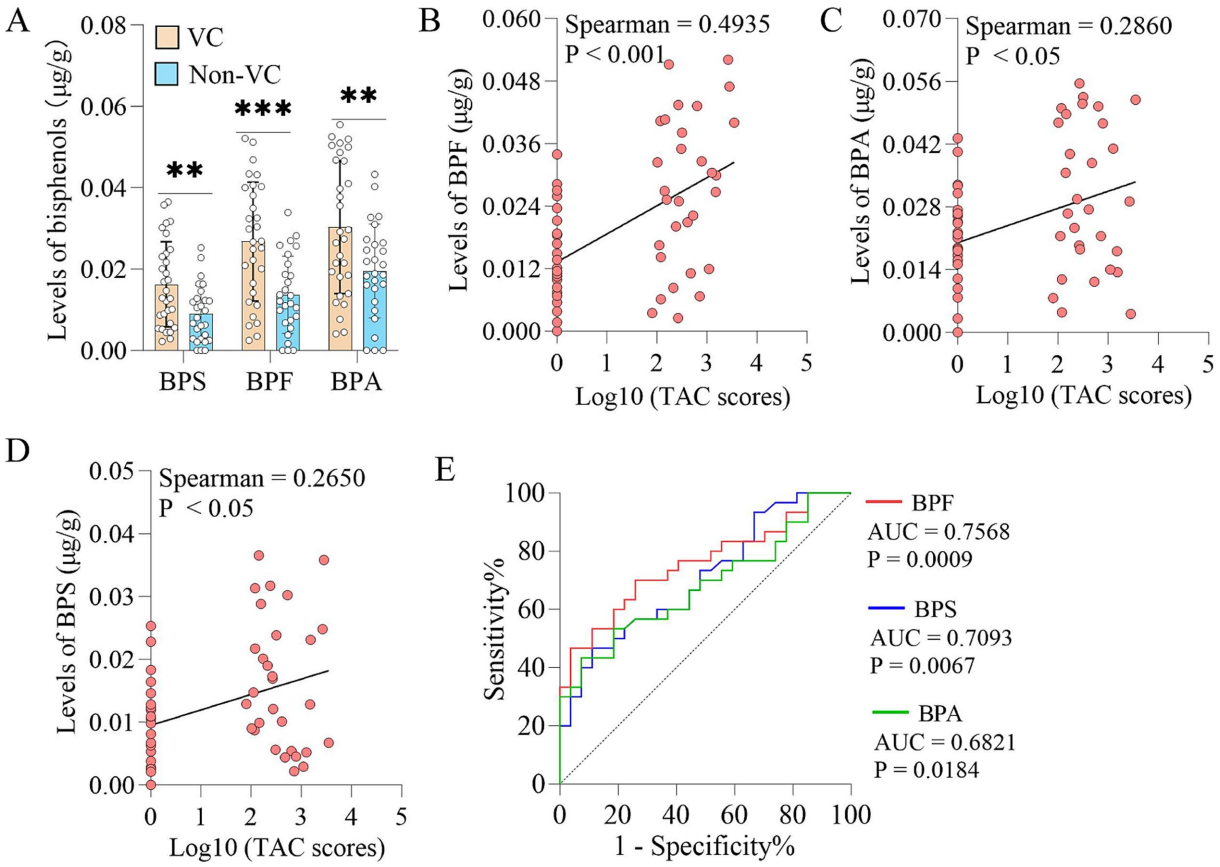

FIGURE 1
Fecal bisphenols in patients with VC. **(A)** Comparison of the abundances of bisphenols in fecal samples from patients with and without VC. **(B–D)** Spearman's correlation analyses of BPF, BPA and BPS levels in fecal samples with TAC scores, respectively. **(E)** Predictive ability of BPF, BPA and BPS levels in fecal samples for vascular calcification, respectively. Continuous and non-normal data were described as median (interquartile range). The Mann–Whitney *U* test was used to analyze the differences of two groups. $^{**}p < 0.01$, $^{***}p < 0.001$. BPA, Bisphenol A; BPF, Bisphenol F; BPS, Bisphenol S; TAC, Thoracic aortic calcification; VC, Vascular calcification.

Anaerovibrio, *Bacteroides*, etc., were variably positively correlated with BPS, BPF, BPA and TAC scores in the VC group and negatively correlated with acetate, propionate and butyrate levels in feces. Additionally, spearman correlation analysis indicated that the abundances of *Bifidobacterium*, *Romboutsia*, *Eubacterium_xylanophilum*, *Turicibacter*, etc., were positively correlated with the levels of acetate, propionate and butyrate and negatively correlated with BPS, BPF, BPA and TAC scores to different degrees in the Non-VC group (Figure 2E). Further analysis found that patients with VC had significantly lower levels of acetate, propionate and butyrate in the fecal samples than Non-VC patients (Figure 2F).

3.4 BPF exposure induced mild VC in normal rats and aggravated VC in VDN-treated rats

Based on the ROC curves results, we selected BPF as the study subject. To elucidate the effect of BPF on VC, we exposed rats to BPF for 120 days, after which pathological changes in the ascending aorta were detected. Alizarin red staining revealed that the ascending aortas of the rats in the normal group had no calcification (Figures 3A,B). Compared with those in the normal group, the ascending aortas of the rats in the normal + BPF group had slight calcification (Figures 3A,B). Compared with those in the VC group, the ascending aortas of the rats in the VC + BPF group had more severe calcification (Figures 3A,B). In addition, relative quantification of the calcium salt showed that compared with those in the normal and VC groups, the calcium contents in the ascending aortas of the normal + BPF and VC + BPF groups were significantly increased (Figure 3C). These results indicate that BPF exposure induces mild calcification of the ascending aorta in normal rats and can aggravate VDN-induced ascending aorta calcification.

3.5 BPF exposure disturbed the gut microbiota

The gut microbiota is a "microbial organ" (Byndloss and Bäumler, 2018) and can be regulated by a variety of exogenous substances. To clarify the effect of BPF on the gut microbiota, we used 16S rRNA gene sequencing to analyze the structure and abundance of the gut microbiota. After 120 days of BPF treatment, the gut microbiota of the rats were significantly disrupted. PCoA at the phylum level revealed

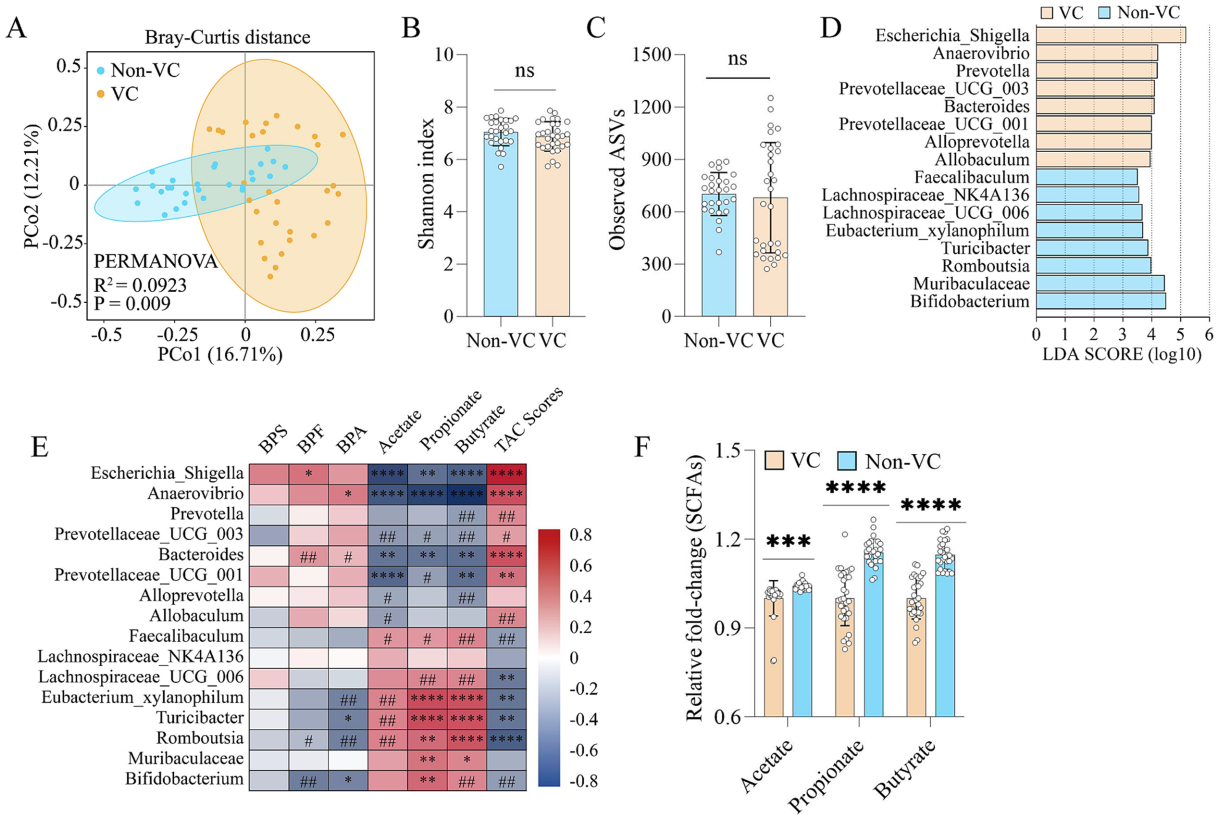

FIGURE 2
Association between fecal bisphenols and gut microbiota in patients with VC. **(A)** PCoA plot showing changes in the β-diversity of the gut microbiota in patients with and without VC. **(B)** α-diversity of the gut microbiota (Shannon index). **(C)** α-diversity of the gut microbiota (Observed ASVs). **(D)** LEfSe (linear discriminant analysis (LDA) coupled with exact size measurements) for the analysis of differences between the gut microbiota of VC group and Non-VC group (LDA > 3.5). **(E)** Spearman's correlation analysis of the relationship of the intestinal microbiota with BPF, BPA, BPS, acetate, propionate, butyrate and TAC scores. Negative and positive correlations are denoted in blue and red, respectively. The adjusted *p*-value was calculated with the Benjamini–Hochberg false discovery rate (FDR) method to correct the multiple comparisons and Spearman's correlations. **(F)** Comparison of the differences in fecal acetate, propionate, and butyrate levels, respectively. Continuous data were described as mean ± standard deviation or median (interquartile range) as appropriate. The *t*-test for normally distributed data and with the Mann–Whitney *U* test for non-normally distributed data. $^{\#}p < 0.25$, $^{\#\#}p < 0.1$, $^{*}p < 0.05$, $^{**}p < 0.01$, $^{***}p < 0.001$, $^{****}p < 0.0001$, ns > 0.05.

differences in the structure of the gut microbiota after BPF treatment ($R^2 = 0.4173$, $p = 0.012$) (Figure 3D) and that BPF treatment reduced the α diversity of the gut microbiota (observed ASVs) (Figure 3E); however, no significant difference was observed in the Shannon index (Figure 3F). Furthermore, LEfSe revealed that both normal rats and VDN-treated rats exposed to BPF exhibited enrichment of the genus Escherichia_Shigella (LDA > 3.5), while rats not exposed to BPF did not show enrichment of this genus (Figures 3G,H).

3.6 BPF exposure promoted systemic inflammatory responses

Escherichia_Shigella is one of the main sources of the intestinal endotoxin LPS (Wang et al., 2022). Therefore, we further analyzed the LPS level in plasma and found that they were significantly higher in the normal + BPF group and the VC + BPF group than in the normal group and VC group (Figure 4A). In addition, we measured the plasma levels of biological factors associated with inflammation to assess the effect of BPF on systemic inflammation. Compared with those in the normal group and VC group, the plasma concentrations of IL-6, IL-1β, and TNF-α in the normal + BPF group and the VC + BPF group were significantly increased (Figures 4B–D). LPS and short-chain fatty acids (SCFAs) are two types of metabolites derived from the gut microbiota that reflect the status of the intestinal system and the functional status of the gut microbiota (Zhang X. Y. et al., 2020; Zhang X. et al., 2020). We detected the main SCFAs in feces, and the results showed that, compared with the normal group and VC group, the normal + BPF group and the VC + BPF group had decreases in the contents of acetic acid, propanoic acid, and butyric acid to varying extents (Figures 4E–G). Taken together, these results reveal that BPF exposure causes drastic changes in the gut microbiota and promotes inflammation in the body.

3.7 BPF promotes VC through the gut microbiota

To study the key role of the gut microbiota in promoting VC, we transplanted the fecal microbiota from the rats in the VC + BPF group to the rats in the VC group (named the VC + FMT group). After FMT, VC in the VC + FMT group was exacerbated (Figures 5A–C).

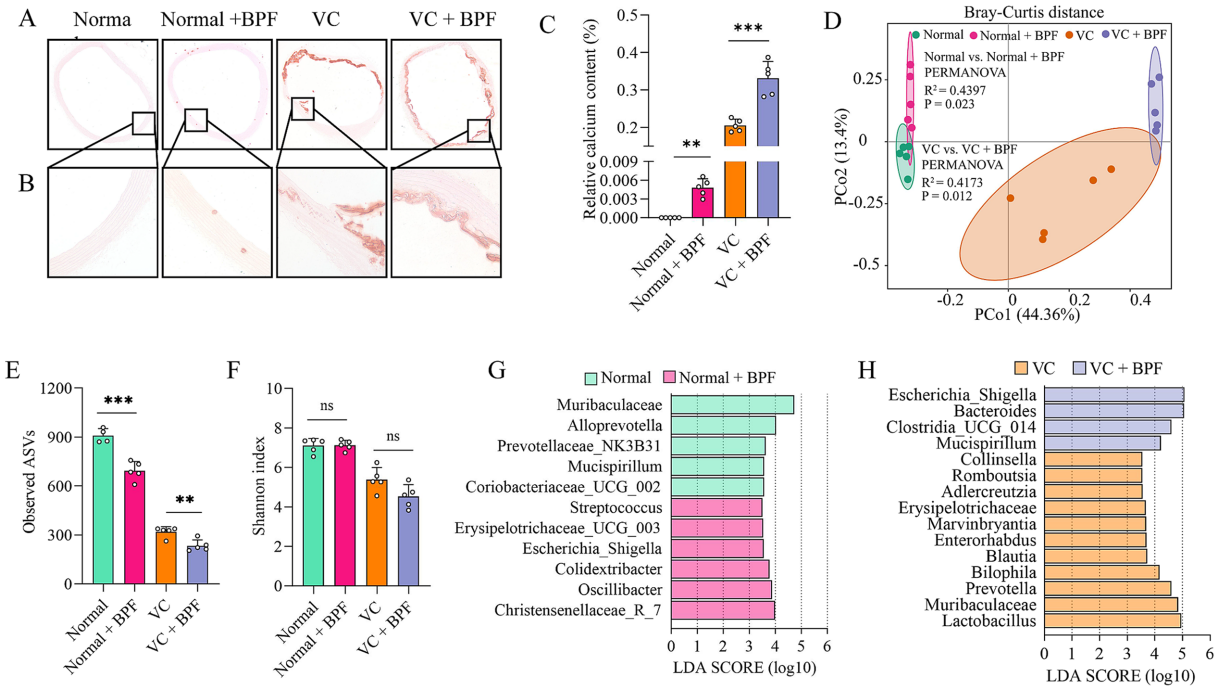

FIGURE 3
BPF exposure promoted VC and disturbed the gut microbiota. **(A)** Alizarin red staining of ascending aorta calcification (original magnification, 40×) (n = 5). **(B)** Alizarin red staining of ascending aorta calcification (original magnification, 200×) (n = 5). **(C)** Relative quantification of calcium content for the vessel sections of the ascending aorta (n = 5). **(D)** PCoA plot showing changes in the β-diversity of the gut microbiota after BPF treatment (n = 5). **(E)** α-diversity of the gut microbiota (Observed ASVs) (n = 4 ~ 5). **(F)** α-diversity of the gut microbiota (Shannon index) (n = 5). **(G)** LEfSe [linear discriminant analysis (LDA) coupled with exact size measurements] for the analysis of differences between the gut microbiota of the normal group and the normal + BPF group (LDA > 3.5) (n = 5). **(H)** LEfSe analysis of the differences between the gut microbiota of the VC group and the VC + BPF group (LDA > 3.5) (n = 5). The t-test was used to analyze the differences of two groups. ns > 0.05, $^{**}p < 0.01$, $^{***}p < 0.001$.

In contrast, the rats in the VC + BPF group received antibiotic cocktail (ABX) treatment (named the VC + BPF + ABX group). Compared with that in the VC + BPF group, VC in the VC + BPF + ABX group was significantly reduced (Figures 5A–C). We further analyzed the factors associated with inflammation in plasma, and the results showed that compared with those in the VC group, the plasma concentrations of LPS, IL-6, IL-1β, and TNF-α in the rats in the VC + FMT group increased to different degrees (Figures 5D–G), while the concentrations of LPS, IL-6, IL-1β and TNF-α in the VC + BPF + ABX group decreased to different degrees when compared with that in the VC + BPF group (Figures 5D–G). These results indicate that BPF promotes VC through the gut microbiota.

4 Discussion

Bisphenols, a well-known class of endocrine-disrupting chemicals, are widely used in various fields of industry and life. Humans are frequently exposed to bisphenols in daily life, which continuously poses an enormous threat to their health. To our knowledge, this study is the first to report the presence of different concentrations of Bisphenols (BPF, BPF and BPA) in the feces of patients with VC. BPF exposure induced mild VC in normal rats and aggravated VC of VDN-treated rats. The mechanisms may involve BPF exposure-induced perturbation of the gut microbiota and promotion of inflammatory responses.

To our knowledge, only one prior study has reported bisphenol levels in human feces. That study found bisphenols undetectable in some samples. In detectable samples, concentrations ranged as follows: BPA from 47.9 to >500 ng/g; BPF between 28.8 and 400.1 ng/g; and BPS between 43.6 and 83.8 ng/g (Moscoso-Ruiz et al., 2024). Consistent with our findings, BPA showed the highest concentrations, followed by BPF, with BPS being the lowest. However, the bisphenol levels detected in our study were significantly lower than those reported in that research. This discrepancy may stem from differences in the study populations and their environmental exposures (Kang et al., 2006; Liao et al., 2012; Liao and Kannan, 2014; Rochester and Bolden, 2015).

In addition to genetic factors, environmental factors are important in triggering or aggravating CVDs (Lin et al., 2019) that also affect the composition and diversity of gut microbes (Tan et al., 2022). This study revealed that the intestines of rats exposed to BPF were enriched in the genera Escherichia and Shigella, which are associated with the endotoxin LPS and can cause the body to develop a significant inflammatory response. The intestines of BPF-exposed rats were enriched in the gut microbiota associated with the production of SCFAs, such as Alloprevotella, Muribaculaceae, Lactobacillus, Prevotella, Bilophila, Blautia, and Romboutsia; the absence of these symbiotic bacteria is unfavorable for the production of SCFAs (Koh et al., 2016). Our metabolomics data also demonstrated that the SCFA contents in the intestines of rats exposed to BPF were significantly reduced. LPS and SCFAs are two types of important metabolites

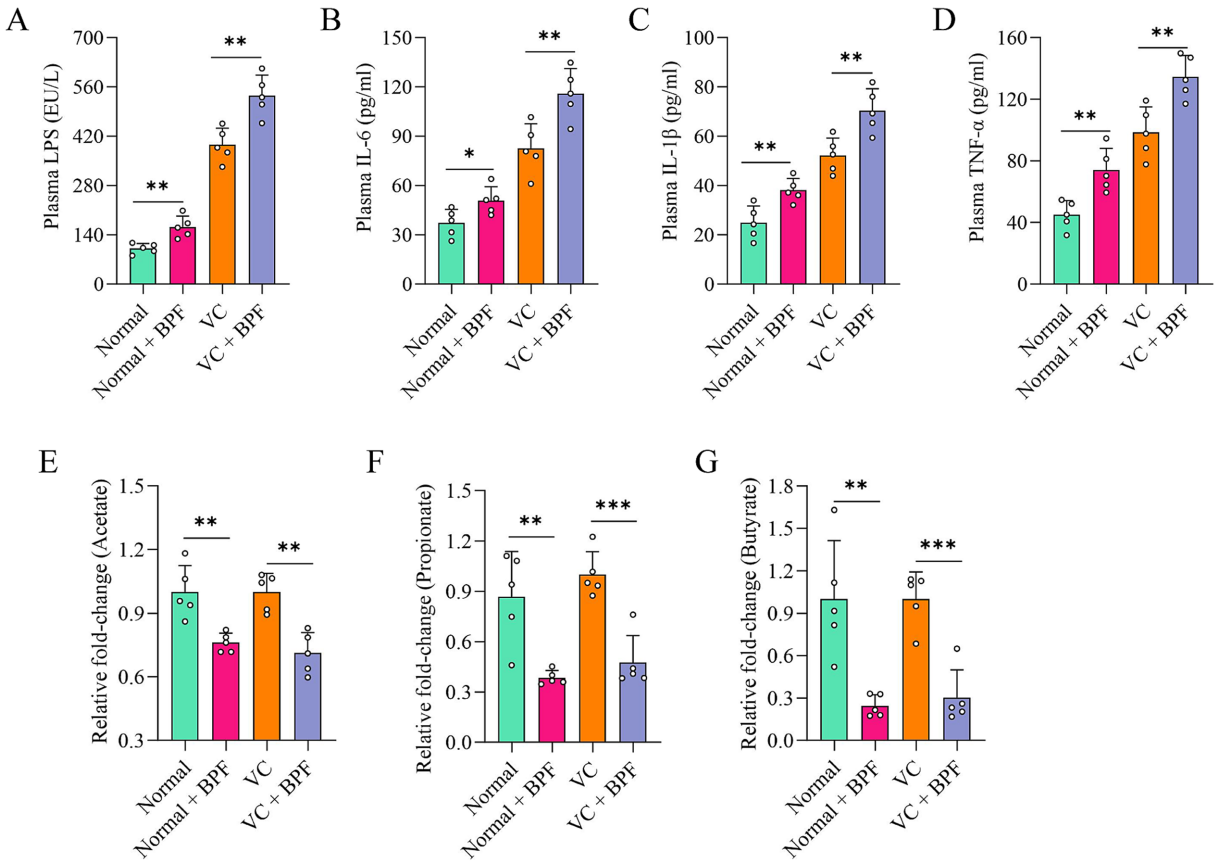

FIGURE 4
BPF exposure promoted systemic inflammatory responses. **(A)** Comparison of the differences in plasma LPS levels (n = 5). **(B–D)** Comparison of the differences in plasma levels of IL-6, IL-1β and TNF-α, respectively (n = 5). **(E–G)** Comparison of the differences in fecal acetate, propionate, and butyrate levels, respectively (n = 5). The t-test for normally distributed data and with the Mann–Whitney U test for non-normally distributed data. *p < 0.05, **p < 0.01, ***p < 0.001.

derived from the gut microbiota that reflect the intestinal system status and the functional status of the gut microbiota (Zhang X. Y. et al., 2020; Zhang X. et al., 2020). Therefore, our study indicated that BPF-related gut microbiota dysbiosis leads to the excessive release of LPS and a deficiency in SCFAs, which may be an important mechanism leading to VC.

To better explain the role of BPF-associated gut microbiota dysbiosis in VC, we transplanted fecal bacteria from BPF-exposed rats to rats with VC and found that FMT significantly aggravated VC and increased the production of inflammatory cytokines. In contrast, Abx treatment depleted the gut microbiota and significantly reduced VC and the production of inflammatory cytokines. Therefore, our study indicated that the exacerbation of VC was dependent on BPF-related gut microbiota dysbiosis, especially the increased abundance of pathogenic Escherichia and Shigella. Escherichia and Shigella, the main members of Proteobacteria, are the main sources of gut-derived LPS (Wang et al., 2022). LPS enters the systemic circulation and activates the Toll-like receptor 4 (TLR4) signaling pathway and TNF-α, IL-1β, and IL-6. The transcription of inflammatory cytokines amplifies the inflammatory response, triggering chronic inflammation in the body (Yan et al., 2023). The development of VC is closely related to the activation of chronic, non-specific inflammation in the body. The results of this study showed that the levels of proinflammatory cytokines, such as LPS, IL-6, IL-1β, and TNF-α, in the systemic circulation of rats exposed to BPF were significantly increased. Consistent with this, BPF exposure disrupted the zebrafish gut microbiota and promoted the expression of the inflammatory cytokines IL-1β and TNF-α (Wang et al., 2021). Inflammatory mediators can activate the inflammation-related transcription factor NF-kB pathway to promote the expression of bone morphogenetic protein-2 (BMP-2), Runt-related transcription Factor 2 (RUNX2) and alkaline phosphatase (ALP) (Panizo et al., 2009; Deuell et al., 2012; Zhang X. Y. et al., 2020; Zhang X. et al., 2020), thereby promoting VC. In summary, exposure to BPF can lead to gut microbiota dysbiosis and the excessive production of LPS, which triggers chronic inflammation in the body and eventually induces or aggravates VC.

The SCFAs are metabolites produced by the gut microbiota that regulate gut microbiota homeostasis (Yan et al., 2022). Our previous study showed that exogenous supplementation with SCFAs (such as propionate) could improve gut microbiota homeostasis (Yan et al., 2022). Studies have shown that when intestinal SCFAs are lacking or insufficient, the pH increases, which is unfavorable for the growth of beneficial bacteria and instead promotes the growth of harmful bacteria, leading to gut microbiota dysbiosis and promoting the development and progression of gut microbiota-related diseases (Wang and Zhao, 2018), such as heart failure (Madan and Mehra,

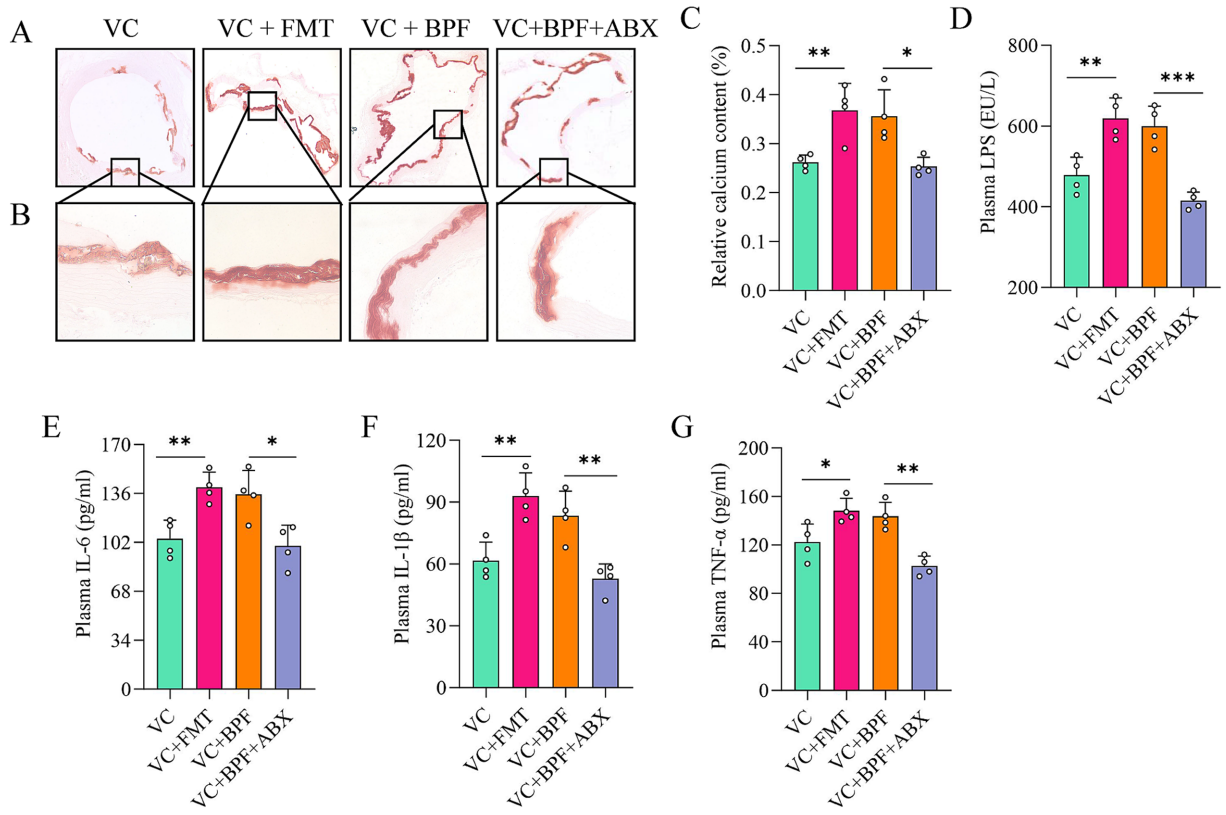

FIGURE 5
BPF promotes VC through the gut microbiota. **(A)** Alizarin red staining of ascending aorta calcification (original magnification, 40×) (n = 4). **(B)** Alizarin red staining of ascending aorta calcification (original magnification, 200×) (n = 4). **(C)** Relative quantification of calcium content for the vessel sections of the ascending aorta (n = 4). **(D)** Comparison of the differences in plasma LPS levels (n = 4). **(E–G)** Comparison of the differences in plasma levels of IL-6, IL-1β and TNF-α, respectively (n = 4). The t-test was used to analyze the differences of two groups. *p < 0.05, **p < 0.01, ***p < 0.001.

2020), hypertension (Yan et al., 2020), and cerebral infarction (Xu et al., 2021). In summary, exposure to BPF can lead to a decrease in the production of SCFAs by the gut microbiota, which may be another mechanism for the induction or aggravation of VC.

Vascular calcification represents a pathological alteration fundamentally driven by chronic inflammation and immune dysregulation (Wu et al., 2013), with its pathogenesis closely linked to the functional interplay between the spleen and liver as pivotal immunomodulatory organs (Emami et al., 2015; Brummer et al., 2025). The unique anatomical connection wherein splenic venous blood directly converges into the liver via the portal vein establishes the physiological foundation of the "spleno-hepatic axis" Research indicates that bisphenol compounds can exploit this axis to trigger systemic chronic inflammatory-immune responses, ultimately impacting the cardiovascular system: First, splenic-derived myeloid-derived suppressor cells (MDSCs) and natural killer T (NKT) cells rapidly infiltrate the liver through portal circulation (Brummer et al., 2025). Simultaneously, damaged hepatocytes release IL-6, GM-CSF, and lipotoxic antigens that retrograde via the portal vein to activate splenic myeloid precursor cells, promoting the expansion and differentiation of MDSCs and NKT cells. This bidirectional pathological cycle leads to the cascade amplification of inflammatory cytokines (TNF-α, IL-1β, IL-6) between the liver and spleen, persistently exacerbating systemic inflammatory processes (Tarantino et al., 2021; Sangwan et al., 2024; Zhu et al., 2024; Brummer et al., 2025). Second, bisphenols synergistically intensify inflammation by disrupting the "gut-spleen axis" Perinatal BPA exposure not only significantly disturbs maternal gut microbiota (e.g., reduced Akkermansia, aberrant Dubosiella) and impairs offspring splenic immune development, but also diminishes the differentiation capacity of splenic regulatory T cells (Tregs) due to decreased microbial metabolite short-chain fatty acids (SCFAs) (López-Moreno et al., 2025). Critically, BPA-induced intestinal barrier damage allows pathogen-associated molecular patterns (PAMPs) like lipopolysaccharide (LPS) to enter the spleen via the portal vein, activating Toll-like receptor 4 (TLR4) and provoking systemic inflammation (López-Moreno et al., 2025). Furthermore, quinone metabolites generated from bisphenol compounds within the spleen deplete antioxidant enzymes (superoxide dismutase, glutathione), inducing lipid peroxidation and DNA damage (Jalal et al., 2018). This subsequently activates the NF-κB pathway and upregulates key inflammatory mediators including cyclooxygenase-2 and inducible nitric oxide synthase, establishing a third independent inflammatory amplification pathway distinct from the aforementioned axes (Jalal et al., 2018). Collectively, bisphenol compounds synergistically drive vascular calcification through three interconnected mechanisms: the spleno-hepatic axis bidirectional pathology, gut-spleen axis disruption, and splenic oxidative stress.

In this study, BPF was selected as the research object based on the ROC curves results. In fact, BPF, BPA, and BPS have similar chemical

structures and thus similar physicochemical properties. There is a growing body of evidence that indicates that BPF, BPA and BPS have different degrees of toxicity to organisms. Therefore, we speculate that BPF, BPA and BPS produce the same effect. We look forward to follow-up studies on the roles of BPA and BPS in CVDs. In addition, how BPF causes gut microbiota dysbiosis and how body inflammation triggers VC are worthy of more in-depth study in the future.

5 Conclusion

Overall, our results demonstrate that BPF exposure induces mild VC in normal rats and exacerbates VC in VDN-treated rats, mediated through gut microbiota dysbiosis via the gut–vascular axis. This dysbiosis, characterized by elevated lipopolysaccharide (LPS) and reduced short-chain fatty acid (SCFA) levels, triggers inflammatory responses in normal rats and aggravates inflammation in VDN-treated rats. These findings establish a mechanistic link between gut microbiota disruption and BPF-induced VC, providing novel insights into the role of LPS/SCFA imbalance in VC pathogenesis and a theoretical basis for incorporating BPF exposure into cardiovascular disease risk assessments.

Data availability statement

The raw 16S rRNA sequencing data have been deposited in the NCBI Sequence Read Archive (SRA) under BioProject accession PRJNA1287671.

Ethics statement

This observational study was registered under trial NCT04864457. All selected participants provided informed consent, and the research protocol was approved by the Ethics Committee of Shenzhen People's Hospital. The studies were conducted in accordance with the local legislation and institutional requirements. The participants provided their written informed consent to participate in this study.

Author contributions

JYa: Funding acquisition, Writing – review & editing, Methodology, Investigation, Writing – original draft, Data curation. YP: Funding acquisition, Writing – review & editing, Writing – original draft, Methodology, Data curation, Investigation. HL: Investigation, Writing – review & editing. JYu: Supervision, Writing – review & editing. JC: Supervision, Writing – review & editing. YG: Writing – review & editing, Validation. CL: Validation, Writing – review & editing. FL: Writing – review & editing, Validation. RW: Investigation, Validation, Writing – review & editing. YH: Funding acquisition, Writing – review & editing. CW: Validation, Investigation, Writing – review & editing. CX: Formal analysis, Writing – review & editing. TL: Writing – review & editing, Formal analysis. PZ: Formal analysis, Writing – review & editing. YL: Writing – original draft, Writing – review & editing, Investigation. WS: Writing – review & editing, Writing – original draft, Investigation. XP: Writing – review & editing, Resources, Funding acquisition. DY: Funding acquisition, Writing – review & editing, Project administration. XS: Funding acquisition, Writing – review & editing, Conceptualization, Project administration, Resources. WL: Conceptualization, Writing – review & editing, Resources, Project administration, Funding acquisition.

Funding

The author(s) declare that financial support was received for the research and/or publication of this article. This work was supported by Guangdong Basic and Applied Basic Research Foundation (2023A1515110916, 2025A1515010555), Shenzhen Science and Technology Program (JCYJ20230807112301002, JCYJ20240813103820027, JCYJ20230807112110022, JCYJ20220530151804009), Shenzhen Health Economics Association Research Foundation (HLJJYJ2023-N006), Shenzhen People's Hospital Nursing Research Fund Project (SYHL2024-N0001), Shenzhen Science and Technology Innovation Committee (SZSTI) (RCYX20221008092950121), Major scientific research project of Shenzhen People's Hospital (SYWGSJCYJ202202, SYWGSCGZH202301), the National Natural Science Foundation of China (82070517), Shenzhen Key Medical Discipline Construction Fund (No. SZXK003), and the Sanming Project of Medicine in Shenzhen (No. SZSM201412012).

Acknowledgments

We thank all technicians from the Translational Medicine Collaborative Innovation Center, the Second Clinical Medical College (Shenzhen People's Hospital), Jinan University, Shenzhen 518020, China, who helped with the experiment. We thank all the medical staff in the Cardiovascular Medicine Department of Shenzhen People's Hospital for their support of this work.

Conflict of interest

The authors declare that the research was conducted in the absence of any commercial or financial relationships that could be construed as a potential conflict of interest.

Generative AI statement

The authors declare that no Gen AI was used in the creation of this manuscript.

Publisher's note

All claims expressed in this article are solely those of the authors and do not necessarily represent those of their affiliated organizations, or those of the publisher, the editors and the reviewers. Any product that may be evaluated in this article, or claim that may be made by its manufacturer, is not guaranteed or endorsed by the publisher.

References

Agatston, A. S., Janowitz, W. R., Hildner, F. J., Zusmer, N. R., Viamonte, M., and Detrano, R. (1990). Quantification of coronary artery calcium using ultrafast computed tomography. *J. Am. Coll. Cardiol.* 15, 827–832. doi: 10.1016/0735-1097(90)90282-t

Ardissino, D., Berzuini, C., Merlini, P. A., Mannuccio Mannucci, P., Surti, A., Burtt, N., et al. (2011). Influence of 9p21.3 genetic variants on clinical and angiographic outcomes in early-onset myocardial infarction. *J. Am. Coll. Cardiol.* 58, 426–434. doi: 10.1016/j.jacc.2010.11.075

Arrokhman, S., Luo, Y. H., and Lin, P. (2023). Additive cardiotoxicity of a bisphenol mixture in zebrafish embryos: the involvement of calcium channel and pump. *Ecotoxicol. Environ. Saf.* 263:115225. doi: 10.1016/j.ecoenv.2023.115225

Brummer, C., Singer, K., Renner, K., Bruss, C., Hellerbrand, C., Dorn, C., et al. (2025). The spleen-liver axis supports obesity-induced systemic and fatty liver inflammation via MDSC and NKT cell enrichment. *Mol. Cell. Endocrinol.* 601:112518. doi: 10.1016/j.mce.2025.112518

Byndloss, M. X., and Bäumler, A. J. (2018). The germ-organ theory of non-communicable diseases. *Nat. Rev. Microbiol.* 16, 103–110. doi: 10.1038/nrmicro.2017.158

Castro, B., Sánchez, P., Torres, J. M., and Ortega, E. (2015). Bisphenol a, bisphenol F and bisphenol S affect differently 5α-reductase expression and dopamine-serotonin systems in the prefrontal cortex of juvenile female rats. *Environ. Res.* 142, 281–287. doi: 10.1016/j.envres.2015.07.001

Chen, Y., Fang, J., Ren, L., Fan, R., Zhang, J., Liu, G., et al. (2018). Urinary bisphenol analogues and triclosan in children from South China and implications for human exposure. *Environ. Pollut.* 238, 299–305. doi: 10.1016/j.envpol.2018.03.031

Cheng, M. D., Li, C. L., Pei, X. Y., Zhang, Y. F., Jia, D. D., Zuo, Y. B., et al. (2023). Integrative analysis of DNA methylome and transcriptome reveals epigenetic regulation of bisphenols-induced cardiomyocyte hypertrophy. *Ecotoxicol. Environ. Saf.* 263:115391. doi: 10.1016/j.ecoenv.2023.115391

Czarny-Krzymińska, K., Krawczyk, B., and Szczukocki, D. (2023). Bisphenol a and its substitutes in the aquatic environment: occurrence and toxicity assessment. *Chemosphere* 315:137763. doi: 10.1016/j.chemosphere.2023.137763

Deuell, K. A., Callegari, A., Giachelli, C. M., Rosenfeld, M. E., and Scatena, M. (2012). RANKL enhances macrophage paracrine pro-calcific activity in high phosphate-treated smooth muscle cells: dependence on IL-6 and TNF-α. *J. Vasc. Res.* 49, 510–521. doi: 10.1159/000341216

Dias, P., Tvrdý, V., Jirkovský, E., Dolenc, M. S., Peterlin Mašič, L., and Mladěnka, P. (2022). The effects of bisphenols on the cardiovascular system. *Crit. Rev. Toxicol.* 52, 66–87. doi: 10.1080/10408444.2022.2046690

Emami, H., Singh, P., MacNabb, M., Vucic, E., Lavender, Z., Rudd, J. H., et al. (2015). Splenic metabolic activity predicts risk of future cardiovascular events: demonstration of a cardiosplenic axis in humans. *JACC Cardiovasc. Imaging* 8, 121–130. doi: 10.1016/j.jcmg.2014.10.009

Gao, C., He, H., Qiu, W., Zheng, Y., Chen, Y., Hu, S., et al. (2021). Oxidative stress, endocrine disturbance, and immune interference in humans showed relationships to serum bisphenol concentrations in a dense industrial area. *Environ. Sci. Technol.* 55, 1953–1963. doi: 10.1021/acs.est.0c07587

Hu, J., Zhao, H., Braun, J. M., Zheng, T., Zhang, B., Xia, W., et al. (2019). Associations of trimester-specific exposure to bisphenols with size at birth: a Chinese prenatal cohort study. *Environ. Health Perspect.* 127:107001. doi: 10.1289/EHP4664

Huang, G. M., Tian, X. F., Fang, X. D., and Ji, F. J. (2016). Waterborne exposure to bisphenol F causes thyroid endocrine disruption in zebrafish larvae. *Chemosphere* 147, 188–194. doi: 10.1016/j.chemosphere.2015.12.080

Jalal, N., Surendranath, A. R., Pathak, J. L., Yu, S., and Chung, C. Y. (2018). Bisphenol a (BPA) the mighty and the mutagenic. *Toxicol. Rep.* 5, 76–84. doi: 10.1016/j.toxrep.2017.12.013

Ji, G., Gu, J., Guo, M., Zhou, L., Wang, Z., Shi, L., et al. (2022). A systematic comparison of the developmental vascular toxicity of bisphenol a and its alternatives in vivo and in vitro. *Chemosphere* 291:132936. doi: 10.1016/j.chemosphere.2021.132936

Kang, J. H., Asai, D., and Toita, R. (2023). Bisphenol a (BPA) and cardiovascular or Cardiometabolic diseases. *J Xenobiot* 13, 775–810. doi: 10.3390/jox13040049

Kang, J. H., Kondo, F., and Katayama, Y. (2006). Human exposure to bisphenol a. *Toxicology* 226, 79–89. doi: 10.1016/j.tox.2006.06.009

Koh, A., De Vadder, F., Kovatcheva-Datchary, P., and Bäckhed, F. (2016). From dietary Fiber to host physiology: short-chain fatty acids as key bacterial metabolites. *Cell* 165, 1332–1345. doi: 10.1016/j.cell.2016.05.041

Lambré, C., Barat Baviera, J. M., Bolognesi, C., Chesson, A., Cocconcelli, P. S., Crebelli, R., et al. (2023). Re-evaluation of the risks to public health related to the presence of bisphenol a (BPA) in foodstuffs. *EFSA J.* 21:e06857. doi: 10.2903/j.efsa.2023.6857

Lee, S., An, K. S., Kim, H. J., Noh, H. J., Lee, J., Lee, J., et al. (2022). Pharmacokinetics and toxicity evaluation following oral exposure to bisphenol F. *Arch. Toxicol.* 96, 1711–1728. doi: 10.1007/s00204-022-03246-w

Li, J., Zhang, Z., Zhang, C., Zhu, Q., Zhao, J., Zong, H., et al. (2023). Association between urinary bisphenols and body composition among American adults: cross-sectional National Health and nutrition examination survey study. *JMIR Public Health Surveill.* 9:e49652. doi: 10.2196/49652

Liao, C., and Kannan, K. (2014). A survey of alkylphenols, bisphenols, and triclosan in personal care products from China and the United States. *Arch. Environ. Contam. Toxicol.* 67, 50–59. doi: 10.1007/s00244-014-0016-8

Liao, C., Liu, F., Guo, Y., Moon, H. B., Nakata, H., Wu, Q., et al. (2012). Occurrence of eight bisphenol analogues in indoor dust from the United States and several Asian countries: implications for human exposure. *Environ. Sci. Technol.* 46, 9138–9145. doi: 10.1021/es302004w

Lin, P. D., Cardenas, A., Hauser, R., Gold, D. R., Kleinman, K. P., Hivert, M. F., et al. (2019). Per- and polyfluoroalkyl substances and blood lipid levels in pre-diabetic adults-longitudinal analysis of the diabetes prevention program outcomes study. *Environ. Int.* 129, 343–353. doi: 10.1016/j.envint.2019.05.027

López-Moreno, A., Torres-Sánchez, A., Suárez, A., Ruiz-Rodríguez, A., and Aguilera, M. (2025). Perinatal bisphenol a exposure impairs gut microbial colonization: implications for offspring obesity and neurodevelopment. *Ecotoxicol. Environ. Saf.* 298:118295. doi: 10.1016/j.ecoenv.2025.118295

Lu, X., Liu, Z., Cui, Q., Liu, F., Li, J., Niu, X., et al. (2022). A polygenic risk score improves risk stratification of coronary artery disease: a large-scale prospective Chinese cohort study. *Eur. Heart J.* 43, 1702–1711. doi: 10.1093/eurheartj/ehac093

Madan, S., and Mehra, M. R. (2020). Gut dysbiosis and heart failure: navigating the universe within. *Eur. J. Heart Fail.* 22, 629–637. doi: 10.1002/ejhf.1792

Mahmood, S. S., Levy, D., Vasan, R. S., and Wang, T. J. (2014). The Framingham heart study and the epidemiology of cardiovascular disease: a historical perspective. *Lancet* 383, 999–1008. doi: 10.1016/S0140-6736(13)61752-3

Meng, Z., Tian, S., Yan, J., Jia, M., Yan, S., Li, R., et al. (2019). Effects of perinatal exposure to BPA, BPF and BPAF on liver function in male mouse offspring involving in oxidative damage and metabolic disorder. *Environ. Pollut.* 247, 935–943. doi: 10.1016/j.envpol.2019.01.116

Moscoso-Ruiz, I., Cantarero-Malagón, S., Rivas, A., and Zafra-Gómez, A. (2024). New analytical method for the determination of endocrine disruptors in human faeces using gas chromatography coupled to tandem mass spectrometry. *Anal Bioanal Chem.* 416, 1085–1099. doi: 10.1007/s00216-023-05087-7

Mu, X., Liu, J., Wang, H., Yuan, L., Wang, C., Li, Y., et al. (2022a). Bisphenol F impaired zebrafish cognitive ability through inducing neural cell heterogeneous responses. *Environ. Sci. Technol.* 56, 8528–8540. doi: 10.1021/acs.est.2c01531

Mu, X., Qi, S., Liu, J., Wang, H., Yuan, L., Qian, L., et al. (2022b). Environmental level of bisphenol F induced reproductive toxicity toward zebrafish. *Sci. Total Environ.* 806:149992. doi: 10.1016/j.scitotenv.2021.149992

Münzel, T., Hahad, O., Daiber, A., and Landrigan, P. J. (2023). Soil and water pollution and human health: what should cardiologists worry about. *Cardiovasc. Res.* 119, 440–449. doi: 10.1093/cvr/cvac082

Panizo, S., Cardus, A., Encinas, M., Parisi, E., Valcheva, P., López-Ongil, S., et al. (2009). RANKL increases vascular smooth muscle cell calcification through a RANK-BMP4-dependent pathway. *Circ. Res.* 104, 1041–1048. doi: 10.1161/CIRCRESAHA.108.189001

Pedrosa, J. F., Barreto, S. M., Bittencourt, M. S., and Ribeiro, A. (2019). Anatomical references to evaluate thoracic aorta calcium by computed tomography. *Curr. Atheroscler. Rep.* 21:51. doi: 10.1007/s11883-019-0811-9

Ripatti, S., Tikkanen, E., Orho-Melander, M., Havulinna, A. S., Silander, K., Sharma, A., et al. (2010). A multilocus genetic risk score for coronary heart disease: case-control and prospective cohort analyses. *Lancet* 376, 1393–1400. doi: 10.1016/S0140-6736(10)61267-6

Rochester, J. R., and Bolden, A. L. (2015). Bisphenol S and F: a systematic review and comparison of the hormonal activity of bisphenol a substitutes. *Environ. Health Perspect.* 123, 643–650. doi: 10.1289/ehp.1408989

Sangwan, S., Bhattacharyya, R., and Banerjee, D. (2024). Plastic compounds and liver diseases: whether bisphenol a is the only culprit. *Liver Int.* 44, 1093–1105. doi: 10.1111/liv.15879

Staley, C., Kaiser, T., Beura, L. K., Hamilton, M. J., Weingarden, A. R., Bobr, A., et al. (2017). Stable engraftment of human microbiota into mice with a single oral gavage following antibiotic conditioning. *Microbiome* 5:87. doi: 10.1186/s40168-017-0306-2

Tan, R., Jin, M., Shao, Y., Yin, J., Li, H., Chen, T., et al. (2022). High-sugar, high-fat, and high-protein diets promote antibiotic resistance gene spreading in the mouse intestinal microbiota. *Gut Microbes* 14:2022442. doi: 10.1080/19490976.2021.2022442

Tarantino, G., Citro, V., and Balsano, C. (2021). Liver-spleen axis in non-alcoholic fatty liver disease. *Expert Rev. Gastroenterol. Hepatol.* 15, 759–769. doi: 10.1080/17474124.2021.1914587

Ullah, A., Pirzada, M., Afsar, T., Razak, S., Almajwal, A., and Jahan, S. (2019). Effect of bisphenol F, an analog of bisphenol a, on the reproductive functions of male rats. *Environ. Health Prev. Med.* 24:41. doi: 10.1186/s12199-019-0797-5

Ullah, A., Pirzada, M., Jahan, S., Ullah, H., Shaheen, G., Rehman, H., et al. (2018). Bisphenol a and its analogs bisphenol B, bisphenol F, and bisphenol S: comparative in vitro and in vivo studies on the sperms and testicular tissues of rats. *Chemosphere* 209, 508–516. doi: 10.1016/j.chemosphere.2018.06.089

Wang, P., Guo, R., Bai, X., Cui, W., Zhang, Y., Li, H., et al. (2022). Sacubitril/valsartan contributes to improving the diabetic kidney disease and regulating the gut microbiota in mice. *Front Endocrinol* 13:1034818. doi: 10.3389/fendo.2022.1034818

Wang, Y., Wang, B., Wang, Q., Liu, Y., Liu, X., Wu, B., et al. (2021). Intestinal toxicity and microbial community disorder induced by bisphenol F and bisphenol S in zebrafish. *Chemosphere* 280:130711. doi: 10.1016/j.chemosphere.2021.130711

Wang, Z., and Zhao, Y. (2018). Gut microbiota derived metabolites in cardiovascular health and disease. *Protein Cell* 9, 416–431. doi: 10.1007/s13238-018-0549-0

Wu, M., Rementer, C., and Giachelli, C. M. (2013). Vascular calcification: an update on mechanisms and challenges in treatment. *Calcif. Tissue Int.* 93, 365–373. doi: 10.1007/s00223-013-9712-z

Xu, K., Gao, X., Xia, G., Chen, M., Zeng, N., Wang, S., et al. (2021). Rapid gut dysbiosis induced by stroke exacerbates brain infarction in turn. *Gut* 70, 1486–1494. doi: 10.1136/gutjnl-2020-323263

Yan, X., Jin, J., Su, X., Yin, X., Gao, J., Wang, X., et al. (2020). Intestinal Flora modulates blood pressure by regulating the synthesis of intestinal-derived corticosterone in high salt-induced hypertension. *Circ. Res.* 126, 839–853. doi: 10.1161/CIRCRESAHA.119.316394

Yan, J., Pan, Y., He, J., Pang, X., Shao, W., Wang, C., et al. (2023). Toxic vascular effects of polystyrene microplastic exposure. *Sci. Total Environ.* 905:167215. doi: 10.1016/j.scitotenv.2023.167215

Yan, J., Pan, Y., Shao, W., Wang, C., Wang, R., He, Y., et al. (2022). Beneficial effect of the short-chain fatty acid propionate on vascular calcification through intestinal microbiota remodelling. *Microbiome* 10:195. doi: 10.1186/s40168-022-01390-0

Yang, Y., Lu, L., Zhang, J., Yang, Y., Wu, Y., and Shao, B. (2014). Simultaneous determination of seven bisphenols in environmental water and solid samples by liquid chromatography-electrospray tandem mass spectrometry. *J. Chromatogr. A* 1328, 26–34. doi: 10.1016/j.chroma.2013.12.074

Yuan, L., Qian, L., Qian, Y., Liu, J., Yang, K., Huang, Y., et al. (2019). Bisphenol F-induced neurotoxicity toward zebrafish embryos. *Environ. Sci. Technol.* 53, 14638–14648. doi: 10.1021/acs.est.9b04097

Yuan, B. F., Zhu, Q. F., Guo, N., Zheng, S. J., Wang, Y. L., Wang, J., et al. (2018). Comprehensive profiling of fecal metabolome of mice by integrated chemical isotope labeling-mass spectrometry analysis. *Anal. Chem.* 90, 3512–3520. doi: 10.1021/acs.analchem.7b05355

Zhang, X. Y., Chen, J., Yi, K., Peng, L., Xie, J., Gou, X., et al. (2020). Phlorizin ameliorates obesity-associated endotoxemia and insulin resistance in high-fat diet-fed mice by targeting the gut microbiota and intestinal barrier integrity. *Gut Microbes* 12, 1842990–1842918. doi: 10.1080/19490976.2020.1842990

Zhang, X., Li, Y., Yang, P., Liu, X., Lu, L., Chen, Y., et al. (2020). Trimethylamine-N-oxide promotes vascular calcification through activation of NLRP3 (nucleotide-binding domain, leucine-rich-containing family, pyrin domain-Containing-3) Inflammasome and NF-κB (nuclear factor κB) signals. *Arterioscler. Thromb. Vasc. Biol.* 40, 751–765. doi: 10.1161/ATVBAHA.119.313414

Zhang, X. M., Lou, X. Y., Wu, L. H., Huang, C., Chen, D., and Guo, Y. (2018). Urinary phthalate metabolites and environmental phenols in university students in South China. *Environ. Res.* 165, 32–39. doi: 10.1016/j.envres.2018.04.006

Zhao, S., Jang, C., Liu, J., Uehara, K., Gilbert, M., Izzo, L., et al. (2020). Dietary fructose feeds hepatic lipogenesis via microbiota-derived acetate. *Nature* 579, 586–591. doi: 10.1038/s41586-020-2101-7

Zhao, C., Xie, P., Wang, H., and Cai, Z. (2018). Liquid chromatography-mass spectrometry-based metabolomics and lipidomics reveal toxicological mechanisms of bisphenol F in breast cancer xenografts. *J. Hazard. Mater.* 358, 503–507. doi: 10.1016/j.jhazmat.2018.05.010

Zheng, S. J., Liu, S. J., Zhu, Q. F., Guo, N., Wang, Y. L., Yuan, B. F., et al. (2018). Establishment of liquid chromatography retention index based on chemical labeling for Metabolomic analysis. *Anal. Chem.* 90, 8412–8420. doi: 10.1021/acs.analchem.8b00901

Zheng, Q., Xiao, J., Zhang, D., Li, X., Xu, J., Ma, J., et al. (2024). Bisphenol analogues in infant foods in South China and implications for infant exposure. *Sci. Total Environ.* 910:168509. doi: 10.1016/j.scitotenv.2023.168509

Zheng, H., Xu, P., Jiang, Q., Xu, Q., Zheng, Y., Yan, J., et al. (2021). Depletion of acetate-producing bacteria from the gut microbiota facilitates cognitive impairment through the gut-brain neural mechanism in diabetic mice. *Microbiome* 9:145. doi: 10.1186/s40168-021-01088-9

Zhu, B., Wu, H., Li, K. S., Eisa-Beygi, S., Singh, B., Bielenberg, D. R., et al. (2024). Two sides of the same coin: non-alcoholic fatty liver disease and atherosclerosis. *Vasc. Pharmacol.* 154:107249. doi: 10.1016/j.vph.2023.107249

Zhu, Q. F., Zhang, Z., Liu, P., Zheng, S. J., Peng, K., Deng, Q. Y., et al. (2016). Analysis of liposoluble carboxylic acids metabolome in human serum by stable isotope labeling coupled with liquid chromatography-mass spectrometry. *J. Chromatogr. A* 1460, 100–109. doi: 10.1016/j.chroma.2016.07.017

frontiers | Frontiers in Microbiology

TYPE Original Research
PUBLISHED 12 August 2025
DOI 10.3389/fmicb.2025.1607045

Check for updates

OPEN ACCESS

EDITED BY
Yu Pi,
Chinese Academy of Agricultural Sciences, China

REVIEWED BY
Andreas Martin Grabrucker,
University of Limerick, Ireland
Qinrui Li,
Peking University People's Hospital, China

*CORRESPONDENCE
Michael W. Taylor
✉ mw.taylor@auckland.ac.nz

RECEIVED 07 April 2025
ACCEPTED 24 July 2025
PUBLISHED 12 August 2025

CITATION
Wong GC, Jung Y, Lee K, Fourie C, Handley KM, Montgomery JM and Taylor MW (2025) Effect of dietary zinc supplementation on the gastrointestinal microbiome and host gene expression in the *Shank3B*$^{-/-}$ mouse model of autism spectrum disorder.
Front. Microbiol. 16:1607045.
doi: 10.3389/fmicb.2025.1607045

COPYRIGHT
© 2025 Wong, Jung, Lee, Fourie, Handley, Montgomery and Taylor. This is an open-access article distributed under the terms of the Creative Commons Attribution License (CC BY). The use, distribution or reproduction in other forums is permitted, provided the original author(s) and the copyright owner(s) are credited and that the original publication in this journal is cited, in accordance with accepted academic practice. No use, distribution or reproduction is permitted which does not comply with these terms.

Effect of dietary zinc supplementation on the gastrointestinal microbiome and host gene expression in the *Shank3B*$^{-/-}$ mouse model of autism spectrum disorder

Giselle C. Wong[1,2], Yewon Jung[2,3], Kevin Lee[2,3], Chantelle Fourie[2,3], Kim M. Handley[1], Johanna M. Montgomery[2,3] and Michael W. Taylor[1,2]*

[1]School of Biological Sciences, University of Auckland, Auckland, New Zealand, [2]Centre for Brain Research, University of Auckland, Auckland, New Zealand, [3]Department of Physiology, University of Auckland, Auckland, New Zealand

Shank gene variants are implicated in ~1% of people with autism, and mice lacking *Shank3* exhibit autism-like behaviours. Zinc deficiency and gastrointestinal problems can be common among people with autism, and zinc is a key element required for SHANK protein function and gut development. In *Shank3B*$^{-/-}$ mice, a supplementary zinc diet reverses autism-like behaviours. We hypothesise that dietary zinc may alter the gut microbiome, potentially affecting the gut-microbiome-brain axis, which may contribute to changes in autism-like behaviours. To test this, four types of gastrointestinal samples (ileum, caecum, colon, faecal) were collected from *Shank3B*$^{-/-}$ wild-type and knock-out mice on either control or supplemented-zinc diets, enabling us to examine the influence of—and interactions between—dietary zinc, the gut microbiome, and ASD-linked host genotype. Cage, genotype, and zinc diet each contributed significantly to bacterial community variation (accounting for 12.8, 3.9, and 2.3% of the variation, respectively). Fungal diversity was significantly lower in *Shank3B*$^{-/-}$ compared with wild-type mice on the control zinc diet, with specific fungal biota signatures detected among gut locations. Host metabolic genes, which may be regulated by the gut microbiota, and host genes involved in antimicrobial interactions were more highly expressed in *Shank3B*$^{-/-}$ mice. Metagenomic analyses revealed differential abundance of bacterial fatty acid biosynthesis and transporters (including zinc transport and neurotransmitter receptors) among our experimental groups. Overall these suggested increased activity of, or a switch towards, metabolic and microbial-host interactions that may benefit both host and microbe, in the presence of zinc. This raises the potential of manipulating both dietary zinc and the gut microbiota itself to ameliorate ASD-related behaviours and associated gastrointestinal issues. These data broaden understanding of the gut microbiome in autism and pave the way towards potential microbial therapeutics for gastrointestinal problems in people with autism.

KEYWORDS

autism spectrum disorder, mouse model, *Shank3*, gut microbiome, host gene expression, bacteria, fungi, zinc

1 Introduction

Autism spectrum disorder (ASD) is a neurodevelopmental condition that is clinically diagnosed by persistent deficits in three areas of social communication and interaction plus at least two of four types of restricted repetitive behaviours (American Psychiatric Association, 2013). Recent data indicate that ASD prevalence may be as high as 1 in 54 people (Maenner et al., 2020). It is clear that genetics play an important role in ASD causation (Abrahams and Geschwind, 2008; Sanders et al., 2012), while the potential influence of environmental factors has also come under increased scrutiny (Grabrucker, 2012; Karimi et al., 2017). One group of genes implicated in ASD encodes for the SH3 and multiple ankyrin (SHANK) repeat domain proteins. The SHANK protein family represents a group of important synaptic proteins localised in the post-synaptic density of the excitatory glutamatergic synapses in the brain (Naisbitt et al., 1999; Vyas and Montgomery, 2016), and mutations in the *Shank3* gene are associated with ~1% of all ASD cases (Leblond et al., 2014). Animal models of ASD have been created with ASD-*Shank* mutations to facilitate study of ASD mechanisms (Jiang and Ehlers, 2013; Nithianantharajah et al., 2017), including the *Shank3B*$^{-/-}$ mutant mouse model (ex13-16) which displays ASD-like characteristics including repetitive behaviours (grooming), anxiety, and deficits in social interaction (Peca et al., 2011). The *Shank3B*$^{-/-}$ knockout (KO) mouse model enables exploration of the interplay between the gut, the gut microbiota, and ASD. Indeed, a recent study of the microbiota of *Shank3B*$^{-/-}$ mice concluded that there was an imbalance, or dysbiosis, within the gut bacterial community, but that probiotic treatment with *L. reuteri* ameliorated ASD-like behaviours (Tabouy et al., 2018). SHANK3 may also play a role in gut permeability changes in ASD, with *Shank3* KO mice exhibiting decreased expression of the tight junction protein ZO-1 in the gut (Wei et al., 2017).

The micronutrient zinc is required for many processes in the body, including gastrointestinal (GI) epithelial barrier function (Skrovanek et al., 2014), gut permeability (Sturniolo et al., 2002), and enzyme functionality (McCall et al., 2000). Dietary zinc is mainly absorbed in the small intestine, where intestinal mucosa metallothionein proteins, zip proteins, and zinc transporters control zinc homeostasis (Maret, 2000; Dufner-Beattie et al., 2003; Liuzzi et al., 2004). Dietary zinc supplementation also confers protection against colitis along with zinc-mediated anti-inflammatory effects, improving gastrointestinal barrier function (Sturniolo et al., 2001; Sturniolo et al., 2002; Foligne et al., 2020; Souffriau et al., 2020). Zinc deficiency has been reported in the ASD population (Faber et al., 2009; Grabrucker et al., 2011b; Yasuda et al., 2015), potentially due to or leading to compromised nutrient acquisition from an individual's diet (Gebhard et al., 1983), diarrhoea, and malnutrition due to reduced integrity of the gut epithelial barrier (Wapnir, 2000), and increased susceptibility to gut pathogens.

Gastrointestinal disorders (ranging from severe constipation to diarrhoea) are common in people with ASD (Buie et al., 2010; Babinska et al., 2020). In at least some cases this may be related to a compromised intestinal epithelial barrier ("leaky gut") through which dietary products and/or bacterial metabolites may pass to enter into the bloodstream (D'Eufemia et al., 1996; Horvath and Perman, 2002; de Magistris et al., 2010; Kushak et al., 2016). Once in the bloodstream, immune responses and direct interactions with the central nervous system may be elicited. This brings into focus a potential contributing role for the gut microbiota in ASD. The gut-microbiota-brain axis refers to the bidirectional communication between gut microbes and the brain (Rhee et al., 2009; Cryan and O'Mahony, 2011; O'Mahony et al., 2015; Cryan et al., 2019), and there is evidence from both humans (De Angelis et al., 2015; Strati et al., 2017) and animal models (Hsiao et al., 2013; Buffington et al., 2016) for a link between the gut microbiota and ASD. Buffington et al. (2016) were able to reverse ASD-associated behaviours and elicit changes in brain neuronal activity in a mouse model of autism by reintroducing the probiotic bacterium *Lactobacillus reuteri*. Numerous studies have reported distinct gut microbiotas (including both bacteria and fungi) in people with and without ASD, while others report no such difference (Gondalia et al., 2012; Son et al., 2015; Strati et al., 2017; Kang et al., 2018; Liu et al., 2019). Nonetheless, the malleability of the gut microbiota, through for example diet changes, probiotics, or even faecal microbiota transfers between individuals, makes this an attractive option to explore in terms of developing potential microbiota-based therapies for ASD and the associated GI issues.

The SAM domain of SHANK3 proteins contains a zinc-binding site, which requires zinc to create structural homomers that act as a scaffold in the post-synaptic density (Grabrucker et al., 2011a), and to build post-synaptic protein complexes (Arons et al., 2016). SHANK3 deficiencies have also been associated with leaky gut and changes to the gut microbiome in a mouse model of ASD (Sauer et al., 2019). Zinc deficiency and loss-of-function *Shank* gene mutations have implications for assembly, localisation, and neurotransmission at the synapse (Rubenstein and Merzenich, 2003). Neurophysiology studies have shown that zinc is responsible for stabilising SHANK3 at the post-synaptic density and regulating excitatory glutamatergic synaptic transmission (Arons et al., 2016; Tao-Cheng et al., 2016). Disruption of this zinc-sensitive signalling system has been observed in *Shank3* mutations related to ASD, which may impact the functionality and plasticity of synapses in the brain and potentially result in ASD-like behaviours (Grabrucker, 2014; Arons et al., 2016). Supplementation of zinc in the diet is beneficial in the *Shank3B*$^{-/-}$ KO mouse model of ASD, with 6 weeks of postnatal supplemented dietary zinc resulting in the reversal of ASD-like behaviours as well as changes in the strength and structure of glutamatergic synaptic transmission in the striatum (Fourie et al., 2018). Moreover, zinc supplementation in pregnant *Shank3B*$^{-/-}$ KO mice can prevent the development of ASD-related behaviours in the offspring (Vyas and Montgomery, 2016). Taken together, these studies show the importance of zinc-dependent signalling in not only regulating SHANK at the synapse but also how this manifests as ASD deficits at the behavioural level.

The importance of diet (Yap et al., 2021) and other potential confounders (Vujkovic-Cvijin et al., 2020) to ASD have recently been highlighted. Disparities among previous studies with regards to methodologies and different populations also raise the question of whether the *identities* of the microorganisms present is the most important factor to consider. Rather, the *function* of the gastrointestinal microbiome could potentially be more informative when investigating differences among cohort or experimental groups. Indeed, the prevalence of GI disorders among many on the autism spectrum (Coury et al., 2012; Babinska et al., 2020) indicates the potential contribution of a dysbiotic microbiome. How these gastrointestinal microbes interact with the host, and the mechanism(s) by which dietary zinc treatment influences gut inflammation, are yet to be determined.

The link between dietary zinc and ASD behaviour suggests that the gut-microbiota-brain axis is a target for zinc-dependent signalling pathways in ASD. Based on this, along with known influences of the gut microbiota on gut-brain communications (Hsiao et al., 2013), we hypothesised that the synaptic and behavioural changes observed with dietary zinc in *Shank3B*$^{-/-}$ KO mice are linked to changes in the gut microbiota. Employing a combination of amplicon, metagenomic and metatranscriptomic sequencing, we sought to determine the effect of dietary zinc and host genotype on (1) the gut microbiota composition (bacteria and fungi), (2) host gene expression in the gut, and (3) microbiome-level functional differences.

2 Materials and methods

2.1 Animals

This study was approved by the University of Auckland's Animal Ethics Committee (AEC#1299 and AEC#1969) and experimental procedures were in adherence to the ARRIVE guidelines. Shank3$^{ex13-16-/-}$ mice (B6.129-Shank3^{tm2Gfng}/J), created by deleting exons 13–16 in the *Shank3* gene (Peca et al., 2011), were imported from Jackson Laboratories, Bar Harbor, ME, United States and housed in the Vernon Jansen Unit animal facility at the Faculty of Medical & Health Sciences, University of Auckland. Heterozygous x heterozygous breeding pairs were bred to generate wild type (WT), heterozygous and homozygous knockout (KO) offspring mice. WT and KO were genotyped by PCR as described previously [52]. After weaning (~20 days post-birth), wild-type *Shank3B*$^{+/+}$ (WT) mice and *Shank3B*$^{-/-}$ knockout (KO) mice were randomly assigned to one of two dietary experimental groups: a control zinc diet [30 ppm; (Tallman and Taylor, 2003; Vyas and Montgomery, 2016; Fourie et al., 2018)] or a supplemented zinc diet (150 ppm), for 6 weeks (Research Diets, Brunswick, NJ, United States) (D19410B and D06041101, Supplementary Table 1). Diets were identical in composition except for the zinc level. Four experimental groups were examined: (1) WT30 (wildtype control mice fed 30 ppm zinc; $n = 46$); (2) WT150 (wildtype control mice fed 150 ppm zinc; $n = 48$); (3) KO30 (*Shank3B*$^{-/-}$ mice fed 30 ppm zinc; $n = 38$); (4) KO150 (*Shank3B*$^{-/-}$ mice fed 150 ppm zinc; $n = 46$). Knockout and wildtype mice of the same sex were housed together in individually ventilated cages (maximum of 6 mice/cage), with a 12:12 h light:dark cycle and food available *ad libitum*.

2.2 Sample collection and DNA/RNA extraction

After 6 weeks on the control or supplemental zinc diet, faecal samples from 9-week-old WT and *Shank3B*$^{-/-}$ KO mice were collected and immediately frozen at −20°C. Mice were euthanised by CO_2 and cervical dislocation, then gut tissue samples (ileum, caecum, colon) were collected into tubes containing RNA*later* (Ambion, Inc.).

The Qiagen AllPrep DNA/RNA Mini Kit (Qiagen, United States) was used to extract DNA and RNA according to the manufacturer's instructions, with minor alterations as follows. Firstly, bead beating was carried out using MP Biomedicals lysing matrix E bead tubes (containing 1.4 mm ceramic spheres, 0.1 mm silica spheres, and one 4 mm glass bead) in the Qiagen TissueLyser II at a frequency of 30 Hz for 2 min. Extracted RNA was treated with DNaseI (Life Technologies, Auckland, New Zealand) and checked for DNA contamination using long cycle PCR targeting the V3-V4 region of the 16S rRNA gene with the following conditions: 95°C for 3 min, 50 cycles consisting of 30 s at 95°C, 30 s at 55°C, and 30 s at 72°C, followed by 72°C for 5 min.

2.3 PCR and amplicon sequencing

The hypervariable V3-V4 region of bacterial 16S rRNA genes was amplified using primers 341F and 785R (Klindworth et al., 2013) synthesised with an Illumina adaptor for multiplex sequencing (Supplementary Table 2). The fungal Internal Transcribed Spacer 2 (ITS2) genomic region was amplified using the ITS4 and ITS3mix1–5 primers with an Illumina adaptor (Supplementary Table 1) (Hoggard et al., 2018). Paired-end sequencing generating 2 × 300 bp reads was conducted by Auckland Genomics Ltd. (University of Auckland, New Zealand) on an Illumina MiSeq with V3 chemistry.

2.4 RNA sequencing

Extracted RNA of intestinal tissue from a subset of mice (4 treatment groups × 2 gut locations (ileum, colon) × 3 replicates = 24 samples) was sent to Otago Genomics (University of Otago, New Zealand) for ribosomal depletion (Ovation Complete Prokaryotic with mouse AnyDeplete module add-in, Tecan, United States), generation of one equimolar library pool, and paired-end sequencing generating 2 × 125 bp reads, using four lanes of two rapid flow cells on an Illumina HiSeq 2500 with V4 chemistry.

2.5 Shotgun metagenome sequencing

A subset of faecal and ileum samples was selected for shotgun DNA metagenomic sequencing, matching the samples selected for RNA sequencing but with additional ileum samples due to low DNA concentration (3 faecal samples per experimental group; 6 ileum samples for WT150 & KO 30; 7 ileum samples for WT30 & KO150). Rubicon Thruplex DNA nano libraries were prepared to create 550 bp fragments for 2 × 125 bp paired-end sequencing using the Illumina HiSeq 2500 platform with V4 chemistry at Otago Genomics.

2.6 Bioinformatics and statistical analyses

2.6.1 Bacterial amplicon analyses

Amplicon sequence variants (ASVs) were generated from the 16S rRNA gene paired-end sequence files using the DADA2 package [v1.14.0; (Callahan et al., 2016)] in the R environment [v3.6.1; (RCoreTeam, 2019)]. Sequences were quality filtered, dereplicated, and merged, with merged sequences of 400–430 bp retained. Chimaeras, singletons, and ASVs representing less than 0.00001% of total sequences were removed. The remaining ASVs were taxonomically assigned using the SILVA database [v132; (Quast et al., 2013)]. A rarefaction threshold of 8,000 reads/sample was applied, leading to the exclusion of two ileum samples and one colon sample from subsequent analyses. Permutational multivariate analysis of

variance (PERMANOVA) with 999 permutations of the data using the 'vegan' package (Oksanen et al., 2019) was undertaken to determine significant sources of variation within the microbial data. Kruskal-Wallis and Dunn tests (Dinno, 2017), with false discovery rate-adjusted *p*-values to account for multiple pairwise comparisons, were used to identify differentially abundant taxa across experimental groups.

2.6.2 Fungal amplicon analyses

Zero-radius operational taxonomic units (ZOTUs) with 100% ITS2 sequence similarity were generated using a customised pipeline with USEARCH [v11; (Edgar, 2010)]. After primer removal, forward reads were trimmed to a maximum length of 220 bp, filtered with a maximum expected error rate of 1 and singletons were removed. The unoise3 algorithm and sintax classifier (Edgar, 2016a,b) were used to assign taxonomy with the UNITE reference database [UNITE_22.08.2016; (Nilsson et al., 2019)]. The ZOTU tables were further refined by removing ZOTUs which did not reach a minimum 0.001% relative abundance threshold across the entire dataset (Edgar, 2017). The data were subsampled to a depth of 500 reads/sample.

2.6.3 RNA sequencing analyses

RNA sequencing files were processed using sickle [v1.33; (Joshi, 2011)] and trimmomatic [v0.38; (Bolger et al., 2014)] to trim adaptor sequences and quality trim reads with a minimum Phred quality score of 30 and a minimum length of 80 bp. Bacterial, archaeal and eukaryotic ribosomal RNA reads were removed using SortMeRNA [v2.1; (Kopylova et al., 2012)]. The STAR aligner [v 2.7.0, (Dobin et al., 2013)] was used to align the remaining reads to the Ensembl 84 mouse reference genome (Mus_musculus. GRCm38). Reads were then quantified using the feature counts software (Liao et al., 2014) and analysed using R [v3.6.1; (RCoreTeam, 2019)]. The R package edgeR (Robinson et al., 2010) was used to identify differentially expressed genes, and specific gene analysis was carried out using transcripts per million (TPM) units and the KEGG database (Kanehisa and Goto, 2000).

2.6.4 Shotgun metagenome analyses

Adaptor sequences were removed using trimmomatic [v0.38; (Bolger et al., 2014)] from the raw sequencing data. Reads were trimmed based on a minimum Phred score of 30 with sickle [v1.33; (Joshi, 2011)], and co-assembled using metaSPAdes [v3.11.0; (Nurk et al., 2017)] with *k-mer* values 41, 51, 61, 81, 101. The 58,151 (>2 kb) assembled scaffolds were binned to create metagenome-assembled genomes (MAGs) using MetaBAT [v2.13; (Kang et al., 2019)], MaxBin [v2.2.6; (Wu et al., 2016)] and CONCOCT (v1.1.0); then dereplicated using DASTool [v1.1.1; (Sieber et al., 2018)] and dRep [v2.3.2; (Olm et al., 2017)]. Bins were validated using VizBin [v1.0.0; (Laczny et al., 2015)], resulting in 124 bacterial bins with >75% completeness, determined via CheckM [v1.0.13; (Parks et al., 2015)]. Of these MAGs, 83 were nearly complete (>95% completeness) and 7 bins were estimated to be 100% complete. Prodigal [v2.6.3; (Hyatt et al., 2010)] was used to predict open reading frames and protein sequences. Protein-coding sequences were annotated using UniProt (UniProt, 2021), UniRef100 (Suzek et al., 2007) and KEGG Orthologous groups databases (Kanehisa and Goto, 2000; Kanehisa et al., 2016) using USEARCH [v9.0.2132; (Edgar, 2010); minimum of 50% identity and e-value cutoff of 0.00]. Additionally, TIGRFAM [v14.0; (Li et al., 2021)] and Pfam [v32.0; (Mistry et al., 2021)] using HMMER [v3.1b2; (Finn et al., 2011); e-value cutoff of 0.001] were used for annotation and the Genome Taxonomy Database Toolkit [GTDB-Tk v1.5.0; (Chaumeil et al., 2019)] was used to assign taxonomy. A phylogenetic tree was created by identifying markers in genomes and creating a representative protein alignment of the main alignment used by GTDB. This alignment was inserted into a guide tree and the most likely taxonomy for each genome calculated by the placement of the genome in the tree, and the length of its branch from nearest neighbours. Bootstrapping (100 bootstraps) to test evolutionary models with IQ-TREE [v1.6.12; (Minh et al., 2020; Letunic and Bork, 2021)] were carried out and the tree was visualised and annotated using iTOL [v5; (Letunic and Bork, 2021)].

2.6.5 Metagenome mapping to MAGs

Trimmed DNA sequence reads were subjected to removal of mouse reads with STAR (Dobin et al., 2013). Reads were mapped to MAGs using Bowtie [v1.2.0; (Langmead et al., 2009)] (WT30: 14 samples, 7 faecal & 11 ileum; WT150: 11 samples, 5 faecal & 6 ileum; KO30: 11 samples, 6 faecal & 5 ileum; KO150: 13 samples, 7 faecal & 6 ileum) (Bushnell, 2014). Mapped reads were normalised to 50,000,000 (number of reads/mapped read size * 1,000,000).

3 Results

3.1 Influence of mouse genotype and dietary zinc supplementation on bacterial and fungal community composition and diversity

Amplicon sequencing of 16S rRNA genes and ITS2 genomic regions was carried out to describe the bacterial and fungal communities, respectively. We observed that there was considerable overlap in bacterial (Figure 1) and fungal (Supplementary Figure S1) community compositions among the four experimental groups. The dominant bacterial phyla across the entire dataset were *Verrucomicrobia* (35.3 mean ± 7.8% S.D.), *Bacteroidetes* (31.9 ± 6.2%) and *Firmicutes* (22.2 ± 8.4%) (Figure 1A). The genus *Akkermansia* dominated across the entire dataset regardless of genotype or dietary zinc level (35.0 mean ± 8.1% S.D.), with *Faecalibaculum* (6.8 ± 6.5%), *Muribaculum* (4.4 ± 3.6%), *Escherichia/Shigella* (4.3 ± 2.6%) and *Dubosiella* (4.1 ± 3.8%) also abundant (Figure 1B).

Although the majority of detected fungal ZOTUs (67.3 mean ± 39.9% S.D.) could not be classified beyond kingdom level, the phylum *Ascomycota* was dominant among those taxa that could be assigned (20.1 ± 31.9%), with other ZOTUs classified to the phyla *Basidiomycota* (9.6 ± 25.7%) and *Zygomycota* (3.0 ± 8.1%) (Supplementary Figure S1). At genus level, the fungi *Rhodotorula* (6.4 ± 22.4%) and *Cyberlindnera* (6.2 ± 20.0%) were most prevalent among those identified, with nine other genera ranging from 0.01–2.70% relative abundance across the data set (Supplementary Figure S1B).

The lack of distinct microbial (bacterial and fungal) signatures among the four experimental groups, as shown by the taxonomic bar charts, was also evident in the non-metric multidimensional scaling plots for both bacteria and fungi (Figures 2A,B). Nevertheless, there were marked differences among communities from different gut sections, with the fungal communities notably differing along the gastrointestinal tract and even more so between gut sections and faecal

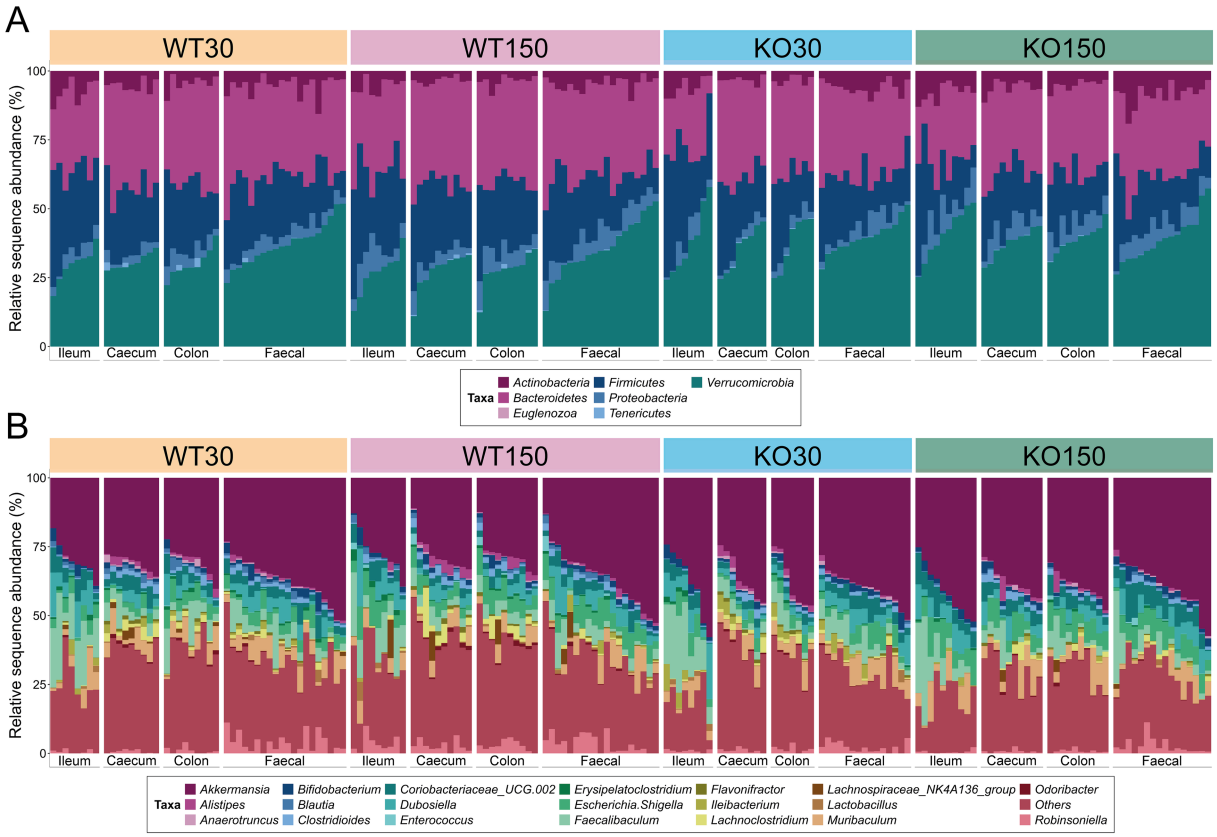

FIGURE 1
16S rRNA gene-based taxonomic summary plot of the relative abundance of bacterial phyla **(A)** and 20 most abundant genera **(B)** in each of the four experimental groups (wild-type control zinc diet WT30 n = 46, wild-type supplementary zinc diet WT150 n = 48, Shank3B$^{-/-}$ KO control zinc diet KO30 n = 38, Shank3B$^{-/-}$ KO supplementary zinc diet KO150 n = 46). All other genera and 'unknown' genus-level taxonomic assignments are grouped in 'Others'. Gastrointestinal sections are noted as I (ileum), Ce (caecum), Co (colon), F (faecal).

samples (Figure 2B). Additionally, bacterial communities associated with ileum samples were overall less similar compared to those from the caecum, colon and faecal samples within an individual mouse, indicating a longitudinal shift in community compositions (Figure 2A).

Bacterial community richness and diversity varied among samples, with 74 to 148 distinct bacterial ASVs observed per sample (Figure 3A). When aggregating samples from all gut locations for a given experimental group, there was significantly higher ($p < 0.05$) bacterial diversity in the WT compared to the *Shank3B*$^{-/-}$ KO mice (Figure 3A), irrespective of alpha-diversity metric and zinc diet. For the fungal ITS2 data, significantly lower diversity—supported by all four alpha-diversity metrics—was observed in the *Shank3B*$^{-/-}$ KO mice fed 30 ppm zinc compared to the wild-type mice fed the same amount of zinc (WT30) (Figure 3B), showing that gut fungal diversity was significantly decreased in *Shank3B*$^{-/-}$ KO mice. However, this difference in fungal diversity was no longer observed when *Shank3B*$^{-/-}$ KO mice were fed the supplemented zinc diet (KO150) and there was no significant difference in alpha diversity compared to WT30 control mice. This suggests that dietary zinc may aid in the increase of fungal diversity to levels observed in WT mice.

In this study, mice of different genotypes were cage housed together and fed one of the treatment diets (control or supplemented zinc), with each cage comprising members of one sex. Based on bacterial 16S rRNA gene amplicon data, individual cages contributed the greatest amount (12.8%) of microbiota compositional variation ($p = 0.001$; Table 1). Gut sample location, mouse genotype, dietary zinc level and the interaction between genotype and zinc diet were also significant ($p \leq 0.008$), explaining 11.4, 3.9, 2.3 and 1.1% of microbiota variation, respectively. A broadly similar trend was observed for the fungal data, whereby dietary zinc levels explained 3.7% of observed variation overall ($p = 0.007$), while gut sample location accounted for almost one-quarter (23.4%, $p = 0.001$) of variation (Table 2; Figure 2B). These results reflect substantially greater discrimination of fungal communities based on gut location than was observed for bacteria.

3.2 Specific microbial taxa as biomarkers for experimental groups

We identified specific microbial taxa that were differentially abundant among the four experimental groups, using Kruskal-Wallis rank-sum and Dunn tests with adjustments for multiple pairwise comparisons. A total of 74 bacterial ASVs differed significantly in abundance between the WT30 controls and the KO30 groups (Supplementary Table 2), with the majority classified as members of the phyla *Bacteroidetes* and *Firmicutes*, and the families *Muribaculaceae* and *Lachnospiraceae*. Individual ASVs with the lowest p-values, indicative of between-treatment differences ($p < 3.78 \times 10^{-9}$) were

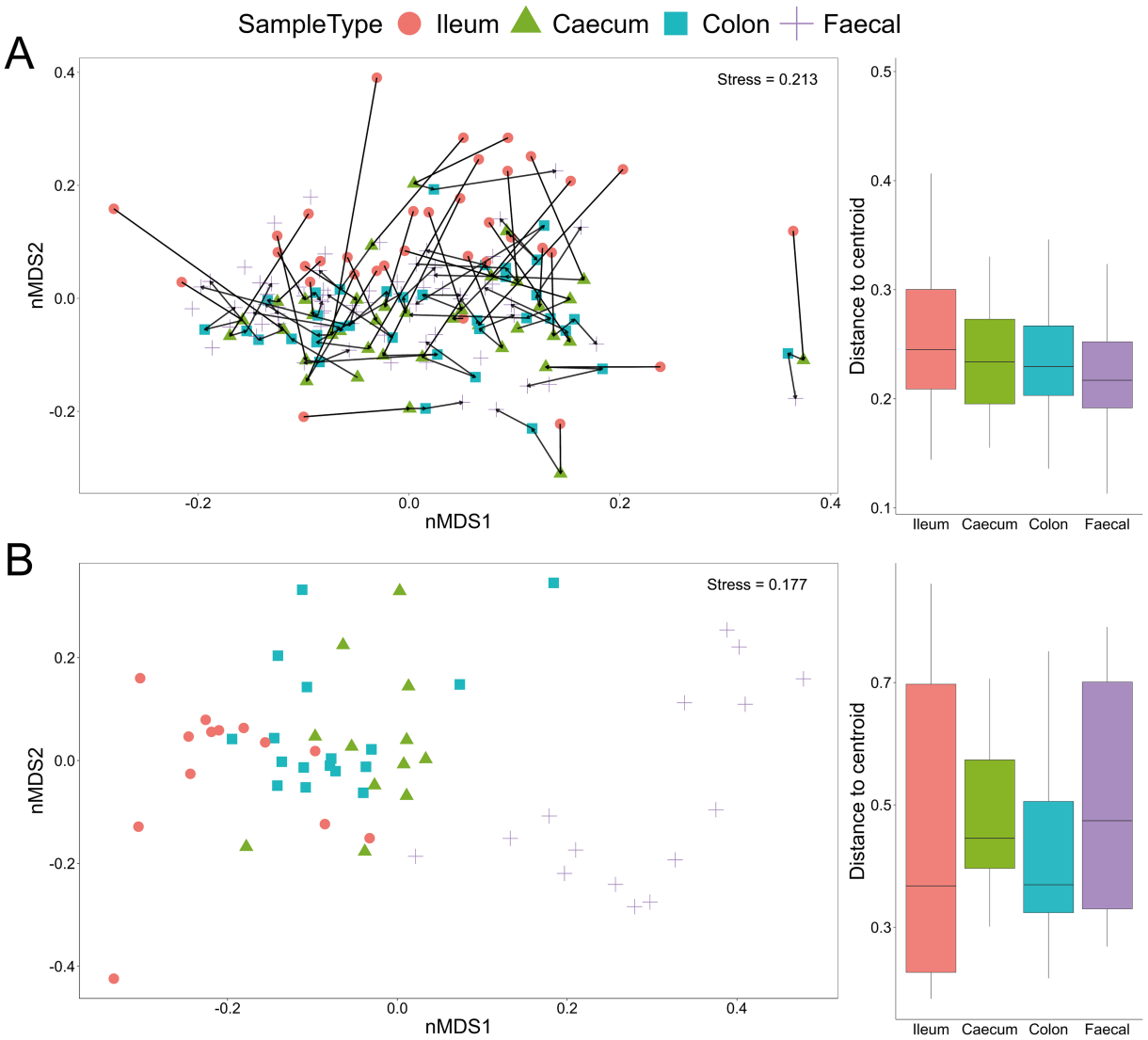

FIGURE 2
Beta-diversity Bray–Curtis dissimilarity non-metric multidimensional scaling (nMDS) plot from all samples with indicated sample type (ileum, caecum, colon and faecal) based on bacterial **(A)** and fungal **(B)** communities. Each line in **(A)** links the four GI samples for an individual mouse. Box and whisker plots show the distance from the centroid for the different sample types.

ASVs 182/155/135 (all *Akkermansia*), ASV 90 (*Lachnoclostridium*) and ASV 69 (*Muribaculaceae*). Sixty-five ASVs differed significantly ($p < 0.05$) in relative abundance between the KO30 and KO150 groups, and 65 ASVs also differed between the WT30 and KO150 groups, including the aforementioned bacterial taxa (Supplementary Table 2). Across all experimental groups, 24 fungal ZOTUs were identified as being differentially abundant (Supplementary Table 3). Only five of these ZOTUs could be classified below kingdom level: *Rhizopus* ZOTUs 5, 7 and 502, and *Aspergillus* ZOTUs 11 and 19 (Supplementary Table 3).

3.3 Effect of mouse genotype and dietary zinc supplementation on host gene expression

Differences in host gene expression were observed between gut sections and treatment groups. Host gene expression patterns correlated strongly with gut section (colon versus ileum). Compared to the colon, ileal samples exhibited lower expression of functional gene groups related to the digestive system, cell motility, and metabolism of amino acids, while genes relating to energy metabolism were typically more highly expressed in the colon (Figure 4). KEGG functional groups of genes related to signal transduction, endocrine and metabolic diseases, and neurodegenerative diseases were also highly expressed in all colon and ileum samples, encompassing ~ 86–89% of all mouse-associated transcripts (KEGG Level 2, Figure 4).

There were differences in KEGG functional groups associated with host gene expression between the WT and *Shank3B*$^{-/-}$ KO genotypes as well as between the zinc diets within a genotype, with differences most notable among colon samples. Genes involved in energy metabolism were enriched in the colon of *Shank3B*$^{-/-}$ KO mice (on both zinc diets) compared to wild-type mice on the control zinc diet. Additionally, there was decreased expression of immune disease genes on the supplemented zinc diet (150 ppm) in both KO and WT

10.3389/fmicb.2025.1607045

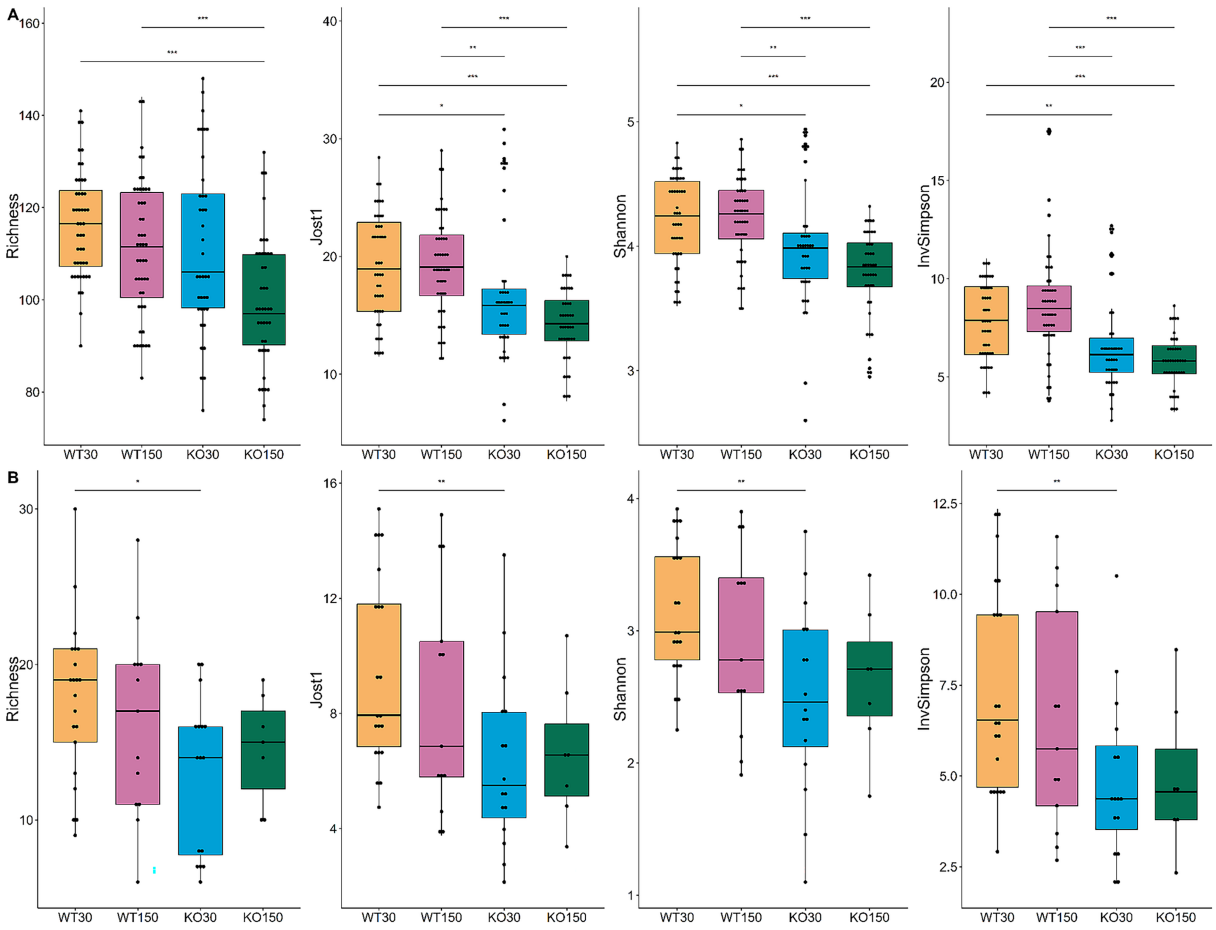

FIGURE 3
Alpha-diversity box and whisker plots based on Richness (observed taxa), Jost1, Shannon and Inverse Simpson index for bacteria **(A)** with WT30 n = 46, WT150 n = 47, KO30 n = 38, KO150 n = 43, and fungi **(B)** WT30 n = 21, WT150 n = 13, KO30 n = 16, KO150 n = 7. Statistical testing was carried out using the Kruskal-Wallis rank sum test with Wilcoxon test (3 degrees of freedom); *$p \leq 0.05$, **$p \leq 0.01$, ***$p \leq 0.001$.

TABLE 1 PERMANOVA showing factors influencing 16S rRNA gene-based bacterial ASV composition, with 999 permutations.

Source	Df	SumsOfSqs	MeanSqs	F.Model	R^2	Pr(>F)
Cage	1	1.5843	1.5844	31.8620	0.1284	0.0010
Sample type	3	1.4028	0.4676	9.4040	0.1137	0.0010
Genotype	1	0.4803	0.4803	9.6580	0.0389	0.0010
Zinc diet	1	0.2883	0.2883	5.7970	0.0234	0.0010
Genotype: Zinc diet	1	0.1324	0.1324	2.6630	0.0107	0.0080
Residuals	170	8.4533	0.0497	0.6850		
Total	177	12.3414	1.0000			

Sample type refers to sample location along the GI tract.

TABLE 2 PERMANOVA showing factors influencing fungal ZOTU composition, with 999 permutations.

Source	Df	SumsOfSqs	MeanSqs	F.Model	R^2	Pr(>F)
Zinc diet	1	0.6988	0.6988	2.6457	0.03709	0.007
Sample type	3	4.4062	1.4687	5.5609	0.23389	0.001
Residuals	52	13.7340	0.2641		0.72902	
Total	56	18.8390			1.0000	

Sample type refers to sample location along the GI tract.

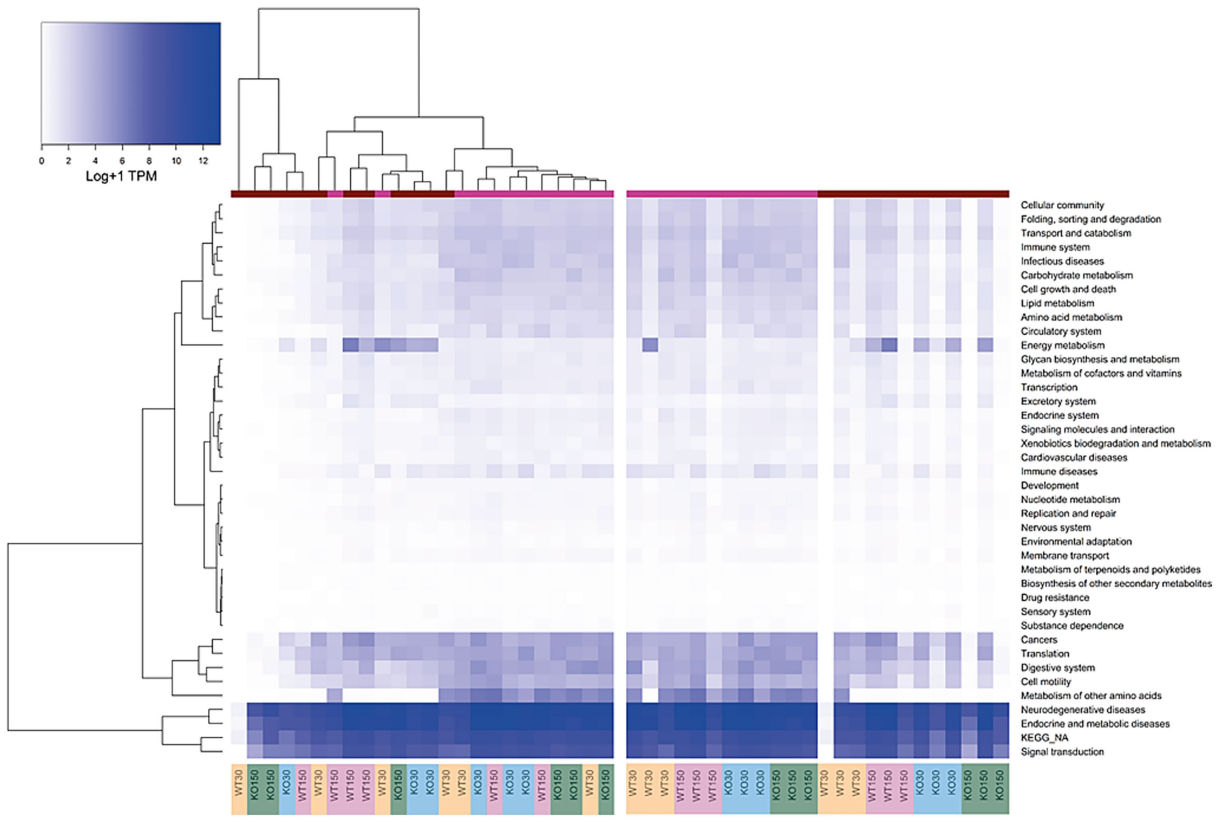

FIGURE 4
Heatmap of KEGG orthologous groups (level 2) expressed by the host (mouse) across the four experimental groups and two sample types (ileum and colon). RNA-seq data were normalised to total counts and presented as log +1 transcripts per million. Sample types are represented by the coloured bar at the top (pink = ileum, red = colon). Samples are re-ordered to allow clustering in the left panel, whereas the same samples without ordering are shown in the right-hand panel.

mice compared to the control zinc diet (30 ppm) in the colons of mice with these genotypes (Figure 4).

Across the mouse host-associated data set, a total of 1,387 genes were significantly differentially expressed. Consistent with the clustering shown in Figure 4, ileum and colon samples were clearly separated in two-dimensional space (Figure 5A), with greater variability in the expression of these genes in the colon. There were 1,271 genes among the ileum samples and 741 genes among the colon samples which were significantly differentially expressed. Many of these were related to antimicrobial interactions (alpha-defensins, mucin 2, carbonic anhydrase 1, intelectin) and host metabolism genes that may be regulated by the gut microbiota (e.g., NADH dehydrogenases). By contrast, distribution of samples in the ordination did not correlate with experimental group, which encompasses zinc diet and mouse genotype (Figure 5B).

Therefore, to further investigate differences between experimental groups, linear discriminant analysis of effect size (LEfSe) was used with host and microbiome gene transcript data. This identified 54 genes (biomarkers) that were significantly differentially expressed between the KO30 and KO150 groups (Figure 6A). NADH dehydrogenases, DNA/RNA binding proteins, zinc finger and transmembrane proteins were among the most differentially expressed gene categories. We focused our subsequent analysis on two main categories: alpha defensins, due to their importance in the control of bacteria at the mucosal barrier, and genes related to tight junction proteins, which play an integral role in mediating gastrointestinal permeability (Chelakkot et al., 2018). Overall, alpha defensin genes were more highly expressed in the ilea of *Shank3B*$^{-/-}$ (KO) mice compared with the ilea of wild-type mice, with slightly higher expression in the supplemented zinc diet KO mice than without supplementation (Figure 6B). Expression of tight junction genes was significantly and markedly lower in the colon samples from *Shank3B*$^{-/-}$ KO mice receiving zinc supplementation compared to their wild-type counterparts on the same diet ($p = 0.0139$), while the ileum samples showed the opposite trend, and these ilea genes were overall more highly expressed than those in the colon (Figure 6C).

3.4 Genomic reconstructions of mouse gut bacteria, including previously unobserved taxa

DNA shotgun sequencing data were reconstructed into 124 metagenome-assembled genomes (MAGs). Seven were 100% complete (with 0–0.94% contamination), 104 were 90–99.78% complete (0–9.68% contamination), and 13 were 76.62–89% complete (0–14.75% contamination). Of these, 124 MAGs with ≤5% contamination and at least 70% estimated completeness were analysed further (Figure 7). Overall the majority of the MAGs were assigned to the families *Muribaculaceae*, *Lachnospiraceae* and

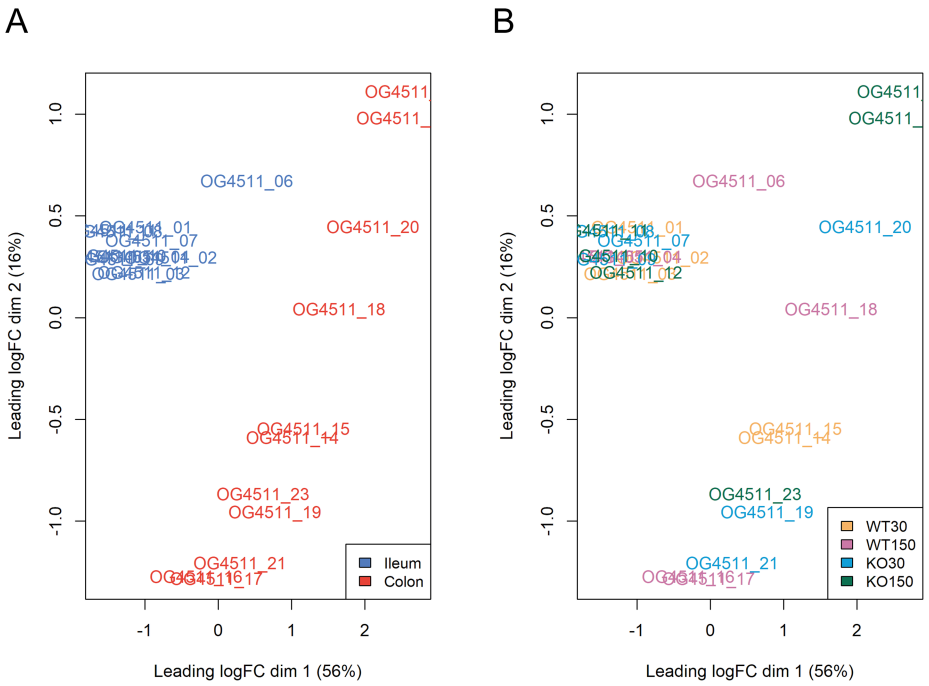

FIGURE 5
Multi-dimensional scaling plots of RNA-seq data, with distances showing leading logFC (the average of the largest absolute log fold changes between each pair of samples) coloured by sample type **(A)** and experimental group **(B)**.

Erysipelatoclostridiaceae (including *Faecalibaculum* and *Clostridium* genera), which was largely consistent with the faecal 16S rRNA gene amplicon data. As expected, general positive gut health indicator taxa *Akkermansia* and *Bifidobacteriaceae* were also present in the MAGs (Figure 7). MAGs were also obtained for members of the *Atopobiaceae*, *Eggerthellaceae*, *Borkfalkiaceae*, *Oscillospiraceae* and *Anaerotignaceae*, despite their not previously being detected in *Shank3*$^{-/-}$ mice bacterial amplicon data (Figure 1). The most highly abundant MAGs belonged to collections of *Akkermansia muciniphila* followed by *Paramuribaculum* (including *P. intestinale*) in faecal samples. In the ileum samples, MAG 22 (*Muricomes* sp900604355) was highly represented in WT30, WT150 and KO150 groups compared to the KO30 group. This same trend was also observed for MAGs representing *Akkermansia*, *Porphyromonas* bacterium UBA7173 and *Faecalibaculum*. Overall, we observed increased abundances of *Akkermansia*, *Porphyromonas* and *Faecalibaculum* in bacterial communities from KO mice on the supplemented zinc diet.

3.5 Major functional differences between experimental groups in microbiome-encoded genes for transporters, zinc-related genes, carbohydrate metabolism, and fatty acid biosynthesis

Differences in bacterial community function were determined using KEGG database annotations of MAGs. In terms of functional capacity, the KO150 group on the supplemented zinc diet displayed a greater relative abundance of genes for metabolism, environmental information processing, and cellular processes than other groups. For example, cellular process gene relative abundances differed significantly between KO150 and the groups KO30 ($p = 0.037$) and WT30 ($p = 0.00018$), and were highest in the KO150 group. Significant genotype differences were observed relating to two of these categories, environmental processing ($p = 0.015$) and cellular processes ($p = 0.039$). Between the dietary zinc treatments, cellular processes ($p = 0.00084$) and environmental processing ($p = 0.0000056$) differed most significantly. Cellular process genes differed significantly between KO150 and the groups KO30 ($p = 0.037$) and WT30 ($p = 0.00018$), with the same trend for environmental processing genes (KO30 $p = 0.000091$; WT30 $p = 0.000021$)—i.e. relative abundances were again highest in the KO150 group. By contrast, the abundance of mucin genes was greater in WT mice compared to KO mice, with increased presence in faecal samples compared to ileum samples within all experimental groups.

While sample location did not significantly affect the distribution of genes involved in carbohydrate metabolism, genotype ($p = 0.0046$), zinc diet ($p = 0.011$) and the interaction between genotype and zinc diet ($p = 0.021$) all significantly affected the number of protein-coding sequences annotated with carbohydrate metabolism in the microbial community. Zinc-related genes, including zinc transporters, metallopeptidases, and zinc-binding cytidine monophosphate, were more abundant in the KO150 group compared to the KO30 group, especially in the ileum. Saturated and unsaturated fatty acid synthesis genes were found in 93 bacterial taxa, with *Akkermansia muciniphila*, *Muribaculum intestinale*, and *Alistipes finegoldii* representing the top three taxa across the entire dataset with these genes. In the ileum samples, normalised count data revealed a lower abundance of fatty acid-related genes in KO30 (total number of genes = 1,346) compared to WT30 (total = 2,371), but an increase in KO150 mice (total = 2,026) towards WT30 levels. This trend was also seen in the faecal samples, WT30 (total = 2,843); KO30 (total = 2,166); KO150 mice

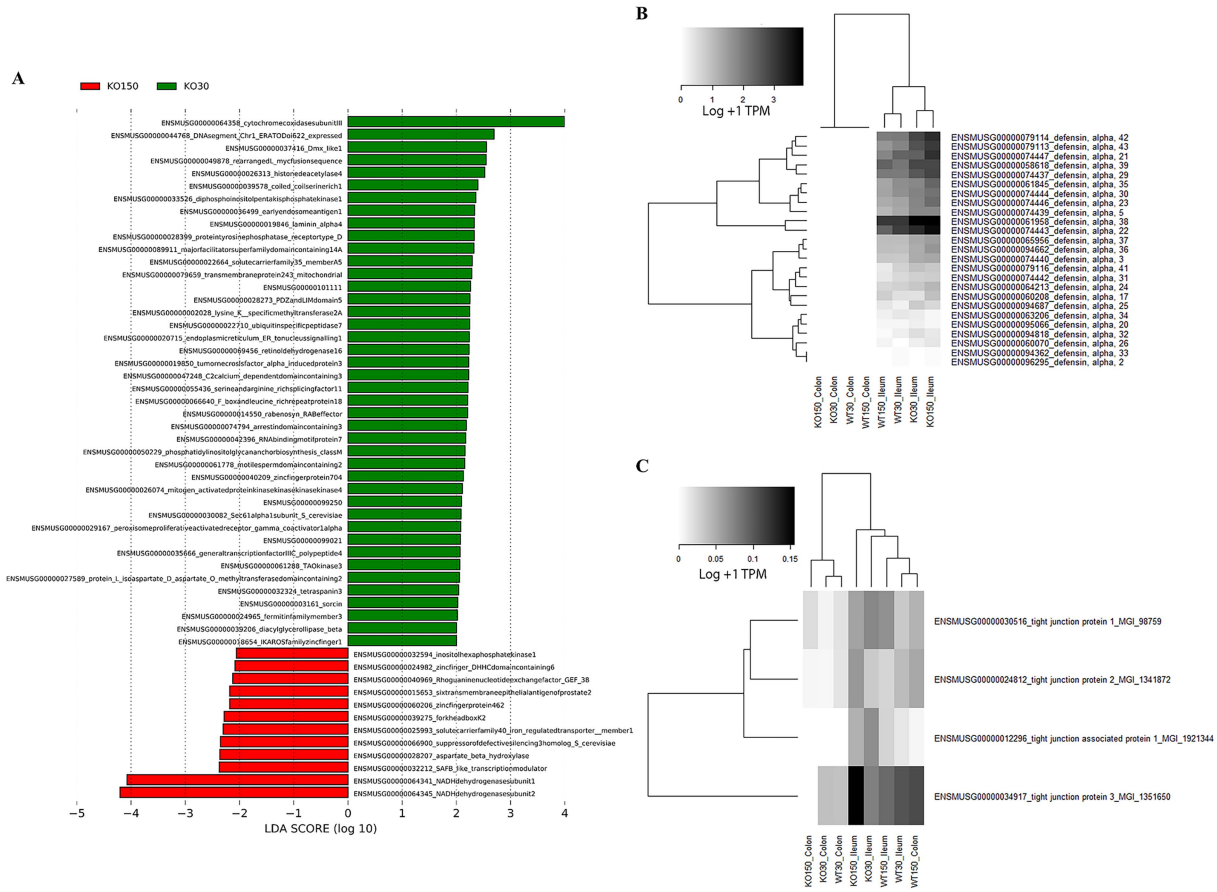

FIGURE 6
RNA-seq analyses of host (mouse) gene expression: **(A)** LEfSe analysis (with Kruskal-Wallis and Wilcoxon testing both set at $p < 0.05$, with the strategy all against all) identifying biomarker differences between KO30 vs. KO150 for both ileal and colon samples combined. Heatmaps of **(B)** alpha defensin genes, and **(C)** tight junction protein genes across the four experimental groups and two sample types. RNA-seq data were normalised to total counts and presented as log +1 transcripts per million. Samples within an experimental group and sample type were pooled together for analysis as biological replicates.

(total = 2,368). Interestingly, in the KO30 faecal samples and KO150 ileum samples, *A. finegoldii* was not among the top three taxa with respect to fatty acid synthesis genes, instead being replaced by *Bacteroides salanitronis* (identified from KO30 faeces) and *Lachnoclostridium* sp. YL32 (KO150 ileum sample). Genes related to synthesis of propionate were significantly different between zinc diets ($p = 0.029$) and the interaction between genotype and zinc diet ($p = 0.033$), but not between the genotypes; these genes were associated with *Escherichia coli* K-12 MG1655, *Desulfitobacterium dehalogenans* and *Flavonifractor plautii*. In KO30 mice, the main propionate-associated organism was *F. plautii*, while *Escherichia coli* K-12 MG1655 was the top bacterium identified that is associated with propionate production and transport in both WT30 and KO150 mice.

4 Discussion

The role of the gut microbiota in ASD has come under considerable scrutiny in the past decade, with evidence for its importance coming from studies of both human populations and animal models (Hsiao et al., 2013; Buffington et al., 2016; Strati et al., 2017). Neural, immunological and hormonal pathways all offer potential mechanisms by which gut microbes may influence neurological development. Changes in gut microbial composition and resulting functional differences have been observed with differential dietary zinc intake in porcine and murine models as well as in human studies (Usama et al., 2018; Foligne et al., 2020; Pieper et al., 2020). We recently described dietary zinc-induced reversal of ASD behaviours in *Shank3B*$^{-/-}$ KO mice (Vyas and Montgomery, 2016; Fourie et al., 2018). Zinc plays a critical role in gut health and, together with published data linking the gut-microbiota-brain axis to ASD, these observations raise the intriguing possibility that the effects of dietary zinc on ASD could be linked to changes in the gut microbiota. In this study, we therefore examined the effects of dietary zinc and host genotype on (1) the gut microbiota in *Shank3B*$^{-/-}$ KO mice, (2) host gene expression in the gut, and (3) microbiome-level functional differences. Our major findings are summarised in Figure 8.

4.1 Zinc supplementation and host genotype influence microbiota composition

When considering the gut-associated microbiota, differences among individual mice were substantial. Even within a given dietary zinc level or genotype group, phylum-and genus-level bacterial community compositions varied greatly, albeit with overall dominance

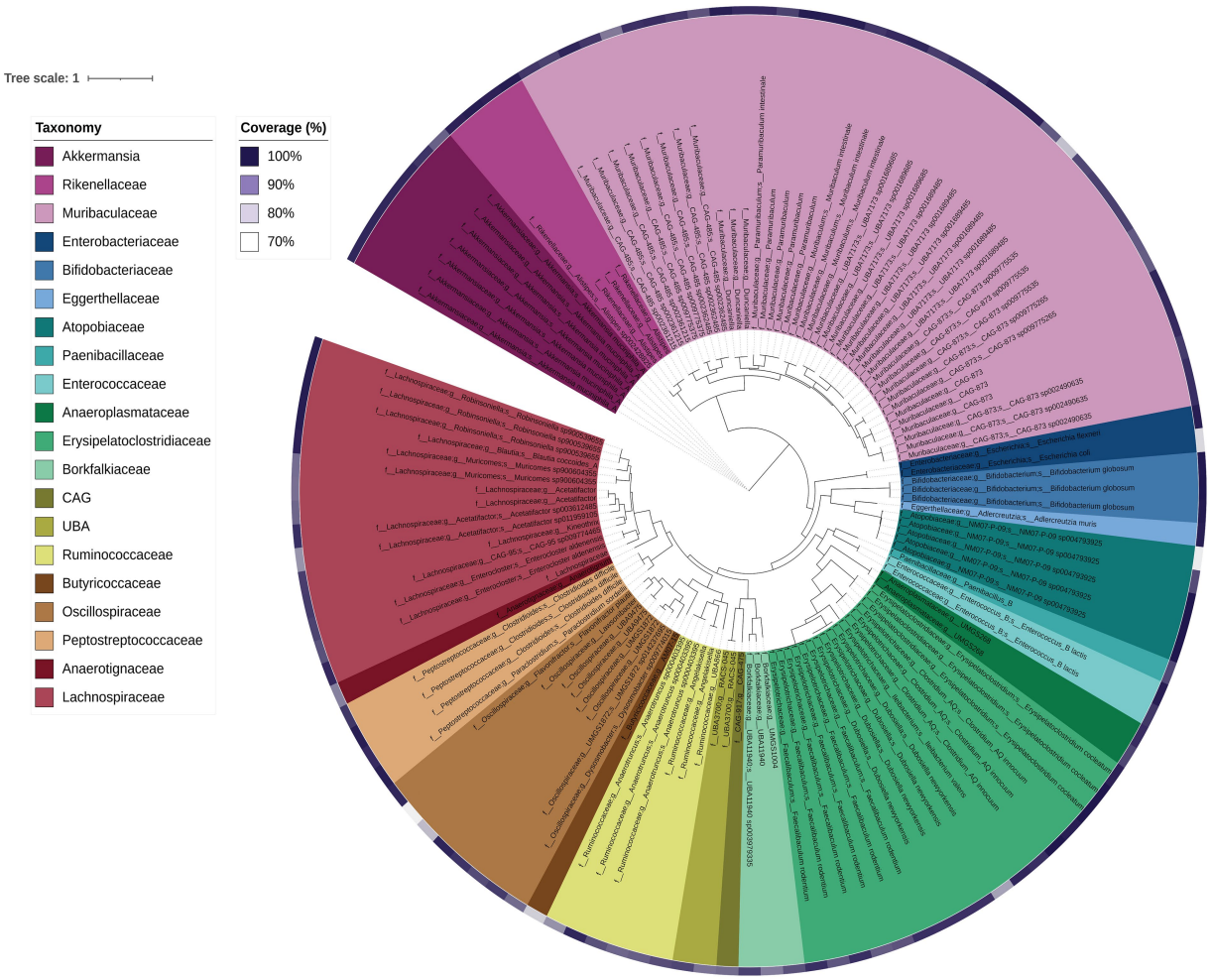

FIGURE 7
Phylogenetic tree of each MAG based on concatenated core genes visualised using iTOL. The colours represent different family groups and genome completeness is indicated by the purple colour gradient outside of the main tree.

by certain taxa, most notably the genus *Akkermansia* (phylum *Verrucomicrobia*). Despite such inter-individual variation, which is consistent with previous autism gut microbiota studies (Bundgaard-Nielsen et al., 2020), our data reveal significant effects of host genotype, dietary zinc level, and their interaction. Specifically, for both bacterial and fungal data, across all alpha-diversity indices WT mice displayed significantly increased diversity compared with *Shank3B*$^{-/-}$ KO mice. This trend of decreased fungal and bacterial alpha-diversity in *Shank3B*$^{-/-}$ KO mice regardless of dietary zinc treatment suggests that host-associated gut microbes may be highly regulated by ASD-linked genetic variations occurring in key synaptic proteins in the central nervous system which can ultimately affect immunological interplay between host and microbe.

Akkermansia muciniphila is a mucin-degrading gut bacterium that improves gut barrier function by stimulating host mucous production and turnover, ultimately reducing GI tract inflammation via regulation of antimicrobial peptides in the gut stimulating host Toll-like receptors that are integral to host immunity (Garcia-Vello et al., 2024). In our study, *Akkermansia* was one of the most dominant bacterial taxa for all experimental groups and was also widely represented in the shotgun metagenomic data. Decreases in *A. muciniphila* have been observed in ASD, irritable bowel syndrome and Crohn's disease, leading to the development of probiotic treatments with this microbe for these gut disorders (Gu et al., 2021).

The clearest differences related to dietary zinc levels and/or genotype were evident not at the level of entire bacterial communities, but rather at the level of specific ASVs, consistent with other gut microbiome studies (de Theije et al., 2014; Chen et al., 2017). For example, 74 ASVs, mostly from the families *Muribaculaceae* and *Lachnospiraceae*, were significantly differentially represented between the WT and KO groups that were both fed 30 ppm zinc. When comparing the two genotypes on the control zinc diet, *Muribaculaceae*, *Blautia* and *Erysipelotrichaceae* were more abundant in WT30 mice than KO30 mice. *Blautia* produces butyrate, a short-chain fatty acid (SCFA), and is considered beneficial for host health. Butyrate has positive anti-inflammatory effects at the mucosa and fortifies the epithelial barrier, with implications for the gut-microbiota-brain axis as it is able to cross the blood–brain barrier and produce neuromodulatory effects (Canani et al., 2011; Oleskin and Shenderov, 2016; Silva et al., 2020). Other SCFAs such as acetate, propionate and succinate can also be produced by members of the family *Muribaculaceae*. This family represents one of the largest proportions of gut bacteria found in mice, and has been suggested to play a similar role

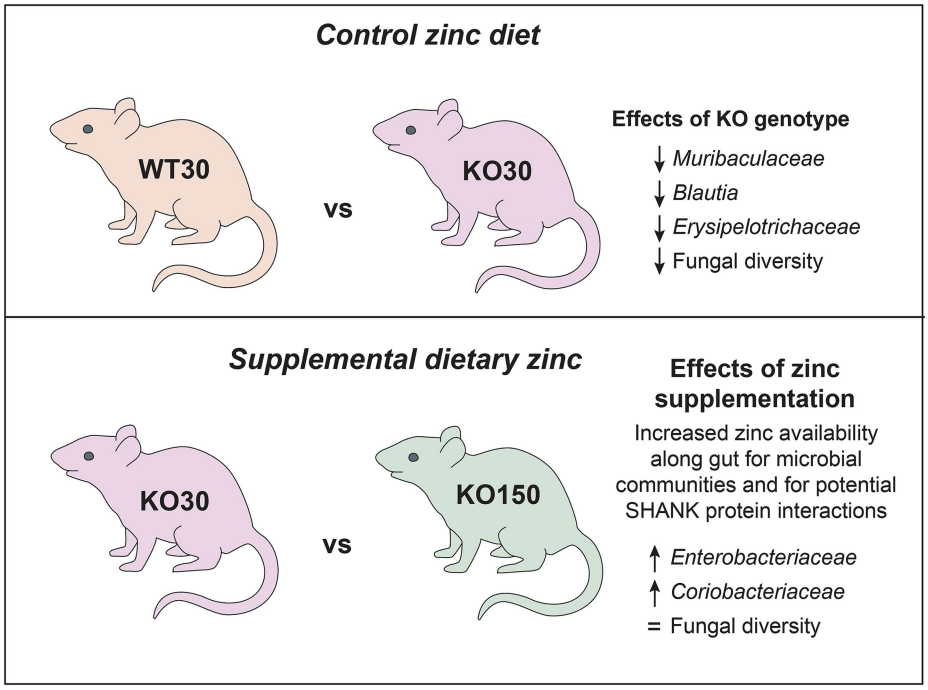

FIGURE 8
Summary of key microbiome findings from this study.

to the genus *Bacteroides* in humans, occupying similar niches and metabolising the same dietary source—complex carbohydrates (Ormerod et al., 2016; Smith et al., 2019). It is worth considering the extent to which the gut microbiota may be directly utilising zinc from the diet, potentially in competition with the host animal. Smith et al. (1972) estimated that GI bacteria utilise 20% of the dietary zinc consumed in a germ-free/pathogen-free rat study (Smith et al., 1972). Zinc supplementation of the host diet (150 ppm) potentially results in increased zinc availability along the GI tract for the microbial community, affecting its overall community structure and function. Microbial high-affinity membrane transport systems and zinc-binding proteins for competitive uptake of zinc between gut microbes are crucial for their persistence and growth along the GI tract. Balancing host and gut microbiome requirements for zinc is therefore essential for survival of both symbiotic components.

Among the *Shank3B*$^{-/-}$ KO mice, the bacterial families *Enterobacteriaceae* and *Coriobacteriaceae* were the top two significant biomarkers that were more abundant in the supplemented zinc diet (KO150) mice compared with the control zinc diet (KO30) mice. KO30 mice, instead, had increased abundances of *Muribaculaceae* and *Ileibacterium*. Diet changes can alter host production of bile acids, which can shift the gut community in favour of organisms that can metabolise bile acids such as members of the *Coriobacteriaceae* (Stenman et al., 2013). This, in turn, can affect gut barrier permeability by interaction of bile acids with the epithelial cells (Raimondi et al., 2008). Similarly, members of *Muribaculaceae*, *Blautia* and *Faecalibaculum* were more abundant in WT30 than KO150 mice, which again had higher abundances of *Coriobacteriaceae* and *Escherichia/Shigella*.

While our main focus was on the influence of dietary zinc on the gut microbiota of *Shank3B*$^{-/-}$ KO mice, this study also provided an opportunity to revisit the association between host genotype and microbiota composition in this animal model. An earlier study by Tabouy et al. (2018) described reduced bacterial alpha-diversity in *Shank3B*$^{-/-}$ KO compared with wild-type mice, as well as differences in the relative abundances of several bacterial genera including *Lactobacillus* and *Prevotella*. The authors interpreted these differences as reflective of a dysbiosis, or dysregulation, of the microbiome. We also observed differences of a comparable magnitude between the *Shank3B*$^{-/-}$ KO and WT mice microbiotas (on the control 30 ppm zinc diet), specifically a decrease in bacterial diversity in KO mice, but contend that these do not necessarily constitute a dysbiosis. Indeed, there were marked similarities at both phylum and genus levels between the *Shank3B*$^{-/-}$ KO and wild-type bacterial communities in our data (Figure 1), as well as in the aggregated genus-level data of Tabouy et al. (2018) (Supplementary Figure 2 in their paper). Moreover, while statistically significant, alpha-diversity in the female mice (which displayed the strongest effect) still only decreased by <10% in Tabouy et al. (2018) data set. Widespread use of the term "dysbiosis" to describe any shift in microbial communities has been criticised (Olesen and Alm, 2016) and we suggest that this term would more appropriately apply to a situation of extreme microbiota depletion, such as seen in *Clostridioides difficile* infection (Antharam et al., 2013), rather than the more subtle changes evident in both our data and those of Tabouy et al. (2018). Nonetheless, whether or not the microbiota differences observed here and by Tabouy et al. (2018) constitute a dysbiosis *per se*, the functional implications of reduced gut-associated microbiota diversity in *Shank3B*$^{-/-}$ KO mice warrant investigation. It is important to note that genotype and dietary zinc factors explained ~7% of variation in the bacterial biota, compared with almost 13%

attributable to individual cage differences. The explanatory power of dietary zinc and genotype was therefore lower, despite striking host behavioural differences associated with zinc supplementation (Fourie et al., 2018), which were not influenced by mouse cage assignment.

While zinc deficiency can be difficult to diagnose in the clinic, plasma serum levels can be influenced by multiple independent factors and use of hair/nail samples have not been conclusive in the literature; therefore proposals for potential microbial biomarkers for zinc deficiency have been suggested (Chen et al., 2021).

Our data also show significant effects of genotype and dietary zinc on fungal diversity. Twenty-four fungal ZOTUs differed significantly in relative abundance across the entire dataset. The five that could be assigned to below kingdom level represented the genera *Rhizopus* and *Aspergillus*. We observed that, on the control diet, KO mice displayed significantly lower fungal diversity compared with WT mice, and moreover that dietary zinc treatment in KO mice reverted fungal diversity towards WT levels. Zinc is key for fungi and has been demonstrated to enhance growth of *Rhizopus* with higher zinc levels (Wegener and Romano, 1963) and *Aspergillus* (Vicentefranqueira et al., 2019) by stimulating RNA synthesis and transcription. Autism-associated behaviours of a child with ASD were reversed following treatment with antifungals to target *Rhizopus*, though the efficacy of this treatment for a wider population is yet to be tested (Baker and Shaw, 2020). Mycotoxins and fungi have been postulated to be involved in the pathobiology of ASD due to their high prevalence in the urine and blood of children on the autism spectrum, but this is largely understudied (De Santis et al., 2019; Markova, 2019). Potential targets for antifungal treatment include zinc transporters (due to their ubiquity and importance in fungi) as well as probiotic treatments such as *Lactobacillus* aimed at adsorbing mycotoxins or altering gut microbial communities (Amich and Calera, 2014; Guo et al., 2014; Vicentefranqueira et al., 2015). Therefore, dietary zinc supplementation may aid in maintaining the balance between a healthy fungal community and its interactions with the *Shank3B*-deficient host which ultimately may affect their phenotype. Together with our data, these findings highlight fungal diversity and zinc as an important focus for future studies.

4.2 Dietary zinc supplementation has a minor but measurable effect on host gene expression in the mouse gut

Consideration of host–microbe interactions demands attention to not only the microbiota, but also the host itself. We therefore utilised RNA-Seq to investigate patterns of host (mouse) gene expression in the ileum and colon of both WT and *Shank3B*$^{-/-}$ KO mice fed either 30 ppm or 150 ppm dietary zinc. As overall gene expression correlated most strongly with gut region (ileum *vs* colon) rather than experimental group (dietary zinc or genotype) (Figure 5), we focused our attention on those genes that were significantly differentially expressed and/or directly relevant to integrity of the gut epithelial barrier.

Alpha defensins are antimicrobial peptides active against a wide range of microorganisms (De Smet and Contreras, 2005). Consistent with their known prevalence in the small intestine (Takakuwa et al., 2019; Nakamura et al., 2020), we documented higher expression of alpha defensin genes in the ileum compared with colon samples. Expression of several alpha defensins was higher in the *Shank3B*$^{-/-}$ KO mice compared to the wild-type mice, especially those on the supplemented zinc diet. Whilst speculative, this could indicate enhanced antimicrobial activity in *Shank3B*$^{-/-}$ KO mice, and that this is further enhanced by high dietary zinc. This suggests that the gut microbiome may be more strictly controlled in *Shank3B*$^{-/-}$ KO mice compared to wild-type mice by various host–microbe interactions.

Given the significant research focus on potential leaky gut in ASD, we also focused our analysis on the expression of tight junction proteins between WT and *Shank3B*$^{-/-}$ KO mice fed control or supplemented zinc levels. Tight junction proteins are crucial for integrity of the gut epithelium, preventing potentially harmful microorganisms or their metabolites from leaking out of the gut and into the bloodstream. Zinc supplementation enhances and maintains the intestinal barrier by regulating expression of several tight junction proteins (Miyoshi et al., 2016). Tight junction expression in the ileum samples from *Shank3B*$^{-/-}$ KO mice was higher than in the corresponding WT30 samples, which may suggest the presence of intestinal inflammation or compromised barrier integrity that can ultimately impact the gut-microbiota-brain axis (Berkes et al., 2003). Additionally, *Shank3B*$^{-/-}$ KO mice can have abnormal GI morphology, with alterations of the gut microbial community and increased bacterial LPS levels in the liver (Sauer et al., 2019); this suggests the importance of the SHANK3 protein in the gut and the consequences of KO SHANK3 involvement in disruption of the mucosal barrier. Dietary zinc supplementation correlated with higher tight junction gene expression, regardless of host genotype, particularly in the ileum. This is intuitive given the greater absorbance of dietary zinc in the small intestine (Maret, 2000; Dufner-Beattie et al., 2003; Liuzzi et al., 2004). Overall, our observations suggest that zinc may be playing a role in reinforcement of the gut epithelial barrier that may help to tightly regulate the gut-microbiota-brain axis and perhaps ameliorate the resulting ASD behaviours.

4.3 Gut region correlates more strongly with fungal than bacterial community composition

We sampled the mouse gut at several regions along the GI tract, namely the ileum, caecum and colon, as well as faecal samples. For bacteria, there was no clear separation of microbiota composition related to gut region in the ordination plot (Figure 3A), although for many individual mice the ileum samples were somewhat distinct. There was much greater separation for fungi, with the fungal composition of faecal samples being markedly different from that of other sample types (Figure 2B) and greater variation explained in the PERMANOVA models compared to the bacterial data. The bacterial community was substantially more diverse than fungal communities across the dataset (Figure 3).

4.4 Gut bacterial communities display functional redundancy

Fatty acids produced from microbial fermentation/metabolism, such as butyrate and propionate, modulate gut

barrier function and provide an anti-inflammatory effect via inhibition of host immune responses, both of which have been linked to the gut-microbiome-brain axis. In particular, *Roseburia* and *Faecalibaculum* were present across samples and sample groups, and encoded genes for fatty acid biosynthesis, with the greatest relative abundance of *Faecalibaculum* in the KO150 group. However, the main fatty acid producers found in this dataset were *Akkermansia muciniphila, Muribaculum intestinale* and *Alistipes finegoldii*. Therefore, important fatty acid functional genes of the gut microbiome may be expressed by different members of the bacterial community. This suggests that bacterial function rather than identity could be a more important contributor to the reversal of ASD-related behaviours observed in this mouse model.

Overall, a potential reciprocal relationship, with *A. muciniphila* degrading mucin and supplying butyrate to the host, may contribute to the observed effects of supplementary dietary zinc, in concert with direct zinc interactions alongside SHANK3 proteins in brain synapses subsequently supporting the ASD behavioural reversal in *Shank3B*$^{-/}$mice. Understanding crosstalk between a host and its gut microbiota is challenging due to the multitude of communication mechanisms across the gut-microbiota-brain axis, however elucidating specific beneficial functions could aid with GI disorders commonly associated with ASD via probiotic supplementation (Zhang et al., 2022).

5 Concluding remarks

To our knowledge this study is the first to investigate the effect of dietary zinc supplementation on the gut microbiota in the context of ASD. By utilising the *Shank3B*$^{-/-}$ KO mouse model we were able to examine the influence of – and interaction between – dietary zinc and ASD-linked host genotype. We found that sample location along the GI tract, as well as genotype and zinc diet, explained some of the variation seen in the microbiota data, with notable bacterial ASV differences between experimental groups. While we observed statistically significant differences between the alpha-diversity of microbiotas from different genotype and dietary zinc treatment groups, we argue that these do not necessarily constitute a major breakdown, or dysbiosis, of the gut microbiota. Interestingly, the observed differences in fungal diversity between *Shank3B* KO mice on different zinc diets are consistent with dietary zinc supplementation maintaining a healthy fungal community and potentially influencing ASD phenotype. Differential expression of host genes among the experimental groups, including antimicrobial interaction genes as well as gut microbiota-regulated host metabolism genes, suggests that the interplay between gut microbes, the gastrointestinal tract and the brain may play a major role towards the observed amelioration of ASD behaviours seen previously with supplemented dietary zinc. Future work, perhaps involving targeted manipulation of the identified genes and/or metabolic processes, would represent a valuable next step. We found differences in bacterial functional capacities among our experimental groups, which notably include fatty acid biosynthesis and transporters (including zinc transport and neurotransmitter receptors). These differences could suggest increased activity of, or a switch towards, specific functions that may benefit both host and microbe, raising the potential of manipulating both dietary zinc and the gut microbiota itself to ameliorate ASD-related behaviours and associated GI issues.

Data availability statement

The sequence data from this study have been deposited in the NCBI Sequence Read Archive under BioProject PRJNA747052 (bacterial and fungal amplicon data) and PRJNA764443 (shotgun metagenome and RNA data).

Ethics statement

This animal study was approved by University of Auckland's Animal Ethics Committee (AEC#1299 and AEC#1969). The study was conducted in accordance with the local legislation and institutional requirements, with experimental procedures in adherence to the ARRIVE guidelines.

Author contributions

GW: Data curation, Formal analysis, Investigation, Methodology, Project administration, Validation, Visualization, Writing – original draft, Writing – review & editing. YJ: Investigation, Methodology, Resources, Writing – review & editing. KL: Investigation, Methodology, Resources, Writing – review & editing. CF: Investigation, Methodology, Resources, Writing – review & editing. KH: Formal analysis, Methodology, Resources, Supervision, Writing – review & editing. JM: Conceptualization, Funding acquisition, Project administration, Resources, Supervision, Writing – review & editing. MT: Conceptualization, Funding acquisition, Project administration, Resources, Supervision, Writing – review & editing.

Funding

The author(s) declare that financial support was received for the research and/or publication of this article. We acknowledge the Marsden Fund (13-UOA-053) and the Health Research Council of New Zealand (17/052) for funding the majority of this study. Additionally, we thank the Minds for Minds Charitable Trust for generously supporting sequencing costs for this research.

Acknowledgments

We gratefully acknowledge the support of the Minds for Minds Charitable Trust.

Conflict of interest

The authors declare that the research was conducted in the absence of any commercial or financial relationships that could be construed as a potential conflict of interest.

Generative AI statement

The authors declare that no Gen AI was used in the creation of this manuscript.

Publisher's note

All claims expressed in this article are solely those of the authors and do not necessarily represent those of their affiliated organizations, or those of the publisher, the editors and the reviewers. Any product that may be evaluated in this article, or claim that may be made by its manufacturer, is not guaranteed or endorsed by the publisher.

Supplementary material

The Supplementary material for this article can be found online at: https://www.frontiersin.org/articles/10.3389/fmicb.2025.1607045/full#supplementary-material

References

Abrahams, B. S., and Geschwind, D. H. (2008). Advances in autism genetics: on the threshold of a new neurobiology. *Nat. Rev. Genet.* 9, 341–355. doi: 10.1038/nrg2346

American Psychiatric Association (2013). Diagnostic and statistical manual of mental disorders (5th ed.). Arlington, VA: American Psychiatric Association.

Amich, J., and Calera, J. A. (2014). Zinc acquisition: a key aspect in *Aspergillus fumigatus* virulence. *Mycopathologia* 178, 379–385. doi: 10.1007/s11046-014-9764-2

Antharam, V. C., Li, E. C., Ishmael, A., Sharma, A., Mai, V., Rand, K. H., et al. (2013). Intestinal dysbiosis and depletion of butyrogenic bacteria in *Clostridium difficile* infection and nosocomial diarrhea. *J. Clin. Microbiol.* 51, 2884–2892. doi: 10.1128/JCM.00845-13

Arons, M. H., Lee, K., Thynne, C. J., Kim, S. A., Schob, C., Kindler, S., et al. (2016). Shank3 is part of a zinc-sensitive signaling system that regulates excitatory synaptic strength. *J. Neurosci.* 36, 9124–9134. doi: 10.1523/JNEUROSCI.0116-16.2016

Babinska, K., Celusakova, H., Belica, I., Szapuova, Z., Waczulikova, I., Nemcsicsova, D., et al. (2020). Gastrointestinal symptoms and feeding problems and their associations with dietary interventions, food supplement use, and behavioral characteristics in a sample of children and adolescents with autism Spectrum disorders. *Int. J. Environ. Res. Public Health* 17:372. doi: 10.3390/ijerph17176372

Baker, S., and Shaw, W. (2020). Case study: rapid complete recovery from An autism Spectrum disorder after treatment of aspergillus with the antifungal drugs Itraconazole and Sporanox. *Integr Med* 19, 20–27

Berkes, J., Viswanathan, V. K., Savkovic, S. D., and Hecht, G. (2003). Intestinal epithelial responses to enteric pathogens: effects on the tight junction barrier, ion transport, and inflammation. *Gut* 52, 439–451. doi: 10.1136/gut.52.3.439

Bolger, A. M., Lohse, M., and Usadel, B. (2014). Trimmomatic: a flexible trimmer for Illumina sequence data. *Bioinformatics* 30, 2114–2120. doi: 10.1093/bioinformatics/btu170

Buffington, S. A., Di Prisco, G. V., Auchtung, T. A., Ajami, N. J., Petrosino, J. F., and Costa-Mattioli, M. (2016). Microbial reconstitution reverses maternal diet-induced social and synaptic deficits in offspring. *Cell* 165, 1762–1775. doi: 10.1016/j.cell.2016.06.001

Buie, T., Campbell, D. B., Fuchs, G. J., Furuta, G. T., Levy, J., Vandewater, J., et al. (2010). Evaluation, diagnosis, and treatment of gastrointestinal disorders in individuals with ASDs: a consensus report. *Pediatrics* 125, S1–S18. doi: 10.1542/peds.2009-1878C

Bundgaard-Nielsen, C., Knudsen, J., Leutscher, P. D. C., Lauritsen, M. B., Nyegaard, M., Hagstrom, S., et al. (2020). Gut microbiota profiles of autism spectrum disorder and attention deficit/hyperactivity disorder: a systematic literature review. *Gut Microbes* 11, 1172–1187. doi: 10.1080/19490976.2020.1748258

Bushnell, B. (2014) BBMap: A Fast, Accurate, Splice -Aware Aligner. Ernest Orlando Lawrence Berkeley National Laboratory, Berkeley, CA.

Callahan, B. J., McMurdie, P. J., Rosen, M. J., Han, A. W., Johnson, A. J., and Holmes, S. P. (2016). DADA2: high-resolution sample inference from Illumina amplicon data. *Nat. Methods* 13, 581–583. doi: 10.1038/nmeth.3869

Canani, R. B., Costanzo, M. D., Leone, L., Pedata, M., Meli, R., and Calignano, A. (2011). Potential beneficial effects of butyrate in intestinal and extraintestinal diseases. *World J. Gastroenterol.* 17, 1519–1528. doi: 10.3748/wjg.v17.i12.1519

Chaumeil, P. A., Mussig, A. J., Hugenholtz, P., and Parks, D. H. (2019). GTDB-Tk: a toolkit to classify genomes with the genome taxonomy database. *Bioinformatics* 36, 1925–1927. doi: 10.1093/bioinformatics/btz848

Chelakkot, C., Choi, Y., Kim, D. K., Park, H. T., Ghim, J., Kwon, Y., et al. (2018). *Akkermansia muciniphila*-derived extracellular vesicles influence gut permeability through the regulation of tight junctions. *Exp. Mol. Med.* 50:e450. doi: 10.1038/emm.2017.282

Chen, T., Long, W., Zhang, C., Liu, S., Zhao, L., and Hamaker, B. R. (2017). Fiber-utilizing capacity varies in *Prevotella-versus Bacteroides*-dominated gut microbiota. *Sci. Rep.* 7:2594. doi: 10.1038/s41598-017-02995-4

Chen, L., Wang, Z., Wang, P., Yu, X., Ding, H., Wang, Z., et al. (2021). Effect of long-term and short-term imbalanced Zn manipulation on gut microbiota and screening for microbial markers sensitive to zinc status. *Microbiol Spectr* 9:e0048321. doi: 10.1128/Spectrum.00483-21

Coury, D. L., Ashwood, P., Fasano, A., Fuchs, G., Geraghty, M., Kaul, A., et al. (2012). Gastrointestinal conditions in children with autism spectrum disorder: developing a research agenda. *Pediatrics* 130, S160–S168. doi: 10.1542/peds.2012-0900N

Cryan, J. F., and O'Mahony, S. M. (2011). The microbiome-gut-brain axis: from bowel to behavior. *Neurogastroenterol. Motil.* 23, 187–192. doi: 10.1111/j.1365-2982.2010.01664.x

Cryan, J. F., O'Riordan, K. J., Cowan, C. S. M., Sandhu, K. V., Bastiaanssen, T. F. S., Boehme, M., et al. (2019). The microbiota-gut-brain Axis. *Physiol. Rev.* 99, 1877–2013. doi: 10.1152/physrev.00018.2018

De Angelis, M., Francavilla, R., Piccolo, M., De Giacomo, A., and Gobbetti, M. (2015). Autism spectrum disorders and intestinal microbiota. *Gut Microbes* 6, 207–213. doi: 10.1080/19490976.2015.1035855

de Magistris, L., Familiari, V., Pascotto, A., Sapone, A., Frolli, A., Iardino, P., et al. (2010). Alterations of the intestinal barrier in patients with autism spectrum disorders and in their first-degree relatives. *J. Pediatr. Gastroenterol. Nutr.* 51, 418–424. doi: 10.1097/MPG.0b013e3181dcc4a5

De Santis, B., Brera, C., Mezzelani, A., Soricelli, S., Ciceri, F., Moretti, G., et al. (2019). Role of mycotoxins in the pathobiology of autism: a first evidence. *Nutr. Neurosci.* 22, 132–144. doi: 10.1080/1028415X.2017.1357793

De Smet, K., and Contreras, R. (2005). Human antimicrobial peptides: defensins, cathelicidins and histatins. *Biotechnol. Lett.* 27, 1337–1347. doi: 10.1007/s10529-005-0936-5

de Theije, C. G., Wopereis, H., Ramadan, M., van Eijndthoven, T., Lambert, J., Knol, J., et al. (2014). Altered gut microbiota and activity in a murine model of autism spectrum disorders. *Brain Behav. Immun.* 37, 197–206. doi: 10.1016/j.bbi.2013.12.005

D'Eufemia, P., Celli, M., Finocchiaro, R., Pacifico, L., Viozzi, L., Zaccagnini, M., et al. (1996). Abnormal intestinal permeability in children with autism. *Acta Paediatr.* 85, 1076–1079. doi: 10.1111/j.1651-2227.1996.tb14220.x

Dinno, A. (2017). Dunn's Test of Multiple Comparisons Using Rank Sums (R package version 1.3.5). Available online at: https://CRAN.R-project.org/package=dunn.test

Dobin, A., Davis, C. A., Schlesinger, F., Drenkow, J., Zaleski, C., Jha, S., et al. (2013). STAR: ultrafast universal RNA-seq aligner. *Bioinformatics* 29, 15–21. doi: 10.1093/bioinformatics/bts635

Dufner-Beattie, J., Wang, F., Kuo, Y. M., Gitschier, J., Eide, D., and Andrews, G. K. (2003). The acrodermatitis enteropathica gene ZIP4 encodes a tissue-specific, zinc-regulated zinc transporter in mice. *J. Biol. Chem.* 278, 33474–33481. doi: 10.1074/jbc.M305000200

Edgar, R. C. (2010). Search and clustering orders of magnitude faster than BLAST. *Bioinformatics* 26, 2460–2461. doi: 10.1093/bioinformatics/btq461

Edgar, R. C. (2016a). SINTAX: a simple non-Bayesian taxonomy classifier for 16S and ITS sequences. bioRxiv [Preprint].

Edgar, R. C. (2016b). UNOISE2: improved error-correction for Illumina 16S and ITS amplicon sequencing. bioRxiv [Preprint].

Edgar, R. C. (2017). Accuracy of microbial community diversity estimated by closed- and open-reference OTUs. *PeerJ* 5:e3889. doi: 10.7717/peerj.3889

Faber, S., Zinn, G. M., Kern, J. C. 2nd, and Kingston, H. M. (2009). The plasma zinc/serum copper ratio as a biomarker in children with autism spectrum disorders. *Biomarkers* 14, 171–180. doi: 10.1080/13547500902783747

Finn, R. D., Clements, J., and Eddy, S. R. (2011). HMMER web server: interactive sequence similarity searching. *Nucleic Acids Res.* 39, W29–W37. doi: 10.1093/nar/gkr367

Foligne, B., George, F., Standaert, A., Garat, A., Poiret, S., Peucelle, V., et al. (2020). High-dose dietary supplementation with zinc prevents gut inflammation: investigation

of the role of metallothioneins and beyond by transcriptomic and metagenomic studies. *FASEB J.* 34, 12615–12633. doi: 10.1096/fj.202000562RR

Fourie, C., Vyas, Y., Lee, K., Jung, Y., Garner, C. C., and Montgomery, J. M. (2018). Dietary zinc supplementation prevents autism related behaviors and striatal synaptic dysfunction in Shank3 exon 13-16 mutant mice. *Front. Cell. Neurosci.* 12:374. doi: 10.3389/fncel.2018.00374

Garcia-Vello, P., Tytgat, H. L. P., Elzinga, J., Van Hul, M., Plovier, H., Tiemblo-Martin, M., et al. (2024). The lipooligosaccharide of the gut symbiont *Akkermansia muciniphila* exhibits a remarkable structure and TLR signaling capacity. *Nat. Commun.* 15:8411. doi: 10.1038/s41467-024-52683-x

Gebhard, R. L., Karouani, R., Prigge, W. F., and McClain, C. J. (1983). The effect of severe zinc deficiency on activity of intestinal disaccharidases and 3-hydroxy-3-methylglutaryl coenzyme a reductase in the rat. *J. Nutr.* 113, 855–859. doi: 10.1093/jn/113.4.855

Gondalia, S. V., Palombo, E. A., Knowles, S. R., Cox, S. B., Meyer, D., and Austin, D. W. (2012). Molecular characterisation of gastrointestinal microbiota of children with autism (with and without gastrointestinal dysfunction) and their neurotypical siblings. *Autism Res.* 5, 419–427. doi: 10.1002/aur.1253

Grabrucker, A. M. (2012). Environmental factors in autism. *Front. Psych.* 3:118. doi: 10.3389/fpsyt.2012.00118

Grabrucker, A. M. (2014). A role for synaptic zinc in ProSAP/Shank PSD scaffold malformation in autism spectrum disorders. *Dev. Neurobiol.* 74, 136–146. doi: 10.1002/dneu.22089

Grabrucker, A. M., Knight, M. J., Proepper, C., Bockmann, J., Joubert, M., Rowan, M., et al. (2011a). Concerted action of zinc and ProSAP/Shank in synaptogenesis and synapse maturation. *EMBO J* 30, 569–581. doi: 10.1038/emboj.2010.336

Grabrucker, A. M., Rowan, M., and Garner, C. C. (2011b). Brain-delivery of zinc-ions as potential treatment for neurological diseases: mini review. *Drug Deliv. Lett.* 1, 13–23. doi: 10.2174/2210303111101010013

Gu, Z., Pei, W., Shen, Y., Wang, L., Zhu, J., Zhang, Y., et al. (2021). *Akkermansia muciniphila* and its outer protein Amuc_1100 regulates tryptophan metabolism in colitis. *Food Funct.* 12, 10184–10195. doi: 10.1039/d1fo02172a

Guo, M., Huang, K., Chen, S., Qi, X., He, X., Cheng, W. H., et al. (2014). Combination of metagenomics and culture-based methods to study the interaction between ochratoxin a and gut microbiota. *Toxicol. Sci.* 141, 314–323. doi: 10.1093/toxsci/kfu128

Hoggard, M., Vesty, A., Wong, G., Montgomery, J. M., Fourie, C., Douglas, R. G., et al. (2018). Characterizing the human Mycobiota: a comparison of small subunit rRNA, ITS1, ITS2, and large subunit rRNA genomic targets. *Front. Microbiol.* 9:2208. doi: 10.3389/fmicb.2018.02208

Horvath, K., and Perman, J. A. (2002). Autism and gastrointestinal symptoms. *Curr. Gastroenterol. Rep.* 4, 251–258. doi: 10.1007/s11894-002-0071-6

Hsiao, E. Y., McBride, S. W., Hsien, S., Sharon, G., Hyde, E. R., McCue, T., et al. (2013). Microbiota modulate behavioral and physiological abnormalities associated with neurodevelopmental disorders. *Cell* 155, 1451–1463. doi: 10.1016/j.cell.2013.11.024

Hyatt, D., Chen, G. L., Locascio, P. F., Land, M. L., Larimer, F. W., and Hauser, L. J. (2010). Prodigal: prokaryotic gene recognition and translation initiation site identification. *BMC Bioinformatics* 11:119. doi: 10.1186/1471-2105-11-119

Jiang, Y. H., and Ehlers, M. D. (2013). Modeling autism by SHANK gene mutations in mice. *Neuron* 78, 8–27. doi: 10.1016/j.neuron.2013.03.016

Joshi, N. F., (2011). Sickle: A sliding-window, adaptive, quality-based trimming tool for FastQ files (Version 1.33) [Software]. Available at https://github.com/najoshi/sickle (Accessed August 20, 2020).

Kanehisa, M., and Goto, S. (2000). KEGG: Kyoto encyclopedia of genes and genomes. *Nucleic Acids Res.* 28, 27–30. doi: 10.1093/nar/28.1.27

Kanehisa, M., Sato, Y., Kawashima, M., Furumichi, M., and Tanabe, M. (2016). KEGG as a reference resource for gene and protein annotation. *Nucleic Acids Res.* 44, D457–D462. doi: 10.1093/nar/gkv1070

Kang, D. W., Ilhan, Z. E., Isern, N. G., Hoyt, D. W., Howsmon, D. P., Shaffer, M., et al. (2018). Differences in fecal microbial metabolites and microbiota of children with autism spectrum disorders. *Anaerobe* 49, 121–131. doi: 10.1016/j.anaerobe.2017.12.007

Kang, D. D., Li, F., Kirton, E., Thomas, A., Egan, R., An, H., et al. (2019). MetaBAT 2: an adaptive binning algorithm for robust and efficient genome reconstruction from metagenome assemblies. *PeerJ* 7:e7359. doi: 10.7717/peerj.7359

Karimi, P., Kamali, E., Mousavi, S. M., and Karahmadi, M. (2017). Environmental factors influencing the risk of autism. *J. Res. Med. Sci.* 22:27. doi: 10.4103/1735-1995.200272

Klindworth, A., Pruesse, E., Schweer, T., Peplies, J., Quast, C., Horn, M., et al. (2013). Evaluation of general 16S ribosomal RNA gene PCR primers for classical and next-generation sequencing-based diversity studies. *Nucleic Acids Res.* 41:e1. doi: 10.1093/nar/gks808

Kopylova, E., Noe, L., and Touzet, H. (2012). SortMeRNA: fast and accurate filtering of ribosomal RNAs in metatranscriptomic data. *Bioinformatics* 28, 3211–3217. doi: 10.1093/bioinformatics/bts611

Kushak, R. I., Buie, T. M., Murray, K. F., Newburg, D. S., Chen, C., Nestoridi, E., et al. (2016). Evaluation of intestinal function in children with autism and gastrointestinal symptoms. *J. Pediatr. Gastroenterol. Nutr.* 62, 687–691. doi: 10.1097/MPG.0000000000001174

Laczny, C. C., Sternal, T., Plugaru, V., Gawron, P., Atashpendar, A., Margossian, H. H., et al. (2015). VizBin—an application for reference-independent visualization and human-augmented binning of metagenomic data. *Microbiome* 3:1. doi: 10.1186/s40168-014-0066-1

Langmead, B., Trapnell, C., Pop, M., and Salzberg, S. L. (2009). Ultrafast and memory-efficient alignment of short DNA sequences to the human genome. *Genome Biol.* 10:R25. doi: 10.1186/gb-2009-10-3-r25

Leblond, C. S., Nava, C., Polge, A., Gauthier, J., Huguet, G., Lumbroso, S., et al. (2014). Meta-analysis of SHANK mutations in autism spectrum disorders: a gradient of severity in cognitive impairments. *PLoS Genet.* 10:e1004580. doi: 10.1371/journal.pgen.1004580

Letunic, I., and Bork, P. (2021). Interactive tree of life (iTOL) v5: an online tool for phylogenetic tree display and annotation. *Nucleic Acids Res.* 49, W293–W296. doi: 10.1093/nar/gkab301

Li, W., O'Neill, K. R., Haft, D. H., DiCuccio, M., Chetvernin, V., Badretdin, A., et al. (2021). Ref seq: expanding the prokaryotic genome annotation pipeline reach with protein family model curation. *Nucleic Acids Res.* 49, D1020–D1028. doi: 10.1093/nar/gkaa1105

Liao, Y., Smyth, G. K., and Shi, W. (2014). featureCounts: an efficient general purpose program for assigning sequence reads to genomic features. *Bioinformatics* 30, 923–930. doi: 10.1093/bioinformatics/btt656

Liu, F., Li, J., Wu, F., Zheng, H., Peng, Q., and Zhou, H. (2019). Altered composition and function of intestinal microbiota in autism spectrum disorders: a systematic review. *Transl. Psychiatry* 9:43. doi: 10.1038/s41398-019-0389-6

Liuzzi, J. P., Bobo, J. A., Lichten, L. A., Samuelson, D. A., and Cousins, R. J. (2004). Responsive transporter genes within the murine intestinal-pancreatic axis form a basis of zinc homeostasis. *Proc. Natl. Acad. Sci. USA* 101, 14355–14360. doi: 10.1073/pnas.0406216101

Maenner, M. J., Shaw, K. A., Baio, J., Washington, A., Patrick, M., DiRienzo, M., et al. (2020). Prevalence of autism Spectrum disorder among children aged 8 years — autism and developmental disabilities monitoring network, 11 sites, United States, 2016. *Surveill Summar* 69, 1–12. doi: 10.15585/mmwr.ss6904a1

Maret, W. (2000). The function of zinc metallothionein: a link between cellular zinc and redox state. *J. Nutr.* 130, 1455S–1458S. doi: 10.1093/jn/130.5.1455S

Markova, N. (2019). Dysbiotic microbiota in autistic children and their mothers: persistence of fungal and bacterial wall-deficient L-form variants in blood. *Sci. Rep.* 9:13401. doi: 10.1038/s41598-019-49768-9

McCall, K. A., Huang, C., and Fierke, C. A. (2000). Function and mechanism of zinc metalloenzymes. *J. Nutr.* 130, 1437S–1446S. doi: 10.1093/jn/130.5.1437S

Minh, B. Q., Schmidt, H. A., Chernomor, O., Schrempf, D., Woodhams, M. D., von Haeseler, A., et al. (2020). IQ-TREE 2: new models and efficient methods for phylogenetic inference in the genomic era. *Mol. Biol. Evol.* 37, 1530–1534. doi: 10.1093/molbev/msaa015

Mistry, J., Chuguransky, S., Williams, L., Qureshi, M., Salazar, G. A., Sonnhammer, E. L. L., et al. (2021). Pfam: the protein families database in 2021. *Nucleic Acids Res.* 49, D412–D419. doi: 10.1093/nar/gkaa913

Miyoshi, Y., Tanabe, S., and Suzuki, T. (2016). Cellular zinc is required for intestinal epithelial barrier maintenance via the regulation of claudin-3 and occludin expression. *Am. J. Physiol. Gastrointest. Liver Physiol.* 311, G105–G116. doi: 10.1152/ajpgi.00405.2015

Naisbitt, S., Kim, E., Tu, J. C., Xiao, B., Sala, C., Valtschanoff, J., et al. (1999). Shank, a novel family of postsynaptic density proteins that binds to the NMDA receptor/PSD-95/GKAP complex and cortactin. *Neuron* 23, 569–582. doi: 10.1016/s0896-6273(00)80809-0

Nakamura, K., Yokoi, Y., Fukaya, R., Ohira, S., Shinozaki, R., Nishida, T., et al. (2020). Expression and localization of Paneth cells and their alpha-Defensins in the small intestine of adult mouse. *Front. Immunol.* 11:570296. doi: 10.3389/fimmu.2020.570296

Nilsson, R. H., Larsson, K. H., Taylor, A. F. S., Bengtsson-Palme, J., Jeppesen, T. S., Schigel, D., et al. (2019). The UNITE database for molecular identification of fungi: handling dark taxa and parallel taxonomic classifications. *Nucleic Acids Res.* 47, D259–D264. doi: 10.1093/nar/gky1022

Nithianantharajah, J., Balasuriya, G. K., Franks, A. E., and Hill-Yardin, E. L. (2017). Using animal models to study the role of the gut-brain Axis in autism. *Curr. Dev. Disord. Rep.* 4, 28–36. doi: 10.1007/s40474-017-0111-4

Nurk, S., Meleshko, D., Korobeynikov, A., and Pevzner, P. A. (2017). metaSPAdes: a new versatile metagenomic assembler. *Genome Res.* 27, 824–834. doi: 10.1101/gr.213959.116

Oksanen, J., Blanchet, F. G., Friendly, M., Kindt, R., Legendre, P., and McGlinn, D. (2019) Vegan: Community Ecology Package. R package version 2.5-6. Available online at: https://CRAN.R-project.org/package=vegan

Olesen, S. W., and Alm, E. J. (2016). Dysbiosis is not an answer. *Nat. Microbiol.* 1:16228. doi: 10.1038/nmicrobiol.2016.228

Oleskin, A. V., and Shenderov, B. A. (2016). Neuromodulatory effects and targets of the SCFAs and gasotransmitters produced by the human symbiotic microbiota. *Microb. Ecol. Health Dis.* 27:30971. doi: 10.3402/mehd.v27.30971

Olm, M. R., Brown, C. T., Brooks, B., and Banfield, J. F. (2017). dRep: a tool for fast and accurate genomic comparisons that enables improved genome recovery from

metagenomes through de-replication. *ISME J.* 11, 2864–2868. doi: 10.1038/ismej.2017.126

O'Mahony, S. M., Clarke, G., Borre, Y. E., Dinan, T. G., and Cryan, J. F. (2015). Serotonin, tryptophan metabolism and the brain-gut-microbiome axis. *Behav. Brain Res.* 277, 32–48. doi: 10.1016/j.bbr.2014.07.027

Ormerod, K. L., Wood, D. L., Lachner, N., Gellatly, S. L., Daly, J. N., Parsons, J. D., et al. (2016). Genomic characterization of the uncultured Bacteroidales family S24-7 inhabiting the guts of homeothermic animals. *Microbiome* 4:36. doi: 10.1186/s40168-016-0181-2

Parks, D. H., Imelfort, M., Skennerton, C. T., Hugenholtz, P., and Tyson, G. W. (2015). Check M: assessing the quality of microbial genomes recovered from isolates, single cells, and metagenomes. *Genome Res.* 25, 1043–1055. doi: 10.1101/gr.186072.114

Peca, J., Feliciano, C., Ting, J. T., Wang, W., Wells, M. F., Venkatraman, T. N., et al. (2011). Shank3 mutant mice display autistic-like behaviours and striatal dysfunction. *Nature* 472, 437–442. doi: 10.1038/nature09965

Pieper, R., Dadi, T. H., Pieper, L., Vahjen, W., Franke, A., Reinert, K., et al. (2020). Concentration and chemical form of dietary zinc shape the porcine colon microbiome, its functional capacity and antibiotic resistance gene repertoire. *ISMEJ* 14, 2783–2793. doi: 10.1038/s41396-020-0730-3

Quast, C., Pruesse, E., Yilmaz, P., Gerken, J., Schweer, T., Yarza, P., et al. (2013). The SILVA ribosomal RNA gene database project: improved data processing and web-based tools. *Nucleic Acids Res.* 41, D590–D596. doi: 10.1093/nar/gks1219

Raimondi, F., Santoro, P., Barone, M. V., Pappacoda, S., Barretta, M. L., Nanayakkara, M., et al. (2008). Bile acids modulate tight junction structure and barrier function of Caco-2 monolayers via EGFR activation. *Am. J. Physiol. Gastrointest. Liver Physiol.* 294, G906–G913. doi: 10.1152/ajpgi.00043.2007

RCoreTeam (2019). R: A language and environment for statistical computing. Vienna, Austria: R Foundation for Statistical Computing.

Rhee, S. H., Pothoulakis, C., and Mayer, E. A. (2009). Principles and clinical implications of the brain-gut-enteric microbiota axis. *Nat. Rev. Gastroenterol. Hepatol.* 6, 306–314. doi: 10.1038/nrgastro.2009.35

Robinson, M. D., McCarthy, D. J., and Smyth, G. K. (2010). edgeR: a Bioconductor package for differential expression analysis of digital gene expression data. *Bioinformatics* 26, 139–140. doi: 10.1093/bioinformatics/btp616

Rubenstein, J. L., and Merzenich, M. M. (2003). Model of autism: increased ratio of excitation/inhibition in key neural systems. *Genes Brain Behav.* 2, 255–267. doi: 10.1034/j.1601-183x.2003.00037.x

Sanders, S. J., Murtha, M. T., Gupta, A. R., Murdoch, J. D., Raubeson, M. J., Willsey, A. J., et al. (2012). De novo mutations revealed by whole-exome sequencing are strongly associated with autism. *Nature* 485, 237–241. doi: 10.1038/nature10945

Sauer, A. K., Bockmann, J., Steinestel, K., Boeckers, T. M., and Grabrucker, A. M. (2019). Altered intestinal morphology and microbiota composition in the autism Spectrum disorders associated SHANK3 mouse model. *Int. J. Mol. Sci.* 20:2134. doi: 10.3390/ijms20092134

Sieber, C. M. K., Probst, A. J., Sharrar, A., Thomas, B. C., Hess, M., Tringe, S. G., et al. (2018). Recovery of genomes from metagenomes via a dereplication, aggregation and scoring strategy. *Nat. Microbiol.* 3, 836–843. doi: 10.1038/s41564-018-0171-1

Silva, Y. P., Bernardi, A., and Frozza, R. L. (2020). The role of short-chain fatty acids from gut microbiota in gut-brain communication. *Front Endocrinol* 11:25. doi: 10.3389/fendo.2020.00025

Skrovanek, S., DiGuilio, K., Bailey, R., Huntington, W., Urbas, R., Mayilvaganan, B., et al. (2014). Zinc and gastrointestinal disease. *World J. Gastrointest. Pathophysiol.* 5, 496–513. doi: 10.4291/wjgp.v5.i4.496

Smith, J. C., McDaniel, E. G., McBean, L. D., Doft, F. S., and Halsted, J. A. (1972). Effect of microorganisms upon zinc metabolism using germfree and conventional rats. *J. Nutr.* 102, 711–719. doi: 10.1093/jn/102.6.711

Smith, B. J., Miller, R. A., Ericsson, A. C., Harrison, D. C., Strong, R., and Schmidt, T. M. (2019). Changes in the gut microbiome and fermentation products concurrent with enhanced longevity in acarbose-treated mice. *BMC Microbiol.* 19:130. doi: 10.1186/s12866-019-1494-7

Son, J. S., Zheng, L. J., Rowehl, L. M., Tian, X., Zhang, Y., Zhu, W., et al. (2015). Comparison of fecal microbiota in children with autism Spectrum disorders and Neurotypical siblings in the Simons simplex collection. *PLoS One* 10:e0137725. doi: 10.1371/journal.pone.0137725

Souffriau, J., Timmermans, S., Vanderhaeghen, T., Wallaeys, C., Van Looveren, K., Aelbrecht, L., et al. (2020). Zinc inhibits lethal inflammatory shock by preventing microbe-induced interferon signature in intestinal epithelium. *EMBO Mol. Med.* 12:e11917. doi: 10.15252/emmm.201911917

Stenman, L. K., Holma, R., Eggert, A., and Korpela, R. (2013). A novel mechanism for gut barrier dysfunction by dietary fat: epithelial disruption by hydrophobic bile acids. *Am. J. Physiol. Gastrointest. Liver Physiol.* 304, G227–G234. doi: 10.1152/ajpgi.00267.2012

Strati, F., Cavalieri, D., Albanese, D., De Felice, C., Donati, C., Hayek, J., et al. (2017). New evidences on the altered gut microbiota in autism spectrum disorders. *Microbiome* 5:24. doi: 10.1186/s40168-017-0242-1

Sturniolo, G. C., Di Leo, V., Ferronato, A., D'Odorico, A., and D'Inca, R. (2001). Zinc supplementation tightens "leaky gut" in Crohn's disease. *Inflamm. Bowel Dis.* 7, 94–98. doi: 10.1097/00054725-200105000-00003

Sturniolo, G. C., Fries, W., Mazzon, E., Di Leo, V., Barollo, M., and D'Inca, R. (2002). Effect of zinc supplementation on intestinal permeability in experimental colitis. *J. Lab. Clin. Med.* 139, 311–315. doi: 10.1067/mlc.2002.123624

Suzek, B. E., Huang, H., McGarvey, P., Mazumder, R., and Wu, C. H. (2007). UniRef: comprehensive and non-redundant UniProt reference clusters. *Bioinformatics* 23, 1282–1288. doi: 10.1093/bioinformatics/btm098

Tabouy, L., Getselter, D., Ziv, O., Karpuj, M., Tabouy, T., Lukic, I., et al. (2018). Dysbiosis of microbiome and probiotic treatment in a genetic model of autism spectrum disorders. *Brain Behav. Immun.* 73, 310–319. doi: 10.1016/j.bbi.2018.05.015

Takakuwa, A., Nakamura, K., Kikuchi, M., Sugimoto, R., Ohira, S., Yokoi, Y., et al. (2019). Butyric acid and leucine induce alpha-defensin secretion from small intestinal Paneth cells. *Nutrients* 11:2817. doi: 10.3390/nu11112817

Tallman, D. L., and Taylor, C. G. (2003). Effects of dietary fat and zinc on adiposity, serum leptin and adipose fatty acid composition in C57BL/6J mice. *J. Nutr. Biochem.* 14, 17–23. doi: 10.1016/s0955-2863(02)00228-0

Tao-Cheng, J. H., Toy, D., Winters, C. A., Reese, T. S., and Dosemeci, A. (2016). Zinc stabilizes Shank3 at the postsynaptic density of hippocampal synapses. *PLoS One* 11:e0153979. doi: 10.1371/journal.pone.0153979

UniProt, C. (2021). UniProt: the universal protein knowledgebase in 2021. *Nucleic Acids Res.* 49, D480–D489. doi: 10.1093/nar/gkaa1100

Usama, U., Khan, M. J., and Fatima, S. (2018). Role of zinc in shaping the gut microbiome; proposed mechanisms and evidence from the literature. *J. Gastrointest. Dig. Syst.* 8:548. doi: 10.4172/2161-069X.1000548

Vicentefranqueira, R., Amich, J., Laskaris, P., Ibrahim-Granet, O., Latge, J. P., Toledo, H., et al. (2015). Targeting zinc homeostasis to combat *Aspergillus fumigatus* infections. *Front. Microbiol.* 6:160. doi: 10.3389/fmicb.2015.00160

Vicentefranqueira, R., Leal, F., Marin, L., Sanchez, C. I., and Calera, J. A. (2019). The interplay between zinc and iron homeostasis in *Aspergillus fumigatus* under zinc-replete conditions relies on the iron-mediated regulation of alternative transcription units of zafA and the basal amount of the ZafA zinc-responsiveness transcription factor. *Environ. Microbiol.* 21, 2787–2808. doi: 10.1111/1462-2920.14618

Vujkovic-Cvijin, I., Sklar, J., Jiang, L., Natarajan, L., Knight, R., and Belkaid, Y. (2020). Host variables confound gut microbiota studies of human disease. *Nature* 587, 448–454. doi: 10.1038/s41586-020-2881-9

Vyas, Y., and Montgomery, J. M. (2016). The role of postsynaptic density proteins in neural degeneration and regeneration. *Neural Regen. Res.* 11, 906–907. doi: 10.4103/1673-5374.184481

Wapnir, R. A. (2000). Zinc deficiency, malnutrition and the gastrointestinal tract. *J. Nutr.* 130, 1388S–1392S. doi: 10.1093/jn/130.5.1388S

Wegener, W. S., and Romano, A. H. (1963). Zinc stimulation of Rna and protein synthesis in *Rhizopus nigricans*. *Science* 142, 1669–1670. doi: 10.1126/science.142.3600.1669

Wei, S. C., Yang-Yen, H. F., Tsao, P. N., Weng, M. T., Tung, C. C., Yu, L. C. H., et al. (2017). *SHANK3* regulates intestinal barrier function through modulating *ZO-1* expression through the PKCepsilon-dependent pathway. *Inflamm. Bowel Dis.* 23, 1730–1740. doi: 10.1097/MIB.0000000000001250

Wu, Y. W., Simmons, B. A., and Singer, S. W. (2016). MaxBin 2.0: an automated binning algorithm to recover genomes from multiple metagenomic datasets. *Bioinformatics* 32, 605–607. doi: 10.1093/bioinformatics/btv638

Yap, C. X., Henders, A. K., Alvares, G. A., Wood, D. L. A., Krause, L., Tyson, G. W., et al. (2021). Autism-related dietary preferences mediate autism-gut microbiome associations. *Cell* 184, 5916–5931. doi: 10.1016/j.cell.2021.10.015

Yasuda, K., Oh, K., Ren, B., Tickle, T. L., Franzosa, E. A., Wachtman, L. M., et al. (2015). Biogeography of the intestinal mucosal and lumenal microbiome in the rhesus macaque. *Cell Host Microbe* 17, 385–391. doi: 10.1016/j.chom.2015.01.015

Zhang, L., Xu, Y., Li, H., Li, B., Duan, G., and Zhu, C. (2022). The role of probiotics in children with autism spectrum disorders: a study protocol for a randomised controlled trial. *PLoS One* 17:e0263109. doi: 10.1371/journal.pone.0263109

frontiers | Frontiers in Microbiology

TYPE Original Research
PUBLISHED 13 August 2025
DOI 10.3389/fmicb.2025.1626941

Check for updates

OPEN ACCESS

EDITED BY
Federica Savini,
University of Bologna, Italy

REVIEWED BY
Marco Pane,
Probiotical SpA, Italy
Arindam Dhali,
National Dairy Research Institute (Southern Regional Station), India

*CORRESPONDENCE
Haiyan Gao
✉ gaohaiyan127@163.com
Xiaobing Jiang
✉ jxb841001@163.com

RECEIVED 12 May 2025
ACCEPTED 25 July 2025
PUBLISHED 13 August 2025

CITATION
Zhao L, Wei Z, Wang Y, Chen W, Zhang W, Xie M, Chen H, Zhang Y, Gao H and Jiang X (2025) *Lactiplantibacillus plantarum* ZP-6 mitigates polystyrene nanoplastics-induced liver damage in colitis mice via the gut-liver axis. *Front. Microbiol.* 16:1626941. doi: 10.3389/fmicb.2025.1626941

COPYRIGHT
© 2025 Zhao, Wei, Wang, Chen, Zhang, Xie, Chen, Zhang, Gao and Jiang. This is an open-access article distributed under the terms of the Creative Commons Attribution License (CC BY). The use, distribution or reproduction in other forums is permitted, provided the original author(s) and the copyright owner(s) are credited and that the original publication in this journal is cited, in accordance with accepted academic practice. No use, distribution or reproduction is permitted which does not comply with these terms.

Lactiplantibacillus plantarum ZP-6 mitigates polystyrene nanoplastics-induced liver damage in colitis mice via the gut-liver axis

Lili Zhao[1], Zihan Wei[1], Yibin Wang[1], Wanrong Chen[1], Wenjing Zhang[1], Mengfei Xie[1], Hong Chen[1], Yiping Zhang[1], Haiyan Gao[2]* and Xiaobing Jiang[1,3]*

[1]College of Life Sciences, Henan Normal University, Xinxiang, China, [2]School of Food Science, Henan Institute of Science and Technology, Xinxiang, China, [3]Henan Engineering Laboratory for Bioconversion Technology of Functional Microbes, College of Life Sciences, Henan Normal University, Xinxiang, China

Introduction: Nanoplastics (NPs) have become a ubiquitous environmental pollutant that exhibits a tendency to accumulate in large quantities in the tissues of the host body (enteritis patients) with intestinal damage and poses a serious health risk, for which there is currently no suitable method for *in vivo* clearance. Studies have found that lactic acid bacteria has the potential to eliminate pollutants from the body.

Methods: In this study, we investigated the capacity of *Lactiplantibacillus plantarum* ZP-6, a strain isolated from human feces with demonstrated *in vitro* microplastic-binding activity, to alleviate the physiological toxicity of polystyrene nanoplastics (PS-NPs) in healthy and colitic murine models. Then, we investigated the capacity of *Lactiplantibacillus plantarum* ZP-6 to alleviate the physiological toxicity of polystyrene nanoplastics (PS-NPs) in healthy and colitic murine models.

Results: Our findings revealed that PS-NPs exposure resulted in systemic accumulation, triggering organ pathology and inflammatory responses in the liver and colon. Dietary intervention with *Lactiplantibacillus plantarum* ZP-6 significantly reduced PS-NPs retention in blood and tissues while enhancing fecal excretion, restoring hepatic, renal, and colonic histopathology to baseline levels. Mechanistically, ZP-6 downregulated pro-inflammatory cytokines (IL-1β, IL-6, TNF-α) and anti-inflammatory IL-10 in affected tissues. Gut colonization dynamics demonstrated transient enrichment of ZP-6, which facilitated PS-NPs adsorption and fecal clearance. Concurrently, ZP-6 upregulated mucin gene *Muc2* and tight junction components (*OCLN*, *CLDN1*), reinforcing the intestinal epithelial barrier and impeding PS-NPs translocation. Metabolomic analysis further indicated that ZP-6 rectified PS-NPs-induced hepatic metabolic dysregulation via the gut-liver axis.

Conclusion: These results elucidate a multifaceted probiotic mechanism for NPs detoxification, providing a promising translational strategy to counteract nanoplastic-related health hazards.

KEYWORDS

***Lactiplantibacillus plantarum*, polystyrene nanoplastic, inflammatory factors, metabonomics, colitic murine, gut-liver axis**

1 Introduction

Nanoplastics (NPs), defined as plastic particles with diameters below 100 nm (Mitrano et al., 2021), have become ubiquitous due to the extensive use of plastic products. These particles are readily ingested by organisms and have now been detected in a wide range of species, including humans (Schwabl et al., 2019). Substantial animal studies demonstrate that NPs can disrupt intestinal epithelial permeability, trigger gut inflammation, impair normal intestinal function, and even promote the development of chronic diseases (Hirt and Body-Malapel, 2020). In toxicological studies of marine organisms, NPs exposure has been shown to reduce digestive enzyme secretion, induce hepatic lipid metabolism disorders (Gonzalez-Fernandez et al., 2021; Lai et al., 2021; Li et al., 2021), upregulate antioxidant gene expression, cause immune dysregulation, and suppress muscle growth (Brandts et al., 2021), ultimately decreasing survival rates. Notably, polystyrene nanoplastics (PS-NPs) accumulate in the gut, reducing mucus secretion and compromising intestinal barrier integrity (Jin et al., 2019). Deng et al. (2017) detected NPs in mouse tissues, with significant accumulation observed in the liver, kidneys, and intestines. Metabolomic analyses further reveal that NPs exposure alters hepatic metabolic profiles in fish, disrupting lipid and energy metabolism (Lu et al., 2016). While growing concerns over the adverse effects of NPs have spurred increasing research into their toxicity mechanisms, few studies have explored potential defense strategies against NPs-induced damage. Consequently, there is an urgent need to identify effective approaches to mitigate NPs toxicity.

Inflammatory bowel disease (IBD), a chronic inflammatory disorder encompassing ulcerative colitis (UC) and Crohn's disease, has rising global prevalence. While Crohn's disease involves transmural inflammation across the gastrointestinal tract, UC specifically targets the colonic mucosa — making it pathologically congruent with experimental colitis models (Xavier & Podolsky, 2007). This UC pathology is characterized by diffuse inflammation and epithelial barrier disruption in the colon, which may facilitate systemic translocation of environmental contaminants (Sandys and Te Velde, 2022). NPs, pervasive foodborne pollutants, accumulate in the gut and exhibit enhanced penetration through the compromised intestinal barrier in UC/colitis (Pironti et al., 2021). Notably, the increasing environmental burden of plastic particles correlates with IBD incidence trends, particularly UC (Molodecky et al., 2012). Epidemiological evidence from Taiwan, China reveals that in regions with high consumption of seafood from polluted waters, UC incidence surged 1.5-fold (1998-2008) (Tong et al., 2013). Critically, Yan et al. (2022) demonstrated elevated NPs in feces of IBD patients, with the highest particle loads observed in UC subgroups—positively correlating with disease severity. These findings establish a focused research imperative: UC-associated colitis creates a "leaky gut" permissive to NPs translocation, potentially driving extra-intestinal damage via portals like the gut-liver axis.

The gut and liver maintain intricate physiological and pathological connections through the "gut-liver axis." Gut microbiota-derived products, including bioactive metabolites and microbe-associated molecular patterns, can traverse the intestinal barrier, enter the portal circulation, and subsequently modulate hepatic pathophysiology during disease progression (Lin et al., 2025). The intestinal barrier serves as a crucial defense system that prevents the translocation of harmful substances such as toxins into systemic tissues and microcirculation, pathological conditions including trauma, stress, and inflammatory responses can compromise intestinal barrier integrity to varying degrees, thereby exacerbating primary disease conditions (Allaire et al., 2018). As the primary detoxification organ, the liver is continuously exposed to numerous endogenous and exogenous toxins that may induce hepatic damage. Emerging evidence suggests that maintaining gut microbial symbiosis may enhance hepatic anti-inflammatory and antioxidant responses, consequently protecting against acute hepatotoxicity. For instance, probiotic administration has been demonstrated to ameliorate aflatoxin B1 (AFB1)-induced toxicity in humans (Mohd Redzwan et al., 2016). These findings highlight the pivotal role of gut microbiota and intestinal homeostasis in modulating toxin-mediated acute liver injury.

Lactiplantibacillus plantarum (*L. plantarum*), a prominent probiotic species within the gut microbiota, is ubiquitously present in various food products and the gastrointestinal tract (Nordström et al., 2021). Accumulating evidence demonstrates its pivotal role in mitigating the detrimental effects of food contaminants on host health. Specifically, *L. plantarum* facilitates heavy metal excretion and reduces tissue accumulation, thereby attenuating metal toxicity. The protective mechanisms include preservation of intestinal barrier integrity and modulation of oxidative stress to inhibit intestinal heavy metal absorption (Duan et al., 2020). *In vivo* murine studies reveal that *L. plantarum* CCFM8610 significantly decreases cadmium accumulation in cadmium-exposed mice while enhancing fecal cadmium elimination (Zhai et al., 2013). Furthermore, *L. plantarum* exhibits multi-faceted therapeutic potential in inflammatory bowel disease through: regulation of inflammatory cytokines; potentiation of anti-inflammatory factor secretion; amelioration of intestinal inflammation (Mishima et al., 2019); Notably, oral administration of *L. plantarum* 06CC2 stimulates IL-10 production in the colon, alleviating dextran sulfate sodium (DSS)-induced colitis in mice (Tanaka et al., 2020). Similarly, *L. plantarum* CBTLP3 restores goblet cell populations and suppresses pro-inflammatory cytokine secretion in DSS-induced colitis models (Kim et al., 2020). Building upon preliminary findings that *L. plantarum* ZP-6 (isolated from human feces) exhibits nanoplastic clearance capacity *in vitro*, we subsequently investigated its therapeutic potential for eliminating NPs *in vivo* using murine models.

Given the escalating burden of plastic pollution, PS-NPs serve as a model to investigate NPs toxicity and remediation. Building upon our previous isolation of *L. plantarum*—a human fecal strain demonstrating *in vitro* NPs adsorption capacity—this study aimed to quantify the effect of ZP-6 on *in vivo* fecal PS-NPs excretion, assess its ability to restore PS-NPs-compromised intestinal barrier integrity, evaluate its anti-inflammatory effects against systemic inflammation, and examine its capacity to rectify PS-NPs-induced metabolic dysregulation via the gut-liver axis. Here, we hypothesize that ZP-6 mitigates PS-NPs-induced damage by: (i) enhancing fecal NP excretion, (ii) restoring gut barrier integrity, (iii) modulating inflammation, and (iv) rectifying metabolic dysregulation via the gut-liver axis. By testing this hypothesis in healthy and colitic mice, we aim to develop a probiotic-based dietary strategy to counteract NPs toxicity.

2 Materials and methods

2.1 Tested strains and materials

The study utilized *L. plantarum* (strain ZP-6), previously isolated from infant feces in our laboratory. Commercial 100 nm polystyrene microspheres were obtained from Dongguan Mingyuxing Plastic Raw Materials Co., Ltd. Five-week-old male mice were supplied by Henan Xincheng Youkang Biotechnology Co., Ltd. The animals were housed under controlled conditions: temperature maintained at 23 ± 1°C, relative humidity at 50% ± 5%, with natural light cycles. Mice had ad libitum access to food and water throughout the study period.

2.2 Preparation of fluorescent PS-NPs

Nile red dye (0.01 mg) was dissolved in chloroform (1 mL) to prepare the Nile red dye solution (0.01 mg/mL) that was kept in dark. Separately, PS-NPs solution was made by dispersing 250 mg of PS-NPs in water-DMSO (v:v = 1:1) mixture. The Nile red dye solution was then added to the PS-NPs dispersion, and the mixture was heated at 75°C for 30 min. Immediately after heating, the solution was rapidly cooled in an ice-water bath. The cooled suspension was filtered through a polycarbonate membrane (30 nm pore size), after which the retained PS-NPs were transferred to pure water and stored protected from light.

2.3 Animal experimental methods

Animal experiments were approved by the Animal Ethics Committee of Henan Normal University, China. Twenty 5-week-old male SPF grade C57BL/6 mice were purchased from Henan Xincheng Youkang Biotechnology Co., Ltd. The mice underwent a 1-week adaptation period under free access to food and water. Subsequently, the mice were divided into a healthy group and a colitis model group (Figure 1a). The healthy group consisted of four groups (n = 5 in each group): control group (Con): 0.2 mL PBS was administered orally daily; *L. plantarum* ZP-6 group (LP): 0.2 mL *L. plantarum* ZP-6 bacterial solution was administered orally daily (5×10^9 CFU/mL, the dose of *L. plantarum* ZP-6 was determined by the previous research of the research group); PS-NPs group (NPs): 0.2 mL fluorescent PS-NPs (10 mg/kg BW) were administered by gavage every day; PS-NPs + *L. plantarum* ZP-6 group (NL): 0.2 mL fluorescent PS-NPs + 0.2 mL *L. plantarum* ZP-6 solution were intragastrically administered every day.

Colitis model group consisted of three groups (n = 5 in each group): ① colitis group (dextran sulfate sodium, DSS): refer to previous studies for the modeling method of acute colitis mice. Specifically, mice were free to drink water containing 3% DSS (w/v; mw36,000–50,000) for 7 days, provided with maintenance feed for mice, and gavaged with 0.2 mL PBS every day; ② Colitis + PS NPs group (DN): on the basis of drinking 3% DSS, 0.2 mL fluorescent PS-NPs (10 mg/kg BW) was administered by gavage every day; ③ Colitis + PS NPs + *L. plantarum* ZP-6 group (DNL): on the basis of drinking 3% DSS, mice were given 0.2 mL of fluorescent PS-NPs (10 mg/kg BW) + *L. plantarum* ZP-6 solution by gavage every day.

The dose of *L. plantarum* ZP-6 was determined as the optimal concentration through previous research and exploration by our research team. The experimental period was 5 weeks. At the end of the 5th week, the mice were anesthetized with isoflurane, and blood was collected from the orbit. The mice were euthanized by cervical dislocation. The liver, kidney, spleen, colon and small intestine were removed, part of which was fixed with 4% paraformaldehyde, and the rest was quickly frozen with liquid nitrogen and stored in a −80°C refrigerator.

2.4 Determination of body weight and organ coefficient of mice

The weight of the mice was measured before the experiment, and the weight of the mice was recorded every 7 days after the start of intragastric administration. The weight of the mice was measured before the mice were killed. After the mice were dissected, the liver, spleen and kidney were collected, weighed, and divided by the weight of the mice to obtain the organ coefficient. The length of the small intestine and colon were measured respectively.

2.5 Distribution of PS-NPs in mice

Mouse liver, kidney, spleen, small intestine, and colon were fixed, dehydrated, and embedded. Tissue sections (5 μm) were prepared using a Leica CM1860 cryostat. Sections were examined under a fluorescence microscope (Leica DMIL Microsystems) equipped with: TRITC filter (Excitation: 550/20 nm; Emission: 630/40 nm), 20× objective and 10× eyepiece (Total magnification: 200×).

2.6 Content of PS-NPs in organs, blood and fecal tissues

After intragastric administration of fluorescent PS-NPs in mice, the blood of mice in NPs group and NL group was obtained by orbital blood collection at 0, 4, 8, 12 and 24 h, and the blood of mice in DN group and DNL group was collected at 3, 5, 7, 9, 11 and 13 h after the start of modeling. The blood volume was 200 μL, and the feces of mice were collected at the same time point. Blood, liver, kidney, spleen, small intestine, colon and fecal tissues were collected after 5 weeks of intragastric administration. Approximately 0.2 g of sample was dissolved in a mixture of HNO_3 and H_2O_2 until no visible solid residue remained, followed by dilution to volume with deionized water. The fluorescence value of the sample was measured at the excitation/emission wavelength of 543 nm/620 nm using a microplate reader (Agilent Technologies SH1M2F). The standard curve was obtained by a series of concentrations of fluorescent PS-NPs (0, 0.1, 0.2, 0.4, 0.6, 0.8 mg/mL). The value of PS-NPs level in the sample was obtained by offsetting the value of the control group. The fluorescence value of the control group (representing untreated sample) was subtracted from the sample fluorescence value to correct for background interference. The PS-NPs concentration in the sample was then determined by interpolating this corrected fluorescence value onto the standard curve.

10.3389/fmicb.2025.1626941

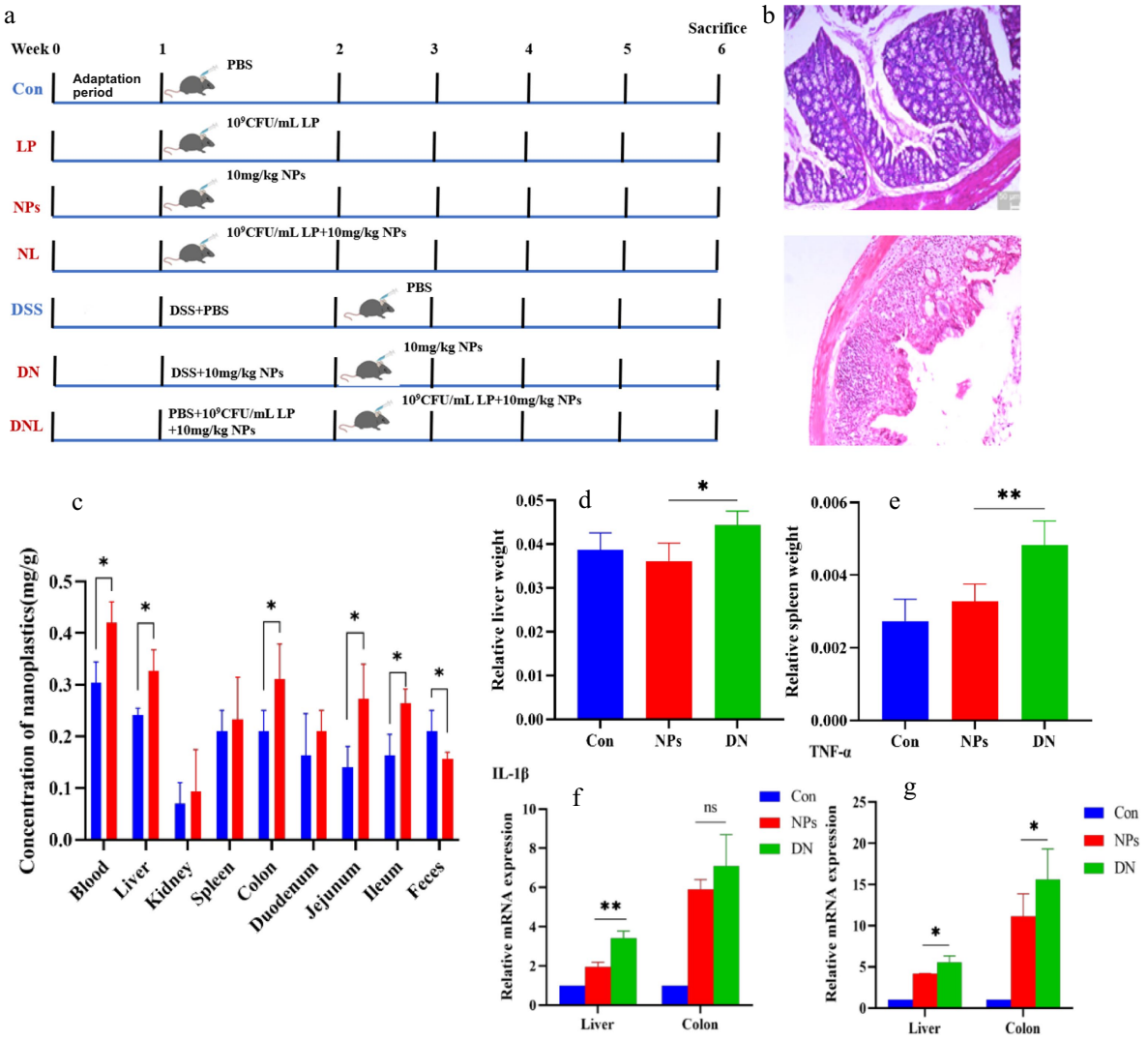

FIGURE 1
(a) Experimental design. Con—control group; LP—*L. plantarum* group; NPs—nanoplastic group; NL—nanoplastic + *L. plantarum* group; DSS—acute colitis group; DN—colitis + nanoplastic group; DNL—colitis + nanoplastic + *L. plantarum* group. **(b)** Colon pathological sections of health mice and mice with colitis. **(c)** Content of PS-NPs in mouse tissues. **(d,e)** Changes in mice body weight and organ coefficients. **(f,g)** Expression of inflammatory factors in mouse liver and colon. ns express $p > 0.05$, *express $p < 0.05$, **express $p < 0.01$, $n = 5$.

2.7 Histopathological analysis

The intact liver, kidney, spleen and colon tissues of mice were fixed in 4% paraformaldehyde for 24 h at room temperature. Fixed tissues were then dehydrated through a graded ethanol series (70–100%, 35 min per concentration). Following dehydration, samples were cleared using sequential xylene incubations: first in a 1:1 (v/v) ethanol-xylene mixture for 10 min, followed by two changes of pure xylene. Tissue infiltration was performed with molten paraffin wax at 65°C. Organs were subsequently embedded in paraffin blocks, solidified at −20°C. Serial sections of 5 μm thickness were cut using a Leica CM1860 microtome. The tissue sections were stained with Hematoxylin and Eosin (H&E) Staining, and permanently mounted with neutral balsam under coverslips. Stained tissue sections were visualized using an OLYMPUS BX43 brightfield microscope for comprehensive histopathological assessment.

2.8 Expression analysis of inflammatory factors and intestinal barrier related factors

The fresh tissues of liver, colon and duodenum of mice were ground and added with RNA extract to extract total RNA, and the RNA concentration was determined by micro spectrophotometer. Reverse transcription was performed according to the instructions of the cDNA reverse transcription kit. The expression of *IL-1β* (Interleukin-1β), *IL-6* (Interleukin-6), *IL-10* (Interleukin-10), *TNF-α* (Tumor Necrosis Factor-α) and intestinal barrier related factors *OCLN* (Occludin), *CLDN1* (Claudin 1), *Muc2* (Mucin 2) were detected by fluorescent quantitative PCR using cDNA as template.

2.8.1 RNA extraction and quantification

Fresh tissues (liver, colon, duodenum; 0.1 g each) were homogenized in 200 μL RNA lysis buffer on ice using a tissue grinder, followed by addition of 800 μL lysis buffer and centrifugation

(12,000 rpm, 4°C, 10 min). The supernatant was transferred to a new tube, mixed with chloroform (20% v/v), vortexed for 15 s, incubated for 5 min, and centrifuged (12,000 rpm, 4°C, 15 min). The aqueous phase was collected, combined with an equal volume of isopropanol, inverted to mix, incubated for 5 min, and centrifuged (12,000 rpm, 4°C, 10 min). After discarding the supernatant, the RNA pellet was washed with 1 mL 75% ethanol (7,500 × g, 4°C, 5 min), air-dried, and dissolved in 30 μL DEPC-H_2O. RNA concentration was determined using a Nanodrop ND-2000 spectrophotometer (Thermo Fisher) with DEPC-H_2O as blank and 1 μL sample loading volume.

2.8.2 cDNA synthesis via reverse transcription

Genomic DNA was removed from RNA templates (1 μg) using a 10 μL reaction containing 1 μL 10 × gDNA remover mix in nuclease-free H_2O. Reactions were incubated at 42°C for 2 min (metal bath), then immediately cooled on ice. Reverse transcription was performed by adding 4 μL 5 × M5 RT Super Plus Mix and 6 μL nuclease-free H_2O to the 10 μL gDNA-cleared RNA, yielding a 20 μL total volume. After gentle mixing and brief centrifugation, samples were incubated at 37°C for 15 min followed by enzyme inactivation at 85°C for 5 s. Synthesized cDNA was stored at −20°C.

2.8.3 Real-time PCR

The primers were synthesized by Shanghai Sanggong Bioengineering Co., Ltd., and the specific sequences are shown in Table 1. Real-time PCR reaction system: 10 μL 2 × SGExcel FastSYBR Mixture; 0.4 μL each forward/reverse primer (10 μM); 5 μL cDNA template; Nuclease-free water to 20 μL final volume. qPCR was performed using SYBR Green Master Mix (Applied Biosystems) with primers validated against Primer Bank sequences. Amplification conditions: 95°C (3 min); 40 cycles of 95°C (5 s)/60°C (20 s); melt curve analysis. Relative expression was normalized to β-actin using the $2^{-\Delta\Delta CT}$ method. Amplicon sizes were confirmed by agarose gel electrophoresis. Primer efficiencies (98–102%) were determined from standard curves ($R^2 > 0.99$) using serial cDNA dilutions.

2.9 Analysis of intestinal colonization of *L. plantarum* ZP-6

FITC (fluorescein isothiocyanate) solid powder was mixed in dimethyl sulfoxide to form a staining solution with a concentration of 0.1 mg/mL, and then added to the suspension of *L. plantarum* ZP-6 for staining. *L. plantarum* ZP-6 (200 μL) was fed into mice by gavage, and six time gradients of 0, 2, 4, 8, 12, and 24 h were set. At these six time points, the mice were euthanized, the colon tissue was taken, cut and spread on the slide, and then the existence of *L. plantarum* ZP-6 in the colon was observed under the inverted fluorescence microscope.

2.10 Analysis of PS-NPs adsorption by *L. plantarum* ZP-6

Mice were intragastrically administered with fluorescent PS-NPs and *L. plantarum* ZP-6 2 h later. Feces were collected within 2 h after intragastric administration of *L. plantarum* ZP-6. The feces were prepared into fecal suspension, and the upper turbid liquid smear was taken to observe the fluorescence under the laser scanning confocal microscope.

2.11 Analysis of intestinal mucus secretion

The method provided by AB-PAS (Alcian Blue-Periodic Acid Schiff) staining kit was used to stain the colonic tissue sections of mice. After staining, the secretion of colonic mucus in each group was

TABLE 1 Primer sequences and amplification parameters.

Genes	Direction	Sequence (5′ → 3′)	Product length (bp)	Annealing temperature (°C)	Efficiency (%)
IL-1β	Forward	GAAATGCCACCTTTTGACAGTG	116	58	101
	Reverse	TGGATGCTCTCATCAGGACAG			
IL-6	Forward	CTGCAAGAGACTTCCATCCAG	131	57	103
	Reverse	AGTGGTATAGACAGGTCTGTTGG			
IL-10	Forward	CTTACTGACTGGCATGAGGATCA	101	58	103
	Reverse	GCAGCTCTAGGAGCATGTGG			
TNF-α	Forward	CCTGTAGCCCACGTCGTAG	148	59	101
	Reverse	GGGAGTAGACAAGGTACAACCC			
β-actin	Forward	GGGAAATCGTGCGTGAC	176	55	105
	Reverse	AGGCTGGAAAAGAGCCT			
OCLN	Forward	TGAAAGTCCACCTCCTTACAGA	128	55	102
	Reverse	CCGGATAAAAAGAGTACGCTGG			
CLDN1	Forward	GCCTTGATGGTAATTGGCATCC	165	58	105
	Reverse	GGCCACTAATGTCGCCAGAC			
Muc2	Forward	AGGGCTCGGAACTCCAGAAA	106	59	102
	Reverse	CCAGGGAATCGGTAGACATCG			

observed under the microscope, and the area of the mucus part was quantified by ImageJ software to obtain the mucus coverage rate for comparison.

2.12 Hepatic metabonomic analysis

Fifty milligrams of liver and pre cooled mixture (methanol: acetonitrile: water = 2:2:2, v/v/v) were treated with vortex and ultrasound, incubated at −20°C for 10 min, and then centrifuged for 20 min. The supernatant was dried under vacuum, redissolved in 600 μL solvent (acetonitrile: water = 1:1, v/v) and centrifuged. Then the supernatant was collected for subsequent analysis. The metabolites were quantified by Thermo Fisher vanquish ultra performance liquid chromatography-q active focus electrostatic field orbital trap mass spectrometry (LC-MS/MS). Metaboanalyst 6.0 was used for metabolomic data analysis (Fu et al., 2022). Partial least squares discriminant analysis (PLS-DA) was performed to visualize the metabolic differences between the experimental groups after mean centralization and unit variance scaling (Zhao et al., 2019).

2.13 Data processing and analysis

Data are expressed as mean ± standard error. At least 3 replicates shall be set for each test. Graphpad prism 8.4.0 (LA Jolla, CA, United States) was used for data analysis. Tukey test was used for one-way analysis of variance (ANOVA). When $p < 0.05$, the results were considered statistically significant.

3 Results

3.1 Impact of PS-NPs on colitis progression in murine models

Unlike previous studies that administered NPs after colitis onset, this investigation employed a concurrent exposure model where PS-NPs were administered via intragastric gavage simultaneously with DSS-induced colitis modeling. This experimental paradigm allows for comprehensive evaluation of NP effects during: (i) the pre-inflammatory phase, (ii) acute colitis manifestation, and (iii) the subsequent recovery period. Importantly, this approach better recapitulates real-world scenarios where environmental NP exposure coincides with colitis development in human patients, thereby enhancing the clinical relevance of our findings. DSS-induced colitis, characterized by pronounced epithelial damage, crypt loss, inflammatory cell infiltration, and mucosal thickening (Figure 1b), was successfully established as evidenced by histopathological confirmation. To assess the potential exacerbating effects of PS-NPs on colitis progression, we conducted comparative analyses between healthy controls (NP_S group) and PS-NP-treated colitis mice (DN group).

The results revealed that PS-NPs exposure significantly ($p < 0.05$) increased: hepatosplenic indices (liver and spleen coefficients) in colitis mice compared to healthy controls; PS-NPs accumulation in systemic circulation (blood) and target organs (liver, colon, jejunum, and ileum); pro-inflammatory cytokine levels in colitis-affected animals (Figures 1c–g). These data collectively demonstrate that PS-NPs exert more pronounced pathological effects in the context of intestinal inflammation, potentially through enhanced tissue accumulation and amplified inflammatory responses. The observed organ coefficient changes suggest possible systemic involvement beyond the gastrointestinal tract.

3.2 *L. plantarum* ZP-6 modulates systemic distribution and fecal excretion of PS-NPs in mice

3.2.1 Systemic circulation analysis

To investigate the pharmacokinetics of orally administered polystyrene nanoparticles (PS-NPs), we quantified their temporal distribution in blood and feces during the first 24 h post-administration (Figure 2). Pharmacokinetic analysis revealed rapid absorption of PS-NPs, with blood concentration peaking at 4 h (0.0884 ± 0.0315 mg/g) followed by gradual decline, suggesting subsequent tissue redistribution (Figure 2a). Notably, prophylactic administration of *L. plantarum* ZP-6 (initiated 4 h post-PS-NPs exposure) significantly attenuated systemic PS-NPs accumulation compared to NPs-only controls ($p < 0.05$, Figure 2b).

In DSS-induced colitis models (DN group), we observed exacerbated PS-NPs absorption kinetics, with peak blood concentrations (0.3224 ± 0.0700 mg/g) coinciding with maximal disease severity on day 9 (Figure 2b). This temporal correlation suggests compromised intestinal barrier integrity facilitates enhanced systemic nanoparticle translocation. The subsequent decline in circulating PS-NPs after day 10 paralleled clinical improvement (body weight recovery, reduced hematochezia), while *L. plantarum* ZP-6 supplementation (DNL group) showed limited efficacy during active inflammation, indicating gut barrier integrity modulates probiotic-mediated nanoparticle clearance.

3.2.2 Fecal excretion dynamics

The pharmacokinetic analysis revealed distinct patterns of fecal PS-NPs excretion contingent upon intestinal health status. In healthy mice, PS-NPs excretion followed a biphasic kinetic profile, characterized by a sharp peak (0.0883 ± 0.0372 mg/g) within 8 h post-exposure, followed by a subsequent decline (Figure 2c). Critically, administration of *L. plantarum* ZP-6 significantly enhanced the magnitude of fecal PS-NPs elimination throughout this excretion timeline without altering its biphasic nature. Conversely, in mice with colitis, the profound impairment of intestinal barrier function severely compromised baseline PS-NPs excretion capacity. While probiotic intervention with ZP-6 significantly increased excretion compared to untreated colitic mice, it achieved only partial restoration, failing to reach the efficiency observed in healthy animals (Figure 2d).

These findings collectively demonstrate that PS-NPs undergo rapid enteric absorption (peak plasma concentration at 4 h) and systemic distribution. The efficacy of *L. plantarum* ZP-6 in enhancing fecal PS-NPs clearance is evident in both healthy and inflamed intestines; however, its therapeutic potential is markedly constrained under conditions of colitis. This differential efficacy directly underscores the paramount importance of gut barrier integrity as a critical determinant governing not only systemic PS-NPs burden but also the success of probiotic-mediated detoxification strategies. Consequently, while *L. plantarum* ZP-6 represents a promising intervention for promoting

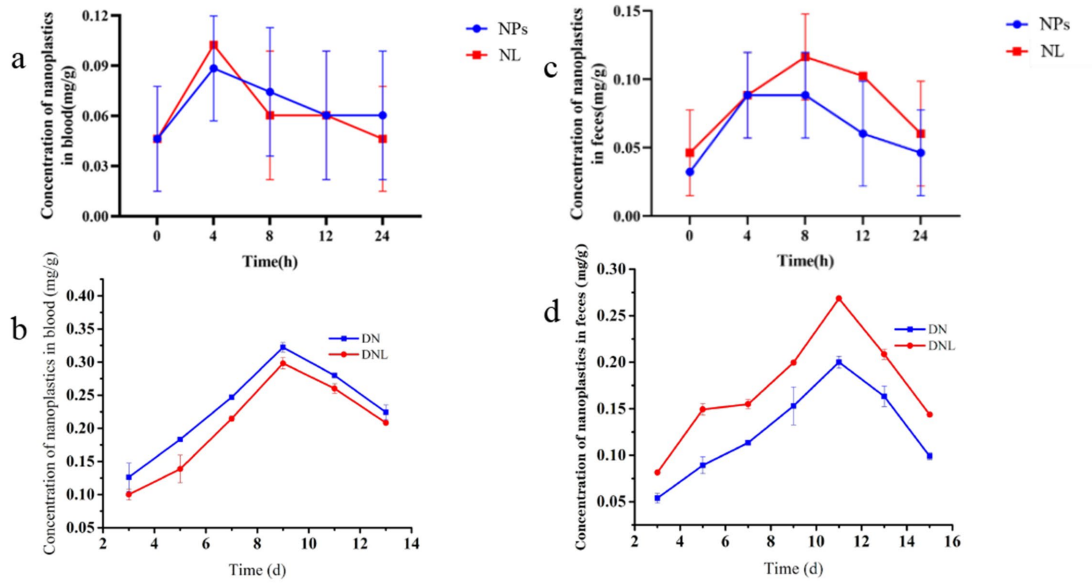

FIGURE 2
(a,b) Changes in nanoplastic content of mice blood. **(c,d)** Changes in nanoplastic content of mice feces. Con—control group; LP—*L. plantarum* group; NPs—nanoplastic group; NL—nanoplastic + *L. plantarum* group; DSS—acute colitis group; DN—colitis + nanoplastic group; DNL—colitis + nanoplastic + *L. plantarum* group; ns express $p > 0.05$, *express $p < 0.05$, **express $p < 0.01$, ***express $p < 0.001$, $n = 5$.

nanoplastic elimination via the fecal route, its detoxification capacity is fundamentally contingent upon the functional status of the intestinal barrier. These results highlight the gut barrier's pivotal role in modulating nanoplastic biodistribution and solidify the rationale for developing probiotic-based approaches to mitigate environmental toxicant exposure, particularly emphasizing the need to consider underlying gut health.

3.3 Effect of *L. plantarum* ZP-6 on the tissue distribution and accumulation of PS-NPs in mice

3.3.1 Tissue distribution analysis

To assess the biodistribution of polystyrene nanoparticles (PS-NPs) in murine tissues, frozen sections of the liver, kidney, spleen, colon, duodenum, jejunum, and ileum were examined via fluorescence microscopy. As depicted in Figure 3a, fluorescent PS-NPs were widely distributed across multiple organs following oral administration. However, treatment with *L. plantarum* ZP-6 significantly attenuated PS-NPs accumulation in these tissues. In the NL group (healthy mice administered *L. plantarum* ZP-6), fluorescent PS-NPs were nearly undetectable in all organs except the ileum. Conversely, in the DNL group (DSS-induced colitis mice treated with *L. plantarum* ZP-6), residual fluorescence was observed in various tissues, particularly in intestinal segments, though at markedly lower intensities compared to the DN group (DSS-induced colitis mice without probiotic intervention). These findings demonstrate that *L. plantarum* ZP-6 effectively mitigates PS-NPs retention in systemic organs.

3.3.2 Quantitative analysis of PS-NPs accumulation

To quantify PS-NPs burdens, tissues (blood, liver, kidney, spleen, colon, duodenum, jejunum, ileum) and fecal samples were collected, digested, and analyzed via fluorometry using a calibrated standard curve ($y = 14.266x - 0.4608$, $R^2 = 0.9972$). In healthy mice (Figure 3b), PS-NPs predominantly accumulated in the circulatory system (highest concentration), followed by hepatic tissue. This distribution pattern suggests that ingested PS-NPs undergo transepithelial uptake in the gastrointestinal tract, entering systemic circulation as nanoparticulate fractions. The liver, while serving as the primary metabolic organ, exhibited significant PS-NPs retention due to its filtration capacity and inability to metabolize synthetic polymers. Colonic accumulation likely reflects prolonged transit time, with partial PS-NPs redistribution into circulation via enterocyte uptake, fecal excretion, or luminal retention.

Notably, *L. plantarum* ZP-6 intervention (NL group) significantly reduced PS-NPs loads in blood, liver, spleen, and colon while enhancing fecal elimination ($p < 0.05$ vs. NP_S controls). In colitis models (Figure 3c), the DNL group showed pronounced reductions in PS-NPs content in blood, liver, colon, and small intestinal segments compared to DN controls ($p < 0.05$), alongside increased fecal excretion. Collectively, these data indicate that *L. plantarum* ZP-6 enhances PS-NPs clearance via the fecal route and reduces systemic bioaccumulation.

3.4 *L. plantarum* ZP-6 attenuates PS-NPs-induced organ damage in mice

3.4.1 Restoration of intestinal morphology

The gastrointestinal tract serves as the primary target for PS-NPs accumulation, with intestinal length serving as a sensitive biomarker of inflammatory severity. As illustrated in Figures 4a,b, chronic (5-week) PS-NPs exposure induced significant colonic shortening ($p < 0.05$ vs. control), a hallmark of intestinal inflammation. Strikingly,

10.3389/fmicb.2025.1626941

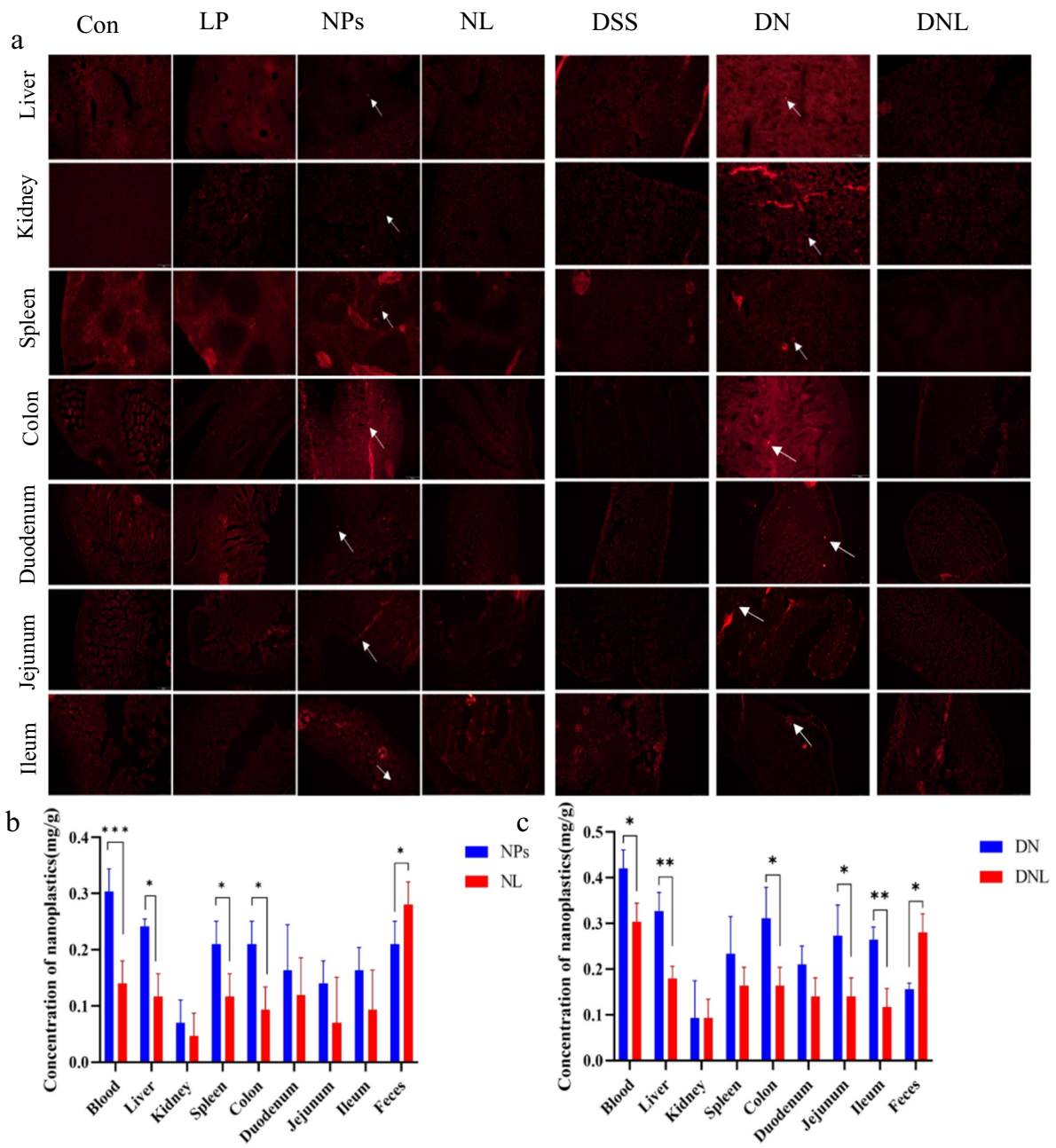

FIGURE 3
(a) Distribution of nanoplastics in various organs of mice. **(b,c)** Content of PS-NPs in mouse tissues. Con—control group; LP—*L. plantarum* group; NPs—nanoplastic group; NL—nanoplastic + *L. plantarum* group; DSS—acute colitis group; DN—colitis + nanoplastic group; DNL—colitis + nanoplastic + *L. plantarum* group; *express $p < 0.05$, **express $p < 0.01$, ***express $p < 0.001$, $n = 5$.

L. plantarum ZP-6 supplementation (NL group) restored colonic length to near-baseline levels, demonstrating therapeutic efficacy.

Unexpectedly, small intestinal morphology exhibited divergent responses (Figure 4c). While PS-NPs exposure (NPs group) triggered significant elongation of the small intestine ($p < 0.05$)—suggesting compensatory hyperplasia or structural remodeling—*L. plantarum* ZP-6 failed to normalize this parameter. These findings indicate that PS-NPs differentially disrupt intestinal homeostasis, with *L. plantarum* ZP-6 selectively mitigating colonic but not small intestinal pathology.

In DSS-induced colitis models, PS-NPs exacerbated disease progression. The DN group (DSS + PS-NPs) exhibited persistent colonic shortening (1.50 cm reduction vs. control, Figure 4d), contrasting with the self-resolving pathology in DSS-only mice. Notably, *L. plantarum* ZP-6 intervention (NDL group) partially reversed this atrophy ($p < 0.05$ vs. DN), underscoring its protective role in inflammatory settings.

3.4.2 Histopathological assessment of systemic organ damage

H&E-stained paraffin sections of major organs revealed distinct PS-NPs-induced pathologies: *Liver*: Parenchymal cell hyperchromasia and nuclear swelling (Figure 4a), indicative of

10.3389/fmicb.2025.1626941

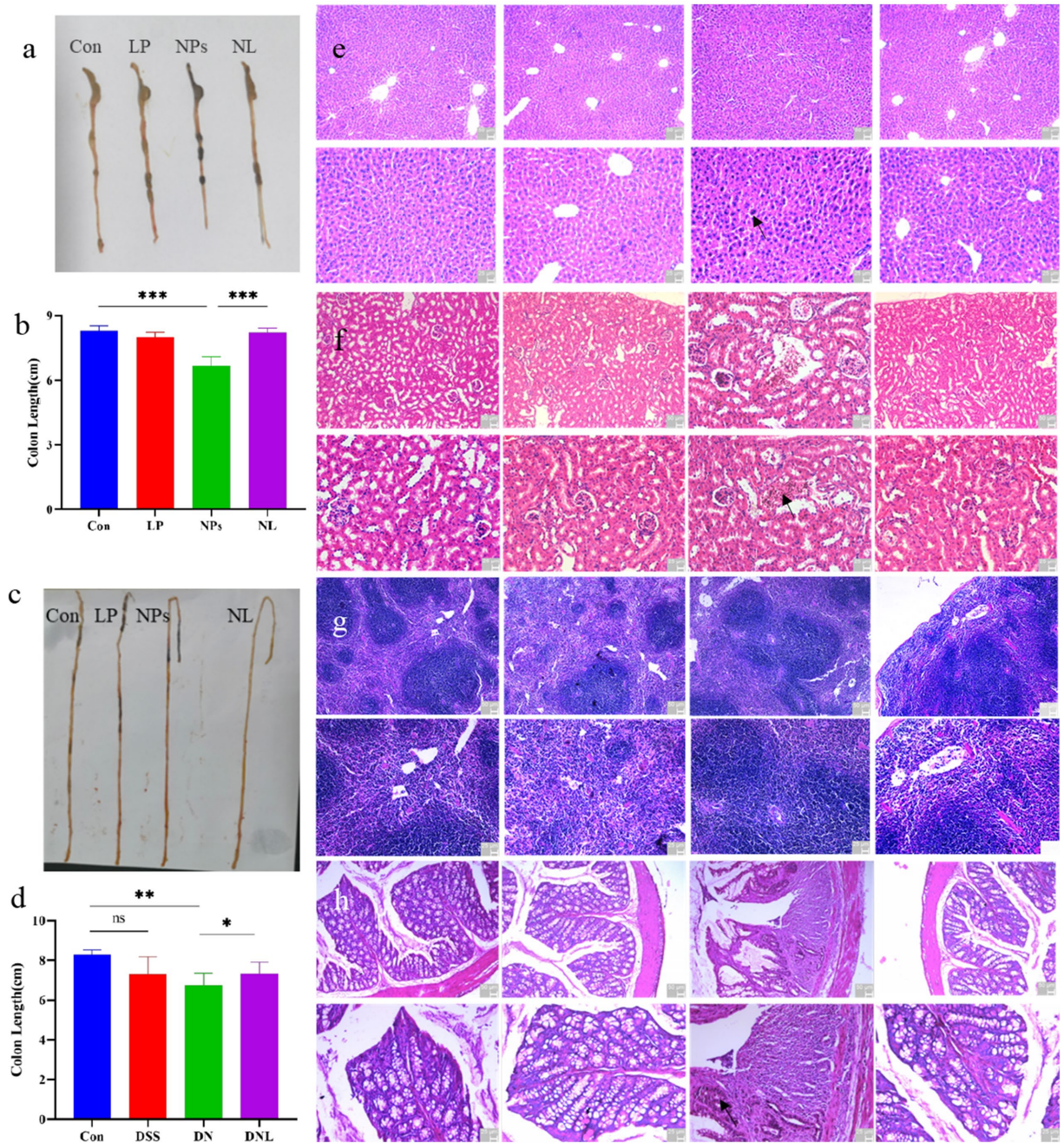

FIGURE 4
(a–d) Changes in mice colon and small intestinal morphology. The organ status of mice **(e)** liver; **(f)** kidney **(g)** spleen; **(h)** colon. Con—control group; LP—*L. plantarum* group; NPs—nanoplastic group; NL—nanoplastic + *L. plantarum* group; DSS—acute colitis group; DN—colitis + nanoplastic group; DNL—colitis + nanoplastic + *L. plantarum* group; *express $p < 0.05$, **express $p < 0.01$, ***express $p < 0.001$, $n = 5$.

hepatocellular stress (Figure 4e); *Kidney*: Proximal tubule dilation and peritubular inflammatory infiltrates (Figure 4f), suggesting acute tubular injury; *Spleen*: No significant microarchitectural alterations (Figure 4g); *Colon*: Crypt distortion, villus blunting, and transmural leukocyte infiltration (Figure 4h), confirming severe colitis. Remarkably, *L. plantarum* ZP-6 treatment (NL group) preserved hepatic, renal, and colonic histoarchitecture at levels indistinguishable from healthy controls. This systemic protection highlights the strain's capacity to counteract PS-NPs toxicity across multiple organ systems.

3.5 Mechanistic insights into *L. plantarum* ZP-6-mediated microplastic clearance

3.5.1 Intestinal colonization dynamics of *L. plantarum* ZP-6

To elucidate the PS-NPs clearance mechanism, we tracked the intestinal colonization pattern of FITC-labeled *L. plantarum* ZP-6 over 24 h (Figure 5a). Fluorescence microscopy revealed: (i) 2 h post-administration: abundant green fluorescent foci appeared in the intestinal lumen, confirming rapid transit of viable bacteria; (ii) 4 h:

fluorescence intensity peaked, indicating maximal bacterial colonization; (iii) 8 h: bacterial counts decreased significantly ($p < 0.05$ vs. 4 h), suggesting initial clearance; (iv) 12 h: only residual fluorescence was detectable, demonstrating near-complete evacuation. This biphasic colonization profile mirrored the temporal excretion pattern of fecal PS-NPs (Figures 1c,d), supporting a potential adsorption-clearance relationship. The synchronized decline in both bacterial counts and intestinal PS-NPs loads implies that *L. plantarum* ZP-6 may physically sequester NPs during transit, facilitating their elimination.

3.5.2 Direct PS-NP adsorption by *L. plantarum* ZP-6

Building on our observation of enhanced fecal PS-NP excretion following *L. plantarum* ZP-6 intervention (Section 3.3.2), we hypothesized direct bacterial adsorption as the underlying mechanism. Confocal microscopy of fecal samples revealed: (i) Spatial co-localization: yellow-green fluorescence (*L. plantarum* ZP-6) and red fluorescence (PS-NPs) exhibited precise overlap (Figure 5b); (ii) Surface binding: PS-NPs adhered extensively to bacterial cell walls, forming distinct aggregates. These findings provide visual evidence that *L. plantarum* ZP-6: physically interacts with PS-NPs via surface adsorption, likely through electrostatic or hydrophobic interactions (given NP surface properties); functions as a biotic vector, transporting immobilized PS-NPs through the gastrointestinal tract for fecal excretion. So, these results revealed that the strain's peptidoglycan layer or extracellular polysaccharides may serve as binding sites, consistent with prior reports of lactic acid bacteria adsorbing environmental pollutants; this "capture-and-remove" mechanism

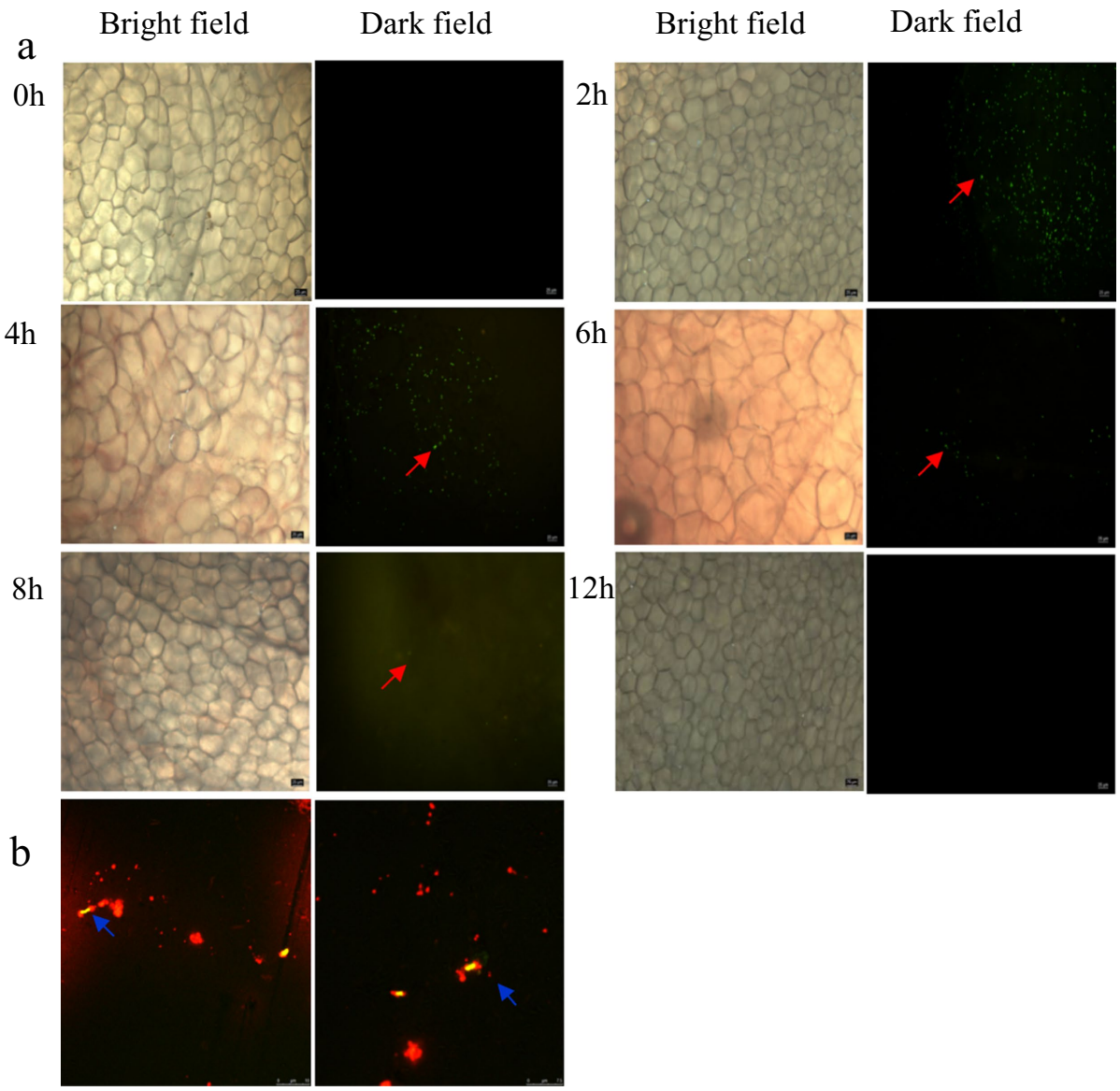

FIGURE 5
(a) Analysis of the colonization of *L. plantarum* ZP-6 in the intestinal tract of mice. **(b)** Combination of *L. plantarum* ZP-6 and nanoplastics in mice feces. Those that emit red fluorescence are PS-NPs, and those that emit yellow-green fluorescence are *L. plantarum* ZP-6.

could explain the reduced systemic NPs accumulation observed in Section 3.3.

3.6 Mechanistic analysis of *L. plantarum* ZP-6 in alleviating PS-NP-induced liver damage via the gut-brain axis

3.6.1 Analysis of intestinal mucus secretion

The intestinal mucus layer constitutes a critical protective barrier against xenobiotic insults. Our investigation of mucus secretion patterns in PS-NPs-exposed mice revealed distinct responses in different physiological states (Figure 6). In healthy mice, PS-NPs exposure (NP_S group) induced a significant 2.3-fold ($p < 0.01$) increase in mucus coverage compared to controls (Figure 6a), suggesting an adaptive mucosal response to nanoparticle challenge.

Interestingly, similar hyper-secretion was observed in enteritis models, where PS-NPs-treated mice (DN group) exhibited 1.7-fold higher ($p < 0.05$) elevated mucus production relative to DSS-only controls. This conserved response across both healthy and inflamed intestines implies a fundamental defensive mechanism against PS-NPs intrusion. Notably, *L. plantarum* ZP-6 administration maintained this elevated mucus secretion without significant suppression, indicating its neutral effect on goblet cell secretory activity.

At the molecular level, we observed that *Muc2* gene expression mirrored these physiological changes (Figures 6b,c). In healthy mice, NP_S treatment upregulated *Muc2* transcription, 19.2-fold upregulation ($p < 0.001$) in colon and 10.06 increase in duodenum, consistent with the observed mucus hypersecretion. However, a paradoxical *Muc2* downregulation occurred in colitic mice following PS-NPs exposure, which was significantly reversed by *L. plantarum* ZP-6 treatment (DNL group), paradoxical about 30% suppression ($p < 0.01$) versus DSS controls. These differential responses suggest that PS-NPs may disrupt mucin homeostasis through distinct mechanisms depending on the inflammatory status of the intestine.

3.6.2 Expression analysis of intestinal barrier-related factors

The integrity of intestinal tight junctions was systematically evaluated through quantification of *OCLN* and *CLDN1* gene expression (Figures 6b,c). PS-NPs exposure induced significant downregulation of these critical barrier proteins in both intestinal segments examined. In healthy mice, we observed tissue-specific suppression, with *CLDN1* most affected in the colon, 55% reduction in colonic *CLDN1* ($p < 0.01$); and *OCLN* in the duodenum, 64% decrease in duodenal *OCLN* ($p < 0.01$).

The compromise of barrier function was more pronounced in enteritis models, where PS-NPs exacerbated the DSS-induced downregulation of both genes, synergistic 60–80% downregulation of both genes ($p < 0.001$). This synergistic effect suggests that inflammatory conditions may potentiate PS-NPs toxicity to the intestinal epithelium. Importantly, *L. plantarum* ZP-6 treatment effectively restored tight junction protein expression in most tissues, though with varying efficacy depending on the specific gene and intestinal segment.

3.6.3 Hepatic metabolomic analysis

PLS-DA of liver metabolic profiles revealed substantial perturbations induced by PS-NPs exposure (Figure 7). The metabolic fingerprints of NPs-treated groups diverged significantly from controls in both healthy and colitic mice, demonstrating systemic metabolic consequences of nanoparticle exposure.

Detailed analysis identified specific metabolic pathways affected: in healthy mice, 14 significantly altered metabolites, including depletion of stachyose and accumulation of guanosine and branched-chain amino acids, the notable changes include stachyose (−3.2-fold), guanosine (+2.8-fold); But in colitic mice, more extensive disturbances with 17 differential metabolites, featuring nucleotide metabolism alterations and widespread amino acid fluctuations, the key alterations include inosine (−4.1-fold), L-methionine (+3.5-fold).

L. plantarum ZP-6 intervention normalized many of these metabolic deviations, 78% reduction in metabolite alterations. Particularly restoring levels of key metabolites like nicotinamide (+2.4-fold) (with known anti-inflammatory properties) and sphingosine (+1.8-fold) (critical for membrane integrity). The partial overlap of confidence ellipses between treated and control groups indicates progressive metabolic recovery.

3.6.4 Modulation of inflammatory responses

PS-NPs exposure triggered robust inflammatory activation in both hepatic and colonic tissues (Figure 8). Pro-inflammatory cytokines (*IL-1β*, *IL-6*, *TNF-α*) were markedly elevated, *IL-1β* was 6.99-fold increase ($p < 0.001$) in colon and 1.9-fold elevation in liver ($p < 0.01$), *TNF-α* was 92.92-fold elevation ($p < 0.001$) in colon and 4.08-fold increase in liver ($p < 0.01$), IL-6 was 5.33-fold upregulation ($p < 0.001$) in colon and 2.29-fold increase in liver ($p < 0.01$), while the anti-inflammatory IL-10 showed more variable responses. This inflammatory signature was particularly pronounced in enteritis models, where PS-NPs amplified DSS-induced cytokine production. *L. plantarum* ZP-6 treatment consistently attenuated these inflammatory responses across tissues and disease states. The probiotic's anti-inflammatory effects were most evident in colitic mice, where it significantly reduced *IL-1β* and *TNF-α* expression in both liver and colon, reduced *IL-1β* by 69% ($p < 0.01$) and normalized colonic *TNF-α* to baseline. Notably, this immunomodulation occurred in parallel with the observed improvements in barrier function and metabolic homeostasis, suggesting coordinated protection across multiple physiological systems (see Figure 9).

Collectively, our findings demonstrate that *L. plantarum* ZP-6 confers comprehensive protection against PS-NPs-induced toxicity through four synergistic mechanisms that collectively preserve gut-liver axis homeostasis. First, the probiotic orchestrates a sophisticated mucosal defense program, initiating rapid mucus hypersecretion followed by sustained Muc2-mediated regulation, with differential modulation observed between healthy and pathological conditions. Second, *L. plantarum* ZP-6 exhibits remarkable tissue specificity in intestinal barrier repair, differentially regulating *CLDN1* and *OCLN* expression to restore tight junction integrity and limit systemic nanoparticle translocation. Third, the strain mediates global metabolic reprogramming, effectively correcting PS-NPs-induced disturbances in nucleotide and amino acid metabolism while restoring critical metabolic pathways. Fourth, it demonstrates potent multi-organ anti-inflammatory activity, simultaneously attenuating pro-inflammatory signaling cascades in both hepatic and intestinal

10.3389/fmicb.2025.1626941

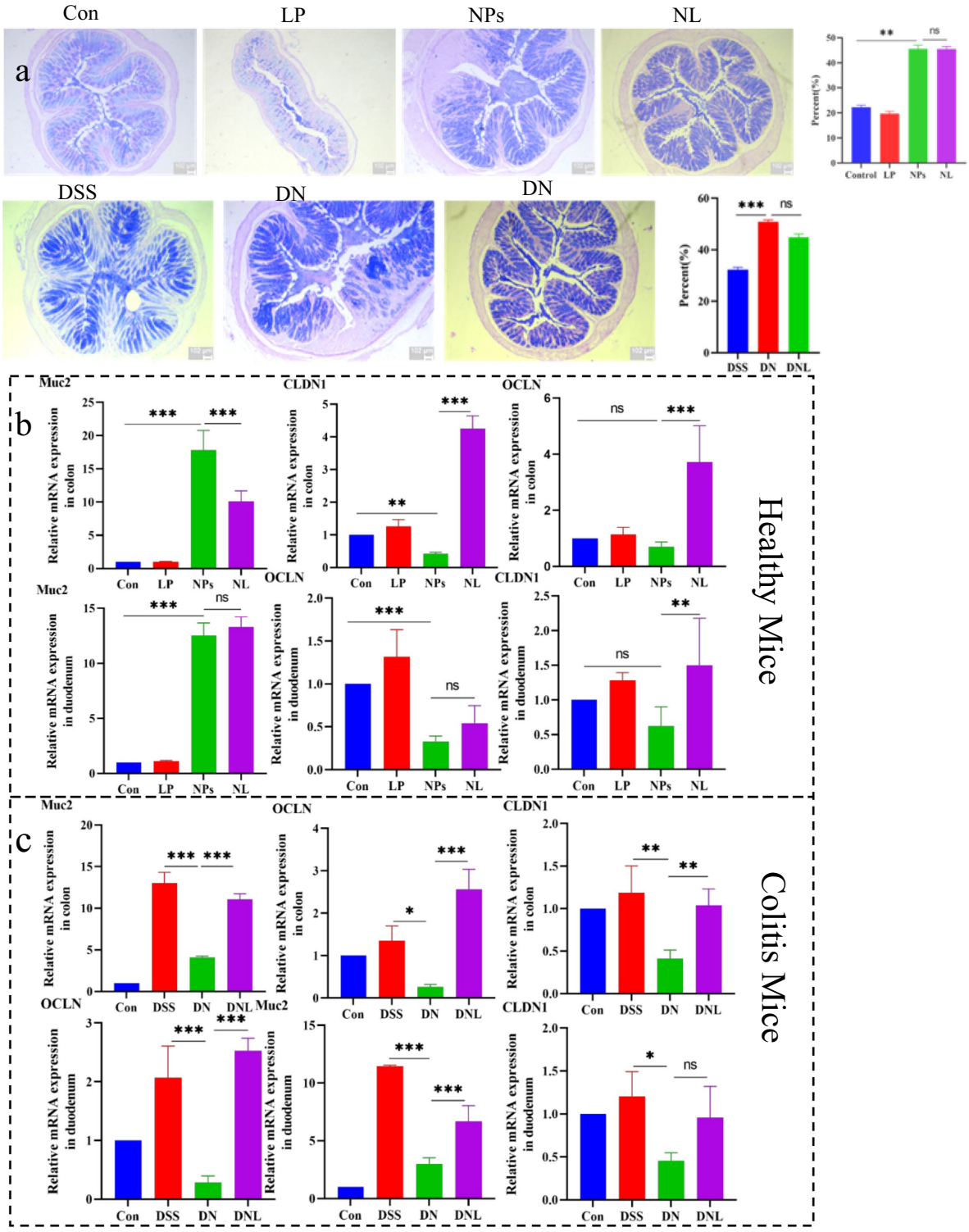

FIGURE 6
(a) Analysis of mucus secretion in mice colon. **(b)** Analysis of expression of mucin and intestinal barrier-related genes in healthy mice. **(c)** Analysis of expression of mucin and intestinal barrier-related genes in Colitis mice colon and duodenum. Con—control group; LP—*L. plantarum* group; NPs—nanoplastic group; NL—nanoplastic + *L. plantarum* group; DSS—acute colitis group; DN—colitis + nanoplastic group; DNL—colitis + nanoplastic + *L. plantarum* group; ns express $p > 0.05$, $^{*}p < 0.05$, $^{**}p < 0.01$, $^{***}p < 0.001$, $n = 5$.

tissues. This multi-omics investigation positions *L. plantarum* ZP-6 as a master regulator of gut-brain-liver communication during nanotoxic stress, highlighting its potential as a novel biotherapeutic agent against environmental pollutant-induced damage. The coordinated nature of these protective mechanisms—spanning mucosal defense, barrier function, metabolic homeostasis, and inflammation

10.3389/fmicb.2025.1626941

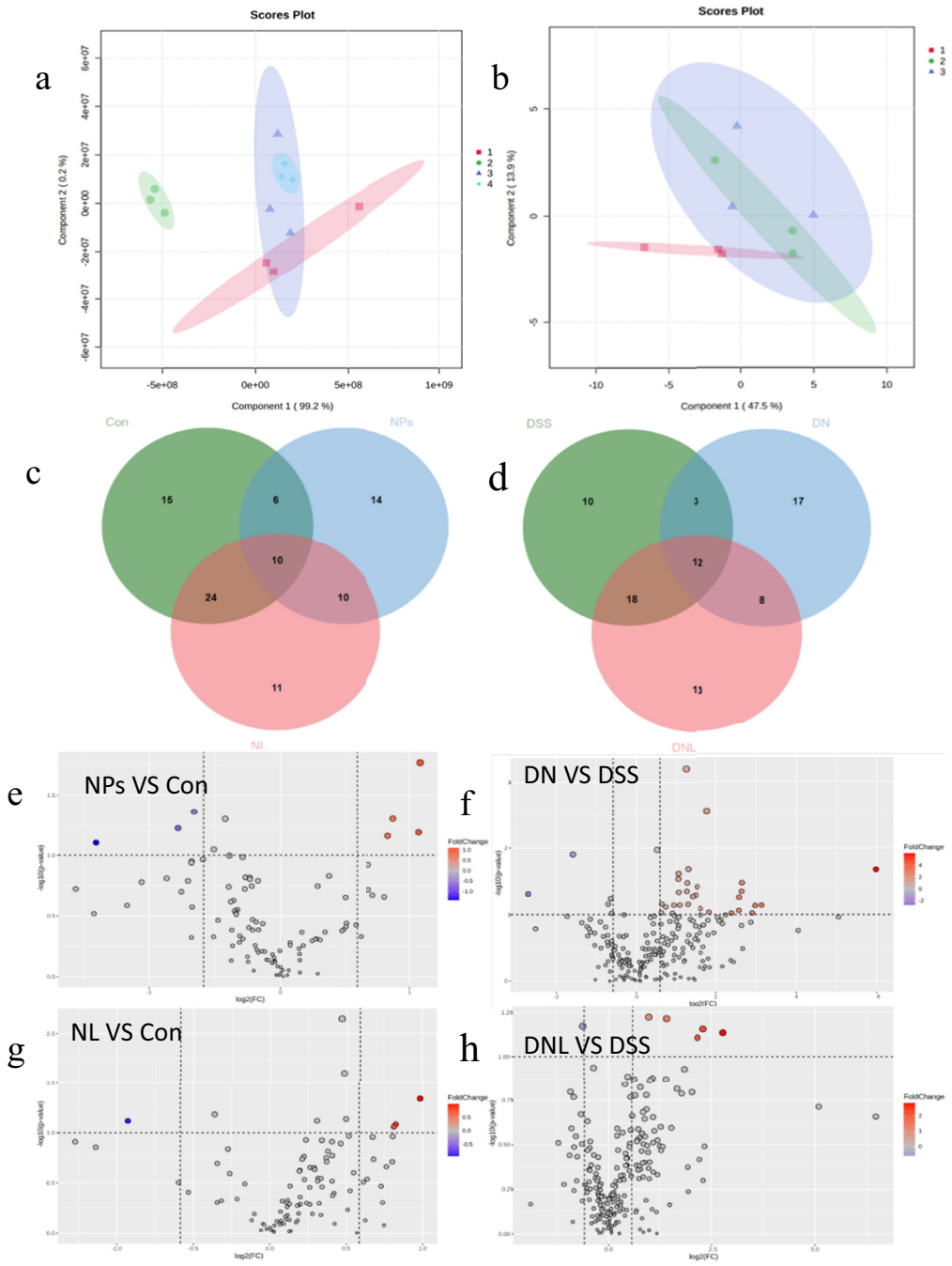

FIGURE 7
Analysis of mice liver metabolic profile. **(a,b)** Analysis of PLS-DA. **(a)** Healthy mice: 1-Con; 2-LP; 3-NL; 4-NPs. **(b)** Enteritis mice: 1-DSS; 2-DN; 3-DNL. **(c,d)** Venn diagram. **(c)** Healthy mice. **(d)** Colitis Mice. **(e–h)** Volcano plot of significantly different metabolite changes in mice liver. Con—control group; LP—*L. plantarum* group; NPs—nanoplastic group; NL—nanoplastic + *L. plantarum* group; DSS—acute colitis group; DN—colitis + nanoplastic group; DNL—colitis + nanoplastic + *L. plantarum* group.

control—underscores the unique capacity of specific probiotic strains to address complex toxicological challenges through microbiome-host crosstalk.

4 Discussion

The mechanisms underlying the hazards of NPs to biological systems are becoming increasingly elucidated. This study, utilizing a 5-week oral exposure protocol, confirmed that 100 nm PS-NPs penetrate the intestinal barrier of mice, enter the systemic circulation, and accumulate primarily in the liver and colon. This observation is highly consistent with the rapid entry into the bloodstream and organ distribution patterns of NPs reported by Im et al. (2022). Accumulated PS-NPs within the organism induced multi-organ damage: manifested as hepatocellular hypertrophy in the liver, mirroring the classic pathological feature of hepatocyte edema caused by MPs in previous studies (Zheng et al., 2021); accompanied by inflammatory cell

10.3389/fmicb.2025.1626941

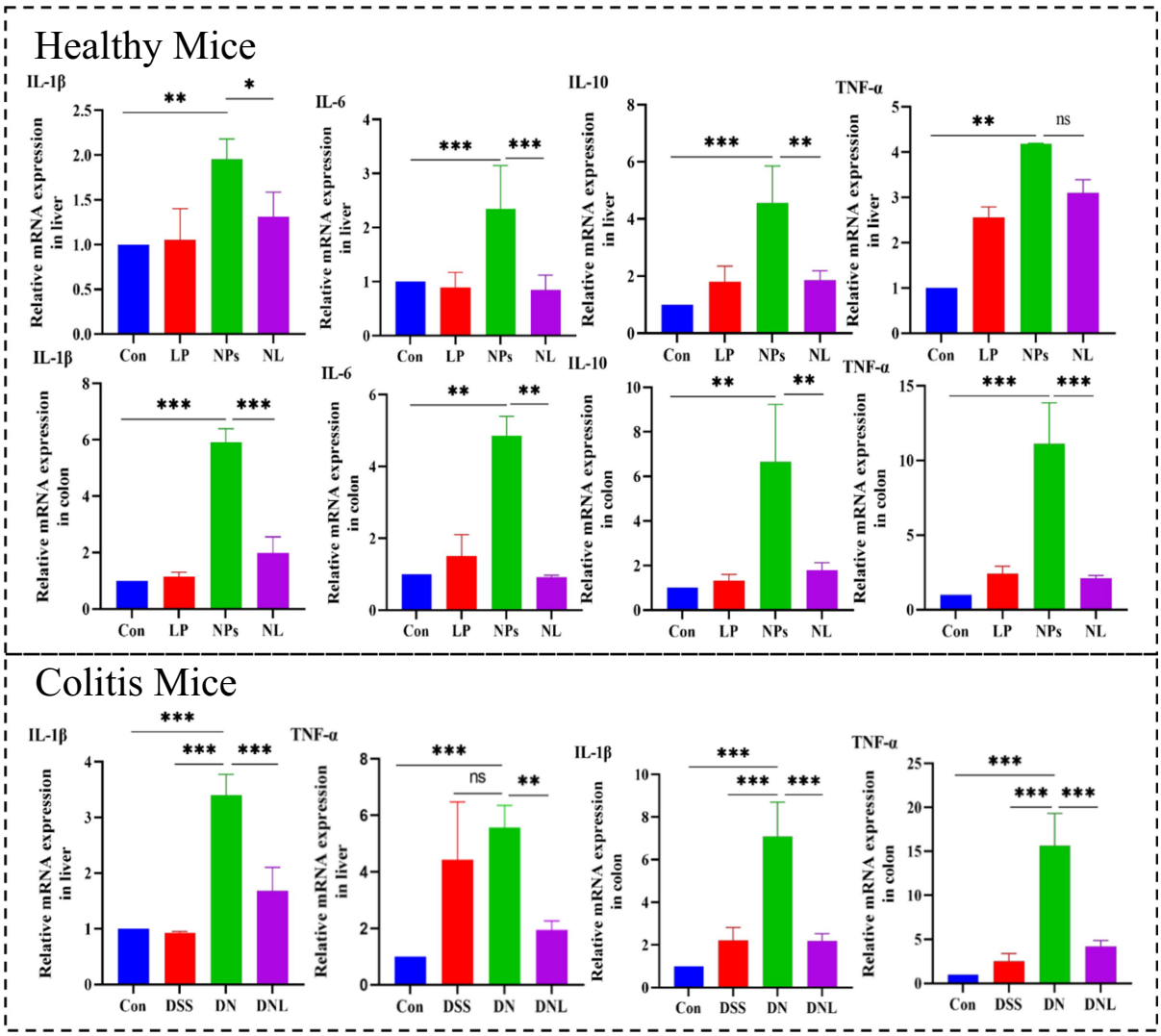

FIGURE 8
Expression of inflammatory factors in mouse liver and colon. Con—control group; LP—*L. plantarum* group; NPs—nanoplastic group; NL—nanoplastic + *L. plantarum* group; DSS—acute colitis group; DN—colitis + nanoplastic group; DNL—colitis + nanoplastic + *L. plantarum* group; ns express $p > 0.05$, *express $p < 0.05$, **express $p < 0.01$, ***express $p < 0.001$, $n = 5$.

infiltration in the kidney, aligning with descriptions of NPs-induced renal tubular necrosis in the study by Meng et al. (2023); and mechanical damage to the intestinal epithelium due to NPs aggregation and physical compression, paralleling the intestinal epithelial injury observed following NPs exposure in the study by Li et al. (2021). These pathological alterations were concomitant with a significant upregulation ($p < 0.05$) of pro-inflammatory cytokines *IL-1β*, *TNF-α*, and *IL-6*, establishing a systemic inflammatory cascade response. This reinforces the critical importance of pro-inflammatory cytokines as biomarkers for NPs exposure (Yu et al., 2018). Notably, the alterations in kidney coefficient and colon shortening identified in this study were not observed in the 28-day short-term exposure conducted by Xu et al. (2021). This discrepancy suggests that prolonged exposure (5 weeks) may trigger progressive, organ-specific damage, highlighting a significant concern for assessing the risks associated with chronic NPs exposure in humans.

Under pathological conditions, the toxicity of NPs exhibited a markedly amplified effect. When mice were in a state of DSS-induced colitis, PS-NPs exposure resulted in exacerbated hepatosplenomegaly, a significant increase in systemic NPs accumulation (approximately 3-fold higher than in healthy exposed mice), and a surge in the inflammatory cytokine *IL-1β* to levels approximately twice those observed in the healthy exposure group. This finding directly corroborates reports by Zheng et al. (2021) on NPs-aggravated hepatic injury in colitis and Luo et al. (2022) on NPs-promoted increases in intestinal permeability, collectively confirming that individuals with intestinal inflammation face a substantially heightened health threat from NPs.

To counteract these toxic effects, this study is the first to reveal that *L. plantarum* ZP-6 achieves potent intervention through multifaceted synergistic mechanisms. Firstly, *L. plantarum* ZP-6 effectively reduces systemic NPs accumulation via a bioadsorption-excretion pathway. ZP-6 facilitates the fecal excretion of adsorbed PS-NPs, leading to a 60–80% reduction ($p < 0.01$) in NPs burden within the liver. This mode of action is analogous to the mechanism reported by Chen et al. (2022), where lactic acid bacteria strains

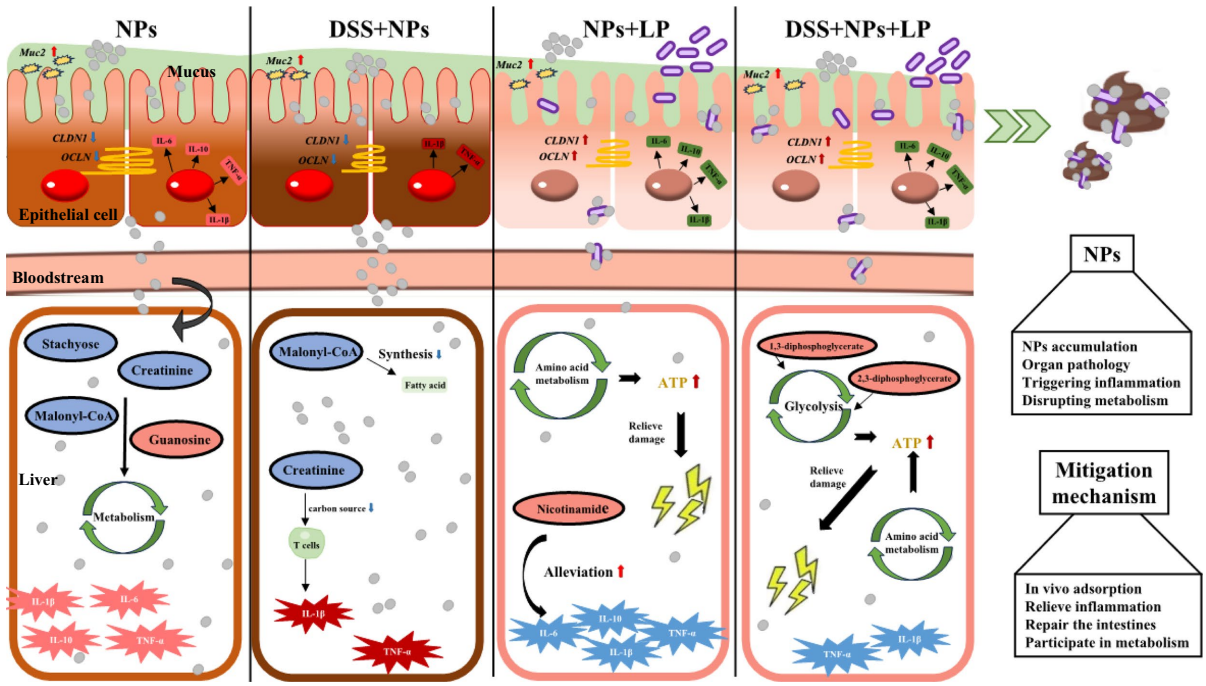

FIGURE 9
Liver damage induced by nanoplastics in mice with inflammatory bowel disease via the gut-liver axis and the alleviating effect of *L. plantarum* ZP-6. LP—*L. plantarum* group; NPs—nanoplastic group; NL—nanoplastic + *L. plantarum* group; DSS—acute colitis group; DN—colitis + nanoplastic group; DNL—colitis + nanoplastic + *L. plantarum* group.

mitigate perfluorooctanesulfonic acid toxicity by promoting its excretion through bio-conjugation. Secondly, *L. plantarum* ZP-6 alleviates nanoplastic toxicity through an anti-inflammatory and barrier-repair pathway. It significantly suppressed the expression of hepatic pro-inflammatory cytokines (reducing *IL-1β* and *TNF-α* by 50–70%, $p < 0.01$), thereby disrupting the vicious cycle of inflammation, a finding consistent with the reported alleviation of intestinal and hepatic inflammation by *L. plantarum* in Zan et al. (2023). Furthermore, *L. plantarum* ZP-6 restored intestinal tight junction proteins, effectively reversing the PS-NPs-induced increase in intestinal permeability. This protective mechanism, akin to the restoration of ZO-1 protein and barrier integrity by *Lactobacillus casei* (Wu et al., 2024), successfully prevented secondary liver injury triggered by endotoxin translocation into the bloodstream (Denker and Nigam, 1998). Finally, at the metabolic level, *L. plantarum* ZP-6 demonstrated a corrective efficacy surpassing previous understanding. PS-NPs exposure profoundly disrupted hepatic metabolism in mice, including dysregulation of nucleotide metabolism (e.g., aberrant elevation of guanosine and significant reduction of inosine), imbalance in amino acid metabolism (e.g., accumulation of leucine/methionine), and impairment of fatty acid synthesis (e.g., decreased malonyl-CoA). These perturbations align with studies in zebrafish models showing PS-NPs interference with metabolic pathways (Liu et al., 2023; Limonta et al., 2019) and reports of NPs-induced metabolic dysregulation in mammals (Zheng et al., 2021). The unique value of *L. plantarum* ZP-6 lies in its ability to: upregulate the anti-inflammatory metabolite nicotinamide, known for its DNA repair functions (Mierzejewska et al., 2018); activate the glycolytic pathway (evidenced by significant increases in 1,3-bisphosphoglycerate), counteracting the energy depletion caused by NPs (Jiang et al., 2022); and reduce the number of significantly altered metabolites in colitic mice by 82%, effectively restoring the hepatic metabolic profile towards near-normal levels. This multi-targeted metabolic remodeling capability represents a more comprehensive homeostatic regulatory advantage compared to previous research on *L. plantarum* FRT10, which focused primarily on modulating amino acid or bile acid metabolism (Cai et al., 2022).

In conclusion, this study not only deepens the understanding of the toxicity associated with long-term exposure to small-sized PS-NPs (particularly the amplified risk in inflammatory bowel states) but also provides an innovative biological intervention strategy against nanoplastic pollution through the tripartite mechanism—"adsorption-excretion," "anti-inflammatory repair," and "metabolic remodeling"—exhibited by *L. plantarum* ZP-6. Compared to the singular toxin-adsorption function traditionally attributed to lactic acid bacteria (Chen et al., 2022), the multi-pathway synergy and metabolic corrective capacity of *L. plantarum* ZP-6 signify a crucial advancement in probiotic-based protective strategies.

5 Conclusion

This study demonstrates that exposure to PS-NPs exacerbates colonic and hepatic pathology in a murine colitis model, primarily mediated via the gut-liver axis. Crucially, *L. plantarum* ZP-6 was found to confer significant protection against PS-NP toxicity through a multi-targeted mechanism. The key findings reveal that ZP-6: (1) effectively sequesters PS-NPs directly, reducing systemic absorption and promoting fecal excretion; (2) modulates immune responses by significantly downregulating pro-inflammatory cytokines in both

colon and liver, thereby restoring intestinal immune homeostasis, and interrupting the inflammation-fibrosis cycle; (3) strengthens the intestinal barrier through upregulation of key tight junction proteins, leading to substantial restoration of barrier integrity, reduced PS-NPs translocation; and (4) restores metabolic homeostasis. Collectively, this study offers a promising probiotic-based therapeutic strategy for mitigating nanoplastic risks in vulnerable populations (e.g., IBD patients). It identifies sensitive biomarkers for nanoplastic exposure assessment. Most importantly, it underscores the critical environmental health implication that pre-existing inflammation significantly amplifies nanoplastic toxicity, demanding urgent attention. While this study delineates compelling protective mechanisms for ZP-6, the findings are based on a mouse model of chemically-induced colitis, extrapolation to human IBD or other inflammatory conditions requires further validation. Future research should focus on conducting longitudinal studies to assess impacts on gut microbiome ecology and long-term health outcomes; and validating these findings in human-relevant models or cohorts.

Data availability statement

The original contributions presented in the study are included in the article/supplementary material, further inquiries can be directed to the corresponding authors.

Ethics statement

All animal experiments were approved by the Henan Normal University Institutional Ethics Committee (Approval No. 2025BS-0425) and conducted in accordance with institutional guidelines and local regulations governing animal welfare and ethical use.

Author contributions

LZ: Conceptualization, Data curation, Formal analysis, Funding acquisition, Investigation, Methodology, Project administration, Supervision, Writing – original draft, Writing – review & editing. ZW: Validation, Writing – original draft. YW: Visualization, Writing – original draft. WC: Conceptualization, Investigation, Methodology, Writing – original draft. WZ: Resources, Writing – original draft. MX: Conceptualization, Writing – original draft. HC: Methodology, Writing – original draft. YZ: Methodology, Writing – original draft. HG: Funding acquisition, Writing – original draft. XJ: Project administration, Writing – original draft.

Funding

The author(s) declare that financial support was received for the research and/or publication of this article. This study was financially supported jointly by the Major Project of Henan Science and Technology Research and Development Joint Fund (245101610008); the Key Scientific Research Project of University in Henan Province (24A550013); the Technology Development Project of Beijing Hongkang Heji Medical Equipment Co., Ltd. (H2024052); the Henan Province project of "Vice President of Science and Technology" (T202421).

Conflict of interest

The authors declare that the research was conducted in the absence of any commercial or financial relationships that could be construed as a potential conflict of interest.

Generative AI statement

The authors declare that no Gen AI was used in the creation of this manuscript.

Publisher's note

All claims expressed in this article are solely those of the authors and do not necessarily represent those of their affiliated organizations, or those of the publisher, the editors and the reviewers. Any product that may be evaluated in this article, or claim that may be made by its manufacturer, is not guaranteed or endorsed by the publisher.

References

Allaire, J. M., Crowley, S. M., Law, H. T., Chang, S. Y., Ko, H. J., and Vallance, B. A. (2018). The intestinal epithelium: central coordinator of mucosal immunity. *Trends Immunol.* 39, 677–696. doi: 10.1016/j.it.2018.04.002

Brandts, I., Barría, C., Martins, M. A., Franco-Martínez, L., Barreto, A., Tvarijonaviciute, A., et al. (2021). Waterborne exposure of gilthead seabream (*Sparus aurata*) to polymethylmethacrylate nanoplastics causes effects at cellular and molecular levels. *J. Hazard. Mater.* 403:123590. doi: 10.1016/j.jhazmat.2020.123590

Cai, H., Li, D., Song, L., Xu, X., Han, Y., Meng, K., et al. (2022). Metabolomic characteristics of liver and cecum contents in high-fat-diet induced obese mice intervened with *Lactobacillus plantarum* FRT10. *Foods* 11:2491. doi: 10.3390/foods11162491

Chen, Q., Sun, S., Mei, C., Zhao, J., Zhang, H., Wang, G., et al. (2022). Capabilities of bio-binding, antioxidant and intestinal environmental repair jointly determine the ability of lactic acid bacteria to mitigate perfluorooctane sulfonate toxicity. *Environ. Int.* 166:107388. doi: 10.1016/j.envint.2022.107388

Deng, Y., Zhang, Y., Lemos, B., and Ren, H. (2017). Tissue accumulation of microplastics in mice and biomarker responses suggest widespread health risks of exposure. *Sci. Rep.* 7:46687. doi: 10.1038/srep46687

Denker, B. M., and Nigam, S. K. (1998). Molecular structure and assembly of the tight junction. *Am. J. Phys.* 274, F1–F9. doi: 10.1152/ajprenal.1998.274.1.F1

Duan, H., Yu, L., Tian, F., Zhai, Q., Fan, L., and Chen, W. (2020). Gut microbiota: a target for heavy metal toxicity and a probiotic protective strategy. *Sci. Total Environ.* 742:140429. doi: 10.1016/j.scitotenv.2020.140429

Fu, Q., Lai, J.-L., Ji, X.-H., Luo, Z. X., Wu, G., and Luo, X. G. (2022). Alterations of the rhizosphere soil microbial community composition and metabolite profiles of *Zea mays* by polyethylene-particles of different molecular weights. *J. Hazard. Mater.* 423:127062. doi: 10.1016/j.jhazmat.2021.127062

Gonzalez-Fernandez, C., Diaz Banos, F. G., Angeles Esteban, M., Esteban, M. Á., and Cuesta, A. (2021). Functionalized nanoplastics (NPs) increase the toxicity of metals in fish cell lines. *Int. J. Mol. Sci.* 22:7141. doi: 10.3390/ijms22137141

Hirt, N., and Body-Malapel, M. (2020). Immunotoxicity and intestinal effects of nano- and microplastics: a review of the literature. *Part. Fibre Toxicol.* 17:57. doi: 10.1186/s12989-020-00387-7

Im, C., Kim, H., Zaheer, J., Kim, J. Y., Lee, Y. J., Kang, C. M., et al. (2022). PET tracing of biodistribution for orally administered ^{64}Cu-labeled polystyrene in mice. *J. Nucl. Med.* 63, 461–467. doi: 10.2967/jnumed.120.256982

Jiang, Q., Chen, X., Jiang, H., Wang, M., Zhang, T., and Zhang, W. (2022). Effects of acute exposure to polystyrene nanoplastics on the channel catfish larvae: insights from energy metabolism and transcriptomic analysis. *Front. Physiol.* 13:923278. doi: 10.3389/fphys.2022.923278

Jin, Y., Lu, L., Tu, W., Luo, T., and Fu, Z. (2019). Impacts of polystyrene microplastic on the gut barrier, microbiota and metabolism of mice. *Sci. Total Environ.* 649, 308–317. doi: 10.1016/j.scitotenv.2018.08.353

Kim, D. H., Kim, S., Ahn, J. B., Kim, J. H., Ma, H. W., Seo, D. H., et al. (2020). *Lactobacillus plantarum* CBT LP3 ameliorates colitis via modulating T cells in mice. *Int. J. Med. Microbiol.* 310:151391. doi: 10.1016/j.ijmm.2020.151391

Lai, W., Xu, D., Li, J., Wang, Z., Ding, Y., Wang, X., et al. (2021). Dietary polystyrene nanoplastics exposure alters liver lipid metabolism and muscle nutritional quality in carnivorous marine fish large yellow croaker (*Larimichthys crocea*). *J. Hazard. Mater.* 419:126454. doi: 10.1016/j.jhazmat.2021.126454

Li, Z., Feng, C., Pang, W., Tian, C., and Zhao, Y. (2021). Nanoplastic-induced genotoxicity and intestinal damage in freshwater benthic clams (*Corbicula fluminea*): comparison with microplastics. *ACS Nano* 15, 9469–9481. doi: 10.1021/acsnano.1c02407

Li, L., Gu, H., Chang, X., Huang, W., Sokolova, I. M., Wei, S., et al. (2021). Oxidative stress induced by nanoplastics in the liver of juvenile large yellow croaker *Larimichthys crocea*. *Mar. Pollut. Bull.* 170:112661. doi: 10.1016/j.marpolbul.2021.112661

Limonta, G., Mancia, A., Benkhalqui, A., Bertolucci, C., Abelli, L., Fossi, M. C., et al. (2019). Microplastics induce transcriptional changes, immune response and behavioral alterations in adult zebrafish. *Sci. Rep.* 9:15775. doi: 10.1038/s41598-019-52292-5

Lin, X., Yu, Z., Liu, Y., Li, C., Hu, H., Hu, J. C., et al. (2025). Gut-X axis. *iMeta* 4:e270. doi: 10.1002/imt2.270

Liu, H., Zhou, W., Zhou, Z., Yu, C., Tye, G. J., Lv, W., et al. (2023). Effects of polystyrene nanoplastic exposure on energy metabolism, lipid metabolism, and amino acid changes in *Monopterus albus*. *Front. Mar. Sci.* 10:1285427. doi: 10.3389/fmars.2023.1285427

Lu, Y., Zhang, Y., Deng, Y., Jiang, W., Zhao, Y., Geng, J., et al. (2016). Response to comment on "uptake and accumulation of polystyrene microplastics in zebrafish (*Danio rerio*) and toxic effects in liver". *Environ. Sci. Technol.* 50, 12523–12524. doi: 10.1021/acs.est.6b04379

Luo, T., Wang, D., Zhao, Y., Li, X., Yang, G., and Jin, Y. (2022). Polystyrene microplastics exacerbate experimental colitis in mice tightly associated with the occurrence of hepatic inflammation. *Sci. Total Environ.* 844:156884. doi: 10.1016/j.scitotenv.2022.156884

Meng, X., Ge, L., Zhang, J., Xue, J., Gonzalez-Gil, G., Vrouwenvelder, J. S., et al. (2023). Systemic effects of nanoplastics on multi-organ at the environmentally relevant dose: the insights in physiological, histological, and oxidative damages. *Sci. Total Environ.* 892:164687. doi: 10.1016/j.scitotenv.2023.164687

Mierzejewska, P., Gawlik-Jakubczak, T., Jablonska, P., Czajkowski, M., Kutryb-Zajac, B., Smolenski, R. T., et al. (2018). Nicotinamide metabolism alterations in bladder cancer: preliminary studies. *Nucleosides Nucleotides Nucleic Acids* 37, 687–695. doi: 10.1080/15257770.2018.1535124

Mishima, Y., Oka, A., Liu, B., Herzog, J. W., Eun, C. S., Fan, T. J., et al. (2019). Microbiota maintain colonic homeostasis by activating TLR2/MyD88/PI3K signaling in IL-10-producing regulatory B cells. *J. Clin. Invest.* 129, 3702–3716. doi: 10.1172/JCI93820

Mitrano, D. M., Wick, P., and Nowack, B. (2021). Placing nanoplastics in the context of global plastic pollution. *Nat. Nanotechnol.* 16, 491–500. doi: 10.1038/s41565-021-00888-2

Mohd Redzwan, S., Abd Mutalib, M. S., Wang, J. S., Ahmad, Z., Kang, M.-S., Abdul Rahman, N., et al. (2016). Effect of supplementation of fermented milk drink containing probiotic *Lactobacillus casei* Shirota on the concentrations of aflatoxin biomarkers among employees of Universiti Putra Malaysia: a randomised, double-blind, cross-over, placebo-controlled study. *Br. J. Nutr.* 115, 39–54. doi: 10.1017/S0007114515004109

Molodecky, N. A., Soon, I. S., Rabi, D. M., Ghali, W. A., Ferris, M., Chernoff, G., et al. (2012). Increasing incidence and prevalence of the inflammatory bowel diseases with time, based on systematic review. *Gastroenterology* 142, 46–54. doi: 10.1053/j.gastro.2011.10.001

Nordström, E. A., Teixeira, C., Montelius, C., Jeppsson, B., and Larsson, N. (2021). *Lactiplantibacillus plantarum* 299v (LP299V®): three decades of research. *Benef. Microbes* 12, 441–465. doi: 10.3920/BM2020.0191

Pironti, C., Ricciardi, M., Motta, O., Miele, Y., Proto, A., and Montano, L. (2021). Microplastics in the environment: intake through the food web, human exposure and toxicological effects. *Toxics* 9:224. doi: 10.3390/toxics9090224

Sandys, O., and Te Velde, A. (2022). Raising the alarm: environmental factors in the onset and maintenance of chronic (low-grade) inflammation in the gastrointestinal tract. *Dig. Dis. Sci.* 67, 4355–4368. doi: 10.1007/s10620-021-07327-1

Schwabl, P., Koeppel, S., Koenigshofer, P., Bucsics, T., Trauner, M., Reiberger, T., et al. (2019). Detection of various microplastics in human stool a prospective case series. *Ann. Intern. Med.* 171, 453–460. doi: 10.7326/M19-0618

Tanaka, A., Kanmura, S., Morinaga, Y., Kawabata, K., Arima, S., Sasaki, F., et al. (2020). Oral administration of *Lactobacillus plantarum* 06CC2 prevents experimental colitis in mice via an anti-inflammatory response. *Mol. Med. Rep.* 21, 1181–1191. doi: 10.3892/mmr.2020.10925

Tong, M., Li, X., Parfrey, L. W., Wegener Parfrey, L., Roth, B., Ippoliti, A., et al. (2013). A modular organization of the human intestinal mucosal microbiota and its association with inflammatory bowel disease. *PLoS One* 8:e80702. doi: 10.1371/journal.pone.0080702

Wu, Y., Zhang, X., Liu, X., Li, Y., Han, D., Pi, Y., et al. (2024). Strain specificity of lactobacilli with promoted colonization by galactooligosaccharides administration in protecting intestinal barriers during Salmonella infection. *J. Adv. Res.* 56, 1–14. doi: 10.1016/j.jare.2023.03.001

Xu, D., Ma, Y., Han, X., and Chen, Y. (2021). Systematic toxicity evaluation of polystyrene nanoplastics on mice and molecular mechanism investigation about their internalization into Caco-2 cells. *J. Hazard. Mater.* 417:126092. doi: 10.1016/j.jhazmat.2021.126092

Yan, Z., Liu, Y., Zhang, T., Zhang, F., Ren, H., and Zhang, Y. (2022). Response to comment on "analysis of microplastics in human feces reveals a correlation between fecal microplastics and inflammatory bowel disease status". *Environ. Sci. Technol.* 56, 12779–12780. doi: 10.1021/acs.est.2c05327

Yu, P., Liu, Z., Wu, D., Chen, M., Lv, W., and Zhao, Y. (2018). Accumulation of polystyrene microplastics in juvenile *Eriocheir sinensis* and oxidative stress effects in the liver. *Aquat. Toxicol.* 200, 28–36. doi: 10.1016/j.aquatox.2018.04.015

Zan, L., Zhang, W., Shang, S., Cui, Y., Pei, J., Yuan, Y., et al. (2023). Alleviating effect of selenium-enriched *Lactobacillus plantarum* 6076 on dextran sulfate sodium-induced colitis and liver inflammation in mice. *Food Funct.* 14, 10151–10162. doi: 10.1039/D3FO03842D

Zhai, Q., Wang, G., Zhao, J., Liu, X., Tian, F., Zhang, H., et al. (2013). Protective effects of *Lactobacillus plantarum* CCFM8610 against acute cadmium toxicity in mice. *Appl. Environ. Microbiol.* 79, 1508–1515. doi: 10.1128/AEM.03417-12

Zhao, L., Zhang, H., White, J. C., Chen, X., Li, H., Qu, X., et al. (2019). Metabolomics reveals that engineered nanomaterial exposure in soil alters both soil rhizosphere metabolite profiles and maize metabolic pathways. *Environ. Sci.: Nano* 6, 1716–1727. doi: 10.1039/C9EN00137A

Zheng, H., Wang, J., Wei, X., Chang, L., and Liu, S. (2021). Proinflammatory properties and lipid disturbance of polystyrene microplastics in the livers of mice with acute colitis. *Sci. Total Environ.* 750:143085. doi: 10.1016/j.scitotenv.2020.143085

frontiers | Frontiers in Microbiology

TYPE Review
PUBLISHED 24 September 2025
DOI 10.3389/fmicb.2025.1602258

Check for updates

OPEN ACCESS

EDITED BY
Mohammad Altamimi,
An-Najah National University, Palestine

REVIEWED BY
Samiullah Khan,
Guizhou University, China
Carlos I. Arbizu,
Universidad Nacional Toribio Rodríguez de Mendoza de Amazonas, Peru
Atif Khurshid Wani,
Lovely Professional University, India

*CORRESPONDENCE
Zhenwei Zhang
✉ qingyibushuo@163.com
Changfa Wang
✉ wangcf1967@163.com
Muhammad Zahoor Khan
✉ zahoorkhattak91@yahoo.com

RECEIVED 29 March 2025
ACCEPTED 08 September 2025
PUBLISHED 24 September 2025

CITATION
Li F, Kong X, Khan MZ, Wei L, Wei J, Zhu M, Liu G, Huang B, Wang C and Zhang Z (2025) Gut microbiome regulation in equine animals: current understanding and future perspectives.
Front. Microbiol. 16:1602258.
doi: 10.3389/fmicb.2025.1602258

COPYRIGHT
© 2025 Li, Kong, Khan, Wei, Wei, Zhu, Liu, Huang, Wang and Zhang. This is an open-access article distributed under the terms of the Creative Commons Attribution License (CC BY). The use, distribution or reproduction in other forums is permitted, provided the original author(s) and the copyright owner(s) are credited and that the original publication in this journal is cited, in accordance with accepted academic practice. No use, distribution or reproduction is permitted which does not comply with these terms.

Gut microbiome regulation in equine animals: current understanding and future perspectives

Fenglin Li[1], Xiangyu Kong[1], Muhammad Zahoor Khan[1]*, Lin Wei[1], Jinjin Wei[1], Mingxia Zhu[1], Guiqin Liu[1], Bingjian Huang[2], Changfa Wang[1]* and Zhenwei Zhang[1]*

[1]Liaocheng Research Institute of Donkey High-Efficiency Breeding and Ecological Feeding, College of Agriculture and Biology, Liaocheng University, Liaocheng, China, [2]State Key Laboratory of Animal Nutrition, College of Animal Science and Technology, China Agricultural University, Beijing, China

The equine intestinal microbiome represents a complex and dynamic ecosystem that fundamentally influences host health and physiological function. This microbial community exhibits distinct compositional and functional variations across different anatomical segments of the intestinal tract, with diversity and abundance patterns shaped by host genetics, dietary inputs, and environmental conditions. The resident microbiota performs essential functions in feed fermentation, nutrient metabolism, pathogen exclusion, and immunological programming. This review synthesizes current knowledge regarding the core taxonomic and functional attributes of the equine intestinal microbiome, examining interspecies variation and conservation patterns. We evaluate key determinants of microbial community assembly and regulation, while examining mechanistic links between microbiota composition and host health outcomes. Through critical analysis of existing literature, this work provides an integrated framework for understanding the equine gut microbiome, with implications for clinical intervention strategies and evidence-based approaches to promote intestinal health in equine.

KEYWORDS

equine, microbial community, metabolism, health, production

1 Introduction

Unlike ruminants, equines use cecal fermentation—a microbial system similar to the rumen that aids digestion, strengthening the intestinal protective barrier and immune (Wunderlich et al., 2023; Zhang et al., 2022a; Kou et al., 2024a; Dicks et al., 2014). The equine gastrointestinal tract represents a complex microecological environment populated by diverse communities of anaerobic bacteria, fungi, parasites, and viruses that collectively enable efficient degradation of low-quality fibrous substrates, thereby providing substantial energy to the host (Raspa et al., 2024; Wunderlich et al., 2023; Liu et al., 2019). The intestinal microbiota serves critical functions beyond nutrient processing, acting as a fundamental determinant of host health through disease prevention and immunomodulatory mechanisms (Sävilammi et al., 2024; Ma et al., 2023; Mach et al., 2022). Initial microbial colonization commences perinatally through vertical transmission via the birth canal, with subsequent community development influenced by maternal contact and environmental exposure (Zhang et al., 2023; Barko et al., 2018).

Consistent with patterns observed across mammalian taxa, the establishment of a diverse and stable gut microbiota is essential for optimal digestive efficiency, nutrient bioavailability,

immune system maturation, and metabolic homeostasis throughout equine development (Xing et al., 2025; Matsuki et al., 2016; Mueller et al., 2015). Contemporary research has elucidated distinct microbial signatures across anatomical compartments of the equine digestive tract (Lan et al., 2025; Wang et al., 2025a, 2025b; Reed et al., 2021). The gastrointestinal system is functionally divided into upper and lower regions, with the foregut (stomach and small intestine) exhibiting greater microbial variability due to the substantial influx of environmental bacteria through dietary intake (Kauter et al., 2019). Microbial community composition demonstrates significant responsiveness to environmental factors and host physiological status (Khan et al., 2025), reflecting the dynamic and symbiotic nature of host–microbe interactions that maintain intestinal homeostasis and systemic health (Ang et al., 2022).

Host-microbe crosstalk is mediated primarily through microbial metabolite production. Intestinal microorganisms catabolize dietary substrates and endogenous compounds to generate bioactive metabolites, including short-chain fatty acids (SCFAs) and phytoestrogens. In equines, microbial fermentation in the cecum and colon contributes approximately 30–40% of total energy requirements through SCFA production (Garber et al., 2020), underscoring the metabolic significance of these compounds for cardiovascular and systemic health (Mach et al., 2022). Additionally, the microbiota orchestrates immune homeostasis by preserving mucosal barrier integrity, promoting immune cell differentiation and activation, and maintaining colonization resistance against pathogenic microorganisms through competitive exclusion and antimicrobial compound synthesis, thereby sustaining microbial equilibrium and preventing disease manifestation.

The intestinal microbiota plays a pivotal role in equine health; however, its composition and functional capacity are significantly modulated by multiple intrinsic and extrinsic factors, including breed characteristics, reproductive status (pregnancy and lactation stage), dietary composition, age, anatomical location within the gastrointestinal tract, and environmental conditions (Qin et al., 2025; Su et al., 2024; Xing et al., 2025; Sha et al., 2024; Zhou et al., 2023a, 2023b; Li et al., 2022a; Zhao et al., 2020). The advent of high-throughput sequencing technologies has revolutionized equine gut microbiome research, enabling increasingly sophisticated analytical approaches. Current methodologies primarily employ 16S rRNA gene amplicon sequencing and shotgun metagenomics, with universal primers targeting conserved regions of the rRNA gene followed by sequencing of internal transcribed spacer regions, techniques extensively validated in fungal taxonomic studies (Zhang et al., 2022b). Recent advances in computational binning algorithms have facilitated the reconstruction of metagenome-assembled genomes (MAGs) from metagenomic datasets, substantially expanding the reference genome repository for mammalian intestinal microorganisms (Kou et al., 2024b). Despite these technological advances, significant knowledge gaps remain regarding the core microbiota of equine species and their functional significance in host physiology.

This review synthesizes current understanding of the fundamental intestinal microorganisms in equine species, elucidates their functional roles, and examines the impact of various intervention strategies on microbial community structure and function. The comprehensive analysis presented herein provides a foundation for developing targeted approaches to optimize microbial-mediated feed utilization efficiency and enhance disease resistance in equine populations.

2 Literature search methodology

A comprehensive literature review was conducted to examine gut microbiome regulation in equine animals using multiple electronic databases, including Google Scholar, PubMed, XMOL, and Web of Science, to ensure comprehensive coverage of relevant publications. The following keywords and search terms were employed in various combinations: "equine gut microbes," "horses," "donkeys," "ruminants," "microbiota effect on equine health and production," "gut microbiota composition," and "factors affecting gut microbiota." Only peer-reviewed articles published in English-language SCI journals were included in this review, focusing specifically on studies examining equine gut microbiome and related health outcomes. Publications in languages other than English, book chapters, conference papers, theses, dissertations, and unpublished data were systematically excluded from the analysis. This systematic approach ensured that only high-quality, peer-reviewed research was included in the review, providing a robust foundation for analysis and synthesis of current knowledge regarding equine gut microbiome regulation.

3 Core microbiota of equine animals

The core microbiota of the equine intestinal tract comprises microbial species that dominate the gut microbial community and significantly influence the health and physiology of equine animals. These microorganisms are characterized by their functional versatility and adaptability, enabling their persistent presence and vital role in the host's digestive system. They contribute to nutrient metabolism, immune modulation, and the maintenance of intestinal homeostasis. However, the specific composition of the core microbiota is not uniform and may vary due to factors such as individual genetic differences, environmental conditions, and dietary practices (Costa and Weese, 2012). Understanding these variations is essential for developing tailored nutritional and management strategies to optimize the health and performance of equine animals. For ease of reference, the comparative abundance of gut microbiota in donkeys and horses has been presented in Table 1 and Figure 1, which are sourced from previously published articles (Liu, 2020; Su et al., 2020; Zhang et al., 2020; Liu et al., 2019).

The intestinal tracts of horses and donkeys are predominantly colonized by two major bacterial phyla: *Firmicutes* and *Bacteroidetes*, which collectively constitute the majority of the microbial community (Zhang et al., 2022c). Notably, Liu (2020) demonstrated significant interspecies variations in the relative abundance of these dominant phyla, reporting that *Firmicutes* and *Bacteroidetes* account for 87.91 and 78.50% of the total microbial population in donkeys and horses, respectively. Furthermore, the ratio of *Firmicutes* to *Bacteroidetes* differs markedly between these species. In donkeys, this ratio approximates 1:1, whereas in horses, it is approximately 0.8:1. These proportional differences are of particular significance, as they are believed to influence the host's capacity for energy extraction from dietary sources and may consequently be associated with metabolic conditions such as obesity. Specifically, an elevated proportion of

10.3389/fmicb.2025.1602258

TABLE 1 Comparison of relative richness (>1%) in the intestinal microbiota of horses and donkeys.

Intestinal area	Jejunum		Ileum		Cecum		Dorsal colon		Abdominal colon		Rectum (feces)	
	Donkey	Horse	Donkey	Horse	Donkey	Horse	Donkey	Horse	Donkey	Horse	Donkey	Horse
Firmicutes	50.3% ~ 85.6%	67.3% ~ 79.3%	60.3% ~ 81.8%	73.5% ~ 78.8%	38.3% ~ 45.0%	38.6% ~ 40.5%	43.2% ~ 56.8%	45.3% ~ 47.6%	45.6% ~ 62.6%	48.1% ~ 54.2%	54.5% ~ 56.1%	50.3% ~ 69.0%
Bacteroidetes phylum	1.0% ~ 9.4%	0.7% ~ 3.7%	<1%	0.7% ~ 1.8%	41.7% ~ 48.6%	45.7% ~ 47.5%	33.6% ~ 42.0%	42.7% ~ 43.4%	31.1% ~ 37.4%	33.5% ~ 36.9%	33.4% ~ 34.2%	5.9% ~ 15.29%
Proteobacteria	11.5% ~ 12.4%	14.1% ~ 15.6%	9.4% ~ 16.2%	17.3% ~ 17.5%	3.1% ~ 4.6%	0.5% ~ 1.7%	3.3% ~ 4.6%	0.3% ~ 1.1%	0.9% ~ 1.7%	0.4% ~ 1.6%	3.4% ~ 4.2%	1.1% ~ 2.82%
Actinobacteria	0.8% ~ 1.7%	0.4% ~ 1.1%	1.1% ~ 1.5%	<1%	<1%	<1%	<1%	<1%	<1%	<1%	<1%	<1%
Clostridium phylum	<1%	0.6% ~ 1.1%	<1%	<1%	<1%	<1%	<1%	<1%	<1%	<1%	5.6% ~ 11%	1.3% ~ 4.53%
Spirobacteria phylum	<1%	<1%	<1%	<1%	3.90% ~ 5.30%	0.3% ~ 3.6%	1.3% ~ 1.5%	1.2% ~ 3.4%	1% ~ 1.8%	0.7% ~ 1.9%	5.32% ~ 5.7%	0.5% ~ 1.24%
Fibrolytic bacteria phylum	<1%	<1%	<1%	<1%	<1%	0.2% ~ 2.5%	0.8% ~ 1.3%	0.4% ~ 1.7%	<1%	0.2% ~ 1.4%	<1%	<1%
Verrucomycota phylum	<1%	<1%	<1%	<1%	<1%	0.8% ~ 3.8%	<1%	0.7% ~ 2.4%	<1%	1.2% ~ 6.1%	2.1% ~ 3.55%	0.4% ~ 3.28%

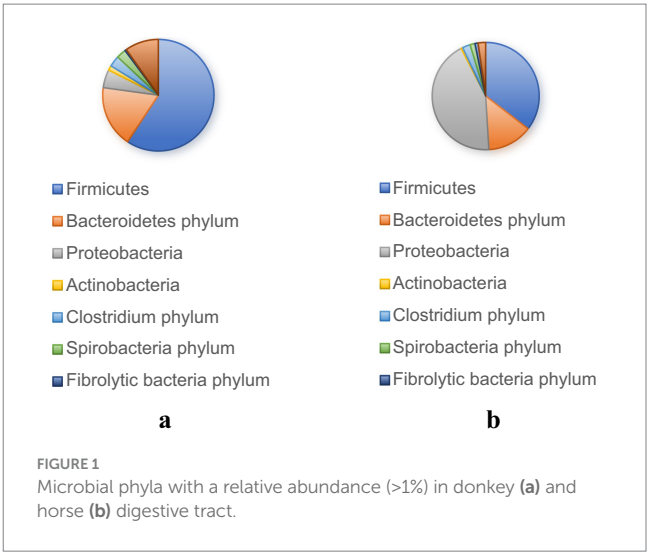

FIGURE 1
Microbial phyla with a relative abundance (>1%) in donkey **(a)** and horse **(b)** digestive tract.

Firmicutes relative to *Bacteroidetes* has been correlated with enhanced energy harvesting capabilities from the diet.

The functional specialization of these bacterial phyla underlies their importance in equine digestive physiology. *Bacteroidetes* serves as a key player in the metabolism of complex compounds, including steroids, bile acids, and polysaccharides, and is particularly crucial for cellulose degradation in herbivorous animals (Costa and Weese, 2012). In contrast, *Firmicutes* primarily functions in the hydrolysis of carbohydrates and proteins (Spence et al., 2006), establishing itself as the predominant bacterial group responsible for carbohydrate utilization in herbivorous species (Xu et al., 2003). Based on these distinct functional characteristics, it has been hypothesized that horses may possess superior metabolic capabilities for processing roughage, while donkeys may demonstrate greater efficiency in metabolizing concentrate feeds. This functional divergence reflects the evolutionary adaptations of these species to their respective dietary niches and feeding behaviors.

The relationship between microbial composition and gastrointestinal health has been well-documented in equine research. Costa et al. (2012), utilizing 16S rDNA sequencing technology, revealed that healthy horses maintain significantly higher concentrations of *Firmicutes* in their intestinal microbiota compared to horses suffering from colitis. This finding suggests a strong association between microbial community structure and gut health status in equine species. Moreover, metagenomic analysis conducted by Guo et al. (2023) identified *Clostridium* and *Bacteroidetes* as the most abundant genera in specific populations. *Clostridium*, classified as cellulose-degrading bacteria, plays a multifaceted role in the intestinal ecosystem. These bacteria not only decompose cellulose to provide fermentation substrates for acid-producing bacteria but also utilize succinate produced by other microorganisms to generate acetate and propionate. Through these metabolic processes, *Clostridium* contributes to gut microbiota stabilization and intestinal pH regulation, thereby creating favorable conditions for microbial growth and host health.

Interspecies and intraspecies variations in gut microbiota composition have been consistently observed across different equine populations. Bulmer et al. (2019) conducted a comprehensive study involving 20 horse populations and found that *Firmicutes* dominated

the microbial community in 18 of these populations. In contrast, *Bacteroidetes* and *Proteobacteria* were less prevalent, with *Proteobacteria* representing less than 1% of the total relative abundance. Within the *Firmicutes* phylum, the class *Clostridia* and the order *Bacillales* were predominantly represented, with additional contributions from *Lactobacillus* species. Similarly, comparative studies between Mongolian horses and purebred horses have revealed that while overall microbial diversity, richness, and uniformity remain relatively consistent, significant differences exist in the specific bacterial species composition (Brulc et al., 2009). These variations likely reflect the unique physiological adaptations that different horse breeds have developed in response to their respective environmental conditions, ultimately influencing the structure and function of their gut microbiota.

Research focusing specifically on donkey populations has provided valuable insights into species-specific microbial patterns. Zhang et al. (2024) investigated the intestinal microbiota of three distinct donkey populations: Yunnan, Dezhou, and Qinghai donkeys. Their findings confirmed that *Firmicutes* and *Bacteroidetes* remain the dominant bacterial groups across all three populations, with *Rikenellaceae* emerging as a notable genus within the *Bacteroidetes* phylum. The predominance of *Firmicutes* in donkey populations may be attributed to the unique cellular structure of these bacteria, which enables them to withstand the harsh intestinal environment while efficiently metabolizing complex carbohydrates such as cellulose and pectin. This metabolic capability is essential for the production of short-chain fatty acids (SCFAs), which are vital for host energy supply and maintenance of intestinal health (Guo et al., 2022).

The comprehensive understanding of intestinal microbiota composition and functional roles in equine species is paramount for advancing scientific breeding practices and developing effective strategies for intestinal disease prevention. The documented differences between horses and donkeys, as well as variations among different breeds, underscore the critical need for species-specific and breed-specific microbiome management approaches to optimize feed utilization efficiency and promote overall gut health. Consequently, continued research efforts are essential to deepen our understanding of these complex microbial communities and their broader implications for equine health, disease prevention, and performance optimization. Future investigations should focus on elucidating the mechanistic relationships between microbiota composition, dietary interventions, and health outcomes to develop evidence-based management strategies for equine populations.

4 Functions of intestinal microbes in equine animals

The hindgut of horses is a complex anaerobic fermentation system that inhabits a large microbial community and is crucial for maintaining health and digestive efficiency. These microorganisms promote nutrient absorption and energy supply by fermenting plant cellulose (Santos et al., 2013) and producing volatile fatty acids (VFAs, such as acetic acid, propionic acid, and butyric acid) (He et al., 2020). The weakly acidic environment of the cecum (pH 6–7) is conducive to microbial activity, and its mucosal epithelium forms a symbiotic barrier with the microbiota, inhibiting pathogens and enhancing immune defense.

In addition, gut microbiota may affect the athletic performance of horses. Research has found that the abundance of bacteria such as *Helicobacter* and *Ruminococcus* in horse racing is relatively high, and the increase in short chain fatty acid (SCFA) production may provide additional energy (Li et al., 2023). However, the widespread use of antibiotics may lead to the accumulation of resistance genes (Pimenta et al., 2023), which requires careful management to maintain microbial community function.

In summary, the gut microbiota of horses has multiple important functions, including digesting nutrients from feed, maintaining gut health, promoting immune protection, and potentially affecting bodily functions. Further research is needed to deepen our understanding of these interactions and their implications for horse health and management.

4.1 Role of gut microbiota in digestion and degradation of nutrients

The gut microbiota of equine species has co-evolved with their hosts and is intricately influenced by their diet. These microorganisms, which evolved alongside the ancestors of horses, have adapted to the challenges posed by the equine digestive system and play a critical role in the digestion and utilization of nutrients. For instance, lipid digestion in the intestinal tract of Equus species is facilitated by microbial communities that not only support the metabolism of fats but also promote fat deposition. Research has demonstrated that the colonization of *Firmicutes* species in the gut is associated with obesity in equines, while the presence of other microbial groups, such as *Bacteroides*, has been linked to reduced fat accumulation. *Firmicutes* are primarily involved in the fermentation of polysaccharides and cellulose, producing SCFAs and other caloric compounds, which contribute to the energy balance and fat storage (Bäckhed et al., 2004; Ley et al., 2005). Consequently, a higher population of *Firmicutes* correlates positively with the degree of obesity in horses. In contrast, *Bacteroidetes* are involved in the breakdown of starch and fiber, yielding energy while simultaneously reducing fat deposition, thus inversely correlating with obesity levels (Araújo et al., 2020). These findings highlight the potential for microbial manipulation to regulate body weight and improve nutritional strategies in equine production (Schwiertz et al., 2010). However, it should be pointed out that the proportion of *Firmicutes/Bacteroidetes* (F/B) in human and animal microbiome research is controversial and requires specific analysis in practical applications.

4.1.1 Role of gut microbiota in lipid metabolism

Gut microbiota plays a crucial role in regulating lipid metabolism through the production of various metabolites. Key microbial species such as *Bifidobacterium*, *Lactobacillus*, *Prevotella*, and *Streptococcus*, as well as *Bacteroides* and *Escherichia coli*, are known to produce SCFAs, which are pivotal in modulating lipid metabolism (Detman et al., 2019; Jian et al., 2022). SCFAs, including acetic acid, propionate, and butyric acid, significantly influence fat metabolism in animals (Li et al., 2022b). These metabolites are absorbed by intestinal cells, where acetate is converted into adenosine monophosphate (AMP) and acetyl-CoA, thereby regulating the AMPK/PGC-1α/PPARα signaling pathway (Jian et al., 2022).

Among the SCFAs, propionate and butyrate play critical roles in maintaining glucose and energy homeostasis by promoting intestinal gluconeogenesis and enhancing sympathetic nervous activity. Additionally, acetate and butyrate have been shown to directly increase the phosphorylation and activity of hepatic AMPK by modulating the AMP/ATP ratio, which in turn upregulates PPARα target genes. This results in enhanced fatty acid oxidation and improved glycogen storage (Yin et al., 2016). Butyrate, in particular, functions as a HDAC inhibitor, thereby influencing lipolysis and promoting fat oxidation. It also plays a significant role in modulating the physiological functions of adipose tissue and other organs, with a noted inhibitory effect on fat deposition (Figure 2; Yin et al., 2016).

Acetic acid, produced by gut microbiota, has been identified as a precursor for the synthesis of long-chain fatty acids such as palmitic acid and stearic acid, which further regulate hepatic fatty acid metabolism (Araújo et al., 2020). Furthermore, *E. coli* strain RB 01 has been shown to produce acetic acid that reduces intracellular triglyceride and cholesterol ester accumulation, as well as decreases lipid droplet size. This mechanism impedes bacterial ability to increase intestinal lipid consumption, thereby reducing lipid accumulation and secretion, and ultimately leading to enhanced lipid utilization within the intestinal tract (Broeders et al., 2015).

4.1.2 Role of gut microbiota in the metabolism of bile acids

The gut microbiota plays a pivotal role in bile acid metabolism through complex biotransformation processes. Primary bile acids, synthesized hepatically from cholesterol, undergo extensive microbial modification within the intestinal tract. Intestinal bacteria facilitate the biotransformation of these primary bile acids through enzymatic processes including deconjugation (hydrolysis), 7α-dehydroxylation, dehydrogenation, and oxidation, resulting in the formation of secondary bile acids such as lithocholic acid (LCA) and deoxycholic acid (DCA). These secondary bile acids function as endogenous ligands for the G-protein coupled bile acid receptor TGR5 (GPBAR1) (Virtue et al., 2019). Upon TGR5 activation, a downstream signaling cascade is initiated that stimulates the secretion of incretin hormones, specifically glucagon-like peptide-1 (GLP-1) and peptide YY (PYY), from intestinal enteroendocrine L cells. This hormonal response subsequently modulates animal appetite and lipid metabolism (Figure 3; Chen et al., 2011). Beyond bile acid biotransformation, the gut microbiota exerts metabolic influence through additional substrate-specific pathways that converge on lipid homeostasis regulation. Complementing the bile acid-TGR5-incretin axis, microbial amino acid metabolism represents another critical mechanism by which the intestinal microbiome modulates host metabolic physiology (Figure 3).

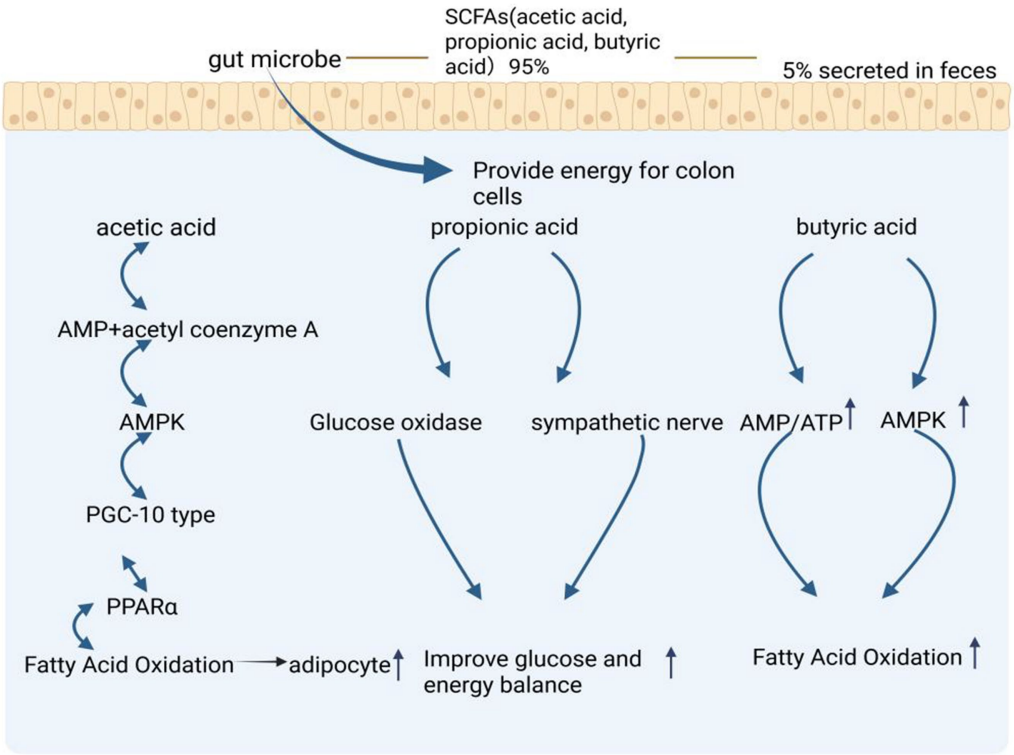

FIGURE 2
Regulation of lipid metabolism mechanism by short chain volatile acids (SCFAs) produced by gut microbiota metabolism. The metabolic pathways of SCFAs- specifically acetic acid, propionic acid, and butyric acid - which are produced by gut microbes, with 95% utilized by colon cells and 5% secreted in feces. The figure shows three main pathways: the acetic acid pathway leading to fatty acid oxidation through AMPK and PPARα, the propionic acid pathway improving glucose and energy balance via glucose oxidase and sympathetic nerve activation, and the butyric acid pathway enhancing fatty acid oxidation through AMP/ATP and AMPK signaling. The figure is created with BioRender.com.

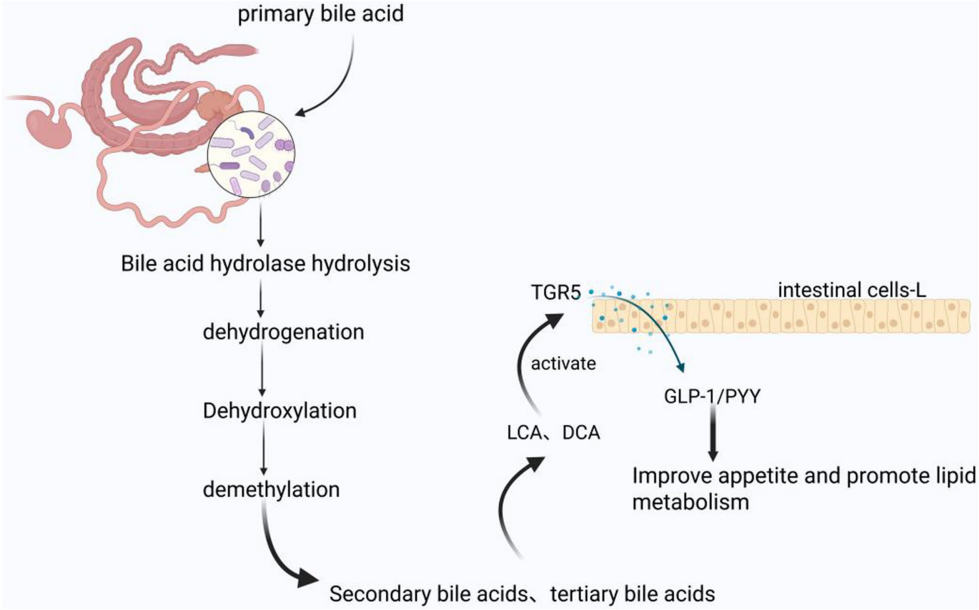

FIGURE 3
Bile acid regulated lipid metabolism mechanism produced by gut microbiota metabolism in equine animals: The products produced by microbial hydrolysis, hydrogenation, dehydroxylation, and demethylation of primary bile acids are activators of TGR5, thereby improving animal appetite and lipid metabolism. The figure is created with BioRender.com.

In addition, studies in mice have demonstrated that approximately 4 to 6% of tryptophan is directly metabolized by gut microbiota into various derivatives, including indole compounds (Neavin et al., 2018). These metabolites affect the expression of small RNA molecules such as miR-181 in adipocytes, and overexpression of miR-181 has been shown to restore adipocyte differentiation and lipid accumulation, indicating that the inhibition of miR-181 mediates some anti adipogenic effects of diet induced obesity (DOS) in cultured white adipocytes (Virtue et al., 2019). These findings indicate that miR-181 plays an important role in fat deposition, and gut microbiota can affect the expression of these small molecules by metabolizing tryptophan. However, further research is needed to determine whether tryptophan and its derivatives regulate fat metabolism through the AhR and miR-181 pathways in horse species.

4.1.3 Role of gut microbiota in nitrogen metabolism

Protein is an essential nutrient for the growth and development of equine species. Nitrogen-containing substances are critical for bacterial protein synthesis. The gut microbiota plays a pivotal role in nitrogen metabolism, particularly through the degradation of amino acids. Most intestinal microorganisms are capable of directly utilizing the free amino acids available in the intestine. Microorganisms in the digestive tract employ various mechanisms to adapt to challenging conditions such as high pH, nutrient scarcity, and digestive enzyme activity. They contribute to the synthesis of essential nutrients, which may be utilized by the host, and facilitate the deamination and decarboxylation of amino acids, resulting in the production of ammonia, short-chain fatty acids, organic acids, phenolic compounds, and gases (Zhang et al., 2025; Chaucheyras-Durand et al., 2022; Lin et al., 2017; Blachier et al., 2007; Radecki and Yokoyama, 2001). While the primary sources of amino acids in monogastric animals are the diet and endogenous proteins, the small intestine in equines is a key site for nutrient metabolism, but its efficiency in utilizing amino acids is limited (Metges, 2000; Torrallardona et al., 2003). In some instances, microbial protein synthesis in the foregut may lead to the excretion of amino acids, which could represent a loss of potential nutrition for the host. However, it remains unclear whether the synthesis of microbial proteins competes with the nutritional demands of the intestinal mucosa, warranting further investigation. Some studies also suggest that the amino acid biosynthesis by intestinal microbes in monogastric animals may help regulate the body's amino acid balance (Metges, 2000; Fuller and Reeds, 1998; Metges and Petzke, 2005), however, the exact role of these newly synthesized microbial amino acids in regulating body amino acid metabolism remains uncertain (Costa et al., 2012). The summary of digestion and degradation of lipid, amino acid and cellulose in feed by equine animals is presented in Figure 4.

4.2 Role of gut microbiota in disease prevention and health maintenance

The gut microbiota plays a central role in maintaining the stability of the microbiota in the health of equine animals, while an imbalance in the microbiota directly leads to various intestinal diseases. The gut of healthy horses is dominated by *Firmicutes* (68%), but in horses with colitis, the abundance of *Bacteroidetes* abnormally increases to 40%, while *Firmicutes* decreases to 30%. The fundamental transformation of the horizontal structure of this phylum leads to a decrease in cellulose degradation ability and an increase in the release of inflammatory factors, directly damaging the colon mucosa, confirming that dysbiosis (rather than a single pathogen) is the core cause of colitis (Costa et al., 2012). The development of diarrhea in foals is directly

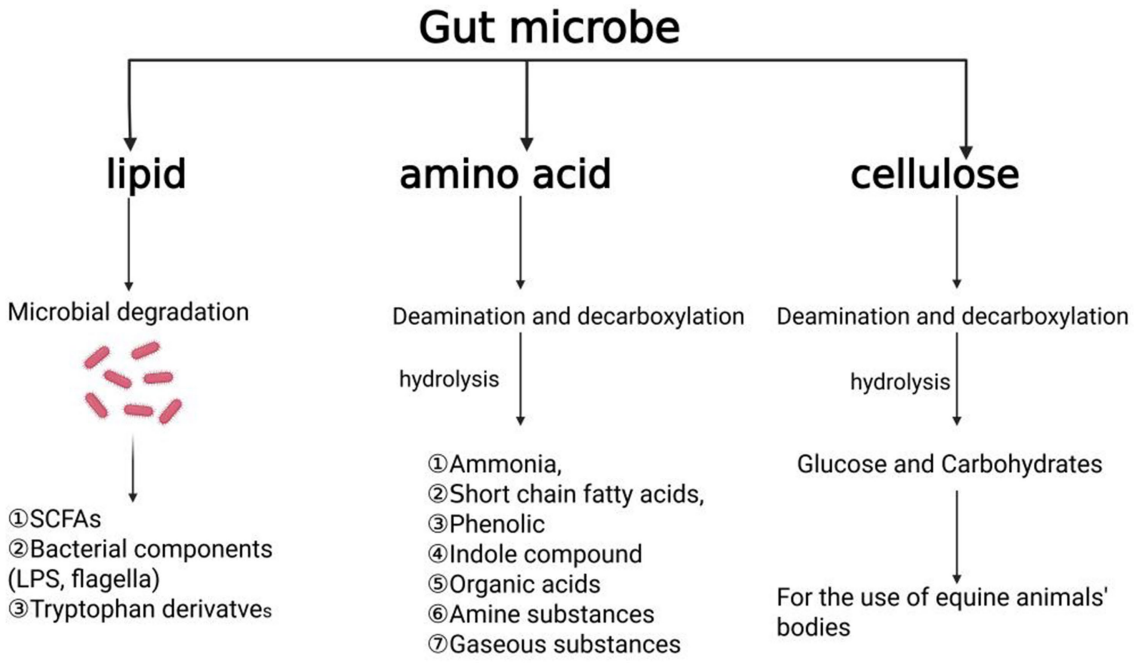

FIGURE 4
Summary of digestion and degradation of three major nutrients in feed by equine animals, including lipid, amino acid and cellulose. The figure is created with BioRender.com.

attributed to the collapse of microbial diversity: the abundance of *Clostridium* and *Lactobacillaceae* in diarrheal foals significantly decreases, weakening the intestinal barrier, while the abundance of *actinomycetes* and *Micrococcus*, which have immune regulatory functions, further weakens the pathogen's resistance, ultimately leading to excessive proliferation of opportunistic pathogens and causing watery diarrhea (Schoster et al., 2017; De la Torre et al., 2019). In the pathogenesis of colic, the ratio of *Firmicutes* to *Proteobacteria* (≥0.95) directly reduces the risk of onset by producing anti-inflammatory short chain fatty acids and stabilizing intestinal peristalsis, while an imbalanced ratio leads to intestinal motility disorders and mucosal inflammation (Stewart et al., 2019); It is worth noting that deworming drugs (such as fenbendazole) further disrupt the buffering capacity of the microbiota by inhibiting the abundance of *Bacteroidetes*, indirectly increasing susceptibility to colic (Hillyer et al., 2002; Walshe et al., 2019). These studies collectively reveal that diseases such as colitis, diarrhea, and colic all begin with dysbiosis of the microbiota structure (inversion of phylum proportions or absence of taxonomic groups), and a decrease in microbial diversity directly weakens the intestinal immune metabolism homeostasis. In the future, it is necessary to focus on analyzing the colonization mechanisms of specific bacterial communities (such as *lactobacilli*), and restore ecological balance through microbial transplantation or targeted probiotic intervention, providing new strategies for disease prevention and control.

4.3 Gut microbiota role in immune response

The intestinal barrier in horses is a dynamic mucosal layer composed of various components that interact with multiple stimuli to elicit an immune response. This barrier covers the entire intestinal surface, serving as the first line of defense, and simultaneously functions as a complex ecosystem consisting of microorganisms, such as bacteria, fungi, and viruses, along with mucus and nutrients (Quigley, 2017). These microorganisms meet their nutritional needs by fermenting indigestible carbohydrates, including oligofructose, inulin, and galactose (Nishida et al., 2018). Intestinal microbiota regulates hormone release within the intestinal tract, contributing to pathogen resistance, promoting vitamin synthesis and absorption, and modulating neural signals that impact metabolism, physiological health, and immune function (Mangiola et al., 2018).

The interaction between gut microbiota and the host immune system occurs through various pathways. Notably, microbial metabolism of SCFAs, such as propionic acid and butyric acid, plays a central role. These SCFAs interact with G protein-coupled receptors (GPCRs), inhibiting histone deacetylase (HDAC) activity and regulating intestinal immune functions. Propionic acid and butyric acid activate GPR43 and GPR109A receptors on the surface of intestinal epithelial cells, respectively. Upon activation, these receptors trigger pro-inflammatory responses and initiate signaling pathways involving interleukin-18 (IL-18), which helps maintain epithelial integrity. Additionally, activation of GPR109A induces the secretion of IL-10, promoting the differentiation of regulatory T cells (Singh et al., 2014; Balakrishnan et al., 2021). SCFAs, as potent HDAC inhibitors, also regulate the expression of transforming growth factor beta (TGF-β) in intestinal epithelial cells (IECs), influencing T-cell differentiation into effector T cells and Tregs (Yang et al., 2020), as well as enhancing mTOR-S6K activity crucial for T-cell differentiation (Park et al., 2015). Thus, SCFAs are vital for maintaining intestinal barrier function by promoting IEC proliferation, differentiation, and reducing apoptosis.

Tryptophan metabolites also play an essential role in immune regulation, enhancing immune function and cell proliferation through activation of the aryl hydrocarbon receptor (AhR) (Ngui et al., 2020). AhR, a sensor for microbial metabolites, protects the host against chemicals and pathogens (Roager and Licht, 2018). In the gut, AhR activation mediates the development of innate and intraepithelial lymphocytes, exerting antibacterial and anti-inflammatory effects (Gutiérrez-Vázquez and Quintana, 2018). Many microbial-derived tryptophan metabolites have been shown to activate AhR, further underscoring the importance of microbial metabolites in host–microbe interactions within the immune system (Figure 5).

Probiotics have been widely studied for their humoral, cellular, and non-specific immune regulatory effects (Gill et al., 2001). Probiotics attach to the animal intestine to form a mucosal barrier, secreting antibiotics and other substances to prevent pathogen and viral infections; Stimulate and regulate various intestinal functions, including digestion, metabolism, immune response, and pathogen elimination, and affect the brain gut axis (Figure 6; Conca, 2016; Kristensen et al., 2016). Probiotics can also release cytokines such as interleukin (IL), tumor necrosis factor (TNF), interferon (IFN), and transforming growth factor (TGF) to regulate innate and adaptive immune responses (Figure 7; Foligné et al., 2010). The

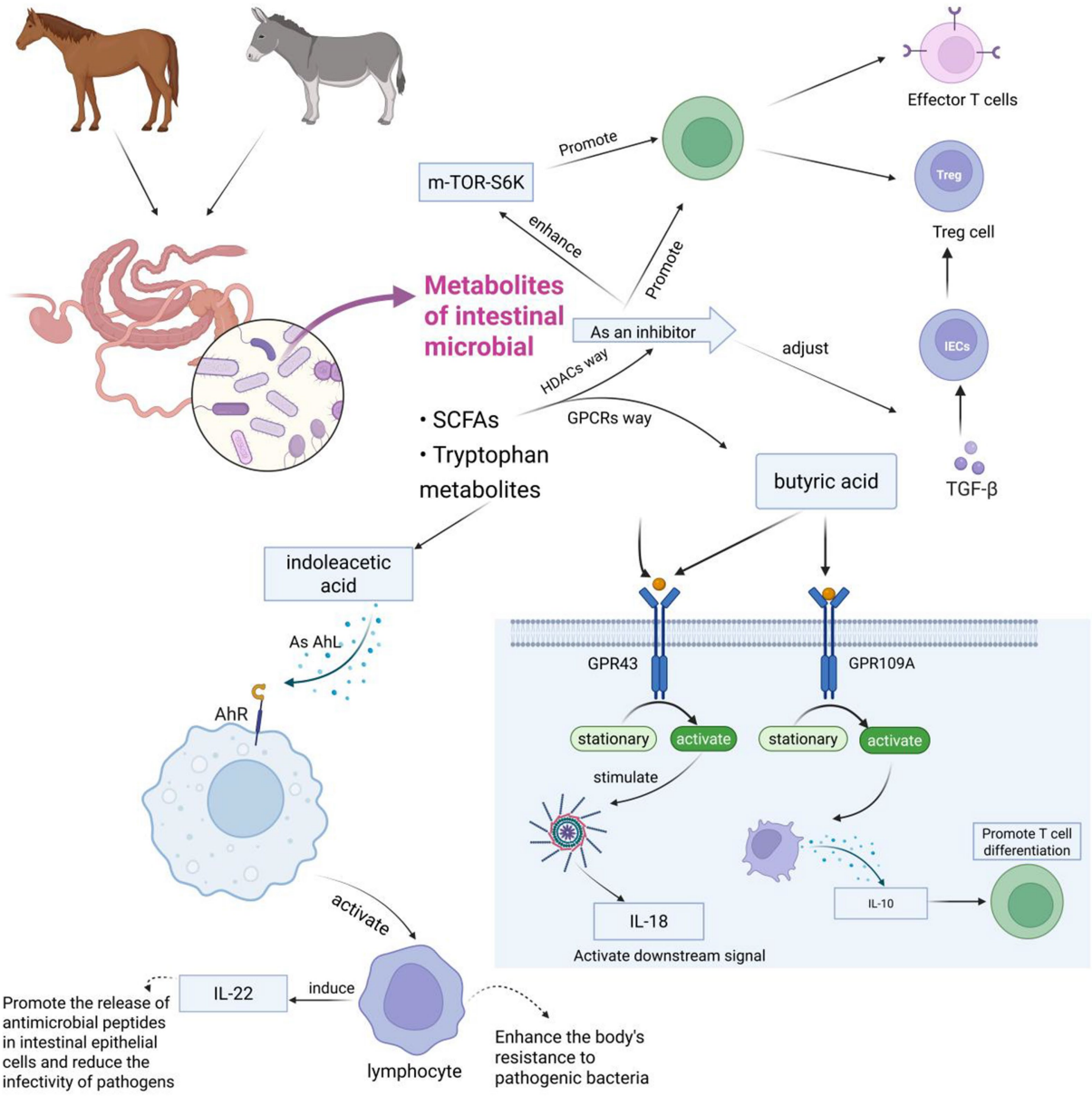

FIGURE 5
This figure illustrates how intestinal microbial metabolites (primarily SCFAs and tryptophan metabolites) from horses and donkeys influence immune responses through various signaling pathways. The diagram shows several key pathways: the mTOR-S6K pathway affecting T cells (Effector T cells and Treg cells), the butyric acid pathway working through GPR43 and GPR109A receptors to produce IL-1β and IL-10 respectively, and the indoleacetic acid pathway activating AHR to stimulate lymphocytes and IL-22 production, ultimately enhancing antimicrobial defense and T cell differentiation. The figure is created with BioRender.com.

non-toxic metabolites produced by the gut microbiota play important roles in both nutritional and clinical environments (Kau et al., 2011; Bermudez-Brito et al., 2012; Bin et al., 2018). By fermenting food that is not easy to digest, probiotics provide energy and show antigenicity, anti-obesity, anti-diabetes and anti-inflammatory properties (Kerry et al., 2018). These findings emphasize the crucial role of gut microbiota metabolites in regulating host immune function and gut immune response. Given the complexity of microbial interactions in mediating these processes, further research on how gut microbiota metabolites affect immune system regulation remains crucial.

The gut microbiota includes multiple types, and different bacterial strains have unique effects on immune regulation. Beneficial bacteria such as *lactobacilli* and *bifidobacteria* can promote intestinal health; Harmful bacteria such as *Escherichia coli* and *Staphylococcus aureus* can damage the intestinal environment; Neutral bacteria such as *Firmicutes* and *Bacteroidetes* are harmless under normal circumstances, but may cause diseases under specific conditions. These microorganisms are crucial for maintaining the intestinal immune barrier. Some typical bacterial strains have been confirmed to have immune regulatory functions. Research has found that *Bifidobacterium* binds tightly to mammalian intestinal mucosal epithelial cells through phosphorylated soap acid, forming a biological barrier on the intestinal mucosal surface together with other anaerobic bacteria, effectively resisting various pathogenic bacteria and harmful microorganisms (Alessandri et al., 2021). This indicates that gut microbiota has multiple effects on the host immune system, but existing research has only revealed a small part of the mechanisms and has not yet formed a complete system. More research is needed in the future to verify the specific roles of different gut microbiota in the immune system of horses.

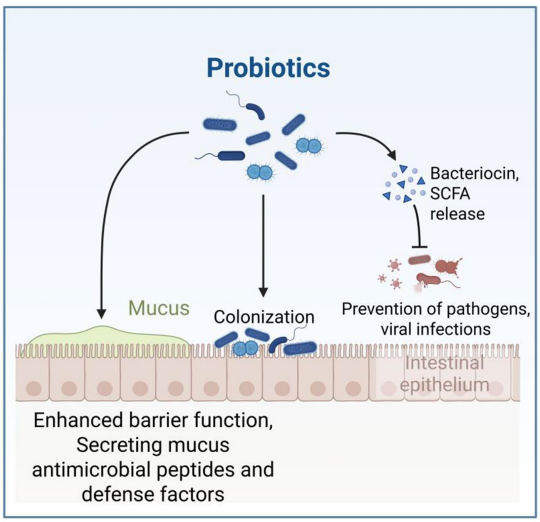

FIGURE 6
This figure demonstrates how probiotics function in the intestinal environment, showing their dual mechanisms of action: direct colonization of the intestinal epithelium and enhancement of the mucosal barrier through bacteriocin/SCFA production that prevents pathogen invasion. The figure is created with BioRender.com.

5 Regulation of gut microbiota in equine animals

5.1 Environmental factors

The gut microbiota is the "extra genome" of horses, which is related to their health through multiple pathways. Under normal circumstances, the composition of the gut microbiota in horses is influenced by various environmental factors, including management factors, seasonal changes, and social interactions, in a symbiotic and dynamic relationship with the host. When designing and interpreting research on the gut microbiota of horses, these factors must be considered. Research has shown that the composition of microbial communities presents a multi-level structure, with significant differences observed at the individual, population, and spatial levels (Antwis et al., 2018). The microbiota of horse feces and skin tends to vary depending on geographical location and habitat. Consistently, Ayoub et al. (2022) found significant differences in protein content in the fecal microbiota of healthy horses (teaching horses vs. client owned) raised in different facilities (Ayoub et al., 2022), demonstrating the impact of management and environment on their fecal microbiota Finally, the higher similarity in the skin microbiota of horses living on the same farm reinforces the conclusion that the environment is an important contributor to the seeding of bacterial species in horses (Kaiser-Thom et al., 2021). It has been reported in study by Salem et al. (2018) that seasonal changes in the fecal microbiota of horses raised on pastures for 12 months, with management measures remaining largely unchanged. Their findings indicate that seasonal changes, weather conditions (temperature and rainfall), and additional feed intake (age) are associated with microbial fluctuations. These results highlight the dynamic characteristics of the gut microbiome in horses and their ability to respond to environmental changes. To evaluate whether these seasonal effects are consistent over time, further longitudinal studies lasting at least 24 to 36 months are needed.

A study by Salem et al. (2018) demonstrated that the gut microbiota of equines varies throughout the year. Although feed and variety significantly affect gut microbiota, some microbial food sharing and social interactions may partially explain these changes (Garber et al., 2020). A study investigating semi local Welsh contributions found that although individual variation accounted for 52.6% of gut microbiota variation, group interaction and social behavior also contributed to overall variation (Antwis et al., 2018). Research has found that mother son relationships have a significant impact on microbial community similarity, with foals having a higher similarity to their mother's microbiota than to other mare populations, indicating to some extent that their microbiome composition may be influenced by each other (Boucher et al., 2024).

5.2 Dietary factors

5.2.1 High fiber and starch dietary components

Dietary composition serves as a fundamental regulatory mechanism for equine gut microbiota modulation (Zhang et al., 2022e). Specifically, diets characterized by elevated animal protein and fat content have been demonstrated to promote increased abundance of *Firmicutes* within the rectal microbiota. Conversely, high-fiber dietary regimens facilitate enhanced concentrations of

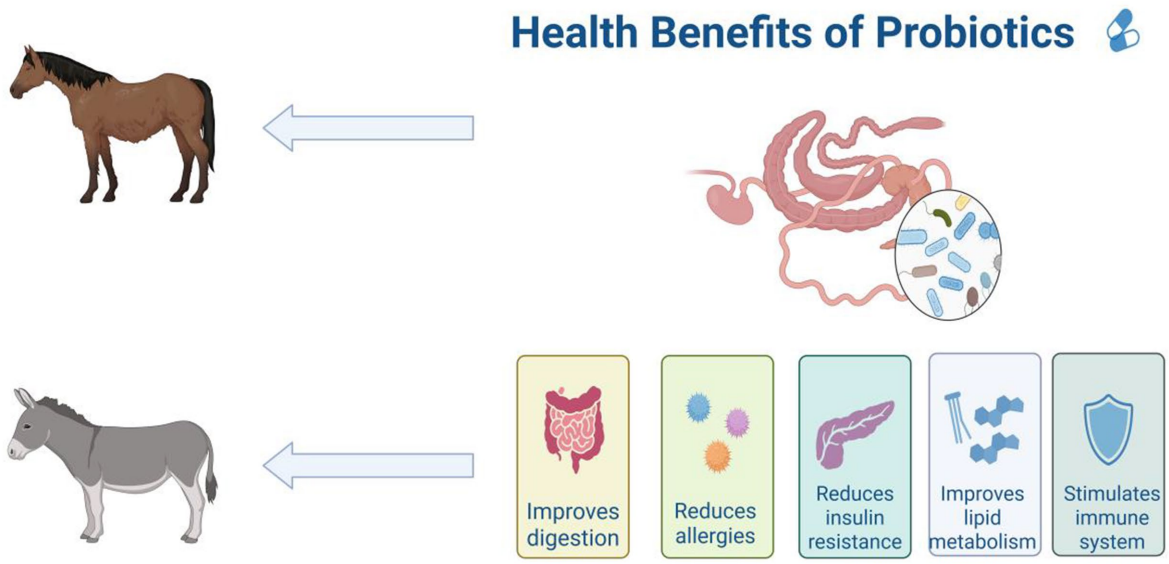

FIGURE 7
Benefits of probiotics in the gut for equine animals, including improved digestion, reduced allergies, reduced insulin resistance, improved lipid metabolism and stimulated immune system. The figure is created with BioRender.com.

Bacteroidetes and fiber-degrading bacterial populations (De Filippo et al., 2010; Wu et al., 2011). Cultivation-based microbial investigations have further elucidated the metabolic shifts occurring during dietary transitions. When equines transition from high-fiber to high-starch diets, a notable increase in the abundance of starch-degrading bacteria, lactic acid-metabolizing bacteria, and Streptococcus species occurs within the gastrointestinal tract. Simultaneously, this dietary shift results in a corresponding decrease in fiber-degrading bacterial populations (Raspa et al., 2024). This microbial transformation can be attributed to the physiological limitations of starch digestion in equines. When horses consume excessive starch quantities (exceeding 1 gram per kilogram of body weight per meal), substantial amounts remain undigested within the foregut (Harris and Dunnett, 2018). Subsequently, this undigested starch undergoes fermentation within the hindgut (Richards et al., 2006), resulting in elevated lactate production. This metabolic environment preferentially supports bacterial communities specialized in starch-to-lactate conversion, while simultaneously creating conditions unfavorable for beneficial fiber-fermenting microorganisms, thereby reducing fiber-degrading bacterial populations. In contrast, high-fiber dietary regimens demonstrate the capacity to enhance fiber-degrading bacterial abundance within equine gut microbiota (Grimm et al., 2017). Comparative studies examining the effects of high-fiber versus high-starch diets on apparent digestibility in donkeys revealed superior digestibility coefficients for high-fiber dietary interventions. Additionally, yeast polysaccharides (YPS) supplementation has been shown to exert beneficial effects on the fecal microbiome, specifically promoting the proliferation of advantageous microorganisms including *Lactobacilli* and *Prevotella* species in donkey foals (Huang et al., 2023). Recent metagenomic analyses conducted by Cai et al. (2024) investigated the influence of concentrate feeding sequences on gut microbiota diversity in fattening donkeys. Their findings demonstrated that initial concentrate feeding resulted in increased abundance of beneficial bacterial phyla, particularly *Bacteroidetes* and *Firmicutes*. These microbial communities play pivotal roles in carbohydrate metabolism and nutrient processing, thereby contributing to the maintenance of optimal digestive function. Furthermore, Zhang et al. (2021) reported that high-energy dietary interventions significantly reduced the *Firmicutes* to *Bacteroidetes* (F/B) ratio. Additionally, high-energy diet administration resulted in decreased alpha diversity within the rectal microbiota, reduced relative abundance of unidentified *Ruminococcaceae* species, and increased abundance of specific microorganisms within the Actinobacteria, *Rikenellaceae,* and *Veillonellaceae* genera.

5.2.2 Methionine supplementation effects on gut microbiota

Methionine supplementation has been demonstrated to enhance lactation performance in donkeys through complex microbiota-mediated mechanisms. Huang et al. (2024) established that dietary methionine addition improves lactation capacity by increasing both milk production and component synthesis. This enhancement occurs through the regulation of serum metabolites, which subsequently improves milk quality and donkey milk metabolite profiles, ultimately optimizing lactation performance. The underlying mechanism involves gut microbiota compositional modifications that influence mammalian milk production and composition. Subsequent research by Huang et al. (2025) revealed that methionine supplementation in lactating donkeys significantly increases the abundance of *Methanococcus, Ruminococcaceae*, and fiber-degrading bacteria, while simultaneously reducing *Ruminococcaceae* populations. Notably, methanogenic bacteria demonstrate associations with organismal antioxidant enzyme systems (Wu et al., 2021). In addition, methionine supplementation significantly enhanced serum antioxidant activity in lactating donkeys, with antioxidant indices (T-AOC and CAT activity) showing correlations with microbial abundance patterns (Guo et al., 2024). Specifically, *Ruminococcus* species exhibited significant positive

correlations with T-AOC and CAT activity, while methanogenic bacteria demonstrated positive correlations with T-AOC levels.

5.2.3 Weaning-associated microbial changes

Weaning represents a critical developmental phase in animal production, characterized by substantial microbial compositional changes within the digestive tract in response to multiple biological and environmental stressors (Zhang et al., 2024). Prior to weaning, *Methanobacterium* constitutes the predominant archaeal genus in both donkey and foal fecal samples, indicating that initial colonization and establishment of methanogenic bacterial populations commence before the weaning process (Zhang et al., 2023). Microbial analysis of donkey and foal fecal samples reveals characteristic diversity patterns during the weaning transition (Yang et al., 2024). Microbial diversity typically exhibits an initial decrease followed by subsequent recovery, with significant reductions observed before and during weaning. This pattern likely reflects effective microbial adjustment and adaptation to environmental changes as foals transition from liquid milk to combined liquid and solid feed consumption. The significant increasing trend observed from weaning through post-weaning periods may be attributed to foal adaptation to solid feed consumption. However, the gut microbiota represents an inherently fragile ecosystem, and the extensive dietary modifications accompanying weaning can precipitate dramatic microbial community alterations. These microbial shifts often result in increased abundance of diarrhea-associated bacteria within the equine intestinal tract, potentially triggering stress-induced diarrheal responses.

Recent investigations by Xie et al. (2023) employed high-throughput 16S rRNA sequencing technology to examine the effects of concentrate feeding sequences on intestinal microbiota richness in weaned donkeys (6-month-old males). Their results demonstrated that the concentrate-crude mixed diet (C3) treatment produced optimal growth performance in weaned donkeys, accompanied by increased relative abundance of *Bacteroidetes* and *Spirochaetes*. Given the high cellulose-degrading capacity of *Spirochaetes*, these findings suggest that concentrate-crude mixed diets promote fibrous substrate degradation by intestinal microbiota through enhanced *Spirochaetes* populations, thereby facilitating optimal nutrient absorption and growth rates in donkeys.

5.3 Genetic and variety factors

Research indicates both similarities and differences in the composition of the gut microbiota across various horse breeds. Comparative studies of Mongolian and Thoroughbred horses have identified notable patterns in microbial communities. The predominant bacterial phyla in both breeds are *Firmicutes* (56% in Mongolian horses, 53% in Thoroughbred horses) and *Bacteroidetes* (33% in Mongolian horses, 32% in Thoroughbred horses), with these taxa constituting the major components of the gut microbiota in both breeds. Despite these similarities, some key differences in bacterial composition were observed. Specifically, Eutrophic bacteria, *Planctomycetes* (floating molds), *Proteobacteria*, *TM7*, and *Chloroflexi* were significantly more abundant in Thoroughbred horses compared to Mongolian horses (Zhao et al., 2016). Conversely, the *Treponema* genus was more abundant in Mongolian horses (43%) compared to Thoroughbreds (29%) (Guo et al., 2022).

Breed-specific differences in the gut microbiota have been linked to distinct clinical conditions. For instance, Arabian horses are predisposed to colic (Gonçalves et al., 2002), while dwarf horses exhibit a higher susceptibility to glucose intolerance, obesity, and metabolic syndrome (Johnson, 2002). These variations in gut microbiota between breeds may influence disease susceptibility and could contribute to the occurrence of stereotypical behaviors in certain equine populations.

A study used high-throughput sequencing to compare the richness of gut microbiota in the 16rDNA V3-V4 variable region between wild and domesticated donkeys (Costa and Weese, 2018). The results indicate that the microbial community structure of wild donkeys is more complex than that of domesticated donkeys, and their dry matter digestibility is also higher. In addition, they found that the composition and functional characteristics of this microbial community may be closely related to its long-term adaptation to the extreme high-altitude environment of the Tibet Plateau under selection pressure, and can be inherited by offspring (Costa et al., 2012). Liu et al. (2020) found that the two dominant phyla of wild donkeys, *Bacteroidetes* and *Firmicutes*, were significantly higher than those of domestic donkeys, while wild donkeys had *Ruminococcocacae NK4A214*, *Phascolarctobacteria*, *Coprostanogenes*, *Lachnospiraceae XPB1014 Akkermansia* is significantly higher than domestic donkeys, highlighting the key role of specific species differences in the gut microbiota of animal physiology and health.

Further studies on different equine animals such as donkeys and horses have shown significant differences in the microbial composition of their gut microbiota. Liu (2020) reported that the ratio of *Firmicutes* to *Bacteroidetes* in donkeys is approximately 1:1, while in horses it is 0.8:1. The ratio of *Firmicutes/Bacteroidetes* has been shown to affect obesity in animals, with higher ratios promoting increased energy absorption and fat storage (Bell, 2015; Ley et al., 2003). Liu (2020) confirmed these findings, demonstrating that under the same feeding conditions, donkeys tend to accumulate more fat than horses. This difference may be due to the specific metabolic functions of these bacterial phyla: *Bacteroidetes* mainly metabolize steroids, bile acids, and polysaccharides, while *Firmicutes* focuses on fermenting carbohydrates. Interestingly, animal methane emissions may be partially influenced by diet, but are also related to genetic factors. Methanogenic bacteria are widely regarded as the most heritable gut microbiota in humans and various animal populations (Grieneisen et al., 2021), and are also representative archaea in the cecum of horses. In the intestine of horses, the fermentation site is mainly in the cecum (pH 6–7), with bacteria dominating (mainly *Firmicutes* and *Bacteroidetes*), a low proportion of archaea, and weak methane production pathways. The dominant metabolites are acetic acid and propionic acid, and the peak gas production during fermentation is early with weak persistence. In contrast, the intestine of donkeys is mainly fermented in the cecum and colon (Zhang et al., 2022d), with a large number of anaerobic fungi (such as *Ruminococcus*). The diversity of archaea is low, and the gas production during fermentation is gentle and long-lasting. It can effectively degrade cellulose, prolong the retention time of chyme, and improve fiber digestion rate. For ease of reference, Table 2 shows the differences in gut fermentation patterns and microbiota between horses and donkeys (supplemented with the fermentation patterns of ruminants as a reference). These data are sourced from previously published articles (Liu, 2020; Li et al., 2023; Beckers et al., 2017; McCann et al., 2017). Stothart et al. (2024) found

TABLE 2 Differences in gut fermentation patterns and microbiota between horses and donkeys.

Feature	Horse	Donkey	Ruminant
Fermentation site	Posterior intestine (mainly cecum)	Posterior intestine (cecum+colon)	Rumen (front-end fermentation)
Advantageous metabolites	Acetic acid, propionic acid	Acetic acid and butyric acid (higher in low-quality feed)	Acetic acid, propionic acid, methane
Microbial diversity	Bacteria dominate, with a low proportion of archaea	Anaerobic fungi are abundant, while archaeal diversity is low	High proportion of archaea (methanogens)
PH adaptability	Cecum pH 6–7 (weakly acidic)	Similar to horses, but with stronger acid resistance	Rumen pH 5.5–6.5 (acidic)
Fermentation persistence	Early peak gas production with weak sustainability	Smooth gas production with a long duration	Continuous high gas production (dependent on fiber degradation)

in their study of Sable Island horses that microbiome characteristics closely related to survival have higher interannual reproducibility among individuals. This result may indicate that, like other mammals, microorganisms associated with intestinal methane production may have a partially accumulated genetic basis or be influenced by the preferential effect of Sebur Island horses.

Additionally, it is important to consider the impact of factors such as the health status and management of equine animals on their gut microbiota composition and structure. The gut microbiota of different breeds of animals can also vary greatly in an unhealthy state, so individual and breed differences, as well as differences between age groups, can also make the process of defining the microbiota of "healthy" or "diseased" equines complex (Murcia, 2019). It is noteworthy that metagenomic studies alone cannot provide a complete understanding of the functional pathways of microbial communities (Marchesi and Ravel, 2015). Without complementary metabolomic analyses, it is difficult to establish causal relationships between changes in microbial composition and physiological outcomes in horses. Metabolomics, which provides direct insights into cellular activity by profiling metabolites in a given environment, holds significant potential for elucidating the functional significance of microbial communities and their impact on host physiology (Garber et al., 2020; Li et al., 2023). For ease of reference, Table 3 and Figure 1 show various comparisons of regulatory factors of the gut microbiota in equine animals, and list the references.

Recent studies have significantly advanced our understanding of the complex and diverse microbial communities in the equine intestinal tract, which not only enhances our comprehension of the role of gut microbiota in animal health but also provides a theoretical framework for future interventions. In equines, the core microbial flora of the intestinal tract is essential for the digestion and breakdown of feed nutrients, immune regulation, disease prevention, and overall health maintenance (Guo et al., 2022). These microbial communities play a crucial role in cellulose degradation and the production of short-chain fatty acids, which are vital for nutrient absorption and energy metabolism in equine species (Liu, 2020). Furthermore, the core microbiota contributes to host resistance against pathogen invasion, supports immune system function, and maintains intestinal health by regulating immune responses and preserving the integrity of the intestinal barrier.

Notably, the composition of the intestinal microbiota has been closely associated with the health status of equines. Future research should focus on the influence of environmental factors—such as geographical location, seasonal variations, and dietary composition—on the core microbial flora of equines. This could offer insights into how to optimize equine health and performance. Additionally, understanding the diversity and richness of the gut microbiota, as well as its impact on nutrient absorption, will be instrumental in improving the management practices of equine animals.

6 Differences in digestive capacity between horses, ruminators, and humans

When comparing the intestinal microbiota of equines with other species, such as ruminants and humans, notable differences arise. While equines, like ruminants (e.g., cattle, sheep), and humans possess complex microbial communities, the specific functions and mechanisms of action vary. The intestinal system of equines differs from that of ruminants, particularly in the absence of a rumen, reticulum, omasum, and abomasum. These specialized compartments in ruminants facilitate the efficient digestion of cellulose-rich plant materials, supported by abundant microbial populations that break down indigestible plant fibers and produce volatile fatty acids as a primary energy source (Campos et al., 2016). In contrast, equines have a relatively small stomach but a relatively long small and large intestine, particularly the highly developed cecum, which compensates for the lack of a rumen by facilitating cellulose digestion. However, this digestive process is less efficient than in ruminants due to the absence of rumination, which allows for additional chewing and reprocessing of food to enhance microbial action (David et al., 2014).

Equine species primarily rely on microbial fermentation to digest plant fibers, while humans utilize digestive enzymes for food breakdown. This structural and functional divergence reflects an adaptive specialization of equines for plant fiber digestion, although this may limit their efficiency in digesting other food types. The human digestive system, by contrast, is relatively short and adaptable, optimized for a varied diet. While equine digestive systems are designed for fibrous plant material, they are less flexible for processing other food types, highlighting the concept of structural adaptation to dietary function.

At present, there is a lack of detailed comparative data on the intestinal microbiota of equine animals versus other species. Future studies could provide valuable insights into the similarities and differences between the gut microbiota of equines and other animals, contributing to the enhancement of equine health, productivity, and evolutionary understanding. Such research could also deepen our knowledge of intestinal microbiomes in other species, facilitating a broader understanding of host–microbe interactions.

TABLE 3 Factors affecting gut microbiota in equine animals.

Factors	Comparison of different factors in the same aspect	Effect on gut microbiota	Species	Reference
Environmental factors	Management factors	• Protein content in fecal microbiota varies among horses raised in different facilities • Hay feeding increases the relative abundance of *filamentous bacteria* and *spirulina* • Wild donkeys are superior to domestic donkeys in terms of dry matter digestion, gut microbiota composition, and function	Horse and Donkey	Ayoub et al. (2022), Kaiser-Thom et al. (2021), and Khan et al. (2024)
	Seasonal changes	• Weather conditions influence both feed availability and quality for horses, as well as environmental microbial populations. • Ingested environmental bacteria can colonize the hindgut, leading to changes in the gut microbiota.	Horse	Salem et al. (2018)
	Social interactions	• Individual variation accounts for 52.6% of the variation in the gut microbiota • Group interaction leads to overall variation in gut microbiota • Social behavior leads to overall variation in gut microbiota	Horse	Antwis et al. (2018)
Dietary factors	High fiber and high starch	• A high starch diet has a high abundance of starch degrading bacteria, lactic acid degrading bacteria, and streptococcus • A high fiber diet with a large number of fiber degrading bacteria • A high fiber diet has higher apparent digestibility than a high starch diet • A high energy feed significantly reduces the ratio of *Firmicutes* to *Bacteroidetes* (F/B)	Horse	De Filippo et al. (2010), Wu et al. (2011), Raspa et al. (2024), and Zhang et al. (2021)
	Methionine in the diet	• High Met increases the abundance of ruminant bacteria, methane bacteria, etc. • High Met can enhance the antioxidant capacity of lactating donkeys	Donkey	Huang et al. (2024) and Huang et al. (2025)
	Weaning	• Diversity of microorganisms in weaned donkeys first decreased and then increased • Weaned donkeys and foals fed a mixed diet of fine and coarse grains, with high relative abundance of *Bacteroidetes* and *Spirobacteria*	Horse Donkey	Yang et al. (2024) and Xie et al. (2023)
Genetic and variety factors	Different horse varieties	• *Synergistetes*, *Planctomycetes*, *Proteobacteria*, *TM7*, and *Chloroflexi* were significantly more abundant in Thoroughbred horses • Treponema genus was more abundant in Mongolian horses (43%). • Arabian horses are predisposed to colic • Dwarf horses exhibit a higher susceptibility to glucose intolerance, obesity, and metabolic syndrome	Horse	Gonçalves et al. (2002) and Johnson (2002)
	Different donkey varieties	• Wild donkeys have a high digestibility of dry matter. • Dry matter digestion rate of domestic donkeys is low • Wild donkeys also exhibit more complex microbial communities. • The *Bacteroidetes* and *Firmicutes* phyla of wild donkeys are higher than those of domestic donkeys • The *Ruminococcaceae NK4A214*, *Phascolarctobacteria*, *Coprostanogenes*, *Lachnospiraceae XPB1014*, and *Akkermansia* in wild donkeys are significantly higher than those in domestic donkeys	Donkey	Costa and Weese (2018) and Liu et al. (2020)
	Different equid species	• The ratio of *Firmicutes* to *Bacteroidetes* in donkeys is approximately 1:1, compared to a ratio of 0.8:1 in horses. • Specific metabolic function of the bacterial phylum causes donkeys to accumulate more fat than horses • In the intestines of horses, the proportion of archaea is low and the methane production pathway is weak, while donkeys have a large number of anaerobic fungi in their intestines	Horse and Donkey	Liu (2020), Liu et al. (2020), and Li et al. (2023)

10.3389/fmicb.2025.1602258

7 Future perspectives

Looking ahead, with ongoing advances in research and technological innovation, we anticipate gaining deeper insights into the core gut microbiota of equine animals. This could offer novel strategies for improving animal health, feed efficiency, and exercise performance. The adaptive coevolution of intestinal microbes with their hosts suggests that gut microbiota plays a significant role in host metabolism, immunity, and disease prevention. For example, intestinal microbes are involved in the digestion of plant polysaccharides and the detoxification of food-derived toxins (Kikuchi et al., 2012; Yoo et al., 2020). They also influence host metabolism, immune responses, and cardiovascular health, with emerging evidence showing that dysbiosis of the gut microbiota may contribute to conditions like hypertension (Li et al., 2017; Wilck et al., 2017). During animal evolution, the gut microbiota has played an integral role in the development of host species (Belkaid and Hand, 2014). Therefore, intestinal microbes should be viewed not only as symbiotic organisms but as essential components of animal physiology and behavior. Future research could explore the dynamics of gut microbial communities in equines, particularly their relationships with host immune systems, and how they contribute to maintaining intestinal homeostasis.

To advance our understanding, future studies could investigate the diversity and functional roles of microbial communities across different equine species, management practices, and environmental conditions. Metagenomic approaches can be employed to study the intestinal microbiota in more detail, helping to elucidate the specific contributions of microorganisms to host health. Additionally, regulating the gut microbiota through feed additives or probiotics could be explored as a potential means of enhancing equine health, performance, and feed efficiency. Understanding how microbial communities respond to seasonal and dietary changes and their associated physiological effects is another critical area for investigation.

Therefore, in the future, research on the gut microbiota of equine animals can make breakthrough progress through multi omics techniques. By integrating spatial transcriptomics and single-cell metabolomics, a spatial localization map of microbial host cell interactions can be drawn to reveal the molecular mechanism of key metabolites (such as butyrate) activating the intestinal epithelial energy pathway through G protein coupled receptors. At the same time, we need to break through the bottleneck of anaerobic bacteria *in vitro* culture technology and establish a single-cell database of equine animals; Based on cross species comparative genomics, screening for host genetic microbial co evolutionary markers (such as the synergistic relationship between *KEAP1* gene mutations and abundance of Mongolian horse butyric acid producing bacteria) provides a new target for stress resistant breeding.

At the application level of transformation, the focus will be on precise regulation of athletic performance: based on the enrichment of butyric acid producing bacteria in horse racing, engineering microbial preparations against gastric acid embedding will be developed to promote the biosynthesis of muscle mitochondria through the "gut muscle axis" mechanism; For metabolic diseases, we will analyze the interference mechanism of the microbiota bile acid axis on the FXR/FGF19 pathway under high-fat diet, and use bacteriophages to selectively clear pathogenic streptococcus to inhibit inflammation; We aim to enhance the stress resistance of domestic donkeys through microbiota transplantation by utilizing the characteristic of Akman bacteria to enhance the intestinal barrier of wild donkeys.

Specific intervention measures for equine animals require multidimensional strategies, such as developing tannin cellulose composite slow-release feed to balance the microbial community, adding seasonally adapted microbial agents (such as succinic acid metabolizing bacteria) to stabilize intestinal pH, constructing a comprehensive prevention and control system for antibiotic resistance genes, replacing antibiotics with antimicrobial peptides, targeting CRISPR-Cas9 nanoparticles to eliminate antibiotic resistance plasmids, and introducing anaerobic bacterial niches to inhibit the spread of antibiotic resistant bacteria; Optimize microbiome transplantation technology, establish screening criteria for "super donors," and develop oxygen tolerant bacterial powder capsules.

Applying synthetic biology to construct engineering yeast for large-scale production of short chain fatty acids, while establishing a "microbial diversity red line" for wild horse species to maintain ecological adaptability, ultimately forming a three-dimensional mechanism analysis precise intervention ecological maintenance model: the basic layer draws host microbial holograms, the application layer develops targeted delivery systems and gene editing tools to prevent metabolic diseases, and the ecological layer establishes a germplasm resource microbial library to support genetic diversity protection, thereby connecting the causal chain of "microbial gene host phenotype" and promoting the transformation of the horse industry towards data-driven management.

8 Conclusion

In conclusion, the investigation of the core gut microbiota in equine animals holds significant scientific and practical value. A deeper understanding of the microbial composition and functional dynamics of the equine intestinal tract offers potential for the regulation and optimization of gut health. By refining environmental conditions and dietary strategies, it may be possible to prevent or treat gut-related disorders effectively. This approach promises to enhance the health management and sustainable development of the equine industry. As research advances and technologies progress, the ability to harness and manipulate intestinal microbial resources will likely play a pivotal role in furthering the welfare and productivity of equine populations, contributing to the long-term success of the industry.

Author contributions

FL: Conceptualization, Data curation, Investigation, Methodology, Writing – original draft, Writing – review & editing, Formal analysis. XK: Conceptualization, Investigation, Methodology, Writing – review & editing, Software. MK: Conceptualization, Investigation, Methodology, Writing – review & editing, Data curation, Supervision, Validation, Visualization, Writing – original draft. LW: Data curation, Investigation, Methodology, Writing – review & editing. JW: Investigation, Methodology, Validation, Writing – review & editing. MZ: Conceptualization, Investigation, Visualization, Writing – review & editing. GL: Investigation, Validation, Visualization, Writing – review & editing. BH: Conceptualization, Data curation, Validation, Writing – review & editing. CW: Conceptualization, Funding acquisition, Project administration, Resources, Supervision,

Validation, Visualization, Writing – original draft, Writing – review & editing. ZZ: Conceptualization, Data curation, Funding acquisition, Investigation, Methodology, Project administration, Resources, Software, Supervision, Validation, Visualization, Writing – original draft, Writing – review & editing.

Funding

The author(s) declare that financial support was received for the research and/or publication of this article. This study was funded by the National Key R&D Program of China (grant nos. 2023YFD1302004 and 2022YFD1600103); Shandong Province Modern Agricultural Technology System Donkey Industrial Innovation Team (grant number SDAIT-27), Livestock and Poultry Breeding Industry Project of the Ministry of Agriculture and Rural Affairs (grant no. 19211162), Shandong Province Agricultural Major Technology Collaborative Promotion Plan (SDNYXTTG-2024-13); The Open Project of Liaocheng University Animal Husbandry Discipline (grant no. 319312101-14), The Open Project of Shandong Collaborative Innovation Center for Donkey Industry Technology (grant no. 3193308), Research on Donkey Pregnancy Improvement (grant number K20LC0901), Key R&D Program Project of Shandong Province (2021TZXD012); and Liaocheng University Scientific Research Fund (grant no. 318052025).

Conflict of interest

The authors declare that the research was conducted in the absence of any commercial or financial relationships that could be construed as a potential conflict of interest.

Generative AI statement

The authors declare that no Gen AI was used in the creation of this manuscript.

Any alternative text (alt text) provided alongside figures in this article has been generated by Frontiers with the support of artificial intelligence and reasonable efforts have been made to ensure accuracy, including review by the authors wherever possible. If you identify any issues, please contact us.

Publisher's note

All claims expressed in this article are solely those of the authors and do not necessarily represent those of their affiliated organizations, or those of the publisher, the editors and the reviewers. Any product that may be evaluated in this article, or claim that may be made by its manufacturer, is not guaranteed or endorsed by the publisher.

References

Alessandri, G., Van Sinderen, D., and Ventura, M. (2021). The genus bifidobacterium: from genomics to functionality of an important component of the mammalian gut microbiota running title: Bifidobacterial adaptation to and interaction with the host. *Comput. Struct. Biotechnol. J.* 19, 1472–1487. doi: 10.1016/j.csbj.2021.03.006

Ang, L., Vinderola, G., Endo, A., Kantanen, J., Jingfeng, C., Binetti, A., et al. (2022). Gut microbiome characteristics in feral and domesticated horses from different geographic locations. *Commun Biol* 5:172. doi: 10.1038/s42003-022-03116-2

Antwis, R. E., Lea, J. M. D., Unwin, B., and Shultz, S. (2018). Gut microbiome composition is associated with spatial structuring and social interactions in semi-feral Welsh Mountain ponies. *Microbiome* 6:207. doi: 10.1186/s40168-018-0593-2

Araújo, J. R., Tazi, A., Burlen-Defranoux, O., Vichier-Guerre, S., Nigro, G., Licandro, H., et al. (2020). Fermentation products of commensal bacteria alter enterocyte lipid metabolism. *Cell Host Microbe* 27, 358–375.e7. doi: 10.1016/j.chom.2020.01.028

Ayoub, C., Arroyo, L. G., Mac Nicol, J. L., Renaud, D., Weese, J. S., and Gomez, D. E. (2022). Fecal microbiota of horses with colitis and its association with laminitis and survival during hospitalization. *J. Vet. Intern. Med.* 36, 2213–2223. doi: 10.1111/jvim.16562

Bäckhed, F., Ding, H., Wang, T., Hooper, L. V., Koh, G. Y., Nagy, A., et al. (2004). The gut microbiota as an environmental factor that regulates fat storage. *Proc. Natl. Acad. Sci. USA* 101, 15718–15723. doi: 10.1073/pnas.0407076101

Balakrishnan, B., Luckey, D., Bodhke, R., Chen, J., Marietta, E., Jeraldo, P., et al. (2021). *Prevotella histicola* protects from arthritis by expansion of *Allobaculum* and augmenting butyrate production in humanized mice. *Front. Immunol.* 12:609644. doi: 10.3389/fimmu.2021.609644

Barko, P. C., McMichael, M. A., Swanson, K. S., and Williams, D. A. (2018). The intestinal microbiome: a review. *J. Vet. Intern. Med.* 32, 9–25. doi: 10.1111/jvim.14875

Beckers, K. F., Schulz, C. J., and Childers, G. W. (2017). Rapid regrowth and detection of microbial contaminants in equine fecal microbiome samples. *PLoS One* 12:e0187044. doi: 10.1371/journal.pone.0187044

Belkaid, Y., and Hand, T. W. (2014). Role of the microbiota in immunity and inflammation. *Cell* 157, 121–141. doi: 10.1016/j.cell.2014.03.011

Bell, D. S. (2015). Changes seen in gut bacteria content and distribution with obesity: causation or association? *Postgrad. Med.* 127, 863–868. doi: 10.1080/00325481.2015.1098519

Bermudez-Brito, M., Plaza-Díaz, J., Muñoz-Quezada, S., Gómez-Llorente, C., and Gil, A. (2012). Probiotic mechanisms of action. *Ann. Nutr. Metab.* 61, 160–174. doi: 10.1159/000342079

Bin, P., Azad, M. A. K., Liu, G., Zhu, D., Kim, S. W., and Yin, Y. (2018). Effects of different levels of methionine on sow health and plasma metabolomics during late gestation. *Food Funct.* 9, 4979–4988. doi: 10.1039/C8FO01477A

Blachier, F., Mariotti, F., Huneau, J. F., and Tomé, D. (2007). Effects of amino acid-derived luminal metabolites on the colonic epithelium and physiopathological consequences. *Amino Acids* 33, 547–562. doi: 10.1007/s00726-006-0477-9

Boucher, L., Leduc, L., Leclère, M., and Costa, M. C. (2024). Current understanding of equine gut Dysbiosis and microbiota manipulation techniques: comparison with current knowledge in other species. *Animals (Basel)* 14:758. doi: 10.3390/ani14050758

Broeders, E. P., Nascimento, E. B., Havekes, B., Brans, B., Roumans, K. H., Tailleux, A., et al. (2015). The bile acid chenodeoxycholic acid increases human brown adipose tissue activity. *Cell Metab.* 22, 418–426. doi: 10.1016/j.cmet.2015.07.002

Brulc, J. M., Antonopoulos, D. A., Miller, M. E., Wilson, M. K., Yannarell, A. C., Dinsdale, E. A., et al. (2009). Gene-centric metagenomics of the fiber-adherent bovine rumen microbiome reveals forage specific glycoside hydrolases. *Proc. Natl. Acad. Sci. U. S. A.* 106, 1948–1953. doi: 10.1073/pnas.0806191105

Bulmer, L. S., Murray, J. A., Burns, N. M., Garber, A., Wemelsfelder, F., McEwan, N. R., et al. (2019). High-starch diets alter equine faecal microbiota and increase behavioural reactivity. *Sci. Rep.* 9:18621. doi: 10.1038/s41598-019-54039-8

Campos, C. F., Duarte, M. S., Guimarães, S. E., Verardo, L. L., Wei, S., Du, M., et al. (2016). Review: Animal model and the current understanding of molecule dynamics of adipogenesis. *Animal.* 10, 927–32. doi: 10.1017/S1751731115002992

Cai, C., Xie, L., Xing, J., Lu, T., Qi, X., Li, L., et al. (2024). Effects of concentrate feeding sequence on VFA production, and cecal microbiota of Dezhou donkeys by metagenomic technology. *Front. Vet. Sci.* 11:1401980. doi: 10.3389/fvets.2024.1401980

Chaucheyras-Durand, F., Sacy, A., Karges, K., and Apper, E. (2022). Gastro-intestinal microbiota in equines and its role in health and disease: the black box opens. *Microorganisms* 10:2517. doi: 10.3390/microorganisms10122517

Chen, X., Lou, G., Meng, Z., and Huang, W. (2011). TGR5: a novel target for weight maintenance and glucose metabolism. *Exp. Diabetes Res.* 2011:853501. doi: 10.1155/2011/853501

Conca, N. (2016). Probiotic supplementation and late-onset sepsis in preterm infants: a meta-analysis. *Rev. Chilena Infectol.* 33:239. doi: 10.4067/S0716-10182016000200016

Costa, M. C., Arroyo, L. G., Allen-Vercoe, E., Stämpfli, H. R., Kim, P. T., Sturgeon, A., et al. (2012). Comparison of the fecal microbiota of healthy horses and horses with

colitis by high throughput sequencing of the V3-V5 region of the 16S rRNA gene. *PLoS One* 7:e41484. doi: 10.1371/journal.pone.0041484

Costa, M. C., and Weese, J. S. (2012). The equine intestinal microbiome. *Anim. Health Res. Rev.* 13, 121–128. doi: 10.1017/S1466252312000035

Costa, M. C., and Weese, J. S. (2018). Understanding the intestinal microbiome in health and disease. *Vet. Clin. North Am. Equine Pract.* 34, 1–12. doi: 10.1016/j.cveq.2017.11.005

David, L. A., Maurice, C. F., Carmody, R. N., Gootenberg, D. B., Button, J. E., Wolfe, B. E., et al. (2014). Diet rapidly and reproducibly alters the human gut microbiome. *Nature* 505, 559–563. doi: 10.1038/nature12820

De Filippo, C., Cavalieri, D., Di Paola, M., Ramazzotti, M., Poullet, J. B., Massart, S., et al. (2010). Impact of diet in shaping gut microbiota revealed by a comparative study in children from Europe and rural Africa. *Proc. Natl. Acad. Sci. USA* 107, 14691–14696. doi: 10.1073/pnas.1005963107

De La Torre, U., Henderson, J. D., Furtado, K. L., Pedroja, M., Elenamarie, O., Mora, A., et al. (2019). Utilizing the fecal microbiota to understand foal gut transitions from birth to weaning. *PLoS One* 14:e0216211. doi: 10.1371/journal.pone.0216211

Detman, A., Mielecki, D., Chojnacka, A., Salamon, A., Błaszczyk, M. K., and Sikora, A. (2019). Cell factories converting lactate and acetate to butyrate: Clostridium butyricum and microbial communities from dark fermentation bioreactors. *Microb. Cell Factories* 18:36. doi: 10.1186/s12934-019-1085-1

Dicks, L. M., Botha, M., Dicks, E., and Botes, M. (2014). The equine gastro-intestinal tract: an overview of the microbiota, disease and treatment. *Livest. Sci.* 160, 69–81. doi: 10.1016/j.livsci.2013.11.025

Foligné, B., Dewulf, J., Breton, J., Claisse, O., Lonvaud-Funel, A., and Pot, B. (2010). Probiotic properties of non-conventional lactic acid bacteria: immunomodulation by *Oenococcus oeni*. *Int. J. Food Microbiol.* 140, 136–145. doi: 10.1016/j.ijfoodmicro.2010.04.007

Fuller, M. F., and Reeds, P. J. (1998). Nitrogen cycling in the gut. *Annu. Rev. Nutr.* 18, 385–411. doi: 10.1146/annurev.nutr.18.1.385

Garber, A., Hastie, P., and Murray, J. A. (2020). Factors influencing equine gut microbiota: current knowledge. *J. Equine Vet. Sci.* 88:102943. doi: 10.1016/j.jevs.2020.102943

Gill, H. S., Cross, M. L., Rutherfurd, K. J., and Gopal, P. K. (2001). Dietary probiotic supplementation to enhance cellular immunity in the elderly. *Br. J. Biomed. Sci.* 58, 94–96

Gonçalves, S., Julliand, V., and Leblond, A. (2002). Risk factors associated with colic in horses. *Vet. Res.* 33, 641–652. doi: 10.1051/vetres:2002044

Grieneisen, L., Dasari, M., Gould, T. J., Björk, J. R., Grenier, J. C., Yotova, V., et al. (2021). Gut microbiome heritability is nearly universal but environmentally contingent. *Science* 373, 181–186. doi: 10.1126/science.aba5483

Grimm, P., Philippeau, C., and Julliand, V. (2017). Faecal parameters as biomarkers of the equine hindgut microbial ecosystem under dietary change. *Animal* 11, 1136–1145. doi: 10.1017/S1751731116002779

Guo, R., Sun, Y. J., Zhang, G. L., Huang, J. J., and Liu, S. Q. (2022). Progress on factors influencing intestinal microbial diversity in equine animals. *Chin. Livest. J.* 58, 28–34. doi: 10.19556/j.0258-7033.20210630-07

Guo, Y., Yin, G., Hui, F., Guo, X., Shi, B., Zhao, Y., et al. (2024). Effects of dietary energy level on antioxidant capability, immune function and rectal microbiota in late gestation donkeys. *Front. Microbiol.* 15:1308171. doi: 10.3389/fmicb.2024.1308171

Guo, R., Zhang, W., Shen, W., Zhang, G., Xie, T., Li, L., et al. (2023). Analysis of gut microbiota in Chinese donkey in different regions using metagenomic sequencing. *BMC Genomics* 24:524. doi: 10.1186/s12864-023-09575-z

Gutiérrez-Vázquez, C., and Quintana, F. J. (2018). Regulation of the immune response by the aryl hydrocarbon receptor. *Immunity* 48, 19–33. doi: 10.1016/j.immuni.2017.12.012

Harris, P., and Dunnett, C. (2018). Nutritional tips for veterinarians. *Equine Vet. Educ.* 30, 486–496. doi: 10.1111/eve.12657

He, J., Zhang, P., Shen, L., Niu, L., Tan, Y., Chen, L., et al. (2020). Short-chain fatty acids and their association with Signalling pathways in inflammation, glucose and lipid metabolism. *Int. J. Mol. Sci.* 21:6356. doi: 10.3390/ijms21176356

Hillyer, M. H., Taylor, F. G., Proudman, C. J., Edwards, G. B., Smith, J. E., and French, N. P. (2002). Case control study to identify risk factors for simple colonic obstruction and distension colic in horses. *Equine Vet. J.* 34, 455–463. doi: 10.2746/042516402776117746

Huang, F., Du, X., Ma, Z., Liu, G., Wang, C., and Zhou, M. (2024). Effects of methionine on Milk performance and Milk constituents of lactating donkeys. *Animals (Basel)* 14:3027. doi: 10.3390/ani14203027

Huang, B., Khan, M. Z., Chen, Y., Liang, H., Kou, X., Wang, X., et al. (2023). Yeast polysaccharide supplementation: impact on lactation, growth, immunity, and gut microbiota in Dezhou donkeys. *Front. Microbiol.* 14:1289371. doi: 10.3389/fmicb.2023.1289371

Huang, F., Ma, Z., Du, X., Wang, C., Liu, G., and Zhou, M. (2025). Methionine alters the fecal microbiota and enhances the antioxidant capacity of lactating donkeys. *Animals* 15:648. doi: 10.3390/ani15050648

Jian, Z., Zeng, L., Xu, T., Sun, S., Yan, S., Zhao, S., et al. (2022). The intestinal microbiome associated with lipid metabolism and obesity in humans and animals. *J. Appl. Microbiol.* 133, 2915–2930. doi: 10.1111/jam.15740

Johnson, P. J. (2002). The equine metabolic syndrome peripheral Cushing's syndrome. *Vet. Clin. North Am. Equine Pract.* 18, 271–293. doi: 10.1016/S0749-0739(02)00006-8

Kaiser-Thom, S., Hilty, M., Axiak, S., and Gerber, V. (2021). The skin microbiota in equine pastern dermatitis: a case-control study of horses in Switzerland. *Vet. Dermatol.* 32, 646–e172. doi: 10.1111/vde.12955

Kau, A. L., Ahern, P. P., Griffin, N. W., Goodman, A. L., and Gordon, J. I. (2011). Human nutrition, the gut microbiome and the immune system. *Nature* 474, 327–336. doi: 10.1038/nature10213

Kauter, A., Epping, L., Semmler, T., Antao, E. M., Kannapin, D., Stoeckle, S. D., et al. (2019). The gut microbiome of horses: current research on equine enteral microbiota and future perspectives. *Anim Microbiome* 1:14. doi: 10.1186/s42523-019-0013-3

Kerry, R. G., Patra, J. K., Gouda, S., Park, Y., Shin, H. S., and Das, G. (2018). Benefaction of probiotics for human health: a review. *J. Food Drug Anal.* 26, 927–939. doi: 10.1016/j.jfda.2018.01.002

Khan, M. Z., Chen, W., Wang, X., Liang, H., Wei, L., Huang, B., et al. (2024). A review of genetic resources and trends of omics applications in donkey research: focus on China. *Front Vet Sci* 11:1366128. doi: 10.3389/fvets.2024.1366128

Khan, M. Z., Li, Y., Zhu, M., Li, M., Wang, T., Zhang, Z., et al. (2025). Advances in donkey disease surveillance and microbiome characterization in China. *Microorganisms* 13:749. doi: 10.3390/microorganisms13040749

Kikuchi, Y., Hayatsu, M., Hosokawa, T., Nagayama, A., Tago, K., and Fukatsu, T. (2012). Symbiont-mediated insecticide resistance. *Proc. Natl. Acad. Sci. USA* 109, 8618–8622. doi: 10.1073/pnas.1200231109

Kou, X., Liu, Y., Xiang, F., Zhang, X., Khan, M. Z., Wu, B., et al. (2024a). Insights into the donkey hindgut microbiome using metagenome-assembled genomes. *Animals (Basel)* 14:3625. doi: 10.3390/ani14243625

Kou, X., Ma, Q., Liu, Y., Khan, M. Z., Wu, B., Chen, W., et al. (2024b). Exploring the effect of gastrointestinal Prevotella on growth performance traits in livestock animals. *Animals* 14:1965. doi: 10.3390/ani14131965

Kristensen, N. B., Bryrup, T., Allin, K. H., Nielsen, T., Hansen, T. H., and Pedersen, O. (2016). Alterations in fecal microbiota composition by probiotic supplementation in healthy adults: a systematic review of randomized controlled trials. *Genome Med.* 8:52. doi: 10.1186/s13073-016-0300-5

Lan, Y., Li, Y., and Wang, Y. (2025). Microbiome analysis reveals dynamic changes of gut microbiota in Guizhou horse and Dutch warmblood horses. *Front. Microbiol.* 16:1562482. doi: 10.3389/fmicb.2025.1562482

Ley, R. E., Bäckhed, F., Turnbaugh, P., Lozupone, C. A., Knight, R. D., and Gordon, J. I. (2005). Obesity alters gut microbial ecology. *Proc. Natl. Acad. Sci. USA* 102, 11070–11075. doi: 10.1073/pnas.0504978102

Ley, R. E., Hamady, M., Lozupone, C., Turnbaugh, P. J., Ramey, R. R., Bircher, J. S., et al. (2003). Evolution of mammals and their gut microbes. *Science* 320, 1647–1651. doi: 10.1126/science.1155725

Li, C., Li, X., Guo, R., Ni, W., Liu, K., Liu, Z., et al. (2023). Expanded catalogue of metagenome-assembled genomes reveals resistome characteristics and athletic performance-associated microbes in horse. *Microbiome* 11:7. doi: 10.1186/s40168-022-01448-z

Li, Y., Ma, Q., Liu, G., Zhang, Z., Zhan, Y., Zhu, M., et al. (2022a). Metabolic alternations during gestation in Dezhou donkeys and the link to the gut microbiota. *Front. Microbiol.* 13:801976. doi: 10.3389/fmicb.2022.801976

Li, Y., Ma, Q., Shi, X., Liu, G., and Wang, C. (2022b). Integrated multi-omics reveals novel microbe-host lipid metabolism and immune interactions in the donkey hindgut. *Front. Immunol.* 13:1003247. doi: 10.3389/fimmu.2022.1003247

Li, J., Zhao, F., Wang, Y., Chen, J., Tao, J., Tian, G., et al. (2017). Gut microbiota dysbiosis contributes to the development of hypertension. *Microbiome* 5:14. doi: 10.1186/s40168-016-0222-x

Lin, R., Liu, W., Piao, M., and Zhu, H. (2017). A review of the relationship between the gut microbiota and amino acid metabolism. *Amino Acids* 49, 2083–2090. doi: 10.1007/s00726-017-2493-3

Liu, G. Q. (2020). *Distribution pattern and function prediction of intestinal microorganisms in donkeys (Doctoral dissertation)*. Inner Mongolia Agricultural University.

Liu, G., Bou, G., Su, S., Xing, J., Qu, H., Zhang, X., et al. (2019). Microbial diversity within the digestive tract contents of Dezhou donkeys. *PLoS One* 14:e0226186. doi: 10.1371/journal.pone.0226186

Liu, H., Zhao, X., Han, X., Xu, S., Zhao, L., Hu, L., et al. (2020). Comparative study of gut microbiota in Tibetan wild asses (*Equus kiang*) and domestic donkeys (*Equus asinus*) on the Qinghai-Tibet plateau. *PeerJ* 8:e9032. doi: 10.7717/peerj.9032

Ma, Q., Yue, Y., Kou, X., Hou, W., Wang, M., Yang, X., et al. (2023). Dynamic distribution of skin microorganisms in donkeys at different ages and various sites of the body. *Animals* 13:1566. doi: 10.3390/ani13091566

Mach, N., Midoux, C., Leclercq, S., Pennarun, S., Le Moyec, L., Rué, O., et al. (2022). Mining the equine gut metagenome: poorly-characterized taxa associated with cardiovascular fitness in endurance athletes. *Commun. Biol.* 5:1032. doi: 10.1038/s42003-022-03977-7

Mangiola, F., Nicoletti, A., Gasbarrini, A., and Ponziani, F. R. (2018). Gut microbiota and aging. *Eur. Rev. Med. Pharmacol. Sci.* 22, 7404–7413. doi: 10.26355/eurrev_201811_16280

Marchesi, J. R., and Ravel, J. (2015). The vocabulary of microbiome research: a proposal. *Microbiome* 3:31. doi: 10.1186/s40168-015-0094-5

Matsuki, T., Yahagi, K., Mori, H., Matsumoto, H., Hara, T., Tajima, S., et al. (2016). A key genetic factor for fucosyllactose utilization affects infant gut microbiota development. *Nat. Commun.* 7:11939. doi: 10.1038/ncomms11939

McCann, J. C., Elolimy, A. A., and Loor, J. J. (2017). Rumen microbiome, probiotics, and fermentation additives. *Vet. Clin. North Am. Food Anim. Pract.* 33, 539–553. doi: 10.1016/j.cvfa.2017.06.009

Metges, C. C. (2000). Contribution of microbial amino acids to amino acid homeostasis of the host. *J. Nutr.* 130, 1857S–1864S. doi: 10.1093/jn/130.7.1857S

Metges, C. C., and Petzke, K. J. (2005). Utilization of essential amino acids synthesized in the intestinal microbiota of monogastric mammals. *Br. J. Nutr.* 94, 621–622. doi: 10.1079/BJN20051509

Mueller, N. T., Bakacs, E., Combellick, J., Grigoryan, Z., and Dominguez-Bello, M. G. (2015). The infant microbiome development: mom matters. *Trends Mol. Med.* 21, 109–117. doi: 10.1016/j.molmed.2014.12.002

Murcia, P. R. (2019). Clinical insights: the equine microbiome. *Equine Vet. J.* 51, 714–715. doi: 10.1111/evj.13165

Neavin, D. R., Liu, D., Ray, B., and Weinshilboum, R. M. (2018). The role of the aryl hydrocarbon receptor (AHR) in immune and inflammatory diseases. *Int. J. Mol. Sci.* 19:3851. doi: 10.3390/ijms19123851

Ngui, I. Q. H., Perera, A. P., and Eri, R. (2020). Does NLRP3 Inflammasome and aryl hydrocarbon receptor play an interlinked role in bowel inflammation and colitis-associated colorectal Cancer? *Molecules* 25:2427. doi: 10.3390/molecules25102427

Nishida, A., Inoue, R., Inatomi, O., Bamba, S., Naito, Y., and Andoh, A. (2018). Gut microbiota in the pathogenesis of inflammatory bowel disease. *Clin. J. Gastroenterol.* 11, 1–10. doi: 10.1007/s12328-017-0813-5

Park, J., Kim, M., Kang, S. G., Jannasch, A. H., Cooper, B., Patterson, J., et al. (2015). Short-chain fatty acids induce both effector and regulatory T cells by suppression of histone deacetylases and regulation of the mTOR-S6K pathway. *Mucosal Immunol.* 8, 80–93. doi: 10.1038/mi.2014.44

Pimenta, J., Pinto, A. R., Saavedra, M. J., and Cotovio, M. (2023). Equine gram-negative Oral microbiota: an antimicrobial resistances watcher? *Antibiotics (Basel)* 12:792. doi: 10.3390/antibiotics12040792

Qin, X., Xi, L., Zhao, L., Han, J., Qu, H., Xu, Y., et al. (2025). Exploring the distinctive characteristics of gut microbiota across different horse breeds and ages using metataxonomics. *Front. Cell. Infect. Microbiol.* 15:1590839. doi: 10.3389/fcimb.2025.1590839

Quigley, E. M. M. (2017). Microbiota-brain-gut Axis and neurodegenerative diseases. *Curr. Neurol. Neurosci. Rep.* 17:94. doi: 10.1007/s11910-017-0802-6

Radecki, S. V., and Yokoyama, M. T. (2001). "Intestinal Bacteria and their influence on swine nutrition-science direct" in Swine Nutrition. ed. S. V. Radecki (Boca Raton, FL: CRC Press), 439–447.

Raspa, F., Chessa, S., Bergero, D., Sacchi, P., Ferrocino, I., Cocolin, L., et al. (2024). Microbiota characterization throughout the digestive tract of horses fed a high-fiber vs. a high-starch diet. *Front Vet Sci* 11:1386135. doi: 10.3389/fvets.2024.1386135

Reed, K. J., Kunz, I. G., Scare, J. A., Nielsen, M. K., Turk, P. J., Coleman, R. J., et al. (2021). The pelvic flexure separates distinct microbial communities in the equine hindgut. *Sci. Rep.* 11:4332. doi: 10.1038/s41598-021-83783-z

Richards, N., Hinch, G., and Rowe, J. (2006). The effect of current grain feeding practices on hindgut starch fermentation and acidosis in the Australian racing thoroughbred. *Aust. Vet. J.* 84, 402–407. doi: 10.1111/j.1751-0813.2006.00059.x

Roager, H. M., and Licht, T. R. (2018). Microbial tryptophan catabolites in health and disease. *Nat. Commun.* 9:3294. doi: 10.1038/s41467-018-05470-4

Salem, S. E., Maddox, T. W., Berg, A., Antczak, P., Ketley, J. M., Williams, N. J., et al. (2018). Variation in faecal microbiota in a group of horses managed at pasture over a 12-month period. *Sci. Rep.* 8:8510. doi: 10.1038/s41598-018-26930-3

Santos, A. S., Jerónimo, E., Ferreira, L. M., Rodrigues, M. A., and Bessa, R. J. (2013). Technical note: fatty acids and purine profile of cecum and colon bacteria as indicators of equine microbial metabolism. *J. Anim. Sci.* 91, 1753–1757. doi: 10.2527/jas.2011-4892

Sävilammi, T., Alakangas, R. R., Häyrynen, T., and Uusi-Heikkilä, S. (2024). Gut microbiota profiling as a promising tool to detect equine inflammatory bowel disease (IBD). *Animals* 14:2396. doi: 10.3390/ani14162396

Schoster, A., Staempfli, H. R., Guardabassi, L. G., Jalali, M., and Weese, J. S. (2017). Comparison of the fecal bacterial microbiota of healthy and diarrheic foals at two and four weeks of life. *BMC Vet. Res.* 13:144. doi: 10.1186/s12917-017-1064-x

Schwiertz, A., Taras, D., Schäfer, K., Beijer, S., Bos, N. A., Donus, C., et al. (2010). Microbiota and SCFA in lean and overweight healthy subjects. *Obesity (Silver Spring)* 18, 190–195. doi: 10.1038/oby.2009.167

Sha, Y., Yu, J., Xia, D., Zhang, Y., Liu, J., and Wang, H. (2024). Remodeling of intestinal bacterial community and metabolome of Dezhou donkey induced by corn silage. *Sci. Rep.* 14:17032. doi: 10.1038/s41598-024-67869-y

Singh, N., Gurav, A., Sivaprakasam, S., Brady, E., Padia, R., Shi, H., et al. (2014). Activation of Gpr 109a, receptor for niacin and the commensal metabolite butyrate, suppresses colonic inflammation and carcinogenesis. *Immunity* 40, 128–139. doi: 10.1016/j.immuni.2013.12.007

Spence, C., Wells, W. G., and Smith, C. J. (2006). Characterization of the primary starch utilization operon in the obligate anaerobe *Bacteroides fragilis*: regulation by carbon source and oxygen. *J. Bacteriol.* 188, 4663–4672. doi: 10.1128/JB.00125-06

Stewart, H. L., Southwood, L. L., Indugu, N., Vecchiarelli, B., Engiles, J. B., and Pitta, D. (2019). Differences in the equine faecal microbiota between horses presenting to a tertiary referral hospital for colic compared with an elective surgical procedure. *Equine Vet. J.* 51, 336–342. doi: 10.1111/evj.13010

Stothart, M. R., McLoughlin, P. D., Medill, S. A., Greuel, R. J., Wilson, A. J., and Poissant, J. (2024). Methanogenic patterns in the gut microbiome are associated with survival in a population of feral horses. *Nat. Commun.* 15:6012. doi: 10.1038/s41467-024-49963-x

Su, L., Guo, J., Shi, W., Tong, W., Li, X., Yang, B., et al. (2024). Metagenomic analysis reveals the community composition of the microbiome in different segments of the digestive tract in donkeys and cows: implications for microbiome research. *BMC Microbiol.* 24:530. doi: 10.1186/s12866-024-03696-5

Su, S., Zhao, Y., Liu, Z., Liu, G., Du, M., Wu, J., et al. (2020). Characterization and comparison of the bacterial microbiota in different gastrointestinal tract compartments of Mongolian horses. *Microbiology* 9, 1085–1101. doi: 10.1002/mbo3.1020

Torrallardona, D., Harris, C. I., and Fuller, M. F. (2003). Lysine synthesized by the gastrointestinal microflora of pigs is absorbed, mostly in the small intestine. *Am. J. Physiol. Endocrinol. Metab.* 284, E1177–E1180. doi: 10.1152/ajpendo.00465.2002

Virtue, A. T., McCright, S. J., Wright, J. M., Jimenez, M. T., Mowel, W. K., Kotzin, J. J., et al. (2019). The gut microbiota regulates white adipose tissue inflammation and obesity via a family of micro RNAs. *Sci. Transl. Med.* 11:eaav1892. doi: 10.1126/scitranslmed.aav1892

Walshe, N., Duggan, V., Cabrera-Rubio, R., Crispie, F., Cotter, P., Feehan, O., et al. (2019). Removal of adult cyathostomins alters faecal microbiota and promotes an inflammatory phenotype in horses. *Int. J. Parasitol.* 49, 489–500. doi: 10.1016/j.ijpara.2019.02.003

Wang, Y., Hu, T., Liang, K., Li, S., Zhang, Q., Li, W., et al. (2025a). Spatial variations in the microbiota: comparative analysis of microbial composition and predicted functions across different intestinal segments and feces in donkeys. *Front. Microbiol.* 15:1494926. doi: 10.3389/fmicb.2024.1494926

Wang, Y., Li, X., Li, Z., Han, Q., Hu, T., Zhang, Q., et al. (2025b). Comparative analysis of composition and spatial variations in the foregut microbiota of male and female donkeys. *Front. Microbiol.* 16:1532265. doi: 10.3389/fmicb.2025.1532265

Wilck, N., Matus, M. G., Kearney, S. M., Olesen, S. W., Forslund, K., Bartolomaeus, H., et al. (2017). Salt-responsive gut commensal modulates TH17 axis and disease. *Nature* 551, 585–589. doi: 10.1038/nature24628

Wu, G. D., Chen, J., Hoffmann, C., Bittinger, K., Chen, Y. Y., Keilbaugh, S. A., et al. (2011). Linking long-term dietary patterns with gut microbial enterotypes. *Science* 334, 105–108. doi: 10.1126/science.1208344

Wu, Z., Nguyen, D., Lam, T. Y. C., Zhuang, H., Shrestha, S., Raskin, L., et al. (2021). Synergistic association between cytochrome bd-encoded Proteiniphilum and reactive oxygen species (ROS)-scavenging methanogens in microaerobic-anaerobic digestion of lignocellulosic biomass. *Water Res.* 190:116721. doi: 10.1016/j.watres.2020.116721

Wunderlich, G., Bull, M., Ross, T., Rose, M., and Chapman, B. (2023). Understanding the microbial fibre degrading communities & processes in the equine gut. *Anim. Microbiome* 5:3. doi: 10.1186/s42523-022-00224-6

Xie, L., Xing, J., Qi, X., Lu, T., Jin, Y., Akhtar, M. F., et al. (2023). Effects of concentrate feeding sequence on growth performance, nutrient digestibility, VFA production, and fecal microbiota of weaned donkeys. *Animals* 13:2893. doi: 10.3390/ani13182893

Xing, J., Jia, M., Zhang, G., Li, L., Liu, S., Li, G., et al. (2025). The composition and predictive function of the fecal microbiota in female donkeys across different reproductive cycles. *Front. Microbiol.* 16:1565360. doi: 10.3389/fmicb.2025.1565360

Xu, J., Bjursell, M. K., Himrod, J., Deng, S., Carmichael, L. K., Chiang, H. C., et al. (2003). A genomic view of the human-*Bacteroides thetaiotaomicron* symbiosis. *Science* 299, 2074–2076. doi: 10.1126/science.1080029

Yang, Q., Liu, H., Jafari, H., Liu, B., Wang, Z., Su, J., et al. (2024). Metabolic changes before and after weaning in Dezhou donkey foals in relation to gut microbiota. *Front. Microbiol.* 14:1306039. doi: 10.3389/fmicb.2023.1306039

Yang, W., Yu, T., Huang, X., Bilotta, A. J., Xu, L., Lu, Y., et al. (2020). Intestinal microbiota-derived short-chain fatty acids regulation of immune cell IL-22 production and gut immunity. *Nat. Commun.* 11:4457. doi: 10.1038/s41467-020-18262-6

Yin, F., Yu, H., Lepp, D., Shi, X., Yang, X., Hu, J., et al. (2016). Correction: transcriptome analysis reveals regulation of gene expression for lipid catabolism in young broilers by butyrate glycerides. *PLoS One* 11:e162150. doi: 10.1371/journal.pone.0162150

Yoo, J. Y., Groer, M., Dutra, S. V. O., Sarkar, A., and McSkimming, D. I. (2020). Gut microbiota and immune system interactions. *Microorganisms* 8:1587. doi: 10.3390/microorganisms8101587

Zhang, W., Guo, R., Song, F. F., Wang, Y. Y., Sun, Y. J., and Liu, S. Q. (2024). Analysis of the characteristic microflora of fecal microorganisms in Yunnan donkeys. *Chin. Livest. J.* 6, 160–170. doi: 10.19556/j.0258-7033.20230512-05

Zhang, Z., Huang, B., Gao, X., Shi, X., Wang, X., Wang, T., et al. (2023). Dynamic changes in fecal microbiota in donkey foals during weaning: from pre-weaning to post-weaning. *Front. Microbiol.* 14:1105330. doi: 10.3389/fmicb.2023.1105330

Zhang, Z., Huang, B., Shi, X., Wang, T., Wang, Y., Zhu, M., et al. (2022a). Comparative analysis of bacterial diversity between the liquid phase and adherent fraction within the donkey Caeco-colic ecosystem. *Animals (Basel)* 12:1116. doi: 10.3390/ani12091116

Zhang, Z., Huang, B., Wang, Y., Zhan, Y., Zhu, M., and Wang, C. (2022b). Dynamic alterations in the donkey fecal bacteria community and metabolome characteristics during gestation. *Front. Microbiol.* 13:927561. doi: 10.3389/fmicb.2022.927561

Zhang, Z., Huang, B., Wang, Y., Zhu, M., and Wang, C. (2022c). Could weaning remodel the oral microbiota composition in donkeys? An exploratory study. *Animals (Basel)* 12:2024. doi: 10.3390/ani12162024

Zhang, Z., Wang, Y., Huang, B., Zhu, M., and Wang, C. (2022d). The Fibrolytic enzyme profiles and the composition of fungal communities in donkey cecum-Colon ecosystem. *Animals (Basel)* 12:412. doi: 10.3390/ani12040412

Zhang, Z., Wang, Y., Zhu, M., and Wang, C. (2022e). The in vitro digestion and fermentation characteristics of feedstuffs inoculated with cecal or colic fluid of Dezhou donkey. *J. Equine Vet. Sci.* 110:103864. doi: 10.1016/j.jevs.2022.103864

Zhang, R., Zhang, J., Dang, W., Irwin, D. M., Wang, Z., and Zhang, S. (2020). Unveiling the biogeography and potential functions of the intestinal Digesta- and mucosa-associated microbiome of donkeys. *Front. Microbiol.* 11:596882. doi: 10.3389/fmicb.2020.596882

Zhang, C., Zhang, C., Wang, Y., Du, M., Zhang, G., and Lee, Y. (2021). Dietary energy level impacts the performance of donkeys by manipulating the gut microbiome and metabolome. *Front. Vet. Sci.* 8:694357. doi: 10.3389/fvets.2021.694357

Zhang, C., Zhen, Y., Weng, Y., Lin, J., Xu, X., Ma, J., et al. (2025). Research progress on the microbial metabolism and transport of polyamines and their roles in animal gut homeostasis. *J. Anim. Sci. Biotechnol.* 16:57. doi: 10.1186/s40104-025-01193-x

Zhao, F., Jiang, G., Ji, C., Zhang, Z., Gao, W., Feng, P., et al. (2020). Effects of long-distance transportation on blood constituents and composition of the nasal microbiota in healthy donkeys. *BMC Vet. Res.* 16:338. doi: 10.1186/s12917-020-02563-5

Zhao, Y., Li, B., Bai, D., Huang, J., Shiraigo, W., Yang, L., et al. (2016). Comparison of fecal microbiota of Mongolian and thoroughbred horses by high-throughput sequencing of the V4 region of the 16S rRNA gene. *Asian Australas. J. Anim. Sci.* 29, 1345–1352. doi: 10.5713/ajas.15.0587

Zhou, M., Huang, F., Du, X., Liu, G., and Wang, C. (2023b). Analysis of the differentially expressed proteins in donkey milk in different lactation stages. *Foods* 12:4466. doi: 10.3390/foods12244466

Zhou, M., Huang, F., Du, X., Wang, C., and Liu, G. (2023a). Microbial quality of donkey milk during lactation stages. *Foods* 12:4272. doi: 10.3390/foods12234272

frontiers | Frontiers in Microbiology

TYPE Original Research
PUBLISHED 29 September 2025
DOI 10.3389/fmicb.2025.1615297

Check for updates

OPEN ACCESS

EDITED BY
Mohammad Altamimi,
An-Najah National University, Palestine

REVIEWED BY
Yina Huang,
Anhui Polytechnic University, China
Zixu Chen,
Shandong University, China

*CORRESPONDENCE
Weihua Chu
✉ chuweihua@cpu.edu.cn
Tianyu Bai
✉ baitianyu19821025@163.com

†These authors have contributed equally to this work

RECEIVED 21 April 2025
ACCEPTED 08 September 2025
PUBLISHED 29 September 2025

CITATION
Bai X, Wang Y, Wang K, Chu W and Bai T (2025) Guiren Runchang granules alleviate slow transit constipation in mice by modulating gut microbiota and short-chain fatty acids.
Front. Microbiol. 16:1615297.
doi: 10.3389/fmicb.2025.1615297

COPYRIGHT
© 2025 Bai, Wang, Wang, Chu and Bai. This is an open-access article distributed under the terms of the Creative Commons Attribution License (CC BY). The use, distribution or reproduction in other forums is permitted, provided the original author(s) and the copyright owner(s) are credited and that the original publication in this journal is cited, in accordance with accepted academic practice. No use, distribution or reproduction is permitted which does not comply with these terms.

Guiren Runchang granules alleviate slow transit constipation in mice by modulating gut microbiota and short-chain fatty acids

Xinfeng Bai[1†], Yachao Wang[1†], Kai Wang[1], Weihua Chu[1,2*] and Tianyu Bai[1*]

[1]Microecological Medicine Research Center, Shandong Provincial Third Hospital, Shandong University, Jinan, China, [2]Department of Microbiology and Synthetic Biology, School of Life Science and Technology, China Pharmaceutical University, Nanjing, China

Guiren Runchang Granules (GRG), a traditional Chinese medicine (TCM) formulation, has demonstrated effectiveness in treating slow transit constipation (STC). This study investigated the therapeutic effects of GRG on constipated mice, focusing on its role in restoring intestinal micro-ecology. The results showed that GRG treatment significantly improved defecation in STC mice and ameliorated intestinal histopathological damage. GRG effectively normalized colonic and serum motility-related hormone levels (5-HT, SP, MTL, and SS) with comparable efficacy to mosapride, a prokinetic agent. In addition, GRG treatment restored the balance of the gut microbiota and increased the levels of short-chain fatty acids (SCFAs). Specifically, the relative abundance of the genera *Alloprevotella* and *Muribaculum* increased, while that of *Prevotellaceae_NK3B31_group*, *Ruminococcus*, and *Lachnospiraceae_UCG-001* decreased. These microbiota changes were significantly correlated with SCFAs level, motility-related hormone concentrations, and defecation phenotype. Our findings highlight GRG's multi-target mode of action involving microbiota modulation, SCFAs restoration, and hormonal regulation, positioning it as a promising alternative to conventional therapies for STC.

KEYWORDS

traditional Chinese medicine, Guiren Runchang granule, constipation, gut microbiota, SCFAs

1 Introduction

Functional constipation, a prevalent gastrointestinal disorder affecting over 15% of the global population (Barberio et al., 2021), imposes significant socioeconomic burdens and compromises quality of life (Harris and Chang, 2022). Chronic constipation can damage the intestinal wall and promote the accumulation of harmful substances and pathogenic bacteria, which are critical risk factors for colorectal cancer (Song et al., 2021). Constipation is also associated with an increased risk of cardiovascular disease, Parkinson's disease, and depression (Sumida et al., 2019).

The pathogenesis of STC involves intricate interactions among neurological disorders, hormonal imbalances, smooth muscle dysfunction, abnormal interstitial cells of Cajal (ICCs), and disruptions in the gut microbiota (Bharucha and Lacy, 2020). The gut microbiota plays a central role in regulating gastrointestinal physiology and maintaining intestinal function (Fan

and Pedersen, 2021). The gut microbiota contributes to suppressing pathogen overgrowth, maintaining the integrity of the mucosal barrier (Martens et al., 2018), and supporting the development of the enteric nervous system (Vicentini et al., 2021). Moreover, bacterial metabolites such as SCFAs, bile acids, and tryptophan derivatives are closely linked to intestinal integrity and motility (Bhattarai et al., 2018). Accumulating evidence positions the gut microbiota dysbiosis as a major risk factor for constipation (Ohkusa et al., 2019). Clinical evidence showing abnormal gut microbiota profiles in constipated patients (Shin et al., 2019), suggesting microbiota-directed therapies could offer novel therapeutic avenues.

Current pharmacological interventions, mainly including osmotic laxatives, secretagogues, and prokinetic agents (Pannemans et al., 2020; Gao et al., 2022), primarily target symptom relief but exhibit limited long-term efficacy and safety concerns, such as electrolyte imbalance and tachyphylaxis effects (Vriesman et al., 2020). TCM formulations, characterized by multi-component synergism, have been widely used to treat digestive disorders (Wang et al., 2022). Unlike conventional monotherapies, TCM exerts holistic effects by modulating gut microbiota, enhancing beneficial intestinal metabolites, promoting intestinal mucosal secretion, and protecting the epithelial barrier. GRG, a TCM compound, has shown clinical efficacy in alleviating STC symptoms. Previous studies attribute GRG's activity to aquaporin modulation and ICCs protection (Sun et al., 2020). However, its interplay with the microbiota remains unexplored. This study established a loperamide-induced STC mouse model to evaluate the therapeutic effects of GRG, focusing on its effects on intestinal motility, gut microbiota, and SCFAs production.

2 Materials and methods

2.1 Chemicals and reagents

Guiren Runchang granules were prepared by the Traditional Chinese Medicine Pharmacy of Shandong Provincial Third Hospital, following previously published methods (Sun et al., 2020). GRG is a compound TCM formula composed of 10 medicinal materials, as detailed in Supplementary Table S1. Loperamide hydrochloride was obtained from Xi'an Yang Sen Pharmaceutical Co. Ltd. (Xi'an, China), and mosapride citrate was purchased from Shandong New Time Pharmaceutical Co., Ltd. (China). Kits for enzyme-linked immunosorbent assays (ELISA), specifically for motilin (MTL), substance-P (SP), somatostatin (SS), vasoactive intestinal peptide (VIP), and serotonin (5-HT), were sourced from Cusabio Biotech (Wuhan, China). SCFA standards (acetic acid, propionic acid, butyric acid, isobutyric acid, valeric acid, isovaleric acid, and hexanoic acid) were procured from Sigma-Aldrich Co. LLC (Shanghai, China). India ink was obtained from Sangon Biotech (Shanghai, China). All additional reagents and chemicals employed in this study were of analytical grade.

Abbreviations: 5-HT, Serotonin; GRG, Guiren Runchang granules; HD, High-dose group; ICCs, Interstitial cells of Cajal; LD, Low-dose group; MD, Medium-dose group; MO, Mosapride-treated positive control; MTL, Motilin; NC, Normal control; SCFAs, Short-chain fatty acids; SP, Substance-P; SS, Somatostatin; STC, Slow transit constipation; TCM, Traditional Chinese medicine; VIP, Vasoactive intestinal peptide.

2.2 Animal experiment

Male BALB/c mice (6 weeks old, weighing 18–20 g, Jinan Pengyue Experimental Animal Co., Ltd., Jinan, China) were housed in a specific pathogen-free environment at 20–25°C with 40–60% relative humidity and a 12-h light/dark cycle. During the experiment, the mice were provided with unrestricted access to both food and water.

After a week of acclimation, 60 mice were randomized into six groups (10 mice per group): the normal control (NC), STC model, mosapride-treated positive control (MO), and low-dose (LD), medium-dose (MD), and high-dose (HD) GRG treatment groups. Mice within each group were housed in two cages (5 mice per cage). The STC model was established as previous study (Liu et al., 2023). All groups except NC were administered 10 mg/kg loperamide daily for 14 days. Therapeutic interventions commenced the day after model establishment and continued for 14 days. The dosages of GRG for intragastric administration were determined by converting the standard human clinical dose of GRG to a mouse equivalent dose (MED) using body surface area normalization. The LD, MD, and HD groups were treated by gavage with 4.72 g/kg/d, 9.44 g/kg/d, and 18.88 g/kg/d GRG, respectively, which were comparable to adult clinical sub effective, equivalent, and super therapeutic doses (Sun et al., 2020). The MO group received mosapride suspension, and the NC and STC groups were treated with saline.

On day 36, fresh fecal samples were firstly collected for microbiota and SCFA analysis. Mice were then transferred to clean cages to collect 1 h fresh feces and 12 h feces for defecation parameters. Subsequently, mice underwent a 12 h fasting period. Intestinal motility tests were performed on day 37, and mice were then euthanized under anesthesia for serum and colon tissue collection. Subsequently, these samples were subjected to experimental test.

2.3 Measurement of defecation parameters

After daily gavage, fresh feces produced over 1 h were collected, and their wet and dry weights were recorded. Fecal water content was calculated: Water content of the feces (%) = (wet weight-dry weight)/wet weight × 100% and the total feces produced during this period were collected for further analysis.

2.4 Determination of intestinal motility

Intestinal motility in mice was evaluated utilizing a small intestine transit rate test and a first black defecation experiment. Post 12 h fasting, 2 mice per cage (4 mice/group) were randomly selected using stratified sampling for the small intestine transit rate test. Each mouse received 0.2 mL of India ink via oral gavage. After 30 min, four mice were euthanized, and the small intestines were excised from the pylorus to the cecum. The intestinal transit rate was calculated: Intestinal transit rate (%) = transited distance by the Indian ink/total length of the small intestine × 100%.

Subsequently, another 2 mice per cage (4 mice/group) were randomly chosen for the first black defecation experiment. The mice were individually placed in clean cages to record the time to first black defecation.

2.5 Measurement of serum and colon hormones

Blood samples were obtained through retro-orbital collection following anesthesia. The samples were allowed to clot at ambient temperature for 2 h, then centrifuged at 3000 × g for 15 min at 4°C to separate the serum. The proximal colon tissue was dissected, washed with saline, and divided into three parts: two portions were stored at −80°C for hormone analysis and RNA extraction, while the third portion was fixed in 4% paraformaldehyde.

The contents of the MTL, SP, SS, VIP and 5-HT in the serum and colon samples Serum and colonic concentrations of MTL, SP, SS, VIP, and 5-HT were determined using a commercially ELISA kits.

2.6 Histopathological examination

Colon tissue sections were evaluated by independent pathologist blinded to the experimental group assignments. Fixed colon tissues were used to assess morphological changes. The tissues were dehydrated for 24 h, embedded in paraffin, sectioned, and stained with hematoxylin and eosin (H&E). Histological features were examined under an optical microscope.

2.7 16S rRNA sequencing and fecal microbiota analysis

The composition of fecal microbiota was analyzed by 16S rRNA gene-based amplicon sequencing method. Bacterial DNA was extracted from fecal samples using the ZR Fecal DNA Extraction Kit (Zymo Research, CA, USA). The variable V4 region of the 16S rRNA gene was amplified with barcoded specific bacterial primers 515F (5′-GTGCCAGCMGCCGCGGTAA-3′) and 806R (5′-GGACTA CHVGGGTWTCTAAT-3′). The amplicons were purified utilizing a DNA gel extraction kit (OMEGA, USA). Sequencing libraries were prepared employing the TruSeq® DNA PCR-Free Sample Preparation Kit (Illumina, USA). Paired-end sequencing was performed on an Illumina HiSeq 2,500 platform (Illumina Inc., San Diego, CA, USA). Sequencing data processing and microbial composition analysis were conducted as previously described (Jia et al., 2024). QIIME II software (version 1.9.1) was used for data processing and analysis. The raw data underwent denoising to generate amplicon sequence variants using the DADA2 algorithm.

Community richness and diversity were quantified using the Chao1 and Shannon indices, respectively. To evaluate the relationships between samples, principal coordinate analysis (PCoA) was performed, providing insights into sample clustering in a low-dimensional space. Differential species were identified using t-test analysis. Microbial metabolic functions were inferred using PICRUSt 2, which maps species composition from 16S rRNA sequencing data to Kyoto Encyclopedia of Genes and Genomes (KEGG) metabolic pathways.

2.8 Quantification of SCFAs in fecal samples

The levels of SCFAs, including acetic acid, propionic acid, butyric acid, isobutyric acid, valeric acid, isovaleric acid, and caproic acid, in fecal samples were measured utilizing gas chromatography–mass spectrometry. Immediately after collection, fecal samples were promptly frozen and preserved at −80°C. Approximately 30 mg of each sample was suspended in 900 μL of 0.5% phosphoric acid and homogenized with a tissue grinder for 3 min. After centrifugation at 10,000 × *g* for 10 min, the clear supernatant was collected. An 800 μL aliquot of the supernatant was combined with an equal volume of ethyl acetate, vortexed for 5 min, and then centrifuged at 14,000 × *g* for 10 min. A 600 μL aliquot of the organic phase was extracted for analysis. SCFA concentrations were determined employing an Agilent 7890A/5975C GC–MS system (Agilent Technologies, USA) equipped with a DB-WAX capillary column (30 m × 0.25 mm, ID × 0.25 μm). Quantification was performed by comparing sample peak areas to standard calibration curves (Guo et al., 2022).

2.9 Statistical analysis

The data were analyzed using GraphPad Prism 9.0. The experiment data were expressed as mean ± standard deviation. Differences among multiple groups were assessed by one-way ANOVA followed by the Tukey–Kramer post-hoc test. The student's t-test was used to analyze the comparison between the two groups. A value of $p < 0.05$ was considered statistically significant. Comparison with the NC group is denoted as #, with #$p < 0.05$, ##$p < 0.01$, and ###$p < 0.001$. Comparison with the MC group is denoted as *, with * $p < 0.05$, ** $p < 0.01$, and *** $p < 0.001$.

3 Results

3.1 GRG treatment improves constipation phenotype

The experimental work flow is outlined in Figure 1A. The therapeutic effects of GRG on constipated mice were evaluated following treatment. In terms of defecation phenotype, compared to the healthy group, model mice exhibited significantly smaller fecal pellets, reduced fecal moisture content, and a lower total fecal output over 12 h ($p < 0.001$). Treatment with GRG or mosapride significantly alleviated these symptoms (Figures 1B–D). In terms of gastrointestinal motility phenotype, loperamide administration markedly impaired gastrointestinal motility, evidenced by prolonged defecation time and a reduced intestinal transit rate ($p < 0.001$). Both GRG and mosapride significantly improved these motility impairments (Figures 1E–G). A dose-dependent effect was observed for GRG across all phenotypes. Notably, high-dose GRG exhibited therapeutic efficacy comparable to, or even exceeding, that of the positive control drug, mosapride.

3.2 GRG treatment repairs colon damage caused by constipation

H&E staining was employed to assess morphological changes in the colon (Figure 2). Constipation induced significant damage to the colonic tissue, characterized by irregular glandular arrangement, apparent reduction in goblet cells, and inflammatory cell infiltration. Treatment with GRG or mosapride effectively ameliorated these structural abnormalities, showing a trend towards

10.3389/fmicb.2025.1615297

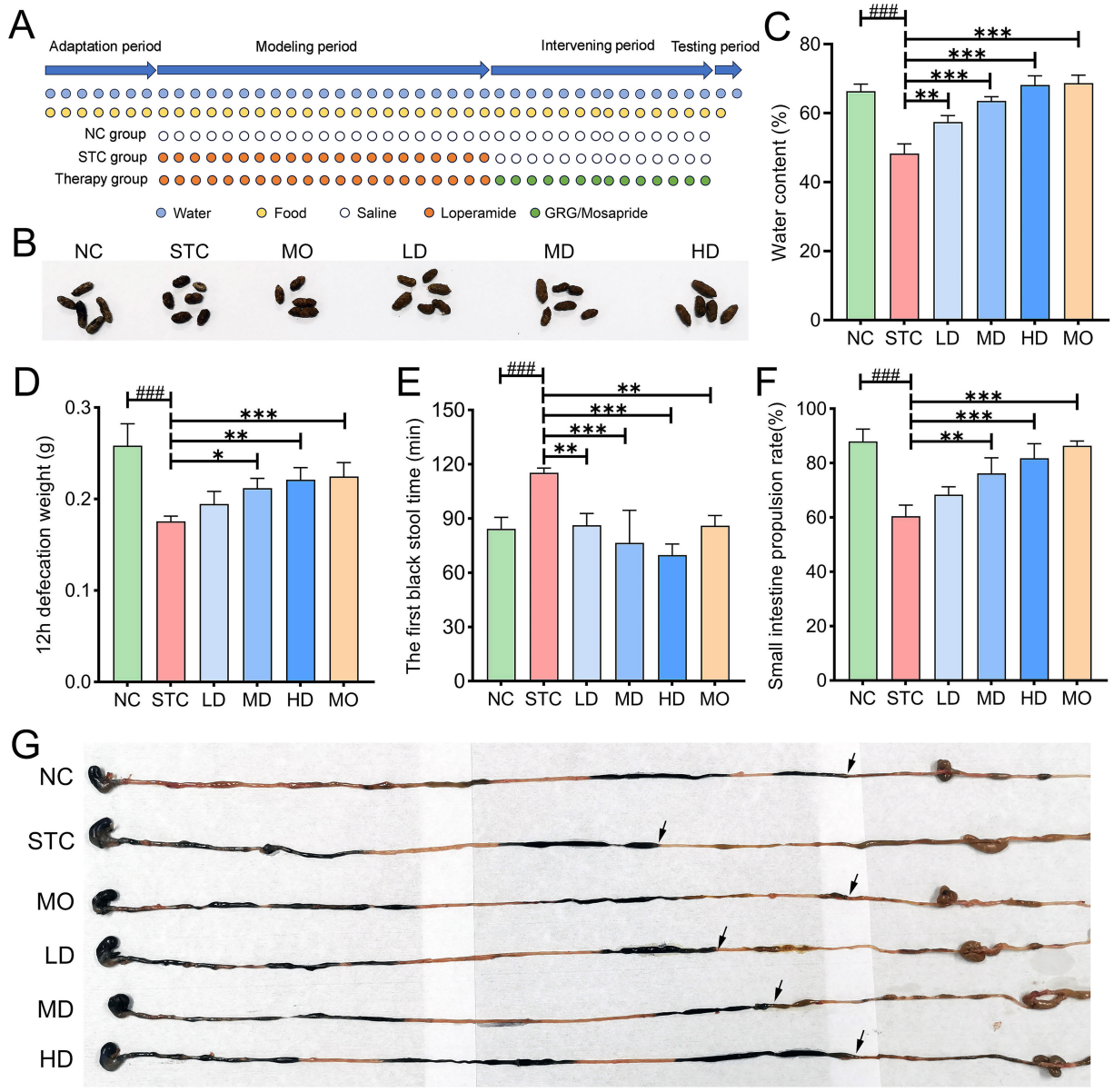

FIGURE 1
Effects of GRG on loperamide-induced constipation mice. **(A)** Experimental design. **(B)** The shape of collected feces. **(C)** Fecal water content. **(D)** The weight of 12 h feces. **(E)** The first black stool defecation time. **(F)** Gastrointestinal transit rate. **(G)** The intestinal propelling length of ink. Values are presented as mean ± SD, $n = 4$. ###$p < 0.001$, NC vs. STC. *$p < 0.05$, **$p < 0.01$, ***$p < 0.001$, LD, MD, HD and MO vs. STC.

restoration of a more normal colonic architecture with clearer glandular structure and a visible increase in goblet cells compared to the STC group.

3.3 GRG regulates motility-related hormone levels in colonic tissue and serum

Gastrointestinal motility is closely regulated by gut hormones. This study measured hormone levels in colonic tissue and serum using ELISA. As shown in Figure 3, loperamide significantly disrupted hormone levels, leading to decreased stimulatory hormones (5-HT, MTL, and SP) and increased inhibitory hormones (SS and VIP) in both colonic tissue and serum. Medium- and high-dose GRG treatments effectively restored the levels of all five hormones in colonic tissue ($p < 0.05$). The reparative effects of GRG on 5-HT, SP, and SS were comparable to those of mosapride, while high-dose GRG demonstrated a significantly stronger effect on MTL compared to mosapride. However, GRG's impact on VIP was less pronounced than mosapride. A clear dose–response effect was observed for MTL and VIP. In serum, medium- and high-dose GRG treatments significantly restored 5-HT, MTL, and SS levels, while high-dose GRG also restored SP and VIP levels. High-dose GRG exhibited comparable effects to mosapride on serum 5-HT and VIP levels, with a more pronounced impact on SP and SS levels. Notably, the dose–response effect of GRG on hormone regulation was more pronounced in

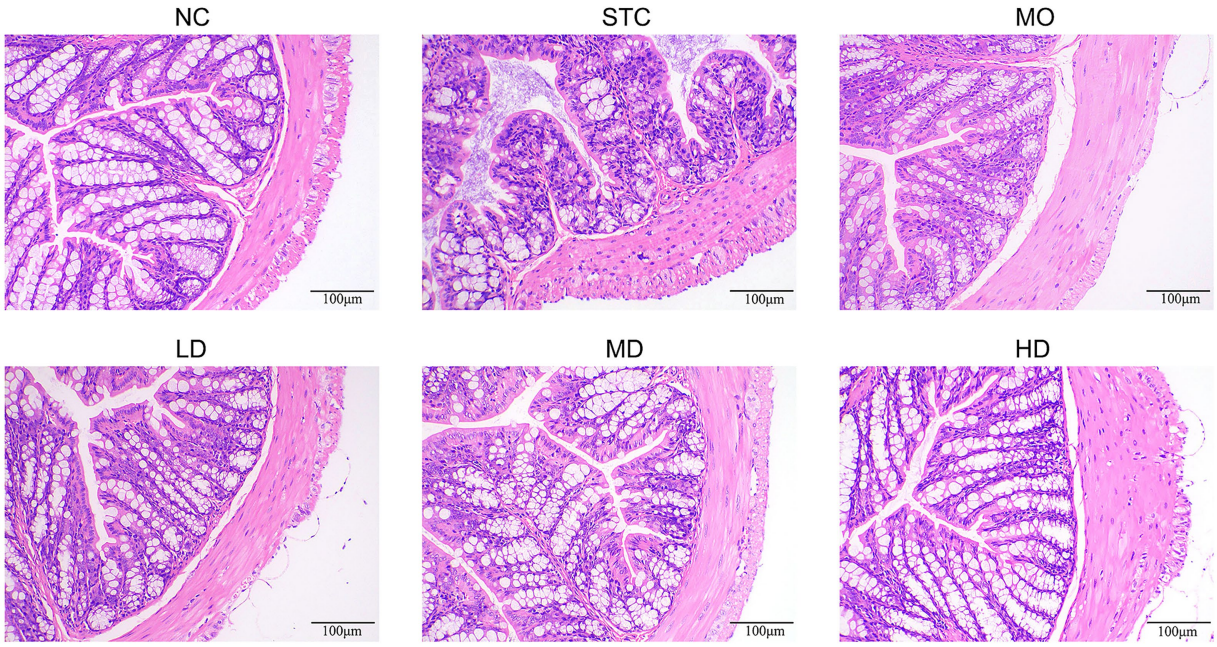

FIGURE 2
Effects of GRG on histology of colonic tissue.

serum than in colonic tissue. These results indicate that GRG significantly regulates motility-related hormone secretion in both colonic tissue and serum, exhibiting a clear dose-dependent therapeutic effect.

3.4 GRG treatment improves the composition of the gut microbiota

The effect of GRG on gut microbiota was evaluated by analyzing the microbiome of fecal samples. Alpha diversity, assessed using the Chao1 index, showed a notable increase in microbial abundance in the STC group relative to the NC group ($p < 0.01$) (Figures 4A,B). Mosapride treatment significantly reversed this change ($p < 0.001$). GRG treatment at low and medium doses significantly reduced microbial abundance ($p < 0.01$), while high-dose GRG also decreased abundance, though not significantly ($p > 0.05$). PCoA based on weighted UniFrac distances revealed significant differences in gut microbiota structure between the STC and NC groups. GRG treatment restored these structural changes (Figure 4C). Inter-group differences, analyzed using ANOSIM, confirmed significant dissimilarities between the microbiota of constipated mice and other groups ($R > 0.72$, $p < 0.01$) (Supplementary Table S2).

To reveal the specific impact of GRG on the microbiome, the composition of the dominant microbiota was analyzed. At the phylum level, Bacteroidota was the dominant phylum across all groups, accounting for 89.9, 65.9, 88.7, 89.7, 81.8, and 91.0% in the NC, STC, LD, MD, HD, and MO groups, respectively, followed by Firmicutes, which showed relative abundances of 9.6, 33.5, 10.5, 9.3, 17.1, and 8.3%. Significant differences in the abundances of Bacteroidota and Firmicutes were noted between the NC and STC groups ($p < 0.01$), with all treatments effectively reversing these changes ($p < 0.01$) (Figure 4D).

At the family level (Figure 4E), Muribaculaceae was the most abundant family in all groups, accounting for 66.5, 37.2, 65.9, 67.7, 64.8, and 74.6% in the NC, STC, LD, MD, HD, and MO groups, respectively. The STC group showed a notable reduction in Muribaculaceae and an elevation in Lachnospiraceae abundance compared to other groups ($p < 0.05$).

At the genus level (Figure 4F), *Alloprevotella*, *Prevotellaceae_UCG-001*, *Bacteroides*, and *Alistipes* were dominant across all groups. Differential analysis using a *t*-test revealed significant differences between the NC group, the MD group, and the STC group. Compared to the STC group, the NC and MD groups showed significant enrichment of *Alloprevotella* and *Muribaculum* (Figures 4G–H). Conversely, genera such as *Prevotellaceae_NK3B31_group*, *Ruminococcus*, *Lachnospiraceae_UCG-001*, *Parabacteroides*, *Eubacterium_xylanophilum_group*, and *Colidextribacter* were significantly enriched in the STC group. Additionally, *Odoribacter* was predominantly enriched in the STC group, while *Parasutterella* was distinctly reduced compared to the NC group. To further investigate the role of these genera in GRG-mediated constipation treatment, Pearson correlation analysis was performed between bacterial abundance and constipation-related indicators. As shown in Figure 4I, bacteria enriched in the NC and MD groups-such as *Alloprevotella*, *Parasutterella*, and *Muribaculum*-were positively correlated with defecation-promoting indicators and excitatory hormones, such as MTL, 5-HT, and SP. These genera were also negatively correlated with inhibitory hormones and defecation time, suggesting their role in promoting defecation. In contrast, bacteria enriched in the STC group-such as *Prevotellaceae_NK3B31_group*, *Ruminococcus*, and *Colidextribacter*-showed the opposite correlations, indicating a potential link to constipation. Notably, *Parasutterella* abundance was positively

10.3389/fmicb.2025.1615297

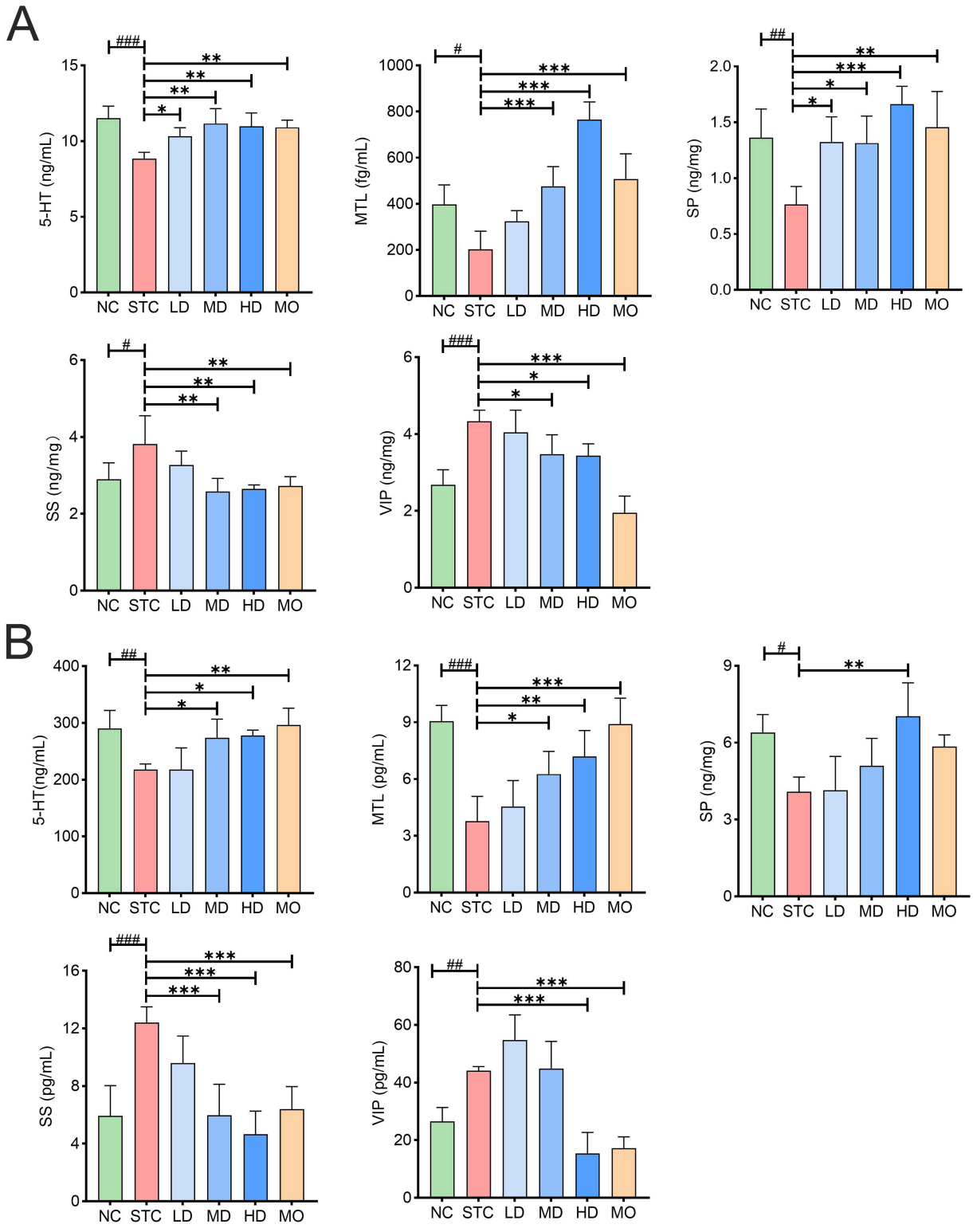

FIGURE 3
The effect of GRG treatment on the motility-related hormone in mice. **(A)** Hormone concentration in colon tissue. **(B)** Hormone concentration in serum. Values are presented as mean ± SD, $n = 4$. #$p < 0.05$; ##$p < 0.01$, ###$p < 0.001$, NC vs. STC. *$p < 0.05$, **$p < 0.01$, ***$p < 0.001$, LD, MD, HD and MO vs. STC.

correlated with MTL levels ($p < 0.01$), while *Muribaculum* abundance was positively correlated with 5-HT and SP levels. In contrast, *[Eubacterium]_xylanophilum_group*, *Colidextribacter*, *Ruminococcus*, and *Prevotellaceae_NK3B31_group* showed negative correlations with 5-HT and SP concentrations ($p < 0.1$). *Parabacteroides* was negatively correlated with MTL levels ($p < 0.05$).

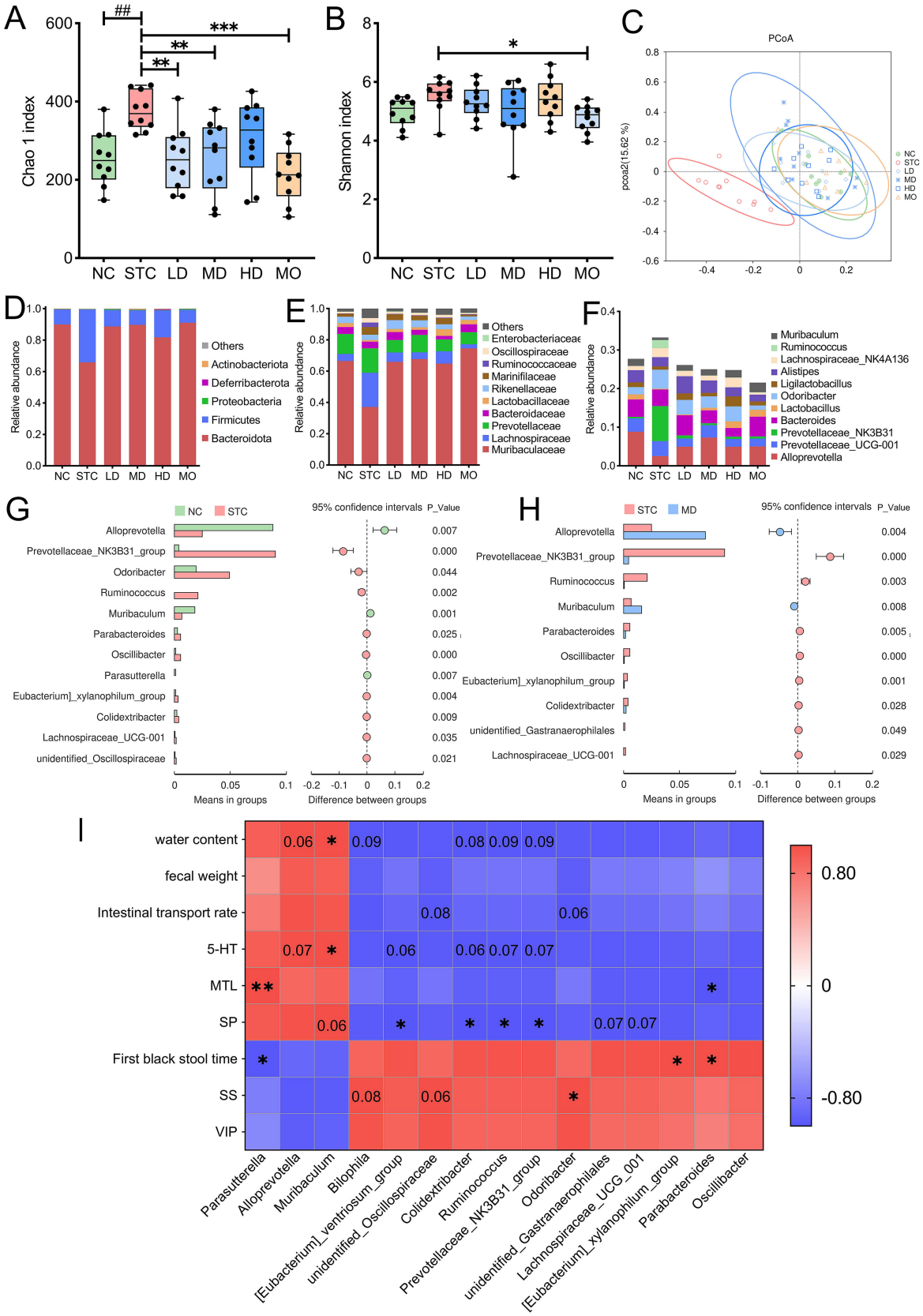

FIGURE 4
Effects of GRG treatment on fecal gut microbiota in mice. Alpha diversity measured by the Chao1 index **(A)** and Shannon index **(B)**, # $p < 0.05$; ## $p < 0.01$, ### $p < 0.001$, NC vs. STC. *$p < 0.05$, **$p < 0.01$, ***$p < 0.001$, LD, MD, HD and MO vs. STC. **(C)** Principal coordinate analysis (PCoA) based on weighted UniFrac distances. Taxonomic distribution of bacterial communities at the phylum level **(D)**, family level **(E)**, and genus level **(F)**. *T*-test analysis of differential bacterial genera at the genus level, NC vs. STC groups **(G)** and MD vs. STC groups **(H)**. The left panel shows the relative abundance ratios of different genera in the two samples, the middle panel indicates the proportion of functional abundance differences within the 95% confidence interval, and the right panel displays the *p*-value. **(I)** Pearson correlation analysis between key differential genera abundance and constipation-related

(Continued)

FIGURE 4 (Continued)
indicators. Red and blue indicate positive and negative correlations between indicators, respectively. *$p < 0.05$; **$p < 0.01$. Values within the squares indicate results with a p-value between 0.05 and 0.1. Values are presented as mean ± SD, $n = 10$.

3.5 GRG therapy restores the metabolic function of gut microbiota

To explore the functional changes in gut microbiota associated with GRG treatment, PICRUSt2 was employed to predict bacterial metabolic functional profiles. KEGG pathway enrichment analysis identified 13 pathways with significant alterations (Figure 5). In the STC group, pathways related to carbohydrate metabolism, cell motility, and cellular community–prokaryotes were significantly upregulated, while metabolic pathways involved in glycan biosynthesis and metabolism, lipid metabolism, and metabolism of other amino acids were markedly suppressed ($p < 0.01$). After GRG treatment, these functional abnormalities were significantly restored ($p < 0.01$). Additionally, GRG therapy notably enhanced the biosynthesis of other secondary metabolites. These findings indicated that GRG treatment effectively regulated the metabolic functions of gut microbiota in constipated mice.

3.6 GRG treatment enhances SCFAs content in feces

Short-chain fatty acids are essential secondary metabolites of the gut microbiota. The fecal levels of SCFAs were measured. As shown in Figure 6A, the total SCFAs content in the feces of constipated mice was notably reduced compared to the healthy group ($p < 0.001$). Specifically, the levels of acetic acid, propionic acid, butyric acid, isobutyric acid, and caproic acid were markedly decreased ($p < 0.001$), while valeric acid and isovaleric acid showed a declining trend ($p < 0.05$). Treatment with medium and high doses of GRG significantly increased the levels of all SCFAs except valeric acid ($p < 0.01$). Low-dose GRG treatment only significantly increased butyrate and isobutyrate levels ($p < 0.01$).

Pearson correlation analysis was implemented to examine the relationship between SCFAs level and the abundance of key bacterial genera. As illustrated in Figure 6B, the abundance of *Parasutterella*, *Alloprevotella*, and *Muribaculum* was positively correlated with SCFAs content, indicating their potential role in SCFAs synthesis. Notably, *Parasutterella* showed a significant positive correlation with acetate, propionate, valerate, and caproate ($p < 0.01$), while *Alloprevotella* was significantly correlated with butyrate and isobutyrate levels ($p < 0.01$). In contrast, genera such as *Prevotellaceae_NK3B31_group*, *Oscillibacter*, *[Eubacterium]_xylanophilum_group*, *[Eubacterium]_ventriosum_group*, *Ruminococcus*, *Lachnospiraceae_UCG-001*, and *Colidextribacter* exhibited a significant negative correlation with the content of most SCFAs ($p < 0.01$).

4 Discussion

4.1 TCM GRG exhibits substantial therapeutic efficacy in constipation management

Traditional Chinese medicine has been used for thousands of years to treat diseases in Asia, emerging clinical and preclinical evidence underscores the therapeutic potential of TCM formulations in constipation management. Clinically, TCM formulations, such as Shouhui Tongbian Capsules, has demonstrated significant therapeutic effects, improving clinical outcomes such as spontaneous bowel movement frequency, stool consistency, the sensation of complete evacuation, and overall quality of life, with durability surpassing conventional therapies (Guo et al., 2023). Preclinical investigations utilizing animal models of constipation further corroborate these findings and highlight its potential impact on various physiological and pathological factors, including gut motility hormones, mucosal barriers, aquaporins, inflammation, gut microbiota, and microbial metabolites (Tuohongerbieke et al., 2024).

Previous research revealed that GRG effectively alleviated morphine-induced STC symptoms in mice by downregulating colonic aquaporin 4 (AQP4) expression and restoring the SCF/c-kit pathway (Sun et al., 2020). In the current investigation, GRG administration significantly ameliorated defecation parameters in loperamide-induced constipated mice, evidenced by elevated fecal water content, augmented fecal output, enhanced colonic motility, and histological restoration of intestinal integrity. Notably, this study highlights the therapeutic mechanism of GRG in the treatment of constipation, focusing on its role in restoring the gut microbiota.

4.2 Gut microbiota as a pivotal mediator in constipation pathogenesis and TCM therapeutic mechanisms

The intricate interplay between gut microbiota and human health has been widely recognized in recent decades (Lynch and Pedersen, 2016). As the largest microbial reservoir in humans, the intestinal ecosystem maintains dynamic equilibrium through symbiotic relationships with its microbial inhabitants (Ohkusa et al., 2019). Emerging evidence positions gut dysbiosis as a hallmark feature of STC. Clinical researches has identified distinct microbial signatures in STC patients (Guo et al., 2020; Han K. et al., 2024). Furthermore, transferring the gut microbiota from constipated patients to mice has been shown to induce constipation-like symptoms, causally linking microbial dysbiosis to constipation pathogenesis. Gut microbiota restoration interventions, including probiotics and fecal microbiota transplantation, have shown remarkable efficacy in alleviating constipation (Ma et al., 2023). Dietary changes and prebiotics treatments for target constipation, have been shown to restore gut microbiota (Lai et al., 2023). These findings underscore the microbiota's dual role as both a disease modulator and therapeutic target. Restoring the balance of the microbiota not only alleviates symptoms, but also serves as a key indicator of treatment efficacy (Schupack et al., 2022; Sorbara and Pamer, 2022).

Metabolic disorders such as constipation often have multifactorial causes. TCM formulas contain various bioactive components such as polysaccharides, polypeptides, and alkaloids. These components enable TCM to exert therapeutic effects via multi-target and multi-pathway mechanisms, providing a holistic treatment strategy for constipation management. Numerous studies highlight TCM exert

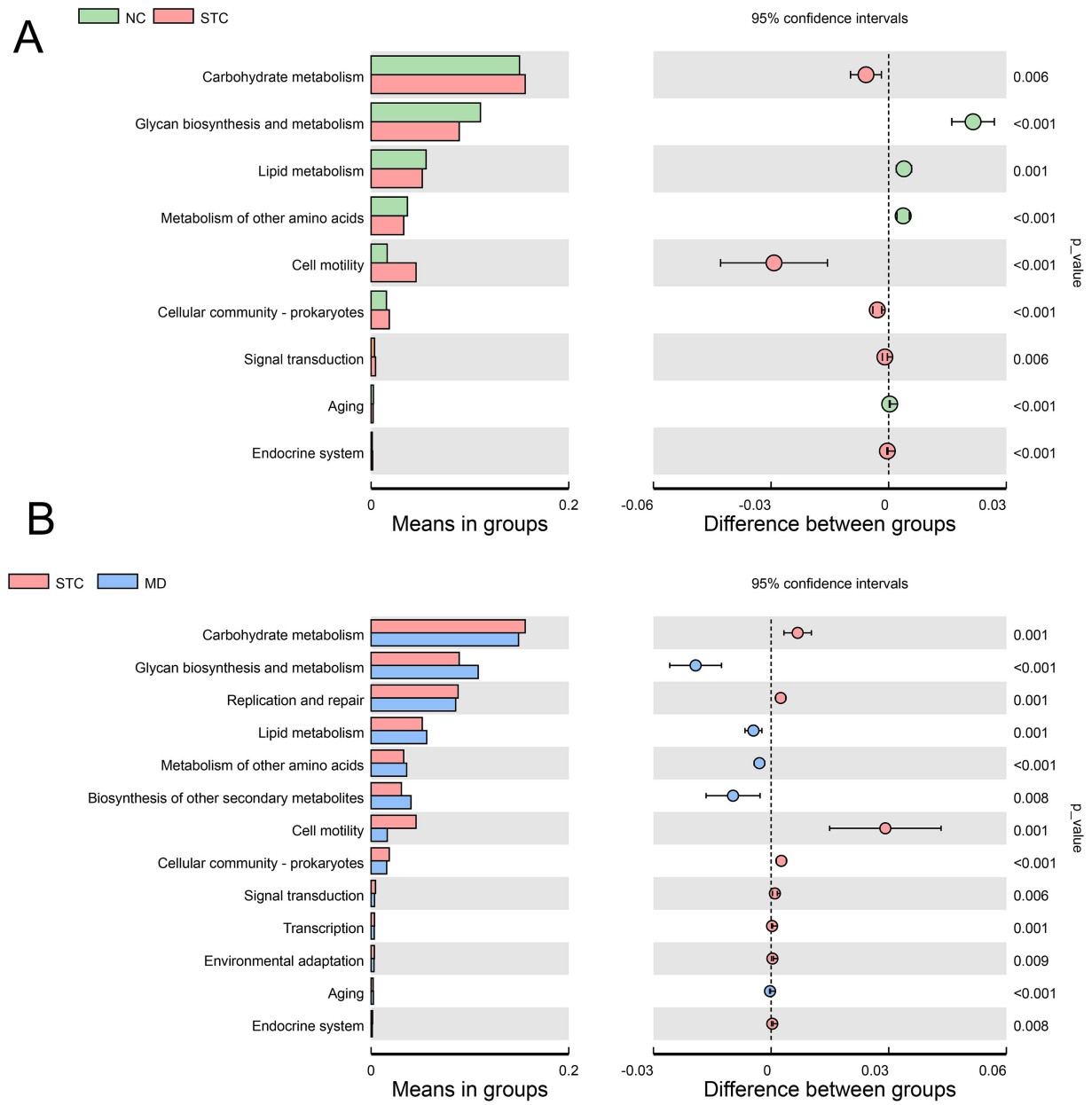

FIGURE 5
GRG therapy improved the metabolic function of gut microbiota. Picrust 2 predicted significantly changed KEGG pathways between NC vs. SC groups **(A)** and MD vs. STC groups **(B)**. The figure on the left shows the abundance ratio of different functions in two groups. In the middle is the proportion of differences in functional abundance within the 95% confidence interval. The right is the *p*-value.

multimodal therapeutic effects by simultaneously restoring microbial ecology, enhancing beneficial metabolites, and repairing mucosal integrity (Zhan et al., 2022; Gou et al., 2023). Central to this paradigm is the bi-directional crosstalk between TCM phytochemicals and gut microbiota (Cheng et al., 2023). For instance, polysaccharides in TCM formulas can promote the growth of beneficial gut bacteria, restore intestinal homeostasis, while also being metabolized by microorganisms to produce active metabolites such as SCFAs (Yue et al., 2022). Microbiota-derived SCFAs play a multifaceted role by serving as an energy source for gastrointestinal neurons, suppressing inflammation, stimulating the secretion of gastrointestinal regulatory peptides, enhancing gastrointestinal motility, and ultimately promoting defecation (Martin-Gallausiaux et al., 2021). Given the crucial role of gut microbiota in mediating the therapeutic effect of traditional Chinese medicine, gut microbiota restoration has become an important direction for studying the mechanisms of traditional Chinese medicine in treating metabolic diseases such as constipation (Zhang et al., 2021; Wang et al., 2024).

4.3 GRG regulates gut microbiota and metabolites to treat constipation

The strong correlations observed between the enrichment of beneficial bacteria (e.g., Alloprevotella and Muribaculum), the rise in SCFAs, and the normalization of motility-related hormones suggest a

10.3389/fmicb.2025.1615297

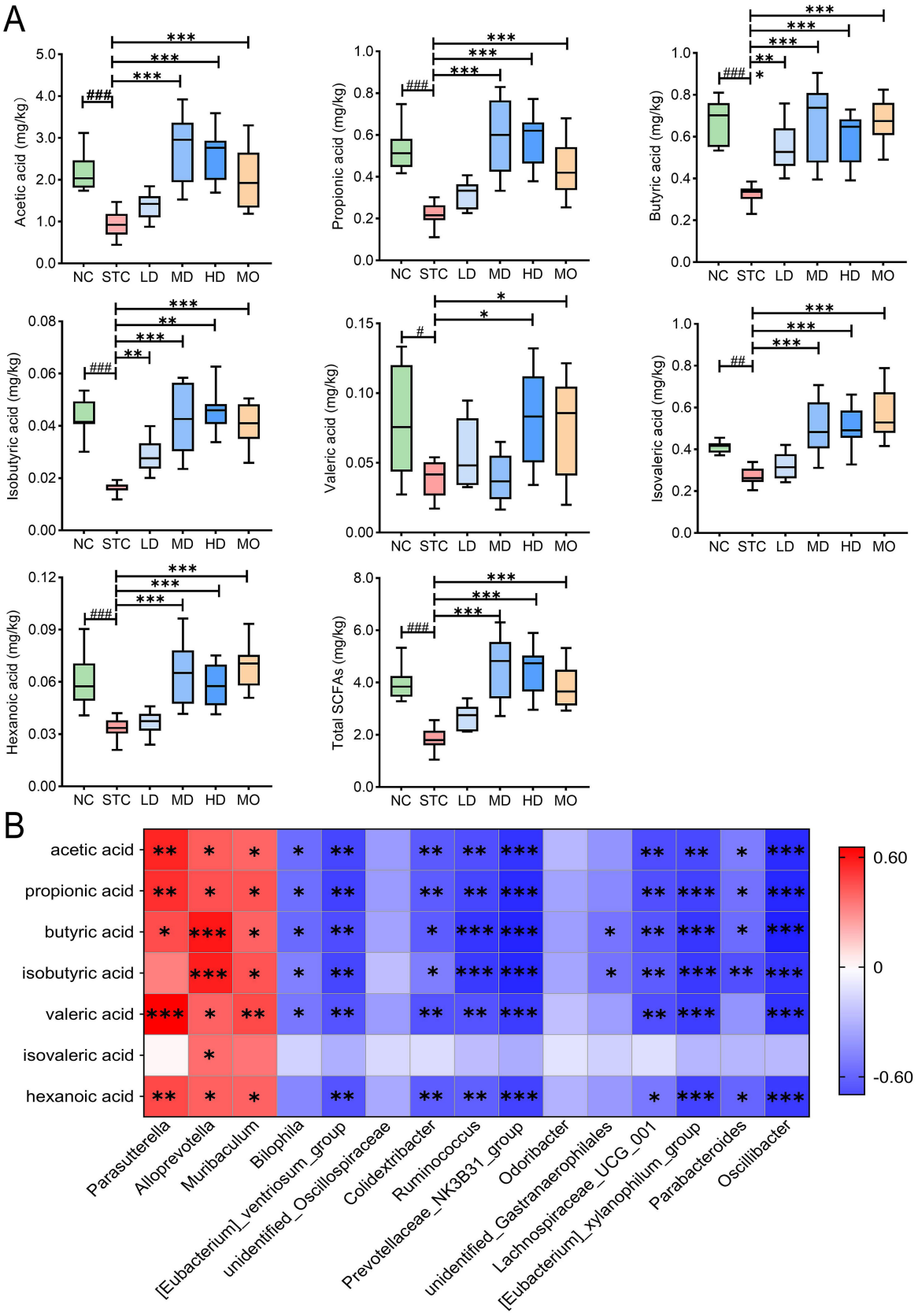

FIGURE 6
GRG treatment affects fecal SCFA contents. **(A)** Fecal SCFA contents in different groups. Total SCFAs stand for the total content of all the seven SCFAs. #$p < 0.05$; ##$p < 0.01$, ###$p < 0.001$, NC vs. STC. *$p < 0.05$, **$p < 0.01$, ***$p < 0.001$, LD, MD, HD and MO vs. STC. **(B)** Correlation analysis between

(Continued)

FIGURE 6 (Continued)
differential genus microbiota and SCFA abundance. Correlation analysis was performed by the Pearson method. The red and blue colors stand for the positive and negative correlation between the two indicators, respectively. Values are presented as mean ± SD, $n = 10$. *$p < 0.05$; **$p < 0.01$; ***$p < 0.001$.

potential mechanistic cascade whereby GRG modulates the gut microbiome, leading to changes in microbial metabolites that in turn influence host hormone secretion and gut function. Our results strongly support this hypothesis and provide a framework for future mechanistic investigations. GRG treatment effectively reversed constipation-induced gut microbiota dysbiosis, characterized by increased *Alloprevotella* and *Muribaculum* abundance and reduced *Ruminococcus*, *Prevotellaceae_NK3B31_group*, *Lachnospiraceae_UCG-001*, *Parabacteroides*, and *Colidextribacter*. The abundance of key microbial taxa strongly correlated with constipation-related phenotypes, suggesting their important roles in GRG's therapeutic effects for STC. Among these key bacteria, *Alloprevotella* was considered a producer of SCFAs (Han B. et al., 2024). In this study, *Alloprevotella* abundance positively correlated with butyrate and isobutyrate levels ($p < 0.001$). Similarly, reduced *Muribaculum* abundance has been observed in constipated mice. *Prevotellaceae_NK3B31_group* presents a more complex relationship with constipation. Yang et al. found it significantly enriched in constipated rats and positively correlated with inflammation markers (Yang et al., 2021). However, other studies reported a decrease in *Prevotellaceae_NK3B31_group* abundance in constipated group (Tuohongerbieke et al., 2024). In this study, the *Prevotellaceae_NK3B31_group* was significantly enriched in constipated mice and negatively correlated with SCFA levels ($p < 0.001$). Clinical research has also identified increased *Ruminococcus* abundance in elderly patients with constipation (Guo et al., 2020). TCM treatments have been shown to significantly reduce *Ruminococcus* levels in constipated rats, leading to changes in metabolite levels and therapeutic benefits (Li et al., 2023). However, variations in key microbial taxa, such as *Alloprevotella*, *Prevotellaceae_NK3B31_group*, and *Ruminococcus*, across different constipation studies highlight the complexity of their relationship with constipation. Further research is needed to clarify these associations and better understand their roles in TCM's treatment mechanisms.

The gut microbiota produced secondary metabolites playing essential roles in regulating host physiology (Krautkramer et al., 2021). This study identified significant changes in the metabolic functions of the gut microbiota in constipated mice. GRG treatment enhanced microbiota functions related to glycan biosynthesis and metabolism, lipid metabolism, metabolism of other amino acids, and biosynthesis of secondary metabolites, highlighting the critical role of microbial metabolites in the therapeutic effects of GRG on constipation. Additionally, GRG treatment significantly increased SCFAs level in constipated mice, consistent with the observed improvement in glycan biosynthesis and metabolism. In this study, GRG treatment restored the abundance of SCFA-producing bacteria such as *Alloprevotella*, which was positively correlated with butyrate and other SCFAs level. Research suggested that TCM could regulate gut motility related hormones by improving gut microbiota (Gao et al., 2022). Besides, GRG treatment significantly increased the levels of stimulating hormones such as 5-HT and SP, which was positively correlated with the increased abundance of bacteria such as *Muribaculum* and *Alloprevotella*. Both 5-HT and SP are critical hormones associated with colonic motility. SP enhances smooth muscle contraction, stimulates gastrointestinal peristalsis, and promotes intestinal secretion (Wang et al., 2023a), while 5-HT facilitates intestinal secretion and motility (Israelyan et al., 2019). Notably, this observation aligns with prior demonstrations that *Alloprevotella*-derived butyrate potentiates enterochromaffin cell activity, thereby amplifying serotonin signaling to enhance intestinal motility (Vincent et al., 2018; Han et al., 2024a). Furthermore, the potential mechanism by which SCFAs like butyrate influence motility may extend beyond hormonal secretion to direct effects on the enteric nervous system (ENS). Research has shown that chronic constipation is associated with ENS dysfunction, including neurochemical abnormalities, loss of nerve fibers, and a reduction in ICC (Bassotti et al., 2011). Notably, impaired butyrate metabolism has been implicated in causing ENS damage, which may be a critical factor in functional constipation (Wang et al., 2023b). Given that GRG treatment in our study significantly increased butyrate-producing bacteria (*Alloprevotella*) and fecal butyrate levels, it is plausible that the amelioration of constipation symptoms was partly mediated through the restoration of butyrate-supported ENS function. These findings suggested that the gut microbiota and its metabolites play an integral role in the mechanisms underlying the efficacy of GRG in treating constipation.

However, this study has several limitations that should be considered. The experiments were conducted exclusively in male mice, which precludes exploration of potential sex-specific differences in GRG's therapeutic effects. And functional predictions via PICRUSt2 depend on the completeness of reference databases and phylogenetic inference; horizontal gene transfer, uncultured microbes, and unannotated genomes may bias pathway predictions. Additionally, although H&E staining indicated that GRG ameliorated histopathological damage, the assessment remained morphological. A more quantitative and mechanistic assessment of intestinal barrier repair, using mucin-specific stains (e.g., PAS) or immunohistochemistry for tight junction proteins (e.g., ZO-1, occludin) would offer deeper mechanistic insight into intestinal barrier repair. Moreover, while GRG modulated overall gut microbiota structure, its key active ingredients and their specific roles were not elucidated. Finally, although compelling systemic correlations were observed, the spatial and cellular mechanisms within the gut wall, such as involvement of specific enteroendocrine cells or enteric neurons, remain unclear.

These limitations highlight the need for future studies incorporating both sexes and employing metagenomic or metabolomic profiling to resolve strain-specific functions and validate microbial metabolite–host interactions. Furthermore, advanced metabolomics should be applied to characterize the chemical profile of GRG, identify its key pharmacological components, and evaluate their effects on specific bacterial groups, SCFA production, and intestinal motility. In addition, future studies utilizing techniques such as immunohistochemistry for neuronal markers (e.g., PGP9.5) and key hormones (e.g., 5-HT) are crucial to visualize and confirm these

interactions directly at the cellular level, moving from correlation to definitive causation. Such approaches would strengthen causal interpretations of GRG's microbiota-mediated mechanisms in constipation management.

5 Conclusion

GRG treatment significantly improved defecation phenotypes and increased intestinal motility in loperamide-induced constipated mice. It also effectively regulated the levels of motility-related hormones levels. The gut microbiota appears to play a key role in the therapeutic effects of GRG. By modulating gut microbiota composition, restoring SCFAs level, and restoring intestinal motility hormones, GRG offers a promising approach for the treatment of constipation.

Data availability statement

The datasets presented in this study are publicly available. This data can be found at: https://www.ncbi.nlm.nih.gov/sra, accession numbers PRJNA1203378 and PRJNA1119701.

Ethics statement

The animal study was approved by Shandong Provincial Third Hospital Animal Ethics Committee. The study was conducted in accordance with the local legislation and institutional requirements.

Author contributions

XB: Data curation, Investigation, Methodology, Funding acquisition, Writing – original draft, Formal analysis. YW: Investigation, Software, Writing – review & editing, Methodology, Visualization. KW: Methodology, Writing – review & editing, Investigation, Supervision. WC: Writing – original draft, Project administration, Conceptualization, Writing – review & editing. TB: Resources, Project administration, Conceptualization, Writing – review & editing.

Funding

The author(s) declare that financial support was received for the research and/or publication of this article. This work was supported by Traditional Chinese Medicine Technology Project of Shandong Province (M-2022193).

Conflict of interest

The authors declare that the research was conducted in the absence of any commercial or financial relationships that could be construed as a potential conflict of interest.

Publisher's note

All claims expressed in this article are solely those of the authors and do not necessarily represent those of their affiliated organizations, or those of the publisher, the editors and the reviewers. Any product that may be evaluated in this article, or claim that may be made by its manufacturer, is not guaranteed or endorsed by the publisher.

Supplementary material

The Supplementary material for this article can be found online at: https://www.frontiersin.org/articles/10.3389/fmicb.2025.1615297/full#supplementary-material

References

Barberio, B., Judge, C., Savarino, E. V., and Ford, A. C. (2021). Global prevalence of functional constipation according to the Rome criteria: a systematic review and meta-analysis. *Lancet Gastroenterol. Hepatol.* 6, 638–648. doi: 10.1016/s2468-1253(21)00111-4

Bassotti, G., Villanacci, V., and Rostami, N. M. (2011). Chronic constipation: no more idiopathic, but a true neuropathological entity. *Gastroenterol. Hepatol. Bed Bench* 4, 109–115.

Bharucha, A. E., and Lacy, B. E. (2020). Mechanisms, evaluation, and management of chronic constipation. *Gastroenterology* 158, 1232–1249.e3. doi: 10.1053/j.gastro.2019.12.034

Bhattarai, Y., Williams, B. B., Battaglioli, E. J., Whitaker, W. R., Till, L., Grover, M., et al. (2018). Gut microbiota-produced tryptamine activates an epithelial G-protein-coupled receptor to increase colonic secretion. *Cell Host Microbe* 23, 775–785.e5. doi: 10.1016/j.chom.2018.05.004

Cheng, H., Zhang, D., Wu, J., Liu, J., Zhou, Y., Tan, Y., et al. (2023). Interactions between gut microbiota and polyphenols: a mechanistic and metabolomic review. *Phytomedicine* 119:154979. doi: 10.1016/j.phymed.2023.154979

Fan, Y., and Pedersen, O. (2021). Gut microbiota in human metabolic health and disease. *Nat. Rev. Microbiol.* 19, 55–71. doi: 10.1038/s41579-020-0433-9

Gao, X., Hu, Y., Tao, Y., Liu, S., Chen, H., Li, J., et al. (2022). *Cymbopogon citratus* (DC.) Stapf aqueous extract ameliorates loperamide-induced constipation in mice by promoting gastrointestinal motility and regulating the gut microbiota. *Front. Microbiol.* 13:1017804. doi: 10.3389/fmicb.2022.1017804

Gou, H., Su, H., Liu, D., Wong, C. C., Shang, H., Fang, Y., et al. (2023). Traditional medicine Pien Tze Huang suppresses colorectal tumorigenesis through restoring gut microbiota and metabolites. *Gastroenterology* 165, 1404–1419. doi: 10.1053/j.gastro.2023.08.052

Guo, X., Li, R., Huang, N., Zhang, T., Li, J., Gong, L., et al. (2023). Efficacy and safety of Shouhui Tongbian capsules in the treatment of constipation: a systematic review and meta-analysis. *Phytomedicine* 108:154541. doi: 10.1016/j.phymed.2022.154541

Guo, Y., Song, L., Huang, Y., Li, X., Xiao, Y., Wang, Z., et al. (2022). *Latilactobacillus sakei* Furu2019 and stachyose as probiotics, prebiotics, and synbiotics alleviate constipation in mice. *Front. Nutr.* 9:1039403. doi: 10.3389/fnut.2022.1039403

Guo, M., Yao, J., Yang, F., Liu, W., Bai, H., Ma, J., et al. (2020). The composition of intestinal microbiota and its association with functional constipation of the elderly patients. *Future Microbiol.* 15, 163–175. doi: 10.2217/fmb-2019-0283

Han, K., Kuo, B., Khalili, H., and Staller, K. (2024). Metagenomics analysis reveals unique gut microbiota signature of slow-transit constipation. *Clin. Transl. Gastroenterol.* 15:e1. doi: 10.14309/ctg.0000000000000766

Han, B., Shi, L., Bao, M. Y., Yu, F. L., Zhang, Y., Lu, X. Y., et al. (2024). Dietary ellagic acid therapy for CNS autoimmunity: targeting on *Alloprevotella rava* and propionate metabolism. *Microbiome* 12:114. doi: 10.1186/s40168-024-01819-8

Harris, L. A., and Chang, C. H. (2022). Burden of constipation: looking beyond bowel movements. *Am. J. Gastroenterol.* 117, S2–s5. doi: 10.14309/ajg.0000000000001708

Israelyan, N., Del Colle, A., Li, Z., Park, Y., Xing, A., Jacobsen, J. P. R., et al. (2019). Effects of serotonin and slow-release 5-Hydroxytryptophan on gastrointestinal motility in a mouse model of depression. *Gastroenterology* 157, 507–521.e4. doi: 10.1053/j.gastro.2019.04.022

Jia, A., Niu, X., Zhang, M., Liu, X., Cui, T., Liu, C., et al. (2024). Integrated microbiomics and metabolomics analysis reveals the influence of gut microbiota on the growth and metabolism of sea cucumber seedlings. *J. Appl. Microbiol.* 135:lxae006. doi: 10.1093/jambio/lxae006

Krautkramer, K. A., Fan, J., and Bäckhed, F. (2021). Gut microbial metabolites as multi-kingdom intermediates. *Nat. Rev. Microbiol.* 19, 77–94. doi: 10.1038/s41579-020-0438-4

Lai, H., Li, Y., He, Y., Chen, F., Mi, B., Li, J., et al. (2023). Effects of dietary fibers or probiotics on functional constipation symptoms and roles of gut microbiota: a double-blinded randomized placebo trial. *Gut Microbes* 15:2197837. doi: 10.1080/19490976.2023.2197837

Li, X., Wang, X., Wang, Z., and Guan, J. (2023). Baizhu-Baishao herb pair ameliorates functional constipation and intestinal microflora disorder in rats. *Animal Model Exp Med* 6, 598–608. doi: 10.1002/ame2.12351

Liu, B., Zhang, Z., Liu, X., Hu, W., and Wu, W. (2023). Gastrointestinal fermentable polysaccharide is beneficial in alleviating loperamide-induced constipation in mice. *Nutrients* 15:4364. doi: 10.3390/nu15204364

Lynch, S. V., and Pedersen, O. (2016). The human intestinal microbiome in health and disease. *N. Engl. J. Med.* 375, 2369–2379. doi: 10.1056/NEJMra1600266

Ma, T., Yang, N., Xie, Y., Li, Y., Xiao, Q., Li, Q., et al. (2023). Effect of the probiotic strain, *Lactiplantibacillus plantarum* P9, on chronic constipation: a randomized, double-blind, placebo-controlled study. *Pharmacol. Res.* 191:106755. doi: 10.1016/j.phrs.2023.106755

Martens, E. C., Neumann, M., and Desai, M. S. (2018). Interactions of commensal and pathogenic microorganisms with the intestinal mucosal barrier. *Nat. Rev. Microbiol.* 16, 457–470. doi: 10.1038/s41579-018-0036-x

Martin-Gallausiaux, C., Marinelli, L., Blottière, H. M., Larraufie, P., and Lapaque, N. (2021). SCFA: mechanisms and functional importance in the gut. *Proc. Nutr. Soc.* 80, 37–49. doi: 10.1017/s0029665120006916

Ohkusa, T., Koido, S., Nishikawa, Y., and Sato, N. (2019). Gut microbiota and chronic constipation: a review and update. *Front Med (Lausanne)* 6:19. doi: 10.3389/fmed.2019.00019

Pannemans, J., Masuy, I., and Tack, J. (2020). Functional constipation: individualising assessment and treatment. *Drugs* 80, 947–963. doi: 10.1007/s40265-020-01305-z

Schupack, D. A., Mars, R. A. T., Voelker, D. H., Abeykoon, J. P., and Kashyap, P. C. (2022). The promise of the gut microbiome as part of individualized treatment strategies. *Nat. Rev. Gastroenterol. Hepatol.* 19, 7–25. doi: 10.1038/s41575-021-00499-1

Shin, A., Preidis, G. A., Shulman, R., and Kashyap, P. C. (2019). The gut microbiome in adult and pediatric functional gastrointestinal disorders. *Clin. Gastroenterol. Hepatol.* 17, 256–274. doi: 10.1016/j.cgh.2018.08.054

Song, E. M., Lee, H. J., Jung, K. W., Kim, M. J., Hwang, S. W., Park, S. H., et al. (2021). Long-term risks of Parkinson's disease, surgery, and colorectal cancer in patients with slow-transit constipation. *Clin. Gastroenterol. Hepatol.* 19, 2577–2586.e6. doi: 10.1016/j.cgh.2020.08.059

Sorbara, M. T., and Pamer, E. G. (2022). Microbiome-based therapeutics. *Nat. Rev. Microbiol.* 20, 365–380. doi: 10.1038/s41579-021-00667-9

Sumida, K., Molnar, M. Z., Potukuchi, P. K., Thomas, F., Lu, J. L., Yamagata, K., et al. (2019). Constipation and risk of death and cardiovascular events. *Atherosclerosis* 281, 114–120. doi: 10.1016/j.atherosclerosis.2018.12.021

Sun, Y., Yan, C., Jin, S., Shi, C., Zhao, J., and Li, G. (2020). Curative effect and mechanism of Guiren Runchang granules on morphine-induced slow transit constipation in mice. *Evid. Based Complement. Alternat. Med.* 2020:5493192. doi: 10.1155/2020/5493192

Tuohongerbieke, A., Wang, H., Wu, J., Wang, Z., Dong, T., Huang, Y., et al. (2024). Xiao Cheng Qi decoction, an ancient Chinese herbal mixture, relieves loperamide-induced slow-transit constipation in mice: an action mediated by gut microbiota. *Pharmaceuticals (Basel)* 17:153. doi: 10.3390/ph17020153

Vicentini, F. A., Keenan, C. M., Wallace, L. E., Woods, C., Cavin, J. B., Flockton, A. R., et al. (2021). Intestinal microbiota shapes gut physiology and regulates enteric neurons and glia. *Microbiome* 9:210. doi: 10.1186/s40168-021-01165-z

Vincent, A. D., Wang, X. Y., Parsons, S. P., Khan, W. I., and Huizinga, J. D. (2018). Abnormal absorptive colonic motor activity in germ-free mice is rectified by butyrate, an effect possibly mediated by mucosal serotonin. *Am. J. Physiol. Gastrointest. Liver Physiol.* 315, G896–g907. doi: 10.1152/ajpgi.00237.2017

Vriesman, M. H., Koppen, I. J. N., Camilleri, M., Di Lorenzo, C., and Benninga, M. A. (2020). Management of functional constipation in children and adults. *Nat. Rev. Gastroenterol. Hepatol.* 17, 21–39. doi: 10.1038/s41575-019-0222-y

Wang, L., Lv, W. Q., Yang, J. T., Lin, X., Liu, H. M., Tan, H.-J., et al. (2023b). Enteric nervous system damage caused by abnormal intestinal butyrate metabolism may lead to functional constipation. *Front. Microbiol.* 14:1117905. doi: 10.3389/fmicb.2023.1117905

Wang, K., Qiu, H., Chen, F., Cai, P., and Qi, F. (2024). Considering traditional Chinese medicine as adjunct therapy in the management of chronic constipation by regulating intestinal flora. *Biosci. Trends* 18, 127–140. doi: 10.5582/bst.2024.01036

Wang, L., Wu, F., Hong, Y., Shen, L., Zhao, L., and Lin, X. (2022). Research progress in the treatment of slow transit constipation by traditional Chinese medicine. *J. Ethnopharmacol.* 290:115075. doi: 10.1016/j.jep.2022.115075

Wang, L., Xie, S., Jiang, X., Xu, C., Wang, Y., Feng, J., et al. (2023a). Therapeutic effects of *Bombax ceiba* flower aqueous extracts against loperamide-induced constipation in mice. *Pharm. Biol.* 61, 125–134. doi: 10.1080/13880209.2022.2157841

Yang, Z., Ye, S., Xu, Z., Su, H., Tian, X., Han, B., et al. (2021). Dietary synbiotic ameliorates constipation through the modulation of gut microbiota and its metabolic function. *Food Res. Int.* 147:110569. doi: 10.1016/j.foodres.2021.110569

Yue, B., Zong, G., Tao, R., Wei, Z., and Lu, Y. (2022). Crosstalk between traditional Chinese medicine-derived polysaccharides and the gut microbiota: a new perspective to understand traditional Chinese medicine. *Phytother. Res.* 36, 4125–4138. doi: 10.1002/ptr.7607

Zhan, Y., Wen, Y., Du, L. J., Wang, X. X., Tang, S. Y., Kong, P. F., et al. (2022). Effects of Maren pills on the intestinal microflora and short-chain fatty acid profile in drug-induced slow transit constipation model rats. *Front. Pharmacol.* 13:804723. doi: 10.3389/fphar.2022.804723

Zhang, H. Y., Tian, J. X., Lian, F. M., Li, M., Liu, W. K., Zhen, Z., et al. (2021). Therapeutic mechanisms of traditional Chinese medicine to improve metabolic diseases via the gut microbiota. *Biomed. Pharmacother.* 133:110857. doi: 10.1016/j.biopha.2020.110857

frontiers | Frontiers in Microbiology

TYPE Review
PUBLISHED 21 October 2025
DOI 10.3389/fmicb.2025.1642377

Check for updates

OPEN ACCESS

EDITED BY
Guiguo Zhang,
Shandong Agricultural University, China

REVIEWED BY
Xiao Ma,
Chengdu University of Traditional Chinese Medicine, China
Xiaoyong Yu,
Shaanxi Provincial Hospital of Traditional Chinese Medicine, China

*CORRESPONDENCE
Fugang Huang
✉ hermanh1218@163.com
Ke Sun
✉ txmarina@163.com

RECEIVED 06 June 2025
ACCEPTED 30 September 2025
PUBLISHED 21 October 2025

CITATION
Li J, Diao L, Li M, Huang F and Sun K (2025) Unraveling the mysteries of the gut-kidney axis: the protective role of traditional Chinese medicine in chronic kidney disease. *Front. Microbiol.* 16:1642377. doi: 10.3389/fmicb.2025.1642377

COPYRIGHT
© 2025 Li, Diao, Li, Huang and Sun. This is an open-access article distributed under the terms of the Creative Commons Attribution License (CC BY). The use, distribution or reproduction in other forums is permitted, provided the original author(s) and the copyright owner(s) are credited and that the original publication in this journal is cited, in accordance with accepted academic practice. No use, distribution or reproduction is permitted which does not comply with these terms.

Unraveling the mysteries of the gut-kidney axis: the protective role of traditional Chinese medicine in chronic kidney disease

Jiahui Li[1], Lijia Diao[2], Menglin Li[3], Fugang Huang[2]* and Ke Sun[4]*

[1]Haiyan Hospital of Traditional Chinese Medicine, Haiyan, China, [2]The First School of Clinical Medicine, Zhejiang Chinese Medical University, Hangzhou, China, [3]Jinhua Fifth Hospital, Jinhua, China, [4]The Third School of Clinical Medicine, Zhejiang Chinese Medical University, Hangzhou, Zhejiang, China

Chronic kidney disease (CKD) constitutes a globally progressive nephropathy orchestrating inexorable deterioration of renal architecture. The paradigmatic gut-kidney axis unveils sophisticated bidirectional interplay between enteric microbiome and renal homeostatic equilibrium. Dysbiotic perturbations catalyze aberrant accumulation of gut-derived uremic metabolites, attenuate intestinal epithelial fortification, and propagate subclinical inflammatory cascades, synergistically precipitating CKD trajectory acceleration. Contemporary therapeutic arsenals targeting this axis encompass probiotic reconstitution, prebiotic orchestration, synbiotic hybridization, precision nutritional calibration, and enteral sequestrants including AST-120. Traditional Chinese Medicine (TCM) paradigms deploy multifaceted strategies through meticulous microbiota choreography, mucosal barrier reinforcement, and renal fibrogenesis attenuation. Distinguished phytotherapeutics including Rhubarb (Rhei Radix et Rhizoma), *Salvia miltiorrhiza*, and Poria cocos, synergized with bioactive constituents curcumin and punicalagin, orchestrate nephroprotective virtuosity via intricate microbiome-metabolome networks. Sophisticated polyherbal architectures, exemplified by YQHG and YSHS, harmoniously fortify intestinal impermeability while nullifying uremic translocation. These revelations substantiate the transformative potential of integrative paradigms amalgamating TCM-based phytomedicine with microbiota-directed precision therapeutics for CKD stewardship.

KEYWORDS

chronic kidney disease, traditional Chinese medicine, gut-kidney axis, therapeutic strategy, gut microbiota, uremic toxins, prebiotic and probiotic foods

1 Introduction

Chronic Kidney Disease (CKD) constitutes a multifaceted clinical entity characterized by the inexorable deterioration of renal architecture and physiological function, representing one of the most formidable challenges in contemporary nephrology (D'Arrigo et al., 2025; Tsinari et al., 2025). This complex pathological syndrome may manifest as a sequela to diverse primary renal pathologies, including diabetic nephropathy (DN) and IgA nephropathy (IgAN), with its relentless progression orchestrated through cascading mechanisms of irreversible nephron depletion, progressive glomerular sclerosis, and extensive tubulointerstitial fibrosis, inevitably culminating in end-stage renal disease (ESRD) (Huang et al., 2025; Kitamura et al., 2025; Tang et al., 2025). The clinical phenotype of CKD is predominantly characterized by the triad of persistent proteinuria, hematuria, and progressive decline in estimated glomerular filtration

rate (eGFR). Contemporary epidemiological surveillance reveals an alarming trajectory of escalating global CKD prevalence, currently imposing its burden upon more than 10% of the worldwide adult demographic (Selby and Taal, 2024). Particularly noteworthy is CKD's propensity to transcend the boundaries of isolated renal dysfunction, precipitating a constellation of cardiovascular complications and metabolic derangements that collectively contribute to substantially elevated all-cause mortality, thereby underscoring the imperative for innovative therapeutic paradigms.

Contemporary therapeutic modalities remain predominantly anchored to renal replacement strategies, encompassing dialysis and renal transplantation; however, the inherent limitations of these interventions—including their invasive nature, prohibitive healthcare expenditures, and fundamental inability to reverse underlying pathophysiological processes—severely constrain their therapeutic utility and accessibility (Wieringa et al., 2025). Within this therapeutic lacuna, personalized treatment strategies rooted in traditional medicinal systems, particularly the sophisticated theoretical framework of Traditional Chinese Medicine (TCM), have emerged as compelling alternatives. TCM's therapeutic philosophy, predicated upon multi-target synergistic modulation and holistic restoration of physiological equilibrium, demonstrates considerable promise in attenuating CKD progression and ameliorating symptomatic burden, thereby providing a robust theoretical foundation for integrative Chinese-Western medical approaches.

The paradigmatic evolution of CKD pathogenesis research has witnessed a transformative shift from reductionist single-organ conceptualization toward sophisticated multi-systemic network modeling, epitomized by the revolutionary "gut-kidney axis" hypothesis (Tsuji et al., 2024; Kemp et al., 2025). This groundbreaking theoretical construct elucidates the intricate bidirectional regulatory networks governing intestinal microecological dynamics and renal physiological homeostasis. Within the pathological milieu of uremia-associated CKD, the intestinal microbiome undergoes profound compositional dysregulation, manifesting as precipitous depletion of beneficial microbial taxa—particularly short-chain fatty acid (SCFA)-producing genera including *Faecalibacterium prausnitzii*, Roseburia, Bifidobacterium, and Lactobacillus—concomitant with the aberrant proliferation of opportunistic pathogenic species such as *Escherichia coli*, Shigella, and Enterococcus (Lyu et al., 2023; Atzeni et al., 2024; Wakino et al., 2025). This dysbiotic transformation precipitates compromised SCFA biosynthetic capacity, disruption of intestinal epithelial barrier integrity, and the pathological phenomenon of intestinal hyperpermeability or "leaky gut syndrome." The consequent translocation of gut-derived pathogen-associated molecular patterns (PAMPs), exemplified by lipopolysaccharides, orchestrates chronic low-grade inflammation through Toll-like receptor (TLR) activation and cascading pro-inflammatory cytokine release, thereby accelerating epithelial-mesenchymal transition within renal tubular epithelium and promoting progressive interstitial fibrogenesis (Rukavina Mikusic et al., 2020; Stasi et al., 2025). Moreover, the accumulation of deleterious microbial metabolites—including indoxyl sulfate (IS), p-cresyl sulfate (PCS), and trimethylamine N-oxide (TMAO)—exerts direct nephrotoxic effects through sophisticated mechanisms involving epigenetic dysregulation and oxidative stress amplification, establishing a self-perpetuating pathological feedback circuit of aberrant "gut-kidney crosstalk" (Alvarenga et al., 2025). Within the context of ESRD and maintenance dialysis, microbial community architecture exhibits additional layers of complexity, characterized by disease-specific, stage-dependent, and etiology-related compositional signatures. This revolutionary theoretical framework not only provides unprecedented insights into the systemic pathophysiology of CKD but also establishes a conceptual bridge between the holistic therapeutic principles of TCM and precision microbiome-targeted interventional strategies.

2 The gut-kidney axis: orchestrating the pathogenesis of CKD

2.1 Disrupted gut microbiota: a catalyst for CKD onset

The perturbation of gut microbiota homeostasis has emerged as a pivotal orchestrator in the pathogenesis of CKD, manifesting through temporally-orchestrated microbial compositional metamorphoses characterized by the quintessential depletion of SCFA-producing commensals and the concomitant proliferation of opportunistic pathogens (Evenepoel et al., 2023; Krukowski et al., 2023; Zheng et al., 2023; Stepanova, 2024; Zhao B. et al., 2025).

Foundational investigations in animal paradigms have elucidated that renal deterioration in membranous nephropathy rodents correlates with the precipitous decline of *Lactobacillus* and *Bifidobacterium* populations (Miao et al., 2024b). The 5/6 nephrectomy murine archetype demonstrated amplified colonization by *Allobaculum*, *Bifidobacterium*, and *Turicibacter*, juxtaposed with the attenuation of *Lactobacillus* and *Rikenellaceae* constituents (Chen F. et al., 2025). The adenine-induced paradigm exhibited taxonomically-selective enrichment of genera encompassing *Dorea*, *Escherichia*, *Clostridium*, and *Ruminococcus* (Li et al., 2025). Nevertheless, the inherent physiological divergence between rodents—functioning as cecal fermenters with coprophagic proclivities—and humans, who rely predominantly on colonic fermentation, presents formidable translational impediments that may circumscribe the clinical applicability of these experimental findings (Jensen et al., 2023). From an anatomical and physiological perspective, the rodent cecum presents itself as a formidable digestive powerhouse, commanding substantial territorial dominance within the abdominal cavity. In the murine paradigm, this remarkable organ claims an impressive 30%–40% of the entire gastrointestinal real estate, orchestrating vigorous peristaltic symphonies (Bolsega et al., 2023). Despite the ephemeral nature of luminal transit, this biological reactor sustains extraordinarily dynamic fermentative processes within its capacious chambers. The meticulously maintained acidic milieu creates an optimal sanctuary for specialized fibrolytic consortia, notably fostering the proliferation of *Akkermansia muciniphila* and allied mucin-degrading virtuosos that flourish in remarkable abundance. The intricate labyrinthine architecture of the cecal mucosa exponentially amplifies the colonization landscape for microbial inhabitants, while the delicately thin cecal epithelium facilitates the expeditious translocation of fermentation-derived SCFAs into systemic circulation. In striking contradistinction, the human colonic architecture embodies a more contemplative digestive philosophy, characterized by leisurely luminal transit and progressively constricting diameters that sculpt the distinctive haustral topography. This anatomical masterpiece orchestrates prolonged substrate

retention, enabling the methodical and comprehensive deconstruction of complex carbohydrate matrices. The human colon manifests an elegant pH gradient cascade, thereby creating distinct ecological niches that strategically compartmentalize butyrate-producing populations proximally while concentrating ammonia-generating microorganisms distally (Cheng and Zhou, 2024; Xie Z. et al., 2024). The metabolomic fingerprints of these two biological systems reveal fascinatingly divergent signatures. Rodent fermentation chambers predominantly synthesize acetate-rich SCFA portfolios, with propionate occupying secondary prominence and butyrate assuming a more modest role—a metabolic choreography that epitomizes rapid high-fiber processing capabilities. Conversely, the human colonic fermentome exhibits a more sophisticated equilibrium, demonstrating reduced acetate predominance while elevating butyrate to greater prominence. This harmonious SCFA architecture reflects the complexity of omnivorous dietary adaptations and the intricate ecological networks governing human intestinal ecosystems, with butyrate emerging as an indispensable guardian of colonic epithelial barrier integrity through compelling clinical evidence. The secondary metabolite landscapes further illuminate these interspecies distinctions. Rodent bile acid biotransformation follows relatively streamlined pathways, predominantly yielding deoxycholic and lithocholic acid derivatives, whereas the human colonic microbiome orchestrates a more elaborate repertoire of secondary bile acid synthesis, encompassing ursodeoxycholic acid and numerous sophisticated metabolic derivatives. Similarly, tryptophan metabolic networks in human intestinal ecosystems generate remarkably diverse indole and derivative spectra, showcasing enhanced biochemical versatility. Despite these profound distinctions, both systems converge upon fundamental functional paradigms, particularly in energy metabolism orchestration, where both rodent and human microbiomes masterfully transform recalcitrant carbohydrates into bioavailable SCFAs, delivering vital energetic substrates to their respective hosts. Butyrate production exemplifies this functional convergence, serving as a pivotal homeostatic regulator that maintains intestinal equilibrium through the elegant induction of regulatory T-cell differentiation cascades in both species (Zhu et al., 2021), while propionate simultaneously modulates insulin sensitivity and lipid metabolism across phylogenetic boundaries (Jiao et al., 2021). The translational paradigm from rodent models to human clinical applications, while foundational to mechanistic understanding and therapeutic development, confronts formidable challenges rooted in these anatomical and physiological divergences. Probiotic strains demonstrating remarkable efficacy in murine systems may encounter colonization barriers or fail to replicate beneficial effects within the distinctive human intestinal landscape. Consequently, the scientific community must embrace increasingly sophisticated experimental architectures: deploying humanized microbiota mouse models to authentically recapitulate human intestinal ecosystems, implementing advanced *in vitro* colonic simulation platforms that faithfully mirror human fermentative environments, and pioneering novel biomarker discovery initiatives to enhance predictive accuracy of translational outcomes. Through these refined methodological innovations, researchers can architect more precise translational strategies, dramatically elevating the success trajectory from fundamental discovery to clinical implementation.

Clinical investigations have unveiled distinctive microbial trajectories in CKD cohorts: the inaugural disease phases are marked by profound diminution of SCFA-synthesizing taxa (encompassing *Prevotellaceae*, *Enterococcus*, and *Lactobacillus*), with the magnitude of this depletion demonstrating positive correlation with eGFR deterioration (Atzeni et al., 2024). Simultaneously, pathogenic bacterial assemblages (including *Enterobacteriaceae*, *E. coli*, and *Clostridioides*) undergo exponential expansion, perpetuating nephrotoxicity through the biosynthesis of uremic toxins including ammonia, indole, and para-cresol (Gryp et al., 2020b; Ahmed and Al-Massri, 2023). Particularly noteworthy is the elevation of *Bacteroidaceae* abundance, which demonstrates direct causality with uric acid/urea metabolic aberrations (Gryp et al., 2020b). As renal functionality undergoes progressive deterioration, anti-inflammatory microbial species such as *Roseburia* and *Faecalibacterium prausnitzii* experience sequential depletion (Yang C.-Y. et al., 2021; Cabała et al., 2024), while toxigenic *Clostridium* species undergo further amplification (Yang C.-Y. et al., 2021). Furthermore, the taxonomic lineage *Bacilli-Lactobacillales-Lactobacillaceae-Lactobacillus-Lactobacillus johnsonii* demonstrates positive correlation with CKD progression in clinical populations, with its abundance correlating with serum creatinine concentrations, and therapeutic supplementation of this strain conferring nephroprotective benefits (Miao et al., 2024a). This microbial dysregulation additionally predisposes to nephrolithiasis through oxalate metabolism perturbations, manifesting as augmented urinary oxalate excretion consequent to *Bifidobacterium* depletion and *Bacteroides* dominance (Cabała et al., 2024).

However, given the etiological heterogeneity encompassing primary and secondary CKD manifestations, the resultant gut microbiota perturbations exhibit pathophysiologically-distinct signatures (Li J. et al., 2024). In primary CKD complicated by nephrotic syndrome, patients afflicted with idiopathic membranous nephropathy (IMN) demonstrate pronounced enrichment of gram-negative pathogenic constituents including *Shigella* spp., *Streptococcus* spp., *Enterobacter* spp., *Enterococcus* spp., and *Escherichia coli*, while experiencing marked attenuation of beneficial taxa such as *Lachnospira*, *Lachnospiraceae*, and *Veillonella*, accompanied by compromised SCFA biosynthesis, attenuated immunomodulatory capacity, and heightened inflammatory cascades (Zhang J. et al., 2020; Motavalli et al., 2021; Doré et al., 2022). Minimal change disease (MCD) patients manifest diminished microbial biodiversity with depleted butyrate-producing genera including *Faecalibacterium* and *Prevotella*, contrasted by pathogenic bacterial amplification such as *Escherichia-Shigella* (Zhang Y. et al., 2022). Focal segmental glomerulosclerosis (FSGS) paradigms demonstrate enhanced *Bifidobacterium*, *Collinsella*, and *Candida* colonization, while experiencing significant depletion of beneficial taxa including *Granulicatella, Christensenella, Turicibacter*, and *Rikenella*, culminating in elevated deleterious metabolite concentrations, compromised intestinal barrier integrity, endotoxemia, and sustained mTORC1 signaling pathway activation that perpetuates glomerular sclerosis and fibrogenesis (Parker et al., 2020; Nakano et al., 2021; Shi et al., 2023). Mesangial proliferative glomerulonephritis (MsPGN) patients exhibit augmented *Bradyrhizobium* and *Hyphomicrobium* populations, concomitant with diminished *Ruminococcaceae*, *Alistipes*, and *Lachnospira* representation (He et al., 2021).

Predominant secondary CKD etiologies encompass DN and lupus nephritis (LN). DN patients manifest attenuated gut microbial biodiversity, with pronounced Actinobacteria elevation at the

phylogenetic level, accompanied by decreased *Alphaproteobacteria* and *Clostridia* populations. At the genus level, *Christensenella*, *Clostridium-XIVa*, and *Eisenbergiella* demonstrate enhanced abundance, with *Eisenbergiella* exhibiting positive correlation with glomerular sclerosis and basement membrane thickening (Lu et al., 2023). Gut microbial perturbations in DN demonstrate 63% metabolic association (Zhang B. et al., 2022; Zhao et al., 2024), characterized by diminished SCFA-producing bacteria (*Butyricicoccus*, *Faecalibacterium*, *Lachnospira*, *Roseburia*, *Ruminococcus*, *Coprococcus*, *Eubacterium*, and *Clostridium leptum*) and pronounced enrichment of pathogenic taxa *Hungatella*, *Bilophila*, and *Escherichia*, compromising serum and fecal SCFA concentrations, with this decline demonstrating positive correlation with renal dysfunction (Zhong et al., 2021). LN patients exhibit gut microbial dysregulation characterized by diminished Firmicutes/Bacteroidetes ratios, accompanied by enhanced *Proteobacteria*, *Streptococcus*, *Lactobacillus*, *Ruminococcus gnavus*, and *Lactobacillus reuteri* populations. *R. gnavus* abundance demonstrates nephrotrophic pathological predisposition, correlating positively with systemic inflammatory cascades, dysregulated inflammatory immune cell differentiation patterns, and autoantibody concentrations, while multi-strain *Lactobacillus* therapeutic intervention facilitates intestinal barrier restoration in LN murine models (Nepal and Gazeley, 2023; Wang A. et al., 2023; Hosseini et al., 2024). Additionally, IgA nephropathy, constituting a primary etiology with CKD progression potential, demonstrates elevated *Escherichia coli* abundance in affected patients relative to healthy controls, while altered *Enterococcaceae*, *Moraxella*, and *Acinetobacter* populations associate with renal dysfunction (Li X.-J. et al., 2024). IgA vasculitis with nephritis (IgAV-N) similarly progresses to CKD, exhibiting gut microbial dysbiosis characterized by enhanced potentially pathogenic bacteria including *Shigella* and *Streptococcus*, juxtaposed with diminished beneficial taxa such as *Prevotella* (Tan et al., 2022).

CKD patients advancing to ESRD necessitate dialytic intervention for survival. Microbial dysregulation in dialysis populations presents modality-specific perturbations: comprehensive *Firmicutes* depletion at the phylum level, accompanied by enhanced *Proteobacteria* and *Fusobacteria* abundance; diminished *Clostridia* representation at the class level with augmented *Gammaproteobacteria*; reduced *Clostridiales* abundance at the order level with enhanced *Enterobacteriales*; attenuated abundance of *Lactobacillaceae*, *Lachnospiraceae*, *Ruminococcaceae*, and *Bifidobacteriaceae* at the family level, contrasted by amplified *Enterobacteriaceae*, *Pseudomonadaceae*, and *Enterococcaceae*; diminished *Faecalibacterium*, *Roseburia*, *Bifidobacterium*, and *Prevotella* representation at the genus level, with enhanced *Escherichia*, *Shigella*, *Pseudomonas*, and *Enterococcus*; and reduced *Faecalibacterium prausnitzii* abundance at the species level accompanied by enhanced *Escherichia coli* (Bao et al., 2022; Shivani et al., 2022; Li J. et al., 2023; Teixeira et al., 2023; Stepanova, 2024). Distinct dialytic modalities generate divergent manifestations: hemodialysis patients characteristically exhibit *Actinobacteria*, *Firmicutes*, and *γ-Proteobacteria* proliferation, accompanied by pronounced depletion of butyrate-synthesizing taxa (including *Faecalibacterium* and *Roseburia*) (Gao et al., 2024; Yasuno and Ito, 2024), while peritoneal dialysis patients demonstrate *Enterobacteriaceae* amplification and *Bifidobacterium/Lactobacillus* depletion (James et al., 2025). These perturbations not only compromise intestinal barrier integrity but also exacerbate microinflammatory cascades through lipopolysaccharide (LPS) translocation, establishing a pernicious "gut-kidney axis deterioration cycle." Furthermore, gut microbial dysregulation constitutes a cardinal pathogenic determinant in CKD-associated cardiorenal syndrome (CRS), with microbial metabolites such as TMAO compromising cardiac and renal functionality, precipitating inflammatory cascades and fibrogenesis (Zhao B. et al., 2025).

In synthesis, CKD-associated microbial dysregulation manifests through a paradigmatic trajectory of "beneficial taxa depletion—pathogenic taxa hegemony," propelling disease progression via multifaceted mechanisms encompassing uremic toxin biosynthesis, metabolic dysfunction, and immunological dysregulation. Comprehensive elucidation of gut microbiota pathophysiological contributions in CKD establishes the theoretical foundation for revolutionary therapeutic paradigms predicated upon microbiome modulation (Gryp et al., 2020b; Yang C.-Y. et al., 2021; Cabała et al., 2024).

2.2 Dysbiosis-induced metabolic disruption and escalation of inflammatory responses

CKD patients manifest profound microbial biodiversity attenuation, accompanied by pathological proliferation of urease-synthesizing bacteria and proteolytic bacterial consortia. This ecological perturbation orchestrates intestinal homeostatic collapse through multifarious pathophysiological cascades (Li X.-J. et al., 2024). Bacterial urease-mediated ammonia (NH_3) biosynthesis precipitates dramatic colonic pH alkalinization (transitioning from physiological mild acidification to pathological alkalinity), consequently triggering aberrant goblet cell hypersecretion, compromising colonic epithelial barrier architectural integrity, and culminating in catastrophic intestinal permeability augmentation (Rukavina Mikusic et al., 2020). These pathological metamorphoses facilitate the systematic translocation of protein-bound uremic toxins (encompassing IS and PCS) and bacterial-derived metabolites (including LPS) into systemic circulation via portal venous networks. Concomitantly, CKD patients exhibit profound downregulation of organic anion transporter OAT1/OAT3 expression within renal and hepatic parenchyma, accompanied by compromised efflux pump BCRP and MRP2/4 functionality, ultimately precipitating catastrophic systemic uremic toxin bioaccumulation (Masereeuw, 2022; Spicher et al., 2025; You et al., 2025). These accumulated nephrotoxic moieties demonstrate remarkable capacity to traverse formidable biological barriers including the blood–brain and blood-pancreatic barriers, orchestrating deleterious multi-organ system perturbations encompassing the central nervous system, pancreas, and skeletal musculature through sophisticated epigenetic modifications and pivotal signaling pathway dysregulation, ultimately catalyzing systemic endotoxemia characterized by relentless low-grade inflammatory cascades and profound immunological dysregulation, establishing a pernicious pathophysiological vortex that exponentially accelerates renal functional deterioration (Bossola and Picconi, 2024; Cabała et al., 2024; He et al., 2024; Xie H. et al., 2024; Chen M.-C. et al., 2025).

Urea, functioning as the quintessential uremic metabolite orchestrating CKD progression, undergoes profound metabolic pathway remodeling during renal functional decimation: as estimated

glomerular filtration rate (eGFR) experiences precipitous decline, urea excretory mechanisms undergo dramatic transition from renal dominance to compensatory colonic clearance modalities (Tsuji et al., 2024). This pathological compensatory paradigm precipitates dose-dependent colonic urea concentration escalation, systematically inhibiting SCFA-producing bacterial proliferation while selectively promoting urease-producing pathogenic bacterial colonization supremacy, establishing a devastating "urea bioaccumulation–dysbiotic amplification" positive feedback vortex (Li Y. et al., 2023; Pyatchenkov et al., 2023). Urea and its cytotoxic degradation product ammonia orchestrate submucosal M1 macrophage polarization and catalyze pro-inflammatory mediator cascade release (González-Guerrero et al., 2017; Qian, 2017; Kim et al., 2025; Shentu et al., 2025); simultaneously, these metabolites systematically downregulate tight junction protein Claudin-1 and ZO-1 phosphorylation homeostasis, inducing epithelial cell junctional complex architectural disintegration and exponentially augmenting bacterial DNA and endotoxin translocation vulnerability (Wang and Gao, 2022; Kane et al., 2023). Remarkably, reactive oxygen species (ROS) generated through colonic urea metabolic processes demonstrate capacity to induce renal tubular epithelial cell mitochondrial functional catastrophe, exponentially accelerating tubulointerstitial fibrotic transformation and establishing a devastating "gut-derived urea–renal injury" pathophysiological cascade amplification phenomenon (Rukavina Mikusic et al., 2020; Pissas et al., 2024; Yang et al., 2025).

Intestinal microbial dysregulation additionally orchestrates protein-bound toxin biosynthetic amplification through aberrant aromatic amino acid metabolism (encompassing tryptophan, tyrosine, and phenylalanine), synthesizing IS, indole-3-acetic acid (IAA), PCS, and phenylacetylglutamine. Sophisticated clinical cohort investigations have definitively established that plasma concentrations of these nephrotoxic moieties demonstrate profound positive correlation with complication incidence trajectories and all-cause mortality paradigms in CKD populations (Yang C.-Y. et al., 2021; Cabała et al., 2024), with IS and PCS functioning as sophisticated biomarkers that exquisitely reflect renal functional decline kinetics, assess renal functionality and disease severity gradations, demonstrating exceptional concordance with CKD staging classifications (Corradi et al., 2024).

IS orchestrates endothelium-dependent vasodilation impairment through sophisticated AhR receptor binding mechanisms and nitric oxide synthase activity inhibition; its extraordinary albumin-binding affinity renders it virtually recalcitrant to conventional hemodialytic clearance modalities (Gryp et al., 2020a; Nguyen et al., 2022; Sánchez-Ospina et al., 2024). At the molecular architectural level, IS executes extraordinarily inflammatory signaling orchestration within renal parenchymal microenvironments through multifarious convergent pathophysiological cascades: it facilitates NF-κB nuclear translocation dynamics via toll-like receptor 4 (TLR4) activation paradigms in renal tubular epithelial cellular matrices (Pei et al., 2022), concurrently catalyzing NLRP3 inflammasome architectural assembly and subsequent IL-1β and IL-18 cytokine liberation cascades (Yamaguchi et al., 2022). Furthermore, IS orchestrates p38 MAPK and ERK1/2 phosphorylation signaling networks, culminating in amplified biosynthesis of pro-inflammatory cytokine arsenals encompassing TNF-α, IL-6, and MCP-1 (Ribeiro et al., 2023). This nephrotoxic moiety additionally activates aryl hydrocarbon receptor (AhR) signaling architectures within podocyte and mesangial cellular compartments, inducing CYP1A1 expression paradigms while exacerbating oxidative stress microenvironments and promoting TGF-β1 transcriptional upregulation, thereby exponentially accelerating glomerulosclerotic progression and tubulointerstitial fibrotic transformation trajectories (Iwashima et al., 2024; Nanto-Hara and Ohtsu, 2024).

p-Cresol (PCS), constituting a sophisticated tyrosine metabolism byproduct, systematically compromises renal functionality through oxidative stress amplification and inflammatory response orchestration, with its sulfate and glucuronide derivatives exhibiting extraordinary nephrotoxic potency and demonstrating relentless systemic bioaccumulation, exponentially exacerbating tissue injury (Sánchez-Ospina et al., 2024; Renaldi et al., 2025). PCS demonstrates extraordinary proficiency in activating renal inflammatory network architectures through complementary yet mechanistically distinct pathophysiological paradigms: it promotes ROS generation via NADPH oxidase activation cascades within renal tubular epithelial cellular matrices, simultaneously catalyzing JNK and p38 MAPK signaling pathway orchestration (Chang et al., 2020). PCS additionally activates NF-κB pathway architectures through IκB kinase (IKK) phosphorylation mechanisms, precipitating enhanced transcriptional activation of pro-inflammatory genetic programs encompassing COX-2, iNOS, and diverse chemokine repertoires (Kuang et al., 2022). This metabolite further disrupts mitochondrial bioenergetic homeostasis through complex III inhibition paradigms, precipitating amplified superoxide production cascades and subsequent activation of redox-sensitive transcription factor networks, ultimately culminating in enhanced expression of profibrotic mediator arsenals (Al Khamici et al., 2022; Mishra et al., 2024).

Sophisticated research paradigms have elucidated that plasma tryptophan concentrations demonstrate positive correlations with *Turicibacter*, *Clostridium IV*, *Pseudomonas*, and *Lactobacillales,* while exhibiting inverse correlations with *Blautia*, *Oscillibacter*, and *Intestinimonas*. These latter genera harbor sophisticated genetic arsenals encoding pivotal tryptophan metabolism enzymes (including tryptophan synthase K16187, indoleamine-2,3-dioxygenase IDO K00463, and tryptophan-2,3-dioxygenase TDO K00453) and their corresponding enzymatic machinery (EC:1.13.11.52 and EC:1.13.11.11), which systematically amplify tryptophan metabolite biosynthesis, thereby exponentially accelerating renal fibrotic progression trajectories. In 5/6 nephrectomy rodent paradigms, attenuated serum tryptophan concentrations and elevated plasma concentrations of tryptophan metabolites demonstrate positive correlations with intestinal *Clostridium IV* abundance while exhibiting inverse correlations with *Blautia*, *Enterorhabdus*, *Allobaculum*, *Clostridium sensu stricto*, and *Escherichia shigella* populations (Selby and Taal, 2024). Furthermore, tryptophan metabolic aberrations have been meticulously characterized in DN and membranous nephropathy paradigms (Gooding et al., 2019). In DN pathophysiology, amplified *Escherichia* abundance intensifies tryptophan metabolic cascades, generating nephrotoxic indole and its derivative IS, exponentially exacerbating renal functional deterioration (Li J. et al., 2024); in membranous nephropathy contexts, diminished *Lactobacillus johnsonii, L. reuteri, L. vaginalis, L. murinus*, and *Bifidobacterium animalis* populations demonstrate positive correlations with IAld, indole-3-pyruvate, and tryptamine mortality trajectories while exhibiting inverse correlations with elevated IAA and ILA concentrations (Miao et al., 2024b).

Additionally, TMAO (synthesized through microbial metabolism of dietary choline and carnitine precursors) demonstrates profound associations with atherosclerotic progression trajectories and cardiovascular risk amplification (Zhen et al., 2023). Within renal cellular microenvironmental, TMAO orchestrates extraordinarily inflammatory activation paradigms through multifarious complementary mechanistic networks: it amplifies scavenger receptor CD36 expression dynamics within macrophage populations infiltrating renal interstitial compartments, promoting foam cell morphological transformation and subsequent inflammatory mediator liberation cascades (Luo et al., 2024). TMAO additionally catalyzes NLRP3 inflammasome pathway activation within renal tubular epithelial cellular matrices through potassium efflux-dependent mechanistic paradigms, precipitating caspase-1 activation cascades and enhanced IL-1β processing machinery (Kapetanaki et al., 2021). Furthermore, TMAO promotes endoplasmic reticulum stress responses within podocyte cellular compartments via IRE1α and PERK pathway activation architectures, culminating in amplified production of inflammatory cytokine arsenals and accelerated apoptotic cell death trajectories (Pan et al., 2023). This metabolite concurrently activates vascular smooth muscle cell proliferative cascades through PDGF receptor signaling orchestration while promoting endothelial dysfunction via eNOS uncoupling mechanisms and enhanced superoxide production paradigms (Brunt et al., 2020). In DN pathophysiology, intestinal *Hungatella* populations and their progenitor bacterium *Clostridium hathewayi* orchestrate TMAO biosynthetic amplification, catalyzing inflammatory cascade activation and augmenting oxidative stress paradigms alongside renal fibrotic transformation (Li J. et al., 2024); altered *Streptococcus* abundance demonstrates positive correlations with hypoalbuminemic states and hematuria manifestations in IgAV-N patients, while *Escherichia–Shigella* populations synthesize LPS that achieves systemic circulation, activating sophisticated immune response cascades and directly orchestrating glomerular endothelial and renal tubular epithelial cell injury (Li J. et al., 2024). In advanced CKD necessitating dialytic intervention, the metabolic landscape undergoes catastrophic transformation, with previously delineated trends in SCFA, TMAO, IS, and p-cresol concentrations becoming exponentially severe (Bao et al., 2022; Li J. et al., 2023). Illustratively, diminished beneficial bacterial populations including *Faecalibacterium*, *Roseburia*, and *Bifidobacterium*-induced SCFA biosynthetic deficiency precipitates systemic inflammatory cascade activation and cardiovascular risk amplification in PD patients (Jiang et al., 2021; Li J. et al., 2023). Conversely, pathological expansion of potentially pathogenic bacterial populations including *Escherichia*, *Shigella*, and *Enterococcus* may exponentially augment peritonitis susceptibility and infection vulnerability in PD populations (Zhou et al., 2022). Phenylacetylglutamine (derived through phenylalanine metabolic pathways) demonstrates profound elevation in advanced CKD and dialytic patients, augmenting arrhythmic vulnerability through cardiomyocyte calcium homeostatic disruption (Wang and Gao, 2022; Kane et al., 2023).

The pathophysiological manifestations of these gut-derived nephrotoxic moieties exhibit sophisticated multi-organ network characteristics: within intestinal microenvironments, toxin bioaccumulation exacerbates barrier dysfunction through tight junction protein complex architectural disruption and intestinal epithelial cell apoptotic cascade induction; systemically, these toxins orchestrate chronic inflammatory microenvironmental establishment through monocyte surface TLR activation and NF-κB signaling cascade initiation; within renal parenchymal architecture, toxins exponentially accelerate tubular atrophic transformation and interstitial fibrotic progression through mitochondrial oxidative phosphorylation uncoupling mechanisms and endoplasmic reticulum stress pathway activation (Chermiti et al., 2024; Frąk et al., 2024; Li X.-J. et al., 2024; Peris-Fernández et al., 2024a, 2024b). Furthermore, the prevalent delayed colonic transit phenomenon in CKD populations systematically exacerbates microbial dysbiotic states and metabolic perturbations by prolonging toxin-mucosa interface duration (Talamantes et al., 2024). Contemporary mechanistic investigations have revealed that IS orchestrates sophisticated disruption of mitochondrial fission/fusion architectural dynamics, systematically impedes physiological mitochondrial biogenetic processes, interferes with mitochondrial electron transport chain functionality, while compromising mitochondrial quality control homeostatic mechanisms, fundamentally remodeling gut microbiota metabolic phenotypic expressions, illuminating the pivotal significance of "microbiota–mitochondria cross-talk" paradigms in uremic toxin bioaccumulation phenomena (Lu et al., 2025; Rumanli et al., 2025).

This "intestinal microbial dysregulation–uremic toxin bioaccumulation–multi-organ injury cascade" constitutes the cardinal pathophysiological circuitry orchestrating CKD progression trajectories (Figure 1). Comprehensive elucidation of the sophisticated molecular mechanisms governing pivotal nodes within this intricate system (encompassing urease activity regulatory paradigms, tight junction protein post-translational modification networks, and toxin receptor signal transduction cascades) will establish the theoretical foundation for developing revolutionary multi-target therapeutic strategies specifically targeting the sophisticated "gut–kidney axis" pathophysiological network.

2.3 Technological insights into gut-kidney crosstalk

Contemporary breakthroughs in organ-on-a-chip biotechnology have unveiled the exquisitely orchestrated bidirectional crosstalk networks between gastrointestinal and renal physiological systems (Wang et al., 2024). Pioneering experimental paradigms utilizing gut-on-a-chip microfluidic platforms have demonstrated that exposure to intestinal barrier-compromising agents, encompassing bacterial lipopolysaccharides and pro-inflammatory cytokine cascades, precipitates quantifiable augmentation of epithelial barrier permeability dynamics. Concurrent investigations employing cutting-edge kidney-on-a-chip architectures have revealed that renal parenchymal tissues demonstrate remarkable adaptive responsiveness to gut-derived metabolic signaling through modulation of transport protein expression repertoires, representing an elegant adaptive mechanism meticulously calibrated to preserve systemic metabolic equilibrium (Jochems et al., 2019; Langerak et al., 2020).

This revolutionary technological paradigm has catalyzed unprecedented revelations into the intricate molecular choreography governing inter-organ communication networks, particularly illuminating the cardinal significance of microbiota-derived metabolites in orchestrating both physiological homeostatic maintenance and CKD pathogenesis trajectories. The seamless integration of these sophisticated microfluidic organ modeling

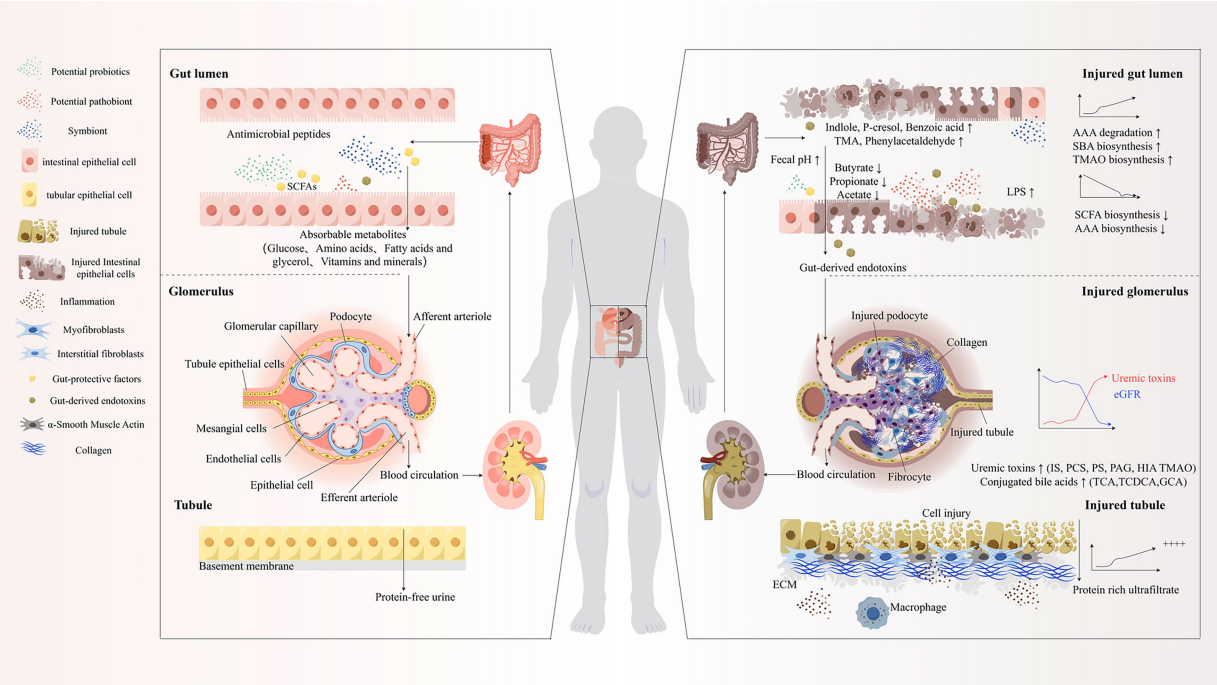

FIGURE 1
"Gut-Kidney Axis" theory. SCFAs, Short-Chain Fatty Acids; TMA, Trimethylamine; AAA, Aromatic Amino Acids; SBA, Secondary Bile Acids; TMAO, Trimethylamine N-oxide; eGFR, Estimated Glomerular Filtration Rate; IS, Indoxyl Sulfate; PCS/PS, p-Cresyl Sulfate; PAG, Phenylacetic Acid; HIA, Hippuric Acid; TCA, Tricarboxylic Acid; TCDCA, Taurochenodeoxycholic Acid; GCA, Glycocholic Acid; ECM, Extracellular Matrix; LPS, Lipopolysaccharide.

systems establishes an extraordinarily refined experimental framework for elucidating the mechanistic foundations underlying gut-kidney axis dysregulation phenomena, potentially catalyzing the emergence of precision-targeted therapeutic interventions specifically designed to combat chronic kidney disease pathophysiology.

3 Therapeutic strategies targeting the gut-kidney axis: current advances

Therapeutic paradigms predicated upon gut-kidney axis pathophysiology have undergone sophisticated evolution into comprehensive, multidimensional intervention architectures. This encompasses an arsenal of microbiota-modulatory agents (encompassing probiotics, prebiotics, and synbiotic formulations), precision dietary compositional strategies, physisorption-based therapeutic modalities (including advanced adsorption technologies), and sophisticated uremic toxin elimination protocols. Each therapeutic modality demonstrates distinctive mechanistic profiles and clinical applications, collectively establishing a holistic therapeutic framework for optimizing renal functionality through meticulously calibrated interventions.

3.1 Microbiota-modulating agents

3.1.1 Probiotic orchestration of intestinal homeostasis

Probiotics constitute an elite consortium of beneficial bacterial assemblages endowed with extraordinary capacity to orchestrate comprehensive intestinal microecological architectural transformation through colonization dynamics and competitive exclusion of deleterious pathogenic entities, thereby catalyzing profound enhancement of intestinal metabolic functionality and conferring multidimensional health optimization benefits (Ghasemzadeh, 2024). Distinguished probiotic taxonomic lineages encompass *Lactobacillus*, *Bifidobacterium*, *Propionibacterium*, *Bacillus*, *Akkermansia muciniphila*, *yeast species*, and *Streptococcus thermophilus* (Yang et al., 2022). Among these microbial virtuosos, *Lactobacillus* and *Bifidobacterium* are universally acclaimed as the foundational architectural cornerstones for engineering efficacious probiotic therapeutic masterpieces (Huang and Chen, 2024).

Lactobacillus demonstrates exquisite functionality through sophisticated lactic acid biosynthetic orchestration, precipitating strategic intestinal pH acidification that systematically inhibits acid-susceptible pathogenic proliferation while cultivating extraordinarily favorable intestinal microbial ecosystems (Leska et al., 2022). In elegant counterpoint, *Bifidobacterium* operates through sophisticated uremic metabolite biotransformation cascades, systematically attenuating toxin bioaccumulation while catalyzing SCFA biosynthesis through intricate carbohydrate fermentation choreography, further suppressing deleterious bacterial expansion (Anjana and Tiwari, 2022; de Carvalho et al., 2024). The exquisite synergistic interplay between *Lactobacillus* and *Bifidobacterium* transcends mere intestinal acid–base equilibrium maintenance, orchestrating comprehensive systemic health optimization through mechanisms encompassing antimicrobial compound biosynthesis, competitive nutritional and binding site monopolization, immune regulatory cellular activation cascades, and essential enzymatic and vitamin synthetic pathways (Tian et al., 2022).

The extraordinary therapeutic potential of probiotic interventions in end-stage CKD management has been meticulously substantiated through comprehensive research paradigms, demonstrating profound positive impacts on clinical trajectories (Soleimani et al., 2017; Yu et al., 2022; Huang and Chen, 2024; Ribeiro et al., 2024). Exemplifying this therapeutic excellence, clinical investigations in CKD stage 3–4 populations revealed that daily administration of meticulously engineered capsules containing 9 billion CFU probiotic consortiums (encompassing *Lactobacillus acidophilus KB27, Bifidobacterium longum KB31*, and *Streptococcus thermophilus KB19*) achieved remarkable reductions in blood urea nitrogen (BUN), creatinine, and uric acid concentrations while dramatically enhancing quality of life parameters with exceptional safety profiles (Ranganathan et al., 2010; Rahman et al., 2024). Particularly noteworthy, *Streptococcus thermophilus*, distinguished by extraordinary urease enzymatic activity, assumes pivotal significance in urea biotransformation and metabolic optimization choreography; its synergistic collaboration with *Lactobacillus* and *Bifidobacterium* generates superior metabolic byproducts, orchestrates intestinal environmental amelioration, and amplifies overall probiotic combination therapeutic magnificence (Arioli et al., 2024; Huang et al., 2024). Furthermore, probiotics facilitate comprehensive gastrointestinal symptom resolution in CKD populations (Yu et al., 2022) and potentially mitigate renal colic vulnerability associated with nephrolithiasis (Wigner et al., 2022). For advanced CKD patients, particularly those requiring hemodialytic interventions, pioneering research has demonstrated that *Bifidobacterium* encapsulation in acid-resistant delivery systems maintains extraordinary viability within hostile gastric acidic environments, enabling triumphant intestinal colonization and subsequent dramatic reductions in serum homocysteine, IS, and triglyceride concentrations while orchestrating profound renal functional restoration (Juárez-Trujillo et al., 2024; Schlienger de Alba and Espinosa Andrews, 2024). Wang et al.'s groundbreaking investigations demonstrated that probiotic interventions ameliorate GFR deterioration trajectories while achieving profound reductions in serum pro-inflammatory cytokine cascades, encompassing TNF-α, IL-6, and IL-18, in ESRD patients receiving hemodialytic therapy (Wang et al., 2021). Probiotics additionally orchestrate intestinal microbiota regulation to dramatically reduce peritonitis incidence, preserve residual kidney function, modulate inflammatory cascades, optimize nutritional parameters, and enhance health-related quality of life in advanced CKD patients requiring dialytic interventions (Stepanova, 2024).

Nevertheless, probiotic applications encounter sophisticated challenges requiring strategic resolution. Certain elite bacterial strains demand extraordinarily stringent survival parameters, including precisely calibrated pH environments or specialized hypoxic conditions, imposing elevated requirements for probiotic formulation engineering excellence and stability maintenance (Wigner et al., 2022). Despite extensive research establishing remarkable therapeutic potential in CKD management, consensus regarding optimal dosing paradigms, strain combination architectures, and treatment duration protocols remains elusive, while individual patient responses to probiotic interventions exhibit significant variability, further complicating standardized treatment protocol development. With revolutionary advancement in formulation biotechnologies, particularly groundbreaking achievements in strain stability enhancement and bioactivity amplification, alongside personalized probiotic combination engineering for CKD populations, probiotics are destined to assume transformative leadership roles in future nephrology therapeutics.

3.1.2 Prebiotic ecological niche engineering mastery

Prebiotics constitute an elite class of functional non-viable substrates endowed with extraordinary capacity to undergo selective fermentation orchestration by specific intestinal probiotic virtuosos (particularly *Bifidobacterium* and *Lactobacillus*), thereby achieving profound intestinal microecological architectural metamorphosis. Prebiotics demonstrate ubiquitous presence within natural botanical matrices and, functioning as precision nutritional intervention modalities, exhibit unparalleled advantages in CKD populations confronting dietary protein restriction challenges (Tsai et al., 2019). This compound classification encompasses extraordinary diversity, including long-chain polyunsaturated fatty acids, fructooligosaccharide complexes, extended-chain inulin architectures, and resistant starch formulations, each possessing distinctive biochemical characteristics and therapeutic signatures (Gibson et al., 2017).

Prebiotics orchestrate probiotic proliferation enhancement, systematically inhibiting uremic toxin biosynthesis within colonic environments while dramatically amplifying SCFA generation cascades, thereby establishing intricate synergistic mechanisms specifically engineered to combat CKD-associated nephropathic processes (Tsai et al., 2019). Clinical investigations have demonstrated that meticulously engineered fructooligosaccharide-inulin composite prebiotic formulations achieve remarkable reductions in PCS biosynthetic rates and serum concentrations in advanced CKD populations (Mitrović et al., 2024; Yin et al., 2024). However, consequent to extraordinary compositional heterogeneity and sophisticated physiological interaction networks inherent to prebiotic architectures, definitive daily intake dosing paradigms specifically applicable to CKD populations remain unestablished. Clinical efficacy demonstrates profound influence from multifarious parameters, encompassing average polymerization degrees, dosing regimen protocols, treatment duration paradigms, and individual patient CKD disease progression stages, with these variables collectively orchestrating prebiotic intervention therapeutic performance trajectories.

3.1.3 Synbiotic symphonic therapeutic orchestration

Synbiotics represent the absolute pinnacle of renal disease microecological intervention sophistication, constructing extraordinary synergistic therapeutic ecosystems through precision molecular matching of elite probiotic populations with meticulously targeted prebiotic substrate architectures. This revolutionary strategic paradigm generates sophisticated biological "symphonic masterpieces" within intestinal microecological landscapes, achieving unprecedented multi-dimensional precision interventions across comprehensive CKD pathophysiological networks. Synbiotic therapeutic excellence manifests through dual-mechanism orchestration: selective amplification of glycolytic beneficial bacterial populations while systematically suppressing proteolytic pathogenic bacterial consortiums characterized by potent protease enzymatic activity, thereby fundamentally reconstructing metabolic

architectural landscapes within intestinal microenvironments, dramatically reducing uremic toxin burdens, restoring sophisticated immune homeostatic equilibrium, suppressing inflammatory cascade networks, and orchestrating profound renal functional restoration (Kieffer et al., 2016; Plaza-Díaz et al., 2017; Liu et al., 2024).

Synbiotic therapeutic magnificence has been comprehensively validated through clinical research paradigms. Illustratively, meticulously engineered synbiotic formulations encompassing *Lactobacillus*, *Bifidobacterium breve*, and galactooligosaccharide complexes achieve remarkable reductions in patient serum toxic metabolite concentrations, particularly demonstrating extraordinary PCS elimination efficacy (Mitrović et al., 2024; Anegkamol et al., 2025). Diverse synbiotic combination architectures exhibit unique therapeutic signature profiles, exemplified by sophisticated formulations containing *Lactobacillus*, *Bifidobacterium*, *Streptococcus*, and inulin complexes effectively reducing indole-producing bacterial abundance, thereby dramatically attenuating indole-class metabolites intimately associated with renal injury cascades (Yang C.-Y. et al., 2021).

Synbiotic therapeutic actions transcend conventional toxin elimination paradigms, demonstrating extraordinary multidimensional advantages at metabolic regulatory orchestration levels. They catalyze intestinal microbial biosynthesis of essential B-complex vitamin complexes (encompassing folate and niacin architectures), thereby elevating serum folate concentrations while dramatically reducing triglyceride and homocysteine levels—the latter constituting critical cardiovascular risk determinants in CKD populations. Additionally, synbiotics enhance calcium bioavailability through sophisticated intestinal pH regulatory orchestration, thereby strengthening calcium-phosphorus binding dynamics and ameliorating phosphorus metabolic disorders ubiquitous in CKD pathophysiology. Most remarkably, synbiotics orchestrate enhanced intestinal microbiota oxalate metabolic capacity, achieving profound reductions in urinary oxalate excretion, thereby assuming pivotal significance in nephrolithiasis prevention and associated renal injury mitigation (Rossi et al., 2015a). This comprehensive synergistic mechanism constellation establishes synbiotics as revolutionary therapeutic paradigms in comprehensive renal disease management architectures.

Contemporary network meta-analytical investigations have unveiled therapeutic spectrum differentiations among diverse microecological intervention modalities: prebiotics demonstrate maximal efficacy in uremic toxin elimination, achieving standardized mean differences of −1.24 for IS concentrations; synbiotics exhibit extraordinary advantages in microinflammatory regulatory orchestration, achieving remarkable 28.6% CRP concentration reductions; while probiotics demonstrate exceptional efficacy in gastrointestinal symptom amelioration, exhibiting relative risk ratios of 2.17 (Yu et al., 2022). Contemporary research trajectories are advancing toward two pioneering frontiers: individualized treatment strategy engineering predicated upon sophisticated microbiome precision stratification paradigms, and revolutionary nanotechnology utilization for optimizing active ingredient colonic-targeted delivery system architectures to enhance bioavailability and stability parameters. These groundbreaking advancement trajectories are destined to elevate "gut-kidney axis" interventions from adjunctive therapeutic modalities to cardinal pillars of comprehensive CKD treatment paradigms, inaugurating a transformative renaissance era in sophisticated nephrology therapeutic excellence.

3.2 Dietary composition: the molecular symphony of therapeutic nutrition

Dietary intervention emerges as the cardinal therapeutic paradigm within contemporary precision medicine, constituting the architectural foundation of CKD management. Through the meticulous orchestration of bespoke nutritional algorithms—particularly the synergistic convergence of low-protein dietary regimens (LPD) and dietary fiber modalities (DF)—clinicians achieve unprecedented manipulation of gut microbiome plasticity, catalyzing the biosynthesis of salutogenic metabolites (notably SCFAs) while simultaneously orchestrating the systematic suppression of deleterious proteolytic fermentation cascades. This sophisticated intervention matrix stabilizes pathophysiological trajectories, decelerates nephrosclerotic progression, and fundamentally reconstitutes prognostic landscapes in CKD populations (Serrano et al., 2022; Watanabe et al., 2022; Chang et al., 2023).

3.2.1 The metabolic virtuosity of low-protein dietary architecture

The therapeutic magnificence of LPD paradigms resides in their exquisite choreography of nutritional homeostasis and metabolic refinement—achieved through precision-engineered protein restriction synergistically enhanced by essential amino acid (EAA) and ketoacid analogue supplementation. Within its biochemical nucleus, this intervention masterfully attenuates intestinal protein hydrolytic fermentation substrates, eloquently diminishing the genesis of nephrotoxic nitrogenous metabolites including ammonia and hydrogen sulfide, thereby dramatically alleviating renal metabolic burden (Watanabe et al., 2022; Wang et al., 2023b).

This sophisticated nutritional strategy operates through an intricate constellation of variables governing intestinal protein assimilation dynamics—encompassing quantitative intake parameters, protein conformational architectures (particularly thermodynamic denaturation profiles), phylogenetic origins (botanical versus zoological), and the complex matrix of concurrent dietary constituents. This multidimensional orchestration profoundly modulates small intestinal absorption kinetics and colonic transit dynamics, ultimately determining therapeutic magnitude for CKD populations (Di Iorio et al., 2019).

Compelling evidence demonstrates this dietary paradigm's extraordinary capacity to recalibrate the delicate equilibrium between protein catabolism and amino acid salvage networks, facilitating adaptive responses to protein-restricted nutritional landscapes while preserving fundamental physiological integrity (Garibotto et al., 2018).

Within the microbial dimension, low-protein intervention precipitates a remarkable architectural transformation of intestinal microbial ecosystems in advanced CKD (stages 3B-4): initially, it orchestrates strategic depletion of pro-inflammatory *Proteobacteria* populations while concurrently amplifying anti-inflammatory *Actinobacteria* representation; subsequently, it catalyzes selective proliferation of butyrate-synthesizing bacterial consortiums (encompassing *Lachnospiraceae*, *Prevotellaceae*, *Bifidobacteriaceae*, *Faecalibacterium*, and *Roseburia*) alongside anti-inflammatory genera

(notably *Blautia* and *Bacteroides*); finally, it systematically suppresses colonization of pathogenic microorganisms implicated in uremic toxin synthesis, including *Akkermansia*, *Streptococcus*, and *Escherichia* (Di Iorio et al., 2019). This microbial metamorphosis manifests clinically as simultaneous attenuation of circulating uremic toxins and D-lactic acid—with therapeutic efficacy exhibiting precise dose-dependency relative to dietary protein consumption (Di Iorio et al., 2019).

Pioneering investigations into amino acid pharmacological nutrition reveal the extraordinary therapeutic potential of sulfur-enriched amino acid regimens (featuring methionine and cysteine). These molecular entities execute post-translational modifications that fundamentally reconstitute the functional landscape of intestinal microbiota in experimental CKD paradigms. Their biochemical signature manifests as pronounced attenuation of tryptophanase enzymatic activity, effectively disrupting uremic toxin biosynthetic cascades and ultimately preserving host physiological integrity (Lobel et al., 2020).

Advanced pharmacological elucidation illuminates the metabolic elegance of ketoacid analogues, which—through their sophisticated transamination chemistry—sequester excess amino nitrogen reservoirs, channeling them toward *de novo* essential amino acid biosynthesis. This remarkable biochemical transformation not only diminishes nitrogenous waste streams and uremic toxin production but significantly decompresses renal metabolic burden. The metabolic reprogramming orchestrated by ketoacids transcends mere protein catabolism inhibition, extending to comprehensive optimization of protein metabolic networks and amino acid recycling efficiency in CKD patients, culminating in enhanced renal function preservation and disease trajectory modification (Ammar, 2022; Faerber et al., 2023; Chen Z. et al., 2024).

3.2.2 The metabolic orchestration of dietary fiber therapeutics

Dietary Fiber (DF) crystallizes as the quintessential therapeutic cornerstone within the nutritional architecture for CKD patients—a therapeutic modality whose profound clinical significance transcends its humble molecular origins. At its structural essence, DF encompasses an elegant consortium of carbohydrate architectures that ingeniously circumvent human digestive enzymatic systems (Jensen et al., 2024), functioning as molecular sentinels that fortify gastrointestinal barrier integrity, orchestrate intricate microecological symphonies within the gut, and dramatically decompress renal metabolic pathways. Meticulously engineered high-fiber nutritional protocols achieve masterful equilibrium—delivering abundant fiber while deftly navigating the treacherous terrain of potassium and phosphorus accumulation, thus epitomizing precision in dietary therapeutics.

Through modulation of intestinal microbial constellations responsible for uremic toxin metabolism and renal metabolite transformation, DF reveals its extraordinary therapeutic potential within CKD's clinical landscape. At the molecular frontier, DF artfully reprograms the nitrogen metabolism blueprint of gut flora: primarily, it catalyzes metabolic alchemy wherein intestinal microorganisms transmute urea and amino acids into vital anabolic building blocks, thereby refining the architectural and functional elegance of microbial ecosystems (Bergen, 2015); secondarily, it strategically curtails indigestible carbohydrate availability within colonic environments, imposing selective pressure against amino acid fermentation pathways, consequently diminishing nephrotoxic metabolite biosynthesis (De Vadder et al., 2014; Rossi et al., 2015b).

This harmonized biological choreography enables DF to recalibrate intestinal pH homeostasis, safeguard molecular integrity of tight junction proteins (notably ZO-1 and Occludin), and ultimately fortify barriers against pathological intestinal permeability (Yokoo et al., 2021; Skinner et al., 2025). Concurrently, DF employs sophisticated nitrogen chelation chemistry to dramatically reduce hepatorenal nitrogen burden (Mardinoglu et al., 2015; Yang H. L. et al., 2021), attenuating systemic inflammatory cascades and culminating in profound reductions of all-cause mortality among CKD populations (Chen Y. et al., 2024; Rispoli et al., 2025).

Resistant Starch (RS)—a distinguished member of the DF therapeutic pantheon—demonstrates extraordinary clinical virtuosity. Compelling evidence illuminates RS's capacity to significantly diminish circulating IS and PCS concentrations in end-stage CKD patients undergoing hemodialysis (Jia et al., 2021). In preclinical investigations, RS intervention demonstrates remarkable restorative potential, rehabilitating renal function and intestinal barrier architecture in adenine-induced CKD models, while concurrently reducing tubulo-interstitial pathology scores and eliminating uremic toxins from circulatory systems (Kingra et al., 2022; Shamloo et al., 2022; Zhang Y. et al., 2024).

The specialized fermentable fiber compounds Guar Gum (GG) and Partially Hydrolyzed Guar Gum (PHGG) reveal multidimensional therapeutic virtuosity in experimental CKD paradigms: initially, they engineer strategic reductions in serum nitrogenous waste products (urea/creatinine); subsequently, they selectively silence pro-inflammatory cytokine expression (TNF-α, IL-1β, IL-6) and fibrogenic molecular pathways (TGF-β1, Col1a1); finally, they cultivate beneficial microbiotic transformations—enhancing Lactobacilli colonization and SCFA (acetate, propionate, butyrate) production—thereby orchestrating comprehensive recalibration of intestinal microbial ecology (Hung and Suzuki, 2018). This multifaceted mechanistic constellation illuminates DF's position as an unparalleled therapeutic modality in sophisticated CKD management.

3.2.3 Avant-garde nutritional intervention paradigms

Additional personalized dietary intervention strategies demonstrate remarkable potential in reconstituting intestinal flora architecture and metabolic homeostasis in CKD populations. Research illuminates that sodium propionate (SP)—a distinguished SCFA representative—when administered via encapsulated formulations to maintenance hemodialysis patients, orchestrates immune-metabolic equilibrium through multidimensional pathways: it significantly attenuates pro-inflammatory parameters including CRP, IL-1, and IL-17, while simultaneously upregulating anti-inflammatory mediators such as IL-10, concurrently reducing gut-derived uremic toxin production (IS and PCS), neutralizing oxidative stress markers including malondialdehyde, and rebalancing insulin resistance and iron metabolism perturbations (Marzocco et al., 2018).

The therapeutic constellation of natural dietary compounds reveals honey polyphenols as extraordinary microbiome architects—these bioactive molecules fundamentally reconstitute intestinal microbial communities, particularly enriching *Bifidobacteriales* and S24_7 bacterial populations, thereby

amplifying SCFA production cascades. This microbial metamorphosis translates into quantifiable improvements in renal structural integrity and metabolic parameters within experimental CKD paradigms (Cao et al., 2024).

Perhaps most compelling is the vegetarian dietary paradigm—a comprehensive nutritional approach associated with dramatically reduced CKD prevalence and progression trajectories (Liu et al., 2019; Hao et al., 2024). Its multifaceted nephroprotective mechanism emerges through dual pathways: initially, the inherently minimal endogenous acid load characteristic of plant-predominant nutrition effectively counterbalances metabolic acidosis that typically accelerates renal functional deterioration in CKD (Chauveau et al., 2019; Carrero et al., 2020); subsequently, this dietary architecture dramatically attenuates circulating concentrations of nephrotoxic metabolites, including IS, PCS, and nitrogenous waste products such as serum urea (Kandouz et al., 2016; Cases et al., 2019).

While these personalized nutritional strategies illuminate a revolutionary therapeutic horizon in nephrology, critical challenges persist at the intersection of scientific understanding and clinical implementation. The mechanistic convergence between these diverse dietary interventions and prebiotic approaches necessitates more precise delineation of their unique therapeutic contributions. Furthermore, the translational pathway from compelling research findings to standardized clinical protocols remains incompletely navigated. The future research imperative lies in systematically validating these interventions through rigorous clinical trials, establishing evidence-based guidelines that stratify patients according to optimal intervention profiles, and exploring synergistic combinations with pharmacological approaches—ultimately elevating personalized nutritional medicine from a promising adjunct to the cornerstone of comprehensive CKD management.

3.3 Physisorption

AST-120, an ingeniously engineered oral activated carbon adsorbent, orchestrates the selective molecular capture of uremic toxin precursors (including indole and p-cresol) within the intestinal luminal microenvironment through physical adsorption mechanisms. This elegant intervention paradigm prevents transcellular absorption across intestinal epithelial barriers and subsequent hepatic sulfation cascades, culminating in dramatic attenuation of circulating indoxyl sulfate (IS) and p-cresyl sulfate (PCS) concentrations (Asai et al., 2019).

The therapeutic virtuosity of this extraordinary pharmaceutical compound transcends conventional renal boundaries, as illuminated by preclinical investigations that reveal a comprehensive constellation of multi-organ cytoprotective effects. Through its strategic molecular sequestration capabilities, AST-120 orchestrates a protective shield encompassing not merely renal parenchymal tissues, but extends its cytoprotective aegis to cardiac myocytes, cerebral neural networks, and skeletal muscle fiber architectures—collectively neutralizing the cytotoxic onslaught of uremic metabolites (Sato et al., 2017).

Expansive clinical investigations substantiate that AST-120 significantly decelerates eGFR deterioration through intricate mechanistic pathways involving systematic suppression of inflammatory cascades and oxidative stress networks (Cha et al., 2016; Chen et al., 2019). This nephroprotective efficacy emerges from the compound's extraordinary capacity to disrupt the pathophysiological axis linking gut-derived toxin generation with systemic organ dysfunction.

While this therapeutic modality exemplifies an exceptional safety architecture—with adverse manifestations predominantly circumscribed to transient and benign gastrointestinal perturbations—the pursuit of optimized clinical outcomes reveals substantial interindividual heterogeneity in therapeutic responsiveness. This pharmacological variability illuminates the imperative for strategic therapeutic synergy with complementary interventions, particularly LPD regimens and precision-targeted pharmacological approaches, to achieve maximal therapeutic convergence across phenotypically diverse patient populations.

Through this orchestrated multimodal therapeutic convergence, AST-120 emerges as the quintessential cornerstone within the revolutionary paradigm of comprehensive uremic toxin neutralization—representing not merely an adjunctive intervention, but rather the architectural foundation upon which next-generation nephroprotective strategies are constructed.

3.4 Precision-orchestrated therapeutic architectures for uremic toxin neutralization

A constellation of pharmacological interventions orchestrates colonic uremic toxin metabolism through exquisitely distinct mechanistic pathways: the synergistic convergence of folic acid and methylcobalamin administration catalyzes homocysteine metabolic recalibration, systematically attenuating serum asymmetric dimethylarginine (ADMA) concentrations—a formidable mediator of endothelial dysfunction and cardiovascular pathophysiology (Angelini et al., 2021; Mohan et al., 2023); acarbose—the quintessential α-glucosidase inhibition virtuoso—precipitates a profound colonic metamorphosis by enriching the luminal microenvironment with undigested carbohydrate substrates, thereby amplifying SCFA biosynthetic cascades while simultaneously orchestrating the systematic suppression of bacterial deamination processes (Evenepoel et al., 2006); allopurinol, with its exquisite mechanistic precision, conducts a targeted biochemical silencing of xanthine oxidase enzymatic networks, fundamentally disrupting the pathophysiological cascade responsible for uric acid generation (Shuvo et al., 2025); meclofenamate emerges as a molecular disruptor, interfering with sulfotransferase-mediated sulfate conjugation mechanisms, thereby systematically reducing indolic toxin biosynthesis within intestinal compartments (Saigo et al., 2014); cilastatin orchestrates a strategic interruption of OAT1/3 functionality, constructing a protective molecular barrier that shields vital renal architectural elements from the cytotoxic assault of nephrotoxic pharmaceutical compounds (Huo et al., 2019).

These precision-engineered therapeutic modalities transcend the inherent limitations of conventional dialytic approaches in protein-bound toxin elimination, establishing a revolutionary multidimensional framework for toxin neutralization that surpasses the physical constraints of extracorporeal filtration methodologies. Through this orchestrated pharmacological symphony, clinicians achieve unprecedented control over uremic toxin burden, fundamentally redefining the therapeutic landscape of advanced CKD management.

3.5 Vanguard technologies and their revolutionary therapeutic potential

Within the pioneering realm of experimental therapeutics, fecal microbiota transplantation (FMT) crystallizes as a paradigmatic biologic intervention—orchestrating the systematic transfer of intricate microbial ecosystems from meticulously screened healthy donors to recipients harboring dysbiotic intestinal landscapes. This revolutionary approach to ecological restoration precipitates a comprehensive architectural reconfiguration of the intestinal microbiome, demonstrating extraordinary capacity to systematically diminish uremic toxin biosynthesis through precision-guided microbial community engineering (Caggiano et al., 2023). This living pharmaceutical paradigm harnesses the metabolic virtuosity of indigenous microbial consortiums to address the fundamental dysbiotic pathophysiology underlying uremic toxin generation networks. Nevertheless, the translational trajectory of FMT within CKD therapeutic paradigms confronts extraordinarily formidable multidimensional impediments that attenuate its immediate clinical implementation prospects. The exquisite sophistication of donor-recipient microbiome compatibility necessitates revolutionary algorithmic matching architectures that remain fundamentally underdeveloped, while the conspicuous absence of comprehensive longitudinal safety databases introduces profound uncertainty regarding potential iatrogenic consequences, encompassing the catastrophic risk of transmitting multidrug-resistant pathogenic organisms or occult oncogenic microbial constituents. Furthermore, the standardization of microbial preparation protocols presents unprecedented technical complexities, as the viability and therapeutic efficacy of transplanted microorganisms demonstrate extraordinary sensitivity to processing methodologies, cryopreservation technologies, and delivery system architectures. Bioethical considerations encompass intricate informed consent paradigms when implementing living microbial therapeutics of indeterminate compositional profiles, while regulatory frameworks encounter profound challenges accommodating this revolutionary therapeutic paradigm that transcends conventional pharmacological categorization schemas.

Organ-on-chip technology emerges as the quintessential masterpiece of biomimetic engineering—recreating the dynamic physiological interplay between intestinal and renal tissue architectures within exquisitely controlled microfluidic environments. These ingeniously engineered microphysiological systems have illuminated previously invisible pathways of organ crosstalk, revealing with unprecedented molecular clarity how intestinal barrier compromise initiates catastrophic signaling cascades across the gut-kidney physiological axis. Through these *in vitro* architectural platforms, researchers have achieved real-time visualization of how disrupted intestinal epithelial barriers facilitate the systematic translocation of inflammatory orchestrators (TNF-α, IL-6) and nephrotoxic mediators (IS) into systemic circulation, subsequently triggering progressive renal structural deterioration and functional collapse (Guo et al., 2023; Mou et al., 2024). However, the technical sophistication and prohibitive manufacturing expenditures associated with these microfluidic platforms severely circumscribe their accessibility and scalability for widespread research deployment across diverse institutional environments. Moreover, despite their biomimetic architectural excellence, these systems inevitably constitute simplified approximations of the extraordinarily complex *in vivo* physiological milieu, potentially obscuring critical intercellular communication networks, systemic immunological responses, and multi-organ interaction paradigms that characterize authentic pathophysiological processes. The standardization of experimental protocols across heterogeneous research institutions remains profoundly problematic, introducing significant methodological variability that compromises reproducibility standards and inter-laboratory validation paradigms. Perhaps most critically, the translation of promising organ-on-chip discoveries to successful clinical therapeutic interventions confronts the formidable challenge of traversing the substantial chasm between controlled in vitro microenvironments and the unpredictable complexity of human pathophysiological landscapes, where genetic polymorphisms, comorbidity interactions, and individual phenotypic variability introduce confounding variables that cannot be adequately recapitulated within microfluidic architectural systems.

Transcending their mechanistic revelations, these pioneering technological platforms function as extraordinary molecular discovery engines—unveiling novel therapeutic targets at the gut-kidney interface while enabling high-throughput screening of innovative therapeutic candidates under physiologically authentic conditions. These platforms represent the convergence of bioengineering excellence and translational medicine, establishing unprecedented opportunities for therapeutic innovation.

3.6 The translational imperative: navigating clinical implementation complexities

Contemporary gut-kidney axis interventional strategies confront formidable implementation challenges across multiple therapeutic dimensions: probiotic and prebiotic therapeutic efficacy demonstrates substantial variability contingent upon host microbiota individuality and metabolic phenotypic diversity; LPD regimens necessitate sophisticated, real-time nutritional status surveillance to prevent iatrogenic sarcopenia and protein-energy malnutrition; long-term fecal microbiota transplantation safety profiles remain incompletely characterized, particularly regarding immunological tolerance and microbiome stability.

Despite these translational complexities, these innovative therapeutic modalities represent a quantum leap in expanding the therapeutic armamentarium for chronic kidney disease management. The convergence of advancing precision medicine technologies, sophisticated microbiome characterization platforms, and personalized metabolic profiling heralds the emergence of individualized therapeutic protocols based on patient-specific gut microbiota signatures and host metabolic phenotypes as the paramount research imperative for future investigation (Figure 2).

This therapeutic evolution transcends conventional one-size-fits-all approaches, ushering in an era of precision gut-kidney axis medicine where therapeutic interventions are meticulously tailored to individual microbiome architectures and metabolic landscapes. The successful navigation of these translational challenges will fundamentally redefine chronic kidney disease management, transforming it from a reactive, symptom-driven discipline to a proactive, mechanism-based therapeutic science.

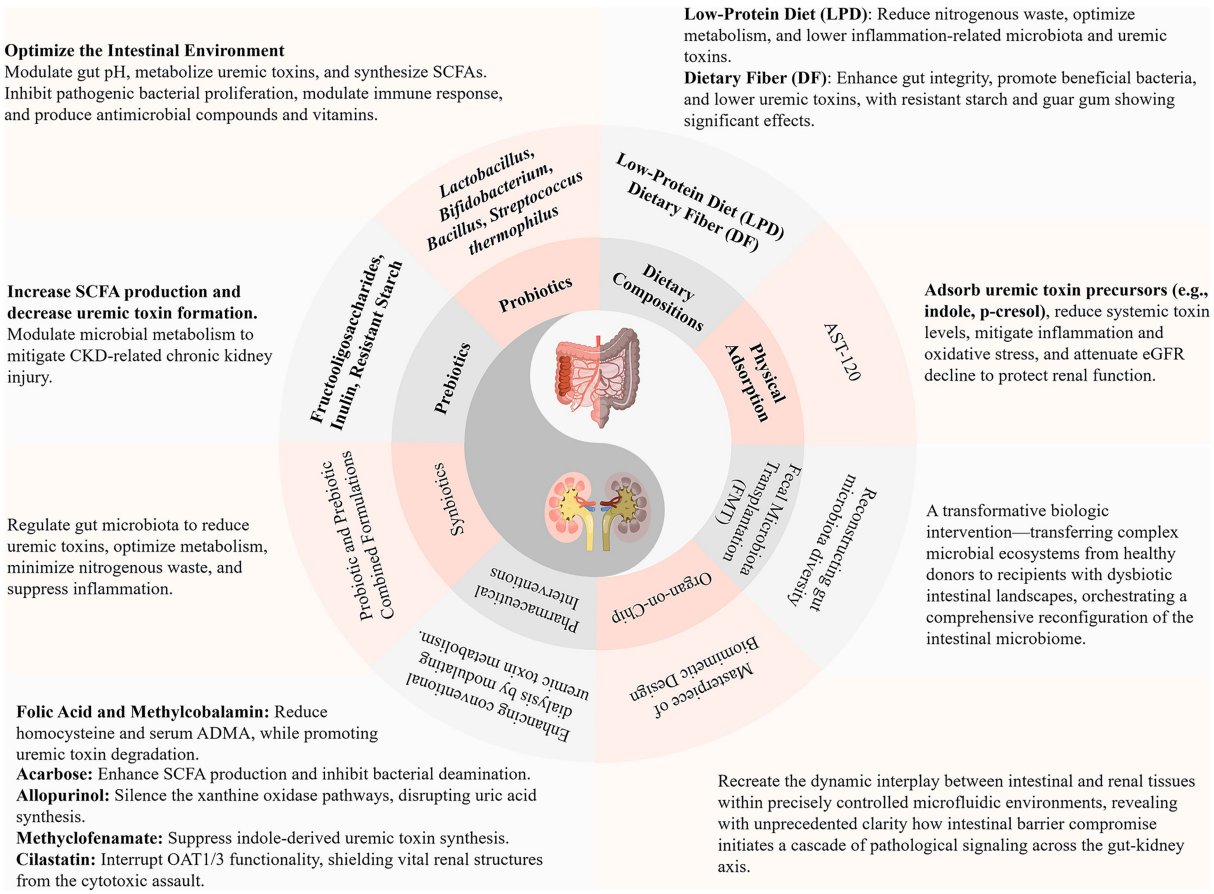

FIGURE 2
Therapeutic strategies targeting the gut-kidney axis: current advances. SCFAs, Short-Chain Fatty Acids; CKD, Chronic Kidney Disease; eGFR, Estimated Glomerular Filtration Rate; ADMA, Asymmetric Dimethylarginine; OAT1/3, Organic Anion Transporter 1/3.

4 Therapeutic innovations and paradigmatic advances in traditional Chinese medicine: evidence-based insights through the gut-kidney axis framework

Contemporary evidence-based medical research has unequivocally established TCM as a therapeutic modality of unprecedented sophistication in CKD management—its integrative, precision-oriented, and holistic philosophical paradigm fundamentally transcends conventional therapeutic frameworks, effectuating profound amelioration of uremic toxin homeostasis and nephroprotective mechanisms (Li et al., 2019). This millennia-old medical tradition derives its conceptual edifice from the seminal classical compendium "Huangdi Neijing" (The Yellow Emperor's Internal Canon), which articulates the foundational doctrine of "renal governance of congenital essence and splenic dominion over acquired essence," demonstrating prescient recognition of the intricate visceral interconnectivity among spleen, kidney, and intestinal organ systems. The modern biomedical paradigm of the "gut-kidney axis" exhibits remarkable consonance with TCM's integrative conceptual framework, elucidating the pathophysiological mechanisms underlying bidirectional renal-intestinal interactions in CKD pathogenesis. TCM therapeutic interventions provide multidimensional therapeutic strategies for comprehensive CKD management through sophisticated modulation of intestinal microbial ecosystems, fortification of intestinal mucosal barrier integrity, and nuanced regulation of inflammatory cascades. Spanning from meticulously isolated singular bioactive phytochemicals to synergistically formulated polyherbal compounds, Chinese medicinal preparations demonstrate extraordinary polypharmacological therapeutic capabilities characterized by multi-target engagement in CKD therapeutics (Ji et al., 2020; Wang et al., 2020).

4.1 Elucidating the therapeutic pharmacodynamics of individual botanical medicines

Rhubarb (Rhei Radix et Rhizoma) constitutes one of the most comprehensively investigated phytotherapeutic agents in CKD management, manifesting therapeutic efficacy through dual mechanistic pathways: facilitation of metabolic waste elimination and cultivation of balanced intestinal microbial ecosystems. Cutting-edge pharmacological investigations have elucidated rhubarb's remarkable capacity to accelerate uremic toxin and creatinine clearance, thereby effectively mitigating the deleterious consequences of nitrogenous retention characteristic of renal insufficiency (Zeng et al., 2021). Of

particular clinical significance is rhubarb's profound modulatory influence on intestinal microbiome composition, demonstrating selective reduction of pathogenic bacterial genera including *Desulfovibrio*, *Clostridium*, and *Ruminococcus*, concurrent with enhancement of beneficial microbial populations such as *Parabacteroides*. Through inhibition of dysbiotic microbial proliferation, this intervention restores intestinal ecological equilibrium, attenuating aberrant protein fermentation processes and amino acid metabolic dysregulation (Wang et al., 2022). This sophisticated microbial homeostatic recalibration not only reinforces colonic barrier architectural integrity but also initiates cascading protective mechanisms, encompassing substantial reduction of uremic toxins. Consequently, rhubarb exerts pleiotropic therapeutic effects—simultaneously decelerating glomerulosclerotic progression and preventing renal interstitial fibrogenesis—thereby providing comprehensive therapeutic modalities for nephroprotection and functional preservation. Within the intricate gut-kidney axis pathological framework, these therapeutic mechanisms collectively demonstrate rhubarb's multifaceted intervention across four critical junctures: orchestrating intestinal microbiome remodeling through selective bacterial modulation, reinforcing intestinal barrier integrity via colonic epithelial strengthening, optimizing microbial metabolite profiles through uremic toxin reduction and correction of aberrant fermentation processes, and ultimately providing direct renal cellular protection by attenuating both glomerulosclerotic progression and interstitial fibrogenesis.

Analogous to rhubarb's regulatory mechanisms, Poria cocos exhibits distinctive targeted modulatory characteristics in optimizing the renal microenvironment. Experimental evidence substantiates Poria's selective capacity to diminish bacterial populations intimately associated with proteinuric metabolism, specifically *Blautia*, *Escherichia-Shigella*, and *Bacteroides* (Guo et al., 2025). This precision-targeted regulation not only attenuates intestinal uremic toxin biosynthesis but also ameliorates renal metabolic burden through preservation of intestinal mucosal tight junction protein architecture. By alleviating metabolic burden, Poria facilitates renal stress mitigation, potentiating synergistic therapeutic effects, optimizing protein-energy utilization efficiency, and maintaining homeostatic fluid balance. The therapeutic trajectory of Poria cocos thus strategically targets three interconnected nodes within the gut-kidney pathological network: implementing selective microbiome modulation through specific reduction of proteinuria-associated bacterial populations, preserving intestinal barrier function via maintenance of tight junction protein architecture, and optimizing metabolite homeostasis through attenuation of intestinal uremic toxin biosynthesis, ultimately culminating in comprehensive renal stress alleviation and metabolic burden reduction.

Moreover, Danshen (*Salvia miltiorrhiza*) demonstrates exceptional bidirectional regulatory properties in the modulation of intestinal microbiome homeostasis. This botanical agent exhibits remarkable proficiency in significantly suppressing potentially pathogenic bacteria including *Bifidobacterium*, *Turicibacter*, *Streptococcaceae*, and *Desulfovibrio*, while concurrently promoting proliferation of beneficial microbial consortia, encompassing *Lactobacillus*, *Clostridium*, and *Ruminococcaceae* (Han et al., 2021). This equilibrium-oriented regulatory capacity not only rectifies aberrant amino acid metabolic pathway activation but also establishes systemic metabolic network modulation foundations for ameliorating renal functional impairment through restoration of energetic homeostasis. Danshen and Eucommia have additionally demonstrated significant nephroprotective functionality in diabetic nephropathy-related experimental models, inhibiting TGF-β/Smad signaling cascades to attenuate renal fibrogenesis progression (Wang et al., 2023a). The comprehensive therapeutic architecture of Danshen thus orchestrates intervention across four pivotal stages of the gut-kidney axis continuum: executing bidirectional microbiome regulation through simultaneous suppression of pathogenic bacteria and promotion of beneficial microbial consortia, correcting metabolic pathway dysfunction via rectification of aberrant amino acid metabolic networks, modulating inflammatory signaling cascades through targeted inhibition of TGF-β/Smad pathways, and providing direct renal cellular protection by attenuating fibrogenesis progression while restoring systemic metabolic homeostasis.

4.2 Pharmacochemical characterization of bioactive phytoconstituents

In contradistinction to crude botanical preparations, concentrated herbal extracts manifest substantially enhanced therapeutic efficacy, particularly in targeting specific pathophysiological mechanisms. Exemplifying this phenomenon, rhubarb's anti-fibrotic properties are primarily attributable to its diverse anthraquinone constituents, encompassing emodin, rhein, aloe-emodin, chrysophanol, and physcion. These bioactive compounds synergistically exert anti-fibrotic, anti-inflammatory, antioxidant, and anti-apoptotic effects through multiple intracellular signaling cascades (Bi et al., 2025). Emodin demonstrates particularly pronounced efficacy in renal interstitial fibrosis inhibition (Xu L. et al., 2021; Feng et al., 2024), suppressing fibrogenetic progression through Klotho activation, SIRT3/FOXO3a pathway modulation, microbiota-endotoxin axis regulation, and epigenetic mechanisms including the lincRNA-ANRIL/let-7a/TGF-β1 network; rhein significantly inhibits TGF-β1/Smad2/3 signaling, blocking epithelial-mesenchymal transition in renal tubular epithelial cells while attenuating inflammatory mediator expression through NF-κB pathway suppression and enhancing autophagy via AMPK activation to ameliorate hyperglycemia-induced glomerulosclerosis; aloe-emodin regulates renal tubular cell apoptosis and proliferation through PI3K/Akt/mTOR pathway modulation, alleviating oxidative stress and interstitial fibrogenesis while conferring cytoprotection through mitochondrial functional stabilization; chrysophanol primarily activates the Keap1/Nrf2/HO-1 pathway to augment intracellular antioxidant capacity, diminish reactive oxygen species generation, and suppress TGF-β1 and α-SMA expression; physcion predominantly exerts anti-inflammatory and anti-fibrotic effects through STAT3 signaling pathway inhibition while concurrently modulating TLR4/MyD88/NF-κB cascades, demonstrating superior immunomodulatory efficacy in IgA nephropathy and nephrotoxic injury models (Feng et al., 2025).

Concerning the aforementioned Poria, its cortical tissues contain abundant tetracyclic triterpenoid compounds, particularly Pachymic acid and Poricoic acids, which confer significant nephroprotective effects against acute and chronic kidney injury through modulation of pivotal signaling networks including TGF-β1/Smad, Wnt/β-catenin, NF-κB, Keap1/Nrf2, and AQP2/ENaC pathways, effectively suppressing inflammatory responses and fibrogenesis while

ameliorating acute or chronic renal functional and histopathological alterations (Guo et al., 2025).

Curcumin exemplifies this pharmacological paradigm with extraordinary precision and clarity. Curcumin administration orchestrates intestinal microbiome compositional remodeling through selective *Prevotellaceae* suppression while promoting *Bacteroidaceae* and *Ruminococcaceae* proliferation (Shen et al., 2017). Additionally, this polyphenolic compound combats opportunistic pathogen overgrowth including *Bacteroides* and *Escherichia-Shigella* while facilitating expansion of beneficial SCFA -synthesizing bacteria such as *Lactobacillus* (Xu X. et al., 2021). Through inhibition of excessive lipopolysaccharide and inflammatory mediator production, curcumin fortifies intestinal barrier integrity, attenuates uremic toxin translocation, and mitigates renal fibrogenesis and NLRP3 inflammasome activation (Xu X. et al., 2021).

Panax notoginseng saponins represent another therapeutically significant class of botanical extracts, conferring profound nephroprotection through sophisticated microbial community modulation. Investigations demonstrate these triterpene saponins reduce phylogenetic abundance across multiple bacterial phyla including *Firmicutes*, *Bacteroidetes*, *Proteobacteria*, and *TM7*, while substantially promoting beneficial bacterial species proliferation encompassing *Bacteroides*, *Lactobacillus*, *Butyrivibrio*, and *Eubacterium*. Concurrently, they attenuate pathogenic bacterial populations including *Escherichia-Shigella* and *Ruminococcaceae* (Mafra et al., 2021). This precision modulatory mechanism not only reestablishes microbial homeostasis but also plays instrumental roles in decelerating renal fibrogenesis progression in CKD patients through pro-inflammatory factor inhibition and intestinal barrier permeability protection (Mafra et al., 2021).

Hirudin demonstrates remarkable capacity for intestinal microbiome abundance modulation, encompassing *Lactobacillus reuteri*, *Escherichia coli*, *Ruminococcus callidus*, and *Clostridium celatum*, effectuating normalization of their ecological proportions. Furthermore, while preserving colonic tight junction protein expression, it inhibits NLRP3-ASC-caspase-1 inflammasome pathway activation in intestinal epithelial cells, thereby diminishing epithelial barrier compromise and uremic toxin translocation (Long et al., 2024).

Punicalagin (PU), a potent polyphenolic compound extracted from *Punica granatum*, exerts profound influences on intestinal microbiome architecture. This bioactive constituent significantly reduces *Proteobacteria* abundance while augmenting SCFA-producing bacterial proportions, including *Akkermansia*, *Lachnospiraceae*, and *Eubacterium_coprostanoligenes_group*. This ecological transformation results in elevated cecal SCFA concentrations, concomitant with reduced abundance of endotoxin-producing bacteria (*Desulfovibrionaceae*) and pathogenic species (*Ruminococcaceae_RC9_gut_group* and *Helicobacter*). Through comprehensive intestinal microbiome ecological restructuring, PU efficaciously reduces circulating lipopolysaccharide and diamine oxidase (DAO) concentrations, ameliorating inflammatory responses and alleviating metabolic dysregulation in DN models. Through these mechanisms, it reestablishes gut-kidney axis equilibrium, providing promising therapeutic strategies for managing renal dysfunction associated with metabolic pathologies (Hua et al., 2022).

Certain individual botanical extracts exhibit prebiotic characteristics. Exemplarily, polysaccharides derived from *Achyranthes bidentata* (ABPW1) function as prebiotics through selective *Bacteroides* abundance enhancement while diminishing *Rikenella*, *Alistipes*, *Laedolimicola*, and *Faecalibaculum* populations. This polysaccharide undergoes intestinal microbial degradation for SCFA biosynthesis, particularly facilitating propionate and isobutyrate production (Si et al., 2024). Another sulfated polysaccharide—fucoidan extracted from marine kelp—can reverse high-fat diet-induced intestinal microbiome diversity reduction. Following fucoidan supplementation, beneficial probiotic abundance including *Streptococcus*, *Lactobacillaceae*, and *Christensenellaceae* significantly increased. This was accompanied by substantial elevations in cecal SCFA concentrations, particularly acetate. SCFAs subsequently attenuate inflammation and oxidative stress through G protein-coupled receptor (GPR43) activation in renal tubular cells and podocytes, enhance mitochondrial functionality, and ameliorate renal complications including glomerular hyperfiltration and renal fibrogenesis (Zhong Z. et al., 2024).

Furthermore, in the extensively investigated CKD primary etiology of DN, herbal extracts demonstrate profound and comprehensive research foundations due to their phytochemical diversity and exceptional metabolic modulatory capabilities. Among polyphenolic compounds, Curcumins, Epigallocatechin-3-gallate, Resveratrol, and Chlorogenic acid; flavonoid constituents including Chrysin, Naringenin, and Total flavones of *Abelmoschus manihot*; quinone compounds exemplified by Tanshinone IIA; alkaloids typified by Berberine; and terpene compounds with Astragaloside IV demonstrating paramount efficacy—all achieve nephroprotection through endoplasmic reticulum stress pathway modulation. Lignan compounds such as Arctigenin and compound extracts including *Ginkgo biloba* extract EGB761 and total paeony glucosides similarly demonstrate therapeutic potential. These agents inhibit cellular apoptosis, augment antioxidant defense systems, attenuate inflammatory responses, and fundamentally ameliorate DN glucose metabolic dysregulation, thereby mitigating renal injury (Wei et al., 2023). Additional compounds including Acetylshikonin, *Abelmoschus esculentus*, Bupleurum polysaccharides, Notoginsenoside R1, *Coreopsis tinctoria*, Taxus chinensis, Dioscoreae Rhizoma, hedera saponin, and Acteoside have all demonstrated exceptional anti-fibrotic capabilities in experimental models (Wang et al., 2023a, 2025; Zhong X. et al., 2024).

This comprehensive phytoconstituent characterization unveils an extraordinarily sophisticated therapeutic paradigm wherein these meticulously orchestrated bioactive compounds execute precision-guided interventions across the quintessential sequential stages of gut-kidney axis pathophysiological cascades. At the primordial stage of intestinal microbiome dysbiosis, an elite cadre of compounds—encompassing curcumin, Panax notoginseng saponins, hirudin, and punicalagin—orchestrates exquisitely selective microbial community architectural remodeling, while specialized polysaccharide matrices, notably ABPW1 and fucoidan, manifest sophisticated prebiotic functionalities that catalyze the strategic proliferation of beneficial bacterial consortia. Progressing to the critical juncture of intestinal barrier dysfunction amelioration, this therapeutic triumvirate of curcumin, hirudin, and Panax notoginseng saponins functions as molecular guardians, meticulously preserving the structural sanctity of tight junction protein complexes and epithelial architectural integrity, thereby establishing formidable barriers against the pathological permeability escalation that epitomizes CKD pathogenesis. The subsequent phase of microbial metabolite dysregulation rectification involves polysaccharide-mediated facilitation of SCFA biosynthetic machinery—particularly optimizing propionate, acetate, and isobutyrate metabolic flux—while punicalagin concurrently executes precision targeting of circulating endotoxin neutralization and diamine oxidase

level modulation. During the pivotal inflammatory cascade activation phase, a sophisticated arsenal of anthraquinone constituents, exemplified by rhein and physcion, implements strategic suppression of NF-κB and STAT3 signaling networks, while hirudin provides targeted inhibition of NLRP3 inflammasome activation, and triterpenoid compounds orchestrate comprehensive modulation of TLR4/MyD88 cascades, collectively establishing a coordinated attenuation of pro-inflammatory mediator expression throughout the entire gut-kidney axis continuum. Culminating in the resolution of renal cellular pathology, emodin, aloe-emodin, and chrysophanol deploy highly specialized mechanisms targeting renal fibrogenesis through synchronized TGF-β1/Smad pathway inhibition, Keap1/Nrf2 antioxidant axis activation, and mitochondrial functional stabilization, while an expansive therapeutic armamentarium—incorporating tanshinone IIA, berberine, and astragaloside IV—delivers comprehensive nephroprotective efficacy through an intricate symphony of synergistic mechanisms encompassing cellular apoptosis suppression, antioxidant capacity amplification, and fundamental metabolic dysregulation resolution, ultimately establishing a paradigmatic framework for precision medicine in CKD management.

4.3 Synergistic pharmacodynamics of botanical pair combinations

Based upon the classical TCM "sovereign-minister-assistant-courier" compatibility doctrine, traditional herbal pairs in CKD therapeutics demonstrate significant synergistic pharmacological effects. The Astragalus-Danshen combination has been definitively proven to substantially reverse intestinal microbial dysbiosis, characterized by increased Firmicutes/Bacteroidetes ratios and enhanced abundance of butyrate-producing bacterial species including *Akkermansia* and *Lactobacillus*. The mechanistic foundation of this synergistic interaction involves tryptophan metabolism regulation and butyrate biosynthetic pathway modulation, not only ameliorating renal metabolic dysregulation but also playing pivotal roles in decelerating renal fibrogenesis progression (Han et al., 2021). Another therapeutically potent combination—Astragalus and Panax notoginseng—suppresses NF-κB signaling pathway activity through *Bifidobacterium*-mediated Mincle receptor modulation, resulting in diminished M1 macrophage proportions while promoting M2 polarization. This immunomodulatory process significantly attenuates both renal and intestinal inflammatory responses, emphasizing this combination's dual therapeutic roles in managing inflammation and fibrogenesis throughout CKD progression (Rui-Zhi et al., 2020). The Astragalus-Cordyceps combination effectively reverses intestinal microenvironmental dysbiosis in DN, significantly improving renal functional parameters with superior therapeutic efficacy compared to Astragalus monotherapy (Li J. et al., 2024).

4.4 Pharmacological investigations of polyherbal formulations and proprietary medicines

Classical TCM polyherbal formulations, predicated upon "syndrome differentiation and treatment" principles, generate synergistic therapeutic outcomes through harmonious multi-constituent interactions. Formulation ratios and therapeutic strategies are meticulously designed with profound scientific foundations and mathematical precision, establishing widespread clinical recognition. Exemplarily, Fuzheng Huayu Jiangzhuo Tongluo Decoction represents a sophisticated nine-herb formulation that exerts specific intestinal microbiome modulatory effects through selective reduction of *Monosporaceae*, *Lactobacillus*, and *Eubacterium nodatum* abundance. Additionally, this polyherbal compound significantly diminishes circulating concentrations of renal injury-associated metabolites including citric acid and bile acids. Its mechanistic therapeutic foundation correlates intimately with inflammatory cascade modulation and renal tubulointerstitial fibrogenesis inhibition, providing comprehensive therapeutic pathways for nephroprotection (Chen et al., 2022). Shulifenxiao Formula demonstrates potential as an alternative therapeutic option for hormone- and immunosuppressant-resistant nephrotic syndrome in refractory idiopathic membranous nephropathy, effectively ameliorating renal histopathological conditions (Cui et al., 2021). Mahuang Fuzi and Shenzhuo Decoction, targeting primary membranous nephropathy (MN), facilitate renal microenvironmental optimization and immune regulatory enhancement, thereby attenuating proteinuria and stabilizing renal functional parameters (Zhang N. et al., 2024). Extra formulations including Xiexin Decoction, ErHuang Formula, Qi-dan-di-huang Decoction, Danggui-Shaoyao-San, Danggui Buxue Decoction, and Sanzi Guben Decoction have been empirically validated in experimental models to confer nephroprotective effects through multiple mechanisms encompassing inflammatory attenuation, inflammatory cell chemotaxis and homing amelioration, NF-κB pathway activation suppression, and endoplasmic reticulum stress and apoptotic inhibition, thereby decelerating renal functional deterioration and preventing progressive fibrogenetic histopathological alterations (Wang et al., 2023a; Wei et al., 2023).

Traditional Chinese patent medicines (TCPMs), conceptually rooted in classical polyherbal formulations and refined through contemporary pharmaceutical technologies, provide standardized therapeutic approaches for specific pathological conditions while seamlessly integrating with modern medical practice. Yishen Qingli Heluo Granules (YQHG), representing a flagship TCM preparation for CKD management, serves as an exemplary model. Investigations demonstrate that YQHG treatment significantly enhances relative abundance of SCFA-producing bacterial species including *Lactobacillaceae*, *Lactobacillus*, and *Lactobacillus gasseri* in experimental CKD models. Furthermore, it elevates total intestinal SCFA concentrations (particularly acetate and butyrate), fortifying intestinal barrier integrity through permeability reduction and microbial translocation limitation. Microbiome transplantation studies further elucidate that YQHG's nephroprotective mechanisms are partially mediated through intestinal microbiome modulation, specifically through bacterial populations involved in SCFA biosynthesis (Sun et al., 2022).

Hibiscus Capsules primarily comprise *Hibiscus mutabilis* floral extracts, abundant in diverse flavonoid compounds (Cai et al., 2017). These bioactive constituents undergo *in vivo* biotransformation to glucuronide-sulfate conjugates, possessing multifaceted pharmacological properties including metabolic enhancement, antihypertensive effects, antioxidative stress amelioration, and anti-inflammatory activities, conferring crucial nephroprotective roles in DN, hypertensive nephropathy, glomerulonephritis, and LN (Chen et al., 2016; Cao et al., 2022; Vagopoulou et al., 2024). Hibiscus Capsules demonstrate remarkable antiproteinuric efficacy and have received approval from the China National Medical Products Administration for

chronic nephritis treatment (Li et al., 2021). Multicenter randomized controlled trials substantiate their profound antiproteinuric effects in patients with early-stage primary glomerulonephritis (Zhang et al., 2014) and IgA nephropathy (Li et al., 2020). In adenine-induced chronic renal failure experimental models, Hibiscus Capsules effectively prevent renal tubulointerstitial fibrogenesis through NADPH/ROS/Erk signaling pathway inhibition (Cai et al., 2017). Moreover, in 5/6 nephrectomy experimental models, they alleviate renal burden through tryptophan transport disruption and microbial metabolic modulation, thereby diminishing uremic toxin accumulation (Lu et al., 2021).

Yishen Huashi Granules (YSHS) demonstrate comparably impressive nephroprotective characteristics. Research reveals that YSHS treatment significantly reduces 24-h proteinuria in non-dialysis CKD patients while promoting beneficial intestinal microbial growth (e.g., *Faecalibacterium*, *Lachnospiraceae*, *Lachnoclostridium*, *Sutterella*) and inhibiting potentially pathogenic bacterial species (e.g., *Eggerthella*, *Clostridium innocuum*). Subsequent analysis demonstrates that *Lachnoclostridium* and *Lachnospiraceae* increases negatively correlate with 24-h proteinuria reduction. Additionally, YSHS intervention modulates multiple metabolic pathways encompassing N-glycan synthesis, steroid hormone biosynthesis, and biotin metabolism. Notably, microbial alterations associated with steroid hormone synthesis regulation exhibit gender-specific differences, with male patients demonstrating increased *Lachnoclostridium* and *Lachnospiraceae*, while female patients experience significant *Prevotella* elevations (Dong et al., 2024).

Additional commonly utilized TCM patent medicine formulations including Sanzi Guben Polysaccharides (SZPs), Fufang Zhenzhu Tiaozhi Capsules (FTZ) & FTZ Polysaccharides (FTZPs), QiDiTangShen granules (QDTS), Moshen granule (MSG), Qiwei granule, Tongxinluo, Liuwei Dihuang Pill, Chaihuang-Yishen granule, The Tangshen Formula, and Huangkui Capsule demonstrate capacity to attenuate renal fibrogenesis and histostructural damage in pathological conditions of CKD primary etiologies through modulation of diverse mechanistic pathways (Wang et al., 2023a, 2025; Li J. et al., 2024; Miao et al., 2024b, 2025).

TCM confers substantial therapeutic advantages in CKD management, primarily attributable to its polypharmacological capacity to engage multiple molecular targets and signaling pathways, functioning across diverse pathophysiological levels throughout disease progression. Whether through botanical decoctions, sophisticated formulations, or standardized patent medicines, TCM demonstrates therapeutic versatility through intestinal microbiome modulation, intestinal barrier integrity enhancement, and renal metabolic optimization. These multifaceted therapeutic effects precisely target pathophysiological mechanisms, providing efficacious and personalized treatment modalities. The pharmacoeconomic advantages and relatively minimal adverse reaction profiles associated with TCM are largely attributable to their compositional complexity and multi-target synergistic mechanisms. Chinese botanical medicines contain abundant bioactive compounds including phenolics, saponins, glycosides, flavonoids, alkaloids, tannins, steroids, and terpenes, each exhibiting distinct physiological effects. Exemplarily, botanical agents including rhubarb, Danshen, and turmeric demonstrate exceptional phenolic compound concentrations, exhibiting potent antioxidant and anti-inflammatory properties that underscore their tremendous potential in nephropathic management. In renal disease pathophysiology, oxidative stress and inflammatory responses play pivotal roles in mediating glomerular and tubular damage, ultimately precipitating renal functional decline. Excessive reactive oxygen species accumulation and antioxidant enzyme inhibition (particularly superoxide dismutase) can activate crucial signaling cascades including NF-κB and MAPK, subsequently promoting pro-inflammatory mediator synthesis and release (Tarek et al., 2023; Chu et al., 2024). Phenolic compounds in Chinese botanical medicines can ameliorate these pathological effects through ROS production inhibition and inflammatory signaling cascade suppression, thereby conferring therapeutic benefits in nephropathic conditions (Sahakyan et al., 2022). Additionally, Astragalus contains abundant saponins and glycosides, with specific astragalosides exhibiting potent anti-inflammatory and anti-fibrotic properties, while flavonoid constituents possess significant antimicrobial characteristics (Cui et al., 2023; Su et al., 2023; Ning et al., 2024). In AKI and CKD contexts, these compounds promote nephroprotection through diuretic, natriuretic, and direct renoprotective mechanisms, substantially improving renal functional parameters.

4.5 Acupuncture and moxibustion: non-pharmacological therapeutic modalities for CKD

Acupuncture and moxibustion, constituting non-pharmacological therapeutic modalities within TCM, represent integral components of Complementary and Alternative Medicine (CAM) in comprehensive CKD management. Acupuncture's effectiveness has been rigorously validated through randomized controlled trials (Yu et al., 2017), while moxibustion's therapeutic benefits are substantiated by numerous meta-analytical investigations (Lu et al., 2021). In CKD patients, acupuncture stimulation of specific acupoints (e.g., Hegu, Zusanli, Taixi) enhances renal hemodynamics and ameliorates renal functional parameters, encompassing eGFR elevation and serum creatinine reduction (Yu et al., 2017). Acupuncture additionally exerts profound modulatory influences on inflammatory biomarkers and immunological responses, attenuating intrarenal inflammation and immune-mediated injury. Through neuroendocrine system modulation, acupuncture alleviates oxidative stress, thereby addressing CKD-associated complications including hypertension, proteinuria, and fatigue, ultimately enhancing patient quality of life (Xiong et al., 2018).

Moxibustion involves combustion of *Artemisia vulgaris* (moxa) upon acupuncture needles, utilizing thermal energy, photonic radiation, and aromatic constituents' therapeutic properties to generate beneficial physiological effects. Investigations demonstrate moxibustion's capacity to improve local renal microcirculation and confer podocyte cytoprotection (Lu et al., 2021). Meta-analytical evidence demonstrates moxibustion significantly ameliorates serum creatinine concentrations, reduces urinary protein excretion, diminishes BUN levels, and enhances overall quality of life in CKD patients (Li et al., 2017; Zhou et al., 2020). Although effects on eGFR, creatinine clearance, and hemoglobin concentrations remain limited, moxibustion's circulatory enhancement and inflammatory modulation capabilities establish it as a valuable adjunctive therapeutic modality for managing renal functional decline and alleviating CKD-associated symptomatology (Zhou et al., 2020).

4.6 Integrative therapeutic paradigms in contemporary CKD management

TCM provides comprehensive and holistic therapeutic paradigms for CKD through synergistic integration of pharmacological and non-pharmacological interventions. Whether through botanical medicines that modulate gut-kidney axis functionality and restore intestinal barrier integrity, or through acupuncture and moxibustion that attenuate inflammatory responses and enhance circulation, TCM demonstrates remarkable therapeutic efficacy in mitigating nephropathic pathological progression. TCM's patient-centric approach transcends conventional disease management, emphasizing holistic health optimization and quality of life enhancement, thereby providing comprehensive supportive care systems for CKD patients.

However, the clinical implementation of TCM therapeutics in CKD populations necessitates extraordinary vigilance regarding safety profiles, pharmacokinetic alterations, and potential therapeutic interactions, particularly given the compromised renal clearance capacity and complex polypharmacy regimens characteristic of this patient demographic. CKD patients exhibit profound alterations in drug metabolism and elimination pathways, with significant reductions in renal organic anion transporter (OAT1/OAT3) and organic cation transporter (OCT2) functionality, potentially precipitating unexpected bioaccumulation of herbal constituents and their metabolites. The nephrotoxic potential of certain botanical compounds presents particular concern: aristolochic acid-containing herbs have been definitively associated with progressive tubulointerstitial nephritis and urothelial carcinogenesis, necessitating absolute contraindication in renal disease contexts (Dickman et al., 2023). Similarly, rhubarb's oxalate content may exacerbate hyperoxaluria and calcium oxalate nephrolithiasis in susceptible individuals, while prolonged usage can precipitate electrolyte imbalances and melanosis coli (Kumar et al., 2021).

Herb-drug interactions constitute a critical consideration in CKD therapeutic paradigms, where patients typically require multiple concurrent medications including ACE inhibitors, ARBs, diuretics, phosphate binders, and immunosuppressive agents. Danshen demonstrates significant anticoagulant properties that may potentiate warfarin effects, increasing hemorrhagic risks (Zhang Y. et al., 2020), while Astragalus may enhance hypoglycemic medication effects, necessitating careful glucose monitoring in DN patients. Panax notoginseng exhibits antiplatelet aggregation properties that contraindicate concurrent usage with anticoagulant therapies (Zhao C. et al., 2025), while certain TCM formulations containing licorice may precipitate pseudohyperaldosteronism, exacerbating hypertension and fluid retention in volume-sensitive CKD patients (Sabbadin et al., 2024). The hepatic cytochrome P450 system, crucial for herbal constituent metabolism, demonstrates altered functionality in advanced CKD, potentially compromising the biotransformation of complex phytochemical matrices and increasing susceptibility to hepatotoxic reactions (Chen et al., 2021). Polyherbal formulations present additional complexity, as synergistic interactions among multiple bioactive constituents may unpredictably modulate pharmacokinetic profiles and therapeutic windows. Quality control concerns regarding standardization, adulteration with undisclosed synthetic compounds, and contamination with heavy metals or microbial pathogens represent persistent challenges in herbal medicine implementation, particularly problematic in CKD populations with compromised immune function and reduced toxin clearance capacity. Individualized therapeutic approaches must incorporate comprehensive assessment of residual renal function, concurrent medication regimens, and patient-specific risk factors including age, comorbidity burden, and genetic polymorphisms affecting drug metabolism. Regular monitoring of renal function parameters, electrolyte balance, liver enzymes, and complete blood counts becomes imperative during TCM intervention, with dose adjustments or discontinuation protocols established based on clinical response and adverse event emergence. The integration of traditional diagnostic methodologies with contemporary biomarker assessment and pharmacogenomic profiling may optimize therapeutic outcomes while minimizing iatrogenic complications.

Professional supervision by qualified TCM practitioners with specialized nephrology expertise, in close collaboration with conventional nephrologists, represents the optimal paradigm for safe and effective herbal medicine implementation in CKD management. Patient education regarding potential adverse effects, drug interaction recognition, and the importance of full therapeutic disclosure to all healthcare providers constitutes an essential component of responsible integrative care. This multidimensional therapeutic approach, founded upon integrative philosophical principles while acknowledging inherent safety considerations and the imperative for rigorous clinical monitoring, represents a promising yet cautiously implemented paradigmatic advancement for future CKD therapeutic strategies, wherein the pursuit of therapeutic efficacy must be meticulously balanced against patient safety and the fundamental principle of "primum non nocere" (Figure 3).

5 Conclusion

The explication of the gut-kidney axis constitutes a transformative paradigmatic shift in our conceptualization of CKD pathophysiology, transcending conventional reductionist frameworks to embrace a more nuanced understanding of inter-organ metabolic orchestration. The metagenomic perturbations characteristic of CKD—manifesting as attenuated microbial biodiversity, compromised fermentative functionality, and deteriorated epithelial barrier architecture—precipitate a deleterious cascade whereby intestinal dysbiosis perpetuates and amplifies the uremic milieu through enhanced nephrotoxin biosynthesis and systemic pro-inflammatory signaling.

Traditional Chinese Medicine, distinguished by its intrinsic systems-based epistemological foundation and polypharmacological therapeutic sophistication, presents a uniquely advantageous pharmacological framework for modulating gut-kidney axis dysfunction. The phytochemical virtuosity inherent in TCM manifests through strategic reconstitution of intestinal microbial ecosystems, reinforcement of mucosal barrier homeostasis, and selective inhibition of uremic metabolite biosynthetic cascades. Archetypal botanical agents and their constituent bioactive principles—notably Rhubarb, Poria cocos, and *Salvia miltiorrhiza*—exhibit remarkable regulatory precision in orchestrating microbial community restructuring and metabolic equilibrium restoration. Sophisticated polyherbal formulations, exemplified by Yishen Qingli Heluo Granule and Yi-Shen-Hua-Shi Granule, actualize multidimensional therapeutic intervention through synergistic phytochemical architectures that harmonize intestinal-renal metabolic dialogue.

The contemporary convergence of cutting-edge computational intelligence and sophisticated bioengineering methodologies heralds

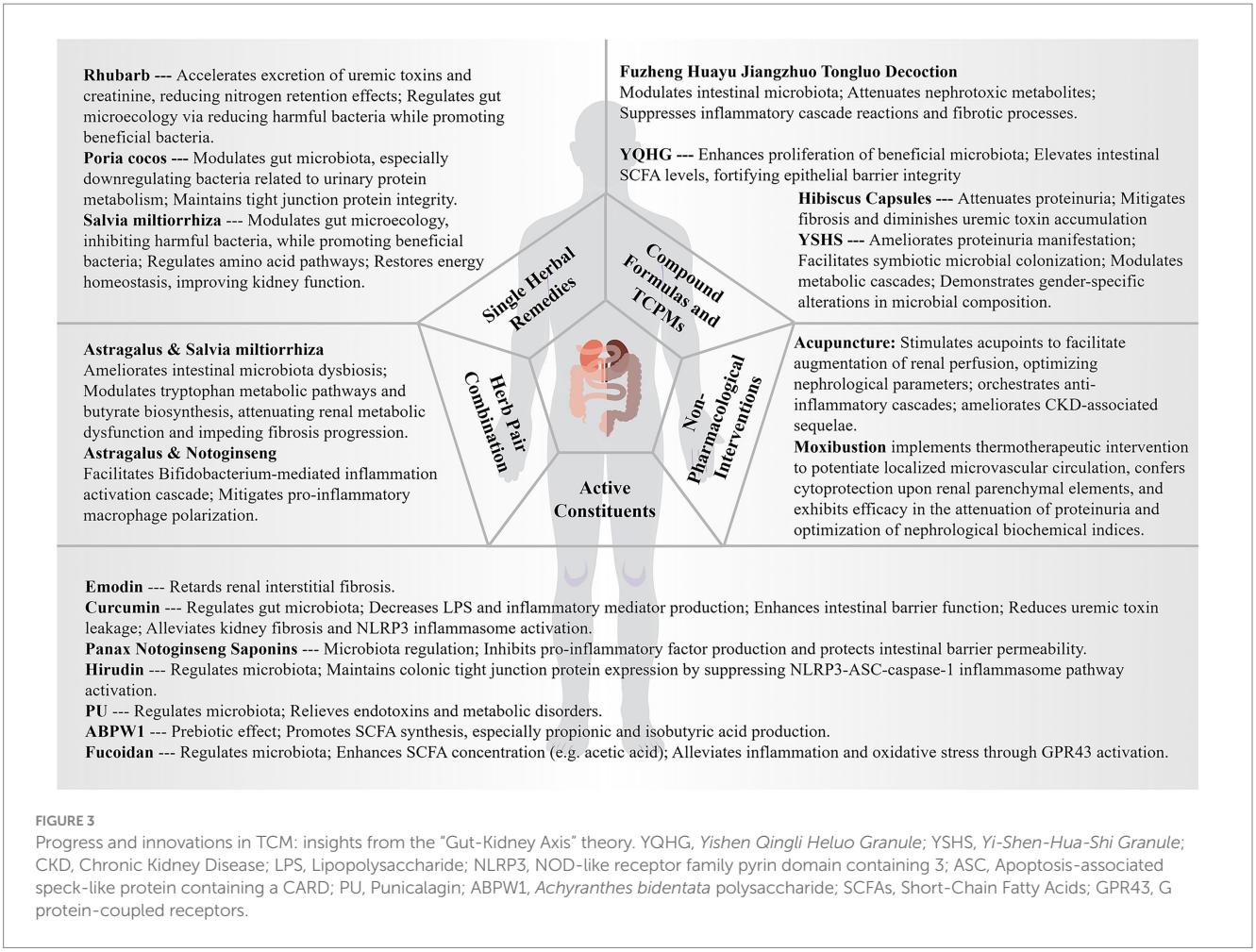

FIGURE 3
Progress and innovations in TCM: insights from the "Gut-Kidney Axis" theory. YQHG, *Yishen Qingli Heluo Granule*; YSHS, *Yi-Shen-Hua-Shi Granule*; CKD, Chronic Kidney Disease; LPS, Lipopolysaccharide; NLRP3, NOD-like receptor family pyrin domain containing 3; ASC, Apoptosis-associated speck-like protein containing a CARD; PU, Punicalagin; ABPW1, *Achyranthes bidentata* polysaccharide; SCFAs, Short-Chain Fatty Acids; GPR43, G protein-coupled receptors.

transformative prospects for advancing TCM investigation within the gut-kidney axis paradigmatic framework. Artificial intelligence architectures facilitate extraordinarily nuanced deconvolution of the intricate tripartite relationships encompassing microbiome dynamics, metabolomic signatures, and therapeutic responsiveness, while intestinal organoid biotechnology furnishes physiologically authentic, high-throughput screening matrices for phytochemical evaluation, synergistically enabling the architectural construction of predictive algorithmic models for precision medicine implementation. Nevertheless, several formidable challenges persist in translating this paradigmatic understanding into clinically validated therapeutic interventions. The inherent heterogeneity of TCM formulations presents significant obstacles to standardization and reproducibility, while the intricate dose–response relationships governing phytochemical-microbiome interactions remain incompletely elucidated. Furthermore, the considerable inter-individual variability in baseline microbiome compositions and metabolic phenotypes complicates the development of universally applicable therapeutic protocols, necessitating more nuanced personalization strategies. Future investigative endeavors must prioritize the development of multi-omics integration platforms that can simultaneously capture microbiome taxonomic profiling, metabolomic fingerprinting, and pharmacokinetic-pharmacodynamic modeling to decipher the complex mechanistic networks underlying TCM efficacy. The emergence of precision fermentation technologies and synthetic biology approaches offers unprecedented opportunities for producing standardized bioactive compounds while preserving their therapeutic synergies. Additionally, the implementation of adaptive clinical trial designs, coupled with real-time microbiome monitoring and machine learning-guided dose optimization, promises to revolutionize the clinical validation of gut-kidney axis-targeted interventions.

This integrative therapeutic paradigm, synthesizing millennia of empirical pharmacological wisdom with contemporary microbiome genomics and cutting-edge technological innovations, illuminates a revolutionary approach to CKD therapeutics—one that targets fundamental pathophysiological mechanisms rather than superficial symptomatic amelioration through precision-guided intervention strategies. The gut-kidney axis thereby furnishes both mechanistic validation of TCM's theoretical constructs and elucidates the molecular basis underlying its documented clinical efficacy, while advanced technologies provide the analytical framework necessary for translating traditional wisdom into contemporary precision medicine applications. These technological convergences, when synergistically integrated with traditional pharmacological wisdom, herald a new epoch in nephrology therapeutics wherein personalized, mechanistically-informed treatment paradigms will supplant conventional one-size-fits-all approaches, ultimately transforming CKD management through precision-guided restoration of gut-kidney metabolic homeostasis, establishing a

robust foundation for the continued convergence of traditional and contemporary therapeutic modalities in nephrology practice.

Author contributions

JL: Conceptualization, Funding acquisition, Writing – original draft, Resources, Formal analysis, Writing – review & editing. LD: Formal analysis, Writing – review & editing, Software. ML: Writing – original draft. FH: Conceptualization, Writing – original draft, Supervision, Project administration, Formal analysis, Writing – review & editing. KS: Writing – original draft, Project administration, Formal analysis, Writing – review & editing, Conceptualization, Supervision.

Funding

The author(s) declare that financial support was received for the research and/or publication of this article. The Zhejiang Chinese Medical University Postgraduate Scientific Research Fund Project (No.: 2025YKJ01).

Acknowledgments

All illustrations were created using materials from Figdraw under authorized permission.

Conflict of interest

The authors declare that the research was conducted in the absence of any commercial or financial relationships that could be construed as a potential conflict of interest.

Generative AI statement

The authors declare that no Gen AI was used in the creation of this manuscript.

Any alternative text (alt text) provided alongside figures in this article has been generated by Frontiers with the support of artificial intelligence and reasonable efforts have been made to ensure accuracy, including review by the authors wherever possible. If you identify any issues, please contact us.

Publisher's note

All claims expressed in this article are solely those of the authors and do not necessarily represent those of their affiliated organizations, or those of the publisher, the editors and the reviewers. Any product that may be evaluated in this article, or claim that may be made by its manufacturer, is not guaranteed or endorsed by the publisher.

References

Ahmed, L. A., and Al-Massri, K. F. (2023). Gut microbiota modulation for therapeutic management of various diseases: a new perspective using stem cell therapy. *Curr. Mol. Pharmacol.* 16, 43–59. doi: 10.2174/1874467215666220222105004

Al Khamici, H., Sanchez, V. C., Yan, H., Cataisson, C., Michalowski, A. M., Yang, H. H., et al. (2022). The oxidoreductase CLIC4 is required to maintain mitochondrial function and resistance to exogenous oxidants in breast cancer cells. *J. Biol. Chem.* 298:102275. doi: 10.1016/j.jbc.2022.102275

Alvarenga, L., Kemp, J. A., Schultz, J., Cardozo, L. F. M. F., Nakao, L. S., Ribeiro-Alves, M., et al. (2025). Potential trimethylamine (TMA)-producing bacteria in patients with chronic kidney disease undergoing hemodialysis. *Int. Urol. Nephrol.* 57, 535–544. doi: 10.1007/s11255-024-04191-6

Ammar, D. (2022). The role of ketoacid analogs with dietary protein restriction in chronic kidney disease patients. *Int. J. Res. Publ.* 100, 1–7. doi: 10.47119/ijrp100931120222788

Anegkamol, W., Bowonsomsarit, W., Taweevisit, M., Tumwasorn, S., Thongsricome, T., Kaewwongse, M., et al. (2025). Synbiotics as a novel therapeutic approach for hyperphosphatemia and hyperparathyroidism in chronic kidney disease rats. *Sci. Rep.* 15:7493. doi: 10.1038/s41598-025-91033-9

Angelini, A., Cappuccilli, M. L., Magnoni, G., Croci Chiocchini, A. L., Aiello, V., Napoletano, A., et al. (2021). The link between homocysteine, folic acid and vitamin B12 in chronic kidney disease. G. Ital. Nefrol. 38:2021-vol4. Available online at: https://pubmed.ncbi.nlm.nih.gov/34469084/ (Accessed August 9, 2025).

Anjana, A., and Tiwari, S. K. (2022). Bacteriocin-producing probiotic lactic acid bacteria in controlling dysbiosis of the gut microbiota. *Front. Cell. Infect. Microbiol.* 12:851140. doi: 10.3389/fcimb.2022.851140

Arioli, S., Mangieri, N., Zanchetta, Y., Russo, P., and Mora, D. (2024). Substitution of Asp29 with Asn29 in the metallochaperone UreE of *streptococcus thermophilus* DSM 20617T increases the urease activity and anticipates urea hydrolysis during milk fermentation. *Int. J. Food Microbiol.* 416:110684. doi: 10.1016/j.ijfoodmicro.2024.110684

Asai, M., Kumakura, S., and Kikuchi, M. (2019). Review of the efficacy of AST-120 (KREMEZIN®) on renal function in chronic kidney disease patients. *Ren. Fail.* 41, 47–56. doi: 10.1080/0886022X.2018.1561376

Atzeni, A., Díaz-López, A., Cacho, A. H., Babio, N., García-Gavilán, J. F., Cornejo-Pareja, I., et al. (2024). Gut microbiota dynamics and association with chronic kidney disease: A longitudinal study within the PREDIMED-plus trial. *Life Sci.* 351:122863. doi: 10.1016/j.lfs.2024.122863

Bao, M., Zhang, P., Guo, S., Zou, J., Ji, J., Ding, X., et al. (2022). Altered gut microbiota and gut-derived p-cresyl sulfate serum levels in peritoneal dialysis patients. *Front. Cell. Infect. Microbiol.* 12:639624. doi: 10.3389/fcimb.2022.639624

Bergen, W. G. (2015). Small-intestinal or colonic microbiota as a potential amino acid source in animals. *Amino Acids* 47, 251–258. doi: 10.1007/s00726-014-1875-z

Bi, Z., Li, H., Liang, Y., Sun, D., Liu, S., Chen, W., et al. (2025). Emerging paradigms for target discovery of traditional medicines: a genome-wide pan-GPCR perspective. *Innovation* 6:100774. doi: 10.1016/j.xinn.2024.100774

Bolsega, S., Smoczek, A., Meng, C., Kleigrewe, K., Scheele, T., Meller, S., et al. (2023). The genetic background is shaping cecal enlargement in the absence of intestinal microbiota. *Nutrients* 15:636. doi: 10.3390/nu15030636

Bossola, M., and Picconi, B. (2024). Uremic toxins and the brain in chronic kidney disease. *J. Nephrol.* 37, 1391–1395. doi: 10.1007/s40620-024-01929-4

Brunt, V. E., Gioscia-Ryan, R. A., Casso, A. G., VanDongen, N. S., Ziemba, B. P., Sapinsley, Z. J., et al. (2020). Trimethylamine-N-oxide promotes age-related vascular oxidative stress and endothelial dysfunction in mice and healthy humans. *Hypertension* 76, 101–112. doi: 10.1161/HYPERTENSIONAHA.120.14759

Cabała, S., Ożgo, M., and Herosimczyk, A. (2024). The kidney-gut Axis as a novel target for nutritional intervention to counteract chronic kidney disease progression. *Meta* 14:78. doi: 10.3390/metabo14010078

Caggiano, G., Stasi, A., Franzin, R., Fiorentino, M., Cimmarusti, M. T., Deleonardis, A., et al. (2023). Fecal microbiota transplantation in reducing uremic toxins accumulation in kidney disease: current understanding and future perspectives. *Toxins (Basel)* 15:115. doi: 10.3390/toxins15020115

Cai, H.-D., Su, S.-L., Qian, D.-W., Guo, S., Tao, W.-W., Cong, X. D., et al. (2017). Renal protective effect and action mechanism of Huangkui capsule and its main five flavonoids. *J. Ethnopharmacol.* 206, 152–159. doi: 10.1016/j.jep.2017.02.046

Cao, Y.-L., Lin, J.-H., Hammes, H.-P., and Zhang, C. (2022). Flavonoids in treatment of chronic kidney disease. *Molecules* 27:2365. doi: 10.3390/molecules27072365

Cao, X., Xu, F., Zhao, H., Zhang, J., and Liu, C. (2024). An extra honey polyphenols-rich diet ameliorates the high-fat diet induced chronic kidney disease via modulating

gut microbiota in C57BL/6 mice. *Ren. Fail.* 46:2367700. doi: 10.1080/0886022X.2024.2367700

Carrero, J. J., González-Ortiz, A., Avesani, C. M., Bakker, S. J. L., Bellizzi, V., Chauveau, P., et al. (2020). Plant-based diets to manage the risks and complications of chronic kidney disease. *Nat. Rev. Nephrol.* 16, 525–542. doi: 10.1038/s41581-020-0297-2

Cases, A., Cigarrán-Guldrís, S., Mas, S., and Gonzalez-Parra, E. (2019). Vegetable-based diets for chronic kidney disease? It is time to reconsider. *Nutrients* 11:1263. doi: 10.3390/nu11061263

Cha, R.-H., Kang, S. W., Park, C. W., Cha, D. R., Na, K. Y., Kim, S. G., et al. (2016). A randomized, controlled trial of Oral intestinal sorbent AST-120 on renal function deterioration in patients with advanced renal dysfunction. *Clin. J. Am. Soc. Nephrol.* 11, 559–567. doi: 10.2215/CJN.12011214

Chang, J.-F., Hsieh, C.-Y., Liou, J.-C., Liu, S.-H., Hung, C.-F., Lu, K.-C., et al. (2020). Scavenging intracellular ROS attenuates p-cresyl sulfate-triggered osteogenesis through MAPK signaling pathway and NF-κB activation in human arterial smooth muscle cells. *Toxins* 12:472. doi: 10.3390/toxins12080472

Chang, L., Tian, R., Guo, Z., He, L., Li, Y., Xu, Y., et al. (2023). Low-protein diet supplemented with inulin lowers protein-bound toxin levels in patients with stage 3b-5 chronic kidney disease: A randomized controlled study. *Nutr. Hosp.* 40, 819–828. doi: 10.20960/nh.04643

Chauveau, P., Koppe, L., Combe, C., Lasseur, C., Trolonge, S., and Aparicio, M. (2019). Vegetarian diets and chronic kidney disease. *Nephrol. Dial. Transplant.* 34, 199–207. doi: 10.1093/ndt/gfy164

Chen, Y., Cai, G., Sun, X., and Chen, X. (2016). Treatment of chronic kidney disease using a traditional Chinese medicine, Flos *Abelmoschus manihot* (Linnaeus) Medicus (Malvaceae). *Clin. Exp. Pharmacol. Physiol.* 43, 145–148. doi: 10.1111/1440-1681.12528

Chen, M.-C., Kuo, C.-H., Lin, Y.-L., and Hsu, B.-G. (2025). Gut-derived uremic toxins and cardiovascular health in chronic kidney disease. *Tzu Chi Med. J.* 37, 264–274. doi: 10.4103/tcmj.tcmj_293_24

Chen, Z., Lin, Y., Wang, J., Yao, K., Xie, Y., Chen, X., et al. (2024). Relationship between compound α-ketoacid and microinflammation in patients with chronic kidney disease. *Curr. Pharm. Des.* 30, 589–596. doi: 10.2174/0113816128291248240131102709

Chen, J., Liu, J., Huang, Y., Li, R., Ma, C., Zhang, B., et al. (2021). Insights into oral bioavailability enhancement of therapeutic herbal constituents by cytochrome P450 3A inhibition. *Drug Metab. Rev.* 53, 491–507. doi: 10.1080/03602532.2021.1917598

Chen, Y., Nie, Y., Wu, J., Li, C., Zheng, L., Zhu, B., et al. (2024). Association between systemic inflammatory indicators with the survival of chronic kidney disease: a prospective study based on NHANES. *Front. Immunol.* 15:1365591. doi: 10.3389/fimmu.2024.1365591

Chen, Y.-C., Wu, M.-Y., Hu, P.-J., Chen, T.-T., Shen, W.-C., Chang, W.-C., et al. (2019). Effects and safety of an Oral adsorbent on chronic kidney disease progression: A systematic review and Meta-analysis. *J. Clin. Med.* 8:1718. doi: 10.3390/jcm8101718

Chen, Z., Wu, S., Zeng, Y., Chen, Z., Li, X., Li, J., et al. (2022). FuZhengHuaYuJiangZhuTongLuoFang prescription modulates gut microbiota and gut-derived metabolites in UUO rats. *Front. Cell. Infect. Microbiol.* 12:837205. doi: 10.3389/fcimb.2022.837205

Chen, F., Zhang, H., Wei, Q., Tang, J., Yin, L., Ban, Y., et al. (2025). Disrupted gut microbiota promotes the progression of chronic kidney disease in 5/6 nephrectomy mice by *bacillus pumilus* gavage. *Front. Cell. Infect. Microbiol.* 15:1548767. doi: 10.3389/fcimb.2025.1548767

Cheng, J., and Zhou, J. (2024). Unraveling the gut health puzzle: exploring the mechanisms of butyrate and the potential of high-amylose maize starch butyrate (HAMSB) in alleviating colorectal disturbances. *Front. Nutr.* 11:1285169. doi: 10.3389/fnut.2024.1285169

Chermiti, R., Burtey, S., and Dou, L. (2024). Role of uremic toxins in vascular inflammation associated with chronic kidney disease. *J. Clin. Med.* 13:7149. doi: 10.3390/jcm13237149

Chu, C., Ru, H., Chen, Y., Xu, J., Wang, C., and Jin, Y. (2024). Gallic acid attenuates LPS-induced inflammation in Caco-2 cells by suppressing the activation of the NF-κB/MAPK signaling pathway. *Acta Biochim. Biophys. Sin. Shanghai* 56, 905–915. doi: 10.3724/abbs.2024008

Corradi, V., Caprara, C., Barzon, E., Mattarollo, C., Zanetti, F., Ferrari, F., et al. (2024). A possible role of P-cresyl sulfate and indoxyl sulfate as biomarkers in the prediction of renal function according to the GFR (G) categories. *Integr. Med. Nephrol. Androl.* 11:e24. doi: 10.1097/IMNA-D-24-00002

Cui, H., Fu, F. Q., Liu, B., Liu, W. J., and Liu, Y. N. (2021). Herbal medicine "shulifenxiao" formula for nephrotic syndrome of refractory idiopathic membranous nephropathy. *Front. Pharmacol.* 12:675406. doi: 10.3389/fphar.2021.675406

Cui, L., Ma, Z., Li, W., Ma, H., Guo, S., Wang, D., et al. (2023). Inhibitory activity of flavonoids fraction from Astragalus membranaceus Fisch. Ex Bunge stems and leaves on Bacillus cereus and its separation and purification. *Front. Pharmacol.* 14:1183393. doi: 10.3389/fphar.2023.1183393

D'Arrigo, G., Marino, C., Pizzini, P., Caridi, G., Marino, F., Parlongo, G., et al. (2025). Quality of life and kidney function in CKD patients: a longitudinal study. *Clin. Kidney J.* 18:sfae429. doi: 10.1093/ckj/sfae429

de Carvalho, B. T., Subotić, A., Vandecruys, P., Deleu, S., Vermeire, S., and Thevelein, J. M. (2024). Enhancing probiotic impact: engineering *Saccharomyces boulardii* for optimal acetic acid production and gastric passage tolerance. *Appl. Environ. Microbiol.* 90:e0032524. doi: 10.1128/aem.00325-24

De Vadder, F., Kovatcheva-Datchary, P., Goncalves, D., Vinera, J., Zitoun, C., Duchampt, A., et al. (2014). Microbiota-generated metabolites promote metabolic benefits via gut-brain neural circuits. *Cell* 156, 84–96. doi: 10.1016/j.cell.2013.12.016

Di Iorio, B. R., Rocchetti, M. T., De Angelis, M., Cosola, C., Marzocco, S., Di Micco, L., et al. (2019). Nutritional therapy modulates intestinal microbiota and reduces serum levels of total and free indoxyl sulfate and P-Cresyl sulfate in chronic kidney disease (Medika study). *J. Clin. Med.* 8:1424. doi: 10.3390/jcm8091424

Dickman, K. G., Chen, C.-H., Grollman, A. P., and Pu, Y.-S. (2023). Aristolochic acid-containing Chinese herbal medicine and upper urinary tract urothelial carcinoma in Taiwan: a narrative review. *World. J. Urol.* 41, 899–907. doi: 10.1007/s00345-022-04100-5

Dong, X., Zhang, J., Li, W., Li, Y., Jia, L., Liu, Z., et al. (2024). Yi-Shen-Hua-Shi regulates intestinal microbiota dysbiosis and protects against proteinuria in patients with chronic kidney disease: a randomized controlled study. *Pharm. Biol.* 62, 356–366. doi: 10.1080/13880209.2024.2345080

Doré, E., Joly-Beauparlant, C., Morozumi, S., Mathieu, A., Lévesque, T., Allaeys, I., et al. (2022). The interaction of secreted phospholipase A2-IIA with the microbiota alters its lipidome and promotes inflammation. *JCI Insight* 7:e152638. doi: 10.1172/jci.insight.152638

Evenepoel, P., Bammens, B., Verbeke, K., and Vanrenterghem, Y. (2006). Acarbose treatment lowers generation and serum concentrations of the protein-bound solute p-cresol: a pilot study. *Kidney Int.* 70, 192–198. doi: 10.1038/sj.ki.5001523

Evenepoel, P., Stenvinkel, P., Shanahan, C., and Pacifici, R. (2023). Inflammation and gut dysbiosis as drivers of CKD-MBD. *Nat. Rev. Nephrol.* 19, 646–657. doi: 10.1038/s41581-023-00736-7

Faerber, V., Kuhn, K. S., Garneata, L., Kalantar-Zadeh, K., Kalim, S., Raj, D. S., et al. (2023). The microbiome and protein carbamylation: potential targets for protein-restricted diets supplemented with ketoanalogues in predialysis chronic kidney disease. *Nutrients* 15:3503. doi: 10.3390/nu15163503

Feng, L., Lin, Z., Tang, Z., Zhu, L., Xu, S., Tan, X., et al. (2024). Emodin improves renal fibrosis in chronic kidney disease by regulating mitochondrial homeostasis through the mediation of peroxisome proliferator-activated receptor-gamma coactivator-1 alpha (PGC-1α). *Eur. J. Histochem.* 68:3917. doi: 10.4081/ejh.2024.3917

Feng, H.-Y., Wang, Y.-Q., Yang, J., Miao, H., Zhao, Y.-Y., and Li, X. (2025). Anthraquinones from *rheum officinale* ameliorate renal fibrosis in acute kidney injury and chronic kidney disease. *Drug Des. Devel. Ther.* 19, 5739–5760. doi: 10.2147/DDDT.S521265

Frąk, W., Dąbek, B., Balcerczyk-Lis, M., Motor, J., Radzioch, E., Młynarska, E., et al. (2024). Role of uremic toxins, oxidative stress, and renal fibrosis in chronic kidney disease. *Antioxidants* 13:687. doi: 10.3390/antiox13060687

Gao, Q., Li, D., Wang, Y., Zhao, C., Li, M., Xiao, J., et al. (2024). Analysis of intestinal flora and cognitive function in maintenance hemodialysis patients using combined 16S ribosome DNA and shotgun metagenome sequencing. *Aging Clin. Exp. Res.* 36:28. doi: 10.1007/s40520-023-02645-y

Garibotto, G., Sofia, A., Parodi, E. L., Ansaldo, F., Bonanni, A., Picciotto, D., et al. (2018). Effects of low-protein, and supplemented very low-protein diets, on muscle protein turnover in patients with CKD. *Kidney Int. Rep.* 3, 701–710. doi: 10.1016/j.ekir.2018.01.003

Ghasemzadeh, Y. (2024). Probiotics and fecal microbiota transplants: Mechanisms underlying the therapeutic benefits in manipulating the gut microbiome. *Qapsule: Queen's Undergrad. Health Sci. J.* 1. doi: 10.24908/qap.v1i2.17348

Gibson, G. R., Hutkins, R., Sanders, M. E., Prescott, S. L., Reimer, R. A., Salminen, S. J., et al. (2017). Expert consensus document: the international scientific Association for Probiotics and Prebiotics (ISAPP) consensus statement on the definition and scope of prebiotics. *Nat. Rev. Gastroenterol. Hepatol.* 14, 491–502. doi: 10.1038/nrgastro.2017.75

González-Guerrero, C., Cannata-Ortiz, P., Guerri, C., Egido, J., Ortiz, A., and Ramos, A. M. (2017). TLR4-mediated inflammation is a key pathogenic event leading to kidney damage and fibrosis in cyclosporine nephrotoxicity. *Arch. Toxicol.* 91, 1925–1939. doi: 10.1007/s00204-016-1830-8

Gooding, J., Cao, L., Whitaker, C., Mwiza, J.-M., Fernander, M., Ahmed, F., et al. (2019). Meprin β metalloproteases associated with differential metabolite profiles in the plasma and urine of mice with type 1 diabetes and diabetic nephropathy. *BMC Nephrol.* 20:141. doi: 10.1186/s12882-019-1313-2

Gryp, T., De Paepe, K., Vanholder, R., Kerckhof, F.-M., Van Biesen, W., Van de Wiele, T., et al. (2020a). Gut microbiota generation of protein-bound uremic toxins and related metabolites is not altered at different stages of chronic kidney disease. *Kidney Int.* 97, 1230–1242. doi: 10.1016/j.kint.2020.01.028

Gryp, T., Huys, G. R. B., Joossens, M., Van Biesen, W., Glorieux, G., and Vaneechoutte, M. (2020b). Isolation and quantification of uremic toxin precursor-generating gut Bacteria in chronic kidney disease patients. *Int. J. Mol. Sci.* 21:1986. doi: 10.3390/ijms21061986

Guo, Y., Chen, X., Gong, P., Li, G., Yao, W., and Yang, W. (2023). The gut-organ-Axis concept: advances the application of gut-on-Chip Technology. *Int. J. Mol. Sci.* 24:4089. doi: 10.3390/ijms24044089

Guo, Z.-Y., Wu, X., Zhang, S.-J., Yang, J.-H., Miao, H., and Zhao, Y.-Y. (2025). Poria cocos: traditional uses, triterpenoid components and their renoprotective pharmacology. *Acta Pharmacol. Sin.* 46, 836–851. doi: 10.1038/s41401-024-01404-7

Han, C., Jiang, Y.-H., Li, W., and Liu, Y. (2021). Astragalus membranaceus and *salvia miltiorrhiza* ameliorates cyclosporin a-induced chronic nephrotoxicity through the "gut-kidney axis.". *J. Ethnopharmacol.* 269:113768. doi: 10.1016/j.jep.2020.113768

Hao, X.-T., Peng, R., Guan, M., Zhang, H.-J., Guo, Y., Shalapy, N. M., et al. (2024). The food and medicinal homological resources benefiting patients with hyperlipidemia: categories, functional components, and mechanisms. *Food Med. Homol.* 1:9420003. doi: 10.26599/FMH.2024.9420003

He, H., Lin, M., You, L., Chen, T., Liang, Z., Li, D., et al. (2021). Gut microbiota profile in adult patients with idiopathic nephrotic syndrome. *Biomed. Res. Int.* 2021:8854969. doi: 10.1155/2021/8854969

He, M., Wei, W., Zhang, Y., Xiang, Z., Peng, D., Kasimumali, A., et al. (2024). Gut microbial metabolites SCFAs and chronic kidney disease. *J. Transl. Med.* 22:172. doi: 10.1186/s12967-024-04974-6

Hosseini, S., Mahmoudi, M., Rezaieyazdi, Z., Shapouri-Moghaddam, A., Hosseinzadeh, A., Arab, F. L., et al. (2024). Lupus mice derived mesenchymal stromal cells: beneficial or detrimental on SLE disease outcome. *Int. Immunopharmacol.* 126:111306. doi: 10.1016/j.intimp.2023.111306

Hua, Q., Han, Y., Zhao, H., Zhang, H., Yan, B., Pei, S., et al. (2022). Punicalagin alleviates renal injury via the gut-kidney axis in high-fat diet-induced diabetic mice. *Food Funct.* 13, 867–879. doi: 10.1039/d1fo03343c

Huang, H.-W., and Chen, M.-J. (2024). Exploring the preventive and therapeutic mechanisms of probiotics in chronic kidney disease through the gut-kidney axis. *J. Agric. Food Chem.* 72, 8347–8364. doi: 10.1021/acs.jafc.4c00263

Huang, J., Zhang, M., Mujumdar, A. S., Wang, Y., and Li, C. (2024). Improvement of 3D printing age-friendly brown rice food on rough texture, swallowability, and in vitro digestibility using fermentation properties of different probiotics. *Food Chem.* 460:140701. doi: 10.1016/j.foodchem.2024.140701

Huang, J., Zhu, H., Li, S., Qiu, J., Yang, H., Zheng, F., et al. (2025). Proteomic insights into IgA nephropathy: A comprehensive analysis of differentially expressed proteins in the kidney. *ACS Omega* 10, 17208–17220. doi: 10.1021/acsomega.4c07827

Hung, T. V., and Suzuki, T. (2018). Dietary fermentable fibers attenuate chronic kidney disease in mice by protecting the intestinal barrier. *J. Nutr.* 148, 552–561. doi: 10.1093/jn/nxy008

Huo, X., Meng, Q., Wang, C., Zhu, Y., Liu, Z., Ma, X., et al. (2019). Cilastatin protects against imipenem-induced nephrotoxicity via inhibition of renal organic anion transporters (OATs). *Acta Pharm. Sin. B* 9, 986–996. doi: 10.1016/j.apsb.2019.02.005

Iwashima, T., Takemura, Y., Kishimoto, Y., Ono, C., Watanabe, A., and Iida, K. (2024). Natural antagonistic flavones for AhR inhibit indoxyl sulfate-induced inflammatory gene expression in vitro and renal pathological damages in vivo. *Food Nutr. Res.* 68. doi: 10.29219/fnr.v68.10032

James, P., Stanford, J., Dixit, O. V. A., Nicdao, M. A., McWhinney, B., Sud, K., et al. (2025). Associations between uraemic toxins and gut microbiota in adults initiating peritoneal dialysis. *Toxins* 17:334. doi: 10.3390/toxins17070334

Jensen, B. A. H., Heyndrickx, M., Jonkers, D., Mackie, A., Millet, S., Naghibi, M., et al. (2023). Small intestine vs. colon ecology and physiology: why it matters in probiotic administration. *Cell Rep., Med.* 4:101190. doi: 10.1016/j.xcrm.2023.101190

Jensen, N., Maldonado-Gomez, M., Krishnakumar, N., Weng, C.-Y., Castillo, J., Razi, D., et al. (2024). Dietary fiber monosaccharide content alters gut microbiome composition and fermentation. *Appl. Environ. Microbiol.* 90:e0096424. doi: 10.1128/aem.00964-24

Ji, C., Deng, Y., Yang, A., Lu, Z., Chen, Y., Liu, X., et al. (2020). Rhubarb Enema improved Colon mucosal barrier injury in 5/6 nephrectomy rats may associate with gut microbiota modification. *Front. Pharmacol.* 11:1092. doi: 10.3389/fphar.2020.01092

Jia, L., Dong, X., Li, X., Jia, R., and Zhang, H. L. (2021). Benefits of resistant starch type 2 for patients with end-stage renal disease under maintenance hemodialysis: a systematic review and meta-analysis. *Int. J. Med. Sci.* 18, 811–820. doi: 10.7150/ijms.51484

Jiang, N., Zhang, C., Feng, H., Yuan, J., Ding, L., Fang, W., et al. (2021). Clinical characteristics associated with the properties of gut microbiota in peritoneal dialysis patients. *Perit. Dial. Int: J. Int. Soc. Perit. Dial.* 41, 298–306. doi: 10.1177/0896860820976983

Jiao, A., Yu, B., He, J., Yu, J., Zheng, P., Luo, Y., et al. (2021). Sodium acetate, propionate, and butyrate reduce fat accumulation in mice via modulating appetite and relevant genes. *Nutrition (burbank Angeles Cty. Calif)* 87–88:111198. doi: 10.1016/j.nut.2021.111198

Jochems, P. G. M., van Bergenhenegouwen, J., van Genderen, A. M., Eis, S. T., Wilod Versprille, L. J. F., Wichers, H. J., et al. (2019). Development and validation of bioengineered intestinal tubules for translational research aimed at safety and efficacy testing of drugs and nutrients. *Toxicol. In vitro* 60, 1–11. doi: 10.1016/j.tiv.2019.04.019

Juárez-Trujillo, N., Peredo-Lovillo, A., Martínez-Gutiérrez, F., Pérez-Armendáriz, B., Ortiz-Basurto, R. I., and Jiménez-Fernández, M. (2024). Encapsulation of *lactobacillus acidophilus* or *bifidobacterium longum* using whey protein concentrate and fructans as wall materials: properties, stability, and viability in simulated gastrointestinal tests. *ACS Food Sci. Technol.* 4, 1881–1889. doi: 10.1021/acsfoodscitech.4c00235

Kandouz, S., Mohamed, A. S., Zheng, Y., Sandeman, S., and Davenport, A. (2016). Reduced protein bound uraemic toxins in vegetarian kidney failure patients treated by haemodiafiltration. *Hemodial. Int.* 20, 610–617. doi: 10.1111/hdi.12414

Kane, J., den Toom, M., Bosmans, L., van Os, B., Vos, W., Beckers, L., et al. (2023). Inflammation secondary to chronic kidney disease and peritoneal dialysis accelerates atherosclerosis in a new mouse model. *Nephrol. Dial. Transplant.* 38:gfad063c_3330. doi: 10.1093/ndt/gfad063c_3330

Kapetanaki, S., Kumawat, A. K., Persson, K., and Demirel, I. (2021). The fibrotic effects of TMAO on human renal fibroblasts is mediated by NLRP3, caspase-1 and the PERK/akt/mTOR pathway. *Int. J. Mol. Sci.* 22:11864. doi: 10.3390/ijms222111864

Kemp, J. A., Ribeiro, M., Borges, N. A., Cardozo, L. F. M. F., Fouque, D., and Mafra, D. (2025). Dietary intake and gut microbiome in CKD. *Clin. J. Am. Soc. Nephrol.* 20, 1003–1013. doi: 10.2215/CJN.0000000705

Kieffer, D. A., Martin, R. J., and Adams, S. H. (2016). Impact of dietary fibers on nutrient management and detoxification organs: gut, liver, and kidneys. *Adv. Nutr.* 7, 1111–1121. doi: 10.3945/an.116.013219

Kim, Y.-I., Ko, I., Yi, E.-J., Kim, J., Hong, Y. R., Lee, W., et al. (2025). NAD+ modulation of intestinal macrophages renders anti-inflammatory functionality and ameliorates gut inflammation. *Biomed. Pharmacother.* 185:117938. doi: 10.1016/j.biopha.2025.117938

Kingra, K., Curtis, S., Mollard, R. C., Shamloo, M., Askin, N., Tangri, N., et al. (2022). The effects of resistant starch consumption in adult patients with chronic kidney disease: a systematic review. *Can. J. Kidney Health Dis.* 9. doi: 10.1177/20543581221100023

Kitamura, H., Tanaka, S., Hiyamuta, H., Tsuruya, K., Kitazono, T., and Nakano, T. (2025). Associations of causes of chronic kidney disease with disease progression and mortality: insights from the Fukuoka kidney disease registry study. *Am. J. Nephrol.* 56, 366–376. doi: 10.1159/000543201

Krukowski, H., Valkenburg, S., Madella, A.-M., Garssen, J., van Bergenhenegouwen, J., Overbeek, S. A., et al. (2023). Gut microbiome studies in CKD: opportunities, pitfalls and therapeutic potential. *Nat. Rev. Nephrol.* 19, 87–101. doi: 10.1038/s41581-022-00647-z

Kuang, Q.-X., Lei, L.-R., Li, Q.-Z., Peng, W., Wang, Y.-M., Dai, Y.-F., et al. (2022). Investigation of the anti-inflammatory activity of fusaproliferin analogues guided by transcriptome analysis. *Front. Pharmacol.* 13:881182. doi: 10.3389/fphar.2022.881182

Kumar, P., Saini, K., Saini, V., and Mitchell, T. (2021). Oxalate alters cellular bioenergetics, redox homeostasis, antibacterial response, and immune response in macrophages. *Front. Immunol.* 12:694865. doi: 10.3389/fimmu.2021.694865

Langerak, N., Ahmed, H. M. M., Li, Y., Middel, I. R., Eslami Amirabadi, H., Malda, J., et al. (2020). A theoretical and experimental study to optimize cell differentiation in a novel intestinal chip. *Front. Bioeng. Biotechnol.* 8:763. doi: 10.3389/fbioe.2020.00763

Leska, A., Nowak, A., Szulc, J., Motyl, I., and Czarnecka-Chrebelska, K. H. (2022). Antagonistic activity of potentially probiotic lactic acid Bacteria against honeybee (*Apis mellifera* L.) pathogens. *Pathogens* 11:1367. doi: 10.3390/pathogens11111367

Li, C., Chen, X., Yao, J., Zha, W., Li, M., Shen, J., et al. (2025). Curcumin modulated gut microbiota and alleviated renal fibrosis in 5/6 nephrectomy-induced chronic kidney disease rats. *PLoS One* 20:e0314029. doi: 10.1371/journal.pone.0314029

Li, P., Lin, H., Ni, Z., Zhan, Y., He, Y., Yang, H., et al. (2020). Efficacy and safety of *Abelmoschus manihot* for IgA nephropathy: A multicenter randomized clinical trial. *Phytomedicine* 76:153231. doi: 10.1016/j.phymed.2020.153231

Li, Y., Lu, H., Guo, J., Zhang, M., Zheng, H., Liu, Y., et al. (2023). Gut microbiota-derived trimethylamine N-oxide is associated with the risk of all-cause and cardiovascular mortality in patients with chronic kidney disease: a systematic review and dose-response meta-analysis. *Ann. Med.* 55:2215542. doi: 10.1080/07853890.2023.2215542

Li, H.-D., Meng, X.-M., Huang, C., Zhang, L., Lv, X.-W., and Li, J. (2019). Application of herbal traditional Chinese medicine in the treatment of acute kidney injury. *Front. Pharmacol.* 10:376. doi: 10.3389/fphar.2019.00376

Li, X.-J., Shan, Q.-Y., Wu, X., Miao, H., and Zhao, Y.-Y. (2024). Gut microbiota regulates oxidative stress and inflammation: a double-edged sword in renal fibrosis. *Cell. Mol. Life Sci.* 81:480. doi: 10.1007/s00018-024-05532-5

Li, Y., Sun, Y., Zhang, C., Wang, K., Shen, P., Huang, D., et al. (2017). Moxibustion alleviates injury in a rat focal segmental Glomerulosclerosis model. *Evid. Based Complement. Alternat. Med.* 2017:7169547. doi: 10.1155/2017/7169547

Li, N., Tang, H., Wu, L., Ge, H., Wang, Y., Yu, H., et al. (2021). Chemical constituents, clinical efficacy and molecular mechanisms of the ethanol extract of *Abelmoschus manihot* flowers in treatment of kidney diseases. *Phytother. Res.* 35, 198–206. doi: 10.1002/ptr.6818

Li, J., Xing, H., Lin, W., Yu, H., Yang, B., Jiang, C., et al. (2023). Specific gut microbiome and metabolome changes in patients with continuous ambulatory peritoneal dialysis and comparison between patients with different dialysis vintages. *Front. Med.* 10:1302352. doi: 10.3389/fmed.2023.1302352

Li, J., Xu, Y., Sun, T., Zhang, X., Liang, H., Lin, W., et al. (2024). Exploration of the pathogenesis of nephrotic syndrome and traditional Chinese medicine intervention based on gut microbiota. *Front. Immunol.* 15:1430356. doi: 10.3389/fimmu.2024.1430356

Liu, H.-W., Tsai, W.-H., Liu, J.-S., and Kuo, K.-L. (2019). Association of vegetarian diet with chronic kidney disease. *Nutrients* 11:279. doi: 10.3390/nu11020279

Liu, C., Yang, L., Wei, W., and Fu, P. (2024). Efficacy of probiotics/synbiotics supplementation in patients with chronic kidney disease: A systematic review and meta-analysis of randomized controlled trials. *Front. Nutr.* 11:1434613. doi: 10.3389/fnut.2024.1434613

Lobel, L., Cao, Y. G., Fenn, K., Glickman, J. N., and Garrett, W. S. (2020). Diet posttranslationally modifies the mouse gut microbial proteome to modulate renal function. *Science* 369, 1518–1524. doi: 10.1126/science.abb3763

Long, C., Zhang, C., and Xie, Y. (2024). Study on the mechanism of hirudin multi target delaying renal function decline in chronic kidney disease based on the "gut-kidney axis" theory. *Naunyn Schmiedeberg's Arch. Pharmacol.* 397, 7951–7962. doi: 10.1007/s00210-023-02888-6

Lu, X., Ma, J., and Li, R. (2023). Alterations of gut microbiota in biopsy-proven diabetic nephropathy and a long history of diabetes without kidney damage. *Sci. Rep.* 13:12150. doi: 10.1038/s41598-023-39444-4

Lu, P.-H., Yu, M.-C., Wei, M.-J., and Kuo, K.-L. (2021). The therapeutic strategies for uremic toxins control in chronic kidney disease. *Toxins (Basel)* 13:573. doi: 10.3390/toxins13080573

Lu, W., Zhang, H., Guo, J., Qin, X., and Liu, Y. (2025). Investigation of "microbial-mitochondrial" cross-talk to explore the compatibility mechanism of Xiaojianzhong Tang against chronic atrophic gastritis rats. *Arab. J. Chem.* 18:652024. doi: 10.25259/ajc_65_2024

Luo, Z., Yu, X., Wang, C., Zhao, H., Wang, X., and Guan, X. (2024). Trimethylamine N-oxide promotes oxidative stress and lipid accumulation in macrophage foam cells via the Nrf2/ABCA1 pathway. *J. Physiol. Biochem.* 80, 67–79. doi: 10.1007/s13105-023-00984-y

Lyu, D., He, G., Zhou, K., Xu, J., Zeng, H., Li, T., et al. (2023). Identification of immune-related genes as biomarkers for uremia. *Int. J. Gen. Med.* 16, 5633–5649. doi: 10.2147/IJGM.S435732

Mafra, D., Borges, N. A., Lindholm, B., Shiels, P. G., Evenepoel, P., and Stenvinkel, P. (2021). Food as medicine: targeting the uraemic phenotype in chronic kidney disease. *Nat. Rev. Nephrol.* 17, 153–171. doi: 10.1038/s41581-020-00345-8

Mardinoglu, A., Shoaie, S., Bergentall, M., Ghaffari, P., Zhang, C., Larsson, E., et al. (2015). The gut microbiota modulates host amino acid and glutathione metabolism in mice. *Mol. Syst. Biol.* 11:834. doi: 10.15252/msb.20156487

Marzocco, S., Fazeli, G., Di Micco, L., Autore, G., Adesso, S., Dal Piaz, F., et al. (2018). Supplementation of short-chain fatty acid, sodium propionate, in patients on maintenance hemodialysis: beneficial effects on inflammatory parameters and gut-derived uremic toxins, a pilot study (PLAN study). *J. Clin. Med.* 7:315. doi: 10.3390/jcm7100315

Masereeuw, R. (2022). The dual roles of protein-bound solutes as toxins and signaling molecules in uremia. *Toxins (Basel)* 14:402. doi: 10.3390/toxins14060402

Miao, H., Liu, F., Wang, Y.-N., Yu, X.-Y., Zhuang, S., Guo, Y., et al. (2024a). Targeting *lactobacillus johnsonii* to reverse chronic kidney disease. *Signal Transduct. Target. Ther.* 9:195. doi: 10.1038/s41392-024-01913-1

Miao, H., Wang, Y.-N., Yu, X.-Y., Zou, L., Guo, Y., Su, W., et al. (2024b). Lactobacillus species ameliorate membranous nephropathy through inhibiting the aryl hydrocarbon receptor pathway via tryptophan-produced indole metabolites. *Br. J. Pharmacol.* 181, 162–179. doi: 10.1111/bph.16219

Miao, H., Zhang, S.-J., Wu, X., Li, P., and Zhao, Y.-Y. (2025). Tryptophan metabolism as a target in gut microbiota, ageing and kidney disease. *Int. J. Biol. Sci.* 21, 4374–4387. doi: 10.7150/ijbs.115359

Mishra, S., Kapoor, R., Sushma, N., Kanchan, S., Jha, G., Sharma, D., et al. (2024). Deoxynivalenol induces drp-1-mediated mitochondrial dysfunction via elevating oxidative stress. *Chem. Res. Toxicol.* 37, 1139–1154. doi: 10.1021/acs.chemrestox.4c00066

Mitrović, M., Dimkovic, N., and Popovic, V. S. (2024). The impact of synbiotics on the uremic toxins, inflammation, and gut microbiome of CKD patients—randomized, double-blind, placebo-controlled trial. *Nephrol. Dial. Transplant.* 39:gfae069-156-279. doi: 10.1093/ndt/gfae069.156

Mohan, A., Kumar, R., Kumar, V., and Yadav, M. (2023). Homocysteine, vitamin B12 and folate level: possible risk factors in the progression of chronic heart and kidney disorders. *Curr. Cardiol. Rev.* 19:e090223213539. doi: 10.2174/1573403X19666230209111854

Motavalli, R., Etemadi, J., Soltani-Zangbar, M. S., Ardalan, M.-R., Kahroba, H., Roshangar, L., et al. (2021). Altered Th17/treg ratio as a possible mechanism in pathogenesis of idiopathic membranous nephropathy. *Cytokine* 141:155452. doi: 10.1016/j.cyto.2021.155452

Mou, X., Shah, J., Roye, Y., Du, C., and Musah, S. (2024). An ultrathin membrane mediates tissue-specific morphogenesis and barrier function in a human kidney chip. *Sci. Adv.* 10:eadn2689. doi: 10.1126/sciadv.adn2689

Nakano, T., Watanabe, H., Imafuku, T., Tokumaru, K., Fujita, I., Arimura, N., et al. (2021). Indoxyl sulfate contributes to mTORC1-induced renal fibrosis via the OAT/NADPH oxidase/ROS pathway. *Toxins (Basel)* 13:909. doi: 10.3390/toxins13120909

Nanto-Hara, F., and Ohtsu, H. (2024). In laying hens, chronic heat stress-induced renal fibrosis is potentially promoted by indoxyl sulfate. *Sci. Rep.* 14:23213. doi: 10.1038/s41598-024-75066-0

Nepal, D., and Gazeley, D. (2023). Role of IL-6 and IL-6 targeted therapy in systemic lupus erythematosus. *Rheumatology* 62, 3804–3810. doi: 10.1093/rheumatology/kead416

Nguyen, C., Edgley, A. J., Kelly, D. J., and Kompa, A. R. (2022). Aryl hydrocarbon receptor inhibition restores indoxyl sulfate-mediated endothelial dysfunction in rat aortic rings. *Toxins* 14:100. doi: 10.3390/toxins14020100

Ning, E.-J., Sun, C.-W., Wang, X.-F., Chen, L., Li, F.-F., Zhang, L.-X., et al. (2024). *Artemisia argyi* polysaccharide alleviates intestinal inflammation and intestinal flora dysbiosis in lipopolysaccharide-treated mice. *Food Med. Homol.* 1:9420008. doi: 10.26599/FMH.2024.9420008

Pan, S., Zhao, D., Duan, S., and Chen, X. (2023). The role of gut-dependent molecule trimethylamine N-oxide as a novel target for the treatment of chronic kidney disease. *Int. Urol. Nephrol.* 55, 1747–1756. doi: 10.1007/s11255-023-03500-9

Parker, B. J., Wearsch, P. A., Veloo, A. C. M., and Rodriguez-Palacios, A. (2020). The genus alistipes: gut bacteria with emerging implications to inflammation, cancer, and mental health. *Front. Immunol.* 11:906. doi: 10.3389/fimmu.2020.00906

Pei, M. X., Dong, S. J., Gao, X. Y., Luo, T., Fan, D., Jin, J. F., et al. (2022). Salvianolic acid B attenuates iopromide-induced renal tubular epithelial cell injury by inhibiting the TLR4/NF-κB/NLRP3 signaling pathway. *Evid. Based Complement. Alternat. Med.* 2022:8400496. doi: 10.1155/2022/8400496

Peris-Fernández, M., Roca-Marugán, M., Amengual, J. L., Balaguer-Timor, Á., Viejo-Boyano, I., Soldevila-Orient, A., et al. (2024a). Uremic toxins and inflammation: metabolic pathways affected in non-dialysis-dependent stage 5 chronic kidney disease. *Biomedicine* 12:607. doi: 10.3390/biomedicines12030607

Peris-Fernández, M., Roca-Marugán, M., Amengual-Roig, J. L., Balaguer-Timor, Á., Viejo-Boyano, I., Sánchez-Pérez, P., et al. (2024b). Uremic toxins and inflammation: metabolic pathways affected in stage 5 kidney disease. *Nephrol. Dial. Transplant.* 12, 607. doi: 10.1093/ndt/gfae069.483

Pissas, G., Tziastoudi, M., Divani, M., Poulianiti, C., Konsta, M. A. P., Lykotsetas, E., et al. (2024). Malate dehydrogenase-2 inhibition shields renal tubular epithelial cells from anoxia-reoxygenation injury by reducing reactive oxygen species. *J. Biochem. Mol. Toxicol.* 38:e23854. doi: 10.1002/jbt.23854

Plaza-Díaz, J., Ruiz-Ojeda, F. J., Vilchez-Padial, L. M., and Gil, A. (2017). Evidence of the anti-inflammatory effects of probiotics and synbiotics in intestinal chronic diseases. *Nutrients* 9:555. doi: 10.3390/nu9060555

Pyatchenkov, M. O., Vlasov, A., Sherbakov, E., Salikova, S., Пятченков, М. О., Власов, А. А., et al. (2023). Microbial-derived uremic toxins: role in the pathogenesis of comorbidities in patients with chronic kidney disease. *Ross. Zh. Gastroenterol. Gepatol. Koloproktol.* doi: 10.22416/1382-4376-2023-33-3-7-15

Qian, Q. (2017). Inflammation: A key contributor to the genesis and progression of chronic kidney disease. *Contrib. Nephrol.* 191, 72–83. doi: 10.1159/000479257

Rahman, W. K., Rabea, I. S., and Meizel, M. M. (2024). Protective effect of probiotic against progression of chronic kidney disease: a randomized clinical study. *Med. J. Babylon* 21:560. doi: 10.4103/MJBL.MJBL_676_23

Ranganathan, N., Ranganathan, P., Friedman, E. A., Joseph, A., Delano, B., Goldfarb, D. S., et al. (2010). Pilot study of probiotic dietary supplementation for promoting healthy kidney function in patients with chronic kidney disease. *Adv. Ther.* 27, 634–647. doi: 10.1007/s12325-010-0059-9

Renaldi, R., Wiguna, T., Persico, A. M., and Tanra, A. J. (2025). P-cresol and p-cresyl sulphate boost oxidative stress: A systematic review of recent evidence. *Basic Clin. Pharmacol. Toxicol.* 137:e70065. doi: 10.1111/bcpt.70065

Ribeiro, F. P. B., de Luna Freire, M. O., de Oliveira Coutinho, D., de Santana Cirilo, M. A., and Brito Alves, J. L. (2024). Gut dysbiosis and probiotic therapy in chronic kidney disease: a comprehensive review. *Probiotics Antimicrob. Proteins* 17, 1797–1819. doi: 10.1007/s12602-024-10427-9

Ribeiro, A., Liu, F., Srebrzynski, M., Rother, S., Adamowicz, K., Wadowska, M., et al. (2023). Uremic toxin indoxyl sulfate promotes macrophage-associated low-grade inflammation and epithelial cell senescence. *Int. J. Mol. Sci.* 24:8031. doi: 10.3390/ijms24098031

Rispoli, R. M., Popolo, A., De Fabrizio, V., d'Emmanuele di Villa Bianca, R., Autore, G., Dalli, J., et al. (2025). Targeting inflammatory imbalance in chronic kidney disease: focus on anti-inflammatory and resolution mediators. *Int. J. Mol. Sci.* 26:3072. doi: 10.3390/ijms26073072

Rossi, M., Johnson, D. W., and Campbell, K. L. (2015a). The kidney-gut axis: implications for nutrition care. *J. Ren. Nutr.* 25, 399–403.

Rossi, M., Johnson, D. W., Xu, H., Carrero, J. J., Pascoe, E., French, C., et al. (2015b). Dietary protein-fiber ratio associates with circulating levels of indoxyl sulfate and p-cresyl sulfate in chronic kidney disease patients. *Nutr. Metab. Cardiovasc. Dis.* 25, 860–865. doi: 10.1016/j.numecd.2015.03.015

Rui-Zhi, T., Hui, D., Jian-Chun, L., Xia, Z., Xiao-Jia, W., Dan, W., et al. (2020). *Astragalus mongholicus* Bunge and Panax Notoginseng formula (A&P) combined with Bifidobacterium contribute a Renoprotective effect in chronic kidney disease through

inhibiting macrophage inflammatory response in kidney and intestine. *Front. Physiol.* 11:583668. doi: 10.3389/fphys.2020.583668

Rukavina Mikusic, N. L., Kouyoumdzian, N. M., and Choi, M. R. (2020). Gut microbiota and chronic kidney disease: evidences and mechanisms that mediate a new communication in the gastrointestinal-renal axis. *Pflugers Arch.* 472, 303–320. doi: 10.1007/s00424-020-02352-x

Rumanli, Z., Vural, I. M., and Avci, G. A. (2025). Chronic kidney disease, uremic toxins and microbiota. *Microbiota Host.* doi: 10.1530/mah-24-0012

Sabbadin, C., Graziani, A., Bavaresco, A., Mazzeo, P., Tizianel, I., Ceccato, F., et al. (2024). Pseudohyperaldosteronism due to licorice: a practice-based learning from a case series. *Int. J. Mol. Sci.* 25:7454. doi: 10.3390/ijms25137454

Sahakyan, G., Vejux, A., and Sahakyan, N. (2022). The role of oxidative stress-mediated inflammation in the development of T2DM-induced diabetic nephropathy: possible preventive action of tannins and other Oligomeric polyphenols. *Molecules* 27:9035. doi: 10.3390/molecules27249035

Saigo, C., Nomura, Y., Yamamoto, Y., Sagata, M., Matsunaga, R., Jono, H., et al. (2014). Meclofenamate elicits a nephropreventing effect in a rat model of ischemic acute kidney injury by suppressing indoxyl sulfate production and restoring renal organic anion transporters. *Drug Des. Devel. Ther.* 8, 1073–1082. doi: 10.2147/DDDT.S67456

Sánchez-Ospina, D., Mas-Fontao, S., Gracia-Iguacel, C., Avello, A., González de Rivera, M., Mujika-Marticorena, M., et al. (2024). Displacing the burden: A review of protein-bound uremic toxin clearance strategies in chronic kidney disease. *J. Clin. Med.* 13:1428. doi: 10.3390/jcm13051428

Sato, E., Saigusa, D., Mishima, E., Uchida, T., Miura, D., Morikawa-Ichinose, T., et al. (2017). Impact of the oral adsorbent AST-120 on organ-specific accumulation of uremic toxins: LC-MS/MS and MS imaging techniques. *Toxins (Basel)* 10:19. doi: 10.3390/toxins10010019

Schlienger de Alba, B. N., and Espinosa Andrews, H. (2024). Benefits and challenges of encapsulating bifidobacterium probiotic strains with bifidogenic prebiotics. *Probiotics Antimicrob. Proteins* 16, 1790–1800. doi: 10.1007/s12602-024-10269-5

Selby, N. M., and Taal, M. W. (2024). What every clinician needs to know about chronic kidney disease: detection, classification and epidemiology. *Diabetes Obes. Metab.* 26, 3–12. doi: 10.1111/dom.15683

Serrano, M., Srivastava, A., Buck, G., Zhu, B., Edupuganti, L., Adegbulugbe, E., et al. (2022). Dietary protein and fiber affect gut microbiome and treg/Th17 commitment in chronic kidney disease mice. *Am. J. Nephrol.* 53, 646–651. doi: 10.1159/000526957

Shamloo, M., Mollard, R., Wang, H., Kingra, K., Tangri, N., and MacKay, D. (2022). A randomized double-blind cross-over trial to study the effects of resistant starch prebiotic in chronic kidney disease (ReSPECKD). *Trials* 23:72. doi: 10.1186/s13063-022-06009-1

Shen, L., Liu, L., and Ji, H.-F. (2017). Regulative effects of curcumin spice administration on gut microbiota and its pharmacological implications. *Food Nutr. Res.* 61:1361780. doi: 10.1080/16546628.2017.1361780

Shentu, J., Xu, H., and Zhu, F. (2025). Ammonia-induced lysosomal and mitochondrial damage: A novel perspective on T cell-based cancer immunotherapy. *J. Natl. Cancer Cent.* 5, 105–107. doi: 10.1016/j.jncc.2025.01.004

Shi, X., Zhang, Y., Shi, Y., Zhang, Q., Duan, H., Liu, J., et al. (2023). Analysis of the alleviating effect of modified Huangqi Chifeng decoction on rats with focal segmental glomerulosclerosis based on gut microbiota and fecal metabolomics. *J. Appl. Microbiol.* 134:lxad205. doi: 10.1093/jambio/lxad205

Shivani, S., Kao, C.-Y., Chattopadhyay, A., Chen, J.-W., Lai, L.-C., Lin, W.-H., et al. (2022). Uremic toxin-producing bacteroides species prevail in the gut microbiota of Taiwanese CKD patients: an analysis using the new Taiwan microbiome baseline. *Front. Cell. Infect. Microbiol.* 12:726256. doi: 10.3389/fcimb.2022.726256

Shuvo, A. U. H., Alimullah, M., Jahan, I., Mitu, K. F., Rahman, M. J., Akramuddaula, K., et al. (2025). Evaluation of xanthine oxidase inhibitors febuxostat and allopurinol on kidney dysfunction and histological damage in two-kidney, one-clip (2K1C) rats. *Scientifica* 2025:7932075. doi: 10.1155/sci5/7932075

Si, H., Chen, Y., Hu, D., Yao, S., Yang, J., and Wen, X. (2024). A graminan type fructan from *Achyranthes bidentata* prevents the kidney injury in diabetic mice by regulating gut microbiota. *Carbohydr. Polym.* 339:122275. doi: 10.1016/j.carbpol.2024.122275

Skinner, A. G., Malik, A., Siddiqui, M. R., Singh, V., and Akhtar, S. (2025). Inulin protects caco-2 cells against lipopolysaccharide-induced epithelial barrier dysfunction. *Food Sci. Nutr.* 13:e70046. doi: 10.1002/fsn3.70046

Soleimani, A., Zarrati Mojarrad, M., Bahmani, F., Taghizadeh, M., Ramezani, M., Tajabadi-Ebrahimi, M., et al. (2017). Probiotic supplementation in diabetic hemodialysis patients has beneficial metabolic effects. *Kidney Int.* 91, 435–442. doi: 10.1016/j.kint.2016.09.040

Spicher, P., Brazier, F., Laville, S. M., Liabeuf, S., Kamel, S., Culot, M., et al. (2025). Transporter-mediated interactions between uremic toxins and drugs: a hidden driver of toxicity in chronic kidney disease. *Int. J. Mol. Sci.* 26:6328. doi: 10.3390/ijms26136328

Stasi, A., Franzin, R., Sallustio, F., Scagliotti, A., Cappello, P., Squiccimarro, E., et al. (2025). mTOR inhibition limits LPS induced acute kidney injury and ameliorates hallmarks of cellular senescence. *Sci. Rep.* 15:9635. doi: 10.1038/s41598-025-93815-7

Stepanova, N. (2024). Probiotic interventions in peritoneal dialysis: A review of underlying mechanisms and therapeutic potentials. *World J. Nephrol.* 13:98719. doi: 10.5527/wjn.v13.i4.98719

Su, X., Guo, H., Zhou, Y., Cao, A., Shen, Q., Zhu, B., et al. (2023). Astragaloside IV attenuates high glucose-induced NF-κB-mediated inflammation through activation of PI3K/AKT-ERK-dependent Nrf2/ARE signaling pathway in glomerular mesangial cells. *Phytother. Res.* 37, 4133–4148. doi: 10.1002/ptr.7875

Sun, X., Chen, J., Huang, Y., Zhu, S., Wang, S., Xu, Z., et al. (2022). Yishen Qingli Heluo granule ameliorates renal dysfunction in 5/6 Nephrectomized rats by targeting gut microbiota and intestinal barrier integrity. *Front. Pharmacol.* 13:858881. doi: 10.3389/fphar.2022.858881

Talamantes, S., Steiner, F., Spencer, S., Neshatian, L., and Sonu, I. (2024). Intestinal methanogen overgrowth (IMO) is associated with delayed small bowel and colonic transit time (TT) on the wireless motility capsule (WMC). *Dig. Dis. Sci.* 69, 3361–3368. doi: 10.1007/s10620-024-08563-x

Tan, J., Zhong, Z., Tang, Y., and Qin, W. (2022). Intestinal dysbiosis featuring abundance of streptococcus associates with Henoch-Schönlein purpura nephritis (IgA vasculitis with nephritis) in adult. *BMC Nephrol.* 23:10. doi: 10.1186/s12882-021-02638-x

Tang, H., Li, K., Shi, Z., and Wu, J. (2025). G-protein-coupled receptors in chronic kidney disease induced by hypertension and diabetes. *Cells* 14:729. doi: 10.3390/cells14100729

Tarek, H., Cho, S. S., Hossain, M. S., and Yoo, J. C. (2023). Attenuation of oxidative damage via upregulating Nrf2/HO-1 signaling pathway by protease SH21 with exerting anti-inflammatory and anticancer properties in vitro. *Cells* 12:2190. doi: 10.3390/cells12172190

Teixeira, R. R., de Andrade, L. S., Pereira, N. B. F., Montenegro, H., Hoffmann, C., and Cuppari, L. (2023). Gut microbiota profile of patients on peritoneal dialysis: comparison with household contacts. *Eur. J. Clin. Nutr.* 77, 90–97. doi: 10.1038/s41430-022-01190-7

Tian, N., Li, L., Ng, J. K.-C., and Li, P. K.-T. (2022). The potential benefits and controversies of probiotics use in patients at different stages of chronic kidney disease. *Nutrients* 14:4044. doi: 10.3390/nu14194044

Tsai, Y.-L., Lin, T.-L., Chang, C.-J., Wu, T.-R., Lai, W.-F., Lu, C.-C., et al. (2019). Probiotics, prebiotics and amelioration of diseases. *J. Biomed. Sci.* 26:3. doi: 10.1186/s12929-018-0493-6

Tsinari, A., Roumeliotis, S., Neofytou, I. E., Varouktsi, G., Veljkovic, A., Stamou, A., et al. (2025). The clinical utility and plausibility of oxidative and antioxidant variables in chronic and end-stage kidney disease: A review of the literature. *Int. J. Mol. Sci.* 26:3376. doi: 10.3390/ijms26073376

Tsuji, K., Uchida, N., Nakanoh, H., Fukushima, K., Haraguchi, S., Kitamura, S., et al. (2024). The gut-kidney axis in chronic kidney diseases. *Diagnostics* 15:21. doi: 10.3390/diagnostics15010021

Vagopoulou, A., Theofilis, P., Karasavvidou, D., Haddad, N., Makridis, D., Tzimikas, S., et al. (2024). Pilot study on the effect of flavonoids on arterial stiffness and oxidative stress in chronic kidney disease. *World J. Nephrol.* 13, 95262. doi: 10.5527/wjn.v13.i3.95262

Wakino, S., Hasegawa, K., Tamaki, M., Minato, M., and Inagaki, T. (2025). Kidney-gut axis in chronic kidney disease: therapeutic perspectives from microbiota modulation and nutrition. *Nutrients* 17:1961. doi: 10.3390/nu17121961

Wang, Y., and Gao, L. (2022). Inflammation and cardiovascular disease associated with hemodialysis for end-stage renal disease. *Front. Pharmacol.* 13:800950. doi: 10.3389/fphar.2022.800950

Wang, R., Hu, B., Ye, C., Zhang, Z., Yin, M., Cao, Q., et al. (2022). Stewed rhubarb decoction ameliorates adenine-induced chronic renal failure in mice by regulating gut microbiota dysbiosis. *Front. Pharmacol.* 13:842720. doi: 10.3389/fphar.2022.842720

Wang, Y., Li, J., Chen, C., Lu, J., Yu, J., Xu, X., et al. (2020). Targeting the gut microbial metabolic pathway with small molecules decreases uremic toxin production. *Gut Microbes* 12, 1823800–1823819. doi: 10.1080/19490976.2020.1823800

Wang, X., Miao, Y.-H., Zhao, X.-M., Liu, X., Hu, Y.-W., and Deng, D.-W. (2024). Perspectives on organ-on-a-chip technology for natural products evaluation. *Food Med. Homol.* 1:9420013. doi: 10.26599/FMH.2024.9420013

Wang, S., Qin, S., Cai, B., Zhan, J., and Chen, Q. (2023a). Promising therapeutic mechanism for Chinese herbal medicine in ameliorating renal fibrosis in diabetic nephropathy. *Front. Endocrinol. (Lausanne)* 14:932649. doi: 10.3389/fendo.2023.932649

Wang, S., van Geffen, M., Venema, K., Mommers, A., Jonkers, D., van Schooten, F.-J., et al. (2023b). Effect of protein fermentation products on gut health assessed in an in vitro model of human colon (TIM-2). *Mol. Nutr. Food Res.* 67:e2200574. doi: 10.1002/mnfr.202200574

Wang, Y.-N., Wu, X., Shan, Q.-Y., Yang, Q., Yu, X.-Y., Yang, J.-H., et al. (2025). Acteoside-containing caffeic acid is bioactive functional group of antifibrotic effect by suppressing inflammation via inhibiting AHR nuclear translocation in chronic kidney disease. *Acta Pharmacol. Sin.* doi: 10.1038/s41401-025-01598-4

Wang, I.-K., Yen, T.-H., Hsieh, P.-S., Ho, H.-H., Kuo, Y.-W., Huang, Y.-Y., et al. (2021). Effect of a probiotic combination in an experimental mouse model and clinical patients

with chronic kidney disease: A pilot study. *Front. Nutr.* 8:661794. doi: 10.3389/fnut.2021.661794

Wang, A., Zhao, J., Qin, Y., Zhang, Y., Xing, Y., Wang, Y., et al. (2023). Alterations of the gut microbiota in the lupus nephritis: A systematic review. *Ren. Fail.* 45:2285877. doi: 10.1080/0886022X.2023.2285877

Watanabe, S., Adachi, K., Wakino, S., Hisada, T., and Mochizuki, J. (2022). Dietary therapy with low protein Genmai (brown rice) to improve the gut-kidney axis and reduce CKD progression. *Asia Pac. J. Clin. Nutr.* 31, 341–347. doi: 10.6133/apjcn.202209_31(3).0001

Wei, M., Liu, X., Li, M., Tian, X., Feng, M., Pang, B., et al. (2023). The role of Chinese herbal medicine in the treatment of diabetic nephropathy by regulating endoplasmic reticulum stress. *Front. Pharmacol.* 14:1174415. doi: 10.3389/fphar.2023.1174415

Wieringa, F. P., Suran, S., Søndergaard, H., Ash, S., Cummins, C., Chaudhuri, A. R., et al. (2025). The future of technology-based kidney replacement therapies: an update on portable, wearable, and implantable artificial kidneys. *Am. J. Kidney Dis.* 85, 787–796. doi: 10.1053/j.ajkd.2024.10.015

Wigner, P., Bijak, M., and Saluk-Bijak, J. (2022). Probiotics in the prevention of the calcium oxalate urolithiasis. *Cells* 11:284. doi: 10.3390/cells11020284

Xie, Z., He, W., Gobbi, A., Bertram, H. C., and Nielsen, D. S. (2024). The effect of in vitro simulated colonic pH gradients on microbial activity and metabolite production using common prebiotics as substrates. *BMC Microbiol.* 24:83. doi: 10.1186/s12866-024-03235-2

Xie, H., Yang, N., Yu, C., and Lu, L. (2024). Uremic toxins mediate kidney diseases: the role of aryl hydrocarbon receptor. *Cell. Mol. Biol. Lett.* 29:38. doi: 10.1186/s11658-024-00550-4

Xiong, W., He, F.-F., You, R.-Y., Xiong, J., Wang, Y.-M., Zhang, C., et al. (2018). Acupuncture application in chronic kidney disease and its potential mechanisms. *Am. J. Chin. Med.* 46, 1169–1185. doi: 10.1142/S0192415X18500611

Xu, L., Gao, J., Huang, D., Lin, P., Yao, D., Yang, F., et al. (2021). Emodin ameliorates tubulointerstitial fibrosis in obstructed kidneys by inhibiting EZH2. *Biochem. Biophys. Res. Commun.* 534, 279–285. doi: 10.1016/j.bbrc.2020.11.094

Xu, X., Wang, H., Guo, D., Man, X., Liu, J., Li, J., et al. (2021). Curcumin modulates gut microbiota and improves renal function in rats with uric acid nephropathy. *Ren. Fail.* 43, 1063–1075. doi: 10.1080/0886022X.2021.1944875

Yamaguchi, K., Yisireyili, M., Goto, S., Cheng, X. W., Nakayama, T., Matsushita, T., et al. (2022). Indoxyl sulfate activates NLRP3 inflammasome to induce cardiac contractile dysfunction accompanied by myocardial fibrosis and hypertrophy. *Cardiovasc. Toxicol.* 22, 365–377. doi: 10.1007/s12012-021-09718-2

Yang, C.-Y., Chen, T.-W., Lu, W.-L., Liang, S.-S., Huang, H.-D., Tseng, C.-P., et al. (2021). Synbiotics alleviate the gut indole load and dysbiosis in chronic kidney disease. *Cells* 10:114. doi: 10.3390/cells10010114

Yang, H. L., Feng, P., Xu, Y., Hou, Y. Y., Ojo, O., and Wang, X. H. (2021). The role of dietary fiber supplementation in regulating uremic toxins in patients with chronic kidney disease: a meta-analysis of randomized controlled trials. *J. Ren. Nutr.* 31, 438–447. doi: 10.1053/j.jrn.2020.11.008

Yang, Y., Gong, S., Zhou, C., Xin, W., Qin, S., Yao, M., et al. (2025). REST contributes to renal fibrosis through inducing mitochondrial energy metabolism imbalance in tubular epithelial cells. *Cell Commun. Signal* 23:176. doi: 10.1186/s12964-025-02166-3

Yang, J., Qin, S., and Zhang, H. (2022). Precise strategies for selecting probiotic bacteria in treatment of intestinal bacterial dysfunctional diseases. *Front. Immunol.* 13:1034727. doi: 10.3389/fimmu.2022.1034727

Yasuno, T., and Ito, K. (2024). Dysbiosis of gut microbiota in patients with chronic kidney disease. *Nephrol. Dial. Transplant.* 39, 347–352 doi: 10.1093/ndt/gfae069.1359

Yin, P., Yi, S., Du, T., Zhang, C., Yu, L., Tian, F., et al. (2024). Dynamic response of different types of gut microbiota to fructooligosaccharides and inulin. *Food Funct.* 15, 1402–1416. doi: 10.1039/d3fo04855a

Yokoo, K., Yamamoto, Y., and Suzuki, T. (2021). Ammonia impairs tight junction barriers by inducing mitochondrial dysfunction in caco-2 cells. *FASEB J.* 35:e21854. doi: 10.1096/fj.202100758R

You, C., Guo, J., and Xun, Y. (2025). Renal organic anion transporter 1: clinical relevance and the underlying mechanisms in chronic kidney disease. *BMC Nephrol.* 26:93. doi: 10.1186/s12882-025-03974-y

Yu, J.-S., Ho, C.-H., Wang, H.-Y., Chen, Y.-H., and Hsieh, C.-L. (2017). Acupuncture on renal function in patients with chronic kidney disease: A single-blinded, randomized, preliminary controlled study. *J. Altern. Complement. Med.* 23, 624–631. doi: 10.1089/acm.2016.0119

Yu, Z., Zhao, J., Qin, Y., Wang, Y., Zhang, Y., and Sun, S. (2022). Probiotics, prebiotics, and synbiotics improve uremic, inflammatory, and gastrointestinal symptoms in end-stage renal disease with dialysis: a network meta-analysis of randomized controlled trials. *Front. Nutr.* 9:850425. doi: 10.3389/fnut.2022.850425

Zeng, J.-Y., Wang, Y., Miao, M., and Bao, X.-R. (2021). The effects of rhubarb for the treatment of diabetic nephropathy in animals: a systematic review and meta-analysis. *Front. Pharmacol.* 12:602816. doi: 10.3389/fphar.2021.602816

Zhang, Y., Hu, X. Y., Yang, S. Y., Hu, Y. C., and Duan, K. (2024). Effects of resistant starch supplementation on renal function and inflammatory markers in patients with chronic kidney disease: a meta-analysis of randomized controlled trials. *Renal Fail.* 46:2416609. doi: 10.1080/0886022X.2024.2416609

Zhang, N., Jiang, H., Dai, H., Huang, S., Zhao, Q., Zhang, N., et al. (2024). Efficacy and safety of Mahuang Fuzi and Shenzhuo decoction for treatment of primary membranous nephropathy: A multicenter prospective trial. *Ren. Fail.* 46:2320834. doi: 10.1080/0886022X.2024.2320834

Zhang, L., Li, P., Xing, C., Zhao, J., He, Y., Wang, J., et al. (2014). Efficacy and safety of *Abelmoschus manihot* for primary glomerular disease: a prospective, multicenter randomized controlled clinical trial. *Am. J. Kidney Dis.* 64, 57–65. doi: 10.1053/j.ajkd.2014.01.431

Zhang, J., Luo, D., Lin, Z., Zhou, W., Rao, J., Li, Y., et al. (2020). Dysbiosis of gut microbiota in adult idiopathic membranous nephropathy with nephrotic syndrome. *Microb. Pathog.* 147:104359. doi: 10.1016/j.micpath.2020.104359

Zhang, B., Wan, Y., Zhou, X., Zhang, H., Zhao, H., Ma, L., et al. (2022). Characteristics of serum metabolites and gut microbiota in diabetic kidney disease. *Front. Pharmacol.* 13:872988. doi: 10.3389/fphar.2022.872988

Zhang, Y., Yang, M., Ho, N. J., Mok, R. Y., Zhang, Z., Ge, B., et al. (2020). Is it safe to take radix *salvia miltiorrhiza* – radix pueraria lobate product with warfarin and aspirin? A pilot study in healthy human subjects. *J. Ethnopharmacol.* 262:113151. doi: 10.1016/j.jep.2020.113151

Zhang, Y., Zhou, Y., Cui, W., Wang, Z., Wang, X., Wu, F., et al. (2022). Characterization and diagnostic value of the gut microbial composition in patients with minimal change disease. *Front. Physiol.* 13:1070569. doi: 10.3389/fphys.2022.1070569

Zhao, C., Fu, J., Wang, Y., and Zhou, Y. (2025). Latest evidence and perspectives of panax notoginseng extracts and preparations for the treatment of cardiovascular diseases. *J. Cardiovasc. Pharmacol.* 85, 248–260. doi: 10.1097/FJC.0000000000001670

Zhao, B., Hu, X., Wang, W., and Zhou, Y. (2025). Cardiorenal syndrome: clinical diagnosis, molecular mechanisms and therapeutic strategies. *Acta Pharmacol. Sin.* 46, 1539–1555. doi: 10.1038/s41401-025-01476-z

Zhao, H., Zhao, T., and Li, P. (2024). Gut microbiota-derived metabolites: a new perspective of traditional Chinese medicine against diabetic kidney disease. *Integr. Med. Nephrol. Androl.* 11:e23-00024. doi: 10.1097/IMNA-D-23-00024

Zhen, J., Zhou, Z., He, M., Han, H.-X., Lv, E.-H., Wen, P.-B., et al. (2023). The gut microbial metabolite trimethylamine N-oxide and cardiovascular diseases. *Front. Endocrinol. (Lausanne)* 14:1085041. doi: 10.3389/fendo.2023.1085041

Zheng, L., Luo, M., Zhou, H., and Chen, J. (2023). Natural products from plants and microorganisms: novel therapeutics for chronic kidney disease via gut microbiota regulation. *Front. Pharmacol.* 13:1068613. doi: 10.3389/fphar.2022.1068613

Zhong, C., Dai, Z., Chai, L., Wu, L., Li, J., Guo, W., et al. (2021). The change of gut microbiota-derived short-chain fatty acids in diabetic kidney disease. *J. Clin. Lab. Anal.* 35:e24062. doi: 10.1002/jcla.24062

Zhong, X., Jia, J., Tan, R., and Wang, L. (2024). Hederagenin improves adriamycin-induced nephropathy by inhibiting the JAK/STAT signaling pathway. *Integr. Med. Nephrol. Androl.* 11:e22-00016. doi: 10.1097/IMNA-D-22-00016

Zhong, Z., Zhang, Y., Wei, Y., Li, X., Ren, L., Li, Y., et al. (2024). Fucoidan improves early stage diabetic nephropathy via the gut microbiota-mitochondria axis in high-fat diet-induced diabetic mice. *J. Agric. Food Chem.* 72, 9755–9767. doi: 10.1021/acs.jafc.3c08503

Zhou, X., Wu, Q., Wang, Y., Ren, Q., Zhu, W., Yao, Z., et al. (2020). Moxibustion as an adjuvant therapy for chronic kidney disease: A systematic review and Meta-analysis of 23 randomized controlled trials. *Evid. Based Complement. Alternat. Med.* 2020:6128673. doi: 10.1155/2020/6128673

Zhou, J., Yang, C., Lei, W., Yang, Z., Chen, J., Lin, H., et al. (2022). Exploration of the correlation between intestinal flora and *escherichia coli* peritoneal dialysis-related peritonitis. *BMC Nephrol.* 23:76. doi: 10.1186/s12882-022-02704-y

Zhu, L.-B., Zhang, Y.-C., Huang, H.-H., and Lin, J. (2021). Prospects for clinical applications of butyrate-producing bacteria. *World J. Clin. Pediatr.* 10, 84–92. doi: 10.5409/wjcp.v10.i5.84

Glossary

ABPW1 - *Achyranthes bidentata* polysaccharide

ACE - Angiotensin-Converting Enzyme

ADMA - Asymmetric dimethylarginine

AhR - Aryl hydrocarbon receptor

AKI - Acute Kidney Injury

Akt - Protein Kinase B

AQP2 - Aquaporin-2

ARE - Angiotensin II Receptor Blocker

ASC - Apoptosis-associated speck-like protein containing a CARD

BCRP - Breast cancer resistance protein

BUN - Blood urea nitrogen

CAM - Complementary and Alternative Medicine

CFU - Colony forming unit

CKD - Chronic Kidney Disease

Col1a1 - Collagen type I alpha 1 chain

COX-2 - Cyclooxygenase-2

CRP - C-reactive protein

CRS - Cardiorenal Syndrome

CYP1A1 - Cytochrome P450 1A1

DAO - Diamine oxidase

DF - Dietary fiber

DN - Diabetic nephropathy

EAA - Essential amino acid

ECM - Extracellular matrix

eGFR - Estimated glomerular filtration rate

ENaC - Epithelial Sodium Channel

eNOS - Endothelial Nitric Oxide Synthase

ESRD/ESKD - End-stage renal disease/End-stage kidney disease

F/B - Firmicutes/Bacteroidetes

FMT - Fecal microbiota transplantation

FOXO3a - Forkhead Box O3a

FSGS - Focal Segmental Glomerulosclerosis

FTZ - Fufang Zhenzhu Tiaozhi Capsules

FTZP - FTZ Polysaccharides

GCA - Glycocholic acid

GFR - Glomerular filtration rate

GG - Guar Gum

GPR43 - G protein-coupled receptor 43

HIA - Hippuric Acid

HO-1 - Heme Oxygenase-1

IAA - Indole-3-acetic acid

IDO - Indoleamine 2,3-Dioxygenase

IgAN - IgA nephropathy

IgAV-N - IgA vasculitis with nephritis

IKK - IκB kinase

IL-1/6/10/17 - Interleukin-1/6/10/17

IMN - Idiopathic Membranous Nephropathy

iNOS - Inducible Nitric Oxide Synthase

IRE1α - Inositol-requiring enzyme 1α

IS - Indoxyl sulfate

JNK - c-Jun N-terminal kinase

Keap1 - Kelch-like ECH-associated Protein 1

LN - Lupus Nephritis

LPD - Low-protein diet

LPS - Lipopolysaccharide

MAPK - Mitogen-activated protein kinase

MCD - Minimal Change Disease

MN - Membranous Nephropathy

MRP2/4 - Multidrug resistance-associated protein 2/4

MSG - Moshen Granule

MsPGN - Mesangial proliferative glomerulonephritis

mTOR - Mechanistic Target of Rapamycin

NADPH - Nicotinamide adenine dinucleotide phosphate

NF-κB - Nuclear factor kappa B

NH_3 - Ammonia

NLRP3 - NOD-like receptor family pyrin domain containing 3

Nrf2 - Nuclear Factor Erythroid 2–Related Factor 2

NO - Nitric oxide

OAT1/3 - Organic anion transporter 1/3

OCT2 - Organic cation transporter

PAG - Phenylacetic acid

PAMPs - Pathogen-Associated Molecular Patterns

PCS/PS - p-Cresyl sulfate

PD - Peritoneal Dialysis

PERK - PKR-like ER kinase

PHGG - Partially hydrolyzed guar gum

PI3K - Phosphoinositide 3-Kinase

PU - Punicalagin

QDTS - QiDiTangShen Granules

RCT - Randomized controlled trial

ROS - Reactive oxygen species

RS - Resistant starch

SCFA - Short-chain fatty acid

SBA - Secondary bile acid

SIRT3 - Sirtuin 3

SP - Sodium propionate

STAT3 - Signal Transducer and Activator of Transcription 3

SZP - Sanzi Guben Polysaccharides

TCA - Tricarboxylic acid

TCDCA - Taurochenodeoxycholic acid

TCM - Traditional Chinese Medicine

TCPM - Traditional Chinese Patent Medicine

TDO - Tryptophan 2,3-Dioxygenase

TGF-β1 - Transforming growth factor beta 1

TLR - Toll-like receptor

TMA - Trimethylamine

TMAO - Trimethylamine N-oxide

TNF-α - Tumor necrosis factor alpha

YQHG - Yishen Qingli Heluo Granule

YSHS - Yi-Shen-Hua-Shi Granule

ZO-1 - Zonula occludens-1

frontiers | Frontiers in Microbiology

TYPE Review
PUBLISHED 28 October 2025
DOI 10.3389/fmicb.2025.1630823

Check for updates

OPEN ACCESS

EDITED BY
Junling Shi,
Northwestern Polytechnical University, China

REVIEWED BY
Lie Zheng,
Shaanxi Provincial Hospital of Traditional Chinese Medicine, China
Yongpeng Shi,
University of Science and Technology of China, China

*CORRESPONDENCE
Qiao Zhang
✉ 18700081184@163.com

RECEIVED 16 June 2025
ACCEPTED 23 September 2025
PUBLISHED 28 October 2025

CITATION
Tian R, Chong C-J, Bai Y-Y, Chen N, Qiao R-R, Wang K, Wang Y-W, Zhao P, Zhao C-B, Tang Y-P, Zhang L and Zhang Q (2025) The role of gut microbiota in diarrhea and its alleviation through microbiota-targeted interventions. *Front. Microbiol.* 16:1630823. doi: 10.3389/fmicb.2025.1630823

COPYRIGHT
© 2025 Tian, Chong, Bai, Chen, Qiao, Wang, Wang, Zhao, Zhao, Tang, Zhang and Zhang. This is an open-access article distributed under the terms of the Creative Commons Attribution License (CC BY). The use, distribution or reproduction in other forums is permitted, provided the original author(s) and the copyright owner(s) are credited and that the original publication in this journal is cited, in accordance with accepted academic practice. No use, distribution or reproduction is permitted which does not comply with these terms.

The role of gut microbiota in diarrhea and its alleviation through microbiota-targeted interventions

Rui Tian[1], Chu-Jun Chong[1], Ya-Ya Bai[1], Ni Chen[1], Rui-Rui Qiao[1], Kan Wang[2], Yu-Wei Wang[1], Peng Zhao[1], Chong-Bo Zhao[1], Yu-Ping Tang[1], Li Zhang[3] and Qiao Zhang[1]*

[1]Key Laboratory of Shaanxi Administration of Traditional Chinese Medicine for TCM Compatibility, and State Key Laboratory of Research & Development of Characteristic Qin Medicine Resources (Cultivation), and Shaanxi Collaborative Innovation Center of Chinese Medicinal Resources Industrialization, and Shaanxi Traditional Chinese Medicine Processing Technology Heritage Base, Shaanxi University of Chinese Medicine, Xi'an, China, [2]College of Sports and Health, Nanjing Sport Institute, Nanjing, Jiangsu, China, [3]Hanlin College Nanjing University of Chinese Medicine, Taizhou, Jiangsu, China

Diarrhea is a common gastrointestinal disease and closely related to the balance of the gut microbiota (GM). In turn, dysregulation of the GM can affect the onset and progression of diarrhea through regulating the metabolism, intestinal immune function, intestinal barrier function and changes in the brain-gut axis of host. Although increasing evidence suggests that GM is associated with gastrointestinal homeostasis and disease, the underlying mechanisms are not fully understood. GM disorder was often accompanied by diarrhea patients and animals, and the diarrhea caused by GM imbalance mainly involved the effects on short chain fatty acids (SCFAs), bile acids (BAs), intestinal barrier, immune system, and brain-gut microbiota axis (BGMA). In addition, intervening in the GM (probiotics, fecal microbiota transplantation and bacteriophage therapy) has been shown to be an effective way to alleviate diarrhea. In this review, the mechanism of diarrhea occurrence, probiotics, fecal microbiota transplantation and bacteriophage therapy intervene in diarrhea by regulating GM from basic and clinical research were summarized and discussed. We aim to provide the latest reference for studying the mechanism of treating diarrhea from the perspective of GM, and provide data support for clinical treatment of diarrhea.

KEYWORDS

diarrhea, gut microbiota, metabolites, probiotics, fecal microbiota transplantation, bacteriophage therapy

1 Introduction

Despite improvements in living conditions and widespread vaccination, diarrhea remains one of the most prevalent global health issues, resulting in approximately 1.3 million deaths annually (Collaborators G.D.D, 2017; Stockmann et al., 2017). Diarrhea is an intestinal disorder characterized by increased gastrointestinal motility, leading to elevated stool frequency and higher water content, often presenting as watery stools. It can be caused by a variety of pathogens and other factors (Brehm et al., 2020; Schiller et al., 2017). Common forms of diarrhea include infectious diarrhea (caused by bacteria, viruses, parasites, or fungi), organic-associated diarrhea, antibiotic-associated diarrhea (AAD), functional diarrhea, and diarrhea-predominant irritable bowel syndrome (IBS-D) (Wilkins and Sequoia, 2017).

Although the current pharmaceuticals for diarrhea includes various agents from traditional Chinese (e.g., Shen-Ling-Bai-Zhu-San) and Western medicine (e.g., loperamide, diphenoxylate), the development of novel, safer, and more effective treatment strategies is urgently required (Ali et al., 2020; Khan et al., 2019; Wang et al., 2020).

The gut microbiota (GM) is increasingly recognized as a pivotal factor in human health, influencing nutrient absorption, immune regulation and gastrointestinal homeostasis (Paul et al., 2025). Alterations in the composition and function of the GM, often termed GM dysregulation, are closely linked to the development of gastrointestinal diseases (Quaglio et al., 2022). The onset of diarrhea is frequently accompanied by GM disturbances, aberrant metabolite levels, reduced immune function, and impaired intestinal barrier function (Anbazhagan et al., 2018; Wu et al., 2022).

For instance, patients with IBS-D exhibit an increased relative abundance of *Shigella, Enterococcus, Streptococcus* and *Ruminococcus,* alongside a decreased abundance of *Faecalibacterium* (Wei et al., 2020). Notably, *Faecalibacterium* is a dominant butyric acid-producing genus. Butyric acid serves as a crucial energy source for colonocytes and can exert anti-inflammatory, immunomodulatory, and intestinal barrier-protecting functions by inhibiting the activation of the toll-like receptor 4-myeloid differentiation factor 88-nuclear factor-κB (TLR4-MyD88-NF-κB) signaling pathway. However, a decline in *Faecalibacterium* abundance is frequently associated with diarrheal symptoms and intestinal inflammation (Anbazhagan et al., 2024; Karim et al., 2024). Moreover, it was found that the occurrence of IBS-D was closely related to the expression of 5-Hydroxytryptamine (5-HT) in the brain-gut microbiota axis (BGMA), and *Ruminococcus* can regulate the production of 5-HT through Trace Amine-Associated Receptor 1 (TAAR1) signaling mediated by phenethylamine and tryptamine, which can stimulate gastrointestinal transit and lead to diarrhea in patients with IBS-D (Shen et al., 2022; Zhai et al., 2023). Studies in AAD models have shown reduced GM richness and diversity, downregulation of the tight junction (TJ) protein zonula occluden 1 (ZO-1) in the colon, and elevated levels of pro-inflammatory cytokines including interleukin-2 (IL-2), interleukin-1β (IL-1β), and tumor necrosis factor-α (TNF-α) (Cui et al., 2021; Xu H. et al., 2023). Collectively, these findings highlight the pivotal role of GM in the pathogenesis of diarrhea (Gallardo et al., 2020; Mei et al., 2021).

Recently, probiotic interventions, fecal microbiota transplantation (FMT) techniques and bacteriophage therapy have demonstrated considerable potential in the treatment of diarrhea (Fujimoto and Uematsu, 2022; Lai et al., 2019; Liu M. et al., 2024). *Lactiplantibacillus plantarum* P9 has been shown to alleviate diarrhea by regulating the composition of GM and increasing the patient's functional intestinal metabolites. The specific action mechanisms include increased the relative abundances of *Butyricicoccus_A* sp002395695 and *Streptococcus thermophilus*, reduced the relative abundances of *Phascolarctobacterium faecium* and *Faecalibacterium* sp., increased the content of acetic acid and butyric acid in short chain fatty acids (SCFAs), and decreased the level of deoxycholic acid (Yang et al., 2024). Additionally, studies have reported that transplantation of fecal fluid from healthy donors into AAD patients alleviated GM disorders, modulated GM composition and quantity, and lowered interleukin-8 (IL-8) and C-reactive protein (CRP). These changes thereby enhanced intestinal immune function and alleviated AAD symptoms (Wang L. et al., 2024). Furthermore, the study found that phage A221 effectively treated diarrhea caused by *Escherichia coli* (*E. coli*) GXXW-1103 in weaned piglets, increased their daily weight gain, and reduced the proportion of Enterobacteriaceae in the duodenum to 0.64%, thereby alleviating lesions in the cecum and duodenum (Mao et al., 2023). Thus, targeted modulation of the GM represents a promising therapeutic strategy for alleviating diarrhea.

Therefore, in this review, we summarize the regulatory mechanisms of GM and its metabolites in diarrhea. Specifically, we discuss the mechanisms of probiotics, FMT and bacteriophage in the treatment of diarrhea, aiming to provide insights for future research on targeted modulation of the GM as a therapeutic strategy for diarrheal diseases.

2 The pivotal role of GM in diarrhea related diseases

As a complex and diverse ecosystem, the GM colonizes the entire gastrointestinal tract in a symbiotic fashion, participating in the growth and development of the host organism while regulating the body's immune system (Takiishi et al., 2017). The GM is crucial for maintaining host homeostasis and overall health. Its diversity and abundance have direct implications for disease pathogenesis and clinical treatment outcomes (Chen et al., 2021). Under normal physiological conditions, the species composition and proportional distribution of GM remain in a homeostatic balance, and it exerts multiple pivotal functions in the host, including modulating immune responses, mediating metabolic processes, and sustaining the homeostasis of the intestinal barrier (Jandhyala et al., 2015; Wu and Wu, 2012). In contrast, under pathological circumstances, perturbations to the intestinal microecosystem can disrupt this balance, ultimately resulting in GM dysbiosis. This dysbiosis subsequently impairs host health via a variety of mechanisms, including alterations in SCFAs metabolism (Morrison and Preston, 2016), BAs (Cai et al., 2022), intestinal barriers (Allam-Ndoul et al., 2020), the immune system (Donald and Finlay, 2023), and BGMA (Hillestad et al., 2022). Such alterations may contribute to the development of diseases such as diarrhea (Shao et al., 2020), inflammatory bowel disease (Quaglio et al., 2022), and cardiovascular diseases (Witkowski et al., 2020).

2.1 Effect on the composition of the GM

Under physiological conditions, a homeostatic GM supports key host functions including immune regulation, metabolic processes, and the maintenance of intestinal barrier integrity (Yue et al., 2019).

In healthy individuals, the GM is predominantly composed of the phyla Firmicutes and Bacteroidetes, followed by Actinobacteria and Verrucomicrobia (Hollister et al., 2014). Under normal physiological conditions, GM is in homeostasis and plays functions of immunity, metabolism and maintenance of intestinal barrier homeostasis in the body (Yue et al., 2019). However, the composition and diversity of GM is easily influenced by various factors (such as diet, drugs, pathogens, and environmental factors), further affecting human and animal health (Cryan et al., 2019; Lange et al., 2016; Zhang, 2022). Compelling evidence indicates that GM dysbiosis increases host vulnerability to a broad spectrum of

pathogens and promotes the development of diverse diseases, including diarrhea, IBS, and allergies (Leong et al., 2018; Shchikota et al., 2021).

Despite improvements in living conditions and healthcare in recent years, diarrhea remains a globally prevalent issue (Wolf et al., 2022). A topic of growing interest currently is the interplay between diarrhea and the GM, which is featured by pathogen-dominated GM dysregulation, encompassing bacterial, fungal, and viral etiologies (Li et al., 2021). Invasive pathogens suppress the proliferation of commensal bacteria, thereby reducing beneficial gut microbiota and increasing pathogenic strains. This imbalance further induces intestinal dysfunction and activates immune responses, ultimately culminating in diarrhea (Czepiel et al., 2019; Jesser et al., 2023).

Furthermore, it has been observed that other types of diarrhea are also closely associated with alterations in the GM (Table 1). Thus, it is evident that dysbiosis of the GM exists across various forms of diarrhea.

2.2 Effect on metabolites of the GM

SCFAs, including acetate, propionate, and butyrate (Liu et al., 2021), are mainly produced by GM via anaerobic fermentation of indigestible carbohydrates and host-derived substrates (Zhang et al., 2023). SCFAs contribute to the enhancement of intestinal barrier function, exhibit anti-inflammatory effects, and participate in

TABLE 1 Changes of GM in diarrhea.

Type of diarrhea		Classification level	Changes in microbiota	Reference
Infectious diarrhea	Bacterial diarrhea (*E. coli* O_{101})	Phylum level	Proteobacteria and Actinobacteria increased; Firmicutes and Verrucomicrobia decreased.	Sun et al. (2019)
		Genus level	*Escherichia* and *Shigella* increased; *Prevotella*, *Enterococcus* and *Akkermansia* decreased.	
	Virus diarrhea (Rotavirus)	Genus level	*Acinetobacter* increased; Ruminococcaceae NK4A214 decreased.	Mizutani et al. (2021)
	Virus diarrhea (Norovirus)	Genus level	*Holdemanella*, *Staphylococcus*, *Howardella*, *Corynebacterium*, and *Massilia* increased.	
	Parasitic diarrhea (Giardia)	Phylum level	Proteobacteria increased, Firmicutes and Melainabacteria decreased.	Barash et al. (2017)
Organic - associated diarrhea	Post-cholecystectomy diarrhea	Phylum level	Bacteroidota increased, Firmicutes decreased.	Xu Y. et al. (2022)
		Genus level	*Prevotella* and *Enterococcus* increased, *Alistipes*, *Lactobacillus*, *Ruminococcus* and *Bacteroides* decreased.	
Antibiotic - associated diarrhea (AAD)		Phylum level	Proteobacteria increased, and Firmicutes, Bacteroidetes, Actinobacteria and Planctomycetes decreased.	Shao et al. (2020)
		Genus level	*Enterococcus* and *Clostridium* increased, *Lactobacillus* decreased.	
Functional diarrhea		Phylum level	*Bacteroides* increased, Firmicutes and Proteobacteria decreased.	Li X. T. et al. (2023)
		Genus level	*Akkermansia* increased, *Lactobacillus*, *Ruminococcus* and *Allobaculum* decreased.	
IBS-D		Phylum level	Proteobacteria increased, Firmicutes, Fusobacteria, and Actinobacteria decreased.	Mei et al. (2021)
		Genus level	Enterobacteriaceae increased, *Alloprevotella* and *Fusobacterium* decreased.	

immunomodulation (Parada Venegas et al., 2019). Specifically, acetate and propionate serve as energy sources for peripheral tissues (den Besten et al., 2013). A recent study demonstrated that acetic acid mediates crosstalk between epithelial and immune cells and promotes T cell-dependent immunoglobulin A (IgA) production by stimulating $CD4^+$ T cells (Takeuchi et al., 2021). Moreover, propionate has been shown to prevent the reduction of TJ proteins, such as ZO-1 and occludin, in colon tissue, and to suppress the mRNA expression of pro-inflammatory cytokines IL-1β, IL-6, and TNF-α (Tong et al., 2016). Butyrate also exerts anti-inflammatory effects by inhibiting the secretion of IL-8, IL-6, IL-12, and TNF-α, while promoting the production of the anti-inflammatory cytokine IL-10, thereby contributing to the maintenance of the intestinal epithelial barrier (Lee et al., 2017). Additionally, they promote the growth of beneficial bacteria, improve GM composition, and help regulate host immune homeostasis (Fukuda et al., 2011; Mann et al., 2024). Moreover, a separate study demonstrated that propionic acid, secreted by *Akkermansia muciniphila*, binds to G-protein-coupled receptor 43 on the surface of intestinal epithelial cells. This interaction enhances histone acetylation, which in turn upregulates the expression of TJ proteins occludin and ZO-1 and increases mucin levels, ultimately improving the integrity of the intestinal epithelial barrier (He et al., 2023). In addition, another study demonstrated that, relative to healthy calves, calves with diarrhea induced by bovine rotavirus (BRV) exhibited significantly reduced concentrations of total SCFAs, acetic acid, propionic acid, and isocaproic acid; in contrast, only propionic acid concentrations were markedly decreased in calves with diarrhea caused by bovine coronavirus. Notably, the depletion of *Parabacteroides* and *Ruminococcus* was strongly associated with reduced acetic acid levels, while declines in isocaproic acid content were closely linked to the loss of *Parabacteroides*, *Ruminococcus*, *Fournierella*, and *Rikenellaceae_RC9_gut_group*. Furthermore, a significant reduction in propionic acid concentrations showed a positive correlation with the depletion of *Collinsella* (Cui et al., 2023). Both propionic and butyric acids are believed to enhance the integrity of epithelial cells, with butyric acid serving as the primary energy source for colonocytes (Furusawa et al., 2013; Tong et al., 2016). Reduced butyrate levels have been shown to elevate intestinal oxygenation, which not only drives gut microbial dysbiosis and promotes the expansion of aerobic pathogens but also disrupts intestinal homeostasis (Handa et al., 2023). SCFAs are absorbed by epithelial cells, which in turn stimulates Na^+-dependent absorption of water and electrolytes, thereby mitigating diarrhea symptoms (Binder, 2010). Several studies have indicated that ADD-type mice exhibit reduced levels of SCFAs (Min et al., 2024; Yang L. et al., 2021; Zhan et al., 2023). Furthermore, piglets infected with *E. coli* developed diarrhea and exhibited decreased levels of SCFAs in their feces (Liu et al., 2019).

Bile acids (BAs) serve as essential signaling molecules that significantly regulate glucose homeostasis, lipid metabolism, and energy expenditure (Sah et al., 2022; Yu et al., 2023). They consist of primary bile acids (PBAs), which are synthesized by the liver, and secondary bile acids (SBAs), which are metabolized by the GM. Among them, PBAs include chenodeoxycholic acid (CDCA) and cholic acid (CA), while SBAs comprise lithocholic acid (LCA) and deoxycholic acid (DCA). Nearly 95% of luminal BAs are reabsorbed in the distal ileum, while the remainder undergoes microbial modification by the GM prior to excretion or passive absorption. In humans, the GM is instrumental in the generation of SBAs via a series of enzymatic reactions, including deconjugation, 7α-dehydroxylation, oxidation, epimerization, desulfation, and esterification. Of these, deconjugation and 7α-dehydroxylation are the most physiologically significant processes (Ridlon et al., 2016; Wahlström et al., 2017). When intestinal homeostasis is disrupted, dysbiosis of the GM affects BAs metabolism and ultimately alters the host response. In IBS-D, excessive fecal BAs are considered a contributing factor to pathogenesis, and there are higher levels of PBAs in fecal samples of IBS-D patients compared to healthy subjects (Duboc et al., 2012; Wei et al., 2021; Wei et al., 2020). However, research has indicated that a microbiota rich in Clostridia can promote BAs excretion in IBS-D patients (Zhao et al., 2020). It is well established that BAs modulate intestinal mucosal permeability and participate in inflammatory responses. Specifically, CDCA and DCA exert their effects by promoting epidermal growth factor receptor (EGFR) autophosphorylation and occludin dephosphorylation, leading to the reorganization of occludin within TJs and a consequent increase in paracellular permeability (Raimondi et al., 2008). Additionally, CDCA contributes to pro-inflammatory responses by stimulating the release of IL-8 and reactive oxygen species (ROS), as well as amplifying the effects of TNF-α and IL-1β on interferon-γ (IFN-γ) production (Sarathy et al., 2017). Ursodeoxycholic Acid (UDCA) has been shown to reduce the production of inflammatory cytokines by participating in the BA receptor Farnesoid X Receptor (FXR), while inhibiting NF-κB activation in macrophages (Pi et al., 2023). BAs metabolites were found to be excessive in the feces of Primary Sclerosing Cholangitis (PCD) patients and PCD mice, and SBAs [DCA, LCA and Hyodeoxycholic Acid (HDCA)] were found to be associated with the onset of diarrhea. These SBAs shortened the gastrointestinal transit time by 0.6-fold, increased the fecal water content by 1.3-fold and stimulated 5-HT levels *in vitro* and *in vivo* (Xu Y. et al., 2023). However, blocking BAs conjugated Takeda G protein-coupled receptor 5/Transient Receptor Potential Ankyrin 1 (TGR5/TRPA1) receptors significantly alleviated PCD GM-induced diarrhea. The present study demonstrates that GM and BA metabolism play a role in diarrhea. These results offer promising biomarkers for diagnosing and treating diarrhea and lay the groundwork for further investigation.

Branched chain amino acids (BCAAs), which include leucine (Leu), isoleucine (Ile), and valine (Val), are essential amino acids for the human body (Peng et al., 2020). These amino acids exert direct or indirect effects on diverse physiological functions, including energy metabolism, protein synthesis, and immune responses (Ma et al., 2018; Stipanuk, 2007). Similarly, BCAAs function as modulators that promote intestinal development and enhance gut health (Ren et al., 2016; Ren et al., 2015). Currently, the majority of research has concentrated on the function of Leu, with less attention paid to Val and Ile in the gut. Leu can maintain intestinal health by enhancing TJ in fish (Jiang et al., 2015). Additionally, it has been shown to improve intestinal epithelial cell proliferation, increase villus height, and promote growth in the small intestine of pigs. However, intestinal growth was inhibited when Leu levels were as high as 2.57% (Ren et al., 2015). Dietary Ile improves intestinal immune function and microbial population, and regulates gene expression of antioxidant enzymes, TJ, Nuclear factor erythroid 2-related factor 2 (Nrf2), Kelch-like ECH-associated protein 1 (Keap1), p38, and Extracellular Signal-regulated Kinase 1 (ERK1) in the intestine of Jian carp (Zhao et al., 2014). Additionally, BCAAs have been significantly linked to

diarrhea; a decreasing trend in BCAA levels was observed in both the functional diarrhea group and the IBS-D group (James et al., 2023). Rotavirus infection induces diarrhea in weaned pigs via systemic protein metabolic disorders and jejunal mucosal dysfunction. However, dietary supplementation with 1% leucine alleviated rotavirus-induced diarrhea in weaned pigs, potentially due to leucine's roles in enhancing protein metabolism, improving intestinal digestive and absorptive capacities, and reinforcing the non-specific barrier function of the intestinal mucosa (Mao et al., 2015). Furthermore, L-isoleucine supplementation has been found to significantly reduce stool output and fluid intake in children suffering from non-cholera acute watery diarrhea (Alam et al., 2011). More recently, a study demonstrated that supplementation with Ile increased the relative abundance of *Prevotella* and decreased the relative abundance of Rikenellaceae in the colon of diarrhea piglets infected with rotavirus, increased the secretion of interleukin-4 (IL-4), IL-10, and Secretory Immunoglobulin A (sIgA), and increased the expression of Claudin-3, Occludin, ZO-1 and mucin 1 (MUC-1), improved the immunity, colon barrier function and colon GM of piglets with diarrhea (Jiang C. et al., 2024; Jiang C. Y. et al., 2024). Nevertheless, the existing literature displays a striking imbalance toward Leu, leaving the mechanisms and efficacy of Val and Ile underexplored. Future studies should thus prioritize elucidating the individualized and synergistic contributions of all three BCAAs—particularly Val and Ile—ac different physiological and pathological contexts, to enable more precise and effective nutritional strategies for intestinal health.

2.3 Effect on intestinal barrier function

The intestinal barrier is a complex physiological structure that serves as a physical, biological, chemical, and immunological barrier. It interacts with the external environment and regulates host health (Zhou et al., 2024). The intestinal barrier, being semi-permeable, serves a dual function: it safeguards the internal milieu against the potential translocation of pathological molecules and microorganisms, while facilitating the absorption of nutrients and water (Martini et al., 2017). However, in pathological conditions, the integrity of the intestinal barrier can be compromised, leading to many local and systemic diseases (Aleman et al., 2023; Wang et al., 2022). TJs serve as a crucial form of connection between intestinal epithelial cells.

The proteins ZO-1 and occludin are key structural components of TJs. They are essential for maintaining cellular morphology and TJ structural integrity, and are widely used as indicators for assessing intestinal barrier function (Al-Sadi et al., 2011; Haas et al., 2022). Mucins are the primary glycoproteins that constitute the intestinal mucosal barrier. Among them, Mucin 2 (MUC2) is the most secreted mucin in the gastrointestinal tract and maintains the integrity of the mucus barrier, which is closely related to GM homeostasis (Liu et al., 2023; Yao et al., 2021). Tropini et al. demonstrated that diarrhea is closely related to the GM and the intestinal mucus barrier (Tropini et al., 2018). Diarrhea significantly disrupts the GM and is associated with thinning or loss of the intestinal mucus layer. This effect may be linked to dysregulated expression of the tight junction proteins ZO-1 and occludin, which compromises intestinal barrier integrity and increases permeability (Chen H. R. et al., 2024; Tropini et al., 2018).

Impaired intestinal mucosal barrier function serves as the primary pathological basis for the development of IBS-D (Shi et al., 2023). Upon the onset of IBS-D, patients exhibit a significant reduction in the expression of occludin, ZO-1, and other epithelial tight junction proteins, resulting in compromised intestinal epithelial barrier integrity and elevated intestinal permeability (Guo et al., 2023; Wang L. et al., 2023). Recent studies have found that *Lactobacillus* promotes occludin and ZO-1 expression and improves diarrheal symptoms (Hou et al., 2020). Related studies have further demonstrated that in diarrheic piglets infected with *E. coli*, increased abundances of *Lactobacillus* and *Cyanobacterium* are associated with reduced intestinal permeability and enhanced barrier repair, with *Lactobacillus* showing a particularly strong correlation with key intestinal barrier markers (Luo et al., 2022). Xu et al. found that MUC2 is a crucial protein in the prevention and treatment of rotavirus infections and diarrhea. It functions by safeguarding the epithelial barrier and enhancing intestinal permeability resistance (Xu et al., 2016). Wang et al. further observed that elevated MUC2 content in the ileum of diarrheal rats enhances intestinal barrier defense and confers intestinal protection (Wang et al., 2019). Furthermore, MUC2 concentration was significantly lower in AAD mice than in normal mice. A significant negative correlation was also identified between MUC2 and two gut microbial taxa, *Prevotellaceae_NK3B31_group* and *Rothia* (Li C. et al., 2023; Li X. T. et al., 2023). Collectively, these findings demonstrate a close association between diarrhea development, GM composition, and intestinal barrier function.

2.4 Effects on intestinal immune function

The GM intricately interacts with the host immune system. The crosstalk between the GM and enterocytes plays a crucial role in shaping the intestinal environment, thereby profoundly influencing intestinal immune homeostasis (Hold, 2016). Different types of diarrhea induce alterations in GM composition, which in turn modulates the expression of inflammatory factors. For example, in patients with diarrhea-predominant IBS-D, levels of IL-8 and TNF-α are elevated, while IL-10 is reduced; in mice with AAD, GM dysbiosis is observed, characterized by a marked increase in Proteobacteria and decreases in Bacteroidetes and Firmicutes, accompanied by upregulated IL-1 and IL-6 levels (Chen et al., 2022; Zhen et al., 2015; Zhu et al., 2022). It was observed that *E. coli* O_1 caused diarrhea in calves with disturbances in the GM and an increased abundance of Proteobacteria and Clostridiales. This condition was accompanied by a decreased expression of $CD4^+$ T and an elevated expression of Cluster of Differentiation 8 Positive T Lymphocyte ($CD8^+$ T) and CD11c-positive T lymphocyte ($CD11c^+$ T) in the ileum. Additionally, there were reduced serum levels of IgA and Immunoglobulin G (IgG), alongside heightened levels of IL-6 and TNF-α (Chen H. et al., 2023). T helper cell 17 (Th17) contribute to the maintenance of host intestinal immune homeostasis through interleukin-17A (IL-17A)-induced expression of the epithelial polymeric immunoglobulin receptor (Cao et al., 2012). In colonic tissues of IBS-D mice, the Th17/Tregs ratio was found to be significantly altered, characterized by reduced Tregs and $IL\text{-}10^+Foxp3^+T$ cells alongside increased Th17 cells. Correlation analysis further revealed positive associations between *Ruminococcus_gnavus* with the Th17/Tregs ratio (Zhang M. M. et al., 2024; Zhang Y. et al., 2024; Zhang Z. et al., 2024).

It is thus clear that GM plays an important role in regulating intestinal immune homeostasis during diarrhea.

2.5 Effects on BGMA

In recent years, this concept has expanded to include BGMA, prompted by the growing recognition of the gut microbiota's critical role in human health and disease (Lee et al., 2023). The BGMA acts as a bidirectional communication pathway between the central nervous system (CNS) and the gastrointestinal tract. It mediates interactions involving the CNS, enteric nervous system (ENS), neuroendocrine system, and immune system, with signals being transmitted either directly or indirectly between the CNS and ENS (Arneth, 2018; Grenham et al., 2011; Morais et al., 2021).

Notably, microbial metabolic activity profoundly shapes brain–gut signaling. For example, disruptions in tryptophan metabolism impact the synthesis of serotonin (5-HT), a key intermediate, which can activate brain–gut neural circuits and precipitate diarrheal responses (Morais et al., 2021; Spencer and Hu, 2020). Furthermore, central processes modulate gut function via the hypothalamic–pituitary–adrenal (HPA) axis: psychological stress triggers cortisol release, altering intestinal permeability and compounding gut dysfunction (Chen H. et al., 2023; Chen X. et al., 2023; Chen J. et al., 2023; Morais et al., 2021). Evidence underscores a robust association between functional diarrhea and impairment of the BGMA. Notably higher rates of this condition occur in patients with mental disorders, with GM-CNS crosstalk serving as a potential mediator of this comorbidity (Zhang et al., 2021). The pathogenesis of IBS-D involves multifaceted interactions among brain–gut peptides, immune activation, and microbial composition (Li et al., 2020). For instance, Gao et al. demonstrated that dampening HPA axis activity via CRHR1 downregulation alleviates diarrheal symptoms in IBS models, underscoring the therapeutic relevance of BGMA modulation (Gao et al., 2023). Wu et al. provided further mechanistic insight, identifying correlations between specific microbial genera and neuro-immune markers in IBS-D rats. The genus *Paraprevotella* was positively associated with elevated 5-HT, CRF, and NPY, suggesting its potential role in modulating the HPA axis via serotonergic pathways (Wu et al., 2022). Additionally, microbial metabolites such as SCFAs and 5-HT are implicated in bidirectional BGMA communication, and their aberrant levels have been consistently reported in IBS-D patients (Dinan and Cryan, 2017; Luo et al., 2021). Interventions including probiotic supplementation have shown promise in reducing 5-HT levels and ameliorating IBS-D symptoms, highlighting the translational potential of targeting microbial components (Gu et al., 2022; Wu et al., 2024). Another compelling example comes from Chen et al. reported that alkaline mineral complex (AMC) water improved diarrhea resistance in stressed piglets by rebalancing the HPA axis and enriching beneficial bacteria such as *Lactobacillus helveticus* and *Ruminococcus gnavus*. This reinforces the notion that BGMA-oriented interventions can restore gut homeostasis through multifactorial mechanisms (Chen H. et al., 2023; Chen X. et al., 2023; Chen J. et al., 2023).

Overall, research on the BGMA provides critical insights into the mechanisms underlying diarrhea and reveals promising therapeutic potential. Current evidence suggests that targeting the BGMA—through modulation of microbial metabolites, neuroendocrine pathways, and immune signaling—may alleviate both intestinal and psychiatric symptoms. However, most studies to date remain correlative or reliant on animal models, highlighting a need for causal validation and clinical translation. Future work should integrate multi-omics approaches to elucidate precise molecular targets within the BGMA, ultimately facilitating the development of personalized therapies and bridging the gap between mechanistic discovery and clinical application.

In summary, the occurrence of diarrhea can alter the composition of the gut microbiota and the levels of its metabolites, regulate immune function, affect the gut-brain axis, and impair intestinal barrier integrity. The potential mechanisms mediating these effects are illustrated in Figure 1.

3 Impact of interventions targeting GM on diarrhea

3.1 Probiotic interventions

Probiotics are defined as beneficial, viable microorganisms, and a growing body of evidence has shown that numerous probiotic strains alleviate diarrhea by modulating the GM (Wieërs et al., 2019), regulation of inflammatory factor production (Wang F. et al., 2023), and enhancement of the intestinal mucosal barrier function (Camilleri, 2021; Su et al., 2022).

Lactobacillus and *Bifidobacterium* are widely employed as probiotics in the treatment of diarrhea, owing to their crucial functions in alleviating inflammation and promoting the balance of the intestinal microbiota. Lactoferricin produced by *Lactobacillus reuteri* CO21 was found to be able to modulate the intestinal physical barrier function by inhibiting the TLR4, Myd88 and Myosin light-chain kinase (MLCK) pathways and up-regulating the expression of the TJ proteins ZO-1 and claudin-2, thereby increasing piglets' resistance to Enterotoxigenic *E. coli* and alleviating diarrhea (Xie et al., 2021). *Lactobacillus* and *Saccharomyces boulardii* have also shown effectiveness in the prevention or treatment of AAD (Doar and Samuthiram, 2023; Yang Y. et al., 2023; Yang Q. et al., 2023). *Saccharomyces boulardii* alleviates GM disorders and improves intestinal barrier function (Bustos Fernández et al., 2023). *Saccharomyces boulardii* mitigates mucosal injury by modulating intestinal mucin composition and secretion, strengthening the mucin barrier, and reducing SN-38 penetration into epithelial cells (Sezer et al., 2009).

In conclusion, probiotics exert beneficial effects on both the prevention and treatment of diarrhea, with such effects being strain-and dose-dependent. Thus, further studies are required to identify and optimize the selection and application of probiotics for managing different types of diarrhea.

3.1.1 Basic experiments

During animal development, exposure to various pathogenic bacteria and toxic compounds often leads to intestinal barrier dysfunction, thereby contributing to the onset of diarrhea and impaired growth (Kovanda et al., 2023; Satitsri et al., 2016). However, probiotics can modulate intestinal barrier function, alleviate intestinal injury, and mitigate diarrhea.

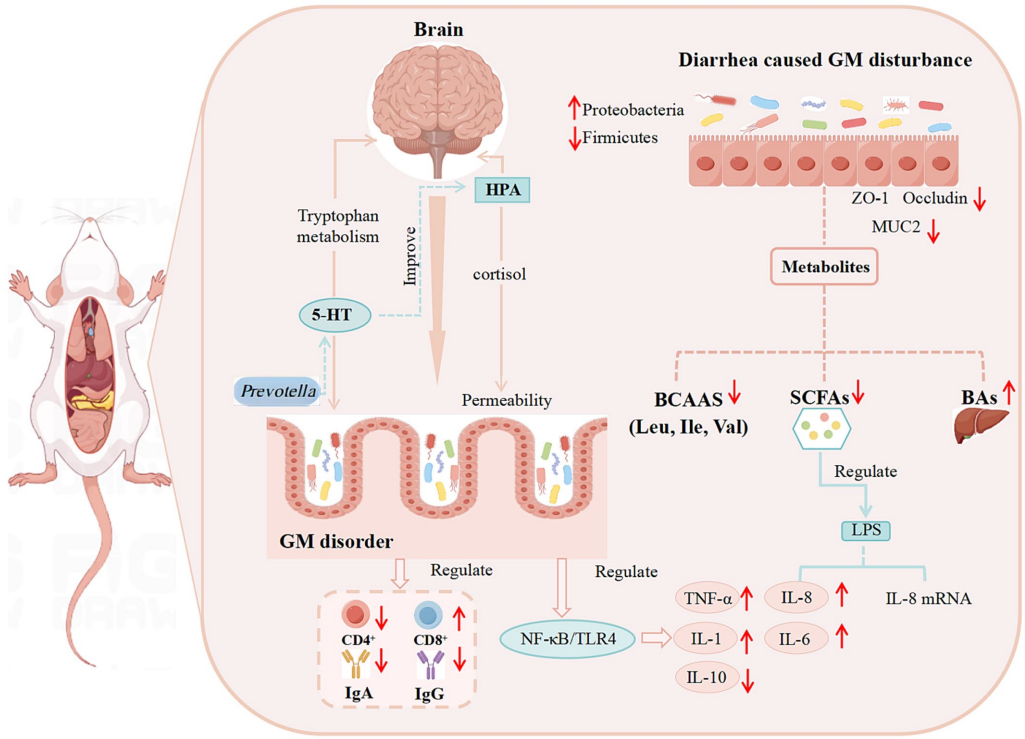

FIGURE 1
The potential mechanism of diarrhea development. (The relationship between diarrhea and GM, GM metabolites, the immune system, the intestinal barrier, and BGMA).

ETEC is a major pathogen of animal diarrhea (Xu C. et al., 2023; Xu Y. et al., 2023; Xu H. et al., 2023), which disrupts the intestinal epithelial barrier through adhesins and enterotoxins (Zhu et al., 2018). It has been found that *Lactobacillus plantarum* ZLP001 has antimicrobial activity, which prevents ETEC growth by producing certain antimicrobial substances and generating a relatively acidic environment (Wang et al., 2018b). Treatment with *L. plantarum* ZLP001 alleviated ETEC-induced intestinal damage by preserving the expression of TJ proteins (claudin-1, occludin, ZO-1), downregulating pro-inflammatory cytokines (IL-6, IL-8, TNF-α), and strengthening the intestinal barrier via enhancing epithelial defense and modulating the GM (Wang et al., 2018a). AAD triggered by GM dysbiosis post-antibiotic therapy, poses serious threat to human and animal health. However, *Lactobacillus plantarum* H-6 was found to modulate the colonic microbial composition in mice by increasing the abundance of *Lactobacillus* and *Akkermansia*, decreasing that of *Bacteroides*, downregulating the expression of pro-inflammatory factors (e.g., IL-1β, IL-6), and elevating the levels of L-tryptophan and LysoPC. These changes improve serum metabolism, thereby alleviating AAD (Yan et al., 2023). In addition, *Akkermansia muciniphila* was able to reduce the relative abundance of *Citrobacter* at the genus level, inhibit intestinal inflammation by up-regulating the expression of G protein-Coupled Receptor 109A (GPR109A) and Solute Carrier family 5 member 8 (SLC5A8) and down-regulating the expression of TNF-α, IFN-γ, IL-1β, and IL-6, and at the same time improve the down-regulation of ZO-1, Occludin, Claudin-4 (CLDN4), and Muc2 in AAD model mice, restore the intestinal barrier function and optimize intestinal health to prevent AAD (S. Liu et al., 2024). *Saccharomyces boulardii* can upregulate Serotonin Transporter (SERT) through activation of epidermal growth factor receptor and modulate GM to inhibit gut motility to alleviate IBS-D symptoms (Gu et al., 2022). The efficacy of other probiotics in modulating the GM for diarrhea treatment is summarized in Table 2, while the potential mechanisms underlying probiotic-mediated diarrhea management are illustrated in Figure 2.

3.1.2 Clinical experiments

Clinical studies have extensively documented the efficacy of probiotics in managing diarrhea. *Bifidobacterium bifidum* G9-1 was reported to reduce serum pro-inflammatory cytokine (Monocyte Chemoattractant Protein-1, IL-8 and Macrophage Inflammatory Protein-1β) levels and increase the abundance of *Bifidobacterium*, alleviating diarrhea in IBS-D patients (Tomita et al., 2023). Similarly, longum ES1 significantly lowered serum IL-6 and TNF-α levels in IBS-D patients compared to baseline (Caviglia et al., 2020). *Clostridium butyricum* ameliorated diarrhea in IBS-D patients by decreasing stool frequency and modulating GM composition (Sun et al., 2018). *Lactobacillus plantarum* LRCC5310 improved diarrhea and Vesikari scores in rotavirus-infected children while suppressing viral proliferation (Shin et al., 2020). *Alkalihalobacillus clausii 088AE* exerts a therapeutic effect on diarrhea in children, adolescents, and adults. Specifically, in the treatment of AAD, it has been demonstrated to be safe and effective in reducing diarrhea episodes and alleviating associated severe symptoms, such as abdominal discomfort, pain, bloating, and flatulence (Maity and Gupta, 2021). However, supplementation with *Bifidobacterium breve* BB05 can partially restore the disrupted GM at both the phylum and genus levels, notably by

TABLE 2 Basic studies on the potential mechanisms of probiotics against diarrhea.

Types of probiotics	Type of diarrhea	Effect on GM	Relief or treatment of symptoms	Reference
Lactobacillus reuteri DSM 17938	*E. coli*-induced diarrhea	Unclassified_Lachnospiraceae and *Anaerostipes* increased, *Escherichia_Shigella* decreased.	Restored the expression of inflammatory factors (IL-6, IL-10, TNF-α, and IFN-γ), reduced the colon inflammatory damage, maintained the integrity of the intestinal barrier, and regulated the composition of GM to alleviate diarrhea.	Wang D. et al. (2024)
Lactobacillus paracasei	Diarrhea caused by *E. coli* O8	Lactobacillus increased, Enterobacter decreased.	Elevated the TJ protein levels and downregulated proinflammatory cytokines IL-6, IL-1β, TNF-α, and p65, Myosin Regulatory Light Chain (MLC2), MLCK.	Ren et al. (2022)
Lactobacillus plantarum CCFM1143	Diarrhea caused by ETEC	*Odoribacter*, *Bifidobacterium*, *Allobaculum* and *Pediococcus* increased, *Blautia* and *Pseudomonas* decreased.	Reduced TNF-α, IFN-γ and IL-6 as well as jejunal damage, rebalanced the GM and modulated the production of SCFAs.	Yue et al. (2020)
Lactobacillus reuteri HCM2	Diarrhea caused by ETEC	*Lactobacillus* increased, Enterobacteriaceae decreased.	Inhibited the growth of ETEC, prevented ETEC infection-induced dysbiosis by stabilizing the relative abundance of the dominant bacteria.	Wang T. et al. (2018)
Lactobacillus	AAD	Muribaculaceae, *Bacteroides*, *Bifidobacterium*, *Lactobacillus* and *Akkermansia* increased, *Klebsiella*, *Parabacteroides*, and Clostridia_vadinBB60_group decreased.	Regulated the microbiota-SCFAs signaling cascade, improved SCFAs levels, inhibited the activation of the TLR4/NF-κB pathway, relieved the intestinal inflammation in AAD.	Xu et al. (2024)
Limosilactobacillus fermentum N-30	Diarrhea caused by rotavirus	Firmicutes increased, Bacteroidota and Proteobacteria decreased.	Improve diarrhea symptoms caused by rotavirus infection.	Murtaza et al. (2024)
Bifidobacterium. bifidum FSDJN7O5	Diarrhea caused by ETEC	*Bifidobacterium* and *Lactobacillus* increased, Escherichia–Shigella decreased.	Reduced the water content of the feces, restored the villi structure in the jejunum, and improved the content of SCFAs in the feces.	. Yang et al. (2021a)
Bifidobacterium bifidum G9-1	Phytohemagglutinin-induced diarrhea	Rikenellaceae decreased.	Inhibited the excessive proliferation of *E. coli*, restored the length of jejunum villi and relieved diarrhea symptoms.	Makizaki et al. (2019)
Bifidobacterium animalis subsp. *lactis* XLTG11	AAD	Muribaculaceae, *Bacteroides*, *Bifidobacterium*, *Lactobacillus* and *Akkermansia* increased, *Klebsiella*, *Parabacteroides* and Clostridia_vadinBB60_group decreased.	Increased the expression of TJ protein, inhibited the activation of TLR4/NF-κB signaling pathway, increased the level of anti-inflammatory cytokines, decreased the level of pro-inflammatory cytokines, increased the production of SCFAs, and decreased the permeability of the intestine.	Xu B. et al. (2022)
Bacteroides uniformis FGDLZ48B1 *and Bifidobacterium adolescentis* FHNFQ48M5	AAD	Restoring the diversity of GM.	Decreased IL-6 levels, restored occludin expression in the colon, increased Mucin-2 expression, and increased concentrations of acetic acid, propionic acid, isobutyric acid, and isovaleric acid in the cecum.	Guo et al. (2021)

(Continued)

10.3389/fmicb.2025.1630823

TABLE 2 (Continued)

Types of probiotics	Type of diarrhea	Effect on GM	Relief or treatment of symptoms	Reference
Weizmannia coagulans WC10	AAD	*Bifidobacterium* and *Roseburia* increased.	Decreased diarrhea status score and fecal water content. Decreased the levels of serum enterotoxin and Diamine Oxidase (DAO), increased the expression of intestinal mucosal immune factors sIgA and occludin, decreased the expression of pro-inflammatory cytokines.	Wang Z. et al. (2024)
Pediococcus pentosaceus Li05	IBS-D	*Alloprevotella*, *Anaerotruncus* and *Mucispirillum* increased. [*Ruminococcus*] *gauvreauii*, *Dubosiella*, *Erysipelatoclostridium* and *Blautia* decreased.	It ameliorated intestinal and systemic inflammation by decreasing the levels of chemokines and pro-inflammatory cytokines. Regulated on Activation, Normal T cell Expressed and Secreted (RANTES), IL-1β, IL-7, and IL-18, and effectively reduced the expression of intestinal 5-Hydroy-tryptamine 3B (5-HT3B) receptor, regulated excessive intestinal motility and secretion in patients with IBS-D.	Wu et al. (2024)
Lactiplantibacillus plantarum ELF051	AAD	*Oscillospira* and *Prevotella* increased, *Allobaculum*, *Desulfovibrio* and *Akkermansia* decreasd.	Improved the pathological changes of colon tissue, down-regulated IL-1β and TNF-α, up-regulated IL-10, increased the level of intestinal SCFAs, and regulated TLR4/MyD88/NF-κB and PI3K/AKT/NF-κB signaling pathways, thereby reducing inflammation.	Liang et al. (2023)
Lactiplantibacillus plantarum 2-33	AAD	*Lactobacillus* increased, *Enterococcus* and *Bacillus* decreased.	Increased the levels of anti-inflammatory cytokines IL-4 and IL-10, reduced the levels of proinflammatory cytokines TNF-α and IFN-γ, and also adjusted carbohydrate metabolism, amino acid metabolism, restored energy metabolism to normal level, accelerated the recovery of intestinal bacterial structure in AAD mice, alleviated AAD.	Bao et al. (2022)

10.3389/fmicb.2025.1630823

elevating the abundances of *Bifidobacterium* and *Roseburia*. In the probiotic-supplemented group, fecal 5-HT concentration was increased, whereas levels of acetylcholine, epinephrine, and norepinephrine were reduced—suggesting that *Bifidobacterium breve* BB05 may alleviate anxiety and diarrhea by BGMA (Wang Y. et al., 2024).

Most existing literature has only summarized the therapeutic effects of probiotics on clinical diarrhea (focusing on diarrhea alleviation) and their safety profiles in patients, with relatively few studies investigating their specific efficacy and underlying mechanisms of action. Supplementary details regarding the clinical application of probiotics for diarrhea treatment and their corresponding mechanisms are provided in Table 3, while the potential mechanisms through which probiotics may exert anti-diarrheal effects in clinical settings are illustrated in Figure 3.

3.2 FMT

FMT is a procedure that involves transferring GM from healthy donors into the gastrointestinal tract of patients to restore a balanced microbial community and treat diseases, particularly those associated with gut dysbiosis such as diarrhea (Almeida et al., 2022; Li et al., 2022).

The therapeutic efficacy of FMT in diarrhea alleviation is closely linked to the modulation of GM composition. On one hand, FMT reintroduces a healthy microbial community that competes for ecological niches in the gastrointestinal tract, thereby suppressing pathogen colonization-this process further facilitates the restoration of immune function and mitigates host tissue damage. On the other hand, FMT aids in replenishing essential metabolites for host metabolism, such as SCFAs, antimicrobial peptides, bacteriocins, and BAs (Ademe, 2020). IBS-D is a common gastrointestinal disorder and is characterized by altered GM, especially involving Firmicutes and Bacteroidetes (Mei et al., 2021; Zhen et al., 2021). However, FMT can reduce intestinal permeability and alleviate the diarrheal effects of IBS-D by modulating GM disorders and affecting GM-produced metabolites such as increasing the production of SCFAs (Lin et al., 2021; Singh et al., 2022; Song et al., 2023). *Clostridium difficile* infection (CDI) is considered a common cause of AAD (Bosnjak et al., 2023; Tubau-Juni et al., 2023). One study demonstrated that FMT administration to children with recurrent CDI enhanced GM diversity while driving shifts in GM composition and function toward those of the donor (Fareed et al., 2018). During the weaning transition, piglets are prone to diarrhea, which is related to the damaged state of the microbiome and immature immune system (Han et al., 2024). In diarrheal piglets infected with *E. coli* K88, the application of FMT increased the number of beneficial bacteria in the gut and reduced the number of harmful bacteria, and further research found that FMT triggered intestinal mucosal autophagy and reduced the damage of *E. coli* K88 to the intestinal barrier (Cheng et al., 2018).

Currently, research on the underlying mechanisms of FMT remains limited. Available evidence suggests that alterations in the GM following FMT play a significant role in the pathogenesis of diarrhea. However, several studies indicate that the therapeutic efficacy of FMT may be constrained. Additionally, to date, FMT has

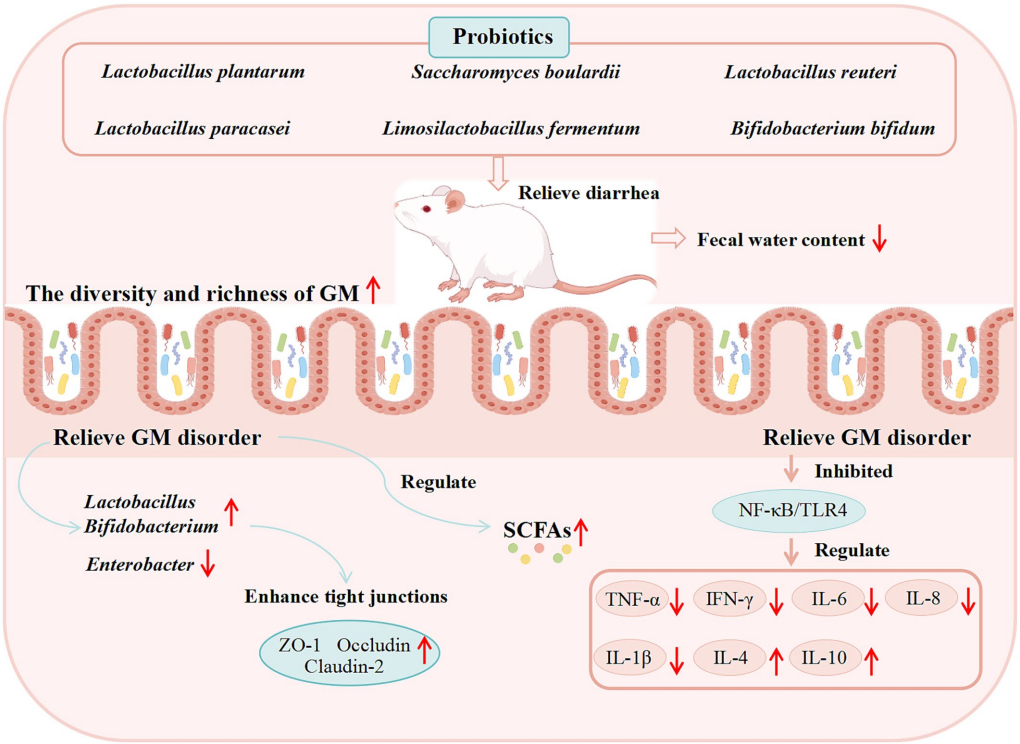

FIGURE 2
Proposed mechanisms of action of probiotics against diarrhea derived from basic studies. (These potential mechanisms mainly involve the GM, SCFAs, the immune system, and intestinal barrier function).

TABLE 3 Clinical studies on the potential mechanisms of probiotics against diarrhea.

Types of Probiotics	Type of diarrhea	Effect on GM	Relief or treatment of symptoms	Reference
Combined *B. infantis, L. acidophilus, E. faecalis,* and *B. cereus* tablets	Chemotherapy-induced diarrhea in patients with rectal cancer	*Streptococcus*, *Blautia* and *Bifidobacterium* increased.	Alleviated chemotherapy-induced diarrhea in Colorectal Cancer (CRC) patients by modulating the GM and promoting SCFA production.	Huang et al. (2023)
Lactobacillus plantarum CCFM1143	Chronic Diarrhea	*Akkermansia*, *Anaerostipes*, *Terrisporobacter*, *Escherichia*, and *Shigella* increased, *Bacteroides*, *Eggerthella*, *Lachnoclostridium*, and *Lachnospira* decreased.	Reduced the clinical symptoms of chronic diarrhea. In addition, it inhibited the elevation of IL-6 and the reduction of motilin; and regulated the production of SCFAs.	Yang et al. (2021b)
Lacticaseibacillus paracasei Zhang, *Lactiplantibacillus plantarum* p-8, and *Bifidobacterium animalis* subsp. *lactis* V9	Chronic diarrhea	*Dysosmobacter welbionis* and *Faecalibacterium prausnitzii* increased, *Megamonas funiformis* decreased.	Alleviated diarrhea by modulating the tryptophan-5-hydroxytryptophan and tryptophan-kynurenine pathways, and improved the patients' Bristol Stool Scale scores, frequency of defecation, and urgency to defecate.	Guo et al. (2024)
Lactiplantibacillus plantarum CJLP243	Functional diarrhea	*Leuconostoc* increased.	Improved diarrhea symptoms.	Jung M. et al. (2022)
Lacticaseibacillus rhamnosus LRa05	AAD	*Faecalibacterium*, *Lachnospira*, *Parabacteroides*, *Phascolarctobacterium*, *Fusicatenibacter*, *Alistipes*, *Coprococcus*, *Oscillibacter*, *Parasutterella*, and *Megamonas* increased.	Relieved adverse symptoms, regulated the inflammatory response.	Niu et al. (2024)
Lactiplantibacillus plantarum APsulloc 331261	IBS-D	Firmicutes increased, Bacteroidetes decreased.	Reduced the severity and frequency of abdominal pain, bloating, and feeling of incomplete evacuation.	Jung K. et al. (2022)
Bifidobacterium animalis subsp. *lactis* BLa80	Acute diarrhea in children	*Bifidobacterium breve* and *Lactobacillus murinus* increased, *Bifidobacterium longum* decreased.	Reduced duration of diarrhea, accelerated improvement in stool consistency and alteration of the gut microbiome.	Chen K. et al. (2024)

been predominantly investigated for the treatment of CDI and diarrhea-predominant IBS-D, while its efficacy in diarrhea of other etiologies remains less established. Thus, further clinical trials are warranted to validate the potential benefits of FMT across diverse forms of diarrhea and to better define its role in managing diarrhea-related disorders. It is also important to note that the limited efficacy of FMT in some cases of diarrhea may be attributable to insufficient donor-recipient matching, among other factors, highlighting the need for more personalized approaches in future studies.

3.2.1 Basic experiment

Diarrhea in animals, triggered by multiple etiologies, is highly prevalent and remains a major challenge afflicting the animal husbandry industry. To address this issue, FMT-an emerging therapeutic technology-has been increasingly applied to the treatment of animal diarrhea in recent years.

Advances in modern genetics and enhanced sow reproductive performance have facilitated the widespread implementation of artificial lactation systems in commercial swine production. However, these systems are linked to a high incidence of diarrhea in piglets. To tackle this challenge, researchers have utilized FMT as a therapeutic strategy to alleviate diarrhea induced by artificial feeding. Results demonstrated that FMT modulates the composition of colonic microbiota and its metabolites, promotes tryptophan metabolism and 5-hydroxyindoleacetic acid (5-HIAA) production, enhances intestinal mucosal barrier function, inhibits the activation of the Jun N-terminal kinase (JNK) pathway and the expression of matrix metalloproteinases (MMPs), reduces the secretion of proinflammatory cytokines and

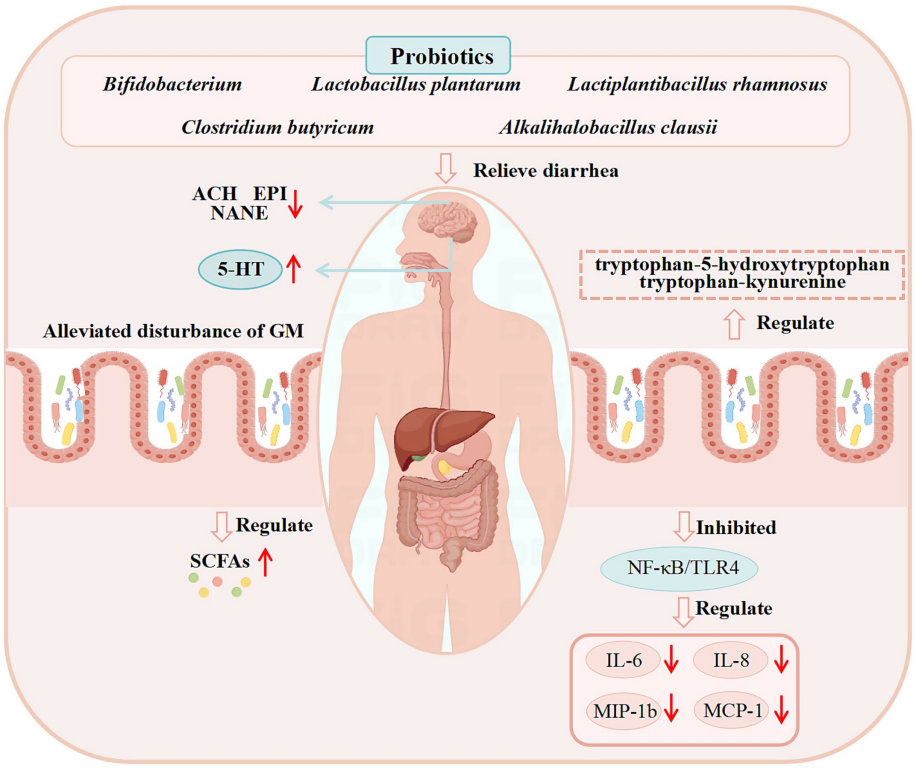

FIGURE 3
Demonstrated mechanisms of probiotics against diarrhea from clinical studies. (These potential mechanisms mainly involve GM, SCFAs, the immune system, and BGMA).

chemokines, and ultimately alleviates artificial feeding-induced diarrhea in piglets (Han, 2023). Bovine viral diarrhea virus (BVDV) is widespread throughout the world and has caused significant economic losses to animal husbandry (Pang et al., 2023). BVDV infection significantly decreased the diversity and changed the composition of GM in mice. However, after FMT, BVDV RNA and protein levels in duodenum, jejunum, spleen and liver were significantly inhibited, Interferon-α (IFN-α) and Interferon-β (IFN-β) mRNA levels were increased, and Interferon Regulatory Factor 1 (IRF1) and Interferon Regulatory Factor 7 (IRF7) mRNA levels were increased. The expression of Toll-Like Receptor 7 (TLR7) and Toll-Like Receptor 9 (TLR9) was restored, the proportion of Cluster of Differentiation 3 (CD3) and CD8 T cells was restored, the expression of ZO-1 protein was increased, and the proliferation of Peripheral Blood Leukocytes (PBL) was restored (Zhang Z. et al., 2024). FMT significantly alleviates symptoms of IBS-D, potentially through modulating the 5-HT signaling pathway within the BGMA. It was found that after FMT, the mental condition of IBS-D mice was improved, the diarrhea was improved, and the fecal water content was significantly reduced. Additionally, the expression levels of 5-HT and SP in brain tissue and serum were significantly decreased, the expression levels of SERT and 5-Hydroxytyryptamine Receptor 4 (5-HT4R) proteins in colon and brain tissues were increased, and the expression levels of Tryptophan Hydroxylase 1 (THP1) and (5-Hydroxytyryptamine Receptor 3) 5-HT3R proteins were significantly reduced (Ouyang et al., 2022).

Basic experimental data on the use of FMT for diarrhea treatment in other studies are presented in Table 4, while the potential mechanisms underlying FMT's therapeutic effects on diarrhea are illustrated in Figure 4.

3.2.2 Clinical experiments

FMT has emerged as a novel clinical strategy for treating diarrhea. As an intestinal microecological therapy with proven efficacy, FMT entails the transfer of GM from healthy donors to patients with diarrhea, which modulates GM composition, restores the intestinal mucosal immune barrier, and thereby exerts therapeutic effects.

CDI is the main cause of nosocomial infectious diarrhea and a high proportion of clinical cure rates have been achieved by restoring the GM with FMT in CDI therapy (Chen and Chiu, 2022; Roshan et al., 2020). Shao et al. found a significant increase in a diversity of GM in CDI patients after FMT, with GM composition more similar to that of healthy donors, increased the abundances of families Ruminococcaceae, Prevotellaceae, Coriobacteriaceae, Porphyromonadaceae, Bacteroidaceae, Bifidobacteriaceae, and Eubacteriaceae, and reduced the abundance of Enterobacteriaceae, Veillonellaceae, Enterococcaceae, and Peptostreptococcaceae (Wei et al., 2022). Clinically, FMT alleviates IBS-D symptoms and improves patients' quality of life by restoring a balanced GM (Fu and Huang, 2022). Studies have shown that GM and SCFAs in patients with IBS-D differ from those of donors at baseline, such as decreased levels of Actinobacteria and *Bifidobacterium* and increased levels of Bacteroidetes and Proteobacteria, however these differences gradually return to normal after 3 weeks after FMT, while patients also have improved symptoms and quality of life of IBS-D during the same period (Mazzawi et al., 2019). However, some studies have also shown

conflicting results. For example, studies in the treatment of IBS-D have shown that both FMT and placebo recipients showing improvements in irritable bowel syndrome-Severity Scoring System (IBS-SSS) and irritable bowel syndrome-Quality of Life (IBS-QOL) scores and reporting improvements in fecal morphology, however, no differences were found between the two groups (Aroniadis et al., 2019). Therefore, more research is needed to determine the efficacy of FMT for IBS-D.

Currently, FMT has shown expanding clinical applications across various diseases. However, clinical evidence supporting FMT for diarrhea remains limited, with existing studies reporting inconsistent therapeutic outcomes. Most available literature has documented improvements in clinical symptoms, FMT safety, and the efficacy and duration of single or multiple transplantation regimens in diarrhea patients, while studies investigating its specific mechanisms of action remain scarce. Additional information on FMT-induced symptomatic improvements and mechanisms in diarrhea treatment is presented in Table 5, and the potential mechanisms underlying FMT's clinical efficacy in diarrhea are illustrated in Figure 5.

3.3 Bacteriophage therapy

Bacteriophages, viruses that specifically infect and lyse bacteria, offer a promising therapeutic strategy by precisely targeting pathogenic bacteria while preserving the commensal GM (Chen H. et al., 2023; Chen X. et al., 2023; Chen J. et al., 2023; Strathdee et al., 2023).

Antibiotics have always been the cornerstone of treating diarrhea, but rising antimicrobial resistance (AMR) has diminished their efficacy (Baran et al., 2023). Moreover, antibiotics disrupt the commensal GM, leading to dysbiosis and increased susceptibility to recurrent infections (Ramirez et al., 2020). Phage therapy, which uses viruses to specifically infect and kill bacteria, has re-emerged as a promising alternative due to its specificity, self-replicating nature, and ability to disrupt biofilms (Duan et al., 2022).

Multiple *in vitro* studies have demonstrated the effectiveness of phage therapy for treating diarrheal pathogens. Research has shown that a phage cocktail targeting *E. coli*, such as a combination of six bacteriophages, can reduce bacterial load by 3 log CFU/mL in vitro

TABLE 4 Basic studies on the application of FMT technique in the treatment of diarrhea.

Type of diarrhea	Donor	Changes in microbiota	Relief or treatment of symptoms	Reference
Horse with diarrhea	Healthyage-matched control horses	Verrucomicrobia increased and Proteobacteria decreased.	Reduced the severity of diarrhea.	McKinney et al. (2020)
Foals with diarrhea	Healthy calves	Verrucomicrobiota and *Akkermansia* increased.	Alleviated the symptoms of weaning diarrhea in calves.	Bell et al. (2024)
Cynomolgus monkeys with diarrhea	Healthy human donors	Firmicutes and *Lactobacillus* increased, *Lactobacillus fermentum* and *Lactobacillus ruminis* CAG_367 increased.	Increased serum levels of IL-10 and decreased levels of IL-6, IL-8, IL-1β and IFN-γ in monkeys with chronic diarrhea.	Tian et al. (2022)
Calves suffering from intractable diarrhea	Healthy calves	*Lactobacillus*, Veillonellaceae, *Selenomonas*, *Acidaminococcus*, and *Collinsella* increased.	Increased the content of SCFAs (especially butyric acid) and medium-chain fatty acids (e.g., octanoic acid) after FMT treatment. Decreased the fecal content of most amino acids in successful recipients.	Islam et al. (2022)
Post-weaning diarrhea in piglets	Healthy Tibetan pigs	Firmicutes, Euryarchaeota, and Tenericutes increased, Proteobacteria and Melainabacteria decreased. *Lactobacillus* and *Methanobrevibacter* increased, *Campylobacter* decreased.	Reduced the incidence of diarrhea, which attenuated the reduction of CD4 T cells and CD4/CD8 ratio in peripheral blood. Down-regulation of mRNA expression of Toll-Like Receptor 2 (TLR2) and NF-κB.	Tang et al. (2020)
IBS-D rats	Healthy rat	Firmicutes and *Bacteroides* increased, Proteobacteria and *Prevotella* decreased.	Inhibited visceral hypersensitivity and regulated GM balance to relieve diarrhea.	Jiang C. Y. et al. (2024)
Oligofructose-induced diarrhea in horses	Healthy horse	Patescibacteria and Planctomycetota increased, Proteobacteria, Desulfobacterota, and Fusobacteriota decreased. *Streptococcus* and *Lactobacillus* decreased.	Decreased body temperature and diarrhea score, and increased fecal pH, decreased inflammatory responses such as increased serum Lipopolysaccharide (LPS), IL-17A, lactic acid and total protein.	Tuniyazi et al. (2024)

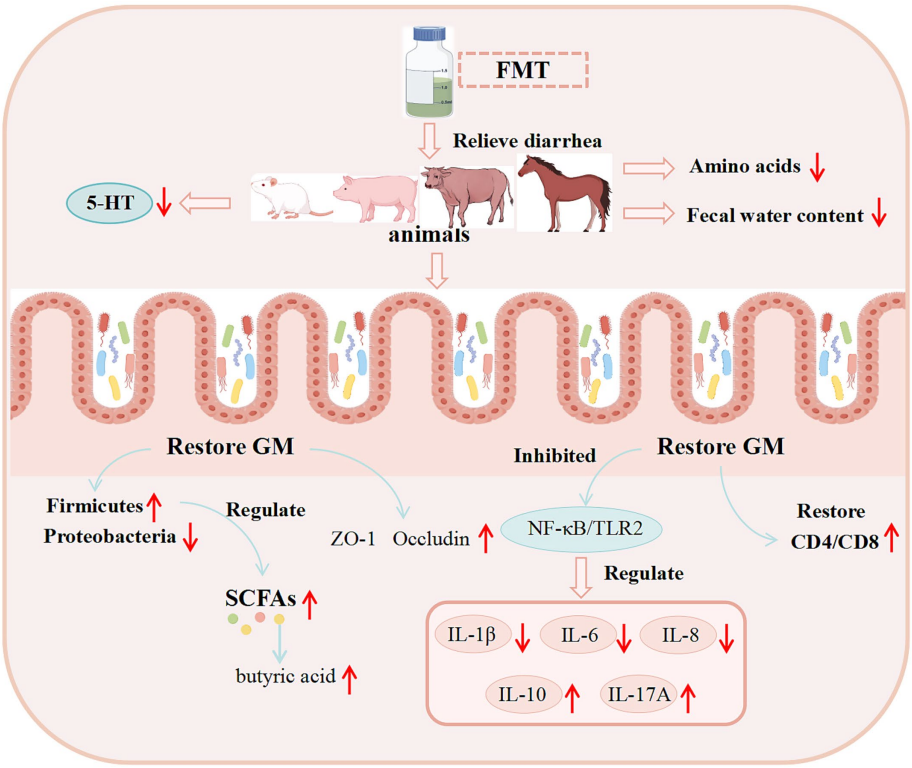

FIGURE 4
Potential mechanisms of FMT in treating diarrhea revealed by basic research. (These potential mechanisms mainly involve GM, SCFAs, the immune system, and intestinal barrier function).

and effectively inhibit biofilm formation (Youssef et al., 2025). In addition, a 2023 study utilized a resource library termed the gut phage isolate collection (GPIC)—composed of bacteriophages isolated from healthy human guts—to demonstrate that a bacteriophage cocktail targeting *Bacteroides fragilis* significantly reduced the abundance of the target bacteria in in vitro fecal cultures, highlighting the potential of bacteriophages in modulating the GM (Shen et al., 2023). In animal model studies, phage therapy has also shown promising effects. Research has shown that the microencapsulated bacteriophage A221 is as effective as the antibiotic florfenicol in treating piglet diarrhea models (Youssef et al., 2025). In addition, phage cocktail therapy targeting *Klebsiella pneumoniae* associated with inflammatory bowel disease can alleviate intestinal inflammation and tissue damage in mouse models (Fuerte-Stone and Mimee, 2022). These studies indicate that bacteriophages can not only effectively reduce the load of pathogenic bacteria, but also alleviate the inflammatory response and tissue damage caused by it.

In recent years, clinical trials of phage therapy for diarrhea have also made some progress. A phase 1 clinical trial in 2022 tested two bacteriophages targeting *Klebsiella pneumoniae* associated with inflammatory bowel disease on 18 healthy volunteers. The results showed that when taken together with antacids such as $CaCO_3$, the bacteriophages not only survived at high levels but also remained active throughout the gastrointestinal tract without affecting the resident GM. All participants did not experience any serious treatment-related adverse events, laying the foundation for further research in patients (Federici et al., 2022).

Although these studies indicate that bacteriophages have great potential in treating diarrhea, a critical translational challenge involves phage instability in the harsh gastrointestinal environment. Gastric acidity and digestive enzymes rapidly denature phage particles, compromising therapeutic efficacy. Advanced encapsulation strategies using electrospun fibers, liposomes, or pH-responsive hydrogels are being developed to shield phages during transit and ensure targeted colonic release (Yang Y. et al., 2023; Yang Q. et al., 2023). Additionally, the field must address the complexity of phage ecology, particularly the potential for temperate phages to facilitate horizontal gene transfer of virulence or resistance genes. Careful selection of obligately lytic phages is therefore essential for clinical safety and efficacy (Gummalla et al., 2023).

3.3.1 Basic experiment

Diarrhea is now a significant public health concern. Consequently, bacteriophage therapy has emerged as a promising therapeutic strategy. Phages modulate the composition and abundance of the GM, which in turn alters the expression of intestinal proteins and inflammatory factors, ultimately alleviating various forms of diarrhea.

The mechanism of action of bacteriophages against diarrhea is multifaceted. It begins with the specific lysis of bacterial pathogens, which in turn drives the recovery of healthy GM. This rebalancing directly leads to a reduction in inflammation, an enhancement of the intestinal barrier, and a positive regulation of the immune response, collectively alleviating the symptoms and pathology of diarrhea. Specifically, bacteriophage vB_Ecos_ULIM2 effectively lysed F18

TABLE 5 Clinical study on the application of FMT technique in the treatment of diarrhea.

Type of diarrhea	Donor	Changes in microbiota	Relief or treatment of symptoms	Reference
IBS-D	Healthy 36-year-old men	*Faecalibacterium*, *Eubacterium* and *Escherichia* decreased.	Relieved diarrhea and anxiety symptoms in IBS-D patients and reduced fecal isovaleric and valeric acid levels.	Lin et al. (2021)
Clostridium difficile infection (CDI)	Healthy donor	Lactobacillaceae, Ruminococcaceae, Desulfovibrionaceae, Sutterellaceae and Porphyromonadaceae increased, Enterobacteriaceae and Veillonellaceae decreased.	Decreased serum proinflammatory cytokines (TNF-α, IL-1β, IL-6, IL-8 and IL-12), returned CRP and fecal calcarein to normal. Increased LL-37 in plasma of successfully treated patients were monitored 3 months after FMT.	Konturek et al. (2016)
AAD	Healthy donor	Firmicutes, Bacteroidota, and Actinobacteriota increased, Proteobacteria decreased. *Bacteroides* and *Faecalibacterium* increased, *Escherichia-Shigella* and *Veillonella* decreased.	Reduced inflammatory markers IL-8 and CRP and alleviated diarrhea symptoms in patients.	Wang L. et al. (2024)
IBS-D	FMT was prepared from one or two healthy unrelated donors	*Lawsonibacter* increased, *Ruminococcus gnavus* decreased.	Relieved the patients' abdominal distension and general symptoms.	Yau et al. (2023)
IBS-D	Screening of eligible faecal donors, and matched by donor-recipient	*Gemella* in donor-recipient-matched group and *Acidovorax* and *Klebsiella* in random-donor group were decreased.	Compared with random-donor FMT, donor-recipient-matched FMT significantly improves the clinical symptoms of patients with IBS-D.	Zhang Y, et al. (2024)
IBS-D	Healthy donor	*Weissella*, *Bacteroides*, *Escherichia-Shigella*, *Akkermansia*, *Enterococcus*, *Parabacteroides*, *Collinsella* and *Dorea* increased, *Streptococcus*, *Lactobacillus*, *Romboutsia*, *Bifidobacterium*, *Subdoligranulum*, *Pediococcus*, *Blautia*, *Faecalibacterium*, and *Fusobacterium* decreased.	Improved the patient's QOL, and also improved Hamilton anxiety scale and Hamilton depression scale scores, and was effective in the following 4 dimensions: interference with activities, health concerns, food avoidance, and interpersonal relationships.	Huang et al. (2022)

ETEC strain (Navez et al., 2023), ZC22 bacteriophage specifically targeted and reduced the load of *Salmonella typhimurium* in organs (Sun et al., 2025), and broad-spectrum cocktail reduced fecal *E. coli* count by 1.33 logarithmic units (Sun et al., 2025).

In addition to direct killing, bacteriophages also significantly regulate the GM to restore health: (1) Reduce pathogenic bacteria: Multiple studies have shown that bacteriophages effectively reduce the abundance of pathogenic families such as Enterobacteriaceae (Li et al., 2024; Mao et al., 2023) and specific genera such as Shigella, Clostridium, and Desulfovibrio (Chen et al., 2025; Choi et al., 2023). (2) Promotion of beneficial bacteria: A key finding is that targeted phage therapy can reduce or even promote the growth of beneficial bacteria. Research consistently reports an increase in the abundance of *Lactobacillus* (Canibe et al., 2022; Castro et al., 2022; Chen J. et al., 2025; Choi et al., 2023; Feng et al., 2025; Mao et al., 2023) and *Bifidobacterium* (Chen J. et al., 2025; Choi et al., 2023), which is crucial for gut health. (3) Increasing diversity: Phage cocktails can increase the richness and diversity of microorganisms that are infected and destroyed (such as Chao1 index) (Zeng et al., 2021).

Continuous treatment with bacteriophages can also lead to significant reductions in pro-inflammatory cytokines such as IL-1β, IL-6, IL-8, and TNF-α (J. Chen et al., 2025; Choi et al., 2023; Dong et al., 2024; Kim et al., 2022; Sun et al., 2025; Zeng et al., 2021). On the contrary, they can increase the levels of anti-inflammatory cytokines such as IL-10 (Zeng et al., 2021). A reduction in inflammation often correlates with decreased intestinal damage. Bacteriophages contribute to the restoration of intestinal barrier integrity, they upregulated the expression of TJ proteins, including ZO-1, Occludin, and Claudin-1/3 (Choi et al., 2023; Dong et al., 2024; Feng et al., 2025; Kim et al., 2022). This will lead to a decrease in intestinal permeability (Kim et al., 2022). In addition, there will also be improvements in intestinal morphology, with studies showing an increase in villus height and a

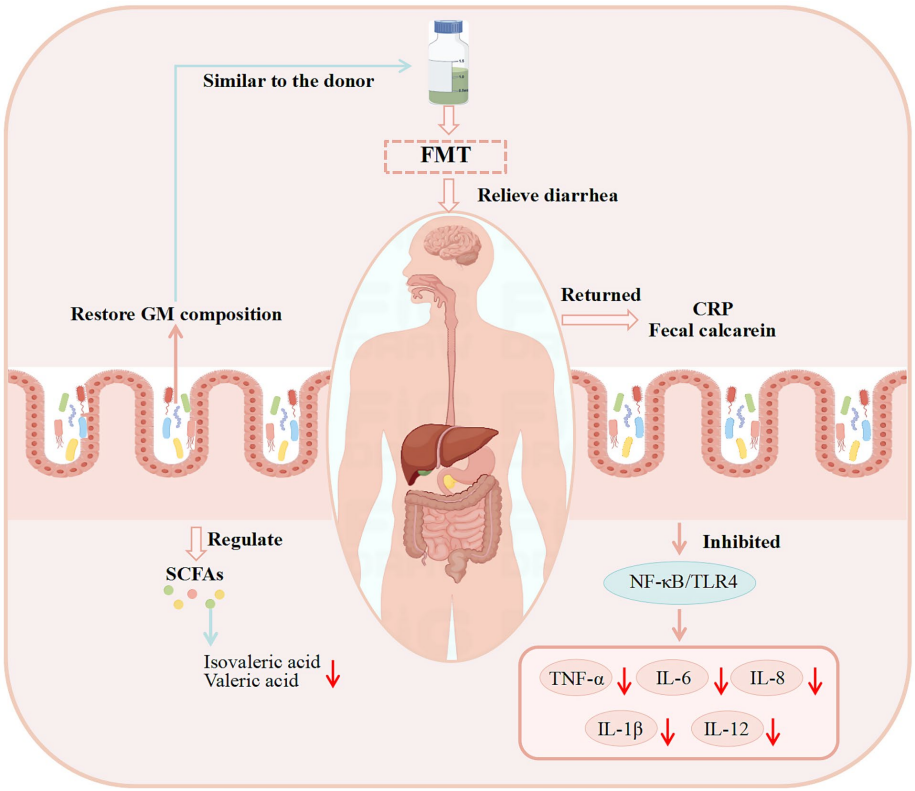

FIGURE 5
Observed outcomes and proposed mechanisms of FMT for diarrhea in clinical studies. (These potential mechanisms mainly involve GM, SCFAs, and immune system).

decrease in crypt depth (Chen J. et al., 2025; Choi et al., 2023; Zeng et al., 2021), indicating enhanced nutrient absorption and intestinal health.

In addition to the above, bacteriophages can regulate the host's immune response, including enhancing specific immunity (increasing IgA and IgG levels) and non-specific immunity (such as increasing IFN-γ and lysozyme activity) (Alomari et al., 2021). Bacteriophages can also indirectly affect the intestinal environment, and some therapies lead to an increase in SCFAs (Dong et al., 2024), which are beneficial metabolites produced by intestinal bacteria, supporting barrier function and reducing inflammation.

The specific basic experiments of bacteriophages in the treatment of diarrhea were shown in Table 6, and the potential mechanism of bacteriophages in the treatment of diarrhea were shown in Figure 6.

3.3.2 Clinical experiments

At present, in addition to probiotics, FMT and other important treatments for diarrhea, phage therapy is also used in clinical diarrhea diseases.

Based on a randomized, double-blind, placebo-controlled clinical trial conducted in Bangladesh, oral bacteriophage therapy was evaluated as a method for treating acute bacterial diarrhea in children. These studies aim to evaluate the safety, *in vivo* kinetics, and clinical efficacy of a customized T4 like *E. coli* phage cocktail and a commercial Russian phage product (Microgen ColiProteus). A total of 120 male children aged 6–24 months hospitalized for acute diarrhea received phage or placebo treatment, as well as standard oral rehydration and zinc therapy. The results indicate that oral phage administration is safe, with no evidence of systemic phage exposure, endotoxin release, or immune response (such as anti phage or anti LPS antibodies) detected, and no serious adverse events or systemic inflammatory reactions observed. These studies emphasize the inherent instability of the gut microbiota in Bangladeshi children, which should be considered in future research on the association of microbiota diseases (Sarker et al., 2017; Sarker and Brüssow, 2016; Sarker et al., 2016). Another study conducted safety testing of phage therapy, which was designed as a single center, randomized, placebo-controlled study. Fifteen healthy volunteers received higher doses of bacteriophages (dose A, 105 PFU/ml), lower doses of bacteriophages (dose B, 103 PFU/ml), and placebo (dose C). The subjects were randomly assigned to one of the following treatment sequences: ABC, BCA, or CAB. During the study, participants provided all fecal samples produced daily. The incidence of adverse events in the high-dose phage group was comparable to that in the low-dose and placebo groups. Ultimately, no adverse events were found to be related to phage administration (Bruttin and Brüssow, 2005).

Although phage therapy is safe and has the potential to serve as an alternative to antibiotic treatment for drug-resistant infections, its efficacy in treating diarrhea has not been confirmed in controlled trials. In the future, we need to conduct pre-screening of phage susceptibility and pathogen dominance, and further fundamental research on phage bacterial dynamics in the human gut. The reason

TABLE 6 Basic studies on the potential mechanisms of bacteriophages against diarrhea.

Types of bacteriophages	Type of diarrhea	Effect on GM	Relief or treatment of symptoms	Reference
Microencapsulated Phage A221	*E. coli*-induced PWD (Post-Weaning Diarrhea)	Reduced Enterobacteriaceae abundance in duodenum to 0.64%; Increased Lactobacillaceae and Oscillospiraceae.	Reduced bacterial load in jejunal lymph nodes, cecum, and spleen, and alleviated intestinal lesions (villi atrophy, gland degeneration, bleeding).	Mao et al. (2023)
Phage ZK22	*Salmonella*-induced diarrhea	Highly specific to *Salmonella Typhimurium*; no significant disruption to normal GM expected due to narrow host range.	Increased survival rate in mice; reduced bacterial load in blood, heart, liver, and spleen; alleviated inflammatory response (IL-2, IL-6, TNF-α).	Sun et al. (2025)
Unclassified *Caudoviricetes*, *Siphoviridae*	Early-onset diarrhea	Increased viral heterogeneity; reduced *Clostridium perfringens* and *Escherichia*; constrained bacterial composition.	Reduced NEC severity, intestinal inflammation, and levels of IL-1β and IL-8; decreased abundance of pathobionts.	Spiegelhauer et al. (2025)
Mixed bacteriophage (Targeting *Salmonella*, *E. coli*, *Clostridium perfringens*, *S. aureus*)	Post-weaning diarrhea	Altered relative abundance of Firmicutes, Bacteroidetes, and Tenericutes.	Reduced feed/gain ratio and diarrhea incidence; Enhanced intestinal morphology (increased villus height, decreased crypt depth); modulated inflammatory response (decreased IL-1*β*, TNF-α; increased IL-10); enhanced intestinal barrier function (increased ZO-1, Claudin-1, Occludin).	Zeng et al. (2021)
φ26, φ27, φ29 (All belonging to Myoviridae)	*E. coli*-induced diarrhea	Reduced pathogenic *E. coli*; no effect on commensal *E. coli*	Reduced duration of diarrhea; enhanced specific (IgA, IgG) and nonspecific (IFN-*γ*, lysozyme) immune response; reduced inflammatory damage; maintained intestinal barrier integrity.	Alomari et al. (2021)
Myovirus phage vB_AccP_PAc	*Aeromonas caviae*-induced diarrhea	Lactobacillaceae increased	Alleviated diarrhea, reduced inflammatory cytokines, increased TJ molecules, and improved intestinal barrier function.	Feng et al. (2025)
Bacteriophage EK99P-1	ETEC K99-induced diarrhea	Reduction of ETEC K99 colonization	Restored intestinal barrier integrity (ZO-1, occludin, claudin-3), reduced intestinal permeability, decreased pro-inflammatory cytokines (IL-8, MCP-1, IL-1*β*).	Kim et al. (2022)
Broad-spectrum phage cocktail (vs. multiple pathogens)	Non-sanitary environment diarrhea	Decreased Proteobacteria, *Desulfovibrio*, *Escherichia-Shigella*, *Clostridium* spp.; increased *Eubacterium* and *Lactobacillus* spp.	Increased ADG, G/F; decreased fecal score; decreased serum IL-1β, IL-6, TNF-α; increased intestinal barrier function; improved microbiota diversity.	Chen J. et al. (2025)
Microencapsulated phage cocktail (NJ12 + EP01)	Mixed *E. coli* O157: H7 and *Salmonella Typhimurium*-induced diarrhea	Reduced the relative abundance of *Enterobacteriaceae*	Reduced diarrhea incidence and severity; increased fecal score; decreased bacterial load in jejunum; attenuated intestinal inflammation and damage; improved weight gain in weaned piglets.	Li et al. (2024)
Bacteriophage cocktail (targeting *E. coli*, *Salmonella*, *Clostridium perfringens*)	Post-weaning diarrhea (mainly *E. coli* and *Clostridium* spp. induced)	Decreased Proteobacteria; *Escherichia-Shigella*; increased *Eubacterium*; *Lactobacillus* spp.; *Bifidobacterium* spp.; decreased *Clostridium* spp.; coliforms; *Desulfovibrio*.	Improved growth performance (final BW, ADG, G/F); reduced pro-inflammatory cytokines (IL-1β, IL-6, TNF-α); decreased myeloperoxidase (MPO) and zonulin; enhanced antioxidant capacity (increased SOD, decreased MDA); improved intestinal morphology, reduced diarrhea incidence and fecal score.	Choi et al. (2023)
Unclassified *Caudoviricetes*, *Siphoviridae*	Early-onset diarrhea	Reduced *Clostridium perfringens* and *Escherichia*	Reduced NEC severity, intestinal inflammation, and levels of IL-1*β* and IL-8; decreased abundance of pathobionts.	Kreis and Soutourina (2022)
Bacteriophage cocktail (*Salmonella*, *E. coli*, etc.)	ETEC-induced diarrhea	Increased *Lactobacillus* concentration	Improved average daily gain, feed intake, and nutrient digestibility; enhanced villus height in duodenum and jejunum.	Castro et al. (2022)
Bacteriophage cocktail (*E. coli* strains K88, K99, F18, F41, 987P, O78)	ETEC-induced diarrhea	Increased the relative abundance of Bacteroidota and Muribaculaceae, decreased the relative abundance of Verrucomicrobiota and Akkermans	Reduced serum DAO level and increased the expression of Claudin-1, Occludin, and ZO-1. Decreased TNF-α, IL-1β and IL-6 levels, and inhibited TLR-4/NF-κB pathway activation induced by ETEC infection. Moreover, the bacteriophage administration increased the levels of acetic acid, propionic acid, butyric acid, and total SCFAs.	Dong et al. (2024)

10.3389/fmicb.2025.1630823

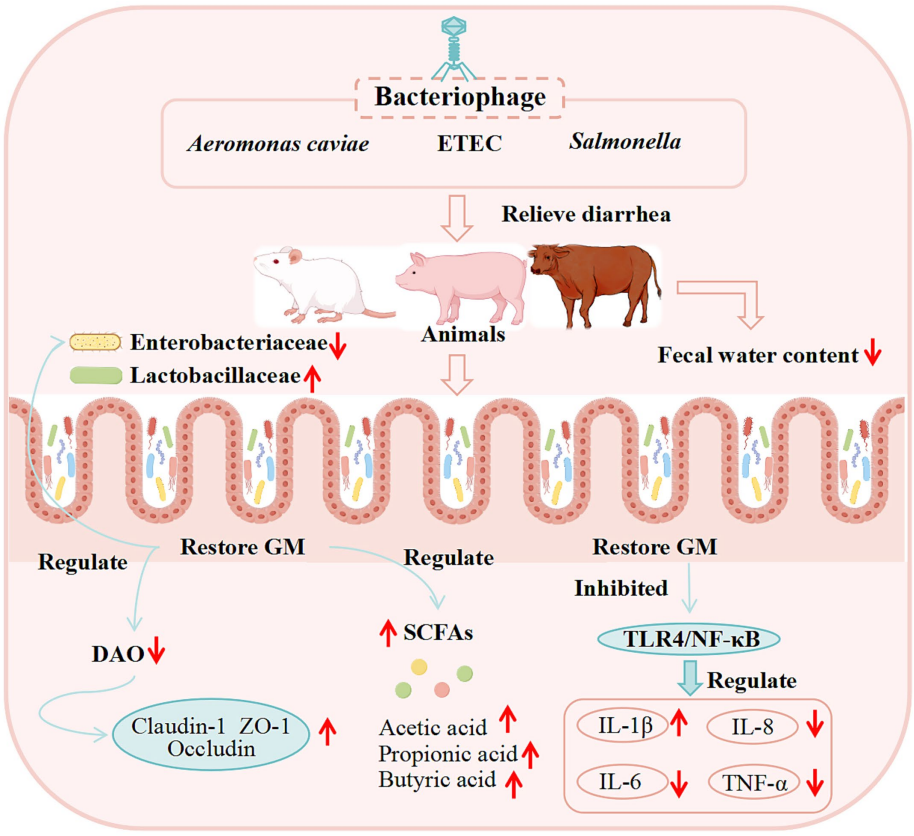

FIGURE 6
Potential mechanisms of bacteriophage therapy for diarrhea from basic studies. (These potential mechanisms mainly involve GM, SCFAs, the immune system, and intestinal barrier function).

for poor efficacy in the diarrhea test described above may be that some patients have low abundance of the target pathogen (*E. coli*). There are other pathogens that bacteriophages do not target, such as streptococcus. Possible issues with phage stability, dosage, or delivery to the site of infection. Future research on phage therapy for diarrhea should incorporate more rigorous randomized controlled trials, improved phage characterization, comprehensive sensitivity testing, and optimized dosage regimens.

4 Discussion

Diarrhea, induced by diverse pathogens or contributing factors, is closely associated with alterations in the GM. As a complex and diverse ecosystem, the GM resides symbiotically within the gastrointestinal tract and plays critical roles in host immunity, metabolism, and the maintenance of intestinal barrier homeostasis (Riccio and Rossano, 2020). During episodes of diarrhea, however, disruption of this microbial ecosystem leads to GM dysbiosis, which impairs metabolite production and immune responses, thereby compromising intestinal barrier function (Rengarajan et al., 2020; Shi Z. et al., 2023). Deficiency of beneficial bacteria and overgrowth of certain pathogens (e.g., *E. coli* and *Shigella*) is one of the important pathogenic mechanisms of diarrhea (Baker and The, 2018; Khan et al., 2022).

Diarrhea can alter the composition of the GM, and in turn, the application of probiotics, FMT or bacteriophage can directly or indirectly influence the GM and the therapeutic outcome of diarrhea. Currently, probiotics, FMT and bacteriophage have demonstrated considerable anti-diarrheal potential, which can regulate the immune response and enhance intestinal barrier function by regulating the diversity and composition of GM and the content of metabolites, and effectively improving diarrhea symptoms (Pilla and Suchodolski, 2019; Sánchez et al., 2017). Notably, the use of probiotics for treating diarrhea is well-documented. These interventions broadly fall into three categories: single-strain preparations, multi-strain mixtures, or probiotics used in conjunction with conventional therapy. Probiotic supplementation not only helps prevent the occurrence of diarrhea but also enhances overall therapeutic efficacy and clinical cure rates, while shortening the duration of symptoms. Importantly, probiotic interventions are associated with a low incidence of adverse reactions (Liu et al., 2022; Steyer et al., 2022). Commonly used probiotics including *Lactobacillus* and *Bifidobacterium*, etc. Probiotics can gain a competitive advantage by altering the intestinal environment, e.g., inhibiting the growth of pathogenic bacteria through the competitive exclusion of intestinal binding sites; probiotics can up-regulate the synthesis of TJ proteins and then protect the intestinal barrier; and they can inhibit the production of pro-inflammatory cytokines to regulate intestinal immune function (Du et al., 2023). In addition, the application of FMT for the treatment of diarrhea has gained increasing attention in recent years owing to its favorable safety profile. The infusion of fecal material from healthy donors can help restore the GM of diarrhea patients to a state resembling that of the donor, thereby

alleviating diarrheal symptoms (Li et al., 2019; Zheng et al., 2020). Currently, most studies have documented and summarized the phenomenon of healing in patients with diarrhea after treatment with FMT, such as clinical cure rate and duration of action (Lee et al., 2018; Pereira et al., 2018). Other investigations have explored alterations in the composition and structure of the GM post-FMT, as well as its effects on intestinal immune-inflammatory responses and barrier function, to elucidate the mechanisms underlying the alleviation of diarrhea (Li, 2020; Tian et al., 2022). Compared to probiotics and FMT, phage therapy demonstrates unique application value in the treatment of diarrhea due to its highly specific antibacterial effects (Chen X. et al., 2023). Phages can precisely recognize and lyse specific pathogenic bacteria (such as diarrheagenic *E. coli* and *Salmonella*), while preserving the stability of beneficial bacterial communities, thereby enabling precise modulation of the GM (Battistelli et al., 2024; Cui et al., 2022). Research has demonstrated that phage therapy can effectively alleviate symptoms of bacterial diarrhea, reduce levels of inflammatory cytokines, and promote the repair of the intestinal mucosal barrier (Dong et al., 2024). However, despite these results indicating the significant potential of phages in combating diarrhea, their clinical application still faces a critical translational challenge: the relatively poor stability of phages in the hostile gastrointestinal environment. Gastric acid and digestive enzymes can readily cause rapid denaturation of phage particles, thereby compromising therapeutic efficacy (Nobrega et al., 2016). Current research primarily focuses on the clearance of pathogens by phages and preliminary evaluation of clinical efficacy, while studies on post-treatment changes in gut microbiota diversity, metabolite profiles, and immune mechanisms remain relatively limited. Future efforts should involve more rigorous randomized controlled trials, along with optimization of phage characterization, sensitivity detection, and dosing regimens.

A review of the relationship between GM and disease reveals that GM dysbiosis is a critical factor in the pathogenesis of diarrhea. Alterations in the GM can lead to abnormal levels of microbial metabolites, such as SCFAs and BAs. These changes in the GM and its metabolites may further modulate immune cell functions and inflammatory factor levels, ultimately contributing to the onset of diarrhea. Although probiotics, FMT, and bacteriophage have been widely used in the treatment of diarrhea, and their efficacy and safety have encouraged the development of therapeutic approaches for gastrointestinal and other systemic diseases, there are still some issues that need to be addressed. Firstly, there is a scarcity of large-scale clinical trials, and secondly, the underlying mechanisms have not been sufficiently clarified through basic experimental research. Therefore, probiotic and bacteriophage interventions, as well as fecal microbiota transplantation, as safe and effective anti-diarrheal treatment strategies still need to go through a long journey.

5 Conclusion

Overall, GM alterations represent a crucial factor in diarrhea pathogenesis and a key target for its treatment. Diarrhea incidence has been closely linked to elevated levels of Proteobacteria and reduced Firmicutes; thus, targeted GM modulation aids in alleviating diarrhea symptoms. Currently, based on the principle of alleviating gut microbiota disorders, the use of probiotics (such as *Lactobacillus* and *Bifidobacterium*), FMT, and bacteriophages has been demonstrated to have definite effects on diarrhea. However, substantial clinical and basic research is still required to elucidate the optimal selection of these interventions, such as screening probiotic strains, FMT donors, and bacteriophages with superior pathogen-targeting advantages, as well as to investigate their long-term safety and efficacy in the treatment of diarrhea. Encouragingly, advances in multi-omics technologies have greatly facilitated investigations into diarrhea treatment mechanisms. Future studies should actively employ diverse research approaches to explore the potential mechanisms of different interventions in various diarrheal diseases and other related conditions, thereby providing data support for clinical diarrhea management and a foundation for the development of novel anti-diarrheal agents.

Author contributions

RT: Writing – original draft, Data curation, Investigation. C-JC: Data curation, Writing – original draft. Y-YB: Data curation, Writing – original draft. NC: Investigation, Writing – original draft. R-RQ: Writing – original draft, Investigation. KW: Writing – review & editing. Y-WW: Writing – review & editing. PZ: Writing – review & editing. C-BZ: Writing – review & editing. Y-PT: Writing – review & editing. LZ: Writing – review & editing. QZ: Writing – review & editing, Formal Analysis, Conceptualization.

Funding

The author(s) declare that financial support was received for the research and/or publication of this article. This research was funded by the Key Research and Development plan project of Shaanxi Province (2025SF-YBXM-257), The Natural Science Foundation of the Jiangsu Higher Education Institutions of China (Numbers: 21KJB360014), Key Disciplines of High-level Traditional Chinese Medicine in Shaanxi Province for Science of Chinese Medicinal Preparation, Key Research and Development plan project of Shaanxi Province (2024SF2-GJHX-67), and Key Disciplines of High-level Traditional Chinese Medicine in Shaanxi Province for Science of Chinese Medicinal Preparation.

Conflict of interest

The authors declare that the research was conducted in the absence of any commercial or financial relationships that could be construed as a potential conflict of interest.

Generative AI statement

The authors declare that no Gen AI was used in the creation of this manuscript.

Any alternative text (alt text) provided alongside figures in this article has been generated by Frontiers with the support of artificial intelligence and reasonable efforts have been made to ensure accuracy, including review by the authors wherever possible. If you identify any issues, please contact us.

Publisher's note

All claims expressed in this article are solely those of the authors and do not necessarily represent those of their affiliated organizations, or those of the publisher, the editors and the reviewers. Any product that may be evaluated in this article, or claim that may be made by its manufacturer, is not guaranteed or endorsed by the publisher.

References

Ademe, M. (2020). Benefits of fecal microbiota transplantation: a comprehensive review. *J. Infect. Dev. Ctries.* 14, 1074–1080. doi: 10.3855/jidc.12780

Alam, N. H., Raqib, R., Ashraf, H., Qadri, F., Ahmed, S., Zasloff, M., et al. (2011). L-isoleucine-supplemented oral rehydration solution in the treatment of acute diarrhoea in children: a randomized controlled trial. *J. Health Popul. Nutr.* 29, 183–190. doi: 10.3329/jhpn.v29i3.7864

Aleman, R. S., Moncada, M., and Aryana, K. J. (2023). Leaky gut and the ingredients that help treat it: a review. *Molecules* 28:619. doi: 10.3390/molecules28020619

Ali, M., Mujahid, A., Bulathsinghala, C. P., and Surani, S. (2020). Cardiac arrhythmia secondary to Loperamide abuse and toxicity. *Cureus* 12:e6936. doi: 10.7759/cureus.6936

Allam-Ndoul, B., Castonguay-Paradis, S., and Veilleux, A. (2020). Gut microbiota and intestinal trans-epithelial permeability. *Int. J. Mol. Sci.* 21:6402. doi: 10.3390/ijms21176402

Almeida, C., Oliveira, R., Baylina, P., Fernandes, R., Teixeira, F. G., and Barata, P. (2022). Current trends and challenges of fecal microbiota transplantation-An easy method that works for all? *Biomedicine* 10:2742. doi: 10.3390/biomedicines10112742

Alomari, M. M. M., Dec, M., Nowaczek, A., Puchalski, A., Wernicki, A., Kowalski, C., et al. (2021). Therapeutic and prophylactic effect of the experimental bacteriophage treatment to control diarrhea caused by *E. coli* in newborn calves. *ACS Infect. Dis.* 7, 2093–2101. doi: 10.1021/acsinfecdis.1c00010

Al-Sadi, R., Khatib, K., Guo, S., Ye, D., Youssef, M., and Ma, T. (2011). Occludin regulates macromolecule flux across the intestinal epithelial tight junction barrier. *Am. J. Physiol. Gastrointest. Liver Physiol.* 300, G1054–G1064. doi: 10.1152/ajpgi.00055.2011

Anbazhagan, A. N., Ge, Y., Priyamvada, S., Kumar, A., Jayawardena, D., Palani, A. R. V., et al. (2024). A direct link implicating loss of SLC26A6 to gut microbial Dysbiosis, compromised barrier integrity, and inflammation. *Gastroenterology* 167, 704–717.e3. doi: 10.1053/j.gastro.2024.05.002

Anbazhagan, A. N., Priyamvada, S., Alrefai, W. A., and Dudeja, P. K. (2018). Pathophysiology of IBD associated diarrhea. *Tissue Barriers.* 6:e1463897. doi: 10.1080/21688370.2018.1463897

Arneth, B. M. (2018). Gut-brain axis biochemical signalling from the gastrointestinal tract to the central nervous system: gut dysbiosis and altered brain function. *Postgrad. Med. J.* 94, 446–452. doi: 10.1136/postgradmedj-2017-135424

Aroniadis, O. C., Brandt, L. J., Oneto, C., Feuerstadt, P., Sherman, A., Wolkoff, A. W., et al. (2019). Faecal microbiota transplantation for diarrhoea-predominant irritable bowel syndrome: a double-blind, randomised, placebo-controlled trial. *Lancet Gastroenterol. Hepatol.* 4, 675–685. doi: 10.1016/s2468-1253(19)30198-0

Baker, S., and The, H. C. (2018). Recent insights into Shigella. *Curr. Opin. Infect. Dis.* 31, 449–454. doi: 10.1097/qco.0000000000000475

Bao, W., He, Y., Yu, J., Liu, M., Yang, X., Ta, N., et al. (2022). Regulatory effect of Lactiplantibacillus plantarum 2-33 on intestinal microbiota of mice with antibiotic-associated diarrhea. *Front. Nutr.* 9:921875. doi: 10.3389/fnut.2022.921875

Baran, A., Kwiatkowska, A., and Potocki, L. (2023). Antibiotics and bacterial resistance-a short story of an endless arms race. *Int. J. Mol. Sci.* 24:5777. doi: 10.3390/ijms24065777

Barash, N. R., Maloney, J. G., Singer, S. M., and Dawson, S. C. (2017). Giardia alters commensal microbial diversity throughout the murine gut. *Infect. Immun.* 85:e00137-18. doi: 10.1128/iai.00948-16

Battistelli, N., Tittarelli, F., Ruffini, F., Gavazzi, L., Scattolini, S., Acciari, V. A., et al. (2024). In vitro characterization and genome sequencing of two novel lytic phages against Salmonella Infantis isolated from poultry feces. *Front. Microbiol.* 15:1479700. doi: 10.3389/fmicb.2024.1479700

Bell, J., Radial, S. L., Cuming, R. S., Trope, G., and Hughes, K. J. (2024). Effects of fecal microbiota transplantation on clinical outcomes and fecal microbiota of foals with diarrhea. *J. Vet. Intern. Med.* 38, 2718–2728. doi: 10.1111/jvim.17185

Binder, H. J. (2010). Role of colonic short-chain fatty acid transport in diarrhea. *Annu. Rev. Physiol.* 72, 297–313. doi: 10.1146/annurev-physiol-021909-135817

Bosnjak, M., Karpe, A. V., Van, T. T. H., Kotsanas, D., Jenkin, G. A., Costello, S. P., et al. (2023). Multi-omics analysis of hospital-acquired diarrhoeal patients reveals biomarkers of enterococcal proliferation and Clostridioides difficile infection. *Nat. Commun.* 14:7737. doi: 10.1038/s41467-023-43671-8

Brehm, T. T., Lütgehetmann, M., Tannich, E., Addo, M. M., Lohse, A. W., Rolling, T., et al. (2020). Risk factors for different intestinal pathogens among patients with traveler's diarrhea: a retrospective analysis at a German travel clinic (2009-2017). *Travel Med. Infect. Dis.* 37:101706. doi: 10.1016/j.tmaid.2020.101706

Bruttin, A., and Brüssow, H. (2005). Human volunteers receiving *Escherichia coli* phage T4 orally: a safety test of phage therapy. *Antimicrob. Agents Chemother.* 49, 2874–2878. doi: 10.1128/AAC.49.7.2874-2878

Bustos Fernández, L. M., Man, F., and Lasa, J. S. (2023). Impact of Saccharomyces boulardii CNCM I-745 on bacterial overgrowth and composition of intestinal microbiota in diarrhea-predominant irritable bowel syndrome patients: results of a randomized pilot study. *Dig. Dis.* 41, 798–809. doi: 10.1159/000528954

Cai, J., Sun, L., and Gonzalez, F. J. (2022). Gut microbiota-derived bile acids in intestinal immunity, inflammation, and tumorigenesis. *Cell Host Microbe* 30, 289–300. doi: 10.1016/j.chom.2022.02.004

Camilleri, M. (2021). Human intestinal barrier: effects of stressors, diet, prebiotics, and probiotics. *Clin. Transl. Gastroenterol.* 12:e00308. doi: 10.14309/ctg.0000000000000308

Canibe, N., Højberg, O., Kongsted, H., Vodolazska, D., Lauridsen, C., Nielsen, T. S., et al. (2022). Review on preventive measures to reduce post-weaning Diarrhoea in piglets. *Animals (Basel).* 12:2585. doi: 10.3390/ani12192585

Cao, A. T., Yao, S., Gong, B., Elson, C. O., and Cong, Y. (2012). Th17 cells upregulate polymeric Ig receptor and intestinal IgA and contribute to intestinal homeostasis. *J. Immunol.* 189, 4666–4673. doi: 10.4049/jimmunol.1200955

Castro, J., Barros, M. M., Araújo, D., Campos, A. M., Oliveira, R., Silva, S., et al. (2022). Swine enteric colibacillosis: current treatment avenues and future directions. *Front Vet Sci.* 9:981207. doi: 10.3389/fvets.2022.981207

Caviglia, G. P., Tucci, A., Pellicano, R., Fagoonee, S., Rosso, C., Abate, M. L., et al. (2020). Clinical response and changes of cytokines and Zonulin levels in patients with Diarrhoea-predominant irritable bowel syndrome treated with *Bifidobacterium longum* ES1 for 8 or 12 Weeks: a preliminary report. *J. Clin. Med.* 9:2353. doi: 10.3390/jcm9082353

Chen, H. R., An, J. R., Yang, Y. F., Liu, J. T., and Shi, Y. (2024). Discussion on the repairing effect and mechanism of traditional Chinese medicine compound Yitangkang on intestinal barrier damage in small intestine of db/db mice. *J. Liaoning Univ. Tradit. Chin. Med.* 26, 31–36. doi: 10.13194/j.issn.1673-842x.2024.07.007

Chen, C. C., and Chiu, C. H. (2022). Current and future applications of fecal microbiota transplantation for children. *Biom. J.* 45, 11–18. doi: 10.1016/j.bj.2021.11.004

Chen, J., Han, J., Yang, Z., Zhou, W., He, Y., Chen, X., et al. (2025). Bacteriophages as potential anti-pathogenic agents for intestinal health of weaned piglets in the post-antibiotic era: an updated review. *Animals (Basel)* 15:1713. doi: 10.3390/ani15121713

Chen, H., Jia, Z., He, M., Chen, A., Zhang, X., Xu, J., et al. (2023). Arula-7 powder improves diarrhea and intestinal epithelial tight junction function associated with its regulation of intestinal flora in calves infected with pathogenic *Escherichia coli* O(1). *Microbiome* 11:172. doi: 10.1186/s40168-023-01616-9

Chen, K., Jin, S., Ma, Y., Cai, L., Xu, P., Nie, Y., et al. (2024). Adjudicative efficacy of *Bifidobacterium animalis* subsp. lactis BLa80 in treating acute diarrhea in children: a randomized, double-blinded, placebo-controlled study. *Eur. J. Clin. Nutr.* 78, 501–508. doi: 10.1038/s41430-024-01428-6

Chen, Y. M., Limaye, A., Chang, H. W., and Liu, J. R. (2022). Screening of lactic acid bacterial strains with antiviral activity against porcine epidemic diarrhea. *Probiotics Antimicrob Proteins* 14, 546–559. doi: 10.1007/s12602-021-09829-w

Chen, X., Mendes, B. G., Alves, B. S., and Duan, Y. (2023). Phage therapy in gut microbiome. *Prog Mol Biol Transl Sci.* 201, 93–118. doi: 10.1016/bs.pmbts.2023.04.005

Chen, J., Zhao, B. C., Dai, X. Y., Xu, Y. R., Kang, J. X., and Li, J. L. (2023). Drinking alkaline mineral water confers diarrhea resistance in maternally separated piglets by maintaining intestinal epithelial regeneration via the brain-microbe-gut axis. *J. Adv. Res.* 52, 29–43. doi: 10.1016/j.jare.2022.12.008

Chen, Y., Zhou, J., and Wang, L. (2021). Role and mechanism of gut microbiota in human disease. *Front. Cell. Infect. Microbiol.* 11:625913. doi: 10.3389/fcimb.2021.625913

Cheng, S., Ma, X., Geng, S., Jiang, X., Li, Y., Hu, L., et al. (2018). Fecal microbiota transplantation beneficially regulates intestinal mucosal autophagy and alleviates. *Gut Barrier Injury* 3:e00137-18. doi: 10.1128/mSystems.00137-18

Choi, Y., Hosseindoust, A., Ha, S. H., Kim, J., Min, Y., Jeong, Y., et al. (2023). Effects of dietary supplementation of bacteriophage cocktail on health status of weanling pigs in a non-sanitary environment. *J Anim Sci Biotechnol.* 14:64. doi: 10.1186/s40104-023-00869-6

Collaborators G.D.D (2017). Estimates of global, regional, and national morbidity, mortality, and aetiologies of diarrhoeal diseases: a systematic analysis for the global

burden of disease study 2015. *Lancet Infect. Dis.* 17, 909–948. doi: 10.1016/s1473-3099(17)30276-1

Cryan, J. F., O'Riordan, K. J., Cowan, C. S. M., Sandhu, K. V., Bastiaanssen, T. F. S., Boehme, M., et al. (2019). The microbiota-gut-brain Axis. *Physiol. Rev.* 99, 1877–2013. doi: 10.1152/physrev.00018.2018

Cui, S., Guo, S., Zhao, Q., Li, Y., Ma, Y., and Yu, Y. (2023). Alterations of microbiota and metabolites in the feces of calves with diarrhea associated with rotavirus and coronavirus infections. *Front. Microbiol.* 14:1159637. doi: 10.3389/fmicb.2023.1159637

Cui, J. Q., Liu, W. H., Zang, Y. X., Zhang, C., Zou, L., Sun, H. Z., et al. (2022). Characterization and complete genome analysis of a bacteriophage vB_EcoM_DE7 infecting donkey-derived *Escherichia coli*. *Virus Res.* 321:198913. doi: 10.1016/j.virusres.2022.198913

Cui, M., Wang, Y., Elango, J., Wu, J., Liu, K., and Jin, Y. (2021). Cereus sinensis polysaccharide alleviates antibiotic-associated diarrhea based on modulating the gut microbiota in C57BL/6 mice. *Front. Nutr.* 8:751992. doi: 10.3389/fnut.2021.751992

Czepiel, J., Dróżdż, M., Pituch, H., Kuijper, E. J., Perucki, W., Mielimonka, A., et al. (2019). *Clostridium difficile* infection: review. *Eur. J. Clin. Microbiol. Infect. Dis.* 38, 1211–1221. doi: 10.1007/s10096-019-03539-6

den Besten, G., van Eunen, K., Groen, A. K., Venema, K., Reijngoud, D. J., and Bakker, B. M. (2013). The role of short-chain fatty acids in the interplay between diet, gut microbiota, and host energy metabolism. *J. Lipid Res.* 54, 2325–2340. doi: 10.1194/jlr.R036012

Dinan, T. G., and Cryan, J. F. (2017). The microbiome-gut-brain Axis in health and disease. *Gastroenterol. Clin. N. Am.* 46, 77–89. doi: 10.1016/j.gtc.2016.09.007

Doar, N. W., and Samuthiram, S. D. (2023). Qualitative analysis of the efficacy of probiotic strains in the prevention of antibiotic-associated diarrhea. *Cureus* 15:e40261. doi: 10.7759/cureus.40261

Donald, K., and Finlay, B. B. (2023). Early-life interactions between the microbiota and immune system: impact on immune system development and atopic disease. *Nat. Rev. Immunol.* 23, 735–748. doi: 10.1038/s41577-023-00874-w

Dong, C., Chen, Y., Ding, M., Liu, Y., Chen, X., He, Y., et al. (2024). Dietary bacteriophage administration alleviates Enterotoxigenic *Escherichia coli*-induced diarrhea and intestinal impairment through regulating intestinal inflammation and gut microbiota in a newly weaned mouse model. *Int. J. Mol. Sci.* 25:10736. doi: 10.3390/ijms251910736

Du, W., Wang, X., Hu, M., Hou, J., Du, Y., Si, W., et al. (2023). Modulating gastrointestinal microbiota to alleviate diarrhea in calves. *Front. Microbiol.* 14:1181545. doi: 10.3389/fmicb.2023.1181545

Duan, Y., Young, R., and Schnabl, B. (2022). Bacteriophages and their potential for treatment of gastrointestinal diseases. *Nat. Rev. Gastroenterol. Hepatol.* 19, 135–144. doi: 10.1038/s41575-021-00536-z

Duboc, H., Rainteau, D., Rajca, S., Humbert, L., Farabos, D., Maubert, M., et al. (2012). Increase in fecal primary bile acids and dysbiosis in patients with diarrhea-predominant irritable bowel syndrome. *Neurogastroenterol. Motil.* 24, 513–520. doi: 10.1111/j.1365-2982.2012.01893.x

Fareed, S., Sarode, N., Stewart, F. J., Malik, A., Laghaie, E., Khizer, S., et al. (2018). Applying fecal microbiota transplantation (FMT) to treat recurrent *Clostridium difficile* infections (rCDI) in children. *PeerJ* 6:e4663. doi: 10.7717/peerj.4663

Federici, S., Kredo-Russo, S., Valdés-Mas, R., Kviatcovsky, D., Weinstock, E., Matiuhin, Y., et al. (2022). Targeted suppression of human IBD-associated gut microbiota commensals by phage consortia for treatment of intestinal inflammation. *Cell* 185, 2879–2898.e24. doi: 10.1016/j.cell.2022.07.003

Feng, C., Wang, L., Bai, H., Huang, Q., Liang, S., Liang, R., et al. (2025). The high efficiency protective effectiveness of a newly isolated myoviruses bacteriophage vB_AceP_PAc in protecting mice from *Aeromonas caviae* infection in mice. *BMC Microbiol.* 25:112. doi: 10.1186/s12866-025-03796-w

Fu, W. Q., and Huang, C. B. (2022). Progress in the study of fecal microbiota transplantation for the treatment of diarrhea-type irritable bowel syndrome. *Pract. Clin. Med.* 23, 122–127. doi: 10.13764/j.cnki.lcsy.2022.03.035

Fuerte-Stone, J., and Mimee, M. (2022). Host happy hour: phage cocktail targets IBD-associated microbes. *Cell Host Microbe* 30, 1352–1353. doi: 10.1016/j.chom.2022.09.010

Fujimoto, K., and Uematsu, S. (2022). Phage therapy for Clostridioides difficile infection. *Front. Immunol.* 13:1057892. doi: 10.3389/fimmu.2022.1057892

Fukuda, S., Toh, H., Hase, K., Oshima, K., Nakanishi, Y., Yoshimura, K., et al. (2011). Bifidobacteria can protect from enteropathogenic infection through production of acetate. *Nature* 469, 543–547. doi: 10.1038/nature09646

Furusawa, Y., Obata, Y., Fukuda, S., Endo, T. A., Nakato, G., Takahashi, D., et al. (2013). Commensal microbe-derived butyrate induces the differentiation of colonic regulatory T cells. *Nature* 504, 446–450. doi: 10.1038/nature12721

Gallardo, P., Izquierdo, M., Vidal, R. M., Soto, F., Ossa, J. C., and Farfan, M. J. (2020). Gut microbiota-metabolome changes in children with diarrhea by Diarrheagenic *E. coli*. *Front. Cell. Infect. Microbiol.* 10:485. doi: 10.3389/fcimb.2020.00485

Gao, F., Yuan, W. H., Wu, S. B., Wang, Z. B., Zhu, G. Q., and Zhou, M. Q. (2023). Electroacupuncture in the treatment of IBS in rats: investigation of the mechanisms of CRH(+) neurons in the paraventricular nucleus. *J. Neurophysiol.* 130, 380–391. doi: 10.1152/jn.00156.2023

Grenham, S., Clarke, G., Cryan, J. F., and Dinan, T. G. (2011). Brain-gut-microbe communication in health and disease. *Front. Physiol.* 2:94. doi: 10.3389/fphys.2011.00094

Gu, Y., Wang, C., Qin, X., Zhou, B., Liu, X., Liu, T., et al. (2022). Saccharomyces boulardii, a yeast probiotic, inhibits gut motility through upregulating intestinal serotonin transporter and modulating gut microbiota. *Pharmacol. Res.* 181:106291. doi: 10.1016/j.phrs.2022.106291

Gummalla, V. S., Zhang, Y., Liao, Y. T., and Wu, V. C. H. (2023). The role of temperate phages in bacterial pathogenicity. *Microorganisms* 11:541. doi: 10.3390/microorganisms11030541

Guo, S., Ma, T., Kwok, L. Y., Quan, K., Li, B., Wang, H., et al. (2024). Effects of postbiotics on chronic diarrhea in young adults: a randomized, double-blind, placebo-controlled crossover trial assessing clinical symptoms, gut microbiota, and metabolite profiles. *Gut Microbes* 16:2395092. doi: 10.1080/19490976.2024.2395092

Guo, J. G., Rao, Y. F., Jiang, J., Li, X., and Zhu, S. M. (2023). MicroRNA-155-5p inhibition alleviates irritable bowel syndrome by increasing claudin-1 and ZO-1 expression. *Ann Transl Med.* 11:34. doi: 10.21037/atm-22-4859

Guo, H., Yu, L., Tian, F., Zhao, J., Zhang, H., Chen, W., et al. (2021). Effects of Bacteroides-based Microecologics against antibiotic-associated diarrhea in mice. *Microorganisms* 9:2492. doi: 10.3390/microorganisms9122492

Haas, A. J., Zihni, C., Krug, S. M., Maraspini, R., Otani, T., Furuse, M., et al. (2022). ZO-1 guides tight junction assembly and epithelial morphogenesis via cytoskeletal tension-dependent and -independent functions. *Cells* 11:3775. doi: 10.3390/cells11233775

Han, Q. (2023) Studies on the mechanism of action of fecal microbiota transplantation in alleviating diarrhea in artificially lactating piglets. Heilongjiang china: Northeast Agricultural University.

Han, X., Hu, X., Jin, W., and Liu, G. (2024). Dietary nutrition, intestinal microbiota dysbiosis and post-weaning diarrhea in piglets. *Anim Nutr.* 17, 188–207. doi: 10.1016/j.aninu.2023.12.010

Handa, O., Miura, H., Gu, T., Osawa, M., Matsumoto, H., Umegaki, E., et al. (2023). Reduction of butyric acid-producing bacteria in the ileal mucosa-associated microbiota is associated with the history of abdominal surgery in patients with Crohn's disease. *Redox Rep.* 28:2241615. doi: 10.1080/13510002.2023.2241615

He, K. Y., Lei, X. Y., Wu, D. H., Zhang, L., Li, J. Q., Li, Q. T., et al. (2023). *Akkermansia muciniphila* protects the intestine from irradiation-induced injury by secretion of propionic acid. *Gut Microbes* 15:2293312. doi: 10.1080/19490976.2023.2293312

Hillestad, E. M. R., van der Meeren, A., Nagaraja, B. H., Bjørsvik, B. R., Haleem, N., Benitez-Paez, A., et al. (2022). Gut bless you: The microbiota-gut-brain axis in irritable bowel syndrome. *World J. Gastroenterol.* 28, 412–431. doi: 10.3748/wjg.v28.i4.412

Hold, G. L. (2016). Gastrointestinal microbiota and Colon Cancer. *Dig. Dis.* 34, 244–250. doi: 10.1159/000443358

Hollister, E. B., Gao, C., and Versalovic, V. (2014). Compositional and functional features of the gastrointestinal microbiome and their effects on human health. *Gastroenterology.* 146, 1449–58. doi: 10.1053/j.gastro.2014.01.052

Hou, Q., Huang, Y., Wang, Y., Liao, L., Zhu, Z., Zhang, W., et al. (2020). *Lactobacillus casei* LC01 regulates intestinal epithelial permeability through miR-144 targeting of OCLN and ZO1. *J. Microbiol. Biotechnol.* 30, 1480–1487. doi: 10.4014/jmb.2002.02059

Huang, F., Li, S., Chen, W., Han, Y., Yao, Y., Yang, L., et al. (2023). Postoperative probiotics administration attenuates gastrointestinal complications and gut microbiota Dysbiosis caused by chemotherapy in colorectal Cancer patients. *Nutrients* 15:356. doi: 10.3390/nu15020356

Huang, H. L., Zhu, J. Q., Yang, L. S., Wu, Q., Shou, D. W., Chen, H. T., et al. (2022). Fecal microbiota transplantation combined with a low FODMAP diet for the treatment of irritable bowel syndrome with predominant diarrhea. *Oxidative Med. Cell. Longev.* 2022:5121496. doi: 10.1155/2022/5121496

Islam, J., Tanimizu, M., Shimizu, Y., Goto, Y., Ohtani, N., Sugiyama, K., et al. (2022). Development of a rational framework for the therapeutic efficacy of fecal microbiota transplantation for calf diarrhea treatment. *Microbiome.* 10:31. doi: 10.1186/s40168-021-01217-4

James, S. C., Fraser, K., Cooney, J., Günther, C. S., Young, W., Gearry, R. B., et al. (2023). Concentrations of plasma amino acids and neurotransmitters in participants with functional gut disorders and healthy controls. *Meta* 13:313. doi: 10.3390/metabo13020313

Jandhyala, S. M., Talukdar, R., Subramanyam, C., Vuyyuru, H., Sasikala, M., and Nageshwar Reddy, D. (2015). Role of the normal gut microbiota. *World J. Gastroenterol.* 21, 8787–8803. doi: 10.3748/wjg.v21.i29.8787

Jesser, K. J., Trueba, G., Konstantinidis, K. T., and Levy, K. (2023). Why are so many enteric pathogen infections asymptomatic? Pathogen and gut microbiome characteristics associated with diarrhea symptoms and carriage of diarrheagenic *E. coli* in northern Ecuador. *Gut Microbes* 15:2281010. doi: 10.1080/19490976.2023.2281010

Jiang, C., Chen, W., Yang, Y., Li, X., Jin, M., Ghonaim, A. H., et al. (2024). Regulation of isoleucine on colonic barrier function in rotavirus-infected weanling piglets and analysis of gut microbiota and metabolomics. *Microorganisms.* 12:2396. doi: 10.3390/microorganisms12122396

Jiang, W. D., Deng, Y. P., Liu, Y., Qu, B., Jiang, J., Kuang, S. Y., et al. (2015). Dietary leucine regulates the intestinal immune status, immune-related signalling molecules and tight junction transcript abundance in grass carp (*Ctenopharyngodon idella*). *Aquaculture* 444, 134–142. doi: 10.1016/j.aquaculture.2015.04.005

Jiang, C. Y., Wang, X. X., Zhang, S. S., Wang, Y., Wen, D., and Fei, S. J. (2024). Effect of fecal microbiota transplantation modulating PAR2-TRPV1 pathway on visceral hypersensitivity, mast cell activation and intestinal flora in an irritable bowel syndrome model rat. *Prog. Mod. Biomed.* 24, 2417–2422+2407. doi: 10.13241/j.cnki.pmb.2024.13.003

Jung, M., Jung, S., Kim, N., Ahn, H., Yun, H., and Kim, K. N. (2022). A randomized, double-blind, placebo-controlled trial to assess the efficacy and safety of Lactiplantibacillus plantarum CJLP243 in patients with functional diarrhea and high fecal calprotectin levels. *Nutrients* 14:389. doi: 10.3390/nu14020389

Jung, K., Kim, A., Lee, J. H., Cho, D., Seo, J., Jung, E. S., et al. (2022). Effect of oral intake of *Lactiplantibacillus plantarum* APsulloc 331261 (GTB1(TM)) on diarrhea-predominant irritable bowel syndrome: a randomized, double-blind, placebo-controlled study. *Nutrients* 14:2015. doi: 10.3390/nu14102015

Karim, M. R., Iqbal, S., Mohammad, S., Morshed, M. N., Haque, M. A., Mathiyalagan, R., et al. (2024). Butyrate's (a short-chain fatty acid) microbial synthesis, absorption, and preventive roles against colorectal and lung cancer. *Arch. Microbiol.* 206:137. doi: 10.1007/s00203-024-03834-7

Khan, H. R., Ali Asghar, S., Kanwal, S., Qadar, L. T., and Qadri, K. H. (2019). Diphenoxylate-atropine (Lomotil) toxicity in infantile diarrhea: a case report of therapeutic failure. *Cureus* 11:e5875. doi: 10.7759/cureus.5875

Khan, J. R., Hossain, M. B., Chakraborty, P. A., and Mistry, S. K. (2022). Household drinking water *E. coli* contamination and its associated risk with childhood diarrhea in Bangladesh. *Environ. Sci. Pollut. Res. Int.* 29, 32180–32189. doi: 10.1007/s11356-021-18460-9

Kim, N., Gu, M. J., Kye, Y. C., Ju, Y. J., Hong, R., Ju, D. B., et al. (2022). Bacteriophage EK99P-1 alleviates enterotoxigenic *Escherichia coli* K99-induced barrier dysfunction and inflammation. *Sci. Rep.* 12:941. doi: 10.1038/s41598-022-04861-4

Konturek, P. C., Koziel, J., Dieterich, W., Haziri, D., Wirtz, S., Glowczyk, I., et al. (2016). Successful therapy of *Clostridium difficile* infection with fecal microbiota transplantation. *J. Physiol. Pharmacol.* 67, 859–866. Available online at: https://www.jpp.krakow.pl/

Kovanda, L., Park, J., Park, S., Kim, K., Li, X., and Liu, Y. (2023). Dietary butyrate and valerate glycerides impact diarrhea severity and immune response of weaned piglets under ETEC F4-ETEC F18 coinfection conditions. *J. Anim. Sci.* 101:skad401. doi: 10.1093/jas/skad401

Kreis, V., and Soutourina, O. (2022). Clostridioides difficile - phage relationship the RNA way. *Curr. Opin. Microbiol.* 66, 1–10. doi: 10.1016/j.mib.2021.11.012

Lai, H. H., Chiu, C. H., Kong, M. S., Chang, C. J., and Chen, C. C. (2019). Probiotic *Lactobacillus casei*: effective for managing childhood diarrhea by altering gut microbiota and attenuating fecal inflammatory markers. *Nutrients* 11:1150. doi: 10.3390/nu11051150

Lange, K., Buerger, M., Stallmach, A., and Bruns, T. (2016). Effects of antibiotics on gut microbiota. *Dig. Dis.* 34, 260–268. doi: 10.1159/000443360

Lee, S., Drennan, K., Simons, G., Hepple, A., Karlsson, K., Lowman, W., et al. (2018). The 'ins and outs' of faecal microbiota transplant for recurrent *Clostridium difficile* diarrhoea at Wits Donald Gordon medical Centre, Johannesburg, South Africa. *S. Afr. Med. J.* 108, 403–407. doi: 10.7196/SAMJ.2018.v108i5.12367

Lee, C., Kim, B. G., Kim, J. H., Chun, J., Im, J. P., and Kim, J. S. (2017). Sodium butyrate inhibits the NF-kappa B signaling pathway and histone deacetylation, and attenuates experimental colitis in an IL-10 independent manner. *Int. Immunopharmacol.* 51, 47–56. doi: 10.1016/j.intimp.2017.07.023

Lee, A., Lee, J. Y., Jung, S. W., Shin, S. Y., Ryu, H. S., Jang, S. H., et al. (2023). Brain-Gut-Microbiota Axis. *Korean J. Gastroenterol.* 81, 145–153. doi: 10.4166/kjg.2023.028

Leong, K. S. W., Derraik, J. G. B., Hofman, P. L., and Cutfield, W. S. (2018). Antibiotics, gut microbiome and obesity. *Clin. Endocrinol.* 88, 185–200. doi: 10.1111/cen.13495

Li, X. L. (2020). Multi-omics study on the effects of fecal microbiota transplantation on piglets with diarrhea after weaning. Chongqing, 9–25.

Li, L., Cui, H., Li, T., Qi, J., Chen, H., Gao, F., et al. (2020). Synergistic effect of Berberine-based Chinese medicine assembled nanostructures on diarrhea-predominant irritable bowel syndrome in vivo. *Front. Pharmacol.* 11:1210. doi: 10.3389/fphar.2020.01210

Li, L., Han, K., Mao, X., Wang, L., Cao, Y., Li, Z., et al. (2024). Oral phages prophylaxis against mixed *Escherichia coli* O157:H7 and *Salmonella Typhimurium* infections in weaned piglets. *Vet. Microbiol.* 288:109923. doi: 10.1016/j.vetmic.2023.109923

Li, X. T., Li, J. L., Cao, Z. Q., Kang, N., and Kong, W. Z. (2023). Based on 16S rRNA sequencing technology, the effect of Shenling Atractylodes medicinal diet paste on the intestinal microbiota of rats with functional diarrhea and spleen deficiency syndrome was explored. *Lishizhen Med. Mater. Med. Res.* 34, 3046–3051. doi: 10.3969/j.issn.1008-0805.2023.12.59

Li, N., Tian, H. L., Chen, Q. Y., Yang, B., Ma, C. L., Lin, Z. L., et al. (2019). Efficacy analysis of fecal microbiota transplantation in the treatment of 2010 patients with intestinal disorders. *Zhonghua Wei Chang Wai Ke Za Zhi* 22, 861–868. doi: 10.3760/cma.j.issn.1671-0274.2019.09.011

Li, Y., Xia, S., Jiang, X., Feng, C., Gong, S., Ma, J., et al. (2021). Gut microbiota and diarrhea: An updated review. *Front. Cell. Infect. Microbiol.* 11:625210. doi: 10.3389/fcimb.2021.625210

Li, C., Xiao, N., Deng, N., Li, D., Tan, Z., and Peng, M. (2023). Dose of sucrose affects the efficacy of Qiweibaizhu powder on antibiotic-associated diarrhea: association with intestinal mucosal microbiota, short-chain fatty acids, IL-17, and MUC2. *Front. Microbiol.* 14:1108398. doi: 10.3389/fmicb.2023.1108398

Li, K., Yang, J., Zhou, X., Wang, H., Ren, Y., Huang, Y., et al. (2022). The mechanism of important components in canine fecal microbiota transplantation. *Vet Sci.* 9:695. doi: 10.3390/vetsci9120695

Liang, W., Gao, Y., Zhao, Y., Gao, L., Zhao, Z., He, Z., et al. (2023). *Lactiplantibacillus plantarum* ELF051 alleviates antibiotic-associated diarrhea by regulating intestinal inflammation and gut microbiota. *Probiotics Antimicrob. Proteins* 16, 1996–2006. doi: 10.1007/s12602-023-10150-x

Lin, H., Guo, Q., Wen, Z., Tan, S., Chen, J., Lin, L., et al. (2021). The multiple effects of fecal microbiota transplantation on diarrhea-predominant irritable bowel syndrome (IBS-D) patients with anxiety and depression behaviors. *Microb. Cell Factories* 20:233. doi: 10.1186/s12934-021-01720-1

Liu, C. S., Liang, X., Wei, X. H., Jin, Z., Chen, F. L., Tang, Q. F., et al. (2019). Gegen Qinlian decoction treats diarrhea in piglets by modulating gut microbiota and short-chain fatty acids. *Front. Microbiol.* 10:825. doi: 10.3389/fmicb.2019.00825

Liu, M., Ma, J., Xu, J., Huangfu, W., Zhang, Y., Ali, Q., et al. (2024). Fecal microbiota transplantation alleviates intestinal inflammatory diarrhea caused by oxidative stress and pyroptosis via reducing gut microbiota-derived lipopolysaccharides. *Int. J. Biol. Macromol.* 261:129696. doi: 10.1016/j.ijbiomac.2024.129696

Liu, B., Wang, C., Huasai, S., Han, A., Zhang, J., He, L., et al. (2022). Compound probiotics improve the diarrhea rate and intestinal microbiota of newborn calves. *Animals (Basel).* 12:322. doi: 10.3390/ani12030322

Liu, P., Wang, Y., Yang, G., Zhang, Q., Meng, L., Xin, Y., et al. (2021). The role of short-chain fatty acids in intestinal barrier function, inflammation, oxidative stress, and colonic carcinogenesis. *Pharmacol. Res.* 165:105420. doi: 10.1016/j.phrs.2021.105420

Liu, Y., Yu, Z., Zhu, L., Ma, S., Luo, Y., Liang, H., et al. (2023). Orchestration of MUC2 - the key regulatory target of gut barrier and homeostasis: a review. *Int. J. Biol. Macromol.* 236:123862. doi: 10.1016/j.ijbiomac.2023.123862

Liu, S., Zhao, S., Cheng, Z., Ren, Y., Shi, X., Mu, J., et al. (2024). *Akkermansia muciniphila* protects against antibiotic-associated diarrhea in mice. *Probiotics Antimicrob Proteins.* 16, 1190–1204. doi: 10.1007/s12602-023-10101-6

Luo, Z., Liu, C., Hu, Y., Xia, T., Zhang, B., Chen, F., et al. (2022). Gegen Qinlian decoction restores the intestinal barrier in bacterial diarrhea piglets by promoting Lactobacillus growth and inhibiting the TLR2/MyD88/NF-κB pathway. *Biomed. Pharmacother.* 155:113719. doi: 10.1016/j.biopha.2022.113719

Luo, M., Zhuang, X., Tian, Z., and Xiong, L. (2021). Alterations in short-chain fatty acids and serotonin in irritable bowel syndrome: a systematic review and meta-analysis. *BMC Gastroenterol.* 21:14. doi: 10.1186/s12876-020-01577-5

Ma, N., Guo, P., Zhang, J., He, T., Kim, S. W., Zhang, G., et al. (2018). Nutrients mediate intestinal Bacteria-mucosal immune crosstalk. *Front. Immunol.* 9:5. doi: 10.3389/fimmu.2018.00005

Maity, C., and Gupta, A. K. (2021). Therapeutic efficacy of probiotic *Alkalihalobacillus clausii* 088AE in antibiotic-associated diarrhea: a randomized controlled trial. *Heliyon* 7:e07993. doi: 10.1016/j.heliyon.2021.e07993

Makizaki, Y., Maeda, A., Oikawa, Y., Tamura, S., Tanaka, Y., Nakajima, S., et al. (2019). Probiotic *Bifidobacterium bifidum* G9-1 ameliorates phytohemagglutinin-induced diarrhea caused by intestinal dysbiosis. *Microbiol. Immunol.* 63, 481–486. doi: 10.1111/1348-0421.12743

Mann, E. R., Lam, Y. K., and Uhlig, H. H. (2024). Short-chain fatty acids: linking diet, the microbiome and immunity. *Nat. Rev. Immunol.* 24, 577–595. doi: 10.1038/s41577-024-01014-8

Mao, X., Liu, M., Tang, J., Chen, H., Chen, D., Yu, B., et al. (2015). Dietary leucine supplementation improves the mucin production in the Jejunal mucosa of the weaned pigs challenged by porcine rotavirus. *PLoS One* 10:e0137380. doi: 10.1371/journal.pone.0137380

Mao, X., Wu, Y., Ma, R., Li, L., Wang, L., Tan, Y., et al. (2023). Oral phage therapy with microencapsulated phage A221 against *Escherichia coli* infections in weaned piglets. *BMC Vet. Res.* 19:165. doi: 10.1186/s12917-023-03724-y

Martini, E., Krug, S. M., Siegmund, B., Neurath, M. F., and Becker, C. (2017). Mend your fences: The epithelial barrier and its relationship with mucosal immunity in inflammatory bowel disease. *Cell. Mol. Gastroenterol. Hepatol.* 4, 33–46. doi: 10.1016/j.jcmgh.2017.03.007

Mazzawi, T., Hausken, T., Hov, J. R., Valeur, J., Sangnes, D. A., El-Salhy, M., et al. (2019). Clinical response to fecal microbiota transplantation in patients with diarrhea-predominant irritable bowel syndrome is associated with normalization of fecal microbiota composition and short-chain fatty acid levels. *Scand. J. Gastroenterol.* 54, 690–699. doi: 10.1080/00365521.2019.1624815

McKinney, C. A., Oliveira, B. C. M., Bedenice, D., Paradis, M. R., Mazan, M., Sage, S., et al. (2020). The fecal microbiota of healthy donor horses and geriatric recipients undergoing fecal microbial transplantation for the treatment of diarrhea. *PLoS One* 15:e0230148. doi: 10.1371/journal.pone.0230148

Mei, L., Zhou, J., Su, Y., Mao, K., Wu, J., Zhu, C., et al. (2021). Gut microbiota composition and functional prediction in diarrhea-predominant irritable bowel syndrome. *BMC Gastroenterol.* 21:105. doi: 10.1186/s12876-021-01693-w

Min, S. J., Kim, H., Yambe, N., and Shin, M. S. (2024). Ameliorative effects of Korean-red-ginseng-derived polysaccharide on antibiotic-associated diarrhea. *Polymers (Basel).* 16:231. doi: 10.3390/polym16020231

Mizutani, T., Aboagye, S. Y., Ishizaka, A., Afum, T., Mensah, G. I., Asante-Poku, A., et al. (2021). Gut microbiota signature of pathogen-dependent dysbiosis in viral gastroenteritis. *Sci. Rep.* 11:13945. doi: 10.1038/s41598-021-93345-y

Morais, L. H., Schreiber, H. L. T., and Mazmanian, S. K. (2021). The gut microbiota-brain axis in behaviour and brain disorders. *Nat. Rev. Microbiol.* 19, 241–255. doi: 10.1038/s41579-020-00460-0

Morrison, D. J., and Preston, T. (2016). Formation of short chain fatty acids by the gut microbiota and their impact on human metabolism. *Gut Microbes* 7, 189–200. doi: 10.1080/19490976.2015.1134082

Murtaza, N., Nawaz, M., Yaqub, T., and Mehmood, A. K. (2024). Impact of Limosilactobacillus fermentum probiotic treatment on gut microbiota composition in sahiwal calves with rotavirus diarrhea: a 16S metagenomic analysis study. *BMC Microbiol.* 24:114. doi: 10.1186/s12866-024-03254-z

Navez, M., Antoine, C., Laforêt, F., Goya-Jorge, E., Douny, C., Scippo, M. L., et al. (2023). In vitro effect on piglet gut microbiota and in vivo assessment of newly isolated bacteriophages against F18 enterotoxigenic *Escherichia coli* (ETEC). *Viruses* 15:1053. doi: 10.3390/v15051053

Niu, Y., Li, J., Qian, H., Liang, C., Shi, X., and Bu, S. (2024). Evaluation of efficacy and safety of *Lacticaseibacillus rhamnosus* LRa05 in the eradication of *Helicobacter pylori*: a randomized, double-blind, placebo-controlled trial. *Front. Immunol.* 15:1450414. doi: 10.3389/fimmu.2024.1450414

Nobrega, F. L., Costa, A. R., Santos, J. F., Siliakus, M. F., van Lent, J. W., Kengen, S. W., et al. (2016). Genetically manipulated phages with improved pH resistance for oral administration in veterinary medicine. *Sci. Rep.* 6:39235. doi: 10.1038/srep39235

Ouyang, Y. W., Li, Z. T., Lv, J., Zhao, G. H., Wang, Y. L., and Cui, X. Y. (2022). Effect of fecal microbiota transplantation on 5-HT signaling pathway in the brain-gut axis of rats with diarrhea-type irritable bowel syndrome model. *Int. J. Lab. Med.* 43, 1994–1999. doi: 10.3969/j.issn.1673-4130.2022.16.01

Pang, F., Long, Q., and Wei, M. (2023). Immune evasion strategies of bovine viral diarrhea virus. *Front. Cell. Infect. Microbiol.* 13:1282526. doi: 10.3389/fcimb.2023.1282526

Parada Venegas, D., De la Fuente, M. K., Landskron, G., González, M. J., Quera, R., Dijkstra, G., et al. (2019). Short chain fatty acids (SCFAs)-mediated gut epithelial and immune regulation and its relevance for inflammatory bowel diseases. *Front. Immunol.* 10:277. doi: 10.3389/fimmu.2019.00277

Paul, J. K., Azmal, M., Haque, A., Meem, M., Talukder, O. F., and Ghosh, A. (2025). Unlocking the secrets of the human gut microbiota: comprehensive review on its role in different diseases. *World J. Gastroenterol.* 31:99913. doi: 10.3748/wjg.v31.i5.99913

Peng, H., Wang, Y., and Luo, W. (2020). Multifaceted role of branched-chain amino acid metabolism in cancer. *Oncogene* 39, 6747–6756. doi: 10.1038/s41388-020-01480-z

Pereira, G. Q., Gomes, L. A., Santos, I. S., Alfieri, A. F., Weese, J. S., and Costa, M. C. (2018). Fecal microbiota transplantation in puppies with canine parvovirus infection. *J. Vet. Intern. Med.* 32, 707–711. doi: 10.1111/jvim.15072

Pi, Y., Wu, Y., Zhang, X., Lu, D., Han, D., Zhao, J., et al. (2023). Gut microbiota-derived ursodeoxycholic acid alleviates low birth weight-induced colonic inflammation by enhancing M2 macrophage polarization. *Microbiome* 11:19. doi: 10.1186/s40168-022-01458-x

Pilla, R., and Suchodolski, J. S. (2019). The role of the canine gut microbiome and metabolome in health and gastrointestinal disease. *Front. Vet. Sci.* 6:498. doi: 10.3389/fvets.2019.00498

Quaglio, A. E. V., Grillo, T. G., De Oliveira, E. C. S., Di Stasi, L. C., and Sassaki, L. Y. (2022). Gut microbiota, inflammatory bowel disease and colorectal cancer. *World J. Gastroenterol.* 28, 4053–4060. doi: 10.3748/wjg.v28.i30.4053

Raimondi, F., Santoro, P., Barone, M. V., Pappacoda, S., Barretta, M. L., Nanayakkara, M., et al. (2008). Bile acids modulate tight junction structure and barrier function of Caco-2 monolayers via EGFR activation. *Am. J. Physiol. Gastrointest. Liver Physiol.* 294, G906–G913. doi: 10.1152/ajpgi.00043.2007

Ramirez, J., Guarner, F., Bustos Fernandez, L., Maruy, A., Sdepanian, V. L., and Cohen, H. (2020). Antibiotics as major disruptors of gut microbiota. *Front. Cell. Infect. Microbiol.* 10:572912. doi: 10.3389/fcimb.2020.572912

Ren, S., Wang, C., Chen, A., Lv, W., and Gao, R. (2022). The probiotic *Lactobacillus paracasei* ameliorates diarrhea cause by *Escherichia coli* O(8) via gut microbiota modulation(1). *Front. Nutr.* 9:878808. doi: 10.3389/fnut.2022.878808

Ren, M., Zhang, S., Liu, X., Li, S., Mao, X., Zeng, X., et al. (2016). Different lipopolysaccharide branched-chain amino acids modulate porcine intestinal endogenous β-defensin expression through the Sirt1/ERK/90RSK pathway. *J. Agric. Food Chem.* 64, 3371–3379. doi: 10.1021/acs.jafc.6b00968

Ren, M., Zhang, S. H., Zeng, X. F., Liu, H., and Qiao, S. Y. (2015). Branched-chain amino acids are beneficial to maintain growth performance and intestinal immune-related function in weaned piglets fed protein restricted diet. *Asian Australas. J. Anim. Sci.* 28, 1742–1750. doi: 10.5713/ajas.14.0131

Rengarajan, S., Knoop, K. A., Rengarajan, A., Chai, J. N., Grajales-Reyes, J. G., Samineni, V. K., et al. (2020). A potential role for stress-induced microbial alterations in IgA-associated irritable bowel syndrome with diarrhea. *Cell Rep Med.* 1:100124. doi: 10.1016/j.xcrm.2020.100124

Riccio, P., and Rossano, R. (2020). The human gut microbiota is neither an organ nor a commensal. *FEBS Lett.* 594, 3262–3271. doi: 10.1002/1873-3468.13946

Ridlon, J. M., Harris, S. C., Bhowmik, S., Kang, D. J., and Hylemon, P. B. (2016). Consequences of bile salt biotransformations by intestinal bacteria. *Gut Microbes* 7, 22–39. doi: 10.1080/19490976.2015.1127483

Roshan, N., Clancy, A. K., and Borody, T. J. (2020). Faecal microbiota transplantation is effective for the initial treatment of *Clostridium difficile* infection: a retrospective clinical review. *Infect. Dis. Ther.* 9, 935–942. doi: 10.1007/s40121-020-00339-w

Sah, D. K., Arjunan, A., Park, S. Y., and Jung, Y. D. (2022). Bile acids and microbes in metabolic disease. *World J. Gastroenterol.* 28, 6846–6866. doi: 10.3748/wjg.v28.i48.6846

Sánchez, B., Delgado, S., Blanco-Míguez, A., Lourenço, A., Gueimonde, M., and Margolles, A. (2017). Probiotics, gut microbiota, and their influence on host health and disease. *Mol. Nutr. Food Res.* 61:10. doi: 10.1002/mnfr.201600240

Sarathy, J., Detloff, S. J., Ao, M., Khan, N., French, S., Sirajuddin, H., et al. (2017). The Yin and Yang of bile acid action on tight junctions in a model colonic epithelium. *Physiol. Rep.* 5:e13294. doi: 10.14814/phy2.13294

Sarker, S. A., Berger, B., Deng, Y., Kieser, S., Foata, F., Moine, D., et al. (2017). Oral application of *Escherichia coli* bacteriophage: safety tests in healthy and diarrheal children from Bangladesh. *Environ. Microbiol.* 19, 237–250. doi: 10.1111/1462-2920.13574

Sarker, S. A., and Brüssow, H. (2016). From bench to bed and back again: phage therapy of childhood *Escherichia coli* diarrhea. *Ann. N. Y. Acad. Sci.* 1372, 42–52. doi: 10.1111/nyas.13087

Sarker, S. A., Sultana, S., Reuteler, G., Moine, D., Descombes, P., Charton, F., et al. (2016). Oral phage therapy of acute bacterial diarrhea with two Coliphage preparations: a randomized trial in children from Bangladesh. *EBioMedicine* 4, 124–137. doi: 10.1016/j.ebiom.2015.12.023

Satitsri, S., Pongkorpsakol, P., Srimanote, P., Chatsudthipong, V., and Muanprasat, C. (2016). Pathophysiological mechanisms of diarrhea caused by the *Vibrio cholerae* O1 El Tor variant: an in vivo study in mice. *Virulence* 7, 789–805. doi: 10.1080/21505594.2016.1192743

Schiller, L. R., Pardi, D. S., and Sellin, J. H. (2017). Chronic diarrhea: diagnosis and management. *Clin. Gastroenterol. Hepatol.* 15, 182–193.e3. doi: 10.1016/j.cgh.2016.07.028

Sezer, A., Usta, U., and Cicin, I. (2009). The effect of Saccharomyces boulardii on reducing irinotecan-induced intestinal mucositis and diarrhea. *Med. Oncol.* 26, 350–357. doi: 10.1007/s12032-008-9128-1

Shao, H., Zhang, C., Xiao, N., and Tan, Z. (2020). Gut microbiota characteristics in mice with antibiotic-associated diarrhea. *BMC Microbiol.* 20:313. doi: 10.1186/s12866-020-01999-x

Shchikota, A. M., Pogonchenkova, I. V., Turova, E. A., Starodubova, A. V., and Nosova, N. V. (2021). COVID-19-associated diarrhea. *Vopr. Pitan.* 90, 18–30. doi: 10.33029/0042-8833-2021-90-6-18-30

Shen, J., Zhang, B., Chen, J., Cheng, J., Wang, J., Zheng, X., et al. (2022). SAHA alleviates diarrhea-predominant irritable bowel syndrome through regulation of the p-STAT3/SERT/5-HT signaling pathway. *J. Inflamm. Res.* 15, 1745–1756. doi: 10.2147/jir.S331303

Shen, J., Zhang, J., Mo, L., Li, Y., Li, Y., Li, C., et al. (2023). Large-scale phage cultivation for commensal human gut bacteria. *Cell Host Microbe* 31, 665–677.e7. doi: 10.1016/j.chom.2023.03.013

Shi, L. T., Peng, Z. Y., Tan, Q., Yin, J. L., Chen, C. Q., and Li, G. X. (2023). Progress of the study on the addition and subtraction of SiniSan to mediate the intestinal mucosal barrier against diarrhea-type irritable bowel syndrome. *Asia-Pacific Traditional Medicine.* 19, 218–222. doi: 10.11954/ytctyy.202304048

Shi, Z., Wang, Y., Yan, X., Ma, X., Duan, A., Hassan, F.u., et al. (2023). Metagenomic and metabolomic analyses reveal the role of gut microbiome-associated metabolites in diarrhea calves. *mSystems* 8:e0058223. doi: 10.1128/msystems.00582-23

Shin, D. Y., Yi, D. Y., Jo, S., Lee, Y. M., Kim, J. H., Kim, W., et al. (2020). Effect of a new *Lactobacillus plantarum* product, LRCC5310, on clinical symptoms and virus reduction in children with rotaviral enteritis. *Medicine (Baltimore)* 99:e22192. doi: 10.1097/md.0000000000022192

Singh, V., Lee, G., Son, H., Koh, H., Kim, E. S., Unno, T., et al. (2022). Butyrate producers, "The sentinel of gut": their intestinal significance with and beyond butyrate, and prospective use as microbial therapeutics. *Front. Microbiol.* 13:1103836. doi: 10.3389/fmicb.2022.1103836

Song, M., Zhang, Z., Li, Y., Xiang, Y., and Li, C. (2023). Midgut microbiota affects the intestinal barrier by producing short-chain fatty acids in *Apostichopus japonicus*. *Front. Microbiol.* 14:1263731. doi: 10.3389/fmicb.2023.1263731

Spencer, N. J., and Hu, H. (2020). Enteric nervous system: sensory transduction, neural circuits and gastrointestinal motility. *Nat. Rev. Gastroenterol. Hepatol.* 17, 338–351. doi: 10.1038/s41575-020-0271-2

Spiegelhauer, M. R., Offersen, S. M., Mao, X., Gambino, M., Sandris Nielsen, D., Nguyen, D. N., et al. (2025). Protection against experimental necrotizing enterocolitis by fecal filtrate transfer requires an active donor virome. *Gut Microbes* 17:2486517. doi: 10.1080/19490976.2025.2486517

Steyer, A., Mičetić-Turk, D., and Fijan, S. (2022). The efficacy of probiotics as antiviral agents for the treatment of rotavirus gastrointestinal infections in children: An updated overview of literature. *Microorganisms* 10:2392. doi: 10.3390/microorganisms10122392

Stipanuk, M. H. (2007). Leucine and protein synthesis: mTOR and beyond. *Nutr. Rev.* 65, 122–129. doi: 10.1111/j.1753-4887.2007.tb00289.x

Stockmann, C., Pavia, A. T., Graham, B., Vaughn, M., Crisp, R., Poritz, M. A., et al. (2017). Detection of 23 gastrointestinal pathogens among children who present with diarrhea. *J. Pediatr. Infect. Dis. Soc.* 6, 231–238. doi: 10.1093/jpids/piw020

Strathdee, S. A., Hatfull, G. F., Mutalik, V. K., and Schooley, R. T. (2023). Phage therapy: from biological mechanisms to future directions. *Cell* 186, 17–31. doi: 10.1016/j.cell.2022.11.017

Su, W., Gong, T., Jiang, Z., Lu, Z., and Wang, Y. (2022). The role of probiotics in alleviating Postweaning diarrhea in piglets from the perspective of intestinal barriers. *Front. Cell. Infect. Microbiol.* 12:883107. doi: 10.3389/fcimb.2022.883107

Sun, X., Gao, Y., Wang, X., Hu, G., Wang, Y., Feng, B., et al. (2019). *Escherichia coli* O(101)-induced diarrhea develops gut microbial dysbiosis in rats. *Exp. Ther. Med.* 17, 824–834. doi: 10.3892/etm.2018.6997

Sun, Y. Y., Li, M., Li, Y. Y., Li, L. X., Zhai, W. Z., Wang, P., et al. (2018). The effect of *Clostridium butyricum* on symptoms and fecal microbiota in diarrhea-dominant irritable bowel syndrome: a randomized, double-blind, placebo-controlled trial. *Sci. Rep.* 8:2964. doi: 10.1038/s41598-018-21241-z

Sun, Y., Qu, Q., Huang, Y., Zhou, S., Xiang, H., and Wang, W. (2025). Isolation, characterization and therapeutic efficacy of lytic bacteriophage ZK22 against *Salmonella Typhimurium* in mice. *BMC Microbiol.* 25:39. doi: 10.1186/s12866-025-03772-4

Takeuchi, T., Miyauchi, E., Kanaya, T., Kato, T., Nakanishi, Y., Watanabe, T., et al. (2021). Acetate differentially regulates IgA reactivity to commensal bacteria. *Nature* 595, 560–564. doi: 10.1038/s41586-021-03727-5

Takiishi, T., Fenero, C. I. M., and Câmara, N. O. S. (2017). Intestinal barrier and gut microbiota: shaping our immune responses throughout life. *Tissue Barriers.* 5:e1373208. doi: 10.1080/21688370.2017.1373208

Tang, W., Chen, D., Yu, B., He, J., Huang, Z., Zheng, P., et al. (2020). Capsulized faecal microbiota transplantation ameliorates post-weaning diarrhoea by modulating the gut microbiota in piglets. *Vet. Res.* 51:55. doi: 10.1186/s13567-020-00779-9

Tian, P., Gao, J., Liang, L., Cui, B., Hu, Q., Zhou, W., et al. (2022). Fecal microbiota transplantation could improve chronic diarrhea in Cynomolgus monkey by alleviating inflammation and modulating gut microbiota. *Biomedicine* 10:3016. doi: 10.3390/biomedicines10123016

Tomita, T., Fukui, H., Okugawa, T., Nakanishi, T., Mieno, M., Nakai, K., et al. (2023). Effect of *Bifidobacterium bifidum* G9-1 on the intestinal environment and diarrhea-predominant irritable bowel syndrome (IBS-D)-like symptoms in patients with quiescent Crohn's disease: a prospective pilot study. *J. Clin. Med.* 12:3368. doi: 10.3390/jcm12103368

Tong, L. C., Wang, Y., Wang, Z. B., Liu, W. Y., Sun, S., Li, L., et al. (2016). Propionate ameliorates dextran sodium sulfate-induced colitis by improving intestinal barrier function and reducing inflammation and oxidative stress. *Front. Pharmacol.* 7:253. doi: 10.3389/fphar.2016.00253

Tropini, C., Moss, E. L., Merrill, B. D., Ng, K. M., Higginbottom, S. K., Casavant, E. P., et al. (2018). Transient osmotic perturbation causes Long-term alteration to the gut microbiota. *Cell* 173, 1742–1754.e17. doi: 10.1016/j.cell.2018.05.008

Tubau-Juni, N., Bassaganya-Riera, J., Leber, A. J., Alva, S. S., Baker, R., and Hontecillas, R. (2023). Modulation of colonic immunometabolic responses during Clostridioides difficile infection ameliorates disease severity and inflammation. *Sci. Rep.* 13:14708. doi: 10.1038/s41598-023-41847-2

Tuniyazi, M., Tang, R., Hu, X., Fu, Y., and Zhang, N. (2024). Carbonate buffer mixture and fecal microbiota transplantation hold promising therapeutic effects on oligofructose-induced diarrhea in horses. *Front Vet Sci.* 11:1388227. doi: 10.3389/fvets.2024.1388227

Wahlström, A., Kovatcheva-Datchary, P., Ståhlman, M., Bäckhed, F., and Marschall, H. U. (2017). Crosstalk between bile acids and gut microbiota and its impact on Farnesoid X receptor Signalling. *Dig. Dis.* 35, 246–250. doi: 10.1159/000450982

Wang, Z., Guo, Z., Liu, L., Ren, D., Zu, H., Li, B., et al. (2024). Potential probiotic Weizmannia coagulans WC10 improved antibiotic-associated diarrhea in mice by regulating the gut microbiota and metabolic homeostasis. *Probiotics Antimicrob Proteins.* doi: 10.1007/s12602-024-10308-1

Wang, L., Guo, G., Xu, Y., Li, L., Yang, B., Zhao, D., et al. (2024). The effect of fecal microbiota transplantation on antibiotic-associated diarrhea and its impact on gut microbiota. *BMC Microbiol.* 24:160. doi: 10.1186/s12866-024-03261-0

Wang, J., Ji, H., Wang, S., Liu, H., Zhang, W., Zhang, D., et al. (2018a). Probiotic *Lactobacillus plantarum* promotes intestinal barrier function by strengthening the epithelium and modulating gut microbiota. *Front. Microbiol.* 9:1953. doi: 10.3389/fmicb.2018.01953

Wang, L., Lei, J., Zhao, Z., Jia, J., and Wang, L. (2023). Therapeutic effects of paeoniflorin on irritable bowel syndrome in rats. *J. Vet. Sci.* 24:e23. doi: 10.4142/jvs.22083

Wang, Y. F., Liang, F. M., Liu, M., Ding, L. C., Hui, J. J., Xu, H. Y., et al. (2022). Is compromised intestinal barrier integrity responsible for the poor prognosis in critically ill patients with pre-existing hyperglycemia? *Diabetol. Metab. Syndr.* 14:172. doi: 10.1186/s13098-022-00943-5

Wang, F., Mei, X., Wang, Q., Zhao, P., Zhou, Y., Tang, L., et al. (2023). Compound Bacillus alleviates diarrhea by regulating gut microbes, metabolites, and inflammatory responses in pet cats. *Anim Microbiome.* 5:49. doi: 10.1186/s42523-023-00270-8

Wang, Y. Y., Tang, L. J., Li, J., Wang, J., Yan, X., Han, D. P., et al. (2019). Effect of *Lactobacillus casei* on the structure of ileal mucosa and MUC2 content in developmental diarrhea model rats. *J. China Agric. Univ.* 24, 94–101. doi: 10.11841/j.issn.1007-4333.2019.08.11

Wang, T., Teng, K., Liu, G., Liu, Y., Zhang, J., Zhang, X., et al. (2018). *Lactobacillus reuteri* HCM2 protects mice against Enterotoxigenic *Escherichia coli* through modulation of gut microbiota. *Sci. Rep.* 8:17485. doi: 10.1038/s41598-018-35702-y

Wang, Y., Wang, Y., Ding, K., Liu, Y., Liu, D., Chen, W., et al. (2024). Effectiveness of psychobiotic *Bifidobacterium breve* BB05 in managing psychosomatic diarrhea in college students by regulating gut microbiota: a randomized, double-blind, placebo-controlled trial. *Nutrients* 16:106541. doi: 10.3390/nu16131989

Wang, J., Zeng, Y., Wang, S., Liu, H., Zhang, D., Zhang, W., et al. (2018b). Swine-derived probiotic *Lactobacillus plantarum* inhibits growth and adhesion of Enterotoxigenic Escherichia coli and mediates host defense. *Front. Microbiol.* 9:1364. doi: 10.3389/fmicb.2018.01364

Wang, D., Zeng, J., Wujin, C., Ullah, Q., and Su, Z. (2024). *Lactobacillus reuteri* derived from horse alleviates *Escherichia coli*-induced diarrhea by modulating gut microbiota. *Microb. Pathog.* 188:106541. doi: 10.1016/j.micpath.2024.106541

Wang, Y., Zhang, S., Zhou, Q., Meng, M., and Chen, W. (2020). Efficacy of Shenlingbaizhu formula on irritable bowel syndrome: a systematic review. *J. Tradit. Chin. Med.* 40, 897–907. doi: 10.19852/j.cnki.jtcm.2020.06.001

Wei, S., Bahl, M. I., Baunwall, S. M. D., Dahlerup, J. F., Hvas, C. L., and Licht, T. R. (2022). Gut microbiota differs between treatment outcomes early after fecal microbiota transplantation against recurrent Clostridioides difficile infection. *Gut Microbes* 14:2084306. doi: 10.1080/19490976.2022.2084306

Wei, W., Wang, H., Zhang, Y., Zhang, Y., Niu, B., Chen, S., et al. (2021). Faecal bile acids and colonic bile acid membrane receptor correlate with symptom severity of diarrhoea-predominant irritable bowel syndrome: a pilot study. *Dig. Liver Dis.* 53, 1120–1127. doi: 10.1016/j.dld.2021.04.022

Wei, W., Wang, H. F., Zhang, Y., Zhang, Y. L., Niu, B. Y., and Yao, S. K. (2020). Altered metabolism of bile acids correlates with clinical parameters and the gut microbiota in patients with diarrhea-predominant irritable bowel syndrome. *World J. Gastroenterol.* 26, 7153–7172. doi: 10.3748/wjg.v26.i45.7153

Wieërs, G., Belkhir, L., Enaud, R., Leclercq, S., Philippart de Foy, J. M., Dequenne, I., et al. (2019). How probiotics affect the microbiota. *Front. Cell. Infect. Microbiol.* 9:454. doi: 10.3389/fcimb.2019.00454

Wilkins, T., and Sequoia, J. (2017). Probiotics for gastrointestinal conditions: a summary of the evidence. *Am. Fam. Physician* 96, 170–178. Available online at: http://www.aafp.org/afp

Witkowski, M., Weeks, T. L., and Hazen, S. L. (2020). Gut microbiota and cardiovascular disease. *Circ. Res.* 127, 553–570. doi: 10.1161/circresaha.120.316242

Wolf, J., Hubbard, S., Brauer, M., Ambelu, A., Arnold, B. F., Bain, R., et al. (2022). Effectiveness of interventions to improve drinking water, sanitation, and handwashing with soap on risk of diarrhoeal disease in children in low-income and middle-income settings: a systematic review and meta-analysis. *Lancet* 400, 48–59. doi: 10.1016/s0140-6736(22)00937-0

Wu, Y., Li, S., Lv, L., Jiang, S., Xu, L., Chen, H., et al. (2024). Protective effect of *Pediococcus pentosaceus* Li05 on diarrhea-predominant irritable bowel syndrome in rats. *Food Funct.* 15, 3692–3708. doi: 10.1039/d3fo04904c

Wu, H. J., and Wu, E. (2012). The role of gut microbiota in immune homeostasis and autoimmunity. *Gut Microbes* 3, 4–14. doi: 10.4161/gmic.19320

Wu, H., Zhan, K., Rao, K., Zheng, H., Qin, S., Tang, X., et al. (2022). Comparison of five diarrhea-predominant irritable bowel syndrome (IBS-D) rat models in the brain-gut-microbiota axis. *Biomed. Pharmacother.* 149:112811. doi: 10.1016/j.biopha.2022.112811

Xie, W., Song, L., Wang, X., Xu, Y., Liu, Z., Zhao, D., et al. (2021). A bovine lactoferricin-lactoferrampin-encoding *Lactobacillus reuteri* CO21 regulates the intestinal mucosal immunity and enhances the protection of piglets against enterotoxigenic *Escherichia coli* K88 challenge. *Gut Microbes* 13:1956281. doi: 10.1080/19490976.2021.1956281

Xu, Y., Jing, H., Wang, J., Zhang, S., Chang, Q., Li, Z., et al. (2022). Disordered gut microbiota correlates with altered fecal bile acid metabolism and post-cholecystectomy diarrhea. *Front. Microbiol.* 13:800604. doi: 10.3389/fmicb.2022.800604

Xu, R., Lei, Y. H., Shi, J., Zhou, Y. J., Chen, Y. W., and He, Z. J. (2016). Effects of lactadherin on plasma D-lactic acid and small intestinal MUC2 and claudin-1 expression levels in rats with rotavirus-induced diarrhea. *Exp. Ther. Med.* 11, 943–950. doi: 10.3892/etm.2016.3015

Xu, B., Liang, S., Zhao, J., Li, X., Guo, J., Xin, B., et al. (2022). *Bifidobacterium animalis* subsp. lactis XLTG11 improves antibiotic-related diarrhea by alleviating inflammation, enhancing intestinal barrier function and regulating intestinal flora. *Food Funct.* 13, 6404–6418. doi: 10.1039/d1fo04305f

Xu, C., Peng, K., She, Y., Fu, F., Shi, Q., Lin, Y., et al. (2023). Preparation of novel trivalent vaccine against enterotoxigenic *Escherichia coli* for preventing newborn piglet diarrhea. *Am. J. Vet. Res.* 84, 1–9. doi: 10.2460/ajvr.22.10.0183

Xu, H., Wang, S., Jiang, Y., Wu, J., Chen, L., Ding, Y., et al. (2023). Poria cocos polysaccharide ameliorated antibiotic-associated diarrhea in mice via regulating the

homeostasis of the gut microbiota and intestinal mucosal barrier. *Int. J. Mol. Sci.* 24:ajvr.22.10.0183. doi: 10.3390/ijms24021423

Xu, B., Wang, Z., Wang, Y., Zhang, K., Li, J., Zhou, L., et al. (2024). Milk-derived Lactobacillus with high production of short-chain fatty acids relieves antibiotic-induced diarrhea in mice. *Food Funct.* 15, 5329–5342. doi: 10.1039/d3fo04706g

Xu, Y., Wang, J., Wu, X., Jing, H., Zhang, S., Hu, Z., et al. (2023). Gut microbiota alteration after cholecystectomy contributes to post-cholecystectomy diarrhea via bile acids stimulating colonic serotonin. *Gut Microbes* 15:2168101. doi: 10.1080/19490976.2023.2168101

Yan, Z., Liu, Z., Ma, Y., Yang, Z., Liu, G., and Fang, J. (2023). Effects of Lactobacillus plantarum and *Weissella viridescens* on the gut microbiota and serum metabolites of mice with antibiotic-associated diarrhea. *Nutrients* 15:4603. doi: 10.3390/nu15214603

Yang, Y., Du, H., Zou, G., Song, Z., Zhou, Y., Li, H., et al. (2023). Encapsulation and delivery of phage as a novel method for gut flora manipulation in situ: a review. *J. Control. Release* 353, 634–649. doi: 10.1016/j.jconrel.2022.11.048

Yang, Q., Hu, Z., Lei, Y., Li, X., Xu, C., Zhang, J., et al. (2023). Overview of systematic reviews of probiotics in the prevention and treatment of antibiotic-associated diarrhea in children. *Front. Pharmacol.* 14:1153070. doi: 10.3389/fphar.2023.1153070

Yang, B., Huang, Z., He, Z., Yue, Y., Zhou, Y., Ross, R. P., et al. (2021a). Protective effect of *Bifidobacterium bifidum* FSDJN7O5 and *Bifidobacterium breve* FHNFQ23M3 on diarrhea caused by enterotoxigenic *Escherichia coli*. *Food Funct.* 12, 7271–7282. doi: 10.1039/d1fo00504a

Yang, N., Ma, T., Xie, Y., Li, Q., Li, Y., Zheng, L., et al. (2024). Lactiplantibacillus plantarum P9 for chronic diarrhea in young adults: a large double-blind, randomized, placebo-controlled trial. *Nat. Commun.* 15:6823. doi: 10.1038/s41467-024-51094-2

Yang, B., Yue, Y., Chen, Y., Ding, M., Li, B., Wang, L., et al. (2021b). *Lactobacillus plantarum* CCFM1143 alleviates chronic diarrhea via inflammation regulation and gut microbiota modulation: a double-blind, randomized, placebo-controlled study. *Front. Immunol.* 12:746585. doi: 10.3389/fimmu.2021.746585

Yang, L., Zhang, Q., Huang, J., Liu, D., Lan, Y., Yuan, L., et al. (2021). Xianglian pill ameliorates antibiotic-associated diarrhea by restoring intestinal microbiota and attenuating mucosal damage. *J. Ethnopharmacol.* 264:113377. doi: 10.1016/j.jep.2020.113377

Yao, D., Dai, W., Dong, M., Dai, C., and Wu, S. (2021). MUC2 and related bacterial factors: therapeutic targets for ulcerative colitis. *EBioMedicine* 74:103751. doi: 10.1016/j.ebiom.2021.103751

Yau, Y. K., Su, Q., Xu, Z., Tang, W., Ching, J. Y. L., Mak, J. W. Y., et al. (2023). Randomised clinical trial: Faecal microbiota transplantation for irritable bowel syndrome with diarrhoea. *Aliment. Pharmacol. Ther.* 58, 795–804. doi: 10.1111/apt.17703

Youssef, R. A., Sakr, M. M., Shebl, R. I., and Aboshanab, K. M. (2025). Recent insights on challenges encountered with phage therapy against gastrointestinal-associated infections. *Gut Pathog.* 17:60. doi: 10.1186/s13099-025-00735-y

Yu, H., Nie, R., and Shen, C. (2023). The role of bile acids in regulating glucose and lipid metabolism. *Endocr. J.* 70, 359–374. doi: 10.1507/endocrj.EJ22-0544

Yue, Y., He, Z., Zhou, Y., Ross, R. P., Stanton, C., Zhao, J., et al. (2020). *Lactobacillus plantarum* relieves diarrhea caused by enterotoxin-producing *Escherichia coli* through inflammation modulation and gut microbiota regulation. *Food Funct.* 11, 10362–10374. doi: 10.1039/d0fo02670k

Yue, S. J., Wang, W. X., Yu, J. G., Chen, Y. Y., Shi, X. Q., Yan, D., et al. (2019). Gut microbiota modulation with traditional Chinese medicine: a system biology-driven approach. *Pharmacol. Res.* 148:104453. doi: 10.1016/j.phrs.2019.104453

Zeng, Y., Wang, Z., Zou, T., Chen, J., Li, G., Zheng, L., et al. (2021). Bacteriophage as an alternative to antibiotics promotes growth performance by regulating intestinal inflammation, intestinal barrier function and gut microbiota in weaned piglets. *Front Vet Sci.* 8:623899. doi: 10.3389/fvets.2021.623899

Zhai, L., Huang, C., Ning, Z., Zhang, Y., Zhuang, M., Yang, W., et al. (2023). *Ruminococcus gnavus* plays a pathogenic role in diarrhea-predominant irritable bowel syndrome by increasing serotonin biosynthesis. *Cell Host Microbe* 31, 33–44.e5. doi: 10.1016/j.chom.2022.11.006

Zhan, M., Liang, X., Chen, J., Yang, X., Han, Y., Zhao, C., et al. (2023). Dietary 5-demethylnobiletin prevents antibiotic-associated dysbiosis of gut microbiota and damage to the colonic barrier. *Food Funct.* 14, 4414–4429. doi: 10.1039/d3fo00516j

Zhang, P. (2022). Influence of foods and nutrition on the gut microbiome and implications for intestinal health. *Int. J. Mol. Sci.* 23:9588. doi: 10.3390/ijms23179588

Zhang, M. M., Dang, M., Wu, X., Ou, L., Li, M., Zhao, C. B., et al. (2024). Da-Jian-Zhong decoction alleviates diarrhea-predominant irritable bowel syndrome via modulation of gut microbiota and Th17/Treg balance. *J. Ethnopharmacol.* 331:118275. doi: 10.1016/j.jep.2024.118275

Zhang, Z., Huang, J., Li, C., Zhao, Z., Cui, Y., Yuan, X., et al. (2024). The gut microbiota contributes to the infection of bovine viral diarrhea virus in mice. *J. Virol.* 98:e0203523. doi: 10.1128/jvi.02035-23

Zhang, D., Jian, Y. P., Zhang, Y. N., Li, Y., Gu, L. T., Sun, H. H., et al. (2023). Short-chain fatty acids in diseases. *Cell Commun. Signal* 21:212. doi: 10.1186/s12964-023-01219-9

Zhang, C. Y., Peng, X. X., Shao, H. Q., Li, X. Y., Wu, Y., and Tan, Z. J. (2021). Gut microbiota comparison between intestinal contents and mucosa in mice with repeated stress-related diarrhea provides novel insight. *Front. Microbiol.* 12:626691. doi: 10.3389/fmicb.2021.626691

Zhang, Y., Wang, S., Wang, H., Cao, M., Wang, M., Zhang, B., et al. (2024). Efficacy of donor-recipient-matched faecal microbiota transplantation in patients with IBS-D: a single-Centre, randomized, double-blind placebo-controlled study. *Digestion* 105, 457–467. doi: 10.1159/000540420

Zhao, J., Feng, L., Liu, Y., Jiang, W., Wu, P., Jiang, J., et al. (2014). Effect of dietary isoleucine on the immunity, antioxidant status, tight junctions and microflora in the intestine of juvenile Jian carp (*Cyprinus carpio* var. Jian). *Fish Shellfish Immunol.* 41, 663–673. doi: 10.1016/j.fsi.2014.10.002

Zhao, L., Yang, W., Chen, Y., Huang, F., Lu, L., Lin, C., et al. (2020). A Clostridia-rich microbiota enhances bile acid excretion in diarrhea-predominant irritable bowel syndrome. *J. Clin. Invest.* 130, 438–450. doi: 10.1172/jci130976

Zhen, Y., Chu, C., Zhou, S., Qi, M., and Shu, R. (2015). Imbalance of tumor necrosis factor-α, interleukin-8 and interleukin-10 production evokes barrier dysfunction, severe abdominal symptoms and psychological disorders in patients with irritable bowel syndrome-associated diarrhea. *Mol. Med. Rep.* 12, 5239–5245. doi: 10.3892/mmr.2015.4079

Zhen, Z., Xia, L., You, H., Jingwei, Z., Shasha, Y., Xinyi, W., et al. (2021). An integrated gut microbiota and network pharmacology study on Fuzi-Lizhong pill for treating diarrhea-predominant irritable bowel syndrome. *Front. Pharmacol.* 12:746923. doi: 10.3389/fphar.2021.746923

Zheng, Y. M., He, X. X., Xia, H. H., Yuan, Y., Xie, W. R., Cai, J. Y., et al. (2020). Multi-donor multi-course faecal microbiota transplantation relieves the symptoms of chronic hemorrhagic radiation proctitis: a case report. *Medicine (Baltimore)* 99:e22298. doi: 10.1097/md.0000000000022298

Zhou, Y., Zhang, D., Cheng, H., Wu, J., Liu, J., Feng, W., et al. (2024). Repairing gut barrier by traditional Chinese medicine: roles of gut microbiota. *Front. Cell. Infect. Microbiol.* 14:1389925. doi: 10.3389/fcimb.2024.1389925

Zhu, Y., Luo, Q., Davis, S. M., Westra, C., Vickers, T. J., and Fleckenstein, J. M. (2018). Molecular determinants of Enterotoxigenic *Escherichia coli* heat-stable toxin secretion and delivery. *Infect. Immun.* 86:e00526-18. doi: 10.1128/iai.00526-18

Zhu, S. S., Wang, J. J., Zou, L., Chen, J. Y., Li, K. W., Liao, L. M., et al. (2022). Anti-inflammation effect of moxibustion for rats with diarrhea-predominant irritable bowel syndrome based on multiple miRNAs regulating NF-κB signal pathway. *Zhongguo Zhen Jiu* 42, 654–662. doi: 10.13703/j.0255-2930.20210521-k0002

frontiers | Frontiers in Microbiology

TYPE Original Research
PUBLISHED 31 October 2025
DOI 10.3389/fmicb.2025.1641035

Check for updates

OPEN ACCESS

EDITED BY
Haobin Zhao,
Weifang People's Hospital, China

REVIEWED BY
Soon Yew Tang,
University of Pennsylvania, United States
Wenda Xue,
Nanjing University of Chinese Medicine, China
Priya Raman,
Northeast Ohio Medical University, United States
Boran Zhu,
Nanjing University of Chinese Medicine, China
Yuhong Lin,
The Chinese University of Hong Kong, China

*CORRESPONDENCE
Shuying Feng
✉ fsy@hactcm.edu.cn

RECEIVED 06 June 2025
ACCEPTED 06 October 2025
PUBLISHED 31 October 2025

CITATION
Wang Q, Niu Y, Huang J, Huang J, Zhang J, Zhang B, Guo Z and Feng S (2025) *Amomum tsao-ko Crevost et Lemarie* extract targets the gut-liver axis to combat atherosclerosis in ApoE$^{-/-}$ mice.
Front. Microbiol. 16:1641035.
doi: 10.3389/fmicb.2025.1641035

COPYRIGHT
© 2025 Wang, Niu, Huang, Huang, Zhang, Zhang, Guo and Feng. This is an open-access article distributed under the terms of the Creative Commons Attribution License (CC BY). The use, distribution or reproduction in other forums is permitted, provided the original author(s) and the copyright owner(s) are credited and that the original publication in this journal is cited, in accordance with accepted academic practice. No use, distribution or reproduction is permitted which does not comply with these terms.

Amomum tsao-ko Crevost et Lemarie extract targets the gut-liver axis to combat atherosclerosis in ApoE$^{-/-}$ mice

Qianqian Wang[1,2], Yuanyuan Niu[1], Jiawei Huang[1], Junhong Huang[1], Jiamin Zhang[1], Boyi Zhang[1], Zixuan Guo[1] and Shuying Feng[1,2]*

[1]Medical College, Henan University of Chinese Medicine, Zhengzhou, China, [2]Henan Engineering Research Center for Chinese Medicine Foods for Special Medical Purpose, Zhengzhou, China

Background: *Amomum tsao-ko Crevost et Lemarie* (T-K), a valuable dual-purpose plant used in both medicine and food, exhibits a wide array of bioactivities and pharmacological effects, including the regulation of gastrointestinal function, promotion of weight loss and fat reduction, lowering of blood sugar levels, antioxidant activity. The efficacy of T-K and its underlying mechanism in managing atherosclerosis have rarely been discussed in the literature. This research aimed to evaluate the therapeutic potential of T-K in atherosclerotic mouse models induced by a high-fat high-cholesterol (HFHC) diet and to explore the potential mechanisms involved.

Methods: Atherosclerotic mice were fed with an HFHC diet for 12 weeks, followed by a continuous oral administration of T-K extract via gavage for an additional 8 weeks. Full-length aorta Oil Red O staining, aortic root Oil Red O staining, and hematoxylin–eosin staining of liver tissues were employed to assess the efficacy of T-K. Biochemical methods and enzyme-linked immunosorbent assays were utilized to quantify alterations in inflammatory markers and oxidative stress indicators in serum and liver tissues. 16S rRNA sequencing technology was used to analyze alterations in the composition of the intestinal microbiota in animals following treatment with T-K.

Results: Full-length aorta Oil Red O staining, aortic root Oil Red O staining, and liver hematoxylin–eosin staining effectively evaluated the therapeutic potential of T-K in managing atherosclerosis. Serological tests confirmed T-K's ability to decrease the total serum cholesterol and low-density lipoprotein cholesterol levels. Additionally, gut microbiota showed significant alterations following T-K treatment, which were markedly different from the changes observed after statin therapies. Furthermore, the results from the enzyme-linked immunosorbent assay indicated that T-K significantly reduced inflammation in both the aorta and liver. Oxidative stress assessments revealed that T-K can mitigate oxidative stress and thus improve atherosclerosis.

Conclusion: T-K has demonstrated significant efficacy in the treatment of atherosclerosis, primarily by lowering serum cholesterol levels and modulating intestinal flora at multiple levels to enhance disease management. Moreover, T-K mitigated the disease progression by attenuating oxidative stress and inflammatory responses in both the liver and aorta.

KEYWORDS

atherosclerosis, gut microbiota, oxidative stress, ApoE$^{-/-}$ mice, hepatic inflammation, 16S rRNA sequencing

1 Introduction

Cardiovascular diseases (CVDs) continue to be the leading cause of death worldwide, significantly impacting public health and contributing to excessive healthcare costs. The global incidence of CVDs increased from 271 million (12.1 million death) in 1990 to 523 million (18.6 million death) in 2019, nearly doubling during this period (Roth et al., 2020; Vaduganathan et al., 2022). Atherosclerosis is a major contributor to CVDs globally (Herrington et al., 2016). It is regarded as a multifactorial metabolic condition, with key risk factors comprising hypertension, elevated lipid levels, smoking, diabetes, obesity, and genetic susceptibility (Falk, 2006). The mechanisms underlying atherosclerosis involve multiple factors, such as high cholesterol, inflammation, endothelial dysfunction, immune response, smooth muscle cell dysfunction, and plaque rupture (Libby et al., 2019). In addition, recent studies have increasingly emphasized the role of intestinal microbes in the onset and progression of atherosclerosis (Björkegren and Lusis, 2022). Although pathogenesis of atherosclerosis is complex, multiple treatments are available, including statins that regulate lipid metabolism, antiplatelet drugs, medications that improve endothelial function, and procedures such as stent implantation, interventional surgery, and endarterectomy (Pu et al., 2023; Sahebkar et al., 2023; Wang X. et al., 2025; Wang C. et al., 2025). At present, the use of antiplatelet agents combined with cholesterol-lowering medications, including aspirin and atorvastatin, remains the conventional therapy for atherosclerosis (Castellano et al., 2022; Davidson et al., 2022). Typical treatments in Western medicine for atherosclerosis have shown significant effects in combating atherosclerosis and reducing lipid levels. However, adverse effects, including gastrointestinal discomfort, increased bleeding risk, and potential liver and kidney damage, were observed during treatment, which could restrict their broader clinical use (Thompson, 2016; Ji et al., 2020).

Amomum tsao-ko Crevost et Lemarie (T-K) is processed by sun-drying, stir-frying until it turns to charred golden-yellow, and dehulling. The kernel obtained through this process is then termed as Caoguo Ren in Chinese. This herb has a strong, pungent aroma and is considered warm in nature, primarily acting on the spleen and stomach meridians. Moreover, this herb exerts therapeutic effects, including drying dampness, warming the middle jiao, eliminating phlegm, and intercepting malaria. Clinically, it is used to treat epigastric distension and pain, nausea, vomiting, phlegm-associated cough, and malaria, while also alleviating alcohol toxicity and managing halitosis. Studies have reported that its extract possesses pharmacological activities, including the regulation of gastrointestinal function and possessing antibacterial, anti-inflammatory, hypoglycemic, and lipid-regulating effects. In our study, we aimed to evaluate the efficacy of oral administration of T-K in alleviating atherosclerosis in ApoE knockout (ApoE$^{-/-}$) mice. Given the strong connection between gut microbiota and liver function, we further confirmed how T-K exerts its therapeutic effects by reducing hepatic lipid deposition and inflammatory responses. Using 16S rRNA sequencing and histological techniques, we deeply explored the therapeutic mechanisms of T-K for atherosclerosis in the ApoE$^{-/-}$ mice model.

2 Materials and methods

2.1 Preparation of T-K extract

T-K (batch number: 23060101-1) were procured from Henan Zhangzhongjing Pharmacy Co., Ltd. (Henan, China). Crushed and dried T-K seeds and deionized water were added at a material-to-solvent ratio of 1:20 (g/mL). The extraction was performed by oscillating the mixture in a water bath set to a constant 60 °C for 2 h. After coarse filtration, the filtrate was subjected to centrifugation at 4 °C and 8,000 rpm for 15 min to obtain a clear extract. Subsequently, the extract was concentrated using rotary evaporation and freeze-dried into a powder. The resulting powder was then stored in a sealed container at −20 °C, protecting it from direct light.

2.2 Animal model and drug treatments

Male ApoE$^{-/-}$ mice on a C57BL/6 background (6 weeks old; body weight 20 ± 2 g) were purchased from GemPharmatech Co., Ltd. (Soochow, China; SCXK2023-0009). All mice were housed in a specific pathogen-free environment with ad libitum access to food and water, under controlled conditions of 22–24 °C, 45–60% relative humidity, and a 12-h light/dark cycle. All animal experiments were conducted in accordance with the regulations and guidelines of the Animal Welfare and Ethics Committee of Henan University of Chinese Medicine and were approved by the committee (No. DWLLGZR202303167). A total of 38 mice were randomly assigned to individually ventilated cages (four mice/cage). After a week-long adaptation period, the mice were grouped, and the modeling process commenced. Mice in control (Con) group (n = 11) were fed low-fat low-sugar (LFLS) control diet (TP 26352; 14% protein, 10% fat, and 72% carbohydrates). Mice in model (Mod) group (n = 27) were fed with a high-fat high-cholesterol (HFHC) diet (TP 26304-050; 14% protein, 42% fat, 44% carbohydrates, and 0.5% cholesterol).

After modeling for 12 weeks (Zhang et al., 2021; Wang X. et al., 2025; Wang C. et al., 2025), three mice each from the Mod group and Con group were randomly sacrificed, and the proportion of lipid plaque area to total aortic surface area was quantified using Oil Red O staining (Supplementary Figure 1). Subsequently, 24 mice in from the Mod group were randomly assigned to three subgroups, including Mod group, atorvastatin calcium (ATV) group, and T-K group. The diet of the mice remained unchanged. Con group and Mod group were treated with distilled water, ATV group received 10 mg/kg/d, and the T-K group received 100 mg/kg/d (Zhang et al., 2022). Once-daily intragastric delivery of treatments was carried out over the course of 8 weeks, with a daily dose of 0.1 mL/10 g (Ping et al., 2024). During the final 2 days of experiment, fecal samples were collected, placed into sterile Eppendorf tubes, and subsequently stored at −80 °C. Following the final treatment,

serum samples were collected. After pre-cooling normal saline perfusion, the heart and aorta were collected and then fixed in 4% paraformaldehyde. Liver tissues were immediately excised and processed after sacrifice. Part of liver was fixed in 4% paraformaldehyde, while the remaining tissue was rapidly collected and frozen at −80 °C for future use.

2.3 Materials and reagents

Lipitor (atorvastatin calcium) was purchased from Pfizer Pharmaceutical Co., Ltd. (New York, United States). Kits for measuring triglyceride (TG, A110-1-1), total cholesterol (TC, A111-1-1), high-density lipoprotein (HDL, A112-1-1), low-density lipoprotein (LDL, A113-1-1), aspartate aminotransferase (AST, C010-2-1), alanine aminotransferase (ALT, C009-2-1), reduced glutathione (GSH, A006-2-1) malondialdehyde (MDA, A003-1-2), and superoxide dismutase (SOD, A001-3-2) were supplied by Nanjing Jiancheng Bioengineering Institute (Nanjing, China). BCA protein assay kit (BCA, PC0020), RIPA lysis buffer, and saline (0.9%) were sourced from Solarbio Biotechnology Co., Ltd. (Beijing, China). Polyformaldehyde (4%) was acquired from Biosharp (Anhui, China). Interleukin-1β (IL-1β, kt21178), interleukin-6 (IL-6, kt99854), tumor necrosis factor-α (TNF-α, kt99985), interleukin-17 (IL-17, kt22800) kits were obtained from Moshake Biotechnology Co., Ltd. (Wuhan, China).

2.4 Experimental methods

2.4.1 Assessment of serum and liver biochemical markers

Following collection via enucleation, blood samples were allowed to coagulate at ambient temperature for 40 min. Consequently, samples were centrifuged (3,000 rpm, 10 min, 4 °C) to obtain serum for subsequent analysis. As outlined in prior studies, liver samples were processed into homogenates (Liu F. et al., 2021; Liu L. et al., 2021). The supernatant was then collected for subsequent analysis. Serum levels of TC, TG, HDL, and LDL, as well as liver concentrations of AST, ALT, TC, and TG were determined depending on instructions of the manufacturer.

2.4.2 Assessment of oxidative stress and inflammatory markers in liver and aorta tissue

Aortic tissue samples were homogenized following previously published protocols to obtain tissue homogenates for subsequent analysis (Liu N. et al., 2022; Liu H. et al., 2022). The protein concentration was determined using the BCA assay, with absorbance measured at 562 nm. SOD, GSH activities, and MDA levels in liver and aorta tissue were measured according to the kit instructions. IL-1β, IL-6, TNF-α, and IL-17 were measured in accordance with the manufacturer's instructions.

2.4.3 Atherosclerotic lesion analysis

After the mice were sacrificed, Oil Red O staining was performed on the full-length aortas of four randomly selected mice per group to assess overall lipid deposition. The aorta was carefully dissected under a stereomicroscope to excise surrounding connective tissue, then opened longitudinally. The entire aorta was stained with Oil Red O solution for 10 min and rinsed with 60% isopropyl alcohol for 2 min to remove excess stain. For aortic root analysis, all eight mice in each group were included. The hearts were collected, fixed in 4% paraformaldehyde, embedded in OCT compound, and cryosectioned at a thickness of 5 μm. The sections were subjected to Oil Red O, hematoxylin and eosin (H&E), and Masson's trichrome staining. The stained aortic root sections and whole aorta tissues were scanned and photographed separately. Image-Pro Plus 6.0 software was used to measure the lesion area and collagen-positive area in the aortic root, followed by quantitative analysis (Zhou et al., 2012).

2.4.4 Intestinal injury and liver lesion histology (H&E staining)

Liver and intestinal tissues were subjected to stain following the protocol outlined in prior research (Shi et al., 2021; Yang et al., 2022). The severity of hepatic steatosis was assessed using the NASH Activity Score (NAS) system (Liu F. et al., 2021; Liu L. et al., 2021). In addition, histological features, including steatosis, inflammation, and fibrosis, were evaluated.

2.4.5 Analysis based on 16S rRNA gene sequencing

Following the previously established procedure, the target amplification products were acquired and quantified for use in subsequent sequencing (Lu et al., 2020; Dai et al., 2022). Aata analysis and 16S rRNA gene sequencing were carried out following established methods (Wang Q. et al., 2022; Wang Y. et al., 2022). To explore the functional alterations of gut microbiota, predictive functional profiling was performed using PICRUSt2.

2.4.6 Correlation analysis

To explore potential associations, a correlation analysis was conducted linking physiological indicators, oxidative stress levels, inflammatory cytokines, and gut microbial profiles. The expression correlation coefficients were determined using the Pearson correlation coefficient method. Based on these correlations, a network was constructed to visualize the relationships between these factors.

2.5 Statistical analysis

Quantitative data are presented as mean ± SD. Data normality was assessed using the Shapiro–Wilk test, and homogeneity of variance was evaluated using Levene's test. For data that met both assumptions, one-way ANOVA followed by Tukey's *post hoc* test was used. When the assumption of homogeneity of variance was violated, the Kruskal–Wallis test followed by Dunn's multiple comparisons test was applied. Statistical analyses were performed using SPSS (version 22.0), and graphs were generated with GraphPad Prism (version 9.5.0). A p-value <0.05 was considered statistically significant.

3 Results

3.1 T-K treatment reduced plaque formation in aorta

To assess the anti-atherosclerotic properties of T-K, an ApoE$^{-/-}$ mice model of atherosclerosis was established through a HFHC diet (van Vlijmen et al., 1994). The intake of food and water did not differ significantly across all groups (Supplementary Figure 2). After 12 weeks of modeling, mice in HFHC diet group exhibited a more

10.3389/fmicb.2025.1641035

pronounced rise in body weight contrast to the LFLS group. After 8 weeks of administering T-K, body weight continued to increase, but mice in T-K group exhibited a more gradual gain in body weight relative to the Mod group (Figure 1A). To evaluate lipid accumulation in the entire aorta, en face Oil Red O staining was performed. As shown in Figures 1B,C, the Mod group exhibited increased lipid deposition compared to the Con group. Both ATV and T-K treatment significantly reduced lipid content relative to the Mod group, with no significant difference between ATV and T-K groups ($n = 4$). Histological analysis of aortic root sections ($n = 8$) was further conducted (Figure 1D). H&E staining revealed more extensive plaque formation in the Mod group, while the lesion area was reduced in both the ATV and T-K groups. Consistently, Oil Red O staining (Figure 1E) showed a significant increase in lipid burden in the Mod group compared to the Con group, which was attenuated by ATV and T-K treatment. To assess plaque stability, Masson's trichrome staining was used to evaluate collagen content (Figure 1F). The Mod group exhibited significantly reduced collagen deposition compared to the Con group, whereas both ATV and T-K treatment restored collagen content within the lesions, suggesting improved plaque stability. The results showed

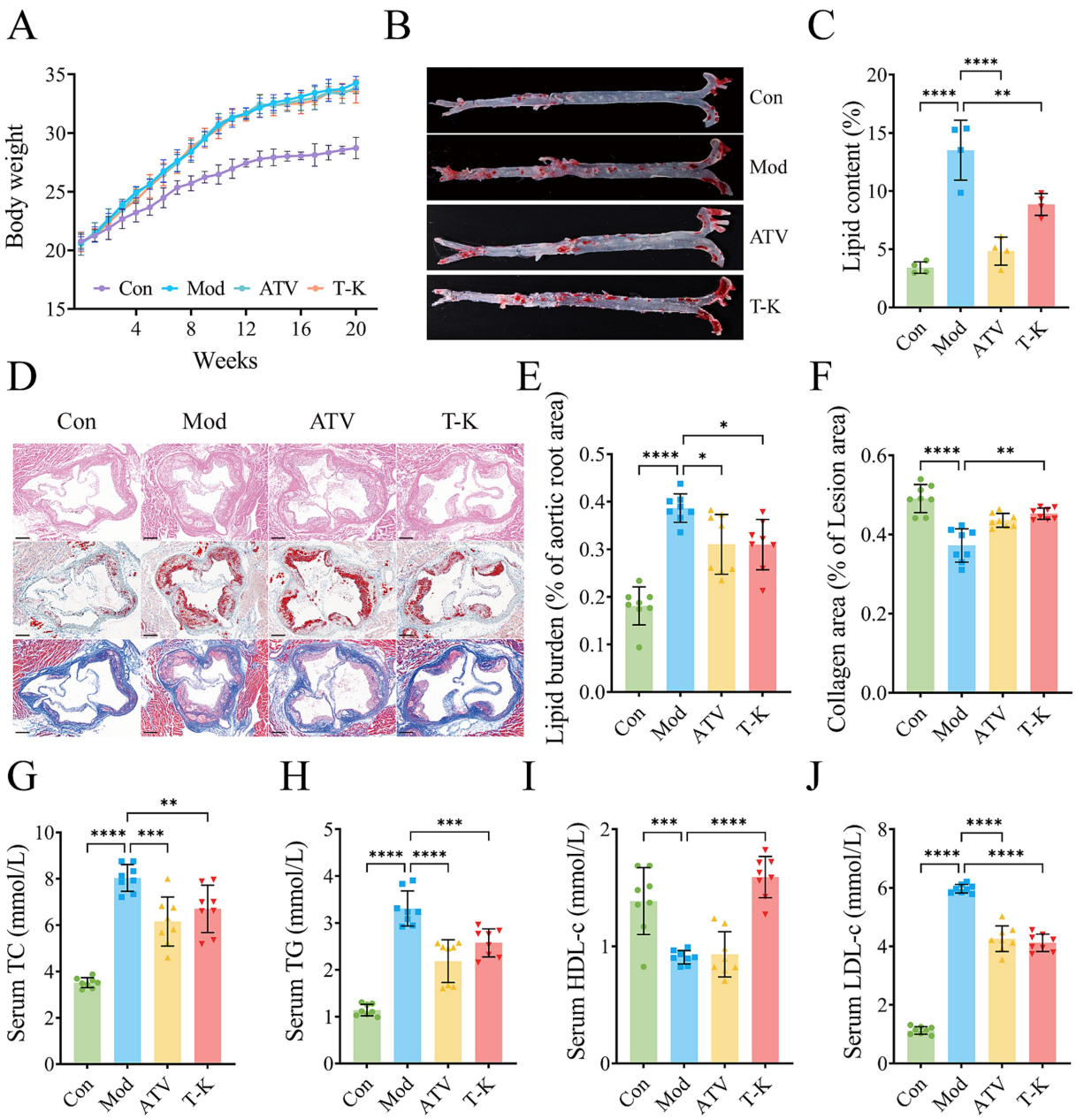

FIGURE 1
Effects of T-K on development of atherosclerotic lesion. **(A)** Body weight changes of mice in each group after different treatments. **(B)** Representative images of Oil Red O staining of aorta. **(C)** Quantitative analysis of plaque area in entire aorta, $n = 4$. **(D)** Represents H&E, Oil Red O, and Masson staining of aortic root sections (scale bar = 200 μm). **(E)** Percentage of lipid burden in aortic root. **(F)** Percentage of collagen area in lesion area. **(G–J)** Represents content determination of total cholesterol, triglyceride, HDL-c, and LDL-c, respectively ($n = 8$). Data are presented as mean ± SD, $^{*}p < 0.05$, $^{**}p < 0.01$, $^{***}p < 0.001$, and $^{****}p < 0.0001$, vs. Mod group.

that T-K treatment has a significant improvement effect on the progression of atherosclerotic plaque formation in ApoE$^{-/-}$ mice.

3.2 T-K regulated lipid metabolism in atherosclerosis mice

Given that atherosclerosis is defined by sustained inflammatory activity in the arterial wall, primarily triggered by lipid accumulation, lipid-lowering therapy remains a fundamental approach in managing atherosclerosis (Libby et al., 2019). Evidence indicates that LDL-C is widely regarded as a causative agent in the onset and progression of CVDs (Penson et al., 2018). As illustrated in Figures 1G–J, serum TC, TG, and LDL levels were elevated, while HDL levels were significantly decreased in the Mod group compared to the Con group ($n = 8$). In contrast, the T-K group exhibited significantly reduced serum TC, TG, and LDL levels along with significantly increased HDL levels when compared to the Mod group. These findings suggest that T-K improved serum lipid profiles and alleviated atherosclerosis in mice.

3.3 T-K reduces oxidative stress and inflammation

The underlying mechanisms of CVDs are closely associated with both oxidative stress and inflammation (Barton et al., 2007; Cheng et al., 2023). Thus, we measured the amounts of MDA, GSH, SOD, TNF-α, IL-6, IL-1β, and IL-17 in liver and abdominal aorta. The results indicated that when compared with LFLS diet of the Con group, HFHC diet substantially raised the levels of MDA ($n = 4$, Supplementary Figure 3A), IL-1β ($n = 4$, Supplementary Figure 3C), TNF-α ($n = 4$, Supplementary Figure 3D), IL-6 ($n = 4$, Figure 2A), and IL-17 ($n = 4$, Supplementary Figure 3E) in aorta of mice at the Mod group. A similar trend was detected in the liver of mice ($n = 8$, Figures 2C–G; Supplementary Figures 3F,G). However, the levels of SOD ($n = 4$, Figure 2B) and GSH ($n = 4$, Supplementary Figure 3B) in aorta of mice in the Mod group were substantially reduced as compared to the Con group. Relative to the Mod group, the T-K group showed certain significance in expression of SOD ($n = 4$, Figure 2B) and IL-6 ($n = 4$, Figure 2A) in aorta. However, it did not show the ability to reduce MDA, SOD, TNF-α, IL-6, IL-1β, and IL-17, and nor did it elevate GSH levels (Figure 2; Supplementary Figure 3B). Test results in mouse livers showed that compared with the Mod group, the T-K group markedly upregulated the expression of MDA ($n = 8$, Figure 2C), IL-6 ($n = 8$, Figure 2F), and IL-17 ($n = 8$, Figure 2G), and substantially elevated SOD levels ($n = 8$, Figure 2D) and GSH ($n = 8$, Figure 2E). No notable alterations were observed in the expression of TNF-α ($n = 8$, Supplementary Figure 3G) and IL-1β ($n = 8$, Supplementary Figure 3F). These findings on oxidative stress and inflammation offer valuable insights for further investigation into the anti-atherosclerotic mechanisms of T-K.

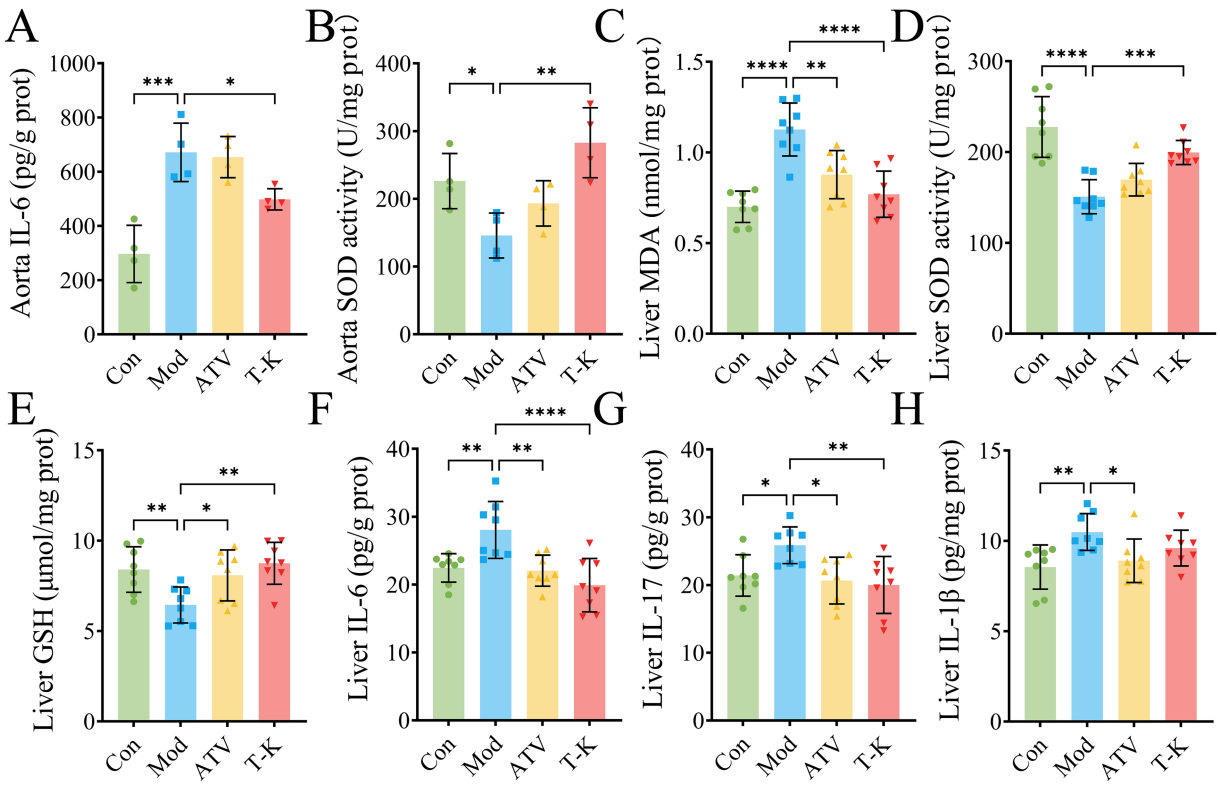

FIGURE 2
T-K decreases the atherosclerosis by diminishing oxidative stress and inflammation in mice. **(A–D)** Represents the levels of IL-6/SOD activity in aorta and MDA/SOD activity in liver, respectively. **(E–H)** Represents the levels of GSH, IL-6, IL-17, and IL-1β in liver, respectively. Data are presented as mean ± SD, $n = 8$, *$p < 0.05$, **$p < 0.01$, ***$p < 0.001$, and ****$p < 0.0001$, vs. Mod group.

3.4 Effects of T-K on histopathology in atherosclerosis mice

As shown by H&E stained liver paraffin sections, HFHC-fed atherosclerosis mice displayed notable histopathological changes in the liver (Figure 3A). Liver tissue of the Mod group mice exhibited extensive hepatocellular steatosis, with cytoplasmic vacuoles of varying sizes observed within the hepatocytes. Ballooning degeneration was evident, characterized by swollen hepatocytes with balloon-like morphology, nucleus centralization, and cytoplasmic vacuolization. Compression of liver sinusoids was noted, and liver cord architecture was disrupted. In addition, focal infiltration of granulocytes and lymphocytes was occasionally observed within liver lobules, suggesting the presence of inflammatory responses and tissue damage. In contrast, the ATV and T-K groups had minimal fat vacuoles, and histological scoring of liver steatosis indicated significant improvement in the pathological features of atherosclerosis in mice (Figures 3A,C). Relative to the Con group, a significant increase in the liver weight index was observed in the Mod group of atherosclerotic mice that was effectively suppressed by T-K and atorvastatin treatments (Figure 3D). Given that T-K's safety requires thorough evaluation, we assessed hepatotoxicity markers following 2 months of drug administration. Specifically, we measured the levels of ALT and AST (n = 8, Figures 3E,F).

H&E staining of mouse colon showed that intestinal gland structure of the Con group was complete, regularly arranged, and the cells were clearly layered, with no evident pathological changes (Figure 3B). In comparison, colon gland morphology of the Mod

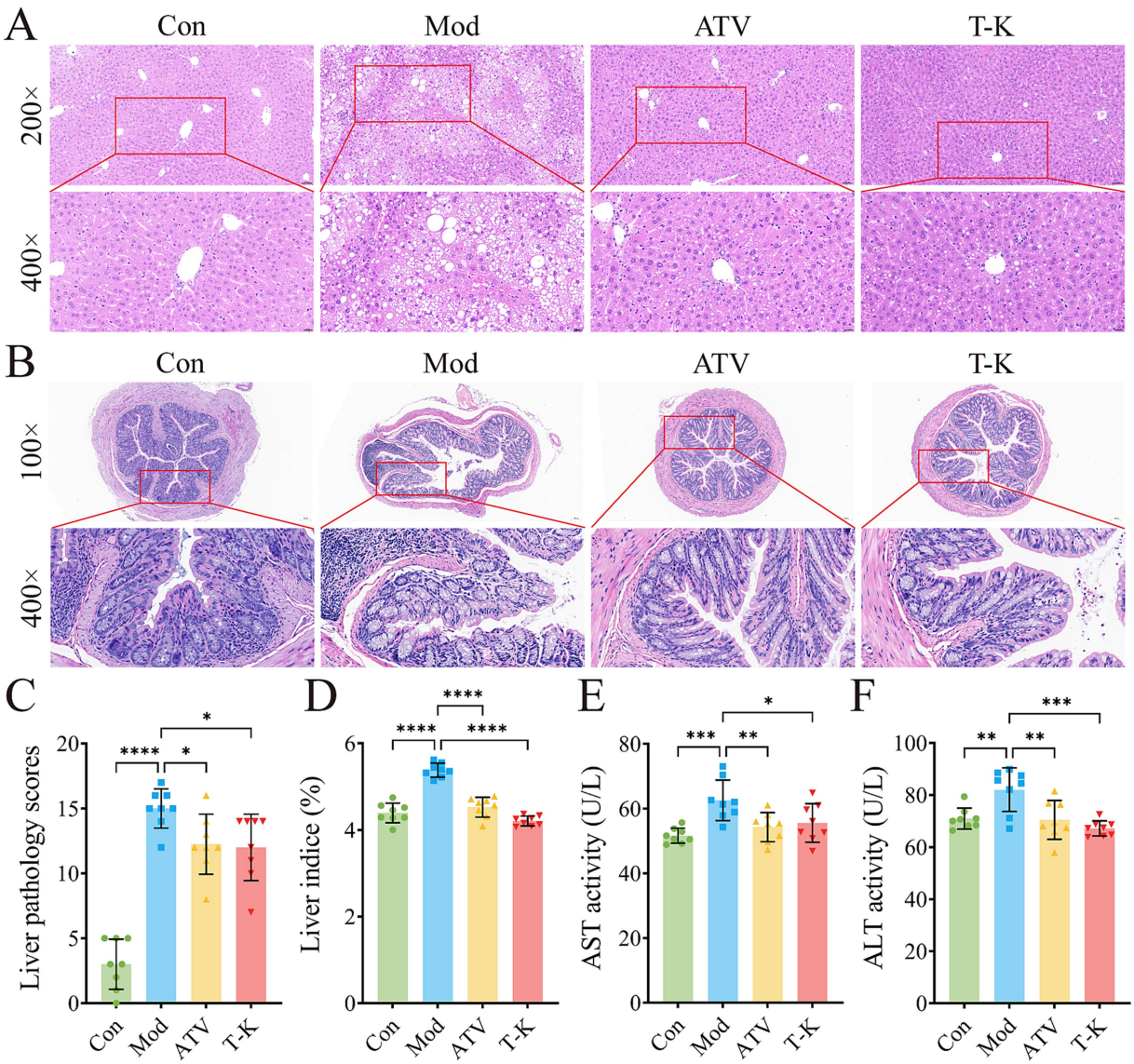

FIGURE 3
Effects of T-K on histopathology of liver and colon in atherosclerotic mice. **(A)** Represents images of liver H&E staining (scale bar is 50 μm and 20 μm separately). **(B)** Represents images of colon H&E staining (scale bars is 100 μm and 20 μm separately). **(C–F)** Represents liver pathology scores, liver weight indexes, ALT, and AST level, respectively. Data are presented as mean ± SD, n = 8, *p < 0.05, **p < 0.01, ***p < 0.001, and ****p < 0.0001, vs. Mod group.

group changed significantly, with expanded glandular spaces, disordered cell arrangement, edema in some areas, and mild inflammatory cell infiltration, suggesting obvious damage or inflammation in intestine. The ATV group showed that colon gland morphology was restored, glands were arranged more regularly, and inflammatory cell infiltration was reduced. Relative to the Mod group, the intestinal tissue structure of the T-K group was relatively complete, glands were tightly arranged, and no significant inflammatory cell infiltration was found, indicating that the drug may have a strong intestinal protective effect and can effectively inhibit the inflammatory response. Overall, the ATV group and the T-K group showed a more significant effect in reducing intestinal inflammatory response and might have contributed positively by modulating the abundance and composition of intestinal microorganisms.

3.5 T-K altered the diversity of the gut microbiota

Alterations in microbial community structure and function have been implicated in numerous disease processes. There is substantial evidence linking gut microbiota-derived processes to the development of atherosclerosis (Witkowski et al., 2020). It is now understood that the gut microbiota influences the progression of atherosclerosis through various mechanisms, for instance, lipid metabolism or other related processes. To investigate these changes, fecal microbiome compositions were analyzed to identify differences and assess the extent of microbiome alterations across different experimental groups. Following the method described earlier, fecal samples were processed for 16S rRNA sequencing ($n = 6$). In Figure 4A, the Shannon curves

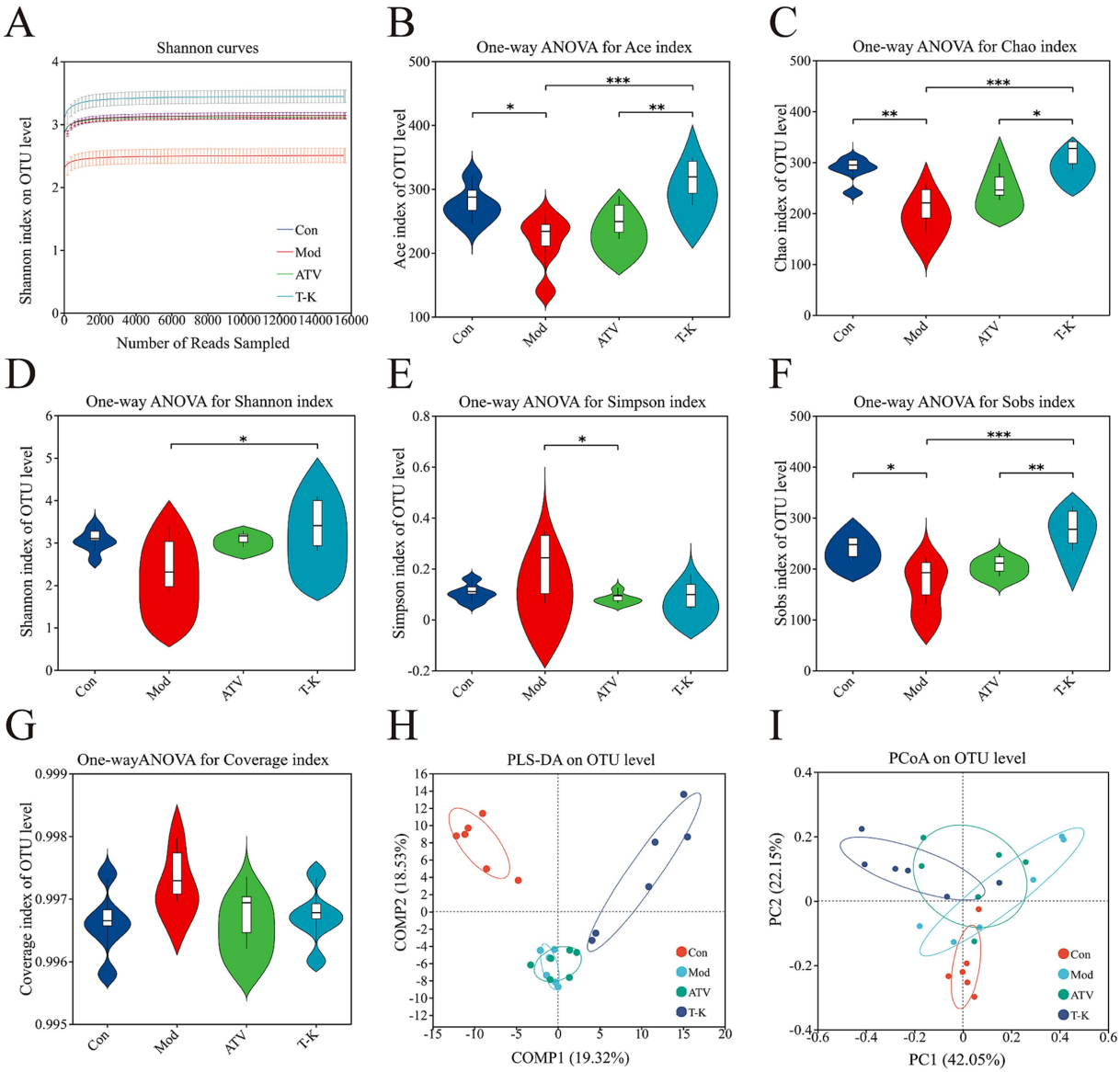

FIGURE 4
Effects of T-K on microbial diversity and community structure in atherosclerotic mice. **(A)** Shannon curves. **(B–G)** Represents the Ace index (reflecting microbial richness), Chao index (indicating species abundance), Shannon index (showing overall microbial diversity), Simpson index (measuring microbial evenness), Sobs index (representing species richness), and Coverage index (indicating sequencing depth and completeness), respectively. **(H,I)** Represents the PLS-DA plot of OTU level (demonstrating distinct clustering of groups) and the PCoA plot of OTU level (showing differences in microbial community composition across the group), respectively ($n = 6$, *$p < 0.05$, **$p < 0.01$, and ***$p < 0.001$, vs. Mod group).

show a tendency to level off, signifying that the test captures most of the microbial composition in the sample.

3.5.1 Alpha diversity

Multiple different alpha diversity analyses, including species observed (Sobs), Shannon–Wiener index (Shannon), Simpson's diversity index (Simpson), Chao1 estimator (Chao1), abundance-based coverage estimator (ACE), and coverage indexes, could reflect the community diversity of gut microbiota. Microbial richness was evaluated using the Sobs, Chao1, and Ace indexes, while microbial diversity was assessed with the Shannon and Simpson indexes. As shown in Figures 4B–E, T-K not only substantially elevated the Ace, Chao1, Sobs, and Shannon indexes of atherosclerosis mice, but the index of T-K group generally exhibited higher values compared to the ATV group, indicating that T-K performed better in terms of microbial richness and diversity and restored the gut microbiota's alpha diversity in mice. The Simpson index of the Mod group is significantly higher, indicating that certain species dominate within this group (Figure 4F). The coverage index can assess the sequencing depth, and the values of these groups approximated 1, indicating successful sequencing and nearly complete coverage of all species within the samples (Figure 4G).

3.5.2 Beta diversity

We further examined the beta diversity to assess how gut microbiota composition differed among the groups. Partial least squares discriminant analysis (PLS-DA) and principal coordinates analysis (PCoA) results (Figures 4H,I) demonstrated a clear distinction among the groups regarding their gut microbiota composition. Notably, as observed in the figure, the groups receiving the T-K treatment formed a distinct cluster, with a clear separation from both the Mod and ATV groups. This indicates that the gut microbiota changes, following the T-K treatment, may exhibit a unique pattern, distinct from the alterations observed in the statin-treated groups.

3.5.3 Gut microbiota abundance

We assessed the relative abundance of taxa at different levels within each group, revealing specific changes in the gut microbiota across the different mouse groups. Figure 5A demonstrated the changes among groups at the phylum levels. *Firmicutes* and *Bacteroidota* were predominant phyla, and T-K decreased both the relative abundance of *Firmicutes* and the ratio of *Firmicutes* to *Bacteroidetes* (Figure 5B), in contrast, the relative abundance of *Bacteroidota* and *Candidatus Melainabacteria* was significantly elevated ($n = 6$, Supplementary Figures 4A,B). Our results demonstrated that T-K corrected intestinal dysbiosis through analysis of F/B ratio for gut microbial dysbiosis (Santisteban et al., 2017). The heatmap of the top 50 genera at the genus level clearly depicts the alterations in gut microbiota composition within each group (Figure 5C). The analysis identified 12 genera that exhibited significant alterations in their abundance (Supplementary Figure 5; Figure 6). We utilized the Disbiome database (Janssens et al., 2018) to extract data on the relationship of these genera with the development of atherosclerotic diseases in humans (Supplementary Table 1). Within available evidence, we identified five genera that showed significant changes in abundance before and after the T-K treatment and were closely associated with atherosclerotic diseases, namely, *Parabacteroides*, *Bacteroides*, *Christensenella*, *Oscillibacter*, and *Alistipes*. Overall, their abundance markedly elevated after the T-K treatment (Figures 5D–H), while the abundance of *Faecalibaculum*, which belongs to the *Lachnospiraceae* family, was significantly decreased.

3.5.4 Gut microbial correlation analysis

T-K treatment significantly altered the gut microbiota composition and abundance in atherosclerotic mice. Concurrently, aortic atherosclerotic area, lipid levels, liver oxidative stress, and body inflammation were improved, showing a favorable trend of change. To figure out whether these favorable changes were associated with gut microbiota alterations, we conducted a correlation analysis between microbiota composition and the above indicators to reveal their potential links. Differences in the fecal microbiota were examined using linear discriminant analysis effect size (LEfSe) (Figure 6A). Pearson's correlation analysis was then performed between the selected genera showing significant differences and the measured indicators (Figure 6B). Among them, relative abundances of *Cuneatibacter* and *Faecalibaculum* were significantly enriched in the Mod group. In addition, *Cuneatibacter* exhibited a significant correlation with serum LDL-C, liver TC, serum TC, and serum TG concentration, and showed a positive association with liver TG levels, while showing an inverse association with liver SOD. *Faecalibaculum* was inversely associated with serum HDL-C levels and exhibited a marked positive relationship with liver MDA concentration. The proportion of *Duncaniella* also displayed significant positive relationships with SOD, liver GSH, and serum HDL-C concentrations. Furthermore, *Duncaniella's* abundance displayed a significant inverse relationship with hepatic ALT, liver MDA, liver IL-17, and liver IL-6 concentrations, and was also negatively correlated with liver AST and liver TG concentrations. Supplementation of T-K significantly enriched the relative abundance of *Christensenella* and *Parabacteroides*. *Christensenella* and *Vampirovibrio* showed positive associations with serum HDL-C concentrations. *Parabacteroides* as well as *Oscillibacter* were negatively associated with liver IL-6 concentrations, while *Oscillibacter* was positively linked positively to serum HDL-C concentrations. *Odoribacter* demonstrated a positive association with liver GSH concentration and serum HDL-C concentration, but exhibited an inverse association with liver ALT, liver MDA, liver IL-17 concentration, and significantly negatively correlated with liver IL-6 concentration. *Alistipes* displayed a positive relationship with serum HDL-C concentrations while showing an inverse relationship with liver ALT, liver IL-17, and liver IL-6 concentrations. *Bacteroides* showed inverse correlations with liver ALT and IL-6 concentrations.

These correlations highlight the interactions between different microbiota and various biomarkers associated with liver function, blood lipids, and inflammation. Collectively, the present findings suggest that the gut microbiota has close associations with these parameters, and alterations in microbial structure and abundance could exert a critical influence on the progression and treatment of atherosclerosis.

3.5.5 Gut microbial functional enrichment analysis

As for functional prediction analysis, PICRUSt2 was used to perform the KEGG pathway annotation and enrichment analysis. At Level 2, a total of 43 functional categories were identified, encompassing major categories such as metabolism, genetic

10.3389/fmicb.2025.1641035

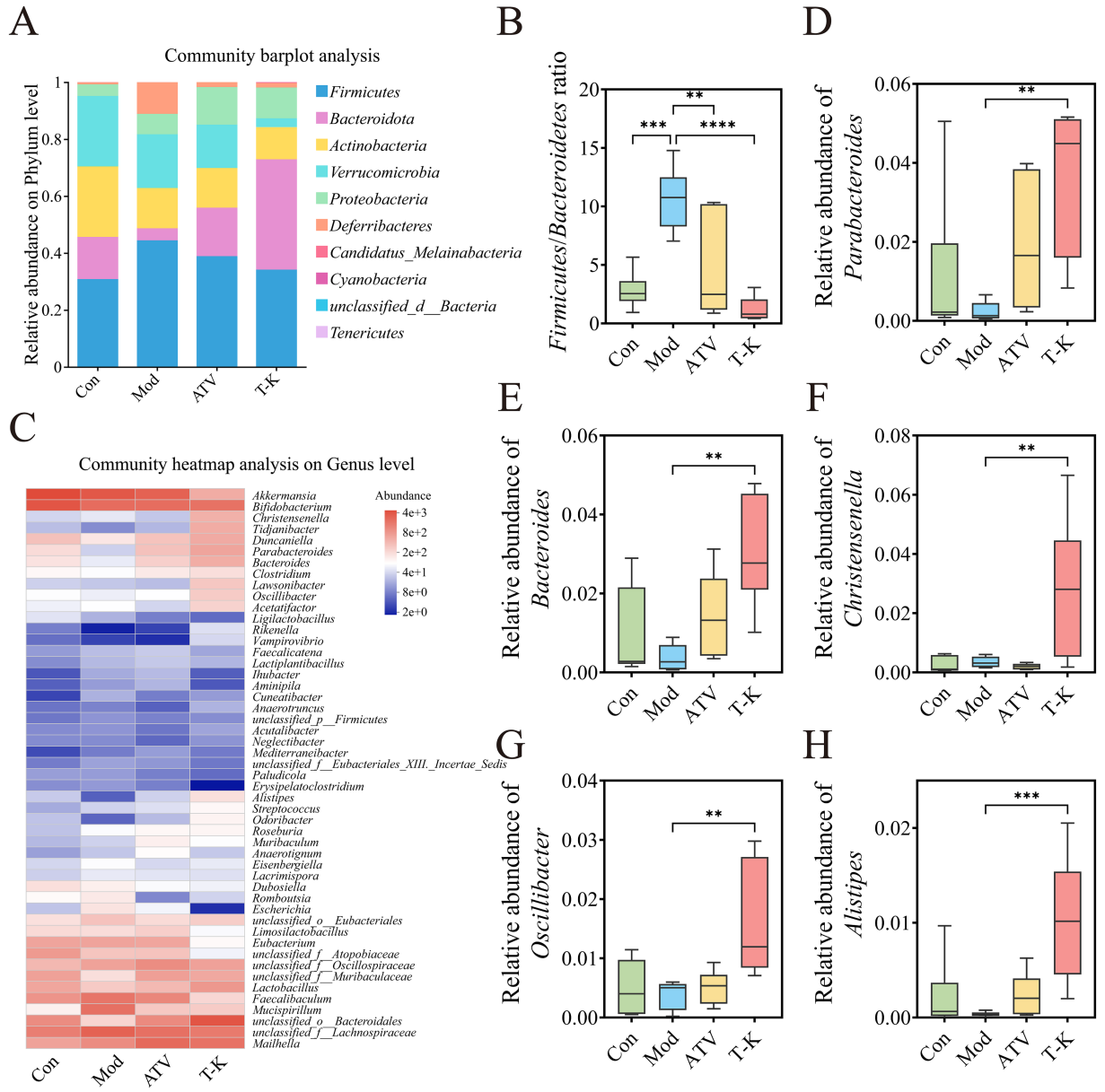

FIGURE 5
Effects of T-K on gut microbiota composition in atherosclerotic mice. **(A)** Community bar plot analysis at the phylum level. **(B)** *Firmicutes/Bacteroidetes* ratio. **(C)** Top 50 genera heatmap. **(D–H)** Represents the relative abundance of *Parabacteroides*, *Bacteroides*, *Christensenella*, *Oscillibacter*, and *Alistipes*, respectively. Data are presented as mean ± SD, $n = 6$, $^{**}p < 0.01$, $^{***}p < 0.001$, and $^{****}p < 0.0001$, vs. Mod group.

information processing, environmental information processing, cellular processes, organismal systems, and human diseases. Overall, after multiple testing correction, most categories showed no significant differences (FDR >0.05). However, as illustrated in Supplementary Figure 6A, nominal significance and intergroup mean trends revealed that the Mod group exhibited general reductions in metabolism-related subclasses, including carbohydrate, lipid, coenzyme and vitamin, and amino acid metabolism, whereas infection- and immune-related categories were relatively elevated. Following intervention, both ATV and T-K showed restorative effects on metabolic and signaling categories and exhibited a regressive trend in cell death-related processes. At the Level 3, 287 pathways were identified, among which 49 showed nominal differences ($p < 0.05$). Supplementary Figure 6B demonstrates that in the Mod group, pathways related to lipid and energy metabolism, including fatty acid degradation, peroxisome, linoleic acid metabolism, one-carbon pool by folate, thiamine metabolism, PPAR signaling, and insulin signaling, were decreased, whereas these pathways were restored to varying extents in the T-K and ATV groups. Conversely, pathways associated with cell death and stress responses, such as apoptosis, ferroptosis, and p53 signaling, were enriched in the Mod group but regressed after T-K intervention. Collectively, these findings indicated that T-K is at least comparable to ATV in reconstructing metabolic homeostasis and suppressing stress responses, and in certain pathways, its effects are even more pronounced.

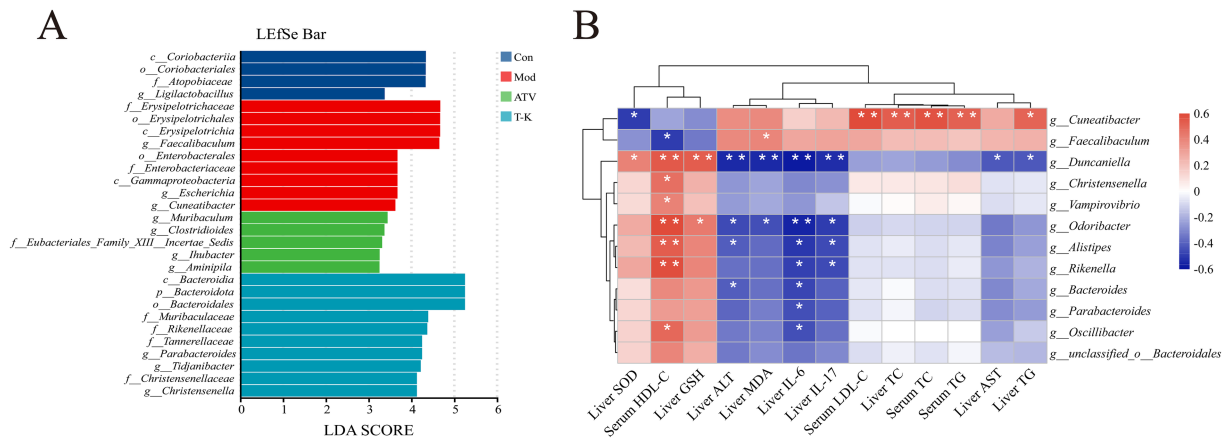

FIGURE 6
Effects of T-K on gut microbiota and its correlation with liver and serum parameters in atherosclerotic mice. **(A)** LEfSe bar plot displaying the LDA scores for the most discriminative taxa between the groups. **(B)** Heatmap showing the correlation between microbial genera and various liver and serum parameters (*$p < 0.05$ and **$p < 0.01$).

4 Discussion

Extensive research has demonstrated that lipid accumulation, oxidative stress, and inflammation responses are key pathogenic mechanisms underlying atherosclerosis (Liu N. et al., 2022; Liu H. et al., 2022). This study systematically evaluated the effects of T-K in ApoE$^{-/-}$ mice with atherosclerosis. T-K significantly reduced lipid deposition in the aortic sinus and increased collagen content within plaques, suggesting improved plaque stability. It also alleviated inflammation in both the liver and aorta. By lowering serum TC, TG, and LDL-C levels and increasing HDL-C, T-K exerted hepatoprotective effects and improved colonic morphology. In addition, T-K enhanced gut microbiota diversity and reshaped microbial community structure. LEfSe analysis identified specific bacterial taxa enriched in the T-K group, potentially associated with its regulatory effects on the gut microbiota. Compared to HFHC diet-fed mice, the T-K treatment led to distinct shifts in gut microbial composition, suggesting that T-K may optimize gut microecology through targeted microbiota modulation, thereby offering new insights into atherosclerosis management. These microbial changes may also contribute to the regulation of host metabolism, immune function, and inflammatory responses. Moreover, correlation heatmap analysis revealed significant associations between specific bacterial taxa and hepatic or serum biomarkers, including SOD, GSH, ALT, MDA, HDL-C, LDL-C, and TG. Collectively, these findings support the therapeutic potential of T-K in the multifactorial management of atherosclerosis, in line with previous reports (Yoshida et al., 2018; Lavillegrand et al., 2024).

Through analysis of gut microbiota abundance and composition, the significantly different species in T-K group include the phyla *Bacteroidota*, *Candidatus Melainabacteria*, and genera *Parabacteroides*, *Bacteroides*, *Christensenella*, *Oscillibacter*, and *Alistipes*. Previous studies have shown that the genus *Bacteroides* is less abundant in individuals with coronary artery disease (CAD) compared to those with risk factors but without CAD or healthy controls. In particular, reduced abundance of *Bacteroides vulgatus* and *Bacteroides dorei* is associated with elevated fecal LPS levels in CAD patients, whereas supplementation with these strains alleviated inflammation and atherosclerotic lesion formation in mice. These findings are consistent with the gut microbiota alterations observed in our experimental mice (Yoshida et al., 2018). It is associated with parameters such as liver IL-6 level, which suggests that gut microbiota might play an indirect role in the pathological process of atherosclerosis by promoting inflammatory responses. After drug treatment in hyperlipidemic mice, levels of *Candidatus Melainabacteria* in microbiota markedly elevated, further confirming the crucial importance of intestinal microbiota to host health (Lu et al., 2022). Emerging evidence suggesting that a *Ganoderma meroterpene* derivative alleviates obesity-related atherosclerosis via enrichment of intestinal *Parabacteroides*. At the same time, supplementation with viable *Parabacteroides* in ApoE$^{-/-}$ mice fed a high-fat diet can reduce the atherosclerotic plaques (Qiao et al., 2022). Evidence suggests that CAD is associated with reductions in *Bacteroidetes* and *Alistipes* populations. In particular, the abundance of *Alistipes* is negatively correlated with liver IL-17 and liver IL-6 levels, while positively correlated with serum HDL-C, indicating that dysbiosis of gut microbiota promotes endothelial inflammation and progression of atherosclerosis (Choroszy et al., 2022). In our study, treatment with T-K extract led to an increased abundance of *Alistipes* in atherosclerotic mice. Similarly, Wang et al. reported that *Ginkgo biloba* extract supplementation in Western diet-fed Ldlr$^{-/-}$ mice elevated *Alistipes*, a shift associated with improved intestinal barrier function and alleviated atherosclerotic lesions (Wang Q. et al., 2022; Wang Y. et al., 2022). These consistent observations suggest that modulation of *Alistipes* may represent a common microbial response to botanical interventions in atherosclerosis, although its functional implications warrant further clarification (Liang et al., 2024). In our study, the relative abundance of *Faecalibaculum* was markedly elevated in atherosclerotic mice but significantly reduced following the treatment with T-K extract. This finding is in line with recent reports indicating that the abundance of *Faecalibaculum* is associated with bile acid dysregulation and activation of the intestinal FXR-FGF19 axis, thereby contributing to lipid metabolism disorders and atherosclerosis progression (Xu et al., 2023). Conversely, suppression of *Faecalibaculum* by T-K extract may attenuate bile acid-driven dysmetabolism, reduce pro-inflammatory

signaling, and ultimately alleviate atherosclerotic lesions (Liang et al., 2024). Nevertheless, the associations of *Christensenella* and *Oscillibacter* with atherosclerosis remain incompletely characterized in current research.

Analysis of the functional prediction results using PICRUSt2 indicated that T-K may ameliorate atherosclerosis by enhancing lipid metabolism pathways, restoring the balance of PPAR and insulin signaling, and suppressing the excessive activation of apoptosis and ferroptosis, thereby exerting coordinated effects on multiple pathological processes. However, it should be noted that the KEGG functional annotation and pathway analysis in this study were primarily based on predictive results, which entails certain uncertainties, particularly as the enrichment significance at Levels 2 and 3 was limited after multiple-testing correction. Therefore, future studies should incorporate transcriptomic, proteomic, or metabolomic data for multi-omics integration to strengthen the reliability of the conclusions.

Recent studies have highlighted the significant role of the gut-liver axis in modulating systemic and hepatic inflammation. Gut microbiota dysbiosis increases intestinal permeability, allowing bacterial products such as lipopolysaccharides (LPS) to translocate into the portal circulation, which subsequently activates hepatic immune responses and promotes liver inflammation and oxidative stress (Anand and Mande, 2022). Moreover, short-chain fatty acids (SCFAs), produced by beneficial gut microbes, exert anti-inflammatory effects and contribute to intestinal barrier integrity (Verhaar et al., 2020). These findings support our observation that T-K improves liver inflammation in parallel with microbiota remodeling. Although our current study is based on correlation analysis, the consistency with previous mechanistic studies suggests a plausible link between microbial modulation and hepatic improvement. In addition, microbiota-derived metabolites such as TMAO and bile acids have been implicated in both cholesterol metabolism and vascular inflammation, indicating that the observed improvement in atherosclerosis may also be partially microbiota-mediated (Mao et al., 2024; Buchynskyi et al., 2025). Notably, the study by Zhu et al. (2020) directly demonstrates that *Alisma orientale* beverage reduces atherosclerotic plaque formation by modulating gut microbiota and lowering TMAO levels in ApoE$^{-/-}$ mice. Together, these findings underscore the importance of gut-derived metabolites such as TMAO in linking intestinal dysbiosis to vascular pathology and suggest that targeting TMAO may be a promising strategy in future anti-atherosclerotic therapies (Liu et al., 2023).

Although this study provides new insights into the atheroprotective effects of T-K via modulation of the gut–liver axis, several limitations should be taken into consideration. The absence of a control + T-K group (healthy mice receiving T-K without disease induction) limits the evaluation of baseline effects of T-K on gut microbiota and host metabolism under physiological conditions. Although no overt toxicity was observed during the 8-week intervention, the long-term safety profile of T-K remains unclear; comprehensive toxicological assessments, including chronic toxicity and organ-specific evaluations, will be important in future studies. Histological analysis was restricted to Oil Red O staining, without cellular characterization of lesions such as smooth muscle cells, macrophages, and leukocytes. These parameters are essential for better understanding the impact of T-K on plaque composition. The relatively small number of animals included in histological evaluation may also reduce statistical power. Moreover, while PLS-DA and LEfSe analyses revealed significant alterations in gut microbiota composition, the absence of microbiota-depleted (pseudo-germ-free) controls prevents definitive conclusions about causality. These limitations highlight the need for more comprehensive experimental designs in future research to fully elucidate the therapeutic potential and underlying mechanisms of T-K.

Till date, the pharmacological research progress of T-K has been systematically summarized by Lu et al. (2022). At least 209 compounds have been isolated and identified from T-K, yet most of these components remain functionally uncharacterized and require further investigation. In the present study, the phytochemical constituents of T-K were identified and are listed in Supplementary Table 2. We have also added a brief summary of several key bioactive constituents that may contribute to the observed pharmacological effects of T-K. For instance, hyperoside (quercetin-3-O-galactoside) has been reported to inhibit LPS-induced NF-κB activation in macrophages, thereby reducing the production of TNF-α, IL-6, and nitric oxide (Kim et al., 2011). It also improves lipid profiles and alleviates hepatic steatosis in high-fat diet-induced models via activation of the PPARγ and FXR/LXRα pathways (Wang et al., 2021). Vanillin and its oxidative metabolite vanillic acid exhibit strong antioxidant and anti-inflammatory activities by scavenging reactive oxygen species and suppressing proinflammatory cytokines, in part through NF-κB inhibition (Kafali et al., 2024). Chlorogenic acid is known to modulate endothelial function, inhibit platelet aggregation, and regulate lipid metabolism, providing cardiovascular protection (Fuentes et al., 2014). In addition, quercetin, a well-studied flavonoid, has been shown to reduce atherosclerotic plaque area in ApoE$^{-/-}$ mice by attenuating oxidative stress and upregulating HO-1 and eNOS expression (Shen et al., 2013). Although some of these components have been functionally validated in *in vitro* or animal studies, clinical evidence remains scarce. This represents an important future direction, as clinical validation will be essential for translating these findings into therapeutic applications (Zhang et al., 2022). Furthermore, the precise mechanisms through which T-K alleviates atherosclerosis remain incompletely understood. Therefore, future studies should focus on the isolation and characterization of individual bioactive compounds, *in vivo* functional validation, and ultimately clinical trials. Such investigations are expected to provide deeper insight into the therapeutic potential of T-K.

In summary, this study indicates that T-K may exert anti-atherosclerotic effects by regulating blood lipid levels, alleviating inflammation, and reshaping the composition of gut microbiota. However, our current research findings are primarily correlational rather than causal, and it is very important to further clarify the mechanisms. In future work, approaches such as fecal microbiota transplantation, antibiotic-induced microbiota depletion, and multi-omics integration will be essential to determine whether the gut microbiota directly mediates the therapeutic effects of T-K. In particular, metabolomics focusing on gut microbiota-derived metabolites, including SCFAs, bile acids and TMAO, will provide mechanistic insight into the microbiota-host interaction. In addition, isolation and functional characterization of individual bioactive compounds will help differentiate the contribution of phytochemical constituents and microbiota-derived mechanisms. By addressing these questions, the therapeutic potential of T-K can be fully elucidated, providing a stronger foundation for its possible use in the prevention and treatment of atherosclerosis and related metabolic disorders.

Data availability statement

The sequencing data have been deposited in the NCBI Sequence Read Archive (SRA) under accession number PRJNA1334592 (BioProject). The dataset includes 24 BioSamples and their corresponding SRA accessions, which can be accessed at https://www.ncbi.nlm.nih.gov/bioproject/PRJNA1334592.

Ethics statement

The animal study was approved by the Animal Welfare and Ethics Committee of Henan University of Chinese Medicine (Approval No. DWLLGZR202303167). The study was conducted in accordance with the local legislation and institutional requirements.

Author contributions

QW: Funding acquisition, Writing – original draft. YN: Writing – original draft, Methodology, Data curation. JiH: Writing – original draft, Data curation. JuH: Investigation, Writing – original draft. JZ: Writing – original draft, Resources. BZ: Writing – original draft, Validation. ZG: Writing – original draft, Software. SF: Writing – original draft, Supervision, Writing – review & editing.

Funding

The author(s) declare that financial support was received for the research and/or publication of this article. This research was supported by the Key Research and Development Special Project of Henan Province (No. 241111311200), the Joint Funds of Science and Technology Research and Development Project of Henan Province (No. 232301420070), the Key Research Project of Colleges and Universities in Henan Province (No. 24A310006), the Natural Science Foundation of Henan Province (No. 242300420498), the Scientific and Technological Attack Project of Henan Province (252102311277).

Conflict of interest

The authors declare that the research was conducted in the absence of any commercial or financial relationships that could be construed as a potential conflict of interest.

Generative AI statement

The authors declare that no Gen AI was used in the creation of this manuscript.

Any alternative text (alt text) provided alongside figures in this article has been generated by Frontiers with the support of artificial intelligence and reasonable efforts have been made to ensure accuracy, including review by the authors wherever possible. If you identify any issues, please contact us.

Publisher's note

All claims expressed in this article are solely those of the authors and do not necessarily represent those of their affiliated organizations, or those of the publisher, the editors and the reviewers. Any product that may be evaluated in this article, or claim that may be made by its manufacturer, is not guaranteed or endorsed by the publisher.

Supplementary material

The Supplementary material for this article can be found online at: https://www.frontiersin.org/articles/10.3389/fmicb.2025.1641035/full#supplementary-material

References

Anand, S., and Mande, S. S. (2022). Host-microbiome interactions: gut-liver axis and its connection with other organs. *npj Biofilms Microbiomes* 8:89. doi: 10.1038/s41522-022-00352-6

Barton, M., Minotti, R., and Haas, E. (2007). Inflammation and atherosclerosis. *Circ. Res.* 101, 750–751. doi: 10.1161/CIRCRESAHA.107.162487

Björkegren, J. L. M., and Lusis, A. J. (2022). Atherosclerosis: recent developments. *Cell* 185, 1630–1645. doi: 10.1016/j.cell.2022.04.004

Buchynskyi, M., Kamyshna, I., Halabitska, I., Petakh, P., Kunduzova, O., Oksenych, V., et al. (2025). Unlocking the gut-liver axis: microbial contributions to the pathogenesis of metabolic-associated fatty liver disease. *Front. Microbiol.* 16:1577724. doi: 10.3389/fmicb.2025.1577724

Castellano, J. M., Pocock, S. J., Bhatt, D. L., Quesada, A. J., Owen, R., Fernandez-Ortiz, A., et al. (2022). Polypill strategy in secondary cardiovascular prevention. *N. Engl. J. Med.* 387, 967–977. doi: 10.1056/NEJMoa2208275

Cheng, C., Zhang, J., Li, X., Xue, F., Cao, L., Meng, L., et al. (2023). NPRC deletion mitigated atherosclerosis by inhibiting oxidative stress, inflammation and apoptosis in ApoE knockout mice. *Signal Transduct. Target. Ther.* 8:290. doi: 10.1038/s41392-023-01560-y

Choroszy, M., Sobieszczańska, B., Litwinowicz, K., Łaczmański, Ł., Chmielarz, M., Walczuk, U., et al. (2022). Co-toxicity of endotoxin and indoxyl sulfate, gut-derived bacterial metabolites, to vascular endothelial cells in coronary arterial disease accompanied by gut dysbiosis. *Nutrients* 14:424. doi: 10.3390/nu14030424

Dai, X., Gu, Y., Guo, J., Huang, L., Cheng, G., Peng, D., et al. (2022). Clinical breakpoint of apramycin to swine salmonella and its effect on ileum flora. *Int. J. Mol. Sci.* 23:1424. doi: 10.3390/ijms23031424

Davidson, K. W., Barry, M. J., Mangione, C. M., Cabana, M., Chelmow, D., Coker, T. R., et al. (2022). Aspirin use to prevent cardiovascular disease: US preventive services task force recommendation statement. *JAMA* 327, 1577–1584. doi: 10.1001/jama.2022.4983

Falk, E. (2006). Pathogenesis of atherosclerosis. *J. Am. Coll. Cardiol.* 47, C7–C12. doi: 10.1016/j.jacc.2005.09.068

Fuentes, E., Caballero, J., Alarcón, M., Rojas, A., and Palomo, I. (2014). Chlorogenic acid inhibits human platelet activation and thrombus formation. *PLoS One* 9:e90699. doi: 10.1371/journal.pone.0090699

Herrington, W., Lacey, B., Sherliker, P., Armitage, J., and Lewington, S. (2016). Epidemiology of atherosclerosis and the potential to reduce the global burden of atherothrombotic disease. *Circ. Res.* 118, 535–546. doi: 10.1161/CIRCRESAHA.115.307611

Janssens, Y., Nielandt, J., Bronselaer, A., Debunne, N., Verbeke, F., Wynendaele, E., et al. (2018). Disbiome database: linking the microbiome to disease. *BMC Microbiol.* 18:50. doi: 10.1186/s12866-018-1197-5

Ji, W., Jiang, T., Sun, Z., Teng, F., Ma, C., Huang, S., et al. (2020). The enhanced pharmacological effects of modified traditional Chinese medicine in attenuation of atherosclerosis is driven by modulation of gut microbiota. *Front. Pharmacol.* 11:546589. doi: 10.3389/fphar.2020.546589

Kafali, M., Finos, M. A., and Tsoupras, A. (2024). Vanillin and its derivatives: a critical review of their anti-inflammatory, anti-infective, wound-healing, neuroprotective, and anti-cancer health-promoting benefits. *Nutraceuticals* 4, 522–561. doi: 10.3390/nutraceuticals4040030

Kim, S.-J., Um, J.-Y., and Lee, J.-Y. (2011). Anti-inflammatory activity of hyperoside through the suppression of nuclear factor-κB activation in mouse peritoneal macrophages. *Am. J. Chin. Med.* 39, 171–181. doi: 10.1142/S0192415X11008737

Lavillegrand, J.-R., Al-Rifai, R., Thietart, S., Guyon, T., Vandestienne, M., Cohen, R., et al. (2024). Alternating high-fat diet enhances atherosclerosis by neutrophil reprogramming. *Nature* 634, 447–456. doi: 10.1038/s41586-024-07693-6

Liang, X., Zheng, X., Wang, P., Zhang, H., Ma, Y., Liang, H., et al. (2024). *Bifidobacterium animalis* subsp. *lactis* F1-7 alleviates lipid accumulation in atherosclerotic mice via modulating bile acid metabolites to downregulate intestinal FXR. *J. Agric. Food Chem.* 72, 2585–2597. doi: 10.1021/acs.jafc.3c05709

Libby, P., Buring, J. E., Badimon, L., Hansson, G. K., Deanfield, J., Bittencourt, M. S., et al. (2019). Atherosclerosis. *Nat. Rev. Dis. Primers* 5:56. doi: 10.1038/s41572-019-0106-z

Liu, N., Qin, H., Cai, Y., Li, X., Wang, L., Xu, Q., et al. (2022). Dynamic trafficking patterns of IL-17-producing γδ T cells are linked to the recurrence of skin inflammation in psoriasis-like dermatitis. *EBioMedicine* 82:104136. doi: 10.1016/j.ebiom.2022.104136

Liu, F., Shan, S., Li, H., Shi, J., Hao, R., Yang, R., et al. (2021). Millet shell polyphenols prevent atherosclerosis by protecting the gut barrier and remodeling the gut microbiota in ApoE$^{-/-}$ mice. *Food Funct.* 12, 7298–7309. doi: 10.1039/d1fo00991e

Liu, L., Yuan, Y., and Tao, J. (2021). Flavonoid-rich extract of *Paeonia lactiflora* petals alleviate d-galactose-induced oxidative stress and restore gut microbiota in ICR mice. *Antioxidants* 10:1889. doi: 10.3390/antiox10121889

Liu, J., Zhou, S., Wang, Y., Liu, J., Sun, S., Sun, Y., et al. (2023). ZeXieYin formula alleviates TMAO-induced cognitive impairment by restoring synaptic plasticity damage. *J. Ethnopharmacol.* 314:116604. doi: 10.1016/j.jep.2023.116604

Liu, H., Zhu, L., Chen, L., and Li, L. (2022). Therapeutic potential of traditional Chinese medicine in atherosclerosis: a review. *Phytother. Res.* 36, 4080–4100. doi: 10.1002/ptr.7590

Lu, X., Han, B., Deng, X., Deng, S.-Y., Zhang, Y.-Y., Shen, P.-X., et al. (2020). Pomegranate peel extract ameliorates the severity of experimental autoimmune encephalomyelitis via modulation of gut microbiota. *Gut Microbes* 12:1857515. doi: 10.1080/19490976.2020.1857515

Lu, X., Qin, Z., Bai, L.-X., Ge, W.-B., Li, J.-Y., and Yang, Y.-J. (2022). Untargeted lipidomics and metagenomics reveal the mechanism of aspirin eugenol ester relieving hyperlipidemia in ApoE$^{-/-}$ mice. *Front. Nutr.* 9:1030528. doi: 10.3389/fnut.2022.1030528

Mao, Y., Kong, C., Zang, T., You, L., Wang, L.-S., Shen, L., et al. (2024). Impact of the gut microbiome on atherosclerosis. *mLife* 3, 167–175. doi: 10.1002/mlf2.12110

Penson, P. E., Long, D. L., Howard, G., Toth, P. P., Muntner, P., Howard, V. J., et al. (2018). Associations between very low concentrations of low density lipoprotein cholesterol, high sensitivity C-reactive protein, and health outcomes in the reasons for geographical and racial differences in stroke (REGARDS) study. *Eur. Heart J.* 39, 3641–3653. doi: 10.1093/eurheartj/ehy533

Ping, L., Zhi-Ming, L., Bi-Shan, Z., Lei, Z., Bo, Y., Yi-Chun, Z., et al. (2024). S-propargyl-cysteine promotes the stability of atherosclerotic plaque via maintaining vascular muscle contractile phenotype. *Front. Cell Dev. Biol.* 11:1291170. doi: 10.3389/fcell.2023.1291170

Pu, Y., Cheng, C. K., Zhang, H., Luo, J.-Y., Wang, L., Tomlinson, B., et al. (2023). Molecular mechanisms and therapeutic perspectives of peroxisome proliferator-activated receptor α agonists in cardiovascular health and disease. *Med. Res. Rev.* 43, 2086–2114. doi: 10.1002/med.21970

Qiao, S., Liu, C., Sun, L., Wang, T., Dai, H., Wang, K., et al. (2022). Gut *Parabacteroides merdae* protects against cardiovascular damage by enhancing branched-chain amino acid catabolism. *Nat. Metab.* 4, 1271–1286. doi: 10.1038/s42255-022-00649-y

Roth, G. A., Mensah, G. A., Johnson, C. O., Addolorato, G., Ammirati, E., Baddour, L. M., et al. (2020). Global burden of cardiovascular diseases and risk factors, 1990–2019. *J. Am. Coll. Cardiol.* 76, 2982–3021. doi: 10.1016/j.jacc.2020.11.010

Sahebkar, A., Foroutan, Z., Katsiki, N., Jamialahmadi, T., and Mantzoros, C. S. (2023). Ferroptosis, a new pathogenetic mechanism in cardiometabolic diseases and cancer: is there a role for statin therapy? *Metabolism* 146:155659. doi: 10.1016/j.metabol.2023.155659

Santisteban, M. M., Qi, Y., Zubcevic, J., Kim, S., Yang, T., Shenoy, V., et al. (2017). Hypertension-linked pathophysiological alterations in the gut. *Circ. Res.* 120, 312–323. doi: 10.1161/CIRCRESAHA.116.309006

Shen, Y., Ward, N. C., Hodgson, J. M., Puddey, I. B., Wang, Y., Zhang, D., et al. (2013). Dietary quercetin attenuates oxidant-induced endothelial dysfunction and atherosclerosis in apolipoprotein E knockout mice fed a high-fat diet: a critical role for heme oxygenase-1. *Free Radic. Biol. Med.* 65, 908–915. doi: 10.1016/j.freeradbiomed.2013.08.185

Shi, S., Verstegen, M. M. A., Roest, H. P., Ardisasmita, A. I., Cao, W., Roos, F. J. M., et al. (2021). Recapitulating cholangiopathy-associated necroptotic cell death in vitro using human cholangiocyte organoids. *Cell. Mol. Gastroenterol. Hepatol.* 13, 541–564. doi: 10.1016/j.jcmgh.2021.10.009

Thompson, P. D. (2016). What to believe and do about statin-associated adverse effects. *JAMA* 316, 1969–1970. doi: 10.1001/jama.2016.16557

Vaduganathan, M., Mensah, G. A., Turco, J. V., Fuster, V., and Roth, G. A. (2022). The global burden of cardiovascular diseases and risk: a compass for future health. *J. Am. Coll. Cardiol.* 80, 2361–2371. doi: 10.1016/j.jacc.2022.11.005

van Vlijmen, B. J., van den Maagdenberg, A. M., Gijbels, M. J., van der Boom, H., HogenEsch, H., Frants, R. R., et al. (1994). Diet-induced hyperlipoproteinemia and atherosclerosis in apolipoprotein E3-leiden transgenic mice. *J. Clin. Invest.* 93, 1403–1410. doi: 10.1172/JCI117117

Verhaar, B. J. H., Prodan, A., Nieuwdorp, M., and Muller, M. (2020). Gut microbiota in hypertension and atherosclerosis: a review. *Nutrients* 12:2982. doi: 10.3390/nu12102982

Wang, X., Cui, J., Gu, Z., Guo, L., Liu, R., Guo, Y., et al. (2025). Aged garlic oligosaccharides modulate host metabolism and gut microbiota to alleviate high-fat and high-cholesterol diet-induced atherosclerosis in ApoE$^{-/-}$ mice. *Food Chem.* 463:141409. doi: 10.1016/j.foodchem.2024.141409

Wang, Q., He, Y., Li, X., Zhang, T., Liang, M., Wang, G., et al. (2022). *Lactobacillus reuteri* CCFM8631 alleviates hypercholesterolaemia caused by the paigen atherogenic diet by regulating the gut microbiota. *Nutrients* 14:1272. doi: 10.3390/nu14061272

Wang, C., Lv, J., Yang, M., Fu, Y., Wang, W., Li, X., et al. (2025). Recent advances in surface functionalization of cardiovascular stents. *Bioact. Mater.* 44, 389–410. doi: 10.1016/j.bioactmat.2024.10.025

Wang, S., Sheng, F., Zou, L., Xiao, J., and Li, P. (2021). Hyperoside attenuates non-alcoholic fatty liver disease in rats via cholesterol metabolism and bile acid metabolism. *J. Adv. Res.* 34, 109–122. doi: 10.1016/j.jare.2021.06.001

Wang, Y., Xu, Y., Xu, X., Wang, H., Wang, D., Yan, W., et al. (2022). *Ginkgo biloba* extract ameliorates atherosclerosis via rebalancing gut flora and microbial metabolism. *Phytother. Res.* 36, 2463–2480. doi: 10.1002/ptr.7439

Witkowski, M., Weeks, T. L., and Hazen, S. L. (2020). Gut microbiota and cardiovascular disease. *Circ. Res.* 127, 553–570. doi: 10.1161/CIRCRESAHA.120.316242

Xu, H., Fang, F., Wu, K., Song, J., Li, Y., Lu, X., et al. (2023). Gut microbiota-bile acid crosstalk regulates murine lipid metabolism via the intestinal FXR-FGF19 axis in diet-induced humanized dyslipidemia. *Microbiome* 11:262. doi: 10.1186/s40168-023-01709-5

Yang, X., Yu, H., Fu, J., Guo, H.-H., Han, P., Ma, S.-R., et al. (2022). Hydroxyurea ameliorates atherosclerosis in ApoE$^{-/-}$ mice by potentially modulating Niemann–Pick C1-like 1 protein through the gut microbiota. *Theranostics* 12, 7775–7787. doi: 10.7150/thno.76805

Yoshida, N., Emoto, T., Yamashita, T., Watanabe, H., Hayashi, T., Tabata, T., et al. (2018). *Bacteroides vulgatus* and *Bacteroides dorei* reduce gut microbial lipopolysaccharide production and inhibit atherosclerosis. *Circulation* 138, 2486–2498. doi: 10.1161/CIRCULATIONAHA.118.033714

Zhang, L., Li, Y., Ma, X., Liu, J., Wang, X., Zhang, L., et al. (2021). Ginsenoside Rg1-notoginsenoside R1-protocatechuic aldehyde reduces atherosclerosis and attenuates low-shear stress-induced vascular endothelial cell dysfunction. *Front. Pharmacol.* 11:588259. doi: 10.3389/fphar.2020.588259

Zhang, X.-F., Tang, Y.-J., Guan, X.-X., Lu, X., Li, J., Chen, X.-L., et al. (2022). Flavonoid constituents of *Amomum tsao-ko Crevost et Lemarie* and their antioxidant and antidiabetic effects in diabetic rats—*in vitro* and *in vivo* studies. *Food Funct.* 13, 437–450. doi: 10.1039/d1fo02974f

Zhou, Q., Mei, Y., Shoji, T., Han, X., Kaminski, K., Taeg, G., et al. (2012). ROCK2 deficiency in bone marrow-derived cells leads to increased cholesterol efflux and decreased atherosclerosis. *Circulation* 126, 2236–2247. doi: 10.1161/CIRCULATIONAHA.111.086041

Zhu, B., Zhai, Y., Ji, M., Wei, Y., Wu, J., Xue, W., et al. (2020). Alisma orientalis beverage treats atherosclerosis by regulating gut microbiota in ApoE$^{-/-}$ mice. *Front. Pharmacol.* 11:570555. doi: 10.3389/fphar.2020.570555

Glossary

T-K - *Amomum tsao-ko Crevost et Lemarie*

H&E - Hematoxylin-eosin

TG - Triglycerides

TC - Total cholesterol

LDL-C - Low-density lipoprotein cholesterol

HDL-C - High-density lipoprotein cholesterol

AST - Aspartate aminotransferase

ALT - Alanine aminotransferase

IL-1β - Interleukin-1β

IL-6 - Interleukin-6

IL-17 - Interleukin-17

TNF-α - Tumor necrosis factor-α

SOD - Superoxide dismutase

MDA - Malondialdehyde

GSH - Glutathione

HFHC - High-fat high-cholesterol diet

LFLS - Low-fat low-sugar diet

ATV - Atorvastatin

ELISA - Enzyme-linked immunosorbent assay

LEfSe - Linear discriminant analysis effect size

Sobs - Species observed

Shannon - Shannon–Wiener index

Simpson - Simpson's diversity index

Chao1 - Chao1 estimator

ACE - Abundance-based coverage estimator

PLS-DA - Partial least squares discriminant analysis

PCoA - Principal coordinates analysis

frontiers | Frontiers in Microbiology

TYPE Original Research
PUBLISHED 18 November 2025
DOI 10.3389/fmicb.2025.1547724

Check for updates

OPEN ACCESS

EDITED BY
Mohammad Altamimi,
An-Najah National University, Palestine

REVIEWED BY
Shalaka Naidu,
Symbiosis International University, India
Gbenga Alabi,
Citrus Research International, South Africa

*CORRESPONDENCE
An Jia
✉ 201208120@hhstu.edu.cn
Wanli Zhao
✉ zhaowanlitcm@126.com

†These authors have contributed equally to this work

RECEIVED 14 January 2025
ACCEPTED 24 October 2025
PUBLISHED 18 November 2025

CITATION
Huang X, Ru G, Tian H, Zhang P, Zhao H, Zhang S, Wang S, Jia A and Zhao W (2025) Chewable tablets containing rape bee pollen and maca attenuate testosterone propionate–induced benign prostatic hyperplasia in Sprague–Dawley rats by regulating the gut microbiota and modulating the IL-6/JAK2/STAT3 signaling pathway. *Front. Microbiol.* 16:1547724. doi: 10.3389/fmicb.2025.1547724

COPYRIGHT
© 2025 Huang, Ru, Tian, Zhang, Zhao, Zhang, Wang, Jia and Zhao. This is an open-access article distributed under the terms of the Creative Commons Attribution License (CC BY). The use, distribution or reproduction in other forums is permitted, provided the original author(s) and the copyright owner(s) are credited and that the original publication in this journal is cited, in accordance with accepted academic practice. No use, distribution or reproduction is permitted which does not comply with these terms.

Chewable tablets containing rape bee pollen and maca attenuate testosterone propionate–induced benign prostatic hyperplasia in Sprague–Dawley rats by regulating the gut microbiota and modulating the IL-6/JAK2/STAT3 signaling pathway

Xiaoqiang Huang[1†], Guohua Ru[1,2†], Hengyun Tian[1†], Pengbo Zhang[1,2], Hongchang Zhao[1,2], Shouren Zhang[1], Sijie Wang[1], An Jia[1*] and Wanli Zhao[3*]

[1]School of Medicine, Henan Provincial Key Laboratory of Nanocomposites and Applications, Institute of Nano-Structured Functional Materials, Huanghe Science and Technology University, Zhengzhou, China, [2]School of Pharmacy, Henan University, Kaifeng, China, [3]Jiangsu Key Laboratory for the Research and Utilization of Plant Resources, Institute of Botany, Jiangsu Province and Chinese Academy of Sciences (Nanjing Botanical Garden, Mem. Sun Yat-Sen), Nanjing, China

Background: Benign prostatic hyperplasia (BPH) significantly compromises patients' quality of life, has detrimental effects on both physical and mental well-being, and poses a substantial economic burden. Current pharmacological interventions primarily focus on symptom relief; nevertheless, their associated adverse effects are evident. Rape bee pollen and maca are both homologous food products, which are not only rich in nutrition, but also have many biological activities. There is no report on the combination of rape bee pollen and maca in benign prostatic hyperplasia therapy, and no report on the molecular mechanism. This study aims to systematically investigate the therapeutic efficacy and underlying molecular mechanisms of a chewable tablet formulation containing rape bee pollen and maca in the management of BPH.

Methods: First, the chewable tablets were prepared from rape bee pollen and maca, and the High Performance Liquid Chromatography (HPLC) fingerprint was established. During a 4-week period, rats were subjected to subcutaneous injections of testosterone propionate solution to establish a BPH model, while simultaneously receiving orally administered chewable tablets for BPH treatment via gavage. We assessed the body weight, prostate tissue index, serum levels of dihydrotestosterone (DHT), testosterone (T), estradiol (E2), interleukin-6 (IL-6), tumor necrosis factor-alpha (TNF-α), interleukin-1beta (IL-1β), superoxide dismutase (SOD), malondialdehyde (MDA) and glutathione (GSH) levels in rats. Prostate tissues were collected for histopathological analysis. The protein expression levels of IL-6, phosphorylated Janus kinase 2 (*p*-JAK2), and phosphorylated signal transducer and activator of transcription 3 (*p*-STAT3) were determined by Western blotting. Rat feces were collected aseptically for

16S rDNA gene sequencing to assess gut microbiota levels. Additionally, our research findings demonstrate that the combined application of rape pollen and maca exhibits superior therapeutic efficacy compared to the individual use of either rape pollen or maca alone.

Results: We prepared the rape bee pollen and maca chewable tablets, established the HPLC fingerprint map, and quantitatively analyzed four of these main components. We found that the rape bee pollen and maca chewable tablets significantly inhibited DHT, T, E2, E2/T ratio, IL-6, TNF-α, and IL-1β and reduced MDA levels and increased SOD, GSH levels. 16S rDNA gene sequencing revealed that the chewable tablet increased the abundance of the beneficial bacteria *Faecalibacterium, Collinsella, Phascolarctobacterium, Kineothrix*, and *Lactobacillus*, and decreased that of the pro-inflammatory *bacterium Prevotella*. Western blot indicated that the chewable tablet could significantly inhibit the IL-6, *p*-JAK2, and *p*-STAT3 protein expression levels.

Conclusion: We found that rape bee pollen and maca chewable tablets had a protective effect on rats with BPH, and also found that the combination of rape bee pollen and maca was better than separate application. The mechanism may be related to the gut microbiota and IL-6/JAK2/STAT3 signaling pathway.

KEYWORDS

benign prostatic hyperplasia, rape bee pollen, maca, gut microbiota, IL-6/JAK2/STAT3 signaling pathway

1 Introduction

Benign prostatic hyperplasia (BPH) is a highly prevalent condition in elderly males, with approximately 30%—40% of men affected by age 40 and 70%—80% of men affected by age 85 (Cannarella et al., 2021; Welén and Damber, 2022). This disorder leads to lower urinary tract symptoms (LUTS), including urinary hesitation, intermittent urinary stream, and straining during urination, thereby significantly compromising patients' quality of life and imposing substantial physical, mental, and economic burdens globally (Ho and Habib, 2011; Song et al., 2023). Recent global statistics indicate that over 94 million men worldwide experience BPH-related symptoms as of 2019 (Awedew et al., 2022). The pathophysiology of BPH involves imbalances in epithelial and stromal cell proliferation and apoptosis within the prostate's transition zone, leading to glandular and stromal hyperplasia (Shah et al., 2021). Specifically, epithelial hyperplasia forms larger glandular nodules, while stromal hyperplasia contributes to diffuse extracellular matrix deposition, particularly of type 1 collagen (Hata et al., 2023). These structural changes collectively disrupt urinary function and exacerbate LUTS severity, underscoring the need for effective therapeutic interventions.

Disease development and treatment are closely intertwined with the gut microbiome. Accumulating evidence has established a bidirectional relationship between BPH and gut microbiota dysregulation. For instance, recent studies elucidating the gut–prostate axis have revolutionized our understanding of BPH pathogenesis (Liu et al., 2021; Li et al., 2024). Animal models further revealed that high-fat diet-induced imbalances in the gut microbiome—particularly elevated ratios of *Bacteroidetes* to *Firmicutes*—are associated with BPH development (Gu et al., 2021). Therapeutic interventions such as finasteride treatment restored the abundance of beneficial gut bacteria, including *Lactobacillus* and *Acetatifactor*, to baseline levels in BPH patients (An et al., 2023). Mechanistically, gut microbiota perturbations may disrupt prostate homeostasis through immune activation and proinflammatory cytokine secretion, thereby promoting pathological inflammation (Russo et al., 2023).

Chronic inflammation has been identified as a key factor in the development and course of certain human illnesses, including prostate cancer and BPH. Interleukin-6 (IL-6) is a cytokine from the gp130 family that mediates the process of inflammation (Staršíchová et al., 2010). The IL-6/JAK2/STAT3 pathway is a key inflammatory signaling pathway. Numerous physiological and pathological processes, including angiogenesis, immunological control, and cell division and proliferation, are influenced by this pathway (Huang et al., 2022). Excessive IL-6 production in response to inflammatory stimulation is an effective stimulator of the JAK/STAT signaling pathway. IL-6 may contribute to inflammation by activating this pathway, which promotes epithelial–mesenchymal transition (Xiao et al., 2017; Singh et al., 2020). Studies have demonstrated that canagliflozin delays the progression of BPH by inhibiting the JAK2/STAT3 pathway (Elbaz et al., 2023).

The primary pharmacological interventions for BPH remain 5α-reductase inhibitors, α1-receptor antagonists, and PDE5 inhibitors (Antoniou et al., 2023). Adverse events associated with 5α-reductase inhibitors encompass erectile dysfunction, ejaculatory disorders, mood disturbances (depression/anxiety), and an elevated risk of prostate cancer progression (Miernik and Gratzke, 2020; Stewart and Lephart, 2023). Meanwhile, α1-receptor blockers are characterized by side effects including orthostatic hypotension, sedation, ejaculatory abnormalities, cognitive impairment, and depressive symptoms. These limitations have catalyzed research interest in complementary/alternative therapies, particularly phytotherapeutic agents (Stewart and Lephart, 2023).

Rape bee pollen (Brassica napus L.) emerges as a dual-use agent in traditional Chinese medicine and functional nutrition. Its bioactive profile comprises polyunsaturated fatty acids, flavonoids, and a comprehensive array of vitamins (Chen et al., 2020; Han et al., 2023), manifesting pleiotropic physiological activities including antioxidative, anti-inflammatory, immunomodulatory, antimicrobial, and organoprotective effects (Rodríguez-Pólit et al., 2023). Specifically, its extract modulates gut microbiota composition in BPH rat models by promoting beneficial taxa (*Coprococcus* and *Jeotgalicoccus*) while suppressing pathogenic microorganisms (*Turicibacter* and *Clostridiaceae_clostridium*) (Qiao et al., 2023). Additionally, rape bee pollen exerts anti-BPH activity through cyclooxygenase-2 (COX-2 pathway inhibition) (Yang et al., 2014). Maca, also known as Peruvian ginseng, was classified as a health food in 2011. Maca root contains numerous bioactive compounds, including macaamide, macaene, glucosinolates, polyphenols, and alkaloids, which can mitigate sexual dysfunction. It also has neuroprotective, memory-enhancing, antidepressant, antioxidant, anti–prostate hyperplasia, anti-inflammatory, and skin-protective properties (Da Silva Leitão Peres et al., 2020). Previous studies have demonstrated that maca can be utilized to treat BPH. Maca can decrease testosterone propionate–induced BPH by preventing dihydrotestosterone conversion (Zou et al., 2017) and can regulate inflammation in patients with BPH by boosting the levels of anti-inflammatory cytokines (IL-4, IFN-γ) and reducing those of pro-inflammatory cytokines (tumor necrosis factor-α) (Vásquez-Velásquez et al., 2020; Ulloa Del Carpio et al., 2024).

In summary, both rape bee pollen and maca exhibit therapeutic potential against BPH. This study formulated chewable tablets using these two ingredients to evaluate their synergistic effects in treating BPH, elucidate the underlying molecular mechanisms, and establish a standardized fingerprint chromatogram for quality control purposes.

2 Materials and methods

2.1 Chemicals and reagents

Testosterone propionate was purchased from Aladdin (Shanghai, China), maca was purchased from Beijing Tongrentang Co., Ltd (Beijing, China), and rape bee pollen was purchased from Henan Mileyuan Beekeeping Specialized Cooperative (Henan, China). Lactose, microcrystalline cellulose and magnesium stearate were purchased from Shaanxi Zhengyi Pharmaceutical Auxiliary Materials Co., Ltd. (Shanxi, China). Citric acid was purchased from Henan Wanbang Chemical Co., Ltd. (Henan, China) and finasteride from HangZhou MSD Pharmaceutical Co., Ltd (Hangzhou China). ELISA kits for the determination of IL-6, TNF-α, and IL-1β in rats were acquired from MultiSciences Lianke Biotech Co., Ltd. (Hangzhou, China). Anti-JAK2, anti–IL-6, anti–phospho-STAT3, anti-STAT3, and anti–phospho-JAK2 were purchased from Chengdu Zhengneng Biotechnology Co., Ltd. (Chengdu, China); Standard products such as rutin, quercetin, kaempferol, Isorhamnetin, etc. were purchased from Shanghai Yuanye Biotechnology Co., Ltd. (Shanghai, China); chromatography-grade phosphoric acid (Tianjin Comio Chemical Reagent Co., Ltd.).

2.2 Chewable tablet preparation

The chewable tablets are prepared using a wet granulation process, with maca water extract and rape bee pollen as principal ingredients, and lactose, microcrystalline cellulose, citric acid, and magnesium stearate as auxiliary components. Each chewable tablet weighs 450 mg and contains the following ingredients: rape bee pollen 136.62 mg, maca 136.62 mg, microcrystalline cellulose 85.545 mg, lactose 83.745 mg, citric acid 2.97 mg, and magnesium stearate 4.5 mg.

2.3 Preparation of the standard solution and sample solution

Take the appropriate amount of each control product, add methanol to make the mixed control solution of rutin, quercetin, kaempferol and Isorhamnetin quality concentration of 12.74 μg/mL, 34.12 μg/mL, 76.56 μg/mL, and 10.23 μg/mL, respectively. Shake well and set aside.

The 10 batches of rape bee pollen maca masticable tablets were prepared according to the "2.2" method. Each sample was weighed 1.0 g, placed in 100 mL round bottom flask, add 50 mL of methanol and 10 mL of 25% hydrochloric acid solution, weighed, heat reflux for 60 min, cool, weigh the mass with methanol, shake well, filter 0.22 μm microporous filter membrane, take the continued filtrate, and set aside.

2.4 Instruments and chromatographic conditions

Chromatographic conditions: Chromatographic column: Agilent ZORBAX SB-C18 column (4.6 × 250 mm, 5 μm), mobile phase: methanol (A)-0.4% phosphoric acid water (B), gradient elution: 0–30 min (A: 30%—50%), 30–50 min (A: 50%—55%), 50–51 min (A: 55%—30%), 51–60 min (A: 30%—30%), detection wavelength: 368 nm, The flow rate was 1 mL/min, the injection volume was 10 μL, and the column temperature was 30°C.

2.5 Animals experiment

After a week-long acclimation period, male Sprague—Dawley rats were randomized into 8 groups with 10 rats per group using a weight-based stratified random sampling technique, which guaranteed that the average weight of rats in each group was the same. Rats were divided into the following 8 groups: control group, model group, finasteride group (0.52 mg/kg), rape bee pollen group (630.0 mg/kg), maca group (630.0 mg/kg), and Chewable Tablets at 3 different dosages groups, namely, low (518.7 mg/kg), middle (1,037.5 mg/kg), and high (2,075.0 mg/kg) dosages. BPH was induced in rats in the model and drug-administered

10.3389/fmicb.2025.1547724

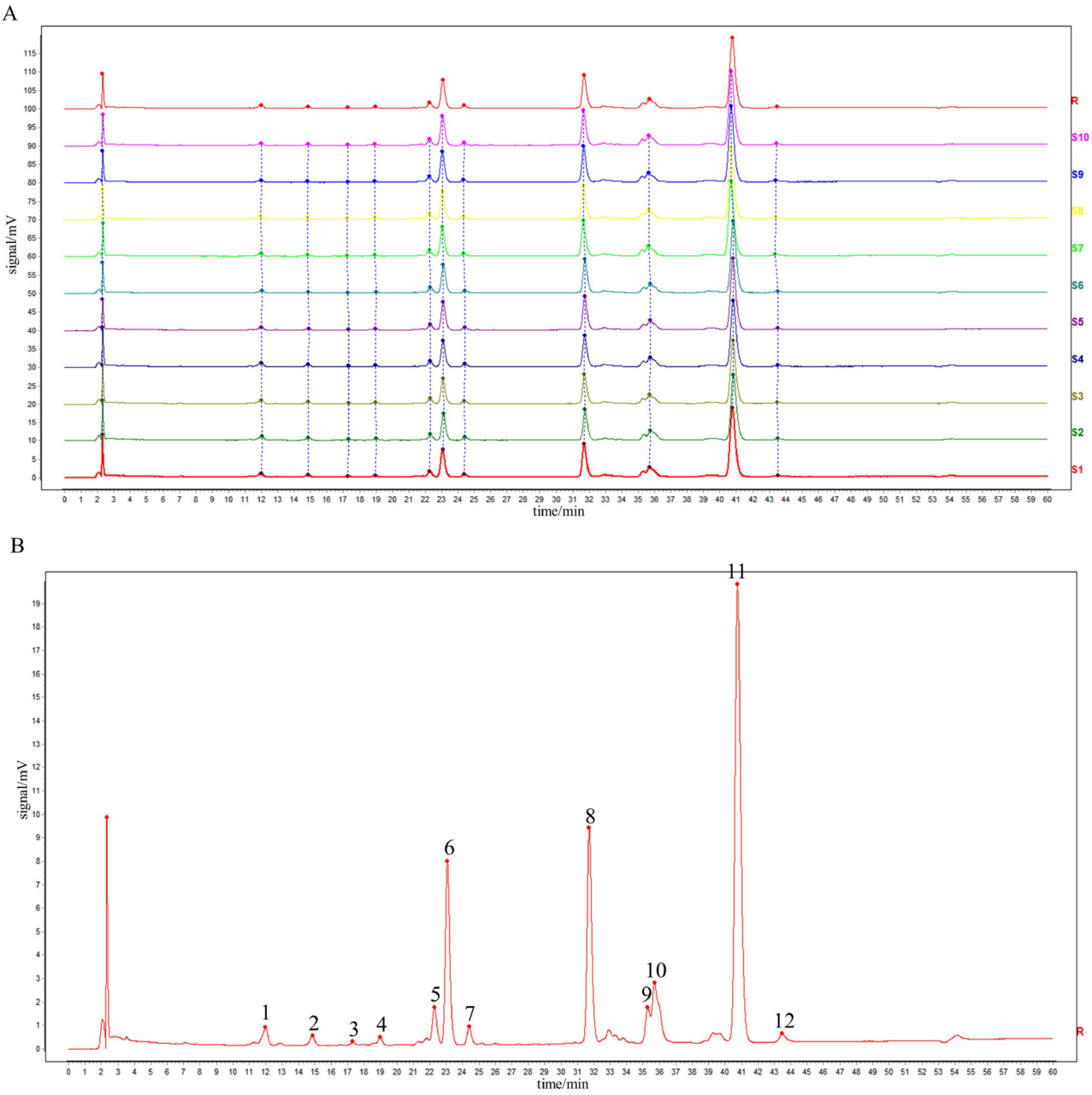

FIGURE 1
HPLC fingerprints of 10 batches of sample **(A)** and reference fingerprint chromatogram **(B)**.

groups using a subcutaneous injection of testosterone propionate (5 mg/kg/day dissolved in olive oil) for 28 consecutive days. Only olive oil was administered subcutaneously for 28 days to rats in the control group. Along with the testosterone propionate injection, rats in the drug-administered groups received daily gavage for 28 days, whereas those in the control group received distilled water following the same protocol. Fecal samples were obtained from each group of rats on the day before the experiment ended. After overnight fasting, blood was drawn from the abdominal aorta under anesthesia with 2% sodium pentobarbital (50 mg). The blood samples were centrifuged at 4,000 rpm for 15 min to obtain the serum. After prostate tissues were imaged for morphological evaluation, they were quickly separated and weighed. The serum was collected and stored at −80°C for ELISA. Rat feces were stored at −80°C until they were used for gut microbiome identification. A part of the prostate tissues was fixed in 4% paraformaldehyde for further histological evaluation. The remaining prostate tissues were promptly stored at −80°C for western blotting.

2.6 Oxidative stress

Serum superoxide dismutase (SOD), malondialdehyde (MDA) and glutathione (GSH) levels were measured using commercial

TABLE 1 Similarity results for the 10-batch samples.

Sample number	Similarity results	Sample number	Similarity results
S1	1.000	S6	0.999
S2	0.999	S7	0.999
S3	1.000	S8	1.000
S4	1.000	S9	1.000
S5	1.000	S10	1.000

reagents (Nanjing Jiancheng Bioengineering Institute, Nanjing, China) according to the manufacturer's recommendations.

2.7 Histopathological analysis

H&E staining was used to determine the morphological characteristics of rat prostate glands that were obtained after treatment with testosterone propionate. The epithelial thickness was determined using ImageJ software.

2.8 Enzyme-linked immunosorbent assay

Three types of pro-inflammatory cytokines, i.e., IL-1β, IL-6, and TNF-α, were measured in serum supernatant using the rat ELISA Commercial Kit (MultiSciences Lianke Biotech, Hangzhou, China) according to the manufacturer's recommendations.

2.9 Gut microbiota analysis

The feces of rats in the control group, model group, chewable tablets middle dosages group, and finasteride group were used as test samples. The gut microbiome samples were sent to BGI Co., Ltd, China (Shenzhen, China) for DNA extraction and sequencing of 16S rRNA gene. Total genomic DNA of the gut microbiome was extracted using E.Z.N.A.® Bacterial DNA Kit (Omega Biotek, Norcross, GA, USA) according to manufacturer's instruction. The V4 of 16S rRNA gene from the single gut microbiome sample was amplified. After genome DNA was normalized to 30 ng per PCR reaction, V4 dual-index fusion PCR primer cocktail and PCR master mix were added, then to run PCR. The melting temperature was 56°C and PCR cycle was 30. The PCR products were purified with AmpureXP beads to remove the unspecific products. The resulting library was used for sequencing on Illumina HiSeq 2500 platform following the standard pipelines of Illumina, and generating 2 × 250 bp paired-end reads (Sinclair et al., 2015).

To obtain clean reads, the raw data were filtered to eliminate the adapter pollution and low-quality reads by an in-house procedure as following (Fadrosh et al., 2014): The clean paired-end reads with overlap were merged to tags using FLASH (fast length adjustment of short reads, v1.2.11) (Magoč and Salzberg, 2011). Then, the tags were clustered to OTUs at 97% sequence similarity by scripts of software USEARCH (v9.1.13) (Edgar, 2013). Taxonomic ranks were assigned to OTUs representative sequence using Greengene (v201305, https://docs.qiime2.org/2024.2/data-resources/#greengenes) (Cole et al., 2014). At last, alpha diversity, beta diversity and the different species screening were analyzed based on OTUs and taxonomic ranks using mother (v1.31.2), software R (v3.1.1), QIIME (v1.80), or metastats (https://huttenhower.sph.harvard.edu/metastats/) (Schloss et al., 2009; White et al., 2009).

2.10 Western blot analysis

The total protein was isolated from prostate tissue homogenate by Radioimmunoprecipitation assay buffer. The protein concentration was then determined using the BCA assay kit (Nanjing Jiancheng Bioengineering Institute, Nanjing, China). Protein samples were separated on a 10% SDS-PAGE gel and transferred to a 0.45 μm polyvinylidene fluoride (PVDF) membrane, and then the PVDF membrane was blocked with 5% skim milk or 5% bovine serum albumin for 2 h. The blocked PVDF membrane were incubated with the following primary antibodies; p-JAK2 (1:1000), JAK2 (1:1000), p-STAT3 (1:1000), STAT3 (1:1000), β-Actin (1:5000) diluted with 5% bovine serum albumin overnight at 4°C, The PVDF membrane was washed 3 times with 1×TBST on a shaker, 10 min each time. The membrane was then incubated with HRP-labeled secondary antibodies for 2 h at room temperature, and the immunobands were visualized using chemiluminescent reagents in the Chemi-Doc XRS system, and the gray value of the protein bands was analyzed by Image J software. All the antibodies listed in this section were obtained from Chengdu Zhengneng Biotechnology Co., Ltd. (Chengdu, China).

2.11 Statistical analysis

Data computations and graphical representations were executed using GraphPad Prism software (version 9.5; San Diego, CA, United States). Intergroup disparities were examined using independent sample t-test, one-way analysis of variance, and Kruskal—Wallis test. Correlation was determined using the Spearman rank correlation coefficient (with a significance threshold of $p < 0.05$) in the corrplot software package of R (v3.4.1). GraphPad Prism v9.5 and R were used for analyses and figure generation. $p < 0.05$ was considered to be statistically significant. The results were expressed as mean ± standard deviations.

3 Results and discussion

3.1 HPLC fingerprint

Prepare 10 batches of rape bee pollen maca chewable tablet test solution (numbered S1~S10), measure according to the chromatographic conditions under item "2.4", and record the chromatogram for 60 min. "Chinese traditional medicine chromatographic fingerprint similarity evaluation system (2012, 1 Edition)" was used to evaluate 10 batches

10.3389/fmicb.2025.1547724

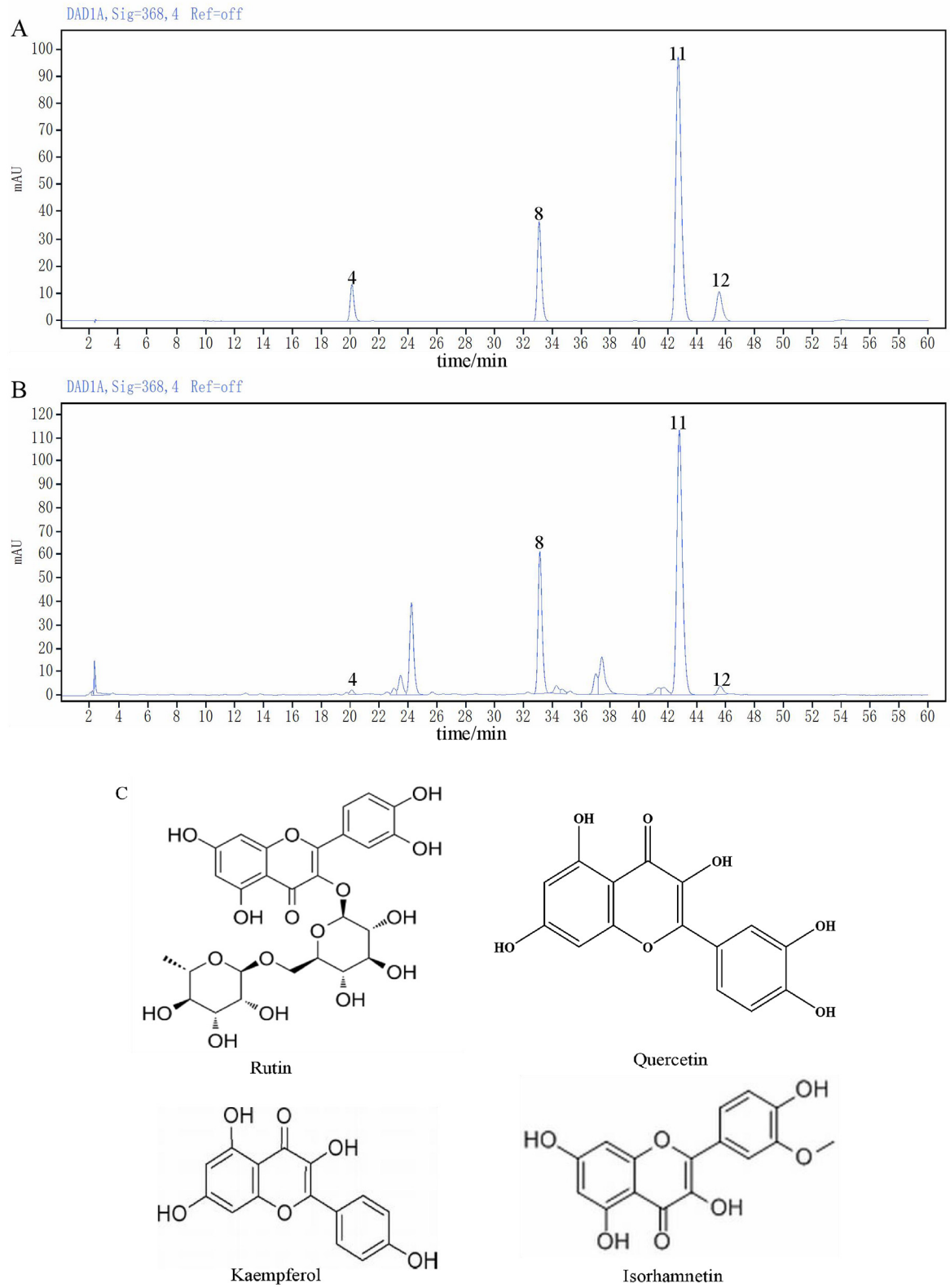

FIGURE 2
The chromatogram of the mixed reference substance **(A)**, the chromatogram of sample **(B)** and Chemical structures of *four* components **(C)**.

of AIA data of sample to be tested. The chromatographic fingerprint of sample S1 was designated as the reference standard. Following multi-point calibrated full-spectrum peak alignment, a consensus fingerprint was generated using the median method, resulting in the identification of 12 characteristic common peaks. Among these, four peaks were structurally authenticated:

TABLE 2 Determination results of component content of sample.

Component	Content (μg/g)
Rutin	15.51 ± 5.69
Quercetin	152.85 ± 3.95
Kaempferol	564.98 ± 1.07
Isorhamnetin	11.73 ± 4.76

Peak 4 (rutin), Peak 8 (quercetin), Peak 11 (kaempferol), and Peak 12 (isorhamnetin). Similarity analysis between the reference fingerprint and those of 10 batches of rape pollen-maca chewable tablets demonstrated high consistency, with similarity indices ranging from 0.999 to 1.000. As shown in Figures 1A, B and Table 1.

3.2 The content of four components in the sample

The content of rape bee pollen maca chewable tablets was analyzed using HPLC method. Quantitative analysis was performed on chromatographic peaks 4 (rutin), 8 (quercetin), 11 (kaempferol), and 12 (isorhamnetin) in the fingerprint spectrum. As illustrated in Figure 2B, these four components constitute the primary constituents of the rape bee pollen maca chewable tablets, with quercetin and kaempferol being particularly prominent. HPLC determination was performed on the sample of rape bee pollen maca chewable tablets and the mixed reference solution separately. The results are shown in Figures 2A, B. In addition, Figure 2C shows the structural formulas of each compound. Simultaneously settle the content of each component, as shown in Table 2.

3.3 Effect of chewable tablets containing rape bee pollen and maca in rats with BPH

To confirm whether rape bee pollen maca chewable tablets decreased BPH, a rat model of BPH was induced by testosterone propionate. Prostate tissues from the control group were light pink in color; they had intact morphology, did not adhere to the surrounding tissues, and had no nodules (Figure 3A). However, prostate tissues from the model group were dark red, had a nonsmooth surface, and showed obvious nodules. Tissues from the finasteride, pollen, and maca groups were lighter red in color and showed no obvious nodules. Tissues from the low-dose group of chewable tablets appeared dark red and showed obvious hyperplastic nodules, whereas tissues from the middle- and high-dose groups from chewable tablets were lighter red in color, had a smooth surface, and showed no obvious nodules. The body weight of rats in the model group was significantly lower ($p < 0.01$) than that of rats in the control group. Intriguingly, we observed that rats in the middle- and high-dose groups of the rape pollen maca chewable tablets exhibited greater body weight compared to those in the rape bee pollen and maca groups, though the difference did not reach statistical significance (Figure 3B). The model group showed a significant increase ($p < 0.01$) in both prostate index and prostate wet weight compared with the control group. The prostate index and prostate wet weight in the finasteride group ($p < 0.01$), pollen group ($p < 0.01$), maca group ($p < 0.01$), and the administration of varying doses of chewable tablets group ($p < 0.01$) were significantly lower than those in the model group (Figures 3C, D). Furthermore, our findings revealed that the middle- and high-dose groups of the rape bee pollen maca chewable tablets demonstrated superior efficacy compared to the rape bee pollen and maca treatment groups (Figures 3C, D).

3.4 Effect of chewable tablets containing rape bee pollen and maca on serum sex hormone levels in rats

Using ELISA, we looked at the variations in serum hormone levels in each group of rats. As demonstrated in Figures 4A–D, serum levels of T, DHT, and E2 were significantly elevated in the model group compared to the control group, along with an increased E2/T ratio ($p < 0.01$). After treatment with different doses of chewable tablets, the levels of T, DHT, and E2 significantly decreased ($p<0.01$), as well as the serum E2/T ratio ($p < 0.01$), but did not fully recover to normal levels (vs control). The collective data indicate that chewable tablets containing rape bee pollen and maca can reduce serum hormone levels in rats with BPH, and the chewable tablet is more efficacious than the use of rape bee pollen and maca as standalone agents.

3.5 Effect of chewable tablets containing rape bee pollen and maca on serum oxidative stress levels in rats

Using the kit, we observed alterations in serum oxidative stress levels across all groups of rats. As shown in Figures 5A–C, compared with the control group, the model group rats exhibited significantly decreased serum levels of SOD and GSH along with markedly elevated MDA levels ($p < 0.01$), demonstrating the occurrence of severe redox imbalance in these experimental animals. After treatment with different doses of chewable tablets, the levels of SOD and GSH significantly increased ($p < 0.01$), Meanwhile, the MDA levels were significantly reduced ($p < 0.01$). Furthermore, we found that the combined application of rape pollen and maca demonstrated superior efficacy compared to the individual use of either rape bee pollen or maca alone.

3.6 Effect of chewable tablets containing rape bee pollen and maca on the histopathology and serum inflammatory factor levels in rats

Figure 6A reflects the histopathologic changes in prostate tissues stained with hematoxylin & eosin (H&E). Prostate tissues were distinctly ordered, had a smooth surface, and exhibited fewer

10.3389/fmicb.2025.1547724

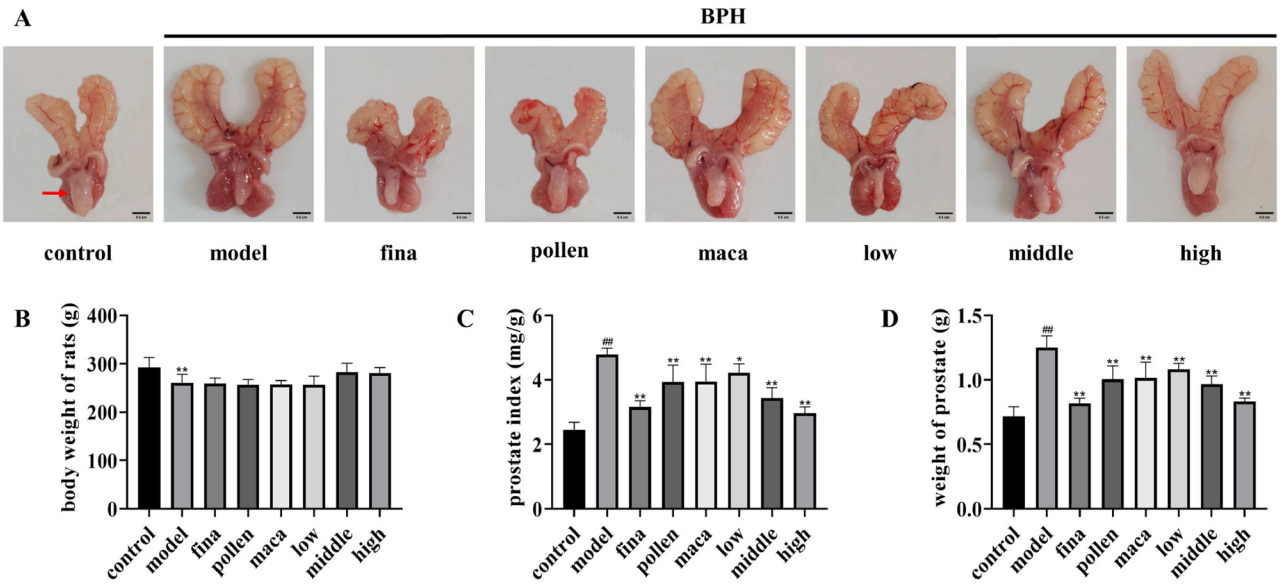

FIGURE 3
(A) Representative images of the prostate from each group. Scale bar = 0.5 cm. (Red arrows indicate rat prostate tissue.) **(B)** Body weight. **(C)** Prostate weight. **(D)** Prostate weight (PW) to body weight (BW) ratio. Data are presented as mean ± standard deviation. $^{\#\#}p < 0.01$ vs. rats that did not receive TP injection, $^{*}p < 0.05$, $^{**}p < 0.01$ vs. rats injected with TP. Low, middle, and high in the figure represent the low, middle, and high the rape pollen maca chewable tablets groups, respectively.

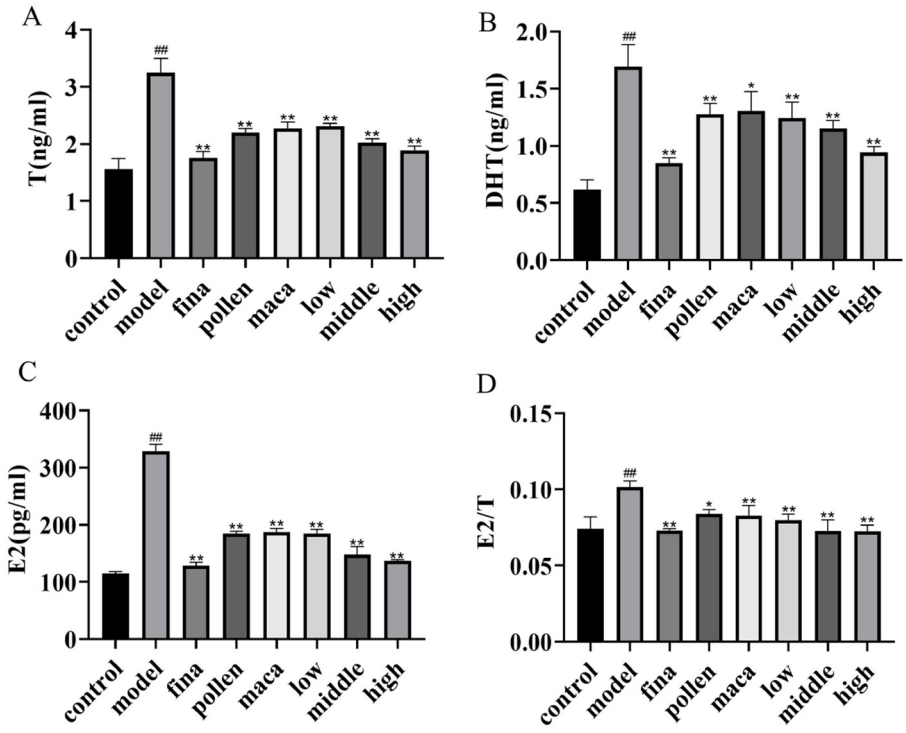

FIGURE 4
(A–C) Serum T, DHT, and E2 levels in rats determined using ELISA. **(D)** The serum E2/T ratio. Data are presented as mean ± standard deviation. $^{\#\#}p < 0.01$ vs. rats that did not receive TP injection, $^{*}p < 0.05$, $^{**}p < 0.01$ vs. rats injected with TP. Low, middle, and high in the figure represent the low, middle, and high chewable tablets groups, respectively.

acinar epithelial folds, and the epithelial cells were firmly packed in a single column in the control group. In contrast, prostate tissues from model rats exhibited considerable hyperplasia compared with that from control rats. Furthermore, the epithelial cells displayed a multilayer arrangement with more rough folds and increased epithelial cell thickness ($p < 0.01$). In addition, rats in the pollen

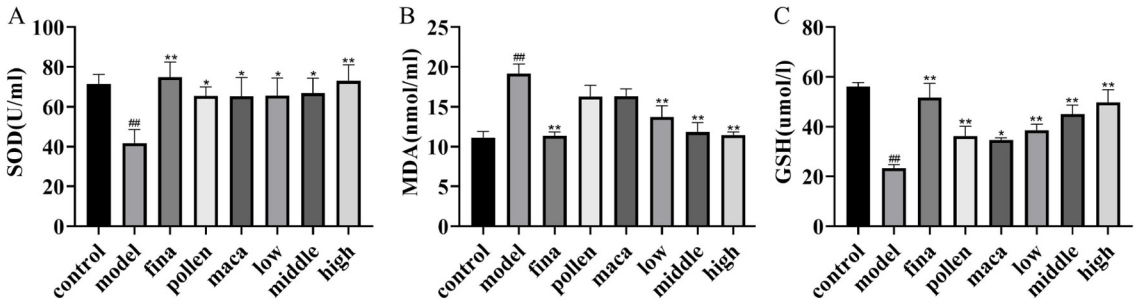

FIGURE 5
(A–C) Serum SOD, MDA and GSH levels in rats determined using Kit. Data are presented as mean ± standard deviation. $^{\#\#}p < 0.01$ vs. rats that did not receive TP injection, $^{*}p < 0.05$, $^{**}p < 0.01$ vs. rats injected with TP. Low, middle, and high in the figure represent the low, middle, and high chewable tablets groups, respectively.

group, maca group, and low-dose group of chewable tablets showed a significant reduction in prostate epithelial cell thickness ($p < 0.01$) and moderate hyperplasia of the prostate gland, whereas rats in the middle-dose group showed mild hyperplasia of the prostate gland and a substantial reduction in epithelial cell thickness ($p < 0.01$) compared with those in rats in the model group. On the other hand, rats in the high-dose group and finasteride group showed normalization of the prostate gland structure and a significant reduction in epithelial cell thickness ($p < 0.01$) (Figure 6B). Enzyme-linked immunosorbent assay (ELISA) was used to determine variations in serum inflammatory factor levels in each group of rats. The chewable tablet significantly decreased IL-6, TNF-α, and IL-1β levels in the blood ($p < 0.01$) (Figures 6C–E). The collective data indicate that chewable tablets containing rape bee pollen and maca could impede the progression of BPH and indicated chewable tablets to be more efficacious than rape bee pollen or maca used singly.

3.7 Effect of chewable tablets containing rape bee pollen and maca on the diversity of gut microbiota of rats

To investigate the effects of rape pollen maca chewable tablets on the gut microbiota in rats with BPH, we selected the following groups as study subjects: the control group, model group, finasteride group, and middle-dose rape bee pollen maca chewable tablet group. Operational taxonomic unit (OTU) data revealed differences in the gut microbiota among the four groups. A total of 941 OTUs were identified by grouping the pristine reads using a 97% threshold as shown in the Venn diagram (Figure 7A). The model, middle-dose chewable tablet group, finasteride, and control groups shared 798 OTUs. A total of 25 unique OTUs in the control group, 46 in the model group, 49 in the middle-dose chewable tablet group, and 23 in the finasteride group were identified. The Chao and Simpson indices, representing the gut microbiota alpha diversity, are commonly used to assess species richness and evenness. The data revealed that the differences in the Chao index among the groups were not statistically significant ($p > 0.05$). Nevertheless, the Chao index demonstrated an increase in the model and treatment groups compared with the control group, implying a higher abundance of intestinal flora compared with that in the control group (Figure 7B). A comparison of the Simpson index of the intestinal flora in the model group with that of the control group revealed a decrease in the former ($p > 0.05$) (Figure 7C). The dissimilarity in microbial communities between samples or populations is referred to as beta diversity. Principal component analysis and partial least squares discriminant analysis revealed variations in gut microbiota between the model group and other groups (Figures 7D, E). Principal coordinates analysis derived from unweighted Unifrac distances revealed that the model group grouped independently, whereas the other groups exhibited partial cross-aggregation. These findings demonstrated that the intestinal flora composition of rats in the model group differed from that of control rats. Furthermore, treatment with finasteride or the middle-dose chewable tablet led to changes in the intestinal flora composition in rats with BPH (Figure 7F).

3.8 Effect of chewable tablets containing rape bee pollen and maca on the composition of gut microbiota

Species difference maps were used to show the constitution of the main gut microbiota in different intervention groups; identify significant changes in the gut microbe at the phylum, and genus levels; analyze the reasons for the differences in the diversity of the gut microbiota in different groups; and explain changes in the structure of the intestinal microbiota. A significant increase in *Bacteroidia* ($p < 0.01$) and a significant decrease in *Bacillus* ($p < 0.05$) were noted at the phylum level in the model group compared with that in the control group (Figures 8A, C, D). At the genus level, significant increases were observed in the abundance of *Segatella* and *Prevotellamassilia*, but substantial decreases in the abundance of *Lactobacillus* ($p < 0.01$), *Phascolarctobacterium*, *Kineothrix*, *Collinsella*, and *Faecalibacterium* were reported in the model group relative to the control group (Figures 8B, E). The middle-dose chewable tablet group showed a reversal in this trend at various taxonomic levels compared with that in the model group.

10.3389/fmicb.2025.1547724

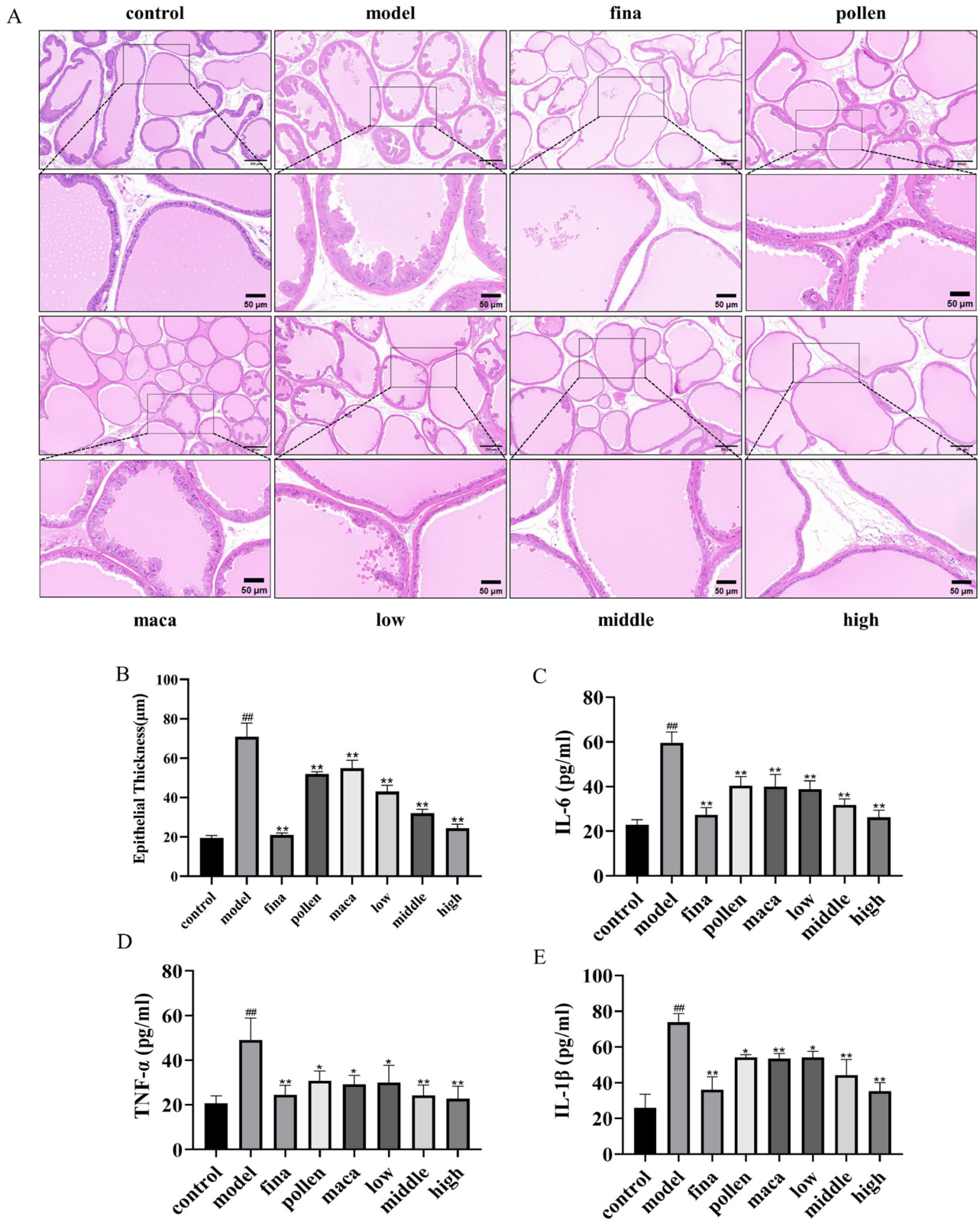

FIGURE 6
(A) H&E staining scale bar = 200 μm. Scale bar = 50 μm. **(B)** Quantification of epithelial thickness. **(C–E)** Serum IL-6, TNF-α, and IL-1β levels in rats determined using ELISA. Data are presented as mean ± standard deviation. $^{\#\#}p < 0.01$ vs. rats that did not receive TP injection; $^{*}p < 0.05$, $^{**}p < 0.01$ vs. rats injected with TP. Low, middle, and high in the figure represent the low, middle, and high chewable tablets groups, respectively.

10.3389/fmicb.2025.1547724

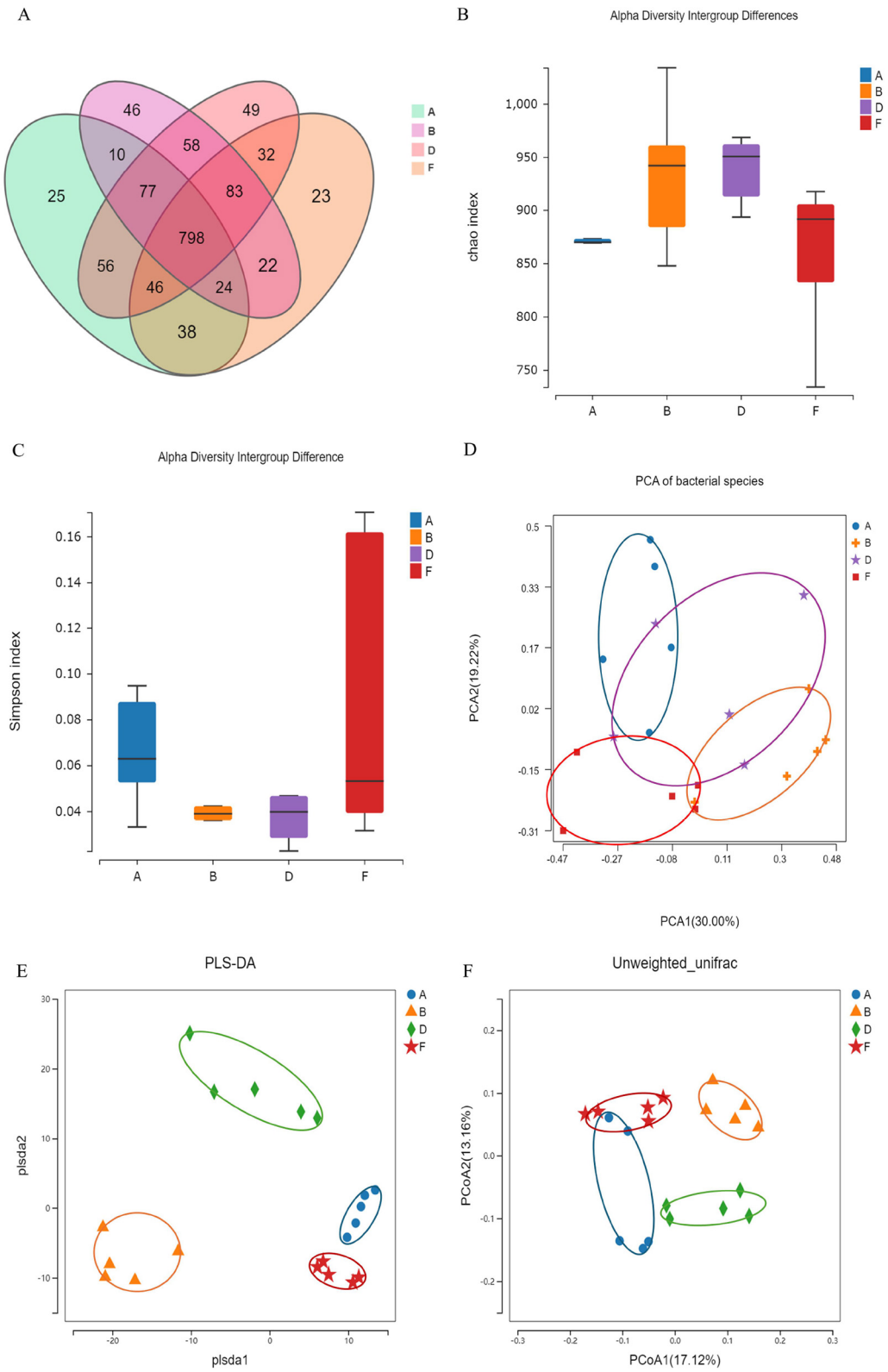

FIGURE 7
(A) Overview of OTUs in diverse groups. **(B)** Chao index. **(C)** Simpson index. Differences were assessed by the Kruskal-Wallis test. **(D)** Principal components analysis (PCA). **(E)** Partial least squares discrimination analysis (PLS-DA). **(F)** Principal Coordinates Analysis (PCoA). **(A, B, D, F)** In the figure represent the control, model, middle-dose chewable tablet, and finasteride groups, respectively.

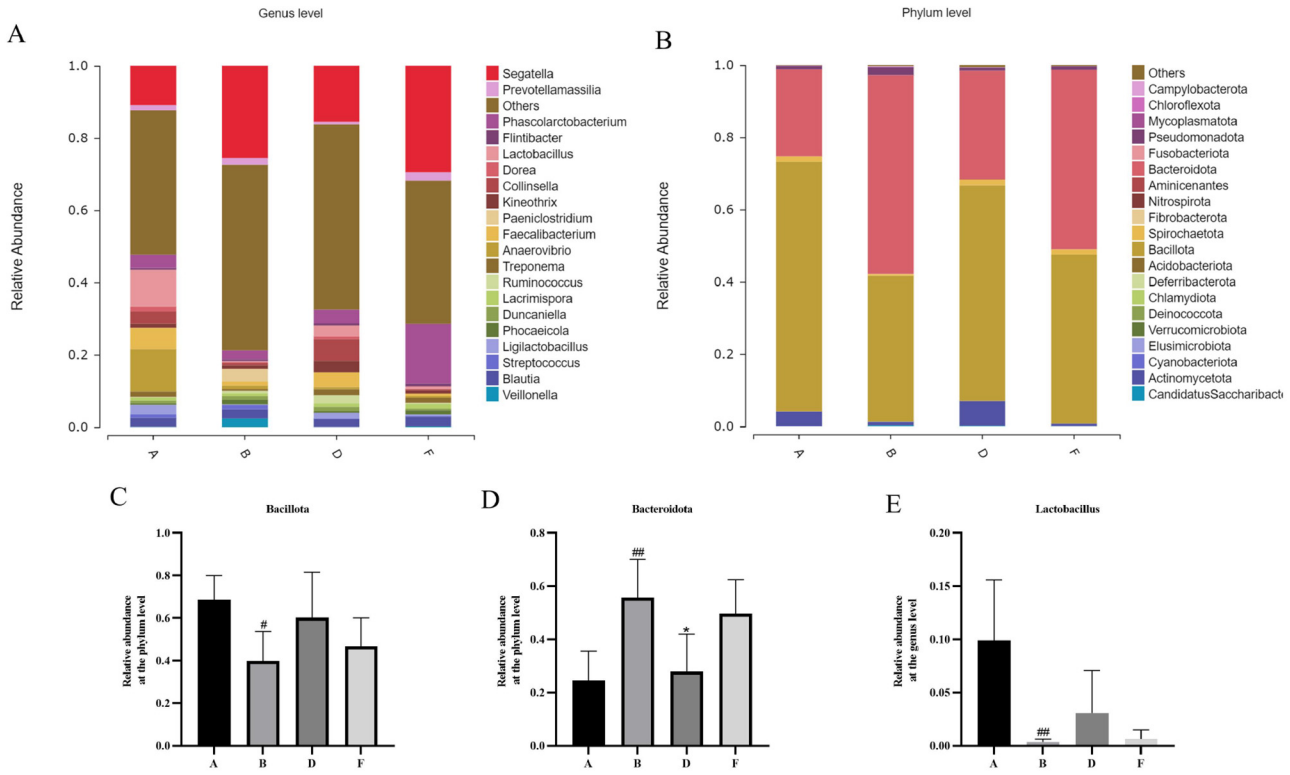

FIGURE 8
(A) Histogram showing the relative abundance of gut bacteria at the phylum level. **(B)** The bar chart shows the relative abundance of intestinal microbes at the genus level. **(C)** relative abundance of bacillota at the phylum level. **(D)** relative abundance of bacteroidota at the phylum level. **(E)** relative abundance of lactobacillus at the genus level. **(A, B, D, F)** in the figure represent the control, model, middle-dose chewable tablet, and finasteride groups, respectively.

3.9 Effect of chewable tablets containing rape bee pollen and maca on the IL-6/JAK2/STAT3 signaling pathway

To further investigate the mechanism of action of rape bee pollen and maca chewable tablets on BPH, we employed Western blotting to detect the expression levels of key proteins in the IL-6/JAK2/STAT3 signaling pathway within prostatic tissues. As shown in Figure 9, compared with the control group, the protein expression levels of IL-6, p-JAK2, and p-STAT3 in the prostatic tissues of model group rats were significantly increased ($p < 0.01$). After drug administration, a marked decrease in the expression levels of IL-6, p-JAK2, and p-STAT3 was observed in the prostate tissues of the treated groups compared to the model group ($p < 0.01$). Our findings indicate that the therapeutic mechanism of rape pollen maca chewable tablets against BPH involves the regulation of the IL-6/JAK2/STAT3 signaling pathway.

4 Discussion

This study established a fingerprint of rape bee pollen maca chewable tablets using HPLC, and 12 common peaks were identified as characteristic peaks. Four known components were identified by comparison with the fingerprint of the mixed control solution, Peak 4 was rutin, peak 8 was quercetin, peak 11 was kaempferol, and peak 12 was isorhamnetin. Their amounts were 15.51 ± 5.69 μg/g, 155.85 ± 3.95 μg/g, 564.98 ± 1.07 μg/g, and 11.73 ± 4.76 μg/g, respectively. The fingerprint spectrum of rape bee pollen maca chewable tablets established in this study is simple, stable, and has good repeatability. It can comprehensively reflect the effective chemical components of rape bee pollen maca chewable tablets, which is conducive to the comprehensive analysis of the quality of rape bee pollen maca chewable tablets. Additionally, studies have reported that quercetin and kaempferol exhibit therapeutic effects on benign prostatic hyperplasia induced by testosterone propionate solution (Wang et al., 2021; Fu et al., 2022).

Our findings revealed that the chewable tablet of rape bee pollen and maca showed better efficacy compared with the use of rape bee pollen or maca alone (Figures 3–5). According to clinical medication observations, excessive consumption of rape bee pollen may lead to gastrointestinal reactions such as nausea, vomiting, and loose stools. Additionally, a small number of patients may develop allergic skin reactions, including rash or pruritus (Hemmer et al., 2004). Therefore, the combined application of rape pollen and maca allows for a reduction in the dosage of rape pollen required, thereby mitigating the occurrence of certain adverse reactions. Since both rape pollen and maca serve dual purposes as medicinal agents and food-grade ingredients, they exhibit a low risk

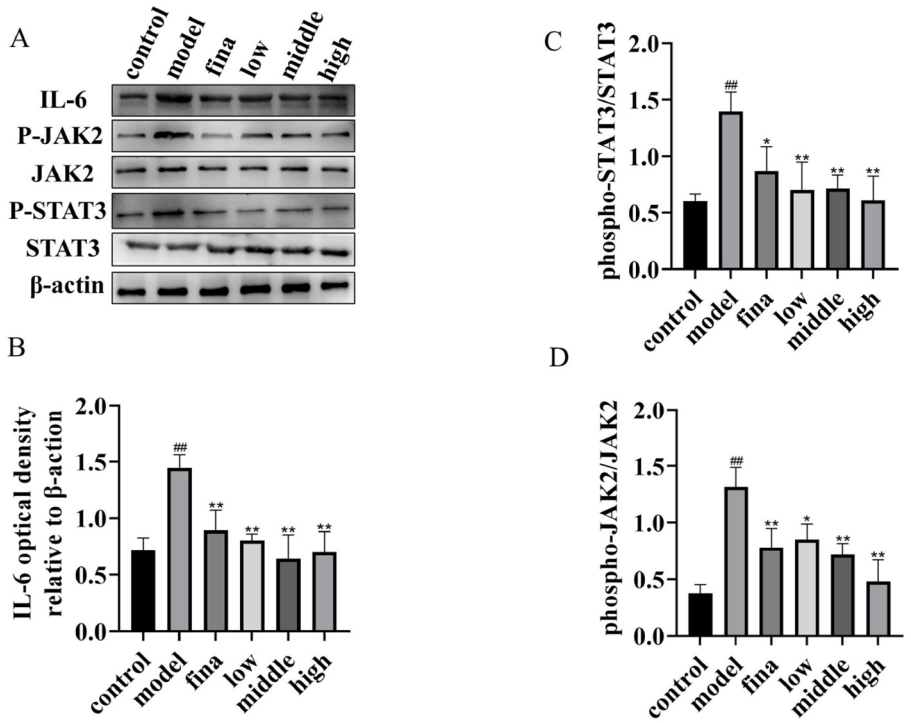

FIGURE 9
(A) Total protein and phosphorylated protein of STAT3 and JAK2, IL-6 proteins. One representative blot was selected from 3 independent experiments. **(B–D)** The relative band intensity was normalized to the relative actin intensity compared with the control. $^{\#\#}p < 0.01$ compared with rats not injected with TP; $^{*}p < 0.05$, $^{**}p < 0.01$ compared with the model group.

of adverse effects and minimal contamination during production processes. Thus, the chewable tablet of rape bee pollen and maca is more widely available than the chemically synthesized drug finasteride. Therefore, this study conducted a pharmacodynamic evaluation of rape pollen maca chewable tablets on benign prostatic hyperplasia, investigated their impact on gut microbiota, and further explored the IL-6/JAK2/STAT3 signaling pathway in prostatic tissues.

It has been established that BPH is influenced by both estrogens and androgens. The prostate's response to estrogens is linked to several processes, such as aromatase expression, apoptosis, and paracrine regulation through prostaglandin E2. E2 to T ratio rises in BPH and malignant prostate tissues due to aberrant expression of aromatase (Wang et al., 2024). 5α reductase (5-AR) converts T, the major circulating androgen in males, to DHT. DHT enters the nucleus by attaching to the AR at the androgen binding site. The DHT/AR complex molecule then attaches to the ARE in the promoter of the target gene, encouraging the growth and survival of prostate epithelial cells (Park et al., 2022; Gong et al., 2023).

In this study, a rat model of testosterone propionate induced BPH was used to determine the efficacy of chewable tablets containing rape bee pollen and maca. Our findings demonstrated that chewable tablets could lead to a notable reduction in prostate volume, epithelial thickness, and serum levels of IL-6, TNF-α, and IL-1β. Inflammation is an important factor in the process of BPH (Cai et al., 2020). Chronic inflammation leads to the overproduction of pro-inflammatory factors, including IL-6, IL-1β, and TNF-α, which induces the overproliferation of prostate epithelial and stromal cells and activates fibrosis to promote signaling and malignant transformation (Cai et al., 2020). We found that chewable tablets group exerted anti-inflammatory activity by significantly inhibiting the IL-6/JAK2/STAT3 signaling pathway. The IL-6/JAK2/STAT3 signaling pathway plays an important role in the development of BPH. IL-6 binds to the IL-6 receptor on the cell membrane and activates intracellular JAK2 and phosphorylating it. Phosphorylated JAK2 further activates STAT3. After dimerization of phosphorylated STAT3, the downstream nuclear transcription factors are activated, which promotes the production and release of IL-6 and exacerbates the inflammatory response (Bowman et al., 2000; Kim et al., 2016; Zhang et al., 2018).

Lactobacillus has anti-inflammatory effects, stimulates brain functions, modulates metabolism, and antagonizes intestinal pathogens (Cai et al., 2020). It can metabolize organic acids such as lactic acid, formic acid, acetic acid, and butyric acid, which reduce the intestinal pH and inhibit the growth of acid-intolerant genera in the host intestine (Petrova et al., 2017; Tramontano et al., 2018). *Faecalibacterium* has been demonstrated to confer protection in several studies owing to its anti-inflammatory and symbiotic characteristics. It plays a role in metabolizing acetate into butyrate, which serves as a primary source of energy for colonocytes and functions as an anti-inflammatory agent (Sha et al., 2020; Maioli et al., 2021; Martín et al., 2023). *Collinsella*

is responsible for the production of butyric acid and reducing inflammatory diseases (Jeong et al., 2019; Qin et al., 2019). The excessive accumulation of succinic acid in the gut can lead to diarrhea, and *Phascolarctobacterium* can use succinic acid to produce propionic acid (Wu et al., 2017). *Kineothrix* can produce butyrate, which plays a role in modulating inflammation (Choi et al., 2023). *Prevotella* has virulence factors, including adhesins, pili, hemolysins, nucleases, proteases, lipopolysaccharides, exopolysaccharides, and other enzymes, which promote its pathogenicity and survival in the host (Sharma et al., 2022). The overgrowth of *Prevotella* or its translocation across the mucosal barrier enhances the immune response and leads to inflammatory diseases (Iljazovic et al., 2021). The genus *Prevotella* exhibited abnormally elevated abundance in the model group, while the SCFA-producing gut microbiota including *Lactobacillus*, *Faecalibacterium*, *Collinsella*, *Phascolarctobacterium*, and *Kineothrix* were significantly reduced. This imbalance led to an overproduction of pro-inflammatory factors and facilitated the development of BPH. In contrast, chewable tablets group demonstrated an increase in the abundance of beneficial bacteria, including *Faecalibacterium, Collinsella, Phascolarctobacterium, Kineothrix,* and *Lactobacillus*, while concurrently demonstrating a decrease in the abundance of the pro-inflammatory bacterial *Prevotella*. The finasteride group demonstrated an increase in the levels of beneficial bacteria, specifically *Phascolarctobacterium* and *Lactobacillus,* while concurrently demonstrating a decrease in the abundance of the pro-inflammatory bacterial *Prevotella*.

5 Conclusion

In conclusion, this study demonstrates that the chewable tablet of rape bee pollen and maca ameliorates testosterone propionate-induced BPH in rats. The protective effects, mediated through the IL-6/JAK2/STAT3 signaling pathway, are associated with reduced inflammation, oxidative stress, and hormonal imbalance, alongside a beneficial modulation of the gut microbiota. In addition, we also established an HPLC fingerprint of rape bee pollen maca chewable tablets. Our findings indicate these chewable tablets containing rape bee pollen and maca as a promising natural therapeutic strategy for BPH management.

Data availability statement

The data presented in the study are deposited in the NCBI Sequence Read Archive (SRA) repository, accession number PRJNA1353094.

Ethics statement

The animal study was approved by the Animal Ethical Committee of Huanghe Science & Technology University approved the Animal Experiments (NO: 2023-011) (Zhengzhou, China). The study was conducted in accordance with the local legislation and institutional requirements.

Author contributions

XH: Funding acquisition, Investigation, Writing – original draft. GR: Investigation, Writing – original draft. HT: Data curation, Writing – review & editing. PZ: Writing – review & editing, Formal analysis. HZ: Formal analysis, Writing – review & editing. SZ: Formal analysis, Validation, Writing – review & editing. SW: Writing – review & editing, Data curation. AJ: Writing – review & editing, Conceptualization, Funding acquisition. WZ: Conceptualization, Writing – review & editing.

Funding

The author(s) declare that financial support was received for the research and/or publication of this article. This work was supported by the Postgraduate Education Reform and Quality Improvement Project of Henan Province (YJS2023JD68); Henan Province Science and Technology Research Project (242102311266, 242400410217, 142102310146); Zhengzhou Science and Technology Research project (2024TLZDJH017); Open Research Project of Henan Provincial Key Laboratory of Nanocomposites and Applications (HKD20240902).

Acknowledgments

We gratefully acknowledge MJEditor (www.mjeditor.com) for providing valuable language support during the preparation of this manuscript.

Conflict of interest

The authors declare that the research was conducted in the absence of any commercial or financial relationships that could be construed as a potential conflict of interest.

Generative AI statement

The author(s) declare that no Gen AI was used in the creation of this manuscript.

Any alternative text (alt text) provided alongside figures in this article has been generated by Frontiers with the support of artificial intelligence and reasonable efforts have been made to ensure accuracy, including review by the authors wherever possible. If you identify any issues, please contact us.

Publisher's note

All claims expressed in this article are solely those of the authors and do not necessarily represent those of their affiliated organizations, or those of the publisher, the editors and the reviewers. Any product that may be evaluated in this article, or claim that may be made by its manufacturer, is not guaranteed or endorsed by the publisher.

References

An, J., Song, Y., Kim, S., Kong, H., and Kim, K. (2023). Alteration of gut microbes in benign prostatic hyperplasia model and finasteride treatment model. *IJMS* 24:5904. doi: 10.3390/ijms24065904

Antoniou, V., Gauhar, V., Modi, S., and Somani, B. K. (2023). Role of phytotherapy in the management of BPH: a summary of the literature. *J. Clin. Med.* 12:1899. doi: 10.3390/jcm12051899

Awedew, A. F., Han, H., Abbasi, B., Abbasi-Kangevari, M., Ahmed, M. B., Almidani, O., et al. (2022). The global, regional, and national burden of benign prostatic hyperplasia in 204 countries and territories from 2000 to 2019: a systematic analysis for the Global Burden of Disease Study 2019. *Lancet Healthy Longev.* 3, e754–e776. doi: 10.1016/S2666-7568(22)00213-6

Bowman, T., Garcia, R., Turkson, J., and Jove, R. (2000). STATs in oncogenesis. *Oncogene* 19, 2474–2488. doi: 10.1038/sj.onc.1203527

Cai, Y., Folkerts, J., Folkerts, G., Maurer, M., and Braber, S. (2020). Microbiota-dependent and -independent effects of dietary fibre on human health. *Br. J. Pharmacol.* 177, 1363–1381. doi: 10.1111/bph.14871

Cannarella, R., Condorelli, R. A., Barbagallo, F., La Vignera, S., and Calogero, A. E. (2021). Endocrinology of the aging prostate: current concepts. *Front. Endocrinol.* 12:554078. doi: 10.3389/fendo.2021.554078

Chen, X., Wu, R., Ren, Z., Tong, Y., Chen, S., Yang, F., et al. (2020). Regulation of microRNAs by rape bee pollen on benign prostate hyperplasia in rats. *Andrologia* 52:e13386. doi: 10.1111/and.13386

Choi, K. J., Yoon, M. Y., Kim, J.-E., and Yoon, S. S. (2023). Gut commensal *Kineothrix alysoides* mitigates liver dysfunction by restoring lipid metabolism and gut microbial balance. *Sci. Rep.* 13:14668. doi: 10.1038/s41598-023-41160-y

Cole, J. R., Wang, Q., Fish, J. A., Chai, B., McGarrell, D. M., Sun, Y., et al. (2014). Ribosomal Database Project: data and tools for high throughput rRNA analysis. *Nucleic Acids Res.* 42, D633–D642. doi: 10.1093/nar/gkt1244

Da Silva Leitão Peres, N., Cabrera Parra Bortoluzzi, L., Medeiros Marques, L. L., Formigoni, M., Fuchs, R. H. B., Droval, A. A., et al. (2020). Medicinal effects of Peruvian maca (*Lepidium meyenii*): a review. *Food Funct.* 11, 83–92. doi: 10.1039/C9FO02732G

Edgar, R. C. (2013). UPARSE: highly accurate OTU sequences from microbial amplicon reads. *Nat. Methods* 10, 996–998. doi: 10.1038/nmeth.2604

Elbaz, E. M., Darwish, A., Gad, A. M., Abdel Rahman, A. A. S., and Safwat, M. H. (2023). Canagliflozin alleviates experimentally induced benign prostate hyperplasia in a rat model: exploring potential mechanisms involving mir-128b/EGFR/EGF and JAK2/STAT3 signaling pathways through in silico and in vivo investigations. *Eur. J. Pharmacol.* 957:175993. doi: 10.1016/j.ejphar.2023.175993

Fadrosh, D. W., Ma, B., Gajer, P., Sengamalay, N., Ott, S., Brotman, R. M., et al. (2014). An improved dual-indexing approach for multiplexed 16S rRNA gene sequencing on the Illumina MiSeq platform. *Microbiome* 2:6. doi: 10.1186/2049-2618-2-6

Fu, W., Chen, S., Zhang, Z., Chen, Y., You, X., and Li, Q. (2022). Quercetin in Tonglong Qibi decoction ameliorates testosterone-induced benign prostatic hyperplasia in rats by regulating Nrf2 signalling pathways and oxidative stress. *Andrologia* 54:e14502. doi: 10.1111/and.14502

Gong, G.-Y., Xi, S.-Y., Li, C.-C., Tang, W.-L., Fu, X.-M., and Huang, Y.-P. (2023). Bushen Tongluo formula ameliorated testosterone propionate-induced benign prostatic hyperplasia in rats. *Phytomedicine* 120:155048. doi: 10.1016/j.phymed.2023.155048

Gu, M., Liu, C., Yang, T., Zhan, M., Cai, Z., Chen, Y., et al. (2021). High-fat diet induced gut microbiota alterations associating with Ghrelin/Jak2/Stat3 up-regulation to promote benign prostatic hyperplasia development. *Front. Cell Dev. Biol.* 9:615928. doi: 10.3389/fcell.2021.615928

Han, Y. Y., Zhang, Q. H., Chen, W. S., Li, Z. L., Xie, D., Zhang, S. L., et al. (2023). Fermented rape pollen powder can alleviate benign prostatic hyperplasia in rats by reducing hormone content and changing gut microbiota. *Benef. Microbes* 14, 503–524. doi: 10.1163/18762891-20230039

Hata, J., Harigane, Y., Matsuoka, K., Akaihata, H., Yaginuma, K., Meguro, S., et al. (2023). Mechanism of androgen-independent stromal proliferation in benign prostatic hyperplasia. *IJMS* 24:11634. doi: 10.3390/ijms241411634

Hemmer, W., Focke, M., Kolarich, D., Dalik, I., Götz, M., and Jarisch, R. (2004). Identification by immunoblot of venom glycoproteins displaying immunoglobulin E-binding N-glycans as cross-reactive allergens in honeybee and yellow jacket venom. *Clin. Exp. Allergy* 34, 460–469. doi: 10.1111/j.1365-2222.2004.01897.x

Ho, C. K. M., and Habib, F. K. (2011). Estrogen and androgen signaling in the pathogenesis of BPH. *Nat. Rev. Urol.* 8, 29–41. doi: 10.1038/nrurol.2010.207

Huang, B., Lang, X., and Li, X. (2022). The role of IL-6/JAK2/STAT3 signaling pathway in cancers. *Front. Oncol.* 12:1023177. doi: 10.3389/fonc.2022.1023177

Iljazovic, A., Amend, L., Galvez, E. J. C., De Oliveira, R., and Strowig, T. (2021). Modulation of inflammatory responses by gastrointestinal *Prevotella* spp. – *From associations to functional studies. Int. J. Med. Microbiol.* 311:151472. doi: 10.1016/j.ijmm.2021.151472

Jeong, Y., Kim, J.-W., You, H. J., Park, S.-J., Lee, J., Ju, J. H., et al. (2019). Gut microbial composition and function are altered in patients with early rheumatoid arthritis. *JCM* 8:693. doi: 10.3390/jcm8050693

Kim, B.-H., Yi, E. H., and Ye, S.-K. (2016). Signal transducer and activator of transcription 3 as a therapeutic target for cancer and the tumor microenvironment. *Arch. Pharm. Res.* 39, 1085–1099. doi: 10.1007/s12272-016-0795-8

Li, J., Li, Y., Zhou, L., Li, C., Liu, J., Liu, D., et al. (2024). The human microbiome and benign prostatic hyperplasia: current understandings and clinical implications. *Microbiol. Res.* 281:127596. doi: 10.1016/j.micres.2023.127596

Liu, Y., Yang, C., Zhang, Z., and Jiang, H. (2021). Gut microbiota dysbiosis accelerates prostate cancer progression through increased LPCAT1 expression and enhanced DNA repair pathways. *Front. Oncol.* 11:679712. doi: 10.3389/fonc.2021.679712

Magoč, T., and Salzberg, S. L. (2011). FLASH: fast length adjustment of short reads to improve genome assemblies. *Bioinformatics* 27, 2957–2963. doi: 10.1093/bioinformatics/btr507

Maioli, T. U., Borras-Nogues, E., Torres, L., Barbosa, S. C., Martins, V. D., Langella, P., et al. (2021). Possible benefits of *Faecalibacterium prausnitzii* for obesity-associated gut disorders. *Front. Pharmacol.* 12:740636. doi: 10.3389/fphar.2021.740636

Martín, R., Rios-Covian, D., Huillet, E., Auger, S., Khazaal, S., Bermúdez-Humarán, L. G., et al. (2023). *Faecalibacterium*: a bacterial genus with promising human health applications. *FEMS Microbiol. Rev.* 47:fuad039. doi: 10.1093/femsre/fuad039

Miernik, A., and Gratzke, C. (2020). Current treatment for benign prostatic hyperplasia. *Dtsch. Arztebl. Int.* 117, 843–854. doi: 10.3238/arztebl.2020.0843

Park, W. Y., Song, G., Park, J. Y., Ahn, K. S., Kwak, H. J., Park, J., et al. (2022). Ellagic acid improves benign prostate hyperplasia by regulating androgen signaling and STAT3. *Cell Death Dis.* 13:554. doi: 10.1038/s41419-022-04995-3

Petrova, M. I., Reid, G., Vaneechoutte, M., and Lebeer, S. (2017). *Lactobacillus iners*: friend or foe? *Trends Microbiol.* 25, 182–191. doi: 10.1016/j.tim.2016.11.007

Qiao, J., Xiao, X., Wang, K., Haubruge, E., Dong, J., and Zhang, H. (2023). Rapeseed bee pollen alleviates chronic non-bacterial prostatitis via regulating gut microbiota. *J. Sci. Food Agric.* 103, 7896–7904. doi: 10.1002/jsfa.12878

Qin, P., Zou, Y., Dai, Y., Luo, G., Zhang, X., and Xiao, L. (2019). Characterization a novel butyric acid-producing bacterium *Collinsella aerofaciens* subsp. *shenzhenensis subsp. nov. Microorganisms* 7:78. doi: 10.3390/microorganisms7030078

Rodríguez-Pólit, C., Gonzalez-Pastor, R., Heredia-Moya, J., Carrera-Pacheco, S. E., Castillo-Solis, F., Vallejo-Imbaquingo, R., et al. (2023). Chemical properties and biological activity of bee pollen. *Molecules* 28:7768. doi: 10.3390/molecules28237768

Russo, G. I., Bongiorno, D., Bonomo, C., Musso, N., Stefani, S., Sokolakis, I., et al. (2023). The relationship between the gut microbiota, benign prostatic hyperplasia, and erectile dysfunction. *Int. J. Impot. Res.* 35, 350–355. doi: 10.1038/s41443-022-00569-1

Schloss, P. D., Westcott, S. L., Ryabin, T., Hall, J. R., Hartmann, M., Hollister, E. B., et al. (2009). Introducing mothur: open-source, platform-independent, community-supported software for describing and comparing microbial communities. *Appl. Environ. Microbiol.* 75, 7537–7541. doi: 10.1128/AEM.01541-09

Sha, S., Ni, L., Stefil, M., Dixon, M., and Mouraviev, V. (2020). The human gastrointestinal microbiota and prostate cancer development and treatment. *Investig. Clin. Urol.* 61, S43–S52. doi: 10.4111/icu.2020.61.S1.S43

Shah, A., Shah, A. A., K, N., and Lobo, R. (2021). Mechanistic targets for BPH and prostate cancer-a review. *Rev. Environ. Health* 36, 261–270. doi: 10.1515/reveh-2020-0051

Sharma, G., Garg, N., Hasan, S., and Shirodkar, S. (2022). *Prevotella*: an insight into its characteristics and associated virulence factors. *Microb. Pathog.* 169:105673. doi: 10.1016/j.micpath.2022.105673

Sinclair, L., Osman, O. A., Bertilsson, S., and Eiler, A. (2015). Microbial community composition and diversity via 16S rRNA gene amplicons: evaluating the illumina platform. *PLoS ONE* 10:e0116955. doi: 10.1371/journal.pone.0116955

Singh, A. K., Bhadauria, A. S., Kumar, U., Raj, V., Rai, A., Kumar, P., et al. (2020). Author correction: novel indole-fused benzo-oxazepines (IFBOs) inhibit invasion of hepatocellular carcinoma by targeting IL-6 mediated JAK2/STAT3 oncogenic signals. *Sci. Rep.* 10:2391. doi: 10.1038/s41598-020-59134-9

Song, G., Tong, J., Wang, Y., Li, Y., Liao, Z., Fan, D., et al. (2023). Nrf2-mediated macrophage function in benign prostatic hyperplasia: novel molecular insights and implications. *Biomed. Pharmacother.* 167:115566. doi: 10.1016/j.biopha.2023.115566

Staršíchová, A., Lincová, E., Pernicová, Z., Kozubík, A., and Souček, K. (2010). TGF-β1 suppresses IL-6-induced STAT3 activation through regulation of Jak2 expression in prostate epithelial cells. *Cell. Signal.* 22, 1734–1744. doi: 10.1016/j.cellsig.2010.06.014

Stewart, K. L., and Lephart, E. D. (2023). Overview of BPH: symptom relief with dietary polyphenols, vitamins and phytochemicals by nutraceutical supplements with implications to the prostate microbiome. *Int. J. Mol. Sci.* 24:5486. doi: 10.3390/ijms24065486

Tramontano, M., Andrejev, S., Pruteanu, M., Klünemann, M., Kuhn, M., Galardini, M., et al. (2018). Nutritional preferences of human gut bacteria reveal their metabolic idiosyncrasies. *Nat. Microbiol.* 3, 514–522. doi: 10.1038/s41564-018-0123-9

Ulloa Del Carpio, N., Alvarado-Corella, D., Quiñones-Laveriano, D. M., Araya-Sibaja, A., Vega-Baudrit, J., Monagas-Juan, M., et al. (2024). Exploring the chemical and pharmacological variability of *Lepidium meyenii*: a comprehensive review of the effects of maca. *Front. Pharmacol.* 15:1360422. doi: 10.3389/fphar.2024.1360422

Vásquez-Velásquez, C., Gasco, M., Fano-Sizgorich, D., and Gonzales, G. F. (2020). Inflammatory pathway employed by red maca to treat induced benign prostatic hyperplasia in rats. *Andrologia* 52:e13516. doi: 10.1111/and.13516

Wang, F., Ma, D., Yang, J., Lyu, D., Gao, Q., Li, C., et al. (2024). Mechanisms and efficacy of Chinese herbal medicines in benign prostatic hyperplasia. *Chin. J. Integr. Med.* doi: 10.1007/s11655-024-3916-0

Wang, X., Zhu, J., Yan, H., Shi, M., Zheng, Q., Wang, Y., et al. (2021). Kaempferol inhibits benign prostatic hyperplasia by resisting the action of androgen. *Eur. J. Pharmacol.* 907:174251. doi: 10.1016/j.ejphar.2021.174251

Welén, K., and Damber, J.-E. (2022). Androgens, aging, and prostate health. *Rev. Endocr. Metab. Disord.* 23, 1221–1231. doi: 10.1007/s11154-022-09730-z

White, J. R., Nagarajan, N., and Pop, M. (2009). Statistical methods for detecting differentially abundant features in clinical metagenomic samples. *PLoS Comput. Biol.* 5:e1000352. doi: 10.1371/journal.pcbi.1000352

Wu, F., Guo, X., Zhang, J., Zhang, M., Ou, Z., and Peng, Y. (2017). *Phascolarctobacterium faecium* abundant colonization in human gastrointestinal tract. *Exp. Ther. Med.* 14, 3122–3126. doi: 10.3892/etm.2017.4878

Xiao, J., Gong, Y., Chen, Y., Yu, D., Wang, X., Zhang, X., et al. (2017). IL-6 promotes epithelial-to-mesenchymal transition of human peritoneal mesothelial cells possibly through the JAK2/STAT3 signaling pathway. *Am. J. Physiol. Renal Physiol.* 313, F310–F318. doi: 10.1152/ajprenal.00428.2016

Yang, B.-C., Jin, L.-L., Yang, Y.-F., Li, K., and Peng, D.-M. (2014). Inhibitory effect of rape pollen supercritical CO2 fluid extract against testosterone-induced benign prostatic hyperplasia in rats. *Exp. Ther. Med.* 8, 31–37. doi: 10.3892/etm.2014.1680

Zhang, X., Lu, H., Hong, W., Liu, L., Wang, S., Zhou, M., et al. (2018). Tyrphostin B42 attenuates trichostatin A-mediated resistance in pancreatic cancer cells by antagonizing IL-6/JAK2/STAT3 signaling. *Oncol. Rep.* 39, 1876–1884. doi: 10.3892/or.2018.6241

Zou, Y., Aboshora, W., Li, J., Xiao, T., and Zhang, L. (2017). Protective effects of *Lepidium meyenii* (Maca) aqueous extract and lycopene on testosterone propionate-induced prostatic hyperplasia in mice. *Phytother. Res.* 31, 1192–1198. doi: 10.1002/ptr.5838

Frontiers in Microbiology

Explores the habitable world and the potential of microbial life

The largest and most cited microbiology journal which advances our understanding of the role microbes play in addressing global challenges such as healthcare, food security, and climate change.

Discover the latest Research Topics

See more →

Frontiers

Avenue du Tribunal-Fédéral 34
1005 Lausanne, Switzerland
frontiersin.org

Contact us

+41 (0)21 510 17 00
frontiersin.org/about/contact